



IMPERIAL INSTITUTE
OF
AGRICULTURAL RESEARCH, PUSA.

PROCEEDINGS
OF THE
ROYAL SOCIETY OF LONDON

SERIES

CONTAINING PAPERS OF A MATHEMATICAL AND
PHYSICAL CHARACTER

VOL. CXLVI.

LONDON:

PRINTED FOR THE ROYAL SOCIETY AND SOLD BY
HARRISON AND SONS, LTD., ST. MARTIN'S LANE
PRINTERS IN ORDINARY TO HIS MAJESTY.

OCTOBER, 1934.

LONDON :
HARRISON AND SONS, LTD., PRINTERS IN ORDINARY TO HIS MAJESTY,
ST. MARTIN'S LANE.

CONTENTS.

SERIES A. VOL. CXLVI.

No. A 856.—August 1, 1934.

	PAGE
Probability Likelihood and Quantity of Information in the Logic of Uncertain Inference. By R. A. Fisher, F.R.S.	1
Probability and Scientific Method. By Harold Jeffreys, F.R.S.....	9
The Refractive Index of an Ionized Medium. By C. G. Darwin, F.R.S.....	17
The Isotopic Constitution and Atomic Weights of the Rare Earth Elements. By F. W. Aston, F.R.S.....	46
Supersonic Dispersion in Gases. By E. G. Richardson. Communicated by T. H. Have- lock, F.R.S.	56
The Kinetics of the Oxidation of Mixtures of Ethylene and Acetaldehyde. By E. W. R. Steacie and A. C. Plewes. Communicated by H. T. Barnes, F.R.S.....	72
On the Stopping of Fast Particles and on the Creation of Positive Electrons. By H. Bethe and W. Heitler. Communicated by P. A. M. Dirac, F.R.S.....	83
The Influence of Pressure on the Spontaneous Ignition of Inflammable Gas-Air Mixtures. III—Hexane- and Isobutane-Air Mixtures. By D. T. A. Townend, L. L. Cohen and M. R. Mandlekar. Communicated by W. A. Bone, F.R.S.....	113
The Sorption of Methyl and Ethyl Alcohol by Silica Gels. By A. G. Foster. Com- municated by A. J. Allmand, F.R.S.....	129
An X-Ray Analysis of the Structure of Chrysene. By J. Iball. Communicated by Sir William Bragg, O.M., F.R.S.	140
The Velocity of Corrosion from the Electrochemical Standpoint—Part III. By U. R. Evans and R. B. Mears. Communicated by Sir Harold Carpenter, F.R.S.....	153
The Excitation of Band Systems by Electron Impact. By G. O. Langstroth. Com- municated by O. W. Richardson, F.R.S.....	166
The Internal Conversion of γ -Rays. By J. B. Fisk and H. M. Taylor. Communicated by R. H. Fowler, F.R.S.....	178
The Nuclear Spins and Magnetic Moments of the Isotopes of Antimony. By S. Tolansky. Communicated by A. Fowler, F.R.S.....	182
The Scattering of Slow Electrons by Organic Molecules. I—Acetylene, Ethylene, and Ethane. By E. C. Childs and A. H. Woodcock. Communicated by Lord Ruther- ford, O.M., F.R.S.....	199
Artificial Radioactivity. By C. D. Ellis, F.R.S., and W. J. Henderson.....	206
Nuclear Spin of Radioactive Elements. By G. Gamow. Communicated by Lord Rutherford, O.M., F.R.S.....	217
The Theory of the Stability of the Benzene Ring and Related Compounds. By W. G. Penney. Communicated by J. F. Lennard-Jones, F.R.S.....	223

No. A 857.—September 1, 1934.

	PAGE
Discussion on Energy Distribution in Molecules in Relation to Chemical Reactions.	
Opening Address by C. N. Hinshelwood, F.R.S.....	239
The Dark Interval in Mercury Fluorescence. By Lord Rayleigh, F.R.S. (Plate 1)...	272
On the Technique of the Counter Controlled Cloud Chamber. By P. M. S. Blackett, F.R.S. (Plates 2-3).....	281
Refractive Dispersion of Organic Compounds. Part V—Oxygenated Derivatives of Cyclohexane. The Inadequacy of the Ketteler-Helmholtz Equation. By C. B. Allsopp. Communicated by Professor T. M. Lowry, F.R.S.	300
Refractive Dispersion of Organic Compounds. Part VI—Refractivities of the Oxygen, Carbonyl, and Carboxyl Radicals. Origin of Optical Rotatory Power and of the Anomalous Rotatory Dispersion of Aldehydes and Ketones. By T. M. Lowry, F.R.S. and C. B. Allsopp	313
The Modes of Activation of Aldehyde Molecules in Decomposition Reactions. By C. N. Hinshelwood, F.R.S., C. J. M. Fletcher, F. H. Verhoek and C. A. Winkler	327
The Kinetics of the Decomposition of Chloral and its Catalysis by Iodine. By F. H. Verhoek and C. N. Hinshelwood, F.R.S.	334
The Thermal Decomposition of Propionic Aldehyde. By C. A. Winkler, C. J. M. Fletcher and C. N. Hinshelwood, F.R.S.	345
The Thermal Decomposition of Formaldehyde. By C. J. M. Fletcher. Communicated by C. N. Hinshelwood, F.R.S.....	357
The Magneto-Caloric Effect and other Magnetic Phenomena in Iron. By H. H. Potter. Communicated by A. M. Tyndall, F.R.S.	362
The Homogeneous Unimolecular Decomposition of Gaseous Methyl Nitrite. By E. W. R. Steacie and G. T. Shaw. Communicated by H. T. Barnes, F.R.S.....	388
Artificial Disintegration by Radium C' α -particles—Aluminium and Magnesium. By W. E. Duncanson and H. Miller. Communicated by J. Chadwick, F.R.S.	396
The Vacuum in Dirac's Theory of the Positive Electron. By R. Peierls. Communicated by P. A. M. Dirac, F.R.S.....	420
The Theory of the Surface Photoelectric Effect in Metals—I. By K. Mitchell. Communicated by R. H. Fowler, F.R.S.....	442
The Resistance of Liquid Metals. By N. F. Mott. Communicated by R. H. Fowler, F.R.S.	465
X-ray Analysis of the Crystal Structure of Dibenzyl. I—Experimental and Structure by Trial. By J. Monteath Robertson. Communicated by Sir William Bragg, O.M., F.R.S.	473
Artificial Radioactivity produced by Neutron Bombardment. By E. Fermi, E. Amaldi, O. D'Agostino, F. Rasetti and E. Segrè. Communicated by Lord Rutherford, O.M., F.R.S.....	483

No. A 858.—October 1, 1934.

	PAGE
The Formation of Emulsions in Definable Fields of Flow. By G. I. Taylor, F.R.S. (Plates 4 and 5).....	501
The Emission of Electrons under the Influence of Chemical Action. Part IV—The Reactions of Liquid NaK ₂ with Gaseous SOCl ₂ , S ₂ Cl ₂ , SO ₂ Cl ₂ , HgCl ₂ , Sulphur Dichloride and with Mixtures of Gases and a New Method of Determining the Contact Potential Difference. By A. K. Denisoff and O. W. Richardson, F.R.S.	524
Studies on Explosive Antimony. I—The Microscopy of Polished Surfaces. By C. C. Coffin and Stuart Johnston. Communicated by A. S. Eve, F.R.S. (Plates 6, 7 and 8)	564
The Crystal Structure of Copper Sulphate Pentahydrate, CuSO ₄ · 5H ₂ O. By C. A. Beevers and H. Lipson. Communicated by W. L. Bragg, F.R.S. (Plate 9).....	570
The Kinetics of the Oxidation of Gaseous Hydrocarbons. II—The Oxidation of Ethane. By E. W. R. Steacie and A. C. Plewes. Communicated by H. T. Barnes, F.R.S.	583
Problem of the Sedimentation Equilibrium in Colloidal Suspensions. By S. Levine. Communicated by J. C. McLennan, F.R.S.	597
Experiments on Heavy Hydrogen. III—The Electrolytic Separation of the Hydrogen Isotopes. By A. Farkas and L. Farkas. Communicated by E. K. Rideal, F.R.S.	623
Experiments on Heavy Hydrogen. IV—The Hydrogenation and Exchange Reaction of Ethylene with Heavy Hydrogen. By A. Farkas, L. Farkas, and E. K. Rideal, F.R.S.	630
The Compressibility of Aqueous Solutions, II. By W. G. Thomas and E. P. Perman. Communicated by A. W. Porter, F.R.S.	640
Approximate Phases in Electron Scattering. By F. L. Arnot and G. O. Baines. Communicated by H. S. Allen, F.R.S.	651
The Scattering of Electrons in Bromine Vapour. By F. L. Arnot and J. C. McLauchlan. Communicated by H. S. Allen, F.R.S.	662
Molecular Structure as Determined by a new Electron Diffraction Method. I—Experimental. By H. De Laszlo. Communicated by F. G. Donnan, F.R.S.....	672
Molecular Structure as Determined by a new Electron Diffraction Method. II—The Halogen-Carbon Bond Distance in some Simple Benzene Derivatives. By H. De Laszlo. Communicated by F. G. Donnan, F.R.S. (Plates 10 and 11).....	690
Wind Structure and Evaporation in a Turbulent Atmosphere. By O. G. Sutton. Communicated by G. C. Simpson, F.R.S.....	701

No. A 859.—October 15, 1934.

The Annihilation of Fast Positrons by Electrons in the K-Shell. By H. J. Bhabha and H. R. Hulme. Communicated by R. H. Fowler, F.R.S.....	723
The Kinetics of the Reaction between Hydrogen and Nitrous Oxide. Part II. By H. W. Melville. Communicated by J. Kendall, F.R.S.	737

	PAGE
The Kinetics of the Reaction between Hydrogen and Nitrous Oxide. III—Effect of Oxygen. By H. W. Melville. Communicated by J. Kendall, F.R.S.	760
The Exchange of Energy between a Platinum Surface and Gas Molecules. By W. B. Mann. Communicated by G. P. Thomson, F.R.S.....	776
The Freezing Point of Platinum. By F. H. Schofield. Communicated by Sir Joseph Petavel, F.R.S.	792
Intensity Measurements in a Fine Structure Multiplet of AsII. By S. Tolansky and J. F. Heard. (Plate 12). Communicated by A. Fowler, F.R.S.....	818
Fluorescent Radiation from N ₂ O. By P. K. Sen Gupta. Communicated by M. N. Saha, F.R.S.	824
Inert Gas Effects in the Photosynthesis of Hydrogen Bromide. By M. Ritchie. Communicated by J. Kendall, F.R.S.	828
The Thermal Decomposition of Ozone. By M. Ritchie. Communicated by J. Kendall, F.R.S.	848
The Physical Basis of the Biological Effects of High Voltage Radiations. By W. V. Mayneord. Communicated by H. Hartridge, F.R.S.....	867
The Collisions of Slow Electrons with Atoms.—IV. By H. S. W. Massey and C. B. O. Mohr. Communicated by R. H. Fowler, F.R.S.....	880
Spectrum of the Afterglow of Sulphur Dioxide. By A. G. Gaydon. (Plates 13 and 14). Communicated by A. Fowler, F.R.S.....	901
The Speed of Positive Ions in Nitrogen. By J. H. Mitchell and K. E. W. Ridler. Communicated by A. M. Tyndall, F.R.S.....	911
Separation of the Isotopes of Lithium and some Nuclear Transformations observed with them. By M. L. Oliphant, E. S. Shire and B. M. Crowther. Communicated by Lord Rutherford, O.M., F.R.S.....	922
On Born's Theory of the Electron. By J. Frenkel. Communicated by P. A. M. Dirac, F.R.S.	930
Index	937

PROCEEDINGS OF THE ROYAL SOCIETY

SECTION A—MATHEMATICAL AND PHYSICAL SCIENCES

Probability Likelihood and Quantity of Information in the Logic of Uncertain Inference

By R. A. FISHER, F.R.S.

(Received December 14, 1933)

In a previous paper H. Jeffreys* put forward a method of obtaining the distribution *a priori* of the precision constant of a hypothetical normal distribution, by means of the principle that if three independent observations are made in succession, from a continuous distribution of any form, the probability that the third observation shall fall between the first two must be one-third (p. 48): "Two measures are made. What is the probability that the third observation will lie between them? The answer is easily seen to be one-third."

This proposition, in the form in which Jeffreys states it as the foundation for his deductions, is ambiguous, and may bear one of two distinct meanings, one true and the other demonstrably false. The proposition may mean:—

(a) If sets of three independent observations are taken from any continuous distribution, the probability that the third observation of any set shall lie between the first two of the same set is one-third.

It is obvious that this proposition is true, since the six orders in which any three specified observations may occur in a set will be realised in different sets in the long run with equal frequency, and in two of these six possibilities the observation with median value will occur last. The probability of any two observations coinciding in value is, of course, zero.

(b) If the first two observations are the same for all sets, and a third observation be chosen at random independently for each set, the probability that the third observation shall lie between the first two is one-third, for all values of the first two observations.

* 'Proc. Roy. Soc.' A, vol. 128, p. 48 (1932).

This proposition (b),^{*} which is that used by Jeffreys in his derivation of the form of the distribution *a priori* of the constant of precision, may be very easily shown to be untrue, save in an exceptional case of zero probability.

If we represent (fig. 1) the probabilities of an observation chosen at random being less, respectively, than the first and the second observation, by the co-ordinates of a point P, then it is easy to see that P will lie with equal probability within any two regions of equal area inside the unit square, for which both co-ordinates lie between 0 and 1. The probability of a third observation lying between the first two will then be the absolute value of the difference between the co-ordinates. This difference will exceed any chosen

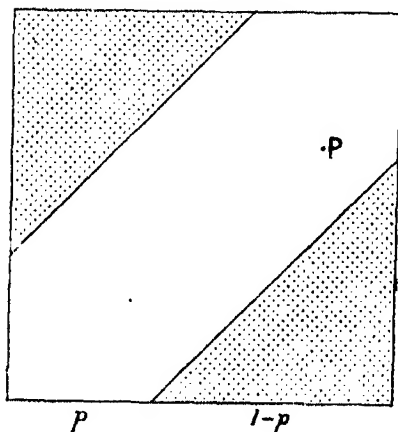


FIG. 1.

value, p , in two regions at opposite corners of the square, the aggregate of which is $(1 - p)^2$. Consequently, in one case out of four p will exceed $\frac{1}{2}$, in four cases out of nine p will exceed $\frac{1}{3}$, and in seven cases out of sixteen p will be less than $\frac{1}{4}$. Obviously, also, the chance of p lying in the range $\frac{1}{2} \pm \frac{1}{2}dp$ will be $\frac{1}{2}dp$, and will tend to zero as dp is decreased indefinitely. The probability, p , is therefore only exceptionally in the near neighbourhood of $\frac{1}{2}$, and in general it takes all values from 0 to 1 with a calculable frequency. It is only its average value that is equal to $\frac{1}{2}$.

In another paper^{*} the author has shown that when, in Jeffreys' analysis, allowance is made for variation in the values of the first two observations by integrating their frequencies over the possible range of these values, the equation arrived at reduces to a mere identity. This was, indeed, to be expected, when a fact, true equally of all the distributions under discussion, is adduced to discriminate the probabilities of each separately.

In a rejoinder,[†] Jeffreys objects to this process of integration:—

“Fisher proceeds to reduce my theory to absurdity by integrating with respect to all values of the observed measures. This procedure involves a fundamental confusion, which pervades the whole of his statistical work, and deprives it of all meaning.”

^{*} ‘Proc. Roy. Soc.’ A, vol. 139, p. 343 (1933).

[†] ‘Proc. Roy. Soc.’ A, vol. 140, p. 532 (1933).

Any defence which Jeffreys might have to offer of his omission to perform these integrations is thus lost in a polemical haze which his subsequent paragraphs do nothing to elucidate. I am not inclined to deny that the integrations reduce Jeffreys' theory to absurdity. Their purpose, however, is merely to justify the principle on which Jeffreys' reasoning is avowedly based, *i.e.*, to draw the conclusions derivable from the true proposition (a) above, in place of those which Jeffreys has derived from the untrue proposition (b).

This point can, I hope, be made plain independently of any general criticism of the system of notions respecting probability, which Jeffreys has elsewhere developed, and which he has reiterated in his rejoinder to my note. Since, however, he seems to complain of my neglect of these notions, I may be permitted to put forward as briefly as possible the reasons which have weighed with me in this neglect.

Criticism of Jeffreys' Theory

Jeffreys' definition of probability is subjective and psychological*: "We introduce the idea of a relation between one proposition p and another proposition q , expressing the *degree* of knowledge concerning p provided by q ." In this it resembles the more expressive phrase used by Keynes, "the degree of rational belief." Obviously no mathematical theory can really be based on such verbal statements. Any such theory which purports to be based upon them must in reality be derived from the supplementary assumptions and definitions subsequently introduced, a "series of conventions, involving no further hypotheses," in Jeffreys' explanatory phrase. Thus Keynes establishes the laws of addition and multiplication of probabilities, by stating these laws in the form of definitions of the processes of addition and multiplication. The important step of showing that, when these probabilities have numerical values, "addition" and "multiplication," as so defined, are equivalent to the arithmetical processes ordinarily known by these names, is omitted. The omission is an interesting one, since it shows the difficulty of establishing the laws of mathematical probability, without basing the notion of probability on the concept of frequency, for which these laws are really true, and from which they were originally derived.

The alternative method of bridging this gulf is adopted by Jeffreys: "The fundamental rule is the Principle of Non-sufficient Reason according to which propositions mutually exclusive on the same data must receive equal probabili-

* 'Proc. Roy. Soc.' A, vol. 140, pp. 527-8 (1933).

ties if there is nothing to enable us to choose between them." It will be noticed that the idea that a probability can have an objective value, independent of the state of our information, in the sense that the weight of an object, and the resistance of a conductor have objective values, is here completely abandoned. The ideas, familiar to all writers on mathematical probability, that a probability may in certain circumstances be unknown and in other circumstances may be known with greater or less accuracy, are quite foreign to Jeffreys' system. His rejection also of frequency as an observational measure of probability ("By 'probability' I mean probability, and not frequency, as Fisher seems to think," p. 523) makes it impossible for any of his deductions to be verified experimentally.

The one merit of a system of thought, founded on Non-sufficient Reason, and denied access to experimental verification, might be its internal consistency. As a succession of writers has shown, however, this supposed principle leads to inconsistencies which seem to be ineradicable, as in the example which Jeffreys quotes from Keynes :—

"Keynes* writes as follows : 'Let us suppose as before that there is no positive evidence relating to the subjects of the propositions under examination which would lead us to discriminate in any way between certain alternative predicates. If, to take an example, we have no information whatever as to the area or population of the countries of the world, a man is as likely to be an inhabitant of Great Britain as of France, there being no reason to prefer one alternative to the other. He is also as likely to be an inhabitant of Ireland as of France. And on the same principle he is as likely to be an inhabitant of the British Isles as of France. And yet these conclusions are plainly inconsistent. For our first two propositions together yield the conclusion that he is twice as likely to be an inhabitant of the British Isles as of France.

"Unless we argue, as I do not think we can, that the knowledge that the British Isles are composed of Great Britain and Ireland is a ground for supposing that a man is more likely to inhabit them than France, there is no way out of the contradiction. It is not plausible to maintain, when we are considering the relative populations of different areas, that the number of *names* of sub-divisions which are within our knowledge, is, in the absence of any evidence as to their size, a piece of relevant evidence.'"

* *Treatise on Probability*, p. 44, 1921.

Jeffreys' attempt to rebut this argument is as follows :—

“ Keynes here commits the fallacy, against which he argues effectively elsewhere, of supposing that the probability of a proposition is a function of that proposition and nothing else, instead of an expression of our state of knowledge of the proposition relative to particular data. Suppose, to make the issue a little more precise, that a man in Buenos Aires receives a message to the effect that a European of unspecified nationality is coming to visit him. He must then assess the probability of the various possible nationalities with respect to his available knowledge. If his data are that Great Britain, Ireland, and France are three different countries, and he has no further information as to the number and mobility of their inhabitants, he must assess their probabilities equally, and the probability that the visitor comes from Great Britain or Ireland is twice the probability that he comes from France. If, on the other hand, he considers that the British Isles are one country, of which Great Britain and Ireland are divisions, he must assign to the British Isles and France the same probability, dividing that assigned to the British Isles equally between Great Britain and Ireland. Keynes's dilemma does not exist and is merely an indication of incomplete analysis of the nature of the data.”

It will be observed that Jeffreys' defence of his principle depends wholly on the verbal use of the word “country,” and has been anticipated and answered by Keynes in the passage quoted, in a way that Jeffreys seems to overlook. Even as a formal solution based on a verbal convention, however, Jeffreys' solution breaks down in the case where the information in the possession of the Argentinian is that the British Isles are one country, in one sense of that word, and two countries in another sense in which the word might be employed; and where he is intelligent enough to recognize that his preferences, if any, among the different definitions of the word “country” are irrelevant to the probability which is under his consideration.

The failure of all assumptions of the same nature as the principle of insufficient reason in logical situations, in which the subject is not only ignorant of the relative probabilities of the different hypotheses he might make, but at the same time knows of his own ignorance, leads naturally to the consideration that the logical situations in which uncertain inference may be attempted are various and diverse in character, and that an initial mistake is introduced in all such definitions as that of Jeffreys in assuming that the degree of knowledge

or degree of rational belief is, in all cases, measurable by a quantity of the same kind. In Jeffreys' definition, indeed, it is evident that at least two different kinds of quantities are admissible :—

- (i) We may consider the amount of information which the proposition, or set of propositions, q , has to offer respecting the truth or falsehood of p ; this is evidently a different quantitative element in the logical relationship from
- (ii) The extent or degree to which the information provided by q favours the truth rather than the falsehood of p .

In the logical situation presented by problems of statistical estimation, I have shown that a mathematical quantity can be identified which measures the quantity of information provided by the observational data, relevant to the value of any particular unknown parameter. That it is appropriate to speak of this quantity as the quantity of information is shown by the three following properties :

- (i) The quantity of information in the aggregate of two independent sets of observations is the sum of the quantities of information in the two sets severally; each observation thus *adds* a certain amount to the total information accumulated.
- (ii) When, on increasing our observations, the sampling error of an efficient estimate tends to normality, the quantity of information is proportional to the precision constant of the limiting distribution.
- (iii) The quantity of information supplied by any statistic or group of statistics can never exceed the total contained in the original data.

Even if, in a logical situation providing a basis for uncertain inference, we confine attention to quantitative characters, measuring the extent to which some inferences are to be preferred to others, different situations, among the kinds which have already been explored, provide measures of entirely distinct kinds. Thus, a knowledge of the construction and working of apparatus, such as dice or roulettes, made for gaming, gives a knowledge of the probabilities of the different events or sequences of events on which the result of the game may depend. This is the form of uncertain inference for which the theory of probabilities was developed, and to which alone the laws of probability are known to apply. Since the term "mathematical probability" and its equivalents in several foreign languages have been used in this sense,

and almost exclusively in this sense, for over 200 years, it is impossible to accept Mr. Bartlett's* suggestion, in his thoughtful discussion of the topic, that only the word "chance" should be used for the objective probabilities with this meaning, and that the word "probability" should be confined to the recent and perhaps ephemeral meaning which Dr. Jeffreys has assigned to it.

It is difficult to understand the difficulty expressed by Jeffreys as to the definition of probability, when incommensurable, as the limit of the ratio of two numbers, when these both become infinite or increase without limit. All the sampling properties of hypothetical infinite populations can be expressed rigorously as limits of the sampling properties of finite populations if, as these are increased indefinitely, the frequency ratios of their elements tend to the values assigned in the hypothetical infinite population. This is quite another matter from the difficulty experienced by those who attempted to define probability as the limit of the frequency ratio of experimental events, for we can have no direct knowledge of the existence, or the nature, of the limits approached when any experimental procedure is repeated indefinitely. In contrast, the limits approached by repeating mathematical operations may be investigated with precision.

The logical situation which arises in the Theory of Estimation is of quite a different character. Here we are provided with a definite hypothesis, involving one or more unknown parameters, the values of which we wish to estimate from the data. We are either devoid of knowledge of the probabilities *a priori* of different values of these parameters, or we are unwilling to introduce such vague knowledge as we possess into the basis of a rigorous mathematical argument. Knowledge *a priori* may be, and often is, used in arriving at the specification of the forms of population we shall consider. The chief logical characteristic of this line of approach is that it separates the question of specification from the subsequent question of estimation, which can arise only when a specification is agreed on.

When a definite specification has been adopted, we can obtain a function of the parameters proportionate to the probability that, had these been the true values, the observations would have been those actually observed. This function is known as the mathematical likelihood of any value of a single parameter, or of a set of values, if the parameters are more than one. With respect to the parametric values the likelihood is not a probability, and does not obey the laws of probability. Maximizing the likelihood provides a

* 'Proc. Roy. Soc.' A, vol. 141, p. 518 (1933).

8 *Probability Likelihood and Quantity of Uncertain Inference*

method of estimation which has been shown to possess the following relevant properties :—

- (i) In certain cases an estimate is possible which, even from finite samples, contains the whole of the information contained in the sample. Such estimates are known as “sufficient.” The method of maximum likelihood provides such sufficient estimates when they exist.
- (ii) When no sufficient estimate is possible, and there exist only estimates which conserve a fraction of the total information, tending to unity as the sample is increased indefinitely, the value with the highest likelihood is one such estimate, and contains not less information than any other estimate of the same kind.
- (iii) When the likelihood function is differentiable at its maximum, ancillary statistics may be formed from its successive differential coefficients, which reduce the amount of information lost, as the sample is indefinitely increased, to zero of any required order.
- (iv) In certain instances, as I have more recently shown, the whole of the information contained in the sample may be recovered by using the whole course of the likelihood function.

Thus we have, in addition to the probability of the classical theory, already two other quantitative characteristics, appropriate to different logical situations admitting of different sorts of uncertain inference. It is to be anticipated that a detailed study of logical situations of other kinds might reveal other quantitative characteristics equally appropriate to their own particular cases. However reasonable such a supposition may have appeared in the past, it is now too late, in view of what has already been done in the mathematics of inductive reasoning, to accept the assumption that a single quantity, whether “probability” or some other word be used to name it, can provide a measure of “degree of knowledge” in all cases in which uncertain inference is possible.

Jeffreys attempts the more difficult task of justifying our procedure in arriving at particular specifications by means of the Theory of Probability. It is not, however, obvious that probability provides our only, or chief, guide in this matter. Simpler specifications are preferred to more complicated ones, not, I think, necessarily because they are more probable or more likely, but because they are simpler. As more abundant data are accumulated certain simplifications are found to be very unlikely, or to be significantly contradicted by the facts, and are, in consequence, rejected; but among the theoretical possibilities which are not in conflict with any existing body of fact, the calculation of probabilities, even if it were possible, would not, in the writer’s opinion, afford any satisfactory ground for choice.

Probability and Scientific Method

By HAROLD JEFFREYS, F.R.S.

(Received April 28, 1934)

I argued in my previous paper* that the opinions (1) that all inference beyond the immediate data of experience is meaningless, and (2) that the whole of scientific knowledge can be established independently of experience, are both logically tenable, at a price, but that neither corresponds with ordinary scientific or common-sense belief. It was obvious that Fisher would be the first to agree with me in rejecting the second alternative; his attitude to the first was less clear. I also maintained that we need a theory of scientific inference that will agree with ordinary beliefs about its validity, and that any such theory would involve as an *a priori* element the notion of probability and some of the fundamental rules for its assessment. By their very nature these rules cannot be established by experience: they must be judged by their plausibility, the internal consistency of the theory based on them, and the agreement or otherwise of the results with general belief. Fisher objects to the introduction of an *a priori* element, and I should agree with him to the extent that *a priori* hypotheses should be reduced to a minimum, but that minimum must be sufficient to give a general theory. I was originally somewhat attracted by the wish to define probability in terms of frequency, but found that the existing theory of Venn failed in its objects. It avoided no *a priori* hypothesis, several having been used but not stated, and its results, when interpreted in terms of the definition, were not in a practically applicable form. As the arguments have already been published twice,† I do not repeat them. Fisher departs from Venn by defining a probability as the ratio of two infinite numbers‡; but then no probability would have a definite value. Later in this paper, however, he obtains definite values for probabilities, and it is not clear how he gets them. (At this stage he generally uses the word "frequency" in place of "probability," but I think he is treating them as synonymous.) There is a gap in his argument at this point; but the results, relating to the prob-

Note.—My practice in giving references is to give initial and final pages where a whole paper or an extended passage is intended; when I refer to a single page, the statement referred to is on that page.

* 'Proc. Roy. Soc.,' A, vol. 140, pp. 523–535 (1933).

† Wrinch and Jeffreys, 'Phil. Mag.,' vol. 38, p. 715 (1919); Jeffreys, "Scientific Inference," p. 218.

‡ 'Phil. Trans.,' A, vol. 222, p. 312 (1922).

ability of a set of observations given the hypothesis, agree in all cases with those of the *a priori* theory, on the supposition, presumably valid, that the probability of any particular observation is determined by the constants of the assumed law of distribution alone, and is not disturbed by the previous observations.

Again, I have no objection to the study of likelihood as such. The theorem of Inverse Probability states that the probability of a hypothesis, given the previous knowledge and the data of experience, is proportional to its probability on the previous knowledge multiplied by the probability of the data of experience given the hypothesis. But the likelihood is simply the probability of the data on the hypothesis, apart from a factor that is the same for all hypotheses. Hence we may state the theorem in the form

$$\text{Posterior probability} \propto \text{prior probability} \times \text{likelihood}$$

One immediate consequence is that the information given by experience is completely summed up in the likelihood, the use of which therefore, on my view, needs no further justification. On the other hand, the prior probability needs further consideration. Dr. Wrinch and I showed that in problems of sampling, provided the sample is large, the likelihood is a small fraction of its maximum, except within a narrow range of hypotheses; provided, therefore, that the prior probability does not vary greatly in this range, the posterior probability is approximately proportional to the likelihood. As large samples are taken in any case to reduce the error of the mean, the precise form of the prior probability is of secondary importance in most practical cases. So far as I can see, this covers all the cases that Fisher and other statisticians consider, and I should be the last person in the world to deny the utility of approximation.

The fact that the distribution of prior probability is of little importance in many cases is, however, no reason for neglecting it. It is easily seen to be relevant to our subsequent opinion by considering extreme cases, such as I have already mentioned. I do not gather what Fisher's attitude to these extreme cases is, but it seems to me that he must agree that likelihood is not always the only thing that matters.

I find it difficult to answer criticisms of the theory, because most of them seem to refer to something different from what I intend, and I cannot see what. It may, however, help to clearness of discussion if I mention a few things that the theory does *not* mean.

It is not claimed that either the laws of probability or the assessment of prior probabilities can be proved, either by logic or by experiment. If they could be proved, the belief that inductive inference is meaningless would be

disproved, and this seems impossible. All we can say is that we do believe that inference is possible, and therefore take this as an axiom. It is a question whether a self-consistent theory can be constructed with a given set of postulates, but enough seems to have been done now to entitle us to answer this question in the affirmative. Prior probabilities could logically be assigned in any way; they must in practice be assigned to correspond as closely as possible to our actual state of knowledge, and in such a way that the sort of general laws that we, in fact, consider capable of being established can acquire high probabilities as a result of sufficient experimental verification. A criticism that is possible, but has not been made, so far as I am aware, is that the argument is circular; the probabilities are assigned to fit the belief that scientific method is valid, and then apparently used to justify it. But we are not trying to prove that it is valid; we know that this cannot be proved. We are trying to find out whether there are general principles that make the method a self-consistent whole. The alternative is that our empirical laws are a haphazard set of guesses, and if that is accepted I cannot see that scientific method is any improvement on primitive superstition. The advantage to science of a general theory of its method is that if *a priori* postulates are needed, discussion is assisted by making them explicit.

The assignment of *a priori* probabilities (*i.e.*, prior probabilities where there is no previous relevant knowledge other than the general principles of the method) has been the chief stumbling-block of the theory in the past. The propositions considered may often be disjunctions of equally probable alternatives and in that case there is no difficulty. I think that a fuller logical analysis than has yet been given may show that this class is much larger than has yet been suspected. But at least one exception exists, possibly two—general laws and quantitative laws. The difficulty about general laws was stated first, with a rather hesitant attempt at a solution, in two important papers by C. D. Broad.* He pointed out that the theory of sampling will never give an appreciable probability for a general law of the form "all crows are black." (A better example in some ways is "All animals with feathers have beaks.") I have suggested a solution† of the apparent paradox, namely, that the logically equivalent alternatives are "all crows are black," "no crows are black," "some crows are black and others are not"; but there may be an alternative solution in terms of Broad's theory of kinds. The definite exception relates to quantitative laws; here there is a solution in terms of the simplicity

* "Mind," vol. 27, pp. 389-404 (1918); vol. 29, pp. 11-45 (1920).

† 'Proc. Camb. Phil. Soc.,' vol. 29, pp. 83-87 (1933).

postulate.* In this case it can be seen unusually clearly that likelihood is not all that matters. We have a set of quantitative observations, which we co-ordinate by means of a simple law. An infinite number of laws could be found that would satisfy them exactly; but we choose one that only satisfies them approximately, because it is the simplest, and we expect that this will give the most accurate results when used for extrapolation. Any of the others would have a greater likelihood; our actual choice of the simplest is due to the principle that it has a greater prior probability and not a much smaller likelihood.

A prior probability is not a statement about frequency of occurrence in the world or in any portion of it. Such a statement, if it can be established at all, must involve experience. The function of the prior probability is to state the alternatives to be tested in such a way that experience will be able to decide between them. I have no *a priori* certainty that the numbers of electrons and protons in the universe are equal, or that the principle of general relativity is true; my respect for both beliefs is due to the fact that they agree better with experience than various other alternatives that I might consider equally likely *a priori*. In the former case I do not consider an indefinite repetition of universes with all ratios of the numbers of electrons and protons equally well represented; this would be as much an *a priori* idea as probability itself, and therefore offers no advantage. I simply state my previous ignorance of the composition, and proceed to consider the consequences of observational data in modifying this ignorance.

Some doubt has been expressed about the postulate that for any two propositions p and q there is a numerical probability of p given q . This can be shown to follow from the postulate that probabilities can be arranged in an order, or, following Bayes and Ramsey, from the postulate that the values of expectations can be arranged in an order.† Ramsey's rules of consistency may be held to assume an ideal man who always makes his decisions for action correctly, according to the value of their consequences. I do not think that this is necessary, but if it is we might equally say that most of pure mathematics assumes an ideal man who always gets his arithmetic right. I am not sure what the objection is, but think it worth while to state that probability is not equivalent to relevance. Thus we may have

$$P(p/q) = P(p/qr)$$

* "Scientific Inference," chapter 4.

† It is not correct that Bayes defined probability in terms of any idea of frequency. He defined it as the ratio of the values of expectations.

for a wide range of values of r ; then r , within limits, is said to be irrelevant to the probability of p given q . Bartlett's notion of chance is an extreme case which is often approximately, but never, I think, exactly, realized in practice.

Again, I do not understand the statement that the prior probability is subjective. The distinction between subjective and objective has been a matter for argument between philosophers for some 2000 years, without, I think, appreciable approach towards agreement. For scientific purposes, our experience reduces on ultimate analysis to sensations, which are largely subjective on almost any philosophical system. It is a fact that different people interpret their essentially private sensations in terms of much the same "reality," but I think I have shown in my book that this interpretation involves the whole procedure of inference, which is therefore more fundamental in knowledge than any question of reality, which is not very important for scientific purposes. (This attitude is a development of that of Karl Pearson.) It is true that different people approaching the same set of new data with different previous knowledge may assess different prior probabilities; but that is a reason for choosing the experiments in such a way that the likelihood will make the posterior probability approximately the same for all, or for exchange of their previous knowledge.

The statement of Fisher and Bartlett that the prior probability is unknown needs more discussion than they give. If the prior probability is interpreted as a statement of the frequencies in the world, or among accessible but unexamined specimens, the statement is true; but that is not my interpretation. I am in full agreement with them about the difficulties of assessing prior probabilities; but these difficulties are of two opposite types, which must be carefully distinguished. It seems to be easier to understand a moderately complicated idea than either a very simple or a very complicated one. The binomial theorem is intelligible to more people than the introduction to "*Principia Mathematica*" or, say, Watson's "*Bessel Functions*." Prior probabilities are subject to the former difficulty when previous relevant knowledge is negligible; then the problem is to clarify our ideas about what really are the equivalent alternatives, but I think solutions can be obtained, and are useful when obtained. When previous knowledge is complex the difficulty of evaluating a prior probability is one of sheer labour; nevertheless, I think that in many cases approximations can be obtained.

I think the above general considerations explain my attitude to most of Fisher's points. I cannot follow his new criticism of my inferred distribution of the prior probability in the theory of errors; it makes no mention of the

postulate that the probability of the errors is distributed according to the normal law about a true value, so I do not see how it can be relevant. I have little to add here to the analysis already given by Bartlett.* There was an unfortunate obscurity in my paper, which is partly removed by a note I had an opportunity of communicating to Bartlett. It is quite true that if we have no previous observations the probability of the third observation lying between the first two is $\frac{1}{2}$, whatever the law of error and the distribution of probability of a and b . But when we have made two observations we have relevant information; the mean gives a clue to the true value, and the difference gives a clue to the standard error. My postulate is that with this extra knowledge the probability that the third observation lies between the first two is still $\frac{1}{2}$, and this is equivalent to the postulate that the standard error is completely unknown until there are two observations. This is a common case, but obviously not universal. If the standard error is known already, the postulate is untrue. To take an extreme case, suppose that the standard error is known before any observations are made, and that the first two observations differ by 6σ . Then there is a high probability that they differ in opposite senses from the mean, and that the third observation will have an error of order σ and will lie between them. On the other hand, if the first two differ by much less than σ , the inference is that their agreement is accidental, and that the next observation will probably not lie between them. In such a case it would only be for some special value of the separation that the probability of the third observation lying between the first two, given the first two, would be $\frac{1}{2}$.

With regard to the quotation from Keynes, I did not overlook Keynes's answer. I do not agree with it. If the word "country" has any intelligible meaning, I think it is a very relevant piece of information whether Great Britain and Ireland are two different countries or two parts of the same country.

I should say here that such assessments of prior probability as an expression of equivalent alternatives afford no basis for the application of the "law of large numbers." Thus, if an Argentinian has no information about the numbers of Englishmen and Frenchmen in his country, the probability on his data that the next foreigner he meets will be English is the same as the probability that he will be French. But this affords no ground for believing that of the next thousand foreigners he meets about as many will be English as French. The law of large numbers depends on the assumption that the probability at every trial is determined completely by information available before any trials

* 'Proc. Roy. Soc.,' A, vol. 141, p. 525 (1933).

are made, as in the case of a throw with perfect dice, and is unaffected by the results of previous trials. In the present case the probability at any trial would be strongly influenced by the results of previous trials, and the conditions for the law break down.

Analogous statements hold for the case of simple sampling. In a more subtle form they arise in a case mentioned by Fisher in a previous paper.* Suppose (a) we deliberately make up classes of 10,000 balls each, such that one contains 10,000 white ones, the next 9999 white and 1 black, and so on. We select one of these at random and extract a sample of 30, 20 of which are found to be white and 10 black. We infer by the rules of probability that in the class sampled about $\frac{2}{3}$ are white and the rest black, the probabilities of various compositions near this being distributed according to a determinate law. But suppose (b) that classes of 10,000 were chosen at random from a class of number 10^{10} , and that we again sampled one of them and found 20 white and 10 black ones. In both cases the prior probabilities of the various compositions are the same, but for different reasons. The posterior probabilities of various compositions of the class sampled are therefore the same in both cases. Fisher, since the original data are different in the two cases, considers it anomalous that the results should be the same; but it is really no more remarkable than that two liquids should have the same density, which sometimes happens. But if we take a sample from a second class, we immediately find a difference. In case (a) the probability that the composition will have any particular value is almost the same as before the first class was sampled; the only change is that since one class, probably with a ratio near 2 : 1, has been excluded, the probability that the second class will yield a sample with a composition in this neighbourhood is slightly less than before. But in case (b) the sample of 30 is effectively a sample from the whole 10^{10} , and its composition therefore implies a high probability that the 2 : 1 ratio holds approximately in this, and therefore in the next 10,000, which are another sample from it. Thus the probability that the second class sampled will have a ratio near 2 : 1 is in case (b) considerably increased by the first sample, whereas in case (a) it is slightly diminished. Fisher is quite right in saying that there is no difference in the result given by sampling one class, but there is a very material difference when we come to consider a second.

At this stage I offer some comments on Bartlett's interesting paper. I have a suspicion that a chance in his sense exists only when inferred from physical

* 'Proc. Camb. Phil. Soc.,' vol. 26, p. 530 (1930), I consider a more special problem than Fisher, but which involves the essential principle.

laws, resting already on such evidence that other knowledge is practically irrelevant; in other words, that the existence of chances can be inferred only by using the general theory of probability. In the throw of an unbiased dice, for instance, the probability of a 6 is $\frac{1}{6}$ on the supposition that the laws of dynamics hold, and that the probability of the rotation during flight is uniformly distributed over a wide range. The latter assumption is an approximation. In the kinetic theory of gases the estimated time needed to establish an approximately Maxwellian distribution depends on the supposition that the molecules do not begin in such paths that the relative velocities at the first collision are in the lines of centres; small deviations in the directions of the initial velocities are required to make the theory work, and the postulate is that within these ranges the probability of the directions is uniformly distributed. This is an approximation of the same character as for dice. The same may be true of the probabilities in wave mechanics.

Towards the end of Bartlett's paper he appears to be arguing for indefiniteness as desirable in itself. I naturally cannot follow him here, but I think a useful purpose would be served in statistical work if posterior probabilities were estimated for the case of previous ignorance. This is usually a fair approximation to the truth when statistical methods are actually used, and it would not be prohibitively difficult to estimate the correction for the effect of a different distribution of prior probability. It is only for small samples that the correction will be important.

I do not follow Bartlett's equation (27). If his (24) was expressed in terms of h instead of σ , the function to be made a maximum is

$$h^{n-1} \exp. \{-\sum h^2 (x_r - m)^2\}$$

and then the maximum is given by

$$2h^2 \sum (x_r - m)^2 - (n - 1) = 0$$

which differs from (27) by the substitution of $n - 1$ for $n + 1$. The fact is that (24) is a probability *density*, and does not give a probability till it is integrated; the difference is simply a matter of change of variable. The quantity whose prior probability is uniformly distributed is $\log h$, or $\log \sigma$; if we take this as our independent variable, we recover Bartlett's equation (26). But the change of variable makes no difference to the posterior probability that an unknown lies between two assigned values.

The only justification of the normal law itself, so far as I can see, is that it is an approximation valid when there are several independent and comparable sources of error. I doubt whether it is ever exact.

The Refractive Index of an Ionized Medium

By C. G. DARWIN, F.R.S.

(Received May 12, 1934)

There has recently been some discussion as to the appropriate formula connecting the refractive index μ of a medium with its atomic characters,* in particular of whether it is the Sellmeyer formula

$$S = \mu^2 - 1 \quad (1)$$

or the Lorentz formula

$$L = \frac{3(\mu^2 - 1)}{\mu^2 + 2} \quad (2)$$

that is related to them.† It has long been accepted that for many substances, in particular for transparent liquids, the L formula is correct, but there are other substances which as certainly demand a formula in S. The distinction is by no means trivial, and it proves a surprisingly subtle matter to find the proper discrimination on theoretical grounds. It will probably come as a surprise to most who have not studied the subject in detail (as it did at first to the present writer) that a question of principle of this kind should still be unsettled, when the main work on it was done more than fifty years ago, for it is not as though it were an obscure point outside the general field of interest of physicists, and, moreover, there has never been any doubt as to the soundness of the basic principles from which one must start.

The present paper really falls into two parts. From § 7 onwards there is presented what appears a satisfactory method of discussing the subject. It is free from the central difficulty, the consideration of the internal electric fields in matter, and supplies sufficient (though perhaps not necessary) conditions for discriminating between substances requiring the two types of formula, and it gives the rule for a mixture of the two kinds of substances, a result I

* Hartree, 'Camb. Phil. Soc. Proc.', vol. 25, p. 47 (1929); vol. 27, p. 143 (1932); 'Nature,' vol. 132, p. 929 (1933); Kronig and Groenewold, 'Proc. K. Akad. Wetens. Amst.,' vol. 35, p. 974 (1932); Tonks, 'Nature,' vol. 132, pp. 101 and 710 (1933); Norton, 'Nature,' vol. 132, p. 676 (1933); Darwin, 'Nature,' vol. 133, p. 62 (1934).

† To those who prefer the modern fashion of nomenclature, in which everyone must be mentioned who has ever thought of a subject, it may be explained that the theme of the present work is the applicability of the Mossotti-Clausius-Lorentz-Lorentz correction to the Maxwell-Sellmeyer-Drude theory!

believe to be new. But it was not possible to be content with these developments without a discussion of the older methods, for the subject has been incorporated in the text-books, and there will be many who have regarded it as a settled question. Therefore it seemed proper to devote some space to the much more formidable task of criticizing these older methods. The chief difficulty of the subject has been that it is only too easy to find arguments, quite as convincing as many of those always accepted in theoretical physics, which lead to either of the two contradictory formulæ. It is quite easy to see weaknesses in these arguments, but it is as easy to see them in the right ones as in the wrong. Now it is probable that for many purposes we shall have to continue to use such rather inadequate arguments, and so it seemed worth while to see whether the discrepancies could be cleared up without a radical change in the method of approach. This is the subject of §§ 3-6, and though the great difficulty in getting clear-cut arguments suggests most of all the need for a wholly different approach to the question, yet such arguments, in a general way and without any precise criteria, do show that a medium with free electrons should obey the S formula and one with isolated atoms the L. It has proved extraordinarily difficult to avoid fallacies in this part of the work, and it is possible that it still contains some; if so, the fact is to be taken chiefly as confirmation of the necessity of having methods free from such troublesome subtlety.

I must express deep thanks to Professor D. R. Hartree for a great deal of valuable criticism, and to Professor E. V. Appleton for giving me much information about the ionosphere.

1—*Review*

The general development of the theory of the refractive index may be read in Chapter IV of Lorentz's "Theory of Electrons." Here it will suffice to recall the main terms that occur.* Consider first a dielectric medium composed of bound oscillating electrons. The electric field is usually analysed into certain parts. E signifies the field strength that would act in a pipe-cavity cut in the material along the line of the force; we shall call it the pipe-force when the fact needs emphasis. P is the dielectric polarization of the medium, and from the electro-magnetic equations we find $E + 4\pi P = \mu^2 E$ for the refractive index. The relation of P to E is the main problem. It is

* The ordinary units, not those of Heaviside, will be used.

determined by the atomic characters, and in the older theories the atoms were regarded as containing oscillating electric dipoles. This assumption has not been essentially altered by the quantum theory; in the old quantum theory there were "virtual electrons," and in the new theory it is still legitimate to speak of them for purposes like the present.

In the earliest theories of refraction it was the pipe-force that was supposed to act on the virtual electrons, with an S formula as the consequence; but Lorentz showed that an allowance must be made for certain other forces given by the mutual influences of the atoms. He separated the forces acting on a virtual electron into three, $E + E' + E''$, by the device of what we shall call the *Lorentz sphere*, a sphere large enough to contain many atoms, but small compared to the wave-length. E the pipe-force is, of course, not merely the external electric field strength, but is that strength reduced by the surface effects of the refractive medium, and to take E as the force acting on an electron is already to allow for the chief part of the mutual influences of the atoms. As to E' (though this is not quite the way Lorentz put it) it may be regarded as the force contributed by the atoms used in filling up the remoter parts of the pipe, while still leaving the Lorentz sphere vacant. Its magnitude is $\frac{4}{3}\pi P$, and we shall refer to it as the *Lorentz force*. E'' is the force from the other atoms inside the sphere; in certain important cases it is zero.* There results from the argument the refraction formula:

$$L = \frac{3(\mu^2 - 1)}{\mu^2 + 2} = \sum_r \frac{4\pi N_r e_r^2}{m_r (\nu_r^2 - \nu^2)}, \quad (1.1)$$

where N_r is the numerical density of the virtual electrons of type r , e_r and m_r their charge and mass, ν_r their natural radiant frequency, and ν the radiant frequency of the incident light.

These results apply strictly only for a medium composed of bound virtual electrons; that is to say, an ordinary transparent medium with absorption lines and if ν lies inside one of those lines, a damping term must be introduced which makes μ complex. A complex μ is sometimes split into its real and imaginary parts, of which the first is called the refractive index and the second the absorption coefficient,† but it is far more convenient to use a single complex

* An excellent discussion of these fields will be found in the paper by Hartree first cited above.

† This is the number of oscillations in 2π seconds. The term frequency will always be used in this sense here.

‡ The absorption coefficient for amplitude; that for intensity is twice as great.

quantity, and we shall speak of this as the refractive index. With the convention that a light wave is written with the factor $e^{+i\omega t}$, the index for an absorbing substance has its imaginary part negative.

If we try to apply the same arguments to a conducting medium we encounter great difficulties. In a dielectric the discussion is helped by thinking of the statical case, but in a conductor this is no use since surface charges annul the internal fields. On the other hand, a free electron is shaken to and fro by an alternating field, and so contributes an alternating electric moment, and so there should be a quantity of the type P for the medium. It seems reasonable therefore to use the same terminology as for a dielectric, and to subdivide the field into the same three parts as before. This, however, is the subject of §§ 3-6.

There is a different way of arriving at the L formula which gives it a somewhat greater generality,* since it calls for no hypothesis about the internal electric fields of a medium or about its atomic structure, but is applicable for any law of atomic scattering. The problem is regarded as one of multiple scattering, in which every atom scatters all the light it receives both from outside and from all the other atoms in a spherical wave that travels away with the ordinary speed of light for free space. The multiple interference of all these waves leads to a retardation of phase which implies a refractive index. The results are more general than those given in Lorentz's book, since there is no restriction of the scattered waves to be of the type that corresponds to a virtual electron. All that is postulated is that any given type of incident wave evokes a definite type of coherent scattered wave, but there is no restriction as to the phase relationship of the two. The solution calls for the summation of all the scattered waves arriving at any atom, and convergence can only be secured by a device that is equivalent to the use of a Lorentz sphere and the assumption that $E'' = 0$. With this method it is seen that the L formula should become applicable to the complex refractive index of a metal; it is the main theme of the present paper to understand why this is not so.

The subject is altogether one in which we do not anticipate any essential difference between the classical and the quantum theories, and as it is easier to carry through the work classically this has been done. I have verified

* See, for example, Darwin, 'Trans. Camb. Phil. Soc.,' vol. 23, p. 137 (1924). I would have preferred to use this method throughout, since it makes much less demand in the way of understanding the field inside a medium; but have refrained from doing so, because the familiarity of Lorentz's method makes it possible to discuss the matter more briefly.

some of the simpler results with the wave-mechanics without finding anything unexpected in the way of differences between the two theories.

2—Experimental Evidence

The ultimate principles determining the refractive index of a medium are completely understood, and so it ought to be possible by purely theoretical argument to give its value in any known case. No appeal to experiment should be necessary, or is indeed legitimate, and yet it is not out of place to review the information given by experiment, since it will show where the interest of the question lies. It furnishes fairly complete answers to the question of what cases call for S and what for L , and one of the main troubles in the discussions of the subject as expounded by various writers (the present one not excepted) is that it has been difficult not to believe some line of reasoning correct, not because of its essential soundness, but merely because it leads to a result agreeing with experiment.

The general analysis of the data of dispersion of ordinary transparent substances makes no discrimination between whether it is S or L that is to be fitted in the dispersion formula (1.1). Indeed, if L has been fitted, it is only a matter of complicated arithmetic to find a corresponding formula for S with changed v_r 's and e 's. It is only if there is some other source of information as to the correct values of v_r 's, etc., that any discrimination can be made from a mere study of the dispersion formula. Lorentz proved the applicability of L for a crystal in cubic array, but since it is hardly possible to imagine that a crystal could be broken into its constituent molecules without a radical change in their nature, such a crystal provides no test. He also applied his theory to an isotropic medium* and verified its correctness in this medium by a comparison of the refractive index of a liquid and its vapour. The verification is not, of course, exact, but that would not be expected; for the Lorentz formula only makes allowance for the mutual perturbations of atoms when their interaction is purely through light waves, and does not take account of the actual deformations due to close collisions, which will be more frequent in the liquid than in the vapour.

In transparent media the numerical difference between S and L is not very great, so that it is possible to think of Lorentz's theory essentially as providing

* See "Theory of Electrons," p. 138. He says " $E'' = sP$ where, for each body, s is a constant which it will be difficult to determine." I have not found in his writings any more detailed discussion of this, and on p. 146, he takes s as zero, the value it would seem that it inevitably ought to have.

a correction to the older theory. But as we have seen the theory is also to be applied for metals and here the change certainly cannot be regarded as a correction. For example, the index of silver for yellow light is $0.177 - i 3.638$, and from this we find $S = -14.21 - i 1.288$, whereas $L = 3.793 - i 0.091$. It is obvious that no theory could regard one of these as a correction of the other. It is easy, however, to see that S must be the right quantity to use, from a comparison of μ^2 with the ohmic resistance. Following the old theory, as developed, for example, in Drude's "Optics," it is seen at once that if σ is the electric conductivity in electrostatic measure, the imaginary part of μ^2 should for low frequencies be equal to $4\pi\sigma/v$. Silver is not quite a normal metal for visible light, but for many metals a very fair agreement can be found, especially in the infra-red. If one tries to make a theory working with L , there is no relation of this kind at all, and we may say that experiment informs us unmistakably that S is right for a metal.

The other interesting case is the ionosphere. Here things are the other way round, for we lack any verification of our theory, but need a valid theory in order that we may derive from experiments information as to the density of free electrons at various high altitudes. It will appear in the course of our argument that the S formula must be used, so that the index for the ionosphere is of the form

$$\mu^2 - 1 = - \frac{4\pi N e^2}{m v^2}. \quad (2.1)$$

3—Contradictory Arguments

The discussion of the optics of a medium containing free electrons centres round the question of how the charge of the electrons is neutralized by positive charges. The whole problem simply does not arise for an unneutralized electron gas; the behaviour of such a gas lies outside the main line of argument and its discussion is deferred to a note at the end of the paper. From the mathematical point of view, as we shall see in § 7, the discussion is easy and rigorous when the electrons are neutralized by a uniform continuous medium of positive electricity, and this case yields the result of a formula in § 8. But the neutralization is, of course, really done by positive ions, and the difficulty is to find under what conditions that these are equivalent to a continuum; much of the writing on the subject has taken this equivalence for granted, and so has really made no contribution to the problem. For the most part we shall suppose the electrons to be neutralized by an equal number of protons, which

will be supposed in fixed positions; this will represent the essence of the matter.

We will now consider the various arguments that may be used to determine the refraction of a proton-electron gas. They are stated here without assessing their value, since that will be made clear later. The crudest argument of all would say that a free electron is not a dipole and so could give rise to no polarization. Hence P vanishes, and the term E' is to be omitted from among the forces acting on an electron. Since E'' vanishes by the isotropy of the gas, we have only E acting and therefore the S formula.

It is easy to find a fallacy in this argument. A free electron describes a succession of straight lines, interrupted occasionally by collisions with protons or other electrons, and under the influence of the incident light the straight lines become slightly sinuous. The mathematical discussion inevitably considers this as a perturbation and represents it as a small term superposed on the unperturbed motion of the electron. This small term corresponds to an oscillating dipole travelling along with the unperturbed electron. The dipole has electric moment and so will contribute to E' , and we still see no reason why E'' should not vanish, so that the improved argument points towards a formula in L .

On the other hand, it is easy to find an argument which points at first to L and then changes round. A free electron may be regarded as the limit of a bound electron when the binding force tends to vanish. If we take a term of (1.1) and put $\nu_r = 0$, we arrive at an expression like (2.1), but with L on the left instead of S . But now we may argue that as the binding force diminishes the amplitude of the electron's motion increases, so that the atom it belongs to will ultimately overlap other atoms or even the Lorentz sphere, and so the whole of Lorentz's argument will fail. But again it is easy to turn the argument back the other way, for the amplitude of light waves is always to be regarded as infinitesimal, so that, in fact, the consequent motion is infinitesimal and will not make the atom unduly large.

It is evident that such arguments are inadequate to decide the matter, though they do not seem inferior to many used in physics. It is easy to find the fallacies in such reasoning, so that by a biassed exercise of judgment one can believe in whatever formula one wishes. But for a proper understanding of the subject it is not enough only to see that the arguments for S for the ionized gas are better than those for L ; it is also necessary to see why those arguments go wrong for an un-ionized gas and why there S is wrong and L right.

4—*Formal Statement of the Dilemma*

We will now work out the matter in closer detail. We shall suppose that each electron undergoes a displacement in the direction of E of length ξ from the position it would instantaneously occupy in the unperturbed motion.* Strictly speaking the ξ of each electron will be different, but we shall suppose that it is legitimate to take the average value for each of them; if this is fallacious, the error is certainly a subtle one. There are two ways of discussing the force on an electron. We may either work out the force at a given place x , and then suppose that there is an electron at that place, or we may work out the force at the position occupied by an electron, making allowance for its shift to $x + \xi$. In both methods the forces of both the protons and the other electrons must be considered, but in the first method the effect that interests us arises directly from the other electrons, while in the second it comes from the protons. Both methods are equally good, and are equivalent, but they must not be confused; we shall adopt the second here, and so have to estimate the field at the place $x + \xi$. We draw a Lorentz sphere of radius a round the place x , and separate the forces acting on the electron at $x + \xi$ into the usual three parts. In making this division we shall make the convention (which is the natural one for any perturbation theory) that the electrons are classified according to their unperturbed positions. The pipe-force E then arises from all the electrons and protons outside the pipe together with the incident external field; the perturbation will leave the electrons outside the pipe. The force E' arises from filling in the pipe while still leaving the Lorentz sphere vacant, but now whereas the protons are omitted from a sphere centred at x , the electrons must be omitted from one centred at $x + \xi$. The contributions of these more distant charges may be smoothed out and yields a force $\frac{1}{3}\pi N e \xi$. Here N is the numerical density of electrons or protons, and e is the charge of the electron. Throughout the paper e is this charge, and so a negative number; the charge of a proton is therefore $-e$.

Next as to the value of E'' , let X_p denote the position of a proton, x_r of one of the other electrons. Then

$$E'' = \frac{\partial}{\partial x} \left\{ \sum_p \frac{e}{|X_p - x - \xi|} - \sum_r \frac{e}{|x_r - x|} \right\}, \quad (4.1)$$

* Throughout the paper symbols like E , x , ξ , etc., will be used in a vector sense. It has not proved necessary to introduce any special notation, beyond the use of $|x|$ for the length of the vector x .

where the summation is over all the protons in the sphere centred at x , and over all the electrons in the sphere centred at $x + \xi$. We have now to take the average of this. Evidently the average of the second term is zero, since it is the force at the centre of the sphere of electrons. The first term is the force at a point distance ξ from the centre of the sphere of protons. Now a spherical shell of electricity exerts no force at any internal point, and so we conclude that the only protons which on the average will exert a force are those inside a sphere of radius ξ round the origin. Since the amplitude is always supposed to be infinitesimal in optical theory, it is hard to see how there can be a proton in this sphere, and hence we should say that the first term of E'' also vanishes. On the other hand, if it is allowable to smooth the protons out into a continuous distribution, then the force E'' at ξ will be $-\frac{4}{3}\pi Ne\xi$. This would be correct if it were allowable to suppose ξ so large that many protons were normally included in the sphere of radius ξ , but that is contrary to the assumption of infinitesimal amplitude for light. Briefly the dilemma is that, if Av stands for the operation of taking the average force, then

$$Av \text{ Lt}_\xi = 0, \quad (4.2)$$

but

$$\text{Lt}_\xi Av = -\frac{4\pi}{3} Ne\xi. \quad (4.3)$$

Though both formulæ are very much open to criticism, yet of the two (4.2) seems on the whole the more natural as may be seen from the following argument. When an electron oscillates in a positive continuum, in the course of its motion it will always be crossing to and fro over some of the positive electricity, and this no matter how small the amplitude of its motion; consequently the force from the positive charges in its immediate neighbourhood will be perpetually reversing their directions. On the other hand, when the electron is among protons there is none of this reversal; indeed what effect there is goes the other way, for as the electron moves to the right it approaches slightly closer to the protons on the right and so gets a stronger force from them, and the contrary when it moves to the left. It is for this reason that it seems that (4.2) is better founded than (4.3).

We can now work out the index for either alternative. The electron under consideration is itself oscillating with amplitude ξ and frequency ν , so that according to (4.2) it should obey

$$-m\nu^2\xi = e \left[E + \frac{4\pi}{3} Ne\xi \right]; \quad (4.4)$$

whereas (4.3) gives

$$-mv^2\xi = eE. \quad (4.5)$$

In both cases $\mu^2 - 1 = 4\pi Ne\xi/E$, so that (4.4) leads to an L and (4.5) to an S standing on the left side of (2.1). As we have seen the L seems rather the more plausible expression, but the S is definitely supported by the experimental evidence of the metals.

5—*The Structure of a Dielectric*

The contradictions of the last section show that it is necessary to examine much more thoroughly what happens when an electron gets near a proton. The understanding of this will be helped by a study of the structure of a dielectric, and we first derive the Lorentz force for a dielectric by a different method from that usually given.

Take an idealized dielectric composed of atoms,* each of which is a sphere of radius d , made of a uniform electrically polarized medium, so that each atom has total electric moment p , and all are pointing in the same direction. The atoms are fixed in arbitrary positions without overlapping, and there are N of them in unit volume. Acting along the same direction there is a pipe-force E . The resulting field in among the atoms is highly irregular. At distance r from a dipole the force is of order p/r^3 , and r can never be a greater distance than $N^{-1/3}$ from some atom, so that the irregular force is never less than Np or P . If the atoms are not packed very close, the field near an atom, being of order p/d^3 , may be thousands of times greater than the Lorentz force, which is thus the average of a quantity that may fluctuate through a very wide range. It will evidently be a delicate matter to argue about such an average, and the result may well depend on exactly how the average is taken.

Suppose now that we have a test electron moving about, and consider what will be the average force on it in various places. Take first a point inside an atom. Here the forces are partly those of the other atoms and the external field, and partly that due to the atom itself. This last force may be compared to the demagnetizing force inside a magnet; it is in a direction opposite to that of the polarization, and is of magnitude $-p/d^3$. We may call it the depolarizing force. Let F be the average of the total force from the other atoms and the external field. Then in the space between atoms, the mean force is F , but inside atoms $F - p/d^3$. The fraction of space occupied by

* It is easy to take a more general type of atom, but the results are the same, and no greater insight into the process is obtained.

atoms is $\frac{4}{3}\pi n^2 N$ and so the average force over space is $F - \frac{4}{3}\pi Np$. In taking the test electron down the field a great distance l the work done will be $l(F - \frac{4}{3}\pi Np)$ and by definition this must be El . We thus have $F = E + \frac{4}{3}\pi Np$ for the average force on an electron, the average being taken over space both outside and inside the atoms, but with the rule that for points inside an atom the forces of that atom are not to be counted as belonging to F , but are to be taken separately.

It is evident that the second term of F is to be identified with the Lorentz force, though it seems to have arisen in a different way, for there has been no use of the Lorentz sphere. If we still want to use the ideas of E , E' , E'' , we must slightly change their meanings. We then identify F with $E + E'$, and have E'' zero for all points outside any atom and $-p/d^3$ for points inside, so that its average value works out at $-\frac{4}{3}\pi P$. This derivation of the Lorentz force brings out one important point, which may be best expressed by saying that the force is an average, but that the average must be honestly taken. For example, suppose the atoms are small though their dipole strength is large, and consider a straight line drawn down the field. There may be quite long paths of this kind which do not cut any atom; the mean force along such a path is not $E + \frac{4}{3}\pi P$, as might be expected at first sight, but E ; or one may say that the Lorentz force is zero even though there has been no atom on the path. To see how this comes about, it is only necessary to remember that the force of a dipole in the equatorial plane is negative, while that on the polar axis is twice as large and positive. If, then, a straight path is chosen to avoid all the atoms it will get none of the polar forces and an undue share of the equatorial, and that will lower the average. An actual electron will not, of course, describe such a straight path, and what we need is the average along its actual path, and this will later receive closer study. But if we wished to believe that it was correct to regard F as the average force for a free electron moving among and through the atoms it would be necessary to show that its actual path had an average that was "honestly" the space average of the space outside all the atoms. We can see no reason whatever why this should be so, and there is thus no reason to believe that a free electron moving among dipole atoms will be affected by the Lorentz force. This will be properly verified in § 10.

We can also see why the Lorentz force is correctly used for neutral atoms or molecules, as in a liquid. In this the E'' is always zero, because what is wanted is the average value for the region in which an atom can lie. Here this is the region outside all the other atoms, and though we have seen that this by

itself does not guarantee the average force to be F , yet since there will be no particular preference for the equatorial planes of other atoms, we conclude that, in fact, the full Lorentz force will be effective. In the same connection it should be noticed that though we have used spherical atoms, the justification of $\frac{4}{3}\pi P$ for the Lorentz force does not depend on this shape. It is the existence of an envelope to the molecule into which others cannot penetrate that matters, and this envelope may be of any form, provided that there are equal numbers orientated in all directions. To establish this we examine the old E'' produced by all the molecules inside the Lorentz sphere. The upper limit for the sum is that sphere, the lower the surface of the molecule. The force at the origin due to a dipole at x is $\frac{\partial^2}{\partial x^2} \frac{p}{r}$ and this is to be summed for all the dipoles. For an isotropic medium the sum may be averaged and replaced by an integral, of which the limits are the same. If now this integral is averaged for all orientations of the molecule, $\frac{\partial^2}{\partial x^2} \frac{1}{r}$ will be replaced by $\frac{1}{3} \nabla^2 \frac{1}{r}$ and the result certainly vanishes, since the origin is excluded from the region of integration.

6—*The Lorentz Force for an Electron Gas*

We have seen that the Lorentz force is not to be counted as acting on an electron moving among dipole atoms, and must now examine the similar question for a proton-electron gas. In this case the whole idea of polarization is a little artificial, and we may say with some confidence that what fails for a genuinely polarized medium will also fail for one in which the polarization is only introduced from the ideas of perturbation theory. Nevertheless, it will be well to consider the point, in order to see better the fallacies in §§ 3, 4. The understanding of these questions is by no means easy, and it must be confessed that the main conclusion to be drawn is that other principles should be used if we are to be quite confident in our results. Here, therefore, we shall be content with indicating two points of failure of the reasoning of §§ 3, 4.

Suppose that we have a number of free electrons more or less at rest between collisions. Under the influence of the light they oscillate to and fro, and we express their motion in two parts: as the unperturbed rectilinear motion of the electrons and as oscillating dipoles of strength $e\xi$ moving with each of them. In conformity with the last section the average force in regions not very close to one of these electrons is $E + \frac{4}{3}\pi Ne\xi$. Consider the effect they will have on another electron B, which we shall specially choose as travelling

rapidly straight down the field. What we require is the difference between the actual averaged force and the force that would have acted if no light were shining. At first sight we would expect the term $\frac{1}{2}\pi Ne\xi$ to be effective, but this would be wrong, for it would be what in the last section was called a dishonest average; only if the proper allowance for collisions of B is made, and if the effect of these is separately estimated is the above the true mean force. Since no allowance was made in § 4 for collisions, there is no validity in its arguments.

Consider another aspect of the matter. In § 4 the calculations were based on the idea that an electron under force F would have amplitude eF/mv^2 and would act as a dipole of moment $-e^2F/mv^2$, which would contribute to the average field of F. Now when an electron collides with a proton the moment of the equivalent dipole is much altered, and so the contribution to F is affected and with it the whole value of F. To see this it will suffice to consider a single type of collision. Consider an electron moving straight down the field towards a proton, and colliding directly with it so as to return along the same path. This motion is to be compared with the corresponding motion unperturbed by F. It is easy to see that the effect of the collision will be to reverse the relative positions of perturbed and unperturbed electrons, so that the moment of the equivalent dipole is reversed by the collision. This effect is roughly analogous to the "depolarizing" effect of the last section, but we shall not pursue the analogy in detail. It is evident that the relation of F to E will be much more complicated than was suggested in § 4.

We may summarize the results of the last two sections. The chief thing they show is that the whole method of analysis by means of Lorentz force, etc., demands great subtlety in its handling, and invites us to seek a better method free from these confusing difficulties. Nevertheless, without these better methods we can see that there is good reason to believe that a free electron is influenced by the pipe-force and not the Lorentz force. The collisions of the electrons with the other particles are an essential feature of the process. If the collisions are frequent, one may say that they make the electrons forget the phases of their oscillations, and this makes it easy to see that there should be no allowance for the Lorentz force. But it was shown in § 5 that even without many collisions the Lorentz force would not be effective, and it will be found in § 9 that the frequency of collisions does not enter into the argument.*

* In my letter to 'Nature' (*loc. cit.*) I referred to the frequency of collisions as a condition for the annulment of the Lorentz force. Through a miscalculation (pointed out to

7—The Index of an Electron-Continuum Gas

Of the many physical problems not completely soluble by mathematics those stand on an altogether firmer basis which can be formulated rigorously, for then the necessary simplifications can be made in the mathematics without the far greater danger and difficulty of physical intuition. One of the main troubles of the present subject is that for technical reasons it is not possible to regard a piece of matter in bulk as a true self-contained dynamical system, so that the methods of general dynamics are not immediately available. Lorentz's method is Newtonian in that the equations of motion of each electron are set down separately, but this sacrifices the generality of Hamiltonian methods. The technical difficulty of using those methods lies in the retardation of the waves arriving at any electron from the more distant ones, for these retarded effects cannot be put into Hamiltonian form. The difficulty of retardation is met by the Lorentz sphere, but since each electron has its own sphere, it is still not possible to group many electrons together as a single system, because there will be electrons outside the Lorentz sphere belonging to one electron which are inside the sphere belonging to one of the others that we want to group with it. It is, however, easy to overcome these difficulties by taking a system for which retardation is unimportant, as it is for a piece of matter small in size compared to the wave-length. It is to be presumed that any shape would do, for which the potential problem has been solved (such as an ellipsoid), but it is, of course, natural to choose the simplest, a sphere. As we shall see the consequence of this choice is, so to speak, to turn the problem inside out, making L the simpler refraction formula and S the more complicated. The great advantage of the present method is that we do not have to think at all about the internal electric fields, which are here represented explicitly by the mutual actions of the electrons.

We suppose that we have a sphere of the material of radius a , containing many atoms but small compared to the wave-lengths, and shall calculate the electric moment excited in it by an external electric field of strength $F \sin vt$; this is the field acting on all the electrons, and we have not now to consider the nature of any internal field. In consequence of its electric moment the sphere scatters light of which the amplitude can be deduced from the moment,

me by several correspondents) I very much overestimated the frequency of collisions in the ionosphere, and so was content with stating this as a sufficient condition, without mentioning that it was not necessary. I also overlooked that with the many collisions "collision damping" would become important.

and this amplitude can also be expressed in terms of the refractive index, so that by a comparison of the two forms we can find the index. When a sphere of dielectric constant μ^2 is placed in a static field of strength F , the moment induced is $\frac{\mu^2 - 1}{\mu^2 + 2} a^3 F$, and it is not hard to show that a similar result holds for a variable electromagnetic field, with μ as the (possibly complex) index. Our task is thus to evaluate the moment and equate it to

$$\frac{\mu^2 - 1}{\mu^2 + 2} a^3 F \sin vt. \quad (7.1)$$

We will first consider a gas composed of n electrons in a uniform continuous positive medium. The medium has total charge $-ne$, and so, since its radius is a , the potential at an internal point is $-e \frac{3a^2 - |x|^2}{2a^3}$. When the electrons have a considerable kinetic energy they may emerge from the surface of the sphere for a short time, but this effect does not interest us, so we shall suppose that the same positive medium extends outwards beyond a so far that there is no need to change the form of the potential. The equations of motion are of the type :

$$m \ddot{x}_f = -\frac{ne^2}{a^3} x_f - \frac{\partial}{\partial x_f} \sum_{g \neq f} \frac{e^2}{|x_g - x_f|} + eF \sin vt, \quad (7.2)$$

and so

$$m \sum_f \ddot{x}_f = -\frac{ne^2}{a^3} \sum_f x_f + neF \sin vt, \quad (7.3)$$

so that

$$e \sum_f x_f = \frac{ne^2 F \sin vt}{-m\nu^2 + (ne^2/a^3)}. \quad (7.4)$$

We thus get

$$\frac{\mu^2 - 1}{\mu^2 + 2} a^3 = \frac{ne^2}{-m\nu^2 + (ne^2/a^3)}, \quad (7.5)$$

and taking N for the numerical density of electrons, so that

$$n = \frac{4\pi}{3} a^3 N, \quad (7.6)$$

we have

$$\mu^2 - 1 = -\frac{4\pi Ne^2}{m\nu^2}. \quad (7.7)$$

This verifies the earlier statement that S is the correct formula for an electron-continuum gas. The same result can be got just as easily by the methods of wave-mechanics.

One important fact, which can be seen from (7.2) and (7.3), is that collisions between pairs of electrons do not need to be considered. During a collision both electrons are under the same external forces, and the sum of their accelerations is unaffected by the collision, so that there is no consequent radiation and so no effect on the refractive index.

8—A Medium Composed of Separate Atoms

We now take a medium composed of ordinary neutral atoms, for which L should be correct. At each atom there is a set of virtual electrons, and the solution is made easy by the assumption, verified afterwards, that all the virtual electrons of each type oscillate with the same amplitude, no matter in which part of the sphere their atoms lie. To find their influence on one of the atoms we surround it by a small sphere of radius b . By virtue of the isotropy we may average the sum and smooth out the distribution of dipoles into a continuous distribution of polarized material throughout a volume composed of a sphere with an eccentric spherical cavity. There is no force from the polarized medium at a point inside the cavity, as may be seen most easily by replacing the polarization by surface charges on the outer and inner surfaces of the sphere; the forces from these are seen to cancel out. Hence each dipole is unperturbed by the other atoms, and so the assumption that the dipoles all had the same amplitude is verified.

Let ξ_r be the displacement of the virtual electron of type r from its position of equilibrium. Then

$$m_r \ddot{\xi}_r = -m_r \nu_r^2 \xi_r + e_r F \sin \nu t, \quad (8.1)$$

and so

$$\xi_r = \frac{e_r F \sin \nu t}{m_r (\nu_r^2 - \nu^2)}. \quad (8.2)$$

Summing over all the types and over all the n_r atoms, we get moment

$$\sum_r n_r e_r^2 F \sin \nu t / m_r (\nu_r^2 - \nu^2), \quad (8.3)$$

and replacing n_r by $\frac{4}{3}\pi a^3 N_r$ we get (1.1). The formula can obviously be extended to cover absorption by including a damping factor in the denominator of each term.

9—The Proton-Electron Gas

We now come to our main problem, the index of an actual ionized gas, which we simplify to be a proton-electron gas. The protons are fixed in arbitrary

positions in the sphere of radius a , but we shall not have to average for varied positions of them; we shall get what we need by taking a dynamical average for the electrons' motions without varying the protons' positions. The essence of the proof is that on account of the attractive force of a proton, an electron moves faster while in its neighbourhood and so the contribution of such regions to any average is less and not more important than that of other regions, and this removes all difficulties of convergence. It will appear that all the dynamical averages do not depend on the adjacent proton, but only on the more distant ones, and since it is possible to regard the effects of these as smoothed out, we may legitimately replace the protons by the continuum of § 7 and so obtain the S formula.

We must, however, here consider a phenomenon not hitherto mentioned, that of "collision damping." Our system contains a force varying explicitly with the time and so is not conservative, and the electric moment has in consequence a component out of phase with the incident light. This is brought about by the collisions of the electrons with the fixed particles (here the protons), and is, of course, closely connected with the electrical conductivity of the medium. The subject will be discussed in § 11, here it suffices to recall that the conductivity is yielded by supposing a slight asymmetry in the distribution function of the velocities of the electrons.

Take a sphere of radius a containing n electrons at x , and n protons fixed at X_p . The Hamiltonian of the system is

$$H = \sum_f \frac{1}{2m} p_f^2 + U - eF \sin vt \sum_f x_f, \quad (9.1)$$

where

$$U = - \sum_f \sum_p \frac{e^2}{|x_f - X_p|} + \sum_{s > f} \sum \frac{e^2}{|x_f - x_s|}.$$

The equations of motion are of the type

$$m\ddot{x}_f = eF \sin vt + \sum_p \frac{\partial}{\partial x_f} \frac{e^2}{|x_f - X_p|} - \sum_{s \neq f} \frac{\partial}{\partial x_f} \frac{e^2}{|x_f - x_s|}, \quad (9.2)$$

and from these we get:

$$m \sum_f \ddot{x}_f = neF \sin vt + \sum_f \sum_p \frac{\partial}{\partial x_f} \frac{e^2}{|x_f - X_p|}. \quad (9.3)$$

We see again that the collisions between pairs of electrons make no direct contribution to the acceleration of charge which is responsible for the light scattering, and so none to the refractive index. They will, however, have the

indirect effect of allowing the electrons to exchange energy and so will produce equipartition among them.

We now set down the formal average of the part of the electric moment that is periodic in ν . Imagine that the motion has been solved in terms of given initial conditions. Then x_f is expressed in terms of the time and of the $6n$ quantities x_{s0} , p_{s0} , the initial co-ordinates and momenta of all the electrons. The periodic part of the electric moment is then, for the in-phase component

$$\frac{2e}{T} \int_0^T \sum_f x_f(x_0, p_0; t) \sin \nu t dt, \quad (9.4)$$

and for the component in quadrature

$$- \frac{2e}{T} \int_0^T \sum_f x_f(x_0, p_0; t) \cos \nu t dt, \quad (9.5)$$

where T is a long time.

We must next average for all possible initial conditions, and the correct process is evidently to average over the whole Gibbsian canonical ensemble of systems. The average amplitude of the in-phase component is thus

$$\frac{\int dx_0^{(3n)} dp_0^{(3n)} e^{-H_0/\Theta} (2e/T) \int_0^T \sum_f x_f(x_0, p_0; t) \sin \nu t dt}{\int dx_0^{(3n)} dp_0^{(3n)} e^{-H_0/\Theta}}, \quad (9.6)$$

where $H_0 = \sum_f \frac{1}{2m} p_{f0}^2 + U(x_0)$ and Θ is the temperature, on Gibbs's scale, at the moment the light is put on.* The theorem of Liouville is valid for a Hamiltonian containing the time, so that we may replace in this $dx_0^{(3n)} dp_0^{(3n)}$ by $dx^{(3n)} dp^{(3n)}$. We ought also to replace H_0 by an expression in x, p , but this cannot be done explicitly because our system is not conservative; so we shall continue to write this factor as before. By partial integrations we can write (9.6) in any of the following forms, all of them useful:—

$$(2e/DT) \int dx^{(3n)} dp^{(3n)} \int_0^T dt \sin \nu t \sum_f x_f e^{-H_0/\Theta} \quad (9.7)$$

$$= (-2e/D\nu^2 T) \int dx^{(3n)} dp^{(3n)} \int_0^T dt \sin \nu t \sum_f \ddot{x}_f e^{-H_0/\Theta} \quad (9.8)$$

$$= (2e/Dm\nu^2 T) \int dx^{(3n)} dp^{(3n)} \int_0^T dt \sin \nu t \sum_f \sum_p \frac{\partial}{\partial x_f} \frac{e^2}{|x_f - X_p|} e^{-H_0/\Theta} \quad (9.9)$$

where

$$D = \int dx^{(3n)} dp^{(3n)} e^{-H_0/\Theta}. \quad (9.10)$$

* The symbols $dx_s^{(3n)}$, etc., signify integration over the $3n$ co-ordinates of type x_s , etc.

The out-of-phase component can be similarly written in the form of (9.7) with $-\cos \nu t$ replacing $\sin \nu t$, and by partial integration this can be transformed to

$$(2e/Dm\nu T) \int dx^{(3n)} dp^{(3n)} \int_0^T dt \sin \nu t \sum_j p_j e^{-H_j/\theta}. \quad (9.11)$$

No progress can be made with these integrals in general, but we can get what we need by dissecting them and estimating the contributions made from certain parts of the phase space. From (9.9) it is evident that the regions of collision, where x_j is near some X_p , call for examination. We define a collision region by drawing a sphere of radius b round each proton, and examine what contributions come from the part of the phase-space for which the configuration-space is inside one of these spheres. We impose the following conditions on b :—

I. The regions of collision do not overlap one another and are a small fraction of the whole space. This is the condition $nb^3 \ll a^3$, or, in terms of the numerical density, $b \ll N^{-1/3}$. This condition implies that there are hardly ever two electrons in collision with the same proton at the same time.

II. The time spent by an electron in a collision is short compared to the period of the light ; this implies that the external force may be taken as constant during a collision. It is expressed by the inequality $b \ll V/\nu$, where V is the mean velocity of the electrons.

III. The radius b is so large that at entry an electron has only imperceptibly greater velocity than it has at infinity. This is the condition $b \gg e^2/mV^2$. It is possible that some of these conditions, though sufficient, are not necessary.

By virtue of I we may regard each collision as taking place independently of the rest of the electrons, so that we may suppose the colliding electron to be moving in a field of force arising from the central proton, the other protons, the other electrons, and the external field. By II the external field may be taken as constant, and the force from the other protons is a function of position only. The force from the other electrons will vary with the time and may do so fairly rapidly, but as they are none of them very close the variation cannot be important and we shall suppose that the forces from all of them can be compounded into a single force that may also be regarded as constant in time during the time of the collision. Under these conditions the electron has a definite energy during the collision, say, W_j . This part of the phase integral can now be factorized into the product of a $(6n - 6)$ -fold integral over the rest of the electrons and a sixfold integral over the colliding electron. We shall

estimate the values contributed to the various integrals by this sixfold integration.

The electron is moving with energy W_r in a field of potential $-\frac{e^2}{r} + U_r$, where U_r is the part due to all the other electrons, the other protons, and the external field. W_r is positive and U_r is supposed to be small by comparison. In view of the collision damping we must allow for an unsymmetrical distribution in the sixfold phase-integral. This will arise from expressing $e^{-\mathbf{H}_e/\theta}$ in (9.8) in terms of x, p , but we cannot find the actual expression for it. Fortunately we do not need to, but may be content to write in a factor $\phi(W_r) + p_r \chi(W_r)$ which will include the dissipative effect, as is well known from the theory of conductivity; χ is here a vector function proportional to the external force, but we do not require its magnitude. We shall suppose in accordance with III that there are only a negligible number of electrons with small energy, so that $\phi(W_r)$ vanishes for small W_r . We have

$$p_r^2 = 2m \left(W_r + \frac{e^2}{r} - U_r \right). \quad (9.12)$$

The integral in the denominator (9.10), thus receives from the region of phase-space considered an amount

$$\int dx_r^{(3)} dp_r^{(3)} \{ \phi(W_r) + p_r \chi(W_r) \}. \quad (9.13)$$

In the numerator (9.8) the integrand must be multiplied by $-\frac{\partial}{\partial x_r} \left(-\frac{e^2}{r} + U_r \right)$ for the in-phase component, and by p_r/mv for the out-of-phase component (9.11).

The integrations are over the inside of the sphere b in x -space, and over all p -space. If W_r were negative, there would be values of x_r inside the sphere b for which no value of p_r existed, and the whole form of the phase integral would be changed; this is as it should be, for we expect our argument to fail for self-contained atoms, since we know that then the L formula is right.

Integrating (9.13) over the directions in p -space we have

$$\int dx_r^{(3)} 4\pi \left\{ 2m \left[W_r + \frac{e^2}{r} - U_r \right] \right\}^{\frac{1}{2}} m \phi(W_r) dW_r. \quad (9.14)$$

Leaving the W_r -integration, we now integrate this for x -space. Expand U_r

in a series of solid spherical harmonics, from which the term of zero order may be omitted as it is included in W_r . Then expand the square root as

$$\left(W_r + \frac{e^2}{r}\right)^{\frac{1}{2}} = \frac{1}{2}U_r \left(W_r + \frac{e^2}{r}\right)^{-\frac{1}{2}},$$

and it is evident that all the harmonics will vanish. The leading term can be integrated accurately, but a sufficient approximation in virtue of III is given by an expansion. Altogether the sixfold integral gives an expression

$$\frac{4\pi}{3} b^3 \cdot 4\pi m \int (2mW_r)^{\frac{1}{2}} \left(1 + \frac{3}{4} \frac{e^2}{bW_r} + \dots\right) \phi(W_r) dW_r. \quad (9.15)$$

For (9.8) we require to evaluate

$$\int dx_r^{(2)} \frac{\partial}{\partial x_r} \left(\frac{e^2}{r} - U_r\right) 4\pi \left\{2m \left[W_r + \frac{e^2}{r} - U_r\right]\right\}^{\frac{1}{2}} m \phi(W_r) dW_r, \quad (9.16)$$

in a similar way. The only harmonic that matters is the first, say, $-Gx_r$, so that G is the mean force arising from all sources except the one central proton. The result is a contribution

$$G \cdot \frac{4\pi}{3} b^3 \cdot 4\pi m \int (2mW_r)^{\frac{1}{2}} \left(1 + \frac{1}{2} \frac{e^2}{bW_r} + \dots\right) \phi(W_r) dW_r. \quad (9.17)$$

Similarly (9.11) yields

$$\frac{1}{mv} \frac{4\pi}{3} b^3 \cdot \frac{4\pi}{3} m \int (2mW_r)^{3/2} \left(1 + \frac{3}{4} \frac{e^2}{bW_r} + \dots\right) \chi(W_r) dW_r. \quad (9.18)$$

Now e^2/bW_r is negligible by virtue of III, and we thus see that in all three integrals the contribution from a collision is just what it would be, if it were taken over the same part of phase space but with no proton at the centre of the sphere. Thus in taking the dynamical average for the force on an electron we need not consider the effect of a very close proton, but only the general force from the more distant ones, and this entirely removes the difficulties stated in § 4. (Indeed from the second order terms in (9.15) and (9.17) we can see that for the in-phase component the neighbourhood of a proton actually makes a smaller contribution to the phase integral than corresponds to its volume in configuration space.) If now the collision damping is negligible we can proceed most simply by averaging the forces from the distant protons, which will give a force like that of a continuum, but still leaving the electrons unaveraged. In this way the system is reduced to that of § 7, for which

we had S rigorously the right formula. The case where the collision damping is not negligible will be discussed in § 11.

One of the most satisfactory features of the present argument is that it gives a natural discrimination between the case when the energy of the electrons is positive and that when it is negative. In the latter the whole argument of this section fails, and that is as it should be, for then we want an L formula. There is no need to study this case in detail. The formal answer is still (9.6), but with strongly negative energy the electrons are all bound and the phase integrals factorize. The calculation corresponding to (9.13) is now the ordinary one for optical dispersion; to be of any use the quantum theory would be demanded, but we do not need to go into this here. The finding of a definite discrimination between the conditions under which the two formulæ apply has been one of the hardest things in the problem.

Our three conditions, though possibly not necessary, do, in fact, hold for the important case of the ionosphere. The electron density at 80 km is about 10^6 , so that I gives $b \ll 10^{-2}$ cm. At temperature 300°C the velocity is about 10^7 cm per second, and the frequencies used are of order 10^6 cycles. This gives $b \ll 1$ cm. Also III gives $b \gg 10^{-6}$ cm; so all three are easily fulfilled. For a metal the conditions are not quite so easy. Take a lattice of 2×10^{-8} cm, with one free electron per atom. The Fermi limit gives a velocity 1.7×10^8 cm per second and the slower electrons do not matter. For visible light $\nu = 4 \times 10^{15}$ radians per second. Then the conditions give I, $b \ll 2 \times 10^{-8}$ cm; II, $b \ll 4 \times 10^{-8}$ cm; III, $b \gg 6 \times 10^{-9}$ cm.

10—*The Addition Formula for a Mixture*

When two media are mixed, for each of which the L formula holds, the refractive index is obtained by adding together the L 's of the two components.* It is interesting to enquire into the corresponding rule when we mix an electron gas with an ordinary gas; we may express this by the question: what is the addition formula of the refractive indices for an L -medium and an S -medium? It does not matter whether we attribute the spectrum of the virtual electrons to the neutral atoms, or in part to the ions; the character of the formula will be given by a mixture of a proton-electron gas with a gas containing virtual electrons, and for simplicity we will suppose that the latter are only of one type, though the generalization is obvious.

* Lorentz, "Theory of Electrons," p. 147.

Take a sphere of radius a and let there be n free electrons as before, typified by co-ordinates x_j . Let there be n' neutral atoms, placed at co-ordinates typified by x' , each of which has a virtual electron e_r of which the displacement is $\xi_r(x')$. In forming the potential energy of the system we take advantage of the previous work. We replace the protons by a continuum, and so get

$$\text{terms } - \sum_j \frac{ne^2(3a^2 - |x_j|^2)}{2a^3} + \sum_{r>j} \frac{e^2}{|x_j - x_r|}. \quad \text{In accordance with § 8 we}$$

omit any term representing the mutual energy of the dipoles, but in doing so we shall have to verify afterwards that under the new conditions the dipoles still all oscillate with the same amplitude, independently of position in the sphere. The new terms that occur are those for the interaction of the free electrons with the atoms. The energy of interaction of one free electron with all the atoms is

$$e \sum_{x'} e_r \left\{ \frac{1}{|x_j - x' - \xi_r(x')|} - \frac{1}{|x_j - x'|} \right\} = -ee_r \sum_{x'} \xi_r(x') \frac{\partial}{\partial x_j} \frac{1}{|x_j - x'|}. \quad (10.1)$$

This has a strong singularity at $x_j = x'$, and the value is at first sight as ambiguous as the matters discussed in § 4; for, in the equation of motion (10.1) must be differentiated, and the resulting sum vanishes if we exclude a small sphere round x' from the summation; whereas if, for no better reason, we sum under the sign of differentiation (10.1) leads to

$$n'ee_r x_j \xi_r / a^3, \quad (10.2)$$

which does not vanish on differentiation.

The ambiguity is resolved by the method of the phase integrals used in § 9. Draw a sphere of radius b round the atom at x' and consider its contribution. We have to replace (9.12) by

$$p_j^2 = 2m \{W_j - eY - U_j\}, \quad (10.3)$$

where Y represents the potential of the dipole. The first point to observe is that if Y represents a point-dipole, there are always regions which cannot be entered by an electron no matter how great its energy; this is an unnecessary complication, and does not correspond to the actual nature of atoms. We therefore suppose that the atomic dipole is represented by a uniform sphere of radius d of polarized matter (as in § 5) centred in the sphere b which we are considering. Then for $r < d$, $Y = px/d^3$, and for $r > d$, $Y = px/r^3$, where x is written for

$x_f - x'$. We may at once drop the general form of U_f , and replace it by the only term that matters — Gx as in § 9. The incident energy W_f is supposed so great that there is no part of the atom that is not easily attained by the free electron; since the dipole p is itself due to the incident light, this condition will be much less exacting than III of § 9. Of the two phase integrals the denominator goes much as before and yields the leading term of (9.15) again. In the numerator, corresponding to (9.16), we have to take

$$\int dx^{(3)} \frac{\partial}{\partial x} (-eY + Gx) \cdot 4\pi \{2m[W_f - eY + Gx]\}^{\frac{1}{2}} m\phi(W_f) dW_f,$$

which becomes

$$[G - ep/b^3] \frac{4\pi}{3} b^3 \cdot 4\pi m \int \sqrt{(2mW_f)} \phi(W_f) dW_f. \quad (10.4)$$

We thus see that the contribution to the phase integral from the volume is the same as though there were no dipole in it but a reduction in the magnitude of the force from G to $G - ep/b^3$. Now since p is the electric moment in the volume $\frac{4}{3}\pi b^3$, the average of p/b^3 will be $n'e_r\xi_r/a^3$, so that the force on the free electron is effectively $G - n'ee_r\xi_r/a^3$. This shows that (10.2) was right for the potential energy of one free electron and all the dipoles.

If we sum (10.2) for all the free electrons we get $-n'ee_r \sum_f x_f/a^3$ for the force on the virtual electron at x' , and since this does not depend on x' , we see the justification of our assumption that all the virtual electrons have the same amplitude. Instead of writing the energy of each atom separately we may simply put down that of a single one and multiply by n' . The total potential energy is thus

$$\begin{aligned} & -F \sin \nu t [e \sum_f x_f + n'e_r\xi_r] + \frac{1}{2}n'm_r\nu_r^2\xi_r^2, \\ & + \frac{1}{2} \frac{ne^2}{a^3} \sum_f x_f^2 + \sum_{\sigma>f} \sum \frac{e^2}{|x_f - x_\sigma|} + \sum_f \frac{n'ee_r}{a^3} \xi_r x_f. \end{aligned} \quad (10.5)$$

The kinetic energy is

$$\frac{1}{2}m \sum_f \dot{x}_f^2 + \frac{1}{2}n'm_r\dot{\xi}_r^2. \quad (10.6)$$

The equations of motion are

$$m\ddot{x}_f = eF \sin \nu t - \frac{ne^2}{a^3} x_f - \frac{\partial}{\partial x_f} \sum_{\sigma \neq f} \frac{e^2}{|x_f - x_\sigma|} - \frac{n'ee_r}{a^3} \xi_r, \quad (10.7)$$

for every free electron, and

$$m_r\ddot{\xi}_r = e_rF \sin \nu t - m_r\nu_r^2\xi_r - \frac{ee_r}{a^3} \sum x_f, \quad (10.8)$$

for the virtual electrons. These easily lead to

$$\left(\frac{ne^2}{a^3} - m\nu^2\right) \sum_f x_f + \frac{nn'e_r}{a^3} \xi_r = ne F \sin \nu t \quad (10.9)$$

$$e_r \xi_r = \frac{e_r^2}{m_r(\nu_r^2 - \nu^2)} \left[F \sin \nu t - \frac{e}{a^3} \sum_f x_f \right]. \quad (10.10)$$

We have to solve these and then form $e \sum_f x_f + n'e_r \xi_r$, which is to be equated to $\frac{\mu^2 - 1}{\mu^2 + 2} a^3 F \sin \nu t$. There is no need to give the reduction, which comes down to quite a simple form. If μ' is the index which the neutral atoms would have if alone at the same density, so that

$$\frac{3(\mu'^2 - 1)}{\mu'^2 + 2} = \frac{3n'}{a^3} \frac{e_r^2}{m_r(\nu_r^2 - \nu^2)}, \quad (10.11)$$

and if μ'' is the index which the free electrons would have if alone at the same density, so that

$$\mu''^2 - 1 = -\frac{3ne^2}{a^3 m \nu^2}, \quad (10.12)$$

then the actual refractive index is simply given by

$$\mu^2 = \mu'^2 + \mu''^2 - 1. \quad (10.13)$$

We may conveniently state the rules for compounding the index of a mixture as follows. Take the L for every type of neutral atom, and add these together. Form the S corresponding to this summed L and add to it the S of the free electron gas; the result will be the S of the whole mixture. It may be possible to test this result from metals when the theory of metals is more perfect than at present; in the case of the ionosphere the frequencies used are far too low to yield any perceptible effect from the atoms.

11—Collision Damping

It was shown in § 9 that all the integrals connected with the interactions of the electrons, both in and out of phase, converged at the origin, but it was not there considered what the actual value of the damping would be. This is usually discussed on the lines worked out by Lorentz,* in which the free electron is regarded as the limit of a bound one, but since we know the limiting

* See Lorentz, "Theory of Electrons," p. 141.

process to be unsatisfactory it will be better to make a new start. It is more natural to proceed on the lines used in the theory of electrical conductivity, by the use of a distribution function for the velocities of the electrons.* The general equation of transport is

$$\frac{\partial f}{\partial t} + u \frac{\partial f}{\partial x} + \frac{X}{m} \frac{\partial f}{\partial u} = N' \int V p d p d \epsilon [f(u') - f(u)], \quad (11.1)$$

where $f(u; x)$ is the distribution function; N' the density of the particles with which the electrons collide; u' the velocity after the collision of one which approached with velocity u ; V the absolute velocity of approach; p, ϵ geometrical quantities defining the collision; and X the total force acting on an electron on account of the external field, the other electrons and the protons or ions.

No progress can be made in the case of a proton-electron gas, since the integral on the right diverges. We shall not attempt this problem, but will take a much simpler one, which corresponds to the practical case of the ionosphere. There the neutral atoms are far more numerous than the ions, and we shall assume that collisions with ions are unimportant without attempting to estimate how far their rarity justifies this.

We adapt (11.1) to this case. The question at once arises what is to be taken for X ; it is indeed primarily this question that brings the problem into our consideration. X is made up of the external field and of forces from the other electrons and protons. To deal with the last two we will again take our sphere of the material of radius a . For damping it is convenient to use complex variables, and we shall denote the external electric field strength by E , supposing it periodically variable in the time with frequency ν . Superposed on this we have the force from the protons, which by § 9 is $-ne^2x/a^3$, and also a force from the other electrons. We did not need this in § 9, but must find it now since we want to consider each electron by itself. It will be derived from the fact that the distribution function f depends on position as well as velocity. The function may be taken as

$$\begin{aligned} f(u; x) &= \phi(V) + uE\chi(V), & |x - \xi| < a \\ &= 0 & |x - \xi| > a \end{aligned} \quad (11.2)$$

There will be a thin transitional region between, which we shall not study. This represents a sphere of electrons oscillating with amplitude ξ through the fixed sphere of protons. At any interior point the force due to the electrons

* See Lorentz, "Theory of Electrons," p. 286.

is $ne^2(x - \xi)/a^3$; so that the total force on an electron is

$$eE - ne^2\xi/a^3. \quad (11.3)$$

There is also a condition to be satisfied at the surface; in detail this would call for the study of the distribution in the transitional region, but it will suffice to take the simpler condition that $d\xi/dt$ must be the mean velocity of the electrons, or

$$i\nu\xi = \int u^2 E\chi(V) du^{(3)} / \int \phi(V) du^{(3)}. \quad (11.4)$$

On the right side of (11.1) we have N' as the numerical density of the atoms. The substitution of (11.2) gives an integral which can be evaluated as soon as the law of collision is known. Here we only take the simplest case, where the atom is regarded as a hard elastic sphere of radius b ; the generalization is easy. Then on the right we get

$$- N'\pi b^2 V u E\chi(V). \quad (11.5)$$

Now $1/N'\pi b^2$ is the mean free path, so that $N'\pi b^2 V$ is the collision frequency for electrons of speed V ; we shall denote this by κ and for convenience shall suppose it averaged so that it no longer depends on the velocity.* Our equation thus is

$$i\nu E\chi(V) + \frac{1}{m} \left(eE - \frac{ne^2}{a^3} \xi \right) \frac{u}{V} \frac{d\phi}{dV} = -\kappa u E\chi(V)$$

and so

$$\chi(V) = - \left(e - \frac{ne^2}{a^3} \frac{\xi}{E} \right) \frac{1}{mV} \frac{d\phi}{dV} / (i\nu + \kappa). \quad (11.6)$$

Substitute this in (11.4) and on performing the integration we find

$$i\nu\xi = \left(Ee - \frac{ne^2}{a^3} \xi \right) / m (i\nu + \kappa). \quad (11.7)$$

The total electric moment of the sphere is $ne\xi$ and so we have

$$\frac{\mu^2 - 1}{\mu^2 + 2} a^3 E = \frac{ne^2 E}{m i\nu (i\nu + \kappa) + ne^2/a^3},$$

* κ is the number of collisions in 1 second, not (like ν) in 2π seconds. Of course κ really depends on the velocity, whereas the mean free path does not, because of the electrons high speed. It is easy to use this fact to improve the formula, but the result is not so simple as (11.8) and will not be given.

from which we derive*

$$\mu^2 - 1 = \frac{4\pi Ne^2}{miv(iv + \kappa)}. \quad (11.8)$$

The importance of damping may be estimated for the ionosphere. The temperature is about 300° , so that V is 10^7 cm per second. The numerical density of the atoms N' is 4×10^{14} and taking atoms of radius 2×10^{-8} cm, we find $\kappa = 5 \times 10^6$ sec $^{-1}$. For waves of 10^6 cycles v is 6×10^8 , and we see that damping may be quite important at this height. At lower heights a similar absorption would occur for longer waves, but there are not enough electrons present to make the imaginary part of μ of sensible magnitude. A similar calculation can be done for metals, and indicates that damping becomes important for visible light, but such a calculation is of course quite inferior to one using the modern theory of electrical conduction, and so it will not be given.

Note on Unneutralized Electron Gas

The discussion of a gas of unneutralized electrons was deferred from § 3 ; it is now shown that the electrons are of necessity undergoing such accelerations that it is impossible to discriminate by experiment whether S or L is right. Consider a uniform sphere of initial numerical density N . An electron at radius r is under a repulsive force of order Ne^2r and so obeys the equation $m\ddot{r} = Ne^2r$. Evidently the radius and with it the density will change considerably in a time of order $\Delta t = \sqrt{(m/Ne^2)}$. The number of oscillations of the light in this time is $v\sqrt{(m/Ne^2)}$, which is also $1/\sqrt{(1 - \mu^2)}$ where μ is the index that the gas would be expected to have. The index cannot possibly be determined unless the light goes through many oscillations during the experiment, so that $1/\sqrt{(1 - \mu^2)}$ must be a large number, and the experiment calls for low density and high frequency. Even so there can be no discrimination between S and L, for if only a time Δt is available the resulting determination of the index must have the same uncertainty as it would have if the frequency were uncertain to a range $\Delta v = 1/\Delta t$, which signifies that

$$\Delta \frac{1}{\sqrt{(1 - \mu^2)}} = \Delta v \sqrt{\frac{m}{Ne^2}} = 1.$$

Hence $\Delta \frac{1}{1 - \mu^2} = \frac{1}{\sqrt{1 - \mu^2}}$, which by hypothesis is a large number. There is

* This agrees with Appleton's result : 'Proc. Phys. Soc.,' vol. 44, p. 248 (1932) which is half as great as that derived from the direct application of Lorentz's formula.

evidently no possibility of discriminating between $\frac{1}{\mu^2 - 1}$ and $\frac{1}{\mu^2 - 1} + \frac{1}{3}$; that is, between S and L.

Such reasoning as this is always open to a little doubt, for it may merely prove that one has chosen a bad experiment. On these lines it is never possible to get a complete proof, but with one or two other devices there are also difficulties which strongly imply that they would yield the same result. For example, we may take the gas in a steady state, say, emitted by a filament, and may try to measure the index by the retardation of phase along a path of uniform density. The attempt fails because the light will not go in a straight line; it would be a formidable and unprofitable task to work out the details.

Summary

The aim of the work is to discriminate what types of medium will have a refractive index of the Lorentz type obeying a formula in

$$L = 3(\mu^2 - 1)/(\mu^2 + 2),$$

and what the Sellmeier type in $S = \mu^2 - 1$. After a review of the information from experiment, it is shown that reasoning of the type hitherto used can be made very plausibly to lead to either result for a medium containing free electrons. These older methods, which depend on a rather close analysis of internal electric fields, require the greatest care in their use and above all suggest the need for methods free from such subtlety, but still the dilemma presented by them can be resolved, and it appears correct that a medium with free electrons should obey S and one with neutral atoms L, though no precise rule of discrimination can be laid down between the two types.

A method is developed free from most of the difficulty, since it does not call for analysis of the internal fields. In this the refractive index is derived from the electric moment of a small sphere of the medium, the size of the sphere being such that the retardation of the waves is negligible. It is then possible to use the machinery of Hamiltonian dynamics so as to formulate correctly the electric moment of the sphere, and by various devices the results are brought to a manageable form. It is confirmed that a gas of electrons neutralized by a continuum of positive electricity will obey the S formula, while a set of self-contained atoms will obey the L. The main problem is that of electrons neutralized by protons. It is shown that, subject to certain prescribed conditions, the contribution to the moment from the collision of an electron with

a proton is on the average the same as that from an empty region of the same size ; this shows that it is legitimate to smooth out the fields produced by the protons and to regard the protons as though they were a continuum. An important point in the argument is that it fails if the electrons have not a certain speed, and the failure leaves room for all those substances which obey the L formula. The conditions for the S formula are fulfilled in the ionosphere and in metals. The mixture of an L medium and an S medium is considered, and it is shown that the correct rule for the index is to add the S's of the two media together. Finally the effects of "collision damping" are considered and previous results are confirmed.

*The Isotopic Constitution and Atomic Weights of the Rare Earth
Elements*

By F. W. ASTON, F.R.S.

(Received May 14, 1934)

Hitherto the widest gap in our knowledge of the isotopic constitution of the elements has been in that part of the Periodic Table containing the rare earths. A means of obtaining the mass rays of these substances was discovered 10 years ago.* By this it was possible to demonstrate the simplicity of lanthanum and praseodymium and to obtain a provisional analysis of the complex elements cerium and neodymium. Beyond these the only positive result was a faint blurr which suggested that erbium was complex and it was decided to postpone further attempts until an instrument of higher resolving power was available.

When this was constructed† it was naturally first applied to the numerous problems which appeared to be of more fundamental importance so that the complete lack of information on elements 62 to 76 remained.

Of recent years such information has become more and more desirable. In order to interpret the hyperfine structure of rare earth spectra some rough data on their isotopic constitution was clearly necessary and in October last experiments on other matters were set aside and efforts were concentrated on applying the second mass-spectrograph to the problem. This paper is an

* Aston, 'Phil. Mag.', vol. 47, p. 385 (1924); vol. 49, p. 1191 (1925).

† Aston, 'Proc. Roy. Soc.,' A, vol. 115, p. 487 (1927).

account of the methods adopted and the results obtained. It forms a continuation to previous communications the last of which dealt with lead.*

Experimental Arrangements

There was no hope of obtaining stable volatile compounds of the rare earths so that these could only be attacked by some method of anode rays. The ordinary apparatus for accelerated anode rays had already been successfully applied to the high resolution mass-spectrograph for certain alkali metals and alkaline earths which were particularly favourable† so that the first problem was how to improve the details of this device so as to increase the intensity of the rays produced and, if possible, to gain a little more insight into the mechanism of the discharge. There is no need to detail the experiments made to this end which were troublesome, tedious, and on the whole disappointing. The form and composition of the anode, its position and that of the subsidiary cathode, the form of the accelerating field and numerous other factors were examined. Additional bulbs and electrodes were introduced and the pressure and intensity of the discharge varied over very wide limits. In the end it was concluded that the most hopeful arrangement was virtually the same as that originally adopted. A full description of this is available in the literature of the subject‡ and it will only be necessary to mention two improvements.

The first of these consisted in the connection of a second bulb of about the same volume to the discharge bulb at a point remote from the cathode. This second bulb, which tended to steady the pressure, contained an electrode originally designed to act as an additional cathode. No particular advantage resulted from its use in this way, but it became valuable as a test anode to be used in place of the working anode while suitable conditions of pressure were being obtained in the discharge. The second and much more important improvement was obtained by the provision of a glass tube containing a small quantity of solid iodine the vapour of which was allowed to flow continually into the discharge through a fine leak. As it was impracticable to control the supply by an ordinary stopcock this reservoir was attached by a wax joint and either immersed in liquid air or removed altogether when not required. The glass leak was carefully chosen in the first place and the rate of flow could be controlled with the greatest convenience and delicacy by immersing the tube

* Aston, 'Proc. Roy. Soc.,' A, vol. 140, p. 535 (1933).

† Aston, 'Proc. Roy. Soc.,' A, vol. 134, p. 571 (1932).

‡ Aston, "Mass-spectra and Isotopes," p. 65 (1933).

of iodine in a thermos bottle containing water at a suitable temperature. The discharge thus took place in pure iodine vapour at a pressure corresponding to a dark space of about 1.5 cm. There is no doubt that an atmosphere of a halogen is one of the most important factors in the production of anode rays, and the arrangement also virtually eliminated the risk of the discharge tube going suddenly hard. When the inflow had been adjusted to balance the natural loss through the cathode slit the discharge could be run with remarkable uniformity over long periods with little or no attention. As in the earlier work a salt of lithium was usually added to the anode mixture and if at the beginning of the run the bright red beam of its anode rays appeared one could be sure at least that the surface of the graphite was working properly.

As regards the main difficulty, namely, the concentration of the beam exactly in the right direction, this still appears almost entirely a matter of pure chance. The apparatus was set up as symmetrically as possible about the axis of the slits and a photograph of the lithium lines taken. If the intensity of these was judged unsatisfactory the apparatus was taken down and any small tentative adjustment which suggested itself was made. This procedure was repeated until a good setting was obtained which could then with reasonable care be used for a considerable time. Thus the first was obtained in the middle of November and yielded the mass spectra of six rare earths before the deposits on the neck of the discharge bulb necessitated dismantling. The second in January was not so good and after some weeks work during which results on thulium and dysprosium were obtained another overhaul was decided upon. This had the most fortunate results, the setting made on February 6, which at the time of writing is still serviceable, is the best so far experienced. With it the survey of the rare earths was completed and many other interesting analyses were made.*

With respect to the discharge itself attempts to use high intensities were soon abandoned as useless. A current of one milliampere was regarded as the upper limit. Fortunately owing to the adoption of a high speed pump the vacuum in the slit system and camera was so excellent that unusually low energy rays could be employed. The potential applied to the deflecting plate was 160 volts corresponding to about 19 kilovolts in the accelerated beam. The discharges actually employed were surprisingly small. Satisfactory effects were obtained with less than 0.5 milliampere with a primary current in the induction coil corresponding to 12 watts. These low values

* Aston, 'Nature,' vol. 133, p. 684 (1934).

were a great technical convenience as they allowed exposures of indefinite periods without the necessity of any cooling devices to protect the wax joints.

The only change in the mass-spectrograph related to the slits employed. Improved vacuum technique had rendered the use of large slits possible and as the object of the work was the revelation of as many isotopes as possible, rather than the measurement of their packing fractions, resolution was deliberately sacrificed to increase the intensity to the utmost possible useful limit. The slits were about 0.1 mm wide and made of steel. The resolution given was still ample for isotopes of the rare earths differing by two units, but where these occurred in a series differing by only one unit identification of faint isotopes was difficult and estimation of relative abundance rough.

For the purpose of discovery and identification of isotopes, as has already been emphasized, the method of accelerated anode rays is practically ideal. The freedom from any trace of lines ascribable to compounds in the spectra obtained during this work was almost incredible. With the best settings the ordinary rays of the discharge were so completely obstructed by the position of the anode that notwithstanding the fact that the bulb was filled with pure iodine, an element abnormally sensitive to positive ray analysis, the line 127 was often too faint to distinguish. In consequence of this entirely unexpected phenomenon it was necessary to add a trace of caesium chloride to provide a standard line with which to identify the mass numbers on the rare earth spectra.

Material Employed in Analysis

From the point of view of mass-spectrum analysis purity of the material is usually of small importance. The most likely impurity, another element of the same chemical group, is generally too far away on the scale of mass to be of any significance. With the rare earths it is otherwise. Any outlying faint line must be looked upon with suspicion as possibly due to a neighbouring element unless and until the constitution of that neighbouring element is known to be such as to disprove this. It was clear that the purest possible material should be used whenever it was reasonably certain that the analysis would be successful. Luckily the method only requires amounts of a few milligrams if things go well and most of this may be recovered as residues if sufficiently valuable. The writer was fortunate in having obtained in 1924, through the kindness of Professor G. v. Hevesy, a presentation set of samples from the late Auer v. Welsbach which contained salts of all the rare earths in the highest state of purity then available. This precious material was only

used when absolutely necessary. A few samples, old but quite pure enough for provisional work, originating from Drossbach & Co., were available through the kindness of Professor Sir William Pope. Other sources of supply will be mentioned under the elements concerned. The rare earths were all added to the anode mixture in the form of bromides. For the photography Ilford "Q" plates were usually used, and occasionally Hilger Schumann plates.

Results

For convenience these will be given in order of atomic number which approximates to that in which the actual analyses were made. As the results obtained from the simple elements (57) *lanthanum* and (59) *praseodymium* by means of the first mass-spectrograph appeared satisfactory these were not repeated.

(58) *Cerium*.—The two isotopes 140, 142 of this element had already been identified but the ratio of their abundance had not been measured. New spectra were obtained from the cerium bromide previously used, and by means of these it was estimated photometrically that 142 was present to the extent of 11% giving a mean mass number 140.22 ± 0.05 .

(60) *Neodymium*.—Some of the bromide, made from Drossbach oxalate, used in the original analysis was available, and with this much improved spectra were obtained. The mass numbers previously identified were confirmed and the element shown to contain five isotopes in the following approximate proportions :—

Mass numbers	142	143	144	145	146
Percentage abundance ..	36	11	30	5	18

These correspond to a mean mass number 143.6 ± 0.2 .

(62) *Samarium*.—For this element bromide made from Drossbach oxalate was used. Samarium is the most complex of the rare earths. The results obtained with the first setting showed five main isotopes and more intense spectra obtained later revealed two more. Photometry gave the following figures :—

Mass numbers	144	147	148	149	150	152	154
Percentage abundance	3	17	14	15	5	26	20

corresponding to a mean mass number 150.2 ± 0.2 .

(63) *Europium*.—The only source of this was the pure sample of sulphate prepared by Welsbach. Some of this was dissolved and treated with strontium bromide. The resulting solution yielded a salt which worked well as an anode. During its use an interesting and unique phenomenon was observed. Under

the impact of the intense beam of cathode rays the surface of the anode, which with other elements merely got red hot, fluoresced strongly and during most of the exposure glowed with a dazzling blue light. This observation is in excellent agreement with the reports on the effect of traces of the element on the blue fluorescence of fluorite which were published soon after.* This remarkable property suggests that europium, the rarest of the known rare earths, may in the future be of great technical importance in obtaining visual effects from cathode rays.

The mass spectrum of europium shows twin lines 151, 153. These are nearly equal in intensity so that their relative abundance can be measured photometrically with the maximum accuracy. The lighter isotope is slightly more abundant the percentage being 50.6 and 49.4 respectively. These give a mean mass number 151.988 ± 0.005 .

(64) *Gadolinium*—This element was first analysed by means of a Drossbach preparation. On the spectra obtained, in addition to a group clearly due to gadolinium, there were two faint lines 152, 154. As their relative intensities corresponded to these two constituents of samarium they were ascribed to traces of that element present as an impurity. This conclusion was confirmed when a more intense spectrum was obtained from a sample prepared by v. Hevesy from the pure Welsbach sulphate which showed no trace of these two lines. Photometry gave the following figures:—

Mass numbers	155	156	157	158	160
Percentage abundance	21	23	17	23	16

corresponding to a mean mass number 157.0 ± 0.2 .

(65) *Terbium*—The Welsbach sample of this element was in the form of the brown superoxide which was easily converted by heating with hydrobromic acid. This gave a single line of satisfactory intensity showing that terbium is a simple element of mass number 159.

(66) *Dysprosium*—The bromide was prepared from a pure sample of the oxide supplied by v. Hevesy. The work with dysprosium was carried out during a rather poor setting of the discharge tube and the spectra obtained were weak. They indicate four isotopes of nearly equal abundance, the estimates being:—

Mass numbers	161	162	163	164
Percentage abundance	22	25	25	28

indicating a mean mass number 162.6 ± 0.2 .

* Haberlandt, Karlik, and Przibram, 'Nature,' vol. 133, p. 99 (1934).

(67) *Holmium*—The bromide was prepared by the action of barium bromide on the Welsbach sample of the sulphate. It gave entirely satisfactory results which showed that holmium is a simple element of mass number 165.

(68) *Erbium*—Erbium bromide had been prepared in 1924 for use with the first mass-spectrograph from an old sample of Drossbach oxalate. As this material had already given positive results it was used in the preliminary work as a convenient indicator to test the efficiency of the apparatus in its various settings as a generator of rays of the rare earths. The spectra obtained were very complex, and at one time it was suspected that erbium might contain even more isotopes than tin, which has eleven. On the other hand, it was quite probable that many of the lines were due to neighbouring rare earth elements present as impurities so that efforts were made to obtain the purest possible sample for the final analyses. A determination of the atomic weight of erbium had recently been made in the laboratory of Honigschmid by means of material purified by Prandtl. Through the kindness of these chemists a sample of this was available in the form of the oxide which was converted into bromide and incorporated in the anode in the usual way. Many spectra were obtained, the best of which gave consistent and convincing results. These showed that erbium contained only four isotopes in any appreciable abundance. Rough estimates by photometry gave the following figures:—

Mass numbers	166	167	168	170
Percentage abundance	36	24	30	10

giving a mean mass number 167.24 ± 0.2 .

There were no indications of any neighbouring lines so that the purity of the sample was amply confirmed, but the isotopic constitution makes the value of the chemical atomic weight 165.204 obtained by Honigschmid* with the same sample impossibly low. No adequate explanation has yet appeared for this remarkable discrepancy.

(69) *Thulium*—Bromide made from the Welsbach sample of oxide was used in the analysis of this element and some trouble was experienced as the apparatus was not working well at the time. In the end a line of satisfactory intensity at 169 was obtained on a Schumann plate. No trace of a companion could be seen so that thulium appears to be simple.

(70) *Ytterbium*—The bromide was prepared by the action of barium bromide on the Welsbach sulphate. Good spectra were obtained, but owing to the

* 'Z. anorg. Chem.,' vol. 214, p. 97 (1933).

closeness of the lines the relative abundance could only be estimated roughly. The results are as follows :—

Mass numbers	171	172	173	174	176
Percentage abundance	9	24	17	38	12

corresponding to a mean mass number 173.3 ± 0.2 .

(71) *Lutecium*—A sample of the pure oxide of this element was supplied by v. Hevesy and the bromide made from this gave good spectra showing conclusively that lutecium is a simple element of mass number 175.

Table I—Showing Constitution of the Rare Earth Elements

Symbol	Mass number	Percentage abundance	Symbol	Mass number	Percentage abundance	Symbol	Mass number	Percentage abundance
La	139	<i>s</i>	Eu	{ 151 153	{ 50.6 49.4	Er	{ 166 167 168 170	{ 36 24 30 10
Ce	{ 140 142	{ 88 11	Gd	{ 155 156 157 158 160	{ 21 23 17 23 16	Tm	169	<i>s</i>
Pr	141	<i>s</i>	Tb	159	<i>s</i>	Yt	{ 171 172 173 174 176	{ 9 24 17 38 12
Nd	{ 142 143 144 145 146	{ 36 11 30 8 18	Dy	{ 161 162 163 164	{ 22 25 25 28	Lu	175	<i>s</i>
Sm	{ 144 147 148 149 150 152 154	{ 3 17 14 15 5 26 20	Ho	165	<i>s</i>			

(*s* = simple)

Atomic Weights deduced from Mass-spectra

In order to obtain these it is only necessary to correct the mean mass numbers for the packing effect and for change of scale. The experiments were not suitable to the determination of the packing fractions, but these can be roughly inferred from the curve. We may expect them to range from about -5 for the lightest to -3 for the heaviest member of the group. There will also be a decrease of about 2 in 10,000 for the change of scale. It is clear that a subtraction of 0.09 of a unit from the mean mass number of each element will give the atomic weight on the chemical scale with sufficient accuracy. The only mean mass number known with high accuracy is that of europium, for both its isotopes have been detected and their relative abundance exactly

determined. The statistics of the isotopes of odd-numbered elements show that the probability of a third isotope being present in abundance too small for detection may be neglected. If only one line is seen the probability of a second isotope two units higher or lower diminishes with the strength of the line but has always to be taken into consideration in estimating the mean mass number. In Table II are given the atomic weights on the chemical scale deduced from the observations on mass-spectra and the latest international values for comparison.

Table II—Atomic Weights

	International values	Mass-spectrum values	Difference
57 La	138.92	138.91 \pm 0.05	—
58 Ce	140.13	140.13 \pm 0.05	—
59 Pr	140.92	140.91 \pm 0.05	—
60 Nd	144.27	143.5 \pm 0.2	0.6
62 Sm	150.43	150.1 \pm 0.2	0.3
63 Eu	152.0	151.90 \pm 0.03	—
64 Gd	157.3	156.9 \pm 0.2	0.4
65 Tb	159.2	158.91 \pm 0.05	0.3
66 Dy	162.46	162.5 \pm 0.2	—
67 Ho	163.5	164.91 \pm 0.05	1.4
68 Er	165.20	167.15 \pm 0.2	1.9
69 Tm	169.4	168.91 \pm 0.05	0.5
70 Yb	173.04	173.2 \pm 0.2	—
71 Lu	175.0	174.91 \pm 0.05	—

The differences are given where these are regarded as serious. It is evident that revision is desirable in several cases, most particularly those of holmium and erbium. The action of the International Committee in changing, for 1934, the atomic weight of Er from 167.64 to 165.20, and that of Os from 190.8 to 191.5 is peculiarly unfortunate. The mass-spectrum data for osmium are quite clear and convincing, and the value deduced 190.31* cannot possibly be out by much more than one-tenth of a unit. It appears that whereas the values previously in use were accurate enough for most chemical purposes the new ones are more than a whole unit out and among the worst in the whole table.

General Conclusions

Elements 57 to 71 form much the largest continuous group differing little in their chemical properties. If there is any direct connection between the latter and the structure of nuclei it was just possible that some unusual regularity might have been detectable in their isotopic constitutions. This does not

* Aston, 'Proc. Roy. Soc.,' A, vol. 132, p. 487 (1931)

appear to occur in any marked degree. It is interesting to note that all the odd ones are simple, except 63, and also that the groups of fairly abundant isotopes dovetail into each other filling up all the available numbers with few isobares. The absence of these must not be unduly stressed, for element 61, if it exists, will provide at least one isobare and there is little doubt that many more isotopes exist than have been detected. The one unique atomic species discovered in this work is samarium 144 which is the only one found so far which differs from its nearest isotope by three units. Which of the numerous isotopes of samarium is responsible for its radioactive properties, recently discovered by v. Hevesy, is an interesting problem which has already received attention.*

In conclusion, the author wishes to express his most cordial thanks to the chemists mentioned who so kindly provided the valuable material with which the work was done.

Summary

Experiments are described by means of which adequately intense beams of anode rays of the rare earth elements have been obtained.

The results of analysis of these by the mass-spectrograph are given providing a provisional survey of the isotopic constitutions of all the elements in the group. During the work more than thirty new isotopes have been discovered.

Estimates of the percentage abundances of each isotope are given from which the chemical atomic weights of the elements are calculated. Serious errors in the international table of atomic weights for 1934 are indicated.

* Curie and Joliot, 'C. R. Acad. Sci. Paris,' vol. 198, p. 360 (1934).

Supersonic Dispersion in Gases

By E. G. RICHARDSON, B.A., Ph.D., D.Sc. (Armstrong College, Newcastle-on-Tyne)

(Communicated by T. H. Havelock, F.R.S.—Received November 9, 1933)

Introduction

The rapid degradation of intensity suffered by compressional waves of high frequency in gases was first observed by Pierce* in carbon dioxide for frequencies in the neighbourhood of $2 \cdot 10^5$ cycles/sec. Although in the last few years a considerable number of measurements of the *velocity* of supersonic waves have been made, less experimental work has been done on the *absorption*. This present paper describes some work aimed at elucidating the mechanism of the phenomenon.†

Consideration was first given to the establishment of a source of vibrations of the requisite frequency. The possible apparatus reduces itself to four types: (1) edge-tones, (2) electric sparks, (3) small resonators of gas, (4) solid resonators; both of the latter types to be maintained by oscillating circuits incorporating valves. The frequency of an edge-tone depends directly on the velocity of the blast, and inversely‡ on the distance from the blower to the edge, so that it should be possible to produce supersonic waves by making the former very large and the latter very small; in fact, Hartmann§ has already used such a source. The difficulty of maintaining constant blast velocity and the complications which the blast introduces in the propagation of such waves would, however, have made such a source unmanageable in the present work. Neklepajev|| has used sparks as sources in the examination of the absorption in air. But here again the frequency is difficult to measure or to maintain constant. Some success was obtained by the author with gaseous resonators consisting of short brass tubes terminated at one end by a brass stopper, and at the other end by a soap film, the distance between the two being half the wave-length at the frequency of excitation. The resonator was maintained in vibration by

* 'Proc. Amer. Acad. Sci.,' vol. 43, p. 375 (1928).

† For a general account and bibliography of supersonics, see Hubbard, 'J. Acoust. Soc.,' vol. 4, p. 99 (1932).

‡ Richardson, 'Proc. Phys. Soc.,' vol. 43, p. 394 (1931).

§ 'Phil. Mag.,' vol. 11, p. 926 (1931).

|| 'Ann. Physik,' vol. 35, p. 175 (1911).

a valve oscillator, of which the plate was connected to a point electrode just above the soap film, while the grid was connected to the brass tube itself. Response of the resonator due to electrostatic attraction of the film was observed by the image of a glowing filament reflected from the slightly concave film on to a scale. By varying the tuning of the oscillator the response curve of the little resonator could be obtained.

It was hoped from such measurements to calculate both the absorption and the velocity of sound in the gas (from the resonant wave-length), but the response was too small for effective use above 10,000 cycles/sec, although resonant half-wave lengths could still be detected down to 2 mm, corresponding to 40,000 cycles/sec in air. Recourse was accordingly had to the fourth method in which, through the piezo-electric, pyro-electric, or magneto-strictive effect, a small solid is maintained in vibration by a tuned valve-oscillator. This has the great disadvantage as against the other three methods, that the frequency cannot be continuously varied. Piezo-electric quartz oscillators have been used by Pielemeier,* Abello,† Kneser,‡ and Groszmann§ for measuring the absorption of supersonic waves in gases. The latter employed two as nearly as possible identical quartz crystals, using one as the sender working through a very small hole to serve as "point source" and the other as receiver of the radiation, and so measured the amplitude at various distances from the source.

Among devices for the detection of the radiation and the measurement of its intensity the present author has used pressure vanes, oil films, and hot-wire anemometers. The pressure on a small vane placed in the path of the radiation has been used since the inception of supersonics, but suffers from inaccuracies owing to the fact that the surface of the vane is usually large compared with the scale of the phenomenon, and is liable to produce resonance between the vane and the quartz. An oil film stretched on a light wire framework serves as a sensitive indicator of supersonic radiation.

A film of oil for this purpose was formed on a metal ring 1 cm diameter, placed parallel to the face of a quartz and held between its electrodes. In a beam of light reflected from the film, interference fringes were observed, but these became broader when the crystal was set in vibration. On moving the crystal away, a series of maxima and minima was observed in the response of

* 'Phys. Rev.', vol. 34, p. 1184 (1929); vol. 36, p. 1005 (1930); vol. 38, p. 1236 (1931); vol. 41, p. 833 (1932).

† 'Phys. Rev.', vol. 31, p. 1083 (1928).

‡ 'Ann. Physik,' vol. 11, pp. 761, 777 (1931); Kneser and Zühlke, 'Z. Physik,' vol. 77, p. 649 (1932).

§ 'Ann. Physik,' vol. 13, p. 681 (1932).

the film, the broadening of the interference fringes being a maximum at places half a wave-length apart. This experiment is, in fact, the acoustical analogue of the device used in A.C. technology in which a line is short-circuited at its terminal through an instrument of known (electrical) impedance in order to determine, from the indications of the instrument, the characteristics of the line. It would be a difficult matter in the present instance to measure the acoustical impedance of the oil film, but the determinations of wave-length by this method were useful for comparison with those given by the hot-wire methods subsequently developed.

Hot-wire Methods in Supersonic Investigations

In the present research, the change of the steady resistance of an electrically heated nickel wire was used as a measure of the amplitude of vibration of the molecules of the gas exposed to the sound. This device has already been used by the author in a number of amplitude measurements in aerial vibrations.* It was found that a 0.001-inch diameter nickel wire, heated just below red heat, the resistance of which had been previously balanced in a simple Wheatstone bridge, would experience a small lowering of resistance, indicated by a change of the galvanometer deflection, when exposed to an oscillating quartz, piezo-electrically maintained, in a chamber sealed against draughts, and lagged with asbestos felt to prevent reflection of the radiation. It was necessary to choose a crystal which did not produce air currents, such as those noticed by Meissner.† It was found that this "wind" was considerable when slabs of quartz whose longitudinal dimension was large compared to the lateral dimensions were used.

The change of resistance which an electrically heated wire experiences when exposed to an alternating draught consists of two parts: (1) a steady drop of resistance; (2) a change alternating with the draught; there may also be variations harmonic to the fundamental frequency. The predominance of the latter effect is favoured by low frequency and fineness of the wire. At these high frequencies, the effect is almost entirely of the first kind, the alternating effect being a very small ripple on the surface of a large steady fall of resistance. Moreover, it can be shown that when the temperature of the wire is sufficiently high, this drop is that which the same wire would experience if exposed to a steady wind of velocity $= 2\pi na$ where n is the frequency and a the amplitude

* Richardson, 'Proc. Roy. Soc.,' A, vol. 112, p. 522 (1926).

† 'Phys. Z.,' vol. 28, p. 621 (1927).

of the alternation.* In the present research a nickel wire of diameter 0.001 inch was used, heated by a current of 0.2 amp, and the calibration was effected by exposing it in a horizontal position to the supersonic radiation at a fixed distance from the face of the quartz. It was hoped at first to measure the amplitude of vibration of the crystal face itself by an optical interferometer, but the work of several experimenters having shown considerable local variation in amplitude across the crystal face, an indirect method was used.

The alternating current across the electrodes was measured by a thermogalvanometer at the same time as the resistance of the wire, and it was assumed

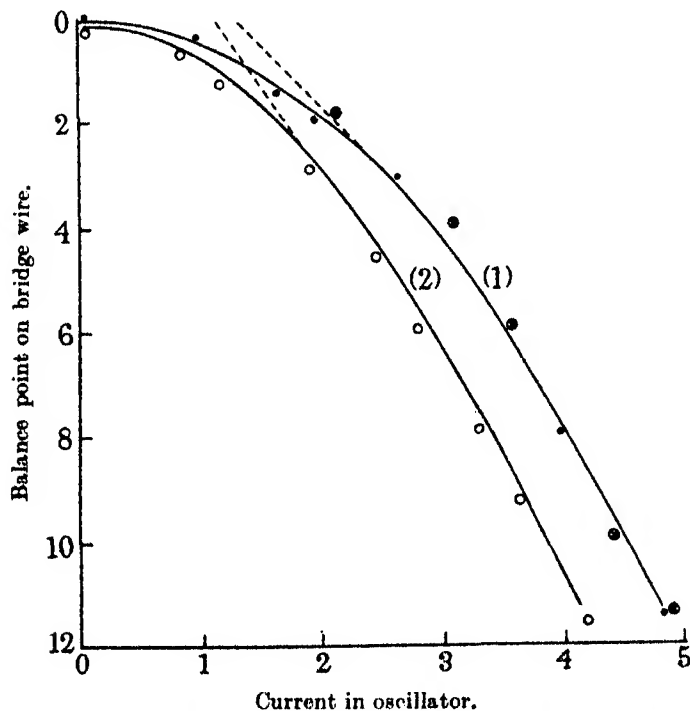


FIG. 1.—Calibration curves of hot-wire detector (1) in oxygen (2) in carbon dioxide.

that in the dynamic piezo-electric effect as in the static effect, the longitudinal elongation was proportional to the lateral applied potential difference. A method to confirm the calibration curves was devised later (*vide infra*).

Fig. 1 shows two typical calibration curves, in oxygen and carbon dioxide at 98 kc/sec. They correspond in shape to those obtained at audible frequencies (*cf.* fig. 2 of the paper just cited). Except at the lowest amplitudes the relation between increase of amplitude and decrease of resistance can be

* Richardson, 'Proc. Roy. Soc.,' *loc. cit.*

taken as linear. The difference in slope is, of course, to be ascribed to the difference in thermal properties of the two gases. The undisturbed resistance served also, in "katharometer" fashion, to test the purity of the gas from time to time.

The calibration curves so obtained for each supersonic source were to be used in two ways: (A) a direct measurement of amplitude in the progressive waves emitted by the source; (B) a measurement of the pseudo-stationary waves between the oscillator and a rigid reflector. Both series of measurements enable one to calculate the coefficient of absorption, k in $I = I_0 e^{-kx}$, as the radiation is propagated in the direction of increasing x . The latter method can also give the wave-length directly, for the distance between successive maxima as the hot wire is moved to and fro is half the wave-length in the gas. During the course of these experiments, it was, in fact, so used independently by Bucks and Müller* to measure the wave-length in air and hence to obtain the frequency of their sources. The method has, however, greater possibilities than this, as we shall show in what follows.

In the second method, either the reflector may be held still, and the hot wire be moved between it and the crystal, or the hot wire can be stationary and the reflector moved. This affords a very sensitive indicator of wave-length; deflections of the galvanometer connected to the hot wire could still be detected under circumstances in which no change in the current through the maintaining oscillator (Pierce method) could be detected. In gases like argon and oxygen (the latter under the proviso that the frequency is not too high in the supersonic gamut) the stationary waves are practically perfect sine-waves, since the measured damping is quite small. Assuming this to be so, the measured resistance of the hot wire in such cases may be correlated with a sine-wave formation to act as a check on the calibration curves obtained by the earlier method. Results so obtained at 98 kc/sec are shown as crosses on the oxygen curve of fig. 1. This method of calibration was suggested by some earlier work of Paris.†

A method (C) of measuring wave-lengths not involving the use of a reflector was found successful at the lower supersonic frequencies. This requires the use of two hot wires and depends on the fact that when these are spaced a half wave-length apart the oscillatory temperature changes in them will be exactly out of phase. The currents from the two hot wires are led to the two halves of a split primary transformer, while the current from a common secondary

* 'Z. Physik,' vol. 84, p. 75 (1933).

† 'Proc. Phys. Soc.,' vol. 39, p. 269 (1927).

is amplified and subsequently passed on to a heterodyne wave meter. This method has been used, without the necessity for amplification, in a number of experiments involving periodic air currents, but it raises new difficulties in the present application, in that the oscillatory currents are so small, and, in fact, are comparable in value with the currents induced in the hot wires by induction from the oscillator, so that this has to be carefully screened. By keeping one hot wire still, and moving the other along the tube, with the wave meter slightly mistuned, waxings and wanings in the heterodyne note may be observed, the maxima occurring when the two wires are one wave-length apart. Sorting out this temperature-fluctuation current from that due to direct induction is assisted to a certain extent by the fact that the strongest

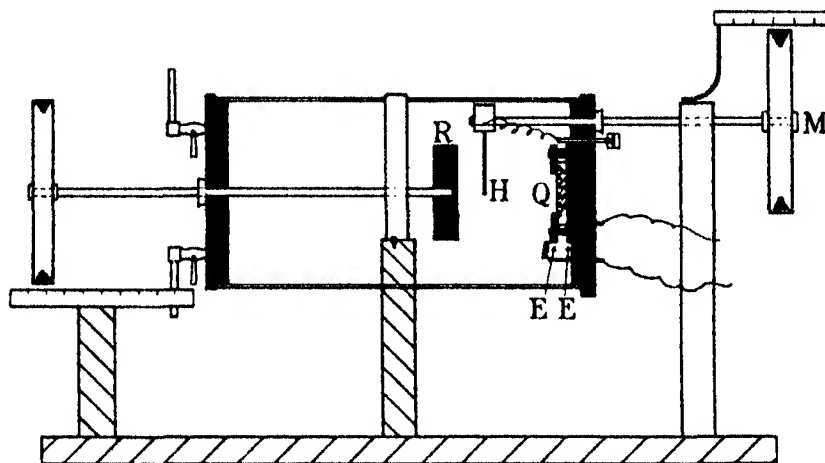


FIG. 2.—Hot-wire apparatus for supersonics

frequency in the former is double that of the crystal, or oscillator frequency, itself. At present, it has not been possible to use this method successfully at the higher frequencies, but some results at frequencies up to 200 kc/sec are included in the table of wave-lengths given later.

The complete apparatus, as mounted for method (B), is shown in fig. 2. The quartz Q is a disc vibrating in the direction of its thickness, held lightly between two polished brass electrodes EE, the outer of which has a hole 2 cm diameter cut in it to let out the radiation. (For frequencies below 500 kc/sec slabs oscillating along their length were used, the holder being modified so that the quartz lay between two horizontal electrodes.) This crystal holder is fixed to an ebonite disc which forms one cap of a glass tube 12 cm \times 6 cm diameter. Through a gland in this cap also passes the rod carrying the hot wire H mounted on a fork of which the upper part is shaped to fit the tube in

such a way that it is merely carried forward or backward on turning the micrometer disc M, marked in degrees. The reflector R, also of ebonite, is carried on the end of a rod screwed through a gland in the cap fitted to the other end of the tube, which also has three gas taps. Both rods, that carrying the reflector, and that carrying the hot wire, are tapped 60 threads to the inch and provided with large micrometer heads. The caps are sealed on with picein. In using method (A), the reflector is removed and the far end of the tube is padded with "paxfelt," a sound absorbing composition of asbestos. With each quartz in position a test was made in argon to find whether any sound was radiated obliquely on to the sides of the tube. Such "spreading" was detected by an apparent decay of amplitude along the tube, such as should not be shown by a normal gas. As a matter of fact, with the fairly wide orifices used, spreading was appreciable only at the lowest (40 kc/sec) frequency in a normal gas.

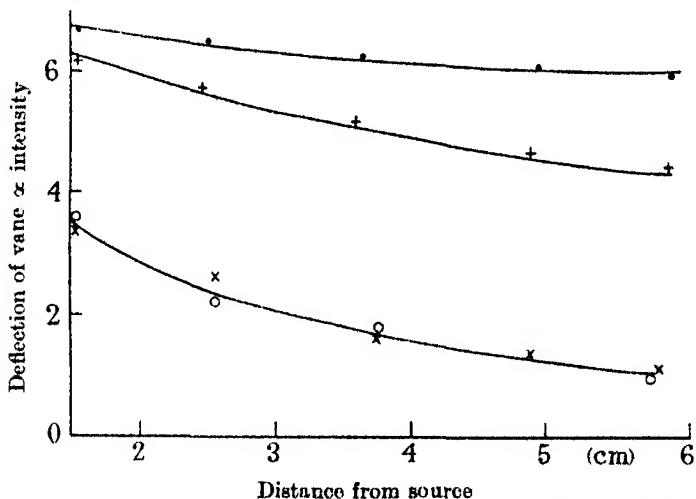


FIG. 3—Measurements with torsion vane at 1000 kc/sec. ● Oxygen ; + sulphur dioxide ; × carbon dioxide and ○ nitrous oxide.

Results of Measurements

Five gases in turn were introduced into the apparatus at each frequency, viz., oxygen, carbon dioxide, nitrous oxide, sulphur dioxide, and argon. They were obtained as commercially available in cylinders and dried before being introduced ; a mercury manometer connected to the apparatus ensured that the pressure was atmospheric. Of the three triatomic gases, sulphur dioxide was expected to behave normally, while the others were known to exhibit

anomalous absorption. Since oxygen showed a little excess of absorption at the higher frequencies, argon was used as a standard. Fig. 3 shows a set of measurements at a frequency of 1000 kc/sec with the earlier torsion vane, a light disc 4 mm in diameter suspended on one side of a quartz fibre and taking the place of the reflector in the tube. It was set vertically, "broadside on" to the radiation, but was pushed back by the pressure of the latter to an extent recorded by a small piece of mirror attached to its rear surface, and by the usual lamp and scale. The pressure on the vane is proportional to the intensity, *i.e.*, to the square of the amplitude. Fig. 4 shows similar measurements with the hot wire at 695 kc/sec plotted in logarithmic form to show that

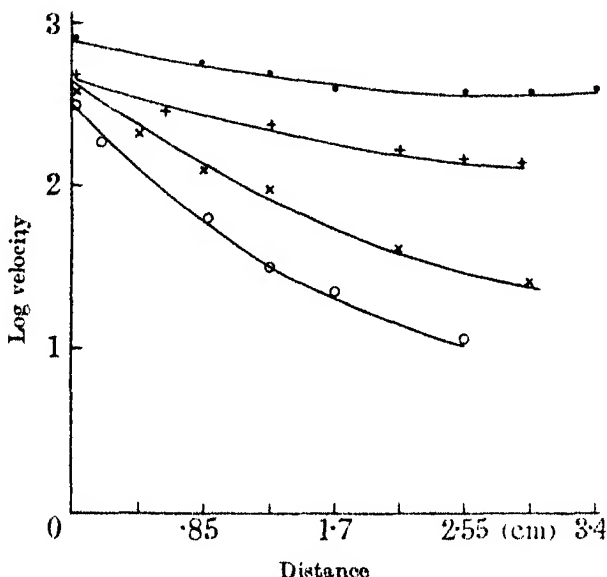


FIG. 4—Measurements with the hot wire at 695 kc/sec. ● Oxygen ; + sulphur dioxide ; × nitrous oxide ; ○ carbon dioxide.

the decay is only approximately exponential. The actual hot-wire measurements have been converted by means of the appropriate calibration curve, although they lie, as a matter of fact, almost entirely on the linear part of the curve. Of the two methods, the hot wire probably gives the more accurate results.

The next two figures show results of the "stationary wave" measurements. Fig. 5 shows detailed results for a few peaks at 98 kc/sec, the recorded points being the actual hot-wire readings, while the lines drawn give the shape of the stationary waves after correction for the curvature in the early part of the

calibration curves. On fig. 6 (at 167 kc/sec) the maxima and minima only are shown, connected by dotted lines. The continuous lines give the general trend of these, from which the wave-length and absorption can be calculated. The change of amplitude with distance in carbon dioxide and nitrous oxide is well marked. Occasionally, the "Meissner wind," already referred to, gave trouble, but its effect, when present, was to raise the general level of the amplitude throughout the curve. After subtracting the direct current, the alternating current remaining was amenable to calculation.

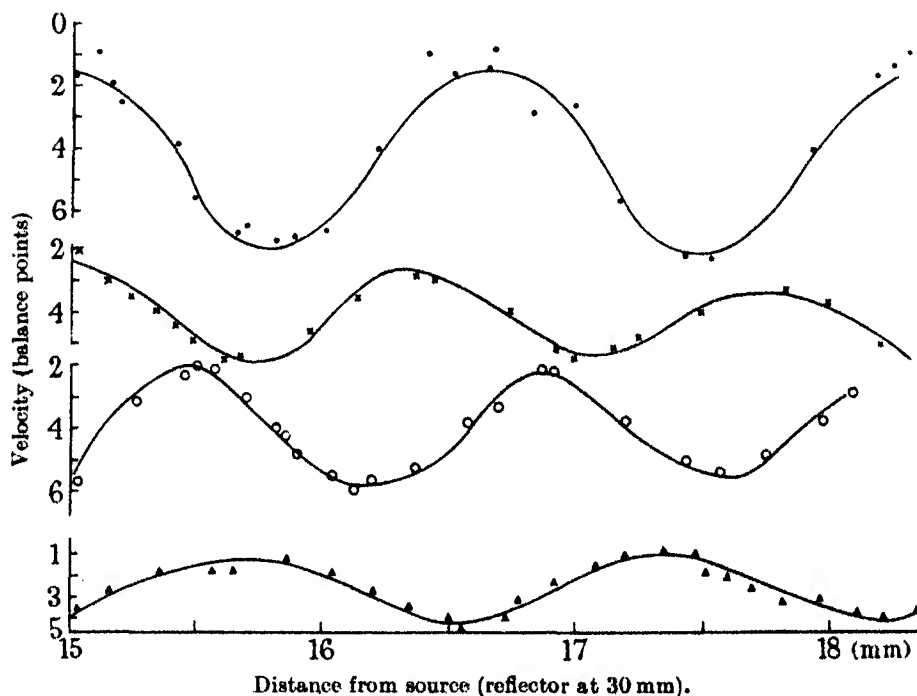


FIG. 5—Stationary waves at 98 kc/sec. ● Oxygen; × nitrous oxide; ○ carbon dioxide; Δ argon.

We may calculate the decay factor from the shape of such curves in the following manner. Let us suppose that the progressive and retrogressive plane waves in a dispersive gas are given by the expression

$$E = Be^{-\alpha x} e^{i(\omega t - \beta x)} + Ce^{\alpha x} e^{i(\omega t + \beta x)}, \quad (1)$$

so that the waves have frequency $\omega/2\pi$, wave-length $2\pi/\beta$ and damping α . Since $E = 0$ at $x = l$ for all values of t ,

$$0 = Be^{-(\alpha + i\beta)l} + Ce^{(\alpha + i\beta)l}.$$

Therefore

$$E = Ce^{(\alpha + i\beta)l} [e^{(\alpha + i\beta)(x-l)} - e^{-(\alpha + i\beta)(x-l)}] e^{i\omega t} \\ = 2Ce^{(\alpha + i\beta)l} \sinh \{(\alpha + i\beta)(x-l)\} e^{i\omega t}.$$

Whence

$$|E|^2 = 2A^2 [\cosh \{2\alpha(x-l)\} - \cos \{2\beta(x-l)\}], \quad (2)$$

where $A = Ce^{i\omega t}$.

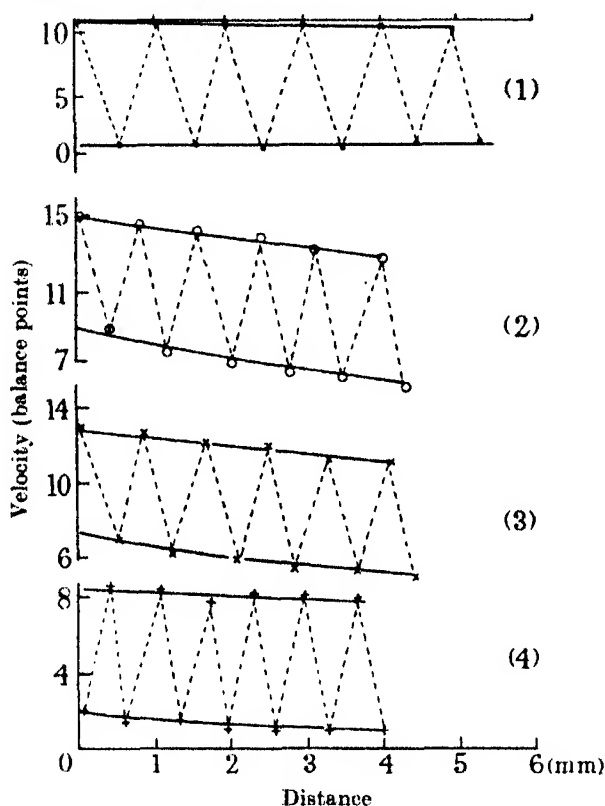


FIG. 6—Maxima and minima at 167 kc/sec. (1) Oxygen (reflector at 16.5 mm); (2) carbon dioxide (reflector at 16.0 mm); (3) nitrous oxide (reflector at 15.5 mm); (4) sulphur dioxide (reflector at 13.5 mm); 2.5 cm from source to reflector in each case.

By taking a number of amplitudes at different distances (x) along the curves, such as those of fig. 5, depicting the stationary waves in the gas, and substituting them in the equation (2), together with the appropriate value of β , α can be calculated. α is usually small compared with β so that the maximum and minimum values of $|E|^2$, as x varies, are given by

$$2A^2 [\cosh \{2\alpha(x-l)\} + 1] \quad \text{and} \quad 2A^2 [\cosh \{2\alpha(x-l)\} - 1] \\ \text{i.e.,} \quad 4A^2 \cosh^2 \{\alpha(x-l)\} \quad \text{and} \quad 4A^2 \sinh^2 \{\alpha(x-l)\},$$

respectively. So that the amplitude in the pseudo-stationary waves varies between $2A \cosh \{\alpha (x - l)\}$ and $2A \sinh \{\alpha (x - l)\}$ as x varies, and these same expressions give the loci of the peaks and troughs respectively. Results calculated from the positions and size of the peaks are given in the tables which follow together with some results obtained with the torsion-vane method. The coefficient actually tabulated is that of energy damping, i.e., k in $I = I_0 e^{-kx}$; $k = 2\alpha$.

On fig. 7 are plotted the absorption coefficients for four gases. According to the recent extensive measurements of Kaye and Sherratt* the normal velocity in

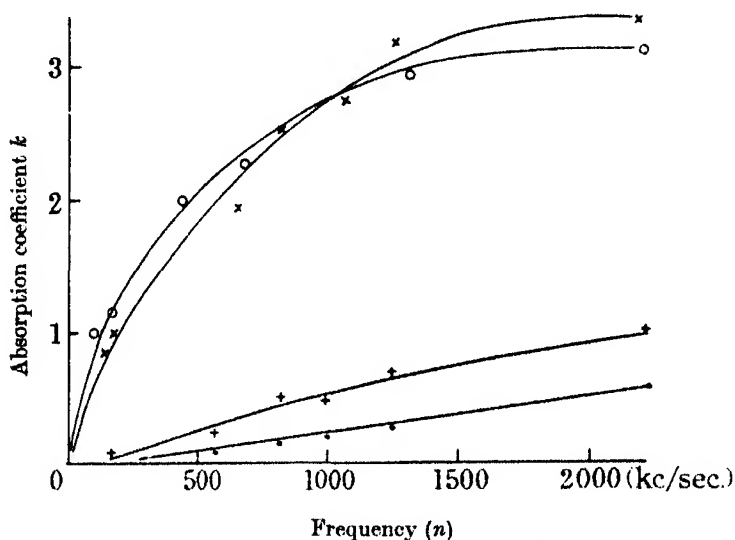


FIG. 7—Absorption curves. ○ Carbon dioxide; × nitrous oxide; + sulphur dioxide; ● oxygen.

carbon dioxide should be 258.8 m/sec, in sulphur dioxide 209.14. Oxygen is the only one of the four in which k/n^2 is approximately constant, this constant being 2×10^{-13} .

Discussion of Results

The anomalous dispersion of supersonic waves in gases may be ascribed to one or more of three factors, viz., (a) lag in the transfer of energy between one and another of the degrees of freedom of the molecules, (b) selective or resonant absorption, (c) abnormal viscosity under high frequency vibration. The theory of the propagation of sound waves in a gas has been treated recently under (a),

* 'Proc. Roy. Soc.,' A, vol. 141, p. 123 (1933).

Table of Results

Frequency (μ) kc/sec	Temperature °C	Wave-length mm	Velocity at 0° C, m/sec	Absorption coefficient k	$k/n^2 \times 10^{12}$
Oxygen					
42.3	19	7.68	314.0	—	—
98.0	18	$\left\{ \begin{array}{l} 3.32 \\ 3.3^* \end{array} \right\}$	315.0	—	—
167	18.5	$\left\{ \begin{array}{l} 1.95 \\ 2.0^* \end{array} \right\}$	315.0	0.05	0.2
695	19	0.467	314.0	0.1, 0.1†	0.2
833	20	0.392	315.2	0.2, 0.15‡	0.2
1000	18	0.325	314.6	0.3†, 0.2‡	0.2
1240	18	0.262	314.5	0.3†, 0.2‡	0.2
1800	19.5	0.182	316.5	—	—
2200	19	(0.150)	(318.9)	0.6†	0.12
Carbon Dioxide					
42.3	19	$\left\{ \begin{array}{l} 6.28 \\ 6.25^* \end{array} \right\}$	256.7	0.3	165
98.0	18	$\left\{ \begin{array}{l} 2.72 \\ 2.7^* \end{array} \right\}$	258.1	1	105
167	18.5	1.62	261.6	1.2	43
465	20	0.587	263.5	2‡	9
695	19	0.40	268.1	2.25, 2.5, † 2‡	4.6
833	18	0.337	270.8	2.5, 2‡	3.6
1000	18	0.280	270.9	2.7†, 2‡	2.7
1240	20	0.228	271.5	3.0†, 2.5‡	2.0
1800	19.5	0.154	267.8	—	—
2200	19	(0.122)	(259.4)	3.1†	0.6
Nitrous Oxide					
42.3	19	$\left\{ \begin{array}{l} 6.27 \\ 6.25^* \end{array} \right\}$	256.5	0.3	165
98.0	18	$\left\{ \begin{array}{l} 2.70 \\ 2.7^* \end{array} \right\}$	256.1	0.8	77
167	18	1.63	262.1	0.1	35
465	20	0.588	263.9	—	—
695	19	0.397	266.0	1.85, 2†	3.8
833	20	0.338	271.0	2.5	3.6
1000	18	0.280	271.1	2.65†	2.65
1240	20	0.228	271.5	3.2†	2.1
1800	19.5	0.154	267.6	—	—
2200	18.5	(0.120)	(257.1)	3.35†	0.7
Sulphur Dioxide					
42.3	19	5.05	207.9	—	—
167	18	1.295	209.2	0.1	0.36
695	19	0.310	208.3	0.3, 0.5‡	0.62
833	19.5	0.260	209.1	0.5, 1‡	0.72
1000	19	0.215	208.1	0.75†, 1‡	0.75
1240	19.5	0.175	209.7	0.75†, 1.5‡	0.5
1800	19.5	0.120	208.7	—	—
2200	18.5	(0.10)	(212.8)	1.0†	0.2
Argon					
42.3	18	7.52	307.8	—	—
98	18	3.25	307.9	—	—
167	19	(1.9)	(308.0)	—	—

* By double hot-wire method.

† By single hot-wire method.

‡ By torsion-vane method.

All other results by hot wire in stationary waves.

by Herzfeld and Rice,* Bourgin,† Kneser,‡ and Henry§ in connection with the results of supersonic velocity measurements made by various workers. The theory had been worked out, before the recent experiments, by Einstein,|| and, apparently unnoticed by recent writers, as early as 1904 by Jeans,¶ who showed that in a gas in which there was delay in the passage of translational into vibrational energy, the velocity of sound would be higher than normal owing to the enhanced ratio of the specific heats, if the source of sound has a period comparable to this "time of relaxation." This will, as Kneser points out, entail a diminishing amplitude (of phase waves). In the words of Hubbard, "one may picture a gas composed of complex molecules as being stiffer for vibrations above a certain frequency than for those below." On this theory a sudden rise in the velocity of propagation should occur when a time period of oscillation equal to the relaxation time is reached. Above this frequency the velocity should remain constant at its new value.

The propagation of sound waves through a medium containing a number of resonators, such as is envisaged under (b) has been examined by Belikov** and Kasterin,†† the latter having also considered the problem theoretically. The absorbing medium consisted of a large number of Helmholtz resonators all tuned to the same frequency and mounted on a lattice; the sound from a loud speaker passed through the system to fall on a Rayleigh disc behind it. Here again, a diminution of amplitude in the neighbourhood of resonance was observed, accompanied by a fall of velocity on the low frequency side of resonance followed by a sharp rise at resonance and a slow fall to normal above resonance—a dispersion curve characteristic of selective absorption. As would be expected from the nature of the phenomenon, selective absorption in sound is characterized by a broader sphere of influence than is the corresponding absorption in light. Even with their tuned resonators Kasterin and Belikov found the effects of dispersion extending to 20% on either side of the maximum.

As to (c) it may be remarked that we know little with respect to the behaviour of gases in the purely viscous damping of waves of even moderate frequency.

* 'Phys. Rev.,' vol. 31, p. 691 (1928).

† 'Phil. Mag.,' vol. 7, p. 821 (1929).

‡ 'Ann. Physik,' vol. 11, p. 761 (1931).

§ 'Proc. Camb. Phil. Soc.,' vol. 28, p. 249 (1932).

|| 'Ber. Berl. Akad. Wiss.,' p. 380 (1920).

¶ "Dynamical Theory of Gases," p. 302 (1904).

** 'Z. Physik,' vol. 39, p. 233 (1926).

†† Thesis, Moscow, quoted in Muller-Pouillet's "Lehrbuch der Physik," vol. 3, p. 406 (1929).

Even if a gas holds to the Kirchhoff formula in respect that the decay of amplitude is proportional to the square of the frequency, the actual coefficient is, in every gas which has been investigated, greater than Kirchhoff's value. This is not surprising when we consider that we have no reason to suppose that the "coefficient of viscosity" to high frequency alternations must be the same as that, as usually measured, in uni-directional flow.

Considering the present results in the light of these three hypotheses, the rise in the velocity of propagation in the neighbourhood of 200 kc/sec shown by carbon dioxide and nitrous oxide is undoubtedly in favour of the Jeans relaxation-time theory. On the other hand, the velocity is not maintained at this value at higher frequencies, and the absorption coefficient is still far above normal up to the limiting frequency at which measurements are possible. There are, in fact, strong indications of a resonant frequency a little above the limit, say, at 5×10^6 cycles/sec. The slight rise in velocity followed by a rapid fall parallels the early part of the dispersion curve obtained by Kasterin with the Helmholtz resonators. If resonance exists, the curve would, of course, again cross the normal velocity at the resonant frequency, while the absorption should fall subsequently to that due to thermal agitation alone. As the latter is a very uncertain quantity at these high frequencies it does not seem fair to subtract the Kirchhoff absorption from the measured values and to call this excess the value of the molecular absorption; but we can compare the absorption shown by the anomalous gases with a normal one like argon, or the nearly normal oxygen. With regard to the latter, its absorption coefficient is about double of that of the Kirchhoff constant over the range investigated, while the trend of its velocity and absorption curves seems to indicate the beginning of abnormality at 2×10^6 cycles/sec. At this frequency, the corresponding curves of carbon dioxide and nitrous oxide have far to go before returning to normality.

If such selective absorption is taking place, it is at frequencies considerably lower than those which have up to the present been considered possible. Considerations of the mean free path of the molecules would point to resonance in the neighbourhood of 10^{10} cycles/sec at ordinary pressures, instead of 10^7 . Some experiments of Altberg* should be cited in this connection. He measured the absorption of high frequency sound in smokes of which the "molecular density" was much greater than that in a gas, and would be expected to show selective absorption at a correspondingly lower frequency. The trend of the absorption curve closely paralleled those given in this paper for gases at

* 'Phys. Z.', vol. 26, p. 153 (1925).

higher frequencies, and leads one to suspect selective absorption in the present instance at about the frequency named. It is unfortunate that the most interesting features of these results appear at such high frequencies, where measurements are admittedly difficult, but by varying the temperature and pressure it should be possible to transfer the selective absorption to a frequency more amenable to treatment.

Whatever explanation we choose to adopt of the marked diminution in amplitude suffered by supersonic waves in such gases as carbon dioxide, it is interesting to speculate on the fate of the kinetic energy which "disappears." Is it all absorbed in molecular motion as heat, or is some of it re-emitted or scattered? Kneser* thinks that some of it may reappear as light quanta. Evidence was found by the present author for scattering of the radiation. Firstly, if the reflector experiments are repeated, using an artificially roughened reflector so as to scatter the radiation that falls on it, a marked smoothing of the antinodal peaks occurs in oxygen as the distance of the reflector from the source is increased. On the other hand, little change is produced in carbon dioxide and nitrous oxide when the scattering reflector is substituted for the plane one. From this one concludes that in the latter gas scattering by the gas itself is already taking place and is increased but a little by the superposed

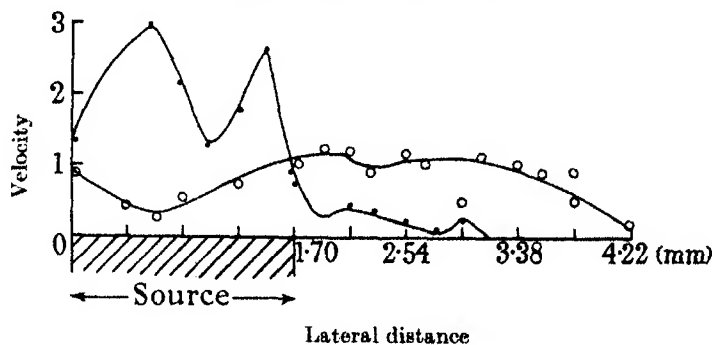


FIG. 8—Lateral traverses at 167 kc/sec. ● Oxygen ; ○ carbon dioxide.

artificial scattering of the reflector. Secondly, traversing of the hot wire from side to side of the tube, at a distance sufficiently great to avoid the region close to the quartz face, showed a spreading of the radiation in carbon dioxide, much greater than in oxygen or argon (*cf.* fig. 8 where cross plots of hot-wire readings at 2 cm from the face of the 167 kc/sec quartz in the two gases are given). From these two experiments we conclude that the observed diminution in amplitude in carbon dioxide is due to dispersion in the complete sense, *i.e.*,

* 'Ann. Physik,' vol. 16, p. 347 (1933).

to both scattering and absorption of energy on the part of the molecules. This leads one to another aspect of the behaviour of these anomalous gases, viz., that the molecules of the gases in which these effects are most marked are all notably anisotropic. They are, in fact, just those which, in view of their limited degrees of freedom, show the Raman effect and allied *light* scattering phenomena most readily. Both effects are, for example, strong in carbon dioxide and nitrous oxide, less in sulphur dioxide and oxygen, negligible in argon.

As to the possibility of a change in wave-length during scattering, this, if it existed, would be difficult to sort out from true absorption. Thus, if an original S.H.M. after dispersion consists of a group of waves covering a small interval of frequency, we should need to take our equation (2), and allow β in the second term to vary within narrow limits, so that the resulting measured velocity would be that of a group. The net effect of true absorption and interference of this type on either stationary or progressive waves will be rather similar to that of absorption alone. Each will produce, in progressive waves, a steady diminution of amplitude, and in stationary waves, a smoothing of the peaks. With the accuracy at present available, the hot wire apparatus could not disentangle the two effects.

Acknowledgments

The author wishes to thank Professor W. E. Curtis for placing every facility of the laboratory at his disposal, also to thank the Senate of the London University and the Council of Armstrong College for making grants for the purchase of apparatus from the Dixon Fund and the College Research Funds respectively.

Summary

The propagation through various gases of supersonic radiation emitted by piezo-electrically maintained quartz crystals is examined experimentally. New methods involving the change of resistance of an electrically heated wire exposed to the radiation are developed, enabling the wave-length and amplitude of the gaseous vibration to be measured. The method of calibrating the apparatus is also described, and the results compared with those obtained by older methods. The anomalous dispersion and absorption shown by certain gases is critically examined, and suggestions put forward to account for it. Evidence is adduced to show that some of the radiation "absorbed" is scattered by the gas.

*The Kinetics of the Oxidation of Mixtures of
Ethylene and Acetaldehyde*

By E. W. R. STEACIE and A. C. PLEWES, Physical Chemistry Laboratory,
McGill University

(Communicated by H. T. Barnes, F.R.S.—Received February 19, 1934)

Introduction

The oxidation of gaseous hydrocarbons has long attracted considerable interest on account of its theoretical and practical importance. Early work was concerned entirely with the identification of the products of oxidation, and the postulation of plausible intermediate steps in their formation. As a result of such work Bone* and his collaborators suggested the so-called "hydroxylation theory," which involved the orderly formation of hydroxyl compounds during oxidation, and their subsequent decomposition or further oxidation. This theory gives an excellent explanation of the intermediate and final products formed in the oxidation of most simple hydrocarbons.

As far as the mechanism of the actual oxidation process is concerned, little progress was made until the development of the idea of thermal chain reactions. It is now generally conceded that the oxidation of most gaseous organic compounds proceeds by a chain mechanism. The main problem at the present time is to obtain some definite information regarding the carriers of the chains. One of the most useful attempts in this direction is the peroxide theory of Egerton,† in which it is assumed that the initial step in the oxidation of organic compounds is the formation of an energy-rich complex with oxygen, which is called a "peroxide." Whether such a complex bears any real relation to actual stable alkyl peroxides is quite unknown.

There have been several attempts to formulate more detailed mechanisms of the chain process and the products formed. One of the most useful of these is that of Bodenstein.‡ The main trouble at present is that all these schemes are necessarily highly speculative in the absence of definite information

* Bone and Drugman, 'J. Chem. Soc.,' vol. 89, p. 676 (1906); Bone, Drugman and Andrew, *ibid.*, vol. 89, p. 1614 (1906); Bone and Drugman, *ibid.*, vol. 89, p. 660 (1906).

† Egerton and Gates, 'Proc. Roy. Soc.,' A, vol. 116, p. 576 (1927); Callendar, 'Engineering,' vol. 123, p. 147 (1927).

‡ 'Z. phys. Chem.,' B, vol. 12, p. 151 (1931).

regarding the carriers of the chains. It is quite possible that the carriers in the oxidation of saturated and unsaturated hydrocarbons are entirely different; and indeed there is no unequivocal proof that the carriers in any one reaction are the same as those in any other. It is known that in certain reactions we may have "sensitized" oxidation of gaseous hydrocarbons. Thus Spence and Taylor* found that the oxidation of ethylene is largely accelerated by the addition of ozone. The fact that a substance will act as a sensitizer does not, of course, prove that it was in any way involved in the original mechanism. However, any substance which acts, or which furnishes products which act, as chain carriers must act as a sensitizer of the oxidation. It is therefore possible to attack the problem by the elimination of those substances which will not affect the rate of reaction. In addition, experiments on the oxidation of mixtures are of interest from the point of view of the specificity of energy exchange between molecules in such reactions.

There is a considerable body of evidence to show that aldehydes and their oxidation products play a considerable part in the oxidation of saturated hydrocarbons.† In fact Bone and Hill‡ showed that the addition of acetaldehyde to ethane-oxygen mixtures caused "instant inflammation." It seems possible that they may be of importance in the oxidation of unsaturated hydrocarbons as well. The oxidation of ethylene is particularly easy to investigate since it is practically independent of the nature of the wall. An investigation is therefore being made of the oxidation of ethylene in the presence of certain substances. The present paper deals with the oxidation of ethylene-acetaldehyde mixtures.

Experimental

Apparatus—Reaction velocities were followed in the usual way by observing the rate of pressure change in a system at constant volume. The reaction vessel was of fused silica and had a capacity of about 125 c.c. The apparatus was similar to one which has been used in a number of previous investigations. The dead space was about 2% of the volume of the reaction vessel.§ The required temperatures were obtained by means of an electric furnace of the type previously described. To secure uniformity of temperature and ease of regulation the reaction bulb was placed in the tube of the furnace and packed

* 'J. Amer. Chem. Soc.,' vol. 52, p. 2399 (1930).

† See especially Pease, 'J. Amer. Chem. Soc.,' vol. 51, p. 1839 (1929).

‡ 'Proc. Roy. Soc.,' A, vol. 129, p. 434 (1930).

§ Steacie, 'Can. J. Res.,' vol. 6, p. 265 (1932); 'J. Phys. Chem.,' vol. 36, p. 1562 (1932).

in with nickel shot. The temperature was hand regulated and could be maintained constant to within $\pm 0.5^\circ$ C. Temperatures were measured with a chromel-alumel thermocouple in conjunction with a Cambridge thermocouple potentiometer. The thermocouple was checked at the boiling points of water and sulphur.

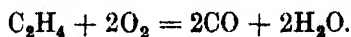
Materials—*Ethylene* was obtained in cylinders from the Ohio Chemical and Manufacturing Company. It was stated to be 99.5% pure. Analysis in the usual way showed it to contain 99.6% C_2H_4 .

Oxygen manufactured by the liquid air process, was obtained from cylinders. It was dried over phosphorus pentoxide. Analysis showed it to be 96% oxygen, the remainder being nitrogen.

Acetaldehyde was obtained by the addition of sulphuric acid to a highly purified sample of paraldehyde. The resulting acetaldehyde was then fractionally distilled.*

The Oxidation of Ethylene

The kinetics of the oxidation of ethylene have been investigated recently by Thompson and Hinshelwood,† who found that, except when ethylene was in excess the main reaction was



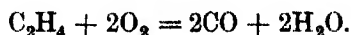
The rate of reaction depended greatly on the concentration of ethylene, but was more or less independent of the oxygen concentration. The reaction was suppressed somewhat by packing and the effect of inert gases was small and suggested short chains. Thompson and Hinshelwood suggested that the initial step is the formation of an unstable peroxide. If this reacts with ethylene the chain is propagated, while if it reacts with more oxygen the chain ends. In the present investigation a considerable part of the work of Thompson and Hinshelwood has been repeated, in order to serve as a basis for comparison in later experiments with added substances.

The Pressure Change Accompanying the Reaction—Thompson and Hinshelwood found that the rate of pressure change in the reaction was approximately proportional to the rate of disappearance of ethylene (except where ethylene was in excess). Consequently the use of pressure change as a measure of the rate of oxidation is justified.

* We are indebted to Mr. C. T. Mason of this Laboratory for the sample of acetaldehyde.

† 'Proc. Roy. Soc.,' A, vol. 125, p. 277 (1927); see also Lenher, 'J. Amer. Chem. Soc.,' vol. 53, p. 3737 (1931).

At completion they found that the pressure increase was 58% of that required by the reaction



The present investigation has been limited to $\text{C}_2\text{H}_4 : 2\text{O}_2$ mixtures. The total pressure change at completion is in good agreement with the values obtained by Thompson and Hinshelwood, as shown in Table I.

Table I

Temperature °C	Initial Pressure		Per cent. increase at completion relative to initial partial pressure of C_2H_4
	C_2H_4 cm	O_2 cm	
452	8.0	16.0	54
452	10.6	20.1	54
452	12.4	24.8	57
452	6.8	13.6	57
430	14.5	29.0	55
430	13.8	27.6	53
430	5.3	10.6	52
430	11.0	22.0	52

The Products of Reaction—Some typical analyses are given in Table II and are compared with the results of Thompson and Hinshelwood.

Table II.— $\text{C}_2\text{H}_4 + 2\text{O}_2$

Temperature °C	Authors		Thompson and Hinshelwood	
	452	452	450	409
CO_2	17.0	16.0	16.95	18.6
CO	41.0	39.0	40.2	59.6
O_2	20.0	19.0	12.65	2.0
C_2H_4	2.0	1.7	12.95	1.0
Residue (partly N_2)	20.0	24.3	8.3	18.8
CO/CO_2	2.35	2.44	2.90	3.22

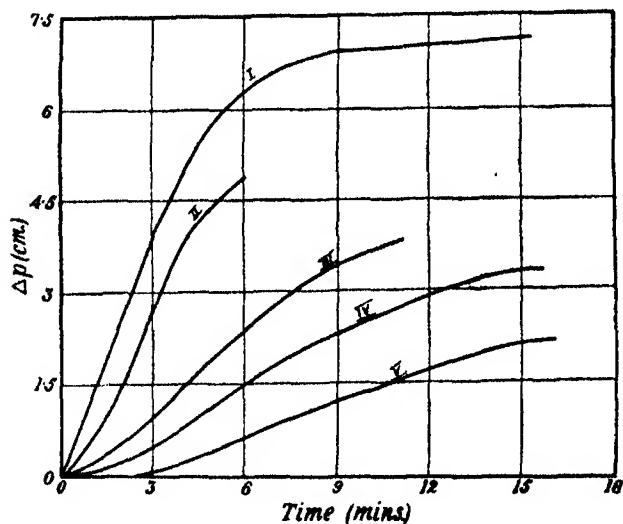
The general trend of these results is in agreement with those of Thompson and Hinshelwood, though there are certain discrepancies. In general we find rather more oxygen left at the end of the reaction, but obtain rather lower CO/CO_2 ratios. Since, however, in either investigation only about 55% of the theoretical pressure change for $\text{C}_2\text{H}_4 + 2\text{O}_2 = 2\text{CO} + 2\text{H}_2\text{O}$ is obtained, minor variations in the products formed are not of very great significance.

The Rate of Reaction—Some typical pressure-time curves are given in fig. 1, and the data are given in Table III.

It will be seen that at the temperatures employed the induction period is not very marked.

Table III.—Typical Pressure-time Data. $C_2H_4 + 2O_2$, $452^\circ C$

12.4		10.6		8.3		6.8		5.4	
Time mins	ΔP cm	Time mins	ΔP cm	Time mins	ΔP cm	Time mins	ΔP cm	Time mins	ΔP cm
0	0	0	0	0	0	0	0	0	0
$\frac{1}{2}$	0.55	$\frac{1}{2}$	0.20	1	0.14	$\frac{1}{2}$	0.08	1	0.0
1	1.12	1	0.46	2	0.45	1	0.12	2	0.03
2	2.57	2	1.60	3	1.02	3	0.58	3	0.20
3	4.00	3	2.73	5	2.00	5	1.24	5	0.53
5	5.80	4	3.68	7	2.82	9	2.32	7	0.96
6	6.25	5	4.34	9	3.40	16	3.34	9	1.29
8	6.80	6	4.83	11	3.80	25	3.77	11	1.61
12	7.04	—	—	—	—	37	3.90	13	1.91
16	7.08	—	—	—	—	42	3.90	16	2.25

FIG. 1.—Typical pressure-time curves for $C_2H_4 + 2O_2$, $452^\circ C$

As is usual in combustion reactions of this type the effect of pressure on the rate of reaction is high. As the data in Table IV show it leads to an apparent order of about 2.5, which is slightly smaller than that found by Thompson and Hinshelwood at corresponding temperatures.

Experiments carried out between 400 and $480^\circ C$ showed that no critical pressure limits existed. As the temperature or pressure was raised the rate of reaction increased progressively until inflammation occurred. Thus with $1C_2H_4:2O_2$ mixtures explosions occurred if the total pressure were above 21 cm at 475° , or above 42 cm at $450^\circ C$. The effect of added nitrogen was very small. With $1C_2H_4:2O_2:2N_2$ mixtures there was a slight retarding

effect, which was, however, not much greater than the experimental error. This presumably indicates a comparatively short chain length.

The surface had little effect on the rate of reaction. Fresh surfaces which had not been cleaned, old surfaces, or surfaces cleaned with aqua regia showed no appreciable difference. It was usually possible to remove reaction bulbs, clean them and replace them, and then check previous runs to within the experimental error.

In general the results of Thompson and Hinshelwood have been confirmed.

Table IV
Temperature 452° C

C_2H_4 pressure cm	T_{30} mins	T_{30} mins	T_{40} mins	Order
5.4	8.0	11.1	15.3	2.8
6.6	5.3	7.6	11.1	
7.1	5.1	7.1	9.8	
8.3	4.3	6.2	8.7	
10.1	3.4	4.6	6.3	
10.4	1.9	2.8	3.9	

Temperature 430° C

C_2H_4 pressure cm	T_{30} mins	T_{30} mins	T_{40} mins	Order
5.3	26.2	35.2	49.4	2.7
6.6	15.0	21.2	31.4	
8.1	9.9	14.7	23.0	
11.0	6.5	9.3	14.2	
12.6	4.9	7.7	12.6	
13.8	4.1	5.9	9.2	
14.5	3.0	4.4	6.9	

The Oxidation of Acetaldehyde

The oxidation of acetaldehyde has been investigated only at low temperatures.* There seems to be little doubt that the initial step is the formation of a peroxide or peracid, which then oxidizes or decomposes. Between 300 and 350° C the reaction occurs practically instantaneously, and is always entirely complete in less than 2 minutes. For a $1CH_3CHO + 2O_2$ mixture at 452° C, explosions occurred if the pressure were greater than about 27 cm. The lack of inflammation at lower pressures is rather surprising in view of the general characteristics of the reaction at lower temperatures.

* Bodenstein, 'SitzBer. preuss. Akad. Wiss.,' No. 3, p. 73 (1931); Hatcher, Steacie, and Howland, 'Can. J. Res.,' vol. 7, p. 149 (1932); Pease, 'J. Amer. Chem. Soc.,' vol. 55, p. 2753 (1933).

At these temperatures the pressure increase at completion for a 1 : 2 mixture was about 50–60%. Some typical analyses at completion for a 1 : 2 mixture at 452° C are given in Table V.

Table V.

CO ₂ %	CO %	O ₂ %	Residue (partly N ₂) %	CO/CO ₂
23	1.0	67	9.0	0.043
24	1.5	66	8.5	0.062

From the point of view of the experiments described in the next section, it is evident that at high temperatures the oxidation of acetaldehyde may be considered to be virtually instantaneous.

The Oxidation of Mixtures of Ethylene and Acetaldehyde

In all the following runs the mixture employed was approximately $1(\text{C}_2\text{H}_4 + \text{CH}_3\text{CHO}) + 2\text{O}_2$. Inasmuch as the rate of oxidation of ethylene is very little influenced by the oxygen concentration, any effect of the acetaldehyde in changing the effective oxygen concentration for the ethylene oxidation will be negligible except at high aldehyde concentrations. In the first series of experiments mixtures of ethylene, acetaldehyde and oxygen were made up externally and introduced into the reaction vessel. The data for a typical run are given in Table VI.

Table VI.—Temperature 452° C, initial partial pressures— $\text{C}_2\text{H}_4 = 9.05$ cm, $\text{CH}_3\text{CHO} = 0.89$ cm, $\text{O}_2 = 21.09$ cm

Time mins	Pressure cm	ΔP cm	ΔP corrected for oxidation of CH_3CHO	% ΔP relative to initial partial pressure of C_2H_4
0	31.03	0.00	—	—
$\frac{1}{2}$	31.58	0.55	—	—
1	32.10	1.07	—	—
$1\frac{1}{2}$	32.61	1.58	1.14	12.6
2	32.93	1.90	1.46	16.1
3	33.68	2.65	2.21	24.4
5	34.54	3.51	3.07	33.8
7	35.08	4.05	3.61	40.0
9	35.33	4.30	3.86	42.6
11	35.43	4.40	3.96	43.8
15	35.63	4.60	4.16	46.0
20	35.73	4.70	4.26	47.1

$T_{40} = 7.0$ mins, T_{40} for corresponding $\text{C}_2\text{H}_4\text{--O}_2$ mixture = 7.4 mins.

The values in the fourth column of Table VI are obtained by assuming that the acetaldehyde is completely oxidized in $1\frac{1}{2}$ minutes, and that the pressure

increase from this cause is 50% of the initial aldehyde pressure. The actual values for the pressure increase at completion as obtained in the last section were from 50–60%. The uncertainty thus introduced into the value of T_{40} is not more than 0.6 minutes.

A summary of the data for various experiments is given in Table VII.

Table VII.— $1(\text{C}_2\text{H}_4 + \text{CH}_3\text{CHO}) + 2\text{O}_2$

Temperature °C	Partial pressures		T_{10} mins	T_{20} for corresponding $\text{C}_2\text{H}_4\text{--O}_2$ mixture mins
	CH_3CHO cm	C_2H_4 cm		
430	0.34	2.49	Very slow	Very slow
430	0.59	4.24	30.0	36.0
430	0.76	5.47	26.8	25.0
430	1.82	6.00	10.4	20.0
452	0.92	9.38	8.3	7.0
452	0.89	9.05	7.0	7.4
452	0.98	11.10	6.1	5.2
452	2.70	9.00	Exploded	7.4
452	2.60	8.70	Exploded	7.8
452	1.88	8.00	9.8	8.9
452	1.63	5.85	11.5	13.0
452	2.25	7.27	6.6	9.9
452	2.60	8.10	Exploded	8.7

In order to make certain that the presence of the ethylene did not affect the acetaldehyde oxidation by an "inert gas" effect, a series of runs were made with a $1(\text{CH}_3\text{CHO} + \text{N}_2) + 2\text{O}_2$ mixture, using nitrogen pressures comparable with the ethylene pressures used above. These showed that there was no appreciable effect.

It is evident from the above experiments that unless the acetaldehyde pressure reaches about one-third that of ethylene, the oxidation of the ethylene is in no way affected by the presence of the aldehyde. At high aldehyde concentrations an accelerating effect comes into play at 430° C, and becomes marked enough to lead to explosions at the higher temperature. The fact that the ethylene oxidation is not in general influenced by the presence of acetaldehyde is shown conclusively by the following experiments: at 430° C an ethylene-oxygen mixture was introduced into the reaction vessel, after reaction had proceeded for 1.5 minutes, acetaldehyde was introduced. The data are given in Table VIII.

In Table VIII data for three runs are given, for each the initial conditions were identical. In run I a comparatively large amount of acetaldehyde was added at the end of 1.5 minutes, in run II about half as much aldehyde was added, and in run III no aldehyde. If the added acetaldehyde is oxidized

independently, without affecting the ethylene, then after, say, 5 minutes the values of ΔP for the three runs should differ by a constant amount. The differences in the last two columns should indicate merely the amount of added aldehyde plus the pressure increase accompanying its oxidation. If, however, the acetaldehyde exerts an accelerating effect on the oxidation of

Table VIII.—Temperature 430° C, $1C_2H_4 + 2O_2$

Time mins	I		II		III		(1)–(3)	(2)–(3)
	$C_2H_4 = 7.38$ cm $O_2 = 14.75$ cm		$C_2H_4 = 7.46$ cm $O_2 = 14.91$ cm		$C_2H_4 = 7.40$ cm $O_2 = 14.80$ cm			
	Pressure cm	ΔP (1)	Pressure cm	ΔP (2)	Pressure cm	ΔP (3)		
0	22.13	0.00	22.37	0.00	22.20	0.00	---	---
0.5	22.15	0.02	22.37	0.00	22.20	0.00	---	---
1	22.17	0.04	22.37	0.00	22.20	0.00	---	---
1.5	(CH ₃ CHO added)		(CH ₃ CHO added)		(NO CH ₃ CHO added)		---	---
2	26.02	3.89	24.05	1.68	22.24	0.04	---	---
3	26.72	4.59	24.59	2.22	22.29	0.09	---	---
5	27.50	5.37	25.39	3.02	22.74	0.54	4.83	2.48
7	28.02	5.89	25.97	3.60	23.13	0.93	4.86	2.67
9	28.42	6.29	26.49	4.12	23.68	1.48	4.81	2.64
11	28.64	6.51	26.81	4.44	24.02	1.82	4.69	2.75
13	28.82	6.69	27.10	4.73	24.30	2.10	4.59	2.63
15	28.97	6.84	27.32	4.95	24.71	2.51	4.33	2.44
20	29.22	7.09	27.62	5.25	25.37	3.17	3.92	2.08
25	29.32	7.19	27.75	5.38	25.58	3.38	3.79	2.00

ethylene, then the values in the last two columns should be very large at the start, and decrease rapidly as reactions I and II approach completion while III is still under way. It will be seen that the differences in the last two columns remain sensibly constant for a considerable time, and then decrease only moderately. Acetaldehyde therefore exerts only a very small effect, a part of which is undoubtedly due to the diminution in oxygen concentration produced by acetaldehyde oxidation. The above data are also plotted in fig. 2. The approximate parallelism of the three curves after 4 or 5 minutes confirms the conclusions of the last paragraph.

Discussion

From the foregoing it may be concluded that acetaldehyde and its products of oxidation have relatively little effect on the oxidation of ethylene. The chain length in the ethylene-oxygen reaction is comparatively short. However, the relative concentrations of aldehyde and ethylene used here were such that if an aldehyde-oxygen chain had been continued in ethylene for even

three or four links, all the ethylene would have been consumed during the aldehyde oxidation. The smallness of the accelerating effect observed at moderate aldehyde concentrations must indicate, therefore, that the efficiency of energy transfer from the carrier in the acetaldehyde-oxygen reaction to ethylene is extremely small. At high aldehyde concentrations a definite accelerating effect was found resulting in either a faster but measurable rate, or an explosion; a considerable amount of aldehyde being oxidized rapidly in the presence of ethylene. It seems probable that isothermal conditions ceased to prevail, and that the resulting acceleration of the ethylene oxidation was due to purely thermal causes.

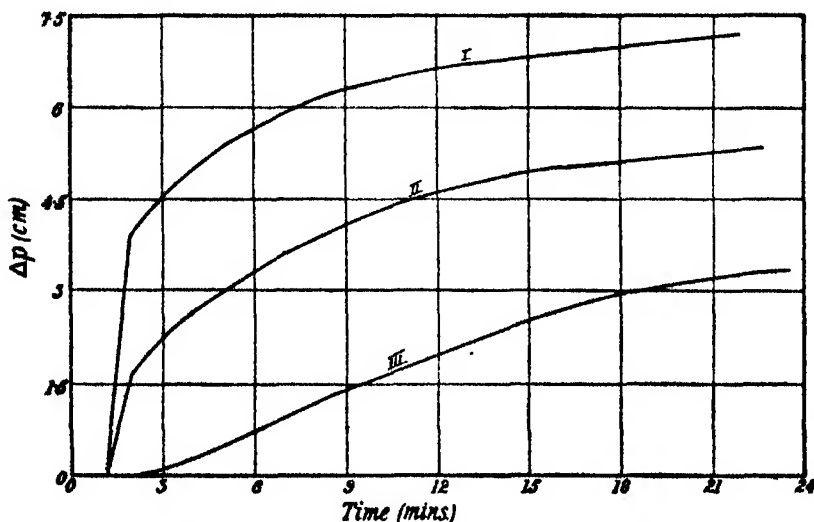


FIG. 2.—The addition of acetaldehyde to $C_2H_4 + 2O_2$ mixture, Table VIII.

After the completion of this work, a paper appeared by Bone, Haffner and Rance* describing an investigation of the oxidation of ethylene, including the effect of 1% of certain foreign substances on the rate of reaction. On p. 37 they state that the "induction period is practically eliminated by a previous addition of 1% of . . . acetaldehyde. The subsequent reaction is accelerated by . . . acetaldehyde." On p. 33 they say "Acetaldehyde practically eliminated the induction without affecting much the subsequent reaction period." The data from which these conclusions are drawn are given only in the form of pressure-time curves, fig. 3 of their paper. If we measure the slope of the lines (in arbitrary units) we find 2.6 ± 0.3 for the reaction with added aldehyde, and 2.5 ± 0.3 for the reaction without added aldehyde. It

* 'Proc. Roy. Soc.,' A, vol. 143, p. 16 (1933).

is evident, therefore, that the aldehyde affects only the induction period, and has no influence on the "stationary" state of the chain process.

The behaviour of ethylene is in sharp contrast to that of ethane, since Bone and Hill (*loc. cit.*) found instant inflammation on adding acetaldehyde to ethane-oxygen mixtures. The work of Pease and others* has indicated that aldehydes are of importance in the oxidation of saturated hydrocarbons. Thus in discussing the question Kassel† says "Taking the results of these two investigations together it is clear that the general nature of hydrocarbon oxidation involves aldehyde formation followed by a chain oxidation of the aldehyde . . . under favourable conditions the excited molecules which carry the chain may crack a considerable amount of the original hydrocarbon."

It appears that the oxidation of saturated and unsaturated hydrocarbons proceeds by quite different mechanisms. From this point of view it should be of interest to examine mixtures of ethane and ethylene to determine whether the chains propagated in one can be continued in the other. Such experiments are in progress.

Summary

An investigation has been made of the kinetics of the oxidation of mixtures of ethylene and acetaldehyde. It is found that, in general, the oxidation of ethylene is not influenced by the presence of acetaldehyde. It is concluded that acetaldehyde and its products of oxidation cannot be of importance in the propagation of chains in ethylene-oxygen mixtures. The oxidation of unsaturated hydrocarbons therefore seems to be of a different character from that of saturated hydrocarbons.

* Pease, 'J. Amer. Chem. Soc.' vol. 51, p. 1839 (1929); Pope, Dykstra, and Edgar 'J. Amer. Chem. Soc.', vol. 51, pp. 1875, 2203, 2213 (1929).

† "Kinetics of Homogeneous Gas Reactions," p. 289 (1932).

On the Stopping of Fast Particles and on the Creation of Positive Electrons

By H. BETHE, Manchester, and W. HEITLER, Bristol

(Communicated by P. A. M. Dirac, F.R.S.—Received February 27, 1934)

Introduction

The stopping power of matter for fast particles is at present believed to be due to three different processes : (1) the ionization ; (2) the nuclear scattering ; (3) the emission of radiation under the influence of the electric field of a nucleus. The first two processes have been treated in quantum mechanics by Bethe,[†] Møller,[‡] and Bloch[§] in a very satisfactory way. A provisional estimation of the order of magnitude to be expected in the third process has been given by Heitler.^{||} The result obtained was that the cross-section ϕ for the energy loss by radiation for very fast particles (if the primary energy $E_0 \gg mc^2$) is of the order

$$\phi \propto \frac{Z^2}{137} \left(\frac{e^2}{mc^2} \right)^2, \quad (1)$$

where Z is the nuclear charge.

It is the aim of the present paper to discuss in greater detail the rate of loss of energy by this third process and its dependence on the primary energy ; in particular we shall consider the effect of *screening*. The results obtained for very high energies ($> 137 mc^2$) seem to be in disagreement with experiments made by Anderson (*cf.* § 7).

By an exactly similar calculation another process can be studied, namely, the “ twin birth ” of a positive and negative electron due to a light quantum in the presence of a nucleus. This process is the converse of the scattering of an electron with loss of radiation, if the final state has *negative energy*. The results are in exact agreement with recent measurements for γ -rays of 3–10 mc^2 . A provisional estimate of the probability of this process has been given by Plesset and Oppenheimer,[¶] who also obtain for the cross-section a quantity of the order of magnitude given by equation (1).

[†] ‘Ann. Physik,’ vol. 5, p. 325 (1930) ; ‘Z. Physik,’ vol. 76, p. 293 (1932).

[‡] ‘Ann. Physik,’ vol. 14, p. 531 (1932).

[§] ‘Z. Physik,’ vol. 81, p. 363 (1933) ; ‘Ann. Physik,’ vol. 16, p. 285 (1933).

^{||} ‘Z. Physik,’ vol. 84, p. 145 (1933). Referred to later as I.

[¶] ‘Phys. Rev.,’ vol. 44, p. 53 (1933).

I. THEORY

§ 1. *The Cross-section for the Energy-loss by Radiation*

1. *General Method.*—In order to obtain the rate of loss of energy of a particle by emission of radiation, we have to calculate the transition probability for the following process : a particle with momentum† \mathbf{p}_0/c and energy E_0 makes a transition to a state with the momentum \mathbf{p}/c and energy E , while a light quantum with the momentum \mathbf{k}/c is emitted, the frequency ν being given by

$$k = h\nu = E_0 - E. \quad (2)$$

The perturbation causing this transition is the interaction of the particle with the nuclear field $V = Ze^2/r$ and with the radiation field $H = -e(\boldsymbol{\alpha}\mathbf{A})$, where \mathbf{A} is the vector potential of the radiation field and $\boldsymbol{\alpha}$ is Dirac's three-dimensional matrix-vector signifying the velocity.

The wave functions of the electron describing the initial and the final state are supposed to be plane waves, the atomic field being only considered as a perturbation. This corresponds to the first approximation of Born's collision theory, which was shown by Bethe (*loc. cit.*) to hold for $Z/137 < v/c$. For fast particles ($v \sim c$) this is always true, if Z is not too large. For lead, however, it is doubtful whether the calculations give quantitatively correct results. But from the experiments it seems that, at least for the twin birth, see § 8, the error is very small.

The transition from the initial to the final state, however, only occurs under the simultaneous action of both the atomic field and that of the light wave. First, the electron goes, under the influence of one of the said perturbations, from the initial state to an intermediate state (conservation of energy does not necessarily hold here); then a second transition immediately happens to the final state, caused by the other perturbation. Since momentum is conserved in the emission of light, it can easily be seen (*cf.* I) that there exist two such intermediate states, where the electron has a momentum \mathbf{p}' , \mathbf{p}'' (energies E' , E'') given by :

$$\left. \begin{array}{ll} \text{I} & \mathbf{p}' = \mathbf{p} + \mathbf{k} \quad \text{no light quantum present} \\ \text{II} & \mathbf{p}'' = \mathbf{p}_0 - \mathbf{k} \quad \text{a light quantum } \mathbf{k} \text{ present} \end{array} \right\}. \quad (3)$$

† It is convenient to express the momentum in energy units $p = c \times \text{momentum}$. Throughout the rest of the paper we shall speak freely of p as the momentum instead of the strictly more correct p/c .

If we denote the initial state (momentum \mathbf{p}_0 , no light quantum) by A, and the final state (momentum \mathbf{p} , \mathbf{k}) by E, the transition probability per unit time becomes (see I, equation (27))

$$w = \frac{2\pi}{\hbar} \rho_E \rho_k dk \left| \sum \frac{H_{EI} V_{IA}}{E' - E_0} + \sum \frac{V_{EI} H_{IA}}{E'' - E} \right|^2, \quad (4)$$

where ρ_E, ρ_k are the numbers of quantum states per unit volume, per unit solid angle and per unit energy interval for the electron and the light quantum in the final state; so that

$$\rho_E dE = \frac{\Omega_E p E dE}{\hbar^3 c^3}, \quad \rho_k dk = \frac{\Omega_k k^2 dk}{\hbar^3 c^3}, \quad (5)$$

(Ω_E, Ω_k being the elements of the solid angle).

The wave functions that occur in the matrix elements in (5) are normalized in such a way that there is one particle per unit volume. The summation in (4) has to be extended over both the spin directions and both signs of the energy of the intermediate states.

To obtain the differential cross-section from (4), we have, according to our method of normalization, to divide by the velocity of the incident electron, $v_0 = cp_0/E_0$. Putting in the values for the matrix elements for a pure Coulomb field (cf. I equations (18)–(21)) we obtain the differential cross-section

$$d\Phi = \frac{Z^2 e^4}{137\pi^2} \frac{\Omega_E \Omega_k p E E_0 k dk}{p_0 q^4} \left| \sum \frac{(u^* \alpha_k u') (u'^* u_0)}{E' - E_0} + \sum \frac{(u^* u'') (u''^* \alpha_k u_0)}{E'' - E} \right|^2, \quad (6)$$

where

$$\mathbf{q} = \mathbf{p}_0 - \mathbf{p} - \mathbf{k}, \quad (7)$$

denotes the momentum transferred to the nucleus in the process. u, u' are the amplitudes of the plane waves with momenta \mathbf{p}, \mathbf{p}' each having four components. u refers to a definite spin direction. α_k is the component of α in the direction of the polarization of the light quantum. $(u^* \alpha_k u') (u'^* u_0)$ depends only upon the angles in terms of which it can easily be expressed. This can be done by the usual method†: first, we carry out the summation Σ over the spin directions and both signs of the energy of the intermediate states (i.e., over all four states having the same momentum \mathbf{p}'):

$$\Sigma \frac{(u^* \alpha_k u') (u'^* u_0)}{E_0 - E'} = \frac{E_0 \Sigma (u^* \alpha_k u') (u'^* u_0)}{E_0^2 - E'^2} + \frac{\Sigma (u^* \alpha_k E' u') (u'^* u_0)}{E_0^2 - E'^2}.$$

In the first term we have simply (Vollständigkeitsrelation)

$$\Sigma (u^* \alpha_k u') (u'^* u_0) = (u^* \alpha_k u_0). \quad (8)$$

† Casimir, 'Helv. Phys. Act.', vol. 6, p. 287 (1933).

For the second we use the wave equation

$$E'u' = [(\alpha \mathbf{p}') + \beta \mu] u' \equiv H'u',$$

where $\mu = mc^2$. This equation holds for both signs of E' , since the operator H' is independent of the sign of E' . Hence

$$\Sigma (u^* \alpha_k E' u') (u'^* u_0) = \Sigma (u^* \alpha_k H' u') (u'^* u_0) = (u^* \alpha_k H' u_0). \quad (9)$$

And finally

$$\Sigma \frac{(u^* \alpha_k u') (u'^* u_0)}{E_0 - E'} = \frac{E_0 (u^* \alpha_k u_0) + (u^* \alpha_k H' u_0)}{E_0^2 - E'^2}. \quad (10)$$

(10) holds for definite spin directions of the initial and the final states. As we are not interested in the probability for special spin directions, we sum also over the spin directions of the final state. Using equation (10) we obtain then from (6) expressions of the form

$$S (u^*_0 A u) (u^* B u_0),$$

where the summation S has to be taken over the spin directions of the final state only, but not over the two signs of the energy. But this sum S can be reduced to a sum Σ over all four states of both spin and energy. For we have

$$Eu = Hu, \quad \text{or} \quad u = \frac{H + E}{2E} u. \quad (11)$$

For the states of *negative energy* with the wave function \tilde{u} the expression $(H + E) \tilde{u}$ vanishes. Introducing the operator $(H + E) u/2E$ instead of u , we may now extend the summation also over both signs of the energy, obtaining

$$S (u^*_0 A u) (u^* B u_0) = \Sigma \left(u^*_0 A \frac{H + E}{2E} u \right) (u^* B u_0) = \left(u^*_0 A \frac{H + E}{2E} B u_0 \right). \quad (12)$$

(12) is the average value of the operator $A (H + E)/2EB$ in the initial state. It can be evaluated by the usual methods.

2. *Differential and Integral Cross-sections.*—If one applies this method to (6) one can easily obtain the differential cross-section

$$\begin{aligned} d\Phi = & \frac{Z^2 e^4}{137 \cdot 2\pi} \frac{dk}{k} \frac{p}{p_0} \frac{\sin \theta \sin \theta_0}{q^4} d\theta d\theta_0 d\phi \left\{ \frac{p^2 \sin^2 \theta}{(E - p \cos \theta)^2} (4E_0^2 - q^2) \right. \\ & + \frac{p_0^2 \sin^2 \theta_0}{(E_0 - p_0 \cos \theta_0)^2} (4E^2 - q^2) - \frac{2p_0 p \sin \theta \sin \theta_0 \cos \phi}{(E - p \cos \theta)(E_0 - p_0 \cos \theta_0)} (4E_0 E - q^2) \\ & \left. + \frac{2k^2 (p^2 \sin^2 \theta + p_0^2 \sin^2 \theta_0 - 2pp_0 \sin \theta \sin \theta_0 \cos \phi)}{(E - p \cos \theta)(E_0 - p_0 \cos \theta_0)} \right\}. \quad (13) \end{aligned}$$

θ , θ_0 are the angles between \mathbf{k} and \mathbf{p} , \mathbf{p}_0 respectively, ϕ the angle between the $(\mathbf{p}\mathbf{k})$ plane and the $(\mathbf{p}_0\mathbf{k})$ plane. The denominators arise from the resonance denominators

$$\left. \begin{aligned} E'^2 - E_0^2 &= (\mathbf{p} + \mathbf{k})^2 - \mathbf{p}_0^2 = -2k(E - p \cos \theta) \\ E''^2 - E^2 &= (\mathbf{p}_0 - \mathbf{k})^2 - \mathbf{p}^2 = 2k(E_0 - p_0 \cos \theta_0) \end{aligned} \right\}. \quad (14)$$

In (14) the summation has already been taken over the directions of polarization, and the spin of the electron in the final state.

In order to obtain the total probability for the emission of a light-quantum of a given frequency ν , one has to integrate (14) over the angles, both of the electron and of the light quantum. This integration is elementary but rather tedious. We shall give only the result.†

$$\begin{aligned} \Phi = \frac{Z^2}{137} \left(\frac{e^2}{mc^2} \right)^2 \frac{p}{p_0} \frac{dk}{k} & \left\{ \frac{1}{4} - 2E_0E \frac{p^2 + p_0^2}{p^2 p_0^2} + \mu^2 \left(\frac{\epsilon_0 E}{p_0^3} + \frac{\epsilon E_0}{p^3} - \frac{\epsilon \epsilon_0}{pp_0} \right) \right. \\ & + \left[\frac{1}{3} \frac{E_0 E}{p_0 p} + \frac{k^2}{p_0^3 p^3} (E_0^2 E^2 + p_0^2 p^2) \right] \cdot \log + \frac{\mu^2 k}{2pp_0} \left[\frac{E_0 E + p_0^2}{p_0^3} \epsilon_0 \right. \\ & \left. \left. - \frac{E_0 E + p^2}{p^3} \epsilon + \frac{2kE_0 E}{p^2 p_0^2} \right] \log \right\}, \quad (15) \end{aligned}$$

with

$$\left. \begin{aligned} \mu &= mc^2, \quad \epsilon = \log \frac{E + p}{E - p} = 2 \log \frac{E + p}{\mu}, \\ \epsilon_0 &= \log \frac{E_0 + p_0}{E_0 - p_0} = 2 \log \frac{E_0 + p_0}{\mu}, \\ \log &= \log \frac{p_0^2 + p_0 p - E_0 k}{p_0^2 - p_0 p - E_0 k} = 2 \log \frac{E_0 E + p_0 p - \mu^2}{\mu k} \end{aligned} \right\}. \quad (15A)$$

For energies large compared with mc^2 , i.e., for

$$E_0 \gg mc^2, \quad E \gg mc^2, \quad k \gg mc^2,$$

(15) reduces to

$$\Phi = \frac{Z^2}{137} \left(\frac{e^2}{mc^2} \right)^2 \frac{dk}{k} \frac{4}{E_0^2} (E_0^2 + E^2 - \frac{1}{2} E_0 E) \left(\log \frac{2E_0 E}{k\mu} - \frac{1}{2} \right). \quad (16)$$

The result will be discussed in § 5, 6, and 7.

† The same formulæ (13), (15), have been obtained by F. Sauter. We are indebted very much to Dr. Sauter for the communication of his results. The comparison with his results has made it possible to avoid some mistakes in the calculations. The same formula has also been obtained by G. Racah. We wish to thank him also for sending us his results.

§ 2. *Creation of Positive Electrons*

The creation of a pair of electrons of opposite charge is considered as a kind of photoelectric process: an electron which is initially in a state of negative energy $E = -|E|$ is excited by a light quantum $h\nu$ to a state of positive energy

$$E_0 = h\nu - |E|.$$

Then it is observed that a negative electron of energy E_0 and a positive one of energy $E_+ = |E|$ are created, the light quantum being absorbed.

The reverse of this process would be the transition of an electron from the state E_0 to a state of negative energy, the energy $E_0 + |E|$ being radiated. This reverse process will not usually occur because the states of negative energy are occupied.† The process is identical with that treated in § 1, the only difference being the sign of the final energy. It is clear that this cannot make any difference in the calculation up to formula (10). One might, however, expect a different value for the quantities $(u^* \alpha_k u_0)$ and $(u^* \alpha_k H' u_0)$.

That this is not so can easily be seen from Casimir's method of evaluating quantities of this kind, which has been used already in § 1, equations (8)–(13). If the momentum \mathbf{p} is given, all considerations leading to (13) remain unchanged, except that we have for the wave amplitude \tilde{u} of a *negative energy state*, instead of (11):

$$\frac{H - |E|}{-2|E|} \tilde{u} = \tilde{u},$$

while for a state of positive energy $(H - |E|) u = 0$. Therefore, in (13) nothing is changed except the sign of the energy, viz.,

$$S(u^*_0 A \tilde{u})(\tilde{u}^* B u_0) = \left(u^*_0 A \frac{H - |E|}{-2|E|} B u_0\right) = \left(u^*_0 A \frac{H + E}{2E} B u_0\right). \quad (17)$$

We conclude that formula (13) holds for the reverse process of the creation of pairs as well as for the "normal" emission of radiation. To calculate the probability of the creation itself, one has only to consider that now there exist *two* electrons in the final state instead of one electron and one light quantum. Instead of $\rho_\nu d\nu$, we must therefore write in (5)

$$\rho_{E_0} dE_0 = \frac{\Omega_0 E_0 p_0 dE_0}{h^3 c^3},$$

i.e., the number of electronic states with energy between E_0 and $E_0 + dE_0$

† It may happen that a positive electron is annihilated in this way by an inner electron of a heavy atom.

per unit volume and per solid angle Ω_0 . Furthermore, one has to divide by the number of incident light quanta per cm^2 and sec., i.e., by c , the density of light quanta being normalized to unity. For the emission of radiation, we had to divide by the velocity $v_0 = cp_0/E_0$ of the primary electron; therefore we get an additional factor $p_0 E_0/k^2 \cdot v_0/c = p_0^2/k^2$ in the cross-section (6) or (13).

There are, however, two points which have to be mentioned. Firstly, one should consider the interaction energy between the two created electrons. Fortunately, it can be seen that this interaction energy V_{+-} does not affect the calculation to our approximation. For the matrix element of $(V_{+-})_{\mathbf{p}_+, \mathbf{p}_-}$ corresponding to the creation is probably the matrix element of a Coulomb interaction belonging to a transition from a positive energy state \mathbf{p}_- to a state with negative energy and momentum $-\mathbf{p}_+$, viz.,

$$(V_{+-})_{\mathbf{p}_+, \mathbf{p}_-} = \int d\tau \left(\exp \frac{i}{\hbar} (\mathbf{p}_- \cdot \mathbf{r}_-) \exp \left(\frac{i}{\hbar} (\mathbf{p}_+ \cdot \mathbf{r}_+) \right) \right) / |\mathbf{r}_+ - \mathbf{r}_-|. \quad (18)$$

But this matrix element vanishes except when momentum is conserved, i.e., $\mathbf{p}_+ + \mathbf{p}_- = 0$. It follows that, if we add to the Coulomb potential V the interaction energy V_{+-} , the latter will not contribute anything to the matrix elements occurring in (4). There will, of course, be a contribution in the next approximation which is only of the order $e^2/\hbar v$ compared with the result of our approximation, while the application of Born's approximation means an error of the order $Zc^2/\hbar v$.

The second point is, that in (13) the momentum and the energy E are the momentum and energy of the hole in the "sea of negative energy electrons" which corresponds to the positive electron. The momentum and energy of the positive electron itself are $-\mathbf{p}$ and $-E$. It is, therefore, physically more significant to introduce

$$E_+ = -E, \quad \mathbf{p}_+ = -\mathbf{p}, \quad \theta_+ = \pi - \theta, \quad \phi_+ = \pi + \phi, \quad p_+ = p, \quad (19)$$

θ_+ being the angle between the direction of motion of the positive electron and that of the incident light quantum, etc. If we introduce these quantities into (13), all terms involving the first power of E or p change sign, thus:

$$\begin{aligned} d\Phi = & -\frac{Z^3}{137} \frac{e^4}{2\pi} \frac{p_0 p_+}{k^2} dE_0 \frac{\sin \theta_0 d\theta_0 \sin \theta_+ d\theta_+ d\phi_+}{q^4} \left\{ \frac{p_+^2 \sin^2 \theta_+ (4E_0^2 - q^2)}{(E_+ - p_+ \cos \theta_+)^2} \right. \\ & + \frac{p_0^2 \sin^2 \theta_0 (4E_+^2 - q^2)}{(E_0 - p_0 \cos \theta_0)^2} + \frac{2p_0 p_+ \sin \theta_0 \sin \theta_+ \cos \phi_+ (4E_0 E_+ + q^2)}{(E_0 - p_0 \cos \theta_0)(E_+ - p_+ \cos \theta_+)} \\ & \left. - \frac{2k^2 (p_+^2 \sin^2 \theta_+ + p_0^2 \sin^2 \theta_0 + 2p_0 p_+ \sin \theta_0 \sin \theta_+ \cos \phi_+)}{(E_0 - p_0 \cos \theta_0)(E_+ - p_+ \cos \theta_+)} \right\}. \quad (20) \end{aligned}$$

The integration over the angles is naturally also identical with that for the radiation case. Formula (15) has, therefore, only to be multiplied by p_0^2/k^2 , dk to be replaced by dE_0 , and E put equal to minus the energy of the positive electron. The cross-section for the creation of a positive electron with energy E_+ and a negative one with energy E_0 by a light quantum $k = h\nu$ then becomes

$$\begin{aligned} \Phi(E_0) dE_0 = & \frac{Z^2}{137} \left(\frac{e^2}{mc^2} \right)^2 \frac{p_0 p_+}{k^3} dE_0 \left\{ -\frac{1}{4} - 2E_0 E_+ \frac{p_0^2 + p_+^2}{p_0^2 p_+^2} \right. \\ & + \mu^2 \left(\frac{\epsilon_0 E_+}{p_0^3} + \frac{\epsilon_+ E_0}{p_+^3} - \frac{\epsilon_+ \epsilon_0}{p_0 p_+} \right) + \left[\frac{k^2}{p_0^3 p_+^3} (E_0^2 E_+^2 + p_0^2 p_+^2) - \frac{E_0 E_+}{p_0 p_+} \right] \log \\ & \left. + \frac{\mu^2 k}{2p_0 p_+} \left[\frac{E_0 E_+ - p_0^2}{p_0^3} \epsilon_0 + \frac{E_0 E_+ - p_+^2}{p_+^3} \epsilon_+ + \frac{2k E_0 E_+}{p_0^2 p_+^2} \right] \log \right\}, \quad (21) \end{aligned}$$

with

$$\epsilon_+ = 2 \log \frac{E_+ + p_+}{\mu}, \quad \log = \log \frac{E_0 k - p_0^2 + p_0 p_+}{E_0 k - p_0^2 - p_0 p_+} = 2 \log \frac{E_0 E_+ + p_0 p_+ + \mu^2}{\mu k}. \quad (21a)$$

This formula is, of course, symmetrical in E_0 and E_+ . An asymmetry would only arise in higher approximations and is small for high energies (*cf.* § 7). If all energies involved are large compared with mc^2 , the formula reduces to

$$\Phi(E_0) dE_0 = \frac{Z^2}{137} \left(\frac{e^2}{mc^2} \right)^2 \frac{1}{4} \frac{E_0 +^2 E_+^2 + \frac{1}{2} E_0 E_+}{(h\nu)^3} dE_0 \left(\log \frac{2E_0 E_+}{h\nu mc^2} - \frac{1}{2} \right). \quad (22)$$

(21) and (22) will be discussed in § 8.

§ 3. Effect of Screening

It could be expected that the screening of the atomic potential by the outer electrons would have a considerable effect on the cross-section for the radiation phenomena considered in this paper, because it may be seen that a large part of the processes take place at big distances from the nucleus of the field-producing atom, *i.e.*, at places where the atomic field is no longer a Coulomb field.

1. *Differential Cross-section.*—The potential which the atom exerts on the electron occurs in formula (4) inside the matrix elements V_{AI} and V_{EII} . Both these matrix elements have the value (besides a factor $(u'u_0)$ and $(u''u)$ respectively)

$$V_{AI} = V_{EII} = \int V \exp \frac{i}{\hbar c} (\mathbf{q}\mathbf{r}) d\tau, \quad (23)$$

where q is the momentum transferred to the atom in the process. Now (23) can be brought into the form

$$V_{AI} = V_{EII} = \frac{4\pi\hbar^2 c^2}{q^2} [Z - F(q)]^2, \quad (24)$$

where F is the well-known atomic form-factor

$$F(q) = \int \rho(r) \exp \frac{i}{\hbar c} (\mathbf{q}\mathbf{r}) d\tau, \quad (25)$$

$\rho(r)$ being the density of the atomic electrons at the distance r from the nucleus. Therefore, we can take account of the screening simply by writing $(Z - F)^2$ instead of Z^2 in formula (13), a change which is familiar from the theory of electron scattering.†

The atomic form-factor F depends on the distribution of the atomic electrons. We assume in our calculations that $\rho(r)$ is the Fermi distribution, which, especially for heavy atoms, should be very accurate. We can, then, write

$$F = Z\mathcal{F}(qZ^{-1}), \quad (26)$$

where \mathcal{F} is a general atomic form-factor valid for all atoms. It is given numerically in several papers.‡

We can easily get an idea under which conditions the screening will have an appreciable effect. The atomic form-factor F becomes comparable with Z , if $q/\hbar c$ is of the order (or smaller than) the reciprocal atomic radius. Now, the radius of the Fermi atom is approximately $a_0 Z^{-1}$, a_0 being the hydrogen radius. Therefore screening is effective if

$$q \leq \alpha = \frac{\hbar c}{a_0} Z^{\frac{1}{2}} = \frac{mc^2}{137} Z^{\frac{1}{2}}. \quad (27)$$

On the other hand, q takes its minimum value if the momentum of the electron is parallel to that of the emitted light quantum both before and after the radiation. Here q is equal to

$$q_{\min} = \delta = p_0 - p - k = E - p - (E_0 - p_0). \quad (28)$$

For energies E_0 and E large compared with mc^2 this reduces to

$$\delta = \frac{(mc^2)^2 \hbar \nu}{2E_0 E}. \quad (29)$$

† Cf., for instance, Mott and Massey, "Atomic Collisions," Oxford Univ. Press, 1934, p. 89.

‡ For instance, Bethe, 'Ann. Physik,' vol. 5, p. 385 (1930).

This formula shows that the minimum momentum transferred to the atom decreases with increasing energy and becomes smaller than α , if

$$E_0 E / h\nu > \frac{1}{2} 137 mc^2 Z^{-\frac{1}{2}}, \quad (30)$$

that is, about $15mc^2$ for heavy atoms. (30) is the condition for the *screening to be effective*. We see from this condition that the screening will only be important for energies large compared with mc^2 , and we can, therefore, assume throughout this section that mc^2 is negligible in comparison with E_0 , E and $h\nu$. This assumption greatly simplifies the calculation.

2. *Integral Cross-section.*—The integration over the angles θ_0 , θ , ϕ is carried out in another paper†. The last part of this integration can only be carried out numerically, since the atomic form factor F of the Fermi atom is only known numerically. The result, *i.e.*, the integral cross-section, can conveniently be written in the form

$$\Phi(\nu) d\nu = \frac{Z^2}{137} r_0^2 \frac{1}{E_0^2} \frac{d\nu}{\nu} [(E_0^2 + E^2) (\phi_1(\gamma) - \frac{1}{2} \log Z) - \frac{2}{3} E_0 E (\phi_2(\gamma) - \frac{1}{2} \log Z)], \quad (31)$$

where

$$r_0 = e^2 / mc^2$$

is the electronic radius and

$$\gamma = 100 \frac{mc^2 h\nu}{E_0 E Z^{\frac{1}{2}}}, \quad (32)$$

and ϕ_1 , ϕ_2 are two functions of γ which are given in fig. 1.‡

The quantity γ is proportional to δ/α and therefore determines the effect of screening. If $\gamma = 0$, we may call the screening “*complete*.” Indeed, the radiation cross-section is then determined entirely by the atomic radius, *i.e.*, by α , whereas the minimum momentum transfer δ (and therefore the energy) has no longer any effect on the cross-section. The values of ϕ_1 , ϕ_2 here are

$$\phi_1(0) = 4 \log 183, \quad \phi_2(0) = \phi_1(0) - \frac{2}{3}, \quad (33)$$

so that for very high energies, $E_0 \gg 137 mc^2 Z^{-\frac{1}{2}}$, the cross-section (31) becomes

$$\Phi(\nu) d\nu = \frac{Z^2}{137} \frac{r_0^2}{E_0^2} \frac{d\nu}{\nu} 4 \left[(E_0^2 + E^2 - \frac{2}{3} E_0 E) \log(183 Z^{-\frac{1}{2}}) + \frac{E_0 E}{9} \right]. \quad (34)$$

For a given ratio $h\nu/E_0$, this cross-section is independent of E_0 . This is not so if the energy becomes smaller ($\gamma > 0$). The cross-section for a given $h\nu/E_0$

† ‘Proc. Camb. Phil. Soc.’ *in press*. Referred to as C.

‡ It would have been more natural theoretically to put $\gamma = \delta/\alpha = 137 mc^2 h\nu / 2 E_0 E Z^{\frac{1}{2}}$. The factor 100 instead of 137/2 has been chosen for convenience in using formula (31).

then decreases, though slowly, with decreasing energy (the ϕ 's decrease with increasing γ). In the limiting case $\gamma \gg 1$, i.e., for energies small compared with $137mc^2 Z^{-1}$ the screening ceases to have any effect, in agreement with our considerations in the preceding section. The cross-section is, then, given by formula (16). For energies that are a little higher, more accurately for values

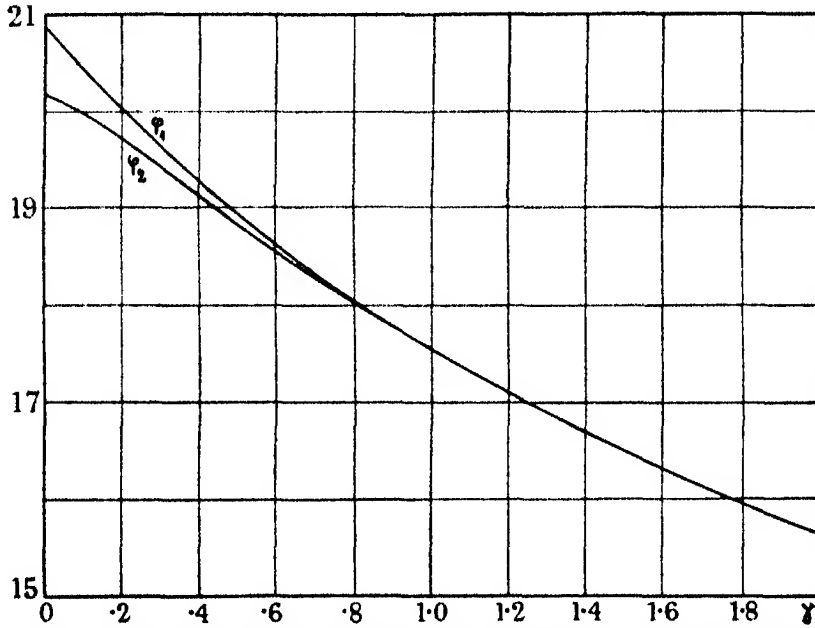


FIG. 1.— ϕ_1 and ϕ_2 (cf. equation (31)) as functions of $\gamma = 100mc^2 \hbar\nu/E_0 E Z^{1/2}$.

of γ between 2 and 15, the screening gives a small correction to formula (16), which may be taken into account by writing instead of (16)

$$\Phi(\nu) d\nu = \frac{Z^2}{137} \frac{r_0^2}{E_0^2} \frac{d\nu}{\nu} 4(E_0^2 + E^2 - \frac{2}{3}E_0 E) \left(\log \frac{2E_0 E}{mc^2 \hbar\nu} - \frac{1}{2} - c(\gamma) \right), \quad (35)$$

and inserting for $c(\gamma)$ the value given in Table I.

Table I.									
$c(\gamma) = 0.21$	0.16	0.13	0.09	0.065	0.05	0.03	0.02	0.01	
$\gamma = 2$	2.5	3	4	5	6	8	10	15	(35A)

For the *creation of pairs* of electrons, all formulæ are exactly similar except for the normalizing factor and for the sign of E . If, in accordance with § 2, we call the energy of the positive electron E_+ , the cross-section for creation becomes

$$\Phi(E_0) dE_0 = \frac{Z^2}{137} r_0^2 \frac{dE_0}{(\hbar\nu)^2} [(E_0^2 + E_+^2) (\phi_1(\gamma) - \frac{1}{2} \log Z) + \frac{2}{3} E_0 E_+ (\phi_2(\gamma) - \frac{1}{2} \log Z)], \quad (36)$$

$\phi_1(\gamma)$ and $\phi_2(\gamma)$ being the functions shown in fig. 1, and

$$\gamma = 100mc^2 \hbar \nu Z^{-1}/E_0 E_+.$$

For small energies the formula

$$\Phi(E_0) dE_0 = \frac{Z^2}{137} r_0^2 \frac{dE_0}{(\hbar \nu)^2} (E_0^2 + E_+^2 + \frac{2}{3} E_0 E_+) \left(\log \frac{2E_0 E_+}{\hbar \nu mc^2} - \frac{1}{2} - c(\gamma) \right), \quad (37)$$

is more convenient, $c(\gamma)$ being given in Table I (35A).

§ 4. Radiation Probability as Function of Impact Parameter

It is possible to get a rough idea about the probability that an electron passing at a given distance r from the nucleus emits radiation during its passage. For the main contribution to the matrix element $V(q) = \int V \exp i(\mathbf{q}\mathbf{r})/\hbar c \cdot d\tau$ arises from the region $r \sim \hbar c/q$, since the contribution of larger r 's nearly vanishes because of interference, while small r 's do not contribute appreciably, because of the smallness of the corresponding volume. Therefore, the radiation emitted in the region between r and $r + dr$ will be equal to the probability of a radiation process in which a momentum between $q = \hbar c/r$ and $q + dq$ is transferred to the atom. This probability $\Phi(q) dq$ has been calculated in the paper (C) referred to above (§ 7), viz.,

$$\Phi(q) dq \sim (1 - \mathcal{N}(q))^2 dq/q \quad \text{if } q \ll \mu, \quad (38)$$

$$\Phi(q) dq \sim (\log(q/\mu) + \text{const}) \cdot dq/q^2 \quad \text{if } q \gg \mu. \quad (39)$$

(cf. C. (67), (66)) since the number of incident electrons having a minimum distance from the nucleus (impact parameter) between r and $r + dr$ is proportional to $r dr$, we get for the probability that an electron passing at a distance r radiates

$$\Phi(r) = \Phi(q) \frac{dq}{r dr} \sim \Phi(q) r^{-2}. \quad (40)$$

If r is smaller than the Compton wave-length \hbar/mc , q will be larger than mc . For this case we take from (39)

$$\Phi(r) = \text{const.} \log \hbar/mc r \quad (\text{for } r \ll \hbar/mc). \quad (39A)$$

That means that for small r the radiation emitted at distances between r and $r + dr$ is nearly independent of r . On the other hand, for r larger than \hbar/mc ,

q will be small compared with μ . If q is still large compared with α , then, according to (27), $\mathcal{R}(q)$ may be neglected in (38). Thus,

$$\Phi(r) \propto 1/r^2 \quad (\text{if } \hbar/mc \ll r \ll a_0 Z^{-1} \quad \text{and} \quad r \ll \hbar/mc \cdot E_0 E / \hbar \nu mc^2). \quad (38A)$$

The second condition follows from (29). If r increases, (38A) will cease to hold. The point at which this occurs depends on whether the energy E_0 is larger or smaller than $137mc^2 Z^{-1}$. In the first case, this limit r_{\max} is given by the atomic radius. Then, for distances larger than $r_{\max} = a_0 Z^{-1}$ screening becomes appreciable and causes $\Phi(q)$ to decrease like q^2 , (cf. C (69) which means

$$\Phi(r) \sim 1/r^6 \quad (\text{for } r \gg a_0 Z^{-1}). \quad (41)$$

If, on the other hand, the energy is small compared with $137mc^2 Z^{-1}$, formula (38A) ceases to be valid already at the point $r_{\max} = \hbar/mc \cdot E_0 E / \hbar \nu mc^2$ (corresponding to q of the order δ).

The main contribution to the total cross-section is given by the region (38A) because the region of smaller r 's (39A) has only a small volume, and for large r 's the radiation probability falls off very rapidly. Therefore the total cross-section will be proportional to

$$\int_{\hbar/mc}^{r_{\max}} \Phi(r) r dr = \log \frac{r_{\max}}{\hbar/mc} = \begin{cases} \log \frac{a_0 Z^{-1}}{\hbar/mc} & \text{for } E_0 > 137mc^2 Z^{-1} \\ \log \frac{E_0 E}{\hbar \nu mc^2} & \text{for } E_0 < 137mc^2 Z^{-1} \end{cases}, \quad (42)$$

which agrees roughly with the results (16), (34) of our exact calculations.

The absolute radiation probability for an electron passing the nucleus at a distance smaller than \hbar/mc is of the order† $Z^2/137^3$, which is very small, even for the heaviest atoms. This behaviour is very different from the result of classical electrodynamics, according to which the total energy radiated should increase as r^{-3} (cf. paper I § 6) if the electron passes near the nucleus, and should become equal to the primary energy of the electron for $r = r_0 Z^{\frac{1}{2}} \left(\frac{E_0}{mc^2} \right)^{\frac{1}{2}}$.

It would seem from this comparison that the quantum mechanical treatment yields a much smaller radiation probability; but nevertheless even this seems to be too large compared with the experiments (cf. § 7‡).

† These electrons form a beam of diameter $2\hbar/mc$. To obtain the radiation probability for a single electron, we have to divide the radiative cross-section for these electrons which is certainly smaller than the total cross-section, i.e., $\propto r_0^2 Z^2/137$, by the area $\pi(\hbar/mc)^2 = \pi \cdot (137 r_0)^2$.

‡ Similar results to those mentioned in this section have been derived by a semi-classical consideration by Weizsäcker, to whom we are indebted for the communication of his results.

II. DISCUSSION

§ 5. *The Radiation Emitted by Fast Electrons*

1. *Intensity Distribution.*—In § 1 and 3, we have calculated the probability that an electron of energy E_0 emits a light quantum of frequency between ν and $\nu + d\nu$ (equations (15) and (31)). This probability is roughly proportional to $1/\nu$ and consequently becomes very large for the emission of quanta of low

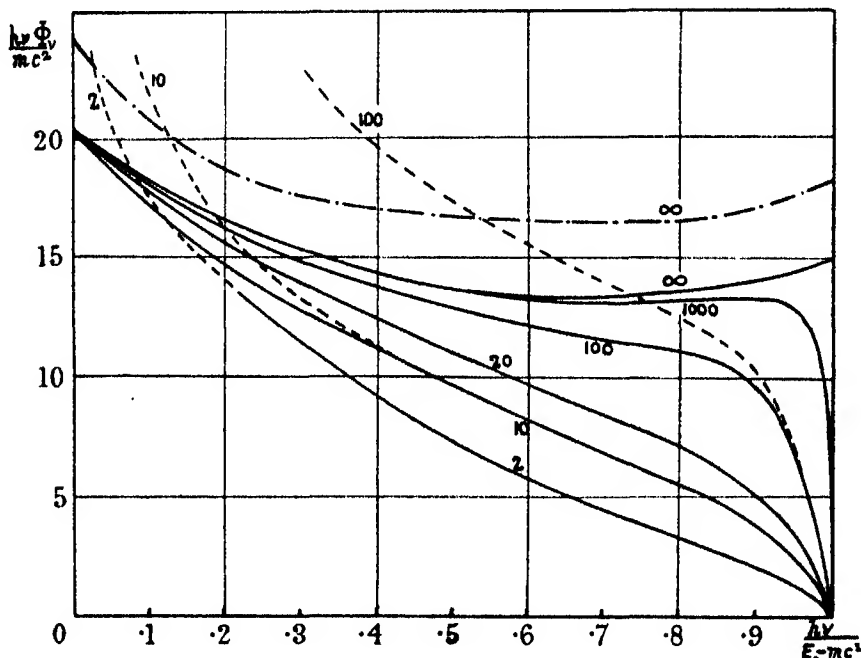


FIG. 2.—Intensity distribution $h\nu\Phi_\nu$ of the emitted radiation for Pb (—), H_2O (---), and with screening neglected (-.-). Φ_ν is the cross-section in units $Z^2r_0^2/137$. The numbers affixed to the curves refer to the primary energy E_0 in units mc^2 .

energy. We have, therefore, plotted in fig. 2 the *intensity* of the emitted radiation, *i.e.*, frequency times the probability of emission, rather than the probability itself as function of the frequency. Fig. 2 shows the intensity distribution for Pb, H_2O and for the case where the screening is neglected.†

† The general behaviour of the intensity frequency curves is similar to that which follows for the radiation of slow electrons ($v \ll c$) from the *exact* but non-relativistic Sommerfeld theory ('Ann. Physik,' vol. 11, p. 302 (1931), fig. 7). The two theories differ, however, for very small and very high frequencies: for $\nu = 0$ the intensity becomes logarithmically infinite in Sommerfeld's theory, finite in ours. This is due to the neglect of screening in Sommerfeld's calculation; in our theory the same infinity appears if we

The cross-section Φ , is expressed in units $Z^2 r_0^2/137$ in order to make its values for different atoms comparable.

The intensity decreases with increasing frequency, and falls to zero at the short wave-length limit $(E_0 - mc^2)/h$.

The intensity of the soft radiation, even in units Z^2 , is dependent on the atomic number Z (increasing for small Z), but independent of the energy E_0 of the incident electron.

The intensity of the harder radiation ($\nu \propto \nu_0$) increases slowly with increasing energy (if ν/ν_0 is kept constant) and reaches a certain asymptotic value for high E_0 , which depends on the atomic number Z .

2. The number of emitted quanta in a given frequency interval ν to $\nu + d\nu$ is

$$n(\nu) = d\nu \int_{h\nu}^{E_i} \frac{N \Phi(\nu, E_0) dE_0}{-dE_0/dx}, \quad (43)$$

where E_i is the initial energy of the emitting electron, $-dE_0/dx$ is its energy loss per centimetre path, $\Phi(\nu, E_0)$ the cross-section for the emission of a quantum of frequency ν by an electron of energy E_0 as given by formulæ (15), (31), and N the number of atoms per unit volume. To a rough approximation, $h\nu \Phi(\nu, E_0) = K$ may be considered as independent of ν and E_0 , fig. 2. The energy loss of the electron is for large energies E_0 mainly due to radiation, as is proved in § 6, if this is so, $-dE_0/dx = KE_0$. This formula holds down to a critical energy $E_c = 1600mc^2/Z$ (equation (52)), below which the energy loss due to collisions becomes important. This latter is, then, much greater than $E_0 K$ so that the contribution of $E < E_c$ to (43) may be neglected. Therefore, roughly, we have

$$\left. \begin{aligned} n(\nu) &= \frac{d\nu}{\nu} \log \frac{E_i}{E_c} & \text{for } h\nu < E_c < E_i \\ n(\nu) &= \frac{d\nu}{\nu} \log \frac{E_i}{h\nu} & \text{for } E_c < h\nu < E_i \end{aligned} \right\}. \quad (44)$$

use the non-screened formula (15) as we see from the dotted curves in fig. 2. On the other hand, at the short wave-length limit our theory is, presumably, not correct. For, we have made use of Born's first approximation which goes wrong if the energy of the electron after the radiation is small (cf. § 1). The exact wave-functions are, in this case, much larger near the nucleus than Born's wave-functions of first approximation. Consequently, the transition probability becomes also much larger, and the intensity of the radiation at any rate does not drop so much as shown in fig. 2. It seems plausible that actually it would tend to a finite limit for $\nu \rightarrow \nu_0$, as it does in Sommerfeld's exact theory.

If an electron of initial energy $E_i = 137mc^2$ (limit of validity of our theory, cf. § 7) is stopped in lead ($E_c = 20mc^2$) there will in the average be emitted:—

quanta of energy	>50	20-50	10-20	5-10	2-5	1-2 mc^2
number	0.5	1.5	1.5	1.5	2	1.5

altogether 8.5 quanta of energy greater than mc^2 .

This table has been calculated from the crude formula (44), since we wanted only to show the order of magnitude; actually there are fewer large quanta and rather more small quanta, owing to the intensity distribution in the spectrum (fig. 2).

3. *Angular Distribution of Emitted Radiation.*—The radiation of fast electrons ($E_0 \gg mc^2$) is emitted mainly in the forward direction. The average angle between the directions of motion of the electron and the emitted light is of the order $\Theta = mc^2/E_0$ (cf. paper C, § 8).

§ 6. Energy Loss of Fast Electrons by Radiation.

1. *Calculation of Energy Loss.*—The average energy radiated by an electron of energy E_0 per centimetre of its path is

$$-\left(\frac{dE_0}{dx}\right)_{\text{rad}} = N \int_0^{\infty} h\nu \Phi_\nu d\nu, \quad (45)$$

N being the number of atoms per cm^3 and Φ_ν the cross-section given by equations (15), (31). The integration over ν can, in general, only be carried out numerically. There are, however, two cases in which analytical integration is possible: (1) if E_0 is so small that screening has no effect at all

$$E_0 \ll 137mc^2Z^{-\frac{1}{2}},$$

and yet E_0 is large compared with mc^2 ; (2) if the energy E_0 is so high that the asymptotic formula (34) is valid for all values of ν (complete screening $E_0 \gg 137mc^2Z^{-\frac{1}{2}}$). In the first case, formula (16) may be used for Φ_ν . The integration yields

$$-\left(\frac{dE_0}{dx}\right)_{\text{rad}} = N \frac{Z^2}{137} r_0^2 E_0 \left(4 \log \frac{2E_0}{mc^2} - \frac{4}{3} \right) \quad (\text{for } mc^2 \ll E_0 \ll 137mc^2Z^{-\frac{1}{2}}). \quad (46)$$

This formula has already been published in a preliminary note by Heitler and Sauter.† It differs from the estimation (1) given in I by the logarithmic term, which varies only very slowly with the primary energy E_0 .

† 'Nature,' vol. 132, p. 892 (1933).

For very high energies (case 2) the integration gives

$$-\left(\frac{dE_0}{dx}\right)_{\text{rad}} = N \frac{Z^2 r_0^2}{137} E_0 \left(4 \log 183Z^{-1} + \frac{2}{9}\right) \quad (\text{for } E_0 \gg 137mc^2Z^{-1}), \quad (47)$$

which means a cross-section independent of E_0 .

The result of the numerical integration in the intermediate range and for small energies is shown in fig. 3. For convenience of representation, we have plotted the "integrated cross-section Φ_{rad} in units $Z^2 r_0^2/137$," defined by

$$-(dE_0/dx)_{\text{rad}} = NE_0 Z^2 r_0^2/137 \cdot \Phi_{\text{rad}}, \quad (48)$$

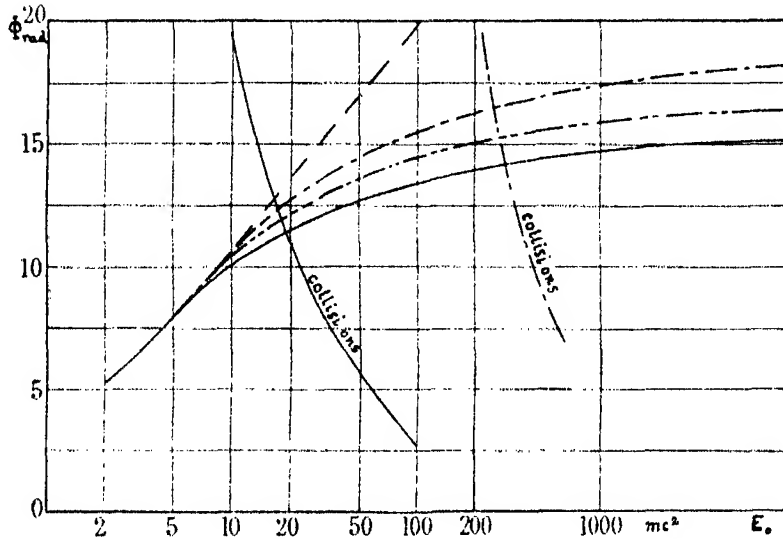


FIG. 3.—Cross-section Φ_{rad} for the energy loss by radiation (defined in equ. 48) as a function of the primary energy for Pb (—), Cu (---), H_2O (- - -) and with screening neglected (· · ·). For comparison the cross-section for the energy loss by collisions for Pb and H_2O are shown on the same scale.

against $\log_{11} E_0$ for three values of Z . Φ_{rad} increases but slowly with increasing energy and decreasing atomic number. For comparison, we have plotted the cross-section for energy-loss by collisions in the same units $Z^2 r_0^2/137$.

Φ_{rad} being a slowly varying function, the radiative energy loss is approximately proportional to the initial energy of the electron E_0 , whereas the energy loss by collisions is approximately constant. Further, the energy loss by radiation is proportional to Z^2 , whereas the energy loss by collisions is proportional to Z . No universal mass absorption-coefficient exists, therefore, for the radiative energy loss.

Table II.—Energy Loss of Fast Electrons by Radiation and Collisions
in millions of volts per centimetre path.

Substance.	Energy loss.	Energy of electron in million volts.						
		5	10	20	50	100	300	1000
H ₂ O	Radiation	0.07	0.16	0.36	0.99	2.07	6.6	22.5
	Collisions	1.98	2.15	2.32	2.55	2.72	2.99	3.29
Cu	Radiation	2.1	4.9	10.9	28.9	61	191	660
	Collisions	12.7	14.0	15.2	0.7	18.2	20.3	22.5
Pb	Radiation	6.4	14.4	31.4	85	177	550	1900
	Collisions	12.5	13.9	15.3	17.3	18.6	20.9	23.4

Table II gives the absolute value of the energy loss for various substances.

The energy loss by radiation is seen to be much greater, for high energies E_0 , than the ordinary energy loss by inelastic collisions. The latter has been calculated from the usual formula for electrons with relativistic energy $> mc^2$, namely,

$$-\left(\frac{dE_0}{dx}\right)_{\text{coll}} = 2\pi r_0^2 mc^2 Z N \log \frac{E_0^3}{2mc^2 I^2}. \quad (49)$$

Following the theory of Bloch (*loc. cit.*), the average ionization potential I was assumed to be proportional to the atomic number Z , explicitly

$$I = 13.5 \cdot Z \text{ volts}, \quad (50)$$

the proportionality factor 13.5 being redetermined for this purpose from the observed energy loss of fast α -particles in gold.[†]

The ratio of radiation and collision energy loss is roughly

$$\frac{-(dE_0/dx)_{\text{coll}}}{-(dE_0/dx)_{\text{rad}}} = \frac{E_0 Z}{1600 mc^2}. \quad (51)$$

This simple formula is due to the fact that the logarithm in (49) varies with E_0 and Z in approximately the same way as that in (48). Radiation and collision become of equal importance at the "critical" energy

$$E_c = 1600 mc^2 / Z, \quad (52)$$

i.e., about $20 mc^2 = 10$ million volts for lead, $55 mc^2$ for copper, $200 mc^2$ for air.

[†] No account was taken of the excitation of nuclear electrons, since it seems highly improbable that the probability of this excitation (if it occurs at all) can be calculated by the simple wave-mechanical formula (49), considering that the electrons presumably do not exist at all in the nucleus. We think that the excitation of nuclear electrons rarely takes place.

2. The range of the electron is determined by the quantity

$$-\left(\frac{dE_0}{dx}\right)_{\text{rad}} - \left(\frac{dE_0}{dx}\right)_{\text{coll}}.$$

For a rough estimate we may consider Φ_{rad} in (48) as a constant and insert for it an average value Φ_0 , say. Then, according to (48), (51), (52), the whole energy loss is given by

$$-\frac{dE_0}{dx} = N \frac{Z^2}{137} r_0^2 \Phi_0 (E_0 + E_c), \quad (53)$$

the first term (E_0) representing the radiation (E_0 being the energy after x cm. path), the second (E_c) the collisions (E_c being constant). Integrating (53) we get for the range the rough formula

$$R = \frac{137}{NZ^2 r_0^2 \Phi_0} \log \frac{E_0 + E_c}{E_c} = \frac{137}{NZ^2 r_0^2 \Phi_0} \log \left(1 + \frac{ZE_0}{1600mc^2}\right). \quad (54)$$

The range of high energy electrons increases, according to (54), only with the logarithm of the energy and remains, therefore, very small even for the fastest electrons. Table III gives the result of an exact numerical calculation of the range in Pb, Cu, H_2O ; for Pb the range calculated by the rough formula (54) is added to show the accuracy of this formula.

Table III.—Average Range of Fast Electrons in cm.

Stopping material.	Energy in million volts.							
	5	10	20	50	100	300	1000	10000
H_2O	2.5	4.8	8.8	18.4	30.4	58	100	195
Cu	0.37	0.67	1.12	1.96	2.78	4.25	6.0	9.4
Pb	0.33	0.54	0.81	1.23	1.68	2.25	2.88	4.08
Pb (calculated by (54))	0.25	0.43	0.68	1.12	1.50	2.14	2.87	4.30

3. *Straggling*.—The effect of radiation is to diminish the energy of an electron suddenly by rather a large fraction of its initial value. Therefore, the actual energy loss may differ very considerably from the average loss. To obtain a rough idea of the effect of this straggling, we assume for the probability of emission of a light quantum $h\nu$ a rough but convenient formula :

$$\Phi(\nu) d\nu = a \frac{d\nu}{E_0 \log E_0/E}, \quad (55)$$

where a is a constant.

(55) may be seen to represent the intensity curves $h\nu \Phi$, of fig. 2 fairly well. If we introduce instead of ν

$$y = \log [E_0/(E_0 - h\nu)] \quad (56)$$

(which is convenient since on the average the log of the electronic energy decreases linearly with the distance), the probability that the electron loses the energy $h\nu$ in travelling an *infinitely short distance* dl is

$$w(y) dy = \Phi(\nu) d\nu dl = a \frac{e^{-\nu} dy}{y} dl. \quad (57)$$

We wish to know the probability for a decrease of the energy of the electron to $e^{-\nu}$ times its initial value after traversing matter of a *finite thickness* l . For this probability we can prove the following formula to be correct:

$$w(y) dy = \frac{e^{-\nu} y^{al-1}}{\Gamma(al)} dy \quad (58)$$

(58) becomes identical with (57) for very small l . For, in this case

$$\Gamma(al) = 1/al \quad \text{and} \quad y^{al} = 1$$

(except for the smallest values of y , i.e., for the smallest values of ν).

To prove that (58) holds for finite l , we let the electron travel first a distance l_1 then a distance l_2 . The log of the energy decreases first by y_1 , then by y_2 altogether by $y = y_1 + y_2$. If (58) is assumed to be correct for the two parts of the path, the probability of the decrease y becomes:

$$w(y) dy = dy \int_0^y w_1(y_1) w_2(y-y_1) dy_1 = dy \frac{e^{-\nu}}{\Gamma(al_1) \Gamma(al_2)} \int_0^y y_1^{al_1-1} (y-y_1)^{al_2-1} dy_1. \quad (59)$$

The integral is evidently proportional to $y^{a(l_1+l_2)-1}$. The numerical factor follows from the fact that $\int_0^\infty w(y) dy = 1$. Therefore, if (58) is valid for the energy losses in the paths l_1 and l_2 , it is also valid for the energy loss in the total path $l = l_1 + l_2$ and is thus proved to hold for any length of the path.

The curves in fig. 4 give the probability that an electron which loses energy only through radiation has, after travelling a certain distance l , still an energy left which is greater than e^{-1}, e^{-2}, \dots , times its initial energy. The abscissa is al . Now the *average energy loss* \bar{y} is exactly equal to al , if the law (57) is accepted. (This can easily be seen by calculating $\int y w(y) dy$ from (58).)

For instance, in the *average* the energy is diminished to e^{-1} times its initial value after travelling a distance $al = 1$, but, as can be seen from fig. 4, even after so great a distance as $la = 2.8$ there still remains a probability of 10% that the energy is higher than $e^{-1} \cdot E_0$. Thus the straggling may increase the

range of some electrons to twice or even three times its average value ; on the other hand, some electrons are stopped much earlier.

The straggling is characteristic of the energy loss by radiation. By this effect, the latter differs from the energy loss by collisions. The unambiguity of this distinction may be seen from Table IV, in which the distribution of energy losses is given for an electron of 50 million volts primary energy traversing $\frac{1}{2}$ mm. of lead, assuming (a) that only collisions take place, (b) only radiation, (c) both. The last two lines give the distribution after traversing 1 mm. lead for initial energies of 50 and 10 million volts.

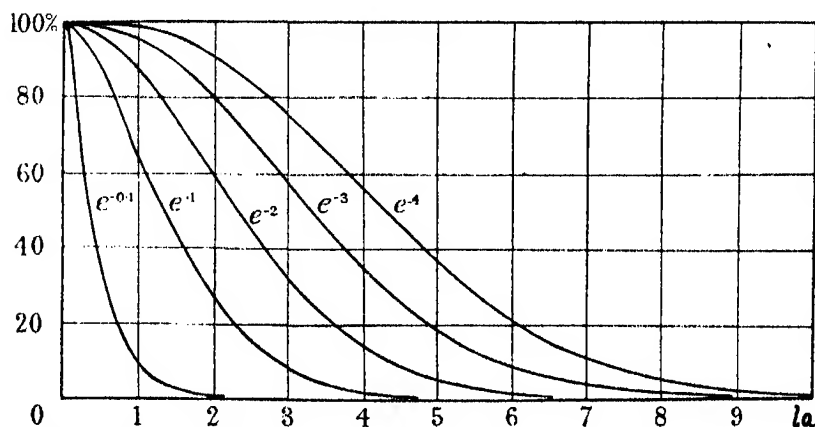


FIG. 4.—Straggling. Probability that an electron after having travelled l cm. has still an energy greater than e^{-1} , e^{-2} , ..., times its initial energy. The scale of the abscissa is chosen so that in the average the energy decreases to e^{-la} .

Table IV.—Probability of different Energy Losses for Electrons passing through Lead (%).

Initial energy.	Thickness of Pb.	Energy lost by	Energy loss in million volts.									
			<0.1	0.1-0.5	0.5-0.7	0.7-1	1-2	2-3	3-5	5-10	10-20	20-50
50	$\frac{1}{2}$ mm.	Collision	0	0	58	32	7.5	1	0.7	0.4	0.2	0.2
50	$\frac{1}{2}$ mm.	Radiation	49	12.4	2.7	2.8	5.9	3.6	4.5	6.2	5.9	6.7
50	$\frac{1}{2}$ mm.	Both	0	0	29	25	14	5.0	7.3	7.0	6.1	6.6
50	1 mm.	Both	0	0	0	0	35	12	11	14	12	16
10	1 mm.	Both	0	0	0	0	57	16	13	14	—	—

§ 7. Comparison with Experiment. Limits of the Quantum Theory.

1. The theoretical energy loss by radiation for high initial energy is far too large to be in any way reconcilable with the experiments of Anderson.† He has measured the energy loss of electrons of initial energy $300 \cdot 10^6$ volts and found

† Anderson, 'Phys. Rev.,' vol. 44, p. 406 (1933).

it to be about $35 \cdot 10^6$ volts per cm. of lead as against $550 \cdot 10^6$ volts given in our theoretical table. The disagreement is definite, although there are several reasons why a more exact theory may give a lower value for the energy loss.

(1) The figures given in Table II apply to electrons having really the energy E_0 . Actually, when the electron has travelled a certain distance, say, 1 mm., it has lost some energy, and therefore the energy loss in the second millimetre will be less than in the first. Thus, the actual range of the electrons will not be $300/550 = 0.55$ cm., but about 2 cm. (cf. Table III). Even so, the electron should lose in 1 cm. of lead about 250 million volts, i.e., nearly all its energy.

(2) It is not quite correct to base the arguments on the average loss of energy, because in each radiation process rather a large fraction of the energy is lost. Therefore, the actual energy loss may for some electrons be considerably smaller than the average (straggling, § 6, section 3). But, since Anderson has measured rather a large number of electron tracks, it seems inconceivable that all his electrons should have lost particularly small amounts of energy.

(3) Our calculations are based on Born's method which may be wrong for such heavy atoms as lead (§ 1). The error, however, should not be appreciable, since the creation of positive electrons seems to be in good accord with our calculation for energies $2-10 mc^2$ (§ 8); in particular the creation probability is found experimentally to be very nearly proportional to Z^2 as required by Born's approximation. Since the calculations for creation of pairs and for emission of radiation are absolutely analogous, it is impossible that Born's approximation can be far wrong for the radiation case. Therefore, even allowing for the three corrections, it seems impossible that the theoretical energy loss can be smaller than about 150 million volts per centimetre lead for Anderson's electrons. The theory gives, therefore, quite definitely a wrong result.†

This can perhaps be understood for electrons of so high an energy. The de Broglie wave-length of an electron having an energy greater than $137 mc^2$ is smaller than the classical radius of the electron, $r_0 = c^2/mc^2$. One should not expect that ordinary quantum mechanics which treats the electron as a point-charge could hold under these conditions. It is very interesting that the energy loss of fast electrons really proves this view and thus provides the *first instance*

† We do not think that the fact that the cosmic radiation reaches the bottom of Lake Constance is equally conclusive. For the highly penetrating radiation may consist of heavy particles; for instance, protons. For these the radiation probability would be almost zero, being inversely proportional to the square of the mass.

in which quantum mechanics apparently break down for a phenomenon outside the nucleus. We believe that the radiation of fast electrons will be one of the most direct tests for any quantum-electrodynamics to be constructed.†

2. It appears, therefore, to be of great importance indeed to test the radiation formulæ for energies for which they should be valid, i.e., $E_0 < 137 mc^2$. Even here there is a region where the *energy loss by radiation is much bigger than the energy loss by collisions*. For lead, this region lies between 10 and 50×10^6 volts. The only electrons at present available in the required energy range seem to be those in the showers of cosmic radiation. Unfortunately they always occur associated with so many other electrons that it should be rather difficult to test directly the emission of radiation by such electrons.

Therefore, the only means of detecting the radiation is the straggling of the energy loss of the shower electrons. To decide unambiguously whether this energy loss is due to ordinary inelastic collisions or to radiation, it would be best to investigate the loss in rather thin metal plates, say, 1 mm. thick. Then most of the electrons will undergo only collisions and will, thus, lose about 1.5 or 2 million volts while a few will lose a considerable fraction of their initial energy (cf. § 6, Table III).

Another test for the energy loss by radiation would be its dependence on the nuclear charge Z^2 . The energy loss per gm./cm.² in Pb would, for electrons of an energy between 10 and 50 million volts, be much bigger than in Al, whereas it would be almost the same if the energy loss were due to collisions only.

The theory could, perhaps, also be proved in the region of fast β -particles for which the radiation probability is already very large. If one chooses a suitable substance which emits no γ -rays, the radiation emitted by the β -particles could be measured directly. Or one could investigate the Wilson tracks in a heavy gas such as xenon or a compound containing lead and detect directly the points where energy is lost without production of a branch track. In xenon the probability that the electron loses more than 1/10 of its energy in a radiation process is about 1 : 1000 per centimetre (electron energy $2-10 mc^2$).

† A very interesting attempt has recently been made by Born to change the classical field equations so as to take the electron radius into account. He found that, for wavelengths $\lambda < r_0$, one has to replace the electronic charge e by an "effective charge" which decreases rapidly with decreasing λ/r_0 . This would, of course, immediately decrease the radiative energy loss. Cf, 'Nature,' vol. 132, pp. 282, 970, 1004 (1933); vol. 133, p. 63 (1934); and 'Proc. Roy. Soc.,' A, vol. 143, p. 410 (1934). An exact comparison with experiments is not yet possible, since up to the present the quantum translation of Born's theory has not been developed sufficiently.

Finally, the stopping in a thin solid plate would give a more conclusive result than for shower-electrons, because many more particles are available. But the experiments with β -particles would, of course, not make experiments on shower-electrons unnecessary, because one wants to see at what energy the quantum theory *begins* to give wrong results.

3. The lowest cosmic ray electron for which the energy loss has been measured was one of 113 million volts. This is still outside the region where quantum mechanics is expected to apply, but not very much above the limit of $137 mc^2$. Anderson found the energy loss in a lead plate of 13.5 mm. thickness to be about $27 \cdot 10^6$ volts, i.e., $20 \cdot 10^6$ volts per centimetre. This is only slightly more than would be expected for collisions only. If other tracks of this energy should give similar results, one would, therefore, conclude that already for this energy the quantum theory gives far too high a radiation probability. But it may be that this particular electron has, by chance, not emitted any large quantum. The question of the validity of our formulæ for the radiation of electrons with energy smaller than $137 mc^2$ can thus only be decided when further experiments are available.

On the other hand, the measured energy loss of $35 \cdot 10^6$ volts for the 300 million volt electron seems to indicate that not only inelastic collisions are effective in the stopping of fast electrons.† We should like to attribute the difference to emission of radiation.

§ 8. Creation of Positive Electrons.

1. *Energy Distribution.*—The probability that a γ -ray-quantum of energy $h\nu$ creates a positive electron with energy between E_+ and $E_+ + dE_0$ and a negative one with energy between E_0 and $E_0 + dE_0$, is given by—

Formula (21), if $h\nu$ is of the order mc^2 ;

Formula (22), if $h\nu \gg mc^2$, but $h\nu \ll 137 mc^2/Z^{\frac{1}{3}}$;

Formula (36), if $E_0 E_+ / h\nu mc^2$ is of the order $137 mc^2 / 2Z^{\frac{1}{3}}$ or larger.

The results of these formulæ are shown in figs. 5 (a) and 5 (b). The quantity actually plotted is the cross-section Φ_{E_+} in units $r_0^2 Z^2 / 137$.

The abscissæ denote $(E_+ - mc^2) / (h\nu - 2mc^2)$, i.e., the kinetic energy of the positive electron as a fraction of the sum of the kinetic energies of both electrons.

† It should be expected that the exact quantum electrodynamics would give rather a lower energy loss in collisions than the quantum theory which itself gives only $20 \cdot 10^6$.

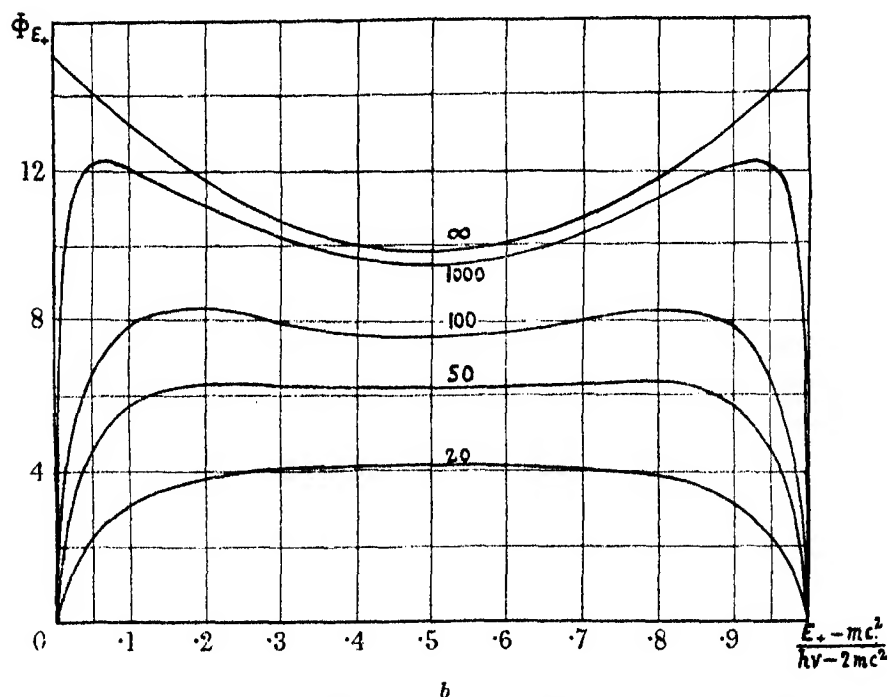
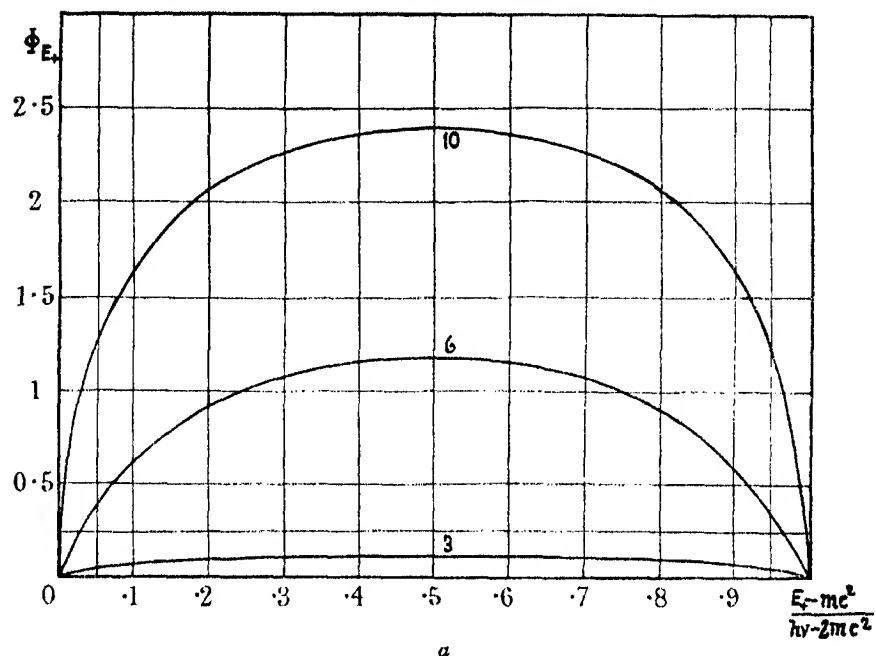


FIG. 5.—Energy distribution of pairs of positive and negative electrons. Φ_{E_+} is the cross-section (units $Z^2 r_0^3 / 137$) for the creation of a positive electron with kinetic energy $E_+ - mc^2$. The numbers affixed to the curves refer to the energy of the light quantum $h\nu$ in units mc^2 . Fig. 5a is valid for any element (screening neglected), fig. 5b refers to lead.

The curves for small values of $h\nu$ are valid for any element, those for $h\nu > 50mc^2$ are calculated for lead, for lighter elements Φ_{E+} would be a little larger because of the smaller effect of screening, but the general form of the curves would be the same.

For quanta of small energy the probability of creation has a broad maximum when both electrons obtain equal energy. The maximum becomes flatter with increasing energy. For higher energies the probability has a flat *minimum* for equal energy and a small maximum when one of the electrons obtains much more energy than the other. This change of the form of the curves can be seen directly from the formulæ (22) and (36).†

The energy distribution is apparently symmetrical in the energies of the two electrons. This is a consequence of the use of Born's approximation. In an *exact* calculation, the positive electron would be found to obtain more energy, on the average, than the negative, as has been pointed out by several authors. This is due to the repulsion of the positive electron and the attraction of the negative by the nucleus. If the electrons are generated at a distance r from the nucleus, the energy difference of the two electrons will be $2Ze^2/r$.

Now according to § 4 the main contribution to the cross-section arises from a region between \hbar/mc and $(\hbar/mc)(h\nu/2mc^2)$ provided that $h\nu \ll 137 mc^2 Z^{-1}$. We, therefore, estimate that the positive electron will obtain about $2mc^2 Z/137$ more energy than the negative for small $h\nu$; for higher $h\nu$ the difference will be smaller.

2. Angular Distribution.—The average angle between the direction of motion of a created electron of energy E_0 and the creating quantum is of the order $\theta \propto mc^2/E_0$. For large energies, therefore, the electrons are emitted mainly in the forward direction. Explicitly, the number of electrons emitted at an angle θ_0 is approximately proportional to

$$\Phi(\theta_0) d\theta_0 = \frac{\theta_0 d\theta_0}{(\Theta^2 + \theta_0^2)} \quad , \quad \Theta = \frac{mc^2}{E_0} . \quad (60)$$

(cf. paper C, (74)). For energies of the order mc^2 , the angular distribution is more complicated and the preponderance of the forward direction less marked.

3. Total Cross-section. Comparison with Experiments.—The total cross-section is found by integrating the cross-sections (21), (22), (36) over all possible

† For high energies $h\nu$ the minimum $E_0 = E_+$ is less marked than in the theory of Oppenheimer and Plesset, who obtain Φ_{E+} proportional to $E_0^3 + E_+^3$ which apparently is due to an error in their calculation.

energies E_0 of the negative electron. Analytical integration is possible in two cases.

(1) If $mc^2 \ll h\nu \ll 137 mc^2 Z^{-1}$, then formula (22) (no screening) has to be integrated, giving

$$\Phi_{\text{pair}} = r_0^2 \frac{Z^2}{137} \left(\frac{28}{9} \log \frac{2h\nu}{mc^2} - \frac{218}{27} \right), \quad (\text{no screening } h\nu \gg mc^2), \quad (61)$$

a result which has been published in the preliminary note by Heitler and Sauter (*loc. cit.*).

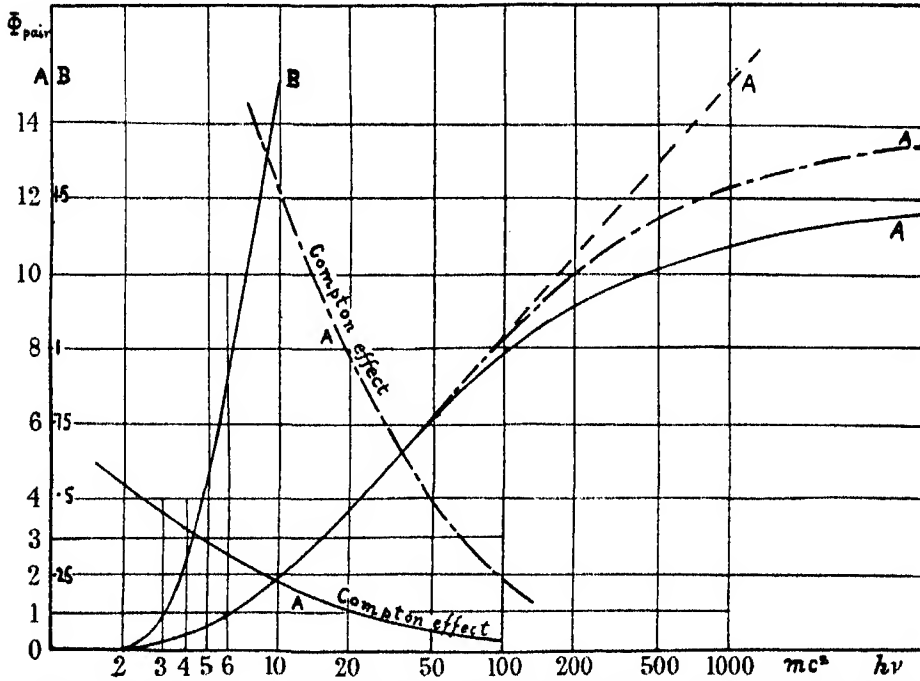


FIG. 6.—Integrated cross-section for the creation of pairs (units $Z^2 r_0^2/137$) as a function of $h\nu$ for lead (—), H_2O (---), and without screening (— · —). The beginning of the curve is also given with 8-fold enlargement (curve B). For comparison the cross-section for the Compton effect is given on the same scale.

(2) If $h\nu \gg 137 mc^2 Z^{-1}$ (complete screening) we find

$$\Phi_{\text{pair}} = r_0^2 \frac{Z^2}{137} \left(\frac{28}{9} \log (183 Z^{-1}) - \frac{2}{27} \right) \quad (\text{complete screening}) \quad (62)$$

For all other values of $h\nu$ the integration must be carried out numerically. The result is shown in fig. 6, which gives the total cross-section for the creation of pairs in lead and aluminium (units $Z^2 r_0^2/137$). For comparison we have plotted the cross-sections for the production of Compton-electrons.

The cross-section is proportional to the square of the atomic number. It also increases rapidly with increasing energy of the quantum $h\nu$ (for small $h\nu$). For very high energies $h\nu$ an asymptotic value is reached which is determined by the ratio of the radius of the atom to \hbar/mc . (In the space between \hbar/mc and the atomic radius the probability for the production of pairs is appreciable.)†

The calculated cross-section is in *good agreement with experiment* as regards both the absolute number of pairs produced and the dependence on energy and atomic number. The direct experiments of Curie and Joliot,‡ Blackett and Occhialini§ and others,|| give the ratio of the number of electron pairs produced by hard γ -rays to the number of Compton plus photo-electrons the Compton effect being calculable from the Klein-Nishina formula.¶ Table V compares the theoretical and experimental values of this ratio for lead and various quantum energies. For the theoretical values an average value of $h\nu$ has been assumed of 3, 5.2, and 11 mc^2 respectively for the three sources.

Table V.—Number of Electrons Pairs produced by γ -rays.

Energy Source	Pb.			Al.	Units. mc^2 .
	2-4.4 Ra mixture.	5.2 ThC''.	10-12 Po + Be.	10-12 Po + Be.	
I—Theoretical cross-section for production of pairs	0.12	0.6	2.0	2.0	} $Z^2 r_0^2 / 137$
II—Theoretical cross-section for production of Compton and photo-electrons.....	4.0	3.0	2.1	12	
III—Ratio of I to II (theoretical)	0.03	0.20	0.95	0.17	—
IV—Ratio (experimental)	(0.03)	0.22	(0.67)	(0.06)	—

The agreement is better than was to be expected. The values in brackets refer to measurements made in rather thick plates of lead,** whereas the value

† Cf. § 4. This fact is in contrast to Oppenheimer and Plesset, who maintain that all pairs are produced at distances \hbar/mc .

‡ 'C. R. Acad. Sci. Paris,' vol. 196, p. 1885 (1933), and p. 1581 (1934).

§ 'Nature,' vol. 132, p. 917 (1933).

|| Grinberg, *ibid.*, vol. 197, p. 318 (1933).

¶ The number of photo-electrons is for lead roughly 10% of the number of Compton electrons, and can be calculated from Sauter's theory.

** A fairly large number of positive and negative electrons is shown to be absorbed in the plate, since very often only one positron appears in the chamber without the accompanying negative electron.

for the $5.2 mc^2$ γ -radiation is reduced to infinitely thin plates.† In particular the increase of the cross-section with increasing energy is very well represented by the theory.

The dependence on the atomic number has been tested by a more indirect method by Heiting.‡ He measures the "excess-scattering" of γ -rays in various elements (beside the Compton-scattering). This effect is known to be due to the recombination of a positive electron (after being stopped by collisions) with a negative electron, the rest energy of both electrons being emitted in two light quanta of energy $h\nu = mc^2$ each. Since all positive electrons die after travelling a comparatively short path, the number of the emitted quanta is just twice the number of positive electrons produced. The intensity of this "scattered" radiation is found to be almost exactly proportional to Z^2 over the whole range of Z from aluminium to lead (the primary radiation had an energy which was $h\nu = 5.2 mc^2$). This agreement proves the validity of Born's approximation for our calculations. This is rather surprising, since Born's approximation means an expansion in a power series in $Ze^2/\hbar c$.

4. *Absorption Coefficient for Light of Short Wave-length.*—If the energy of the quantum becomes high, the probability for the creation of pairs becomes larger than that for the Compton effect (see fig. 6), since the latter decreases with increasing energy as $1/h\nu \cdot \log(2h\nu/mc^2)$. This fact is analogous to the energy loss of particles by radiation (cf. § 6). For lead, the creation of pairs is the more probable process already for $h\nu = 10 mc^2$, for aluminium about $h\nu = 35 mc^2$ is required to make the probability for the two processes equal.

The absorption of light of very short wave-length is, therefore, due to the creation of pairs rather than to the Compton effect. Since the *creation cross-section increases with increasing energy, the same is true for the absorption coefficient*, a behaviour which is rather unfamiliar. Table VI gives the absorption coefficient for hard γ -rays in Pb, Cu, and H_2O ; it rises, for instance, to more than 1 cm^{-1} in lead. It should, however, be considered that for $h\nu > 137 mc^2$ the quantum theory will go wrong, as it does for the radiation of fast electrons. It is to be expected that, as a consequence, the absorption coefficient for quanta of energy greater than $137 mc^2$ will decrease again.§

† We are indebted to Professor Blackett for his kind communication.

‡ 'Z. Physik,' vol. 87, p. 127 (1933).

§ [Note added in proof, May 25, 1934.—In a recently published paper v. Weizsäcker (Z. Physik, vol. 88, p. 612 (1934), cf. footnote‡ at the end §4) came to the conclusion that the theoretical results reached in this paper should be valid also for energies $> 137 mc^2$. If this result should be correct it would be hardly possible to reconcile it with the experiments mentioned in §7.]

112 *Stopping of Fast Particles and Creation of Electron Pairs*

Table VI.—Absorption Coefficient for Hard γ -rays in various Materials in cm^{-1} .

Material.	Absorption due to	Energy in million volts.					
		5	10	20	50	100	1000
Pb	Compton effect....	0.235	0.141	0.082	0.039	0.022	0.003
Pb	Pairs	0.24	0.46	0.68	0.96	1.15	1.43
Pb	Total	0.48	0.60	0.76	1.00	1.17	1.43
Cu	Total	0.292	0.276	0.31	0.36	0.40	0.50
H ₂ O	Total	0.032	0.022	0.017	0.015	0.015	0.017

Summary.

The probability for the emission of radiation by fast electrons passing through an atom is calculated by Born's method (§ 1), the calculations going beyond previous publications mainly by considering the screening of the atomic field (§ 3). The results are discussed in §§ 5 to 7. The total radiation probability (fig. 3) becomes very large for high energies of the electron, indeed the stopping of very fast electrons (energy $> 20 mc^2$ for Pb) is mainly due to radiation, not to inelastic collisions. The theory does not agree with Anderson's measurements of the stopping of electrons of 300 million volts energy, thus showing that the quantum theory is definitely wrong for electrons of such high energy (§ 7) (presumably for $E_0 > 137 mc^2$).

By the same formalism, the probability for the creation of a positive and a negative electron by a γ -ray is calculated (§§ 2, 3). The energy distribution of the electrons is shown in fig. 5, the total creation probability in fig. 6. For γ -rays of $h\nu$ between 3 and 10 mc^2 the theory is in very good agreement with the experiments.

The Influence of Pressure on the Spontaneous Ignition of Inflammable Gas-Air Mixtures III—Hexane- and Isobutane-Air Mixtures

By D. T. A. TOWNEND, D.Sc., L. L. COHEN, M.Sc., and M. R. MANDLEKAR, Ph.D., High Pressure Gas Research Laboratories of the Imperial College of Science and Technology, London

(Communicated by W. A. Bone, F.R.S.—Received March 1, 1934)

Introduction

In two recent communications* we described the results of investigations into the influence of varying initial pressure up to 15 atmospheres on the spontaneous ignition of butane- and pentane-air mixtures, showing that in each case the ignition points were located in two distinct and widely separated temperature ranges, location in the higher range occurring at low pressures and in the lower range at high pressures. Transference of an ignition point from the higher to the lower range occurred sharply, at a critical pressure, which depended upon the hydrocarbon concerned and the composition of its mixture with air. The bearing of these observations upon the problem of knock was also discussed.

A wide range of explosive media, comprising mainly the higher hydrocarbons contained in liquid fuels, is now being systematically studied, and the present paper summarizes the results obtained for hexane- and isobutane-air mixtures. So far, our results support the view (also recently endorsed by Neumann and Estrovitch†) that the lower group of ignition points is the outcome of the survival and further rapid oxidation of certain intermediate bodies, a process favoured by high pressure, whereas the higher group results from ignitions mainly of the products of their thermal decompositions which are favoured by low pressure.

We have refrained from attempting to examine in close detail the mechanism of the processes involved with any of the combustibles referred to because a true interpretation of our observations will be more easily reached by an extension of our investigation, which is now in progress, to the lower hydrocarbons the oxidations of which are less complex. With hexane-air mixtures,

* 'Proc. Roy. Soc.,' A, vol. 141, p. 484 (1933); vol. 143, p. 168 (1933).

† 'Nature,' vol. 133, p. 105 (1934).

however, as opportunity has arisen we have studied such factors as the influence of "surface" and of the replacement of nitrogen diluent by oxygen, etc.

A. Hexane-Air Mixture

Procedure—Our experimental procedure followed closely that previously employed. A new explosion vessel has been brought into use provided with four quartz windows arranged in a horizontal plane along one side, the heating furnace being so constructed as to provide visual access to the interior of the vessel. In all other details the vessel was identical with that previously employed and preliminary trials showed that ignition temperatures determined by means of it agreed closely with those previously reported.

The hexane used was a synthetic product (b.p. 68–69° C) supplied by the Eastman Kodak Company. The gas mixtures were made up and stored as before, both the storage cylinders and the capacity vessel* being now immersed in an oil bath thermostatically regulated at 80° C. At this temperature, which was adequate to maintain the hydrocarbon in the vapour phase at all storage pressures employed, mixing was complete in the course of a few hours and no change in composition on account of stratification was ever detected.

Results—In fig. 1 a series of curves has been plotted showing the observed variation of ignition points with composition for mixtures of hexane content between 1 and 8% at pressures of $\frac{3}{4}$, 1, $1\frac{1}{4}$, $1\frac{1}{2}$, $1\frac{3}{4}$, 2, 3, 5 and 10 atmospheres. The temperature range between the two groups of ignition points extends from 350° to above 495° C for mixtures containing less than about 5.1% of the combustible and from about 290° to approximately 520° C for richer mixtures. This range compares with 350° to 490° C for all pentane-air mixtures and 370° to 450° C for all butane-air mixtures. The sudden widening of the temperature range for mixtures rich in hexane (*see* fig. 1) is an observation to which we shall refer later.

Only at pressures below $\frac{3}{4}$ atmosphere did the ignition points for all hexane-air mixtures lie entirely in the higher range; one atmosphere sufficed to transfer to the lower range those for mixtures containing more than 5.2% of the combustible. This fact no doubt accounts for the conflicting and scanty data in the literature for ignition temperatures with this hydrocarbon at atmospheric pressure.

Similar determinations have been made with the mild steel liner in the explosion vessel replaced by one of glass, the general effect of this change being

* *See* Part I, p. 487.

to lower the ignition points some 20° , whether in the higher or lower ranges ; the pressure requisite to lower them, however, was always slightly greater than with the mild steel liner. The thin-lined curve incorporated in those shown in fig. 1 gives the ignition points determined with the glass liner in use

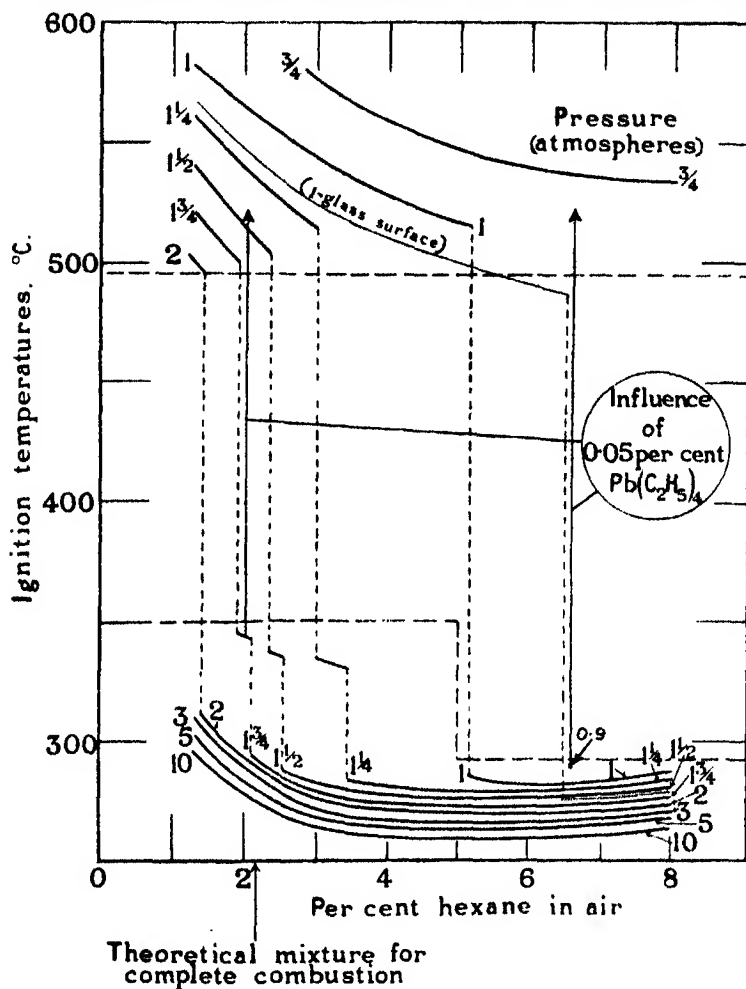


FIG. 1

at atmospheric pressure ; the curves for all other pressures may be taken as showing similar shifts from our normal curves.

As with butane- and pentane-air mixtures the effect of additions of 0.05% of lead tetraethyl to the mixtures (as indicated by the two arrows) was to raise the ignition points in a limited pressure range just above the critical transition pressures from the lower to the higher system.

The Ignition Regions at Pressures above the Critical Transition Pressures— With pentane-air mixtures (Part II), we discovered that at pressures just exceeding the critical transition pressures ignition occurred at first only within limited temperature ranges which widened and ultimately merged with increasing pressure. This phenomenon has been found to be a general feature of our observations and appears to become of increasing importance as the paraffins increase in complexity.

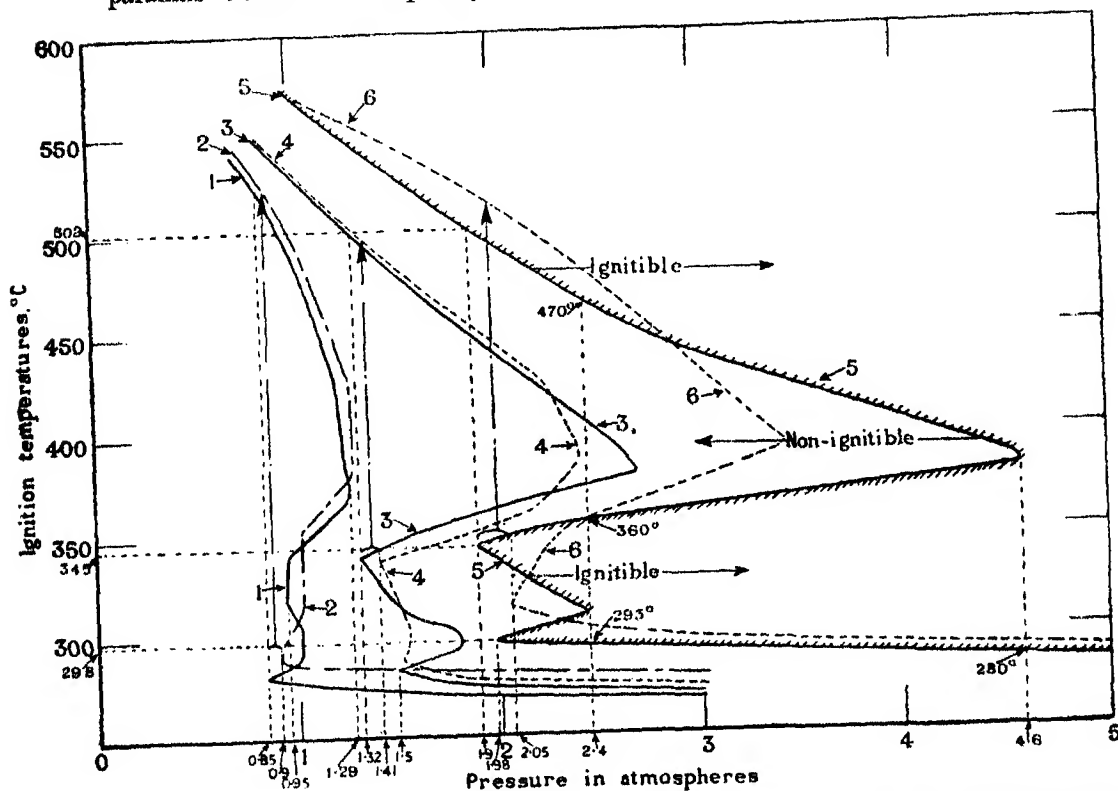


FIG. 2—Percentage mixtures for the curves:—1 = 6.5, 3 = 2.7, 5 = 1.8. The mixtures for curves 2, 4 and 6 were the same as those of 1, 3, 5, but with the addition of 0.05% $\text{Pb}(\text{C}_2\text{H}_5)_4$.

In fig. 2 detailed curves, Nos. 1, 3 and 5, have been drawn showing the influence of progressive increments of initial pressure on the ignition points of mixtures having hexane contents, 6.5, 2.7 and 1.8% respectively. The method employed in plotting these curves was to determine at intervals of every few degrees over the whole temperature range two pressures separated usually by not more than 0.05 to 0.1 atmosphere at the lower of which ignition did not occur and at the higher of which it did. Little difficulty was ever

experienced in repeating the curves closely and certain of the mixtures used for purposes of reference have been examined frequently. To facilitate a proper understanding of the curves No. 5 may best be described.

It should be understood that ignition occurred at any temperature and pressure found in the area to the right of the curve (shaded side). At pressures up to 1.9 atmospheres—the critical transition pressure—the ignition points were located in the top range and fell progressively with increase of pressure to 502° C. At this pressure ignition also became possible at 345° C but not at temperatures between 345° and 502° C. At 1.98 atmospheres ignition was possible at 298°, between 340° and 352°, and at all temperatures above 495° C. At about 2.4 atmospheres pressure the two lower ignition regions merged so that ignition was possible at temperatures between 293° and 360° and above 470°, but not between 360° and 470° C. At 4.6 atmospheres pressure ignition occurred at all temperatures above 280° C.

On comparing curve No. 5 with Nos. 1 and 3 it will be observed that the regions in which the mixtures are non-ignitable are far more extensive for mixtures containing an excess of air than for those containing an excess of combustible; thus with the 6.5% mixture, curve 1, they lie merely between 0.85 and 1.29 atmospheres in contrast to the range 1.9 to 4.6 atmospheres for the 1.7% mixture, curve 5.

An important feature of the curves is the fact that the higher of the two pressure minima of initial ignition in the lower range always lies closely to 350° C; this temperature is characteristic whether the hydrocarbon be propane, butane, isobutane, pentane, hexane or heptane. The lower pressure minimum is less definitely located but is observed with hexane-air mixtures between 280° and 310° C; with other hydrocarbons it is sometimes not observed at all. We incline to regard these temperatures as probably indicative of a rapid thermal breakdown of some intermediate body or bodies, the formation of which is common in each combustion and the survival of which is vital to ignition in the lower temperature range. Attention is also directed to the fact brought out in curve 1 that with rich mixtures ignition at the critical transition pressure occurred first at the lower of the two pressure minima in the lower temperature range, thus effecting a fall in ignition temperatures for these mixtures (*cf.* also fig. 1) of no less than *circa* 230° C.

Curves 2, 4 and 6 have been drawn similarly for 6.5, 2.7 and 1.8% mixtures to which 0.05% of lead tetraethyl had been previously admixed. These curves do not maintain uniformly the precise contour of those of the undoped mixtures, but they reveal among themselves common features when compared

with the latter, namely (1) a general though not invariable increase in ignition temperature over the whole pressure range, and (2) the necessity with the presence of lead tetrathyl for a higher pressure to effect ignition in the lower group. This higher pressure has the effect of raising the ignition temperatures over a narrow pressure range (as shown by the vertical arrows) by about 175°C for weak mixtures and about 230°C for rich mixtures.

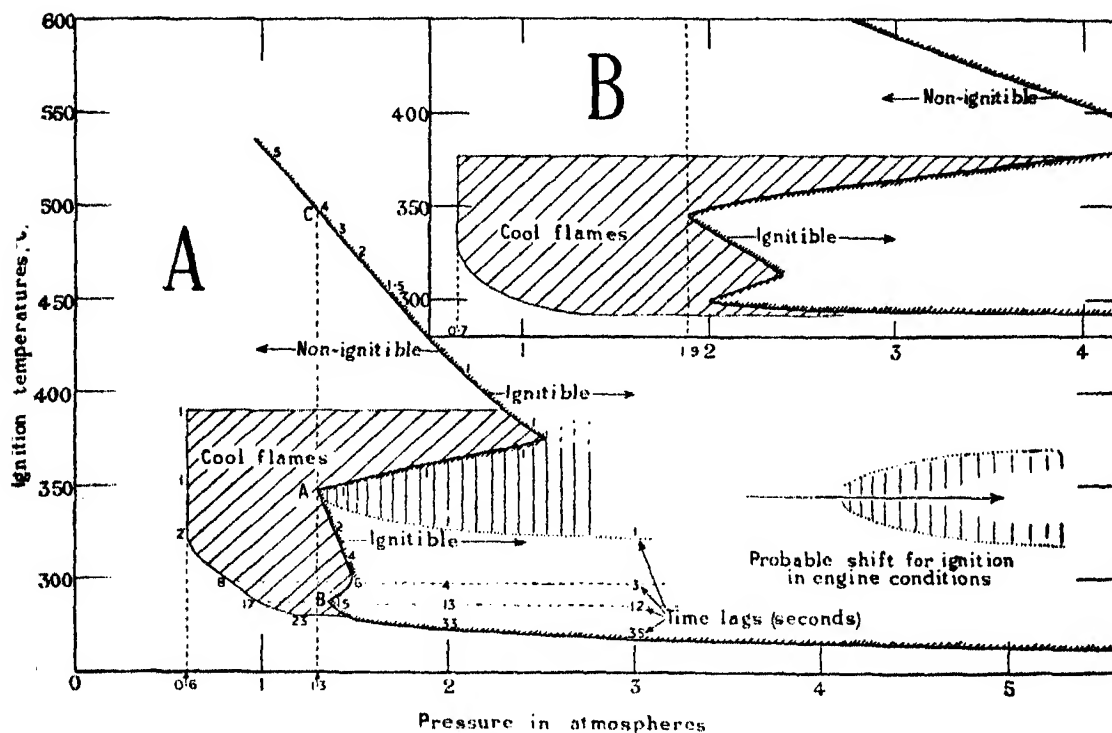


FIG. 3—A, 3.1% mixture; B, 1.8% mixture.

Cool Flames—Following our observation with pentane-air mixtures that in certain circumstances a small pressure pulse was observable which synchronized with the passage of a slow moving bluish flame and the production of a considerable formation of intermediate compounds strongly aldehydic in character, we have studied the extent of this phenomenon with two hexane-air mixtures each containing 3.1 and 1.8% of the combustible, respectively. The temperature and pressure limits within which it could be observed are illustrated in fig. 3 by the diagonally shaded areas. Thus, with the 3.1% mixture, fig. 3, A, cool flames were first observed at 280° and at pressures between about 1.2 and 1.4 atmospheres under which conditions the time lag was about 23 seconds.

Increase of pressure above 1.4 atmospheres at this temperature resulted in true ignition as defined by the shaded boundary curve. Raising the initial temperature widened the lower pressure limit for cool flames to 0.6 atmosphere and progressively decreased the time lags until at 390° C they became very short and the pressure pulses much less intense; at higher temperatures the phenomenon was no longer observable. With a 1.8% mixture, which contained an excess of air, fig. 3, B, the observations were much the same with the exception that cool flames did not occur at pressures below 0.7 atmosphere, and the temperature range was now restricted to between about 290° and 380° C. Also with the weaker mixture the cool flames were very much fainter and at the higher temperatures were detectable by the pressure pulse alone. The temperature ranges referred to did not vary greatly whether either butane, isobutane, pentane, or hexane were used as the combustible.

Fig. 3 also makes clear the relationship between our own determinations and those of Prettre* and more recently of Coffey and Birchall† who have shown that at atmospheric pressure cool flames (so-called "first inflammations" or "ignitions") are observable only within restricted temperature ranges above which ignition is not possible until much higher temperatures have been reached. This matter has recently been referred to elsewhere‡ and it has also been discussed in detail by Beatty and Edgar.§

We have not found in the literature any complete explanation of cool flames. Though hesitating to advance a final opinion at the present stage of our work, we think that they result from the propagation of flames in which the combustion is limited to a definite oxidation, for example, an aldehyde, stage. True ignition does not normally ensue if the pressure and temperature conditions are (a) such as to allow the rapid breakdown of the intermediate body formed, or (b) in other circumstances are inadequate to promote its further rapid oxidation.

Time-Lags and Knock—It should be borne in mind that the ignition points determined in these investigations are defined (Pt. I, p. 486) as "the lowest temperature to which the vessel must be heated for ignition ultimately to occur." In considering our results in the light of their possible application to internal combustion engines the question of time-lag is also one of great importance; for in such conditions the maximum time-lag permissible would

* 'Bull. Soc. Chim. Paris,' vol. 51, p.1132 (1932).

† 'J. Soc. Chem. Ind.,' vol. 53, p. 237 (1934).

‡ *Ibid.*, p. 237.

§ 'J. Amer. Chem. Soc.,' vol. 56, pp. 102-114 (1934).

not then exceed (say) 0.005 second.* It is instructive, therefore, to consider from our curves the likely limiting pressure and temperature conditions for spontaneous ignition to occur in such short time intervals.

In fig. 3, A, the small figures along the ignition point curve relate to the observed time-lags; these are seen to depend mainly upon temperature. Thus at 2 atmospheres pressure, ignition point 274°C , the lag was 33 seconds; this decreased markedly as the temperature was raised, being 15 seconds at B (I.P. 285°C) and approximately 1 second at A (I.P. 374°C). This short lag remained constant until a temperature of approximately 420°C had been reached; thereafter it progressively increased being 4 seconds in the higher group at the critical transition pressure (C). These lags varied little with mixture composition, tending generally to be shorter with mixtures containing an excess of air. There was a marked shortening of the lags, however, as the paraffin series was ascended as the following figures for corresponding points (as in fig. 3, A, B, C) on the curves show:—

Hydrocarbon	Time-lags (secs) at		
	A	B	C
Butane	10 to 15	25	6 to 8
Pentane	6 to 8	15	4 to 6
Hexane	(approx.) 1	15	3 to 6

It is thus seen that the portion of the curve having the shortest lag, and therefore probably of greatest bearing on internal combustion engine practice lies immediately above the point A (at about 350°C). By increasing the pressure at temperatures below 350°C ignition occurred with reduced time-lag and the boundary of the vertically shaded area is approximately the ignition point curve for ignition with minimum lag. It seems probable that for ignition to occur within such a short time-interval as 0.005 second much higher pressures still would have to be employed and we visualize a pressure shift somewhat as indicated by the horizontal arrow; these pressures might then correspond with the "Highest Useful Compression Ratios" observed in engine practice.

"Surface" Influence—Hitherto, while recognizing that our ignitions might be influenced by surface conditions both in their initiation as well as in regard to heat dissipation, we have deferred investigating the matter closely because

* We regard it unlikely that "knock" in an engine is merely spontaneous ignition; the phenomenon may well arise, however, in circumstances responsible for a high rate of chemical reactivity in the explosive medium to which the spontaneous ignition temperature is closely related.

of the known complexity of the combustions of the hydrocarbons under investigation.

In order to obtain some insight into the matter, however, and particularly to see how far our results might be influenced by employing a vessel with a large surface volume ratio, as would obtain in an engine cylinder, we have compared the results obtained with a 2.6% hexane-air mixture when the

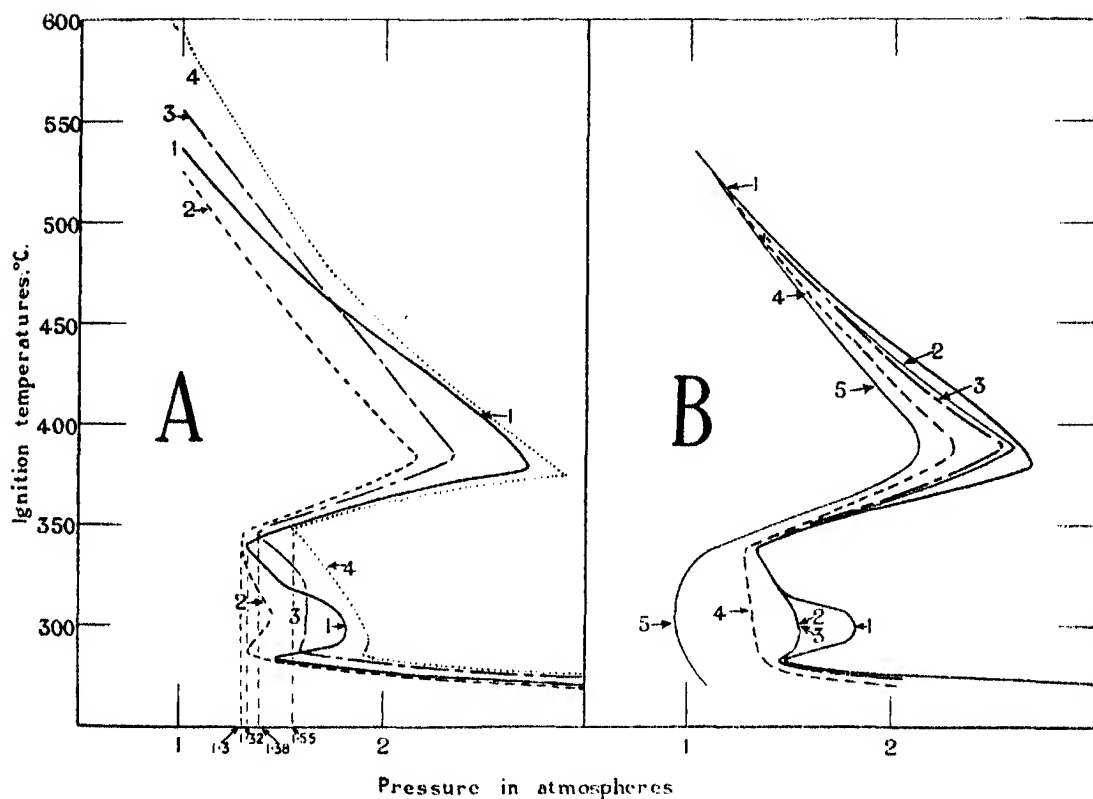


Fig. 4—A: Curves 1, 2, 3 and 4 are for s/v ratios 1.1, 1.23, 1.55 and 2.17. B: Curves 1 = 2.68% mixture; with 0.5% valeraldehyde 2; 0.5% acetaldehyde 3; 1.0% acetaldehyde 4; and 5.0% acetaldehyde 5.

length of the explosion cavity was reduced by means of closely fitting mild steel plugs from the normal 6 inches to $4\frac{1}{2}$ inches, $2\frac{1}{2}$ inches and $\frac{3}{4}$ inch respectively, the diameter remaining constant at $1\frac{1}{2}$ inches. In such circumstances the surface volume ratios were correspondingly increased to 1.1, 1.23, 1.55 and 2.17 respectively, and the curves obtained Nos. 1, 2, 3 and 4 are plotted in fig. 4, A.

Actually the first decrease in volume was found to facilitate ignition, the ignition temperatures being generally lowered, and markedly so in the higher temperature range; the critical transition pressure was also reduced from 1.32 to 1.30 atmospheres. Further increase in surface volume ratio to 1.55 and 2.17, however, progressively raised the ignition points, and the critical transition pressures were increased from 1.32 to 1.38, and 1.55 atmospheres, respectively. It is also interesting to observe that the influence of an increase

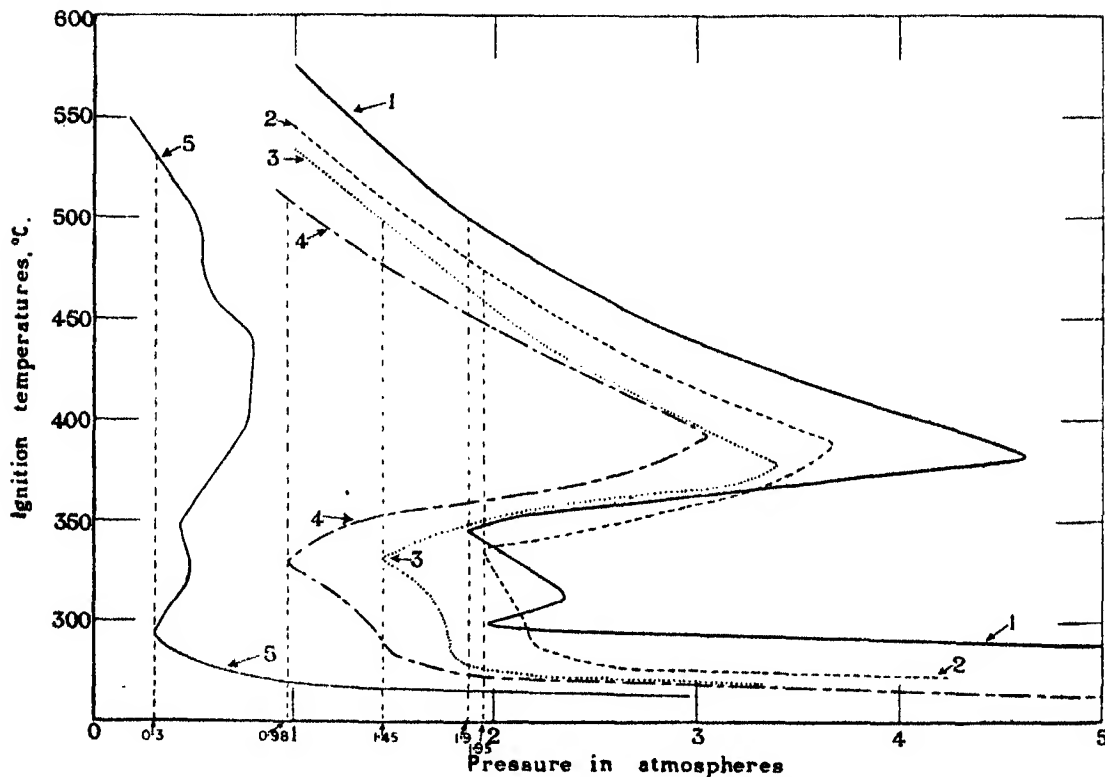


FIG. 5—Curves 1, 2 and 3 are for a 1.8% hexane-air mixture with mild steel, glass, and aluminium liners. Curve 4 = 1.8% hexane-oxygen mixture. Curve 5 = $C_6H_{14} + 9\frac{1}{2}O_2$ mixture.

of surface had much the same effect as the addition of lead tetraethyl to the explosive mixture (*cf.* No. 4, fig. 2 and No. 3, fig. 4, A).

In fig. 5, curves 1, 2 and 3 are in respect of a 1.8% mixture, curve 1 being the normal curve with a mild steel liner; curves 2 and 3 were obtained with the mild steel liner replaced by glass and aluminium, respectively. As already indicated, a glass liner was found to effect a general lowering of the ignition point by about 20° C and with the 1.8% mixture the critical transition pressure

was raised from 1.9 to 1.95 atmospheres. The aluminium liner effected not only a still greater general lowering of the ignition points but also reduced the critical transition pressure from 1.9 to 1.45.

Influence of Nitrogen Replacement by Oxygen—Curve No. 4, fig. 5, shows the ignition points for a 1.8% hexane-oxygen mixture and may be compared with that for the corresponding hexane-air mixture, No. 1. As is usually found with oxygen, the ignition points were all much lower than with air as the diluent; moreover, the critical transition pressure was found at 0.98 atmosphere which compares with 1.9 atmospheres for the corresponding air mixture. This curve also throws light upon the fact that the ignition temperatures of mixtures of the higher hydrocarbons with oxygen at atmospheric pressure are frequently given at *circa* 300° C, whereas those of the corresponding mixture* with air are usually above 500° C.

We have also studied an undiluted theoretical hexane-oxygen mixture ($C_6H_{14} + 9\frac{1}{2}O_2$) and the ignition points have been plotted in fig. 5, curve No. 5. The critical transition pressure was now found at a pressure of 0.3 atmosphere the curve maintaining the characteristic pressure minima in the lower temperature range, first at 295° and subsequently at 350° C. Our results for this mixture thus agree with the observation of Neumann and Estrovitch† who found that with a theoretical pentane-oxygen mixture there was a ‘considerable scattering of their points’ and a sudden fall in ignition temperatures from a higher to a lower system at a pressure of 60 cm of mercury. We think, however, that a more detailed study of their ignitions would show that the points do not drop vertically as in their diagram, but that there is initially over a definite pressure range a narrowing temperature zone in which ignition does not occur although it may do so quite readily in a lower temperature system.

The Influence of Additions of Aldehydes—In Part II, p. 174, in support of our view that the lower group of ignition temperatures arises from the rapid oxidation of certain intermediate oxygenated bodies, we cited the observation of Bone and Hill‡ that 1% of acetaldehyde was able to effect the ignition of a $C_2H_6 + O_2$ mixture at 316° C and 710 mm pressure under conditions when the reaction normally proceeded quite slowly. And we showed that a like amount of the aldehyde was adequate to effect the ignition at atmospheric pressure of a 3.5% pentane-air mixture in the lower group at 318° C where normally a pressure of *circa* 2 atmospheres would have been required.

* cf. Dykstra and Edgar, ‘Ind. Eng. Chem,’ vol. 26, p. 509 (1934).

† *Loc. cit.*

‡ ‘Proc. Roy. Soc.,’ A, vol. 129, p. 474 (1930).

In fig. 4, B, we have plotted curves showing the influence on the ignition points of additions to a 2.6% hexane-air mixture (curve 1), which contains a defect of oxygen, of 0.5% valeraldehyde, curve 2, 0.5% acetaldehyde, curve 3, 1.0% acetaldehyde, curve 4, and 5.0% acetaldehyde, curve 5. While the respective influences of either 0.5% of acetaldehyde or valeraldehyde were much the same, both tending to induce ignition in the lower temperature range, further additions of acetaldehyde had a very marked influence though perhaps not equal to that observed with the 3.5% pentane-air mixture. We would emphasize the fact that at temperatures above 350° C the influence of the aldehyde decreased rapidly, and above 500° C no appreciable lowering of the ignition temperatures was observable, even if the amount of acetaldehyde was greatly increased above the proportions stated. This fact we regard as strongly supporting our view that at low pressures the ignitions in the higher temperature range pertain to the thermal decomponents of the oxygenated bodies the survival of which is responsible for ignition in the lower temperature range.

When using acetaldehyde in these experiments care was always taken, before each determination, to ensure that the surface had been renormalized by admitting compressed air to the vessel and subsequently submitting it to a prolonged evacuation. Failure to carry out this precaution left the surface active, and induced subsequent ignitions at pressures slightly below those usually observed.

B. Isobutane-Air Mixtures

There is a considerable difference between the behaviours on combustion of corresponding straight- and side-chained hydrocarbons. In an engine, for example, whereas *n*-octane is a bad knocking fuel, its isomers are comparatively free from the defect, so much so that 2-2-4 trimethyl pentane (*iso*-octane) is widely employed as a standard for "knock-rating." Until recently no study had been made of the characteristics of the slow combustion of such hydrocarbons but in 1927-29 Edgar* investigated both *n*-octane and its isomers. He found generally that (1) oxygen attacked the methyl group at the end of the longest open chain of the hydrocarbon, the first recognizable products being water and the corresponding aldehyde; (2) the aldehyde was oxidized to a lower aldehyde, water, etc.; (3) with the branched isomers, the process proceeded until a branch in the molecule was reached giving rise to a ketone

* 'Ind. Eng. Chem.,' vol. 19, p. 145 (1927); 'J. Amer. Chem. Soc.,' vol. 51, p. 1875 (1929) and vol. 51, pp. 2203, 2213 (1929). cf. also Pense, *ibid.* vol. 51, p. 1839 (1929).

instead of an aldehyde; and (4) since ketones oxidize more slowly than aldehydes the reaction slowed down.

A comparison of the behaviours of two isomeric hydrocarbons was therefore a matter of great interest because (a) if our view be correct that "knock" in an engine is conditioned by a compression ratio adequate to permit ignition

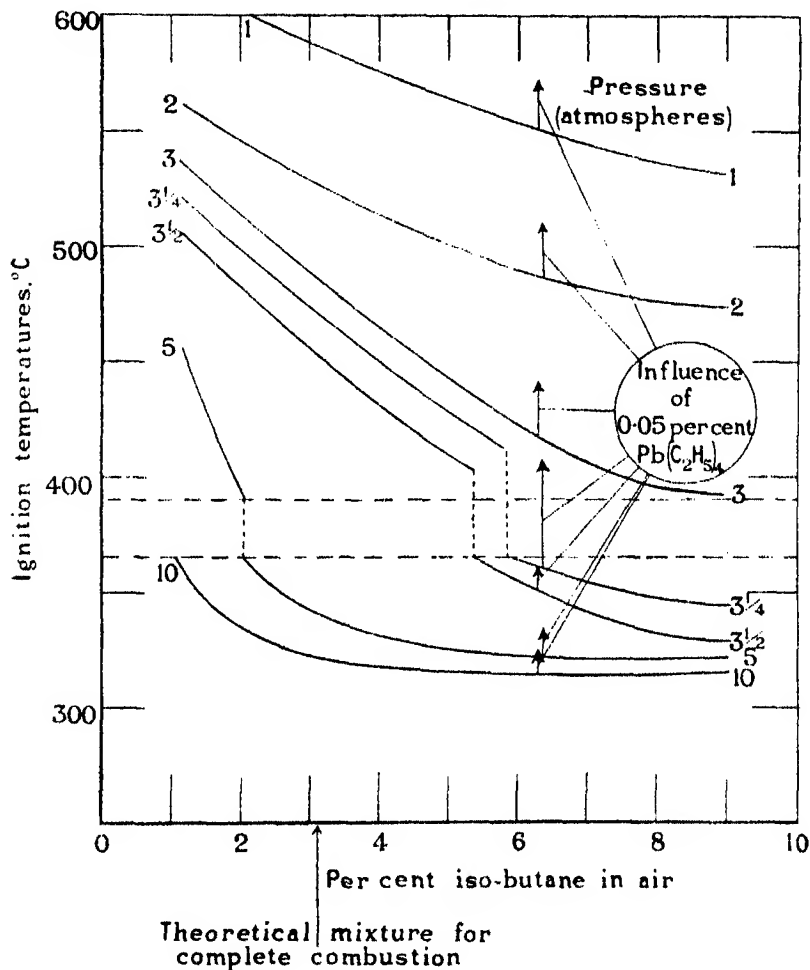


FIG. 6

in the lower of the two temperature ranges, then one would anticipate a higher critical transition pressure in our experiments with a side-chained hydrocarbon than with the corresponding straight-chained isomer; and (b) if this anticipation proved correct support would be forthcoming for the view that ignition in the lower temperature range is the outcome of the survival of some inter-

medially formed body or bodies—probably aldehydes—because of the known difference in the formations of these compounds in the two combustions. It remains to show how our results confirmed this anticipation.

Having already studied butane-air mixtures in detail we were fortunate in obtaining a supply of liquid iso-butane, the simplest side-chained paraffin, from the Ohio Chemical and Manufacturing Company, Cleveland, U.S.A.

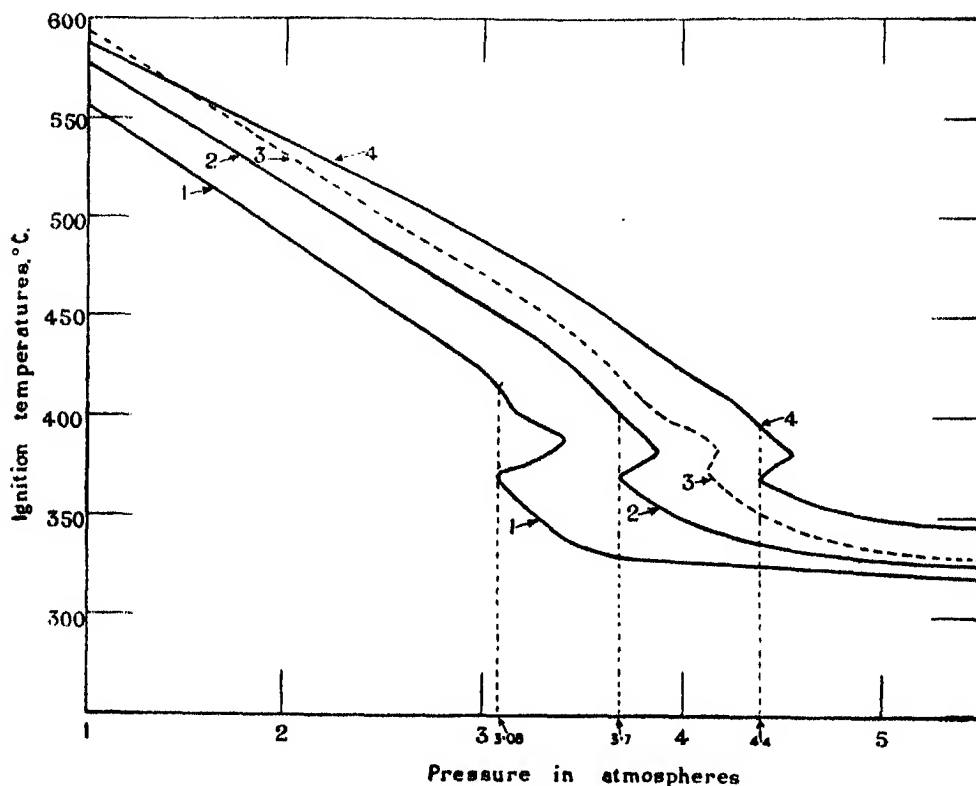


FIG. 7—The iso-butane contents of the mixtures are 1 = 5.8%, 2 = 3.7%, 4 = 2.6%, and 3 = 3.7% with 0.05% $\text{Pb}(\text{C}_2\text{H}_5)_4$.

The purity of the material was checked both by chemical analysis and by its vapour pressure.

We have plotted in fig. 6 a series of curves showing the observed variation of ignition points with composition for mixtures of iso-butane content between 1 and 9%, and at pressures of 1, 2, 3, $3\frac{1}{4}$, $3\frac{1}{2}$, 5 and 10 atmospheres. These may be compared with the corresponding curves for the *n*-butane-air mixtures, Part I, fig. 2. It will be observed that (a) whereas the temperature range between the two ignition systems was 370° to 450° C for the *n*-butane-air

mixtures it was reduced to 365° to 390° C for the iso-butane-air mixtures, and (b) whereas $1\frac{3}{4}$ atmospheres sufficed to transfer the ignition point of rich *n*-butane mixtures from the higher to the lower temperature range, with iso-butane-air mixtures $3\frac{1}{4}$ atmospheres was necessary.

A comparison between the two sets of experiments is perhaps best brought out by studying the detailed curves for individual mixtures in figs. 7 and 8. In fig. 7, curves 1, 2 and 4, show the influence on the ignition points of pro-

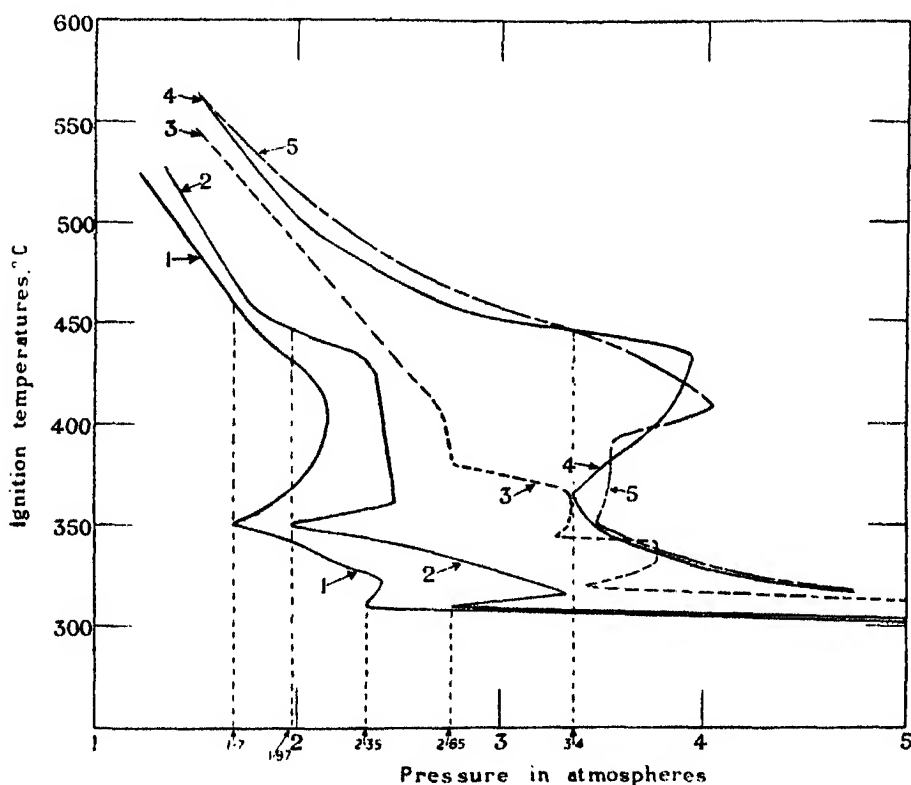


FIG. 8—The butane contents of the mixtures are 1 = 1.54, 2 = 3.8, 4 = 1.8, 3 = 3.8 with 0.05% $\text{Pb}(\text{C}_2\text{H}_5)_4$, and 5 = 1.8 with 0.05% $\text{Pb}(\text{C}_2\text{H}_5)_4$.

gressive increase in pressure for mixtures containing 5.8, 3.7 and 2.6% of iso-butane, respectively. The two ignition systems are almost continuous but definite transition pressures occurred at 3.08, 3.7 and 4.4 atmospheres respectively; ignition commenced in the lower range at about 370° C with each mixture and the ignition points fell progressively therefrom with further increase of pressure, the dual pressure minima phenomenon found with most other paraffins not being now observable. Curve 3 relates to the ignition

128 *Spontaneous Ignition of Inflammable Gas-Air Mixtures*

points of a 3.7% iso-butane-air mixture to which 0.05% of lead tetraethyl had been previously admixed.

By contrast curves 1, 2 and 4, fig. 8, are curves for 5.4, 3.8 and 1.8% *n*-butane-air mixtures. The critical transition pressures occurred at much lower pressures, namely 1.7, 1.97 and 3.4 atmospheres respectively, ignition in the lower temperature range being initiated at 350° C with the 5.4 and 3.8% mixtures, and at 370° C with the 1.8% mixture. It is also interesting to observe that whereas lower pressure minima at 310° C occurred with curves 1 and 2 at 2.35 and 2.65 atmospheres, respectively, curve 4 for the weak 1.8% mixture resembles those of the iso-butane-air mixtures being quite smooth in the lower temperature system. Curves 3 and 5 show the influence of 0.05% of lead tetraethyl on the 5.4 and 3.8% *n*-butane-air mixtures, respectively.

Summary

An investigation into the influence of pressure on the spontaneous ignition of explosive hydrocarbon-air media has been extended to hexane and iso-butane. The ignition points have been found to lie in two well-defined temperature ranges, location in the higher range occurring at low pressures, and in the lower range at higher pressures. Transference of the ignition points from the higher to the lower range occurred at a critical pressure which depended upon mixture composition, and for rich mixtures was as follows:—

	Lower range below ° C	Higher range below ° C	Pressure requisite to effect transfer from higher to lower range atms
Butane	370	450	1.75
Iso-butane	370	390	3.25
Pentane	350	490	1.25
Hexane	350	495	0.9

It is thought that the lower group of ignition points is the outcome of the rapid oxidation of certain intermedially formed oxygenated bodies the survival of which is favoured by high pressures; the higher group results from ignitions of mainly the products of the thermal decompositions which are favoured by low pressures. This is supported by the fact that aldehydes promote ignition in the lower temperature range but hardly at all in the higher range; more-

over, a normal paraffin is far more easily ignitable in the lower temperature system than a corresponding side-chained isomer the oxidation of which is known to give rise to fewer aldehydes.

Knock in an engine is probably conditioned by a compression ratio adequate to promote ignition in the lower temperature range; this compression ratio is raised by the presence in the medium of an antiknock.

The Sorption of Methyl and Ethyl Alcohol by Silica Gels

By A. GRAHAM FOSTER, King's College, London

(Communicated by A. J. Allmand, F.R.S.—Received March 6, 1934)

The original object of the present research was to investigate the sorption of methyl alcohol by silica gel, in order to compare the isothermals with those of water and ethyl alcohol, which had been determined by Lambert and Foster.* Owing to the fact that the supply of gel used for this earlier work had been exhausted, it was necessary to examine a number of other specimens. One of these, which like the original gel, was a commercial product, was found to take up a larger amount at saturation, and also to exhibit hysteresis phenomena which were not observed with the original gel. Unfortunately it was impossible to find a sample giving exactly the same shape of isothermal as the original gel, although some specimens known to belong to the same batch gave very similar curves. One of these was selected for the present work, and an examination has been made of the isothermals of methyl and ethyl alcohols on these two types of silica gel at 25° C.

The fact that one specimen showed hysteresis provided a suitable occasion further to confirm the view, always maintained by Lambert and the author,† that these phenomena are in no way due to incomplete removal of permanent gases or other impurities from the systems. In previous work† with silica and ferric oxide gels, evacuation was carried out at 150° C, which is actually the optimum temperature of activation for the latter gel, the adsorptive capacity of which decreases rapidly when higher temperatures are employed. Silica gels, however, will withstand a much higher temperature

* 'Proc. Roy. Soc.,' A, vol. 134, p. 246 (1931).

† Lambert and Foster, 'Proc. Roy. Soc.,' A, vol. 126, p. 363 (1932).

with comparatively little diminution in capacity, and in the present work it has been shown that the hysteresis phenomena are not affected by raising the temperature of the initial evacuation to 250° C or even to 350° C. It has also been shown that the phenomena persist after continued "flushing out" of the gel with methyl or ethyl alcohol vapour. (McBain* suggested that the hysteresis observed by Lambert and Clark† with benzene on ferric oxide gel would not have occurred if the gel had been flushed out with benzene before the isothermals were determined.)

Experimental

The experimental method employed previously was designed to enable systems to be examined over a wide range of temperature, but although this was extremely simple in operation, a considerable time was required for assembly and evacuation for each series of experiments. In the present work isothermals at 25° C only were required, and it was desired to investigate their structure as closely as possible, in order to determine whether discontinuities were present. For these reasons the static method of Allmand and Burrage‡ was adopted, by which points can be obtained very close together by removing known volumes of vapour from the system. The experimental procedure was exactly similar to that described by these workers and later improved by Burrage,§ but in general this "pressure change" method has been used only to determine those portions of the isothermal where an accurate knowledge of the shape is essential. The majority of points were determined by direct weighing of the gel container after reading the equilibrium pressure.

The gel was evacuated at 150° C by means of a Leybold mercury vapour pump backed by a Hyvac oil pump, and then charged to saturation with the vapour. The container was then transferred, after weighing, to the measuring system, which consisted of a wide bore mercury manometer, the ground joint being sealed with Everett's wax. A number of points were then determined by the pressure change method, opening the container tap to the evacuated manometer and calculating the weight of vapour removed from a previous calibration of the volume of the measuring system. The container was then removed and weighed in order to obtain a check on the calculated quantity

* "Sorption of Gases and Vapours by Porous Solids," p. 191.

† 'Proc. Roy. Soc.,' A, vol. 122, p. 497 (1929).

‡ 'Proc. Roy. Soc.,' A, vol. 130, p. 610 (1931).

§ 'J. Phys. Chem.,' vol. 36, p. 2272 (1932).

values. An example of the agreement between the calculated and observed amounts is given by the following figures obtained with methyl alcohol:—

Calculated loss after 31 points determined by—

Pressure change method	107.42 mg/gm
Actual loss	107.47 „

The methyl alcohol used was specially purified for conductivity work and was kindly supplied by the Balliol College Laboratory, Oxford. The ethyl alcohol was not of quite such a high standard of purity, but it was carefully dried and fractionated before use, and the vapour pressure found to agree with the values given by Ramsay and Young.

The Sorption of Ethyl Alcohol

The isothermals determined in the previous work,* were of rather peculiar shape. At a concentration of about 100 mg/gm the pressure was only about one-fiftieth of the saturation value, whilst at approximately 125 mg/gm, the curve became linear and continued so until about 155 mg/gm where the pressure was about one-half saturation. The isothermal then rose sharply to saturation at 160 mg/gm.

In the present work the sample approximating to the original gel, which will be referred to as "Gel A," has been found to reach a pressure of one-fiftieth saturation at a concentration of about 100 mg/gm and is linear between 145 and 155 mg/gm, the pressure at the latter concentration being about one-third saturation. The quantity of ethyl alcohol adsorbed at saturation is about 180 mg/gm, nearly 12% greater than that of the original gel.

The sample of gel with the higher capacity which will be referred to as "Gel B," gives an isothermal which rises from one-fiftieth saturation at 140 mg/gm, and is linear between 170 and 265 mg/gm, a range of 95 mg/gm, or about one-third of the total amount held at saturation, which is approximately 300 mg/gm. At a pressure of 27 mm the gel A isothermal is rising almost vertically towards saturation, whilst, the gel B isothermal is bending horizontally into the hysteresis area, which follows the linear part.

Gel A.—A sample weighing 4.9620 gm was used and the isothermal was investigated in detail from the saturation pressure, 59.4 mm, down to 2.54 mm by the pressure change method, a total of 75 points being determined, with five weighed points to check the calculated quantity values.

* 'Proc. Roy. Soc.,' A, vol. 134, p. 246 (1931).

Fig. 1 shows the isothermal plotted graphically, and the weighed points are given in Table I.

Table I

q (mg/gm)	Pressure (mm Hg)
174.97	31.10
161.00	14.70
147.82	8.00
141.00	4.80
130.70	2.45

Saturation value 182 mg/gm
 Range of linear portion $q = 143.7$ to 163.0 mg/gm
 $p = 0.05$ to 15.9 mm

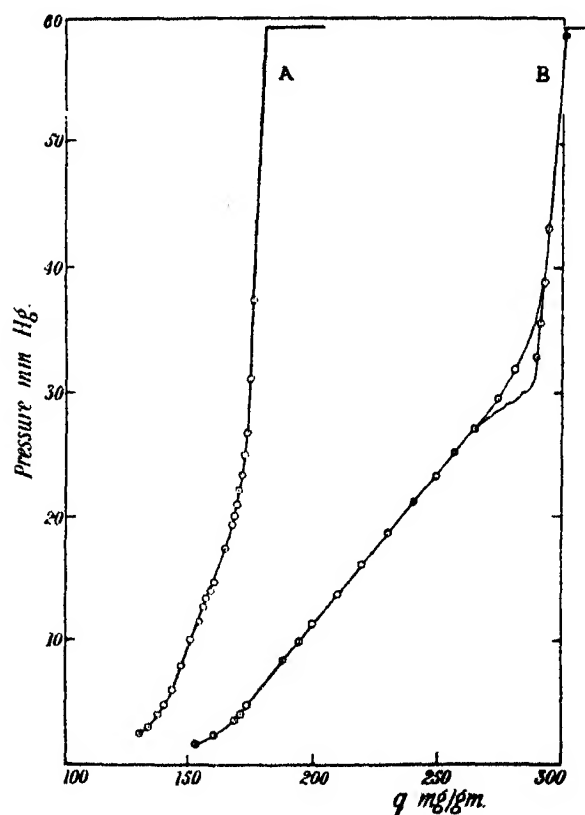


FIG. 1.

Gel B.—The sorption of ethyl alcohol by this gel was investigated in detail from saturation down to 1.6 mm pressure. The sample, weighing 4.952 gm was first evacuated at 150° C and after charging, a series of about 170 points was obtained. The isothermal is plotted in fig. 1.

The "ascending" points were all obtained by charging the gel to the observed pressures and then removing the container for weighing. Nineteen points were determined by the pressure change method without interruption, the gel being maintained isothermally at 25° C throughout the series, two points, determined by weighing, serving as a check upon the calculated quantity values. The remaining points given in the graph are selected from a total of about 150, and serve to define the general shape of the isothermal.

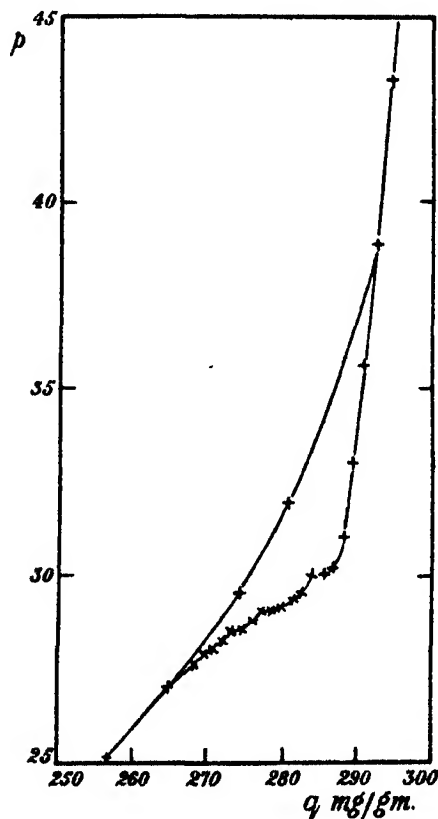


FIG. 2.

In fig. 2 the hysteresis area is shown plotted on a larger scale, and it will be seen that there are three quite definite breaks in the desorption curve; at 30.1, 29.1 and 28.6 mm respectively. Although the isothermal was examined in detail over the entire range, no further evidence of discontinuities was observed except below 2 mm pressure where points taken at intervals of about 0.2 mg/gm do not fall on a smooth curve. There is no indication of any

regular step-like breaks as have been observed with carbon tetrachloride on silica gel and charcoal.*

In order to see whether breaks could be observed after "flushing out" the gel was charged with alcohol vapour at room temperature, and the container heated to 100° C for several hours with the tap closed. The gel was then evacuated as completely as possible at 150° C and recharged. Portions of the isothermal were then examined closely, but showed no signs of irregularities. This treatment was repeated after heating the gel *in vacuo* at 250° C and a series of seventeen desorption points gave readings almost identical with those obtained during the first run, but the low pressure breaks were no more definite than before. The gel was then refluxed with ethyl alcohol for several hours but this treatment also failed to reveal any further breaks, and the discontinuities in the hysteresis area became less definite. A final evacuation at 350° C was also unsuccessful and apart from a shift towards the pressure axis, the shape of the isothermal remained unaltered.

The Sorption of Methyl Alcohol

Gel A.—5.045 gm was evacuated at 150° C and the isothermal was investigated from saturation (116 mm) down to 0.40 mm. The results are shown graphically in fig. 3.

The linear portion of the isothermal is not very well defined, and after several sorption and desorption experiments had been carried out, a shift towards the pressure axis occurred, and the linear part was then observed between 30 and 50 mm pressure, the corresponding *q* values being 150 and 170 mg/gm respectively. The isothermal was examined in detail from about 40 mm pressure up to saturation, during sorption and desorption but there was no evidence of any lack of reversibility in this region, where the hysteresis phenomena occur on the other type of gel.

Gel B.—A sample weighing 5.0082 gm after evacuation at 150° C was charged up to saturation and a desorption curve determined. This is shown graphically in fig. 3, curve I.

The gel was then evacuated, recharged and flushed out at about 80° C for several hours at 150 mm pressure. After evacuation the gel adsorbed practically the same amount at saturation as before (302 mg/gm), but the desorption curve began to shift towards the pressure axis away from the original curve. After about twenty points had been obtained an "ascending" isothermal was commenced. These readings are shown in fig. 4 together with the subse-

* Burrage, 'J. Phys. Chem.,' vol. 37, p. 505 (1933).

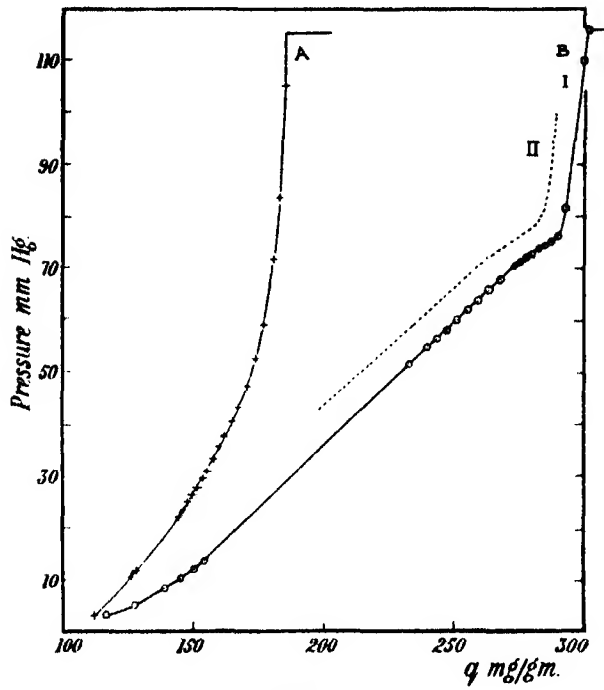


FIG. 3.

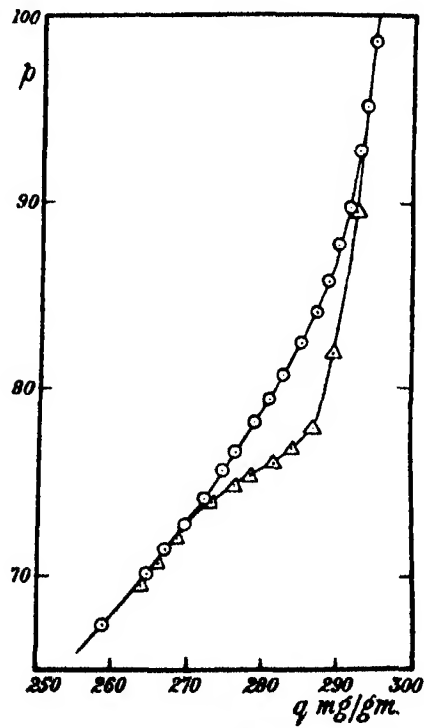


FIG. 4.—○ Ascending points ; △ descending points.

quently determined "descending" points, which showed no further shift. Although the points are not sufficiently close together to reveal any discontinuities the second series of desorption points gave same indication of breaks resembling those obtained with ethyl alcohol, but owing to the shift of the isothermal these readings were rejected. The gel was next evacuated at 250° C and another isothermal determined, which is shown in fig. 3 as curve II; apart from the shift towards the pressure axis there is clearly no alteration in shape.

The behaviour of the methyl alcohol isothermals at low pressures is interesting, since the curves for the two gels tend to coincide below 3 mm pressure. This is illustrated in fig. 5 which shows the lower portions of both isothermals plotted as $\log p - \log q$ curves. Unfortunately the ethyl alcohol isothermals

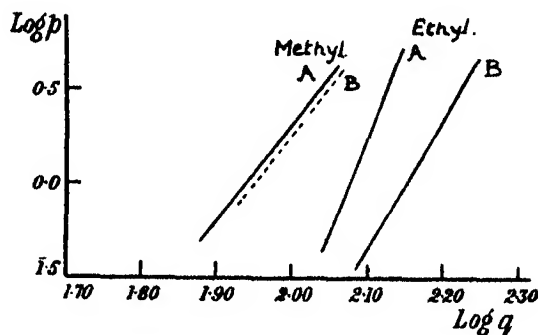


FIG. 5.

were not investigated below 1 mm pressure by the static method, but during the preliminary examination of the gels, data had been obtained by the retentivity method* down to 0.2 mm pressure, which were considered of sufficient accuracy to indicate that there is a considerable separation between the two curves even at 0.3 mm, fig. 5. Below a concentration of about 100 mg/gm, where the pressure is approaching 0.1 mm the curves run together more closely.

Comparative data are given in Table II for the saturation values and the range of the linear portion of the four isothermals which have been studied.

Discussion

An examination of the two types of silica gel isothermals shows that, apart from the hysteresis phenomena exhibited by the "B" gel, they are essentially

* Burrage, 'J. Phys. Chem.,' vol. 37, p. 735 (1933).

similar in shape. The two curves for methyl alcohol, figs. 3 and 5, are practically coincident from 3 mm down to 0.3 mm pressure. If the surfaces of the two gels were similar in nature and extent, one would expect the initial stages of the sorption process to be identical, at least, as far as the formation of the first layer is concerned, but it would appear that the unimolecular layer is already completed even at the lowest pressures observed in these systems, since the Langmuir equation is inapplicable. Capillary condensation in accordance with the Kelvin equation does not generally appear at pressures

Table II

	<i>q</i> (mg/gm)			
	Gel A.		Gel B.	
	MeOH.	EtOH.	MeOH.	EtOH.
Saturation value	185	182	302	301.5
Linear portion begins	145	143	155	170
Linear portion ends	162	165	265	265

below about one-third saturation, so that the major portion of these isothermals must represent some intermediate stage in the sorption process, the mechanism of which is uncertain, but may consist either in the formation of additional layers, or in the filling up of pores of molecular dimensions by a modified condensation process, to which the Kelvin equation is inapplicable. It is hardly to be expected that either process would involve a simple relation between pressure and concentration, and it is therefore surprising to find in the middle of the isothermals a linear portion which, for the "B" gel, extends over a considerable range of pressure. Such a relation is, of course, characteristic of the early stages of layer adsorption where only a small fraction of the surface is covered, but is most unlikely to occur during the last stages of any such process. Nor is it easy to see how a condensation process could lead to such a relation, unless there is a balance between the capillary and the adsorptive forces. It is interesting to note that the isothermals of methyl and ethyl alcohol on ferric oxide gel, which has a coarser structure, do not show this linear part.

The manner in which the size of the adsorbed molecule can influence the shape of the isothermal on a given adsorbent has been discussed elsewhere by the author* and a similar argument may be used to illustrate how the capillary radius of the adsorbent can affect the shape of the isothermal. It has already been suggested that the two gels have essentially the same surface areas, but the saturation volumes are roughly in the ratio 3 to 5; it is therefore

* Foster, 'Trans. Faraday Soc.,' vol. 28, p. 645 (1932).

evident that in a simple structure of cylindrical pores it would be necessary for the capillary radii to be in the same ratio also, so that if the radius of the pores of the B gel were five times the diameter of the adsorbed molecules that of the A gel would be only three diameters. Now, in order to simplify the argument, let it be supposed that the true adsorption process ceases after the formation of a second adsorbed layer, and that further sorption can occur only by capillary condensation: a comparison of the two gels at the stage where layer formation is complete will show that in the A gel there remains unfilled, in the centre of the pores, a space whose radius is equal to only one molecular diameter, whereas in the B gel the radius is three diameters. In the former system it is not to be expected that capillary condensation will take place in accordance with the Kelvin equation, and this final stage will represent only about one-tenth of the total sorption. On the other hand, in the B gel condensation can occur in accordance with the Kelvin equation, and this process will represent a larger proportion of the total than in the A gel. Actually, of course, the true structure of the gels is more complex than has been assumed in this illustration and it is not suggested that the radii of the capillaries are really three or five times the diameter of the adsorbed molecules, but it is quite evident that the pore size may affect the shape of the isothermal to a marked extent. There can be little doubt that the difference between the two gels is due mainly to some simple structural difference of this type, although the mechanism of the sorption process may not be as simple as that assumed.

Since condensation takes place in the last stages of the sorption process of the B gel, it is possible to calculate the capillary radius by means of the Kelvin equation. Similar calculations have been made by the author for ferric oxide gel,* and it has been shown that the point of inflexion which occurs in the middle of the hysteresis area on the desorption curve is the most convenient point from which to make this calculation. The relative pressures at which this inflexion occurs with methyl and ethyl alcohol on the B gel, together with the calculated radii are shown below.

	Rel. pressure. r ($\times 10^{-7}$) cm.	
Methyl alcohol.....	0.64	1.63
Ethyl alcohol	0.49	1.43

The agreement is of the same order as that found for benzene and ethyl alcohol on ferric oxide gel, where the values are 1.6 and $1.8 \cdot 10^{-7}$ cm respectively.

It has been pointed out by the author* that it is impossible to determine how accurately the Kelvin equation holds unless the variation in the thickness of the adsorbed layer can be estimated; because, although the pore size does not alter (unless sorption is accompanied by any marked swelling of the adsorbent), the radius of the space which is filled by condensation diminishes as the thickness of the adsorbed layer increases. It is therefore to be expected that for a given adsorbent, the larger the adsorbed molecule, the lower will be the radius calculated from the Kelvin equation. Qualitatively the results so far obtained support this view, since in the present work ethyl alcohol gives a lower value than methyl alcohol, and on ferric oxide gel, benzene gives a smaller value than ethyl alcohol. It must, however, be remembered that the lack of complete agreement may be due to the fact that the limit of validity of the Kelvin equation has been reached, since the calculated radii are only three or four times the diameter of the adsorbed molecules. If the adsorbed layer on the walls of the capillaries is two molecules thick, the actual pore radius of the B gel must be at least of the order $2.5 \cdot 10^{-7}$ cm, or about five molecular diameters. It is interesting to note that the water isothermals on the "A" type silica gel show an inflexion in the hysteresis area corresponding to a radius of only $1.0 \cdot 10^{-7}$ cm, whence, allowing for a double layer on the walls, the actual pore radius would be about $1.7 \cdot 10^{-7}$ cm. This suggests that the actual capillary radii of the two gels are not vastly different from those which were arbitrarily assumed in the illustration given above.

In order to obtain further information concerning the validity of the Kelvin equation it is proposed to extend this investigation to other alcohols and related compounds so that data may be available for a number of members of a homologous series, and the effect of the gradual increase in molecular size observed.

The author's thanks are due to Dr. B. Lambert for the loan of the samples of silica gel; to Professor A. J. Allmand for providing laboratory accommodation; and to the Department of Scientific and Industrial Research for a Senior Research Award, during the tenure of which this work has been carried out.

Summary

Sorption isothermals of methyl and ethyl alcohol have been determined on two samples of silica gel at 25° C. The isothermals on the two types of

* 'Trans. Faraday Soc.,' vol. 28, p. 645 (1932).

gel are similar at low pressures, and all four show a linear range at intermediate pressures. At higher pressure the gel with the higher capacity exhibits a well defined hysteresis area, which is reproducible, and is not affected by drastic flushing out, or by evacuation at 350° C. The different behaviour of the two types of gel is attributed to a simple difference in capillary structure. The pressures at which hysteresis occurs correspond to a constant capillary radius as calculated by means of the Kelvin equation.

An X-Ray Analysis of the Structure of Chrysene

By JOHN IBALL, M.Sc., Ph.D. (Fellow of the University of Wales)

(Communicated by Sir William Bragg, O.M., F.R.S.—Received March 16, 1934)

Chrysene crystallizes in the monoclinic system. By means of rotation, oscillation, and moving film photographs the following crystal data have been obtained :—

$$a = 8.34 \text{ \AA}, b = 6.18 \text{ \AA}, c = 25.0 \text{ \AA}, \beta = 115.8^\circ.$$

All the planes (hkl) are halved when $h + k + l$ is odd and in addition all the ($h0l$) planes are halved. There are two space groups available, C_{2h}^6 ($I2/c$) and C_4 (Ic). In what follows it will be shown that the former space group is the more probable. The measured density is 1.27 (at room temperature) giving 4 molecules of $C_{18}H_{12}$ per unit cell. Molecular volume = 290 (\AA)³.

Intensity Measurements

The crystals used in this investigation were from material supplied by Dr. O. Rosenheim and Dr. Gilchrist, of the Davy-Faraday laboratory, very kindly crystallized them. Most of the intensity data for the Fourier analysis were obtained with a small crystal weighing approximately 0.037 mg.

The photographs were taken with copper $K\alpha$ radiation on a Weissenberg type of camera and the relative intensity of the spots measured on an integrating photometer designed by Dr. Robinson.* I am indebted to Dr. Robinson for a measurement with Mo radiation of the absolute intensities of reflection from the (002) and (110) planes. This made it possible to put the relative measure-

* 'J. Sci. Instr.' vol. 10, p. 233 (1929).

ments on an absolute scale. This absolute scale was checked with copper radiation by taking photographs on a new spectrometer, designed by Dr. Robertson, which permitted accurate comparisons to be made of the intensities of reflections from any two crystals. In this way two chrysene crystals were compared with a standard crystal. The absolute values of the reflections from the standard crystal were already known. This spectrometer was also used to correlate the intensities of the very strongly reflecting planes with the weakly reflecting planes. A shutter operated by a timing switch made it possible to reduce the intensity of the strong planes by a known factor.

With the size of crystal used the absorption of the X-rays is small and the effect of extinction is negligible. The crystal used for the intensity data of the $(0kl)$ zone was very nearly rectangular in shape and so it was possible to calculate without too much labour an approximate correction for the absorption of rays reflected from each plane in that zone. The maximum correction was for the (002) plane and the minimum that for the (020) , the difference between these two planes being 10%.

No direct measurement of the absorption coefficient was possible as the crystals are too small, so a value was calculated from the mass absorption coefficients of its constituents, carbon and hydrogen. The linear coefficient was obtained from the mass coefficients given in the "New International Tables for Crystal Structure Determination," (μ/ρ for carbon = 5.50 and 0.70 for Cu . K α and Mo . K α respectively. For hydrogen μ/ρ is approximately 0.15 in each case*). The absorption coefficients thus obtained for chrysene are : μ per cm = 6.8 and 0.87 for Cu . K α and Mo . K α respectively.

It is necessary to make a preliminary attempt at the determination of structure by a method of trial and error. The information so gained may then be used for a careful analysis by means of a Fourier analysis

Structure by Trial and Error

From the similarity of the chemical formula of chrysene to that of anthracene it seemed reasonable to assume that chrysene would have a planar molecule as those of anthracene and naphthalene,† and that 1.41 Å would be the benzene ring radius.

As there are only four molecules in the unit cell the space group C^4_{2h} requires either a dyad axis or a centre of symmetry in the molecule, while the space group C^4 , requires no molecular symmetry. With polar molecules it is often

* I am indebted to Dr. Lonsdale for these values from the proofs of the tables.

† Robertson, 'Proc. Roy. Soc.,' A, vol. 140, p. 79 (1933); vol. 142, p. 674 (1933).

possible to show the presence of pyro-electricity when the crystals are cooled in liquid air. This was tried with chrysene and a negative result obtained, but the smallness of the crystals made this of little value. However, since anthracene and naphthalene have centres of symmetry it is not unreasonable to assume that chrysene also has one. The agreement between the observed structure factors and those calculated on this assumption is sufficiently good for it to be said that this is justified as far as the X-ray analysis is concerned.

In order to give the chrysene molecule a dyad axis it would be necessary to make the plane of the molecule coincide with the (010) of the crystal. Intensity considerations rule out this possibility at once, since the (0*h*0) intensities do not fall off "normally."

By far the strongest reflection observed was from the (20 $\bar{2}$) plane and this was taken to indicate that most of the atoms were near to this plane. Also the (060) and the (0317) planes, see figs. 2 and 4, had large structure factors, and, as these are very small spacing planes, it pointed to an enhancement due to the spacing of the planes coinciding with a natural periodicity of the molecule. The molecule was therefore placed with its centre of symmetry at the origin of co-ordinates, the long axis OA, fig. 1, perpendicular to the (001) plane and the short axis OB along the *b* axis of the cell.

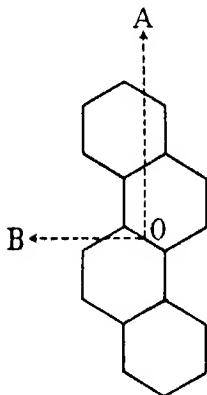


FIG. 1

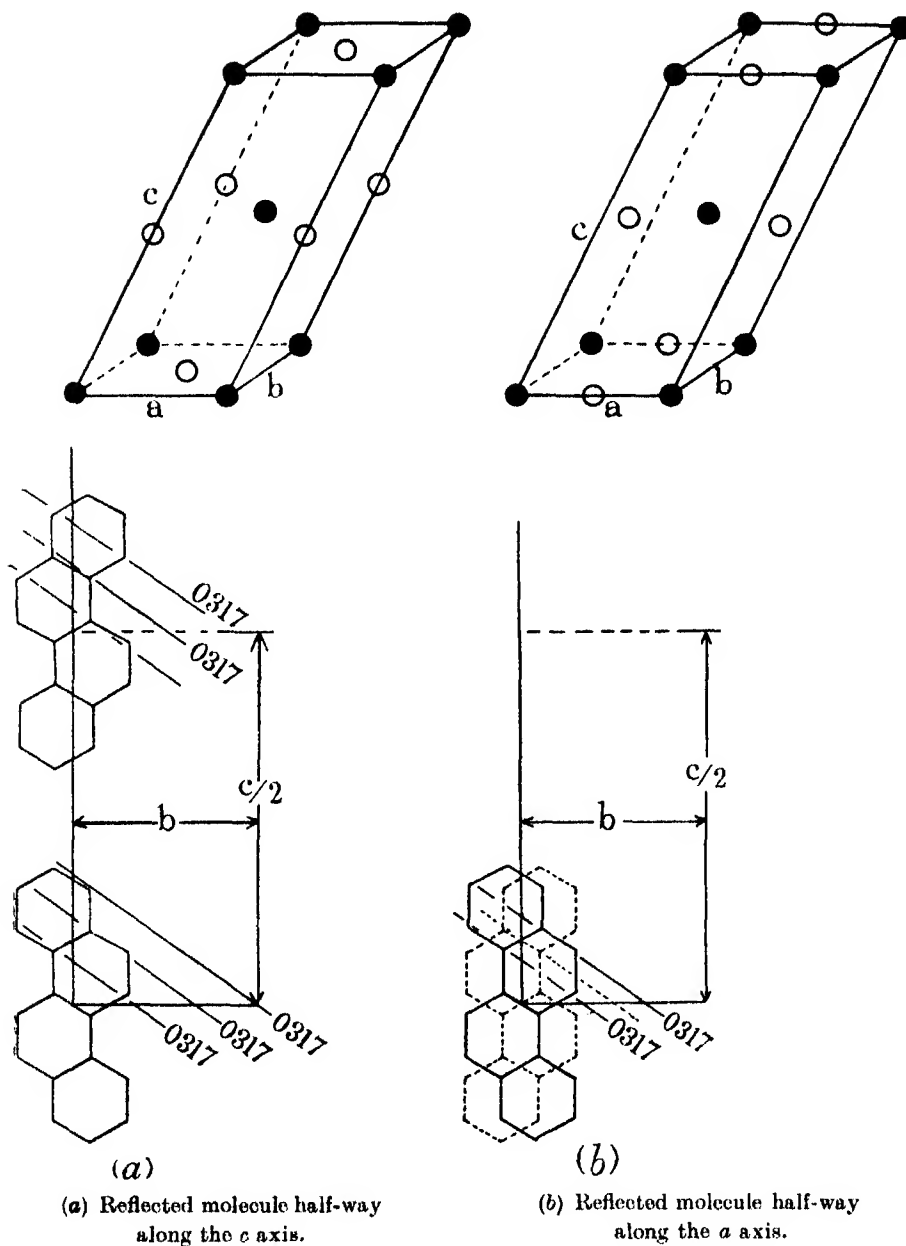
With the molecule in this position it was seen that the spacings of the planes (060) and (0317) showed a fair agreement with periodicities in the molecule. Also the angle between these two planes was about 57° , which seemed to show some coincidence between their position

and the sides of the benzene rings.

In the space group C_{2h}^6 it is possible for the reflected molecule to lie either half-way along the *c* axis of the unit cell (12/*c*), or half-way along the *a* axis (1*o*), i.e., the co-ordinates of the asymmetrical unit can be expressed as follows :

$$\begin{aligned}
 (1) \quad & \left\{ \begin{array}{l} x, y, z; \bar{x}, y, \frac{1}{2} - z; \frac{1}{2} + x, \frac{1}{2} + y, \frac{1}{2} + z; \frac{1}{2} - x, \frac{1}{2} + y, \bar{z}; \\ (12/c) \quad \bar{x}, \bar{y}, \bar{z}; x, \bar{y}, \frac{1}{2} + z; \frac{1}{2} - x, \frac{1}{2} - y, \frac{1}{2} - z; \frac{1}{2} + x, \frac{1}{2} - y, z. \end{array} \right\} \\
 (2) \quad & \left\{ \begin{array}{l} x, y, z; \frac{1}{2} - x, y, \bar{z}; \frac{1}{2} + x, \frac{1}{2} + y, \frac{1}{2} + z; \bar{x}, \frac{1}{2} + y, \frac{1}{2} - z; \\ (12/a) \quad \bar{z}, \bar{y}, \bar{z}; \frac{1}{2} + x, \bar{y}, z; \frac{1}{2} - x, \frac{1}{2} - y, \frac{1}{2} - z; x, \frac{1}{2} - y, \frac{1}{2} + z. \end{array} \right\}
 \end{aligned}$$

However, if the molecule is given a position near to the plane (20 $\bar{2}$) it can be seen that the plane (0317) will be almost exactly halved when the reflected molecule is at half a translation along the *a* axis of the cell (see fig. 2). As this



(b) shows the inter-leaving of the plane (0317) that would take place if the reflected molecule was half-way along the a axis.

FIG. 2

plane is a very strong one it is unlikely that the molecules are arranged in this way. A more convincing proof is given by Table I showing the agreement of the observed and calculated structure factors with the molecules in each of the possible positions. Only those planes having an odd k index are affected.

Table I

$0kl$	Structure factors		
	Observed	Calculated	
		Position (1)	Position (2)
011	20	-30	+127
013	16	+16	-41
015	36	-29	+25
035	84	-70	-2
037	34	-27	-3
0315	43	-34	+3
0317	54	-54	-5

With the plane of the molecule perpendicular to the (001) plane and parallel to the b axis, the structure factors of the (00 l) planes were calculated from the co-ordinates of the atoms and an F-curve for carbon obtained from graphite.* The agreement with the observed values was not very good, but it showed that the orientation of the molecule was not far from this position.

Various positions were now tried, first rotating the long axis about the y -direction and then about the x -direction. It was found that this axis of the molecule could not be moved from the (xz) plane without destroying the agreement between observed and calculated structure factors of the (00 l) planes. The best relative agreement was obtained with an inclination of about 10° from the normal to the (001) plane.

Taking then the (0 k 0) planes, the short axis of the molecule was rotated about the normal to the (001), and the best relative agreement found between observed and calculated structure factors. This was obtained when the short axis was inclined at about 16° to the y axis. With these planes also it was found that the long axis must remain very near to the (xz) plane. With these values it is possible to calculate the co-ordinates of all the atoms.

Using the co-ordinates so found the structure factors for all the planes observed were calculated, neglecting the effect of the hydrogen atoms. The relative agreement for the (0 kl) planes was fairly good, but that for the (h 0 l) planes was not so satisfactory. It was realized that the (0 kl) planes were not sensitive to a movement of the plane of the molecule away from the b axis.

* Bernal, 'Proc. Roy. Soc.,' A, vol. 106, p. 749 (1924); Lonsdale, *ibid.*, vol. 123, p. 499. (1929).

The disagreement between the observed and calculated values for the (*h*0*l*) planes indicated that the molecule was further from this axis than the position given above and that the angle 16° between the short axis of the molecule and the *b* axis should probably be increased. However, as the structure factors of the (0*kl*) planes are very insensitive to such a movement, it seemed safe to assume that the good agreement obtained in the case of these reflections was sufficient to determine the signs of the structure factors. So at this stage of the investigation it was decided to carry out a two-dimensional Fourier analysis about the (0*kl*) zone and obtain refinement of the structure in this way.

Fourier Analysis

The application of the double Fourier series to crystal structures was developed by W. L. Bragg.* In the present investigation the density of scattering matter in the unit cell has been projected on to a plane perpendicular to the *a* axis. The density of scattering matter per unit area is given by :

$$\rho(yz) = \frac{1}{A} \sum_{-\infty}^{\infty} \sum_{-\infty}^{\infty} F(0kl) \cos . 2\pi (ky/b + lz/c) ,$$

for a projection along the *a* axis. The coefficients of the Fourier series are the experimental structure factors whose signs had been determined from the analysis given above.

For the successful application of this method it is necessary to measure reflections sufficiently weak to give structure factors approaching zero. For these measurements on chrysene the ratio of the strongest reflection to that of the weakest is about 3000 to 1. Even so it will be seen in Table II that planes of very small spacing such as (0121) and (062) have fairly large structure factors. The neglecting of planes having structure factors below these will tend to make the outer portions of the atoms in the projection a little uncertain. This probably explains the presence of some negative values of $\rho(yz)$ in the space representing the cleavage plane (001). If the absolute scale is a little too high, this will also tend to give negative values. The centre of the atoms will, however, be fixed by the bigger structure factors.

The density of scattering matter shown in the tables and the contour diagram is in absolute units. The number 480 shown in Table II as $F(000)$ is the total number of electrons in the unit cell. This is the first term in the Fourier series.

* 'Proc. Roy. Soc.,' A, vol. 123, p. 537 (1929).

Table II—Chrysene. Values and signs of $F(0kl)$. When k is odd, l is odd.
 When k is odd, $F(0k\bar{l}) = -F(0kl)$. When k is even, $F(0k\bar{l}) = F(0kl)$

		$\longleftarrow k \longrightarrow$												
		6	5	4	3	2	1	0	1	2	3	4	5	6
$l \downarrow$	0	-45		-14		-56		<u>+480</u>		-56		-14		-45
	1		-7		+12		-20		+20		-12		+7	
	2	-18		—		-36		+76		-36		—		-18
	3		—		—		+16		-16		—		—	
	4	—		—		+35		-64		+35		—		—
	5		—		-84		+36		-36		+84		—	
	6	—		—		—		+25		—		—		—
	7		—		-34		-6		+6		+34		—	
	8	—		—		-5		-27		-5		—		—
	9		—		+8		+12		-12		-8		—	
	10	—		—		—		+88		—		—		—
	11		—		—		+15		-15		—		—	
	12	—		—		-17		+65		-17		—		—
	13		—		+9		—		—		-9		—	
	14	—		—		+12		-25		+12		—		—
	15		—		-43		—		—		+43		—	
	16	—		-5		+32		—		+32		-5		—
	17		—		-54		—		—		+54		—	
	18	—		—		—		—		—		—		—
	19		—		—		—		—		—		—	
	20	—		—		—		—		—		—		—
	21		—		—		-16		+16		—		—	
	22	—		—		—		-18		—		—		—

Table III gives the results of the summation and fig. 3 (a) is the contour diagram obtained from them for one-half the unit cell. Fig. 3 (b) shows the relative positions of the atom centres, the lines drawn in full connect the atoms of the identical molecule the centre of symmetry of which is in the plane of the diagram. The dotted lines join atoms of the reflected and identical molecules which lie at half a translation perpendicular to the paper.

Table III—Projection along the a axis. Density as number of electrons per square $\text{\AA} \times 10$

18	3	6	18	28	31	26	18	10	7	6	5	3	1	10
19	5	2	13	23	26	21	14	8	7	6	6	4	2	5
20	8	3	5	13	17	14	9	6	5	8	6	6	4	8
16	8	4	3	11	16	13	9	6	5	6	7	7	7	5
5	4	6	16	25	29	22	17	14	8	7	8	9	9	2
0	17	22	35	47	50	42	25	20	13	10	2	11	11	7
10	29	35	50	63	65	55	37	29	22	18	17	17	15	10
23	38	41	48	60	62	53	45	34	32	27	21	22	16	9
49	56	49	49	50	47	42	41	43	48	49	42	32	21	9
83	79	60	45	36	31	28	33	46	59	63	53	38	25	8
105	95	66	42	26	17	12	22	42	57	62	53	37	22	5
103	93	62	38	23	11	6	11	27	45	49	42	28	18	5
77	71	48	32	22	13	4	3	14	27	33	28	19	15	4
45	44	30	22	20	13	6	2	9	21	28	22	16	13	5
34	32	20	15	18	14	9	7	16	32	37	31	20	15	4
50	42	26	17	14	10	8	15	34	54	60	49	31	22	5
85	63	43	23	12	7	6	21	49	75	84	68	45	29	11
113	95	58	32	16	8	6	21	52	82	93	80	59	44	29
112	97	65	43	30	20	12	19	43	69	83	78	68	65	58
83	82	62	55	52	43	29	17	24	46	69	64	71	88	89
45	51	53	66	77	70	44	20	14	23	35	47	67	94	107
16	28	43	70	91	85	56	23	8	10	19	31	52	86	75
4	17	32	60	83	79	51	22	8	12	15	21	35	62	74
6	14	21	41	60	58	36	23	11	20	24	22	27	44	51
8	9	7	18	32	29	14	6	7	22	28	24	23	36	36
10	9	3	13	24	22	7	4	4	21	31	31	33	50	55
8	12	11	26	41	38	17	1	1	14	26	35	45	71	86
6	15	25	49	70	66	37	10	1	9	18	32	51	86	106
10	22	36	66	90	86	55	22	11	12	19	29	50	85	95
24	32	41	66	85	82	56	31	24	32	34	36	46	69	81
60	49	43	52	63	60	44	34	44	60	63	52	43	49	60

$\xleftarrow{b/4}$ \times $\xrightarrow{b/4}$
 Centre of symmetry.

It will be seen that there is considerable overlapping of the atoms, the only two which come out entirely separated are two at the end of the molecule. The general appearance indicates the existence of the chrysene molecule as four plane hexagon rings. If we take the distance 1.41 Å found in anthracene and naphthalene* as the correct distance between atoms in the chrysene

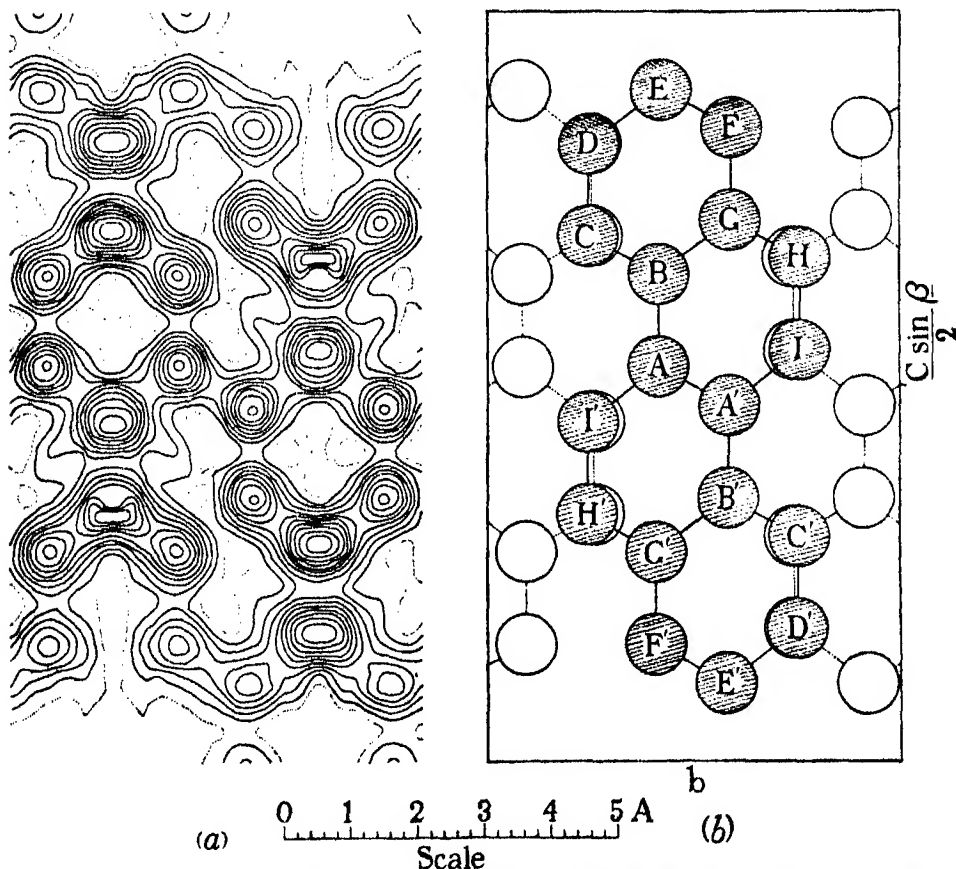


FIG. 3—Projection along the *a* axis. The dotted line represents the one electron line, the other lines are drawn at intervals of one electron per Å². (Only one-half the unit cell is shown.)

molecule, then we can calculate the orientation of the molecule from measurements of the co-ordinates of the atoms in the projection.

It is clear from the diagram that the long axis of the molecule is very near to the (*xx*) plane. Measurements of the diagram give 0.5° as the probable inclination.

* Robertson, 'Proc. Roy. Soc.,' A, vol. 140, p. 79 (1933); vol. 142, p. 674 (1933).

It is possible to measure the y and z co-ordinates of the two atoms E and F with fair accuracy as their centres can be easily estimated and the scale was 5 cm to one Angström unit. From these the inclination of the molecule was calculated. Also, from the length of the long axis, the angle that it makes with the x axis can be calculated. It is more difficult to measure the position and length of the short axis, but by estimating the centres of the two middle atoms it can be done approximately. When this has been done and its true direction in space found it is possible by combining its direction cosines with those of the long axis to find again the orientation of the molecule. The angles thus determined are in good agreement with those calculated from the co-ordinates of the two end atoms.

To simplify the calculations rectangular co-ordinate axes were chosen as follows: x along the a axis of the cell, y along the b axis and z' perpendicular to the $(00l)$ planes. The angles that the long axis of the molecule made with these axes are referred to as χ , ψ , ω respectively, and those that the short axis made as χ' , ψ' , ω' respectively.

The final values obtained for the orientation of the molecule to the above rectangular axes are:—

$$\begin{array}{ll} \chi = 102.0^\circ & \chi' = 118.4^\circ \\ \psi = 90.5^\circ & \psi' = 29.0^\circ \\ \omega = 12.0^\circ & \omega' = 95.4^\circ \end{array}$$

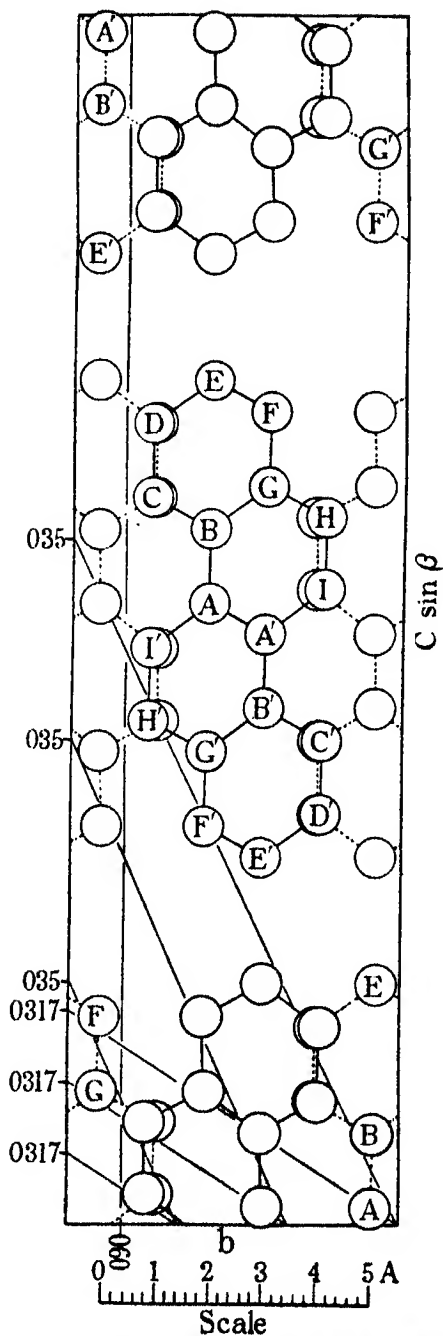


FIG. 4—Projection along the a axis showing the arrangement of the molecules in the complete unit cell.

This showed that the short axis of the molecule was turned through a bigger angle from the y direction than was indicated by the "trial and error" method ($\psi' = 16^\circ$). With this new orientation all the structure factors were recalculated and it will be seen from Table IV that the agreement between these and those observed is quite satisfactory.

Table IV—Measured and Calculated Values of the Structure Factors

hkl	$\sin \theta$ Cu. K α	F calculated	F measured
002	0.068	+92	76
004	0.139	-67	64
006	0.205	+20	25
008	0.274	-23	27
0010	0.342	+64	87
0012	0.411	+57	65
0014	0.479	-16	25
0016	0.547	-21	<15
0018	0.615	-2	<13
0020	0.683	-6	<13
0022	0.752	-20	18
020	0.249	-46	56
040	0.498	+15	14
060	0.747	-60	45
200	0.205	+105	104
400	0.409	-11	9
600	0.615	-34	27
011	0.130	-30	20
013	0.162	+16	16
015	0.213	-29	36
017	0.274	+1	6
019	0.334	+13	12
0111	0.399	+13	15
0113	0.468	+10	<10
0115	0.530	-1	<11
0117	0.597	+9	<13
0119	0.664	+5	13
0121	0.731	-18	16
022	0.260	-30	36
024	0.286	+25	35
026	0.325	+11	<8
028	0.372	-10	5
0210	0.426	+5	<10
0212	0.482	-23	17
0214	0.542	+10	12
0216	0.604	+37	32
031	0.376	+16	12
033	0.387	-5	<9
035	0.412	-70	64
037	0.444	-27	34
039	0.486	+8	8
0311	0.533	-18	<13
0313	0.583	+12	9
0315	0.637	-34	48
0317	0.695	-54	54
0416	0.742	-22	5
051	0.625	-13	7
062	0.753	-11	18
2012	0.365	+57	68
2010	0.308	+2	<12

Table IV—(continued)

<i>hkl</i>	<i>Sin θ</i> Cu. Kα	F calculated	F measured
20 $\bar{8}$	0.258	+8	8
20 $\bar{6}$	0.217	+46	49
204	0.190	—24	29
20 $\bar{2}$	0.175	+159	160
202	0.242	—57	62
204	0.292	+1	<11
206	0.347	—16	23
208	0.404	+9	14
2010	0.466	+24	23
404	0.370	—22	22
40 $\bar{2}$	0.384	—9	13
402	0.443	+33	26
404	0.484	+7	<16
406	0.534	—9	<17
408	0.585	—1	<19
4010	0.640	—18	<20
4012	0.695	+26	25
60 $\bar{2}$	0.735	—24	19
60 $\bar{2}$	0.695	—28	26
601 $\bar{0}$	0.558	—50	38
602	0.650	+27	22
6012	0.875	+40	25
80 $\bar{2}$	0.835	—47	32
801 $\bar{2}$	0.740	—17	20
110	0.161	—133	138
11 $\bar{1}$	0.386	+33	32
111 $\bar{0}$	0.323	+20	<29
11 $\bar{8}$	0.264	—19	<26
11 $\bar{6}$	0.212	+13	<23
114	0.170	—39	40
11 $\bar{2}$	0.150	+89	108
112	0.195	—29	37
114	0.247	+27	31
116	0.303	+7	<29
118	0.365	—5	<32
1110	0.430	+38	42
22 $\bar{8}$	0.340	—30	48
22 $\bar{6}$	0.313	—40	42
224	0.301	—3	<28
22 $\bar{2}$	0.302	+36	36
222	0.351	+15	<31
224	0.393	+53	60

In the zone (0*kl*) the structure factor of the weak plane (040) changes sign and there is some uncertainty about the sign of the structure factor of the still weaker plane (017). These, however, do not affect the summation to any appreciable extent.

The co-ordinates of all the atoms in the asymmetrical unit are given in Table V.

Intermolecular Distances

The closest distance between two atoms in different molecules is between the end atom, E, fig. 3, in the molecule at the centre of the cell, and the end

atom, E', in the identical molecule at the corner of the cell. This distance is 3.42 Å. This is rather smaller than the distance of closest approach found hitherto in aromatic compounds, and it is very nearly that found between layers of atoms in graphite.* It was realized that this distance can be increased very rapidly by tilting the molecule a few degrees further from the yz' plane,

Table V—Co-ordinates of Atoms with respect to Monoclinic Axes. Centre of Symmetry at the Origin

Atom	x Å	y Å	z Å
A	-0.22	0.53	0.32
B	0.15	0.52	1.86
C	-0.30	1.58	2.49
D	0.08	1.57	4.02
E	0.90	0.49	4.91
F	1.34	-0.59	4.27
G	0.97	-0.55	2.74
H	1.42	-1.62	2.10
I	1.04	-1.61	0.57

which can be done by increasing the angle ω . This has a marked effect, however, on the calculated structure factors of the $(h0l)$ zone. The agreement between observed and calculated values becomes worse as this angle is increased.

The distance between the nearest atoms in the molecules at the ends of the b axis is about 3.51 Å and between those in the identical and reflected molecules about 4.17 Å.

It is not possible to make an electron count owing to the overlapping of the molecules. The electron density in the separated atoms rises to a peak value of 6 which is similar to that found in other compounds of this type.†

I desire to express my thanks to the Managers of the Royal Institution and Sir William Bragg for the facilities provided in the Davy-Faraday Laboratory. I am greatly indebted to Dr. J. M. Robertson for his constant help and encouragement throughout the work and to Mrs. Lonsdale for some valuable discussions. I wish also to thank the Council of the University of Wales for a Fellowship which made it possible for me to carry out this work.

Summary

The crystalline structure of chrysene has been determined by a quantitative X-ray analysis. Crystal data: $a = 8.34$ Å, $b = 6.18$ Å, $c = 25.0$ Å,

* Bernal, *loc. cit.*

† Robertson, *loc. cit.*

$\beta = 115.8^\circ$; space group, C_{2h}^6 (I2/c) or C_4 (Ic). Crystal density = 1.27. Four molecules of $C_{18}H_{12}$ per unit cell.

The molecule appears to be planar and to consist of regular hexagons, the interatomic distance being 1.41 Å. The orientation has been found by a combination of the "trial and error" method and a double Fourier analysis about the (0kl) zone. The co-ordinates of each atom are given on p. 152.

*The Velocity of Corrosion from the Electrochemical Standpoint—
Part III*

By U. R. EVANS and R. B. MEARS

(Communicated by Sir Harold Carpenter, F.R.S.—Received March 16, 1934—

Revised May 2, 1934)

The previous paper* comprised a chemical and electrical survey of corroding iron specimens in potassium chloride solution, and indicated that the corrosion observed was quantitatively explained on simple electrochemical principles. Very similar views have been published by Herzog and Chaudron,† Baisch and Werner,‡ and by Schikorr.§ The papers of Bengough, Lee, and Wormwell,|| however, contain criticisms, some depending upon misunderstanding of the opinions criticized. The anomalous distributions of attack, held to disprove the "differential aeration view," have in many cases been described and explained by the Cambridge authors. The sinking of heavy corrosion-products from a point attacked usually causes the rising of columns of oxygen-rich liquid elsewhere, which wash the metal above and on each side of the sinking column, leading to the distributions observed; this will occur even when the source of the oxygen is below the specimen.

* Evans and Hoar, 'Proc. Roy. Soc.,' A, vol. 137, p. 343 (1932).

† 'C. R. Acad. Sci. Paris,' vol. 192, p. 837 (1931); vol. 193, p. 587 (1931); 'Trans. Electrochem. Soc.,' vol. 64, p. 87 (1933).

‡ "Erste Korrosionstagung" (Berlin), p. 83 (1931).

§ 'Z. Phys. Chem.,' A, vol. 160, p. 205 (1932); 'Mitt. Materialprüfungsamt,' Sonderheft, p. 22 (1933).

|| 'Proc. Roy. Soc.,' A, vol. 131, p. 494 (1931); vol. 134, p. 308 (1931); vol. 140, p. 399 (1933); 'Trans. Electrochem. Soc.,' vol. 61, p. 455 (1932); 'J. Soc. Chem. Ind.,' vol. 52, pp. 195, 228 (1933).

The water-line corrosion obtained by lengthy immersion of zinc in potassium chloride* can be explained in many ways, but is probably mainly due to attack by cathodically formed alkali. The distribution obtained by Bengough with Teddington water is the same as that obtained with Cambridge water and many calcium and magnesium salt solutions.†

The anomalous results obtained in Bengough's differential aeration cell‡ are attributable to the high resistance of the cell, which will cut down differential aeration currents in favour of local currents. The argument that the early work on differential aeration was similarly vitiated appears invalid; any correction for cell-resistance would here make the results even more difficult to explain by all theories other than that of differential aeration. In any case, recent studies§ in the absence of a diaphragm confirm the differential aeration view; the velocity obtained electrically agrees well with that measured directly.

The part played by the air-formed film is discussed elsewhere||; some observations by Homer¶ and Tronstad** agree with the views expressed. The role of crevices in metals was probably exaggerated in some early papers from this laboratory, but new researches†† indicate that the attack at crevices caused where glass or other inert substance rests on the metal is mainly due to differential aeration. The partial protection afforded by a corroding point to the area around it will be discussed elsewhere.

The new "Film Distribution View" of Bengough and Wormwell agrees with the view of the present authors in ascribing protection largely to cathodically formed alkali; there are other points of accord concealed by the mode of presentation. Differences of opinion exist on two matters, namely:

- (A) The effect of solid corrosion-products on oxygen-transport, and
- (B) The possible inhibition of corrosion by excess of oxygen.

The research described below was designed to settle these questions.

* Evans, 'J. Chem. Soc.,' p. 114 (1929); Borgmann and Evans, 'Trans. Electrochem. Soc.,' Preprint (1934).

† Evans, 'J. Soc. Chem. Ind.,' vol. 47, p. 57 T (1928).

‡ Bengough, Lee and Wormwell, 'Proc. Roy. Soc.,' A, vol. 131, p. 511 (1931).

§ Evans and Hoar, 'Proc. Roy. Soc.,' A, vol. 137, p. 363 (1932).

|| Britton and Evans, 'Trans. Electrochem. Soc.,' vol. 61, p. 446 (1932).

¶ 'Carnegie Scholarship Memoir,' vol. 21, p. 36 (1932).

** 'J. Iron Steel Inst.,' vol. 127, p. 430 (1933).

†† Mears and Evans, 'Trans. Faraday Soc.,' vol. 30, p. 417 (1934).

Materials—The electrolytic iron E33, kindly prepared by Dr. W. H. Hatfield, contained 0.06% carbon, no manganese, 0.03% silicon, 0.003% sulphur, and 0.017% phosphorus.

(A)—*The Effect of Solid Corrosion Products on Oxygen Transport*

The authors hold the view originally due to Aston* and McKay† that the corrosion set up on iron at points covered by rust coming from some other portion is due to oxygen-screening. Bengough‡ considers that his time-corrosion curves (which are linear or actually increase in slope) show that rust does not obstruct the passage of oxygen. A constant rate of disappearance of oxygen from the gas-space above the liquid can, however, be interpreted in many ways. It may indicate that the obstruction imposed by rust is small compared with the obstruction imposed by the gas-water interface, which obstruction is known to be considerable§ and is probably affected by stirring in the liquid. Miyamoto and Nakata's discovery,|| that the rate of oxidation of sulphite solution by oxygen is independent of sulphite concentration but proportional to the surface area of the liquid, appears to be analogous to Bengough's observation that corrosion is largely independent of the specimen size but is affected by the area of the liquid surface; both phenomena may be due to the failure of the slower molecules to pass the gas-water interface. But even if the total oxygen-entry is fixed by that interface, the *distribution* of oxygen between rusted and unrusted areas may still be affected by "screening." Bengough's view that "wherever metal ions can penetrate . . . dissolved oxygen can do so" seems to make no distinction between natural diffusion under a concentration gradient and ionic migration under a potential gradient.

It was decided to test directly the obstruction imposed on the passage of oxygen by various corrosion-products. The method used to test the passage of oxygen through liquid depended on the use of tubes lined internally with a roll of "ferrous hydroxide paper." This was prepared as follows. A roll of

* 'Trans. Amer. Electrochem. Soc.,' vol. 29, p. 458 (1916).

† 'Ind. Eng. Chem.,' vol. 17, p. 23 (1925).

‡ 'Proc. Roy. Soc.,' A, vol. 140, p. 411 (1933).

§ Lewis and Whitman, 'Ind. Eng. Chem.,' vol. 16, p. 1217 (1924); Whitman and Davis, 'Ind. Eng. Chem.,' vol. 16, p. 1235 (1924); cf. Brimley, 'Chem. Ind.,' vol. 52, p. 472 (1933).

|| 'Bull. Chem. Soc., Japan,' vol. 6, p. 9 (1931) [Abstract, 'Brit. Chem. Abs.,' A, p. 437 (1931)].

filter paper was placed in a test-tube, and the mouth of the tube was closed by a rubber bung furnished with two glass tubes. The test-tube was evacuated and refilled three times with purified nitrogen. About 5 cc of 5% ferrous sulphate solution (oxygen-free) was admitted, and any excess blown out with purified nitrogen. Next, purified nitrogen saturated with ammonia gas was blown in, to precipitate ferrous hydroxide in the filter paper. The tubes were then ready for use. The paper was white at first, but soon became slightly green, possibly because ferrous hydroxide, as shown by Schikorr,* liberates hydrogen from water, passing to a ferroso-ferric product. The tubes could, however, be stored for weeks without any brown appearing.

If oxygen was admitted into such a tube, the whole paper became brown within 15 minutes. If the tube was first partly filled with liquid, and then the space above the liquid was filled with oxygen, the passage of oxygen down into the liquid could be followed by the advance of the brown-green boundary. Several series of comparative experiments were thus conducted on the diffusion of oxygen through test-tubes containing 0.1 N potassium chloride solution, with or without corrosion products. The corrosion-products tested were:—

- (a) Zinc "hydroxide" (or basic chloride) obtained by natural corrosion of the spectroscopically pure metal in 0.1 N potassium chloride solution.
- (b) Zinc "hydroxide" obtained by precipitation from a mixture of 0.2 N zinc chloride and 0.2 N potassium hydroxide.
- (c) Magnetic iron oxide obtained by natural corrosion of electrolytic iron in 0.1 N potassium chloride solution.
- (d) Magnetic iron oxide obtained by mixing ferrous and ferric hydroxides suspended in 0.1 N potassium chloride solution.
- (e) Ferric hydroxide obtained by electrolysing electrolytic iron electrodes in 0.1 N potassium chloride containing hydrogen peroxide.
- (f) Ferric hydroxide obtained by precipitation from a mixture of 0.2 N ferric chloride and 0.2 N potassium hydroxide.
- (g) Ferrous hydroxide obtained by precipitation from an air-free mixture of 0.2 N ferrous sulphate solution and 0.2 N potassium hydroxide solution.
- (h) Aluminium hydroxide obtained by electrolysing specially pure aluminium electrodes in a solution of 0.1 N potassium chloride.

* 'Z. anorg. Chem.,' vol. 212, p. 34 (1933). In this research, Schikorr made his ferrous hydroxide from ferrous salts and alkali, thus meeting Bengough's criticism that the hydrogen came, not from ferrous hydroxide, but from metallic iron.

- (i) Aluminium hydroxide obtained by precipitation from a mixture of 0.2 N aluminium chloride and 0.2 N potassium hydroxide.

In every test, comparative experiments were conducted with clear 0.1 N potassium chloride without corrosion product.

To prevent complications due to the settling of the voluminous precipitate during the experiment, the product was, in most experiments, freed from the entrained liquid by centrifuging until a consistency was reached at which no gravity-settling took place; no attempt was made to express the liquid beyond this point. Special series were conducted on precipitates which had not been settled or centrifuged, and in such cases settling occurred during the experiment.

The conditions of testing were:—

(1) *Liquid stagnant*, the tube being surrounded with a glass water-jacket placed in a thermostat at 25° C.

(2) *Liquid exposed to Adeney convection-streaming* produced by blowing a current of unsaturated air, which had previously passed through 3 N sodium hydroxide solution and a saturated solution of sodium fluoride. This led to much more rapid oxygen-transport than the stagnant conditions.

Two methods of measuring the advance of oxygen were used. In the first, a long roll of ferrous hydroxide paper ran the length of the liquid-filled portion of the tube, the advance of the brown colour indicating the progress of oxygen. This method gives a complete distance-time curve; the absorption of oxygen by the ferrous hydroxide paper may perhaps affect the natural velocity, but, since the experiments with and without corrosion-product will both be affected, the comparison remains valid. In the second method, there was merely one small piece of ferrous hydroxide paper at the bottom of the tube, and although no curve was obtained, the time of arrival of the oxygen at the bottom, unaffected by any unnatural oxygen-loss on the way, could be compared in the various tubes. The times taken were naturally a little shorter than in the first method, but the order of arrival for different products was the same.

Typical results are shown in figs. 1 and 2 and in Table I; every point in fig. 2 represents the mean of two reasonably concordant experiments. Corrosion-products obtained from the metal, fig. 1, produced an effect not very different from similar products obtained by precipitation, fig. 2. In every experiment in which there was *no settling* of corrosion-product, the presence of the product *retarded* notably the passage of oxygen downwards, as compared with the corresponding experiment using clear liquid. This was

equally true for both modes of transport, but in every experiment where there was *settling* during the experiment, the corrosion-product actually *accelerated* the passage of oxygen downwards.

A specially interesting case was that of magnetite, which could not be satisfactorily compacted by centrifuging. Some settling occurred during the

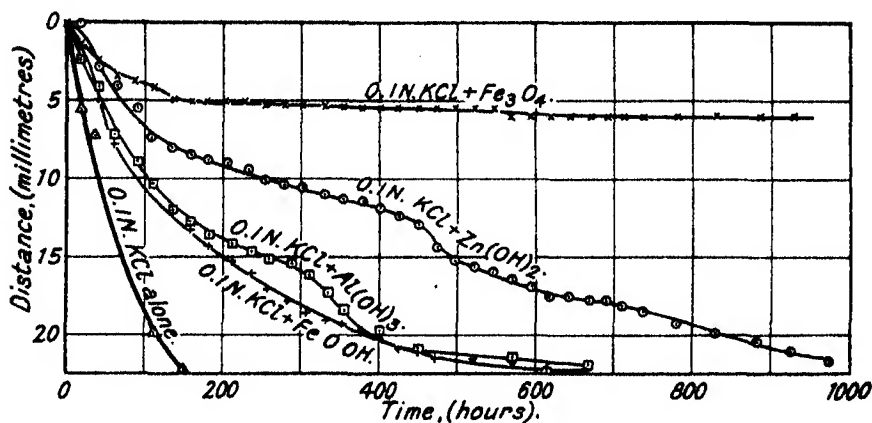


FIG. 1

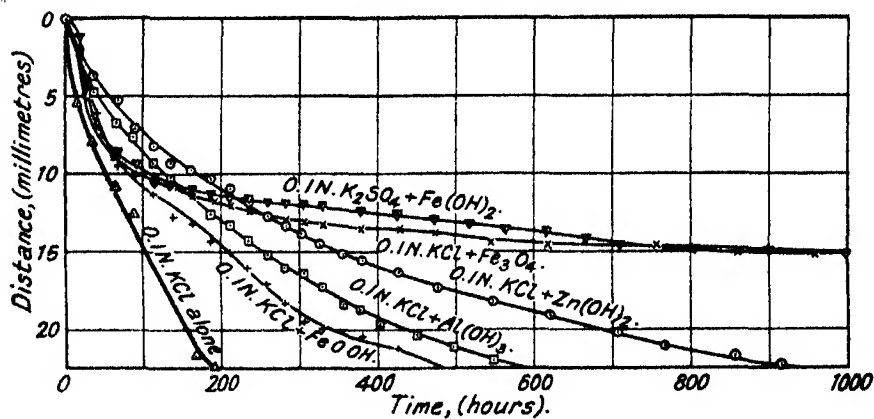


FIG. 2

first part of the experiment, and, whilst this continued, the passage of oxygen downwards was quite rapid. When once the oxygen-front had passed the magnetite-liquid boundary, the passage of oxygen slowed up and became almost stationary. In comparing this result with Bengough and Wormwell's statement* that magnetite layers may be freely pervious to oxygen, it is fair

* 'Proc. Roy. Soc.,' A, vol. 140, p. 419 (1933).

to point out that "aged" magnetite can be very different from the freshly produced body. There appears also a *prima facie* contradiction of the work of Roetheli and Brown,* but here the explanation is apparent; in Roetheli and Brown's experiments, the liquid was in motion, and the granular magnetite would be more readily thrown off than the clinging hydrated ferric oxide, which is then likely to be the more protective.

Table I—Advance of oxygen downwards through 0.1 N potassium chloride containing various solids

Compound tested	Time in hours needed for brown colour on paper to extend 2.0 cm below surface			
	Air current playing on surface; paper down whole side	Stagnant conditions; paper at bottom only	Stagnant conditions; paper down whole side	Paper down whole side (settling during experiment)
None (clear 0.1 N KCl)	43	138	150	—
Hydrated ferric oxide	185	269	326	90
Aluminium hydroxide	117	353	426	—
Zinc hydroxide	—	571	700	42

The passage of oxygen through ferrous hydroxide is extremely slow, undoubtedly because here the precipitate absorbs oxygen; but the magnetite formed occupies a smaller volume than the ferrous hydroxide, so that the settling is renewed; this favours the advance of oxygen, and the resultant rate is similar to that through magnetite. Aluminium hydroxide, which offers a slightly greater obstruction to oxygen under stagnant conditions than hydrated ferric oxide, produces a smaller obstruction under "Adeney streaming" conditions, probably because much of the hydroxide is in the "sol" form and thus shares the motion of the liquid.

In all the experiments in which settling of the product was permitted, the transport of oxygen was stimulated. Now in Bengough's experiments, the specimen does not occupy the whole cross-section of the vessel, and a falling of the product over the edge must occur. It seemed possible that this might be the cause of the maintenance of the rate of oxygen disappearance. To test this explanation, experiments were conducted on the corrosion of horizontal specimens of iron (1) under conditions permitting the rust to fall over the edge, and (2) under conditions not permitting this "falling over." The specimens were discs 2.4 cm diameter, with the bottom and edges protected by wax, set in a vessel of diameter 3.7 cm. Under conditions (1), an annular "ditch,"

* 'Ind. Eng. Chem.,' vol. 23, p. 1010 (1931).

of breadth 0.65 cm and depth 1 cm, surrounded the specimen, but under conditions (2), this was filled with wax up to the level of the surface of the specimen. The absorption of oxygen was measured by Borgmann's modification of the Bengough apparatus*; the solution was 0.1 N potassium chloride, the depth of immersion 1.5 cm, and the temperature controlled at 25.2° C in all experiments.

Three experiments were conducted under each of the two conditions. When the "falling over" of rust was permitted, the curves were nearly straight, curve I, fig. 3, thus confirming Bengough's results. When it was not permitted, the curves soon showed a falling off of oxygen absorption with the time, curve IIa, fig. 3, suggesting that the corrosion-product *does* obstruct the passage

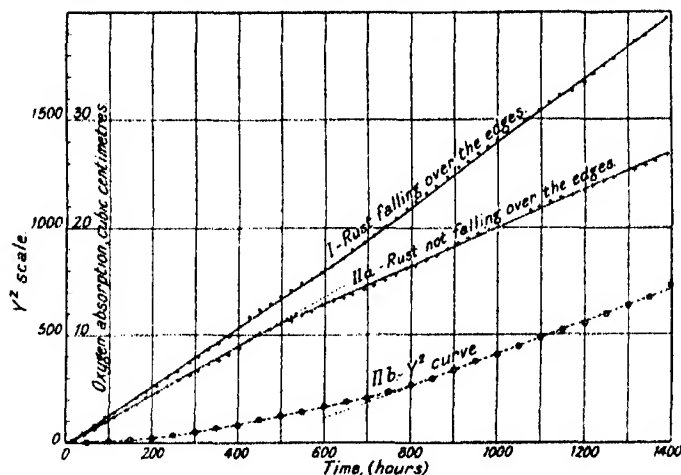


FIG. 3

of oxygen. If the accumulating rust (y) adds to the combined resistances (A) of the liquid-surface and liquid column, an extra resistance, by , proportional to the thickness of the rust-layer, we should expect, under conditions of "oxygen-starvation" where the oxygen-concentration next the metal is small compared to the saturation-value C_s , an equation for the velocity

$$dy/dt = \frac{C_s}{A + by},$$

which is of the form

$$t = \kappa_1 y^2 + \kappa_2 y + \kappa_3.$$

At small values of t , the term $\kappa_2 y$ will predominate over $\kappa_1 y^2$ and the curve connecting y and t will be linear, whilst, at large values, $\kappa_1 y^2$ will predominate,

* 'Trans. Electrochem. Soc.' (preprint) (1934).

and the curve connecting y^2 and t will be linear. Curves IIa and IIb show that both these expectations are realized under the conditions studied. Doubtless they might not always hold good, since the rust-layer is not homogeneous, and several complicating factors have been neglected.

However this may be, the straight and rising curves which form the basis of recent criticisms of the differential aeration view are due to the falling of the corrosion-products over the edges of the specimens. When this is avoided, the gradient diminishes with the time. *So far as time-corrosion curves can give any information at all, they support the view that corrosion-products settled on the surface screen it from oxygen.*

It may be added that weight-loss experiments also showed that the corrosion-rate was depressed when the "falling-over" of rust was avoided. Hydrogen-evolution (measured by Bengough's combustion method) was negligible in the early stages, but always became appreciable later. On this point, Bengough, Lee, and Wormwell's results* were confirmed.

In explaining the delivery of oxygen to corroding metal, some investigators postulate a circulation due to differences in density between oxygen-free and oxygen-saturated water. It was decided to compare these densities. The apparatus used is shown in fig. 4. Both tubes were filled with water previously freed from dissolved gases by boiling under reduced pressure. The water in tube A only was then saturated with purified oxygen, and the whole was allowed to stand for an hour in a thermostat at 25° C. The taps T_1 and T_2 were opened and, after establishment of equilibrium, the difference of levels was recorded photographically.

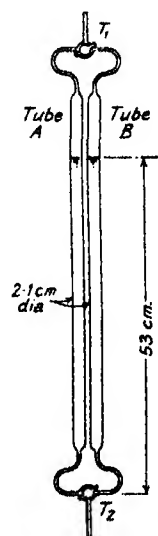


FIG. 4

Experiments were conducted :

- (1) With the level in A higher than in B, before opening the taps.
- (2) With the level in B higher than in A, before opening the taps.
- (3) and (4) As (1) and (2), but using A to hold the gas-free water and B the water containing oxygen.
- (5), (6), (7), and (8) As (1), (2), (3), and (4), but using purified air instead of oxygen.

* 'Proc. Roy. Soc.,' A, vol. 134, p. 328 (1931).

In no case was a difference in height exceeding 0.25 mm observed, and it is concluded that, taking the density of oxygen-free water as 1.0000, that of oxygen-saturated water lies between 0.9995 and 1.0005.

Such a small difference could hardly provide the head demanded for the circulation; in any case the effect must be slight compared with that caused by metallic salts, potassium or sodium hydroxide, and (particularly) solid corrosion-products, descending over the edges of the specimens. The falling of these bodies is undoubtedly responsible for the circulation both with vertical and horizontal specimens.

(B)—*Can Oxygen act as Inhibitor?*

Schikorr* has expressed the view that oxygen can act, not only as a stimulator of corrosion, but also, under other conditions, as an inhibitor. These views have been contested by Lee.† The word "inhibitor" may be used in three senses, as meaning a body which decreases, either (1) the velocity of attack, (2) the area of attack, or (3) the probability of attack. Experiments by Borgmann and one of the authors‡ appears to show that, below oxygen-nitrogen mixtures, the corroded area of iron immersed vertically in potassium chloride solution increases steadily as the proportion of oxygen is decreased, although the velocity of attack diminishes. Lee considers the evidence insufficient and a fuller series of experiments on electrolytic iron E33 with various mixtures of oxygen and nitrogen have now been carried out in triplicate.

The results are shown in fig. 5, each point showing the mean of three experiments. Curve 1 indicates the total corrosion, which falls steadily as the oxygen-concentration is diminished.§ The attack occurs along the edges and bottom portions; at high oxygen-concentrations the line separating the etched area at the bottom is generally horizontal, as in the "ideal distribution" described in an earlier paper.|| The level of this horizontal rises steadily as the oxygen-concentration falls (see Curve 2) reaching the water-level when the oxygen-concentration is about 3%. On certain specimens, attack from central points prevented the level of this horizontal from being ascertained; such experiments

* 'Korr. Met.,' vol. 4, p. 244 (1928); 'Z. Elektrochem.,' vol. 39, p. 409 (1933).

† 'Trans. Faraday Soc.,' vol. 28, p. 707 (1932).

‡ 'Z. Phys. Chem.,' vol. 160, p. 194 (1932); 'Trans. Faraday Soc.,' vol. 28, p. 813 (1932).

§ Cf. Similar results on lead in oxygen-nitrogen mixtures, described by Burns and Salley, 'Ind. Eng. Chem.,' vol. 22, p. 293 (1930).

|| Evans and Hoar, 'Proc. Roy. Soc.,' A, vol. 137, p. 345 (1932).

are necessarily omitted from Curve 2, but Curve 3 comprises *all* the specimens, the level on the "abnormal" specimens being taken as the lowest point reached by the unetched area; the mean level thus obtained also rises as the oxygen-concentration falls. Curve 4 shows the full area affected, including the corroded "wings" extending up the cut edges (these wings actually decrease with diminishing oxygen). The total area *increases* as the oxygen-concentration decreases, and at 3% oxygen represents the whole immersed area of the specimen (at 0% oxygen it is more than 100% of the immersed area, owing to creep). However, in the low-oxygen mixtures, owing to the small total corrosion and the large area affected, the *intensity* of the attack is very

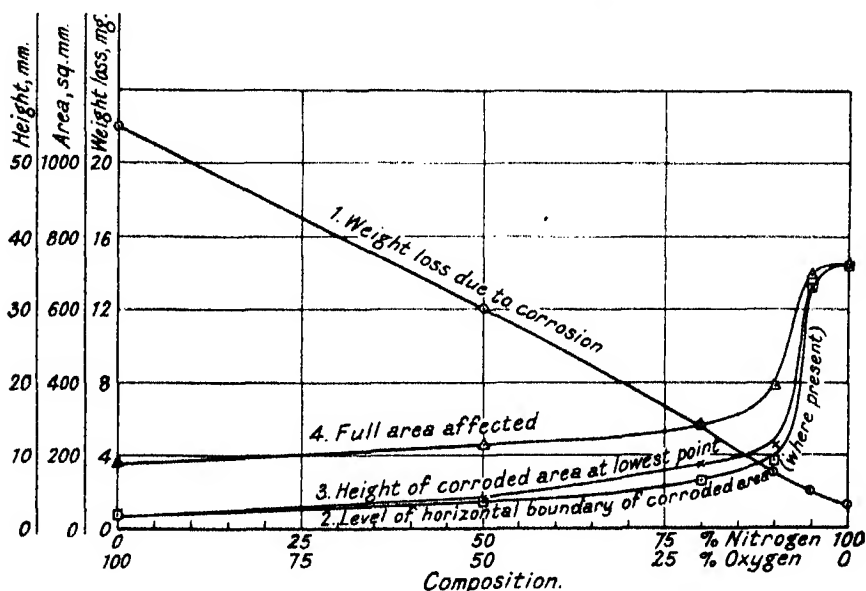


FIG. 5

small, especially at points in the lower parts of the specimen. In the experiments conducted below pure nitrogen, there is no true rust, but only a little dark green matter adhering, especially near to the water-line; the alteration definitely extends over the whole immersed area. The feebleness of the attack below nitrogen explains the apparent contradiction between the two passages quoted by Lee* from two papers by Borgmann and one of the authors.† On all essential points, Borgmann's experimental results are confirmed. The

* 'Trans. Faraday Soc.,' vol. 28, p. 825 (1932).

† 'Z. Phys. Chem.,' A, vol. 160, p. 194 (1932); 'Trans. Faraday Soc.,' vol. 28, p. 813 (1932).

statement of Liebreich,* who claims to have produced the same distribution of attack in absence as in presence of oxygen, and for this reason rejects the differential aeration view, cannot be upheld.

These experiments suggested that if the experimental area were small enough, high oxygen-concentration might sometimes prevent corrosion altogether, at least in dilute solutions. This possibility was tested statistically, using a new method of obtaining large numbers of "square drops" almost simultaneously. A large quantity of electrolytic iron was abraded with No. 3 Hubert emery paper, cut into specimens 2.5 cm by 5 cm, which were "shuffled," degreased twice with carbon tetrachloride, and stored in a desiccator until required. In preparing for a run four specimens were removed, each was abraded with fresh emery paper, wiped with clear cotton wool and weighed.

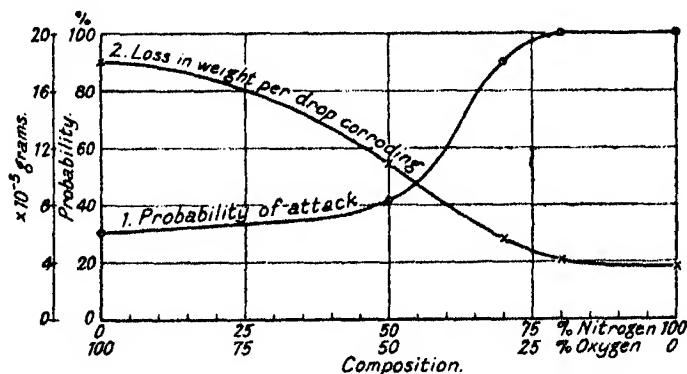


FIG. 6

Then, by means of a closely cropped paint brush, two sets of parallel lines were traced with a solution of paraffin wax in carbon tetrachloride (100 gm per litre), so as to leave 24 unwaxed 3 mm squares on each specimen. After an hour in a desiccator at 25° C, the specimens were attached to a glass plate and introduced into a glass vessel, which was then filled with the mixture of oxygen and nitrogen to be investigated. 0.001 N potassium chloride solution, saturated with the gas mixture under consideration, was introduced into the vessel, allowed to run over the surface of the specimens, and was then sucked out again, leaving 24 independent square drops, separated by the waxed lines, on each specimen. After 22 hours the number which had developed corrosion was counted; in nearly all cases, either a drop developed distinct attack or remained absolutely unchanged. The results, shown in fig. 6, Curve 1,

* 'Z. Phys. Chem.,' A, vol. 155, p. 123 (1931).

indicate that the frequency of attack definitely decreases as the oxygen-concentration is increased. On the other hand, it was obvious to the eye, and verified by loss of weight (fig. 6, Curve 2) that, where corrosion had actually started in a drop, the attack was very much greater in the oxygen-rich mixtures than in the oxygen-poor mixtures. Thus oxygen decreases the "probability" of corrosion, but increases the "conditional velocity."

Evidently, therefore, oxygen is a stimulator of corrosion in some senses of the word and an inhibitor in others. There may be cases where the inhibitor action is unimportant compared to the stimulator action; but the converse is also true. Bryan and Morris,* for instance, have shown that the corrosion of a chromium-nickel alloy and a chromium-nickel steel in dilute citric acid may be greatly *reduced* by the presence of oxygen.

In publishing this work, one of us (U. R. E.) wishes to express sincere thanks for the aid given by the Armourers' and Brasiers' Company.

Summary

1—Bengough's Film Distribution View of Corrosion has much in common with views published by the present authors, and can in part be accepted.

2—Criticisms of the Differential Aeration View based on Bengough's linear corrosion-time curves are invalid; with precautions to prevent rust from falling over the edges of the specimens, the curves soon cease to be straight, and indicate that rust obstructs the passage of oxygen. Direct measurement of oxygen advance through columns of potassium chloride shows that all the corrosion-products tested can cause obstruction to oxygen-transport. The difference in the density of water produced by oxygen is too small to play a serious part in the transport of oxygen to the metal.

3—In the corrosion of iron vertically immersed in potassium chloride below oxygen-nitrogen mixtures, the velocity *increases*, and the area affected *diminishes* with the oxygen-concentration, thus confirming Borgmann.

4—A statistical study of drops of potassium chloride on iron below oxygen-nitrogen mixtures shows that the probability of attack *diminishes* and the conditional velocity *increases* with oxygen-concentration. This confirms the belief of Schikorr that oxygen can be regarded either as a stimulator or inhibitor of corrosion.

* "Report of the Food Investigation Board," pp. 174, 177 (1932).

The Excitation of Band Systems by Electron Impact

By G. O. LANGSTROTH,* Ph.D., 1851 Exhibition Scholar, Rijks Universiteit,
Utrecht, Holland

(Communicated by O. W. Richardson, F.R.S.—Received March 16, 1934)

§1 *Introduction*

The relative positions of the more intense bands of a system† in the usual square array can be predicted by classical methods‡ (the Frank-Condon principle) from the potential curves for the initial and final states. This procedure is upheld in its essentials by wave mechanics,§ and a further wave mechanics development|| permits the calculation of transition probabilities in emission in band systems of symmetric diatomic molecules. The essential features of the theory are that the relatively massive nuclei may be assumed not to respond immediately to changes in the electronic arrangement of the molecule, and that one need not evaluate that part of the electric moment directly concerned with such electronic rearrangements. These circumstances reduce the problem to one for simple oscillators with known potential functions.

For a *complete* theory of the relative *intensities*, however, the details of the accompanying phenomenon of excitation must be known. While these are necessarily extremely complicated for bands emitted from different initial electronic states, a considerable simplification may be expected for bands emitted from the same electronic state. The problem of the relative excitation probabilities then forms the excitation analogue of the Frank-Condon principle.

This paper presents a study of excitation of band systems in nitrogen by impact of electrons of known energy, and also of the complete intensity problem. A simple excitation theory is developed by introducing assumptions (see § 2) analogous to those of the emission treatment. It is possible to show that if these assumptions are valid the intensity ratios of bands having the same electronic transition but different initial vibrational quantum numbers in emission should be independent of the velocity of the exciting electrons. Furthermore, under these conditions the relative excitation probabilities can

* Research Associate, McGill University, Montreal, Canada.

† This term, by definition, includes all bands with the same electronic transition in emission.

‡ Condon, 'Phys. Rev.', vol. 28, p. 1182 (1926).

§ Condon, 'Phys. Rev.', vol. 32, p. 858 (1928).

|| Hutchisson, 'Phys. Rev.', vol. 36, p. 410 (1930).

be calculated, and used with the emission probabilities to furnish predicted complete intensities for comparison with experiment. The assumptions introduced are not limited to the nitrogen molecule, but apply quite generally to symmetric diatomic molecules.

In order to test the validity of the basic assumptions the relative intensities of the second positive bands $0 \rightarrow 2$ (λ 3805), $1 \rightarrow 3$ (λ 3755), and $2 \rightarrow 4$ (λ 3710) with various exciting electron voltages between 14 and 160 volts, and of the negative bands $0 \rightarrow 1$ (λ 4278) and $1 \rightarrow 2$ (λ 4237) with voltages between 21 and 50 volts, were determined.* The optical excitation curves for these bands were also obtained, but the main interest lies in the intensity ratios of the bands at each voltage. It is believed that under the conditions of the experiment practically the entire initial level populations of these bands were due to excitation by electron impact directly from the ground state of the neutral molecule.

The intensity ratio of the negative bands, and the ratios of the positive bands with exciting voltages greater than 30 volts, were found to be independent of the voltage within the experimental error. Below 20 volts, however, the ratios of the positive bands depend strongly on the exciting voltage. There is no corresponding change in the relative development of the rotational structure of the different bands. The voltages at which the bands first appear agree well with those values found by Sponer.†

These results indicate that the assumptions introduced in the excitation treatment are valid (for N_2) with exciting voltages greater than 30 volts. Under these conditions the relative intensities can be calculated by the methods of § 2. It is found that, while the relative emission probabilities calculated from Hutchisson's work are quite opposite in sense to the observed intensities, the calculated complete intensities agree surprisingly well with experiment. Values for the complete intensities were also estimated by the simple graphical method‡ in order to see how well it represents the facts. The values so found are in the right intensity order, but the excitation and emission probabilities taken singly are quite different from those predicted by wave mechanics.

The dependence of the intensity ratios of the second positive bands on the exciting voltage for a range of about 7 volts above the excitation potential

* Some early experimental facts have already been published. Ornstein and Langstroth. 'Proc. Acad. Sci. Amst.,' vol. 36, p. 394 (1933).

† 'Z. Physik,' vol. 34, p. 622 (1925).

‡ With the assumption that in the classically predicted continuum the emitting or excited molecules go to the nearest quantum state.

is probably due entirely to the difference in excitation potential of the initial emission vibrational levels. On the other hand, one should expect a similar dependence in the intensity ratios of the negative bands and this is not found. Owing to the conditions under which the experiments were carried out (*e.g.*, undetermined velocity distribution of the exciting electrons), the present data are not sufficient for a critical discussion of this part of the curves, but they give some ground for suspecting that the "picture" of an excitation transition in this region may differ from that for higher voltages.

§ 2 Formulation of the Problem

Hutchisson (*loc. cit.*) has published formulæ for the electric moment matrix elements for bands of symmetric diatomic molecules. As a result of simplifying assumptions, these were calculable from the wave functions for harmonic oscillators with appropriate potential functions. It was assumed that (1) the complete wave function can be approximately expressed as a product of a function of the electronic co-ordinates only, and one of the nuclear co-ordinates only,* and (2) that the instantaneous electric moment can be approximately written as the sum of two functions dependent on the electronic and nuclear co-ordinates respectively; (2) takes into account the relatively large inertia of the nuclei. As a consequence of (1) and (2), that part of the electric moment directly concerned with the electronic rearrangement of the molecule enters, for bands of a system, only as a constant which need not be evaluated. The expression for the electric moment associated with the transition $n' \rightarrow n''$, is,

$$P_{n'n''} = C \frac{(n'! n''!)^{\frac{1}{2}}}{2^{(n'+n'')/2}} \sum_{l=0}^{n' \text{ or } n''} \sum_{i=0}^{(n'-l)/2} \sum_{j=0}^{(n''-l-1)/2} a_{2l} b_{2i} c_{2j} d_{n'-2i-l} e_{n''-2j-l}, \quad (1)$$

where

$$\begin{aligned} a_{2l} &= \frac{1}{l!} \left(\frac{4\alpha}{1+\alpha^2} \right)^l & b_{2i} &= \frac{1}{i!} \left(\frac{1-\alpha^2}{1+\alpha^2} \right)^i \\ c_{2j} &= \frac{1}{j!} \left(\frac{-(1-\alpha^2)}{1+\alpha^2} \right)^j & d_{n'-2i-l} &= \frac{1}{(n'-2i-l)!} \left(\frac{-2\alpha\delta}{1+\alpha^2} \right)^{(n'-2i-l)} \\ e_{n''-2j-l} &= \frac{1}{(n''-2j-l)!} \left(\frac{2\delta}{1+\alpha^2} \right)^{(n''-2j-l)} \\ \alpha &= (\omega''_0/\omega'_0)^{\frac{1}{2}} & \delta &= 0.1221 (r'_0 - r''_0) (\omega''_0 M)^{\frac{1}{2}}, \end{aligned}$$

n is the vibrational quantum number, ω_0 the "frequency" of vibration for very small amplitudes (in cm^{-1}), M the atomic weight of the nucleus ($O = 16$),

* Born and Oppenheimer, 'Ann. Physik,' vol. 84, p. 457 (1927).

and r_0 the separation (in Angstrom units) of the nuclei in static equilibrium. The primed and doubly primed terms refer respectively to the initial and final emission states. The upper limit of the first sum is the smaller of n' or n'' , and the upper limits of the second and third sums are the upper or lower figures depending on whether $n - k$ is even or odd.

We now attempt to treat the excitation process in a similar way. We assume (a) that the complete excitation function, like the wave function for the molecule, may be written as the product of two functions which depend respectively on the electronic and nuclear co-ordinates, i.e.,

$$G(x, r, v) = G(x, v) \cdot F(r, v), \quad (2)$$

where x and r denote respectively the electronic and nuclear co-ordinates, and v represents the velocity of the exciting electrons.

Neglecting the contribution of recombination and cascade effects to the populations of the initial levels, and omitting for the time a v^4 correction, the relative intensity of any particular band is given by,

$$I_{n'n''} = P_{n'n''}^2 \sum_k N_k \int_0^\infty G_{kn'}(x, v) \cdot F_{kn'}(r, v) \cdot f(v) dv, \quad (3)$$

where N_k denotes the number of molecules in some initial excitation state k , $f(v)$ represents the velocity distribution of the exciting electrons, and $P_{n'n''}^2$ the probability of transition in emission.

Two further assumptions are necessary to simplify the problem; (b) the exciting electrons have no direct effect on the nuclei which are about 26,000 times as massive, and (c) the electronic rearrangement of the molecule takes place so rapidly in excitation that the nuclear co-ordinates may be considered as unchanged during it. With suitably chosen experimental conditions the great majority of the molecules are in the ground state (n), so that equation (3) becomes,

$$I_{n'n''} = N_0 P_{n'n''}^2 \cdot F_{nn'}(r) \int_0^\infty G_{nn'}(x, v) \cdot f(v) dv. \quad (4)$$

For all bands of a system the expression under the integral sign is the same, and under these conditions $P_{n'n''}$ is given by equation (1). Furthermore, a slight consideration shows that $F(r) = P^2(r)$. We then have

$$I_{n'n''} = C_1 P_{n'n''}^2(r) \cdot P_{nn'}^2(r). \quad (5)$$

which gives the complete intensities in terms of the results of equation (1). It should give correct results if equation (4) holds. The latter, based on

assumptions (a), (b), and (c), predicts the constancy of the band intensity ratios within a system with change in exciting voltage. It should be stressed that the validity of (a), (b), and (c) is essential for this prediction, for if they are not correct constancy cannot occur. An experimental test of this point then provides an excellent means of ascertaining whether or not equation (5) may be expected to give correct results. If it is, a comparison with experiment of the intensities calculated from (5) furnishes a complete test of the entire theory.

The values of the molecular constants necessary for the calculations are included in Birge's tables,* with the exception of a value for r_0 of the ground state of the neutral molecule. There seems to be no "observed" value for this in the literature. Morse,† however, has calculated that it should be about 1.09 Å. For reasons to be discussed later the value 1.096 has been used in this paper. The calculated values of α and δ for use in equation (1) are given in Table I.

Table I—Molecular Constants for Intensity Calculations

Process.		Negative initial state.	Second positive initial state.
Emission (from)	$\begin{cases} a \\ \delta \end{cases}$	0.957 -0.899	0.923 -1.19
Excitation (from molecule ground state to)	$\begin{cases} a \\ \delta \end{cases}$	1.01 0.470	0.928 -1.09
Recombination (from ion-molecule ground state to)	$\begin{cases} a \\ \delta \end{cases}$	— —	0.960 -0.651
Excitation (from ion-molecule ground state to).....	$\begin{cases} a \\ \delta \end{cases}$	1.04 0.930	— —

The potential curves which were used in this paper were calculated from Morse's formula‡

$$E = A + D (e^{-2\beta(r-r_0)} - 2e^{-\beta(r-r_0)}), \quad (6)$$

E represents the energy (cm^{-1}), r the distance apart of the nuclei (in Ångström units), and A , D , and β are characteristic constants whose values are tabulated in Morse's paper.

§ 3 Experimental §

The results of these experiments were obtained with two different excitation tubes. The first consisted of a hot filament from which electrons fell through

* 'Int. Crit. Tables,' vol. 5, p. 411 (1929).

† 'Phys. Rev.,' vol. 34, p. 57 (1929).

‡ Cf. Rydberg, 'Z. Physik,' vol. 73, p. 376 (1931).

§ For the details of the experimental technique see Ornstein and Langstroth, 'Proc. Acad. Sci. Amst.,' vol. 36, p. 384 (1933).

a known accelerating field, and passed through a grid into a field-free observation space. In the second a system of rather wide slits was incorporated to define the electron beam. The tubes were filled to 0.1 mm of mercury pressure with purified nitrogen, and were generally operated with tube currents of 0.30 milliamperes.

A Standard Hilger E1 quartz spectrograph, and quartz optics were used. The exposure time was 30 minutes. Intensity marks were put on each plate with a step-slit and quartz band lamp. Exposure times for the intensity marks and for the nitrogen bands were made equal in the way described in a former paper. A wide slit (about 0.5 mm) was used in order to blend the rotational structure. Since maximum blackening measurements may not yield objection free results for bands, integration measurements were also carried out with the aid of an analysing apparatus designed by Wouda.*

No corrections for background or interfering bands or lines were necessary, except for the negative band λ 4237, where a slight correction for the tail of the positive band λ 4269 had to be made.

§ 4 Results

The following tables include determinations made with both experimental tubes. No ν^4 corrections have been made. The intensities are given to the nearest two figure value, but the intensity ratios have been calculated from the original three figure values. Owing to slight variations in the tube current during an exposure, certain plates are not suitable for the determination of the optical excitation functions. They can be used to determine intensity ratios, however, since at a given voltage the ratios are practically independent of slight variations in the current when it is small, as it is in these experiments.

The results of Tables II and III are shown graphically in figs. 1 and 2. All values with accelerating potentials differing by 0.1 volts or less have been averaged for purposes of plotting.

§ 5 Discussion

The optical excitation curves for the second positive bands ($^3\pi \rightarrow ^3\pi$) have the usual form for triplet states, fig. 1. The intensity increase for the negative bands ($^3\Sigma \rightarrow ^3\Sigma$) is not far from linear up to the highest accelerating potential used (50 volts).

* 'Z. Physik,' vol. 79, p. 511 (1932).

Table II—Variation of Intensity with Voltage, and Intensity Ratios at Various Voltages, of the Second Positive Bands

Accelerating potential (volts).	Intensities			Intensity ratios		
	0 → 2.	1 → 3.	2 → 4.	1 → 3/0 → 2.	2 → 4/0 → 2.	2 → 4/1 → 3
12.0	0	0	0	—	—	—
14.0*	25 (25)	14 (15)	3.4 (3.6)	0.55 (0.60)	0.13 (0.14)	0.24 (0.26)
15.0*	64 (64)	38 (40)	9.2 (9.7)	0.58 (0.63)	0.15 (0.16)	0.25 (0.25)
16.0*	95 (95)	69 (70)	19 (19)	0.73 (0.74)	0.21 (0.20)	0.28 (0.28)
18.0*	100 (95)	79 (83)	26 (25)	0.79 (0.88)	0.26 (0.27)	0.33 (0.30)
20.0*	83 (84)	74 (73)	23 (24)	0.90 (0.88)	0.27 (0.29)	0.31 (0.33)
20.0	85	78	25	0.91	0.29	0.32
21.0	—	—	—	0.88	0.28	0.32
22.0	—	—	—	0.89	0.27	0.30
22.2*	79	69	19	0.87	0.24	0.28
25.1*	—	—	—	0.88	0.27	0.30
25.3*	70	65	20	0.90	0.27	0.31
25.3	70	65	20	0.93	0.28	0.30
25.4	67	54	18	0.81	0.27	0.33
30.0	63	56	17	0.90	0.27	0.30
30.0	71	56	18	0.79	0.25	0.32
35.0	63	53	16	0.85	0.26	0.31
35.2	58	47	15	0.82	0.25	0.31
40.0	—	—	—	0.82	—	—
40.2	57	46	13	0.81	0.23	0.28
50.0	48	40	13	0.88	0.25	0.29
50.0	—	—	—	0.84	0.27	0.32
60.0	45	38	12	0.84	0.27	0.32
80.0	—	—	—	0.82	—	—
120.0	—	—	—	0.83	—	—
160.0	—	—	—	0.82	—	—

* The figures in this line are averages of the values given in a previous publication of early experimental results (*loc. cit.*). The values found by integration measurements are given in round brackets.

Table III—Variation of Intensity with Voltage, and Intensity Ratios at Various Voltages, of the Negative Bands

Accelerating potential (volts)	Intensities†		Intensity ratio	
	0 → 1.	1 → 2.	1 → 2/0 → 1.	
21.0	—	—	0.14	
22.0	—	—	0.13	
25.4	45	5.7	0.13	
30.0	75	9.9	0.13	
35.0	106	15	0.14	
40.2	130	17	0.13	
50.0	162	23	0.14	

† These intensities are expressed in approximately the units of those of Table II. The comparison was made from a measurement of the relative intensities of $\lambda 3805$ and $\lambda 4278$ at 50 volts accelerating potential.

In order that the experimental results may be of use in testing the predictions of Section 2, it is necessary that direct excitation by electron impact from the ground state of the neutral molecule should predominate. This should be so in the present experiments because of the low tube current and pressure.

Supporting evidence is furnished by the fact that extrapolation of the excitation function curves to zero intensity gives values for the excitation potentials

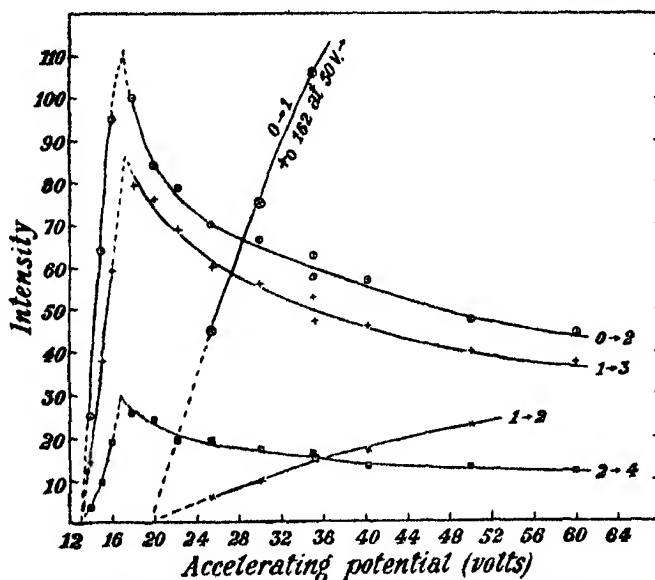


FIG. 1.—Optical excitation functions for the second positive bands $0 \rightarrow 2$, $1 \rightarrow 3$, and $2 \rightarrow 4$, and the negative bands $0 \rightarrow 1$ and $1 \rightarrow 2$.

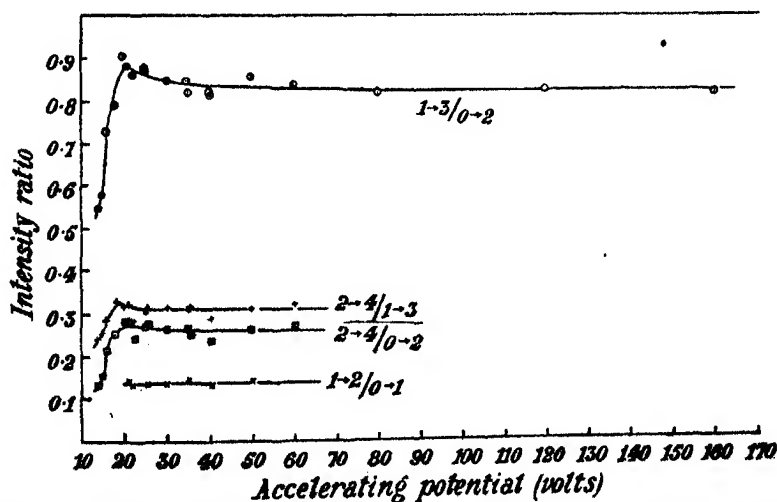


FIG. 2.—Variation of the intensity ratios with voltage for the investigated bands.

in good agreement with those found by Sponer (*loc. cit.*). Furthermore, the following consideration shows that population of the initial levels of the investigated bands by the recombination of an ion molecule with an electron,

or of ions, must play a negligibly small part. At first sight it might be thought that the constancy of the intensity ratios, which sets in shortly after the ionization potential (16.5 volts) is reached, is due to a recombination effect, since the *relative* populations acquired in this way would be independent of the velocity of the exciting electrons. If this were so, recombination would have to predominate in filling the levels, and since the number of molecular ions, and also of ions, increases strongly with the exciting voltage up to at least 100 volts,* the intensities of positive bands should increase proportionally. This is not so, as examination of fig. 1 shows. As pointed out in an earlier paper, the agreement of the relative intensities calculated from maximum blackening and from integration measurements (see Table II) shows that there is no variation with voltage in the *relative* rotational development of the different bands. The experimental results are therefore believed to represent the facts for a symmetric diatomic molecule (for which the rotational characteristics need not be considered) excited by electron impact directly from the ground state. The analysis outlined in Section 2 can therefore be applied as follows.

Inspection of fig. 2 shows that the band intensity ratios are independent of the exciting voltage above 30 volts. This condition was necessary for the validity of equation (4), Section 2, and its underlying assumptions. It is to

Table IV—Comparison of Predicted and Observed Complete Intensities
for Accelerating Potentials greater than 30 volts

	Second positive bands			Negative bands	
	0 → 2.	1 → 3.	2 → 4.	0 → 1.	1 → 2.
Excitation probability, $P_{nn'}^s$	100	63.4	15.1	100	10.7
Emission probability, $P_{n'n''}^s$	43.0	82.2	100	76.1	100
Calculated intensity ratio, $kP_{nn'}^s \cdot P_{n'n''}^s$	66	79	23	100	14
Observed intensity ratio, $1/\nu^4$	100	80	23	100	14

be expected therefore that equation (5) should give correct results for the relative intensities of the bands in this region. The calculated excitation and emission probabilities, and the calculated and observed intensities are given in Table IV.

The agreement is surprisingly good considering the number of assumptions and approximations of the theory, and the error involved in experiment (8% for a single determination). The manner in which strong excitation com-

* The strong increase of the negative bands (ion-molecule) with voltage is seen from fig. 1, and more completely from Lindh's work ('Z. Physik,' vol. 67, p. 67 (1930)) on the excitation function of the negative band λ 3914.

pensates for weak emission to give approximately the observed value is especially interesting. The only discrepancy appears in the value for the $0 \rightarrow 2$ band, which is too low. It may be that the expression used for the potential function does not accurately describe the conditions very near the point of static equilibrium for the second positive initial state. It seems, however, that it is quite adequate for the ground state and initial negative state, for which vibrational levels equally near to the potential curve minimum are considered.

The principal source of error in the numerical calculations lies in evaluating $(r'_0 - r''_0)$ (see equation (1)). While the r_0 values have been given to four figures by Birge (*loc. cit.*), the difference contains only two significant figures. In addition I have been able to find no experimentally determined value for r_0 of the ground state of the neutral molecule. Morse (*loc. cit.*) has calculated a value 1.09 Ångström units from an empirical relation which is expected to hold rather well for nitrogen. The value 1.096 has been used in the calculations of this paper since it gives the best agreement with experiment. This variation is within the limits to which the "observed" and calculated r_0 values for nitrogen usually agree.

Consideration of the effects of other types of excitation on the intensities show that if these are present to a small but appreciable degree, the agreement with theory is not improved, but impaired. For example, the relative transition probabilities from the ground state of the ion-molecule to the initial levels 0, 1, 2 of the second positive bands are 100, 22.9, and 1.8, as calculated from equation (1). The relative amount of recombination (with these probabilities) necessary to improve the agreement in Table IV was calculated. The improvement obtained was very slight. Moreover, a further calculation showed that if this amount of recombination was present at 30 volts, where the constancy of the intensity ratios begins, the intensity of the band $0 \rightarrow 2$ would be stronger by a factor of more than 8 at 160 volts than it was at 30 volts. This follows from the sharp increase of the number of ion-molecules with increase in exciting voltage. It is, of course, not true, for the intensity of the band continues to decrease with increasing voltage in the manner shown in fig. 1 to at least 160 volts.

The relative excitation probabilities of the initial negative states 0 and 1, from the ground state of the ion-molecule are 100 and 40, as calculated using equation (1). Corrections for a partial excitation of this type, therefore, give much poorer agreement in Table IV. One would hardly expect this effect to be appreciable, for the number of neutral molecules in the ground state must be considerably larger than the number of ion-molecules.

In order to ascertain how well the facts were represented by the simple classical picture, estimates were made from the potential curves given by equation (6) by a graphical method. It was assumed that in the predicted continuum excited and emitting molecules go to the nearest quantum state, and that the relative number of transitions taking place when the nucleus is in any small portion of the oscillatory orbit is proportional to the time of stay of an harmonic oscillator in that portion. The values obtained for the complete intensities of the second positive bands $0 \rightarrow 2$, $1 \rightarrow 3$, and $2 \rightarrow 4$ were 100, 48, and 19. The agreement with experiment is quite good (cf. Table IV) considering the roughness of the method. On the other hand, while the classical method and wave mechanics predict complete intensities, which are in rough agreement, they differ in the predicted excitation and emission probabilities. The classical probabilities are 100, 51, and 38 in excitation, and 100, 94, and 50 in emission.

An interesting part of the curves of fig. 2 lies below an accelerating potential of 30 volts. The intensity ratios of the second positive bands exhibit a marked dependence on the exciting voltage for values from about 20 volts down to the excitation potential (13.0 volts*). The energy separation of the 0, 1 and 1, 2 initial emission levels is 0.25 volts. If one corrects for this energy difference by plotting the intensities for the $1 \rightarrow 3$ and $2 \rightarrow 4$ bands with abscissæ respectively 0.25 and 0.50 volts less than the measured accelerating potential, the intensity ratios $1 \rightarrow 3/0 \rightarrow 2$, $2 \rightarrow 4/0 \rightarrow 2$, and $2 \rightarrow 4/1 \rightarrow 3$ become 0.75, 0.23, 0.32 at 14 volts, and 0.78, 0.23, 0.30 at 16 volts. This correction is sufficient to make the band intensity ratios approximately independent of the exciting voltage in this region.

On the other hand, the intensity ratio of the $0 \rightarrow 1$ and $1 \rightarrow 2$ negative bands, whose initial levels have an energy separation of 0.29 volts, is found (without correction) to be constant with exciting voltages down to within 1.4 volts of the excitation potential (19.6 volts*). If the explanation of the curves near the excitation potential were simple, we should expect here a dependence of the intensity ratio on accelerating potential up to 25 or 26 volts, analogous to that of the second positive bands. When the correction for the energy separation of the initial levels 0, 1, is made, the intensity ratio $0 \rightarrow 1/1 \rightarrow 2$ becomes 0.19, 0.15, and 0.13 at 21, 23, and 30 volts, *i.e.*, it introduces a dependence on voltage near the excitation potential in the corrected curve.

The present data are not suitable for further discussion of this point, which requires the results of rather fine measurements with exciting electrons of

* Sponer, *loc. cit.*

narrow velocity distribution. Moreover, the theoretical model used in this work is probably inadequate in this region since according to it an electron capable of exciting the lowest vibrational level of a system is capable of exciting all levels of that system.

In conclusion, I wish to express my thanks to Professor L. S. Ornstein for many discussions, and for extending to me the opportunity of working at his institute. I am also indebted to Mr. H. Brinkman for discussion, to Mr. G. G. Zaalberg for aid in some of the experimental work, and to the Royal Commission for the Exhibition of 1851 for the award of a scholarship.

Summary.

(1) A theory of direct excitation by electron impact for band systems of symmetric diatomic molecules is given. It permits the calculation of the *complete* relative intensities of bands of a system.

(2) The constancy of the band intensity ratios with change in the energy of the exciting electrons is shown to be a criterion for the validity of the assumptions on which the excitation treatment is based.

(3) Measurements were made of the relative intensities of the $0 \rightarrow 2$, $1 \rightarrow 3$, and $2 \rightarrow 4$ bands of the second positive nitrogen system excited by electrons, with accelerating potentials between 14 and 160 volts, and of the $0 \rightarrow 1$ and $1 \rightarrow 2$ bands of the negative nitrogen system with accelerating potentials between 21 and 50 volts.

(4) It is found experimentally that the band intensity ratios are constant with accelerating potentials of more than 30 volts, but that in the second positive system there is a dependence on voltage below this value.

(5) In the former voltage region the calculated and observed complete intensities agree surprisingly well, although the relative emission probabilities alone are quite different in sense from the observed intensities.

(6) The dependence of the intensity ratios of the second positive bands on voltage near the excitation potential may be explained by taking into consideration the energy separation of the initial vibrational levels. This is not, however, sufficient for a complete explanation of all the results obtained near the excitation potential.

(7) The optical excitation functions for the second positive bands are of the usual form for triplet states, and those for the negative bands are of the form found by Lindh (*loc. cit.*).

(8) The complete intensities estimated graphically from the potential curves are in the right order, but the excitation and emission probabilities differ from those predicted by wave mechanics.

The Internal Conversion of γ -Rays

By J. B. FISK, Trinity College, Cambridge, and H. M. TAYLOR, Clare College, Cambridge

(Communicated by R. H. Fowler, F.R.S.—Received March 17, 1934)

§ 1. *Introduction*—Theories of the internal conversion of γ -rays developed by Hulme* and by Taylor and Mott† have met with success in explaining the observed values of the conversion coefficient in the range of wave-lengths of the RaC spectrum. The observed values for RaC lie approximately on two curves of which the one corresponding to lower values of the conversion coefficient is obtained theoretically if it be assumed that the nucleus radiates the field of an electric dipole, while the other is obtained on the assumption that the radiated field is that of an electric quadrupole.

Neither theory, however, is in agreement with the observations on softer γ -rays, such as those from RaB, where the experimental results are about twice as large as the values predicted by the quadrupole theory, and, of course, many times larger than those predicted by the dipole theory.

§ 2. The dipole and quadrupole fields assumed by the above theories to be radiated from the nucleus are, of course, not the only possible fields. Electric multipole fields of higher order are possible, but it is shown by Taylor and Mott‡ that it is improbable that such fields will occur. There are, however, still further possible fields, namely, those associated with oscillating magnetic multipoles. Such a field is in fact associated with the ordinary electric dipole field radiated by a Dirac electron making an “optical” jump.§ In such optical radiation the intensity of the “magnetic” radiation is small compared with the “electric” radiation, but it does not necessarily follow that this would be so in radiation from nuclei, and therefore it becomes of interest to examine what values of the internal conversion coefficient would be given by radiated fields arising from magnetic dipoles and magnetic quadrupoles. The

* ‘Proc. Roy. Soc.,’ A, vol. 138, p. 643 (1932).

† ‘Proc. Roy. Soc.,’ A, vol. 138, p. 665 (1932), referred to as T.M. I; and vol. 142, p. 215 (1933), referred to as T.M. II.

‡ T.M. I, p. 667.

§ Cf. T.M. II. p. 236, and equations (4.18), (4.23). Electric dipole radiation is associated with magnetic quadrupole, and electric quadrupole with either magnetic octopole or magnetic dipole.

calculation has been carried through as in T.M. I assuming in each case that the nucleus radiates a pure magnetic field. Thus for the field perturbing the extra-nuclear electron, and causing its ejection as a β -particle we have taken :

(a) *Magnetic Dipole**

$$\left. \begin{aligned} \mathcal{A}_x &= K \cdot P_1^1(\cos \theta) \cdot \sin \phi \cdot r^{-1} \cdot \left(1 + \frac{i}{qr}\right) \cdot e^{i(qr - \omega t)} \\ \mathcal{A}_y &= -K \cdot P_1^1(\cos \theta) \cdot \cos \phi \cdot r^{-1} \cdot \left(1 + \frac{i}{qr}\right) \cdot e^{i(qr - \omega t)} \\ \mathcal{A}_z &= 0 = \mathcal{A}_0 \end{aligned} \right\} \quad (2.1)$$

or

(b) *Magnetic Quadripole*

$$\left. \begin{aligned} \mathcal{A}_x &= L \cdot P_2^1(\cos \theta) \cdot \sin \phi \cdot r^{-1} \cdot \left(1 + \frac{3i}{qr} - \frac{3}{q^2 r^2}\right) \cdot e^{i(qr - \omega t)} \\ \mathcal{A}_y &= -L \cdot P_2^1(\cos \theta) \cdot \cos \phi \cdot r^{-1} \cdot \left(1 + \frac{3i}{qr} - \frac{3}{q^2 r^2}\right) \cdot e^{i(qr - \omega t)} \\ \mathcal{A}_z &= 0 = \mathcal{A}_0 \end{aligned} \right\} \quad (2.2)$$

The calculations follow closely upon the lines of those of T.M. I and are therefore not reproduced here. The results are shown in fig. 1, where it will be seen that these radiations from magnetic multipoles give rise to conversion coefficients up to fifty times as great as those arising from the electric multipole radiations previously considered.

If then, in the actual nuclear radiation, a small amount of this "magnetic" radiation accompanies what is in the main an electric dipole or quadripole radiation, it is quite possible that the calculated internal conversion coefficient may be raised sufficiently above its value for pure electric radiation to agree with the experimental values in the RaB region, while still leaving unaffected the agreement in the RaC region.

§ 3. *A Simple Nuclear Model*—It thus becomes important to find whether there is in fact any appreciable amount of this "magnetic" type of radiation present in the nuclear radiation. For this purpose we have taken a simple model nucleus for which detailed calculations can be made, namely, a potential hole with vertical walls of depth less than $2Mc^2$, in which is confined a proton of mass M obeying Dirac's relativistic equations. The wave functions for

* Cf. T.M. II, equation (2.23), where an electric quadripole and a magnetic dipole wave are superposed. T.M. (2.23) is the form valid for large values of r and so the term $(1 + i/qr)$ of our (2.1) has been replaced by unity.

such a system can be written down explicitly in terms of Bessel functions, and, assuming the width of the potential hole to be of the order of 10^{-12} cm we obtain a series of energy levels for the proton which are in very rough qualitative agreement with those of the observed γ -ray spectrum. On this crude picture of the nucleus we may now determine the field radiated when the proton makes

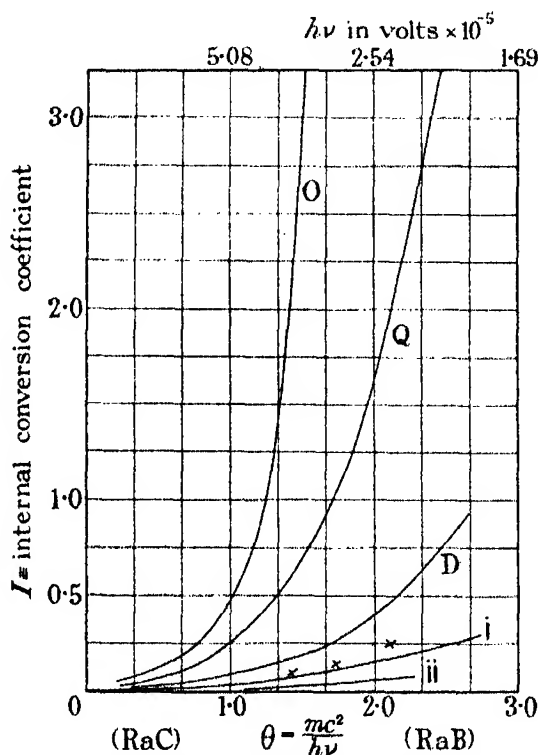


FIG. 1—Curve I—Electric quadrupole; II—Electric dipole; D, Q, O, magnetic dipole, quadrupole, and octopole respectively; \times experimental values in the RaB region. The RaC experimental points are all less than 0.008.

a transition from one energy level to another. For a transition in which $\Delta l = 2$ we find, for points far from the nucleus

$$\left. \begin{aligned} \mathcal{A}_0 &= H \{ 2P_2^0(\cos \theta) + 1 \} \cdot r^{-1} \cdot e^{i(qr - \omega t)} \\ \mathcal{A}_x &= iK \cdot P_1^1(\cos \theta) \cdot \sin \phi \cdot r^{-1} \cdot e^{i(qr - \omega t)} \\ \mathcal{A}_y &= -iK \cdot P_1^1(\cos \theta) \cos \phi \cdot r^{-1} \cdot e^{i(qr - \omega t)} \\ \mathcal{A}_z &= 3H \cdot P_1^0(\cos \theta) \cdot r^{-1} \cdot e^{i(qr - \omega t)} \end{aligned} \right\} \quad (3.1)$$

where the constants H and K determine the relative amounts of "electric" and "magnetic" radiation present. These constants are expressed as integrals

in T.M. II, equation (4.21), and for our simple nuclear model we can evaluate these integrals using the explicit forms for the wave functions concerned. We find that the ratio of H to K is of the order of 4000 to 1, and that the ratio of the amount of electric quadrupole to the associated "magnetic" dipole or octopole is of the same order. Thus on the assumption of such a model nucleus we deduce that the amount of "magnetic" radiation present is always too small to make any appreciable alteration in the conversion coefficients as given by Hulme and by Taylor and Mott.

§ 4. It is possible, however, that an appreciable amount of "magnetic" radiation may arise in other ways. A neutron possessing magnetic moment and no electric charge would radiate a purely "magnetic" radiation. But since the centre of mass of a nucleus remains stationary in a nuclear transition, therefore a transition of a neutron between two quantum states would cause a corresponding change in the remainder of the nucleus and hence a change in the electric centre. Thus such a transition would give rise to a field consisting of both electric and magnetic terms.

Summary

It is shown that in addition to the fields of radiation which have formerly been assumed, namely, those of electric multipoles, a nucleus may also emit those due to magnetic multipoles, and will in fact emit a combination of both. The internal conversion coefficients arising from such magnetic multipole radiations are calculated, and are shown to be much larger than the corresponding values for electric multipole radiation. It is shown that, on the assumption of a simple model nucleus, the proportion of magnetic radiation actually present is too small to affect appreciably the values of internal conversion coefficients calculated on the assumption of purely electric multipole radiation. A more complete theory of the nucleus is needed to predict the relative amounts of magnetic and electric radiation to be expected from an actual nucleus. In order to bring the theoretical values of the conversion coefficient into agreement with the experimental values for RaB this proportion would need to be of the order of 1 to 50.

The Nuclear Spins and Magnetic Moments of the Isotopes of Antimony

By S. TOLANSKY, Ph.D., 1851 Exhibition Senior Student, Imperial College of Science and Technology, South Kensington, London

(Communicated by A. Fowler, F.R.S.—Received March 20, 1934)

Introduction

The first detailed examination of the fine structures occurring in the visible lines of the Sb II spectrum was made by Badami,* who reported extensive structures in many lines. Badami attempted to excite the Sb II spectrum in a hollow cathode discharge, but even a current of 0.4 amp failed to produce sufficiently strong lines. As a source he therefore used a relatively high current arc (carrying 3–5 amps) which necessarily broadened each component so that serious blending often took place, and as many of the structures are complex, the blends introduce considerable ambiguity in analysis. According to Aston,† antimony consists only of two isotopes, 121 and 123, whose abundance ratio is 100 : 78.5. Badami concluded that the nuclear spin of the 121 isotope is $5/2$ and that of the 123 isotope is $7/2$. However, a critical comparison between the experimental data he published, and the theoretically predicted patterns based upon this assumption, shows so much ambiguity in interpretation, that a re-examination of the spectrum was undertaken.

It was apparent that the source to be used must give sharper components than the arc as used by Badami, and for this purpose a hollow cathode appeared to be most suitable. When the author was engaged upon an analysis of the As II fine structures,‡ he encountered the same difficulty as Badami, in failing to excite a sufficiently strong As II discharge in a cooled hollow cathode. Since arsenic and antimony are so closely related in the Periodic Table, it was thought that the phenomenon might be due to inappreciable sputtering in both elements. However, whilst recently engaged upon intensity measurements in the As II structures (together with J. F. Heard) the author found it possible to produce an intense As II spectrum in a cooled hollow cathode, provided the arsenic was free from oxide. This at once suggested that an oxide free antimony hollow cathode ought to yield good results. This was indeed

* 'Z. Physik,' vol. 79, p. 206 (1932).

† 'Proc. Roy. Soc.,' A, vol. 132, p. 487 (1931).

‡ 'Proc. Roy. Soc.,' A, vol. 137, p. 541 (1932).

found to occur, and with only one-seventh of an ampere a brilliant Sb II spectrum was excited. The source is much superior to the arc, not only giving sharper lines, but also appearing to be much stronger.

The analysis of the patterns observed with a hollow cathode, shows without any doubt that the nuclear spins of both of the 121 and 123 isotopes are $5/2$, but that the nuclear magnetic moments are different, that of 121 being 1.37 times that of 123. As a result, the pattern of a line consists of a fine structure multiplet due to 121, and superposed on this is a similar pattern due to 123, approximately three-quarters of the intensity of the main pattern and about five-sevenths of the scale. The patterns for lines involving higher J values are therefore extremely complex.

Experimental

The spectrum was excited in a hollow cathode tube through which pure helium was continuously circulated. To obtain an oxide-free antimony hollow cathode, a simple procedure was employed. Molten antimony was run into a hollow iron cylinder, and on cooling, the solid cylinder of antimony was drilled, exposing a fresh surface. This was immediately introduced into the discharge tube, and after pumping and circulating helium for a few minutes, a brilliant, sharp spectrum could be obtained with currents between 100 and 150 milliamps. The spectrum could be excited equally well in a water cooled or in a hot hollow cathode, but the latter had the advantage of giving a relatively weak helium spectrum and was mainly used. The atomic weight of antimony is sufficiently high not to call for cooling, if small currents are employed.

The lines were examined for fine structure with a silvered Fabry-Perot interferometer crossed with a large aperture two-prism spectrograph. The interferometer gaps employed were $1\frac{1}{2}$, 2, $2\frac{1}{2}$, 3, 4, 5, 6, 8, 11, 15 and 25 mm. The region examined was $\lambda\lambda$ 6800–5000, and when Ilford hypersensitive panchromatic plates were used, the exposure times varied between a few seconds and an hour. Many lines below λ 5000 have complex structures, but the patterns are wide and only small gaps can be employed, so that the combination of diminishing resolving power due to reduction in reflection coefficient, together with the smallness of the gaps, makes resolution extremely difficult; hence observations have not been attempted.

In Table I is given a list of the observed structures. The wave-lengths are taken mainly from Kayser's 'Handbuch der Spektroskopie,' and the allocations where known are those given by Badami (*loc. cit.*). It is possible that one or two of the unallocated lines in the table may belong to the arc spectrum, and

where this is suspected the line has an asterisk against it. The evidence is very indefinite however. The fine structures are given in units of $\text{cm}^{-1} \times 10^{-3}$, and the visually estimated intensities are shown below, as usual, in brackets. The errors in the best of values probably do not exceed three units, but many components are broad and diffuse, and the errors for these must be higher.

If these data are compared with those of Badami, it is seen that the patterns reported by the latter are actually those which arise when the individual components are broad and blending occurs. Comparisons will be made later.

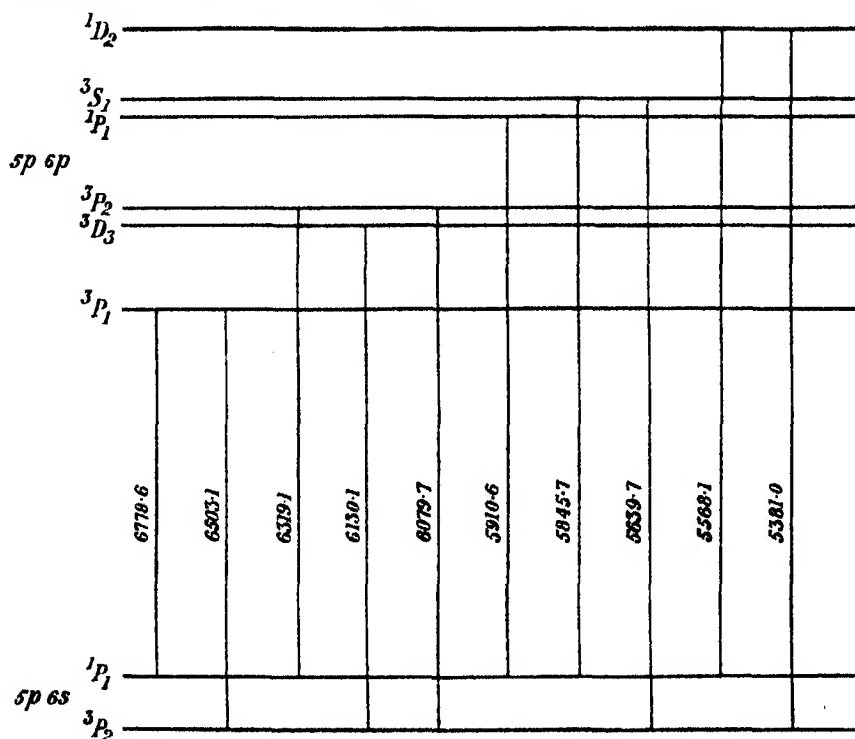


FIG. 1—Allocated lines observed for fine structures.

Analysis of the Structures

Unfortunately the gross structure multiplet analysis in Sb II has only been partially carried out, and about one-third of the observed lines have been classified (Badami, *loc. cit.*). Those classified lines which are studied here are shown in fig. 1, from which it is seen that they involve transitions between S P D terms of the 5p 6p configuration, and 5p 6s 3P_2 and 5p 6s 1P_1 . Each of the last-named two lower terms is involved five times and four of the upper

Table I—Fine Structures of the Lines of Sb II

Wave-length	Int.	Allocation	Structure										Violet	
6806.2	2	—	—	744	615	433	393	72	0	+				
				(5)	(4)	(10)	(8)	(10)	(14)					
6778.6	4	$6s^1P_1-6p^3P_1$	—	110	45	0	+							
				(3)	(5)	(7)								
6713.3	1	—	—	0	70	118	+							
				(4)	(4)	(3)								
6558.5*	1	—	—	195	151	97	0	+						
				(1)	(1)	(2)	(3)							
6513.0	3	—	—	571	484	368	219	184	80	0	+			
				(3)	(2)	(1)	(4)	(4)	(2)	(10)				
6503.1	4	$6s^3P_2-6p^3P_1$	—	0	76	242	275	413	515	630	+			
				(10)	(7)	(8)	(5)	(3)	(5)	(4)				
6417.8	1	—	—	0	29	176	260	310	368	+				
				(10)	(7)	(11)	(3)	(7)	(2)					
6389.4	1	—	—	104	63	0	+							
				(3)	(5)	(7)								
6319.1	3	$6s^1P_1-6p^3P_2$	—	312	230	125	30	0	+					
				(1½)	(2)	(10)	(6)	(8)						
6320.8	8	—	—	86	0	89	433	458	533	628	760	788	928	+
				(6)	(10)	(7)	(4)	(5)	(4)	(4)	(2)	(2)	(4)	
6193.1	3	—	—	148	83	0	+							
				(3)	(5)	(7)								
6130.1	25	$6s^3P_2-6p^3D_2$	—	100	0	31	131	209	314	389	416	516	569	+
				(1)	(10)	(7)	(3)	(8)	(4)	(5)	(3)	(3)	(1½)	
6079.7	20	$6s^3P_2-6p^3P_2$	—	131	0	50	175	229	314	417	521	+		
				(1)	(10)	(10)	(5)	(3½)	(4)	(5)	(3)			
6052.9	10	—	—	131	0	90	506	561	626	755	950	1160	1207	+
				(6)	(10)	(7)	(3)	(4)	(3)	(3)	(3)	(4)	(2)	
6005.2	20	—	—	451	258	123	0	49	214	361	435	560	701	+
				(1)	(5)	(4)	(30)	(20)	(12)	(10)	(16)	(6)	(3)	
5910.6	15	$6s^1P_1-6p^1P_1$	—	0	102	145	188	+						
				(4)	(3)	(2)	(1)							
5895.0	8	—	—	0	108	614	686	966	1175	+				
				(14)	(10)	(8)	(10)	(4)	(5)					
5845.7	5	$6s^1P_1-6p^3S_1$	—	138	68	0	+							
				(2)	(3)	(3)								
5702.4	9	—	—	330	0	240	464	588	813	907	1202	1355	+	
				(1)	(7)	(5)	(1)	(1)	(9)	(7)	(4)	(5)		
5639.7	20	$6s^3P_2-6p^3S_1$	—	0	71	217	319	399	477	605	728	+		
				(10)	(8)	(9)	(3)	(3½)	(6)	(5)	(1½)			
5632.0*	10	—	—	0	180	213	+							
				(10)	(4)	(5)								
5568.1	25	$6s^1P_1-6p^1D_2$	—	224	174	90	0	+						
				(3)	(5)	(7)	(9)							
5556.3*	7	—	—	368	296	226	189	98	0	+				
				(2)	(4)	(1)	(3)	(3½)	(7)					
5464.4	10	—	—	0	244	672	879	1017	1243	1434	1666	1852	+	
				(10)	(7½)	(12)	(1)	(2)	(4½)	(3½)	(3)	(3)		
5381.0	10	$6s^3P_2-6p^1D_2$	—	117	0	36	129	207	268	307	365	465	507	+
				(1)	(10)	(7)	(2)	(4)	(3)	(4)	(4)	(6)	(3)	
5055.9	5	—	—	0	100	557	632	882	1073	+				
				(14)	(10)	(8)	(10)	(4)	(5)					

terms are each involved twice. Opportunity is thus afforded for checking the derived term structures. Coupling theory, and comparison with the analogous As II spectrum, suggest that the $5p\ 6s^3P_2$ term should show a wide fine structure whilst that of $5p\ 6s^1P_1$ should be narrow. Most of the structures

in the $5p\ 6p$ configuration are expected to be smaller than that of the $5p\ 6s\ ^3P_2$ term, for the latter involves an s electron.

As pointed out previously, the patterns produced by lines involving higher J valued terms are expected to be extremely complex, and, indeed, the clue to the analysis is given by a group of relatively simple lines involving terms with $J = 1$. In these lines the terms which produce the fine structures are unknown, but in each the J value must be 1 and the other term must have a minute or zero structure. This will become apparent from the analysis. The three unclassified lines in question are $\lambda\lambda\ 6806\cdot2$, $5895\cdot0$, $5055\cdot9$, and each will now be considered in detail.

$\lambda\ 6806\cdot2$ —The analysed structure is shown in fig. 2. The line consists of six sharp clearly resolved components degrading in intensity to the red. The components, drawn with the straight lines A, B, C, are attributed to the 121 isotope (abundance = 100) whilst the dotted components a , b , c are attributed to the 123 isotope (abundance = 78·5). The estimated intensities fit this scheme very well, and there is no alternative explanation. Since the structure for each isotope consists of a regular degraded triplet, the term possessing the fine structure must have a J value of 1 (the number of components in a term equals $2I + 1$ or $2J + 1$ according to which is smaller). The extreme sharpness of the individual components shows that the other term involved has a very small structure if any at all. Since the structure is entirely due to one term with $J = 1$, the interval ratio in the structure will give the nuclear spin, the ratio $AB : BC$ is $1\cdot39 : 1$ and that of $ab : bc$ is $1\cdot44 : 1$. The following ratios are those given by different nuclear spins :—

Nuclear spin	3/2	5/2	7/2	9/2
Interval ratio	1·66	1·40	1·28	1·22

It is at once obvious that $5/2$ is the nuclear spin for both the isotopes, without any possible ambiguity. The deviations from the theoretical value $1\cdot40$, are probably real. Calculations shows that a small structure in the other term involved has the net effect of slightly increasing one ratio and diminishing the other. There is in addition the experimental difficulty attached to measuring very accurately the separation Bb which is only 40 units ($0\cdot019\text{ \AA}$). There is usually a tendency to underestimate the separation of close components, and this would move the ratios in the observed direction. A check to the analysis is formed by calculating the optical centres of gravity of the structures of each isotope, which ought to coincide, unless there happens to be an isotope displacement. The calculated centres of gravity fall at 309 and 301 respec-

tively for the stronger and weaker patterns. Considering that six components contribute to the calculation of the two centres of gravity, the small difference of 8 units is hardly likely to have such significance, and indeed the centres of gravity may be considered as coincident. There is no reason to expect isotope displacement, so that the coincidence strongly supports the analysis.

Since both the isotopes have the same nuclear mechanical moments, the fact that the patterns have different scales shows that the nuclear magnetic moments of the isotopes are different, for whereas the number of the components in a term is determined by the nuclear spin, the width of the pattern is proportional to the nuclear magnetic moment. From the pattern it is found that $\mu_{121}/\mu_{123} = 1.37$ where μ_{121} and μ_{123} are the respective nuclear

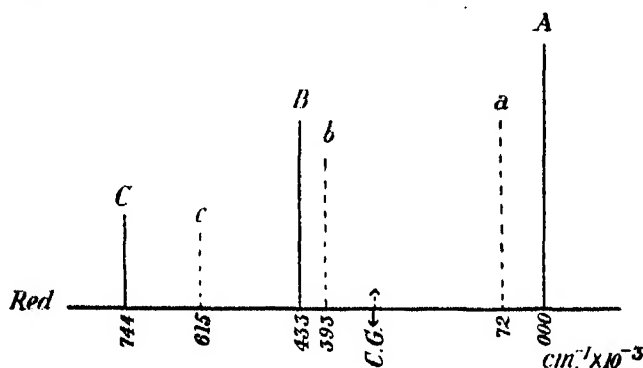


FIG. 2— λ 6806.2.

magnetic moments. The interval factors calculated for the term with the structure are, 124 for the more abundant isotope and 90 for the less abundant.

λ 5895.0—The structure and analysis are shown in fig. 3a. The pattern is identical in appearance with that of the previous line, but is degraded to the violet and about 50% larger. This line has also been observed by Badami but the separations given by him and by the author do not exactly agree. They are as follows :—

	A	a	b	B	c	C
Badami	0	117	589	680	959	1159
Author	0	108	614	686	966	1175

The measurements were made on $1\frac{1}{2}$, $2\frac{1}{2}$, 3, 4, 5 and 6 mm etalons. The largest deviation is in the separation of the closest pair Bb, the difference being 19 units. Owing to the superior source employed by the author, the data presented here are probably more reliable. This is the line upon which Badami

based his analysis, finding the interval ratios as 1.40:1 and 1.28:1 respectively.

It is again apparent that the term possessing the fine structure has a J value = 1. The interval ratios found by the author are 1.40:1 for the stronger isotope and 1.43:1 for the weaker isotope, giving again $5/2$ unambiguously for both isotopes, and thus agreeing with the deduction made from the previous

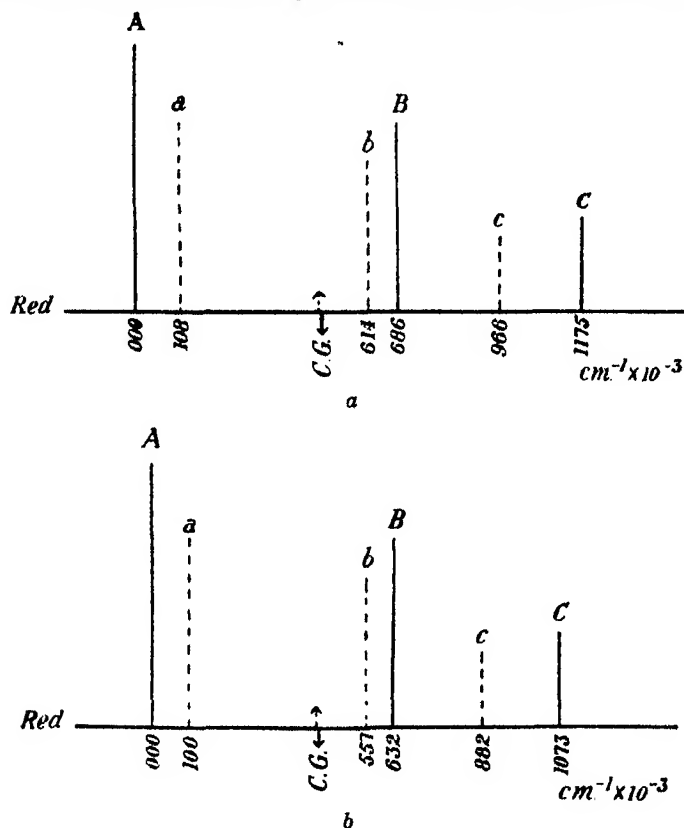


FIG. 3— a , $\lambda 5895.0$; b , $\lambda 5055.9$.

line. The ratio $\mu_{121}/\mu_{123} = 1.36$ which agrees remarkably well with the previous value 1.37.

$\lambda 5055.9$ —The structure and analysis are shown in fig. 3, b . The pattern for this line is closely similar to that of the previous line, but about 10% smaller. The interval ratios are 1.40:1 for the stronger and 1.43:1 for the weaker isotope, giving again a spin of $5/2$. The respective centres of gravity are at 436 and 426 so that again the difference is not very significant. The ratio $\mu_{121}/\mu_{123} = 1.37$; therefore from the three lines, it

can be concluded with certainty that the spin for both isotopes is $5/2$ and that the 121 isotope has a nuclear magnetic moment 1.37 times that of the 123 isotope. The calculated interval factors for the last two lines under consideration are 179 ... 130 and 194 ... 143 respectively, and it is possible that

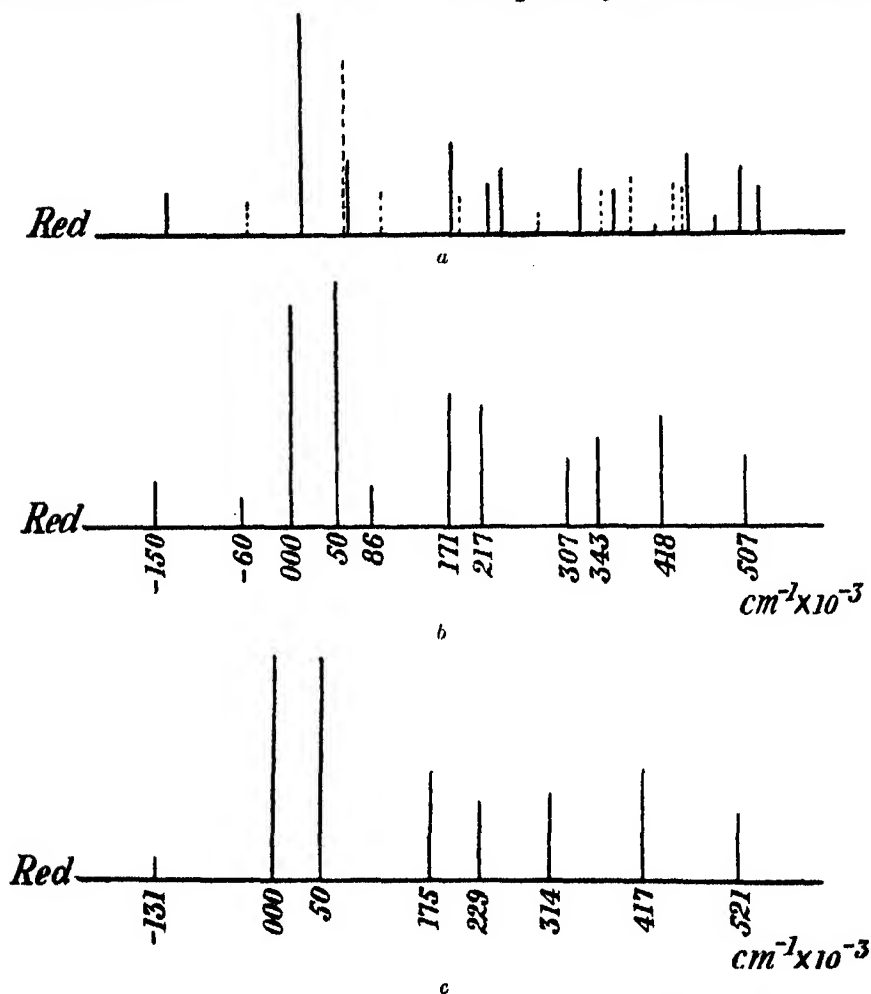


FIG. 4— $\lambda 6079.7$ ($6s\ ^3P_2 - 6p\ ^3P_2$). a, theoretical pattern; b, resultant pattern calculated; c, observed pattern.

both lines involve the same fine structure term. If so the 8% difference is to be attributed to one of the other terms involved. There is no definite evidence of any isotope displacement in the three lines. These considerations will now be applied to the more complex classified lines, and it will be seen that they explain these structures satisfactorily.

λ 6079.7 ($6s\ ^3P_2-6p\ ^3P_2$)—When a highly complex transition such as this is being considered, then the only approach to term analysis that can be made is by means of the Fisher-Goudsmit graphical method* details of which are given in the author's work on arsenic (*loc. cit.*). By means of this, it is possible to calculate both the upper and lower term structures from a line pattern, even if a number of components are blended in the pattern. The observed pattern is fitted into a graphical line complex, and from the position of closest fit the term structures can be calculated. For instance in fig. 4 is shown the observed and the predicted pattern for λ 6079.7. The interval factor for the $6s\ ^3P_2$ term is 74 for the 121 isotope, and 54 for the 123 isotope, and the values for the upper term are 36 and 26. The theoretical line pattern for these interval factors is extremely complex and is shown in fig. 4, *a*. However, the graphical method shows up clearly that the complex pattern can be reduced to that of fig. 4, *b* when the centres of gravity of blends are taken into account. Fig. 4, *c* shows the observed pattern, and the agreement may be considered highly satisfactory, both as regards the intensities and the positions of the components. Certain of the observed components, in all the complex lines, were recognized to be complex from their widths, but owing to overlapping of orders with increasing plate separation, higher resolving powers could not be used.

λ 5639.7 ($6s\ ^3P_2-6p\ ^3S_1$)—The structure of the lower term has already been determined from the previous line. The analysis is shown in fig. 5 and when carried out independently graphically, it is found that within experimental error the same interval factor is obtained as before for the lower term. The predicted and observed patterns agree well, the net resultant theoretical blends being shown in fig. 5, *a*, and the observed pattern in fig. 5, *b*. Owing to the frequent blending of the components, due to the different isotopes, there is very little point in differentiating these by straight and dotted lines as in the simpler structures. In this line, and in the next, only the first two components can be strictly ascribed to 121 and 123 respectively, the remainder being largely blends, although frequently one isotope predominates in the intensity contributions.

λ 6503.1 ($6s\ ^3P_2-6p\ ^3P_1$)—The observed and calculated structures are shown in fig. 6. The agreement is reasonably good.

λ 5381.0 ($6s\ ^3P_2-6p\ ^1D_2$)—The analysis for this line is very satisfactory, fig. 7. The graph predicts eleven observable resultant components, several of which are blends. Ten components were observed, eight of these being

* 'Phys. Rev.,' vol. 137, p. 1059 (1931).

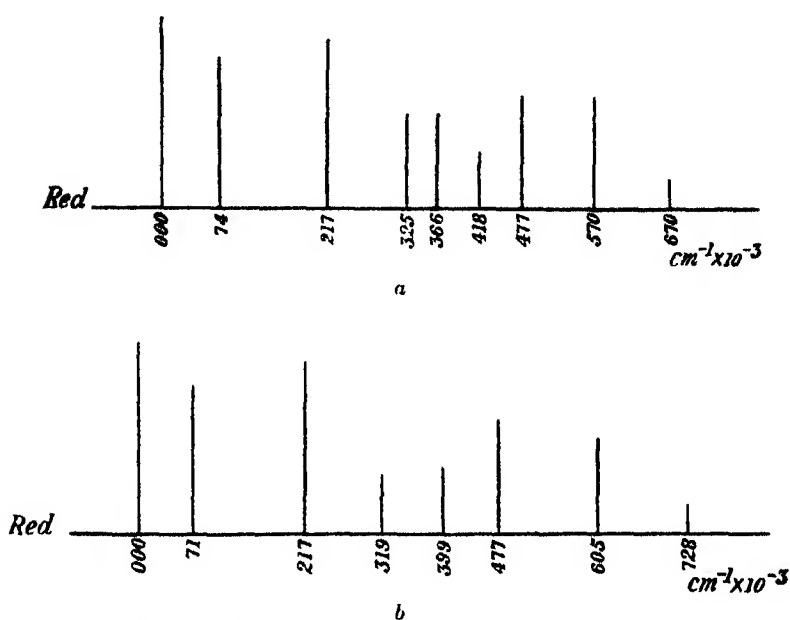


FIG. 5— $\lambda 5639.7$ ($6s\ ^3P_2 - 6p\ ^3S_1$). *a*, calculated resultant; *b*, observed.

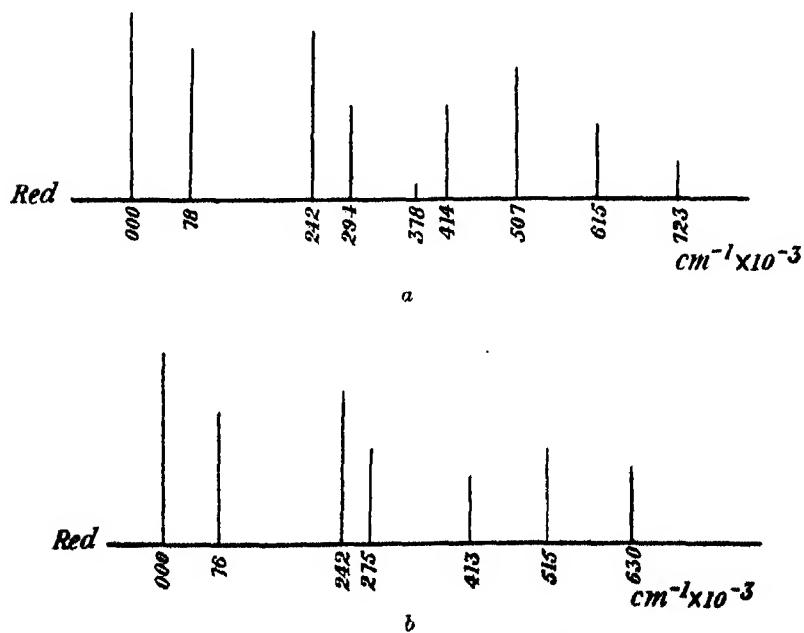


FIG. 6— $\lambda 6603.1$ ($6s\ ^3P_1 - 6p\ ^3P_1$). *a*, calculated resultant; *b*, observed.

very close to the calculated positions (from 0 to 7 units away). The deviations 23 and 25 units in the other two can be explained. The first error arises from the difficulty in measuring accurately the small separation, 59, between the two strongest components, one of which is a blend, and the second error is due to a diffuse tail-end component.

$\lambda 6130.1$ ($6s^3P_2-6p^3D_2$).—This is the last line involving the $6s^3P_2$ term to be considered. Fig. 8, *b* shows the predicted pattern and fig. 8, *c* the observed pattern. Considering the fact that the upper term has a *J* value 3 (the actual total number of components in the pattern being 28) the agreement is as good

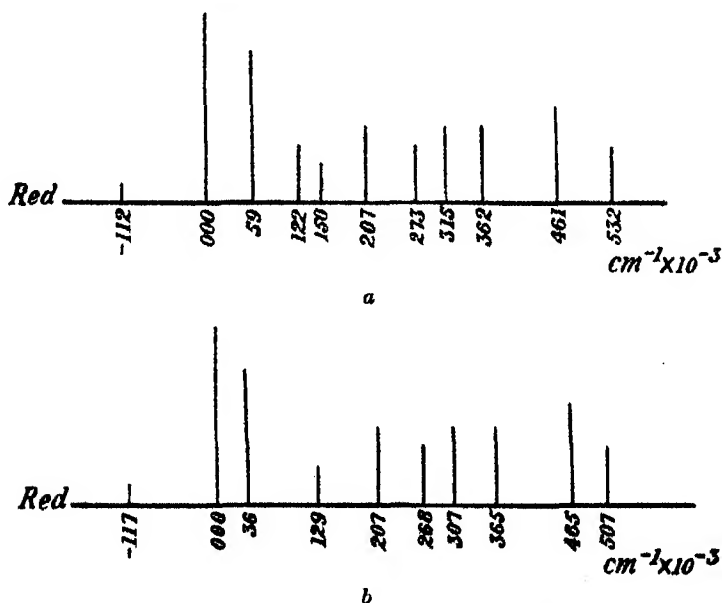


FIG. 7— $\lambda 5381.0$ ($6s^3P_1-6p^3D_2$). *a*, calculated resultant; *b*, observed.

as can be expected. In fig. 8, *a* the pattern reported by Badami is shown, to illustrate the difference in resolution obtained.

This concludes the analysis of the lines involving the $6s^3P_2$ term, and it can be confidently concluded that the interval factors for this term are 74 and 54 for the stronger and weaker isotope respectively. The remaining five classified lines have $6s^1P_1$ as the lower term and four of the five upper term structures have already been determined. The analysis of these lines will therefore afford a check on the previous work.

$\lambda 6319.1$ ($6s^1P_1-6p^3P_2$).—The upper term structure is obtained from the previous analysis of $\lambda 6079.7$. The predicted and observed patterns are

shown in fig. 9. The pattern is degraded to the red because the structure in the upper term is greater than that in the lower term, which is expected also on theoretical grounds. The agreement between observation and prediction is very good, for the structure is not on a large scale. The calculated interval factor for the $6s\ ^1P_1$ term (stronger isotope) is 9.8.

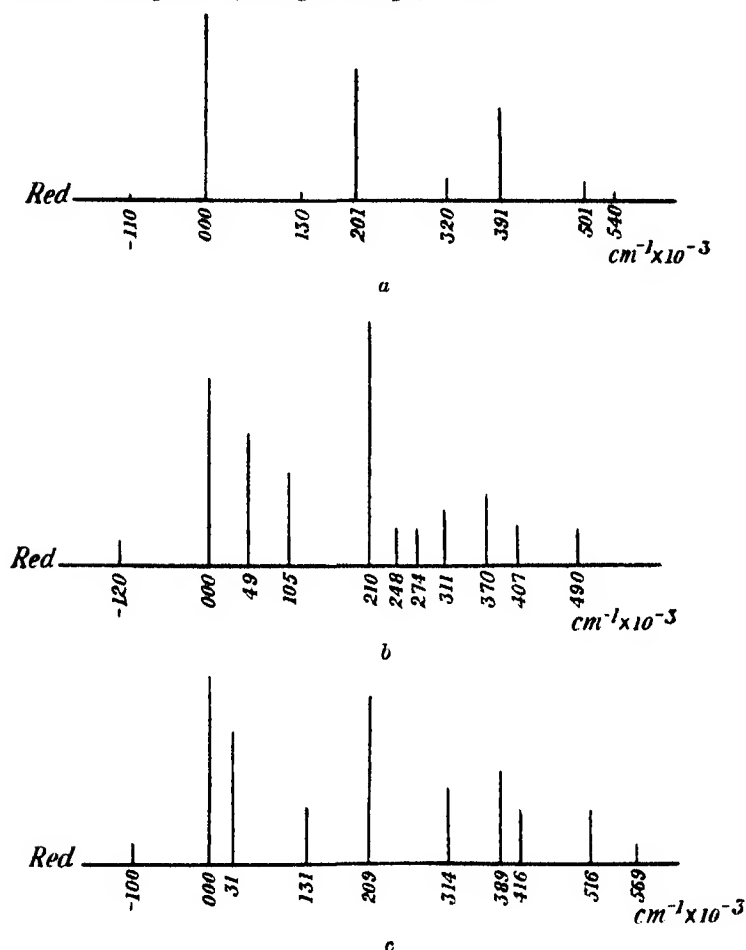
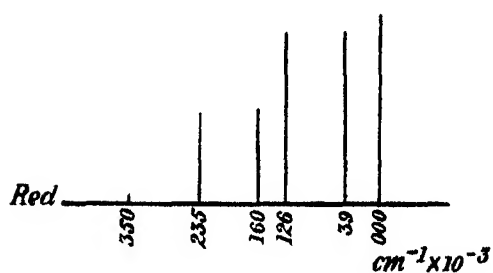


FIG. 8— $\lambda\ 6130.1\ (6s\ ^3P_2-6p\ ^3D_2)$. *a*, structure reported by Badami; *b*, calculated resultant; *c*, observed.

$\lambda\ 5845.7\ (6s\ ^1P_1-6p\ ^3S_1)$ —The structure is very small, and three broadened blended components could only be resolved. The predicted pattern, fig. 10, consists also of three broad patches of blends in good agreement with observation. The calculated interval factor for $6s\ ^1P_1$ is 8.6 which agrees surprisingly well with the previous value 9.8.

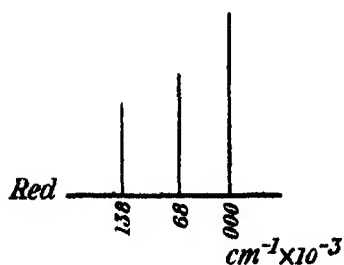


a

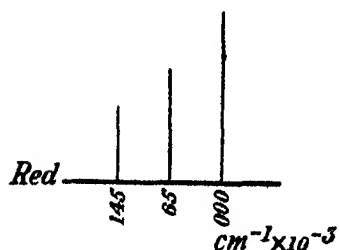


b

FIG. 9— $\lambda 6319.1$ ($6p\ ^1P_1 - 6p\ ^3P_2$). a, observed; b, calculated resultant.

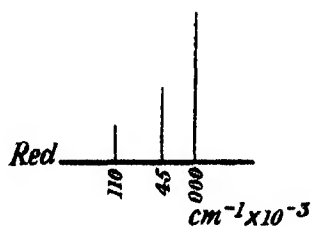


a

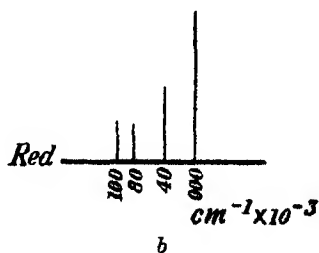


b

FIG. 10— $\lambda 5845.7$ ($6s\ ^1P_1 - 6p\ ^3S_1$). a, observed; b, calculated resultant.



a



b

FIG. 11— $\lambda 6778.6$ ($6s\ ^1P_1 - 6p\ ^3P_1$). a, observed; b, calculated resultant.

$\lambda 5568.1$ ($6s^1P_1-6p^1D_2$)—Like the previous two lines, this has also a very small structure degraded to the red, and analysis gives 8.3 for the interval factor of the lower term, again in good agreement with the previous value.

$\lambda 6778.6$ ($6s^1P_1-6p^3P_1$)—Three close components were measured, fig. 11, and the analysis proved ambiguous. The calculated interval factor for $6s^1P_1$ is 5 but this is unreliable.

$\lambda 5910.6$ ($6s^1P_1-6p^1P_1$)—This line is the only one involving the $6s^1P_1$ term that is degraded to the violet. The previous data show that the lower term has a small interval factor whose value is about 9. This line can therefore only be explained by attributing a negative factor to the upper term. The value deduced for this is -40 , but there is a large uncertainty, perhaps 20%.

Discussion

The concordance between the three relatively simple lines $\lambda\lambda 6806.2$, 5895.0 , 5055.9 shows that the nuclear spins of both the isotopes are $5/2$ and that the ratio $\mu_{121}/\mu_{123} = 1.37$. The five lines involving the $6s^3P_2$ term have all been analysed on the assumption of interval factors of 74 and 54 for the 121 and 123 isotopes, respectively, and agree well with the predicted patterns despite the great complexity expected. The five lines also give the structures for $6p^3P_1$, $6p^3D_3$, $6p^3P_2$, $6p^3S_1$, and $6p^1D_2$. The first four of these terms are involved in the lines coming to $6s^1P_1$ so that the interval factors of the latter can be independently calculated from each. This is only small, yet the values (for 121) obtained from three of the lines are 9.8, 8.6, and 8.3. The second figure has very little significance, and the three values may be considered as identical, affording a verification of the analysis. The complete list of calculated interval factors is given in Table II. The unknown terms a_1 b_1 c_1 each have a J value 1. If the structure in $\lambda 6806.2$ arises from the lower term, then the interval factor is negative, whilst if the lower terms are also responsible for the other two lines, their interval factors are positive. It is possible, as pointed out before, that b_1 and c_1 both refer to the same term.

It is of interest to compare these interval factors with those given by Badami for the 121 isotope. Since Badami calculated the 123 interval factors on the basis of a $7/2$ spin no comparison is necessary for these. The comparison is made in Table III.

An asterisk is placed against the terms in which the agreement is not very good, and it is to be observed that all these are upper terms involving a J value of 1. For a given interval factor the spread of the structure is almost

proportional to the value of J (up to a $J = 3$) which indicates that those lines having the smaller structures in the upper terms, have not been sufficiently well resolved by Badami, so that the interval factors are all underestimated. The deviation in $6p\ ^1P_1$ lies in the fact that the structure in the line involving this term is small.

Table II—Term Interval Factors in Sb II Structures

Term	Interval factors	
	121	123
$6s\ ^3P_2$	74	54
$6s\ ^1P_1$	9	6
$6p\ ^4P_1$	26	19
$6p\ ^3P_2$	36	26
$6p\ ^3D_2$	24	17
$6p\ ^3S_1$	35	26
$6p\ ^1D_2$	26	19
$6p\ ^1P_1$	-40	-29
6806 a_1	124	90
5895 b_1	194	149
5056 c_1	179	130

Table III—Comparison of Interval Factors

Term	Badami	Tolansky
$6s\ ^3P_1$	188	—
$6s\ ^3P_2$	74	74
$\dagger 6s\ ^1P_1$	small	9
$6p\ ^3P_2$	32	36
$6p\ ^1D_2$	26	26
$6p\ ^3D_2$	19	24
$6p\ ^3S_1$	26	35
$6p\ ^3P_1$	19	26
$6p\ ^1P_1$	small	-40
5895 b_1	193	194
$5s\ 5p^3\ ^3D_2$	174	—

† Given by Badami as 3P_1 , no doubt a misprint.

The values given by both observers for the other terms are in good agreement, particularly $6s\ ^3P_2$ and $6p\ ^1D_2$. It is highly probable therefore that the intervals given by Badami for the $6s\ ^3P_1$ and the $5s\ 5p^3\ ^3D_2$ terms are both approximately correct, for the structures in these terms are very wide. The ratio of the factors for the $5s\ ^3P_1$ and $5s\ ^3P_2$ terms found in As II by the author is 1.24, while the ratio between the $6s\ ^3P_2$ term of Sb II and the value given by Badami for $6s\ ^3P_1$ is 1.27. The electron couplings in the two spectra being similar, the closeness of the two ratios enhances the reliability of the value given for $6s\ ^3P_1$ by Badami.

The large interval factors for the terms $a_1\ b_1\ c_1$ indicate that these are probably associated with the $5s\ 5p^3$ configuration, which possesses a deeply

penetrating *s* electron. Amongst the unclassified structures in Table I it is also probable that those in the lines $\lambda\lambda$ 6052.9, 5702.4 and 5464.4 are associated with this configuration. A consideration of the more complex patterns shows that approximately correct values will be obtained for the 121 isotope even with partial resolution, but leaves the analysis of the 123 isotope quite ambiguous. This accounts for the agreements in Table III in spite of the different spins adopted for the 123 isotope.

The line λ 5632.0 is of particular interest. It is suspected to be an arc line with *J* value $\frac{1}{2}$ for the term showing structure. With small gaps the structure is a doublet, intensity ratio about 7:5. With high resolution the weaker component splits up, presumably owing to the unequal magnetic moments. From the structure it is possible to get an approximate value of the ratio μ_{121}/μ_{123} which is found to be 1.4, in good agreement with the much more accurately determined value 1.37.

Nuclear Magnetic Moments

The calculation of nuclear magnetic moments is as important as the determination of the mechanical moment and has been made possible, in favourable cases by making use of the formulæ deduced by Goudsmit.*

For accurate calculation it is necessary to know the type of coupling in the terms and the fine structures, and this enables the interval constants for individual electrons to be determined. Goudsmit* has calculated the nuclear magnetic moments for the antimony isotopes, using Badami's data. From Table III it is seen that Badami's interval factors for the 121 isotope will give the correct value for the magnetic moment, for the formulæ employed by Goudsmit are only approximate when applied to a spectrum like Sb II. The value calculated by Goudsmit for this isotope will therefore be retained. Since $\mu_{121}/\mu_{123} = 1.37$ the magnetic moment for 123 is readily deduced.

If *I* is the nuclear mechanical moment, and μ the nuclear magnetic moment, then if quantum units are used,

$$\mu = I \cdot g(I),$$

where *g* (*I*) is a numerical ratio. For the purpose of comparison with theory, it is simpler to divide the calculated magnetic moment by *I*, and to compare the resultant *g* (*I*) factors. Goudsmit finds $g(I)_{121} = 1.1$, therefore $g(I)_{123} = 0.8$. A theory has been proposed by Landé for the calculation of *g* (*I*) factors† for

* 'Phys. Rev.', vol. 43, p. 636 (1933).

† 'Phys. Rev.', vol. 44, p. 1082 (1933).

certain atoms. The fundamental assumption made, is that in atoms with odd atomic charge and odd atomic number, the nuclear spin properties, are attributed to the single odd proton in the nuclear configuration. This proton is assumed to possess a spin of a $\frac{1}{2}$ and also an orbital angular momentum, which combines with this to give a resultant spin value, which is the nuclear spin. On the basis of this theory there are two possible $g(I)$ factors for antimony, namely, one arising from a nuclear configuration in which the spin of the odd proton couples parallel with an orbital quantum number 2, and one in which it couples antiparallel with an orbital quantum number 3. Both of these arrangements produce a mechanical spin of $5/2$ but the $g(I)$ factor calculated for the first is 1.6 while that for the second is 0.57. These calculated values may be compared with the experimental values 1.1 and 0.8. The theory of Landé is only tentative.

There is one other known atom which possesses two isotopes with the same mechanical moment, but with different magnetic moments. This is gallium, in which the two isotopes 69 and 71 have a spin of $3/2$ but the ratio $\mu_{71}/\mu_{69} = 1.27$.* There is also no isotope displacement effect. In gallium the heavier atom is less abundant (1 : 1.5) and has the larger magnetic moment, while in antimony the heavier atom is also less abundant, but has the smaller magnetic moment.

The Table IV shows the atoms which have isotopes with different nuclear magnetic moments.

Table IV—Isotopes with different Nuclear Magnetic Moments

Atom	H	Ga	Rb	Sb	Xe	Hg
Isotope A	2	71	87	121	129	201
Isotope B	1	69	85	123	131	199
Ratio μ_A/μ_B	<1	1.27	2.0	1.37	-1.1	-1.12

I wish to take this opportunity of expressing my thanks to Professor A. Fowler, F.R.S., for his helpful interest and advice and for the excellent experimental facilities he has afforded me in his laboratory.

Summary

The spark spectrum of antimony has been excited in a hollow cathode discharge and examined for fine structure in the region $\lambda\lambda$ 6800–5000 with a silvered Fabry-Perot interferometer. Structures, most of which are highly complex, were measured in 26 lines.

* Campbell, 'Nature,' vol. 131, p. 204 (1933).

The structures are completely explained by attributing a nuclear spin of $5/2$ to both of the isotopes 121 and 123, but the nuclear magnetic moment of the former is 1.37 times as great as that of the latter.

Fine structure interval factors, for both isotopes, have been calculated for 11 terms.

The $g(I)$ factors are found to be 1.1 and 0.8 for the 121 and 123 isotopes respectively.

The Scattering of Slow Electrons by Organic Molecules
I—Acetylene, Ethylene, and Ethane

By E. C. CHILDS, Ph.D., Exhibition of 1851 Senior Student, and
A. H. WOODCOCK, M.A.

(Communicated by Lord Rutherford, O.M., F.R.S.—Received March 20, 1934)

Introduction

It is now well established that beams of electrons are scattered by atoms to produce diffraction maxima and minima which may be fairly well accounted for by considering the probability of an electron travelling in any particular direction as a wave function. The atom provides a refrangient medium the refractive index of which depends both on the initial energy of the electron and the potential at the region of the atomic field occupied by that electron. In previous papers by Massey and one of us* comparison was drawn between the diffraction patterns for the members of the zinc, cadmium, and mercury group, which are of very similar structure in the outer shells, and the conclusion was drawn that the region in the atomic field which is chiefly responsible for the scattering, is that in which the orbital electron energy is of the order of magnitude of the energy of the incident electrons, shells of similar radius and energy scattering similarly. Hence there is the possibility that the structure of atoms and molecules may be investigated experimentally by a comparison of their electron scattering patterns, using electrons of various energies, with those for atoms of known fields. Since, however, few molecules possess even approximately spherical symmetry, even at considerable distances,

* Childs and Massey, 'Proc. Roy. Soc.,' A, vol. 141, p. 473 (1933); vol. 142, p. 509 (1933).

it is important that the effect of lack of spherical symmetry should be known. For this purpose the group of molecules comprising acetylene, ethylene, and ethane was chosen. The outer field contours of these molecules vary from roughly spheroidal for acetylene to dumb-bell-shaped for ethane.

Description of Apparatus and Experimental Procedure

The quantity measured in the present experiments was the fraction of the incident electron beam scattered into a certain fixed solid angle, and the variation of the scattered electron current with the angle of scattering was investigated using an apparatus similar to that of Bullard and Massey.* This has often been described, and consists of an electron gun providing a narrow beam of electrons, and a Faraday cylinder surrounded by an outer screen containing two slits. The latter is mounted on a ground joint and may thus be rotated. The slits of both the electron gun and the collecting system are aligned on the axis of rotation, so that the latter defines the solid angle of collection while the gun and collector together define the angle of scattering and the scattering volume. After alignment the whole is inserted through a large ground joint in a pyrex tube, which is then evacuated to a pressure of about 10^{-6} mm of mercury and baked at a high temperature to remove back-ground scattering.

The gas investigated was contained in a glass bulb of about 4 litres capacity at a pressure of nearly 2 cm of mercury. It was passed into the scattering chamber through a capillary tube leak, so that a suitable pressure of a few thousandths of a millimetre was maintained against the pumps, a continuous flow of pure gas thus being secured. The liquid air trap between the tube and the McLeod gauge prevented the measurement of the pressure in the scattering chamber, but frequent check measurements were taken to ensure that this was constant. The magnitude of the scattered current was such that the probability of plural or multiple scattering was small. A precise knowledge of the pressure was not important, as absolute measurements cannot be made with the apparatus.

Electrons which had made inelastic collisions were rejected by the Faraday cylinder, to which was applied a retarding potential sufficient to maintain it at a few volts positive with respect to the filament of the gun. When the electron energies were above the ionization energy of the molecules (about 10 volts) the positive ions produced were prevented from reaching the collector

* 'Proc. Roy. Soc.,' A, vol. 130, p. 579 (1931).

by applying a positive potential to the outer case, relative to the potential of the scattering chamber. When this was not effective the ion current was measured separately by rejecting all electrons at the Faraday cylinder, the total current being then corrected by this amount.

Of the gases used, acetylene and ethylene were supplied by the British Oxygen Company, the former dissolved at high pressure in acetone-saturated kapok, and were not further purified. Ethane was not obtainable commercially and was prepared chemically, using the Grignard reaction.

Results and Discussion

The results obtained are shown in fig. 1 and Tables I, II, and III. The form of the curves varied so rapidly with voltage at the lower end of the range studied that it was necessary to obtain results at very small voltage intervals. Angular distribution curves were therefore taken for approximately 4, 6, 8, 10, 12, 15, 20, 25, 30 and 40 volts, represented by v in the tables, θ being the angle of scattering. At the conclusion of these experiments there appeared a description by Hughes and McMillen* of similar experiments with acetylene and ethylene, mainly at higher voltages. Their 10-volt curves (their lowest) agree reasonably well with ours, but rather better for acetylene than for ethylene. Their 25-volt curves, however, indicate larger scattering, relative to the 10-volt ones, than do ours. The same discrepancy is shown when their results for methane are compared with those of Bullard and Massey.† The latter give curves for 20- and 30-volt electrons, from which the 25-volt curve had to be interpolated.

It is apparent that at low voltages there is a steady transition of the form of the angular distribution curves from acetylene, through ethylene, to ethane, but at higher voltages, where comparison is necessarily made mainly by steepness at small angles, the order becomes ethylene, acetylene, ethane. If comparison is also made with methane, which has roughly spherical symmetry, it is found that ethylene bears the greatest resemblance to this gas rather than to the spheroidal molecule acetylene.

In order to discuss the results in the light of molecular fields, we may use the theory of Pauling‡ and Slater,§ or of Hund and Mulliken|| concerning the

* 'Phys. Rev.,' vol. 44, p. 876 (1933).

† 'Proc. Roy. Soc.,' A, vol. 133, p. 637 (1931).

‡ 'J. Amer. Chem. Soc.,' vol. 53, pp. 1367, 3225 (1931).

§ 'Phys. Rev.,' vol. 37, p. 481 (1931).

|| A list of references may be found in Mulliken, 'Phys. Rev.,' vol. 41, p. 751 (1932).

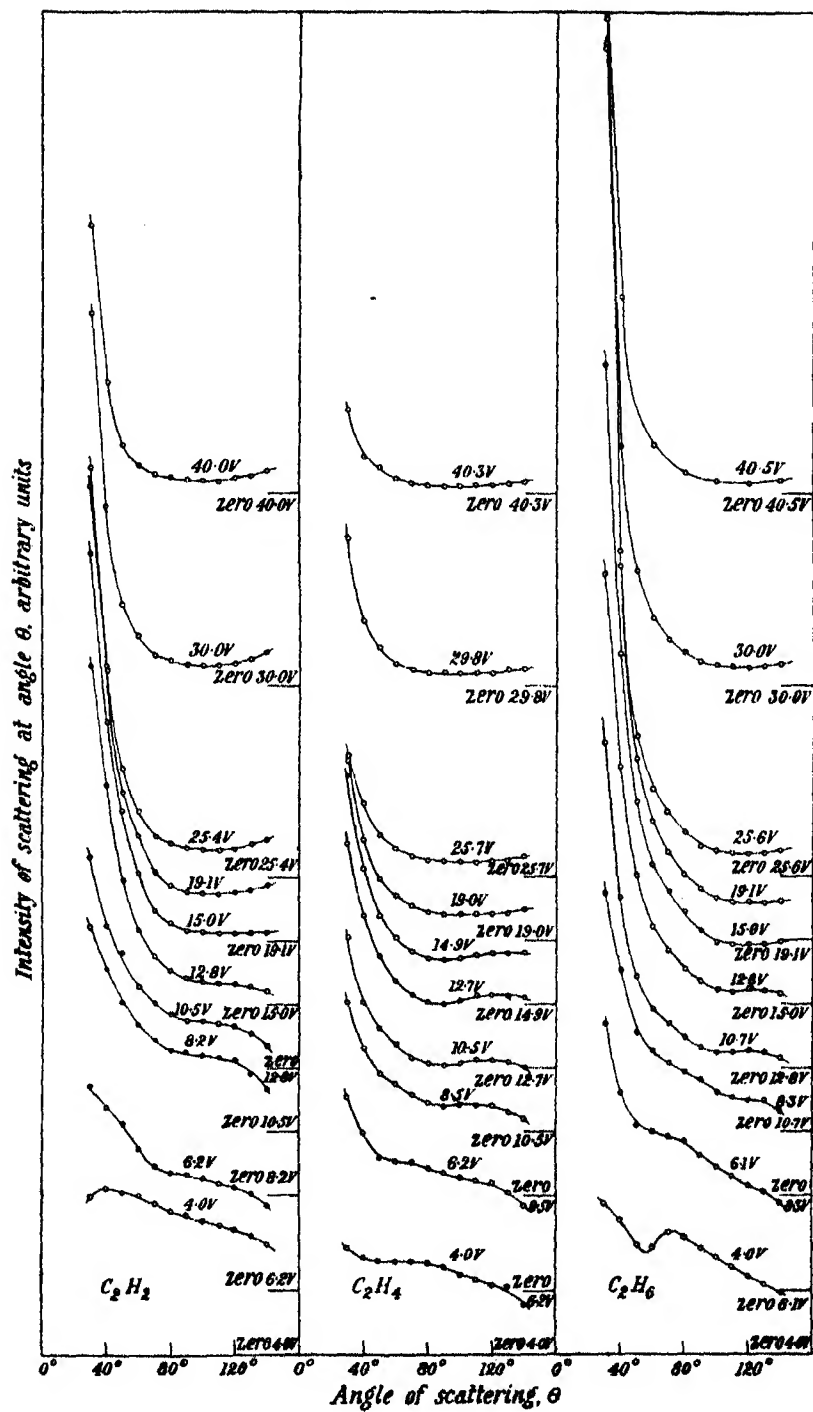


Table I—Acetylene

$\theta^\circ \backslash v$	4.0 v.	6.2 v.	8.2 v.	10.5 v.	12.8 v.	15.0 v.	19.1 v.	25.4 v.	30.0 v.	40.0 v.
30	0.496	0.645	0.845	0.860	1.26	1.41	1.42	1.28	1.16	0.838
40	0.521	0.575	0.713	0.647	0.887	0.887	0.853	0.664	0.559	0.344
50	0.507	0.513	0.612	0.562	0.589	0.605	0.463	0.339	0.266	0.162
60	0.497	0.443	0.540	0.459	0.435	0.415	0.329	0.206	0.153	0.084
70	0.473	0.388	0.489	0.403	0.356	0.297	0.215	0.131	0.094	0.061
80	0.449	0.369	0.458	0.371	0.309	0.254	0.173	0.105	0.080	0.051
90	0.436	0.361	0.453	0.348	0.286	0.232	0.157	0.092	0.070	0.041
100	0.420	0.352	0.439	0.349	0.271	0.220	0.153	0.086	0.064	0.041
110	0.404	0.337	0.435	0.343	0.270	0.224	0.150	0.086	0.064	0.037
120	0.389	0.324	0.425	0.333	0.266	0.223	0.153	0.092	0.073	0.050
130	0.373	0.304	0.383	0.310	0.258	0.224	0.160	0.105	0.085	0.056
140	0.346	0.269	0.335	0.273	0.241	0.227	0.174	0.119	0.102	0.069

Table II—Ethylene

$\theta^\circ \backslash v$	4.0 v.	6.2 v.	8.5 v.	10.5 v.	12.7 v.	14.9 v.	19.0 v.	25.7 v.	29.8 v.	40.3 v.
30	0.336	0.610	0.610	0.610	0.705	0.710	0.594	0.368	0.462	0.262
40	0.305	0.479	0.465	0.408	0.480	0.427	0.317	0.232	0.203	0.115
50	0.293	0.420	0.385	0.325	0.353	0.279	0.191	0.130	0.117	0.081
60	0.293	0.408	0.350	0.275	0.274	0.211	0.139	0.091	0.070	0.045
70	0.293	0.403	0.317	0.231	0.228	0.166	0.107	0.064	0.054	0.031
80	0.288	0.384	0.291	0.214	0.206	0.144	0.088	0.052	0.039	0.025
90	0.274	0.369	0.280	0.207	0.200	0.140	0.082	0.050	0.044	0.021
100	0.253	0.358	0.285	0.216	0.211	0.143	0.082	0.046	0.036	0.022
110	0.236	0.346	0.285	0.226	0.226	0.157	0.084	0.044	0.040	0.026
120	0.220	0.340	0.282	0.223	0.225	0.160	0.082	0.052	0.039	0.029
130	0.214	0.310	0.260	0.221	0.224	0.160	0.086	0.052	0.052	0.031
140	0.161	0.272	0.238	0.201	0.221	0.162	0.100	0.064	0.053	0.037

Table III—Ethane

$\theta^\circ \backslash v$	4.0 v.	6.1 v.	8.3 v.	10.7 v.	12.8 v.	15.0 v.	19.1 v.	25.6 v.	30.0 v.	40.5 v.
30	0.475	0.840	0.950	1.220	1.55	2.00	2.79	2.69	2.03	1.49
40	0.423	0.622	0.707	0.733	0.942	1.10	1.22	0.975	0.750	0.618
50	0.346	0.521	0.509	0.488	0.604	0.633	0.570	0.421	0.360	—
60	0.338	0.498	0.456	0.386	0.444	0.437	0.369	0.274	0.216	0.157
70	0.366	0.484	0.418	0.341	0.366	0.353	0.277	0.201	0.143	—
80	0.369	0.469	0.386	0.295	0.309	0.291	0.203	0.140	0.103	0.065
90	0.334	0.424	0.363	0.262	0.271	0.230	0.161	0.096	0.076	—
100	0.309	0.388	0.324	0.248	0.246	0.196	0.129	0.082	0.063	0.040
110	0.278	0.359	0.311	0.246	0.236	0.185	0.116	0.076	0.059	—
120	0.244	0.331	0.298	0.243	0.244	0.185	0.120	0.073	0.055	0.035
130	0.219	0.312	0.299	0.248	0.243	0.188	0.118	0.074	0.059	—
140	0.196	0.275	0.262	0.228	0.234	0.192	0.120	0.078	0.061	0.041

electronic structure of molecules. According to the former the building of the molecule is considered as a process of overlapping of atomic wave functions. Atoms possessing complete outer shells of eight electrons are inert, while those atoms with incomplete shells have valence bonds formed by the tendency of those wave functions representing orbits lacking electrons to overlap with similar ones in neighbouring atoms. For hydrogen this is a $1s$ electron, with a spherically symmetrical probability distribution. For carbon there are three p bonds forming a mutually perpendicular system, and one s bond, a slight rearrangement producing the well-known tetrahedral model. Acetylene is represented by two such tetrahedra sharing a common base, ethylene by two sharing a common edge, and ethane by two sharing an apex only. According to Hund,* single bonds are always of σ^2 type, double bonds of $\sigma^2\pi^2$ type, and triple bonds of $\sigma^2\pi^4$ type, where σ bonds are symmetrical about the nuclear axis and π bonds have a distribution proportional to $\sin \theta$, θ being the rotation about the axis. Hence we see that ethane is roughly symmetrical about the C—C axis, and is dumb-bell-shaped, acetylene is quite symmetrical about the C—C axis, the two π bonds together being symmetrical, and is roughly spheroidal or cylindrical, while ethylene is unsymmetrical, the π bond giving a charge distribution projecting out of the plane of the atoms. The molecules are all approximately of the same size and have the same ionization potential,† hence differences in the electron diffraction curves are most probably due to differences in shape, and at low voltages we have seen that there is the steady transition expected. When the scattering molecule is not spherically symmetrical, the angular distribution of the scattered electrons depends on the orientation of the molecule relative to the direction of the incident electron beam, and since the molecule is practically stationary during the time in which an electron is in its field, the results obtained are an average over all directions of incidence. At the higher voltages scattering is taking place mainly in the unshared atomic orbits, interference occurring between the waves scattered from the various centres. It seems reasonable to suppose that, with such conditions, the angular distribution of scattering would depend very markedly on the molecular orientation, and that averaging over all directions of incidence would account for the smoothing out of any diffraction maxima and minima. Such arguments may also account for the fact that ethylene does not take its place between acetylene and ethane for the higher

* 'Z. Physik,' vol. 73, p. 565 (1932).

† Hughes and Dixon, 'Phys. Rev.,' vol. 10, p. 495 (1917).

voltages as for the lower. From the atomic configuration point of view, acetylene is cylindrically symmetrical and ethane is roughly so, while ethylene is a plane molecule. Averaging might therefore have a more profound effect for the latter substance than for the former. The similarity between ethylene and methane is not, however, accounted for. It is possibly fortuitous, since the sizes and ionization potentials of the molecules are different, as well as the symmetries.

We wish to express our thanks to Lord Rutherford and to Dr. J. Chadwick for the interest they have shown in the progress of the work, and to Dr. H. S. W. Massey (with whom the experiments were first begun) and Dr. W. G. Penney for discussion of some of the points involved.

Summary

Experiments have been carried out to measure the angular distributions of 4, 6, 8, 10, 12, 15, 20, 25, 30 and 40 volt electrons scattered elastically in acetylene, ethylene, and ethane. The results are discussed in relation to the shapes of the molecular field contours and, at the higher voltages, to the symmetry of the atomic configurations.

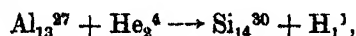
Artificial Radioactivity

By C. D. ELLIS, F.R.S., and W. J. HENDERSON (1851 Exhibitioner)

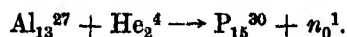
(Received June 21 1934)

§ 1 *Introduction*

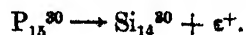
The new phenomenon of induced radioactivity discovered by Curie and Joliot* presents many points of exceptional interest. It appears that when α -particles collide with aluminium nuclei two different processes may occur. A proton may be ejected



leaving a stable isotope of silicon. This is the process which has been investigated in great detail, notably by Chadwick and his collaborators. Alternatively a neutron may be ejected instead of the proton leaving an isotope of phosphorus



This element, called radio-phorus by its discoverers, Curie and Joliot,* disintegrates with emission of positrons with a period of about 3 minutes



Similar phenomena occur using boron nitrogen or magnesium instead of aluminium.

In attempting to obtain more information about this phenomenon we have studied how the production of radio phosphorus from aluminium depends on the energy of the α -particle, and also the relative size of the effects from the other elements. In the course of this work we have had many opportunities of measuring the periods of the radioactive elements produced, and a discussion of our values is given in § 4. We have also investigated the energy of the positrons emitted from radio-phosphorus using both an absorption method and magnetic analysis.

The apparatus we used was of the simplest kind. Our source of α -particles was either Ra(B + C) deposited on a brass disc, or radon contained in a glass tube with walls sufficiently thin to allow the α -particles to escape. The positrons from the activated matter were detected by a Geiger-Müller counter.

* 'J. Phys. Rad.,' vol. 4, p. 153 (1934).

§ 2 Production of Radio-phosphorus by α -particles of Different Energies

In these experiments we used as sources small metal discs coated with either Ra(B + C) or Th(B + C) and the aluminium to be activated, which was also in the form of a disc, was placed within a few millimetres of the radioactive material. To prevent contamination the radioactive source was hermetically sealed in a small container, the α -particles issuing through a window covered with thin mica. Additional mica sheets could be inserted to observe the effects of α -particles of different energies. The procedure was to expose the aluminium discs to the α -rays for 10 minutes, then to remove them and place them in a standard position in front of the counter. Counting was started 30 seconds after removal, and continued for 8 minutes, the total count in this time being noted. It is the average of such total counts which are shown in Table I under the heading of relative yield.

Table I

I	II	III
Energy of α -particle volts $\times 10^{-6}$ E	Relative yield of radio-phosphorus	Absolute yield $q(E) \times 10^7$
8.25	4140	6.4
7.61	3040	4.7
7.06	1290	2.0
6.66	734	1.1
6.33	464	0.7
5.49	86	0.13
4.81	15	0.02
4.20	0	0

Under our conditions of solid angles for activation and measurement we obtained a total count in 8 minutes of 22 particles per milligram activity of the source for α -particles of the maximum energy shown in the above table.

The rapid increase of the yield as the energy of the α -particle increases is similar to that observed in other cases of artificial disintegration and is mainly determined by the probability of the α -particle penetrating the potential barrier surrounding the nucleus.

A more generally useful way of presenting these results is to evaluate the probability $q(E)$ that an α -particle of energy E will at some portion of its range form a radio-phosphorus atom. This quantity, the absolute yield, is shown in column III of Table I and was obtained from the results in column II by taking into account the period of radio-phosphorus, the duration of the periods of activation and measurement, and the solid angles involved.

As an example we may consider the result of exposing a piece of aluminium for a long time to the action of a source emitting n α -particles per second. Then if P denote the equilibrium number of radio-phosphorus atoms formed, and λ the disintegration constant of this body

$$P\lambda = q(E) \cdot n.$$

The initial activity of the radio-phosphorus source is $P\lambda$. If for n we write the number of α -particles emitted per second per millicurie 3.7×10^7 , it can

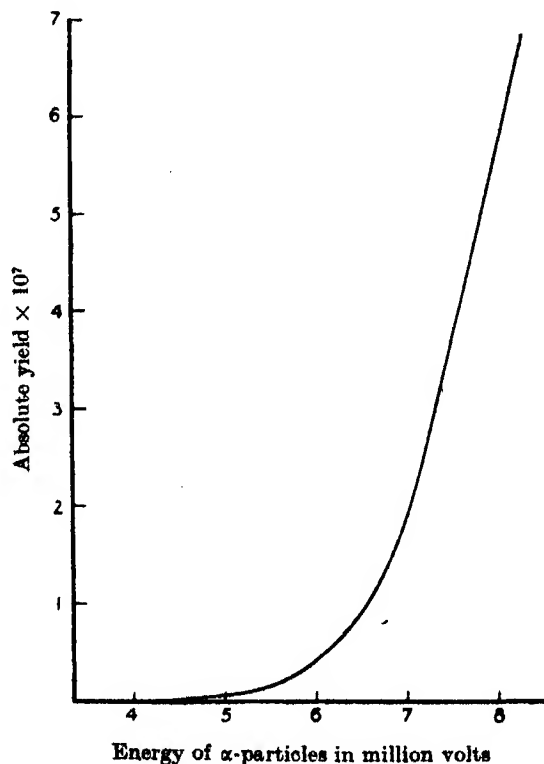


FIG. 1

be seen that initial activities (solid angle 4π) of 4 to 20 positrons per second can be obtained from activation by 1 millicurie of a radioactive substance.

While the excitation curve shown in fig. 1 is not very accurate it is sufficiently dependable to justify a further analysis to determine the excitation probability $Q(E)$. This has the meaning that $Q(E)dE$ is the probability that an α -particle will form a radio-phosphorus atom during its passage through that amount of aluminium which causes its energy to change from E to $E - dE$. The

excitation probability determined by differentiation of the curve in fig. 1 is shown graphically in fig. 2.

The significant feature of this curve is the flattening which starts at an energy of about 8×10^6 volts. We should hesitate to lay much weight on the exact details of this curve, but we feel convinced that at least a pronounced decrease in the rate of rise of the excitation probability $Q(E)$ must commence about here. Detailed information about the potential barrier of the aluminium nucleus has been obtained from observations on the protons emitted under

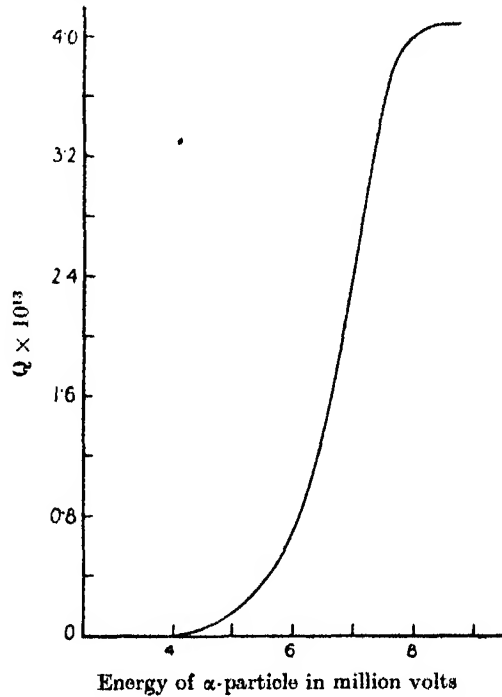


FIG. 2

α -particle bombardment. As is well known these experiments have shown the existence of a number of resonance levels and also that the top of the potential barrier is about 8×10^6 volts. Our experimental conditions were not definite enough, nor the changes in the energy of the α -particle sufficiently small to have any chance of detecting individual resonance levels, but the flattening of the excitation curve at 8.0×10^6 volts is in agreement with the top of the potential barrier having this energy.

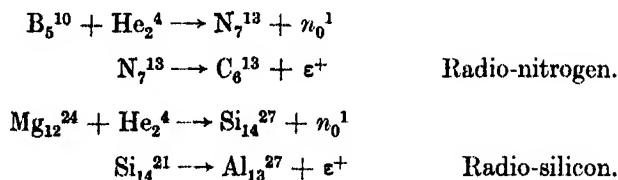
It is interesting to form some estimate of the relative probabilities of proton to neutron emission (leading to the formation of radio-phosphorus), but only

rough data are available. The absolute yield of protons from the complete absorption of one α -particle of 7.6×10^6 volts energy is about 10^{-5} , and contrasting this with the figure 5×10^{-7} for neutrons we find proton emission is twenty times more probable.

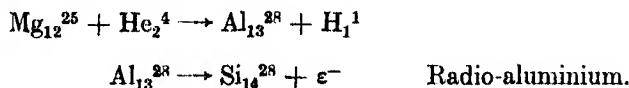
The figures for the excitation probability for neutron disintegration given in Table II lead, in the case of an α -particle of 8×10^6 volts energy, to an effective cross-section of about 10^{-26} cm², whereas the top of the potential barrier of aluminium presents a cross-section of about 6×10^{-25} cm². We can see that if an α -particle hits an aluminium nucleus with enough energy just to pass over the top of the barrier it has a chance of the order of 1 in 60 of ejecting a neutron. It seems probable, and it would fit in with these rough estimates, that the corresponding probability of proton ejection is of the order of unity.

§ 3 *Relative Magnitudes of the Effects from Boron, Aluminium, and Magnesium*

The corresponding effects in boron, nitrogen, and magnesium are believed to be



According to Curie and Joliot (*loc. cit.*) there is also a radioactive body formed from magnesium which emits negative electrons. They suggest that in this case the reaction is



We have not separated these two effects and in what follows the yield from magnesium refers to the sum of the positrons and electrons and for convenience will be referred to as originating from radio-silicon.

We can best compare the efficiencies with which these radio-elements are formed by finding the total number of active atoms formed by a very long exposure to a constant source of α -rays. The experiments were carried out in the same way as for aluminium except that radio-nitrogen with a period of 14 minutes needed a longer exposure. In each experiment the time of exposure was noted to permit of correction to infinitely long exposure, and the positrons

were counted over a period of at least two or three times the half life, and this number corrected to give the total number which would be observed in an infinitely long count.

We shall first consider the results found by comparing the formation of radio-nitrogen, radio-phosphorus, and radio-silicon from boron, aluminium, and magnesium respectively using in each case the complete absorption of α -particles of energy 7×10^6 volts. If as before we denote by q the chance of such an α -particle producing an active atom at some point in its path, and by P the total number of such atoms formed in a long exposure to a constant source of n α -particles per unit time, then $P\lambda = qn$.

In the next table under the heading total yield are shown relative values of the quantity P , and from this values for the initial activity $P\lambda$ were obtained by multiplying by the appropriate decay constant. These figures give relative values for q , the efficiency of production. Assuming that the effective isotope of boron is B^{10} [$B^{10} : B^{11} :: 1 : 4$] we obtain the values under the heading " q corrected." We have not corrected the value for magnesium since we did not separate the positron from the β -disintegration.

Table II—Formation of radio-nitrogen, radio-phosphorus, and radio-silicon by α -particles of energy 7×10^6 volts

Relative values	Radio-nitrogen from boron	Radio-phosphorus from aluminium	Radio-silicon from magnesium
Total yield, P	19	34	6.2
Efficiency of production, q	1.0	7.3	2.0
q (corrected)	5.0	7.3	—

When examining the yield from boron the decay curve was found to consist of two distinct portions of 1.1 minute half period and 14 minutes half period respectively. The effect with a 1.1 minute period was found to occur with a variety of substances including copper and platinum with well-cleaned surfaces. The effect must be due to some common contamination on all surfaces such as occluded gas and is undoubtedly the radio-fluorine reported by Wertenstein* as formed from nitrogen. Using a source consisting of a thick layer of amorphous boron held by celluloid paint to a metal disc the initial intensity from activated nitrogen and activated boron were about equal and corrections had to be applied to calculate the boron yield. Corrections have also been made for this effect in calculating the boron yield, but not for aluminium since here the relative magnitudes of the effect rendered it unnecessary.

* 'Nature,' vol. 133, p. 564 (1934).

§ 4 *Periods of Decay*

We found it a matter of some difficulty to obtain accurate values for the half periods of these radioactive bodies owing to the statistical fluctuations. We counted 12,000 particles from radio-phosphorus using a succession of sources and extending the measurements over 6 to 8 minutes in each case.

Even with this number of particles we are not able to give a closer value than 3.2 ± 0.1 minutes. At one time we thought we had detected a dependence of the period on the energy of the activating α -particle, but subsequently we concluded that if such an effect does exist it must be of the same order as the variation due to statistical fluctuations.

Our values for the periods of the other bodies are :—

Radio-nitrogen (from boron)	14 ± 1 minute
Radio-fluorine (from nitrogen)	1.1 ± 0.1 minute
Radio-silicon and radio-aluminium (from magnesium)	2.1 ± 0.2 minute.

The limits of error assigned to these values may seem large, but we have looked into the question carefully and found that the statistical fluctuations do, in fact, have a larger effect on the period than might at first be anticipated. The values given here agree within the assigned limits of error with those of Curie and Joliot (*loc. cit.*).

§ 5 *Recoil*

The nuclear reaction proposed by Curie and Joliot for the activation of aluminium is that the α -particle penetrates the aluminium nucleus, a neutron is at once emitted and thus a radio-phosphorus atom is formed. Knowing the energy of the α -particle, and the energy released during the reaction the energy of the recoil phosphorus atom can be calculated from the equations expressing the conservation of energy and momentum. It is known that 2.07×10^6 volts are released in the reaction $\text{Al}_{13}^{27} + \text{He}_2^1 \rightarrow \text{Si}_{14}^{30} + \text{H}_1^1$ and taking the value given in § 5 for the upper limit of the continuous spectrum of positrons as the energy released in the reaction $\text{P}_{15}^{30} \rightarrow \text{Si}_{14}^{30} + e^+$ it follows that there must be 0.78×10^6 volts absorbed in the reaction $\text{Al}_{13}^{27} + \text{He}_2^4 \rightarrow \text{P}_{15}^{30} + n_0^1$. Hence, using 7×10^6 volt α -particles the maximum energy of the recoil P_{15}^{30} atom in the forward direction is 1.76×10^6 volts corresponding to a range of about 3.6 mm in air at N.T.P. It is also found that all the recoil radio-phosphorus atoms are knocked forward within an angle of 26° with the

direction of the α -particle. From this it would seem quite an easy matter to collect the recoil radio-phosphorus atoms. A thin piece of aluminium of about 1 mg/cm² was bombarded with α -rays, and about 2 mm from the opposite side was placed a collecting disc of copper or silver. After a 10-minute exposure the disc was found to be active with a period slightly less than radio-phosphorus. When gold was substituted for the aluminium the activity on the disc was greatly reduced and had the period of radio-fluorine which, as mentioned above, is common to all metal surfaces. That the period of the activity collected from aluminium was less than that of radio-phosphorus is explained by the fact that the α -rays are penetrating the aluminium and producing radio-fluorine from the nitrogen occluded on the metal discs. The two effects could not be clearly separated owing to the small intensity. The number of radio-phosphorus atoms collected was slightly increased by making the collecting disc negative with respect to the aluminium. Wertenstein (*loc. cit.*) has also reported briefly that he has detected the recoil.

§ 6 *The Energy of the Positrons Emitted by Radio-phosphorus*

It is obvious that information on the energy of emission of the positrons in these new types of disintegration will be important in obtaining a clearer understanding of the phenomenon, but unfortunately it is not easy to make accurate measurements owing to the relatively small magnitudes of the effects.

We first carried out experiments by a simple absorption method, placing the activated aluminium (source of radio-phosphorus) about 15 mm from the counter and interposing absorbing sheets of aluminium and copper. The absorption curves so obtained are shown in fig. 3 and for comparison absorption curves of the β -particles from Th(C + C'') and ThC''' taken under identical conditions are included in the figure. The β -particles from these two sources form continuous spectra with upper limits at 2.25×10^6 volts and 1.79×10^6 volts respectively.*

The most significant difference between the curves is the initial flat portion of the positron curves. While 0.1 gm/cm² of aluminium absorbs at the most 10% of the positrons it reduces the β -rays of ThC to 45%. This can only mean that there are relatively fewer slow particles in the positron spectrum than in the β -ray spectrum. It appears that there are very few, if any, positrons from radio-phosphorus with a range less than 0.05 gm/cm² which corresponds to about 1700 Hp or $0.2 + 10^6$ volts.

* Henderson, 'Proc. Roy. Soc.,' A (*in the press*).

The absorption curve of the positrons in aluminium has been extended to greater thicknesses until all the positrons were absorbed. At 1.3 gm/cm^2 the intensity has been reduced to between 3% and 4% and from here on the curve becomes nearly flat. The residual intensity through 1.3 gm/cm^2 is presumably at least partly due to radiation produced by the annihilation of a positron and electron.

The range, as with the β -rays is not a very definite quantity, but a point on the absorption curve can be chosen where nearly all positrons have been

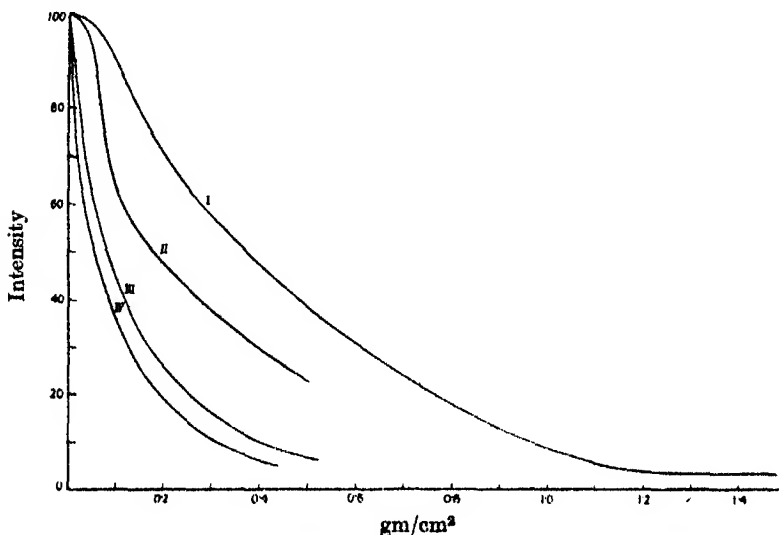


FIG. 3—I, Radio-phosphorus, positrons absorbed in Al; II radio-phosphorus, positrons absorbed in Cu; III, thorium C, β -rays, positrons absorbed in Al; IV, thorium C, β -rays, positrons absorbed in Cu.

absorbed and from this a value can be found for the energy of the fastest positrons in the beam. Taking 1.25 gm/cm^2 as the range, and assuming the energy-range relation is the same as for the β -rays, we find as an upper limit 2.74×10^6 volts from the known data concerning ranges and upper energy limits of the β -ray spectra, and some new measurements by one of us* on the upper energy limits of ThC and ThC''.

An interesting and important point is to see whether the positrons form a continuous energy spectrum as occurs for β -rays. While the absorption curve is compatible with such a distribution the conditions of experiment and also the method itself are not suitable for settling such a question. We

* Henderson, *loc. cit.*

therefore endeavoured to analyse the spectrum by the usual semi-circular magnetic focussing method. Accurate measurements were impossible owing to the small intensities available, and the shortness of the period also introduced difficulties, but we have been able to show that the positrons are distributed in a continuous spectrum extending from $H\beta$ 11,000 to below $H\beta$ 2500. We could not follow the spectrum to lower speeds owing to the presence of absorbing foils through which the positrons had to pass. The value obtained for the upper energy limit is $H\beta$ 11,100 or 2.85×10^6 volts which agrees fairly well with that obtained from the range measurements. This point is of some importance since it indicates that the relation between range and energy is

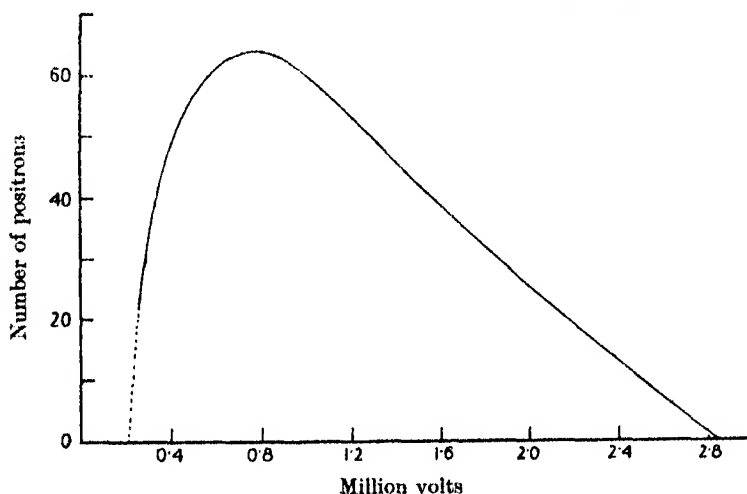


FIG. 4

very similar to that for β -rays. The distribution curve against energy is shown in fig. 4, the dotted portion being sketched in to end at 200,000 volts as suggested by the absorption measurements.*

The two significant features which we can discuss at present are the upper and lower energy limits. The upper energy limit is no doubt analogous to that found for β -rays, and is associated with the total energy of disintegration. We therefore see that the energy difference between P_{15}^{30} and Si_{14}^{30} is 2.85×10^6 volts plus any γ -ray energy that may be emitted corresponding to the mode

* Meitner ('Naturwiss.', vols. 22/24, p. 388 (1934)) has recently described the results of experiments on the formation and disintegration of radio-phosphorus. There appears to be some divergence between her results and ours in that she finds a smaller upper limit for the energy of the positrons— 2×10^6 volts and further her data may suggest a higher yield for the formation of radio-phosphorus than we have reported.

of disintegration giving this end point. We have at present no information on this question.

The lower limit is one feature in which the positron differs from the β -ray disintegration, but while it is clearly connected with the sign of the charge of the emitted particle and possibly its reaction with the Coulomb field, a detailed interpretation scarcely seems possible at present. Fermi* has proposed a theory of these types of disintegration according to which a proton in the nucleus transforms into a neutron with emission of a positron and neutrino. The simplest interpretation of the lower limit would be that this energy represents the potential energy of the positron at the point where it is produced, but it hardly seems likely that the Fermi field can extend out to a point where the potential is only 200,000 volts. It seems more probable that the process is analogous to α -ray decay, the positron being produced inside the nucleus with an energy that varies according to the fraction going to the neutrino. One of the factors tending to make the curve fall off sharply at lower energies will then be the increasing difficulty of penetrating the potential barrier. This point of view would suggest that there should, in fact, be no definite lower limit but merely a marked concavity of the curve corresponding to an exponential factor.

We are very grateful to Dr. Peierls for informing us that Wick† has applied Fermi's theory to positron disintegration and finds, with the simple type of Fermi field assumed up to the present, that the distribution curve would continue to zero energy and there should be no apparent lower limit. Dr. Peierls suggests that the most obvious way of accounting for the form of the curve we find would be to assume a different type of Fermi field.

A feature of the distribution curve against energy of which we feel fairly certain is that it is asymmetrical; that is, that the average energy is less than half the maximum energy. This is the same behaviour as is found with β -ray disintegrations, and hence it would appear that the effect of the Coulomb field on the distribution is not serious. With greater certainty than before we may therefore apply Perrin's argument, and conclude from this asymmetry that the mass of the neutrino is considerably less than that of the electron.

* 'Z. Physik,' vol. 88, p. 161 (1934).

† 'Rend. Acad. Lincei,' vol. 19, p. 319 (1934).

Nuclear Spin of Radioactive Elements.

By G. GAMOW.

(Communicated by Lord Rutherford, O.M., F.R.S.—Received March 20, 1934.)

There seems at present to be rather definite evidence that the rate of radioactive disintegration, and excitation of the product-nucleus usually connected with it, is largely affected by the values of nuclear angular momenta.

It was shown by the author† that the existence of intense components of α -ray-fine-structure indicates that the disintegrating-, and the product-nuclei possess different spins. The angular momenta received in this case by α -particles of the normal group (transitions between normal states of both nuclei) will reduce its probability of escape in favour of other groups corresponding to the formation of the excited product.

From this point of view we have to accept the change of nuclear spins in normal disintegration of radioactive C-products (ThCC''; RaCC''; AcCC'') and also of most members of the actinium-family. Unfortunately the existing formula for decrease of probability does not take into account all the factors influenced by angular momenta of α -particle (only the effect due to increase of potential barrier can be simply evaluated) and therefore the values of spin-differences cannot be exactly estimated.

The role of nuclear spin in the process of β -integration was recently indicated by Fermi‡ in his theory of β -decay. According to this theory the decay constant λ for β -disintegrating bodies depends on the factor :

$$\left| \int u_n v_m^* d\omega \right|^2, \quad (1)$$

where u_n and v_m are the eigenfunctions of nuclear neutron and resultant proton. We may notice, however, that this result is not necessarily connected with the special form of Fermi's theory, and will hold for practically every theory treating the β -decay as the transformation of a nuclear neutron into a proton.

The factor (1) must be of the order of magnitude unity if the initial and resultant nuclei possess the same spin (permitted transitions) :

$$i = i' \quad (2)$$

† 'Nature,' vol. 129, p. 470 (1932); vol. 131, p. 618 (1933); Gamow and Rosenblum, 'C. R. Acad. Sci. Paris,' vol. 197, p. 1620 (1933).

‡ 'Ric. Sci.,' vol. 2, No. 12 (1933); 'Z. Physik,' vol. 88, p. 161 (1934).

and be reduced to the value

$$\left(\frac{\text{radius of the nucleus}}{\text{wave-length of } \beta\text{-particle}} \right)^{2\Delta i} \sim \left(\frac{1}{100} \right)^{\Delta i}$$

if this condition is not fulfilled (non-permitted transitions):

$$i \neq i'. \quad (2')$$

This explains the result found by Sargent† that plotting the logarithms of decay constants against the logarithms of maximum energy of β -particles we get the experimental points distributed between two different curves. We must say that the β -spectra belonging to the class I (RaD, UX₁, ThB, AcB, RaB, AcC'', ThC'', UX₂) correspond to $i = i'$ while those of the class II (RaE, MTh₃, ThC, RaC) to $i \neq i'$ (most probably $i = i' \pm 1$). One would also expect the shape of continuous β -spectra to be different for permitted and non-permitted transitions, although the present experimental evidence is not sufficient to prove that.

Remembering that the product-nucleus can be formed in different excited states, with the energy-excess not greater than the total energy-difference between the two nuclei, we must consider the following possibility. The normal state of the product nucleus possesses a spin different from that of the original one ($i_0 \neq i'_0$) but one of its excited states has the same value of spin ($i_0 = i'_n$). In such cases we must expect that the observed β -spectra will correspond to a permitted transition leading to the formation of an excited nucleus and consequently will be accompanied by a strong γ -line with absolute intensity unity (or by several less strong γ -lines, if different radiative transitions from this completely excited level are equally possible). This has actually been observed by Ellis and Mott‡, for several β -disintegrating bodies (for example, for ThBC and ThC''D). The fact that there are no β -transformations belonging to the non-permitted class and at the same time possessing γ -lines of absolute intensity unity speaks in favour of the exclusion rules (2) and (2').

We shall now apply these considerations to the forking regions of three known radioactive families for which the experimental evidence is rather complete.

In fig. 1 is given the scheme of radioactive decay from ThA to ThD (lead). From the absence of intense fine structure in the α -disintegration-row leading

† 'Proc. Roy. Soc.,' A, vol. 139, p. 659 (1933).

‡ 'Proc. Roy. Soc.,' A, vol. 139, p. 369 (1933).

to the formation of ThB, we conclude that all these nuclei (including ThB) possess the same value of spin, and one can hardly doubt that this value is zero ($i_0(\text{ThB}) = 0$). Now ThB emits a continuous β -spectrum belonging to the class I and possesses a quadrupole γ -line, $\gamma = 0.24 \times 10^6$ e.v., with absolute intensity unity.[†] Thus we must say that observed β -spectra (with $E_{\text{max}} = 0.36 \times 10^6$ e.v.) represents the permitted transformation of the ThB-nucleus into the excited state of the ThC-nucleus, and that this later state

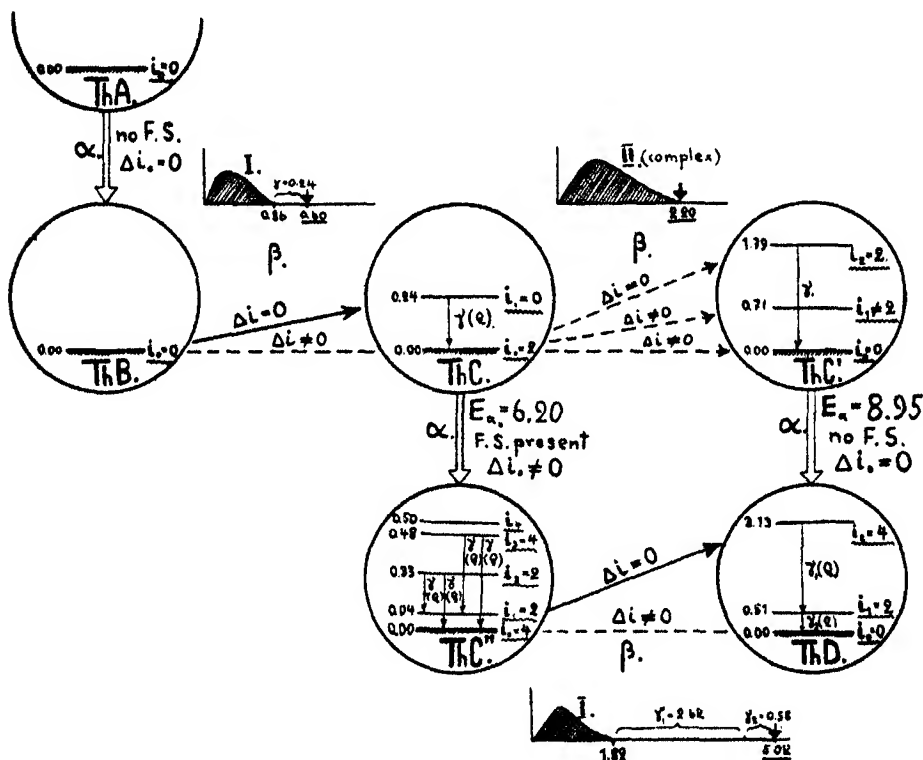


FIG. 1.

possesses the spin $i_n(\text{ThC}) = 0$. The spin of the normal state of ThC must be consequently $i_0(\text{ThC}) = 2$ as the value 0 would permit the β -transformation between the normal state and the value 1 is excluded by the quadrupole character of the γ -ray, 0.24×10^6 e.v.

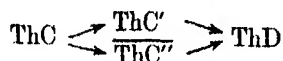
The second β -transformation leads from ThC to ThC'. The absence of the fine-structure of α -rays from ThC' shows that the normal state of this nucleus possesses the same spin as the normal state of ThD. But from spectro-

[†] 'Proc. Roy. Soc., A, vol. 139 p. 639 (1933).

scopic evidence it seems very plausible that $\text{ThD} = {}^{208}\text{Pb}$ possesses no spin. Thus: $i_0(\text{ThC}') = 0$ and the normal β -transformation ThCC' must be not-permitted in agreement with the fact that the observed β -spectra of ThC belongs to the class II. The two levels 0.71×10^6 e.v. and 1.79×10^6 e.v. estimated from ThC' long-range α -groups, correspond respectively to the permitted and not-permitted β -transformations. Thus the corresponding spins are $i_2 = 2$ and $i_1 \neq 2$. There seems to exist in the γ -spectra of ThC' a weak line corresponding to a radiative transition from the level 1.79×10^6 e.v. to the fundamental one,† and we must assume that this line has quadrupole character.

Turning our attention to ThC'' nucleus, we can compare it with ThC and ThD . The presence of strong fine-structure of α -rays from ThC shows that $i_0(\text{ThC}'')$ is in any case different from 2. Comparing ThC'' with ThD , we see that the normal β -transition is not-permitted, and consequently $i_0(\text{ThC}'') \neq 0$. The observed β -spectra of ThC'' belongs to the class I and leads to the totally excited state of the ThD nucleus, for which $i_0(\text{ThC}'') = i'_n(\text{ThD})$. The totally excited state of ThD corresponds to an energy-excess of 3.20×10^6 e.v. and gives rise to two successive γ -lines: quadrupole line $\gamma_1 = 2.62 \times 10^6$ e.v. and dipole line $\gamma_2 = 0.58 \times 10^6$ e.v., both having the absolute intensity unity. This gives to the level 0.58×10^6 e.v. the spin 1 and to the upper level 3.20×10^6 e.v. the spin 1 or 3. These values are hardly possible as it would be difficult to account for the observed fine structure of ThC α -rays if the spin-difference between corresponding normal states is only unity.

We want, therefore, to indicate the other possibility for the level scheme of ThD nucleus. From the upper limit energy-balance for the forking



we obtain for the energy of totally excited state of ThD $2.20 + 8.95 - 6.20 - 1.82 = 3.13 \times 10^6$ e.v., which is more nearly represented by the sum of $\gamma_1 = 2.62 \times 10^6$ e.v. and the other γ -line $\gamma_2 = 0.51 \times 10^6$ e.v., corresponding to the quadrupole-transition and having the absolute intensity 0.3. If we accept the γ -line 0.51×10^6 e.v. instead of 0.58×10^6 e.v. we must give to the first level (0.51) the spin 2 and to the top-level (3.13) the spins 0 or 4. As the value 0 is excluded (otherwise the normal β -transformation $\text{ThC}''\text{D}$ would be permitted), we must accept for the upper level of ThD and, consequently for the normal state of ThC'' , the spin 4, as is indicated in our diagram. This would give the spin-difference $\Delta i_0 = 4 - 2 = 2$ to the normal α -group of ThC .

† Skobelzyn, 'C. R. Acad. Sci. Paris,' vol. 194, p. 1486 (1932).

As, on the other hand, the group α_3 seems to possess the same Δi as α_0 † we must accept for the excited state 0.48 of ThC'' nucleus also the value $i_3 = 4$. This fits with the fact that the γ -transition from this level to a fundamental one has quadrupole character. The levels 0.04 and 0.33, connected with 0.00 and 0.48 by quadrupole γ -transitions, may have $i = 2$ or $i = 4$; we choose $i = 2$, as the corresponding fine-structure α -components are relatively strong. The evidence about the level 0.50 is indecisive as the only known γ -transition can be a quadrupole as well as a dipole one; the extremely high intensity of corresponding α_4 -group is also surprising.‡

It must, however, be noticed that the selection-rule for quadrupole transitions used in the article of Ellis and Mott is correct only for a model of a single radiating particle in a central field, and is not necessarily applicable to real nuclei consisting of a great number of particles. The possibility is not excluded (although not necessarily required) that for real nuclei the transitions $\Delta i = \pm 1$ (except $0 \rightarrow 1$) may be permitted in quadrupole radiation.

The evidence concerning the two other radioactive families is less complete, and we shall mention only the main points. As the β -spectrum of RaB belongs to the class I and also some intense γ -lines are present we must either regard this case as analogous to ThB, and accept the value $i_0(\text{RaC}) \neq 0$ or suppose that the normal and also one or several of the excited states of RaC nucleus possess the spins zero ($i_0(\text{RaC}) = 0$). The second possibility is, however, excluded as RaC' possesses a transition from the level 1.414 to the fundamental one which is, as well known, not permitted in radiation. This means that the fundamental state of RaC' nucleus (and also excited state 1.414) possesses the spin zero and consequently, as RaC β -spectra belongs to the class II, $i_0(\text{RaC}) \neq 0$.

The existence of fine structure of RaC α -rays give us also $i_0(\text{RaC}) \neq i_0(\text{RaC}'')$. The upper limit of the RaC'' β -spectrum is not measured but can be estimated from upper-limit energy balance and belongs to the class II. Thus

† Gamow and Rosenblum, *loc. cit.*

‡ [Note added in proof, May 23, 1934,—The detailed investigation of the relative intensities of different components of β -spectra has shown that it is difficult to account for the observed intensity of the normal β -group of ThC accepting the spin-difference $i_0(\text{ThC}) - i_0(\text{ThC}')$ to be equal to 2 units; it seems necessary to accept for it the value 1. As the value for $i_0(\text{ThC}) = 2$ seems to be rather definite we must accept for $i_0(\text{ThD})$ the value 1 and explain the absence of hyperfine structure in the optical spectra of lead by the vanishing of the corresponding Landé-factor. This will change our arguments concerning this part of the diagram and the spins of the normal and two excited states of ThD-nucleus will now be: 1; 2; 4 (accepting the level 0.58) or 1; 1; 3 (accepting the level 0.51). The first hypothesis seems now to be more probable.]

$i_0(\text{RaC}'') \neq i_0(\text{RaD})$. For RaD we probably have a situation analogous to RaB, and for the RaEF transformation we get $i_0(\text{RaE}) \neq i_0(\text{RaF})$.

The actinium-family is rather analogous to that of thorium and radium with the difference, however, that both the AcCC' and AcC''D β -transformations (upper limit of AcC β -spectra being again estimated from energy-balance†) seems here to belong to permitted transitions. One must, however, be very careful with the upper limits of β -spectra estimated in the above way.

In speaking about the energy-distribution in continuous β -spectra we must conclude that β -spectra of ThB and ThC'' must be simple. On the other hand the spectra of ThC must be constructed from different β -components corresponding to the excitation of different ThC' levels; the same kind of complexity we must also ascribe to continuous β -spectra of RaC leading to strongly excited RaC' nucleus. Ellis and Mott‡ tried to construct these complex spectra from different components with relative intensities defined by the percentage of excitation of corresponding levels of C'-products. Their constructions, however, may not be quite correct, as they assumed that all β -components have the same shape as the second class spectra of RaE, when it seems that some of these components belong to first class transitions (ThC'' component in the mixture ThC-ThC'' and the slowest components of ThC and RaC spectra) and, consequently, may have different shape.

The author is very glad to express his thanks to Professor N. Bohr for the kind interest and helpful discussion of this paper.

† Beck, 'Nature,' vol. 132, p. 967 (1933).

‡ 'Proc. Roy. Soc.,' A, vol. 141, p. 502 (1933).

The Theory of the Stability of the Benzene Ring and Related Compounds

By W. G. PENNEY, 1851 Senior Exhibitioner, Trinity College, Cambridge

(Communicated by J. E. Lennard-Jones, F.R.S.—Received March 20, 1934)

Introduction

There are two fairly distinct problems involved in a treatment of the stability of the benzene ring. The first is to explain why of all the single-ring structures C_nH_n , that of benzene ($n = 6$) is by far the most stable.* The second is to examine the different models proposed by the chemists for the benzene ring in the light of quantum mechanics and to show in fact that they are all represented with varying probabilities in the complete model. Attempts have been made at both problems, but only the second has been worked out satisfactorily. In the present paper we attempt a more accurate solution than has hitherto been given of the first problem. Before commencing this it is necessary to give a description of previous work, since otherwise it is very difficult to see what is already certain and what remains to be done.

In a series of papers Hückel† has discussed at great length both of the problems mentioned above, not only for the simple benzene ring, but also for many of its substitution products. He evaluates the energy of the plane ring compound in two ways, one of which virtually amounts to the method of generalized electron pairs and the other to that of molecular orbitals. The chief weakness in his theory is that he considers only what he calls the p_A electrons, viz., the n $2p$ -electrons whose wave functions are odd for reflection in the plane of the ring. As we shall show, the three remaining bonding electrons on each carbon nucleus have a most important influence on the best value of n . Nevertheless, Hückel's work is quite satisfactory as regards the resonance between the p_A electrons.

Pauling and his co-workers‡ have extended and greatly simplified the work of Hückel on the p_A electrons, and have successfully applied their methods to molecules even more complicated than benzene, which, however, are built

* We use the word *stable* in the mechanical sense of minimum energy rather than in the chemical sense.

† 'Z. Physik,' vol. 70, p. 204 (1931); vol. 72, p. 310 (1931); vol. 76, p. 628 (1932).

‡ Pauling, 'J. Chem. Phys.,' vol. 1, p. 280 (1933); Pauling and Wheland, *ibid.*, vol. 1, p. 362 (1933); Pauling and Sherman, *ibid.*, vol. 1, p. 679 (1933).

up from hexagonal rings of carbon atoms. They explain in greater detail than did Hückel, that with benzene, for example, it is not permissible to assume that the six p_h electrons can be separated into three electron pairs. The coupling can be done in several ways and the proper wave function to take is a linear combination of those of the various models, each with its three electron pairs. Then, in the usual way, the probability of occurrence of any particular arrangement is simply the square of the coefficient associated with it in the complete wave function. Another way of expressing the same idea is to say that the total spin S and the individual spins s_i ($i = 1, 2, \dots, 6$) are good quantum numbers,* but that the resultants of any two of the spins s_i are not.

All previous work assumes, just as we shall do, that the ring $(CH)_n$ is a plane one, with the C atoms forming a regular polygon, and the H atoms a similar but larger polygon located symmetrically around the carbon atoms. Whether this arrangement has less energy than, for example, $n/2$ separate acetylene molecules is too difficult a question to be answered at present. All that we obtain from our theory is that $n = 6$ is the most stable plane ring, and that the various bonds are just about as strong as they could possibly be in any hydrocarbon built up out of CH.

The Resonance of the p_h Electrons

We give now the energies $W_n(p_h)$ for the interaction of the n p_h electrons in the single plane ring C_nH_n . Our purpose in displaying these formulæ is simply to demonstrate that the resonance between the p_h electrons does not decide that the most stable ring is $n = 6$. Clearly, the stability is determined not by $W_n(p_h)$ but by $W_n(p_h)/n$, a quantity which, for the sake of brevity, we denote by W_n . It is found that

$$\left. \begin{aligned} w_3 &= 0, & w_4 &= -0.500 \text{ J}, & w_5 &= -0.413 \text{ J}, \\ w_5 &= -0.248 \text{ J}, & w_6 &= -0.433 \text{ J}, \end{aligned} \right\} \quad (1)$$

The values w_3 to w_6 are taken from the papers of Hückel and Pauling, and w_5 has been calculated by the author using the method developed by Pauling. The quantity J is a certain exchange integral defined in a later section as $C_{\pi\pi\pi}$. The sign of J is positive but its magnitude is a little uncertain. Accord-

* When a dynamical variable of a system is nearly or absolutely constant, either in consequence of general dynamical principles or as a result of some symmetry of the system, the quantum number relating to this variable is, in Mulliken's terminology, "a good quantum number."

ing to Pauling and Wheland* $J = 1.50$ v.e. for benzene. The present author,† however, has shown that in ethylene J must be taken about 0.7 v.e. in order to account for the observed twisting frequency. As it happens, the exact value of J is unimportant for our present purpose, and where numerical values are required $J = 1$ v.e. does very well.

Perhaps it will not be out of place here to say a few words about the determination of w_s . There are 14 canonical structures (i.e., independent singlet states) for the eight p_A electron problem of the plane ring C_6H_6 , but on account of the great symmetry of the ring the secular determinant factorizes considerably. Actually, one is left with a cubic equation to solve. One can see that this must be so in the following way. In the ground state, the two Kekulé structures must occur with equal weight, similarly the eight singly excited structures and similarly the four doubly excited structures. There are therefore only three parameters, and their elimination must lead to a cubic equation. The energy of either Kekulé structure is $-2J$; the resonance between them gives $-8J/3$ for the lower level. The resonance of this level with the eight singly excited structures, reduces the ground state to $-3.290J$. Finally, putting in the four doubly excited structures lowers the energy to $-3.3022J$, corresponding to a value $w_s = -0.413J$ as given above.

Two features stand out clearly in the set of equations (1). Firstly, for n odd and not too large, w_n is small. This would be expected since in this case there is an unbalanced spin, the influence of which on w_n becomes less and less as n increases. Secondly, if only the p_A electrons are taken into account, the ring $n = 4$ is probably the most stable of all the rings for which n is even, and is at any rate more stable than those for which $n = 6$ or $n = 8$. One might have expected $n = 4$ to be the most stable ring from the following considerations. Each ring has only two Kekulé structures and most of the p_A resonance energy comes from the interaction of these two. The stability is determined by the quotient of the resonance energy with n , and the fact that the ring $n = 4$ has the minimum possible value of n (n even) would give this ring as the most stable. It is true that as n increases the number of excited states increases rapidly, and the resonance of these with the two Kekulé structures lowers the energy of the ground state considerably, but not sufficiently rapidly to keep pace with n , and so the stability does fall off as n increases.

* Pauling, 'J. Chem. Phys.' vol. 1, p. 290 (1933); Pauling and Wheland, *ibid.*, vol. 1, p. 362 (1933); Pauling and Sherman, *ibid.*, vol. 1, p. 679 (1933).

† Penney, 'Proc. Phys. Soc. Lond.' vol. 46, p. 333 (1934).

The change in stability as n passes from six to eight is quite small, and cannot account for the experimental fact that these two rings have very different chemical properties. It thus appears necessary to appeal to the bonds in the plane of the ring for an explanation of this phenomenon and for the non-existence of the ring $n = 4$.

The Bonds in the Plane of the Ring

Expression for the Energy—Naturally, it is impossible to get an exact solution for the energy of the ring C_nH_n , and some method of approximation must be adopted. The most promising line of attack seems to be that of electron pairs. We have seen already that this method is not at once applicable to the p_A electrons because of the various ways of arranging the p_A bonds. However, when we confine our attention to the three remaining bonds on each carbon nucleus it is fairly certain that the approximation of localized bonds is a good one, because there is only one sensible way of arranging them. We shall therefore only consider the approximation of perfect electron pairing, using directed wave functions. When we do this the mathematics becomes easily manageable.

It is not proposed to give an explanation of the method since this has been done in the literature so many times already.* The expression for the energy is a sum of exchange integrals

$$W = \sum_i J_{ii} - \frac{1}{2} \sum_{i,j(i \neq j)} J_{ij}, \quad (2)$$

those with coefficient $(+1)$ arising from electron pairs and those with coefficient $(-\frac{1}{2})$ from two electrons in different pairs. The object is to make W a minimum by a suitable choice of directed wave functions. There are two types of exchange integral, the carbon-hydrogen, sufficiently defined by two and the carbon-carbon which need four suffices for their definition. For the convenience of the reader, these diatomic exchange integrals are redefined†

$$\left. \begin{aligned} N_{a\beta} &= - \int \psi_H(1s_1) \psi_C(\alpha_2) H \psi_H(1s_2) \psi_C(\beta_1) dv_1 dv_2 \\ C_{a\beta\gamma\delta} &= - \int \psi_C(\alpha_1) \psi_C(\beta_2) H \psi_C(\gamma_1) \psi_C(\delta_2) dv_1 dv_2 \end{aligned} \right\} \quad (3)$$

* See for example Van Vleck, 'J. Chem. Phys.,' vol. 1, p. 219 (1933) In this paper the directed wave functions which we employ have been used already by Van Vleck to establish the regular tetrahedron structure of methane.

† For a more detailed description and discussion of these integrals see Penney, 'Proc. Roy. Soc.,' A, vol. 144, p. 166 (1934).

Here H is that part of the Hamiltonian which depends on the co-ordinates of electrons 1 and 2, and α, β, \dots denote quantum states referred to the axis joining the two nuclei concerned in the integral.

The Directed Wave Functions in the Plane of the Ring

Our next problem is to discover the three directed wave functions on each carbon nucleus which give a maximum bonding energy. We have for their construction one $2s$ wave function and two $2p$ wave functions, all three being even on reflection in the plane of the ring and each orthogonal to the other two. Let us fix our attention on one particular carbon nucleus C , exhibited

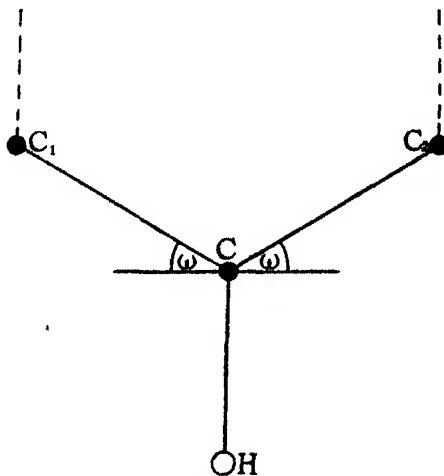


FIG. 1

in fig. 1, and denote its left- and right-hand neighbours by C_1 and C_2 respectively. Introduce an angle ω determined by the number of carbon atoms in the ring from the equation $n\omega = \pi$. Then of the three bonds of C one goes to H , one to C_1 , and the third to C_2 . Let the three directed wave functions which represent these bonds be $\psi_C(H)$, $\psi_C(C_1)$ and $\psi_C(C_2)$ respectively. Then the following give the best choice for these wave functions

$$\left. \begin{aligned} \psi_C(H) &= [k(\omega)]^{\frac{1}{2}} [\operatorname{cosec} \omega \cos 2\omega \psi_C(2p\sigma_H) + (\cos 2\omega)^{\frac{1}{2}} \psi_C(2s)], \\ \psi_C(C_i) &= (1 + \cos 2\omega)^{-\frac{1}{2}} [\psi_C(2p\sigma_{Ci}) + (\cos 2\omega)^{\frac{1}{2}} \psi_C(2s)], \quad (i = 1 \text{ and } 2) \\ 1/k(\omega) &= \operatorname{cosec}^2 \omega \cos^2 2\omega + \cos 2\omega, \quad 0 \leq \omega \leq \pi/4. \end{aligned} \right\} \quad (4)$$

Here, for example, $\psi_C(2p\sigma_H)$ is a $2p$ wave function of origin C and having $m_l = 0$ when viewed along the $C-H$ line. The phase of the wave function is defined such that the positive end encloses the H atom. Similar definitions

apply to $\psi_C(2p\sigma_{C1})$ and $\psi_C(2p\sigma_{C2})$. There will be a set of directed wave functions similar to (4) for each carbon nucleus.

Equation for the Stability

Since we are chiefly interested in the way the stability depends on n , we do not calculate the total energy W_n of the ring, but rather the quantity W_n/n , denoting this latter by S_n for brevity. It is clear that S_n is built up of parts. In the first place there is the contribution from the bonds in the plane of the ring; secondly, there is the contribution w_n from the resonance between the p_n electrons; lastly, there is the contribution from the interaction between the bonds in the plane of the ring and the p_n electrons. We can allow for the second and last of these by writing them as $w_n + K$, where the w_n are given by (1) and K is a constant, the exact expression for which is given later. It remains to estimate the contribution to S_n from the bonds in the plane of the ring. This can be done from a consideration of the interaction of the electrons on C with those on other atoms.

For the present we are going to neglect the interaction between any two hydrogen atoms, between any hydrogen atom and any but the nearest carbon atom, and between any two carbon atoms not contiguous. An estimate of the influence of these neglected terms, as well as that of the Coulomb attractions, will be made later.

A little care is needed in the evaluation of $(S_n - w_n - K)$. If we limit ourselves to the bonds of C in the plane of the ring, we find that their interaction with that of H must be taken with weight unity, but their interaction with those of C_1 and C_2 must be taken with weight one-half, since otherwise these latter would be counted twice in the total energy W_n . Using the wave functions (4) and the hydrogen wave functions $\psi_H(1s)$, we can evaluate the exchange integrals J as linear combinations of the fundamental integrals (3), and then perform the simple addition to obtain the energy $(S_n - w_n - K)$ after the fashion of equation (2). As a matter of fact, the algebra is considerably shortened by writing this latter as $(3\Sigma_i J_{ii} - \Sigma_{ij} J_{ij})/2$. By removing the restriction that $i \neq j$ in the second summation, we can make use of the directional properties of the bonds of sp^2 to obtain the result that the summation is independent of the hybridization.* The result can then be written straight

* *Proof*—Let there be one electron on atom A and four on C, with aggregate configuration sp^2 . Let ψ_i ($i = 1, 2, 3, 4$), be one set of normal orthogonal wave functions for C. Let $\psi_j = \Sigma_i S(j, i) \psi_i$, where $SS^{-1} = 1$. Then

$$\Sigma_i N_{ij} = \Sigma_j \int \psi_A(1) \Psi_j(2) H \psi_A(2) \Psi_j(1) d\nu = \Sigma_{ij} S(j, i) S(j, i) N_{ii} = \Sigma_i N_{ii}$$

down. The integrals J_{ii} , on the other hand, are quite lengthy, but are otherwise easily managed. We find

$$S_n = w_n + K + L + H(\omega) + C(\omega) \quad (5)$$

$$K = 2C_{\pi\pi\pi\pi} + 2C_{\sigma\sigma\sigma\sigma} + 2C_{\pi\pi\sigma\sigma} + \frac{1}{2}N_{\pi\pi},$$

$$L = C_{\pi\pi\pi\pi} + C_{\sigma\sigma\sigma\sigma} + 2C_{\pi\sigma\sigma\pi} + 2C_{\pi\pi\sigma\sigma} + 2C_{\sigma\sigma\pi\pi} + \frac{1}{2}(N_{\pi\pi} + N_{\sigma\sigma} + N_{\pi\sigma}),$$

$$H(\omega) = -3[\cos 2\omega \sec^2 \omega N_{\sigma\sigma} + \tan^2 \omega N_{\pi\pi} + 2 \tan \omega \sec \omega (\cos 2\omega)^{\frac{1}{2}} N_{\pi\sigma}] / 2 \quad (6)$$

$$C(\omega) = -3 \sec^4 \omega [C_{\sigma\sigma\sigma\sigma} + \cos^2 2\omega C_{\pi\pi\pi\pi} + 4(\cos 2\omega)^{\frac{1}{2}} (C_{\pi\sigma\sigma\pi} + \cos 2\omega C_{\pi\pi\sigma\sigma}) + 2 \cos 2\omega (C_{\pi\sigma\sigma\pi} + C_{\pi\pi\sigma\sigma} + C_{\sigma\sigma\pi\pi})] / 8. \quad (7)$$

It will be noticed that we have written S_n as a sum of terms. The reason is that we find it simpler and more instructive to consider them separately than collectively. Our object is to minimize S_n with respect to n , or since ω is directly proportional to n , with respect to ω . The constants K and L can be neglected in the variation problem, and as we have the values of w_n already, it remains only to consider the dependence on ω of the hydrogen-carbon energy $H(\omega)$ and the carbon-carbon energy $C(\omega)$.

Let us examine the dependence of $H(\omega)$ on ω . The exchange integrals N , according to Van Vleck* have the values

$$\text{I} \quad N_{\sigma\sigma} = 2.3, \quad N_{\pi\pi} = 2.0, \quad N_{\pi\sigma} = 1.0 \text{ electron-volts.}$$

However, it seems to us that this does not give enough prominence to $N_{\pi\sigma}$ nor does it differentiate quite enough between $N_{\sigma\sigma}$ and $N_{\pi\pi}$. Therefore we prefer the values

$$\text{II} \quad N_{\sigma\sigma} = 1.70, \quad N_{\pi\pi} = 1.20, \quad N_{\pi\sigma} = 1.43 \text{ electron-volts,}$$

which give equally good agreement for the difference of energy of dissociation of methane and 4CH . In fig. 2 we plot $H(\omega)$ for the two sets of values I and II. It is seen that in both cases there is a decided minimum at about $\omega = 30^\circ$. Finally, let us make the drastic assumption that

$$\text{III} \quad N_{\sigma\sigma} = N_{\pi\pi} = N_{\pi\sigma} = 2 \text{ e.v. (say).}$$

since $S(j, i) = S^{-1}(i, j)$. The proof in no way specifies the type of wave function for A , and therefore the result obtained for the integrals N holds also for the C , as is seen by a double application of the above result, summing first over one carbon atom and then over the other. Q.E.D.

* Van Vleck, 'J. Chem. Phys.', vol. 2, p. 20 (1934). The values used by Van Vleck have been obtained from spectroscopic data and also from the calculated values of Coolidge, Ireland, etc.

In case III we calculate that $H(\omega)$ has a minimum at $\omega = 35^\circ$. Now the true values of the integrals N certainly lie somewhere in the range covered by I, II and III, and must therefore be such that the function $H(\omega)$ has a distinct minimum at about $\omega = 30^\circ$ (i.e., $n = 6$). Fig. 2 does not bring out sufficiently clearly just how strong this minimum is because we have plotted the whole range $0 \leq \omega \leq \pi/4$. Perhaps a numerical example will make this point

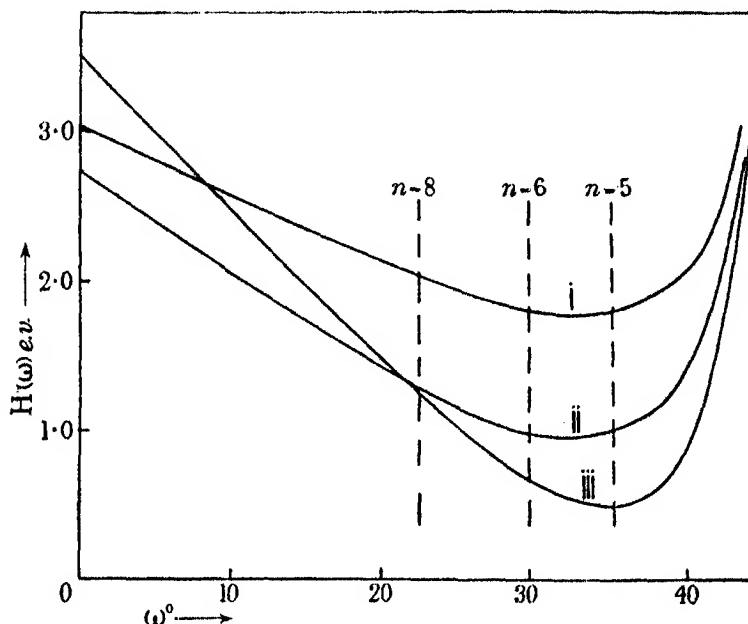


FIG. 2.—The figure illustrates the way the energy of attachment $H(\omega)$ of an H atom depends on ω in the plane ring compound $(CH)_n$. The angle ω is determined from $n\omega = \pi$. Curves I, II and III are obtained by assuming various values for the fundamental C-H exchange integrals, of which II are the most probable. It is seen that of the "even" rings, $n = 6$ is preferred.

clear. The difference between $n = 6$ and $n = 8$ in curve II is 0.30 e.v., a quantity large enough to swamp the variation in w_n .

Let us now examine the dependence of $C(\omega)$ on ω . Here we meet with considerable difficulty because the carbon-carbon exchange integrals which appear in the expression for $C(\omega)$ are practically unknown. Fortunately none of the integrals have any π - but only s - and σ -suffixes. From the usual sort of overlapping consideration we would expect C_{ssss} to be the least of the integrals and the values of the others to increase steadily with the number of σ -suffixes. The variation in the integrals will be further emphasized by the

fact that the screening for the 2s electrons is not quite so large as it is for the 2p electrons. If we assume

$$(1) \quad C_{ssss} = 1.00, \quad C_{ss\sigma\sigma} = 1.37, \quad (C_{s\sigma\sigma s} + C_{ss\sigma\sigma} + C_{s\sigma\sigma\sigma})/3 = 1.75, \\ C_{s\sigma\sigma\sigma} = 2.13, \quad C_{\sigma\sigma\sigma\sigma} = 2.50,$$

then we find that $C(\omega)$ varies with ω in the fashion shown by curve (1) in fig.

3. If we assume the set of values

$$(2) \quad C_{ssss} = 1.00, \quad C_{ss\sigma\sigma} = 1.32, \quad (C_{s\sigma\sigma s} + C_{ss\sigma\sigma} + C_{s\sigma\sigma\sigma})/3 = 1.73, \\ C_{s\sigma\sigma\sigma} = 2.29, \quad C_{\sigma\sigma\sigma\sigma} = 3.00,$$

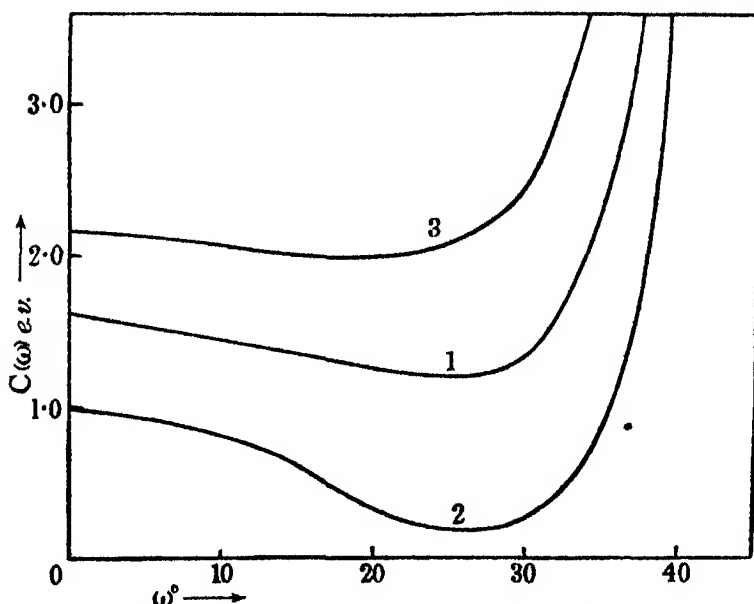


FIG. 3—The figure illustrates the way the binding energy $C(\omega)$ between the carbon atoms per carbon atom, depends on ω . Curves 1, 2 and 3 are obtained with various plausible assumptions for the C-C exchange integrals. Of the "even" rings, it is seen that $n = 6$ (or possibly $n = 8$) is preferred.

we obtain curve (2). If we take a set of values (3), intermediate to those of (1) and (2), this time making the integrals in geometric rather than arithmetic progression

$$(3) \quad C_{ssss} = 1.50, \quad C_{ss\sigma\sigma} = 1.71, \quad (C_{s\sigma\sigma s} + C_{s\sigma\sigma\sigma} + C_{ss\sigma\sigma})/3 = 1.94, \\ C_{s\sigma\sigma\sigma} = 2.20, \quad C_{\sigma\sigma\sigma\sigma} = 2.50$$

we obtain curve (3). If we make the most unlikely assumption that all of the above integrals are equal, we find that the function $C(\omega)$ has a minimum

at $\omega = 0$ and increases steadily with ω . We perceive from the above calculations that it is very probable that the function $C(\omega)$ shows a minimum at about $\omega = 30^\circ$, near enough to ensure that $n = 6$ or possibly that $n = 8$. One conclusive result we obtain is that $C(\omega)$ for $n = 4$ is much greater than the minimum value with any reasonable choice of the exchange integrals.

Discussion

We have seen that the quantity S_n , which determines the most stable ring, depends for its variation with n on the sum of three functions w_n , $H(\omega)$ and $C(\omega)$. The first of these requires that n is even, but providing this condition is satisfied the variation with n is relatively small. The function $H(\omega)$ has the important property that it shows a pronounced minimum at $n = 6$ over a wide range of values of the exchange integrals on which it depends, wide enough certainly to include the true, but unknown, values. The function $C(\omega)$ in all probability has also a minimum at about $n = 6$, but the variation in $C(\omega)$ as n changes from 6 to 8 is small. There is no escape from the conclusion that $C(\omega)$ and $H(\omega)$ are so large with $n = 4$ that the plane ring C_4H_4 is completely ruled out.

For the experimental facts concerning the existence of the rings $(CH)_n$ we refer the reader to Hückel's papers. Sufficient be it to note the following. The ring C_4H_4 is unknown. The benzene ring C_6H_6 is, of course, known and very stable. A ring C_8H_8 (cyclo-octatetrene) is known, but rings of higher order do not seem to exist. Our conclusions are seen to be in excellent accord with the experimental facts.

Cyclo-octatetrene is very different in its chemical properties from benzene, and hydrogenates very easily. It is unknown from experimental evidence whether this molecule is plane or not. Our analysis would seem to indicate that it is slightly buckled out of a plane, alternate C atoms lying equally above and below a central plane. This arrangement enables the CCC angle to be 120° , but impairs the efficiency of the resonance of the p_k electrons. One cannot, however, definitely decide whether the compound is plane or not until the various exchange integrals are known with greater certainty. What is clear, is that the compound must buckle on hydrogenation, but we defer the proof of this to the following section.

The fact that $n = 6$ is the most stable plane ring over wide ranges in the relative magnitudes of the N exchange integrals, has an obvious chemical interpretation. Any or all of the H atoms in benzene can be replaced by

other mono-valent atoms or groups, and the ring still retains its form and stability. If the ratio of the N integrals to one another did have an appreciable effect on the best value of n , one would expect to obtain very stable $n = 8$ or $n = 10$ rings, by a suitable choice of monovalent groups to take the place of H atoms. No such rings, however, have been prepared.

Refinements in the Theory

It is necessary now to investigate whether the choice of the best value of n is influenced by the inclusion of terms which up to now have been neglected. We find that if numerical values are required for the total energies these terms are of considerable importance, but it seems unlikely that they can affect the most important result which our approximate method has given, namely, that benzene is the most stable ring. The types of term now under consideration can be arranged under various headings as follows: (1) steric repulsions between H atoms; (2) steric repulsions between C atoms not contiguous; (3) steric repulsions between H and C atoms not joined by a bond; (4) Coulomb and Van der Waals forces; (5) influence of L-S structure on the energy of the carbon valence state, the wave function for which depends slightly on n . We proceed to a discussion of the separate terms (1)-(5).

If we make the reasonable assumption that the minimum C-C and C-H distances do not depend on n , then terms (1), (2) and (3) vary with n simply on account of the geometry of the rings. For example, the H-H distances vary with n , and therefore the H-H exchange and Coulomb integrals depend on n . We can calculate the effect of terms (1) exactly and the results are listed for $n = 4, 6$ and 8 under the heading W (1). They are based on the Morse function given by Eyring and Polanyi* for the interaction of two hydrogen atoms whose spins are not coupled in any way whatsoever, and C-C and C-H distances of 1.43 and 1.10 Ångströms respectively. It is seen that terms (1) tend to make n as small as possible. The variation with n in the magnitudes of terms (2) and (3) is very difficult to estimate but their net result is towards larger values of n . Fortunately, there are several influences at work which mitigate somewhat the effect of these terms. Firstly, the variation with n ($n \geq 6$) of the internuclear distances involved in (2) and (3) is a good deal smaller than the corresponding variation in those of (1). Secondly, the exchange integrals in (2) vary in sign, those involving two π suffixes probably

* 'Z. phys. Chem.,' B, vol. 12, p. 279 (1931); Eyring, 'J. Amer. Chem. Soc.,' vol. 53, p. 2537 (1931).

being of opposite sign from those involving none. Thirdly, Coulomb and Van der Waals forces are more important in C-C than in H-H interactions, and act against the exchange repulsions.

It is clearly a good approximation to take the Coulomb and Van der Waals energy between atoms coupled by a bond as independent of n . The interactions between atoms not coupled by a bond can be included in (1), (2) and (3), and as already explained, will reduce the effect of these terms.

The influence of the L-S structure can be easily calculated from a formula given by Van Vleck.* The variation of the stability with n due to this type of term is shown in the table under the heading W (5). The dependence on n is very slight provided n is taken greater than 4. The ring $n = 4$ is anomalous because in this case there is no hybridization of the $2s$ and $2p$ wave functions. Of the even n , the ring $n = 6$ gives the best value for the L-S energy, but the variation as n changes from 6 to 8 is indeed very small.

n	4	6	8
W (1) e.v.	0.096	0.224	0.336
W (5) e.v.	0.300	0.033	0.049

Summing up, we see that for the determination of the best value of n , terms (4) and (5) are unimportant. Moreover, (1) acts in the opposite direction from (2) and (3), and the net influence of these three is probably very small. Our earlier work, therefore, on the variation of the stability with n is still valid, and gives benzene as the most stable plane ring.

Application to Cyclo-Hexane

The experimental observation that there are four forms of decahydro β -naphthol and decahydro β -naphthylamine can be explained on the hypothesis that the six carbon atoms in cyclo-hexane are not coplanar. This view is supported by other examples of stereo-isomerism similar to those already mentioned above and by X-ray and electron diffraction measurements.† It is possible to some extent to understand theoretically why the benzene ring should become buckled on hydrogenation. The problem is similar to that of calculating the angles between the bonds in the molecule CX_2Y_2 considered by Van Vleck.‡ The atoms X in this case are hydrogen atoms and the Y are the two neighbouring carbon atoms of the ring.

* 'J. Chem. Phys.,' vol. 2, p. 20 (1934).

† Hassel and Kringstad, 'Tidsskr. Kemi. Bergevesen,' vol. 10, p. 128 (1931); Hassel, 'Z. Elektrochem.,' vol. 37, p. 540 (1931); Wierl, 'Ann. Physik.,' vol. 8, p. 521 (1931).

‡ 'J. Chem. Phys.,' vol. 1, p. 219 (1933).

Consider now one particular C atom in a cyclo-hexane molecule. Call the two attached hydrogen atoms H_1 and H_2 respectively, and the two neighbouring carbon atoms on either side C_1 and C_2 . Denote the $C_1C C_2$ angle by $(\pi - 2\omega)$ and the $H_1C H_2$ angle by $(\pi - 2\omega')$. The choice of directed wave functions is

$$\begin{aligned}\psi_C(C_i) &= (1 + \cos 2\omega)^{-\frac{1}{2}} [\psi_C(2p\sigma_{C_i}) + (\cos 2\omega)^{\frac{1}{2}} \psi_C(2s)], \quad i = 1 \text{ or } 2, \\ \psi_C(H_j) &= (1 + \cos 2\omega')^{-\frac{1}{2}} [\psi_C(2p\sigma_{H_j}) + (\cos 2\omega')^{\frac{1}{2}} \psi_C(2s)], \quad j = 1 \text{ or } 2.\end{aligned}$$

Orthogonality conditions demand

$$\cos 2\omega \cos 2\omega' = \sin^2 \omega \sin^2 \omega', \quad 0 \leq \omega \leq \pi/4, \quad 0 \leq \omega' \leq \pi/4. \quad (8)$$

Evaluating that part of the energy of cyclo-hexane which depends on ω and ω' , we find

$$W(\omega, \omega') = 6 [H(\omega') + C(\omega)],$$

$$H(\omega') = -3 [N_{\sigma\sigma} + 2 (\cos 2\omega')^{\frac{1}{2}} N_{\sigma s} + \cos 2\omega' N_{ss}] / (1 + \cos 2\omega'),$$

and $C(\omega)$ has been given already in equation (7). We have omitted exchange terms between non-neighbours, and steric, Coulomb, ionic, Van der Waals

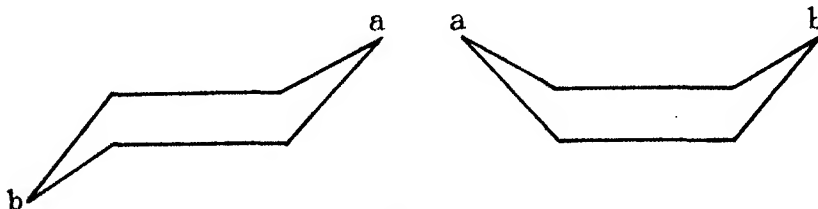


FIG. 4

and L-S terms, just as we did in earlier sections. Presumably, their net influence will be only of subsidiary importance for determining ω and ω' . The steric repulsions will, however, be of primary importance in deciding whether the "chair" or the "boat" form of cyclo-hexane is the more stable. The difference in energy arises only from the interaction of the groups labelled a and b in fig. 4, and must therefore be very small. It seems likely, without making any calculations, that the "chair" form is the more stable since this would minimize the steric repulsions between a and b . This agrees with the rather scanty experimental evidence, Hassel (*loc. cit.*).

Since there is a relation (8) between ω and ω' , the energy $W(\omega, \omega')$ can be expressed in terms of ω only. That value of ω giving a minimum W is required. If it turns out to be exactly 30° , the six carbon atoms of cyclo-

hexane are coplanar; if it is greater than 30° , the ring is buckled; if it is less than 30° , the interpretation is that there is some compound $(\text{CH}_2)_n$ with $n > 6$ more stable than cyclo-hexane and such that the carbon atoms are coplanar.

Once again, we consider the functions $H(\omega')$ and $C(\omega)$ separately, but for convenience we plot them both in fig. 5. On account of the relation between

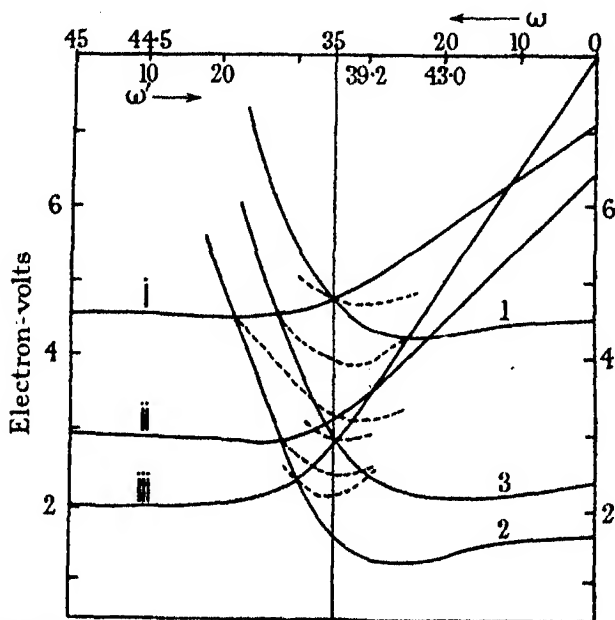


FIG. 5—The figure represents an effort to determine the CCC angle in the ring compounds $(\text{CH}_2)_n$. Curves I, II and III represent the dependence on n of the binding energy $H(\omega')$ of the two H atoms to their C atom, assuming various values for the C-H exchange integrals. Similarly 1, 2, and 3 represent the binding energy $C(\omega)$ between the carbon atoms per carbon atom, as a function of n , assuming various values for the C-C integrals. Here $2\omega = \pi - \text{CCC}$ and $2\omega' = \pi - \text{HCH}$ with ω and ω' related by (8). The value of ω giving a minimum in $H(\omega) + C(\omega)$ is required. It is seen to be within a degree or two of 34° . This result implies that the C atoms in rings $n = 3, 4$ and 5 are coplanar, but in rings $n = 6, 7, \dots$ are staggered alternately above and below a central plane.

ω and ω' , it is not possible to get an even scale for ω' if an even scale for ω is adopted. Consequently, we have plotted fig. 5 in such a way that in the left-hand half ω' increases evenly from 0 to 35° , while in the right-hand half ω decreases evenly from 35° to 0. For reference, certain corresponding values of ω and ω' have been marked. The angle $\omega = \omega' = 35^\circ$ gives the tetrahedral wave functions such as exist in methane. The various curves in the figure

have been obtained using the different sets of exchange integrals already employed with benzene, and to identify them the curves are labelled in the same way as the exchange integrals themselves. It should be mentioned that the curves do not have the same origin of energy; they have been moved up or down arbitrarily so that each can be seen as clearly as possible.

It remains to add the ordinates of H and C in fig. 5 and find where the minimum in W occurs. It is more convenient in the figure to plot $W/2$, and as we have taken three sets of values of both H and C, there are in all nine possible combinations. To prevent confusion only six of the nine curves for $W/2$ are represented in the figure, and the particular H and C involved in any one of these can be determined by tracing the separate curves from the point at which all three intersect. Two features of interest are apparent: (1) The angles ω and ω' can depart but very little from the tetrahedral value. This is imposed, not so much by the relative magnitudes of the exchange integrals, but because of the way the angles themselves appear in the expression for the energy; (2) the minimum for W is very sharp and lies within one or two degrees of 35° , the most probable value being 34° . Therefore all ring compounds $(CH_2)_n$ with $n \geq 6$ are buckled. The rings $n = 3$ and $n = 4$ are necessarily plane and the ring $n = 5$ probably.

It is found experimentally that single ring compounds $(CH_2)_n$ exist from $n = 3$ up to very high values of n ($n = 18$ or 20). Wierl* finds by electron diffraction measurements that C_5H_{10} (cyclo-pentane) is plane but that C_6H_{12} (cyclo-hexane) is angular. These observations are very nicely accounted for by our calculations. In addition, Wierl finds that C_6H_6 (benzene) is plane, in accordance with our initial assumptions.

The rings $(CH_2)_3$ (cyclo-propane) and $(CH_2)_4$ (cyclo-butane) are clearly rather different in character from the higher members of the series. We have seen that the angles between the two bonds from a C atom to the H atoms in a CH_2 group cannot deviate much from the tetrahedral value without involving a large gain in potential energy. This fact keeps the angle between the two remaining bonds also very near the tetrahedral value. Consequently it is not possible to construct a ring $(CH_2)_3$ using for the C-C bonds directed wave functions pointing from one C atom to the next, since this would imply an angle 60° between the bond directions. The geometry of the ring in cyclo-propane and cyclo-butane prevents the C-C bonds from having their best values. In other words, these bonds are "strained," and are not very strong. We see,

* 'Ann. Physik,' vol. 8, p. 521 (1931).

roughly, why heating cyclo-propane changes it over* into $\text{CH}_2 = \text{CH} - \text{CH}_3$ (propylene).

I should like to express my best thanks to Dr. H. W. Melville for helpful discussions on the chemical aspects of problems considered in this paper.

Summary

It is shown that the resonance between the p_n electrons does not select benzene as the most stable of the single-ring structures $(\text{CH})_n$; but that the binding energy of the other three bonds on each carbon nucleus does. The calculations are based on the well-known formula of perfect pairing, with directed wave functions for the C-C and C-H bonds. The energy of the ring $(\text{CH})_n$ is evaluated in terms of n and certain exchange integrals. It is found that $n = 6$ is the most stable ring over wide ranges in the exchange integrals, and this is interpreted to mean that the H atoms can be replaced by any monovalent group with little change in the form and stability of the ring. Improving the calculations by putting in some terms previously omitted does not affect the result that benzene is the most stable ring.

The ring nearest in stability to benzene is $n = 8$ (cyclo-octatetrene). The calculations indicate that this compound is probably slightly buckled out of the plane. One would expect cyclo-octatetrene to hydrogenate very easily, and in fact, it does.

The calculations can be extended to the ring compounds $(\text{CH}_2)_n$. One finds that any value of n greater than 2 can give a ring, but that $n = 3$ and 4 should be rather unstable. Rings $n = 3, 4$ and 5 should have the C atoms coplanar, but rings $n = 6, 7, \dots$, should be buckled. These conclusions are borne out by the observed stereo-isomerism and by X-ray and electron diffraction measurements.

* Chambers and Kistiakowsky, 'J. Amer. Chem. Soc.', vol. 56, p. 399 (1934).

*Discussion on Energy Distribution in Molecules in Relation to
Chemical Reactions*

Opening Address

By C. N. HINSHELWOOD, F.R.S.

(May 10th, 1934)

It often happens that the empirical observations of chemistry reveal the working of principles which can be easily interpreted in terms of physical theories, but which might have been difficult to predict. One need only mention the question of the nature of valency as one of the most conspicuous examples. For this reason it is useful if problems lying on the border line of physics and chemistry are discussed from both points of view.

The present theme is the distribution of energy in molecules and its relation to the phenomena of chemical change. We know that the transference of energy from one molecule to another and, in particular, the accompanying interconversion of translational and internal energy depend upon specific mechanisms which give rise to phenomena of great interest. I need only mention the influence of hydrogen and certain other gases in maintaining the energy distribution in unimolecular reactions, the variation of the velocity of sound with frequency, due to the finite time required for the establishment of equilibrium in the energy distribution among the internal degrees of freedom, and lastly that curious inability of solvent molecules to degrade the light energy absorbed by fluorescent substances.

There are still interesting things to be known about these phenomena, especially on the theoretical side, but I will pass on to some newer problems connected with internal rearrangements of energy which has already been given to a molecule. As we know, one form of this problem has been very prominent of late years in connexion with the type of photochemical decomposition called predissociation.

The first of the chemical problems to which I should like to draw attention is connected with the existence of what we may call independent modes of activation of the molecules taking part in certain reactions. The experimental facts are as follows. If, for a reaction involving the decomposition of a single substance, we plot the reciprocal of the time of half change against the initial pressure we obtain, in general, a curve which first rises and then bends round

to become parallel to the pressure axis. The interpretation of this curve in terms of the activation and deactivation of molecules by collision, and the transformation probability of the activated molecule is well known. Now in certain cases there is clear evidence that the curve is really composed of the superposition of several curves, and does in fact present a well-defined segmented appearance. The interpretation which we have tentatively given to this is that there are several virtually independent reactions taking place at the same time, all unimolecular, and differing only in the values of the various characteristic constants. This type of behaviour is found with nitrous oxide, with acetaldehyde and with propionic aldehyde. With the two former substances at any rate, the chemical nature of the reaction is essentially the same over the whole pressure range, so that we appear to have several physically different mechanisms by which molecules are activated for the same unimolecular chemical transformation. The hypothesis which we have found most useful in explaining this is that once a molecule has received its activation energy, the internal rearrangement of this energy is relatively difficult, and that according to the original way in which the energy was placed in the molecule there will be a different probability of chemical decomposition. To illustrate the point with one very rough example, if the N-N link of nitrous oxide is activated to a high vibrational level the probability of the decomposition $\text{N}_2\text{O} = \text{N}_2 + \text{O}$ will clearly not be the same as when the N-O link is activated. Thus the N-N activated molecules and the N-O activated molecules will undergo what are virtually independent reactions. This is an unduly simplified picture, no doubt, of what constitutes one of these modes of activation. In the hope of throwing further light on this, we have recently been making a comparison of the kinetic behaviour of a series of related compounds to see how the prominence of a given mode varied with the presence of a substituent. The series chosen was HCHO , CH_3CHO , $\text{C}_2\text{H}_5\text{CHO}$ and CCl_3CHO . I will not describe the experimental results in detail here. They form the subject of a paper now in the hands of the Royal Society, and my colleague, Mr. Fletcher, will say something about them in the course of this discussion. But I will summarize certain conclusions upon which the views of theoretical physicists would be helpful. These are (a) the hypothesis that molecules with the activation energy differently located or distributed do seem frequently, and perhaps generally to behave as virtually independent entities for kinetic purposes appears to be confirmed; (b) that, in certain substances at least, although several types of activated molecule are detectable, the number is not indefinitely great, or at any rate the types fall into a few well-differentiated

groups; (c) in a molecule like HCHO the chance that the activation energy is communicated to the molecule in such a way as to cause rapid decomposition is relatively much greater than with substituted molecules such as C_2H_5CHO ; (d) with CCl_3CHO , the CCl_3 part of the molecule is much more likely to be activated than the CHO part. To what extent this is simply a function of the greater mass of the chlorine atoms is an interesting question; (e) from the purely experimental point of view we are not yet able to estimate the relative importance of "valency oscillations" and "deformation oscillations" of the molecule, though on general grounds the importance of the latter appears to be considerable.

The question of the relation between the actual magnitude of the activation energy and the decomposition probability raises interesting questions which, however, cannot be dealt with here, as we must pass on to other matters.

The next group of problems coming within the scope of this discussion I will only just mention. In a large class of reactions it may be ambiguous whether a decomposition occurs by the mechanism $XY_2 = X + Y_2$, or by the alternative $XY_2 = XY + Y$, and subsequent reaction of the active radicle Y. I hope there may be some discussion of the general aspects of this problem, and will only say that in my opinion the dissociation idea is often carried too far, and that frequently interaction between two parts of a molecule is a process occurring more easily than the development of either in a free state.

I will now turn to a rather different type of problem, where transition probabilities of activated molecules are concerned even more intimately. There is a large class of bimolecular reactions in solution where the observed rate is as nearly as may be equal to the rate of encounter of the appropriate activated molecules. There is a second class where the reaction velocity is many powers of ten smaller than the activation rate. (Doubtless there is a continuous transition between the two classes, but we may consider extreme examples. Reactions of the second class are very sensitive to the catalytic action of solvents, and it thus appears probable that a ternary collision involving a solvent molecule is necessary. In one example, namely, the benzylation of amines in organic solvents Mr. E. G. Williams and I have been able to show that even when the condition of a simultaneous collision between two reactant molecules, suitably activated, and a solvent molecule is fulfilled, the transformation probability is still small. I have suggested that perhaps we ought to distinguish two extreme cases in chemical kinetics; the first where the rate of reaction is primarily determined by the acquisition of the necessary activation energy, and the second where a probability factor independent of temperature is of

equal or greater importance. Such a factor would be characteristic of a problem in which a quantum mechanically "forbidden" transition was involved. Such transitions occur when certain types of electronic reorganization are involved. They are greatly facilitated by perturbing forces acting on the molecules. There is a suggestive connexion between this and the remarkable catalytic effect of solvents—often roughly parallel with their polarity—on the one hand and, on the other hand, with the fact that in reactions where one of the reactants is an ion the rate is usually nearly equal to the activation rate, as though the great electrostatic forces contributed a perturbation powerful enough to increase the transformation probability to nearly unity.

(Slides illustrating experimental results were shown.)

Professor J. E. LENNARD-JONES, F.R.S.—It seems to me that there is no branch of chemistry in which it is more important to understand, in a detailed way, the electronic structure of molecules than in the branch under discussion to-day. One of the methods which have been used to determine electron distribution in molecules starts from the assumption that each electron may be regarded as moving independently in the field of the complete nuclear framework. The properties of the various possible states are then determined by the symmetry of the environment in which the electrons move. Some of these states have the same symmetry of the nuclear framework, and may be regarded as symmetrically (though not equally) related to all the nuclei, while others have different symmetry properties and indicate that electrons in those states prefer to avoid certain parts of the molecule (as, for instance, certain planes of symmetry). When one electron of a molecule is excited by light absorption (or other means) from a state which is of the symmetrical type to one of unsymmetrical type, some of the bonds of the molecule are affected to a greater extent than the rest. The effect may sometimes be so drastic as to cause the molecule to dissociate at a particular link or to cause a rearrangement of the valency links.

It is believed that molecules which dissociate in unimolecular reactions do so without light absorption. None the less, a transition may occur from one electronic state to another, if the vibrational energy is such that the nuclei of the molecule can take up certain special configurations. It is, therefore, of importance to know the energy of the various states of the molecule for all possible configurations of the nuclear framework.

Mr. Hinshelwood, in his opening address, has referred to the mechanism of the decomposition of molecules of the type AB_2 . At present it is not yet known whether these molecules decompose into $A + B_2$ or into $AB + B$, or what the factors are which control the products of decomposition. In this connection I may refer to some recent work of mine on the electronic structure of certain molecules of this type for it may suggest the mechanism, by which these molecules decompose. If the molecule AB_2 has the symmetry of the letter Y, the electronic orbitals are of three types. They may most easily be described by reference to three rectangular axes, of which the axis of z is along the axis of the molecule, while the axes of x and y are respectively perpendicular to and parallel to the plane containing the nuclei.

One kind of molecular orbital has the same symmetry as the nuclear framework so that it is unaffected by reflection in the planes xy and yz . This is called an " a_1 " orbital. Another kind is such that the wave function vanishes everywhere in the yz plane, so that reflection of the wave function in the plane causes a change of sign. This is called a " b_1 " orbital. The third type has a nodal plane in the xz plane. This is called a " b_2 " orbital. There are, of course, many orbitals of each type, just as there are many s - and p -orbitals in atoms, each having its characteristic quantum number or nodal surfaces, but all orbitals conform to one of the three types just described.

The wave function of the *whole* electron distribution may be described in an analogous way. It may have a symmetry of the same type as an individual orbital, which we have labelled " a_1 ." It is then described as an " A_1 " state. Similarly there are B_1 and B_2 states.*

The electronic structure of formaldehyde, acetone, and certain other ketones can be described in terms of this notation. I have recently made a study of the electronic states of formaldehyde by correlating them with those of the oxygen molecule, which contains the same number of electrons. It appears that among the low energy levels there are three transitions from the ground state 1A , one to another 1A_1 level, one to a 1B_2 level and one to a 1B_1 level. In the first transition the symmetry of the molecule does not change, while in the second ($^1A_1 \rightarrow ^1B_2$) and third ($^1A_1 \rightarrow ^1B_1$) the symmetry changes in such a way as to correspond to a change of the electric moment in the direction of the y -axis, and x -axis respectively.

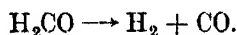
Now Dieke and Kistiakowsky† have recently shown that the characteristic

* For reasons into which I need not enter, there is also another state labelled A_2 .

† 'Phys. Rev.,' vol. 45, p. 4 (1934). I am indebted to Dr. Snow for bringing this reference to my notice and for interesting discussions on this subject.

absorption band of the CO group in formaldehyde in the neighbourhood of 3000 Å does in fact correspond to a change of moment parallel to the y -axis, and we may, accordingly, infer with some degree of certainty that absorption in this region of the spectrum corresponds to the ${}^1A_1 \rightarrow {}^1B_2$ transition. Presumably the characteristic absorption of aldehydes, ketones and all other molecules containing a CO group in the region of 3000 Å corresponds to a transition of this type.

When the detailed electron structure appropriate to each of these states is examined, it is found that the ground state has its two outermost (or most lightly bound) electrons in b_2 orbitals, viz. $(b_2)^2$, while the corresponding electrons in the 1B_2 excited state are (b_2) and (a_1) , one of the electrons having been lifted from a b_2 orbital to an a_1 orbital. This means that the electron distribution has altered in such a way as to throw the H-atoms into a closer relation to each other. It would not be surprising, therefore, if the molecule subject to light in the region of 3000 Å dissociated according to the scheme



I understand that Dr. Norrish has obtained experimental evidence of the decomposition of molecules of this type when subject to radiation of this wave-length.

There may, however, be a difference between the case of formaldehyde and that of other Y-shaped molecules such as acetone, because the H-atoms are in a sense spherically symmetrical and can react with each other whatever their relative orientation, whereas two CH_3 groups can only react to form ethane provided the two groups are oriented in a particular way. Hence it is possible that aldehydes $\text{R} \cdot \text{CHO}$ and ketones $\text{R} \cdot \text{R}'\text{CO}$ may dissociate in different ways. This suggests the necessity of a theoretical investigation of the electronic states of these various molecules and their energies as functions of the internuclear distances.

Even when the energies of the various states of a molecule are known as functions of the internuclear distances (or other suitable parameters), there still remains the difficulty of representing the results in a graphical way so as to facilitate comparison of experimental and theoretical results. One reason why so much progress has been made with diatomic molecules is that energy diagrams are functions of one co-ordinate and can conveniently be represented in a two-dimensional space. The usual method of representing the energies of molecules with two degrees of freedom is by a system of equipotential curves in a two-dimensional space. Each energy state requires one complete

system of curves, so that when a number of such sets of curves are superimposed, the network is so complicated as to be useless. The next method is to represent the energy of each state by a surface, the height of each point above a plane representing the energy appropriate to that molecular configuration. This is most helpful when only one state, say the ground state of a molecule, is being considered. When several states have to be considered simultaneously, it is again impossible, in practice, to construct a number of intersecting surfaces without causing great confusion. Moreover, it is difficult to commit the results of such an analysis to paper.

In order to overcome these difficulties I have found it advantageous for molecules where two degrees of freedom are important, to use the following method. Let x and y be the co-ordinates associated with the two degrees of freedom in which we are most interested. We suppose them measured as usual along two perpendicular directions, and the energy appropriate to any configuration (x, y) is represented by an ordinate (z) perpendicular to the plane xy . In problems of photochemistry interest is usually centred in the possible transitions from a particular state of the molecule (say the ground state) and by the Franck-Condon principle the transitions mostly take place from the neighbourhood of the minimum of the energy surface, whose co-ordinates are (x_0y_0) . It, therefore, seems advantageous to concentrate on the transitions from this neighbourhood and to take a section $x = x_0$ and $y = y_0$ through all other energy surfaces. If, in addition, the parameters are chosen in such a way that all possible configurations of the molecule are represented by a finite range of values of x and y , say from (x_0y_0) to (x_1, y_1) , then the energy surfaces can conveniently be represented by their sections on a four-sided blackboard made in the form of a cylinder of square cross-section.

If, for example, a linear molecule ABC is being considered, then, as long as it is linear, it can be described by two distances, which may describe the length of the link AB and the length of the link BC. Then one side of the blackboard will represent the interaction of A and B when C is at an infinite distance from both. This interaction may be denoted by $(A \leftrightarrow B) + (C)$. The other three sides will represent the interactions

$$(AB \leftrightarrow C), \quad A \leftrightarrow (BC) \quad \text{and} \quad A + (B \leftrightarrow C).$$

An example of a scheme of energy levels for a molecule of this kind is shown in fig. 1. Another method of representing the same set of surfaces is given in fig. 2, where the curves appearing on the four sides of the four-sided blackboard are drawn in four panels in the same plane.

A similar method of representation can be used for a Y-shaped molecule like formaldehyde, if we suppose the CO part of the molecule to remain fixed and the hydrogens to approach and recede from the molecule symmetrically, that is, so as to preserve the symmetry of the Y. Then the distance of the mid-point of the line joining the two H-atoms from the carbon atom can be

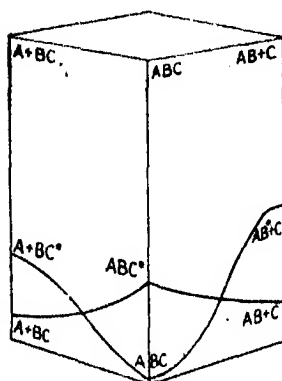


Fig. 1

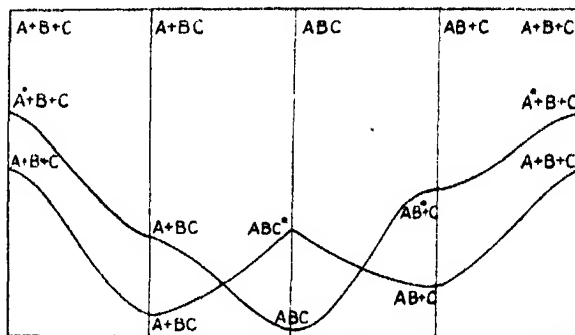


Fig. 2

taken as one co-ordinate (x), and the distance between the H-atoms as the other (y). For molecules of this kind the symbolic representation of the energy levels is of the type shown in fig. 3. Denoting the molecule by XR_2 , the first panel shows the interaction of R and R at an infinite distance from X.

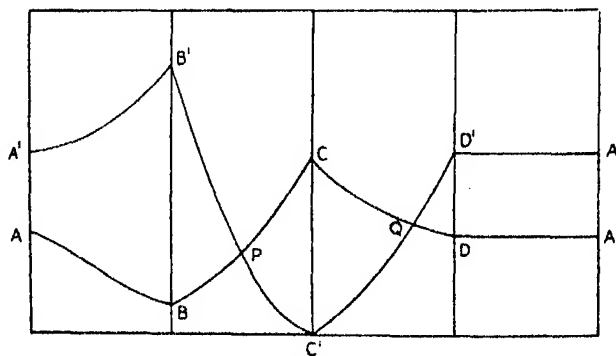


Fig. 3

The second shows the interaction of R_2 and X when the R_2 molecule is brought towards X in such a way that its mid-point moves along the axis of symmetry of X and the correct symmetry of the XR_2 system is preserved; in this process, the internuclear distance of the atoms of R_2 is kept fixed. In the third panel the interaction of R_2 and X is shown where the R atoms are drawn apart

from each other in such a way that their centre of gravity remains fixed at the equilibrium distance from X, and the symmetry of the system $X + R + R$ is preserved. In the last stage the R atoms, already at an infinite distance from each other, are moved so that their centre of gravity recedes from X. During this process the energy does not change but the cycle is completed and the system returned to its original configuration.

In the figure two energy surfaces are represented by the curves ABCDA and A'B'C'D'A' and their curve of intersection by two points P and Q. The point C' represents the minimum of the energy surface and the vibrations of the molecule at low temperatures can be represented by the movement of a point about C'.

If, as a result of collision, the molecule receives sufficient energy to reach the point P, an electronic transition may occur, provided that the intersecting surfaces correspond to states of the same symmetry and the same multiplicity (that is, the same spin vector). The molecule will then decompose into $X + R_2$. Similarly if the molecule receives sufficient vibrational energy to reach the point Q, the molecule will decompose into $X + R + R$. (In order to consider the possibility $XR + R$, a third co-ordinate and therefore a more complex energy diagram would be necessary.) The curve of intersection, of which P and Q are two points, will in general be non-planar and will resemble a rim which has become warped. It will have two minima such as P and Q (not usually at the same height) and two maxima in between them. In consequence, the probability of decomposition and the products of decomposition will depend on the energy. It will increase from zero as the vibrational energy increases from a certain critical value (corresponding to the height of P on the energy diagram) until it reaches a maximum, after which it may decrease again, for, when the vibrational energy of the molecule exceeds that of the highest point of the curve of intersection, the probability of a spontaneous switch from one surface to another will become small. The energy must therefore lie within definite limits for decomposition, which involves a switch between these two energy states.

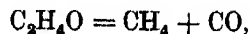
The conditions for decomposition become more complex if the two energy surfaces correspond to states of different multiplicity. If, for example, the lower one is a 1A_1 state, in the notation already explained for a Y-shaped molecule, while the upper one (BCD) is a 3A_1 state, then a switch from one surface to another at P or Q will not always occur. The probability of transition will be very much smaller and may be of the order of 10^{-3} or less, just as transitions from a triplet to a singlet level in emission or absorption are

much less frequent than those between levels of the same multiplicity. The probability of decomposition under these conditions will therefore depend on two factors, viz., (i) the energy, which must lie within prescribed limits, and (ii) a change of spin of the electrons. The latter will be affected by the environment in which the molecule moves and may be accelerated by the presence of electric or magnetic fields. This may be the explanation of the effect of various solvents on decomposition, to which Mr. Hinshelwood has referred.

Professor M. TRAVERS, F.R.S.—The following note is based upon the results of work carried out in the Chemical Laboratories of the University of Bristol conjointly with Dr. T. J. P. Pearce, Mr. R. V. Seddon, B.Sc., and Mr. P. F. Gay. The work involved the study of the pyrolysis of acetaldehyde, and also of ethane and ethylene, and the equilibrium mixtures of these gases with hydrogen. The work on the acetaldehyde is in progress, but the investigation of the hydrocarbons is completed, and will be communicated to the Society in the course of a few days.

It appears from the circular issued to the Fellows of the Society that the ideas which Mr. Hinshelwood proposes to put forward for discussion are based upon the results of a series of investigations, such as that carried out by himself and Mr. Hutchinson* on the pyrolysis of acetaldehyde. It is proposed to put forward some facts which show that the conclusions arrived at from this work may be open to serious question, and that the basis for the present discussion is by no means a sound one.

In the latter investigation the decomposition of acetaldehyde was supposed to proceed according to the equation,



side reactions being negligible. The rate of reaction was measured between 430° and 592° C, and at initial pressures below 479 mm, by first connecting an exhausted silica bulb with a vessel containing pure aldehyde at a known temperature for a moment, and then observing the rate of change of pressure. The half-life period was calculated from the results, and it was concluded that—

- (i) the reaction was bimolecular ;
- (ii) it was practically homogeneous ;

* 'Proc. Roy. Soc.,' A, vol. 111, p. 580 (1926).

- (iii) it was entirely unaffected by the products of decomposition of the acetaldehyde; and
- (iv) no carbon dioxide or unsaturated hydrocarbons were formed.

Using an entirely different method of investigation, we have arrived at conclusions which are generally the reverse of those stated above. Briefly, the method involved the accurate measurement of a volume of acetaldehyde, which was condensed in a silica reaction tube, cooled with liquid air, and then sealed. The tube was then heated for a definite period, and the contents were analysed for methane, carbon monoxide, carbon dioxide, aldehyde, propylene, and propane. The method was laborious but accurate. As some carbon monoxide was formed together with the propylene by a reaction which followed on a condensation process, the rate of formation of methane was taken as indicating the rate of the main reaction.

Now the graphs representing the rate of this main reaction are not continuous, so that the half-life period can have no real meaning. However, the initial portions are nearly linear, so that the initial rates can be determined graphically. It would now seem to be a simple matter to find the variation of the rate of reaction with temperature, but here we encounter another difficulty. The rates of reaction are influenced to a marked extent by the state of the surface.

These facts are well illustrated by the accompanying graphs. At 400° each point on the diagram represents the result of an experiment carried out after the reaction tube had remained heated to 600° overnight while full of hydrogen. At 380° two series of experiments were carried out, A in which the reaction tube was preheated overnight while filled with hydrogen, and B, in which the pretreatment with hydrogen lasted only 2 hours. From the experiments at 400° and series A at 380° the critical increment of the process was found to be 24.6 k. cals., and from the experiments at 400° and series B at 380° it was found to be 31.1 k. cals. Also, with different reaction tubes different rates of reaction were obtained at the same temperature. In silica apparatus, therefore, the process is not mainly homogeneous, but is materially influenced by surface conditions.

The process is very considerably accelerated by the addition of carbon monoxide, methane, or even of hydrogen, and to almost the same extent by any one of these gases. On increasing the quantity of either of the gases it is found that the rate of decomposition of the aldehyde reaches a maximum, and a further addition of the gas leads to a reduction in the apparent rate of

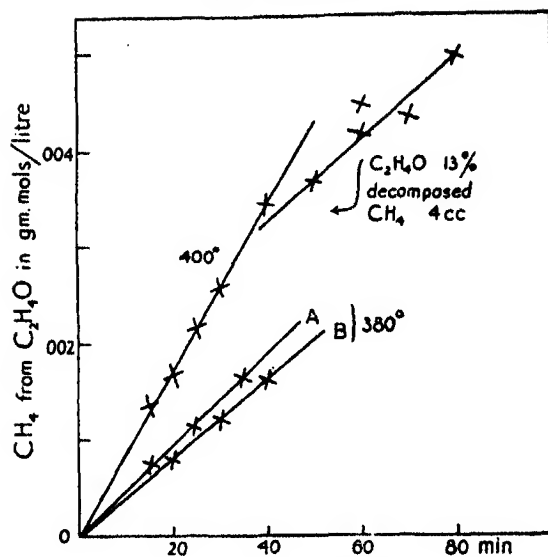


FIG. 4

CH ₄ added	nil	4	4.5	6	7	8	CC
CH ₄ formed	3	3.6	3.4	4	6	8.5	CC

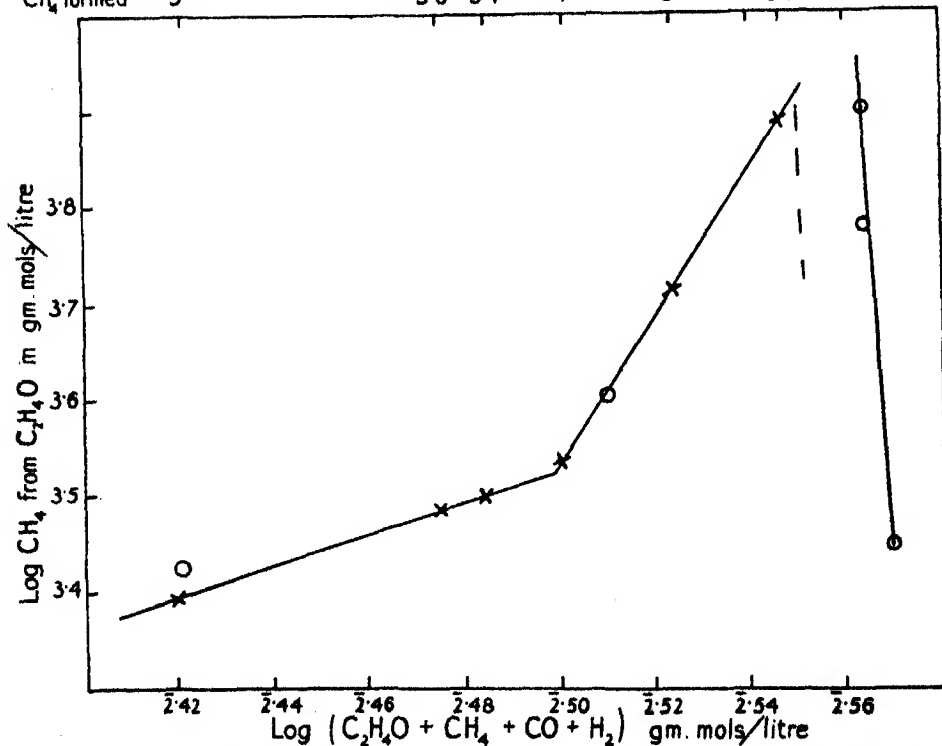


FIG. 5—H₂ series O; CH₄ series ×. Initial C₂H₄ 0.02505 gm. mol/litre; temperature 400° C, time $\frac{1}{2}$ hour.

reaction as is indicated in the diagrams, figs. 5 and 6. We are therefore led to the conclusion that the decomposition of the acetaldehyde is not bimolecular with regard to the aldehyde, but is expressed by,

$$d(C_2H_4O)/dt = K(C_2H_4O)(\phi C_2H_4O + \phi'CH_4 + \phi''CO).$$

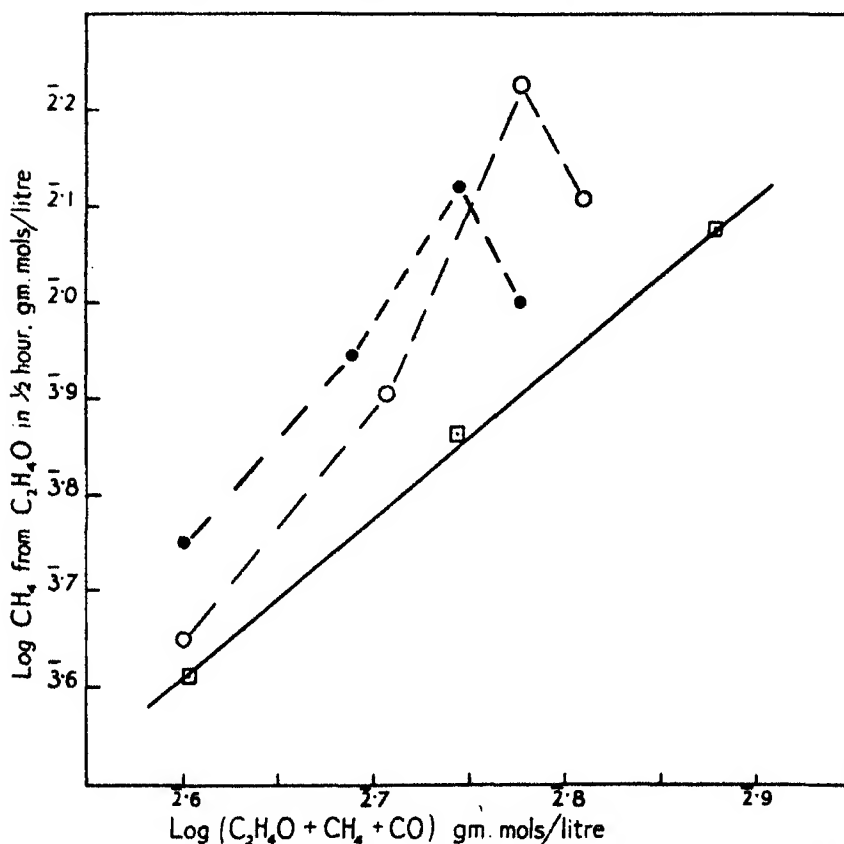


FIG. 6—● CH₄ tube A; ○ CH₄ tube B; □ CO tube B. Initial C₂H₄O 0.03840 gm. mol/litre; temperature 400° C, time $\frac{1}{2}$ hour.

It will now be seen why it is that the initial portions of the graphs representing the rate of decomposition of aldehyde are nearly linear. Also, it is possible to account for the breaks in the graphs without introducing the hypothesis which Mr. Hinshelwood has put forward.

This work was actually undertaken in support of an investigation on the decomposition of ethane and ethylene, and of ethane-ethylene-hydrogen equilibrium mixtures, on which a note was given to the meeting of the Faraday Society at Cambridge in September last. The processes which take place

in the equilibrium mixtures appear to be quite independent of surface conditions, and are therefore most easily studied. The formation of *condensate* appears to be initiated by a *parent* process, the rate of which is measured by the rate of formation of condensate, and which is determined by the ethylene concentration,

$$dR/dt = K_R (C_2H_4)^2.$$

The rate of formation of methane, which takes place simultaneously, follows, in presence of hydrogen, on an activation process similar to that which precedes the decomposition of acetaldehyde, so that

$$d(CH_4)/dt = K_{me} (C_2H_4) (\phi C_2H_6 + \phi' CH_4 + \phi'' H_2).$$

The rate again depending on the ethylene concentration, but now on the sum of the concentrations of the ethane, methane, and hydrogen. Addition of methane increases the rate of the process, a maximum being reached in this case also.

No breaks appear in the graphs representing the rate of either of these processes, when using equilibrium mixtures. Starting with pure ethane or pure ethylene the breaks are very marked. An explanation is given in the paper referred to in the first paragraph of this note, which is now completed.

MR. HINSHELWOOD—I should like to say, in connexion with Professor Travers' paper, that the results are of great interest, but they do not bear on the problem I have been discussing. In our experiments the decomposition of acetaldehyde is an absolutely homogeneous reaction unaffected by the character of the vessel. We have obtained the same results at intervals of two years, with different vessels, different thermocouples and different conditions generally, and the results have remained steady from day to day and from month to month. If Professor Travers is using a vessel in which his results vary from day to day owing to drifts, variations of surface activity or other factors, it is interesting, but the difficulty lies in the variation of the catalytic properties of the surface. With regard to the activation energy, our results for the reaction velocity are depicted by the straight line of the Arrhenius equation over a range of 100 degrees. I may also point out that the experiments of Professor Travers are made at an average temperature over 100° lower than ours, where surface effects may well be more prominent; and that with his method of working it must be very difficult to avoid adsorbed oxygen on the silica, which exerts a pronounced, though transient catalytic effect. I think, therefore, that Professor Travers' results, though extremely

interesting, represent a phase of the behaviour of acetaldehyde quite different from the one which I have discussed.

Dr. M. POLANYI—Mr. Hinshelwood's observations and some other data in recent literature show that the dependence of the reaction rate k on pressure p cannot be represented by the simple formula $k = p/(a - bp)$. Deviations from this formula in a similar direction, as observed by Mr. Hinshelwood have been predicted by O. K. Rice and Ramsperger. However, if Mr. Hinshelwood's claim that a definite number of different activated molecules appear in his reactions, is accepted, the question of the accumulation of energy in a molecule and its transfer into elongation of a certain bond, calls for a renewed and more precise consideration. I wish to outline a treatment which is being worked out at present in collaboration with Professor Wigner, of Princeton.

The energy E which a molecule contains should be considered as being distributed between the different proper vibrations, rather than between bonds or vibrations of pairs of atoms. The former distribution would remain stationary for all times if the vibrations were exactly harmonic. At the same time, the amplitude of the vibration of a certain bond would be subject to fluctuations owing to the interference of the different proper vibrations. These fluctuations would occasionally lead to a chemical change in which the bond under consideration is involved.

The first point we want to emphasize is, that the different proper vibrations are of very different effect on a certain bond. It might be that if a certain proper vibration is excited alone, a certain bond will remain completely unaffected. Obviously, the energy contained in such a proper vibration would be entirely lost for a reaction of these bonds. If the k th proper vibration were alone excited and its energy were ϵ_k , the amplitude of the vibration of the l th bond can be represented by $\sqrt{\epsilon_k} \alpha_{kl}$ where the α_{kl} are determined by the mechanical model of the molecule. If all vibrations are excited simultaneously, the elongation of the l th bond is

$$\chi_l = \sum_k \alpha_{kl} \sqrt{\epsilon_k} \sin \nu_k (t - t_k),$$

where ν_k are the frequencies of the proper vibrations and the t_k are constant phases.

It is evident that these considerations do not affect the theory of reaction rates at high pressure. At low pressures, however, the restriction can be derived that only those states should be considered as activated states, which can lead to the critical elongation without exchange of energy between different

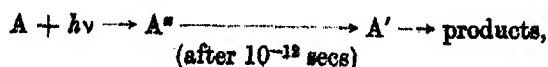
proper vibrations. Activated states with different distributions of energy, would have different reaction rates. On these lines it seems easy to account for the presence of different kinds of activated molecules, as required by the experiments of Mr. Hinshelwood.

A further effect should become appreciable at very low pressures. Since the vibrations of no molecule can be considered as strictly harmonic, there will always be some chance for a redistribution of the energy between all the proper vibrations. Thus no molecule will be absolutely stable, which contains in any distribution whatever the energy necessary for the rupture of the critical bond.

Mr. C. ZENER—I wish to remark that there are two distinct factors which may greatly reduce the probability that a molecule A should dissociate following collision with a second molecule, the combined energy of the two molecules being sufficient for this dissociation. Firstly the probability may be very small that the critical bond would absorb sufficient energy for dissociation. This may arise either because the molecule A has an extreme reluctance to absorb internal energy (the anomalies in the velocity of sound are familiar examples), or because the energy in A has difficulty in becoming concentrated into the critical bond.

Secondly, even though the bond should have sufficient energy to dissociate, specific perturbations may be necessary for dissociation. This occurs when the symmetries of the electron wave functions associated with the undissociated molecule and with the dissociated molecule in its *lowest* state are different. Some external influence, such as the electric field of a neighbouring ion, will then be necessary to allow a transition between the two states of different symmetry. Professor Lennard-Jones has given an example in which dissociation by a particular bond would require such an external influence. I do not know whether in the complicated molecules which have been studied here such symmetry relations exist; that will require further investigation.

Mr. E. J. BOWEN—There is just one feature of the photo-decomposition of gaseous aldehydes and ketones to which Professor Lennard-Jones referred that I should like to develop, and that is their delayed unimolecular decomposition. They all seem to be



similar to the thermal decompositions discussed by Mr. Hinshelwood, except, of course, that the excited levels involved are different. This mechanism agrees with the photo-kinetics; the quantum efficiency is unity or somewhat less, and the reaction rate is independent of the pressure in the gaseous state. There is also strong evidence from work we have been doing with liquid or dissolved substances, such as acetone, glyoxal and diacetyl, which shows that they do not decompose at all unimolecularly in this state, evidently because of the deactivating effect of collisions on the primary excited state A^* .

An important question is, of course, how far the nature of the absorption spectra of these substances, which are all diffuse, can be used to throw further light on the mechanism of the decompositions. At one time the mechanism was interpreted as simple predissociation, because the absorption spectra of these substances in the gaseous state begins with fine structure and passes at shorter wave-lengths into diffuse bands. If one asked the question "Does the molecule in fact dissociate?" the old answer was "Yes—no." Now, however, we know that if the delay period is longer than a rotational period the answer may be "Yes—yes," as with formaldehyde.

Diffuse spectra may also be simulated by close packing of the rotational lines, or may be due to transitions not involving dissociation as in sulphur dioxide. Then the answer to the question "Does the molecule in fact dissociate?" is "No—no." The fact is that a cursory glance at the diffuse spectrum does not answer the question.

One has to conclude that the belief in this phenomenon of time lag is really based on the chemical evidence. This delay feature in the decomposition of aldehydes is common to both thermal and photochemical reactions. With some hesitation, I suggest that we might have a new term for this phenomenon of delayed unimolecular transitions, the existence of which is really inferred from chemical evidence, because the term "predissociation" has rather vague spectral associations. Possibly the word "menolysis" might prove convenient to describe the phenomenon of unimolecular reaction occurring with a delay between excitation and decomposition, common to both thermal and photochemical reactions.

With regard to the nature of the products of decomposition, it cannot be said that the chemical work is entirely satisfactory. The problem is a very difficult one, because in order to get enough of the products to analyse, one is tempted to take the reaction to completion and also to use a high pressure. It is just under these conditions that these molecules polymerize, and the polymerized product decomposes. Therefore, however carefully the analysis is

made, one does not get the true products of unimolecular decomposition. That is what one finds in comparing other people's results. The question of whether hydrogen is or is not formed in the decomposition of acetaldehyde, for example, is very uncertain. I merely want to focus attention on the accuracy of the present chemical work and to emphasize that any experimental work on these more complex substances must be subject to a very close scrutiny indeed before we can really be satisfied with it.

Dr. R. G. W. NORRISH—I should like to touch briefly on the advantages of the photochemical method in studying the energy changes in molecules. First of all, I will illustrate the type of data with which one has to deal. I think it is important in studying any of these reactions to take care to study all the possible aspects of the given reaction. It is necessary to investigate every possible photochemical and spectroscopic aspect: the absorption spectrum, fluorescence, products of decomposition, and also the quantum yield at different wave-lengths.

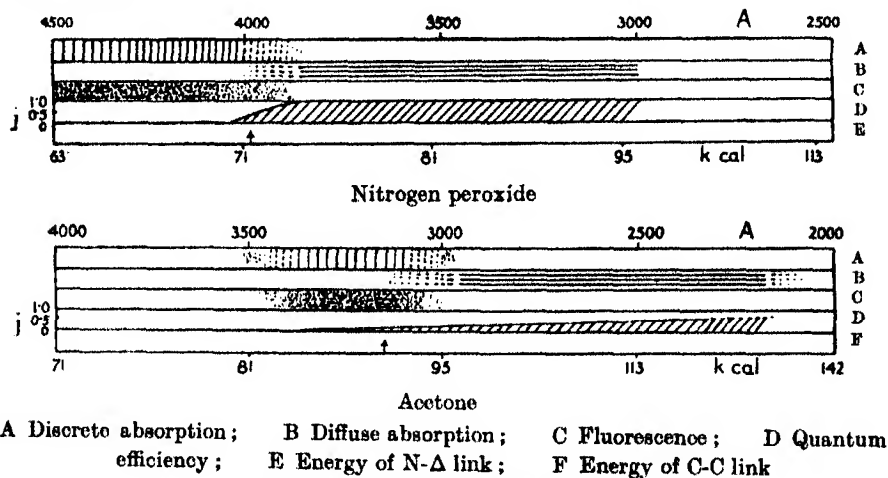


FIG. 7—Nitrogen peroxide acetone

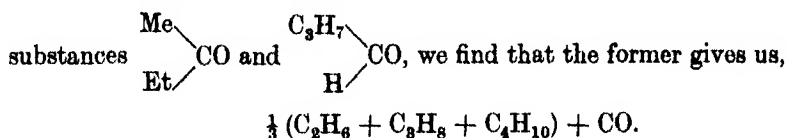
At Cambridge we studied two substances in order to investigate, as far as possible, all these effects together. The first was nitrogen peroxide and the second acetone. (*Slides were shown.*)

In both these substances we have a photochemical threshold of reactivity. This coincides approximately with the onset of diffuseness in the spectrum, and with the cessation of fluorescence. Allowing for a short region of overlap it may be said that fluorescence and fine structure are alternative to diffuseness and reaction. At the photochemical threshold, the energy of the quantum

corresponds fairly closely to the energy of some link in the molecule which is broken. With nitrogen peroxide an oxygen atom splits off; with acetone a free CH_3 radical is eliminated. Now we see how these phenomena are explained; we have the ground state and the upper level; in the upper level it may be possible for an energy switch to occur to an unstable state leading to spontaneous dissociation of the molecule. If this switch occurs within the period of one rotation (10^{-13} sec) we find that the dissociation is evidenced by a diffuse (predissociation) spectrum which has lost its rotational structure. With a polyatomic molecule, however, the energy switch may take place after an interval greater than the period of molecular rotation; the life of a stable excited state is of the order 10^{-8} second, and if during this period the molecule passes through some suitable phase for dissociation, then decomposition may follow even in the region of the spectrum showing fine structure, *e.g.*, as with formaldehyde.

I should therefore like to emphasize that diffuseness is not the best criterion of predissociation. In polyatomic molecules it can be an unreliable guide. The best guide is to be found in the fluorescence. If the fluorescence of a substance is studied at different wave-lengths it is found that the fluorescent limit—the point in the spectrum where fluorescence ceases—is just about coincident with the threshold of photochemical dissociation. Below the threshold the molecule can live again and remit its energy as fluorescence; beyond the threshold it breaks up and fluorescence is no longer possible. That is really a safer criterion of predissociation.

We have studied some other questions relating to aldehydes and ketones. This slide shows that there is essentially a different mechanism in the two cases. When I say "different mechanism" I do not mean that it is very different, but that there are points of difference. If we compare the two



The ethane, propane and butane are present in roughly equal quantities. We have been able partly to separate those substances by fractional distillation in freezing mixtures and to characterize samples of each by explosion. With

isobutaldehyde, however, $\begin{array}{c} \text{C}_3\text{H}_7 \\ \diagdown \\ \text{CO} \\ \diagup \\ \text{H} \end{array}$, which can be compared exactly with the ketone, we have a simpler result. As far as the results of Franck and Pollitzer

go, there are equivalent quantities of CO and propane produced. While the ketone gives a mixture, the aldehyde gives a pure hydrocarbon. This can only be explained by assuming that, instead of coming off as a single molecule as in isobutaldehyde, these two groups in the ketone come off separately. I see no way out of the view that a ketone molecule decomposes either directly into carbon monoxide plus two free radicals (the energy required being 80 kilocalories) or that it breaks up and gives one hydrocarbon radical plus an unstable acyl radical which itself immediately breaks up. It is thus not possible in these experiments to say whether the two radicals come off simultaneously or one after the other, but the chemical effect shows that they must each be liberated separately in the course of the reaction.

The liberation of the radical may be regarded as closely allied to the Auger effect. It is possible to suppose that the carbon atom in the chromophoric group can become excited and then, instead of radiating, can undergo an internal Auger effect which may lead to the rupture of one of its bonds and the decomposition of the molecule.

In contrast to these results, I may mention an interesting result which we obtained when we studied methyl butyl ketone, $\text{CH}_3\text{CH}_2\text{CH}_2\text{CH}_2 \cdot \text{CO} \cdot \text{CH}_3$. This is a ketone with a longer hydrocarbon chain on the one side, and instead of behaving as ketones usually do, to give CO and the hydrocarbons we get nearly quantitatively acetone plus propane—the molecule breaks at a point in the hydrocarbon chain. There is no question about the fact that the quantum is first absorbed by the carbonyl group; the energy for disruption must then be transferred to this bond in the hydrocarbon chain. The question is, how does it get there?

The exact amount of energy involved in this break-down of the hydrocarbon chain is a little difficult to determine. In the analogous reaction of the decomposition of butane, which yields propylene and methane, the energy of activation measured by Pease and Durgan was 65 kilocalories. This measurement does not necessarily give the actual energy which must be applied to that point in the molecule for reaction. It gives an upper limit. The endothermic thermal effect of the reaction is 22 kilocalories, and gives a lower limit. The energy of activation transferred to this point of the molecule must therefore lie between those limits, and in all probability is not less than 30 or 40 kilocalories. That amount of energy has to come out of the original 89 kilocalories which are absorbed by the carbonyl group, and it is more than can be transferred from the excited group to the critical point in the hydrocarbon chain by a pure process of vibration.

We must therefore suggest some other way in which the energy can be degraded. I should like to draw the analogy here, without elaborating it, that we have something akin to an internal collision of the second kind—an "inner sensitization." We are familiar with such processes between two colliding molecules. For example, an excited neon atom may react with a hydrogen molecule to break it into atoms. This only takes place when the excited and unexcited molecules are in close contact, and it is probable that the effect is dependent on resonance between the excited molecule and the primary process; it is not difficult to imagine that the same may also be true here, and that something akin to the radiationless transfer of this kind takes place between the constituent groups of the polyatomic molecule. Further work will be required; we want more data, and these are rather slow to be attained.

Another point to which I should like to draw attention is this: the fluorescent spectrum of acetone has three diffuse bands in the yellow and green. It is difficult at first sight to understand how such diffuse fluorescence can be obtained from a molecule, but provisionally we have come to the conclusion that it may be explained as a type of reversed predissociation; that is to say, that the molecule goes up to a stable upper level and drops back to a lower *unstable* level. This constitutes a new kind of primary process in which a molecule may fluoresce and decompose in one act. By subtracting the emitted quantum from the absorbed quantum, we can calculate the position of this unstable level, and find that it indicates an infra-red absorption between 8000 and 10,000 Å. This we have been able to confirm. It seems possible that this unstable infra-red level is identical with that reached thermally in the thermal decomposition of acetone.

The photochemical method of studying the conditions affecting the interchange of energy within large molecules is valuable because by means of the light quantum we can stimulate a given centre in the molecule, and observe what happens to some other part. In using the better known behaviour of diatomic and triatomic molecules as a prototype however, we must not push the analogy too far; it is probable that with new data now accumulating some new types of photochemical decomposition may appear.

Mr. H. W. THOMPSON—I should like to speak for a few moments on the correlation of certain spectroscopic results with the corresponding photochemical data.

First, however, I would agree with Mr. Bowen about the importance of certain general principles which have hitherto been somewhat obscured.

The first of these is that in polyatomic molecules a diffuse or even continuous absorption spectrum may for a variety of reasons not imply the occurrence of a dissociation process. As Henri has shown* for COCl_2 and some other molecules, the three moments of inertia of a Y-shaped molecule containing relatively heavy nuclei are often so great as to produce a very close packing of rotation lines in the bands. This packing can become such that the thickness of the individual lines is greater than their separation, and even under the highest dispersion available a resolution may not be effected. This consideration might *a priori* be expected to apply to the Y-shaped molecule acetone. With formaldehyde, however, the moments of inertia are smaller and rotational fine structure will be detectable. Measurements on fluorescence may, as Dr. Norrish suggests, help to locate the real limit of predissociation but even here the evidence may be misleading if several neighbouring electronic states of the molecule exist.

A second example in which diffuse bands in absorption do not imply a dissociation process is provided by sulphur dioxide. The spectrum consists of two distinct regions, the first stretching from 3800–2500 Å and the second, quite different in structure, from 2300–higher frequencies. In the first of these regions there are both sharp and diffuse bands, the diffuseness being developed gradually towards higher frequencies over a considerable range. It is now thought that a predissociation limit is not involved here and that the diffuseness is brought about by a close approach of potential energy curves in the manner discussed by Franck, Sponer and Teller.† I shall refer to this again.

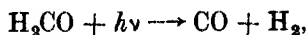
The other general principle which I think it is most important to emphasize is the converse to the above, namely, that the observance of discrete rotational structure does not preclude the possibility of predissociation in the same region. As Mr. Bowen has remarked, this circumstance arises as a result of the greater complexity of polyatomic molecules than diatomic ones. The occurrence of predissociation is determined by whether the vibration of the molecule after initial absorption into such a configuration that a radiationless switch can occur takes place in a time shorter than a natural rotational period. In a polyatomic molecule undergoing a complicated Lissajou motion the time taken to arrive in the switch position may be rather long, giving the molecule time to execute a complete rotation. It is therefore clear that the position of a predissociation limit with a polyatomic molecule will be somewhat ambiguous

* 'Proc. Roy. Soc.,' A, vol. 128, p. 178 (1930).

† 'Z. phys. Chem.,' B, vol. 18, p. 88 (1932).

and often noticeably affected by pressure conditions which may assist or retard the attainment of the switch position.

It seems to me that the case of formaldehyde studied by Dr. Norrish* offers an example of this idea. The quantum efficiency for the photochemical decomposition which, as Dr. Norrish has said, follows the equation



is unaffected as the predissociation limit is passed. It is hardly likely that two essentially different mechanisms, the one in the discrete region, involving a primary excitation process, the other in the diffuse region involving primary dissociation, could be compatible with this result; and it is more reasonable to suppose that in the fine structure region predissociation is incipient, the process in both regions being



Mr. Bowen has suggested the term "menolysis" for this delayed dissociation. I had intended to suggest the word "hysterolysis," in accordance with other lag phenomena such as hysteresis.

With regard to specific matters, I would only mention two series of investigations in which these problems, and others mentioned by Mr. Hinshelwood, arise.

The first is in connexion with the photochemical decomposition of molecules containing the chromophoric group SO_2 . The absorption spectra of SO_2Cl_2 , $(\text{CH}_3)_2\text{SO}_2$, $(\text{C}_2\text{H}_5)_2\text{SO}_2$ and certain other sulphuryl compounds such as $\text{C}_6\text{H}_5 \cdot \text{SO}_2\text{Cl}$ appear to be essentially similar to that of SO_2 itself. As I have already said, this consists of two regions, one of sharp and diffuse bands *ca.* 4000–2500 Å, the other beginning at *ca.* 2300 Å. SO_2Cl_2 is not photochemically decomposed by ultra-violet frequencies corresponding with the first system of diffuse bands at 3000 Å. Photochemical decomposition does, however, occur† with light wave-length 2300 Å, and what appears to be a fairly sharp predissociation limit is observed at about this point.

That a case of delayed dissociation is involved here is strikingly shown by the marked dependence of the position of the predissociation limit upon pressure.

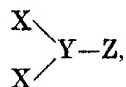
The products of this photodissociation are SO_2 and Cl_2 , and the light energy absorbed by the SO_2 group must therefore be transferred, in part at least, to

* 'J. Chem. Soc.,' p. 1518 (1932).

† Andrich, Kangro and Leblanc, 'Z. Electrochem.,' vol. 25, p. 229 (1919); Traum, 'Z. phys. Chem., A, vol. 105, p. 356 (1922).

the S-Cl links. The quantum efficiency of the process has not yet been determined, and it is not possible to state with certainty whether both Cl atoms leave the molecule simultaneously or not. The energy quantum absorbed is almost certainly sufficient for this.

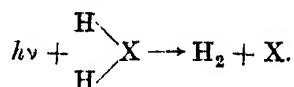
It does seem, to me, important to remember that with many molecules of the type



deformation vibrations of the X-Y links are prominent in the absorption spectra. This will be important in connexion with the photochemical decomposition. With formaldehyde, which decomposes into $\text{H}_2 + \text{CO}$, the magnitude of the $\text{H} \leftrightarrow \text{H}$ deformation oscillation is as Herzberg* showed, *ca.* 830 cm^{-1} . With COCl_2 that of the $\text{Cl} \leftrightarrow \text{Cl}$ is *ca.* 582 cm^{-1} ; with acetaldehyde that of $\text{CH}_3 \leftrightarrow \text{H}$ is *ca.* 825 cm^{-1} ; and with other molecules it is of the same order.

I am inclined to think that deformation vibrations of this kind may be very important in the decomposition of the molecule.

It is interesting to remember that some time ago Goodeve and Stein† suggested that water, hydrogen sulphide, hydrogen selenide, and hydrogen telluride decompose photochemically, thus



Objections have been raised to this, but it is not definitely disproved.

With COCl_2 the absorbed quantum would appear to be quite large enough, taking energy of reorganization into account, for the change $\text{COCl}_2 \longrightarrow \text{CO} + \text{Cl}_2$, and other alternatives such as $\text{COCl}_2 \longrightarrow \text{COCl} + \text{Cl}$ ought to be carefully reconsidered.

I have recently been examining the absorption spectra of a series of compounds in which alkyl radicals are attached to a single atom in the molecule, such as $\text{Zn}(\text{CH}_3)_2$, $\text{Zn}(\text{C}_2\text{H}_5)_2$, $\text{Pb}(\text{C}_2\text{H}_5)_4$. These spectra often have a surprisingly simple appearance, and although their interpretation is less obvious there seem to be indications that deformation oscillations are prominent.‡ Marked dependence of the $\text{Zn}(\text{C}_2\text{H}_5)_2$ continuum upon pressure suggests that collisions are important in the decomposition.

* 'Trans. Faraday Soc.,' vol. 27, p. 393 (1931).

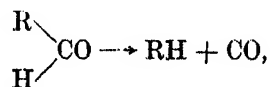
† 'Trans. Faraday Soc.,' vol. 27, p. 378 (1931).

‡ J. Chem. Soc., 1934, p. 790.

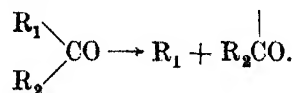
Similar considerations to these appear to apply to the other sulphuryl compounds which I have mentioned. For example, $(C_2H_5)_2SO_2$ is decomposed in the far ultra-violet region into sulphur dioxide and a hydrocarbon residue. As yet the quantum efficiency of this process has not been measured, and the hydrocarbon residue has not been analysed.

With regard to the mechanism of the photochemical decomposition of aldehydes and ketones, I am, as I gather Mr. Bowen is, still a little uncertain of the interpretation of the very extensive and beautiful results described to us by Dr. Norrish. I am of the opinion that these processes involve a primary excitation followed by a dissociation which may be quite considerably delayed. The existence of an excited molecule of relatively long life is in accordance with the fluorescence, the concurrent bimolecular polymerization, and with the very low quantum efficiency resulting from deactivation possibilities. The variation of the quantum efficiency with pressure in the decomposition of acetone, as found by Damon and Daniels,* is also in agreement with the idea of a delayed dissociation.

I find it a little difficult to understand the reason for the essential difference suggested between the mechanism of decomposition for aldehydes and ketones respectively. As Dr. Norrish has shown, all lines of evidence indicate that for aldehydes



but for ketones the intervention of free radicals is suggested :



The spectral evidence cannot decide between the two possibilities, and it seems to me that analysis of the products with mixed ketones must be the deciding criterion.

I am inclined to agree with Mr. Bowen in regard to the difficulties involved in such analyses. It is surprising, if free methyl radicals are first liberated in the decomposition of $(CH_3)_2CO$, that the reaction proceeds as much as 90% towards ethane formation. I think more than 10% of subsidiary products might have been expected.

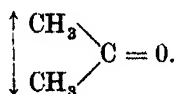
The free radical theory appears to rest mainly on the analyses with methyl ethyl ketone. I have been thinking, quite apart from the points raised by

* 'J. Amer. Chem. Soc.', vol. 55, p. 2363 (1933).

Mr. Bowen, of the difficulties of obtaining specimens of this substance which are quite free from the diethyl ketone. I believe that the purification is particularly difficult owing to the nature of the vapour pressure curves of mixtures of the different homologues and the close similarity of derivatives which might be used in a process of purification.

It is, moreover, not at all clear how the products with methyl butyl ketone comply with the hypothesis of free radicals.

Dr. Norrish has referred to the question of the real nature of the acetone continuum. Some time ago, using a 1-metre column and pressures down to *ca.* 0.5 mm, I took photographs of this continuum under high dispersion. Above 1 mm the absorption was continuous. At the lowest pressures a peculiarly symmetrical recurring system of diffuse bands was obtained. I believe that Dr. Snow has also obtained some indications of maxima in the continuum, but not quite of the same kind. Dr. Norrish has suggested to me that the effect I observed might have been due to an interference phenomenon caused by a slightly incorrect alignment of the quartz end plates of the absorption tube. There are several reasons why this is improbable, but it may be so. But the inferences to be drawn from the presence or not of such diffuse bands does not affect the view of the decomposition mechanism which I have suggested. The only point would be that the structure of the system might give additional evidence for the presence of deformation oscillations



These may still be involved in the region of bands from 3000–3300 Å which have not yet been analysed in detail.

Dr. NORRISH—In answer to Mr. Thompson, we were very careful to purify our methyl ethyl ketone by distillation. The origin of the methyl ethyl ketone (from aceto-acetic ester) ensures the purity from anything but traces of other homologous ketones. The purified product boiled constantly to within a tenth or so of a degree of the boiling point given in the International Critical Tables for the barometric pressure of the day.

With reference to the low quantum yield in the decomposition of acetone—that is a point I rather missed when I spoke. According to the results of Damon and Daniels, there is with dry acetone no polymerization and only decomposition, and in that part of the spectrum which is wholly continuous the quantum yield is no greater than 0.4. With these results our own experiments

are in agreement. There is no fluorescence in this part of the spectrum ; what therefore happens to those molecules which absorb light and do not decompose ? If we have the possibility of an Auger effect in the carbon atom of the excited carbonyl group, leading to the ejection of a CH_3 radical, it is conceivable that only 40% (say) of the molecules will actually decompose, and that this will be conditioned by their internal condition. In a polyatomic molecule such as acetone the several constituent groups are in one sense separate structures with their own rotational and vibrational degrees of freedom. They can thus take from the C-C link some of the energy which would otherwise lead to decomposition, and we get the equivalent of a stabilizing collision. Thus the incipient decomposition is prevented, and we have instead a process of internal degradation to heat. It is possible that external deactivating collisions also play their part.

Mr. C. J. M. FLETCHER—Mr. Hinshelwood has given the conclusions which have been drawn from a study of the aldehydes. I should like to describe briefly the experimental results which form the basis of the association of the energy of activation with different parts of the molecule, for the different activated states which exist for the aldehydes. (*Slides were shown.*)

The slide shows, for the same temperature, the variation with pressure of the rates of reaction of formaldehyde, acetaldehyde, and propionaldehyde. For the last two molecules there are four definite segments, so that four independent modes of decomposition for each molecule may be distinguished. The simplest way to identify the different segments with activation of different parts of the molecule is to compare acetaldehyde on the one hand with formaldehyde, and on the other hand with propionaldehyde.

The decomposition of formaldehyde is a simple bimolecular reaction up to high pressures. For acetaldehyde also, the curve indicates that there is a reaction which remains bimolecular up to the highest pressures used. The rate of reaction of formaldehyde is satisfactorily explained by the simplest type of activation, i.e., of two square terms. At high pressures the same is also true of acetaldehyde. It seems, therefore, that there is a bimolecular decomposition of acetaldehyde, similar to that of formaldehyde, in which the energy of activation goes directly to that part of the molecule, whose activation is responsible for carbon monoxide being split off.

The segment at the lowest pressures measured, may be identified by a comparison of the curves for acetaldehyde and propionaldehyde. As the slope of the line is greatest for this segment, the rate at which activated molecules are

produced is greatest for the associated reaction; however, the energy of activation is considerably larger than at higher pressures. These two facts taken together, mean that the energy of activation is contained in many square terms. As this segment is relatively more important in propionaldehyde than in acetaldehyde, it may be reasonably assumed that activation is concerned with that part of the molecule which is different in the two substances—*i.e.*, with the alkyl group. This hypothesis accounts for the large number of square terms concerned, and also for the fact that as the alkyl group is remote from that part of the molecule which is responsible for decomposition, the probability of decomposition is small, so that the curve becomes horizontal at low pressures. The theory is further confirmed by an entirely different experimental fact. The primary products of decomposition of propionaldehyde at normal pressures are mainly carbon monoxide and ethane; but at lower pressures, hydrogen and ethylene appear in increasing proportions; the extent to which they increase, agrees closely with the extent to which the lowest segment becomes more prominent. The reaction predominating at low pressures must therefore involve activation of the alkyl group, to account for the production of hydrogen and ethylene as primary products in the decomposition of propionaldehyde.

It is not possible to associate the two intermediate segments with activation of any particular vibrations of the acetaldehyde molecule, but they may be connected with activation of the carbonyl group, or other vibrations concerned with the carbon atom of the —CHO group.

Professor E. K. RIDEAL, F.R.S.—Since the time is very late I will shorten my communication to a few remarks.

Ever since Professor Lindemann put forward suggestions for the mechanism of a unimolecular reaction, about thirty have been investigated. They have all involved the inference of a number of squared terms (S). We may note that as the internal energy has to surge into a particular link before deactivation by a secondary collision occurs we are interested not only in the problem whether the necessary amount of energy is actually present in the molecule, but also if this energy be present how long it takes to migrate to the reactive bond. This problem in its turn involves the investigation of the influence of the molecular structure, *i.e.*, the path by which the energy is conveyed both on the probability of energy transfer and on the time required for such transfer.

In respect to the first point, *viz.*, the amount of internal energy actually possessed by the molecules at the reacting temperatures I confess that I am

somewhat sceptical as to the realities of the magnitudes deduced by the application of the collision theory of activation. We may note that 25 squared terms are required for cyclopropane, 38 for tertiary butyl alcohol, 25 for azo-methane and 28 for ethyl azide. I cannot help suspecting that some of these reactions will turn out to involve chains, especially when we recollect that over the usual range of reacting temperature only one CH linkage in seven can contain a quantum of vibrational energy equal to *ca.* 2kT, and the main contribution to the internal energy must come from the heavy atoms in the molecule. More work on the specific heats of these substances is evidently desirable.

The next consideration is, if the energy be really there, what are the relationships between the structure and the conditions of transmission of this energy. In the first place how far can E and S be correlated with constitutional factors.* The ethers (6-12 S terms) and the azo compounds (25-40 S terms) are the only homologous series studied hitherto and the former show no well-defined regularities. The increase in S effected by substitution of —O— for —N=N— would appear to be surprisingly large. The azo decompositions that have been investigated, and the work is being extended to other compounds of this type by Dr. Gwyn Williams in my laboratory, do show a fairly regular change of E and S with increasing molecular complexity, as shown in the following table, all computed with $\sigma = 3.6 \cdot 10^{-8}$ cm.

Structure	Temperature range °C	E Energy of activation cals./gm. mol.	S No. of square terms
$\text{CH}_3\text{--N=N--CH}_3$	270 -- 330	51,200	25
$\text{CH}_3\text{--N=N--C}\begin{array}{l} \text{CH}_3 \\ \text{H} \\ \text{CH}_3 \end{array}$	250 -- 330	47,430	33
$\begin{array}{l} \text{CH}_3 \\ \text{H} \end{array} \text{CN=N}\begin{array}{l} \text{CH}_3 \\ \text{H} \\ \text{CH}_3 \end{array}$	250 -- 290	40,900	> 40
$\text{C}_6\text{H}_5\text{CH=N--N=C.HC}_6\text{H}_5$	318 -- 353	57,000	> 32
$\text{C}_6\text{H}_5\text{CH}_2\text{--N=N--CH}_2\text{C}_6\text{H}_5$	Gaseous decomposition at 200°		

We may note that whilst E changes relatively slightly the number of squared terms rises rapidly with the increase in molecular complexity; also from a study of organic reactions in solution we may conclude that constitutional influences are operative over a considerable distance in the molecule, although damping in a carbon chain usually occurs after the fourth carbon atom. It is, of course, also well known that the relative chain lengths in chain reactions are subject

* The value of S may be affected by a steric factor, and by incomplete redistribution of energy in molecular collisions.

to large variations and a comparison of chain lengths in well-established chain decompositions with molecular complexity would appear important.

Another method of approach to the problem of energy transfer is to ensure that the reacting group is maintained constant, attach to it another group, which can grow in a homologous series, and examine the effect of chain length on E and S. This problem is at present under examination by Dr. Melville, who has commenced a study of a simple polymeric reaction. The scanty evidence derived from technical sources suggests to us that frequently in building up a polymer we are not dealing with a bi-molecular reaction between first of all simple molecules followed by a sequence of bimolecular reactions between bi- and tri-merides (and so on) respectively, but that simple molecules add themselves progressively to growing chains and that as the chain gets longer the facility of addition increases but not indefinitely. If this view be correct the properties of the growing polymer must surely be a continuous function of its size and thus certain generalized equations may be used to describe the behaviour and so yield some information about the mechanism of the growth, the number of squared terms involved, the target area and the energy transfers involved.

Naturally conditions are most favourable in the gas phase at low pressures. The results of a preliminary investigation on the polymerization of acetylene by light from a mercury vapour lamp in the presence of mercury vapour lead to some interesting conclusions.

Without going into experimental details the facts (at pressures from 0.01 to 10 mm) are (a) that the reaction consists in association of an excited mercury atom with an acetylene molecule, this complex then participating in a series of collisions with normal acetylene molecules thus building up a polymer, the photochemical chain length at room temperature being about 10, and rising gradually to about 100 at 250° C., and subsequently decreasing to about 50 at 500° C (b). The chain length is independent of pressure, of intensity of light, and does not appear to depend on whether the tube is packed or not. It may be added that there is evidence for a secondary polymerization of the products of the photo reaction on the walls of the reaction vessel.

The reaction kinetics are thus reasonably simple and permit, therefore, a quantitative enquiry into the details of the process. The experiments lead to the conclusion that termination of the chains, *i.e.*, a cessation of increase in size of the polymer, occurs by the collision of a chain carrier (polymer) with an acetylene molecule and not by the collision of two (polymer) carriers nor by the spontaneous decomposition of the carrier. Similarly, however, the

propagation reaction involves the collision between the chain carrier and an acetylene molecule. The absolute value of the length of the chain, *i.e.*, the polymer size, and its variation with temperature will therefore be determined simply by the nature of the energy transformations involved when an acetylene molecule hits a polymer molecule. The first problem is thus to evaluate the ratio and if possible the absolute value of the velocity coefficients for the propagation and termination reactions.

Two extreme situations may be imagined. (a) There are two separate kinds of collision involving different energies of activation, numbers of square terms and steric factors. (b) There is only one type of collision and the subsequent emergence of a chain carrier from the collision is determined by the probability of the distribution of energy in the collision complex itself, which may vary with temperature.

Suppose k_1, k_2, k_3, \dots , and k'_1, k'_2, k'_3, \dots , denote respectively the velocity coefficients for propagation and for termination then it can be shown, by setting down the equations expressing the stationary concentrations of each individual polymer molecule, that the chain length is given by the equation

$$v = 1 + \left\{ 1 + \frac{k_1}{k_1 + k'_1} + \frac{k_1}{k_1 + k'_1} \times \frac{k_2}{k_2 + k'_2} + \dots \frac{k_1}{k_1 + k'_1} \dots \frac{k_{n-1}}{k_{n-1} + k'_{n-1}} \right\}.$$

If, for simplicity, it is assumed that $k'_1/k_1 = k'_2/k_2 = x$ then

$$v = 1 + \left\{ 1 + \frac{1}{1+x} + \frac{1}{(1+x)^2} + \frac{1}{(1+x)^3} \dots \right\}.$$

If x is not too small the series converges rapidly and therefore summing to ∞ terms

$$v = 2 + 1/x,$$

when the chains are long

$$v = 1/x = k_1/k'_1 = \frac{\alpha e^{-E/RT}}{\alpha' e^{-E'/RT}} = \alpha/\alpha' e^{-(E-E')/RT},$$

where α and α' are coefficients containing (a) the factors to increase the rate of activation when the number of square terms exceeds two, and (b) steric factors. The chain length increases with temperature and hence $E - E'$ must be positive, and is actually at 25° C, 4000 cal. The quantity $e^{-(E-E')/RT}$ is therefore much less than unity, but since v is 10 at 25°, α/α' is very much greater than unity and is equal at 25° C to 3×10^4 .

This calculation rules out the possibility that the propagation or termination of the growth of the polymer is determined by an energy distribution in a given

collision. The next problem is to separate steric and square term factors. Progress is now less certain, but considering the steric factors first, it is probably true to say that only a comparatively small portion of the growing polymer molecule has the property of adding on an acetylene molecule, while termination might occur by partial disintegration of the polymer by an impact of an acetylene molecule at any part of the polymer, and thus there should be a large steric factor for propagation whereas in fact the reverse state of affairs exists since $\alpha \gg \alpha'$.

On account of the chain length reaching a maximum, *i.e.*, $dv/dt = 0$, then

$$\frac{d \ln \alpha / \alpha'}{dT} = - (E - E') / RT^2,$$

and therefore α/α' must be a function of the temperature. Hence it is the variation in this quantity which has the effect of counterbalancing and finally more than counterbalancing the increase in chain length brought about by the factor $e^{-(E-E')/RT}$.

Including square terms and steric factors (F and F')

$$\frac{\alpha}{\alpha'} = \frac{F}{F'} \frac{(E/R)^{(S/2-1)}}{(E'/R)^{(S'/2-1)}} T^{1(S'-S)} \frac{(S'/2-1)!}{(S/2-1)!}$$

whence

$$\frac{d \ln \alpha / \alpha'}{dT} = \frac{\frac{1}{2}(S' - S)}{T}$$

$$\frac{1}{2}(S - S') = (E - E')/RT \quad \text{or} \quad S - S' = 8.$$

Thus at 250° C eight more square terms participate in propagation than in termination.

Until the absolute value of E or E' is determined the absolute value of S, S' and F and F' cannot be determined.

Preliminary experiments using a method which need not be described here, indicate that E is of the order 5000 cal.

It is interesting to note that under these conditions, ethylene does not polymerize in a manner similar to acetylene, and no increase in the velocity of polymerization occurs when the temperature is raised from 15° C to 300° C.

MR. UBBELOHDE—The point of Mr. Hinshelwood's observations has been that in thermal activation there is no evidence that there is anything but an increasing number of vibrations of the molecule in the ground level. Furthermore, the observation of Richards and Reid* likewise only dealt with the ground

* 'Nature,' vol. 130, p. 739 (1932)

level. The curious thing that has been observed there is that not every collision between molecules leads to the transfer of vibrational energy; only one in 10^5 may be effective. Nevertheless, certain impurities, such as hydrogen, are far more efficient in promoting this exchange of the translation of vibration than ethylene itself. Consequently, from the point of view of reaction mechanism, when we find catalysts such as Mr. Hinshelwood has found—hydrogen in the decomposition of aldehydes and ethers and iodine in the decomposition of ethers—it is interesting to enquire whether the physical investigation bears out the simple interpretation that the effect of these catalysts is simply to favour the transmission of vibrational energy in the ground state.

I just want to make one remark about the sort of physical tests we use at the moment to check the chemical equations. The chief method is the change in velocity of sound with frequency. If the impurity which is found to have the catalytic effect promotes exchange of vibrational energy it will, of course, shift the region of dispersion. Another physical check comes from thermo-conductivity. In the same way, if the impurity affects the sound transmission it likewise raises the thermo-conductivity of the gas abnormally.

Another point is that we know from the qualitative theory of the transmission of vibration to molecules that unless the molecules penetrate fairly deeply into one another's fields, transmission will not take place. Consequently, if hydrogen is more effective in exciting vibrations of ethylene than ethylene itself, we expect to find other physical evidence for such a penetration. In the ethers there is indeed evidence that iodine in the vapour state has some very loose combination with ether, with a heat of formation of 3k. cals., this indicates penetration by molecules to an abnormal extent, compared with the ordinary Van der Waals' attraction.

Mr. HINSHELWOOD, in reply—The points raised have been so varied and interesting, and some of them so much beyond my power to deal with, that to summarize would be rather difficult. We have seen what an extraordinary variety of phenomena come within the scope of this discussion. On the question that Mr. Ubbelohde has just asked, I suggested to Dr. Fromherz, of Munich, who worked in my laboratory last summer, that substances which form addition compounds with acetaldehyde at low temperatures might catalyse its decomposition at high temperatures, but experiments which he made gave negative results in this respect.

The Dark Interval in Mercury Fluorescence

By Lord RAYLEIGH, F.R.S.

(Received May 18, 1934)

[PLATE 1]

This phenomenon was originally described by R. W. Wood.* He found that when a rapidly moving current of mercury vapour was excited by the aluminium spark, the green fluorescence did not start at the point at which excitation was applied, but that an interval could be observed in which the vapour was dark. He also found that the fluorescence of wave-length 2537 corresponding to the resonance line, which accompanies the green fluorescence, showed a dark interval. Some other authors have also written on this effect. Pienkowski† obtained it under certain conditions with mercury arc excitation, but left it open whether the excitation was to be considered atomic or molecular. It has also been discussed by Gaviola.‡

It seemed that further work was called for since the dark interval phenomenon may be crucial for determining the real relationship between the numerous and complicated phenomenon of mercury fluorescence.

The methods used are largely the same as those in previous work on kindred subjects,§ but it has been thought best to make the present paper as far as possible self-contained.

The general aim was to separate the various features of the mercury fluorescence spectrum, and to observe the presence or absence of a dark interval in each under varied conditions of excitation. This can be done, at any rate in principle, by the spectroscope, but I have succeeded much better by direct photography through suitable filters. This method allows of a large aperture and comparatively quick exposure. It gives a complete and distinct picture in each spectral region and the results are in practice much more convincing than when we are limited to the narrow section of the field included by a spectro-

* 'Proc. Roy. Soc.,' A, vol. 99, p. 362 (1921).

† 'Ann. Physik,' vol. 50, p. 787 (1928).

‡ 'Phys. Rev.,' vol. 33, p. 1025 (1929).

§ 'Proc. Roy. Soc.,' A, vol. 125, p. 1 (1929), (I); vol. 132, p. 650 (1931), (II); vol. 135, p. 617 (1931), (III); vol. 137, p. 101 (1932), (IV); vol. 139, p. 507 (1932), (V).

scopic slit. Fortunately it is possible to find suitable filters to separate well enough the regions of the fluorescence spectrum to be studied. These are:—

(a) The visual green continuous region, with photographic maximum at 4850. This is isolated with Wratten No. 2 filter (aesculene) cutting off all wave-lengths less than 4000. In some cases a Wratten yellow filter No. 12 is preferable.

(b) The ultra-violet continuous region with maximum at 3300. This is isolated by a silica cell containing bromine vapour, not quite saturated, and 6 cm thick, combined with Schott's blue uviol glass (W.G.3 in his catalogue), 1 mm thick. This has maximum transmission at about 3300, cutting off all visual light, and all light of wave-length less than about 2900.

(c) The resonance line 2537. This is isolated by a chlorine tube 15 cm in length combined with 6 cm of bromine vapour. This combination cuts out the regions (a) and (b).

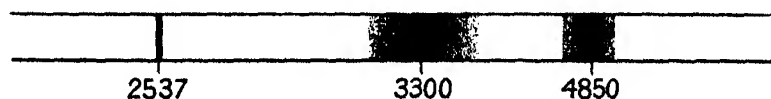


FIG. 1

For taking some of the earlier photographs, a quartz lens was used. This, however, involves rather troublesome refocussing for the ultra-violet, which has to be done by calculation. Later, a quartz-fluorite achromat of 2.5 cm aperture and 10 cm focal length was substituted and proved very useful and convenient.

The present work is essentially exploratory and it is convenient to describe the experiments rather with reference to technique than to logical order. The results will be classified and summarized at the end.

The apparatus first used is shown in fig. 2. It is of fused silica. Mercury vapour passed up from the boiler through a 1 cm square tube made of ground and polished plates. It was condensed above and ran back by a side tube. By introducing gas pressure (nitrogen) into the condenser, the pressure of the vapour is controlled, but owing to the opposing vapour stream, no appreciable admixture of nitrogen is present in the square observation tube. A diaphragm 3 mm square was placed over the entrance wall, and the source focussed on this aperture. Wood's experiment with aluminium spark excitation was repeated, using a quartz lens of 2.5 cm diameter and 2.5 cm focus as condenser. The effect is best developed at as low a pressure as possible, but diminishing

luminosity sets a limit to this, and 5 mm seemed to be about the best compromise under the conditions. The dark interval was well seen, and was also well photographed (reproduction I) Plate 1, using a yellow filter (Wratten 12) over the camera lens and a panchromatic plate. The track along the beam is due to false light reflected by the droplets of condensed mercury. It cannot well

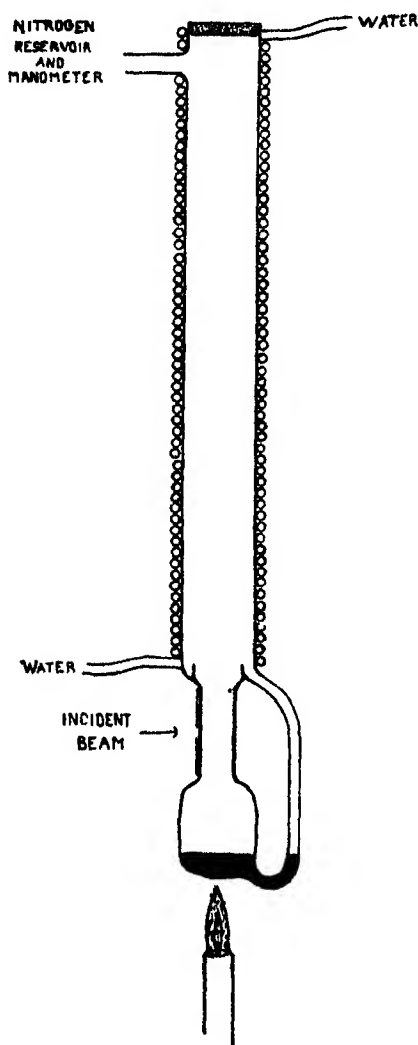


FIG. 2

be avoided, because no filters are available to cut off visual light of the source, while retaining the extreme aluminium lines 1862 and 1854 which are chiefly effective. However, it serves to mark out the track of the exciting light; the dark interval between this and the fluorescence is very conspicuous.

Without altering the conditions of excitation, photographs were taken to bring out the fluorescence in 2537 light, using the combined chlorine and bromine filters. The result is seen in reproduction II, Plate 1. The fluorescence rises as before, but there is no sign of a dark interval, in marked contrast to I. There is a discrepancy here from Wood's conclusion, which certainly seems at first sight to be borne out by the photographs he reproduces. I hardly see at present what the essential difference in the conditions can be, though the optical technique used is somewhat different. But even after allowing for the fact that Wood's evidence has to be judged from the reproduction and not from the actual photograph I think it may perhaps be claimed that the present evidence is clearer, and it is further reinforced by reproductions VIII

and IX, Plate 1, of the present paper (see below).

After these experiments with the aluminium spark, similar ones were made using the mercury arc as a source.

As so often emphasized before* it is necessary to distinguish between the cooled mercury lamp giving the atomic resonance line, 2537 (core excitation) and the hot lamp, in which the core of the atomic line is lost by self-reversal, and the band extending from 2537 on the long wave side is operative (wing excitation).

Many attempts have been made to detect the dark interval in the visual fluorescence, using core excitation, and a variety of conditions, with pressures from 5 mm down to 0.2 mm. A blue corex glass combined with a bromine cell cut down practically all visual light from the source and the exciting beam was in some tests narrowed down to $\frac{1}{2}$ mm vertical light and the intensity made as low as practicable. Reproduction III, Plate 1, shows one of the experiments at 2 mm pressure. No trace of the dark interval was ever seen or photographed.

If the cooling fan was removed, and the mercury lamp allowed to warm up, the wing effect came into evidence, and as soon as this happened the dark interval could be detected. Photographs were taken in visual light through Wratten No. 2 filter to show the distribution of 4850 light. Reproduction IV, Plate 1, is one of these, at 6 mm pressure.

This experiment was repeated with conditions unaltered, except that the photographs were taken in 3300 light, using a bromine cell combined with blue uvioi glass over the camera lens (see reproduction V, Plate 1). There is now little, if any, evidence of a dark interval, and certainly much less than in the light of 4850 (compare IV and V). VI, Plate 1, is taken under the same conditions as IV and V, but in the light of the resonance line, with chlorine and bromine filters over the camera lens. This is introduced for the sake of its remarkable contrast with the result obtained under the same conditions with the aluminium spark (see above comparing II and VI). It has already been shown in detail† that with wing or core excitation the 2537 luminosity does not commence to move along the vapour current until the presence is much lower than is needed to make the 4850 luminosity show this effect.

Finally, visual experiments were made with iron arc excitation. Here again the dark interval was seen and photographed in the light of 4850, see reproduction VII, Plate 1. The dark interval is apparent but less conspicuous than with the aluminium spark, and also, it is thought, less conspicuous than with the wing excitation from mercury.

* Paper I, p. 8, and also in later papers.

† See paper I, Plate 2.

Having got as much as seemed feasible out of this experimental arrangement (fig. 2), I reverted to a different one (fig. 3) which has a much larger boiler, and uses downward instead of upward distillation of the vapour. This is an advantage in that condensed drops do not fall back into the path of the beam and the increased boiler capacity allows of a rapid stream under higher pressure and therefore with improved luminosity.* On the other hand, it does not lend itself so well to continuous circulation of the working fluid, and is somewhat cumbrous and fragile. It has already been figured and described in

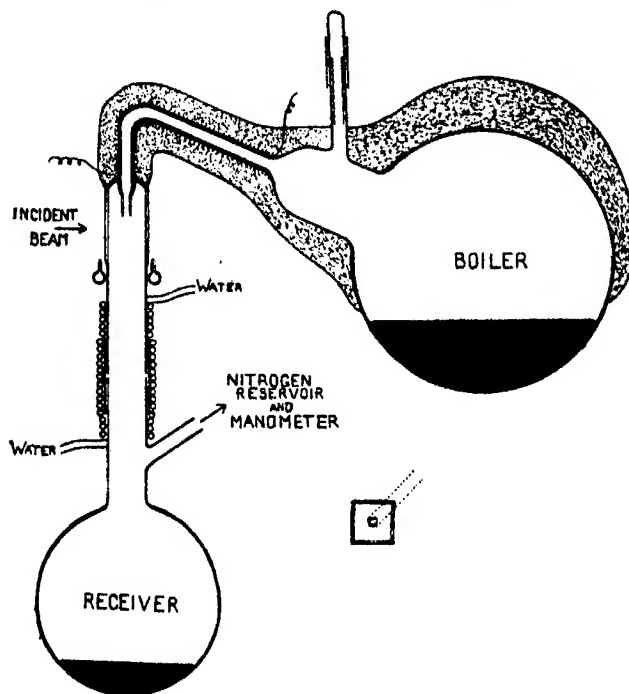


FIG. 3

paper V, p. 512. The nozzle, it may be recalled, has 3 mm square bore and delivers mercury vapour into a casing 20 mm square bore. The latter contains nitrogen at any desired pressure and this pressure determines the pressure of the mercury in the jet which comes out from the nozzle. As shown in the former paper, the mercury vapour by exposure of a strong beam of the exciting light focussed on this nozzle is made luminous, and comes out in a well-defined jet. If the pressure of mercury in the boiler exceeds about double that around the jet, the jet has periodic swellings (paper V, fig. 4), which are of the nature

* Neither arrangement is regarded as having reached a final form.

of stationary sound waves. These, however interesting in themselves, are a source of complication for the immediate purpose, and the heat under the boiler was so regulated that they were not produced.

It is not necessary, however, to apply the exciting beam at the nozzle, as was done in the previous work. The jet of issuing vapour may be made luminous by exposure to the exciting beam *at any part of its course*. It may issue dark from the jet, and be made luminous by crossing the path of the exciting beam *in the open* (fig. 4). In this way we can observe the detailed circumstances right away from the silica walls, and from the false light which they unavoidably introduce. This is an important technical improvement.* Using this method in this form there was no difficulty in observing the delay effect similar to that found by R. W. Wood. In particular, it was

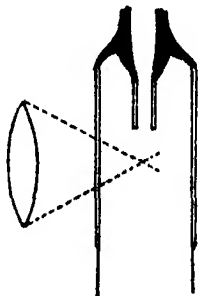


FIG. 4

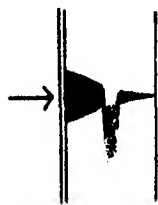


FIG. 5

clearly seen with the aluminium spark and the mercury arc, running hot so as to give molecular excitation. Photographs were also taken with the latter in visual light, and show definitely that there is a dark interval. With this arrangement the rapidly moving mercury stream is quite distinct from the quiescent nitrogen atmosphere all round, but it is difficult to arrange the conditions so that the latter does not contain some mercury vapour, and this mixture gives a strong fluorescence, so that the convergent cone of exciting light is well marked out except where the descending jet crosses it (fig. 5). At this point there is a gap, free from luminosity, and representing the dark interval. Below it, the jet becomes luminous. Under favourable circumstances, this luminosity is outside the track of the original beam, starting at about the lower boundary of this beam. In this

* By this method it may be shown, if indeed that were necessary, that the periodic swellings, when they occur, are already present in the jet of dark mercury vapour, and come into view whenever the exciting radiation is applied, whether at a node or at a loop.

particular form of experiment, I have not been able to get a wider separation. This form of experiment throws some light on the character of the motion near the jet. It is obvious that there cannot be a discontinuity of velocity in the full mathematical sense as we enter the jet laterally; and, in fact, the motion outside the jet is visible by the viscous dragging down of the self-luminous atmosphere on either side of the jet, as indicated in fig. 5.*

I have so far been speaking of experiments in which the principle of working right away from the neighbourhood of solid walls has been fully adhered to. There are advantages, however, in so far departing from this principle as to have the jet of mercury vapour moving very close to the surface of a sheet iron screen and parallel to it. The exciting beam enters through a slit-shaped aperture, measuring 1 mm in the vertical direction (*i.e.*, that of the jet) and open at the front end, so as to allow the level of excitation to be seen. Such a

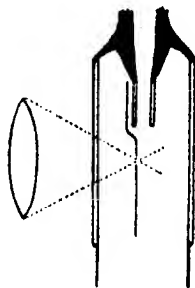


FIG. 6

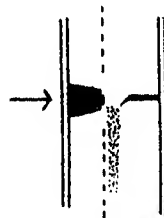


FIG. 7.

screen, placed near the jet, does not seem to affect it in any way and the slit allows of a much more definite limitation of the exciting beam than would otherwise be possible. This is, of course, all-important if a dark interval is to be looked for. Photographs are taken approximately in the plane of the screen, and the point where the jet leaves the exciting beam is very well defined, particularly if we concentrate attention on a stream line as close as possible to the plane of the iron screen.

Using this arrangement (fig. 6) with 2 cm pressure, various sources were examined. The general type of picture is indicated diagrammatically in fig. 7. The plane of the iron screen is indicated by the dotted line, which, however, to avoid confusion, is omitted at what is, in fact, the critical place, namely, in the neighbourhood of the slit. The incident cone is marked out by fluorescence, indicated by heavy shading and the descending jet shows

* The photographs in this case, though clear and unambiguous enough, are not well suited to reproduction, owing to the great range of intensities.

fluorescence indicated by the lighter shading. These features will readily be traced by comparison in the actual photograph (reproduction X, *e.g.*).

With this arrangement (fig. 5) at 2 cm pressure in the receiver various sources were examined. Using a mercury lamp in the ordinary way (not cooled) with 62 volts at the terminals, and with chlorine and bromine filters to cut out stray light, the effect as seen visually was photographed, using a Wratten No. 2 (aesculene) filter to cut out any ultra-violet light. The picture (not reproduced) shows the lag in time of the visual luminosity very clearly.

The same experiment was repeated using iron arc excitation, with chlorine and bromine filters over the source. In this case also the dark interval appears very definitely in the photographs taken in the light of the maximum 4850, though the result was perhaps not quite so conspicuous as in the previous case. The jet becomes luminous as, or after, it leaves the place of excitation (reproduction X). A pair of photographs, reproduction XI, taken in quick succession, and under strictly comparable conditions, in the light of 4850 (left) and 3300 (right) shows the dark interval in the former but not in the latter.

With the aluminium spark, it was found desirable to work at a lower pressure, 1 cm of mercury. Under these conditions, and if the heat under the boiler was suitably regulated, it was found possible to avoid the presence of mercury vapour in the surrounding nitrogen atmosphere, so that there was no fluorescence in the incident cone, but only in the jet itself. This makes the interpretation in some respects clearer.

Satisfactory photographs were taken in the light of 4850 (reproduction VIII) and in the light of 2537 (reproduction IX). They reaffirm even more emphatically the conclusion reached before that 4850 alone shows the dark interval. Photographs were also taken in the light of 3300, but it was found extremely difficult to get rid of false light, for the source has strong lines in this region, and no filter was available to remove them. The trouble was to some extent overcome by the method of focal isolation, combined with various screening devices. The photographs are not clear enough for reproduction, but they gave no suggestion of a dark interval, and were considered to prove that none exists.

Summarizing the above experiments, it appears that the phenomenon of the dark interval only occurs in the visual mercury fluorescence, which has continuous spectrum, photographic maximum 4850, and visual maximum in the green. The ultra-violet maximum at 3300 does not show it, nor does the fluorescence at or near the line 2537. Further, even in the visual fluorescence, the appearance of the dark interval is dependent on the source of excitation.

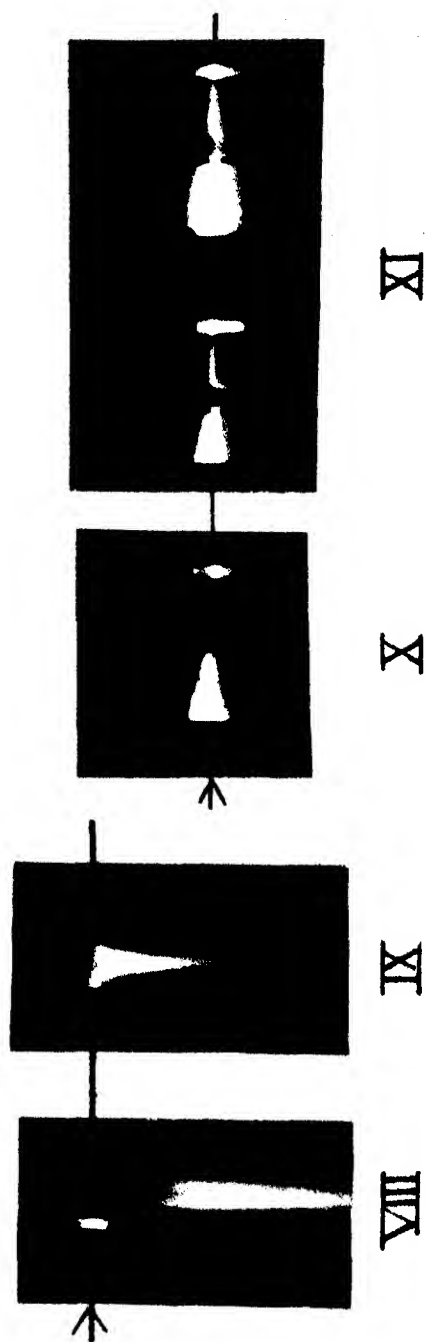
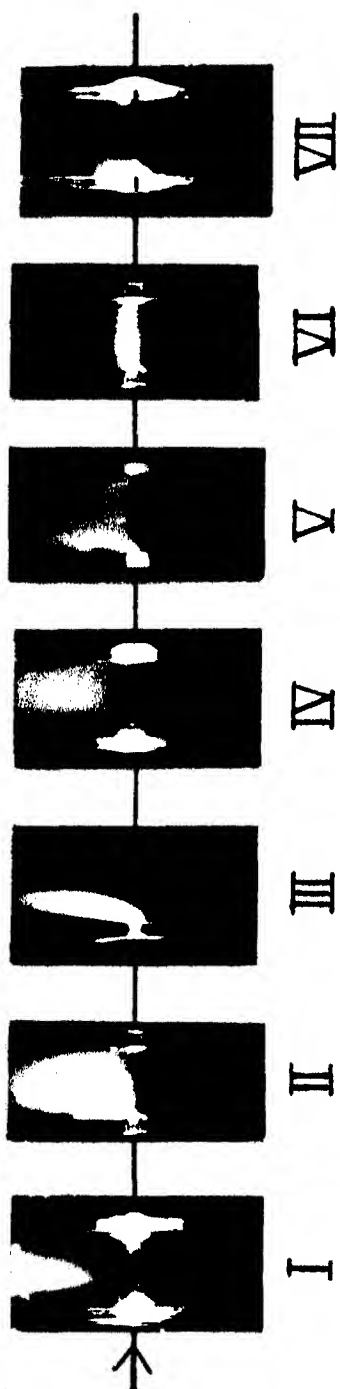
It is most conspicuous when the aluminium, zinc, or cadmium sparks are used, exciting on the long-wave side of the $1^1S_0-1^1P_1$ line of mercury; less conspicuous with the hot mercury lamp or the iron arc exciting on the long wave side of the $1^1S_0-2^3P_1$ line of mercury; and altogether absent with the cooled mercury arc, exciting exactly at the $1^1S_0-2^3P_1$ line of mercury (atomic excitation).

These are the observed facts. Some negative conclusions at any rate may be drawn from them. We cannot attribute the dark interval in general to the time interval required for transition from the 2^1P to the 2^3P state of the molecule; for it occurs in some cases when only the 2^3P state is involved. Further, we cannot attribute it to any delay in forming molecules from 2^3P_1 atoms; for the case when we start from the 2^3P_1 atom is precisely the case when we do not get it. The same argument shows that it is not inherent in the final process which leads to the emission of the green visual fluorescence. I do not think that we have at present the necessary key to a definite explanation.

EXPLANATION OF PLATE

The arrow in each case shows the axis of the exciting beam. All photographs are actual size except VIII and IX, which are enlarged twofold.

- I—Rising stream. Aluminium spark excitation. 5 mm pressure. Visual light. Some stray light in the path of the beam. Above this, note dark interval, then fluorescence.
 - II—The same, in light of λ 2537. Dark interval absent.
 - III—Rising stream. Cooled mercury lamp excitation. 2 mm pressure. Visual light. Dark interval absent.
 - IV—Rising stream. Hot mercury lamp excitation. 5 mm pressure. Visual light. Note dark interval.
 - V—The same in light of λ 3300. Dark interval absent.
 - VI—The same in light of λ 2537. Dark interval absent, the fluorescence scarcely moving along the stream at all.
 - VII—Rising stream. Iron arc excitation. 5 mm pressure. Visual light. Note dark interval.
 - VIII—Descending stream. Aluminium spark excitation. 10 mm pressure. Visual light. Note dark interval.
 - IX—The same in light of λ 2537. Dark interval absent.
 - X—Descending stream. Iron arc excitation. 20 mm pressure. In visual light. Note dark interval.
 - XI—Left Descending stream. Iron arc excitation. 20 mm pressure. In visual light. Note dark interval (not quite so well shown as in previous, but strictly comparable with XI, right).
 - XI—Right. Same. In light of λ 3300. Dark interval absent.
-



On the Technique of the Counter Controlled Cloud Chamber

By P. M. S. BLACKETT, F.R.S.

(Received May 18, 1934)

[PLATES 2 and 3]

1—General Considerations

The method by which very fast atomic particles are made to take their own cloud photographs has proved very useful for the investigation of cosmic rays. A short account of the method and a detailed account of the results obtained by its use have already been given by Blackett and Occhialini.*

Recently Locher† and also Anderson, Millikan, Neddermeyer, and Pickering‡ have used the same method and have obtained some beautiful results.

The method consists in using two or more tube counters to detect the passage of a high energy particle through a cloud chamber. The electrical response of the counters is then made to actuate the cloud chamber by means of relays. In order that the cloud tracks so formed should be fairly fine, it is necessary that supersaturation of the vapour should be attained very quickly after the passage of the ray.

Now when a fast particle traverses a gas, it produces an equal number of positive and negative ions within a narrow cylindrical column. Neglecting, at present, recombination and the effect of the electric field, these ions will diffuse away from their starting-point according to the diffusion equation, so that after a time τ their distribution will be given by§

$$n = \frac{N_0}{4\pi D\tau} e^{-\frac{r^2}{4D\tau}}, \quad (1)$$

where N_0 is the total number of ions of both signs per cm of track and D is the diffusion coefficient of the ions. If at a time τ after the passage of the ray the supersaturation of the vapour reaches the critical value for condensation on the ions, the mobility of the ions will then be suddenly reduced nearly to zero. So a photograph of such a track, taken a short time after the attainment

* 'Nature,' vol. 130, p. 263 (1932); 'Proc. Roy. Soc.,' A, vol. 139, p. 699 (1933).

† 'Phys. Rev.,' vol. 44, p. 779 (1933); 'Phys. Rev.,' vol. 45, p. 979 (1932).

‡ 'Phys. Rev.,' vol. 45, p. 357 (1934).

§ Jaffé, 'Ann. Physik,' vol. 42, p. 303 (1913).

of supersaturation, will give the projection on, say, the zx plane of the instantaneous position of the ions at time τ . The number of ion images in a strip parallel to OZ and of width δx is

$$\frac{N_0}{4\pi D\tau} \delta x \int_{-\infty}^{+\infty} e^{-\frac{x^2+y^2}{4D\tau}} dy,$$

so the superficial density of the ion images $\rho(x) = dn/dx$, at a distance x from the centre of the image on the photographic plate, is given by

$$\rho(x) = \frac{N_0}{\sqrt{4\pi D\tau}} e^{-\frac{x^2}{4D\tau}}, \quad (1)$$

or

$$\rho(x) = \rho_0 e^{-\frac{x^2}{4D\tau}}, \quad (1A)$$

where

$$\rho_0 = \frac{N_0}{\sqrt{4\pi D\tau}}.$$

It is convenient to define what may be called the 90% breadth X_1 , as that width of the image which contains 90% of the ion images. This is found to be given by

$$X_1 = 4.68 \sqrt{D\tau}. \quad (2)$$

Since the mean value of D for the positive and negative ions* in air at N.T.P. is $0.034 \text{ cm}^2 \text{ sec}^{-1}$, we have $X_1 = 0.86\sqrt{\tau} \text{ cm}$ at N.T.P. So if we demand that the tracks shall not be more than 1 mm broad, then we must have τ not more than $1/70$ second.

We can reasonably allow half this time for the release and half for the fall of the piston. If the piston has to move 1 cm in $1/140 \text{ sec}$, then it will require an acceleration of about 50 g , where g is the acceleration of gravity. Since the necessary acceleration a for the piston to move a given distance in a time τ is proportional $1/\tau^2$, and since from (2), $\tau \propto X^2$, we have $a \propto 1/X^4$. So to obtain tracks $\frac{1}{2} \text{ mm}$ broad, one would need an acceleration of 800 g .

From the same considerations it follows that for a given force applied to the piston, the breadth of the tracks is proportional to the fourth root of the mass of the piston.

It is clearly of importance to make the distance the piston has to move as small as possible. For a given initial height of chamber this distance depends on the expansion ratio required, and this depends on the gas and on the vapour used. We have so far used air and water, which require an expansion ratio

* Thomson, "Conduction of Electricity through Gases," vol. 1, p. 77 (1928).

of about 1.30. But by using a monatomic* gas, say, argon, in conjunction with a vapour such as alcohol, the necessary expansion will be about 1.12. This will allow still finer tracks to be obtained, or alternatively a larger and deeper chamber could be made to give the same breadth of track.

Since the diffusion coefficient D is inversely proportional to the pressure, the breadth of the tracks will be inversely proportional to the square root of the pressure of the gas.

2—The Movement of the Piston

There are two main ways of making the piston move. In the first, to which the calculation made above is relevant, the force is applied to the piston previously to the arrival of the ray. The piston is kept from moving by a catch, which is then released when the ray arrives. Now a piston of, say, 13 cm diameter, which is sufficiently rigid for this method to be used, could hardly be made lighter than 1 or 2 kg. Thus to give an acceleration of 50 g a force of 50 to 100 kg is required. It is not quite easy to release such a force by a catch in 1/150 second.

The alternative method is to apply the force only after the ray has arrived, and the simplest method† of doing this is to apply the force by a sudden alteration of the pressure on the two sides of the piston as in C. T. R. Wilson's original technique. With this method a very much lighter piston can be used. Since now the force on the piston increases with the time, its displacement will vary approximately as t^3 , and so the breadth of a track will vary roughly as the sixth root of the mass of the piston.

Since a cloud chamber for use with cosmic rays must be placed in a vertical plane, the liquid seal method of C. T. R. Wilson cannot be used. Hence the piston must be kept tight either by means of oil lubrication between accurately machined surfaces, as was used by Auger‡ and others, by the use of oil lubricated piston rings of some kind, or by the use of a flexible material, such as rubber or thin metal.

Preliminary experiments were made with the first method, but it was found that it was difficult to keep such a ground piston tight except by using an oil of such viscosity that the viscous forces made the expansion rather slow.

* Locher (*loc. cit.*) has recently used argon and water vapour in a tube-controlled cloud chamber.

† Various explosion methods have been considered but none actually tried.

‡ 'Ann. Physique,' vol. 6, p. 184 (1926).

Suppose that the clearance between piston and cylinder is about $25\ \mu$, then at a mean velocity of 150 cm per sec the viscous force on a piston whose cylindrical surface has an area of 300 sq cm and is lubricated by, say, Hyvak pump oil with a viscosity of 10 c.g.s. units is about 180 kg.

The breaking force of a lubricated leather piston ring would certainly be smaller than this, but we doubted whether it would be really tight and therefore did not try it. The new type of chamber using a fixed gauge as the floor of the chamber, recently described by C. T. R. Wilson,* is clearly very suitable for use with the tube controlled method.

3—*The Design of the Chamber*

These various considerations led us therefore to design the chamber shown in fig. 1. The piston, A, was made of aluminium alloy† and together with the hollow piston rod of monel metal weighed only 280 gm. The chamber was made tight by means of the flexible diaphragm B, made of reinforced rubber 1 mm thick. The chamber was usually filled with oxygen at a pressure of about 1.7 atmospheres. The space under the piston which can be closed by a light valve E, is filled with air, before the expansion, to the same pressure as in the chamber. The amount of the expansion is governed by the position of the nut H on the piston rod.

The expansion is made by moving a trigger F holding the valve closed (see also fig. 2). The valve weighs about 20 gm and has an area of 5.3 sq cm. The pressure on it is 0.7 atmosphere so that when released it starts to move with an acceleration of 160 g.

The dead space under the piston is made as small as possible, so that little more air shall have to flow out of the valve than is made necessary by the movement of the piston.

An oscillograph record of the movement of the piston is shown in fig. 18, Plate 3. From this it will be seen that the piston takes 0.005 second to travel its full movement of 1 cm that it then bounces a little and finally comes to rest 0.008 second after the start. Its maximum velocity is about 280 cm per sec, and its initial acceleration is about 80 g.

The quick deceleration of a piston moving with this velocity requires careful consideration. The method adopted was the simplest possible one, that of

* 'Proc. Roy. Soc.,' A, vol. 142, p. 88 (1933).

† A bare aluminium surface has a detrimental effect on the track formation. So the piston was covered with black enamel.

allowing the piston to fall flat with most of its area on to the thin rubber sheet G, which covers the floor of the casting. By this means the piston is brought to rest within less than a millimetre, with not much bounce, and without danger of the distortion that might be introduced by applying the braking force at the rim or at the centre alone. The measured deceleration of the piston at

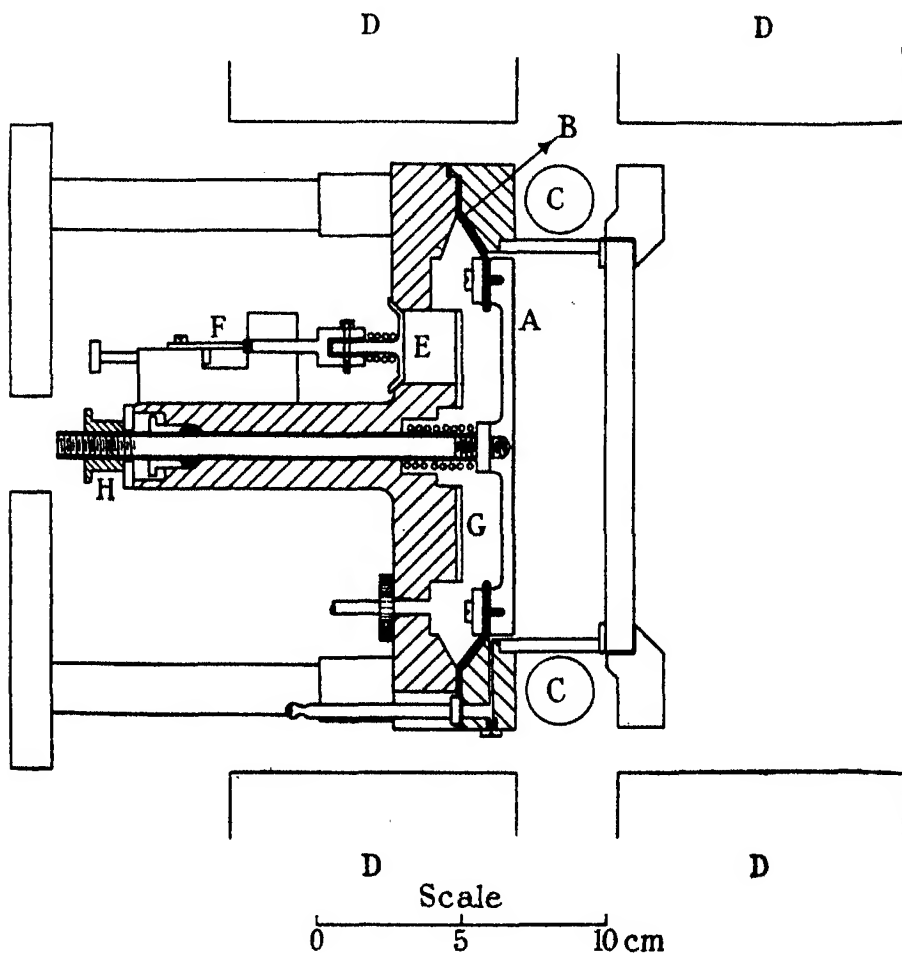


FIG. 1

the bottom of its movement is about 400 g. The piston bounces about $\frac{1}{2}$ mm which corresponds to a momentary 3% reduction in the expansion ratio.

The bounce is much more marked if a heavier piston is used. For instance, a brass piston, three times as heavy, bounced about 1.5 mm; that is, three times as much as the aluminium one.

The Geiger counters C were placed in such a position that any ray passing straight through both must also go through the illuminated part of the chamber. The whole chamber is placed inside a water cooled solenoid D.

The electric field used was usually about 3 volt per cm. Taking the mean mobility* at N.T.P. as about 1.6 cm/sec/volt/cm, we find that the separation of the positive and negative ions is not large enough to make the track double.

4—*The Release Mechanism*

Fig. 2 shows the method of releasing the valve. A continuous current passes through the small electro-magnet G and is of just sufficient magnitude to keep a light armature H attracted to it against a spring J. The electrical impulse from the amplifier connected to the Geiger counters is fed to the grid of a thyatron. When the latter flashes over, it short circuits the small magnet and allows the armature to fly off. The movement of the armature is transmitted by the nut K to the arm M and so to the long wire L, which is already under tension due to the spring N. A small clearance P is provided between the nut and the arm. Without such a clearance the adjustments are very critical and the mechanism therefore uncertain in action. In the arrangements used a movement of the armature of less than $\frac{1}{2}$ mm is sufficient to release the valve.

The method of adjustment is as follows. The two springs N and J are tightened till the catch F is just not released and the armature H just does not leave the magnet. Then the nut K is screwed up till it just does not touch the bar M.

The magnet and its circuit must be designed to make the time from the flashing over of the thyatron to the instant when the valve is released as small as possible.

The circuit used is shown in fig. 3. If the thyatron flashes over at $t = 0$, the current i in the magnet falls from its initial value $i_0 = V/(R + G)$ to its final value $i_1 = VS/R'(S + G)$, where $R' = R + SG/(S + G)$. The time constant T of the decay, before the armature releases, is L/R' .

To get a large change in the current through the magnet we must have $R \gg S$; the value of S is of the order of 20 ohms. Then G must be chosen to limit the current through the thyatron to a safe value. We made F and G both about 600 Ω .

* Dee, 'Proc. Roy. Soc.,' A, vol. 116, p. 664 (1927.)

In order to make T small, it is necessary to make the magnet small with only a few turns, and to use large external resistances.

A consideration of the acceleration of the armature on release also leads to the result that the magnet must be made as small as possible. For the

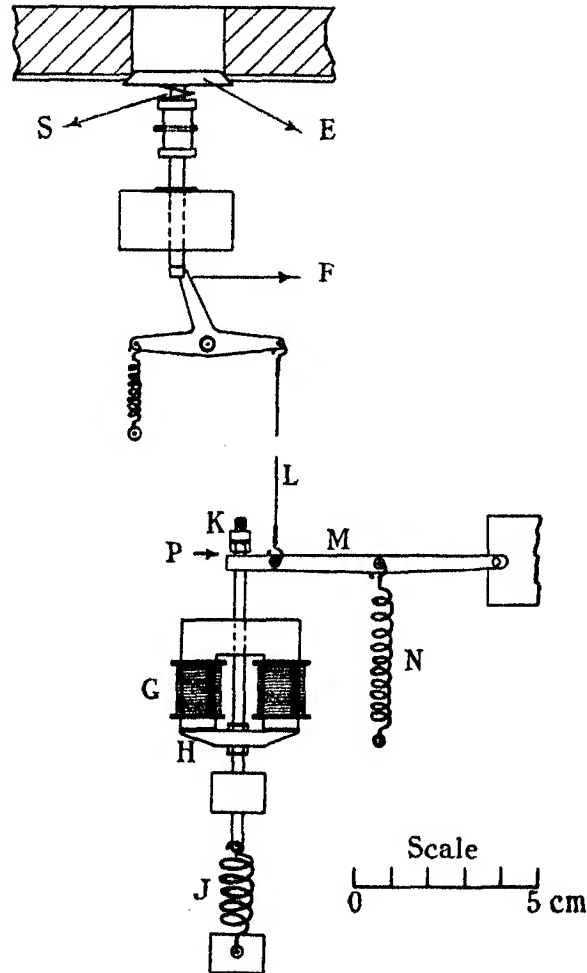


FIG. 2

mechanical force exerted by the magnet on the armature is proportional to the square of the linear dimensions of the magnet, while the mass of the armature is proportional to the cube, so the acceleration at release is inversely proportional to the linear dimensions.

The laminated magnet used, fig. 3, has 250 turns and a cross-section of 1 sq cm. Its calculated inductance is about 0.1 Henries. Since $R' \doteq 600 \text{ } \Omega$, the time constant of the circuit $T \doteq 2 \times 10^{-4}$ seconds.

The armature system had a mass of about 15 gm and the measured pull off force for a current of 0.18 amps was about 3 kg. So an acceleration of the order of 200 g was obtained.

In the construction of such magnets it is very important that the air gap between the armature and the magnet shall be as small as possible, in order to get the greatest possible attractive force.

The whole apparatus was tested by measuring the time from the flashing

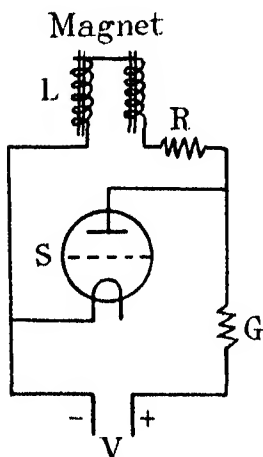


FIG. 3

over of the thyatron to the end of the expansion. This was found to be very nearly 0.010 second. The measurement of the separation of the positive and negative ions of a cosmic ray track, gave a similar value.

5—The Illuminating System

We used the following method of illumination. A capillary mercury lamp was connected directly to the secondary of an 8000 volt transformer connected to the 220 volt mains. To make the flash a large current, 100 to 200 amps, was passed through the primary for 1/50 to 1/20 second. If an A.C. supply is used, the flash is, of course, intermittent. If a D.C. supply is used, the flash is continuous. The illumination from

such a lamp is adequate to allow the photography of single droplets from a direction at right angles to the direction of illumination.

6—The Distortion of the Tracks

One of the chief difficulties of this tube-controlled method is the distortion of the tracks; that is, the final photograph does not represent accurately the original path of the ionizing ray.

(a) In the first place, since the ray goes through the chamber before the expansion, the whole original track is subjected to a simple *strain* by the expansion. Actually, of course, owing to the effect of the walls, etc., the distortion is more complicated than this.

But in addition to this distortion, which occurs *before* the drops are formed at the end of the expansion, there is the distortion which occurs between this

instant and the time when the photograph is taken. There are three main types of this to be considered.

(b) The tracks are distorted by the fall of the drops through the gas. This velocity of fall is approximately *uniform*, and is of the order of $\frac{1}{2}$ cm per second, depending on the size of the drops and so on the expansion ratio and the density of ionization. Owing to this motion it is never possible to photograph later than about $\frac{1}{4}$ second after the expansion without distortion.

(c) After the expansion, the gas near the walls warms up first so that convection currents develop, consisting most obviously in the rapid fall of the central mass of cold gas. This motion is much greater in a vertical than in a horizontal chamber. If it be assumed that the displacement *forces*, causing this motion, increase linearly with the time from the moment of expansion, then the displacement of a drop due to this cause, will vary* as t^3 .

It is a consequence of this rapid increase of distortion with the time that it is necessary, when using a vertical chamber, to take the photograph very soon after the end of the expansion. More illumination is therefore required, since the drops have not grown to their full size in so short a time.

(d) There is a type of distortion which may be called accidental, in contrast to the two former types, and which has caused us considerable trouble. The gas appears sometimes to be subject to a local swirling movement. Marked evidence of this is seen in some of the photographs already published. It is difficult to be quite sure of the cause of this gas motion, but we believe that it is due partly to the electric wind produced by the electrification of hairs, or possibly of the rubber diaphragm. A hair on the piston, for instance, which touches the walls of the chamber during the expansion, may become electrified by friction, and produce a sufficient electric wind to cause serious distortion. Confirmation of this view is obtained from the observation that large numbers of condensation nuclei are often found associated with the swirls. Also the swirling is absent when a slow expansion is made.

It is possible that our chamber is particularly liable to this trouble owing to some fault in the design.

The best way of avoiding errors of measurement arising from distortions (b), (c), and (d) is to start the illumination before the start of growth of the drops.† In this way any distortion, except that of type (a), can be noticed. Anderson uses this method.

* Assuming that viscous damping is not important.

† Anderson and others, *loc. cit.*

7—*The Magnetic Field*

The solenoid used had an internal diameter of 23 cm and consisted of four sectional coils in series, each with 100 turns of copper tube of 7.7 cm external diameter and 4.7 mm bore. The total resistance was 0.34 Ω and the weight of copper was 120 kg. A current of 200 amps was generally used giving 80,000 ampere turns and a field of 2200 gauss at the centre, with a power expenditure of 7 kw. Water was passed through the coils at the rate of 5 litres a minute (the water connections being in parallel), but this flow only sufficed to keep the steady temperature down to about 70° C. Sometimes 300 amps was used, but the current could then only be run for 2 minutes at a stretch.

Since the average time of waiting for a cosmic ray to arrive was 2 minutes, it was not possible conveniently to obtain more than 2200 gauss over the chamber. And since the electric power required varies as the square of the magnetic field, there was no possibility of obtaining, continuously, any great increase of field by using a solenoid of this type, except by the use of very large powers. A new chamber has therefore been made to fit between the poles of a large electro-magnet. With this new arrangement a field of 10,000 gauss could be obtained continuously with the same power required to produce 2000 gauss with the solenoid.

It is of interest to compare these figures with those given by Anderson* for the performance of the magnet used in his experiments. He used 440 kw. of power and a water flow of 160 litres per minute to obtain a field of 15,000 gauss. The ratio H/\sqrt{W} is then nearly the same for Anderson's and our solenoid.

8—*A Cloud Chamber between the Poles of an Electro-magnet*

Through the kindness of the Director of the National Physical Laboratory, an old Poulsen arc electro-magnet, weighing about 5000 kg was lent to the Cavendish Laboratory. This produced a field of nearly 10,000 gauss near the pole face with a gap of 12 cm when using about 100,000 ampere turns. The power consumed was about 6 kw.

The chamber shown in fig. 4 was very like the one already described except for the modification necessary to allow it to go between the pole pieces. The whole object of the design was to reduce, as far as possible, the gap between the

* 'Phys. Rev.', vol. 44, p. 406 (1933).

pole pieces. For, provided the iron is not nearly saturated, the field obtained is inversely proportional to this gap.

As no piston rod could conveniently be used, the piston A was unsupported except by the rubber diaphragm which served to close the chamber. When in the upper position, the piston rested against three brass stops B. When in the expanded position it lay flat on a rubber covered iron plate C. The expansion

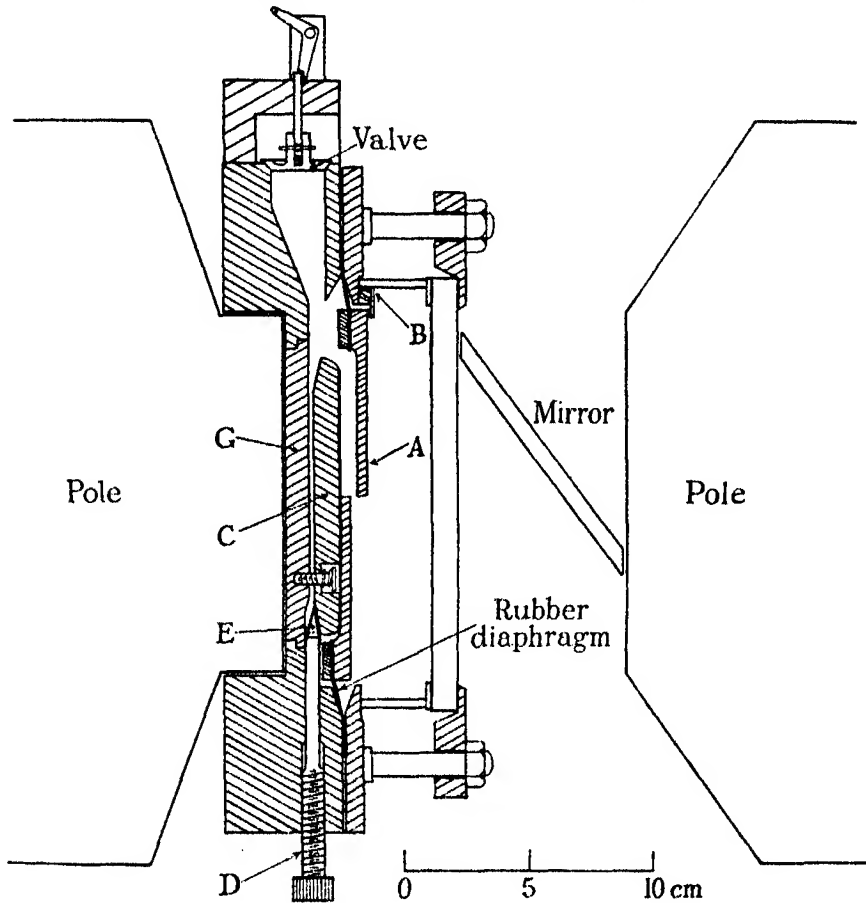


FIG. 4

was changed by altering the position of this iron plate. This was done by means of three long screws, D, with coned ends, E, on which the iron plate rested. The main casting was of brass, but an iron plate G was let into the back so as to form a continuation of the pole piece. Since the top of the iron plate, C, was effectively the pole face, this device enabled the tracks to be photographed within less than a centimetre of the pole face.

The tracks were photographed by two cameras, using a mirror at an angle of about 45° .

The chamber was made originally with two valves placed symmetrically so as to ensure that no large pressure differences developed over the surface of the piston, which would cause it to twist during the expansion. However, one valve proved adequate, presumably owing to the fact that, since the inertia of the air under the piston is very small compared with the inertia of the piston itself, the pressure is equalized underneath the piston before it has twisted appreciably. The release mechanism was identical in principle with that already described.

Many hundreds of photographs have been taken with this apparatus. One is reproduced in fig. 12, Plate 2.

9—The Breadth of the Tracks

Equation (2) gives what has been called the 90% breadth X_1 of the tracks. Below are given the observed and calculated values of X_1 , for tracks in O_2 and H_2 at a mean pressure of 1.5 atmospheres, when the delay $\tau = 0.01$ second.*

Gas.	\bar{D} NTP.	\bar{D} at 1.48 atmos.	X calcs. mm.	X obs. mm.
O_2	0.032	0.022	0.71	0.85
H_2	0.135	0.092	1.42	1.78

It is difficult to measure X_1 at all precisely, but the estimated values given are in rough agreement with the theoretical calculations. Figs. 10a, 10b, Plate 2, show typical electron tracks in oxygen and hydrogen.

Now these measurements were made on fast electron tracks where the number N_0 of ions per cm is of the order of 100. When, however, the particle producing the track is an alpha-particle, or a still more heavily charged particle, N_0 may have a value of the order of 10^6 . With such large values of N_0 , certain other considerations affect the observed breadth of the tracks.

Firstly, a considerable recombination of the positive and negative ions will take place. From Diebner's† measurements, one finds that in our apparatus about half the ions produced by an alpha-particle will disappear by recombination. Jaffé‡ has discussed the question theoretically, and has shown that,

* Thomson, *loc. cit.* \bar{D} assumed inversely proportional to pressure.

† 'Z. Physik,' vol. 10, p. 247 (1931).

‡ 'Ann. Physik,' vol. 42, p. 303 (1913).

even though recombination is taking place, the distribution remains a Gaussian one, though N_0 no longer remains constant but decreases with the time according to the relation

$$N_0' = \frac{N_0}{1 + \frac{\alpha N_0}{4\pi D} \log \left(\frac{4D\tau}{b^2} + 1 \right)},$$

where α is the coefficient of recombination, and b^2 is a constant measuring the initial distribution of ions at the time of their formation, and has a value 3×10^{-6} for air.

The photographic negative of such a heavily ionized track will show a central black part bordered by edges showing a rapid decrease of drop density. The larger the photographic exposure the broader the black part of the track will appear, since the individual drop images will be larger and will therefore the sooner run together, to form a completely black image. Now we find experimentally that with our particular optical arrangement a superficial drop density of about 1000 drops per sq cm gives a practically black image. Hence we can define the photographic breadth X_p of a track, as its breadth up to points where ρ reaches the value 1000 drops per sq cm.

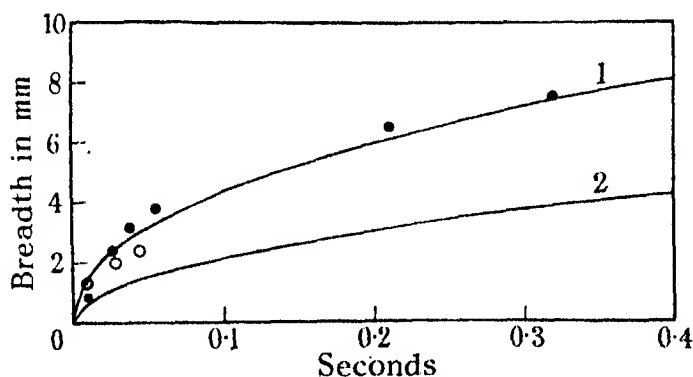


FIG. 5—Breadth of tracks in oxygen at 1.5 atmospheres for different times T of formation. Curve 1, X_p equation (3); 2, X_i equation (2); ● α particles, X_p , ○ protons, X_p ; ■ electrons X_i .

Denoting this value by ρ_1 , we find from (1) and (2) that

$$X_p = 4.0 (D\tau \log \rho_0/\rho_1)^{\frac{1}{2}}. \quad (3)$$

This equation can be tested by measuring the photographic breadth of those alpha-ray tracks for which the positive and negative ions are separated. For the time τ can be calculated from this separation. The curve (a) in fig. 5

shows the calculated value of X_p plotted against τ , for an alpha-particle,* for which $N_0' = 4 \times 10^4$. The points represent the results of measurements on tracks. The agreement is very satisfactory, considering that the conception of a photographic breadth is only a rough one, and the measured value will depend on the strength of the light and many other factors.

Curve (b) shows how the 90% breadth X_1 , calculated from (2), varies with τ .

10—On the Interpretation of some very Broad Tracks

In several of our original series of photographs described in our former paper were found tracks nearly a centimetre broad, such as those reproduced in figs. 8, 14, 15, 16, 17, Plate 2; 19, and 21 Plate 3. These were provisionally attributed to alpha-particles from radio active contamination, which passed through the chamber as much as half a second before the expansion. However, this interpretation presented certain difficulties and the question was left open till a full investigation could be made of the question of the track breadths. Later on, the view was put forward† that such tracks were probably not due to contamination, but might be interpreted as recoil tracks set in motion by the collision of neutrons associated with the cosmic ray showers. This view is almost certainly false, for the calculations of the breadths that have been given above show that such broad tracks as these must, in fact, be due to particles which have passed through the chamber a long time before the expansion, and cannot possibly be explained, as was thought at that time, as due to particles of very great ionizing power passing through at the same time as the cosmic rays, which actuated the counters.

For the number of ions per cm of path due to various types of recoil nuclei can be calculated from the data of Blackett and Lees.‡ It is found, for instance, that a nitrogen nucleus produces about 2×10^5 ion pairs per cm in air over the last half-centimetre of its range. Similarly an argon recoil nucleus ionizes at about the same rate over the last 3 mm of its range.

If we calculate from (3) the value of X_p for $N_0 = 2 \times 10^5$ and $\tau = 0.01$ second, we find a value about 1.9 mm. Again, if N_0 is given the very high value of 10^7 , even then X_p only has the value 2.2 cm. It is therefore quite

* The mean value for N_0 for an alpha particle from RaC in air at N.T.P. is 68,000. Taking recombination into account and allowing for the higher pressure in the chamber we get a value about 40,000.

† Solway Conference, Brussels, October, 1933.

‡ 'Proc. Roy. Soc.,' A, vol. 134, p. 658 (1932).

impossible to attribute a track 1 cm broad to a particle passing 0.01 second before the expansion. The correct interpretation is almost certainly that which attributes the broad tracks to particles of much lower ionizing power passing a much longer time before the expansion.

A confirmation of this view may be obtained as follows. A few of the broad tracks photographed are so good technically that it is possible to count the distribution of drops on the edges of the track. In this way a partial test of the theoretical distribution can be made and the unknown constants τ and N_0 can be obtained directly. One of these tracks is shown in fig. 16, Plate 2, and also very much enlarged in fig. 17, Plate 2.

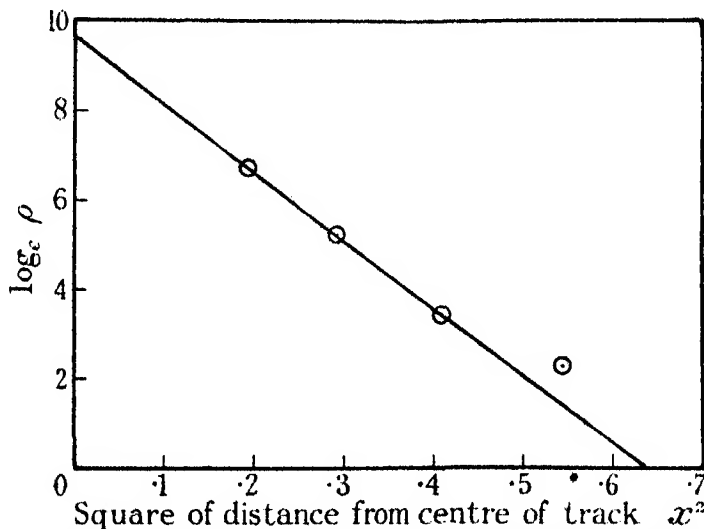


FIG. 6—Observed distribution of drops at edge of the track shown in figs. 16 and 17 Plate 2.

In fig. 6 is shown the observed distribution. The curve shows that the relation between $\log \rho$ and x^2 is linear, as it should be from (1A). The constants are found to be $N_0' = 6700$ and $\tau = 0.78$ seconds. Since the separation of the positive and negative ions for such a long delay is complete, the photograph shows those of one sign only,* so the figure obtained above must be compared with an expected value of about 15,000. The discrepancy is not very serious since the method is rough and gives directly $\log N$ and not N . Several other tracks give comparable values of N_0 and τ .

* The reason why a very broad track is usually single and not double is merely that the positive and negative ion tracks are seldom both in the illuminated part of the chamber.

It can therefore be taken as certain that these very broad tracks have nothing directly to do with the cosmic rays actuating the counters.

If these tracks are due to alpha-particles occurring at random in time—that is, if the number occurring in a time δT is proportional to δT —then from (2) the number of tracks with breadth between X and $X + dX$, is proportional to $X dX$, and so increases linearly with X . The observed distribution of the tracks in breadth shown in fig. 7 is consistent with this view, though there is a slight defect in the numbers between 1 and 2 mm. But this may well be due to chance. More than half of the tracks of less than 1 mm breadth are probably associated with the cosmic rays, the rest being of chance occurrence. The upper limit to the breadth of the tracks is merely that breadth to which

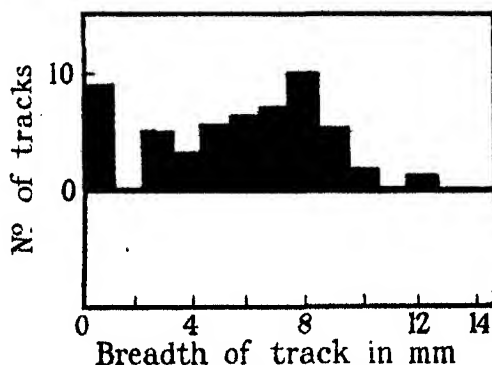


FIG. 7—Number of broad tracks.

they will grow in the time taken for the ions to cross the chamber under the electric field, and so is large when a weak electric field is used.

If the broad tracks are due to alpha rays, then their rate of occurrence in the chamber is about five per minute. This works out at about 70 per hour per 100 sq. cm area, which is of the order of the expected contamination.*

Sometimes quite short tracks are observed, very much shorter than any known alpha-rays, figs. 13, 14 and 15, Plate 2. Some of these may possibly be due to the recoil tracks produced when a neutron collides with a heavy nucleus. But there is often an alternative explanation. The ions move in air at 1.5 atmospheres under the field of about 2.5 volts per cm with a velocity of about 3 cm sec⁻¹. So in a time of $\frac{1}{2}$ second they have moved about 2.3 cm from where they were formed; that is, a distance of the order of half the height of the chamber.

* Beardon, 'Rev. Sci. Instr.', vol. 4, p. 271 (1933).

Suppose an alpha particle happens to be emitted in the material of, say, the piston, so as just to emerge into the gas and produce a track of few millimetres long. Then all the ions of one sign will be drawn into the middle of the chamber and therefore photographed as a short nearly round blob.

So when a *single* small round blob is observed it is not possible always to conclude with certainty that it corresponds to a particle of short range. The occurrence of such short-range particles can only be considered certain when a double track showing both positive and negative ion groups is observed, or when the position in the chamber is such as to exclude the other explanation. It is interesting to compare the tracks in figs. 14, 15, which are probably due to parts of the track of a radio-active contamination alpha-particle, with fig. 13, which was photographed when using a neutron source, and is almost certainly a neutron recoil track.

Some photographs have recently been taken by Locher* with the same counter-controlled method, but with argon in the chamber and three instead of two counters. Locher reports several neutron recoil tracks apparently associated with cosmic ray showers and shows their close resemblance to the recoil tracks produced by a neutron source. It appears that some of the tracks observed by Locher are as broad as 1.5 cm. If the argument given here is valid, such very broad tracks were certainly not due to particles which were contemporary with the cosmic rays. They must, therefore, be attributed to random events, not related to the showers. Locher also observed thinner tracks which may have been contemporary with the cosmic rays.

That neutrons might be associated with the showers and yet occur half a second earlier must be considered as unlikely. It is equally unlikely that such broad tracks are due, not to the diffusion of ions from a line, but to some new form of spatially extended ionizing agent.

I wish to express my pleasure and gratitude derived from the collaboration during the last two years with my colleague G. P. S. Occhialini, who was closely associated with nearly all the work described in this paper.

The cost of the solenoid was met by a grant from the Government Grant Committee of the Royal Society.

I wish to express my appreciation of the interest taken by Lord Rutherford in this work and for the facilities which he has put at our disposal in the Cavendish Laboratory.

* *Loc. cit.*

I also wish to thank the staff of the Laboratory, in particular Messrs. Lincoln, Fuller, and Aves, for their assistance in constructing the apparatus.

Summary

When Geiger counters are used to actuate a cloud chamber, the tracks formed will have a breadth which can be calculated by taking into account the diffusion of the ions, during the time τ from the instant of their formation to the instant of drop formation. The breadth of a track varies as $\tau^{\frac{1}{2}}$. It is found that when $\tau = 0.01$ second, tracks can be obtained in air at 1.5 atmospheres, which are about $\frac{3}{4}$ mm broad. It is almost impossible to obtain tracks, at this pressure, very much finer than this owing to the very large forces required to produce the necessary acceleration of the piston. The breadth of the tracks, for a given delay τ , should inversely be proportional to the pressure of the gas.

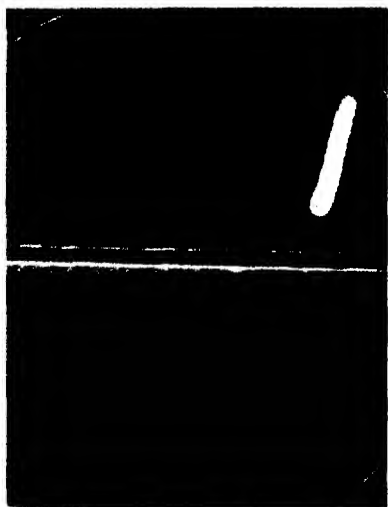
Special care is required in the design of the release mechanism, to reduce as far as possible the time taken to release the valve controlling the expansion. To obtain a quick release, the release magnet must be made quite small and of small inductance.

Since not more than 3000 gauss could be obtained with the water-cooled solenoid used in the first experiment, a new chamber has been made to fit between the pole pieces of a large electro-magnet, which could produce about 10,000 gauss.

The tracks are liable to various kinds of distortion, which may be of great importance as limiting the accuracy of measurement of the tracks.

Measurement of the track breadths in oxygen and hydrogen confirm the theoretical calculations based on the diffusion theory. When the tracks of heavily ionizing particles are considered, it is found that their apparent breadth is greater than that of electron tracks. Their *photographic breadth* depends on the intensity of the light and on the optical arrangement. Measurements confirm the theoretical variation of track breadth with time of formation.

The broad tracks often observed are interpreted, in the light of the discussion, as due mainly to alpha particles from radio-active materials in the walls of the chamber. The numbers observed of different breadths agree with this assumption. It is probable therefore that they have nothing to do with the cosmic radiation.



8



9
0.01 second



10a

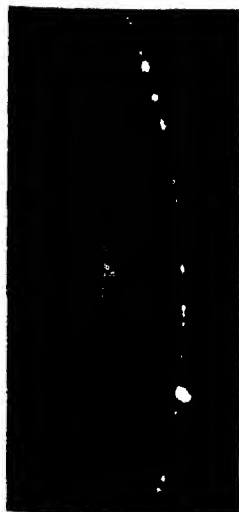


10b

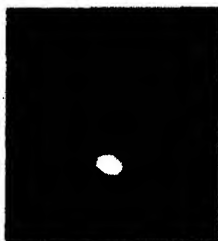


11

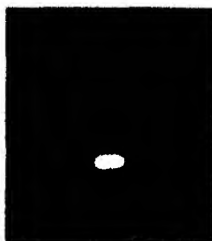
0 1 cm.



12



13



14



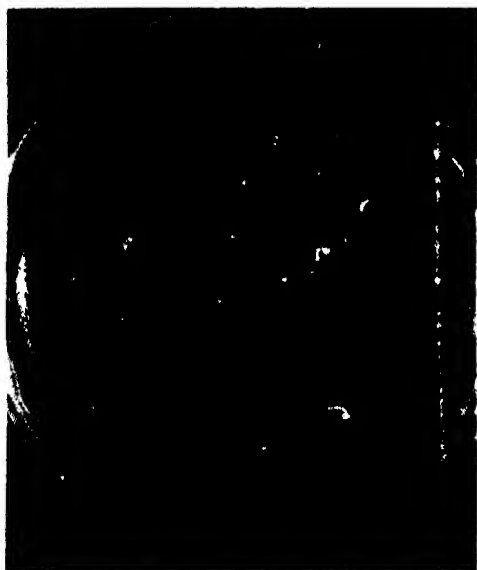
15



16
0 3 cm.



17
0 1 cm.



18



19



20



21

DESCRIPTION OF PLATES

PLATE 2

- FIG. 8—A single cosmic ray track ($E \sim 200 \times 10^6$ volts), and a broad track due probably to an early contamination alpha-particle.
- FIG. 9—An oscillograph record of fall of piston.
- FIG. 10—Enlarged photograph of electron track in oxygen. $X_1 = 0.85$ mm.
- FIG. 10A—Enlarged photograph of electron track in hydrogen, showing clearly the individual droplets. $X_1 = 1.8$ mm.
- FIG. 11—Enlarged photograph of proton track in oxygen. $X_p = 1.3$ mm.
- FIG. 12—Track of particle of energy 45 million volts, taken in a magnetic field of 10,000 gauss, with the chamber described in Section 8.
- FIG. 13—A neutron recoil track using a source of Po + Be. (Chadwick, Blackett, and Occhialini, 'Proc. Roy. Soc.,' A, vol. 144, p. 235 (1934)).
- FIG. 14—Photograph of short track found on photographs of cosmic rays. Although very like fig. 13, which latter is certainly due to a neutron recoil track, it is probable that 14 represents *part* of an early contamination alpha-particle track.
- FIG. 15—A short broad track found on a cosmic ray photograph. The positive and negative ion groups are here both visible so that the time can be calculated $\tau = 0.21$ second $X_p = 0.65$ cm. The two tracks are separated by 1.1 cm and one appears shorter than the other because it has been displaced by the field nearly out of the illuminated part of the chamber.
- FIG. 16—A typical broad track.
- FIG. 17—The same enlarged so as to show the individual droplets. Fig. 4 shows the variation of observed drop direction with distance from the track centre.

PLATE 3

- FIG. 18—A complicated shower, showing about 16 tracks, some of high and some of low energy, in no very simple relation to each other ($H = 2200$ gauss).
- FIG. 19—A shower with four tracks of which two are positrons and two electrons. The energies are 230, 150, 55, and 20 million volts. The round blob probably represents *part* of an early contamination alpha particle ($H = 3300$).
- FIG. 20—Another complicated shower of about 19 tracks, mostly of rather low energy about 6 million volts. It is almost impossible to find any simple characteristics of this shower. It is therefore not possible to tell for certain the direction of the particles or therefore their charge. ($H = 3300$.)
- FIG. 21—A single ray of energy greater than 2×10^8 volts going straight through the chamber. A circular track due to a particle of about 800,000 volts. A broad track probably due to a contamination alpha passing through the chamber about $\frac{1}{2}$ second before the expansion. ($H = 2200$.)
-

*Refractive Dispersion of Organic Compounds. V—Oxygenated
Derivatives of Cyclohexane The Inadequacy of the Ketteler-
Helmholtz Equation*

By C. B. ALLSOPP, M.A., Ph.D., Laboratory of Physical Chemistry, Cambridge

(Communicated by Professor T. M. Lowry, F.R.S.)

(Received February 12, 1934)

In the preceding paper of this series,* refractive indices and molecular extinction coefficients over a wide range of wave-lengths were recorded for the two cyclic hydrocarbons *cyclohexene* and 1:3-*cyclohexadiene*. These observations completed a study of the refractive dispersions of the series of 6-ring compounds C_6H_{12} , C_6H_{10} , C_6H_8 , C_6H_6 ; they also provided a basis for the study of the phenomenon of "optical exaltation," which is exhibited by compounds containing conjugated double bonds, since the last two members of the series belong to this type. Conjugation, however, may be effected, not only between two olefinic double bonds, but also between an olefinic double bond and an oxygenated radical, such as the carboxyl, carbonyl, or hydroxyl group. The present paper, therefore, records the absorption spectra and refractive dispersions of three oxygenated derivatives of cyclohexane, namely, *cyclohexanol*, *cyclohexanone*, and *ethyl hexahydrobenzoate*, in the molecules of which each of the preceding groups is exemplified.

Dispersion curves are thus now available for typical compounds of the cyclohexane series containing "unsaturated" radicals of all the principal types which are used in constructing conjugated systems, and the way has been prepared for a detailed study of conjugation, as exemplified on the one hand by *cyclohexadiene*, and similar compounds containing two olefinic radicals, and on the other hand by a variety of compounds containing a double bond in addition to a hydroxyl, carbonyl, or carboxyl group. It is anticipated that, with the help of the data set out in the preceding and present papers, it will be possible in a later communication to demonstrate in what respect the behaviour of conjugated compounds differs from that which might be anticipated from a merely additive behaviour of the chromophoric radicals, and thus to determine the nature, and if possible to discover the origin, of the phenomenon of optical exaltation.

* Allsopp, 'Proc. Roy. Soc.,' A vol. 143, p. 618 (1934).

The present measurements are also of interest from a different point of view. By taking advantage of the extreme thinness of the films of liquid which are used in the interference method for measuring refractive dispersion,* it was possible to measure the refractive indices of *cyclohexanone* right through the "ketonic" absorption band (between 3000 Å and 2500 Å), which is exhibited by all compounds containing an isolated $>\text{C}=\text{O}$ group. These measurements reveal that, whereas the rotatory dispersion of optically active ketones is largely dominated by the ketonic absorption band, the contribution of this band to the refractive dispersion is extremely small and produces only a slight "ripple" on an otherwise smooth curve (fig. 2).

Materials—(a) Commercially-pure *cyclohexanol* was shaken with caustic soda, extracted with ether, dried over potassium carbonate, and distilled three times *in vacuo* from small pieces of sodium. The product, which melted at 20° was fractionated *in vacuo* in an all-glass apparatus by heating to 30° whilst the receiver was cooled in liquid air. The distillate melted at 11° , whilst the residue solidified to pure white crystals melting at 23.5° . The crystals were allowed to drain for 2 weeks, when a small quantity of a glassy solid separated.

The remaining crystals melted to a liquid of density $d_4^{25} = 0.9255$. A sample used by Auwers and co-workers† melted at 23.0° and had $d_4^{37} = 0.9373$. The highest melting-points hitherto recorded, for samples stored in sealed, evacuated tubes, are 24.9° ‡ and 25.5° §; but the melting-point is extremely sensitive to traces of moisture and dissolved air. The close agreement of our molecular refraction with that found by Auwers for material with a lower melting-point shows that (as with *cyclohexane*) the slight residual impurity has no marked effect on the value of the refractive index.

(b) Commercial *cyclohexanone* was purified through the bisulphite compound, dried and fractionated. A fraction boiling at 156.5° was refractionated immediately before use. Its density was $d_4^{20} = 0.9462$. Auwers (*loc. cit.*) gives the density as $d_4^{15.3} = 0.9503$ and boiling-point as 156.6° to 156.8° .

(c) A specimen of *ethyl hexahydrobenzoate* was kindly supplied by Dr. Komatsu, of the Imperial University of Kyoto,|| who gave its boiling-point as 95° at

* Lowry and Allsopp, 'Proc. Roy. Soc.,' A, vol. 126, p. 165 (1929); vol. 133, p. 26 (1931).

† Auwers, Hinterseber, and Treppman, 'Liebig's Ann.,' vol. 410, p. 257 (1915).

‡ Skau and Meier, Dissertation, Trinity College, Hartford (1931).

§ Lange, 'Z. phys. Chem.,' A, vol. 161, p. 80 (1932).

|| Komatsu and Mitsui, 'Kyoto, Coll. Sci. Mem.,' A, vol. 14, p. 297 (1931).

30 mm, and its density as $d_4^{25} = 0.9562$. At high dilutions the sweet smell of the ester gives place to an intensely disagreeable and persistent odour. For this reason, ethyl isobutyrate, which contains the same chromophoric radical, was substituted for it in the measurements of absorption spectra.

(d) The samples of *ethyl isobutyrate* and *isobutyric acid* after fractionation boiled at 110.5° and 154° , and had $d_4^{20} = 0.8704$ and 0.9486 respectively.

Absorption Spectra

The molecular extinction coefficients of solutions of the above compounds in cyclohexane are plotted against wave-length in fig. 1.

(a) The absorption spectrum of *cyclohexanol* consists of a band with a maximum beyond the present limits of observation ($\log \epsilon = 2.0$ at 1850 Å), together with a slight "step-out," $\log \epsilon = -0.4$, between 2100 and 2200 Å.

(b) The ketonic absorption band of *cyclohexanone* has a maximum intensity $\log \epsilon = 1.10$ at 2880 Å, and is symmetrical on a scale of wave-lengths. A second band with a maximum inside the Schumann region is at least 100 times more intense, since $\log \epsilon = 2.9$ at 1850 Å.*

(c) The absorption spectrum of *ethyl isobutyrate* includes a maximum, $\log \epsilon = 1.82$ at 2075 Å, together with a well-defined "shelf," $\log \epsilon = -0.75$ between 2600 and 2800 Å, where the absorption is about 400 times less than at the principal maximum.

(d) *iso-Butyric acid* gives a maximum, $\log \epsilon = 2.10$ at 1850 Å, of slightly higher intensity and at shorter wave-lengths than the ester. The step-out, $\log \epsilon = -0.5$ at 2500 Å, is also more intense, but the intensity does not fall off so rapidly at longer wave-lengths. Thin films of *ethyl hexahydrobenzoate*, used in the measurement of refractive indices, begin to absorb at about the same wave-length as *isobutyric acid* and its ester.

Refractive Indices

The refractive indices of *cyclohexanol*, *cyclohexanone*, and *ethyl hexahydrobenzoate*, for 24 wave-lengths in the visible spectrum are recorded in Table I, while Tables II, III, and IV contain the ultra-violet values measured photographically for the three compounds at 44, 46, and 40 wave-lengths respectively.

Comparison with other Observations

(a) The refractive indices of *cyclohexanol* and of *cyclohexanone* at four wave-lengths in the visible spectrum were measured by Auwers (who paid

* Cf. Donle and Volkert, 'Z. phys. Chem.', B, vol. 8, p. 60 (1930).

particular regard to the purity of the materials and to accuracy of measurement) in the course of his investigation of the additive relationships in molecular refractivity.* Auwers records the following values for the molecular

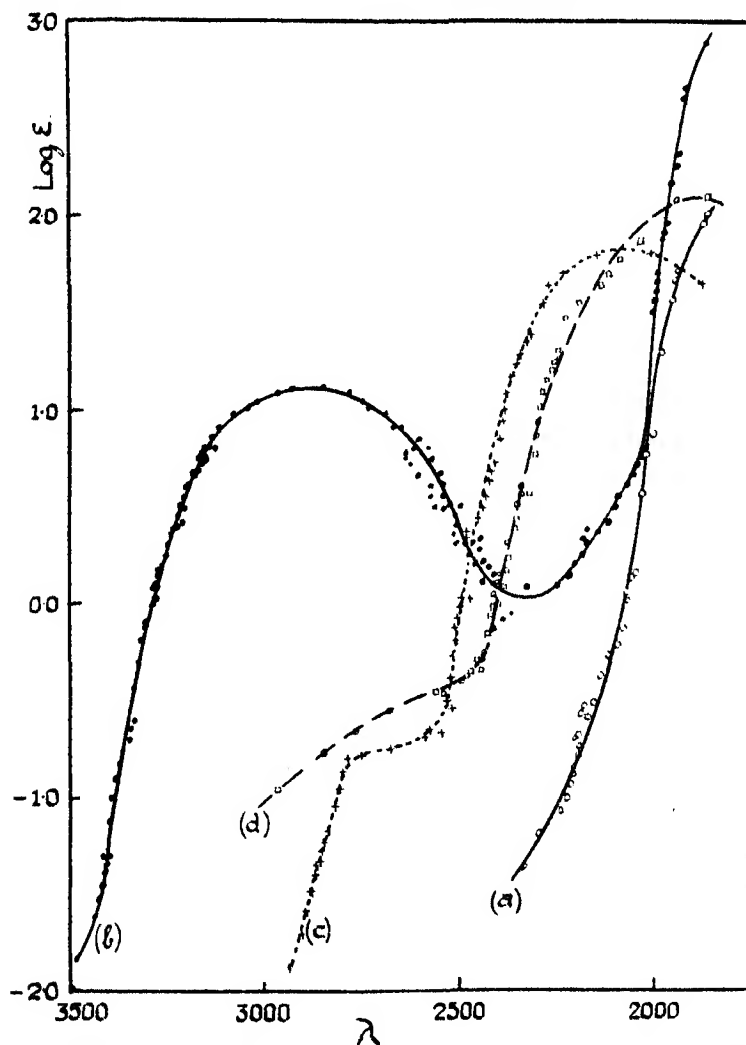


FIG. 1—Molecular extinction coefficients of (a) cyclohexanol, (b) cyclohexanone, (c) ethyl isobutyrate, (d) isobutyric acid, in cyclohexane solution.

refractivities at $\lambda = 5896 \text{ \AA}$: cyclohexanol, $M_D (\text{obs.}) = 29.28$, $(\text{calc.}) = 29.23$; cyclohexanone, $M_D (\text{obs.}) = 27.88$, $(\text{calc.}) = 27.72$, the calculated values

* Auwers, Hinterseber, and Treppmann, *loc. cit.*

Table I.—Refractive Indices of *cyclo*Hexanol at 25° C and of *cyclo*Hexanone and Ethyl Hexahydrobenzoate at 20° C
Pulfrich Refractometer Readings

λ^*	<i>cyclo</i> Hexanol (25° C)				<i>cyclo</i> Hexanone (20° C)				Ethyl hexahydrobenzoate (20° C)			
	n observed	n calculated	Difference (O—C) $\times 10^4$		n observed	n calculated	Difference (O—C) $\times 10^4$		n observed	n calculated	Difference (O—C) $\times 10^4$	
Li 6707.86	1.45218	1.45212	+0.6		1.44878	1.44883	—0.5		1.44312	1.44298	+1.4	
Cd 6438.47	1.45294	1.45289	+0.5		1.44943	1.44961	—1.8		1.44379	1.44378	+0.1	
Zn 6362.34	1.45317	1.45312	+0.5		1.44966	1.44985	—1.9		1.44393	1.44403	—0.5	
Li 6103.6	1.45400	1.45399	+0.1		1.45051	1.45074	—2.3		1.44490	1.44495	—0.5	
Na 5895.93	1.45472	1.45477	—0.5		1.45145	1.45155	—1.0		1.44577	1.44577	\pm	
Hg 5790.68	1.45518	1.45520	—0.2		1.45191	1.45200	—0.9		1.44623	1.44623	\pm	
Cu 5782.15	1.45518	1.45524	—0.6		1.45196	1.45204	—0.8		1.44627	1.44626	+0.1	
Cu 5700.24	1.45548	1.45559	—1.1		1.45237	1.45240	—0.3		1.44667	1.44664	+0.3	
Ag 5471.51	1.45651	1.45667	—1.6		1.45348	1.45352	—0.4		1.44774	1.44778	—0.4	
Hg 5460.73	1.45657	1.45672	—1.5		1.45366	1.45358	—0.2		1.44783	1.44784	—0.1	
Cu 5220.06	1.45800	1.45803	—0.3		1.45500	1.45494	+0.6		1.44933	1.44922	+1.1	
Ag 5209.04	1.45813	1.45810	+0.3		1.45506	1.45500	+0.6		1.44940	1.44929	+1.1	
Cu 5153.26	1.45848	1.45844	+0.4		1.45547	1.45535	+1.2		1.44966	1.44964	+0.2	
Cu 5105.55	1.45869	1.45872	—0.3		1.45574	1.45566	+0.8		1.44995	1.44996	—0.1	
Cd 5085.82	1.45879	1.45885	—0.6		1.45585	1.45579	+0.6		1.45000	1.45006	—0.6	
Ba 4934.10	1.45976	1.45978	—0.2		1.45686	1.45681	+0.5		1.45111	1.45115	—0.4	
Zn 4810.53	1.46084	1.46076	+0.8		1.45786	1.45779	+0.7		1.45207	1.45210	—0.3	
Cd 4799.91	1.46090	1.46083	+0.7		1.45795	1.45785	+1.0		1.45218	1.45219	—0.1	
Zn 4732.16	1.46160	1.46145	+1.5		1.45864	1.45868	—0.6		1.45290	1.45284	+0.6	
Zn 4680.14	1.46184	1.46179	+0.5		1.45896	1.45885	+1.1		1.45323	1.45319	+0.4	
Cd 4678.15	1.46190	1.46183	+0.7		1.45902	1.45895	+0.7		1.45329	1.45321	+0.8	
Li 4603.0	1.46250	1.46246	+0.4		1.45966	1.45943	+2.3		1.45389	1.45389	\pm	
Ba 4534.04	1.46299	1.46287	+1.2		1.46006	1.45996	+0.8		1.45442	1.45436	+0.6	
Hg 4358.34	1.46472	1.46477	—0.5		1.46187	1.46197	—1.0		1.45625	1.45636	—1.1	

* The wave-lengths for the visual readings in Table I are taken from the 'International Critical Tables,' vol. 5 (1929).

Table II—Refractive Indices of *cyclo*Hexanol at 25° C. Photographic Readings

λ^*	Refractive index		Diff. (O - C) $\times 10^4$	λ	Refractive index		Diff. (O - C) $\times 10^4$
	observed	calculated			observed	calculated	
Fe 4890.770 B	1.4601	1.4601	\pm	Fe 3437.045 B	1.4791	1.4791	\pm
W 4600.450	1.4626	1.4625	+1	W 3407.639	1.4797	1.4798	-1
W 4546.498	1.4630	1.4629	+1	Fe 3351.529 B	1.4813	1.4810	+3
W 4493.978	1.4636	1.4634	+2	Fe 3296.806 B	1.4827	1.4825	+2
Fe 4442.345 III	1.4640	1.4639	+1	Fe 3244.186 B	1.4842	1.4840	+2
W 4295.012	1.4654	1.4655	-1	Fe 3192.806 B	1.4855	1.4859	-4
Fe 4248.224 B	1.4659	1.4660	-1	Fe 3167.856 B	1.4861	1.4861	\pm
Fe 4202.032 B	1.4664	1.4665	-1	Fe 3119.495 B	1.4876	1.4877	-1
Fe 4157.805 B	1.4669	1.4670	-1	W 3049.694	1.4898	1.4900	-2
Fe 4071.748 B	1.4681	1.4681	\pm	Fe 2983.571 B	1.4922	1.4924	-2
Fe 3989.861 B	1.4693	1.4692	+1	Fe 2941.347 II	1.4939	1.4940	-1
Fe 3909.834 B	1.4704	1.4704	\pm	Fe 2908.864 B	1.4956	1.4953	+3
Fe 3871.752 III	1.4711	1.4709	+2	Fe 2840.422 B	1.4983	1.4982	+1
Fe 3833.863 B	1.4715	1.4715	\pm	Fe 2808.329 B	1.5003	1.4997	+6
Fe 3797.518 III	1.4723	1.4721	+2	W 2776.091	1.5015	1.5012	+3
Fe 3725.495 B	1.4733	1.4733	\pm	Fe 2746.486 B	1.5037	1.5027	+10
Fe 3690.732 III	1.4738	1.4739	-1	W 2687.389	1.5073	1.5057	+16
Fe 3657.143 B	1.4746	1.4746	\pm	W 2603.567	1.5125	1.5106	+19
W 3629.513	1.4751	1.4752	-1	W 2551.360	1.5162	1.5141	+21
Fe 3559.514 B	1.4768	1.4764	+2	Fe 2501.70 B	1.5201	1.5175	+26
Fe 3497.111 III	1.4779	1.4778	+1	Fe 2453.478 B	1.5236	1.5211	+25
Fe 3466.501 B	1.4784	1.4784	\pm	Fe 2431.05 B	1.5259	1.5228	+31

Table III—Refractive Indices of *cyclo*Hexanone at 20° C. Photographic Readings

λ^*	Refractive index		Diff. (O - C) $\times 10^4$	λ	Refractive index		Diff. (O - C) $\times 10^4$
	observed	calculated			observed	calculated	
W 4680.539	1.4590	1.4589	+1	Fe 3285.425 B	1.4821	1.4813	+8
W 4542.900	1.4603	1.4601	+2	Fe 3250.400 B	1.4833	1.4823	+10
Fe 4476.022 III	1.4606	1.4607	-1	Fe 3219.582 B	1.4843	1.4833	+10
W 4412.206	1.4613	1.4614	-1	Fe 3160.650 B	1.4804	1.4852	+12
Fe 4352.738 II	1.4622	1.4620	+2	Fe 3099.898 B	1.4887	1.4873	+14
W 4234.358	1.4631	1.4634	-3	Fe 3045.082 B	1.4905	1.4893	+12
Fe 4173.925 B	1.4637	1.4641	-4	Fe 2990.394 B	1.4925	1.4915	+10
Fe 4123.759 B	1.4644	1.4648	-4	W 2956.676	1.4928	1.4929	-1
W 4064.799	1.4650	1.4656	-6	W 2935.632	1.4937	1.4938	-1
W 4018.312	1.4656	1.4662	-6	Fe 2904.163 B	1.4945	1.4955	-10
Fe 3919.068 B	1.4670	1.4677	-7	Fe 2853.685 B	1.4962	1.4976	-14
W 3864.334	1.4680	1.4686	-6	Fe 2806.985 B	1.4990	1.5000	-10
Fe 3825.885 III	1.4688	1.4693	-5	W 2789.076	1.5001	1.5009	-8
W 3772.430	1.4699	1.4701	-2	W 2745.111	1.5028	1.5033	-5
W 3736.220	1.4703	1.4708	-5	W 2702.537	1.5055	1.5058	-3
Fe 3651.512 B	1.4720	1.4725	-5	Fe 2661.200 B	1.5080	1.5084	-4
Fe 3602.515 B	1.4734	1.4735	-1	Fe 2635.818 B	1.5099	1.5101	-2
Fe 3571.998 B	1.4742	1.4741	+1	W 2596.460	1.5126	1.5128	-2
Fe 3495.290 III	1.4761	1.4757	+4	Fe 2545.979 B	1.5161	1.5166	-5
Fe 3447.282 III	1.4772	1.4770	+2	W 2510.184	1.5189	1.5195	-6
Fe 3422.665 B	1.4783	1.4776	+7	Fe 2487.069 B	1.5213	1.5214	-1
W 3375.120	1.4795	1.4788	+7	Fe 2442.574 B	1.5249	1.5253	-4
Fe 3305.980 B	1.4814	1.4807	+7	Fe 2366.59 K	1.5324	1.5328	-4

* The wave-lengths of the iron lines are either secondary (II) or tertiary (III) standards selected by Fabry ('International Critical Tables,' vol. 5, pp. 275-276 (1929)), or those recorded by Burns ('Z. wiss. Photogr.,' vol. 12, p. 207 (1913)). The wave-lengths of the tungsten lines are those given by Belke ('Z. wiss. Photogr.,' vol. 17, p. 132 (1917) and vol. 17, p. 144 (1918))

Table IV—Refractive Indices of Ethyl Hexahydrobenzoate at 20°. Photographic Readings

λ^*	Refractive index		Diff. (O - C) $\times 10^4$	λ	Refractive index		Diff. (O - C) $\times 10^4$
	observed	calculated			observed	calculated	
W 4563.602	1.4543	1.4543	\pm	Fe 3413.048 B	1.4719	1.4722	-3
Fe 4482.262 B	1.4549	1.4551	-2	Fe 3312.707 B	1.4747	1.4748	-1
W 4436.912	1.4555	1.4555	\pm	Fe 3280.268 B	1.4757	1.4757	\pm
W 4316.821	1.4565	1.4568	-3	Fe 3249.204 B	1.4765	1.4766	-1
Fe 4248.224 B	1.4577	1.4576	+1	Fe 3217.389 B	1.4776	1.4776	\pm
W 4204.415	1.4580	1.4582	-2	Fe 3188.586 B	1.4786	1.4785	+1
Fe 4140.441 B	1.4592	1.4590	+2	Fe 3157.877 B	1.4795	1.4794	+1
Fe 4098.183 III	1.4596	1.4595	+1	W 3130.164	1.4805	1.4804	+1
Fe 3995.989 B	1.4607	1.4610	-3	Fe 3099.968 B	1.4818	1.4814	+4
Fe 3940.044 B	1.4616	1.4618	-2	Fe 3074.157 B	1.4825	1.4817	+8
W 3847.501	1.4630	1.4633	-3	Fe 3021.076 B	1.4849	1.4844	+5
Fe 3808.732 III	1.4636	1.4640	-4	Fe 2991.648 B	1.4861	1.4855	+6
Fe 3760.054 III	1.4646	1.4648	-2	Fe 2988.473 B	1.4862	1.4856	+6
Fe 3677.309 B	1.4665	1.4664	+1	Fe 2941.347 II	1.4887	1.4876	+11
Fe 3640.392 II	1.4672	1.4671	+1	W 2799.929	1.4975	1.4941	+34
W 3597.271	1.4679	1.4680	-1	Fe 2757.316 B	1.5005	1.4963	+42
Fe 3560.705 B	1.4684	1.4687	-3	Fe 2716.226 B	1.5030	1.4986	+44
Fe 3521.265 III	1.4695	1.4696	-1	Fe 2635.818 B	1.5087	1.5034	+53
W 3485.507	1.4701	1.4704	-3	Fe 2599.577 B	1.5116	1.5057	+59
W 3448.842	1.4713	1.4714	-1	Fe 2527.44 B	1.5178	1.5108	+70

* See footnote on p. 305.

being derived from Eisenlohr's atomic refractivities. The molecular refractivities for the present samples are 29.33 and 27.93 respectively.

(b) In the ultra-violet, the only previous measurements were made by Voellmy,[†] who gives indices for a number of apparently interpolated wave-lengths. (i) Voellmy's materials were probably impure, since he records $M_D = 29.16$ for *cyclohexanol* (his observations being made at 22.3° when both the present sample and that used by Auwers were still solid), and $M_D = 28.07$ for *cyclohexanone*. Both his dispersion curves diverge from the present readings in the same way as was observed with benzene.[‡]

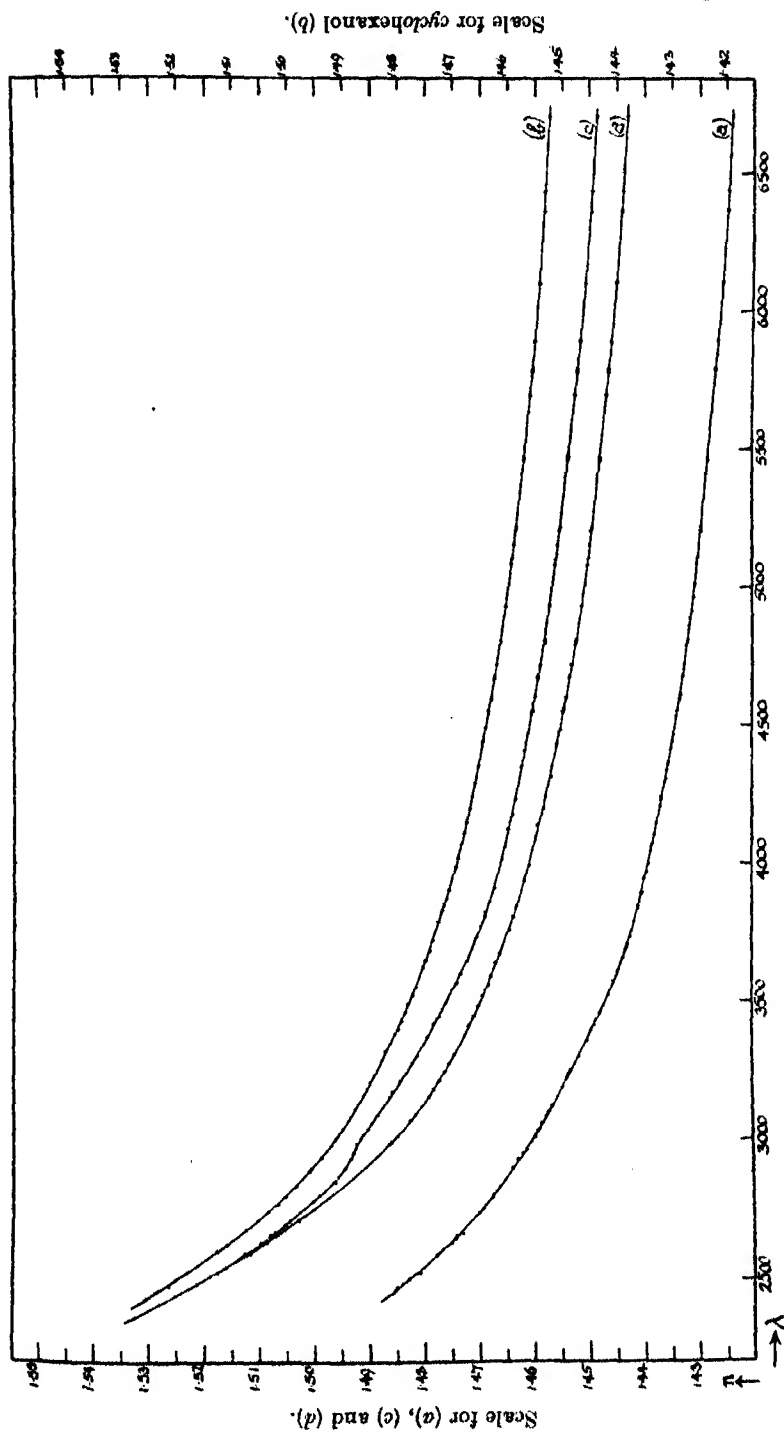
(ii) Voellmy's dispersion curve for *cyclohexanone* shows no anomaly inside the absorption band, since, in a range of 200 Å on either side of the maximum of absorption, he gives data for only two wave-lengths, as compared with seven values in the present series.

(c) No data for the dispersion of ethyl hexahydrobenzoate have been recorded previously. The molecular refraction for the present specimen is $M_D = 43.34$, as compared with 43.10 calculated on the basis of Eisenlohr's atomic equivalents.

Form of the Dispersion Curves—The curves of refractive dispersion of *cyclohexanol* (b), *cyclohexanone* (c), and ethyl hexahydrobenzoate (d), together with that for *cyclohexane* (a), are reproduced in fig. 2.

[†] 'Z. phys. Chem.', vol. 127, p. 305 (1927).

[‡] Lowry and Allsopp, 'Proc. Roy. Soc., A, vol. 133, p. 48 (1931).



(a) The curve for *cyclohexanone* is of special interest since, by using a film of liquid only about 6 μ in thickness, it was possible to record the tiny "ripple" produced by "anomalous dispersion" inside the absorption band. This "ripple" is of very small amplitude; it is therefore not surprising that the refractive indices in the visible spectrum can be represented with fair accuracy by an equation containing only one variable term, namely,

$$n^2 = 1.36014 + \frac{0.713294 \lambda^2}{\lambda^2 - 0.0156233} \quad (1)$$

The characteristic frequency in this equation corresponds to a wave-length of 1250 Å, and does not differ very widely from the corresponding wave-length (1096 Å) in the equation for *cyclohexane*.

The difference curve *a* of fig. 3 shows that the anomaly is of the unsymmetrical type required by the Ketteler-Helmholtz theory, but attempts to represent the "partial refraction" by an expression of the Ketteler-Helmholtz type with a single characteristic frequency were unsuccessful and a complete analysis of the curve has been postponed until more data (particularly for optically active methyl*cyclohexanone*) are available.

(b) *Cyclohexanol*—The refractive dispersion of *cyclohexanol* can be represented over almost the whole range of the observations from 6708 to 2431 Å by the simple equation

$$n^2 = 1.18394 + \frac{0.899514 \lambda^2}{\lambda^2 - 0.0122660} \quad (ii)$$

The variable term in this equation represents the contribution from a natural period at 1109 Å. This is almost identical with that recorded for *cyclohexene* and 1:3-*cyclohexadiene* at 1106 Å, and can again be associated with the saturated methylene groups of the six-membered ring. The values calculated by means of equation (ii), set out in Tables I and II, diverge to a small extent from the observed values below 2900 Å, as can be seen in the difference curve *b* of fig. 3. This divergence may be attributed to the influence of an absorption band in the Schumann region, but attempts to represent it as a partial refraction of the normal type were unsuccessful.

(c) Above 3100 Å the curve of refractive dispersion for ethyl hexahydrobenzoate in fig. 2 can be represented accurately, like that for *cyclohexanol*, by means of a simple equation, namely,

$$n^2 = 1.16800 + \frac{0.887754 \lambda^2}{\lambda^2 - 0.0130026} \quad (iii)$$

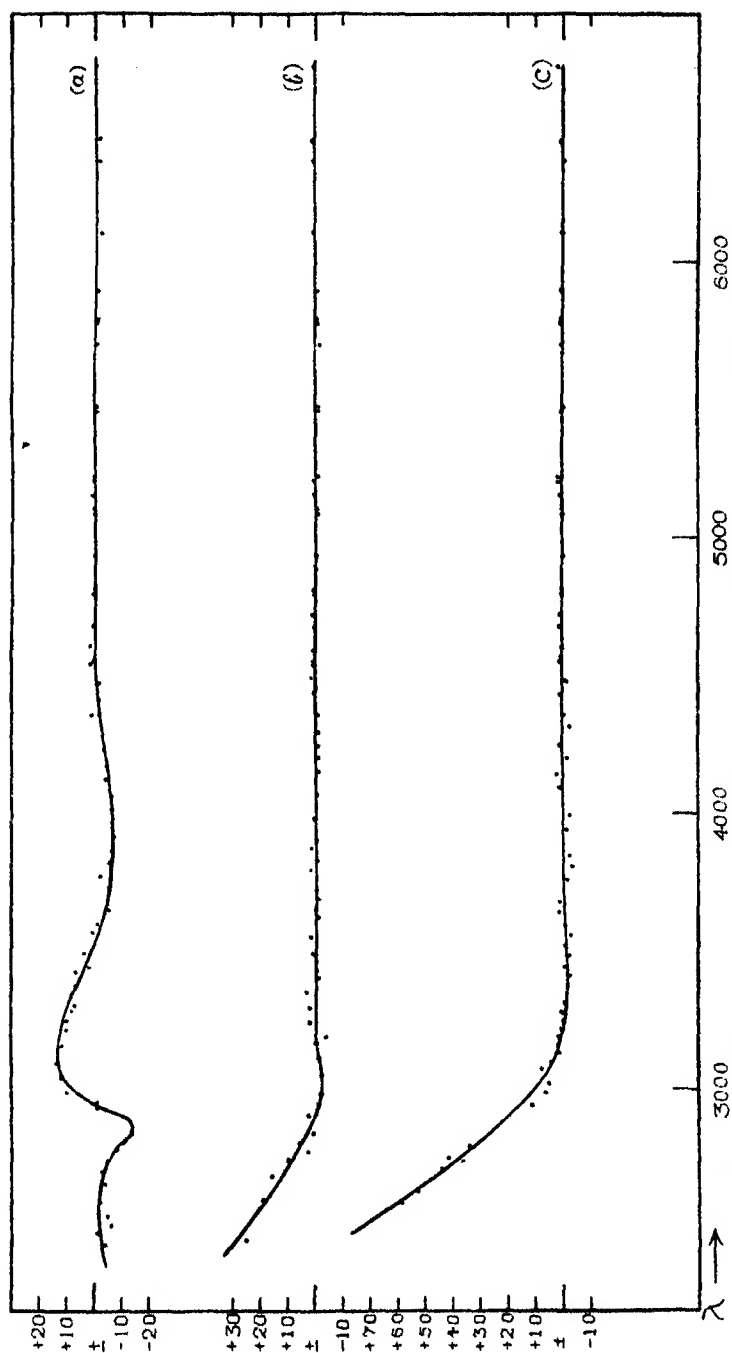


Fig. 3.—Difference Curves for (a) cyclohexanone, (b) cyclohexanol, (c) ethyl hexahydrobenzoate.

in which the characteristic frequency now falls at 1140 Å. Below 3100 Å the observed values diverge from the calculated values much more than those for *cyclohexanol*, as can be seen from the difference curve *c*, fig. 3. This divergence can again be attributed to the influence of an absorption band at about 2075 Å, but it has not been found possible to calculate a partial refraction, from any absorption frequency, which is adequate to correct this divergence.

Inadequacy of the Ketteler-Helmholtz Equation

In the preceding papers of this series, and for the compounds now investigated the curves of refractive dispersion have been expressed either (i) by means of a simplified Ketteler-Helmholtz equation (no damping factor), which gives a hyperbolic curve with an asymptote at the characteristic frequency, as for *cyclohexane*,* or (ii) by the complete Ketteler-Helmholtz equation, in which the "anomalous" refractive indices in the range of wave-lengths covered by the absorption band are represented by means of a damping factor, as for benzene, nicotine,† and *cyclohexene*. The difference curves show, however, that, even when using the complete equation, the agreement between observed and calculated values in the region of absorption is never entirely satisfactory; and for the three compounds described in the present paper and for *cyclohexadiene* in Part IV no agreement whatever could be obtained by means of such equations. This discrepancy can be attributed to the fact that equations of the Ketteler-Helmholtz type, which were designed to express the influence of forced vibrations in increasing the width of a spectrum line, are invalid when applied to an absorption band which may be spread over a width of 1000 Å.

A similar breakdown was observed in 1926 by Bruhat and Panthenier, when studying the anomaly in the curve of refractive dispersion of carbon bisulphide in the region of its absorption band at 3250 Å. Since a single term of the Ketteler-Helmholtz type was inadequate to express the form of the absorption band,‡ they made use of a series of *five* terms, with characteristic frequencies uniformly spaced over the band, and thus obtained a fairly close agreement between the observed and calculated refractive indices.§ It may be added that, in the region of complete transparency, the Ketteler-Helmholtz

* Lowry and Allsopp, 'Proc. Roy. Soc.,' A, vol. 133, p. 36 (1931).

† Lowry and Allsopp, 'J. Chem. Soc.,' p. 1613 (1932).

‡ Cf. Henri, 'Photochimie,' p. 28 (1919).

§ Bruhat and Panthenier, 'Ann. Physik,' vol. 6, p. 440 (1926).

formula is identical in form, though not in the significance of its parameters, with that deduced from the quantum theory,* but the form of the curve in the region of absorption has not yet been deduced in this way.

The inadequacy of the "damping" theory is shown in a most striking way when the theoretical form of the *absorption curves* is compared with those obtained experimentally, and also when these results are applied to the theory of *rotatory dispersion* in the region of absorption. These discrepancies between theory and experiment have led to the introduction of empirical equations of an exponential type for the form of the absorption curves, by Bielecki and Henri, by Kuhn and Brown, and finally by Lowry and Hudson. Corresponding expressions have also been developed for rotatory dispersion.† It is now obvious that similar equations must be devised to represent the form of the curves of refractive dispersion in the region of absorption. This problem can, however, be tackled effectively only when the compounds under investigation are optically active, since only then is it possible to make a complete analysis of the optical constants of the molecule. In the present communication, therefore, the refractive indices in the region of absorption have been recorded, and the contributions of the nearer bands have been plotted, but without attempting at this stage to make a complete mathematical analysis of the curves.

The author desires to place on record his indebtedness to the Department of Scientific and Industrial Research for providing a Research Assistantship during the period in which the investigation described in the present paper was carried out, and to Professor T. M. Lowry, F.R.S., for his continued help and encouragement.

Summary

Values are given for the refractive indices of *cyclohexanol* at 25° C and of *cyclohexanone* and *ethyl hexahydrobenzoate* at 20° C at a series of wavelengths between 6708 Å and 2366 Å.

Molecular extinction coefficients for *cyclohexanol*, *cyclohexanone*, *isobutyric acid*, and *ethyl isobutyrate* in solution in *cyclohexane* are also recorded.

The curve of refractive dispersion for *cyclohexanone* contains only a shallow "ripple" in the region covered by the ketonic absorption band ($\log \epsilon_{\max} = 1.10$

* Kramers, 'Nature,' vol. 113, p. 451 (1924), etc.

† See Lowry and Hudson, 'Phil. Trans.,' A, vol. 232, p. 117 (1933), and Lowry, Hudson, and Wolfrom, 'J. Chem. Soc.,' p. 1179 (1933).

at 2880 Å). The influence of this band on the refractive dispersion is thus remarkably small when compared with the influence on optical rotatory power exerted by the corresponding band in optically active compounds.

At wave-lengths remote from an absorption band, the refractive dispersions can each be represented by an equation containing one variable term of the Ketteler-Helmholtz type, with a characteristic frequency corresponding to that of the saturated 6-membered ring of *cyclohexane*.

At wave-lengths covered by or near to the absorption bands, the Ketteler-Helmholtz equation is no longer adequate. The contribution of the ketonic band to the refractive indices of *cyclohexanone* cannot be represented even approximately by a single term, and evidence is adduced to show that, in the region of absorption, the simple theory of damping breaks down for the refractive dispersion of a liquid just as it has already been shown to do for rotatory dispersion.

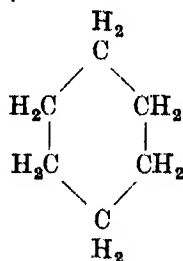
Refractive Dispersion of Organic Compounds Part VI—Refractivities of the Oxygen, Carbonyl, and Carboxyl Radicals. Origin of Optical Rotatory Power and of the Anomalous Rotatory Dispersion of Aldehydes and Ketones

By T. M. LOWRY, F.R.S., and C. B. ALLSOPP, M.A., Ph.D.

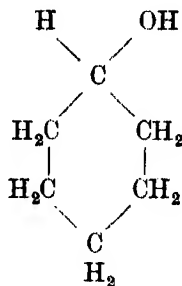
(Received March 29, 1934)

The refractive indices recorded in the preceding paper were determined in order to prepare the way for an attack, which is still in progress, on the problem of optical exaltation in compounds containing conjugated double bonds. They have, however, an immediate value in that, when combined with the refractive indices of *cyclohexane*,* they can be used to determine the refractivities over a wide range of wave-lengths of the three radicals

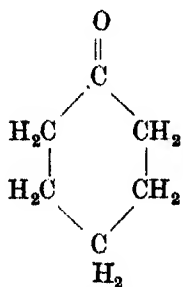
>O , >C=O , and $\text{---C}\begin{smallmatrix} \text{O} \\ \text{O} \end{smallmatrix}$. The formulæ of the compounds in question are set out below :—



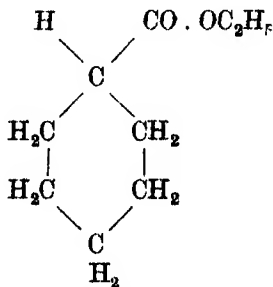
cycloHexane



cycloHexanol



cycloHexanone



Ethyl hexahydrobenzoate

* Lowry and Allsopp, 'Proc. Roy. Soc.,' A, vol. 133, p. 26 (1931).

Refractivities of O, CO, and CO₂

(i) In order to deduce the refractivity of the *oxygen* radical it is only necessary to subtract the refractivity of *cyclohexane* from that of *cyclohexanol*, since these two compounds differ only by a single oxygen atom.

$$R [C_6H_{11}OH] - R [C_6H_{12}] = R [O].$$

(ii) In order to deduce the refractivity of the *carbonyl* radical, we divide the refractivity of *cyclohexane* by *six*, in order to obtain the value for the methylene radical, $>CH_2$; then, since *cyclohexanone* contains *five* methylene radicals, it is only necessary to subtract from the refractivity of this ketone the value for $5CH_2$ in order to give the refractivity of $>C=O$.

$$R [C_6H_{10}O] - \frac{5}{6}R [C_6H_{12}] = R [CO].$$

(iii) In order to deduce the refractivity of the *carboxyl* radical, we note that we can pass from *cyclohexane* to *ethylcyclohexane* by interpolating two additional methylene groups between hydrogen and carbon, and from *ethylcyclohexane* to *ethyl hexahydrobenzoate* by interpolating the CO_2 radical between the ethyl-radical and the ring. On the assumption that the refractivities of carbon and hydrogen remain additive, we can then deduce a value for the carbonyl radical by subtracting from the refractivity of the ester the value for *eight* methylenes

$$R [C_8H_{11} \cdot CO \cdot OC_2H_5] - \frac{4}{3}R [C_6H_{12}] = R [CO_2].$$

The values thus deduced for 18 lines in the visible spectrum and for 39 interpolated wave-lengths in the photographic region are set out in Table I and are plotted in fig. 1.

The inset shows, on a larger scale, the anomaly in the refractivity of the carbonyl group in the region of absorption; the broken line shows the molecular extinction coefficients of the absorption band.

Anomalous Refractivity of the Carbonyl-radical

A principal point of interest arises from the fact that the refractive indices of *cyclohexanone* were measured right through the absorption band, where anomalous refractive dispersion might be expected to occur. Similar, but less exact, measurements have already been made by Voellmy,* but the anomaly produced by the carbonyl-group is so insignificant that no indications of it

* 'Z. phys. Chem.,' vol. 127, p. 324 (1927).

can be seen in his curves for acetone and for cyclohexanone, although a slight displacement can be detected in his curves for methyl ethyl ketone and for methylcyclohexanone.

The data recorded in the preceding paper show that this anomaly has a real existence, but that it produces a fluctuation of only ± 0.0013 on a refractive index of about 1.49. Its course can therefore only be traced when measurements in the region of absorption can be made to *four* places of decimals, as in the fully developed form of the interferometer method. The refractive index of the ketone is mainly composed, however, of the refractivities of the five methylene radicals with which the carbonyl-group is associated, and it is important to be able to dissect out the refractivity of this group in order to secure a clear picture of the magnitude of the anomaly. The results of this analysis in the region of the anomaly are set out in Table II and are shown on a large scale as an inset to fig. 1.

The anomaly still amounts to only about $\pm 1\%$ of the total refractivity of the carbonyl-group, but its real existence appears again to be beyond dispute.

Refractivity of the Oxygen-radical

The data for this radical are of a more unexpected character, since they present several features which could not have been foreseen. Thus the refractivity of the oxygen atom remains constant over the range of wave-lengths from 6708 to 5200 Å; it then increases to a shallow maximum at about 3600 Å and decreases to a shallow minimum at 3100 Å; finally it increases much more rapidly up to the limit of the observations at 2400 Å.

These phenomena show a superficial resemblance to the anomalies in the curve for the carbonyl-radical, but they differ fundamentally from them in that they all occur in a region of complete transparency. Their occurrence in such a region has an important bearing on the whole theory of atomic refractivities, since it suggests that the additive relationships, on which the calculation and use of these quantities is based, may only be valid over a limited range of wave-lengths. This range of wave-lengths appears to correspond approximately with that of our visual observations, which extend to the mercury line Hg 4358. Within this range, our experience shows that the refractive indices of unconjugated compounds can be expressed by equations which include only one variable term, with a characteristic frequency in the Schumann region. In particular, the influence on the dispersion curve of cyclohexanone of the ultra-violet absorption band at 2880 Å appears to have

Table I—Refractivities of the Carbonyl, Oxygen, and Carboxyl Radicals

λ	Refractivities				Difference
	$>C=O$	$-O-$	$>C=O$ + $-O-$	$\sim C \begin{smallmatrix} O \\ \diagup \diagdown \\ O \end{smallmatrix}$	
Li 6708	4.816	1.621	6.437	6.349	-0.088
Cd 6438	4.832	1.638	6.470	6.373	-0.097
Zn 6362	4.839	1.643	6.482	6.372	-0.110
Li 6104	4.841	1.637	6.478	6.386	-0.092
Na 5896	4.841	1.625	6.466	6.392	-0.074
Hg 5791	4.854	1.629	6.483	6.402	-0.081
Cu 5700	4.858	1.622	6.480	6.406	-0.074
Hg 5461	4.869	1.620	6.489	6.418	-0.071
Cu 5220	4.892	1.629	6.521	6.455	-0.066
Cu 5153	4.896	1.637	6.533	6.454	-0.079
Cu 5086	4.898	1.629	6.527	6.452	-0.075
Ba 4934	4.904	1.631	6.535	6.475	-0.060
Cd 4800	4.929	1.650	6.579	6.504	-0.075
Zn 4722	4.935	1.651	6.586	6.517	-0.069
Cd 4678	4.944	1.656	6.600	6.534	-0.066
Li 4603	4.949	1.654	6.603	6.535	-0.068
Ba 4554	4.960	1.667	6.627	6.561	-0.066
Hg 4358	4.977	1.668	6.645	6.590	-0.055
<hr/>					
4300	4.98	1.67	6.65	6.60	-0.05
4250	4.98	1.67	6.65	6.61	-0.04
4200	4.98	1.68	6.66	6.62	-0.04
4150	4.99	1.68	6.67	6.64	-0.03
4100	5.00	1.69	6.69	6.66	-0.03
4050	5.00	1.70	6.70	6.67	-0.03
4000	5.01	1.70	6.71	6.69	-0.02
3950	5.02	1.71	6.73	6.70	-0.03
3900	5.04	1.72	6.76	6.72	-0.04
3850	5.06	1.72	6.78	6.74	-0.04
3800	5.07	1.72	6.79	6.76	-0.03
3750	5.09	1.73	6.82	6.78	-0.04
3700	5.11	1.73	6.84	6.80	-0.04
3650	5.12	1.74	6.86	6.81	-0.05
3600	5.14	1.74	6.88	6.83	-0.05
3550	5.16	1.74	6.90	6.84	-0.06
3500	5.18	1.74	6.92	6.86	-0.06
3450	5.20	1.74	6.94	6.87	-0.07
3400	5.22	1.73	6.95	6.89	-0.06
3350	5.24	1.73	6.97	6.90	-0.07
3300	5.26	1.73	6.99	6.92	-0.07
3250	5.28	1.72	7.00	6.95	-0.05
3200	5.30	1.72	7.02	6.97	-0.05
3150	5.32	1.72	7.04	7.00	-0.04
3100	5.35	1.71	7.06	7.04	-0.02
3050	5.37	1.72	7.09	7.09	±
3000	5.39	1.73	7.12	7.15	+0.03
2950	5.38	1.74	7.12	7.24	+0.12
2900	5.36	1.76	7.12	7.34	+0.22
2850	5.37	1.79	7.16	7.47	+0.31
2800	5.45	1.83	7.28	7.59	+0.31
2750	5.53	1.87	7.40	7.70	+0.30
2700	5.59	1.91	7.50	7.82	+0.32
2650	5.64	1.95	7.59	7.94	+0.35
2600	5.69	1.98	7.67	8.06	+0.39
2550	5.73	2.01	7.74	8.17	+0.43
2500	5.78	2.03	7.81	8.28	+0.47
2450	5.85	2.06	7.91	—	—
2400	5.93	2.08	8.01	—	—

Table II—Refractivity of the $>\text{C}=\text{O}$ Radical in the Region of Absorption

λ	R_{CO}	λ	R_{CO}	λ	R_{CO}	λ	R_{CO}
3375	5.231	3160	5.325	2951	5.358	2718	5.562
3305	5.250	3126	5.324	2936	5.371	2703	5.587
3285	5.260	3100	5.362	2904	5.363	2676	5.608
3250	5.282	3068	5.359	2854	5.371	2661	5.626
3220	5.290	3045	5.376	2807	5.434	2636	5.653
3187	5.296	3003	5.384	2789	6.461	2596	5.692
3178	5.322	2990	5.397	2745	5.528		

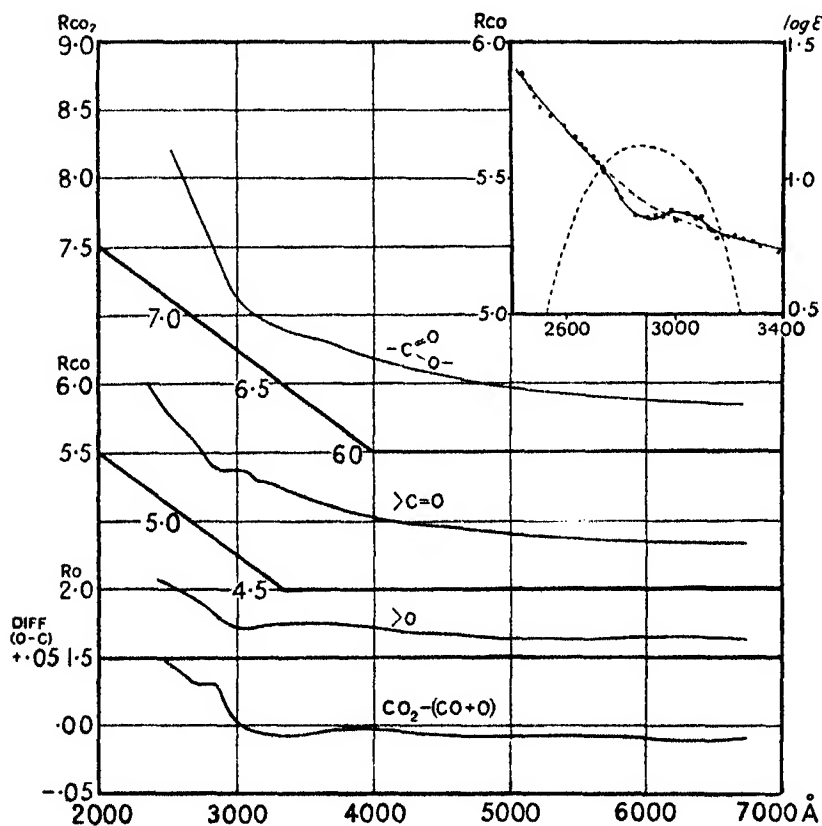


FIG. 1—Refractivities of the Oxygen, Carbonyl, and Carboxyl Radicals

died out completely before the visual region is reached. Within this limit therefore calculations of refractivity may have a validity that they do not appear to possess in the ultra-violet region. The device of extrapolating refractivities to infinite wave-length as used by Bruhl* (1880), Landolt† (1882),

* 'Liebig's Ann.,' vol. 200, p. 139 (1880).

† 'Liebig's Ann.,' vol. 213, p. 75 (1882).

and Eykman* (1893), has much to commend it, since the probability that additive relationships will hold good may be expected to increase progressively as the region of absorption in the ultra-violet becomes more remote.

The occurrence of a shallow maximum and minimum in the experimental data for the refractivity of the oxygen-atom obviously depends on a lack of strict parallelism between the curves of refractive dispersion of *cyclohexane* and of *cyclohexanol*. In the visual region, the refractive indices of both compounds can be expressed by equations containing a single variable term with similar characteristic frequencies in the Schumann region at 1106 and 1109 Å respectively; but there are good reasons for believing that the band system of the polymethylenes must already be complex, and would be rendered still more complex by the introduction of an oxygen atom. The refractive indices are therefore dominated not by a single frequency but by a cluster of frequencies, and must be made up of a bundle of partial refractions. Any alteration in the relative intensity (as well as in the characteristic frequency) of these components would cause a displacement of the minor idiosyncrasies of the dispersion curves, and would thus give rise to ripples (such as are now recorded) in the curves for the differences between the refractivities of two related compounds. These are obviously comparable with the ripples in the curves showing the difference between the observed and calculated refractive indices of each individual compound.

In support of this conclusion attention may be directed to the remarkable irregularities which Voellmy obtained by plotting the differences of refractivity for pairs of homologous ketones, when the absorption band is displaced on the scale of wave-lengths by the introduction of the methyl radicals. Thus, when deduced from the refractions of acetone and of methyl ethyl ketone, the refractivity of the methylene-group passed through a conspicuous maximum at about 2700 and minimum at about 2550 Å, in a region in which the methylene group is itself completely transparent. Even more remarkable anomalies were recorded when the refractivity of the methylene radical was deduced from the difference between *cyclohexanone* and its *o*- and *p*-methyl derivatives, since (in addition to a "step-out" or shelf at 3800 Å) the curves exhibited maxima at 2900 and 2500, and minima at 2800 and 2200 Å, which are much more striking than the real anomalies of the $>CO$ group in the region of absorption, since these can be detected only with difficulty on some of his curves and not at all on others.

* 'Rec. trav. chim.,' vol. 12, pp. 157, 266 (1893).

Refractivity of the Carboxyl-radical

The data for the carboxyl-radical are much more normal. The refractivity rises relatively slowly from 6708 to 3100 Å; but at shorter wave-lengths it increases much more rapidly on approaching an absorption-band with a maximum at about 2075 Å.* The slow increase at longer wave-lengths shows that the carboxyl-group (like the carbonyl and methylene groups) possess a characteristic frequency in the Schumann region, which dominates its refractivity at the longer wave-lengths. The sharp rise on approaching the absorption band takes place at the same wave-length as the breakaway of the curve of refractive indices from the calculated curve for an equation with one variable term,† and can be attributed to the appearance of an additional partial refraction associated with this band.

If their refractivities were strictly additive, it should be possible also to deduce the refractivity of the carboxyl-group from those of the oxygen and carbonyl-radicals

$$R[\text{CO}_2] = R[\text{O}] + R[\text{CO}].$$

It is, however, well known that the carboxyl-radical is abnormal both in its chemical and in its physical properties. Thus, it no longer possesses the chemical properties of the carbonyl-group in aldehydes and ketones; and even the parachor, which is usually so strictly additive a function of the component radicals, gives an abnormal value for the esters, in which $O_2 = 60.0$ instead of $2 \times 20.0 + 23.2 = 63.2$. By comparing the refractivities of the carboxyl-group with those now deduced for the constituent oxygen and carbonyl-radicals, we can obtain a measure of the influence on their optical properties of the close contiguity of these two polar and highly-polarizable groups. This influence is expressed by the differences shown in Table I, and by the corresponding curve in fig. 1.

In the visual region from Li 6708 to Hg 4358 where the additive relations appear to be relatively satisfactory, the interaction of the two radicals has a *negative* influence, since the refractivity of the carboxyl-group is less by about 0.08 units than the sum of the refractivities of the oxygen and carbonyl-radicals. The differences then decrease to zero at a wave-length, 3050 Å, within the range of the absorption band. The *positive* differences then increase rapidly up to the maximum of absorption at 2880 Å, when the difference curve flattens out over a range of about 100 Å. The idiosyncrasies between

* Part V.

† *Ibid.*

3050 and 2750 Å are due to the anomalies in the refractivity of the *carbonyl*-group on passing through the absorption band at 2880 Å ; but they are followed by a rapid increase in the positive differences as the absorption band of the *carboxyl*-group at 2075 Å is approached. It is noteworthy that the interaction which produces a *decrease* of refractivity in the visual region, corresponding with the decrease in the parachor, gives rise to an *increase* in a region of shorter wave-lengths, and that the additive rule is momentarily valid at a wave-length of 3050 Å.

Molecular Theory of the Origin of Optical Rotatory Power

In a paper "Calcul du pouvoir rotatoire d'une molécule tétraédrique," de Malleman* deduced for the rotatory power of a tetrahedral model a formula which contains the factors $(n^2 + 2)^2 A_1 A_2 A_3 A_4 / \lambda^2$, where n is the mean refractive index of the medium and $A_1 A_2 A_3 A_4$ are the "reduced refractivities" of four *atoms* at the corners of the tetrahedron. Calculations of the rotatory power of a compound, CHClBrI , which has not yet been prepared, then showed that the rotation thus deduced ($3 \cdot 2^\circ$ per cm) was of the order of magnitude to be expected in such a compound. A similar model, described by S. F. Boys at a meeting of the Royal Society on February 15, 1934,† gave rise to a formula containing the term $(\mu^2 + 2)(\mu^2 + 5) R_A R_B R_C R_D / \lambda^2$, where μ is the mean refractive index of the medium and $R_A R_B R_C R_D$ are the refractivities of four *radicals* at the corners of a tetrahedron. Calculated values for the rotations of some of the simplest optically active molecules were again shown to be of the right order of magnitude, as compared now with the observed rotations of these compounds. There can therefore be little doubt that this tetrahedral model is adequate to account for the existence and approximate magnitude of the "normal" rotatory power of the simplest dissymmetric compounds, in terms of the linear dimensions of the molecule and the refractive indices of the constituent radicals.

Normal Rotatory Dispersion of Carbinols‡

One of the simplest methods of testing the "molecular theory of optical rotatory power"§ is to ascertain how far it can be used to account for the

* 'C. R. Acad. Sci. Paris,' vol. 181, p. 298 (1925).

† 'Proc. Roy. Soc.,' A, vol. 144, p. 655 (1934).

‡ We are indebted to Mr. H. F. Willis for making the calculations recorded under this heading.

§ de Mallemann, 'Ann. Physique,' vol. 2, p. 137 (1924); 'Trans. Faraday Soc.,' vol. 26, p. 281 (1930).

simple rotatory dispersion of dissymmetric molecules which contain only one asymmetric atom and no unsaturated or chromophoric groups. This test has the advantage of eliminating all hypotheses as to the size and shape of the molecule, since these remain fixed when only the wave-length of the incident light is changed. Calculations of rotatory dispersion are therefore independent of the postulate that the four dissymmetric radicals can be treated as spheres, which may be plausible for atoms such as F, Cl, Br, I, and radicals such as OH, NH₂, and CH₃ (which have a similar electronic structure to the halogens), but is obviously unsound for radicals such as —CH₂ · CH₃ and —CH₂ · OH. Thus, without assuming any knowledge of the linear dimensions of the molecule, or of the nature of the function through which they influence its optical rotatory power, we can calculate from the refractivities of the radicals the values of the product $(n^2 + 2)^2 A_1 A_2 A_3 A_4 / \lambda^2$ or $(\mu^2 + 2)(\mu^2 + 5) R_A R_B R_C R_D / \lambda^2$ for the green and blue mercury lines, and compare the ratio of these two products with known values of the optical rotatory dispersion-ratio $\alpha_{4858} / \alpha_{5461}$.

For the purpose of this test, it is convenient to use the data for the two simple alcohols :

		$\frac{\alpha_{4858}}{\alpha_{5461}}$
<i>sec</i> -Butyl alcohol	$\begin{array}{c} \text{C}_2\text{H}_5 \\ \diagdown \\ \text{CH} \cdot \text{OH} \\ \diagup \\ \text{CH}_3 \end{array}$	1·661
<i>act</i> -Amyl alcohol	$\begin{array}{c} \text{C}_2\text{H}_5 \\ \diagdown \\ \text{CH} \cdot \text{CH}_2 \cdot \text{OH} \\ \diagup \\ \text{CH}_3 \end{array}$	1·700

The dispersion-ratio of *sec*-butyl alcohol differs but little from the average value for several series of secondary alcohols which were examined in 1915 by Lowry, Pickard, and Kenyon,* *e.g.*, 1·652 for the other methyl carbinols, 1·660 for the ethyl carbinols, and 1·663 for the *iso*-propyl carbinols, the lowest member of each homologous series being excluded. *act*-Amyl alcohol, on the other hand, gives a dispersion ratio which is abnormally high, but agrees closely with those of

		$\frac{\alpha_{4858}}{\alpha_{5461}}$
Methyl <i>iso</i> -propyl carbinol	$\begin{array}{c} \text{CH}_3 \\ \diagdown \\ \text{CH} \cdot \text{CHOH} \cdot \text{CH}_3 \\ \diagup \\ \text{CH}_3 \end{array}$	1·697

* 'J. Chem. Soc.,' vol. 105, p. 94 (1915).

		α_{4358}
		α_{5461}
Methyl <i>ter</i> -butyl carbinol	$\begin{array}{c} \text{CH}_3 \diagdown \\ \text{CH}_3 - \text{C} \cdot \text{CHOH} \cdot \text{CH}_3 \\ \text{CH}_3 \diagup \end{array}$	1.707
<i>iso</i> Valeric acid	$\begin{array}{c} \text{C}_2\text{H}_5 \diagdown \\ \text{CH} \cdot \text{CO} \cdot \text{OH} \\ \text{CH}_3 \diagup \end{array}$	1.710

The atomic refractivities of carbon, hydrogen, and oxygen for the two mercury lines are not included in the usual tables, but the values given in Table III have been deduced from the refractivities tabulated by Eisenlohr* for the sodium and hydrogen lines, using for each the formula of Lorentz and Lorenz in which the refractivity is expressed by the function

$$R_L = \frac{n^2 - 1}{n^2 + 2} \frac{M}{d}$$

Table III.

	[H]	[O]	[C]	[OH]	[CH ₃]	[C ₂ H ₅]	[CH ₂ · OH]
Hg 4358	1.122	1.540	2.465	2.662	5.831	10.376	7.371
Hg 5461	1.106	1.527	2.423	2.633	5.741	10.540	7.268
Ratio	1.015	1.009	1.018	1.011	1.016	1.016	1.014

The principal factor in determining the dispersion-ratio is the term $1/\lambda^2$, which for the two wave-lengths in question gives rise to a ratio 1.570. For the carbinols, this ratio has to be increased by 4 to 8% with the help of four refractivities, which provide multipliers ranging from 1.011 for the hydroxyl radical to 1.016 for the alkyl radicals, together with a factor $(n^2 + 2)^2$ or $(\mu^2 + 2)(\mu^2 + 5)$, which provides a further increment of about 0.8 %. As de Malleman† has pointed out, this is sufficient to bring the calculated ratio within the range of the observed values of the rotatory-dispersion ratio in compounds of this class.

The results of this comparison for the product $R_A R_B R_C R_D / \lambda^2$ are :—

Dispersion-ratio		
	(observed)	(calculated)
<i>sec</i> -Butyl alcohol	1.661	1.661 or 1.664
<i>act</i> -Amyl alcohol	1.700	1.666 or 1.668

* "Spektrochemie Organischer Verbindungen," Stuttgart, 1912, p. 48.

† 'Trans. Faraday Soc.,' vol. 26, p. 292 (1930).

In deducing the first pair of values for the refractivity ratio, the central atom of carbon was ignored; in deducing the second pair of values, the shared electrons of the carbon atom were assigned to the octets of the four surrounding radicals, after the manner of Kossel, as used by Boys.

The lower value, 1.661 for *sec*-butyl alcohol is correct to the third decimal, whilst the higher value, 1.664 is perhaps within the limits of experimental error; but the further increase to 1.677, produced by the factor $(\mu^2 + 2)$ $(\mu^2 + 5)$, would make the product definitely incorrect. On the other hand, the dispersion-ratio of *act*-amyl alcohol, 1.700, is too high to be expressed by this formula, since the maximum value given by the product $R_A R_B R_C R_D^2$ for any saturated compound of carbon, hydrogen and oxygen is $1.57 \times (1.016)^4 = 1.673$, and the factor $(\mu^2 + 2)$ $(\mu^2 + 5)$ only increases this to 1.686. Whilst, therefore the formula deduced by Boys can be used to account for the rotatory-dispersion of the simpler secondary alcohols, the experimental values for the primary alcohols, and for the secondary alcohols with branched chains, are outside the range of the formula.

Anomalous Rotatory Dispersion of Aldehydes and Ketones

The anomalies in the rotatory dispersion of optically active ketones and aldehydes in the region of absorption are of a very striking character, especially when contrasted with the minute ripples produced by the ketonic absorption band in the curves which represent the refractivity of the carbonyl-group. Thus the vapour of camphor shows maxima of specific rotation $[\alpha]^{180^\circ} = +2000^\circ$ and -1860° on either side of a zero value at 3020\AA^* as compared with $[\alpha]_D = 55^\circ$ for the yellow sodium line. In the still more remarkable tetra-acetyl- μ -arabinose, $\text{H}[\text{CH} \cdot \text{OAc}]_4 \cdot \text{CHO}$, where the partial rotations of the three fixed asymmetric centres appear to cancel out completely, a solution in chloroform gave equal and opposite maxima, $[\alpha]^{20^\circ} = \pm 1200^\circ$, on either side of a zero value at 2909\AA , as compared with $[\alpha]_D = -61.8^\circ$ and $[\alpha]_{5461} = -76.5^\circ$.† It is indeed remarkable that an absorption band which dominates the optical rotatory power of aldehydes and ketones throughout the visible and ultra-violet spectra, and which also gives rise to profound photochemical decomposition when light of similar frequency is absorbed,‡ should be so weak as to influence the refractivity of the radical by only $\pm 1\%$. Alternatively,

* Lowry and Gore, 'Proc. Roy. Soc.,' A, vol. 135, p. 13 (1932).

† Hudson, Wolfrom, and Lowry, 'J. Chem. Soc.,' p. 1179 (1933).

‡ Norrish, 'Trans. Faraday Soc.,' vol. 27, p. 404 (1931) *et seq.*

if we attribute to the band in the Schumann region an intensity $\log \epsilon = 5$, it would appear that only one molecule in perhaps 10,000 is able to absorb a quantum from incident light of wave-length 2880 Å at the maximum of the ultra-violet band.

Origin of Anomalous Rotatory Dispersion of Aldehydes and Ketones

de Malleman* suggested that "the observed influence of heavy atoms and of specially mobile electrons (double bonds)" could be expressed by means of the product of the reduced refractivities; but in a private communication he restricts his theory specifically to "regions of spectral transparency." On the other hand, in the verbal presentation of his paper to the Royal Society, Boys claimed that the anomalous rotatory dispersion of a ketone such as camphor could be attributed to anomalies in the refractive dispersion of the radical containing the carbonyl-group, and that the theory of "induced dissymmetry," put forward by Lowry and Walker in 1924,† was therefore unnecessary.

The data now recorded show that this claim is entirely unjustified. Thus, on the basis of the formulæ referred to above, *the rotation can only pass through a zero value if the refractivity of the unsaturated radical also becomes zero.* The anomaly in the refractivity of the carbonyl-group on passing through the ultra-violet absorption band is, however, so minute that the refractivity curves of fig. 1 show no tendency to cut the zero axis in the region of absorption, and it is obvious that the absorption is much too feeble to reproduce the phenomena recorded by R. W. Wood in sodium-vapour.‡ It is therefore impossible to account for the observed anomalies in the rotatory dispersion of aldehydes and ketones by means of this factor, since in the aldehydes the refractivities recorded above would be increased by that of a hydrogen atom, and in an optically active ketone by the refractivity of an alkyl radical, and would thus be removed still further from the axis of zero refractivity.

It is of interest to enquire under what conditions the anomalous refractivity of a carbonyl-group could give rise to anomalous rotatory dispersion in terms of the "molecular theory" of optical rotatory power, as expressed in the formulæ cited above. For this purpose, the refractivity of the electrons which are associated with the optically active absorption band must obviously be segregated, in such a way that the tiny ripple due to this band lies on an axis

* 'C. R. Acad. Sci. Paris,' vol. 181, p. 298 (1925).

† 'Nature,' vol. 113, p. 565 (1924); Lowry, 'Nature,' vol. 131, p. 566 (1933).

‡ 'Phil. Mag.,' vol. 8, p. 293 (1904); "Physical Optics," pp. 418-427 (1923).

of zero refractivity, instead of on a curve which is remote from this axis. This might be effected by considering the carbon atom of the carbonyl-radical in an optically-active ketone as an additional asymmetric centre. The radicals R_1 and R_2 in the system $R_1 \cdot CO \cdot R_2$ would then contribute two refractivities A_1 and A_2 or R_A and R_B to the product, whilst the shared electrons of the double bond would contribute two refractivities A_3 and A_4 or R_C and R_D . In an optically active compound the two latter refractivities need not be equal to one another, since the double bond is no longer symmetrical, but is polarized unsymmetrically by the internal field of the molecule. Moreover, since these refractivities need not include any extraneous refractions, one or both of them might pass through a zero value in the middle of the absorption band. Under these conditions, therefore, a feeble anomaly in the curve of refractive dispersion might give rise to the gross anomalies shown by the curves of rotatory dispersion. These conditions are, however, identical with those which were postulated by Lowry and Walker, when they suggested that the carbonyl-radical might itself become optically active in the internal field of the molecule and thus give rise to a separate partial rotation, in addition to those which depend directly on the fixed dissymmetry of the asymmetric atoms.

This suggestion was at that time entirely novel. Thus Tschugaeff in 1913* had suggested that in a coloured compound the partial rotations of the asymmetric centres might include terms "determined by the influence of the chromophores," on very similar lines to the concepts used by de Malleman and by Boys; but no suggestion was made that these chromophores might become optically active under the influence of the asymmetric centres. It is now evident, however, that the "molecular theory" of optical rotatory power can only be extended to cover the phenomena of anomalous rotatory dispersion by replacing de Malleman's *atoms*, or Boys' *radicals*, by *electrons*, as regards at least one of the refractivities, and that this can only be done with the help of *an asymmetric centre within the chromophoric group*, in addition to those which are associated with asymmetric carbon atoms.

Summary

1.—From the refractive indices recorded in Part V, values are deduced for the refractivities of the radicals >O , >C=O , and $\text{—C}\begin{smallmatrix} \text{O} \\ \diagup \diagdown \\ \text{O—} \end{smallmatrix}$ over a range of wave-lengths from 6708 to 2400 Å.

* Tschugaeff and Ogorodnikoff, 'Z. phys. Chem.,' vol. 85, pp. 507-508 (1913).

2—The refractivity of the *carbonyl* radical exhibits an anomalous dispersion in the region covered by the absorption band with maximum at 2880 Å, but this anomaly is represented by a ripple with a range of only ± 0.05 , or $\pm 1\%$ of the total refractivity of the radical.

3—The refractivity of the *oxygen*-radical exhibits a slight anomaly, in a region of complete transparency; this is attributed to small differences of refractive dispersion between *cyclohexane* and *cyclohexanol*, although both can be expressed throughout the visual region by an equation with the same characteristic frequency at about 1100 Å.

4—The refractivity of the *carboxyl*-group is of a normal type, but the values increase very rapidly as the absorption band at about 2075 Å is approached. In the visual region the refractivities are about 0.08 or 1.2% *less* than the sum of the refractivities of the constituent oxygen and carbonyl-radicals, but this difference disappears at 3050 Å. At shorter wave-lengths the refractivity of the carboxyl-group becomes *greater* than the sum of the component refractivities, on account of the growing influence of the carboxyl band, but the difference curve also reproduces the anomaly of the $>\text{CO}$ group on passing through the absorption band at 2880 Å.

5—The rotatory dispersion of *sec*-butyl alcohol, $\alpha_{4358}/\alpha_{5461} = 1.661$ can be accounted for by means of the term $R_A R_B R_C R_D / \lambda^2$, where $R_A R_B R_C R_D$ are the refractivities of the four radicals; but the values given by this formula, even when multiplied by the factor $(\mu^2 + 2)(\mu^2 + 5)$, never reach that observed in *act*-amyl alcohol, for which $\alpha_{4358}/\alpha_{5461} = 1.700$.

6—The anomalous rotatory dispersion of aldehydes and ketones in the region of absorption (which includes two maxima of opposite sign on either side of a zero rotation) cannot be attributed to the anomalous refractive dispersion of the carbonyl-group, since this does not pass through a zero value. This phenomenon might, however, be accounted for by postulating the presence of an additional asymmetric centre *within the chromophoric radical*, as in Lowry and Walker's theory of "induced dissymmetry."

The Modes of Activation of Aldehyde Molecules in Decomposition Reactions

By C. N. HINSHELWOOD, F.R.S., C. J. M. FLETCHER, F. H. VERHOEK, and
C. A. WINKLER

(Received April 18, 1934)

In reactions depending on the decomposition of a single substance the general relation between the rate, as represented by the reciprocal of the time of half change, and the initial pressure is given by a curve which at first rises from the origin and then bends round to become parallel to the pressure axis. The point at which the curve becomes horizontal, and the height of the limiting ordinate depend upon specific constants. Thus, if a molecule suffered a number of alternative decompositions, the total rate of change would be represented by a curve which showed a corresponding number of changes of slope in particular regions of pressure, giving it a segmented appearance.

The curves for nitrous oxide* and for acetaldehyde† show such an appearance, and the decompositions appear to be composite. Yet the products of reaction are the same over the whole pressure range.‡ The same chemical reaction thus occurs by mechanisms which differ in some physical way. This can be interpreted by assuming different types of activated molecule which have widely different decomposition probabilities.

The segmented curve can be roughly analysed into a series of curves each rising at first and then reaching a limiting height, as shown in fig. 6 of the paper of Fletcher and Hinshelwood, each curve corresponding to a different type of activated molecule. The slope of the rising, or "second order," part of each of these fundamental curves is proportional to the rate at which activated molecules are produced, and the limiting height to the probability of the decomposition of the particular type of activated molecule. The reaction corresponding to a small probability of decomposition will be observable experimentally only when the time between collisions is relatively long, that

* Muirgrave and Hinshelwood, 'Proc. Roy. Soc.,' A, vol. 135, p. 23 (1932); Hunter, *ibid.*, vol. 144, p. 386 (1934).

† Fletcher and Hinshelwood, *ibid.*, vol. 141, p. 41 (1933).

‡ At 400 mm acetaldehyde gives carbon monoxide and methane quantitatively. The average of four analyses made on the products from acetaldehyde at 15–18 mm gave:— Gas: contraction on combustion: CO₂ formed = 1.00 : 1.22 : 0.98. Theoretical for CH₄ + CO = 1.00 : 1.25 : 1.00.

is at low pressures, and then only if the rate of activation for that particular mode is greater than that of the other modes of activation. If a long time between collisions is required for reaction, a comparatively low pressure will be sufficient to maintain the equilibrium concentration of activated molecules, so that the curve for the reaction with a small decomposition probability bends over more quickly than that for the reaction with the higher probability. This condition is illustrated by the curves 1 and 2 of the figure above referred to. The curve which rises steeply and bends at low pressures thus means a high rate of activation and a small probability of decomposition.

It was suggested that the different activated states in acetaldehyde correspond to a location of the energy in different parts of the molecule. The essential process in the decomposition of an aldehyde is the migration of a hydrogen atom and the breaking of a C—C bond. Energy of activation communicated by collision to any part of the molecule other than one of the two bonds in question will have to be redistributed before decomposition can occur. Hence the widely varying probabilities of chemical reaction according to the location of the energy.

The problem now arises of attempting to correlate particular parts of the curve with the activation of specific degrees of freedom in the molecules of particular compounds. The most direct method is to investigate changes in the form of the curve when the structure of the molecule is varied in a known way. For this purpose a comparison has been made of the behaviour of acetaldehyde with formaldehyde, propionic aldehyde and chloral. The reaction in each substance consists in the removal of carbon monoxide from the molecule. With formaldehyde the residue is hydrogen, with acetaldehyde, methane, with chloral, chloroform which decomposes further, and with propionic aldehyde, a variety of products of which ethane is the principal one.

The actual experimental results are described in the following papers and in a previous paper.* In the present paper the general conclusions are summarized and discussed. A general comparison of the shape of the curves for the four substances is shown in fig. 1. Except for chloral, which decomposes at a very much lower temperature, all the curves represent decomposition at 556° C.†

* 'Proc. Roy. Soc.,' A, vol. 141, p. 41 (1933).

† The temperatures were compared in terms of the same thermocouple (platinum-platinum-rhodium). The restandardization lowers by 4° the temperatures given by Fletcher and Hinshelwood; 560° of their paper should read 556°. The original temperature scale of Hinshelwood and Hutchison corresponds to a value between the old and the corrected value, but very close to the latter ('Proc. Roy. Soc.,' A, vol. 111, p. 380 (1926)).

The most striking contrast revealed by the curves is the relative increase in the magnitude of the lower segments with increase in the degree of substitution of the aldehyde. With formaldehyde, as far as has been determined, the curve consists of a line passing through the origin and showing no changes of slope. This suggests that in formaldehyde there is a single mode of activation, as might be expected from its simple structure. Acetaldehyde shows additional modes of activation, which are still more pronounced with propionic aldehyde and with chloral. From all the evidence, we shall conclude that those corresponding to the lower segments represent the location of the activation

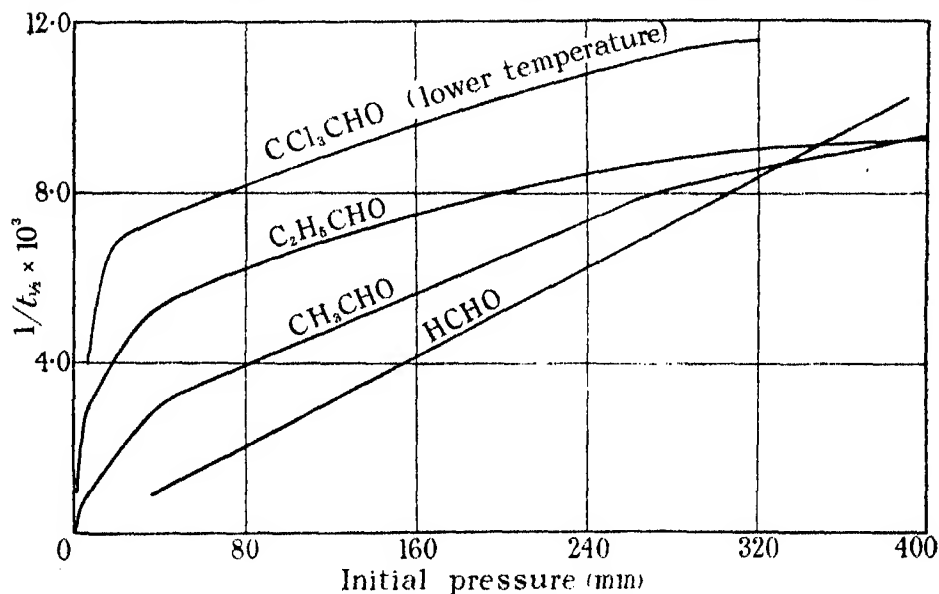


FIG. 1

energy in parts of the molecule remote from the aldehyde group. The residual slope of the lines at high pressures, on the other hand, represents the simplest and most direct mode of activation for the decomposition of an aldehyde.

Although at 556° the rates of reaction at the lower pressures increase from formaldehyde to propionic aldehyde, at higher pressures the curves cross, so that formaldehyde decomposes most readily while with propionic aldehyde the line becomes almost horizontal. The part played by the simple mode of activation thus becomes less in absolute magnitude with increase in length of the hydrocarbon chain. This is in accord with what might be expected, from electronic theories of organic reactions, from the effect of the alkyl group in strengthening the attachment of the aldehyde hydrogen. On the other hand,

the more complex modes of activation, as represented by the lower segments, are much in evidence, and become more so as the molecules are more heavily substituted. This can be understood in terms of our hypothesis, because there are many more ways in which the energy can be given to the molecule, *e.g.*, it can reside in the more remote parts of the alkyl group, and have to find its way to the sensitive part of the molecule before decomposition can occur. As is well known from the general theory of unimolecular reactions, such a state of affairs gives rise to a high rate of reaction, because more degrees of freedom can contribute. For example, even though the energy may reside in the methyl group, the three degrees of freedom of the three C—H bonds give an enormously increased chance that the requisite energy is present, and this more than compensates for the smaller probability that it ultimately finds its way to the right place.

As far as concerns the general thesis that decomposition reactions may be kinetically composite, nothing need be assumed about the energies of activation at different pressures. What has just been said applies specifically to the identification of that mode of activation which happens to predominate at low pressures in the particular example of the aldehydes. This special interpretation is supported by a consideration of the experimental values of the energies of activation. These are given in Table I, which should be considered in conjunction with fig. 1.

Table I

Pressure (mm Hg)....	25	30	100	200	350	450
HCHO	—	—	—	44,000	—	—
CH ₃ CHO	55,000	—	—	50,400	—	47,700
C ₂ H ₅ CHO	—	63,500	61,200	59,500	56,000	—
CCl ₃ CHO	—	—	49,200	49,200	—	—

With formaldehyde the energy of activation corresponds to the simplest mode of activation, the number of molecules reacting being given by $Z \cdot e^{-E/RT}$; in other words, practically every collision between two molecules possessing enough energy to activate one internal degree of freedom (two square terms) can lead to reaction (Fletcher, p. 357). With acetaldehyde the high pressure part of the reaction can be expressed in the same way,* but the energy of activation corresponding to the lower segments of the curve is greater.† To account for the rate of reaction at lower pressures, increasing numbers of degrees of freedom must be brought in.

* Hinshelwood and Hutchison, *loc. cit.*

† Fletcher and Hinshelwood, *loc. cit.*

The same increase in E with decreasing pressure is found with propionic aldehyde, but here the contribution of the "high pressure" part of the reaction is so small that, even at the highest pressures measured, E is still too great to allow the rate to be accounted for by activation in two square terms, p. 356. If the contribution from the "low pressure" mechanisms could be eliminated, it is possible that there might be a residual reaction with a rate given by the simple formula.

With chloral, the decomposition takes place at a comparable rate about 100° lower. This is what might be expected from the loosening of the aldehydic hydrogen by the chlorine atoms. The energy needed in the vital bond must be less, and if the reaction were of the "second order" type, as with formaldehyde, we should expect the E value to be correspondingly small. But, as the curves show, the reaction is predominantly of the type which we are associating with the more complex modes of activation. Accordingly we find, as with acetaldehyde and propionic aldehyde at lower pressures, that the E value is much greater than would correspond to the simple mode of activation. Comparison of chloral with acetaldehyde raises the question why the simple mode itself should not be more in evidence. The explanation may well be that the chlorine atoms, whether by mere size or mass, or by some more specific effect, cause the energy of collision to enter the CCl_3 group preferentially.

So far no distinction has been made between the separate segments into which we consider the low pressure part of the curves for acetaldehyde and propionic aldehyde, p. 345, to be divided.

Although there is no question of any discontinuity in the curves, and it must be emphasized that no such discontinuity has been suggested, nevertheless the changes of slope can hardly be represented except by functions with more than one set of independent constants.

Below 100 mm, with propionic aldehyde and acetaldehyde, there are two distinct regions of changing slope, namely at about 40 mm, and at 1 to 10 mm. The reaction which gives rise to the lowest bend is the one with the smallest transformation probability, as discussed above. In the special example of the aldehydes this reaction is the one with the highest energy of activation. It might therefore be assumed that the energy is located in the region of the molecule most remote from the aldehyde group, namely, the C—H links of the alkyl group. The probability of energy getting from here to the vital link is small, but, since the corresponding degrees of freedom are numerous, a high activation rate is possible. Thus we have a rapid rise with increasing pressure, and the early attainment of the small limiting value. The prominence of the

lowest segment with propionic aldehyde, as compared with acetaldehyde, can be explained by the greater number of alkyl C—H links.

In this connection, we may consider the analysis of the propionic aldehyde reaction products. At the higher pressures the principal products are carbon monoxide and ethane. As the pressure falls ethylene and hydrogen make their appearance in increasing proportion, and they can be proved not to come from any secondary decomposition of the ethane. The increase corresponds more or less exactly to that in the proportion of the reaction corresponding to the lowest segment, p. 355. Without going into details of the process by which an aldehyde molecule at the moment of decomposition yields ethylene and hydrogen rather than ethane, it is reasonable to suppose that this process has involved the activation of one or more atoms of the alkyl group itself.

Having associated the lowest part of the curve with the activation of the alkyl group and the highest part with the direct activation of the vital part of the molecule, we might now suppose that any intermediate segments that are distinguishable arise either from modes of activation involving vibrations of specific linkages such as the C=O bond, or from particular deformation vibrations, or from particular combinations of various types of vibration. From the curves, two extra types of activation apparently have to be provided for, though there may be others not experimentally distinguishable.

One of these could be provided for by the vibrations of the carbonyl-group. Before speculating as to which other might be concerned, we should have to know what constitutes activation in the "vital bond" referred to above. This has been left unspecified because there seems no easy way of deciding whether the "vital bond" is that joining the aldehyde hydrogen to the carbon from which it must migrate in the reaction, or the bond joining the aldehyde carbon to the adjacent carbon from which it must be severed. Whichever it is, one of the others would be available to provide an extra mode of activation, and this would be expected to give the second highest transformation probability, that is, to provide the segment next to the highest.

But the increase in the number of degrees of freedom which must be assumed in order to account for the reaction rate at low pressures shows that, in principle, combinations of different vibrations occur. Thus it may not be justifiable to identify too rigidly a given mode of activation with one single specific link. Even for the simplest mode of activation, the energy may not be definitely localizable either in the C—H or in the C—C link, but may reside in a deformation oscillation in which the angle between these two bonds changes.

In the decomposition of propionic aldehyde, methane is formed in a primary reaction to some extent. It is possible that the corresponding mode of activation involves a bending oscillation, whereby the hydrogen of the aldehyde is brought within reach of the methyl group.

In conclusion, it may be pointed out that the view adopted here of a number of distinct transformation probabilities for various types of activated state is not inconsistent with those theories* which make any one probability a function of the total energy. What have been called transformation probabilities may quite well be energy functions rather than constants. But the point is that, even so, a number of such functions with considerably different mean values are necessary. If the course of the curves discussed above were expressed by one function only, it can be shown that the observed energy of activation would fall at low pressures. Actually it rises.

We are indebted to the Royal Society and to Imperial Chemical Industries, Ltd., for grants by which apparatus for these various investigations has been obtained.

Summary

The curves representing the variation with pressure of the time of half decomposition of acetaldehyde and of nitrous oxide indicate that the reactions are kinetically composite. A number of different modes of activation of the molecules are assumed. By a comparison of the behaviour of differently substituted aldehydes—formaldehyde, acetaldehyde, propionic aldehyde and trichloroacetaldehyde—an attempt is made to characterize some of these various modes of activation.

* Rice and Ramsperger, 'J. Amer. Chem. Soc.,' vol. 49, p. 1617 (1927); Kassel, 'J. Phys. Chem.,' vol. 32, p. 225 (1928).

*The Kinetics of the Decomposition of Chloral and its Catalysis
by Iodine*

F. H. VERHOEK and C. N. HINSHELWOOD, F.R.S.

(Received April 18, 1934)

Introduction

The introduction of chlorine atoms into organic compounds causes marked changes in properties which can often be explained in terms of a displacement of electrons under the influence of the substituent. It is an interesting question how far these influences will show themselves in the kinetic behaviour of the substituted molecules. Accordingly the thermal decomposition of chloral and its catalysis by iodine have been studied. The decomposition is a homogeneous gaseous reaction which can be compared with the decompositions of acetaldehyde and propionic aldehyde.

Apparatus

The apparatus was of the usual type, with a silica reaction vessel heated in an electric furnace. A tube led to a capillary mercury manometer outside the furnace, and the course of the reaction was followed by observing the rate of pressure increase. In view of the relatively high boiling point of chloral it was necessary to keep all the connecting tubes heated to 80°–90° C. Considerable difficulty was experienced with the lubricants for the stop-cocks operating at this temperature. A special high temperature vapourless grease was used, but even this showed a tendency to run and foul the connecting tubes. The reaction products also tended to foul the apparatus so that frequent cleaning of the whole, including the manometer and the mercury pump, was required.

Nature of the Reaction

Since the decomposition of chloral had not been previously studied, it was necessary, first of all, to determine the nature of the reaction.

The decomposition was found to proceed at a conveniently measurable rate in the neighbourhood of 440° C. A typical curve obtained when the ratio of the increase in pressure to the initial pressure ($\Delta p/p_0$) is plotted against time is given for 441° C and 126 mm. in fig. 1. The pressure increase is directly

proportional to time up to about 70% increase; the curve then slopes off rather abruptly and proceeds until $\Delta p/p_0$ is about 1.35.

If chloral decomposes in the same manner as acetaldehyde, we should expect chloroform and carbon monoxide as the products of the reaction. There are also present in the reaction products, however, hydrogen chloride, hexachloroethane, and carbon. The hexachloroethane condenses as a dirty white solid in the cooler parts of the apparatus when the products are pumped out. (It sublimes without melting at about 60°.) Considerable quantities of carbon are formed, appearing as a black deposit on the walls of the reaction vessel. Hexachloroethane and hydrogen chloride are known to be formed by the

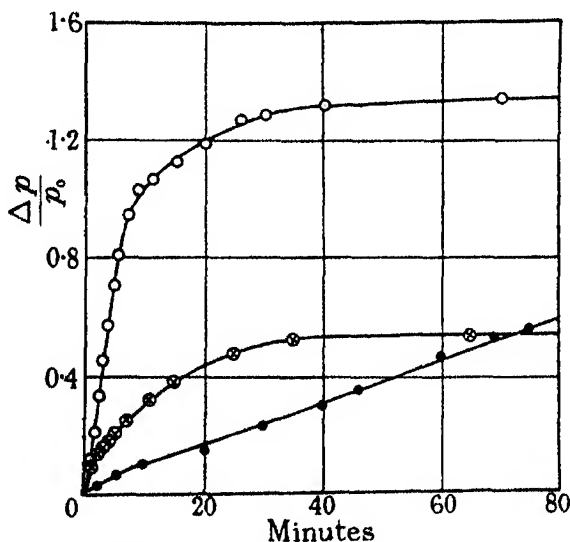


FIG. 1—○ chloral; × chloroform in presence of decomposition products of chloral; ● chloroform alone.

decomposition of chloroform at these temperatures.* That the formation of chloroform and carbon monoxide is the primary reaction in the decomposition of chloral seemed at first unlikely, since, if chloroform alone is allowed to decompose, the reaction proceeds steadily for a considerable time after the decomposition of chloral at the same temperature would have been complete. This may be seen by comparing the lower straight line of fig. 1 with the curve for chloral. At 40 minutes, when the pressure increase for chloral has nearly reached its final value, the decomposition of chloroform has gone barely half way to its end-point (corresponding to $\Delta p/p_0 = 0.60$). If, however, chloral

* Cf. Hurd, 'Pyrolysis of Carbon Compounds,' p. 132, 1929.

is allowed to react until there is no further increase in pressure, and chloroform is then added to the reaction products, the decomposition is found to be markedly accelerated, and the graph of $\Delta p/p_0$ against time is given by the curve with the crosses in fig. 1. The decomposition of the chloroform is now complete in 40 minutes, and the curve resembles the later part of the chloral curve. Thus it is possible to suppose that chloroform is one of the primary decomposition products of chloral. Gas samples taken when $\Delta p/p_0$ was 1.00 showed appreciable amounts, corresponding to as much as 20% of p_0 , of a compound containing

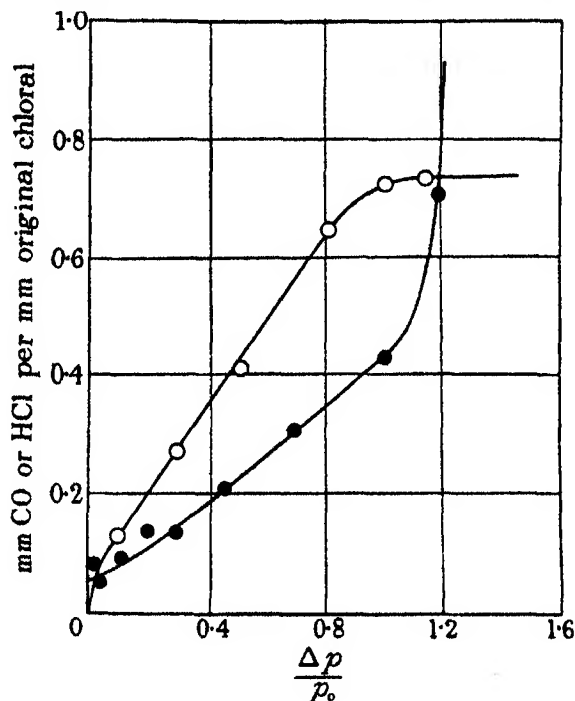


Fig. 2—○ Carbon monoxide; ● hydrogen chloride.

a trichlormethyl group, detected and estimated by the pyridine colorimetric test for chloroform.* At this stage of the reaction the pressure increase has begun to slow up and no further carbon monoxide is being formed, indicating that all the chloral has decomposed. The trichlormethyl compound found is therefore probably chloroform.

The results of analyses showing the amounts of hydrogen chloride and carbon monoxide present at various stages of the reaction are plotted in fig. 2,

* Cole, 'J. Biol. Chem.,' vol. 71, p. 173 (1926).

where the ratio of HCl or CO to the initial pressure of chloral is plotted against $\Delta p/p_0$. The hydrogen chloride was determined by shaking a sample of the gaseous products with water and titrating with baryta. It was difficult to free the chloral from small amounts of hydrogen chloride initially present, and the values given should be corrected for this initial contamination, which is shown by the intercept which the hydrogen chloride line makes with the axis. Rate determinations in the presence of 10 to 15 times as much hydrogen chloride as the initial impurity showed that it did no great harm. The amount of carbon monoxide was determined by allowing the reaction to proceed in the presence of a known quantity of nitrogen, which did not affect the rate, and then analysing for the ratio of carbon monoxide to nitrogen in a Bone and Wheeler apparatus. The gases were first washed with alcohol to remove vapours of chloroform and chloral, which are not soluble in water or dilute sulphuric acid, and which generate appreciable quantities of gas (carbon monoxide) when shaken with the concentrated potash used in the analysis.

The curves in fig. 2 show that hydrogen chloride is formed more and more rapidly as the reaction proceeds; that is, as more and more chloroform accumulates. The shape of the curves indicates that the hydrogen chloride is produced in a subsequent decomposition of this chloroform, and is not part of the primary products from the breakdown of the chloral molecule. Carbon monoxide, on the other hand, appears to be formed from the start and to be a primary product. It may be noted, however, that only 75 mm of carbon monoxide are formed for every 100 mm of chloral decomposing. In other words, about 25% of the chloral molecules form condensation products which do not decompose to form carbon monoxide.

Course of the Reaction at Different Pressures and Temperatures

The combined reactions—decomposition of chloral followed by the decomposition of chloroform—are of the same nature at different initial pressures of chloral and at different temperatures. If the time for a 50% increase in pressure for some given initial pressure and temperature is taken as a "standard value," and the time scales for reactions at other initial pressures and temperatures are changed in the ratio of their half times to the standard half time, so as to make all the half-times coincident, then the whole course of the reaction up to 80% pressure increase is found to be the same for all initial pressures and all temperatures. The result of such a manipulation is given in fig. 3. Pressure increase-time curves were plotted for a range of initial pressures and for two

temperatures; the time scale for each curve was then changed so that all curves should pass through the value 50 at the same time as the curve for 148 mm and 450°. The curves are seen to coincide over their whole course.

This fact simplifies the situation, since the time taken to reach any definite pressure increase will bear a constant relation to the rate of the primary chloral decomposition, the quantity in which we are directly interested.

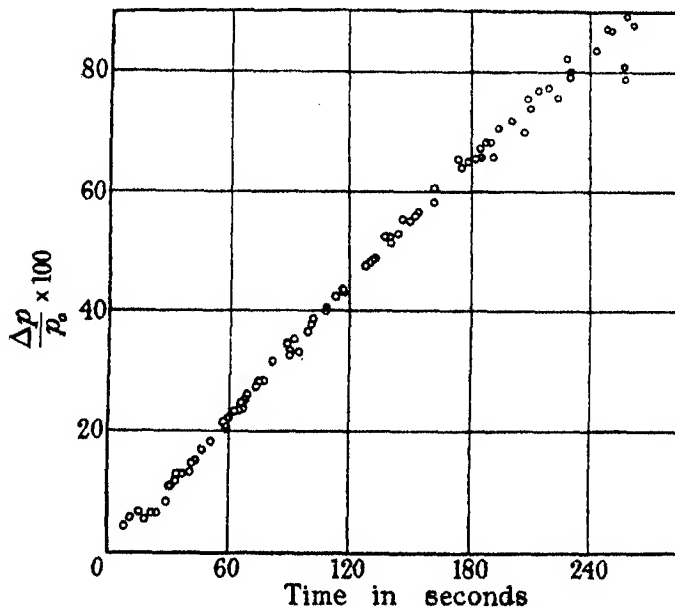


FIG. 3—The points refer to seven experiments at 450° C with p_0 from 38 to 294 mm, and three experiments at 400° C.

Order of Reaction

The order of reaction is best revealed by plotting the reciprocal of the time for a given percentage change against the initial pressure. In the present example, the time for a definite percentage pressure increase will serve the same purpose, as has just been shown. The time chosen is that for a 50% increase, and is designated t_{50} . Curves were determined for 440°, 445°, and 450°. An example is given in fig. 4, and the results are collected in Table I. The curve rises steeply as the pressure increases from zero to 15–20 mm, and then bends over and rises much less steeply.

The determinations of the reaction rate are not as concordant as one might wish, but there were no consistent variations in changing from one sample of chloral to another.

Table I—Relation between Initial Pressure and Rate. Temperature 445°. Pressure in mm, time in seconds

p_0	t_{50}	p_0	t_{50}
6	450	116	174
6.5	418	137	161
9.5	357	153	149
12	350	176	143
12	230	179	171
15	210	193	149
26	214	201	129
31	191	222	152
67	189	228	139
82	175	228	137
100	178	233	136
101	175	261	134
106	174	296	131
		321	123

Essentially similar results were found at 450° and at 400°.

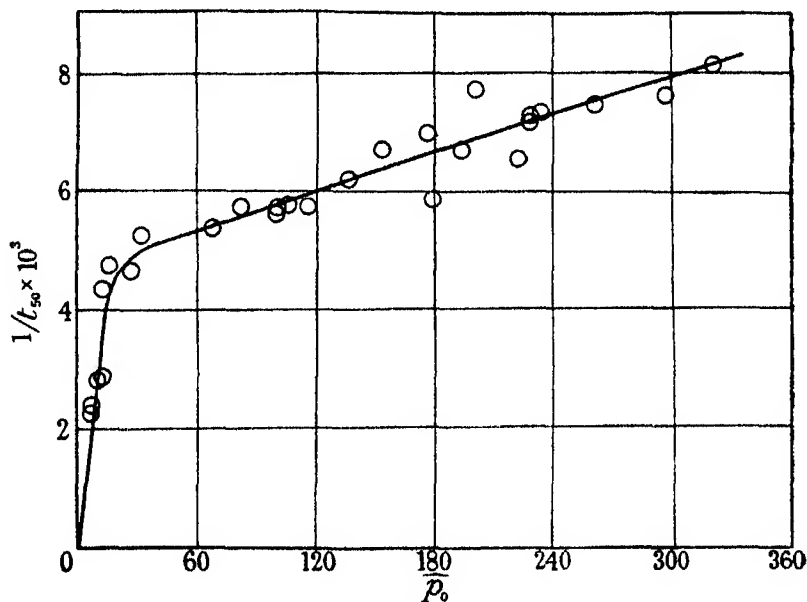


FIG. 4

Homogeneity

The reaction is essentially homogeneous. A series of experiments were made with reaction vessels filled with silica tubes. The surface/volume ratio was about four times as great as for the ordinary reaction bulb, but the increase in rate was not marked. The ratio of t_{50} in the unpacked vessel to that in the packed, at 440°, with chloral pressures between 100 and 200 mm was found

in various experiments to be: 1.49, 1.30, 1.32, 1.28, 1.11, 1.07, 1.21. In a bulb filled with silica balls, and having a surface/volume ratio about 16 times as great as the normal, the increases in rate were given by the factors: 1.08, 1.02, 1.35, 1.27. In this bulb the total increase in pressure was smaller than in the unpacked bulb, indicating that a greater proportion of the chloral was lost in condensation reactions. This means that a 50% increase in pressure represents a greater extent of reaction in the packed bulb, so that the decomposition may be speeded up more than the small change in t_{50} indicates.

Temperature Coefficient

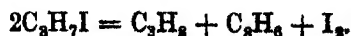
Temperature coefficients were determined for initial pressures of 225 mm and 120 mm. The results are given in Table II. The Arrhenius equation is followed in a satisfactory manner. No difference in the values of E at the two pressures could be detected. Each amounted to 49,200 calories per gram molecule.

Table II—Influence of Temperature

Temperature ° Abs	p_0	t_{50}	p_0	t_{50}
673	119	1118	218	1159
	123	1312	221	1127
			233	1006
685	121	726	226	629
	129	729	228	614
703	118	245	221	221
	120	274	224	225
	129	275		
725	126	93	224	85
	131	93	225	85
736	110	61	232	50
	142	53	232	50
	120	57		

The Decomposition Catalysed by Iodine

The decomposition of chloral is catalysed by iodine, the catalysed reaction proceeding at a conveniently measurable rate at a temperature about 60° below that for the uncatalysed decomposition. The catalyst was introduced in the form of isopropyl iodide, which was allowed a few minutes to decompose before the chloral was added. Isopropyl iodide yields iodine* according to the equation



* Glass and Hinshelwood, 'J. Chem. Soc.', p. 1815 (1929).

When $\Delta p/p_0$ is plotted against time, the shape of the curve is not greatly different from that for the uncatalysed reaction, but the total pressure increase is greater.

Iodine was also found to catalyse the decomposition of chloroform, and to approximately the same extent as it catalyses the chloral decomposition. Thus the effect of the iodine is roughly to transport the whole chloral-chloroform system to a position 60° lower on the temperature scale. The following figures are typical.

Temperature 380° C, chloral 216 mm, catalyst 10 mm

Time (seconds)	47	94	142	203	271	382
$\Delta p/p_0$	0.20	0.40	0.60	0.80	1.00	1.20

The reaction is of the first order with respect to the chloral over a ten-fold range of initial pressures. In Table III are given the values of t_{50} for varying initial pressures of chloral at 380° . The amount of catalyst was 10 mm of the products from isopropyl iodide in each experiment.

Table III—Catalysed Reaction—Influence of Chloral Pressure

p_0 (mm)	54	126	216	296
t_{50} (secs)	148	134	117	131

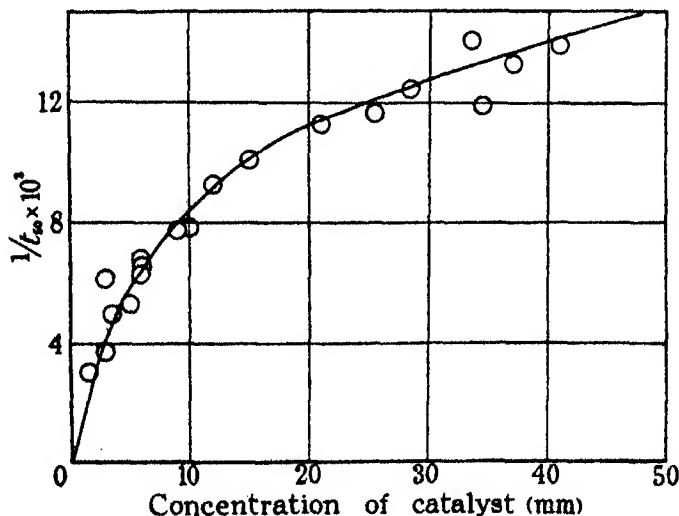


FIG. 5

The reaction velocity increases as the concentration of iodine increases, but not in direct proportion. Fig. 5 shows $1/t_{50}$ at 380° plotted against the concentration of catalyst. This non-linear dependence on the catalyst con-

centration appears to be a general one, and can be given a simple interpretation,* according to which molecules of catalyst can both communicate and remove activation energy. In the light of this theory it can be shown that t_{50} plotted against the reciprocal of the catalyst concentration should give a straight line, a condition which is, in fact, fairly well satisfied by the present results. On the other hand, the graph of $1/t_{50}$ against the square root of the iodine concentration is also a straight line, which would be expected if the catalysis involved simple collision with atoms rather than molecules of iodine. That the catalyst is atomic iodine is unlikely in the present example, since with acetaldehyde and with various ethers there is a linear relation between the rate and the concentration of molecular iodine.†

The temperature coefficient of the catalysed reaction was measured over a 60° range. For these experiments the reservoir of isopropyl iodide was kept in a bath of melting ice to ensure a constant vapour pressure, and a portion of the connecting tubes was used as a pipette to measure a constant amount of catalyst (equivalent to 5 mm of decomposed isopropyl iodide at 380°) into the apparatus at each temperature. The data are given in Table IV. The value of E is 39,000 calories per gram molecule.

Table IV—Temperature Coefficient of the Catalysed Reaction

Temperature ° Abs	t_{50} (mean values)
626	754
636	448
654	183
666	106
685	51

The relation between the number of molecules reacting, the collision number and the energy of activation will be different according to whether the catalysis is due to iodine molecules or iodine atoms.

From the relation between rate and catalyst concentration, and using the fact that the reaction is of the first order with respect to the chloral, it may be calculated that the number of chloral molecules reacting per cc per second when the pressure of chloral is 100 mm at 380° C and the pressure of iodine 1 mm is 4.4×10^{15} . The number of collisions between iodine molecules and chloral molecules at 380° and these pressures is 5.1×10^{24} per cc per second, assuming

* Bairstow and Hinshelwood, 'Proc. Roy. Soc.,' A, vol. 142, p. 77 (1933); 'J. Chem. Soc.,' p. 1159 (1933).

† 'J. Chem. Soc.,' p. 1815 (1929); Clusius, *ibid.*, p. 2607 (1930); Clusius, Hadman, and Hinshelwood, 'Proc. Roy. Soc.,' A, vol. 128, p. 88 (1930).

5×10^{-8} for the diameter of the chloral molecule and using Rankine's value 3.76×10^{-8} for the iodine molecule. According to the simplest possible mechanism, multiplication of this number by $e^{-39,000/RT}$ should give the reaction rate. The value of this product, however, is only 4×10^{11} .

For the hypothesis of reaction on collision with iodine atoms we can calculate the number of iodine atoms per cc at 1 mm and 380° from the equation of Bodenstein and Starck* to be 1.6×10^{14} . The number of collisions between atoms and chloral molecules for a chloral pressure of 100 mm is 5.4×10^{22} , assuming a value of 3×10^{-8} cm for the diameter of the iodine atom. The energy of activation must now be reduced by half the heat of dissociation of iodine: this gives 21,000 calories as the net energy of activation for the collisions. The product $5.4 \times 10^{22} \times e^{-21,000}$ gives 3.8×10^{15} molecules reacting per cc per second.

Discussion

The chief matters of interest emerging from the experiments which have been described are the following. Chloral appears to decompose in a manner analogous to acetaldehyde, but at a much lower temperature. The increased reactivity is what might be expected from the effect of the chlorine atoms in weakening the attachment of the hydrogen atom in the aldehyde group. This, however, is not the whole story, for in spite of the much lower reaction temperature—about 100° lower—the energy of activation is no smaller than that of acetaldehyde. Thus a considerably greater number of degrees of freedom must be invoked to account for the rate of reaction. This is discussed further in the paper in which the behaviour of the various aldehydes is compared, p. 327.

The decomposition resembles that of acetaldehyde and propionic aldehyde in being subject to catalysis by iodine, but the iodine in the present instance is a less effective catalyst, in the sense that it reduces the energy of activation to 39,000 calories only, instead of to about 33,000 as with the other aldehydes. The assumption that the iodine atom is the catalyst explains the influence of the catalyst concentration, and leads to a close agreement between the observed reaction rate and the rate of activation with two square terms. Thus it is quite possible, as far as the direct experimental evidence goes, that the mechanism differs from that of the catalytic decomposition of acetaldehyde or propionic aldehyde and depends upon collision with iodine atoms.

* 'Z. Elektrochem.', vol. 16, p. 966 (1910).

On the other hand, the relation between rate and catalyst concentration can be equally well represented by an expression of the form recently discussed by Bairstow and Hinshelwood (*loc. cit.*), assuming the iodine molecule to be the effective agent. On this hypothesis more than two square terms are needed to account for the rate of activation, as the calculation has shown. This is what might be expected from analogy with the uncatalysed reaction. Furthermore, on the basis of the theory given by Bairstow and Hinshelwood the influence of the C—Cl bonds might prevent the iodine from communicating the activation energy effectively to the sensitive part of the aldehyde molecule, possibly because the large moments of these bonds cause a polarization and attraction of the iodine molecule and divert it from the aldehydic group.

Summary

The thermal decomposition of chloral is predominantly homogeneous, and appears to yield principally carbon monoxide and chloroform—which undergoes subsequent decompositions. Condensation reactions also occur to a considerable extent. So far as the reaction $\text{CCl}_3\text{CHO} = \text{CHCl}_3 + \text{CO}$, is the principal primary change, the decomposition is analogous to that of acetaldehyde and other simple aldehydes.

The relation between reaction rate and initial pressure corresponds most nearly to that characteristic of a “quasi-unimolecular” reaction.

The rate is much greater than that of the acetaldehyde or propionic aldehyde decompositions, as might be expected from the influence of the chlorine atoms on the strength of attachment of the aldehyde hydrogen. The energy of activation, however, is 49,000 calories—as great as for acetaldehyde—and numerous square terms must be taken into account to provide an adequate rate of activation.

The reaction is accelerated by iodine. The catalytic reaction is of the first order with respect to the chloral, and its rate increases in less than direct proportion to the iodine concentration. The catalysis is relatively less effective than with acetaldehyde. The mechanism is discussed.

The Thermal Decomposition of Propionic Aldehyde

By C. A. WINKLER, C. J. M. FLETCHER, and C. N. HINSHELWOOD, F.R.S.

(Received April 18, 1934)

The hypothesis put forward in 1926, namely, that unimolecular reactions are mainly confined to molecules with large numbers of internal degrees of freedom, has proved a great stimulus to the investigation of more complex molecules, such as those encountered in the field of organic chemistry. The hypothesis was suggested by an investigation on the thermal decomposition of propionic aldehyde.* Although this work was detailed enough for its original purpose, a re-investigation has become desirable in view of recent advances in chemical kinetics.

According to the collision theory of activation and deactivation, the unimolecular velocity constant should decrease at low pressures. Reactions which behave in this way (so-called quasi-unimolecular reactions) are kinetically bimolecular at low pressures, but become unimolecular at high pressures. More complex behaviour is observed with gaseous acetaldehyde.† This compound, while decomposing bimolecularly at high pressures, undergoes additional quasi-unimolecular decompositions at low pressures. The occurrence of independent quasi-unimolecular reactions in the acetaldehyde decomposition can be attributed to the existence of different types of activated state in the molecule. The mode of decomposition would be, on this assumption, a function of the manner in which the energy imparted to the molecule is distributed among the various molecular motions, and also the transformation probability characteristic of the different distributions.

A detailed examination of the decomposition of propionic aldehyde in the light of the above ideas became of great interest. The questions arising were the following: To what extent could the theoretical conclusions which had been arrived at from the study of acetaldehyde be confirmed with propionaldehyde? What influence would the introduction of an extra CH_2 group into the molecule exert on the distribution of activation energy? Would the various

* Hinshelwood and Thompson, 'Proc. Roy. Soc.,' A, vol. 113, p. 221 (1926).

† Fletcher and Hinshelwood, *ibid.*, vol. 141, p. 41 (1933).

modes of decomposition, assuming these to exist as with acetaldehyde, be reflected in any way in the products resulting from the decomposition?*

EXPERIMENTAL PROCEDURE

The propionic aldehyde used was obtained commercially, and subjected to careful fractionation in an all-glass apparatus. The fraction boiling between 48.5°C and 49.5°C was used throughout the investigation. Owing to possible polymerization, a given sample of aldehyde was never employed later than 3 weeks after fractionation. Different samples gave identical results.

The apparatus used for the investigation was similar in essential details to that previously employed, the rate of decomposition being measured by change of pressure at constant volume. The aldehyde was decomposed in a silica bulb, of approximately 200 cc capacity, heated in an electric furnace. The "dead space" did not exceed 2% of the volume of the bulb. With the aid of an iron filament lamp in series with the furnace, which served to buffer voltage fluctuations, the current through the furnace could be maintained quite constant, with but little manipulation of a rheostat in series with it. In this way, the maximum error in the temperature was maintained within 1° . Temperatures were measured with a platinum-platinum-rhodium thermocouple, which was checked against the melting point of pure antimony.

For the pressure range 15–400 mm, a mercury manometer of the usual type was employed. Two McLeod gauges† were employed for measuring pressures less than 15 mm, a few determinations also being made above 15 mm with these gauges to serve as a check. The first gauge ("McLeod I") was used over the range 20 mm–1 mm and the second ("McLeod II") over the range 1 mm–0.5 mm.

The "sharing ratios" of both gauges were determined for air at three different temperatures, room temperature, 400°C , and 550°C . A strictly linear relationship held for McLeod I, which was quite independent of the pressure shared. The sharing ratio for propionic aldehyde was found to be the same as that for air, at room temperature and 400°C , and it was assumed that the sharing ratio for the aldehyde was likewise identical with that for air over the working temperature range of 510° – 590°C .

With McLeod II, however, the sharing ratio for air was found to diminish

* The experimental results are given in this paper. The theoretical discussion is given in another paper, p. 327.

† For details of measuring reaction velocities in this way see Fletcher and Hinshelwood 'Proc. Roy. Soc., A, vol. 141, p. 41 (1933).

with decreasing pressure; a curve of the sharing ratio-pressure relationship for air was accordingly constructed at 549° C, the normal working temperature. It was found, moreover, that the sharing ratio for air differed slightly from that of the aldehyde at room temperature and at 400° C, at pressures less than approximately 0.8 mm. The necessary correction was therefore applied, for any given pressure shared, to the sharing ratio for air at 549° C, thus obtaining the sharing ratio for propionic aldehyde at the same pressure, at this temperature.

Care was taken in all McLeod measurements to allow sufficient time for pressure equilibrium between the gauge and the reaction bulb. A correction was applied to the reaction time, to compensate for the small amount of change which occurred in the sharing interval. For pressures less than 0.3 mm, the sharing ratio became somewhat uncertain, possibly on account of effects, or to a Knudsen effect, or both.

The sharing ratio for the products of the reaction was also determined at 549° C. It was found to be the same as that for air at the corresponding pressure, and where the reaction approached completion, the sharing ratio for air was used.

Each gauge was provided with an electrically heated mantle, to prevent condensation of the aldehyde when it was compressed. (Each gauge was calibrated with the mantle heated.) The least sensitive gauge was calibrated against the mercury manometer, at higher pressures (30–40 mm) after which the calibration was extended to lower pressures, and also to the more sensitive gauge. As a check on the accuracy of the calibration, duplicate determinations made on McLeod I and on the manometer were found to agree closely; determinations in which the initial pressure in the reaction bulb was measured on McLeod I, and the pressure after reaction measured on McLeod II, were also found to agree well with determinations made on the gauges individually.

Before starting a series of determinations, the whole apparatus was washed out with propionaldehyde vapour several times to prevent any possible contamination with adsorbed air.

EXPERIMENTAL RESULTS

Variation of End-point with Pressure

The end-point of the reaction is not independent of the initial pressure. Hinshelwood and Thompson* found indications of a variation of end-point

* 'Proc. Roy. Soc.,' A, vol. 113, p. 221 (1926).

with initial pressure, but did not investigate it in detail. The course of the reaction was therefore determined at 549° C for a series of initial pressures from 240 mm–0.5 mm. Pressure-time curves were plotted. It was found that after the greater part of the pressure increase had taken place there was a slow subsequent increase. This very slow reaction was attributed to the decomposition of one or more products of the primary decomposition. This seems quite justifiable, since ethane certainly is formed in relatively large quantities and undoubtedly suffers decomposition at the temperatures used in the investigation (see Table VII). For this reason, the "true" end-points, corresponding to the decomposition of propionic aldehyde itself, were estimated graphically from the pressure-time curves, the portion corresponding to the primary aldehyde decomposition being extrapolated till it became parallel with the time-axis.

Table I $T = 549^{\circ} \text{C}$

P_e (mm)	$(P_e - P_0)P_0$	t_1/t_2
238	1.00	2.20
170	1.03	2.10
125	1.06	2.11
73	1.08	1.90
35	1.14	2.17
20	1.16	2.08
7.8	1.22	2.11
4.0	1.24	2.05
2.8	1.27	1.94
1.70	1.30	2.00
0.50	1.35	2.00

A careful study of the "true end-points" in this way showed that they increased gradually as the initial pressure fell, in the manner shown in Table I. P_e is the final pressure, estimated as explained, and P_0 is the initial pressure. From a knowledge of the end-point-pressure relationship, it was possible to apply the suitable correction in determining the time to half decomposition at a given pressure. No significant variation of the end-point with temperature was observed over a range of 50°.

Order of the Reaction

As may be seen from Table I, the ratio t_1/t_2 does not deviate appreciably from the value 2 over the entire range of initial pressures used, in agreement with earlier work.

Influence of an Increase of Surface on the Velocity of the Reaction

Hinshelwood and Thompson (*loc. cit.*) found the decomposition of propionic aldehyde to be almost entirely homogeneous, by the addition of silica powder

to the reaction vessel. A more detailed examination was made in the present investigation, the surface-volume ratio being increased by a factor of approximately 5, and the time to half decomposition, t_1 , determined over a range of pressure from approximately 20–200 mm. Table II shows that no significant increase or diminution in t_1 is observed. A few experiments made with a bulb

Table II

P_0 (mm)	t_1 (packed) bulb	t_1 (unpacked) bulb
I. Surface : volume ratio increased 5 times— $T = 549^\circ \text{C}$		
206	174	170
195	180	175
103	216	215
40	260	260
20	348	341
II. Surface : volume ratio increased 16 times— $T = 549^\circ \text{C}$		
208	165	170
46	214	240
23	250	312

in which the surface-volume ratio was approximately 16 times that in the unpacked bulb showed a slight acceleration. The extent of the surface reaction in the unpacked bulb, however, would be insufficient even at low pressures to affect seriously the observations recorded in the following sections.

Influence of the Initial Pressure on the Time of Half Change

The time of half change was determined at 549°C , over a range of pressures from 0.5 mm to approximately 400 mm, using the unpacked reaction bulb.

The results are shown in figs. 1, 2, and 3, P_0 being the initial pressure in mm, and t_1 the time for the reaction to proceed half-way to the "true" end-point.

An examination of fig. 1, in which the entire pressure range is included, now reveals that there is a similarity between the behaviour of propionic aldehyde and acetaldehyde, the contrasted behaviour found in earlier investigations being a matter of degree only. With both substances there is a quite definite segmentation of the curve. With propionic aldehyde, the curve is practically parallel to the axis of initial pressure for pressures greater than approximately 300 mm; that is, the reaction is "unimolecular" in this region. As the regions of smaller initial pressure are approached, however, the curve shows marked changes in direction. One of these occurs at an initial pressure of approximately 300 mm, while similar changes in direction are evident in the

neighbourhood of 40 mm and 5 mm initial pressure. Fig. 2 shows the latter more clearly.

The necessity for assuming the existence of marked changes of direction in the curves is further illustrated in fig. 3, a cursory examination of which would lead to the conclusion that the curve tended to become parallel to the pressure axis at pressures not greatly exceeding 10 mm. Comparison of this curve with that in fig. 2 shows, however, that in fact the value of $1/t_1$ increases practically linearly up to a pressure of 40 mm, where its value is practically double that at 10 mm. This leaves little doubt that each "segment" of the

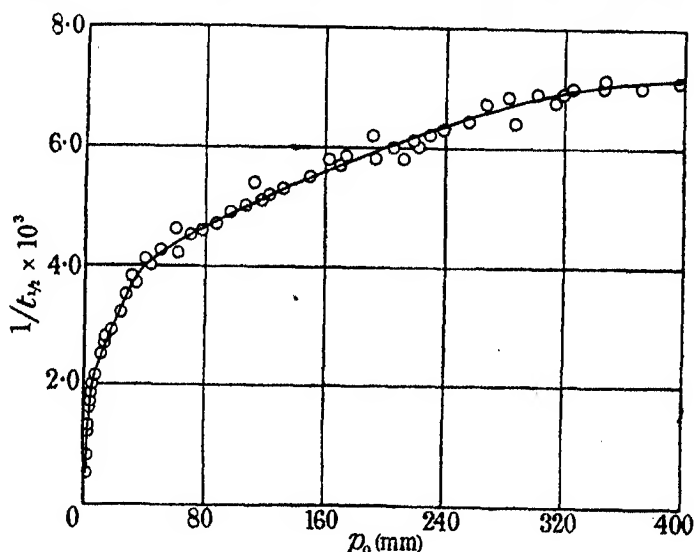


FIG. 1

curve in fig. 1 corresponds to an individual "quasi-unimolecular" mode of reaction. The correspondence between these different modes of reaction and the possible different states of activation, is considered in greater detail elsewhere.

It is not certain that the curve would ultimately pass through the origin, but from fig. 3 it seems very probable. Unfortunately, owing to surface effects, Knudsen effect, etc., it was not possible to extend the investigation to pressures below 0.5 mm with a degree of certainty sufficient to draw definite conclusions.

Temperature Coefficient of the Reaction

The values of t_1 for six different pressures were determined over a temperature range of approximately 90° C. Due corrections were applied for the variation

of end-point with pressure. At least two determinations were made for a given pressure at each temperature, and an average taken for the value of t_1 . If the initial pressures in the duplicate experiments were not exactly the same, a small correction was applied.

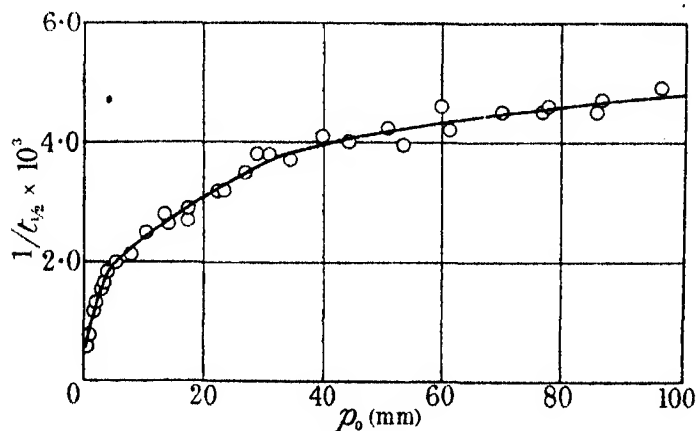


FIG. 2

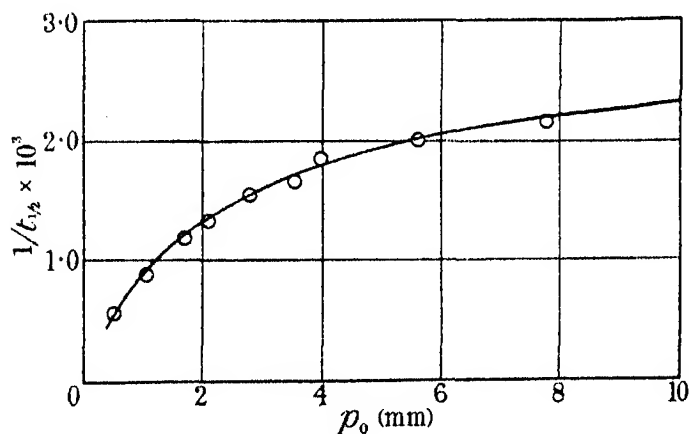


FIG. 3

At each pressure there is a satisfactory linear relation between $1/T$ and $\log_{10}(1/t_1)$. The data are given in Table III.

The variation of E with pressure is evident from Table IV, or from fig. 4. The values shown are uncorrected for variation of the collision rate with temperature. The value found by Hinshelwood and Thompson, namely, 55,000 cal, was not measured at one definite pressure, but represents a value for a mean pressure of 300–350 mm. It is evident that the mean energy of

Table III

Temperature °C	$\text{Log}_{10} (1/k \times 10^4)$				
	30 mm	40 mm	70 mm	100 mm	200 mm
499				0.620	0.750
509	0.610	0.660	0.770	0.820	0.950
519		0.876		1.012	1.156
529	1.030	1.119	1.185	1.233	1.361
539		1.319		1.450	1.544
549	1.439	1.542	1.575	1.667	1.769
559		1.772		1.845	1.921
569	1.860	1.958	2.000	2.022	2.137
579		2.155		2.236	2.328
589	2.240	2.377	2.360	2.420	2.509
599		2.432			

Table IV

P_0 (mm)	E (cal/gm mol)
30	63,500
40	63,900
70	61,400
100	61,200
200	59,500
350	56,000

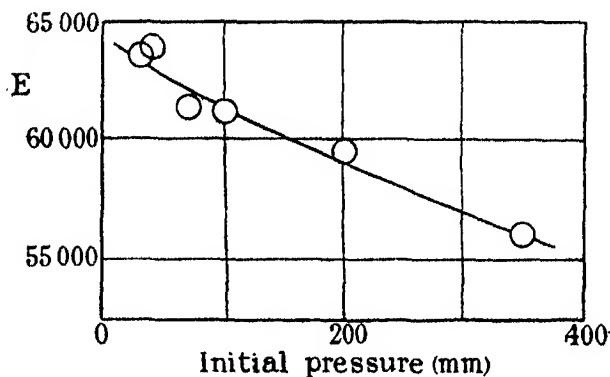


FIG. 4—Variation of activation energy with pressure

activation rises as the initial pressure falls. The significance of this fact is discussed elsewhere.

Influence of Hydrogen on the Velocity of the Reaction

The velocity constant of a unimolecular reaction falls off at some pressure sufficiently low. It has been observed that the addition of sufficient hydrogen will maintain the velocity constant at its "normal," high pressure value, but it has never been found possible to increase the velocity constant above its normal value in this way.*

* Hinshelwood, 'Proc. Roy. Soc.,' A, vol. 114, p. 84 (1927); Hinshelwood and Askey, *ibid.*, vol. 115, p. 215 (1927).

In view of the more or less qualitative nature of the results previously obtained,* it was thought of interest to re-investigate the behaviour of propionic aldehyde in the presence of hydrogen. Pure hydrogen was introduced directly into the reaction bulb through a heated palladium tube, the rest of the experimental arrangements being as before.

The introduction of hydrogen diminished the end-point of the reaction somewhat. The values of $t_{\frac{1}{2}}$ are calculated on the basis of the observed end-points. A small correction was applied for the increased pressure of aldehyde in the "dead space," inasmuch as this would be responsible for a fraction, at least, of the end-point diminution.

Table V $T = 549^{\circ} \text{C}$

P_0 (mm)	P_{H_2} (mm)	$t_{\frac{1}{2}}$ (secs)	$t_{\frac{1}{2}}$ (no H_2)	End-point $(P_0 - P_0)/P_0$
57.5	41.0	228	240	0.96
46.5	82.5	195	250	1.00
40.5	161.0	198	256	0.92
45.5	241.0	183	252	0.92

Limiting value of $t_{\frac{1}{2}}$ for "high pressures" of aldehyde 140 seconds.

The results are given in Table V. For a given aldehyde pressure, increasing pressures of hydrogen successively lower the half time, but never reduce it below the "normal" or high pressure value. It was difficult to work with larger ratios of hydrogen to aldehyde, but it is unlikely that an even greater excess of hydrogen would increase the reaction velocity above its normal value.

It was deemed of interest to ascertain, if possible, the cause of the diminution in end-point caused by the addition of hydrogen. Since unsaturated hydrocarbons are known to be formed, the decrease in the end-point might be due to their hydrogenation. Two samples, collected near the end of the reaction, were therefore analysed. The initial pressure of aldehyde was 40 mm, with 80 mm of hydrogen added in one instance, and none in the other. Analysis showed 11.1% unsaturated hydrocarbons in the sample to which no hydrogen has been added, and in the other 9.0%. This would point to appreciable hydrogenation of unsaturated hydrocarbons, which may explain the observed diminution in the end-point.

Influence of Pressure and Extent of Decomposition on the Products formed during Reaction

Analyses of the products of reaction under different conditions were made in a Bone and Wheeler apparatus. The usual procedure was followed. Hydro-

* Hinshelwood and Askey, 'Proc. Roy. Soc.,' A, vol. 116, p. 163 (1927).

gen was determined by oxidation with copper oxide, at 275° C for 12 minutes, while saturated hydrocarbons were determined by combustion. Unsaturated hydrocarbons were assumed to consist of ethylene only, and saturated hydrocarbons to be entirely methane and ethane.

Analyses were first made to determine the effect of initial pressure (P_0) on the nature of the reaction products. The reaction was always allowed to proceed to approximately 90% completion, at a temperature of 549° C. The results are shown in Table VI. In addition to the products indicated, from 1-2% of "carbon dioxide" were always obtained. This includes the small amount of aldehyde vapour remaining undecomposed and uncondensed.

Table VI $T = 549^\circ \text{C}$

P_0 (mm)	Unsat. %	H_2 %	CO %	CH_4 %	C_2H_6 %
4	18.0	18.0	40.5	7.0	10.2
12	13.0	12.0	44.4	10.8	13.5
40	11.1	9.0	47.2	10.8	16.1
120	8.8	7.5	48.1	6.5	24.6
200	8.5	5.2	48.9	8.5	24.3

Table VII $T = 549^\circ \text{C}$

Decom. %	Unsat. %	H_2 %	CO %	CH_4 %	C_2H_6 %
20	6.2	3.0	48.8	6.4	27.9
40	7.6	2.6	49.4	7.6	26.6
65	8.1	3.4	48.6	5.7	27.3
90	8.5	5.2	48.9	8.5	24.3
2 hr	8.6	6.2	48.3	9.3	22.9
15 hr	7.4	6.3	49.6	15.6	17.1

Table VII shows the results of analyses made at different stages of the reaction, the initial pressure of aldehyde in each test being 200 mm. Undecomposed aldehyde was removed before analysis by passing the gas through a tube immersed in a mixture of solid carbon dioxide and acetone.

The figures given in the tables are those actually measured; the residues include the 1 or 2% carbon dioxide previously mentioned, and a small constant proportion of air introduced, in sampling, from a capillary tube which it was not expedient to evacuate completely. This affects all the values in the same proportion, and is therefore unimportant.

As the initial pressure of the aldehyde decreases, the amount of ethylene in the reaction products increases regularly, and hydrogen appears to increase in equivalent proportion to it. In the early stages of the reaction at 200 mm, however, there is a deficit of hydrogen. From the parallel variations of

ethylene and hydrogen, it is reasonable to suppose that they are produced simultaneously, and to attribute the small loss of hydrogen under certain conditions to secondary changes or adsorption.

When CO is removed from the molecule C_2H_5CHO , the residue is equivalent to C_2H_6 . This residue may appear, from the primary reaction, as ethane, as $C_2H_4 + H_2$, or as $1.5 CH_4 + 0.5 C$. If it appeared wholly in any one of these ways, the ethane, ethylene, or methane would be not less than the CO removed. In general, then, the sum of C_2H_6 , C_2H_4 , and CH_4 should be at least equal to the amount of CO. Actually, the carbon monoxide is in excess of the sum of these three. Hence, some of the fragments left when CO is removed must have formed more complex compounds not appearing in the gas analysis.

The formation of methane must be regarded as a primary process, and not due simply to subsequent decomposition of the ethane. This can be seen from Table VII, which shows that very little decomposition of the ethane occurs, even in two hours the reaction is 90% completed.

The formation of ethylene and hydrogen appears to be characteristic of the lowest of the segments into which the curve in fig. 2 can be analysed. This can be seen from an approximate quantitative treatment. For example, at 5 mm the value of $1/t_1$ is 2 (approx.). By extrapolating the second segment of the curve (5 to 40 mm) to the axis of $1/t_1$ the intercept is found to be 1.5 (approx.). Hence roughly 0.75 of the reaction at $p = 5$ mm corresponds to the lowest segment, and 0.25 to succeeding segments of the curve. Assuming the higher segment to be characterized by the formation of ethane and methane (reaction 1), and the lowest segment by a reaction giving α parts of C_2H_4 to $(1 - \alpha)$ parts of $C_2H_6 + CH_4$ (reaction II), then at 5 mm pressure, from the analyses,

$$\text{total } C_2H_4 / (C_2H_6 + CH_4) = 17/17 = 1.0 = 0.75\alpha / \{0.75(1 - \alpha) + 0.25\},$$

whence $\alpha = 0.67$. Then at, say, 200 mm where $1/t_1$ is 6.0, the proportion of reaction II is $1.5/6.0 = 0.25$ and of reaction I, 0.75. Hence

$$C_2H_4 / (C_2H_6 + CH_4) = 0.25\alpha / \{0.25(1 - \alpha) + 0.75\} = 0.18.$$

From the analytical results, $C_2H_4 / (C_2H_6 + CH_4) = 0.24$.

Similarly at 20 mm pressure the theoretical ratio is 0.47 and that found 0.45.

The increase in end-points observed experimentally would seem to be accounted for by the formation of greater quantities of ethylene and hydrogen

as the pressure is diminished. This can also be shown by approximate calculations.

The observed end-point at 240 mm is a 100% increase. At this pressure the analyses show that about 0.2 of the total reaction goes to form ethylene and hydrogen, and 0.8 goes to form methane and ethane. The former reaction would give 150% increase and the latter 100%. Thus the composite reaction would give $0.2 \times 150 + 0.8 \times 100 = 110\%$ increase. Thus the observed end-point is 91% of the theoretical. The deficit may be attributed to losses by condensation reactions. Assuming that the end-point is always reduced in a constant proportion by these losses, then at 20 mm, for example, where the proportion of the two reactions is approximately 1:1, the end-point should be $\frac{1}{2}(150 + 100) \times 0.91 = 114\%$. Actually it is found to be about 117%. Similarly at 5 mm the calculated end-point is 125% and the observed 124%. Thus the actual increase at lower pressures is accounted for.

Molecular Statistics of the Reaction

The earlier investigation led to the result that to account for the rate of activation a considerable number of square terms must contribute to the activation energy.* The value of E used was 55,000 calories. The present value for higher pressures is 56,000 and for lower pressures greater still. Thus the original result holds good, with the additional conclusion that at low pressures the number of square terms involved rises above the 12 previously postulated.

SUMMARY

The thermal decomposition of propionic aldehyde has been re-investigated over a pressure range from 400 to 0.5 mm. The reaction appears to be kinetically complex, as with acetaldehyde, and to be best interpreted as the resultant of several quasi-unimolecular reactions. These are homogeneous.

The chemical nature of the reaction products varies with the pressure to some extent, which accounts for changes in the "end-point." The influence of hydrogen has been further studied, previous results being confirmed and extended.

The energy of activation shows a well-defined variation with pressure.

* Hinshelwood, 'Proc. Roy. Soc.,' A, vol. 113, p. 230 (1926).

The Thermal Decomposition of Formaldehyde

By C. J. M. FLETCHER

(Communicated by C. N. Hinshelwood, F.R.S.—Received April 18, 1934)

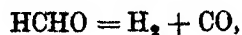
The thermal decomposition of formaldehyde has been studied for comparison with the decomposition of other simple aldehydes. In the decomposition of acetaldehyde the kinetics of the reaction have led to the hypothesis of the existence of a limited number of different activated states of the molecule.* It was of interest to determine whether the kinetics for the simpler molecule of formaldehyde correspond to a smaller number of modes of activation.

EXPERIMENTAL RESULTS

The experimental method was that described previously.* Formaldehyde vapour was introduced into the reaction vessel by heating paraformaldehyde. To prevent condensation in parts of the apparatus outside the furnace, all these were kept above 100° C with heated nichrome wire, a special high temperature grease being used for the taps. As the reaction was unaffected by the presence of water vapour (Tables I and II) elaborate drying of the formaldehyde was not undertaken. Care was taken to avoid traces of air which interfere with the reaction. The vapour first given off from a fresh sample of paraformaldehyde was found to decompose rather more rapidly than paraformaldehyde which had been in use for some time.

The temperature was measured by a platinum-platinum-rhodium thermocouple calibrated in terms of the rate of decomposition of acetaldehyde and propionic aldehyde. The temperature was controlled within 1° by a Cooke and Swallow regulator working in conjunction with an iron wire resistance lamp.

In addition to the predominant decomposition



formaldehyde undergoes at 569° C various condensation reactions. Thus the final increase in pressure is less than 100%. The pressure increase appears to take place in two distinct stages: the first stage is rapid and is succeeded by a slow pressure increase lasting for a number of hours. The percentage

* Fletcher and Hinshelwood, 'Proc. Roy. Soc.,' A, vol. 141, p. 41 (1933).

increase for the first stage diminishes from 83% at 43.5 mm to 59% at 388 mm (Table I). It is also lowered by a 16-fold increase in the surface-volume ratio by approximately 15% at any one pressure. The percentage increase in the second stage of the reaction becomes larger as the first stage becomes smaller.

Analysis of the volatile products after the reaction has gone to its final end-point shows the gas to consist almost entirely of carbon monoxide and hydrogen. The ratio CO/H_2 in two analyses was 1.09 and 1.06. In an analysis of the gas present towards the end of the first stage (when this represented only 41% increase), the ratio CO/H_2 was 1.37. The first pressure increase must include the straightforward decomposition of formaldehyde. At the same time condensation reactions catalysed by the surface seem to be taking place, giving some non-volatile products but mainly a substance which subsequently slowly decomposes. During the condensation some carbon monoxide is formed, so that at first the ratio CO/H_2 is greater than unity. The subsequent slow decomposition must therefore produce more hydrogen than carbon monoxide for the final CO/H_2 ratio to be nearly unity. It is not inconceivable that in the early stages of the reaction two molecules of formaldehyde give carbon monoxide and methyl alcohol by a kind of Cannizzaro reaction, and that the methyl alcohol slowly decomposes according to the equation



Additional evidence for this is provided by a study of the rate of decomposition of methyl alcohol in the presence of the end products from formaldehyde. The rates of reaction and the pressure increase correspond to that of the "second stage." It will be shown that the rate of decomposition of formaldehyde is proportional to the square of the initial pressure. Since the amount of methyl alcohol formed increases with the initial pressure, its production would seem to vary with some power of the initial pressure greater than the second.

As the purpose of the investigation was to study the kinetics of the simple decomposition of formaldehyde, a number of determinations of the pressure increase for the first stage were made from the pressure-time curves for initial pressures from 30 to 400 mm, Table I, and a curve constructed showing the variation of this "end-point" with pressure. For subsequent calculations, the end-point at any pressure was read off from this curve. The considerations that follow apply to this "first stage" of the reaction.

Table II gives some typical results at different initial pressures (p_0) at 569° C. The times for a third, t_1 , and a half, t_2 , change are taken respectively as the time for a pressure increase of a third and a half of that corresponding to

the end-point for the first stage. The initial rate $(dp/dt)_0$, expressed in mm per second, is obtained by drawing a tangent at the origin.

The reciprocal of the half-time plotted against the initial pressure gives an inclined straight line passing very nearly through the origin, fig. 1, and thus corresponding to a "bimolecular" reaction. This is shown by the approximately constant values, Table II, of the expression

$$k_1 = \frac{1}{t_{1/2} \cdot p_0}.$$

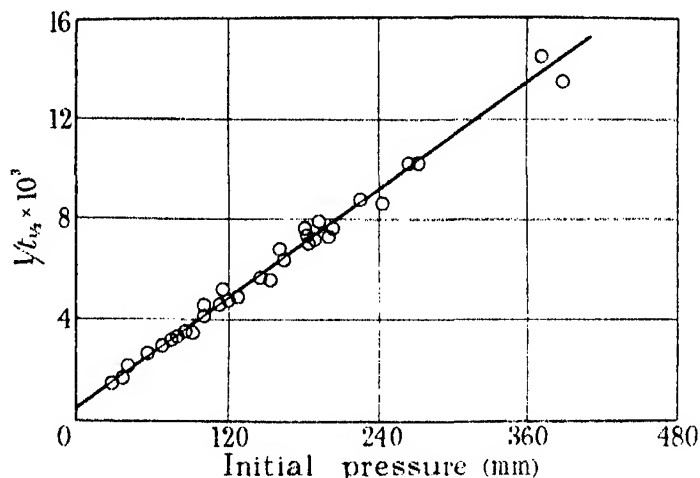


FIG. 1

Table I—Unpacked bulb. % Pressure increase

Initial pressure (mm)	1st stage	2nd stage	Total
28.5	91	—	—
43.5	83	—	—
52	82	12	94
80	79.5	13.5	93
132	74	16	90
*183	68	21	89
203	66	22	88
265	63.5	23.5	87
388	59	26	85
†90	67	—	—
†146	63	—	—

Packed Bulb

89	67.5	—	—
146	58	—	—
217	46	26	72
333	42	29	71
389	41	—	—

* In presence of 6 mm of water vapour.

† In presence of 150 mm of the products of the reaction.

Table II further shows that for different initial pressures, the value of k_1 derived from the expression $\frac{1}{p_0^2} \left(\frac{dp}{dt} \right)_0$ is almost constant. Thus a bimolecular constant can be derived in two independent ways. This makes it unlikely that the result is fortuitous, and due merely to some compensating variations in the complex pressure changes caused by the simultaneous condensation reactions. In view, however, of the empirical way in which the half-times are obtained, it is not surprising that the mean values of k_1 in the two different cases (4.05×10^{-5} and 2.55×10^{-5}) are somewhat different.

The products of the reaction seem to facilitate both decomposition and condensation. Thus in the presence of 150 mm of the reaction products both the half-times and the end-points for the first stage agree approximately with those normally obtained for an initial formaldehyde pressure 150 mm greater, Tables I and II.

Table II — Unpacked Bulb. Temperature 569° C

p_0	$\left(\frac{dp}{dt} \right)_0$	t_1	$\frac{t_1}{t_2}$	$\frac{1}{t_1 p_0} \times 10^5$	$\frac{1}{p_0^2} \left(\frac{dp}{dt} \right)_0 \times 10^5$
mm	mm per sec	secs			
28.5	0.028	705	1.72	4.98	3.5
56	0.12	383	1.84	4.66	3.7
80	0.17	304	1.82	4.12	2.6
101	0.28	244	1.89	4.06	2.8
120	0.42	211	1.95	3.95	2.9
146	0.45	177	1.82	3.87	2.1
165	0.62	158	1.84	3.83	2.3
*183	0.72	137	1.90	3.99	2.1
203	0.78	132	1.89	3.74	1.9
225	0.90	114	1.87	3.90	1.8
265	1.67	98	1.96	3.86	2.4
371	2.83	69	2.00	3.92	2.05
†90	0.27	143	1.74	7.77	3.3
†146	0.63	120	2.00	5.75	3.0

* In presence of 6 mm of water vapour.

† In presence of 150 mm of the products of the reaction.

As the products of the reaction thus appear to activate formaldehyde, the course of the reaction at any given pressure would be nearly unimolecular if no interfering reactions were taking place. Actually the ratios t_1/t_2 given in Table II, and t_1/t_2 , which has a mean value of 1.79, correspond to an order of reaction intermediate between the first and the second.

In a packed reaction bulb, the values of both the initial rate and the reciprocal of the half-time are, at any given pressure, smaller (by a factor of three or four) than the corresponding values in the unpacked bulb. The decomposition of formaldehyde into carbon monoxide and hydrogen is therefore not catalysed

by the surface. In view of the considerably lower end-points in the packed bulb, it is not certain to what extent, if at all, the decomposition is really slower.

The rate of reaction was measured over a temperature range of nearly a 100° at initial-pressures of approximately 200 mm. The end-points for the first stage were evaluated at the highest and lowest temperature used, and found to be within 2% of the end-point pressure curve for 569°C . The t_1/t_2 values were also comparable over the whole temperature range.

The results are given in Table III. The values for k_1 are derived from the half-times, and are corrected for the variation in the initial concentration, $\log_{10} k_1$ plotted against the reciprocal of the absolute temperature gives a good straight line. The energy of activation, uncorrected for variation of the collision rate with temperature, is 45,300 cal. The corrected value, which is $\frac{1}{2}RT$ lower, is 44,500 cal.

Table III

Temperature $^\circ\text{C}$	$\text{Log}_{10} (k_1 \times 10^6)$
607	2.114
599	2.021
569	1.585
550	1.304
531	1.044
513.5	0.770
510.5	0.716

DISCUSSION

As the kinetics of the reaction show that the decomposition is bimolecular, it might be expected that the number of molecules reacting would be given by the simple expression $Z \cdot e^{-E/RT}$, where Z is the number of collisions.

The number of molecules reacting may be derived from the value of k_1 . This constant has been deduced in two ways. Taking the mean of the two values, *i.e.*, 3.3×10^{-5} , the number of molecules reacting per second in 1 cc at 760 mm and at 569°C is 2.20×10^{17} . At 569°C the value of $e^{-E/RT}$ is 2.57×10^{-12} . The number of collisions from the expression $\sqrt{2}\pi\sigma^2\bar{u}n^2$ is 7.12×10^{28} , taking the diameter of the formaldehyde molecule to be 5×10^{-8} cm, and 4.56×10^{28} taking it to be 4×10^{-8} cm. The value for $Ze^{-E/RT}$ in the two cases is therefore 1.83×10^{17} and 1.17×10^{17} . The number of molecules reacting is therefore within a factor of two of the number activated, if the energy of activation is contained in only two square terms.

Owing to the number of complicating features, a complete analysis of this reaction is impossible. The methods of approximation which have been used

are admittedly crude, but different methods of approach lead to the salient fact that the main decomposition into carbon monoxide and hydrogen is a reaction with a rate proportional to the square of the pressure.

SUMMARY

The thermal decomposition of formaldehyde into carbon monoxide and hydrogen has been shown to be a homogeneous bimolecular reaction over the pressure range 30–400 mm. Simultaneous condensation reactions occur. The decomposition has been studied from 510°–607° C, and the energy of activation found to be 44,500 calories. The rate of reaction is approximately equal to the rate of production of activated molecules calculated from the simple expression $Z \cdot e^{-E/RT}$ where Z is the collision number.

The Magneto-Caloric Effect and other Magnetic Phenomena in Iron

By H. H. POTTER, Ph.D., Wills Physical Laboratory, University of Bristol

(Communicated by A. M. Tyndall, F.R.S.—Received March 21, 1934)

According to the Weiss theory a ferromagnetic body is composed of a number of "domains" each magnetized even in the absence of an external field to an intensity dependent on the temperature. At absolute zero this spontaneous magnetization (σ_0) is equal to the saturation intensity (σ_∞) whilst at any other temperature (T) the value of σ_0/σ_∞ is dependent only on the ratio T/θ where θ is the Curie temperature. This is known as the law of corresponding states. At low temperatures the apparent increase in magnetization, accompanying the application of the external field H , is due merely to alignment of the directions of spontaneous magnetization of the various domains. As the temperature rises, however, σ_0 becomes much less than σ_∞ , and the effect of an external field is twofold—(1) an apparent increase of magnetization due to alignment, and (2) a true increase in the degree of magnetization of each domain. Magnetization of a specimen is accompanied by a decrease of magnetic energy and if the experiment is carried out adiabatically a rise in temperature results. This phenomenon is known as the magneto-caloric

effect. Weiss and Forrer* have shown that this temperature increase is given by the equation

$$dT = - \frac{T}{J\rho c_H} \left[\frac{\partial \sigma}{\partial T} \right]_H dH, \quad (1)$$

where c_H is the specific heat at constant external field H , ρ the density, J the mechanical equivalent of heat, and σ the intensity per unit volume. This equation was arrived at thermodynamically without reference to the hypothesis of the intramolecular field. The intramolecular field theory has been attacked by Honda† who develops an equation identical with (1) but in which he states that H is the total field (external + intramolecular). If this were so, equation (1) would be in complete quantitative disagreement with the experiments of Weiss and Forrer on nickel. Honda's argument depends on the use of the equation $dW = pdv + vHd\sigma$, where $vHd\sigma$ is the work done on the body by the field. Honda assumes that H is the total field, but since work can hardly be done on a body by its own internal field, it appears to the writer that the H in Honda's formula is the external field, giving then an equation identical with that of Weiss and Forrer. Equation (1) is further justified by being in excellent agreement with the experimental results of Weiss and Forrer, and with those of the writer given below.

Weiss and Forrer have further shown that the rise of temperature is related to the change in the magnetization by the equation

$$dT = \frac{H + H'}{J\rho c_\sigma} d\sigma, \quad (2)$$

where H' is the internal field, c_σ the specific heat at constant magnetization, and $d\sigma$ the change in volume-intensity accompanying the application of an external field H . This involves no assumption as to the nature of H' , but follows from the statement that the change of energy of the substance per unit volume can be expressed as

$$dU = J\rho c_\sigma dT - H' d\sigma,$$

where this equation may be considered as the definition of H' . In addition the work (dW) done on the body by the external field is $= Hd\sigma$. Since in an adiabatic process the heat dQ communicated to the specimen is zero we have $dQ = dU - dW = 0$ thus leading immediately to equation (2).

* 'Ann. Physique,' vol. 5, p. 153 (1926).

† 'Sci. Rep. Tohoku Univ.,' vol. 21, p. 341 (1932).

H' is then put equal to $N\sigma$, N being called the intramolecular field factor. We have therefore

$$dT = \frac{H + N\sigma}{J\rho c_\sigma} d\sigma. \quad (2A)$$

One of the features of the Weiss theory is the assumption that N is independent of both T and σ . It will be shown below that this assumption is disproved by experiment. The Heisenberg theory does lead to a field factor which depends on both T and σ , but it will be shown that even this theory is inadequate.

Equation (2A) can be integrated if N is independent of σ . Below the Curie point—and, in fact, for some distance above it— H is negligibly small in comparison with H' ($= N\sigma$), and we have

$$\Delta T = \frac{N}{2J\rho c_\sigma} (\sigma^2 - \sigma_0^2), \quad (3)$$

where σ_0 is the value of the spontaneous magnetization. At higher temperatures $\sigma = \chi H$ and $\sigma_0 = 0$. The susceptibility χ also becomes independent of H , so we have

$$\Delta T = \left(N + \frac{1}{\chi}\right) \frac{\sigma^2}{2J\rho c_\sigma} = \frac{N'\sigma^2}{2J\rho c_\sigma}. \quad (4)$$

N' will be a function of the temperature since $1/\chi$ increases with temperature, but in the range of temperatures used in the experiments described below $1/\chi$ never reached 10% of N .

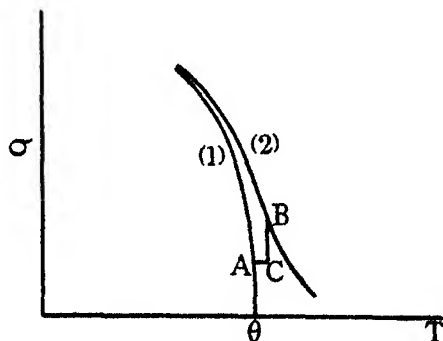


FIG. 1

Equation (3) can be obtained by the following simple argument. Let curves (1) and (2) of fig. 1 represent respectively the variation with temperature of the spontaneous magnetization and the total magnetization in an external field H . θ represents the Curie temperature. Assume that initially the

specimen is in a state represented by the point A, and that a field H is switched on raising the temperature and the magnetization to a point represented by B. The energy is a single valued function of the positions A and B, so that the change of energy in going from A to B will be independent of the path chosen. Suppose that the operation is performed in two stages, AC representing an increase of temperature, but not of magnetization, and CB representing a change of magnetization but not of temperature. If ΔT represents the temperature rise from A to C, and σ and σ_0 the two values of the magnetization at B and A respectively, the energy changes in the two cases will be $\rho J c_\sigma \Delta T$ and $-\frac{1}{2} N (\sigma^2 - \sigma_0^2)$. If the work done by the external field is small, and the total change is adiabatic, we have

$$\Delta T = \frac{N}{2J\rho c_\sigma} (\sigma^2 - \sigma_0^2).$$

If the rise of temperature is plotted against the square of the magnetization the result should therefore be a straight line as shown in fig. 2 with an intercept on the axis equal to σ_0^2 . In practice the relation shows initial curvature as

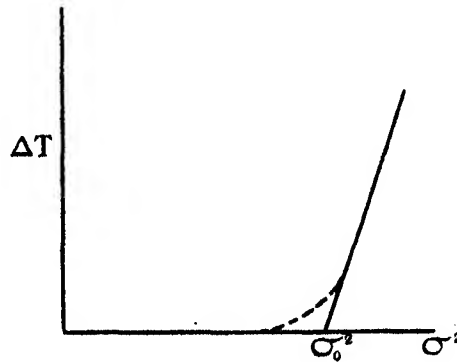


FIG. 2

indicated by the dotted line. This is due to the fact that in all cases it is not σ (the actual degree of magnetization of the domains) which is measured, but the average value of the component of this magnetization for the various domains, in the field direction. If therefore the turning process of these domains into the field direction is not complete before true increase of magnetization begins, a rise of temperature is registered before the apparent magnetization has reached the value of the spontaneous magnetization σ_0 .

The magneto-caloric effect gives the only satisfactory method of determining σ_0 and so of testing the law of corresponding states. The effect has been investi-

gated in great detail by Weiss and Forrer (*loc. cit.*) for nickel, and the theoretical conclusions have, except for a few details, been strikingly verified. Similar experiments have not been made with iron, except for some rough measurement by the writer* for the purpose of comparison of the magneto-caloric and magneto-resistance effects.

The object of the present research is to carry out more accurately magneto-caloric experiments on iron.

Experimental Methods

Certain serious experimental difficulties are immediately encountered. The Weiss-Forrer method of measurement applied to iron would be unsatisfactory. Their method of measuring σ and ΔT consists of removing suddenly from the field of an electromagnet an electric furnace containing the nickel specimen. The change of flux in a coil situated in the field, and the change of temperature of specimen, were measured. This necessitated boring the pole pieces to take the furnace. Although this may be practicable for nickel, it would be impracticable with iron, where the higher Curie temperature makes the use of a bigger furnace essential. Any ballistic method of measuring σ involving switching on or switching off the electromagnet would be useless owing to the great difficulty of obtaining accurate compensation for the field lines. The various torsion methods, which have been used in ferromagnetic measurements, seem equally inapplicable at high temperatures. A new method of measurement has therefore been evolved, based on a method for the measurement of diamagnetic susceptibilities due to Kapitza and Webster,† and a method for the measurement of paramagnetic susceptibilities due to Sucksmith.‡ The principle of the new method is shown in fig. 3.

A is sphere of iron between the poles (N.S.) of an electromagnet. A coil B, of about 150 turns of 36 S.W.G. copper, wound in three layers on an ivory former with its axis parallel to the lines of force of the magnet, was placed above A, and suspended by a quartz tube T from a phosphor-bronze ring carrying two tiny mirrors m_1 and m_2 . An image of a straight filament lamp F was formed by means of a lens L in a telemicroscope M, the beam of light being reflected from both mirrors m_1 and m_2 . The force of attraction (or repulsion) between A and B is directly proportional to the magnetic moment

* 'Phil. Mag.,' vol. 13, p. 233 (1932).

† 'Proc. Roy. Soc.,' A, vol. 132, p. 442 (1931).

‡ 'Phil. Mag.,' vol. 8, p. 158 (1929).

of A, and was measured in terms of a deflection in M, produced by reversing a known current in B. This current was kept constant by measuring it on a high quality milliammeter the pointer being observed under a microscope. The maximum deflection in M at room temperature was about 1 cm, and could be measured to 1/100 mm.

The force of attraction is also dependent on the distance between A and B, but the great advantage of the method lies in the high magnifying power of the system, the actual movements of B being negligibly small. As only comparative values of the magnetization were needed, the distance had merely

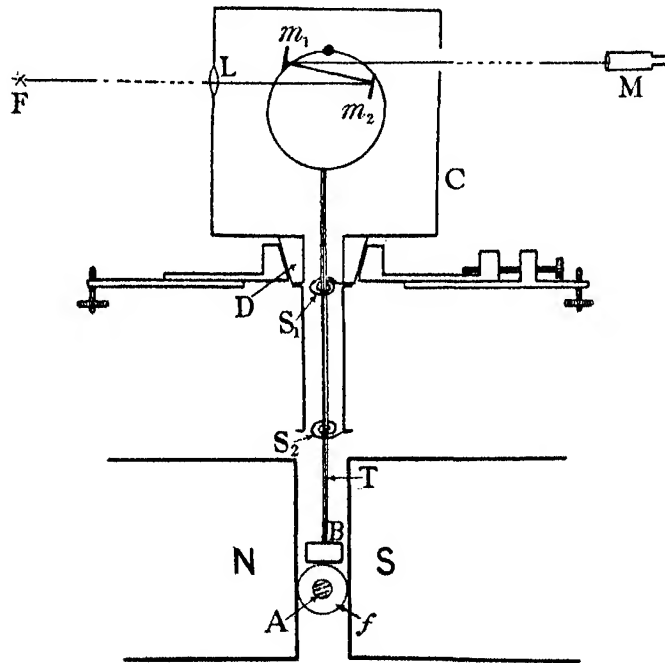


FIG. 3

to be kept fixed during a single group of experiments. Since the measurements are made not on A, but on B, A can be enclosed in a furnace, *f*, and raised to any desired temperature without disturbing the measuring system.

Lateral movement of the coil B relative to the case C was prevented by two flat phosphor bronze spirals S_1 , S_2 , fixed to the quartz tube and on to the case. These spirals were cut from sheet metal 5/1000 of an inch thick, and the two coils were mounted so that their turns ran in opposite directions. These completely prevented lateral movement while exerting very little controlling

force in a vertical direction. The latter amounted to about 5% of the controlling force due to the ring.

In a perfectly uniform field the vertical force on B would be determined entirely by the magnetic moment of A, but in practice there is a small force due to non-homogeneity of the field of the electromagnet. This was reduced as far as possible by using large diameter pole faces turned to be accurately parallel to one another. It was also necessary to have the axis of B accurately parallel to the field, otherwise the torque produced was found to be converted by the elastic ring into a considerable vertical movement. This parallelism was obtained by having the case mounted in a cone bearing, D, free to rotate about a vertical axis. The whole apparatus was turned in this bearing until the pull of the field on the current in B was reduced to a minimum. Lateral and vertical movement was also provided on the case.

It was not found possible to eliminate completely the direct effect of the field, but it was reduced to less than 1% of the pull due to A at room temperature. The pull due to the field varies in a very complicated way with the field, and when reduced to a minimum by proper adjustment of B it invariably changed sign as the value of the field was increased. This is undoubtedly due to a changing inhomogeneity of the field, resulting from the varying importance of the lines of force due to the iron and those due directly to the magnetizing current. The pull of the furnace surrounding A, which is included in the field correction also introduces complications. The pull of the field could, however, be measured to 1 part in 20, so that errors from this cause amounted to less than 1/20% at room temperature.

The Furnace

In the actual experiments A was 1 cm diameter and was enclosed in a highly exhausted quartz furnace 12 mm internal diameter and $\frac{1}{2}$ mm wall. The heating current was supplied to a nichrome wire wound direct on to the quartz, and heat insulation was provided by an asbestos magnesia compound. To obviate convection currents which would disturb the measuring apparatus, the furnace was enclosed in a water jacket consisting of two brass tubes 27 and 30 mm respectively in external diameter, with $\frac{1}{2}$ mm wall and 1 mm gap between them. The water was made to circulate spirally in the gap. It will be seen that the thickness of heat insulation was only about 7 mm, which was very inadequate for high temperature work where very steady temperatures were required. The amount was, however, limited by the pole gap, which was itself determined by the maximum field required.

The method of maintaining the steady temperature by stabilization of the current supply is described elsewhere.* The magnesia-asbestos compound was found to be an excellent heat insulator, but on account of its low density it gave the furnace a low heat capacity. From this point of view ordinary sheet asbestos is much better, but it is unfortunately markedly ferromagnetic. Its effect on the coil B could have been considered as part of the general effect of the field, but unfortunately it changed very considerably and somewhat irregularly with the furnace temperature. The magnesia-asbestos compound was therefore preferred. Even this is slightly magnetic and contributed slightly to the pull on B, but the variation of its magnetization with temperature was found to be definite, and much smaller than for sheet asbestos.

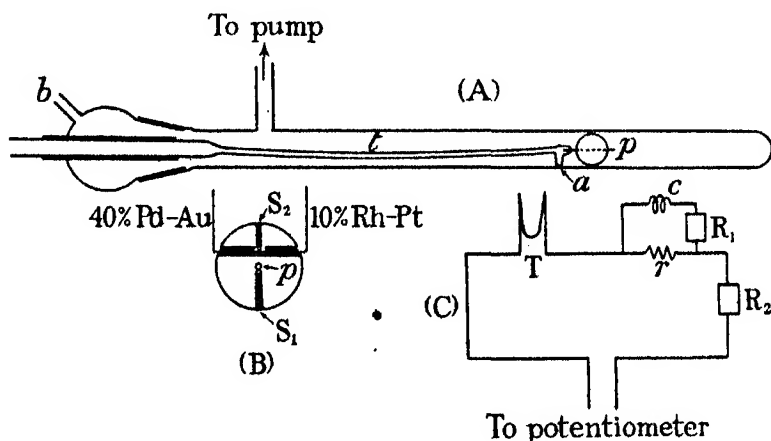


FIG. 4

Mounting of the Specimen

It was very necessary that the position of the specimen should remain absolutely fixed during an experiment, since the pull on the coil B depends on a high power of the distance separating it from the specimen. The specimen, an iron sphere, was mounted by a tiny set-screw, S_1 , fig. 4B, on a tapered tungsten pin, p , figs. 4A and 4B, which was sealed into a small quartz tube, t . This quartz tube was mounted rigidly in the male part of the ground joint connected to the furnace tube. The small tube was slightly curved so that on being slipped into position two small projections on the tube (one only is shown at (a)) pressed firmly against the furnace wall. The specimen was thus held in position by the elastic strain in the quartz tube, t .

* 'J. Sci. Instr.,' vol. 11, p. 95 (1934).

The Thermo-Junction

The temperature of the specimen was given by a thermo-junction of 40% palladium in gold as one element, and 10% rhodium in platinum as the other element. Both wires were 30 S.W.G. The e.m.f. of this thermo-junction is about five times that of platinum-platinum-rhodium, is more nearly a linear function of temperature, and consisting entirely of noble metals it is perfectly constant and easily stands the temperatures demanded in this experiment. The Pd-Au wire can be obtained from Messrs. Johnson Matthey, and, since it is cheaper than platinum, it seems strange that this excellent thermo-junction is not more widely known and used. Its e.m.f. is about equal to that of a Cu-constantin junction, but is of course much more reliable at high temperatures. The Pd-Au wire has excellent mechanical properties, and welds perfectly on to the Pt-Rh element. The thermo-junction was near the centre of the sphere and was held by a tiny set-screw, S_2 , fig. 4B. In order that the temperature registered should be definitely that of the centre of the sphere, the leads out from the iron were insulated by very thin quartz sheaths as shown in fig. 4B.

One of the thermo-junction leads passed out along the small quartz tube which supported the specimen, whilst the other passed through the side tube *b*. They were then joined to copper leads, the junctions being immersed in a water bath. The thermoelectric e.m.f. was measured on a potentiometer combined with a low resistance, low period, sensitive galvanometer specially made by Messrs. Tinsley.

The thermocouple, which was calibrated against a standard Pt, Pt-Rh couple, served to measure the absolute temperature of the iron, as well as the rise of temperature on adiabatic magnetization.

The magnetization process involved sudden changes of the field, and since the thermocouple leads enclosed a certain number of lines of force, each change of the field produced a ballistic throw of the galvanometer. This was compensated in the following way: a small coil C, fig. 4C, was placed in the magnetic field and joined in series with the thermocouple, T. R_1 and R_2 indicate resistance boxes and r was a small fixed resistance. Compensation was obtained by altering the resistance R_1 . Since the resistance of r was small, the changes in R_1 did not affect the thermoelectric current. The resistance R_2 was adjusted until the galvanometer was just aperiodic. The reason for this adjustment was as follows. At the high temperatures at which most of the experiments were made, radiation was so great that the excess temperature of the specimen due to adiabatic magnetization decreased

noticeably within a few seconds, even although this effect was minimized by making sure that the temperature measured was that of the centre of the sphere and not of its surface (see above). The method of measuring the rise was as follows. The field was switched on, and the galvanometer deflection noted. This rapidly reached a maximum, and the field was immediately switched off. The temperature then fell quickly to a value slightly less than the initial value, due to a loss of heat while the specimen was at a temperature above its surroundings. The true temperature change was taken to be the mean of the rise and the fall. The readings should naturally be taken as quickly as possible and consequently the galvanometer was made aperiodic. It was made only just aperiodic, however, since the time required to take up its deflected position is less than for the over-damped case. Owing to the impossibility of compensating the ballistic throws completely, and the time taken to establish the magnet field, there was nothing to be gained by making the galvanometer period very short. The actual value was 4 seconds.

The Electromagnets

Two different electromagnets were used in the experiment. Both were made in the departmental workshop. The first magnet was of the Weiss pattern with two coils each of a thousand turns 12 S.W.G. wire in series, taking a maximum of 20 amps, and giving a maximum field of 9600 gauss in a 3 cm gap over a 10 cm diameter. The second magnet was of the rectangular yoke pattern, having four coils of 2000 turns in parallel. The resistance was about $1\frac{1}{2}$ ohms and the maximum current was 60 amp. A field of 12,800 gauss could be obtained in a gap of 3 cm with a pole diameter of 15 cm. To avoid the building up of large inductive potentials on switching off a resistance of 9 ohms was kept permanently in parallel with the magnet. The control of a current of 60 amp presents some difficulties. For currents above about 30 amps, wire rheostats are unsuitable, and the current was controlled by water-cooled stud rheostats. Two such rheostats were used in series. The first consisted of four 60 cm lengths of 21 S.W.G. eureka wire, and four similar lengths of 19 S.W.G. eureka. Each wire was stretched by a short molybdenum spring along the axis of a 1 cm diameter glass tube. Heavy copper leads carried the current to and from the eureka resistances, which were water cooled. Heavy copper leads went from the ends of each eureka wire to the studs, so that any number of the wires could be brought into circuit. The 21 S.W.G. wires were $\frac{1}{2}$ ohm each, and the 19 S.W.G. wires were $\frac{1}{4}$ ohm each. The thinner wires were

cut out of circuit first, and carried up to 40 amp without giving trouble. The thicker wires were capable of carrying the full 60 amps. Finer adjustment of the current was obtained from the second stud rheostat. This consisted of a number of lengths of water-cooled german silver tube joined in series, with contacts from the ends of each tube to the studs. Eight lengths of tube were used, each being 60 cm long. The first six were 0.375 cm diameter, with a wall thickness of $\frac{1}{4}$ mm, and 1/12 ohm resistance. The last two tubes were double this diameter, but otherwise similar, and therefore were about 1/24 ohm each. This rheostat was used to cover the gaps of the larger resistance. At high values of the current, when very little resistance was in circuit, the 1/12 ohm steps gave considerable jumps in the current values. At large values of the current, however, the electromagnet field does not vary quickly with current, and the steps obtained were quite small enough.

The Image Effect

The attraction or repulsion of the specimen for the coil B is complicated by images of the magnetized sphere in the pole pieces. These images are similar to electrostatic images, and in comparative measurements could be ignored, if they remained a constant percentage of the total effect. If the permeability of the pole faces is infinite, and the pole faces are considered as infinite in extent, the images will be perfect reflections of the specimen in the poles. As the electromagnet field increases, however, the permeability falls, and the image is less perfect. The usual formula $\frac{\mu - 1}{\mu + 2} M$ (μ permeability, M magnetic moment of the specimen) cannot be expected to give the moment of the image, since the problem is complicated by the presence of the powerful electromagnet field. Weiss and Forrer* have given an experimental method of measuring the image effect. They give the correction for changing image effect to four significant figures. The writer has been quite unable to repeat this result with anything approaching this accuracy.

The image effect as measured by this method was certainly a function of the previous history of the magnet, and several other complicated effects seemed to enter into the results. The only point of agreement with Weiss and Forrer was that the change in the image effect was negligible for fields up to 6000 gauss. The actual change in the image effect was, however, very small, even at the highest fields, and was of importance only in the region below the Curie

* 'Ann. Physique,' vol. 12, p. 304 (1929).

point, where the magneto-caloric effect depends on a quite small rise in the magnetization at high fields.

The effect was eventually measured by another method. A magnetization curve for a single crystal at room temperature was taken, the intensity being plotted as a function of the field. Various observers have found that single crystals saturate completely in fields of a few hundred gauss at most. The magnetization curve obtained in the present experiment showed a rise of about $\frac{1}{2}\%$ between 7000 and 12,800 gauss. This was attributed to a decrease in the image effect. (It can easily be shown that the force exerted on the coil by the images is in the opposite direction to the force exerted by the specimen itself. Consequently a decrease in the image effect gives an apparent rise in the total effect.) A correction of the magnitude indicated was applied to all results given below.

Results

The present investigation has been carried out with five different kinds of iron—Armco, Hilger Spectroscopic, Heraeus electrolytic, large grain impure iron, and a single crystal prepared by the method of Edwards and Pfeil, and kindly presented to me by Dr. Gough, of the Metallurgical Department of the N.P.L.

ΔT as a Function of H —These five specimens gave almost identical results, so that only those of the single crystal will be given in any detail.

Results showing ΔT as a function of H are shown in Table I and fig. 5. The equation (1) gives a linear relation between dT and dH provided $\left(\frac{\partial \sigma}{\partial T}\right)_H$ is independent of H . This condition is fulfilled for temperatures below and not too near the Curie point. As the Curie temperature is approached $\left(\frac{\partial \sigma}{\partial T}\right)_H$ decreases with increasing H , and so the curves should be concave to the axis of H .

In Table I and fig. 5 the values of H have been corrected for the end demagnetizing field of the specimen, which for a sphere is $4\pi\sigma/3$. The absolute value of σ was obtained by assuming that the saturation value at room temperature was 1705 c.g.s. units per cc. The temperature indicated on each curve is for zero external field. The straight lines obtained at 523.5° , 716° , 730° , and 734° , and the curves at 744.5° and 756° which show slight concavity to the H axis, are in good agreement with theory. The curves at 620.5° and 663° show convexity towards the H axis, but a corresponding batch of curves

for the Heraeus iron showed a very slight concavity in the same region. This curvature is undoubtedly experimental error, due probably to the demagnetizing factor not being exactly $4\pi\sigma/3$.

The curves may therefore be considered as in good qualitative agreement with equation (1). To test the equation quantitatively, we can calculate the value of c_H , by using the slopes of these $(\Delta T, H)$ curves at the origin, and the

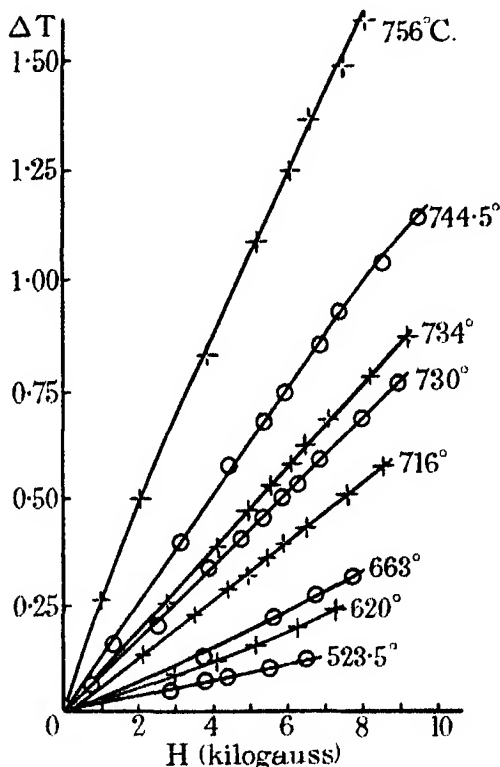


FIG. 5

values of $\left(\frac{\partial\sigma}{\partial T}\right)_{H=0}$ from fig. 9. The values of c_H calculated in this way show a sharp rise as the Curie temperature is approached—corresponding to the well-known specific heat anomaly. The absolute values of c_H determined in this way, were, however, some 15 to 25% higher than those given by Klinkhardt* from direct determination. One can hardly expect much better agreement than this with such an indirect method of determination, involving the

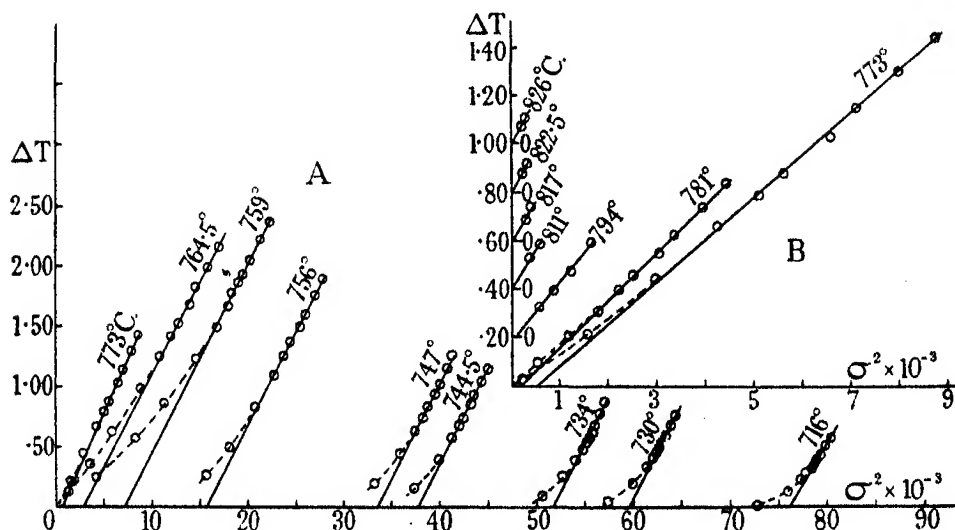
* 'Ann. Physik,' vol. 84, p. 191 (1927).

Table I.

T° C	H corrected	ΔT	σ	σ ² × 10 ⁻³	N	T° C	H corrected	ΔT	σ	σ ² × 10 ⁻³	N
523.5	2860	0.045				747	1457	0.195	577	332.5	
	3790	0.071					3285	0.440	599.5	359	
	4400	0.0795					4630	0.621	612	374.2	
	5530	0.102					5490	0.733	619	383.1	
	6500	0.121	1390				6070	0.828	623.2	388	
620.5							6970	0.931	630	396.5	
	3010	0.083					7570	1.017	633.5	402.8	
	4130	0.115					8670	1.143	639.5	409	
	5150	0.153					9620	1.258	644	414.9	
	6280	0.191				756					
663	7250	0.236	1210				996	0.26	396.8	157.2	
							2087	0.492	425.5	181	
	3470	0.122					3855	0.824	457	208.6	
	5610	0.217					5180	1.083	478.4	228.6	
	6740	0.271					8020	1.246	489	238.9	
716	7710	0.314	1100				8590	1.364	496	245.8	
							7490	1.488	505.5	255.6	
	307	0.019	853	727.5			8070	1.59	511.8	261.7	
	2125	0.129	871.4	758.5			9160	1.75	521.2	271.7	
	3510	0.226	878	771.0			10100	1.89	529	279.6	
	4390	0.283	881.2	776.4		759					
	4980	0.317	884.8	782.8			470	0.245	206	42.4	
	5490	0.357	886.8	786.5			1459	0.568	288.4	83.2	
	5895	0.388	887.8	788.0			2463	0.86	337.7	114.0	
	6490	0.424	890.0	793.2			4109	1.225	384	147.4	
	7010	0.502	892.8	797.0			5465	1.49	412	169.6	
	8570	0.566	896	803.0			6300	1.66	425	180.5	
							6867	1.77	433	184.0	
							7365	1.86	438.5	192.1	
							7755	1.925	443	196.2	
730							8330	2.045	451.5	203.8	
	702	0.062	757.5	573.6			9412	2.215	463	214.3	
	2525	0.198	773.8	598.0			10349	2.36	471	222.0	
	3900	0.333	783.3	613.4		764.5					
	4750	0.402	787.8	620.0			450	0.052	62.8	3.04	
	5350	0.449	790.0	623.9			860	0.121	114.2	13.03	
	5870	0.495	792.2	627.2			1850	0.357	190.3	36.2	
	6260	0.524	793.5	629.3			2840	0.621	243.1	59.15	
	6850	0.581	796	632.8			4480	0.980	299.8	89.8	
	7970	0.674	799	638.3			5720	1.25	331	109.6	
	8930	0.759	802	643.5			6550	1.41	348	121.1	
							7150	1.52	359	128.8	
							8000	1.68	375	140.6	
734							8580	1.82	384	147.2	
	897	0.083	712	506		773	9600	1.99	399.5	159.4	
	2735	0.254	726	527.2			10550	2.15	410	168.0	
	4110	0.385	735	540							
	4980	0.466	740.4	548.2			1140	0.029	46.7	2.18	
	5570	0.526	743	552			2280	0.108	89.8	8.05	
	6080	0.571	745.5	555.5			3300	0.217	125.3	15.71	
	6480	0.616	747	558.5			5000	0.441	172.2	29.65	
	7080	0.674	749	561			6230	0.656	206	42.40	
	8200	0.774	752.8	566.6			7100	0.782	226	51.05	
	9160	0.862	755.5	570.8			7600	0.872	237	56.03	
744.5							8500	1.025	256.7	65.8	
	1307	0.155	611	373			9050	1.14	266.5	71.0	
	3115	0.392	632	399			10100	1.295	282.7	79.8	
	4480	0.569	642.5	412.5			11000	1.43	295.2	87.1	
	5340	0.668	649	420.9		773					
	5920	0.735	652.5	425.5			1140	0.029	46.7	2.18	
	6810	0.845	658	433.0			2280	0.108	89.8	8.05	
	7410	0.921	661.5	436.9			3300	0.217	125.3	15.71	
	8510	1.035	667	444.5			5000	0.441	172.2	29.65	
	9470	1.14	672	451.0			6230	0.656	206	42.40	
							7100	0.782	226	51.05	
							7600	0.872	237	56.03	
							8500	1.025	256.7	65.8	
							9050	1.14	266.5	71.0	
							10100	1.295	282.7	79.8	
							11000	1.43	295.2	87.1	

Table I—(continued)

T° C	H corrected	ΔT	σ	$\sigma^2 \times 10^{-3}$	N	T° C	H corrected	ΔT	σ	$\sigma^2 \times 10^{-3}$	N
781	3570	0.098	73.6	5.41	2300	811	9900	0.128	61.2	3.74	3660
	5300	0.207	109	11.88			11900	0.184	75.6	5.70	
	6600	0.307	134	18.0		817	9980	0.080	52.8	2.78	3800
	7450	0.393	149.5	22.35			12050	0.136	62.7	3.93	
	8000	0.454	158.4	25.06		822.5	10000	0.076	48.1	2.32	3890
	8850	0.545	174	30.3			12100	0.118	56.3	3.25	
	9400	0.621	183	33.5		826	10000	0.069	45.4	2.06	4050
794	10420	0.734	198.7	39.44			12100	0.107	54.2	2.94	
	11400	0.833	210	44.04							
	6800	0.124	76.6	5.85	2780						
	8300	0.191	94.8	8.97							
	9700	0.274	109.5	12.12							
	11600	0.398	129	16.45							

FIG. 6—Rise of temperature as a function of σ^2

measurement of the slopes of two separate curves—a type of measurement which is always open to considerable error.

ΔT as a Function of σ^2 —The variation of ΔT as a function of σ^2 is shown in Table I and figs. 6A and 6B. These curves were obtained in the following way: the furnace temperature was kept as steady as possible so that the condition of the specimen corresponded, say, to the point A, fig. 1. A known field was switched on, bringing the specimen to a different temperature and magnetization indicated by the point B. The magnetization required in plotting figs. 6A and 6B is that corresponding to B, but owing to the rapid decrease in the excess temperature of the specimen, this could not be measured

at the same time as the rise of temperature ΔT . Time was allowed for the specimen to come into equilibrium with its surroundings (with field on) and the magnetization and temperature were noted. In this way the magnetization at any field was obtained at a large number of different temperatures, and that corresponding to any particular required temperature was interpolated.

Curves such as those demanded by equation (2) and fig. 2 are obtained, but a serious discrepancy arises when the actual values of N are calculated from the slopes of these curves, according to equation (4). In the Weiss theory N is assumed to be independent of both σ and T . The former assumption is verified since the linear relation between ΔT and σ^2 is obtained experimentally. If N is independent of T the $(\Delta T, \sigma^2)$ curves should, in the region below the Curie temperature, be a series of parallel straight lines, having the slope $N/2J\rho c_\sigma$. (J , ρ , and c_σ can be considered as constants). At temperatures above the Curie point, where the slope is given by $\frac{1}{2J\rho c_\sigma} (N + 1/\chi)$, the $(\Delta T, \sigma^2)$ curves should still be nearly parallel, since in the range of temperatures used $1/\chi$ was always small compared with N . This parallelism was obtained at temperatures below the Curie temperature, but at higher temperatures the slopes of the lines increased with increasing temperature, indicating a marked increase in the value of N . The variation of N with temperature—as calculated from the curves of figs. 6A and 6B—is given for the single crystal in fig. 7A. Corresponding results are given for the Heraeus iron in fig. 7B. Unfortunately the gradual fall in both σ and ΔT as T increases made it impossible to extend the results to higher temperatures by the present method.

Weiss and Forrer have made no mention of this variation of N with temperature. The value, as calculated from their results on nickel, is plotted in fig. 7C. It shows the same rapid increase above the Curie point as observed by the writer for iron, but there is also indication that N becomes constant again at higher temperatures. Here again, more values would be useful, but as in the case of iron, the experiments are beginning to fail at these temperatures.

The magneto-caloric rise of temperature is plotted in fig. 8 as a function of the temperature for three different values of the field. The field values given represent the internal field, i.e., external field corrected for demagnetizing coefficients.

Law of Corresponding States

The curves of figs. 6A and 6B combined with direct measurements of saturation intensities at lower temperatures enable us to determine the relation

between σ_0/σ_∞ and T/θ . It is already known from the results of Weiss and Forrer, and Hegg, that the theoretical curve based on the modified Weiss theory agrees only approximately with experiment. The collected results are shown in fig. 9, the theoretical curve being that given by the Weiss theory, with the quantum theory modification assuming that the quantum number $j = \frac{1}{2}$.

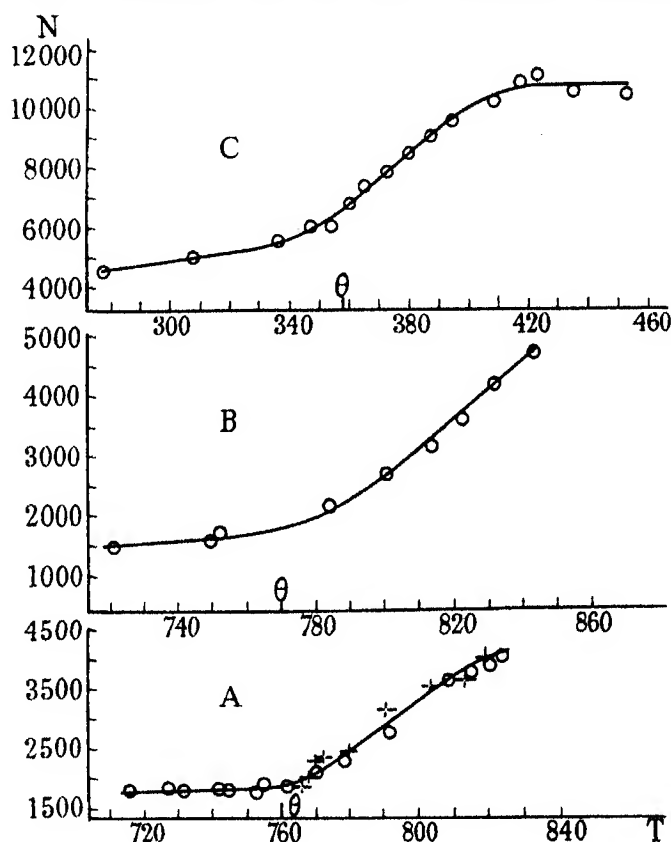


FIG. 7—A, single crystal iron \circ magnet 2; $+$ magnet 1. B, Heraeus electrolytic iron, magnet 2. C, nickel Weiss and Forrer.

It will be seen that for three specimens* of iron used by the writer the curves obtained were identical, showing that the deviation from theory is not a result of impurity or crystalline state. These deviations were slightly greater than those detected by Hegg.† No measurements have been made below room

* Two other specimens (large grain impure iron, and Hilger spectroscopic iron) gave identical curves, but the points have been omitted for the sake of clearness.

† Hegg's curve lies between that of Weiss and Forrer and the writer's curve for iron, but has been omitted for the sake of clarity of the figure.

temperature, the value of σ_0/σ_∞ for that temperature being put = 0.98, in agreement with the results of Weiss and Forrer.

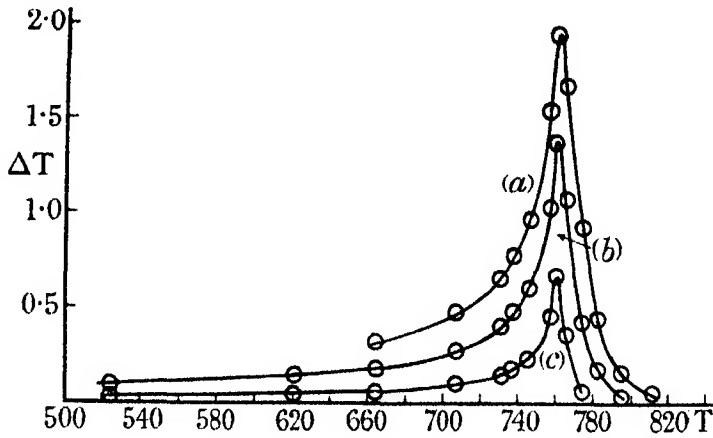


FIG. 8—(a) 8000 gauss, (b) 5000 gauss, (c) 2000 gauss

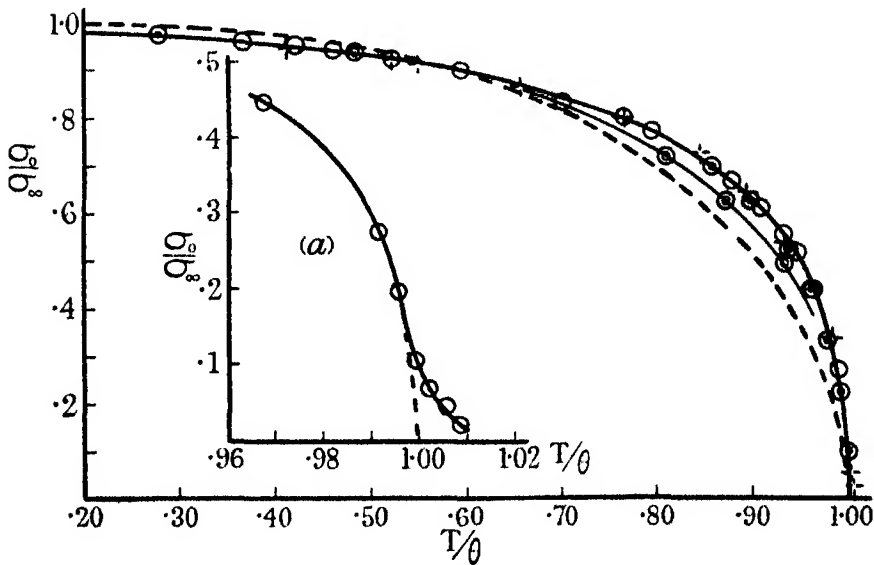


FIG. 9—... theoretical; \odot nickel Weiss and Forrer; \circ Heraeus electrolytic iron; \ominus single crystal iron; + Armco iron.

Several attempts have been made to explain the deviation from the theoretical curve. Neel* has introduced the conception of a fluctuating intramolecular field, but it would appear that the deviation of iron from the theoretical curve

* 'Ann. Physique,' vol. 18, p. 1 (1932).

is much more than predicted by him. Neel's theory seems to limit the deviation to an amount corresponding to the separation between the ferromagnetic and paramagnetic Curie point (see p. 48 of his paper). Stoner* has suggested that the orbital moments may become effective at high temperatures thus increasing the effective value of σ_∞ .

The fact that the value of σ_0/σ_∞ falls below the theoretical value at low temperatures has been emphasized by Weiss and Forrer and by Constant and Allen.† The latter have also pointed out that the deviation is different for different crystal types. Bloch's‡ extension of the Heisenberg theory leads to $(\sigma_0/\sigma_\infty, T/\theta)$ curves which depend on the crystal type, the curve being different even for different kinds of cubic symmetry. Whether the same hypotheses are capable of explaining the difference between the iron and nickel curves at high temperatures is not clear, since the theory is valid only at low temperatures. It is also somewhat discounted by the fact that Weiss and Forrer get identical curves for iron (body-centred) and nickel (face-centred) at low temperatures.

In addition the $(\sigma_0/\sigma_\infty, T/\theta)$ curve was found not to cut the temperature axis at a definite angle but to approach it gradually. This is shown on a larger scale in fig. 9 (a). This "foot" to the curve was present in all specimens tested, but was not always identical. It must be remembered, however, that the magneto-caloric effect gives σ_0^2 , and since σ_0 is already quite small, σ_0^2 is difficult to measure accurately in this region, although it was very definitely not equal to zero. It can always be assumed that this foot is due to impurity, or to the different states of the crystalline grains causing different regions to have different Curie temperatures. The latter suggestion is rather discounted since the "foot" exists even in a single crystal. The Heraeus iron containing only about 1/10% of impurity also gave a pronounced foot. An attempt was made to obtain some of the extremely pure iron prepared by the N.P.L., and sold by Messrs. Hilger, but this cannot as yet be obtained in pieces large enough for the present experiment. There is, however, no experimental evidence, in the writer's opinion, for the assumption of the existence of a definite temperature at which σ_0 can be said to disappear. Weiss and Forrer in their work on nickel assume a definite temperature 357·6, at which the spontaneous magnetism vanishes, but an examination of their curves at temperatures 358·1°, 360°, 361·8°, 365·3°, and 369·07° (fig. 10 of their paper) shows that spontaneous magnetization still exists—or, in other words, the $(\sigma_0/\sigma_\infty, T/\theta)$ curve does not

* 'Phil. Mag.,' vol. 12, p. 760 (1931).

† 'Phys. Rev.,' vol. 44, p. 232 (1932).

‡ See Sommerfeld and Bethe, "Handbuch der Physik,," vol. 24, p. 612 (1933).

approach the axis sharply. In their curve (fig. 16) showing σ_0^2 as a function of T they have omitted all points for temperatures above 355°C .

In the present work the Curie temperature has been determined by extrapolating the steepest part of the (σ_0, T) curve on to the temperature axis. The values of θ for single crystal and electrolytic iron, determined in this way, were 762°C and 769°C respectively.

The Paramagnetic State

Above the Curie temperature the ferromagnetic passes over into a quasi-paramagnetic condition. We shall now consider the properties in this region.

The Weiss-Langevin theory gives

$$\frac{\sigma}{\sigma_\infty} = \coth \alpha - \frac{1}{\alpha}, \quad (5)$$

where

$$\alpha = \frac{\mu (H + N\sigma)}{kT}, \quad (6)$$

μ being the magnetic moment of the carrier of the magnetism and k Boltzmann's constant for the carrier.

The quantum theory modification—assuming only two possible orientations for the elementary magnet—gives in place of (5)

$$\frac{\sigma}{\sigma_\infty} = \tanh \alpha. \quad (7)$$

Equation (7) also results from the Heisenberg theory.

This leads by well-known methods* to

$$\theta = \frac{MN\sigma_\infty^2}{nqR\rho}, \quad (8)$$

where q is the number of elementary magnets per atom, M is the molecular weight, and R is the gas constant per gm mol. On the Weiss-Langevin theory $n = 3$ and on the quantum modification $n = 1$.

Above the Curie temperature we have on both theories

$$\frac{1}{\chi} = \frac{N}{\theta} (T - \theta). \quad (9)$$

This is obtained by putting $\coth \alpha - \frac{1}{\alpha} = \frac{\alpha}{3}$ or $\tanh \alpha = \alpha$, so should be strictly true for small values of H and σ .

* Stoner, 'Phil. Mag.', vol. 12, p. 741 (1931).

By determining the slopes of the $(\sigma, H)_{T=\text{const}}$ curves near the origin, $1/\chi$ can be obtained and equation (9) can be tested. If $(1/\chi)_{H=0}$ is then plotted against T a straight line cutting the temperature axis at $T = \theta$ should be obtained. It is a well-known fact that for nickel this is not so; the curve is asymptotic to a line which cuts the temperature axis at θ_p , which is called the paramagnetic Curie point.* Experiments on iron above its Curie point have been carried out by Weiss and Foex,† and by Terry.‡ Weiss and Foex claim that when $1/\chi$ is plotted against T , two straight lines are obtained, the slope of the line at high temperatures being greater than that at lower temperatures. The two lines meet at 834°C . An examination of the results shows, however, that there is little justification for this interpretation. The number of points is very small, and they fit quite well on a smooth curve which becomes asymptotic to a straight line as the temperature increases.

The results of Terry give a smooth curve, but the results are not entirely satisfactory as a test of (9), since the values of $1/\chi$ are given for fields of 9000 gauss. In such large fields χ is too large—for temperatures near the Curie point—to justify the assumptions involved in developing equation (9). His results indicate, however, that even at the highest temperatures the $(1/\chi, T)$ curve is not a straight line.

Honda and Takagi§ have also made some measurements on the susceptibility above the Curie point, but their results show no sign of the two straight lines.

The writer has examined a portion of the $(1/\chi, T)$ curve for values of T up to 75° above the Curie point. For temperatures near to θ the value of $1/\chi$ was determined from the slope of the (σ, H) curve at the origin. At higher temperatures σ is a linear function of H and this extrapolation to zero H is not necessary. The measurements cannot be extended by the present method above the temperatures given, as it cannot be expected that a method designed for measurements in the ferromagnetic state would be useful over any great range of paramagnetic state. It has nevertheless been possible to trace the course of the $(1/\chi, T)$ curve over the region in which the magneto-caloric experiments indicated a variation of N with temperature. Both for the single crystal, fig. 10, and for the Heraeus iron the curves are smooth, and apparently become asymptotic to a straight line which cuts the temperature axis some

* See Forrer, 'J. Phys. Rad.,' vol. 7, pp. 10, 312 (1931); Neel, Strasbourg Thesis 1932, and 'Ann. Physique,' vol. 18, p. 40 (1932); Bates, 'Proc. Phys. Soc.,' vol. 43, p. 87 (1931).

† 'Arch. Sci. Nat.,' vol. 31, p. 96 (1911).

‡ 'Phys. Rev.,' vol. 9, p. 401 (1917).

§ 'Sci. Rep. Tohoku Univ.,' vol. 1, p. 237 (1911).

14° above the Curie point for the single crystal, and some 20° above for the Heraeus iron. The slope of the straight lines gives $N = 4400$ for the single crystal, and 4600 for the Heraeus iron. These values were calculated using equation (9) with θ equal to the value corresponding to the paramagnetic Curie point. The numerical data for fig. 10 were not taken from Table I, but from a special set of readings carried out in such a way as to get the greatest possible accuracy in the determination of σ at high temperatures. The great majority of the data of Table I do, however, lead to points very near to the curve of fig. 10. The initial curvature of the $(1/\chi, T)$ curve could be explained in terms of a variable N , but direct comparison with the magneto-caloric

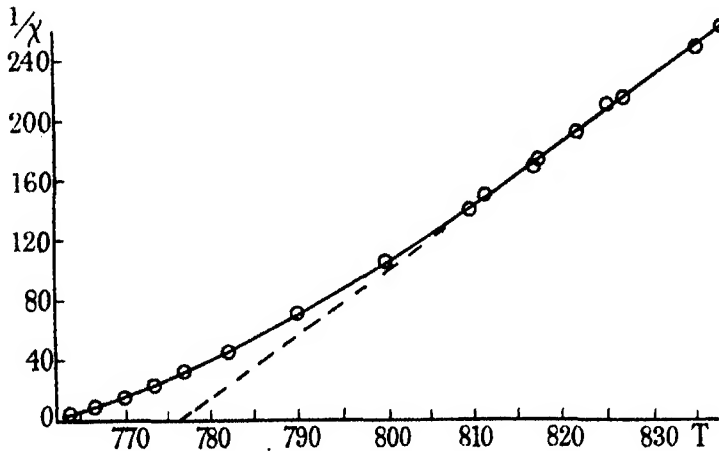


FIG. 10

results is difficult, as the result of the calculation for N depends on such a marked degree on the value of θ . Between the ferro- and paramagnetic Curie temperatures it is impossible to decide which value of θ to use. It is possible that the indefiniteness of the ferromagnetic Curie point is also a contributory factor to the curvature.

Since the $(1/\chi, T)$ curve does eventually reach an asymptote which enables us to calculate N , it appears that the curves 6A and 6B must become horizontal in the same way as 6C. It is most unfortunate that the experiments cannot be extended another 30° C.

Discussion

Magneto-Caloric Effect—The magneto-caloric effect, coupled with the assumption that σ_s is independent of T , gives directly the intramolecular field

$H' = N\sigma$, defined by the equation $dU = J\rho c_s dT - H'd\sigma$. The work of Weiss and Forrer for nickel and of the present writer for iron shows that—

(1) N is independent of σ ;

(2) N is a function of the temperature,* increasing from an approximately constant value below the Curie point to a considerably greater value in the range of some 60° above the Curie point.

Combining equations (8) and (9) we have

$$\frac{1}{\chi} = -N + \frac{MnkT}{\rho Lq\mu^2},$$

where L is the Loschmidt number, and μ the magnetic moment of the elementary magnet. n is a factor depending on the quantum number j ; $n = 1$ for $j = \frac{1}{2}$ and $n = 3$ for $j = \infty$. Professor Mott has pointed out to me that this formula depends only upon the assumption that the elementary magnets obey Boltzmann's law, i.e., that the number inclined at an angle ϕ to the field is proportional to $e^{-(H + H^1)\mu \cos \phi / kT}$. The approximate agreement below the Curie point of the $(\sigma_0/\sigma_\infty, T/\theta)$ curve with that given by the simple Weiss theory with $j = \frac{1}{2}$, indicates that this assumption cannot be very far from the truth.

Now in the region just above the Curie point $1/\chi$ is small compared with N , so that any marked variation in N must be accompanied by a similar variation in $MnkT/\rho Lq\mu^2$. Since k , M , ρ , and L are constants and T does not change more than 6% in the region considered, the variation must take place in $n/q\mu^2$. Let n_c , q_c , μ_c represent the values of these quantities at the Curie temperature, and n_p , q_p , μ_p the values in the paramagnetic state at the maximum temperature of the experiments. As long as spin moment only is effective, μ_p will be equal to μ_c , but if orbital moment also become effective at high temperatures the equality will no longer exist.

Then in iron since, from the magneto-caloric effect, N increases some three-fold.

$$\frac{n_p}{q_p\mu_p^2} \approx 3 \frac{n_c}{q_c\mu_c^2}.$$

Magneton Numbers and the Curie Temperature—The Weiss magneton number (W_p) in the paramagnetic state is defined by the equation

$$1123.5 W_p = \sqrt{3RC_M} = \sqrt{3R\chi_M} (T - \theta_p), \quad (10)$$

* Gerlach, 'Phys. Z.', vol. 33, p. 957 (1932) has already hinted at the necessity of some such assumption in connection with magneto-resistance experiments.

where C_M is the Curie constant per gram molecule, and χ_M the gram molecular susceptibility.

The magneton number (W_r) in the ferro-magnetic state at the absolute zero is given by

$$1123 \cdot 5 W_r = \frac{M}{\rho} \sigma_\infty.$$

It is usually assumed that the paramagnetic magneton number enables us to calculate the saturation intensity per unit volume (σ_p) in the paramagnetic state. This is the maximum moment which could be obtained if a sufficiently large field could be applied to the paramagnetic body. It is not necessarily equal to σ_∞ .

The following are the magneton numbers for iron and nickel :—

<i>Iron</i>	$W_p = 17$	$W_r = 11$
<i>Nickel</i>	$W_p = 8$	$W_r = 3$

Since W_p for both iron and nickel is greater than W_r , it has usually been assumed that $\sigma_p > \sigma_\infty$, or that there is more than one kind of elementary magnet in both iron and nickel.*

We shall now show that σ_p cannot be calculated from W_p unless both n_p and q_p are known.

The value of $\chi_M (T - \theta_p)$ —given from the straight portion of fig. 10—is $Lq_p \mu_p^2 / n_p k$. (The straight line means that N has become constant.)

Substituting in (10)

$$1123 \cdot 5 W_p = \sqrt{3RLq_p \mu_p^2 / n_p k} = \frac{M}{p} \sqrt{3\sigma_p^2 / n_p q_p}. \quad (11)$$

Thus σ_p cannot be obtained from W_p unless $n_p q_p$ is known. Previous workers have taken $n_p = 3$ and $q_p = 1$ —quite unjustifiable assumptions.

Let σ_θ be the saturation intensity at the Curie point. This again is not necessarily equal to σ_∞ . Let $\sigma_\theta = K_\theta \sigma_\infty$ and $\sigma_p = K_p \sigma_\infty$. Then using equation (11) and the magneton numbers given above we have for iron

$$\sqrt{K_p^2 / n_p q_p} = 17/11$$

or

$$K_p^2 / n_p q_p = 0 \cdot 8.$$

The Curie point is given by

$$\theta = \frac{N_p L q_\theta \mu_p^2}{M k n_\theta} = \frac{N M K_\theta^2 \sigma_\infty^2}{\rho L k n_\theta q_\theta}.$$

* See Stoner, 'Magnetism,' p. 72; 'Phil. Mag.,' vol. 12, p. 759 (1931).

Putting $\theta = 1030$, $N = 1600^*$ and using the appropriate values of the other constants for iron we have

$$K_\theta^2/n_\theta q_\theta = 2.65.$$

Since

$$K_p/K_\theta = q_p \mu_p / q_\theta \mu_\theta,$$

we have

$$\frac{n_p}{q_p \mu_p^2} = 3.3 \frac{n_\theta}{q_\theta \mu_\theta^2},$$

in excellent agreement with the results of the magneto-caloric effect.

The agreement for nickel is equally satisfactory. The change in N gives

$$\frac{n_p}{q_p \mu_p^2} = 2 \frac{n_\theta}{q_\theta \mu_\theta^2}.$$

The paramagnetic magneton number and the value of the Curie point give

$$\frac{n_p}{q_p \mu_p^2} = 2.2 \frac{n_\theta}{q_\theta \mu_\theta^2}$$

in excellent agreement with the value given above from the work of Weiss and Forrer on the magneto-caloric effect.

Thus if we are to fit our results into the framework of the Weiss theory we must assume that $n/q\mu^2$ varies rapidly near the Curie point. It is unfortunate that in each case the three quantities enter into the equations together, so that the observed variation cannot be attributed to either quantity separately.

On the Heisenberg theory, in its present state of development, the intra-molecular field factor depends upon both T and σ . Its value is

$$\frac{1}{2\mu\sigma_\infty} \left[zJ \left\{ 1 - \frac{J}{kT} + \frac{J}{2kT} \left(\frac{\sigma}{\sigma_\infty} \right)^2 \right\} \right],$$

where J is the interaction integral, and z the number of neighbours. The second term cannot be responsible for a large change in N in a restricted temperature range. The third term is not in accord with experiment, which gives N independent of σ . Alternatively, if the experiments are not considered final on this point, the term gives a variation of N in the wrong direction since N is measured at large values of σ below the Curie point and at low values above the Curie point.

My best thanks are due to Professor Mott for much helpful discussion on the theoretical aspects of these results, to Professor Tyndall for providing facilities

* The average value found experimentally in this paper.

for the work, and to the Colston Research Society of the University of Bristol for a grant towards the expenses of the investigation.

Summary

Various magnetic phenomena in iron, including the magneto-caloric effect, have been examined in the neighbourhood of the Curie point.

A new method is employed in the measurement of the intensity of magnetization. It is capable of an accuracy of 1 part in 1000 and has various advantages over the older standard methods.

The results demand that the intramolecular field factor N (which in the Weiss theory has been considered as independent of both σ and T) is independent of σ , but in the neighbourhood of the Curie point shows a rapid increase with increasing T . The increase begins near the Curie temperature and the value of N is approximately trebled in a range of 60°C .

The Weiss magneton numbers of nickel and iron in the paramagnetic state are discussed. It is shown that to explain either the magneto-caloric effect or the magneton numbers in terms of the Weiss theory we must assume that $n/q\mu^2$ increases as the temperature is raised above the Curie temperature. (μ is the magnetic moment of the elementary magnet, q the number per atom, and n a factor depending on the quantum number j .) Both in iron and in nickel the same variation is required to explain the magneto-caloric effect as to explain the magneton numbers.

The curvature of the $(1/\chi, T)$ curve just above the Curie point is also attributed to the variation in N .

Magnetization curves of iron are also given as a function of the reduced temperature, T/θ . Five specimens of iron were found to give results which fitted on to one and the same curve, which, however, showed considerable departure for the theoretical Weiss curve for $j = \frac{1}{2}$.

The Homogeneous Unimolecular Decomposition of Gaseous Methyl Nitrite

By E. W. R. STEACIE and G. T. SHAW

(Communicated by H. T. Barnes, F.R.S.—Received March 22, 1934)

Introduction

It is of considerable interest to investigate the homogeneous unimolecular decomposition of a series of related chemical compounds. The only series so far investigated is that of the aliphatic ethers.* On account of their simplicity, low boiling points, and lack of stability, the alkyl nitrites appeared to be worth investigation. The present paper deals with the first member of the series, viz., methyl nitrite. As will be shown, the decomposition of this compound is, in fact, homogeneous and unimolecular.

Experimental Procedure

Reaction velocities were measured in the usual way by observing the rate of pressure change in a system at constant volume. The reaction vessels were pyrex bulbs having a capacity of about 125 cc. The apparatus was similar to those used in a number of previous investigations.† The required temperatures were obtained by the use of a well-stirred oil bath, heated electrically. Temperatures were measured with standard mercury thermometers. The temperature could be maintained constant to within 0.25°C .

Methyl nitrite was prepared by the addition of a solution of nitrous acid to absolute methyl alcohol. The gas evolved was purified by passing it through a 50% sodium hydroxide solution, followed by a 40% ferrous sulphate solution to remove nitrogen oxides. It was then roughly dried by passage over calcium chloride. The gas was then condensed and fractionally distilled twice, the middle 3/5 being retained each time. Samples prepared at various times gave identical results. During the investigation the material was stored as a liquid in a bulb immersed in a solid carbon dioxide-acetone mixture.

* Hinshelwood and co-workers, 'Proc. Roy. Soc.,' A, vol. 114, p. 84 (1927); vol. 115, p. 215 (1927); 'J. Chem. Soc.,' p. 1804 (1929); Steacie, 'J. Phys. Chem.,' vol. 36, p. 1562 (1932); 'J. Chem. Phys.,' vol. 1, pp. 313, 618 (1933); Kassel, 'J. Amer. Chem. Soc.,' vol. 54, p. 3641 (1932).

† Steacie, 'Can. J. Res.,' vol. 6, p. 265 (1932).

Experimental Results

The Products of the Reaction—Since the form of the reaction rate curves and total pressure increase at completion did not vary with temperature or pressure, as will be seen later, it follows that there cannot be much variation in the products of reaction with varying conditions.

Some typical analyses of the gaseous products at completion, under various conditions follow :—

	%	%	%	%	%
NO	86 :	83	88	81	83
CO	10	9	3	6	—
Residue.....	4	8	9	14	—

In the above analyses NO was determined by absorption with slightly acidified ferrous sulphate. Considering the difficulty in gas analysis in the presence of nitrogen oxides, the results show excellent agreement.

The condensable products of the reaction were determined by separate experiments with a 250 cc reaction vessel, the products being washed out with water, or else frozen out in a small side tube after each run. Formaldehyde was always present in large amounts as shown by (1) its odour, (2) the melting point of paraformaldehyde, (3) the resorcinol test. Approximate quantitative determinations showed that formaldehyde constituted about 50% of the condensable products. The remainder of the condensable products consisted almost entirely of a liquid with a very low freezing point, and an odour and vapour pressure corresponding to methyl alcohol.

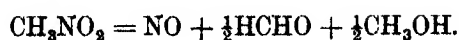
In order to determine the relative amounts of liquid and gaseous products, runs were made at 215° C. At pressures corresponding to 25 and 50% increase over the initial pressure the reaction vessel was suddenly cooled to -80° C, and the residual pressure determined. At this temperature neither methyl alcohol nor paraformaldehyde would have an appreciable vapour pressure. The vapour pressure of methyl nitrite, as determined by blank trials, is about 1.78 cm at -80°. Subtracting this we can find the partial pressure of NO + CO at -80° C, and can then calculate what it was at 215° C. The results given in Table I were obtained.

It appears, therefore, that the gaseous products formed are slightly less than the amount of CH_3NO_2 disappearing. The amounts of gaseous products are probably somewhat too small on account of a certain amount of solubility of NO in the condensed material.

Table I

	I	II	III	IV
Initial pressure, cm	42.19	41.83	36.79	38.72
ΔP , cm	10.53	20.92	18.40	19.36
CH_3NO_2 reacted	12.78	25.35	22.30	23.42
Pressure at -80°C	6.42	10.03	9.05	9.38
Pressure at -80°C corrected for v.p. of CH_3NO_2	4.64	8.25	7.27	7.60
$\text{PCO} + \text{NO}$ at 215°C	11.72	20.85	18.40	19.23

The main reaction is therefore approximately



On the basis of Rice's* theory of free radicals the mechanism can be given as—

- (1) $\text{CH}_3\text{NO}_2 = \text{CH}_3\text{O} + \text{NO}$,
- (2) $\text{CH}_3\text{O} = \text{HCHO} + \text{H}$,
- (3) $\text{H} + \text{CH}_3\text{O} = \text{CH}_3\text{OH}$.

This would lead to a 100% pressure increase at completion; the actual increase is 82.5%. There is therefore a certain amount of condensation of some sort accompanying the reaction.

The Pressure Change Accompanying the Reaction—The mechanism given in the last section would lead to a pressure increase of 100% at completion. Actually the pressure increased regularly in any run up to about 82.5%, and then diminished very slowly owing to some secondary reaction or condensation. The maximum pressure increases obtained under various conditions are given in Table II.

Table II—Maximum Pressure Increase

Temperature, $^\circ\text{C}$	Reaction vessel	Initial pressure, cm	Maximum pressure increase, %
240.7	Unpacked	28.48	82.6
240.7	„	37.69	82.4
240.7	„	11.86	80.6
240.7	„	36.22	81.6
230.2	Packed No. 2	23.01	79.4
219.9	„ No. 1	25.05	80.2
219.9	„ No. 2	26.32	81.8

The cause of the final slow decrease in pressure is probably the gradual formation of paraformaldehyde, a small amount of which condensed out in

* Rice and co-workers, 'J. Amer. Chem. Soc.,' vol. 53, p. 1959 (1931); vol. 55, p. 3035 (1933); vol. 56, p. 284 (1934).

the connecting tubing. In any case the subsequent diminution in pressure occurred very slowly. We have assumed that 82.5% pressure increase corresponds to complete reaction. This is supported by two facts. In the first place good unimolecular constants are obtained in any run on this basis (see Table III). We can also test the assumption as follows. If T_{25} and T_{50} represent the times for 25 and 50% pressure increase, then they should correspond to 30.3 and 60.6% reaction respectively. Theoretically, therefore, T_{50}/T_{25} should be equal to 2.58. Actually the mean ratio for all runs was 2.53. It therefore appears to be justifiable to use the values of T_{25} and T_{50} as a measure of the rate of reaction, and to assume that they correspond to 30.3 and 60.6% reaction respectively.

Complete data for some typical experiments are given in Table III. The values of K are computed on the assumption that the reaction is first order, and that 82.5% pressure increase corresponds to completion. It will be seen that satisfactory first order constants are obtained.

Table III—Data for Typical Experiments

Temperature 209.8° C Initial pressure 23.01 cm				Temperature 240.7° C Initial pressure 18.11 cm			
Time, mins	ΔP cm	% reaction	K	Time, mins	ΔP cm	% reaction	K
0	0	0	—	0	0	0	—
0.5	0.27	1.42	0.0130	0.5	2.37	15.9	0.151
1	0.59	3.11	0.0133	1	4.46	29.8	0.155
1.5	0.79	4.16	0.0120	1.5	6.17	41.2	0.154
2	1.09	5.73	0.0129	2	7.59	50.8	0.154
4	2.19	11.5	0.0132	2.5	8.81	58.9	0.154
7	3.78	19.9	0.0138	3	9.83	65.7	0.169
				4	11.51	77.0	0.159
11	5.49	28.9	0.0135	5	12.74	85.3	0.167
14	6.63	34.8	0.0133	6	13.63	91.1	0.175
16	7.46	39.3	0.0136				
20	8.79	46.3	0.0135				
23	9.73	51.2	0.0136				
27	10.84	57.0	0.0136				
29	11.30	59.4	0.0136				
31	11.90	62.6	0.0138				

The Effect of Pressure on the Rate—The summarized data for all runs are given in Table IV. The constancy of T_{25} and T_{50} with varying pressure indicates that the reaction is first order. There appears to be some indication of a falling off in rate at lower pressures. The effect, however, is of the order of magnitude of the experimental error. The rate at low pressures is now being investigated, and the discussion of the falling off in rate will be deferred until more definite information is available.

Table IV

Reaction vessel	Temperature, °C	Initial pressure, cm	T ₂₅ sec	T ₅₀ sec
Empty.....	189.9	29.99	3750	—
"	199.9	15.13	1740	—
"	199.9	23.77	1725	—
"	199.9	23.80	1717	—
"	199.9	34.34	1720	—
"	199.9	40.77	1689	—
"	209.8	6.80	860	2120
"	209.8	20.94	696	1770
"	209.8	23.01	673	1770
"	209.8	30.21	677	1722
"	209.8	30.91	690	1724
"	209.8	47.79	641	—
"	219.9	5.25	502	1135
"	219.9	8.65	412	1000
"	219.9	8.75	371	944
"	219.9	15.55	357	858
"	219.9	16.35	371	932
"	219.9	19.20	396	1084
"	219.9	21.73	352	882
"	219.9	21.79	349	835
"	219.9	22.20	376	750
"	219.9	22.50	327	736
"	219.9	27.10	384	1002
"	219.9	29.60	301	772
"	219.9	35.45	343	904
"	219.9	41.95	313	758
"	219.9	46.90	410	766
"	219.9	51.35	339	—
"	230.2	3.33	152	426
"	230.2	9.18	167	409
"	230.2	15.35	187	475
"	230.2	16.05	161	380
"	230.2	22.26	150	377
"	230.2	23.76	164	385
"	230.2	24.10	141	373
"	230.2	30.34	144	375
"	230.2	30.87	131	352
"	230.2	31.25	155	380
"	230.2	38.56	121	348
"	230.2	39.55	110	283
"	230.2	41.95	156	407
"	240.7	6.06	101	229
"	240.7	11.86	57.6	150
"	240.7	18.11	62.4	158
"	240.7	25.72	62.4	160
"	240.7	28.48	64.1	161
"	240.7	36.22	65.9	169
"	240.7	37.69	61.3	155
Packed	189.9	33.08	3390	—
"	199.9	20.09	1453	—
"	199.9	30.46	1460	—
"	209.8	13.07	642	1588
"	209.8	15.38	655	1685
"	209.8	17.83	665	1696
"	209.8	24.96	672	1690
"	209.8	25.09	696	1765
"	209.8	36.30	675	1674
"	209.8	43.61	665	1688
"	209.8	48.86	653	—
"	219.9	10.75	315	783
"	219.9	13.25	295	777
"	219.9	18.15	315	838

Table IV—(continued)

Reaction vessel	Temperature, °C	Initial pressure, cm	T ₁₅ , sec	T ₅₀ , sec
Packed	219.9	22.75	301	794
"	219.9	24.06	312	835
"	219.9	25.05	307	798
"	219.9	26.32	304	798
"	219.9	27.15	291	794
"	219.9	27.30	296	762
"	230.2	17.37	128	339
"	230.2	24.56	134	346
"	230.2	30.35	141	354
"	240.7	17.89	69.0	167
"	240.7	19.31	70.3	171

The Effect of Surface

In making comparisons of the rates of reaction at various temperatures and in various vessels, the usual method is to compare the extrapolated values corresponding to infinite pressure. In this paper, since there is no very definite indication of a falling off in rate with diminishing pressure, the mean values of T_{12.5}, T₂₅, and T₅₀ have been used for comparison, neglecting runs made at initial pressures below 10 cm. These values are given in Table V.

Table V—Mean Rates of Reaction

Reaction vessel	Temperature, °C	T _{12.5} , sec	T ₂₅ , sec	T ₅₀ , sec
Empty	189.9	1736	3750	—
Packed	189.9	1458	3390	—
Empty	199.9	804	1718	—
Packed	199.9	635	1457	—
Empty	209.8	315	675	1746
Packed	209.8	288	664	1687
Empty	219.9	156	350	858
Packed	219.9	135	304	798
Empty	230.2	70.2	147	376
Packed	230.2	61.3	134	346
Empty	240.7	—	62.4	159
Packed	240.7	—	69.7	169

The above table gives comparative rates for an empty reaction vessel, and different vessels packed with short lengths of Pyrex tubing so as to increase the surface-volume ratio about nine times. In general packing increased the rate from 10 to 15%. Hence the reaction in the empty bulb is complicated by a small amount of a heterogeneous reaction. The heterogeneous reaction, however, cannot amount to more than 1-2% of the whole process, and hence does not seriously affect the results.

The Temperature Coefficient

The values given in Table V for the empty reaction vessel are shown in fig. 1 in the form of a $\log T_{\infty} - 1/T$ plot. From the slopes of these lines, and of similar ones for the packed vessel, we obtain the values given in Table VI for the heat of activation.

Table VI

From $T_{12.5}$ empty vessel	36500 cal/gm mol
" T_{25} "	36500 "
" T_{50} "	36700 "
" $T_{12.5}$ packed vessel.....	35800 "
" T_{25} "	36200 "
" T_{50} "	36500 "
Mean	36400 "

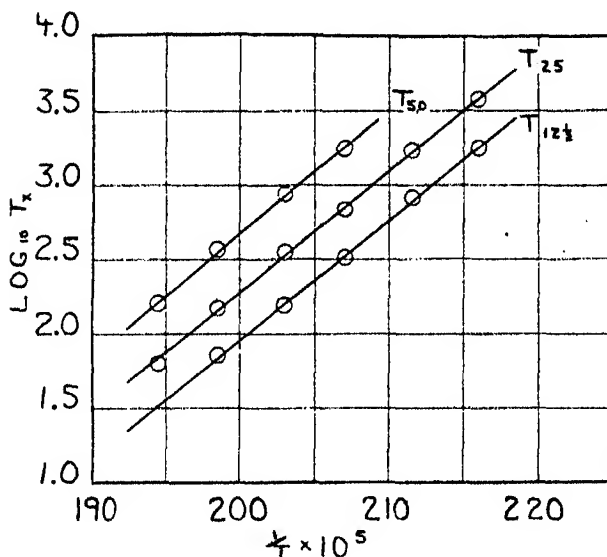


FIG. 1

The rate of the reaction may therefore be expressed by

$$T_{25} = 1.95 \times 10^{-14} e^{36400/RT} \text{ sec.}$$

If we assume that T_{25} represents 30.3% reaction, then we have

$$KT_{25} = 0.36,$$

where K is the velocity constant expressed in reciprocal seconds. Hence

$$K = 1.84 \times 10^{13} e^{-36400/RT} \text{ sec}^{-1}.$$

Since the falling off in rate at low pressures has not yet been definitely established, there is no use making an elaborate calculation of the number of oscillators involved. We may, however, make an approximate calculation on the basis of the simple Hinshelwood theory. If we assume that at 209.8°C the rate begins to fall off at a pressure of 10 cm, we have

$$\frac{\text{Number of molecules reacting per cubic centimetre per second}}{\text{Number of collisions per cubic centimetre per second}}$$

$$= \bar{e} \frac{36400 + \left(\frac{n}{2} - 1\right) RT}{RT} \left\{ \frac{36400 + \left(\frac{n}{2} - 1\right) RT}{RT} \right\}^{\frac{n}{2} - 1},$$

$$\left| \frac{n}{2} - 1 \right|$$

whence $n = 12$.

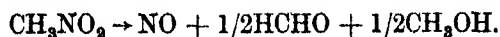
This is a minimum value, since the falling off in rate at low pressures has not been definitely established.

Further work is in progress on the decomposition of methyl nitrite at low pressures. The decompositions of other nitrites are also being investigated.

Summary

The thermal decomposition of gaseous methyl nitrite is a homogeneous first order reaction. It proceeds at a conveniently measurable rate between 190 and 240°C .

The overall reaction is mainly



The rate of reaction is given by

$$K = 1.84 \times 10^{13} e^{-36400/RT} \text{ sec}^{-1}.$$

There is no definite falling off in rate down to 5 cm pressure. On the basis of the Hinshelwood theory, therefore, at least 12 degrees of freedom are required to account for the observed rate.

Artificial Disintegration by Radium C' α -particles—Aluminium and Magnesium

By W. E. DUNCANSON, M.Sc., Ph.D., Trinity College, Cambridge, and
H. MILLER, B.A., Hutchinson Research Student, St. John's College,
Cambridge

(Communicated by J. Chadwick, F.R.S.—Received March 23, 1934)

§ 1 *Introduction*

A study of the protons emitted from certain elements when bombarded by α -particles has yielded valuable information on the structure of the atomic nuclei of light elements. The development of electrical counters for α -particles and protons has provided a method by which the emitted protons can be analysed in a more detailed manner than was possible by the scintillation method. These electrical methods have been applied to the examination of the protons emitted from many elements when bombarded by α -particles. For several elements the absorption curve of these protons reveals the presence of a number of discrete groups of protons each ending at a definite range. It is found that an α -particle of given energy may give rise to one or more groups of protons, each group corresponding to a transmutation process in which a definite amount of nuclear energy is either absorbed or released. It also appears that α -particles of all energies are not equally effective in producing protons, since the energies of the α -particles which produce protons fall into definite discrete groups.

The experimental evidence so far obtained has been co-ordinated by adopting the picture of the nucleus shown in fig. 1.

This figure represents the potential energy of an α -particle in the neighbourhood of an atomic nucleus. If the energies of the ground levels of the proton and α -particle in the nucleus are E_p^0 and E_a^0 respectively, then an incident α -particle of energy E will give rise to a proton of energy $E + E_a^0 - E_p^0$ an amount of nuclear energy $E_a^0 - E_p^0$ being released in the process. Thus the occurrence of a number of groups of protons can be accounted for by assuming that the α -particle may fall into one or other of a few α -particle levels in the nucleus with energies, E_a^0, E_a^1, \dots . It can also be supposed that the α -particle will later pass to the most stable of these levels by one or more transitions accompanied by the emission of γ -ray quanta of the appropriate energy.

On classical grounds, only α -particles of energy greater than the top of the potential barrier, E_m , can enter the nucleus, but from wave mechanical considerations an α -particle of energy less than E_m may have a finite probability of entering the nucleus. Gurney* has pointed out that there may be a resonance effect between the α -particle and the nucleus, which means that an α -particle of the appropriate energy, colliding with the nucleus, will have a very much greater chance of penetrating the potential barrier than if its

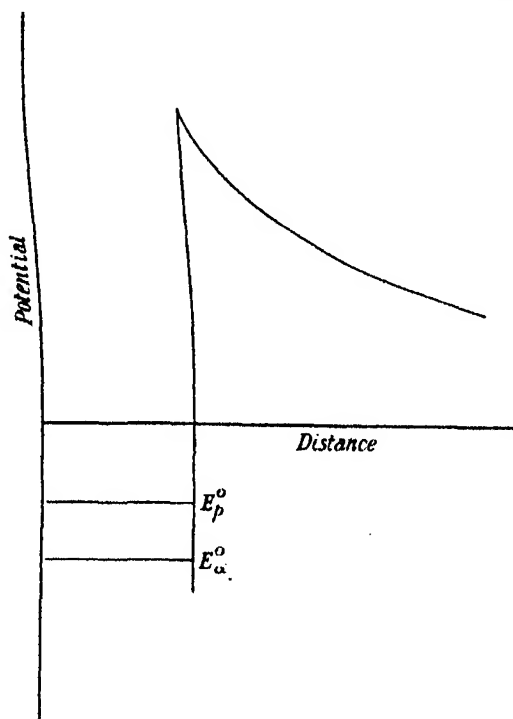


FIG. 1

energy were slightly higher or lower. Evidence† for this effect has been obtained from disintegration experiments, where it is found that protons are produced by α -particles which have entered the nucleus by passing both over the top of the potential barrier and through a series of discrete resonance levels in the barrier itself.

In general, in previous work with electrical counters polonium has been used as the source of the bombarding α -particles. Polonium emits α -particles

* 'Nature,' vol. 123, p. 565 (1929).

† Pose, 'Z. Physik,' vol. 64, p. 1 (1930); Chadwick and Constable, 'Proc. Roy. Soc.,' A, vol. 135, p. 48 (1932).

of mean range 3.8 cm (energy being 5.25×10^6 e-volts) and is free from strong β - and γ -radiation, so that the only ionizing radiations entering the counter are the protons to be observed. For the elements heavier than fluorine, however, the energy of the polonium α -particle is insufficient to reach the top of the potential barrier. Protons observed when elements, such as aluminium, are bombarded with polonium α -particles are therefore produced by α -particles which have passed through the potential barrier at some distance from the top. Hence α -particles of this energy do not permit a complete exploration of the potential barrier. Sometimes where the transmutation of an element is accompanied by an absorption of energy by the nucleus the process is more readily examined by using α -particles of energy greater than the polonium α -particles, since when the nucleus absorbs energy the proton ranges are relatively short. There is some need, therefore, to use the electrical counting methods for experiments in which more energetic α -particles are used for bombardment. Difficulty arises from the fact that all the radioactive sources available which give more energetic α -particles also emit strong β - and γ -radiation, and a counting method had to be developed which would not be disturbed by this ionizing radiation.

In the ordinary parallel plate ionization chamber, used in many experiments, γ -radiation gives rise to β -particles, mainly produced in the walls of the chamber. Superposition of the ionization currents due to these β -particles usually produces a total effect comparable with that due to a single proton whose presence it is required to detect.

Two conditions must be fulfilled in order to count successfully the individual protons in the presence of strong β - and γ -radiation. Firstly, the amplification of the primary ionization must be approximately linear, when the recorded effect of an individual electron, whether a primary β -particle from the source or a secondary particle produced in the chamber, will be negligible compared with that produced by a single α -particle or proton, since the ionization produced per centimetre path is for a proton at least of the order 20 times that produced by a β -particle. Secondly, the time taken to record completely the effect of a single particle must be very short in order to decrease the probability of the superposition of the effects of individual β -particles. The method adopted follows a plan similar to that used by Fränzl,* Bothe and Fränzl,† and Haxel.‡ The protons are collected in a suitable form of ionization chamber,

* 'Z. Physik,' vol. 63, p. 370 (1930).

† 'Z. Physik,' vol. 49, p. 1 (1928).

‡ 'Z. Physik,' vol. 83, p. 323 (1933).

the electrical impulses from which are, after amplification, applied to an oscillograph. A permanent photographic record of the oscillograph deflections is obtained. The various parts of the apparatus used will now be described in detail.

§ 2 Apparatus

1. *Counter*—A Geiger-Klemperer ball counter was used to detect the protons. The counter, fig. 2, consists of a brass cylinder C, 4 cm long and 3 cm in diameter closed at one end by a brass disc having a circular window W. 1.5 cm in diameter, covered with aluminium foil of 8.13 cm stopping power. A highly polished steel ball B, diameter 3 mm, is supported centrally 1 cm away from the window by a brass rod R, diameter 2 mm. This is, in turn,

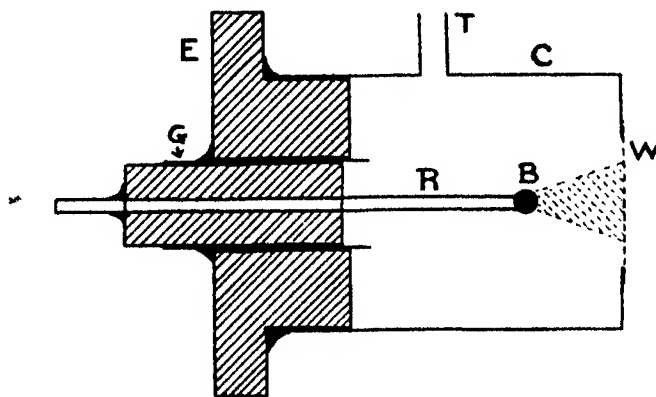


FIG. 2

supported by the ebonite disc E which closes the other end of the cylinder, and G is an earthed guard ring. Tube T is for the purpose of evacuating or admitting gas.

Geiger and Klemperer* have shown that for such a counter, with suitably adjusted negative potentials on the counter case, the initial ionization produced by each individual particle on entering is magnified linearly by collision. The multiplication factor increases with increasing counter potential until a maximum critical potential is reached beyond which the discharge changes character, and the charge collected by the central electrode becomes independent of the initial ionization. The time of collection is extremely rapid so that the counter, working in the linear region described, is suitable for our work.

* 'Z. Physik,' vol. 49, p. 753 (1928).

Since the multiplication factor of the counter, working in the linear region, increases rapidly with the voltage applied, and since the upper limit of the voltage for the linear region is comparatively sharp, a steady source of high potential is required. A suitable source of high potential has been described by Webster,* in which negative voltages up to 5000 volts can be obtained from the ordinary A.C. supply, free from ripple and other electrical disturbances, and which is stabilized so that the output voltages do not vary by more than $\frac{1}{4}\%$. This apparatus proved very satisfactory for the present work.

The counter was filled with dry hydrogen, a gas in which ionic mobilities are high, and the time of collection was thus considerably reduced. It is important in the present work for both the counting area and the multiplication factor of the counter to be as large as possible. These both increase with increasing gas pressure, voltage, and size of ball. With the voltage supply available the most convenient working conditions, with a 3 mm ball, were a pressure of 69 cm and a voltage of 4300 volts. The natural effect of this counter was 6 particles per hour.

The proton gave a maximum deflection of 10 mm on the photographic record. Deflections of appreciable size will occasionally be observed owing to superposition of β -rays in the counter and to avoid these, usually only deflections greater than 2 mm were counted. A consideration of the relation between the range of the proton and its specific ionization indicates that a proton of range greater than about 14 cm in air will have a specific ionization less than $\frac{1}{5}$ of the maximum. Neglecting deflections less than 2 mm, therefore, means that protons with residual range greater than about 14 cm will not be counted. It will be seen later that such an effect is apparent in the experimental curves.

In a counter of the type used in these investigations the size of deflections produced by particles of given velocity depends upon the region of the counter through which the particle passes, and will be a maximum for particles which pass close to the ball. The volume effective in counting is shown shaded in fig. 2. Small kicks will be produced if particles have only a small path in this region. It was found that the number of particles counted by this counter was equal to the number counted by a parallel plate ionization chamber of circular opening of 0.75 cm diameter.

To increase the counting area the counter, shown in fig. 3, was constructed in which seven balls, B_1, B_2, \dots, B_7 , of 3 mm diameter were used. Each is supported at the end of a brass rod of 2 mm diameter A_1, A_2, \dots, A_7 , fixed to a disc D in turn supported by the rod R. The rods A_1 – A_6 are arranged sym-

* 'Proc. Camb. Phil. Soc.,' vol. 28, p. 121 (1931–32).

metrically about A_7 on a circle of 1.5 cm diameter. A_7 is threaded to facilitate the adjustment of the central ball relative to the plane of the other six. The ebonite supports and guard ring are similar to those of the counter shown in fig. 2. The case C is 6 cm long and 5 cm in diameter, with an opening at the front of 2 cm diameter, covered by an aluminium foil. Outside this foil was a mica foil which would support atmospheric pressure, and movements of the aluminium foil on evacuation of the counter were thus avoided. Each of the outer balls was 1 cm and the central ball 0.85 cm from the front of the counter. For a case voltage of 4300 the pressure of hydrogen necessary was 46.5 cm.

2. *Amplifier*—The central electrode of the counter was connected to the grid of the first valve of a resistance-capacity coupled amplifier similar to that described by Wynn-Williams and Ward.* Indirectly heated valves in

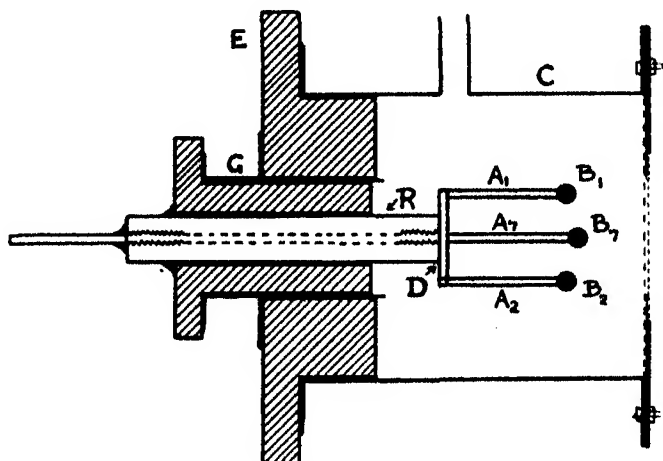


FIG. 3.

the third and fourth stages increased the amplification, while a further increase was obtained by having two pentodes in parallel in the output stage. Wynn-Williams and Ward have discussed at length the conditions necessary to allow an impulse to pass through the amplifier in a very short time. They point out that if the time is made too short the amplification will be seriously reduced, so that a compromise must be effected. In the present experiments it was found possible to use a grid leak of 4 megohms on the first valve without any interference from the Johnson effect, and the impulse was distorted in the last stage by using a coupling resistance and condenser of values 250,000 ohms and 0.001 microfarads respectively.

* 'Proc. Roy. Soc.,' A, vol. 131, p. 391 (1931).

3. *Oscillograph*—It will be seen from previous considerations that the natural frequency of the recording apparatus must be as high as possible. It was found most satisfactory to use a moving iron oscillograph of the type described by Wynn-Williams and Ward (*loc. cit.*). It was fitted with a suspension wire of $125\ \mu$ diameter the tension of which was adjusted until a natural frequency of 3300 was obtained. With the oscillograph element in a magnetic field of about 2000 gauss the sensitivity was 1.2 cm per 100 volts at a distance of 1 metre. The deflections of the oscillograph were recorded on cine-bromide paper moving at a rate of 20 cm per minute.

Before this oscillograph was adopted a number of other possible recording devices were tried, and it seems worth while to give a brief account of these. An Einthoven string galvanometer was modified by replacing the string by a thin phosphor-bronze strip, the thin edge of which covered a fine slit inclined at a small angle to its length. A small deflection of the strip uncovers a long length of the slit thus giving large magnification. A light placed behind the slit allowed a photographic record to be obtained. The slit of light thus photographed varies in intensity along its length and makes it difficult to determine the end point.

A Kerr cell was also tried, consisting of a pair of parallel nickel plates immersed in nitro-benzene. The cell was placed between crossed nicols. When an electric field exists between the plates light passes through the analysing nicol. The cell was connected to a modified output circuit in the amplifier and impulses of varying sizes passing through the amplifier were recorded as variations in intensity of light passing through the analysing nicol. Attempts to convert these intensities into lines of varying length by the use of an optical wedge gave a very uncertain end point to the lines, and for this reason both the Einthoven string galvanometer and the Kerr cell were abandoned.

A cathode ray oscillograph of the von Ardenne type was used in some preliminary experiments and proved to be quite satisfactory. The output circuit of the amplifier had to be adapted for this oscillograph and a step-up transformer was used, the secondary of which was connected across one pair of deflecting plates of the oscillograph. With an accelerating voltage of 3000 volts this instrument had a sensitivity at the fluorescent screen of 1.1 cm per 100 volts. By using a suitable lens the fast deflections of the fluorescent spot could be photographed. However, on account of its more robust nature the moving iron oscillograph was finally adopted.

4. *Arrangement of Source and Target*—Protons emitted in the same direction as the incident α -particles and also at right angles to that direction have been

observed. The arrangement of source and target for these two experiments are shown in figs. 4 and 5 respectively. In fig. 4 B, is a rectangular brass box closed at one end by a plate of ground glass. In the opposite end of brass is a hole W of 1 cm diameter closed with mica of stopping power 3.28 cm. Mica

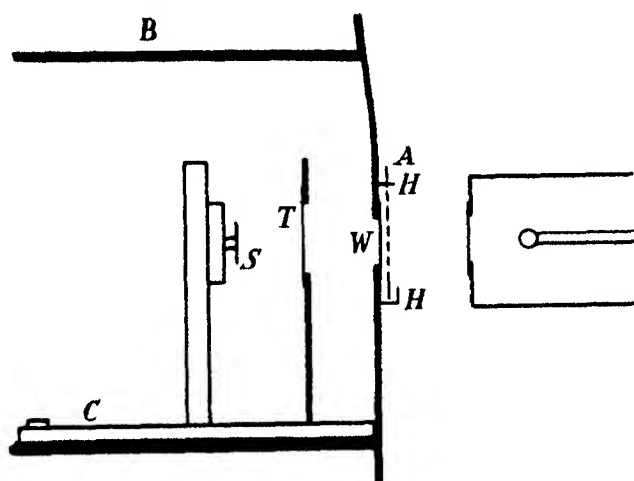


FIG. 4

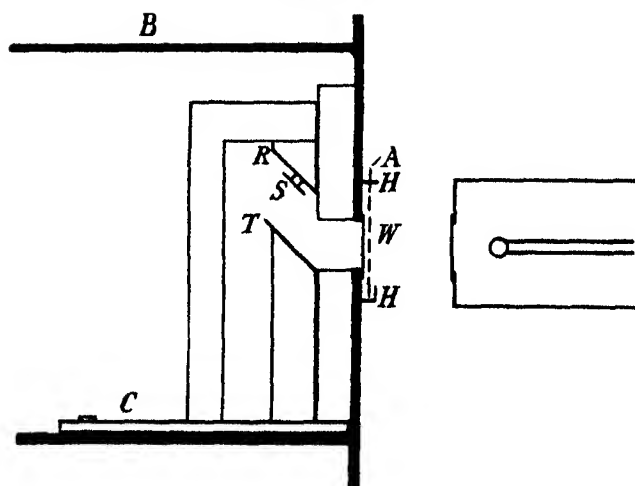


FIG. 5

absorption screens A may be inserted in the holder H. The source of α -particles S, and the target T of the element to be examined, are supported at the same height as W, and are carried on a brass plate C. The distances between the source, target, and counter can be varied at will. It was arranged that the box could be evacuated or gas circulated through it.

For the right angle experiments the supports for the source and target were modified and arranged as shown in fig. 5. S and T are arranged parallel to one another at an angle of 45° to the base of the box, and with their centres 1.5 cm apart. A block of lead 0.85 cm thick serves the twofold purpose of preventing α -particles from the source from striking the mica window W and also cuts down the intensity of the γ -rays reaching the counter. The centre of the target is 1.5 cm from the window. In experiments for both the forward and right angle direction the box B was placed between the poles of a strong electromagnet in order to prevent the β -particles, emitted by the source, from entering the counter.

The range of the α -particles incident on the target may be varied by introducing gas between the source and target or by placing absorption screens over the source. In general a gas is more convenient as it enables the range of the α -particles to be varied by small increments. In the experiments in the forward direction carbon dioxide gas was used for this purpose as neither carbon nor oxygen are disintegrated when bombarded by α -particles.

The source of α -particles was radium (B + C) deposited on a nickel disc of 8 mm diameter. Experiments have been made with sources of initial strength up to 100 millicuries.

§ 3 Aluminium

1. *Introduction*—The experimental observations on protons emitted when elements are bombarded by α -particles give information on two distinct problems connected with the nuclear structure of the bombarded elements. The first problem deals with the nature of the potential barrier of the nucleus for an α -particle and the probability of penetration of the α -particle through this barrier. The second problem is concerned with the α -particle and proton levels in the nucleus.

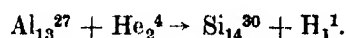
Many investigations have already been made on the structure of the aluminium nucleus by bombarding it with polonium α -particles.* The results of Chadwick and Constable show that in the region of the potential barrier examined (between 3.7×10^6 e-volts and 5.25×10^6 e-volts) the α -particle may enter the nucleus through one of four resonance levels, the maximum energies of which are 4.0, 4.49, 4.86, and 5.25×10^6 e-volts respectively, with width about 250,000 e-volts. The same workers have also

* Poae, 'Phys. Z.', vol. 30, p. 780 (1929); 'Z. Physik,' vol. 64, p. 1 (1930); vol. 67, p. 194 (1931); Chadwick, Constable, and Pollard, 'Proc. Roy. Soc.,' A, vol. 130, p. 463 (1931); Chadwick and Constable, 'Proc. Roy. Soc.,' A, vol. 135, p. 48 (1932).

shown that the α -particle on entering the nucleus may fall into one of two possible levels whose energies are 0 and -2.3×10^6 e-volts relative to the level from which the proton is ejected.*

In some recent experiments by Haxel† in which aluminium is bombarded by radium C' α -particles, a third α -particle level is indicated in the nucleus with an energy 2×10^6 e-volts relative to the proton level. This result will be discussed later in conjunction with the present experimental results.

In the above work, and also in that of the present writers, there has been no indication that the α -particle has not been captured in the transmutation. The following reaction is therefore assumed to take place



The resulting nucleus is therefore Si^{30} .

The relation between the velocities of the incident α -particle and of the emitted proton and the energy released by the nucleus in the transmutation is derived from considerations of energy and momentum relations, assuming that the α -particle is captured in the process. We have

$$Q = \frac{1}{2m_n} [m_p v_p^2 (m_p + m_n) - MV^2 (m_n - M) - 2MVm_p v_p \cos \theta], \quad (1)$$

where

- Q = energy released by the nucleus at a disintegration,
- m_p, v_p = mass and velocity of the emitted proton,
- M, V = mass and velocity of the incident α -particle,
- m_n = mass of the residual nucleus, and
- θ = angle between the direction of the incident α -particle and of the emitted proton.

2. *Nuclear Levels of Proton and α -particle*—Experiments were made to detect the proton groups produced by α -particles of a given energy. This was done by bombarding a thin aluminium foil, 0.4 cm stopping power, with the maximum range α -particles from radium C'. A group of 66 cm range was obtained which gives for the energy Q released at a transmutation a value in good agreement with the value -0.16×10^6 e-volts obtained by Chadwick and Constable. The yield of protons from the thin foil was so small that

* A recently determined range-velocity relation by Duncanson ('Proc. Camb. Phil. Soc.,' vol. 30, p. 102 (1934)) will be used in this paper. Using this relation the values of these nuclear energy changes become -0.16×10^6 and 2.07×10^6 e-volts.

† Haxel, 'Z. Physik,' vol. 83, p. 323 (1933).

a thick foil of aluminium, 8 cm stopping power, had to be used to detect the group corresponding to the second energy change of Chadwick and Constable. In this experiment the source was 0.3 cm from the target and the target 3.8 cm from the counter.

Fig. 6 is the absorption curve of the protons emitted in the forward direction under these geometrical conditions. If the protons of 107 cm range are produced by the maximum range α -particles, then the release of nuclear energy in this process agrees with the value $Q = 2.07 \times 10^6$ e-volts given by Chadwick and Constable. The 66 cm group is again observed. This absorption

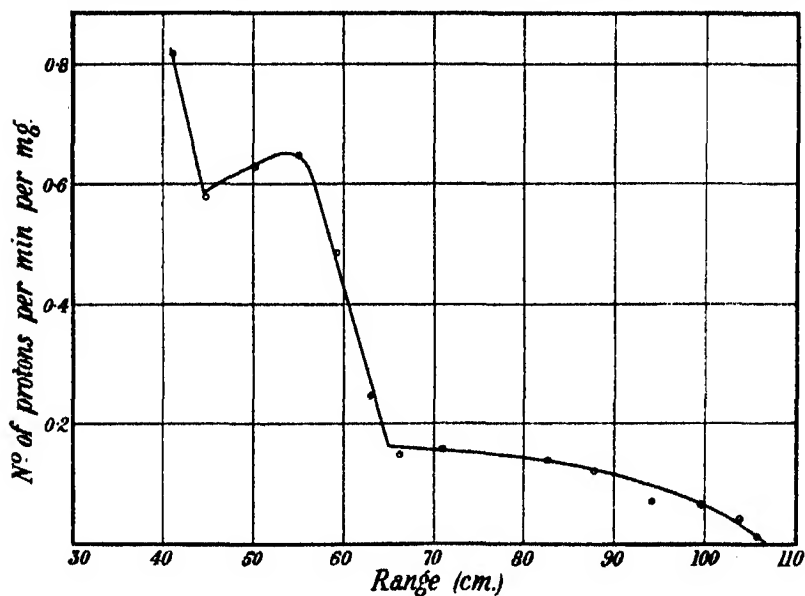


FIG. 6

curve includes groups of protons produced by α -particles entering the nucleus through resonance levels, but the geometrical arrangement was not sufficiently precise to resolve these.

Fig. 6 also suggests a group of protons ending between 40 cm and 45 cm, and to test whether this is due to a third value of the nuclear energy change further experiments were made with a thin aluminium foil, 0.4 cm stopping power, bombarded with 6.87 cm α -particles, both in the forward direction and at right angles. The absorption curve for the forward direction indicated a group of protons ending at 45 cm. Fig. 7 is the absorption curve of the protons in the right angle direction and shows two groups ending at 24.5 cm and 37.7 cm. If the 45 cm group in the forward direction and the 37.7 cm group

in the right angle direction correspond to the same value of the nuclear energy change, then a value of 70° is given for the minimum effective angle between the incident α -particle and the ejected proton, when the appropriate values are substituted in equation (1). This is in good agreement with the value 73° deduced from geometrical considerations. The two groups of fig. 7 therefore correspond to nuclear energy changes of -1.53×10^6 e-volts and -2.67×10^6 e-volts. There is evidence in the curve obtained by Rutherford and Chadwick,* by the scintillation method, for the existence of a group of protons ending at about 20 cm in the right angle direction. The proton group

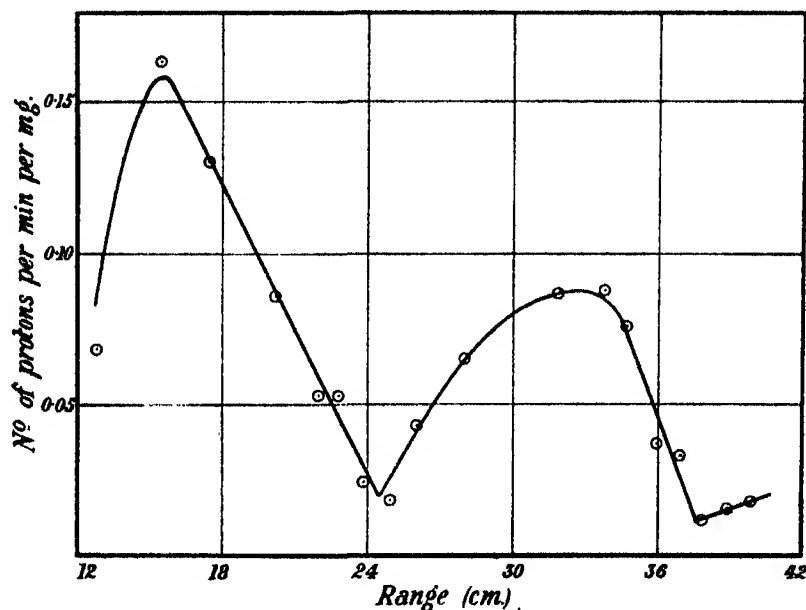


FIG. 7

due to $Q = -2.67 \times 10^6$ e-volts will have a maximum range of 30 cm in the forward direction, but this cannot be detected since it has a range shorter than the natural protons, *i.e.*, protons produced from the hydrogen contamination of the source and target.

The curve of fig. 7 shows the effect due to counting only the deflections which were greater than 2 mm. Deflections due to fast particles do not appear above the background of the records. Evidently only particles having a residual range of less than about 13 cm in the counter were detected and this is in good agreement with the value, 14 cm, obtained earlier from theoretical considerations.

* 'Proc. Camb. Phil. Soc.,' vol. 25, p. 186 (1928-29).

Table I

	I	II	III	IV
Nuclear energy change in 10^6 e-volts.....	2.07	-0.16	-1.53	-2.67
Approximate value of relative proton yield	1	3	3	5

Four possible values for the nuclear energy change at a disintegration are thus indicated and these are given in the second row of Table I; these have been numbered I, II, III, IV. The third row of Table I gives approximate values for the relative number of protons emitted for the respective values of Q . These ratios are obtained on the assumption that they are the same for α -particles of all energies, since the ratio of I to II is taken from the work of Chadwick and Constable,* while the ratios of II, III, and IV have been derived from observations of the protons emitted both in the forward and right angle direction from a thin foil in the present work.

If the ejected proton always arises from the same level, these four values of the nuclear energy change suggest that the α -particle causing the disintegration may fall into one of four levels which are shown diagrammatically in fig. 10. It may be assumed that the resultant nucleus finally settles down to its unexcited state by the passage of the α -particle to its ground state in one or more steps with the consequent emission of γ -radiation. Hence this γ -ray emission of aluminium may be expected to contain quanta of several discrete energies.

If the α -particle passes by a single transition from an excited level to the ground state, then γ -rays of the following quantum energy can be expected 4.74, 3.60, 2.23×10^6 e-volts. On the other hand, if transitions to the intermediate levels take place there will also be present quanta of energies 2.51, 1.37, 1.14×10^6 e-volts. It is possible that some of these transitions may be forbidden. This consideration suggests that the hardest component in the emitted γ -radiation must have an energy of at least 2.23×10^6 e-volts while it may have an energy of 4.74×10^6 e-volts.

Haxel† has recently made some experiments on the disintegration of aluminium using the α -particles from a radon tube and those from a thorium (B + C) active deposit source. In the experiments with the radon tube he obtained proton groups corresponding to the two nuclear energy changes found by Chadwick and Constable and verified by the present writers (present values

* 'Proc. Roy. Soc.,' A, vol. 135, p. 48 (1932).

† 'Z. Physik,' vol. 83, p. 323 (1933).

being now taken as -0.16×10^6 and 2.07×10^6 e-volts). With thorium (B + C) as a source of α -particles he observed a new group of protons which correspond to an energy change of -2×10^6 e-volts. This is not in accord with either of the two values (-1.53×10^6 and -2.67×10^6 e-volts) found in the present work. In the work of Haxel geometrical conditions were such that the minimum angle between the direction of the observed proton and the incident α -particle was 90° . In this direction α -particles of 8.6 cm range would produce protons of ranges 46 cm and 32 cm for nuclear energy changes -1.53×10^6 and -2.67×10^6 e-volts respectively. The 4.6 cm α -particles from thorium (B + C) will produce, with the energy change -0.16×10^6 e-volts, a proton group of range 33 cm. It seems possible that Haxel has been unable to resolve these three groups of protons, and this may account for the discrepancies between his results and ours*.

3. *Resonance Levels*—The second problem, as already indicated, deals with the penetration of the α -particle through the potential barrier. There will now be described experiments on the exploration of the potential barrier of the aluminium nucleus with α -particles of energies between 5.25×10^6 and 7.7×10^6 e-volts.

A thin aluminium foil (0.16 cm stopping power) was bombarded with α -particles of different ranges, and observations were made on the variation of the number of protons with the range of the incident α -particle. The arrangement of the source and target for this experiment is as shown in fig. 4. A thick silver foil was placed behind the aluminium foil to prevent α -particles striking the mica window. The distance between the source and target was 1.6 cm and between target and counter 1.6 cm. The range of the α -particles striking the aluminium target was varied by introducing into the box B, fig. 4, carbon dioxide at different pressures. The stopping power of carbon dioxide relative to air was taken as 1.53. Thus for atmospheric pressure of carbon dioxide, in a distance of 1.6 cm the range of the α -particles is reduced by 2.3 cm. In order to reduce the range still further several gold foils of a total stopping power of 0.85 cm were placed over the source. The α -particle range could then be varied from the maximum 6.87 cm down to 3.72 cm.

The curves obtained are shown in fig. 8. Curve 1 is for an absorption of 42.2 cm in the proton path, and curve 2 is for a corresponding absorption of 34.2 cm. It is seen that the proton yield decreases with decreasing α -particle

[* *Note added in proof*, May, 23, 1934—Haxel ('Z. Physik,' vol. 88, p. 346 (1934)) has recently shown that there are four possible values of the nuclear energy change and obtains results in good agreement with those of Table I.]

range to a minimum at 5.6 cm range, then rises sharply to a maximum at 5.25 cm range, and to a further maximum at 4.25 cm range.

In an interpretation of this excitation curve several points have to be born in mind. Firstly α -particles of a given range produce four groups of protons corresponding to the four values of the nuclear energy release. For 6.87 cm α -particles these ranges are 30 cm, 45 cm, 66 cm, and 107 cm respectively. As there is already 42.2 cm of absorption in the proton path for curve 1, the protons of the smallest range will not be counted. For 6.5 cm α -particles, the next group, now having a range less than 42 cm is not observed, so that the

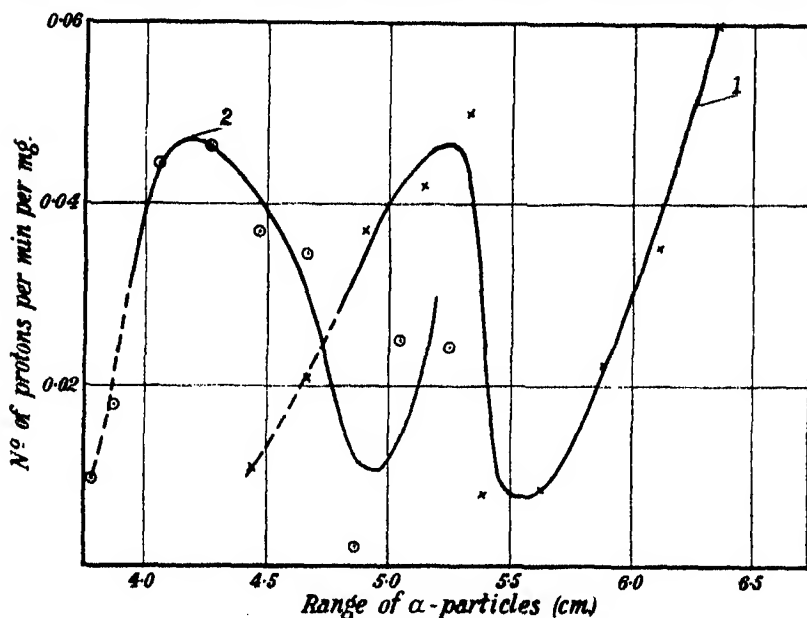


FIG. 8

decrease in the proton yield below 6.5 cm cannot be accounted for by the absorption of this group.

The third group of protons will be completely absorbed when the α -particle has a range of 4.6 cm and absorption will begin at a somewhat higher range, owing to the heterogeneity of the proton group. This fact will contribute to the decrease in curve 1. Comparison with curve 2 shows that the decrease is not wholly accounted for by this effect.

Similarly it can be shown that the only part of curve 2 which can be affected by absorption of the protons is the part below 4.2 cm α -particle range.

A second point to be considered is that only deflections greater than 2 mm have been counted, which means, as has been shown, that protons reaching

the counter with a range greater than 14 cm will not be counted. This accounts for the fact that for α -particle ranges greater than 5 cm the points of curve 2 fall below these of curve 1.

From fig. 8 it can now be deduced that as the range of the α -particle is reduced from 6.5 cm the decrease in proton yield corresponds to a decrease in probability of penetration of the α -particle through the potential barrier. Penetration through the barrier ceases at a range of 5.6 cm (energy equal to 6.7×10^6 e-volts). Riezler* who investigated the scattering by aluminium of α -particles of range 6.5 cm deduced that α -particles making central collisions with an aluminium nucleus must have an energy of at least 7×10^6 e-volts for them to have an appreciable probability of penetrating the top of the potential barrier. The above result is in good agreement with this.

The rise to a maximum at a range of 5.25 cm and again at 4.25 cm indicates the existence of resonance levels in the potential barrier. α -particles entering the nucleus by these levels will each give rise to four groups of protons. Experiments were made to detect the groups due to the nuclear energy change $Q = -0.16 \times 10^6$ e-volts. For this purpose a thick aluminium foil was bombarded by α -particles of maximum range from radium C' and the absorption curve of the emitted protons observed in the region 32 cm–66 cm. The distance of the source from the target was 2.6 cm and the distance of the target from the counter 2.1 cm. The results of this investigation are shown in fig. 9 where the number of particles per milligram per minute is plotted against the range. The upper curve is for deflections greater than 2 mm and the lower one for deflections greater than 5 mm. On the upper curve the low points after the end of a proton group and the general rise of the curve as the end of the next group is approached is due to the failure to count fast protons as has been pointed out earlier. This effect is accentuated in the lower curve of fig. 9. For these experiments about 200 particles were counted on each point of the upper curve, and about 50 to 60 on each point of the lower one.

From the two curves of fig. 9 it is seen that there are four groups of protons ending at 38 cm, 45 cm, 53 cm, and 66 cm respectively. The ranges indicated in the figure are measured from the point at which the α -particles enter the foil of aluminium. If, however, any of the proton groups are produced by α -particles having a range less than the maximum they originate at some point in the aluminium at which the α -particle has lost the required amount of energy. The real range of the proton group will thus be less than that indicated in the curves of fig. 9.

* 'Proc. Roy. Soc.,' A, vol. 134, p. 154 (1931).

Assuming that the group of range 53 cm is due to an energy change -0.16×10^6 e-volts and correcting the range according to the above consideration, which reduces it to 51.5 cm, it can be calculated from equation (1) that the α -particle producing this group has an energy of 6.61×10^6 e-volts, corresponding to a range of 5.45 cm. Referring again to the excitation curve in fig. 8 it is seen that as the α -particle range is decreased the yield of protons reaches a minimum between 5.7 cm and 5.5 cm. On further reduction of the α -particle range the proton yield rises to a maximum for an α -particle range of 5.25 cm (6.45×10^6 e-volts). This maximum in the excitation curve indicates

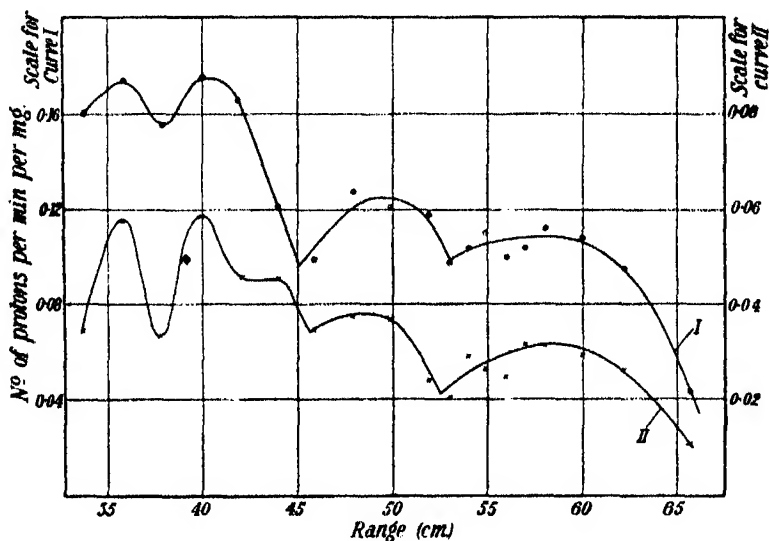


FIG. 9

the energy of the α -particle for which the probability of penetration of the barrier in this region is greatest, whereas the range of the α -particle deduced from the absorption curve, fig. 9, is that of the α -particle of maximum energy which can penetrate the barrier in this region. This would be consistent with the assumption that there is a resonance level in the potential barrier with a maximum energy of 6.61×10^6 e-volts and a width of 300,000 e-volts. However, little reliance can be placed on this method of determining the width of a resonance level as a difference of 1 mm in the position of the maximum in fig. 8 will alter our estimate of the width by about 200,000 e-volts.

After correcting the proton range in a manner similar to the above the range of the group observed at 38 cm becomes 35 cm, which is in good agreement with the group at 34 cm produced by an α -particle of range 3.9 cm, and

with the value of $Q = -0.16 \times 10^6$ e-volts, found by Chadwick and Constable.

Consider now the group ending at 45 cm. From the experiments on the thin aluminium foil it is seen that α -particles of range 6.87 cm produce protons of range 45 cm corresponding to a nuclear energy change of -1.53×10^6 e-volts. The resonance level revealed in fig. 8 at an α -particle range of 4.25 cm would give rise to four groups of protons and one would be expected ending at a range of about 42 cm, corresponding to $Q = -0.16 \times 10^6$ e-volts. In the upper curve of fig. 9 such a group is not separated from the 45 cm group, but there are indications of its presence in the lower curve. These are still more definite in the corresponding curves for deflections greater than 6 mm and 7 mm respectively, where a group ending at 42 cm is apparent. The range of the α -particle producing a group of this range with an energy change of $Q = -0.16 \times 10^6$ e-volts is 4.35 cm, giving an approximate value of 200,000 e-volts for the width of the resonance level concerned. Chadwick and Constable found proton groups of ranges 49 cm and 55 cm produced by α -particles of 2.7 cm and 3.1 cm range respectively and these would appear on our curves, fig. 9, at 53 cm and 59 cm respectively, but no attempt was made to resolve them.

Table II

Maximum range R of α -particle	5.45	4.35	3.9	3.45	3.1	2.7
Corresponding energy in 10^6 e-volts.....	6.61	5.75	5.25	4.86	4.49	4.0

In Table II are collected the results of Chadwick and Constable and the present writers in which is given the maximum range α -particle that can enter the respective resonance levels and their corresponding energies.

4. *Width of Resonance Levels*—Chadwick and Constable have used several methods to obtain information about the width of a resonance level.

(i) By observing the maximum and minimum velocities which the α -particle must have to liberate a certain proton group.

(ii) If for a certain group of protons the ratio of the yields obtained from a thick and thin aluminium foil is determined, then the product of this ratio and the energy the α -particle loses in passing through the thin foil gives an estimate of the width of the resonance level in question.

(iii) By assuming that the resonance level is an S-level, that is, one with angular momentum zero, the probability of α -particles of a given energy entering the nucleus by means of this level can be calculated. As we are dealing with an S-level, only α -particles with angular momentum between 0 and $\hbar/2\pi$ will concern us. Knowing therefore the total number of protons emitted by

α -particles entering at a given level the width of this level can then be calculated. This gives a minimum value for the width since it has been assumed that all α -particles which enter the nucleus cause a disintegration. Chadwick and Constable, using this method deduced a value of 230,000 e-volts for the width of the levels found in their experiments. However, they assumed that all protons emitted from the nucleus were confined to two groups produced by the energy changes I and II of Table I. It is seen from Table I that the total yield of protons from the groups I, II, III, and IV will be three times the total yield from I and II. This would lead to a value of 690,000 e-volts for the minimum width of the resonance level which cannot be reconciled with the estimates obtained from the two previous methods. If, on the other hand, it is assumed that the resonance level is a P-level—that is, α -particles entering the nucleus through this level have angular momentum between $\hbar/2\pi$ and $2\hbar/2\pi$ —the calculations give a value of 230,000 e-volts for the minimum width, in good agreement with the other estimates.

The same argument can be applied to the results of the present experiments. The width of the upper level of maximum energy 6.61×10^6 e-volts can be determined from the observed yield of the 53 cm group from the thick foil, fig. 9. Assuming this level to be a P-level a minimum value of 200,000 e-volts is given for its width, while an S-level gives a minimum width of 600,000 e-volts. Deductions from figs. 8 and 9 have led to an approximate value of 300,000 e-volts for its width. Thus it is not certain whether this is an S- or a P-level, though it seems more likely to be a P-level since an S-level would have a minimum width of 600,000 e-volts.

Since no group of protons produced by the entry of α -particles through the 5.75×10^6 e-volts level is resolved in the absorption curve, fig. 9, the width cannot be estimated from arguments based on the proton yields, though an approximate value of 200,000 e-volts has already been indicated for the width of this level.

A diagrammatic representation of the interaction field between the α -particle and the aluminium nucleus is given in fig. 10, showing the position of the resonance levels and the position of the α -particle levels in the nucleus relative to an arbitrary position of the proton level.

§ 4. *Magnesium*

The scintillation method has already been used* to detect the protons emitted when magnesium is bombarded with α -particles from Ra C', and

* Rutherford and Chadwick, 'Proc. Phys. Soc. Lond.,' vol. 36, p. 417 (1924).

protons up to about 40 cm range have been observed. The use of electrical counters enables a more detailed investigation to be made.

The present work on magnesium has been mostly confined to an examination of the protons emitted in a direction approximately at right angles to the incident α -particles, since the disintegration is accompanied by an absorption of energy by the nucleus and the ranges of most of the protons in the forward

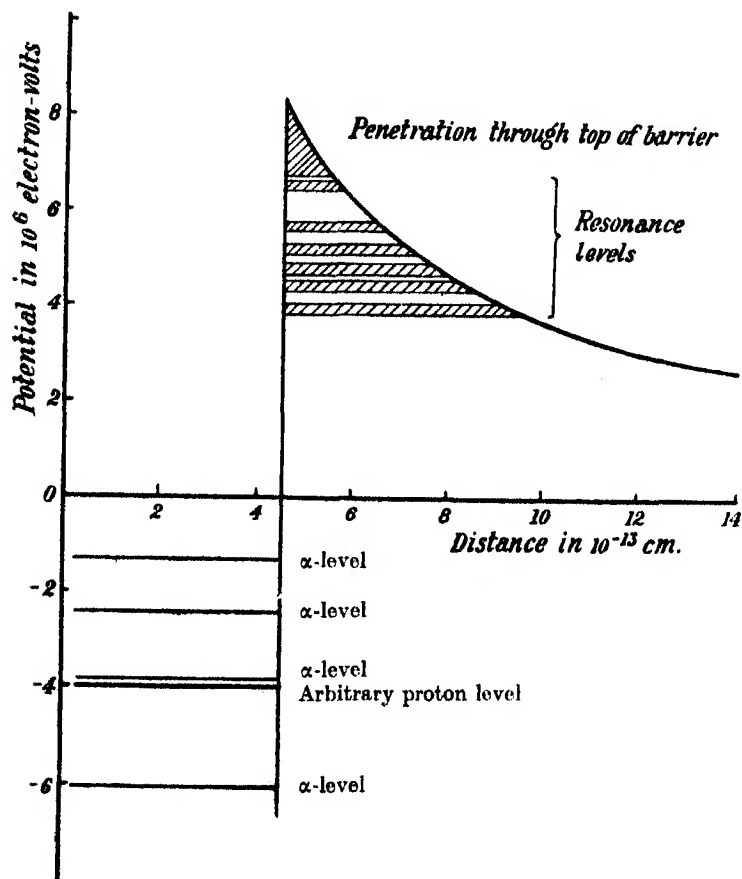


FIG. 10

direction are shorter than those of the natural protons. The interpretation of the results cannot be conclusive until it is known whether one, two, or all the isotopes of magnesium are concerned in the disintegration.

Valuable information can be obtained by observing the protons produced by α -particles of a given energy. In practice this was nearly realized by bombarding a foil of magnesium of 2 mm stopping power. The loss of energy of an

α -particle from Ra C', of energy 7.7×10^6 e-volts, in this foil is only about 200,000 e-volts. The foil was prepared by depositing magnesium on a sheet of silver foil by evaporation in a vacuum.

α -particle Levels in the Nucleus—Fig. 11 is an absorption curve of protons emitted in the right angle direction from a thin magnesium foil of stopping power 0.2 cm with the arrangement of source, target, and counter as shown in fig. 5. The effect of the failure to count protons of range greater than 14 cm, which has been discussed earlier, is apparent in the curve. From geometrical considerations the minimum angle between the proton and the incident α -particle is 75° . Fig. 11 reveals two proton groups ending at 21 cm and 31 cm.

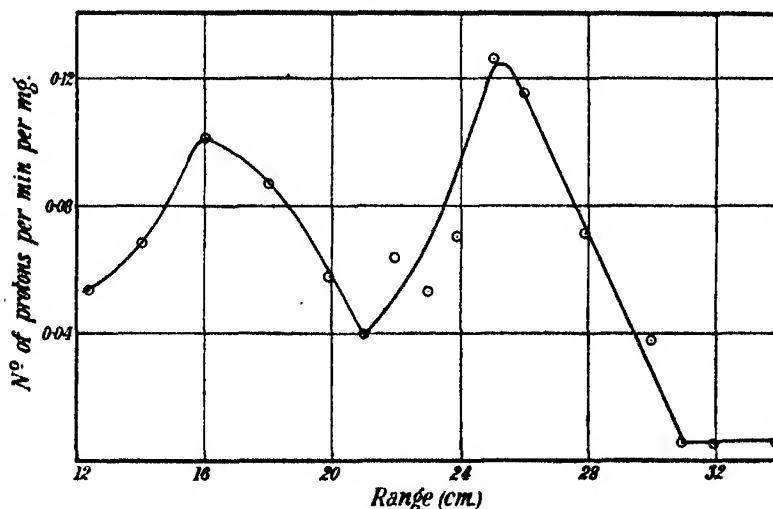


FIG. 11

There was also some evidence for a group of still greater range, but as its yield was so small the group was looked for in the forward direction from a thick magnesium foil. The absorption curve of protons thus obtained revealed a group ending at 39.5 cm, which corresponds to the 31 cm group in the right angle direction, and a much weaker one ending at about 50 cm. It was difficult to determine accurately the end point of this latter group as its yield was so small.

Since magnesium consists of three isotopes Mg_{24} , Mg_{25} , and Mg_{26} , it is not possible at present to decide which isotope or isotopes are involved in the production of these protons and the curves will be interpreted with reference to each one. In Table III the results are collected for these two experiments

in the right angle and forward direction. In columns 4, 5, and 6 are given the energy changes for each isotope corresponding to the various proton groups.*

Table III.

Range of α -particle in cm	Range of proton in forward direction, cm	Range of proton in right angle direction	Energy change in 10^6 e-volts		
			Mg ₂₄	Mg ₂₅	Mg ₂₆
6.87	50	—	-1.15	-1.16	-1.18
6.87	39.5	31	-1.90	-1.91	-1.93
6.87	—	21	-2.87	-2.88	-2.91

No deductions can be made about the emission of a γ -radiation as it is not known whether all the energy changes belong to the one isotope.

Resonance Levels—Experiments were also made to investigate the penetration of the α -particle through the potential barrier of the magnesium nucleus. A thin film (0.2 cm stopping power) of magnesium was bombarded by α -particles from Ra C' and protons which were emitted in the right angle direction counted. The apparatus used was that of fig. 5. A brass cylinder was fitted on the source holder R in order to hold mica screens in the path of the bombarding α -particles. The α -particle range was varied from about 6 cm to 4 cm and fig. 12 shows the variation of the proton yield with α -particle range. The absorption in the path of the protons was 12.1 cm.

This curve reveals two resonance levels in the potential barrier for α -particles of range greater than 4 cm. The ranges of the α -particles for maximum probability of penetration through the resonance levels are 5.0 cm, energy = 6.3×10^6 e-volts, and 4.25 cm, energy = 5.7×10^6 e-volts, respectively. The curve also indicates that penetration through the top of the potential barrier stops for an α -particle range of 5.25 cm, energy = 6.5×10^6 e-volts.

The α -particles entering the nucleus through each resonance level will produce three groups of protons corresponding to the three values of the nuclear energy change, and an attempt was made to detect these by bombarding a thick magnesium foil with Ra C' α -particles and observing the protons emitted in the right angle direction. It was found difficult to separate with

* Klarmann ('Z. Physik,' vol. 87, p. 411 (1934)) has recently described some experiments in which magnesium has been bombarded by polonium α -particles. There are considerable differences between his results and ours, but both sets of experiments give an energy change of -1.9×10^6 e-volts. We have observed no protons corresponding to the energy change -0.6×10^6 e-volts deduced from his experiments, although the yield of the corresponding group in his experiments was quite large. With such an energy change α -particles of 6.87 cm range would have given a proton group of about 60 cm range in the forward direction.

certainly the individual groups of this curve, and it did not seem profitable to pursue the investigations further at this stage, particularly as there is no means of deciding which isotope or isotopes of magnesium are responsible for the observed effects.

No accurate measurements have been made of the masses of these isotopes and it can only be assumed that the mass defects of Mg_{24} , Mg_{25} , Mg_{26} lie on the curves for elements of mass numbers $4n$, $4n + 1$, and $4n + 2$ respectively,* where n is the number of α -particles in the nucleus. If this assumption is

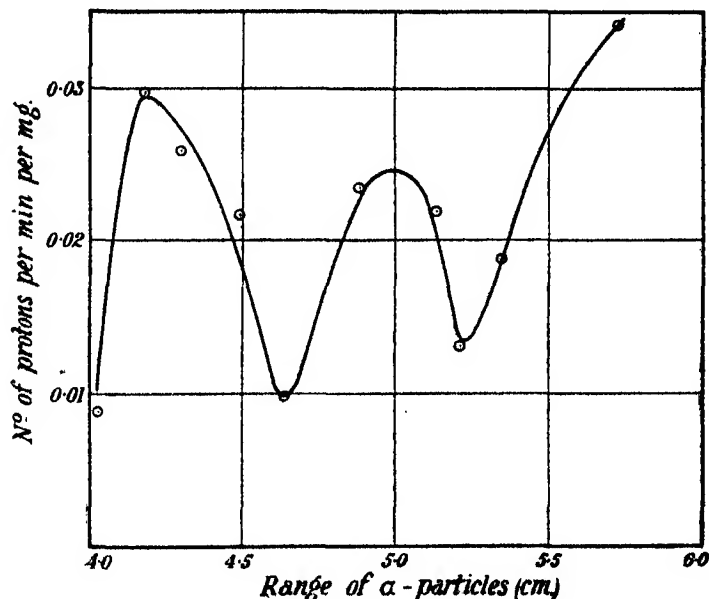


FIG. 12

correct, the transmutations $\text{Mg}_{24} \rightarrow \text{Al}_{27}$, $\text{Mg}_{25} \rightarrow \text{Al}_{28}$, and $\text{Mg}_{26} \rightarrow \text{Al}_{29}$ would each be accompanied by the absorption of energy of a few million volts (that is, assuming that the aluminium isotopes also lie on their appropriate mass defects curve). Consideration of the relative abundance of the three isotopes† suggests that the most likely transformation is $\text{Mg}_{24} \rightarrow \text{Al}_{27}$, but either of the two other isotopes may also be concerned in the production of the protons.

The writers wish to express their thanks to Lord Rutherford for his interest in the work, and to Dr. Chadwick for suggesting the problem and for his

* Chadwick, Constable, and Pollard, 'Proc. Roy. Soc.,' A, vol. 130, p. 463 (1931).

† The isotopes Mg_{24} , Mg_{25} , Mg_{26} are present in the ratio 77.4 : 11.5 : 11.1 (Aston, "Mass Spectra and Isotopes," p. 236).

The quantum mechanical perturbation theory can be applied in two distinct ways, which we may call the stationary and non-stationary methods, to the problem considered. In the former the whole system, metal and light wave and photoelectric current, is assumed to be in a stationary state, while in the latter the metal alone is supposed to be in a stationary state, and the light wave is suddenly turned on at a definite time. After a long time we should expect a steady state to be reached, and would naturally expect the properties of this state to be the same as those of the state considered by the stationary method. Mathematically the two differ only in the methods adopted to solve the same differential equation, the first order equation of the perturbation theory. In the stationary method, the total wave function is written down directly, appealing to physical considerations to justify the exclusion of those parts of it representing electrons moving towards the surface of the metal. In the non-stationary method, the total wave function is determined as an expansion in a series of solutions of the unperturbed problem. These partial wave functions then have no direct physical significance, and we cannot exclude any of them on *a priori* grounds. It is here that Tamm and Schubin fall into error. Remarking that the total wave function must represent a stream of electrons moving outwards from the surface of the metal, they conclude wrongly that the same must be true of each partial wave function entering into the expansion. This evidently amounts to arguing that "the group velocity must be outwards from the surface, hence so must the wave velocity of every wave"—a well-known *non sequitur*.†

In the present paper the correct result for the surface effect, using the proposed model, is derived by the two methods outlined above, and the results of more general calculations, in which account is taken of the refraction and reflection of light at the metal surface, are quoted and shortly discussed. A later paper will present a more detailed comparison with experimental results.

Calculation by the Stationary Method

3.1. *The Method*—We consider the behaviour of a single electron in the metal, using the model proposed in the preceding section, and calculate the

† In a metal bounded by an infinite plane, where the wave equation separates in rectangular Cartesian co-ordinates, a certain arbitrariness remains in the wave functions representing free states, in that we can have outward and inward moving waves of the same energy, both of which must be included in our expansion. In an atom, with the wave equation separating in spherical polar co-ordinates, the behaviour of the wave function at the origin determines a definite combination of the inward and outward waves, and the same difficulty does not arise.

perturbation produced by an incident light wave. The metal is taken to occupy all space to the negative side of the plane of yz , and the light wave, of frequency ν , is supposed to be incident upon the surface in a direction making an angle θ with the x -axis. For convenience, the plane of incidence is supposed to be the plane of xy , and refraction and reflection of the light will be neglected.

The initial wave functions are determined, and the light wave is considered to act as a small perturbation. Two equations are found to determine this, to the first order, inside and outside the metal, and these are to be solved in such a way that the perturbed wave function and its first derivatives shall be continuous at the surface. The general solution obtained in this way still contains two arbitrary constants. These are determined from the condition that the total wave function must represent electrons moving away from the surface, both inside and outside the metal. The current outside the metal due to the given initial state can then be calculated, and the result summed over the conducting electrons to obtain the total emission.

3.2. *The Initial Wave Functions*—The wave equation for an electron in the metal, under the influence of a light wave whose vector potential is \mathbf{A} and scalar potential zero, is

$$\frac{\hbar^2}{8\pi^2m} \nabla^2 u + \frac{\hbar}{2\pi i} \frac{\partial u}{\partial t} - Vu = -\frac{ie}{2\pi mc} (\mathbf{A}, \text{grad } u), \quad (1)$$

where V is the potential energy of the electron in the metal,

$$\left. \begin{aligned} V &= -h\nu_a, & x < 0 \\ V &= 0, & x > 0 \end{aligned} \right\}, \quad (2)$$

and e is the charge on the electron.

We replace \mathbf{A} by zero to obtain the equation for the initial wave functions. Setting

$$u = u_k = \psi_k \exp(2\pi i E_k t / \hbar), \quad (3)$$

we obtain the ordinary Schrödinger equation for an electron in a field V ,

$$\nabla^2 \psi_k + \frac{8\pi^2m}{\hbar^2} (E_k - V) \psi_k = 0. \quad (4)$$

As V is a function of x alone, this equation is separable.

Equation (4) is to be solved for bound states, for which

$$E_k < 0 \leq E_k + h\nu_a, \quad (5)$$

subject to the conditions that ψ_k must be everywhere finite, and ψ_k and

$\partial\psi_k/\partial x$ must be continuous on the plane $x = 0$. We introduce three quantities k_x, k_y, k_z , such that

$$\frac{8\pi^2m}{h^2} (E_k + h\nu_a) = k_x^2 + k_y^2 + k_z^2, \quad (6)$$

and denote by p the positive value of the expression

$$p = (\mu\nu_a - k_x^2)^{\frac{1}{2}}, \quad (7)$$

where

$$\mu = \frac{8\pi^2m}{h}. \quad (8)$$

The appropriate solution of (4) is then seen to be

$$\left. \begin{aligned} \psi_k &= \alpha_k (e^{-ik_x x} + a_k e^{ik_x x}) e^{ik_y y + ik_z z}, & x < 0 \\ \psi_k &= \alpha_k b_k e^{-px} e^{ik_y y + ik_z z}, & x > 0 \end{aligned} \right\}, \quad (9)$$

where α_k is an undetermined constant, and a_k and b_k are constants determined by the continuity relations at $x = 0$,

$$\left. \begin{aligned} b_k &= 1 + a_k \\ pb_k &= ik_x (1 - a_k) \end{aligned} \right\}. \quad (10)$$

Evidently k_x, k_y , and k_z must all be real, and k_x may be restricted to positive values only.

3.31. *The Perturbation produced by the Light Wave*—We will suppose now that the amplitude of the light wave is small. Then in equation (1) we set

$$u = u_k + v, \quad (11)$$

where u_k is given by (3) and (9). Terms in u_k on the left-hand side of (1) will go out, and hence, neglecting products of v and terms involving Λ , we obtain the first order equation of the perturbation theory,

$$\frac{h^2}{8\pi^2m} \nabla^2 v + \frac{h}{2\pi i} \frac{\partial v}{\partial t} - Vv = -\frac{i\hbar e}{2\pi mc} (\Lambda, \text{grad } u_k). \quad (12)$$

Suppose now that the vector potential of the light wave is given by

$$\Lambda = 2\mathbf{a} \cos 2\pi\nu \left\{ t + \frac{x \cos \theta + y \sin \theta}{c} \right\}, \quad (13)$$

where \mathbf{a} is a constant vector. Replacing the cosine by its exponential expression, we see that the right-hand side of (12) will fall into two parts, having the time factors $\exp \{2\pi i (E_k \pm h\nu) t/h\}$, and so v will also fall into two parts

having these same time factors. These parts evidently correspond to photo electric excitation and to stimulated emission; the latter may be neglected immediately, by omitting the corresponding term from (12). Setting

$$v = \phi(x, y, z) \exp \{2\pi i (E_k + h\nu) t/h\}, \quad (14)$$

we obtain the equation for ϕ ,

$$\begin{aligned} \nabla^2 \phi + \frac{8\pi^2 m}{h^2} (E_k + h\nu - V) \phi \\ = - \frac{4\pi i e}{hc} (\mathbf{a}, \text{grad } \psi_k) \exp \left(2\pi i \nu \frac{x \cos \theta + y \sin \theta}{c} \right). \end{aligned} \quad (15)$$

Again, the right-hand side of (15) is the sum of three terms, involving respectively, $\mathbf{a}_x, \mathbf{a}_y, \mathbf{a}_z$, which can be regarded as independent, since both the angle of incidence and the plane of polarization of the light wave can be varied independently. The corresponding contributions to ϕ will then be additive, and they may be determined separately by setting

$$\phi = \lambda_x \phi_x + \lambda_y \phi_y + \lambda_z \phi_z, \quad (16)$$

where the λ_i are constants, and ϕ_i corresponds to \mathbf{a}_i , for $i = x, y, z$.

3.32. We proceed to the determination of ϕ_x . Setting

$$\lambda_x = - \frac{4\pi i e}{hc} \mathbf{a}_x \alpha_k, \quad (17)$$

$$q = (k_x^2 + \mu\nu)^{\frac{1}{2}}, \quad (18)$$

$$r = \{k_x^2 + \mu(\nu - \nu_0)\}^{\frac{1}{2}}, \quad (19)$$

where in (18) and (19) the positive values of the roots are to be taken, and r is supposed to be real, the equations obtained are

$$\begin{aligned} \nabla^2 \phi_x + (q^2 + k_y^2 + k_z^2) \phi_x \\ = - ik_x (e^{-ik_x x} - \alpha_k e^{ik_x x}) e^{ik_y y + ik_z z} \exp \left(2\pi i \nu \frac{x \cos \theta + y \sin \theta}{c} \right), \\ x < 0, \end{aligned} \quad (20)$$

$$\begin{aligned} \nabla^2 \phi_x + (r^2 + k_y^2 + k_z^2) \phi_x \\ = - pb_k e^{-\nu x} e^{ik_y y + ik_z z} \exp \left(2\pi i \nu \frac{x \cos \theta + y \sin \theta}{c} \right), \quad x > 0. \end{aligned} \quad (21)$$

The solutions ϕ_x are required to be everywhere finite, to represent waves moving outwards from the surface, both inside and outside the metal, and further to be such that ϕ_x and $\partial \phi_x / \partial x$ are continuous on the plane $x = 0$.

We will now neglect $2\pi\nu/c$ in comparison with k_x and k_y . This is permissible for the majority of electrons in the metal, the order of magnitude of

$2\pi\nu/c$ being 10^5 and that of k_x for the important electrons being 10^8 cm^{-1} . The particular integrals of (20) and (21) then depend upon y and z through the factor $\exp(ik_y y + ik_z z)$, and it is found that they do not by themselves satisfy the continuity relations. We must then add to them those parts of the complementary functions having the same y - and z -factors, and representing outgoing waves. The solutions thus obtained are†

$$\phi_x = \left\{ c_x e^{iqx} - \frac{ik_x}{\mu\nu} (e^{-ik_x x} - a_k e^{ik_x x}) \right\} e^{ik_y y + ik_z z}, \quad x < 0, \quad (22)$$

$$\phi_x = \left\{ b_x e^{-irx} - \frac{pb_k}{\mu\nu} e^{-px} \right\} e^{ik_y y + ik_z z}, \quad x > 0, \quad (23)$$

where b_x and c_x are constants determined by the continuity relations,

$$\left. \begin{aligned} c_x - \frac{ik_x}{\mu\nu} (1 - a_k) &= b_x - \frac{pb_k}{\mu\nu} \\ iq c_x - \frac{k_x^2}{\mu\nu} (1 + a_k) &= -ir b_x + \frac{p^2 b_k}{\mu\nu} \end{aligned} \right\} \quad (24)$$

Elimination of c_x , using (10), leads to the result

$$b_x = \frac{\nu_a b_k}{i\nu(q+r)} = \frac{2k_x(p - ik_x)}{\mu\nu(q+r)}. \quad (25)$$

3.33. ϕ_y and ϕ_z can be determined similarly. In these cases, however, it is easily seen that the equations corresponding to (20) and (21) have as inhomogeneous terms the expressions for $\partial\psi_k/\partial y$ or $\partial\psi_k/\partial z$ in the two regions, when $2\pi\nu/c$ is again neglected. The particular integrals, then, are the expressions for $(1/\mu\nu) \partial\psi_k/\partial y$ or $(1/\mu\nu) \partial\psi_k/\partial z$, and these, as well as their first derivatives with respect to x , are already continuous at $x=0$. No term from the particular integral is then needed, and the contribution to the current vanishes.

This result will be modified by taking into account the neglected term $2\pi\nu/c$, but the resulting current will still be very small in comparison with that given by the term ϕ_x .

3.34. In the region $x > 0$ the whole wave function is now

$$u = \left[\alpha_k b_k e^{-px} e^{2\pi i E_k t/h} + \lambda_x \left\{ b_x e^{-irx} - \frac{pb_k}{\mu\nu} e^{-px} \right\} e^{2\pi i (E_k + h\nu) t/h} \right] e^{ik_y y + ik_z z}, \quad (26)$$

† There is nothing to prevent us from adding on further parts of the complementary functions, with different y - and z -factors. These, however, must satisfy the conditions at $x=0$ separately, whence it is seen that the current due to them must be continuous in crossing the boundary, and hence everywhere zero, since it is outwards in both regions. This argument plainly involves no confusion between group and wave velocities.

omitting terms coming from ϕ_y and ϕ_z , which involve the factor $\exp(-px)$. The current density can now be calculated from the general expression

$$\mathbf{j}_x = \frac{eh}{4\pi mi} \left(u \frac{\partial u^*}{\partial x} - u^* \frac{\partial u}{\partial x} \right), \quad (27)$$

where the asterisk denotes the conjugate complex. Evidently, then, the only term in (26) giving a non-zero contribution to the current will be the term in $\exp(-irx)$, provided r is real. We thus obtain the results

$$\mathbf{j}_x = \frac{ehr}{2\pi m} |\lambda_x b_x|^2, \quad \text{if } k_x^2 + \mu v > \mu v_a, \quad (28)$$

$$\mathbf{j}_x = 0, \quad \text{if } k_x^2 + \mu v \leq \mu v_a. \quad (29)$$

The current density thus obtained is due to the initial state given by (9), for which the electron density inside the metal has the mean value

$$2 |\alpha_k|^2. \quad (30)$$

3.41. *Summation over the Conducting Electrons*—According to the electron theory of metals, the mean number of electrons in unit volume having momenta in the ranges $hk_x/2\pi$ to $h(k_x + dk_x)/2\pi$, etc., is given by the Fermi-Dirac distribution function

$$\frac{2}{8\pi^3} \frac{dk_x dk_y dk_z}{1 + \exp\{h^2(k_x^2 + k_y^2 + k_z^2 - \mu\bar{v})/8\pi^2 mkT\}}, \quad (31)$$

where k is Boltzmann's constant, T is the absolute temperature, and

$$\mu\bar{v} = (3\pi^2 n)^{\frac{2}{3}}, \quad (32)$$

n being the number of conducting electrons in unit volume. We now equate the two expressions (30) and (31) for the electron density of the state considered, and substitute the resulting value of $|\alpha_k|^2$ in (28) or (29) to obtain the current due to the electrons in the metal with momenta in the above ranges. The result is then integrated over all possible momenta to obtain the total photoelectric current density,

$$J_x = \frac{e^3 a_x^2 v_a}{2\pi^4 m^2 c^2 v^2} \iiint \frac{dk_x dk_y dk_z}{1 + \exp\{h^2(k_x^2 + k_y^2 + k_z^2 - \mu\bar{v})/8\pi^2 mkT\}} \cdot \frac{rk_x^2}{(q + r)^2}. \quad (33)$$

This is to be integrated over all states for which r is real, that is

$$k_x^2 + \mu v > \mu v_a.$$

3.42. For all ordinary temperatures, the emission will be given with sufficient accuracy, except in the immediate neighbourhood of the threshold, by taking T to be zero in (33). The exponential is then to be replaced by zero or infinity according as $k_x^2 + k_y^2 + k_z^2 - \mu\bar{v}$ is negative or positive. The symbols k_y and k_z then disappear from the integrand, and the integrations with respect to these variables can be carried out by introducing plane polar co-ordinates.

$$dk_y dk_z = \rho d\rho d\phi, \quad (34)$$

and integrating between the limits 0 to 2π , for ϕ , and 0 to $(\mu\bar{v} - k_x^2)^{\frac{1}{2}}$, for ρ . We thus obtain, using (18) and (19),

$$J_x = \frac{e^2 a_x^2 v_a}{2\pi^3 m^2 c^2 v^2} \int_0^{(\mu\bar{v})^{\frac{1}{2}}} \int_{[\mu(v_a - v)]^{\frac{1}{2}}} dk_x \frac{k_x^2 (\mu\bar{v} - k_x^2) \{k_x^2 + \mu(v - v_a)\}^{\frac{1}{2}}}{[(k_x^2 + \mu v)^{\frac{1}{2}} + \{k_x^2 + \mu(v - v_a)\}^{\frac{1}{2}}]^2}, \quad (35)$$

the lower limit being 0, if $v > v_a$, and $\{\mu(v_a - v)\}^{\frac{1}{2}}$, if $v < v_a$.

Calculation by Variation of Constants

4.1. In the calculation to be given now it is assumed that the light is turned on at an arbitrary time, conveniently $t = 0$, and the change in the wave function at a later time t is determined. Starting from equation (12), we seek to obtain a complete space-time description of events by expanding v in a series of solutions of the unperturbed problem, whereas previously $u_k + v$ was regarded as representing a stationary state of the whole system. It is shown here that in the limit as t tends to infinity, the value of v calculated by the method of variation of constants tends into agreement with the value obtained by the stationary method.

We commence by determining the free states for the unperturbed problem. As regards their x -factors, these are not now completely determined, but we can conveniently separate them into two sets, representing outgoing and ingoing waves outside the metal. The expansion can then be made in terms of these. Alternatively, we may determine suitable linear combinations of outgoing and ingoing waves of the same energy, so that the usual normalization and orthogonality conditions are satisfied. The two methods are precisely equivalent, but the former seems clearer, and will be adopted here.

4.2. *The Free States*—We proceed to solve equation (4) for

$$E_r > 0. \quad (36)$$

To avoid confusion we write a suffix f in place of the previous k . Introducing quantities g, g_v, g_s , such that

$$\frac{8\pi^2 m}{h^2} (E_f + h\nu_a) = g^2 + g_v^2 + g_s^2, \quad (37)$$

and denoting by f the positive value of the expression

$$f = (g^2 - \mu\nu_a)^{\frac{1}{2}}, \quad (38)$$

the outgoing waves are given by

$$\left. \begin{aligned} \psi_f^+ &= (e^{-i\theta x} + a_f e^{i\theta x}) e^{i\theta_v y + i\theta_s z}, & x < 0 \\ \psi_f^+ &= b_f e^{-i f x} e^{i\theta_v y + i\theta_s z}, & x > 0 \end{aligned} \right\}, \quad (39)$$

and the inward moving waves by

$$\left. \begin{aligned} \psi_f^- &= (a_f e^{-i\theta x} + e^{i\theta x}) e^{i\theta_v y + i\theta_s z}, & x < 0 \\ \psi_f^- &= b_f e^{i f x} e^{i\theta_v y + i\theta_s z}, & x > 0 \end{aligned} \right\}, \quad (40)$$

where

$$\left. \begin{aligned} 1 + a_f &= b_f \\ g(1 - a_f) &= f b_f \end{aligned} \right\}. \quad (41)$$

u_f^+ and u_f^- will be used to denote $\psi_f^+ \exp(2\pi i E_f t/h)$ and $\psi_f^- \exp(2\pi i E_f t/h)$ respectively.

4.31. *Determination of the Expansion*—We seek to solve (12) by assuming for v an expansion of the form†

$$v = \int_{-\infty}^{\infty} dg_v \int_{-\infty}^{\infty} dg_s \int_0^{\infty} df C_f^+(t) u_f^+ + \int_{-\infty}^{\infty} dg_v \int_{-\infty}^{\infty} dg_s \int_0^{\infty} df C_f^-(t) u_f^-. \quad (42)$$

Inserting this expansion in (12), and assuming the validity of inverting the order of integrating and operating by

$$\left(\frac{h^2}{8\pi^2 m} \nabla^2 + \frac{h}{2\pi i} \frac{\partial}{\partial t} - V \right), \quad (43)$$

it is found that the right-hand side is an expansion like (42), but with $C_f(t)$ replaced by dC_f/dt . We then multiply both sides by $u_{f'}^{\alpha*}$, where α denotes

† We omit the part of the expansion due to the bound states, which must also be inserted. It can easily be verified, however, that this gives the term in $\exp(-px)$ obtained in (26), and this makes no contribution to the current.

+ or —, and integrate over all space, inverting the order of the space and momentum integrations to obtain the result

$$\int_{-\infty}^{\infty} dg_y \int_{-\infty}^{\infty} dg_z \left\{ \int_0^{\infty} df \frac{dC_f^+(t)}{dt} \int d\tau u_f^+ u_f^{**} + \int_0^{\infty} df \frac{dC_f^-(t)}{dt} \int d\tau u_f^- u_f^{**} \right\} \\ = \frac{e}{mc} \int d\tau (A, \text{grad } u_k) u_f^{**}. \quad (44)$$

The orthogonality relations subsisting between the free states (39) and (40) can be written in the form

$$\left. \begin{aligned} \int d\tau u_f^+ u_f^{**} &= \int d\tau u_f^- u_f^{**} = N_f^{(1)} \delta(f-f') \delta(g_y - g'_y) \delta(g_z - g'_z) \\ \int d\tau u_f^+ u_f^{-*} &= \int d\tau u_f^- u_f^{-*} = N_f^{(2)} \delta(f-f') \delta(g_y - g'_y) \delta(g_z - g'_z) \end{aligned} \right\}, \quad (45)$$

where $N_f^{(1)}$ and $N_f^{(2)}$ are to be determined, and $\delta(f-f')$ denotes the Dirac δ -function. Inserting these values in (44), and replacing α by + and — in turn, we obtain the simultaneous equations

$$\left. \begin{aligned} N_f^{(1)} \frac{dC_f^+(t)}{dt} + N_f^{(2)} \frac{dC_f^-(t)}{dt} &= \frac{e}{mc} \int d\tau (A, \text{grad } u_k) u_f^{**} \\ N_f^{(2)} \frac{dC_f^+(t)}{dt} + N_f^{(1)} \frac{dC_f^-(t)}{dt} &= \frac{e}{mc} \int d\tau (A, \text{grad } u_k) u_f^{-*} \end{aligned} \right\}. \quad (46)$$

Eliminating $dC_f^-(t)/dt$, and performing the time-integration, assuming that at time $t = 0$, when the light is turned on, the electron is in the state k , we obtain the result

$$C_f^+(t) = \frac{\exp\{2\pi i (E_k + h\nu - E_f)t/h\} - 1}{2\pi i (E_k + h\nu - E_f)/h} (k | a | f)^+, \quad (47)$$

where

$$(k | a | f)^+ = \frac{e/mc}{\{N_f^{(1)}\}^2 - \{N_f^{(2)}\}^2} \int d\tau (a, \text{grad } \psi_k) \{N_f^{(1)} \psi_f^{**} - N_f^{(2)} \psi_f^{-*}\} \\ \times \exp 2\pi i \nu (x \cos \theta + y \sin \theta)/c. \quad (48)$$

Here, as in the stationary method, we have omitted a further term which has the time-factor $\exp 2\pi i (E_k - E_f - h\nu)t/h$, and which corresponds to stimulated emission.

Neglecting the exponential term $\exp 2\pi i \nu (x \cos \theta + y \sin \theta)/c$, we see that $(k | a | f)^+$ will involve the factors $\delta(k_y - g_y) \delta(k_z - g_z)$. We shall then write

$$(k | a | f)^+ = (k | a | f)_0^+ \delta(k_y - g_y) \delta(k_z - g_z). \quad (49)$$

4.32. We now insert (47) in (42), and carry out the resulting integrations to obtain the value of v . In virtue of (49), the integrations with respect to

g_s and g_r can be carried out at once, leading to the result for v , outside the metal,

$$v = \int_0^\infty df \frac{\exp \{2\pi i (E_k + h\nu - E_f) t/h\} - 1}{2\pi i (E_k + h\nu - E_f)/h} (k|a|f)_0^+ b_f e^{-ifx + ik_y y + ik_z z} e^{2\pi i E_f t/h} \\ + \int_0^\infty df \frac{\exp \{2\pi i (E_k + h\nu - E_f) t/h\} - 1}{2\pi i (E_k + h\nu - E_f)/h} (k|a|f)_0^- b_f e^{ifx + ik_y y + ik_z z} e^{2\pi i E_f t/h}, \quad (50)$$

where $(k|a|f)_0^-$ is the corresponding matrix element to $(k|a|f)_0^+$, in the expression for $C_f(t)$.

In both the integrals occurring in (50), we may suppose x and t to be great. The factors occurring can then be split up into those varying quickly or slowly with f . The entire contribution to both integrals will come from the immediate neighbourhood of the resonance value given by

$$E_f = E_k + h\nu. \quad (51)$$

We can then give the slowly varying factors their values at the resonance point, and put them outside the sign of integration. Denoting by r the value of f at this point, we have

$$v = b_r e^{ik_y y + ik_z z + 2\pi i (E_k + h\nu) t/h} \{e^{-irx} (k|a|r)_0^+ \Psi + e^{irx} (k|a|r)_0^- \Psi'\}, \quad (52)$$

$$\text{where} \quad \left. \begin{aligned} \Psi &= \int_0^\infty df \frac{1 - \exp 2\pi i (E_f - E_r) t/h}{2\pi i (E_f - E_r)/h} e^{-i(f-r)x} \\ \Psi' &= \int_0^\infty df \frac{1 - \exp 2\pi i (E_f - E_r) t/h}{2\pi i (E_f - E_r)/h} e^{i(f-r)x} \end{aligned} \right\}. \quad (53)$$

Making the substitution

$$(f - r) t = \eta, \quad (54)$$

and taking η between the limits $\pm \infty$, on account of the greatness of t , we can reduce Ψ and Ψ' to the forms

$$\left. \begin{aligned} \Psi &= \frac{h}{2\pi} \cdot \frac{4\pi^2 m}{h^2 r} \int_{-\infty}^\infty \frac{d\eta}{\eta} \left\{ i \cos \frac{x}{t} \eta - i \cos \left(\frac{hr}{2\pi m} - \frac{x}{t} \right) \eta \right. \\ &\quad \left. + \sin \frac{x}{t} \eta + \sin \left(\frac{hr}{2\pi m} - \frac{x}{t} \right) \eta \right\} \\ \Psi' &= \frac{h}{2\pi} \cdot \frac{4\pi^2 m}{h^2 r} \int_{-\infty}^\infty \frac{d\eta}{\eta} \left\{ i \cos \frac{x}{t} \eta - i \cos \left(\frac{hr}{2\pi m} + \frac{x}{t} \right) \eta \right. \\ &\quad \left. - \sin \frac{x}{t} \eta + \sin \left(\frac{hr}{2\pi m} + \frac{x}{t} \right) \eta \right\} \end{aligned} \right\}, \quad (55)$$

whence we deduce that for positive x and t

$$\left. \begin{aligned} \Psi &= \frac{4\pi^2 m}{hr}, & \frac{x}{t} &< \frac{hr}{2\pi m} \\ \Psi &= 0, & \frac{x}{t} &> \frac{hr}{2\pi m} \\ \Psi' &= 0, & \text{for all values of } x/t \end{aligned} \right\}. \quad (56)$$

Hence, making t infinite, we find that outside the metal v has the form

$$v = \frac{4\pi^2 m}{hr} b_r (k | a | r)_0^+ e^{-ix + ik_y y + ik_z z} e^{2\pi i (E_k + h\nu) t / h}. \quad (57)$$

4.4. We must now evaluate $(k | a | r)_0^+$ to show that the results obtained by both methods are the same. In the first place we remark that $N_r^{(1)}$ and $N_r^{(2)}$, defined in (45), will contain factors due to the x -, y -, and z -integrations separately. If, then, in (48) we neglect $\exp 2\pi i \nu (x \cos \theta + y \sin \theta)/c$ it will be seen that the factors in $N_r^{(1)}$ and $N_r^{(2)}$ due to the y - and z -integrations will disappear from the result, and we need calculate only the factor due to the x -integration. From (4) we separate out an equation for the x -factor of the wave function. Writing down the resulting equations for the x -factors X_r and $X_{r'}^*$ of two wave functions ψ_r and $\psi_{r'}^*$, multiplying by $X_{r'}^*$ and X_r respectively, and subtracting, we deduce

$$(g^2 - g'^2) X_r X_{r'}^* = (f^2 - f'^2) X_r X_{r'}^* = \frac{d^2 X_r}{dx^2} X_{r'}^* - \frac{d^2 X_{r'}^*}{dx^2} X_r. \quad (58)$$

Integrating with respect to x between the limits $\pm R$, where R is very large and positive, and remembering that X and dX/dx are continuous at $x = 0$,

$$\begin{aligned} \int_{-R}^R dx X_r X_{r'}^* &= \frac{1}{f^2 - f'^2} \left(\frac{dX_r}{dx} X_{r'}^* - \frac{dX_{r'}^*}{dx} X_r \right)_{x=R} \\ &\quad - \frac{1}{g^2 - g'^2} \left(\frac{dX_r}{dx} X_{r'}^* - \frac{dX_{r'}^*}{dx} X_r \right)_{x=-R}. \end{aligned} \quad (59)$$

In (59) we insert explicit expressions for X_r and $X_{r'}^*$, and then integrate the resulting equation with respect to f' over a range including $f' = f$. Since $f'^2 = g'^2 - \mu \nu_0$, we have $f' df' = g' dg'$. Then we set $R(f' - f) = \eta$ and $R(g' - g) = \zeta$ in the first and second terms of (59) respectively, and take η and ζ between the limits $\pm \infty$, on account of the greatness of R . As we see from (45), the integral with respect to f' of the left-hand side of (59) will be

equal to either $N_f^{(1)}$ or $N_f^{(2)}$, depending upon the particular X_f and $X_{f'}$ chosen, and hence we find after some reduction, using (41), the results

$$\left. \begin{aligned} N_f^{(1)} &= \frac{2\pi g}{f} \\ N_f^{(2)} &= \frac{2\pi g}{f} \cdot a \end{aligned} \right\}. \quad (60)$$

Substitution of (60) into (48) then gives

$$(k|a|f)_0^+ = \frac{e/mc}{1-a_f^2} \cdot \frac{f}{2\pi g} \int_{-\infty}^{\infty} dx \left\{ a_x \frac{dX_k}{dx} + (a_y ik_y + a_z ik_z) X_k \right\} (X_f^{+*} - a_f X_f^{-*}), \quad (61)$$

with an obvious notation. That the terms in a_y and a_z go out is evident from the fact that the bound states are orthogonal to all the free states. Replacing X_k , X_f^{\pm} by the x -factors of (9), (39), and (40), the integrations in (61) can be easily carried out, using a convergence factor $\exp \varepsilon^2 x$ for the range $x < 0$, and finally, replacing f by r , we obtain the result

$$(k|a|r)_0^+ = -\frac{e}{mc} \cdot \frac{r}{2\pi q} \cdot \frac{v_a}{v} \cdot \alpha_k b_k a_x. \quad (62)$$

Evidently then

$$\frac{4\pi^2 m}{hr} b_r (k|a|r)_0^+ = -\frac{4\pi ie}{hc} a_x \alpha_k \cdot \frac{2k_x(p - ik_x)}{\mu v(q + r)} = \lambda_a b_x, \quad (63)$$

and the two methods of calculation are in agreement, as we see by comparing (57) and (26).

4.5. *Comparison with the Result of Tamm and Schubin*—Tamm and Schubin, using the method of variation of constants, obtain a result differing from our formula (35) by having an extra factor

$$\frac{4(k_x^2 + \mu v)}{[(k_x^2 + \mu v)^{\frac{1}{2}} + \{k_x^2 + \mu(v - v_a)\}^{\frac{1}{2}}]^2} \quad (64)$$

in the integrand. Their calculation differs from ours in the following respect†: in place of the full expansion (42), they omit the second integral over the inward-moving waves, and then determine C_f^+ by the usual argument, as given in Section 4.31, leading to the result

$$(k|a|f)^+ = \frac{e/mc}{N_f^{(1)}} \int d\tau (a, \text{grad } \psi_k) \psi_f^{+*} \exp 2\pi i v(x \cos \theta + y \sin \theta)/c, \quad (65)$$

† For details of the calculation see Blochinzev, 'Phys. Z. Sowjet Union,' vol. 1, p. 781 (1931).

where

C_f^+ and $(k|a|f)^+$ are connected by (47).

Since the incoming waves actually make no contribution to the current, this would be correct if the ingoing and outgoing wave functions of the same energy were orthogonal; that is, if $N_f^{(2)}$ were zero. Since, however, this is not so, C_f^+ is given by (48) rather than by (65), and since the final results are different it is evident that the result deduced from (65) must be wrong.

Discussion

5.1. *Interpretation of the Results*—It is interesting to investigate in some detail the expression (33) for the current. If we suppose the incident light wave, whose vector potential \mathbf{A} is given by (13), is polarized with the electric vector in the plane of incidence, so that

$$\mathbf{a} = |\mathbf{a}| (-\sin \theta, \cos \theta, 0), \quad (66)$$

then the rate at which light energy is incident upon the surface will be

$$\frac{2\pi\nu^3 \cos \theta}{c} |\mathbf{a}|^2 = \frac{2\pi\nu^3 \cos \theta \cdot a_x^2}{c \sin^2 \theta}. \quad (67)$$

Dividing the expression (33) by (67) we obtain the emission per unit incident energy, P_x , which can be written

$$P_x = \frac{e^3 \nu_a \sin^2 \theta}{4\pi^2 m^2 c \cos \theta} \iiint \frac{2}{8\pi^3} \frac{dk_x dk_y dk_z}{1 + \exp h^2 (k_x^2 + k_y^2 + k_z^2 - \mu \bar{\nu}) / 8\pi^2 m k T} \\ \times \frac{1}{\nu^4} \cdot \frac{k_x^2}{(k_x^2 + \mu \nu)^{\frac{1}{2}}} \cdot \frac{4 (k_x^2 + \mu \nu)^{\frac{1}{2}} \{k_x^2 + \mu (\nu - \nu_a)\}^{\frac{1}{2}}}{[(k_x^2 + \mu \nu)^{\frac{1}{2}} + \{k_x^2 + \mu (\nu - \nu_a)\}^{\frac{1}{2}}]^2}, \quad (68)$$

where the integrations are to extend over all electrons in the metal whose normal velocities are sufficient to enable them to escape, after absorbing a quantum.

The integrand of (68) can be split into three factors, the Fermi-Dirac distribution function

$$\frac{2}{8\pi^3} \frac{dk_x dk_y dk_z}{1 + \exp h^2 (k_x^2 + k_y^2 + k_z^2 - \mu \bar{\nu}) / 8\pi^2 m k T}, \quad (69)$$

the boundary transmission coefficient for the simple potential step

$$\frac{4 (k_x^2 + \mu \nu)^{\frac{1}{2}} \{k_x^2 + \mu (\nu - \nu_a)\}^{\frac{1}{2}}}{[(k_x^2 + \mu \nu)^{\frac{1}{2}} + \{k_x^2 + \mu (\nu - \nu_a)\}^{\frac{1}{2}}]^2}, \quad (70)$$

and a residual factor

$$\frac{1}{v^4} \cdot \frac{k_x^2}{(k_x^2 + \mu v)^{\frac{1}{2}}}, \quad (71)$$

which, in the factor v^{-4} , is reminiscent of the excitation probability for the atomic photoelectric effect. On purely *a priori* grounds, we should have expected the factor (69), an inverse power of v , as in (71), and perhaps the boundary transmission coefficient; the modifications of these factors could hardly have been foreseen.

5.21. *Effect of Refraction and Reflection of the Light*—The result (68) suffers from the same failing as that pointed out in the theory of Sommerfeld and Bethe, that it makes the emission per unit incident energy infinite for grazing incidence. This disadvantage can be removed by taking into account the effect of refraction and reflection of the incident light, when we may hope to obtain a more correct dependence upon the angle of incidence. This same modification will also increase the order of magnitude of the results in about the ratio $(E_x + E_x')^2 : E_x^2$, where E_x, E_x' refer to the incident and reflected beams, the effect of this being much the same as that of the extra factor (64) occurring in Tamm and Schubin's result. We may then expect this modification to give improved results in these two respects.

An exact theory can be given, assuming that the surface of the metal behaves as a simple discontinuity towards the light wave, and the calculations being made in the simple manner presented in Section 3. We use symbols $\mathbf{a}_i, \mathbf{a}_r, \mathbf{a}_t$ to denote the vector potentials of the incident, reflected, and transmitted beams respectively (when multiplied by the appropriate exponential factors), and obtain in place of (24) the equations

$$\left. \begin{aligned} c_x - \frac{ik_x}{\mu v} (1 - a_k) &= b_x - \frac{pb_k}{\mu v} \frac{\mathbf{a}_{tx} + \mathbf{a}_{rx}}{\mathbf{a}_{tx}} \\ iq c_x - \frac{k_x^2}{\mu v} (1 + a_k) &= -ir b_x + \frac{p^2 b_k}{\mu v} \frac{\mathbf{a}_{tx} + \mathbf{a}_{rx}}{\mathbf{a}_{tx}} \end{aligned} \right\}, \quad (72)$$

giving the result

$$b_x = \frac{(k_x^2 - ipq) + p(p + iq)(\mathbf{a}_{tx} + \mathbf{a}_{rx})/\mathbf{a}_{tx}}{i\mu v(q + r)} b_k, \quad (73)$$

where we have taken for λ_x , in place of (17), the value

$$\lambda_x = -\frac{4\pi i e}{hc} \mathbf{a}_{tx} \alpha_k. \quad (74)$$

We then obtain the result

$$J_x = \frac{e^3 |a_{tx}|^2 v_a}{2\pi^3 m^2 c^2 v^2} \int_{(1, [\mu(\nu_a - \nu)]^{\frac{1}{2}})}^{(\mu \bar{\nu})^{\frac{1}{2}}} dk_x \frac{k_x^2 (\mu \bar{\nu} - k_x^2) r}{(q + r)^2} \times \frac{|(k_x^2 - ipq) + p(p + iq)(a_{tx} + a_{rx})/a_{tx}|^2}{\mu^2 v_a^2}, \quad (75)$$

which reduces to (35) for $a_{tx} = a_x$, $a_{rx} = 0$. The contributions to the current due to the y - and z -components of vector potential again vanish, on account of the continuity relations

$$\left. \begin{aligned} a_{ty} + a_{ry} &= a_{ty} \\ a_{tz} + a_{rz} &= a_{tz} \end{aligned} \right\}, \quad (76)$$

which are established below.

a_r and a_t can be calculated in terms of a_i and the optical constants n and κ of the metal, by the classical electromagnetic theory. Only the case where the electric vector vibrates in the plane of incidence need be considered. Using the conditions that the tangential components of the electric and magnetic intensities are continuous at the surface, we find the vector potentials must be given by the real parts of the expressions

$$\left. \begin{aligned} A_i &= (a_{ix}, -a_{ix} \cot \theta, 0) \exp 2\pi i \nu (x \cos \theta + y \sin \theta + ct)/c \\ A_r &= (a_{rx}, a_{rx} \cot \theta, 0) \exp 2\pi i \nu (-x \cos \theta + y \sin \theta + ct)/c \\ A_t &= (a_{tx}, -a_{tx} \frac{n - i\kappa}{\sin \theta}, 0) \exp 2\pi i \nu \{(n - i\kappa)x + y \sin \theta + ct\}/c \end{aligned} \right\}, \quad (77)$$

where

$$\left. \begin{aligned} \frac{a_{rx}}{a_{tx}} &= \frac{\sin^2 \theta + (n - i\kappa)^2 - (n - i\kappa)/\cos \theta}{\sin^2 \theta + (n - i\kappa)^2 + (n - i\kappa)/\cos \theta} \\ \frac{a_{tz}}{a_{tx}} &= \frac{2}{\sin^2 \theta + (n - i\kappa)^2 + (n - i\kappa)/\cos \theta} \end{aligned} \right\}. \quad (78)$$

It can be easily verified that the first of equations (76) holds, and the second follows from the continuity of E_z when the incident light is polarized in the plane of incidence.

From equations (78) it is found that the rate at which energy is incident upon the surface is

$$\frac{\pi v^2 |a_{tx}|^2}{2c \cos \theta \sin^2 \theta} \cdot \{(n^2 + \kappa^2 + \sin^2 \theta)^2 \cos^2 \theta + 2n \cos \theta (n^2 + \kappa^2 + \sin^2 \theta) + n^2 + \kappa^2 \cos^2 2\theta\}, \quad (79)$$

and the rate at which energy is absorbed is

$$\frac{\pi v^2 |a_{tx}|^2}{2c \cos \theta \sin^2 \theta} \cdot 4n (n^2 + \kappa^2 + \sin^2 \theta) \cos \theta. \quad (80)$$

We also find

$$\frac{a_{tx} + a_{rx}}{a_{tx}} = \sin^2 \theta + (n - i\kappa)^2. \quad (81)$$

Dividing (75) by (79) or (80) we obtain expressions for the emission referred to unit incident or absorbed energy. It is evident that these expressions will remain finite for all angles of incidence, as of course they must.

The final result is most conveniently expressed in terms of certain reduced variables. We use the notation

$$\left. \begin{aligned} v_\sigma &= v_a - \bar{v} \\ k_x^2 &= \mu v_\sigma X^2 \\ \bar{v} &= \varepsilon v_\sigma \\ v &= \eta v_\sigma \end{aligned} \right\}, \quad (82)$$

and convert the emission per unit incident energy into coulombs per calorie by multiplying by $1.395 \cdot 10^{-2}$. Giving all the absolute constants their appropriate numerical values, the result is

$$P_\sigma = C \left[\frac{\sin^2 \theta \cos \theta [(n^2 + \kappa^2)^2 - 2(n^2 - \kappa^2) \cos^2 \theta + \cos^4 \theta] \zeta_1(\eta) + \{2(n^2 - \kappa^2 - \cos^2 \theta) + 1\} \zeta_2(\eta) + n\kappa \zeta_3(\eta) + \zeta_4(\eta)}{v_\sigma \{(n^2 + \kappa^2 + \sin^2 \theta)^2 \cos^2 \theta + 2n \cos \theta (n^2 + \kappa^2 + \sin^2 \theta) + n^2 + \kappa^2 \cos^2 2\theta\}} \right], \quad (83)$$

where

$$C = \frac{64c^3}{h^2c} \cdot 1.395 \cdot 10^{-2} = 7.537 \cdot 10^{13}, \quad (83A)$$

and

$$\zeta_1(\eta) = \frac{1 + \varepsilon + \eta}{(1 + \varepsilon) \eta^4} \int_0^{\frac{1}{2}} dX \cdot \frac{X^2 (\varepsilon - X^2) (1 + \varepsilon - X^2) (X^2 + \eta - 1 - \varepsilon)^{\frac{1}{2}}}{\{(X^2 + \eta)^{\frac{1}{2}} + (X^2 + \eta - 1 - \varepsilon)^{\frac{1}{2}}\}^2}, \quad (84)$$

$$\zeta_2(\eta) = \frac{1 + \varepsilon}{1 + \varepsilon + \eta} \zeta_1(\eta), \quad (85)$$

$$\zeta_3(\eta) = \frac{4}{\eta^4} \int_0^{\frac{1}{2}} dX \cdot \frac{X^2 (\varepsilon - X^2) (X^2 + \eta - 1 - \varepsilon)^{\frac{1}{2}} (X^2 + \eta)^{\frac{1}{2}} (1 + \varepsilon - X^2)^{\frac{1}{2}}}{\{(X^2 + \eta)^{\frac{1}{2}} + (X^2 + \eta - 1 - \varepsilon)^{\frac{1}{2}}\}^2}, \quad (86)$$

$$\zeta_4(\eta) = \frac{1}{\eta^4} \int_0^{\frac{1}{2}} dX \cdot \frac{X^4 (\varepsilon - X^2) (X^2 + \eta - 1 - \varepsilon)^{\frac{1}{2}}}{\{(X^2 + \eta)^{\frac{1}{2}} + (X^2 + \eta - 1 - \varepsilon)^{\frac{1}{2}}\}^2}. \quad (87)$$

Equation (83) gives P_z , the emission per unit incident energy, in coulombs per calorie, in terms of the optical constants and angle of incidence, the threshold frequency, and the dimensionless integrals $\zeta_i(\eta)$.

5.22. The above method of taking into account the effect of refraction and reflection needs a certain amount of justification. The objection of Tamm and Schubin, that the absorption of light by the metal is in part due to photoelectric processes, is seen to be unimportant when it is remembered that the photoelectric emission of a metal is rarely as great as one electron per 200 quanta, and is generally very much less. Undoubtedly our ideal must be a single theory yielding results for the optical constants and for the photoelectric emission at the same time, but as this is unattainable at present, we must content ourselves with the theory presented above. We can always conceive of the optical constants being calculated without reference to the emission from the surface, and can suppose the values thus obtained to be inserted above.

Another objection is, however, certainly valid. The abrupt transition at the surface is only an approximation, and in reality there will be a gradual change in the constants of the light wave over a region of the order of the wave-length of the incident light. This is large compared to the wave-length of the electrons in the metal, hence also to the region from which the main parts of the matrix elements come. We might then expect to obtain a closer approximation to the true state of affairs by averaging over the position of the surface of discontinuity for the light. We will avoid this further complication for the present.

5.3. *The Spectral Distribution Curve*—We will content ourselves, in the present paper, with an examination of the form of the spectral distribution curve given by (83). Since the integrals $\zeta_i(\eta)$ involve the quantity $\epsilon = \bar{\nu}/\nu_0$, which depends upon the metal chosen, it is essential to make the calculations for a particular metal.

Our choice must evidently fall upon an alkali metal, in spite of the uncertain knowledge as to their thresholds, and the conflicting experimental results for them. The reason for this is that the thresholds of the heavier metals lie in the ultra-violet, and their properties have been investigated only over a frequency range too small to be of interest. With the alkalis, however, the thresholds lie in the visible part of the spectrum, and spectral distribution curves have been obtained over quite wide frequency ranges.

We use the values of $\bar{\nu}$ obtained from formula (32), assuming that there is one free electron per atom, and use the experimental values of ν_0 , the threshold

frequency. As, however, the latter are not accurately known, we have evaluated the integrals $\zeta_i(\eta)$ on the assumption (which is probably nearly true for the alkali metals) that $\bar{\nu}$ and ν_g are equal, and their values are shown in fig. 1 as functions of $\eta = \nu/\nu_g$.

It will be observed that the forms of these curves, and in particular the positions of their maxima, are rather different, and that accordingly the form of the resulting spectral distribution curve cannot be deduced without taking a particular metal. Potassium is suitable. Suhrmann and Theissing† have reported a value of $4.84 \cdot 10^{14}$ for the threshold frequency for this metal, and this lies sufficiently close to the calculated value of $\bar{\nu}$, namely $4.96 \cdot 10^{14}$, for the assumption that $\bar{\nu}$ and ν_g are equal to be reasonably accurate. Taking the near value $\nu_g = 5 \cdot 10^{14}$, assuming for the angle of incidence θ the value 60° , and using for the optical constants the measured values‡ for $\nu = 5.1 \cdot 10^{14}$,

$$\left. \begin{aligned} n &= 0.068 \\ \kappa &= 1.5 \end{aligned} \right\}, \quad (88)$$

the emission per unit incident energy has been calculated, and is given in fig. 2 as a function of frequency. The curve given by Suhrmann and Theissing is also shown in fig. 2 for purposes of comparison.

In the first place, we may remark that the order of magnitude is reasonably correct, for not too great frequencies. In this connection, however, it must be remarked that Suhrmann and Theissing fail to state the angle of incidence or the state of polarization of the light. The dependence upon the former of our result (83) is, however, rather insensitive in the neighbourhood of $\theta = 60^\circ$, and values in this neighbourhood are usual in experimental work since they give the greatest emission.

The form of the theoretical curve, on the other hand, is in not too good agreement with experimental results. The general trend is correct, but the curve is too flat, and its maximum occurs at higher frequencies than observed maxima. These features could, however, be altered by variations in the optical constants, and hence the form of the curve cannot be taken as conclusive until more is known of these quantities. The form of the curve, in particular the position of the maximum, depends also upon the value of $\bar{\nu}$, which in its turn depends upon the binding of the conducting electrons. The effect of this can be considered formally as causing an increase in the effective

† 'Z. Physik,' vol. 52, p. 453 (1928-29).

‡ 'Int. Critical Tables,' vol. 5, p. 249.

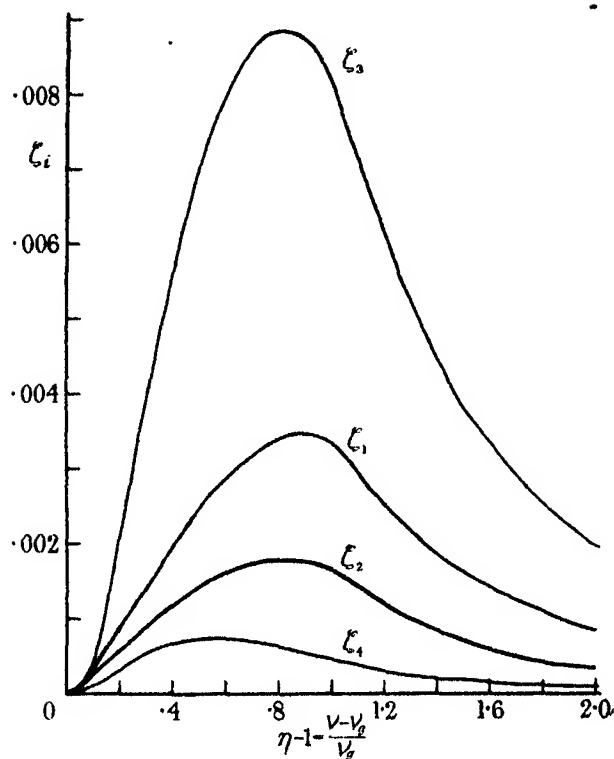


FIG. 1—The functions $\zeta_i(\nu)$ for $\tilde{\nu} = \nu_j$.

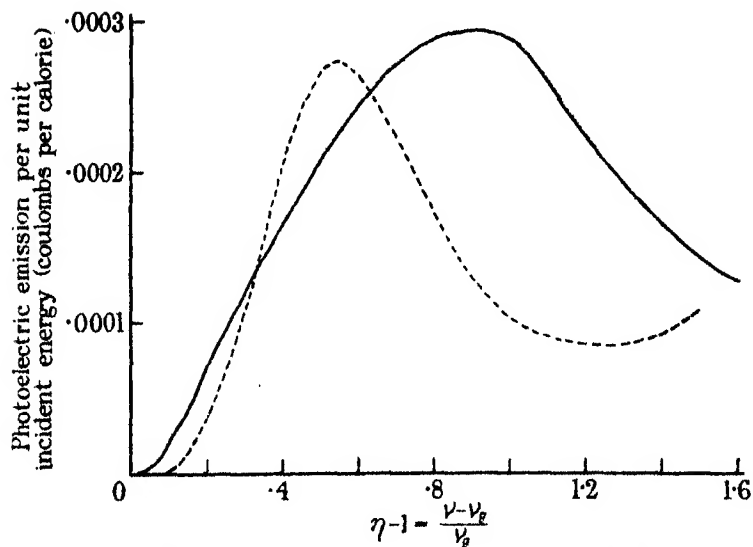


FIG. 2—Theoretical and experimental spectral distribution curves for potassium.
— theoretical (equation (83)) ; - - - experimental (Suhrmann and Theissing).

mass of the electrons, causing $\bar{\nu}$ to decrease, and shifting the maximum towards the threshold. This and other points will be discussed in a subsequent paper.

The author wishes to thank Professor R. H. Fowler, F.R.S., and Mr. A. H. Wilson for their constant interest and for many illuminating discussions; as well as the Master and Fellows of Peterhouse, and the Goldsmiths' Company, for studentships during the tenure of which the work was carried out.

Summary

6. The theoretical position of the surface photoelectric effect in metals is discussed, and objections are raised against the theories of Wentzel and Fröhlich.

The photoelectric emission due to a single surface is calculated by two methods, and the results obtained are in agreement. Tamm and Schubin, using the same assumptions, obtained a different result, which is shown to be incorrect.

The results of a more general calculation of the effect due to a single surface, taking into account the effect of reflection and refraction of the light wave, are quoted, and the theoretical spectral distribution curves given for potassium, and compared with experiment.

The Resistance of Liquid Metals

By N. F. MOTT, the H. H. Wills Physical Laboratory, University of Bristol

(Communicated by R. H. Fowler, F.R.S.—Received March 28, 1934)

The electrical resistance of most normal metals in the liquid state just above the melting point is about twice as great as that of the solid metal just below the melting point. Certain abnormal metals, however, such as bismuth, gallium and antimony, which are rather poor conductors in the solid state, increase their conductivity on melting. The purpose of this paper is to discuss this change of resistance from the point of view of the modern theory of electronic conduction which is based on the wave mechanics, and to obtain a formula for the change of resistance which is in quantitative agreement with experiment for normal metals. No quantitative theory can as yet be given for the abnormal metals, but we shall show that their behaviour is explicable in a qualitative way.

In a solid the atoms vibrate about mean positions which are fixed in the solids in a liquid at temperatures near the melting point, it is now generally recognized that the atoms vibrate about mean positions which, though not fixed, move slowly compared with the velocity, of order of magnitude $\sqrt{(kT/M)}$, with which the atoms vibrate. The most direct evidence for this is afforded by the specific heats of monatomic metals, which have, within the limits of experimental error ($\sim 7\%$), the same values (in the neighbourhood of $3R$) for a given metal in the solid and liquid states near the melting point.* Further evidence is given by the rates of diffusion of gold in mercury† (0.72 sq cm/day) or of thorium B (Pb) in non-radioactive liquid lead‡ (2.2 sq cm/day). If one compares these numbers with the formula for the diffusion coefficient in gases,

$$D = \frac{1}{3}lc,$$

where l is the mean free path, and c the mean molecular velocity, one finds, on setting c equal to a quantity of the order of magnitude of $\sqrt{(kT/M)}$, that l must be taken to be about one-hundredth of the interatomic distance.

* Eucken, 'Handb. exp. Physik,' vol. 6/I, p. 333 (1929).

† Cf. Landolt-Börnstein's 'Tables,' 5th ed., vol. I, p. 249.

‡ Groh and von Hevesy, 'Ann. Physik,' vol. 63, p. 85 (1920).

A theory of the viscosity of liquids has recently been given by Andrade,* based on the same hypothesis.

In discussing the phenomenon of melting, therefore, and the accompanying change of resistance, we shall treat the atoms of the liquid as though they were vibrating about mean positions which remain fixed. We shall also suppose that each atom vibrates with a definite frequency ν_L , which is the same for each atom, although it is probable that in a real liquid the frequencies will not all be exactly the same. We shall denote by ν_S the frequency with which the atoms vibrate in the solid, so that

$$\Theta_S = h\nu_S/k,$$

is the characteristic temperature of the solid, if Einstein's rather than Debye's formula for the specific heats is used.

We shall denote by U the work required to remove an atom at rest in the solid to a position of equilibrium in the liquid. If the temperature of melting T_M is such that $kT_M \gg h\nu_S$, then for both solid and liquid the mean energy of vibration is $3kT_M$ per atom, so that U is equal to the latent heat of fusion, expressed in ergs per atom.

At the temperature T_M at which the liquid and solid are in equilibrium at zero pressure, the free energy F is a minimum. Thus, if one atom is transferred from the liquid to the solid, the change in the free energy must vanish. It is a well-known result of statistical mechanics that, for a body consisting of N atoms,

$$F = N(-kT \log f + E),$$

where f is the partition function of each atom, and E the energy of an atom at rest in its position of equilibrium. Thus, if N_S atoms are in the solid phase and N_L in the liquid, the free energy is

$$N_S(-kT \log f_S) + N_L(-kT \log f_L + U),$$

where f_S, f_L are the partition functions of atoms in the solid and liquid respectively. At the melting point, $T = T_M$, this must be a minimum for any change in N_S and N_L , subject to the condition that $N_S + N_L$ must remain constant. We obtain

$$kT_M \log f_S = kT_M \log f_L - U,$$

whence

$$\frac{f_L}{f_S} e^{-U/kT_M} = 1.$$

* 'Phil. Mag.' vol. 17, p. 698 (1934).

Since, for a simple harmonic oscillator at temperatures such that $kT \gg h\nu$, f is proportional to $(kT/\nu)^2$, we have*

$$\frac{v_L}{v_S} = e^{-\frac{1}{2}U/kT_M}, \quad (1)$$

or

$$\frac{v_L}{v_S} = e^{-40(L/T_M)},$$

if L is the latent heat in kilojoules† per gram atom and T_M the melting point in degrees K.

According to the theory of metallic conduction developed‡ by Bloch and others, electrons can pass freely through a perfect crystal lattice, which consequently has infinite conductivity. Resistance is due to irregularities in the lattice, which may be due to the heat motion of the atoms, or to the presence of impurities or foreign atoms in solid solution. The theory shows that the resistance due to heat motion is proportional to the square of the distance through which the atoms vibrate; at temperature T , this distance x is given by

$$\frac{1}{2}fx^2 = kT \quad (f/M = 4\pi^2\nu^2)$$

f being the restoring force; hence,§ if σ is the conductivity,

$$\begin{aligned} 1/\sigma &\propto x^2 \propto T/M\nu^2 \\ &\propto k^2 T/M\Theta^2, \end{aligned} \quad (2)$$

where M is the mass of an atom.

The conductivity also depends on the extent to which the electrons may be considered "free," *i.e.*, to the ease with which they move from atom to atom under the influence of an electric field. Bethe|| gives the following formula for the conductivity:

$$\sigma = \frac{2n_0}{\pi^2} \frac{M}{m} \left(\frac{K}{C} \frac{dE}{dK} \right)^2 \frac{1}{hKa_0} \frac{k\Theta^2}{T}. \quad (3)$$

* Cf. Ratnowsky, 'Verh. deuts. phys. Ges.', vol. 16, p. 1033 (1914), who obtains the same formula. Ratnowsky calculates v_L/v_S for various metals; his experimental values for L , however, are not the same as those used here.

† A kilojoule is 10^{10} ergs.

‡ 'Z. Physik,' vol. 59, p. 208 (1930).

§ A formula of this type was proposed by Wien ('Sitzber. Preuss. Akad. Wiss,' p. 184 (1913)) before the application of quantum mechanics; Gruneisen, 'Verh. deuts. phys. Ges.', vol. 15, p. 194 (1913); Bridgeman ('Phys. Rev.', vol. 9, p. 269 (1917), and Beckman ('Phys. Z.', vol. 16, p. 59 (1917)) have shown that the change of conductivity under pressure $d\sigma/dp$ can be explained for many (but not all) metals, by taking for $d\Theta/dp$ a value deduced from the compressibility and thermal expansion coefficient.

|| 'Handb. Physik,' vol. 24/II, p. 507 (1933).

Here n_0 denotes the number of free electrons per atom; M , m are the masses of a vibrating atom and of an electron respectively, and a_0 is the radius of the first Bohr orbit. K denotes the wave number of an electron at the top of the Fermi distribution, and E the kinetic energy of such an electron. C is a constant depending on the interaction between the metallic ion and a free electron, and is a property of the ion rather than of the crystal structure.

We must now ask which of the properties of (3) may be expected to alter when the metal melts. K depends only on the specific volume, and so will not alter appreciably. dE/dK , on the other hand, depends on the structure, and will alter considerably on melting, if the arrangement of the atoms relative to each other alters. However, for good conductors, and especially for monovalent conductors, E and K are likely to have values approximating to the values for free electrons, namely

$$E = \frac{1}{2}mv^2, \quad K = 2\pi mv/h;$$

so that $E = \hbar^2 K^2 / 8\pi^2 m$, and

$$K \frac{dE}{dK} = 2E = \text{twice the maximum energy of the Fermi distribution.}$$

Since the energy of the Fermi distribution depends only on the volume, we should not expect any great change on melting.

For strongly diamagnetic metals, such as bismuth, it is well known* that the diamagnetism and low conductivity are related to an abnormally small value of dE/dK . Since the diamagnetism disappears on melting, we should expect an increase of dE/dK .

We therefore suggest the hypothesis† that in normal metals the change of resistance on melting is due mainly to the change in v , or Θ , discussed above. We should therefore expect that

$$\frac{\sigma_L}{\sigma_S} = \left(\frac{v_L}{v_S} \right)^2 = e^{-U/RT_M} = e^{-80L/T_M},$$

where L is the latent heat, in kilojoules per gram atom. Table I shows the extent to which this hypothesis is in agreement with experiment. The values

* Peierls, 'Z. Physik,' vol. 80, p. 763 (1933).

† Simon, 'Z. Physik,' vol. 27, p. 157 (1924), has suggested that the change of resistance is proportional to v_L/v_S , and has remarked that the observed change of resistance is of the same order of magnitude as the change in v_L/v_S deduced by Ratnowsky (*loc. cit.*).

of T_M and L are taken from the International Critical Tables,† the values of σ_S/σ_L from Grüneisen.‡

Table I— σ_L , σ_S are the conductivities of the liquid and solid respectively ; L is the latent heat in kilojoules per gram atom, and T_M the melting point.

Element	L	T_M (degrees K)	Θ	$\left(\frac{\sigma_S}{\sigma_L}\right)_{\text{calc.}}$	$\left(\frac{\sigma_S}{\sigma_L}\right)_{\text{obs.}}$
Li	3.2	459	510	1.84	1.68
Na	2.65	370.5	200	1.77	1.45
K	2.35	335.3	126	1.75	1.55
Rb	2.15	311.5	85	1.76	1.61
Cs	2.1	299	68	1.75	1.66
Cu	11.5	1356	310	1.97	2.07
Ag	11	1233.5	215	2.0	1.9
Au	13.3	1336	175	2.22	2.28
Al	8.0	933	400	2.0	1.64
Cd	6.2	593.9	168	2.3	2.0
Pb	4.70	600.5	90	1.87	2.07
Sn	(7)*	504.8	—	(3)*	2.1
Tl	6.15	580.5	96	2.3	2.0
Zn	7.1	692.4	235	2.3	2.09
Hg	2.33	234	97	2.23	3.2-4.9
Bi	10.9	544	—	5.0	0.43
Ga	5.55	302.7	—	4.5	0.58
Sb	19.5	903.5	—	5.6	0.67
Fe	11.2	1808	—	1.65	—
Ni	18.1,	1725	—	2.34	—
Pt	22	2028	—	2.40	—

* L not known accurately.

Table I shows also the Debye temperature Θ of some of the metals. For Li, Na, K and Al the assumption upon which the calculation is based, namely $T_M \gg \Theta$, is hardly justified. It would therefore be more correct to use, instead of (1)

$$\frac{e^{h\nu_S/kT_M} - 1}{e^{h\nu_L/kT_M} - 1} = e^{hU/kT_M} \quad (1.1)$$

This formula gives rather smaller values of ν_S/ν_L than those shown in Table I. Assuming as before that $\sigma_S/\sigma_L = (\nu_S/\nu_L)^2$, one obtains the following values :—

	Li	Na	K	Al
σ_S/σ_L calc. from (1)	1.84	1.77	1.75	2.0
σ_S/σ_L calc. from (1.1)	1.50	1.58	1.67	1.8
(1.57)				
σ_S/σ_L observed	1.68	1.45	1.55	1.64

† Approximately the same figures are given by Eucken, 'Handb. exp. Physik,' vol. 8/I, p. 592 (1929).

‡ 'Handb. exp. Physik,' vol. 13, pp. 28, 29 (1928) ; cf. Landolt-Börnstein, vol. 2, p. 1052.

The agreement with experiment is improved. On the other hand, a small correction must be applied in the other direction to take account of the fact that the law, $\sigma \propto \Theta^2/T$, depends also on the assumption that $T \gg \Theta$. However, according to the formulæ of Bloch, which are in agreement with experiment* as regards the temperature variation of resistance of copper and gold in the region $T \sim \Theta$, this correction† is only about 1% when $T \simeq 2\Theta$ and 5% when $T \simeq \Theta$. For lithium this correction is appreciable, and the corrected value is shown in brackets above.

For the monovalent metals, considering the considerable experimental uncertainties in the measurement of the latent heats and of σ_s/σ_L , the agreement is good, and is fair for some of the other metals. For bismuth, gallium and antimony, $\sigma_s < \sigma_L$, and we must conclude that the effective number of free electrons, $(dE/dK)^2$, increases by a factor of about 10 when the metal melts.

Of the metals for which σ_s/σ_L has been measured, mercury is the only one in which the increase of resistance on melting is considerably greater than that predicted by the theory, so that we must conclude that dE/dK is smaller in the liquid than in the solid state. This view is supported by the fact that the admixture of a small quantity of Au, Cd, Sn, Pb or Bi increases the conductivity, whereas in most other liquid metals, as in solids, the resistance is raised by the presence of foreign atoms.

The agreement obtained between theory and experiment for the normal metals is rather surprising, since it shows that the extra resistance in the liquid is due to the greater amplitude of the atomic oscillations, and not, to any large extent, to the irregularity of the arrangement of the atoms, as contrasted with their regular arrangement in the crystalline solid. From this we must, I think, conclude that, in a region large compared with the electron's wave-length (*i.e.*, the interatomic distance) the atoms of the liquid are arranged in a regular way, as in a crystal; and also that these small crystals are not separated by sharp surfaces, as are the crystallites of a polycrystalline metal, but merge gently into one another. Any *gradual* change of crystalline phase would not have the effect of scattering the electron waves as they travel through the liquid. This view is strengthened by the fact recorded by Norbury‡ that the addition of about 1% of Al, Ni, Ag, Sn or other metals to molten copper resulted in a rise of resistance, independent of temperature, of about

* Grüneisen, 'Ann. Physik,' vol. 16, p. 530 (1933).

† *cf.* Bethe, *loc. cit.* p. 532.

‡ 'Proc. Faraday Soc.,' vol. 16, p. 581, fig. 6 (1920).

the same amount as for solid copper. Thus it appears that foreign atoms have the same scattering power in the solid and liquid states, showing that the disorder in a liquid is not so great that it cannot be increased by the pressure of foreign atoms.

The change of electrical resistivity with temperature has been measured for very few liquid metals. For the resistivity, $\rho = 1/\sigma$, just above the melting point, Northrup* finds for liquid Cu, Ag, Au, and Bridgeman* for Li, Na, K, the following values :—

	Li	Na	K	Cu	Ag	Au
$10^8 \frac{1}{\rho} \frac{d\rho}{dT} \left\{ \begin{array}{l} \text{exp.} \\ \text{calc.} \end{array} \right.$	1.45	3.2	3.6	0.38	0.71	0.46
	2.2	2.7	3.0	0.74	0.81	0.75

On the theory given above,

$$\rho = \text{const } T,$$

and hence, as for a solid

$$\frac{1}{\rho} \frac{d\rho}{dT} = \frac{1}{T} \quad (4)$$

The values calculated from (4) at the melting point are shown above. The theoretical formula gives at any rate the order of magnitude of the observed effect.

On the other hand, the temperature coefficient of liquid mercury is equal to about one quarter of the theoretical value (4), and various investigators* have found that the resistance of liquid zinc is almost independent of temperature. One can only interpret these facts by assuming that the effective number of free electrons increases with T , which is, *a priori*, quite probable for a divalent metal.

[*Note added in proof, May 15, 1934*—While this paper was in press, a paper by Schubin ('Phys. Z. Sowjet Union,' vol. 5, p. 83, 1934) has appeared, dealing with the same subject. Schubin considers that the extra resistance in liquids is due to a process in which the electrons are scattered without loss of energy, the configuration of the ions changing at the same time from one state of relative equilibrium to another. The probability of such a process is shown to be independent of temperature.

If Schubin's explanation of the resistance is correct, the temperature coefficient should be less than that given by (4), as is in fact the case for a great many metals. On the other hand, it seems to the author that, except for the

* References in 'Handb. Exp. Physik,' vol. 13, p. 28 (1928).

monovalent metals silver and the alkalis, it is rather dangerous to assume that the free electron number in a liquid is independent of temperature, since, according to the theory of Bloch, when an allowed zone of energies is nearly full, the number of electrons which are free to move depends rather sensitively on the structure. According to the experimental values given above, however, it seems that it is just for the monovalent metals that (4) is approximately valid.

Schubin also considers, in agreement with the present author, that the type of disorder which exists in a liquid is unlikely to increase the resistance appreciably.]

Summary

It is assumed that the atoms in a liquid metal vibrate about slowly varying mean positions with a frequency ν_L ; the ratio of ν_L to the atomic frequency of the solid is calculated from the observed latent heat and melting point. It is shown that the change of resistance on melting can be accounted for by the change in atomic frequency, for normal metals; and the bearing of this fact on theories of liquid structure is discussed.

X-ray Analysis of the Crystal Structure of Dibenzyl I—Experimental and Structure by Trial

By J. MONTEATH ROBERTSON, M.A., Ph.D., D.Sc.

(Communicated by Sir William Bragg, O.M., F.R.S.—Received May 9, 1934)

The molecules of those aromatic compounds such as naphthalene, durene, and diphenyl which have been examined in detail by the X-ray method are all found to possess a planar structure to within the limits of the respective experimental errors. Dibenzyl, the analysis of which is described below, now proves to be an interesting exception to this rule because the molecule is found to extend in three dimensions. A planar structure would be quite in keeping with the chemical formula, but the X-ray evidence seems to point conclusively to an alternative structure in which the benzene rings though parallel occupy different planes (see fig. 3); those planes being at right angles to the plane containing the zig-zag of the connecting CH_2 groups.

Crystal Data—Space Group

Dibenzyl belongs to the monoclinic prismatic class. Good crystals were easily obtained from alcohol or ether solution, and the form is a familiar one; being very similar to the naphthalene and diphenyl series except that there is a somewhat greater tendency for the crystals to elongate along the b axis. The (001), (110), and (201) faces are most frequently developed, particularly the former. The axial ratios are given by Groth* as

$$a : b : c = 2.0806 : 1 : 1.2522. \quad \beta = 115^\circ 54'.$$

Hengstenberg and Mark† have made an X-ray examination and give

$$a = 12.82, b = 6.18, c = 7.74 \text{ \AA}, \beta = 116^\circ; \text{ density} = 1.105,$$

the space group being C_{2h}^5 ($\text{P2}_1/a$) with two molecules in the unit cell. But it is hard to reconcile the visual estimates of intensities recorded by these authors with the values now measured and given below. It seems possible that their indices may have been incorrectly assigned to the various reflections.

* 'Chem. Krystallog.', vol. 5, p. 191 (1919).

† 'Z. Krystallog.', vol. 70, p. 283 (1929).

For the purpose of this work the cell dimensions have been remeasured, chiefly by means of single crystal rotation photographs, with the following results:—

$$a = 12.77 \pm 0.05 \text{ \AA}$$

$$b = 6.12 \pm 0.03 \text{ \AA}$$

$$c = 7.70 \pm 0.03 \text{ \AA}$$

$$\beta = 116.0^\circ \pm 0.2.$$

The $\{hol\}$ reflections are halved when h is odd, and the (010) is halved. The space group is thus C_{2h}^5 ($P2_1/a$), as recorded above, and the two molecules in the unit cell must each possess a centre of symmetry.

Experimental—Measurement of Intensities

Certain difficulties were encountered in dealing with the crystals of this compound with regard to quantitative intensity measurement. When mounted in the ordinary way and exposed to the X-ray beam the crystal surfaces gradually become white and after some days the whole crystal crumbles away. The nature of this change was not ascertained, but it was found that it could be greatly diminished by sealing the specimens off in small glass tubes. Specially thin Lindemann glass tubes* were used for this purpose, which stopped only a small fraction of the X-rays—copper radiation.

Small crystal specimens (0.1–0.4 mg) were now rotated while completely immersed in the X-ray beam, and the integrated reflections recorded by the photographic method. Most of the work was carried out on the new two-crystal moving film spectrometer† which had three distinct applications to the present work.

1—By exposing a standard crystal and the crystal under investigation in alternation to the X-ray beam, reflections of known absolute intensity were recorded side by side with the dibenzyl reflections on the moving film, thus ensuring correct calibration with absolute values.

2—The automatic shutters were employed to reduce the intensity of the more powerful dibenzyl reflections by a factor of 12 and so make their comparison with the weaker reflections more accurate.

3—Reflections from two dibenzyl crystals set about different zone axes were recorded on the same film to ensure a correct correlation. The various films were then carefully measured with Robinson's integrating photometer.

* For the preparation of these tubes I am much indebted to Mr. H. Smith of this laboratory.

† Described in a later paper in the 'Phil. Mag.'

In order to calculate the values of the structure factors it was further necessary to know the absorption of the crystals and of the glass containers for the X-ray beam. These were measured by exploration with a fine pinhole beam of monochromatic rays. The glass containers were found to stop about 10% of the X-rays, and for the absorption coefficient of the crystal a value of about 5.0 per cm was obtained. This is somewhat less than the calculated value of $\mu = 5.7$ for $\lambda = 1.54$. A rough correction was now applied to allow for the different paths presented by the crystal specimen when oriented for the various reflections in the zone, but as care had been taken to cut the specimens to a nearly square section (side about 0.4 mm) this correction did not amount to much.

The values of the structure factors were now obtained by the usual formulæ for the "imperfect crystal" and are given in Table I under the heading "F measured."

Table I—Measured and Calculated Values of the Structure Factor

<i>hkl</i>	$\sin \theta$ $\lambda = 1.54$	F measured	F calculated	<i>hkl</i>	$\sin \theta$ $\lambda = 1.54$	F measured	F calculated
200	0.134	38	-40	051	0.640	<3	-1
400	0.268	7	-10	052	0.669	4	-6
600	0.402	16	+12	053	0.713	<3	+0
800	0.536	14	+23				
1000	0.670	11	-22	206	0.732	<3	+2
020	0.252	10	+5	205	0.624	<3	+2
040	0.504	9	-8	204	0.515	17	+18
060	0.755	<3	-3	203	0.409	13	+13
001	0.110	20	+16	202	0.305	15	-14
002	0.221	20	-10	201	0.409	23	+16
003	0.332	7	+6	201	0.133	13	+15
004	0.442	12	-13	202	0.204	70	+66
005	0.553	3	+2	203	0.300	6	+5
006	0.664	<3	-8	204	0.404	11	+15
				205	0.511	<2	-3
011	0.168	59	+52	206	0.619	5	-1
012	0.255	18	-13	207	0.728	<3	-4
013	0.355	3	+7	405	0.713	3	+6
014	0.460	4	-7	404	0.609	<3	-5
015	0.568	5	-2	403	0.510	<3	+3
016	0.676	<3	0	402	0.416	34	+30
021	0.276	19	+19	401	0.333	25	+14
022	0.336	6	0	401	0.243	12	+8
023	0.418	3	0	402	0.264	3	-6
024	0.510	3	0	403	0.323	<2	+1
025	0.609	5	-8	404	0.405	<2	-12
026	0.710	<3	+6	405	0.498	<2	-2
031	0.394	15	+11	406	0.598	11	+10
032	0.488	<2	-1	407	0.700	<3	-4
033	0.504	8	-8	604	0.717	6	+12
034	0.583	<3	+3	603	0.625	6	+6
035	0.670	2	-7	602	0.538	2	+6
041	0.516	5	-4	601	0.462	2	+5
042	0.550	<2	+2	601	0.370	11	+4
043	0.605	5	-6	602	0.366	18	-24
044	0.672	<3	-2	603	0.396	4	-4

Table I—(continued)

hkl	$\sin \theta$ $\lambda = 1.54$	F measured	F calculated	hkl	$\sin \theta$ $\lambda = 1.54$	F measured	F calculated
604	0.450	13	+10	510	0.359	16	+10
605	0.523	<3	-5	520	0.420	5	-7
606	0.607	9	-18	530	0.505	<5	+3
607	0.700	<3	-3	540	0.605	<6	-3
803	0.745	<3	+1	550	0.714	<6	-4
802	0.605	<3	-3	610	0.422	<5	+4
801	0.595	<3	-3	620	0.475	9	-11
901	0.500	5	+1	630	0.551	<6	+1
902	0.485	<2	+2	640	0.645	<6	-5
903	0.495	2	-3	710	0.485	6	-8
904	0.527	17	-23	720	0.533	<5	+7
905	0.580	6	-6	730	0.602	<6	-1
906	0.647	3	-1	740	0.689	<6	+4
907	0.726	<3	-3	810	0.550	5	+9
1001	0.728	<3	+3	820	0.592	<6	+2
1001	0.632	9	-9	830	0.657	<6	+6
1002	0.610	12	+15	840	0.736	<6	+1
1003	0.608	4	-4	910	0.617	<6	+7
1004	0.625	<3	+4	920	0.653	9	+6
1005	0.659	<3	-4	930	0.711	<6	-2
1006	0.710	6	-5	1010	0.683	<6	-4
1202	0.738	10	-18	1020	0.716	<6	-1
1203	0.727	9	-6				
1204	0.732	<3	-2	111	0.199	8	+6
				111	0.161	37	+35
110	0.144	15	+11	112	0.238	59	+50
120	0.260	4	+1	113	0.333	<2	+3
130	0.385	7	-2	223	0.480	3	-4
140	0.510	9	+12	222	0.396	13	+15
160	0.633	<6	-3	221	0.327	8	+6
210	0.185	<3	+3	221	0.284	7	-8
220	0.286	10	-4	222	0.322	9	-6
230	0.402	4	+5	223	0.390	21	+23
240	0.522	<5	0	224	0.475	<3	+2
250	0.645	10	-12	333	0.593	<3	+4
310	0.238	15	+15	332	0.520	10	+13
320	0.323	18	+19	331	0.464	8	+9
330	0.428	<3	+1	331	0.419	10	-7
340	0.542	<6	+5	332	0.439	<3	+3
350	0.661	<6	-3	333	0.484	5	-7
410	0.295	<4	+1	334	0.548	10	-11
420	0.368	25	+25	441	0.556	8	+14
430	0.465	10	+8	442	0.567	<3	-3
440	0.571	<3	+1	443	0.598	11	-9
450	0.685	<6	+7				

Analysis of the Structure

Basing the calculations on the atomic f -curve for carbon obtained first from graphite and later modified slightly to fit the anthracene and naphthalene measurements, it is found that few of the dibenzyl structure factors attain a value of more than 50% of their possible maxima. This indicates at once that as in the vast majority of organic structures the atoms in the dibenzyl molecule do not lie in any simple relation to any of the crystallographic planes. The

strongest reflections are given by the (20 $\bar{2}$) and the (011) planes with structure factors of 70 and 59 comparing with possible maxima of about 113 and 126 units respectively. The molecules must thus be oriented so that the atoms concentrate to some extent on these planes.

It is now necessary to consider the relative positions of the atoms as given by the chemical structure. Unlike naphthalene and the other condensed ring structures already studied, there are in this substance several alternative models, owing to the possibility of free rotation about the single bonds between the CH₂ groups and between these and the benzene rings. The centre of

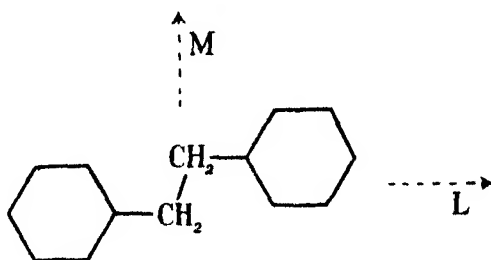


FIG 1—Model A

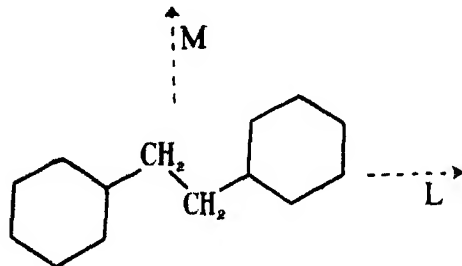


FIG 2—Model A'

symmetry which must exist in the molecule between the CH₂ groups disposes at once of certain possibilities. Thus there is only one planar configuration as illustrated in figs. 1 and 2. These two diagrams represent the same model, but one is turned over and then rotated in the plane of the paper until the ring occupy as nearly as possible the same positions as before. For the purpose of this analysis it is convenient to consider these as separate models. (It may be noted that owing to the higher symmetry inherent in the naphthalene, anthracene, and duren structures of our earlier analyses alternatives of this kind did not arise.)

With regard to non-planar models, the planes of the benzene rings might make any angle with the plane of the central zig-zag, but the most symmetrical

model is obtained when they are placed at right angles, as illustrated in fig. 3.

Another possibility to be kept in mind is that of actual rotation or other large movement of the groups about the single bonds. But such a possibility seems rather remote as it would involve quite a large motion of the benzene rings as a whole in the crystal.

Although models A and B are radically different yet if they are brought as nearly as possible into coincidence it is found that the difference in position of corresponding atoms is not a large one, certainly much smaller than the over-all dimensions of the molecule. Thus it is not surprising to find that each of the models can be oriented with respect to the crystal axes in a manner which gives quite a fair quantitative explanation of the intensities of all the

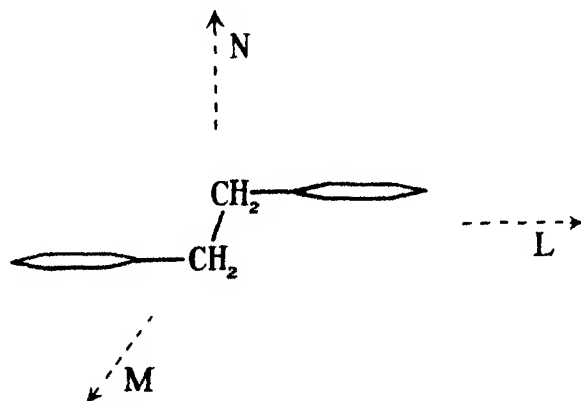


FIG 3—Model B

larger spacing reflections. These orientations can be found by concentrating first of all on the strongest reflections like the $(20\bar{2})$ and the (011) already mentioned, and gradually refining the positions by passing to a study of the higher order reflections. It is when we reach these smaller spacing planes that the difference between the models begins to show itself. With A and A', fig. 1 and 2, it is found to be quite impossible to get good agreements between the calculated and observed values for *all* the reflections, no matter how the models are moved about. But with model B it is possible to obtain the same order of agreement for all the reflections as has already been found for anthracene, naphthalene, and other structures.

Table II contains reflections representative of four different zones and shows the extent of the agreements obtained for the different models when each is moved into the orientation most suited to it. A more complete list of the

measured values of F and those calculated from model B is given in Table I.

The orientations found may be described as follows. χ , ψ , and ω are the angles which the direction L, see figs. 1, 2, and 3, makes with the a , b , and c' crystal axes (c' is perpendicular to a and b). χ' , ψ' , ω' and χ'' , ψ'' , ω'' are the corresponding angles for the directions M and N. M in fig. 3 is supposed to be perpendicular to the plane of the paper and parallel to the planes of the rings. Then

Models A and A'			Model B		
$\chi = 30^\circ$	$\chi' = 117.5^\circ$		$\chi = 49.5^\circ$	$\chi' = 126.1^\circ$	$\chi'' = 61.3^\circ$
$\psi = 75^\circ$	$\psi' = 42^\circ$		$\psi = 75^\circ$	$\psi' = 40^\circ$	$\psi'' = 54^\circ$
$\omega = 64.7^\circ$	$\omega' = 61^\circ$		$\omega = 44.4^\circ$	$\omega' = 75.1^\circ$	$\omega'' = 130.5^\circ$

A movement of a few degrees from these values is not important at the present stage. The figures are given in more detail in order to be mutually consistent.

Table II—Comparison of the Structure Factors Calculated from Different Models

hkl	F measured	F calc. model B	F calc. model A	F calc. model A'	hkl	F measured	F calc. model B	F calc. model A	F calc. model A'
200	38	-40	-39	-43	202	15	-14	-4	-3
400	7	-10	-10	-19	201	23	+16	+14	+11
600	16	+12	+29	+5	201	13	+15	+16	+12
020	10	+5	-1	+7	202	70	+66	+53	+55
040	9	-8	-17	-6	403	<3	+3	+1	+3
001	20	+16	+22	+23	402	34	+30	+29	+19
002	20	-10	-29	-20	401	25	+14	+9	+3
003	7	+6	+4	+9	401	12	+8	+13	+2
004	12	-13	-18	-7	402	3	-6	+20	+10
005	3	+2	-5	+6	602	18	-24	-9	-34
006	<3	-8	+3	+2	603	4	-4	+2	-10
					803	2	-3	+3	-6
110	15	+11	+20	+22	804	17	-23	0	-12
210	<3	+3	-1	-5	1002	12	+15	+29	-6
310	15	+15	+6	+2	1003	4	-4	+9	-6
410	<4	+1	+2	-3	1202	10	-18	-5	+2
510	16	+10	+13	+10	1203	9	-6	0	0
120	4	+1	+1	-2	1204	<3	-2	+18	-12
220	10	-4	-6	-3					
320	18	+19	+9	+2	111	8	+6	+5	+8
420	25	+25	+24	+26	111	37	+35	+24	+27
					112	59	+50	+55	+61
011	59	+52	+68	+63	113	<2	+3	+5	+10
012	18	-13	0	-5	222	13	+15	+6	+11
021	19	+19	+15	+22	221	8	+6	-2	+2
022	6	0	+2	+23	223	21	+23	+12	+18
031	15	+11	+18	+11	224	<3	+2	+16	+19
032	<2	-1	+14	+5	332	10	+18	+10	+12
					332	<3	+3	-6	+8
205	<3	+2	-3	+7	442	<3	-3	-8	+9
204	17	+18	+7	+22	443	11	-9	-16	-1

In the models we have assumed the benzene rings to be regular plane hexagons of 1.41 Å between the carbon atoms, the angles between the bonds of the CH₂ groups to have the tetrahedral value of 109½°, the distance between the CH₂ groups to be 1.54 Å, and the distance between these groups and the benzene rings to be 1.47 Å. A refinement of these figures will be attempted at a later stage by the method of Fourier analysis.

In discussing these results it must be remembered that no attempt has yet been made to refine the shape of the model, the angle of the bonds, etc., and that no account has been taken of the effect of the hydrogen atoms or allowance made for any difference in scattering power between aromatic and aliphatic carbon atoms. Even so it is found that the discrepancies for model B (the three-dimensional structure) are of just about the same order as in our previous analyses. But for the planar models, A and A', these discrepancies, when summed, are found to be more than twice as great. The conclusion, therefore, must be that the X-ray evidence points quite definitely to the three-dimensional model.

It may be of interest to mention that in carrying out this analysis the planar models were tested first, and a considerable time was spent in trying to get agreements, and a large number of orientations were studied. But when the three-dimensional model was adopted at a later stage the orientation given above was found in a comparatively short time.

The minimum distance between the atoms on adjacent molecules obtained from this structure is found to be of the order of 3.7 Å, the same as for the other hydrocarbons which have been analysed.

Evidence from other Physical Properties

Very few data are available on the optical properties of this crystal, but the observations recorded by Groth* seem to be consistent with the present structure.

More detailed work has been done, however, on the magnetic properties of the crystal by Krishnan† and his collaborators, who have calculated the orientation of the molecules by making a correlation between the magnetic anisotropy of the crystal and that of the individual molecules. Their orientation is described by first placing the molecule with its plane parallel to the (100) plane, and its length along the *c* axis, then rotating about *c* through an angle λ

* 'Chem. Krystallog.', vol. 5, p. 191 (1919).

† 'Phil. Trans.,' A, vol. 231, p. 235 (1933).

and about b through an angle μ (towards a through the obtuse angle β). The molecule is next rotated through an angle ν about the normal to the plane containing b and the length of the molecule (after the rotation μ has been performed). They then find that $\lambda = 30^\circ$, $\mu = 83.9^\circ$, $\nu = 0^\circ$.

In our structure, the three-dimensional molecule has no longer a unique plane and so the above description is hardly applicable. But if we take the "plane" of the molecule to be the mean plane through the centre of symmetry and parallel to the planes of the benzene rings, we find,* in the above notation, that $\lambda = 37.5^\circ$, $\mu = 68.2^\circ$, $\nu = 15^\circ$. Although our figures differ from those quoted above, it is satisfactory to find that the orientation obtained from the X-ray analysis bears at least considerable resemblance to that deduced from the magnetic measurements.†

Our figures, of course, may be subject to an alteration of a few degrees when the structure is further refined by a Fourier analysis, but not by as much as is required to bring them into really close agreement with the results obtained from the magnetic measurements. Rather than question these measurements, which have been very carefully performed, we would suggest that the values used for the principal susceptibilities of the individual molecules along their lengths, breadths, and the normals to their planes, upon which the calculations are based, may require some modification. There is no doubt that when quantitative intensity measurements are employed, X-ray analysis is an exceedingly accurate method of determining even a complex structure like that of dibenzyl. When complete it is then possible to work back and express the various physical properties of the crystal, such as the optical and magnetic anisotropies, as properties of the individual molecules. This is, of course, one of the most valuable results of the X-ray investigation of these organic structures.

In conclusion, I wish to thank Sir William Bragg, O.M., F.R.S., and the Managers of the Royal Institution for the facilities afforded me at the Davy

* Employing the relations :—

$$\begin{aligned}\cos \chi &= \cos \nu \cdot \cos (\beta - \mu) \\ \cos \psi' &= \cos \nu \cdot \cos \lambda \\ \psi &= 90^\circ - \nu.\end{aligned}$$

† Through an oversight the writer was not aware of the magnetic measurements and deduced orientation of dibenzyl until the X-ray analysis was complete. In the present work, therefore, the X-ray results were arrived at quite independently. But in general even a rough knowledge of the magnetic susceptibilities is a valuable aid in the preliminary stages of X-ray analysis.

Faraday Laboratory for carrying out this work. I am also indebted to Miss I. Woodward for assistance with the numerical work involved.

Summary

An X-ray investigation of the crystal structure of dibenzyl is described. The space group is $P2_1/a$, and the two molecules in the unit cell each possess a centre of symmetry.

Quantitative intensity measurements have been made of the reflections from about a hundred crystal planes.

In the analysis of the structure it is shown that the molecule extends in three dimensions instead of being planar as in the aromatic compounds already examined. The planes of the benzene rings, though parallel to each other, are at right angles to the plane containing the zig-zag of the connecting CH_2 groups. The orientation of this molecule in the crystal has been determined and is stated on p. 479.

The relation with Krishnan's work on the magnetic susceptibilities of the crystal is discussed.

Artificial Radioactivity produced by Neutron Bombardment

By E. FERMI, E. AMALDI, O. D'AGOSTINO, F. RASETTI, and E. SEGRÈ

(Communicated by Lord Rutherford, O.M., F.R.S.—Received July 25, 1934)

I—Introduction

This paper aims at giving a fuller account of experiments made in the Physical Laboratory of the University of Rome, on new radio-elements produced by neutron bombardment. Preliminary results have already been announced in short communications.*

Curie and Joliot† first discovered that the product atom of an artificial disintegration need not always correspond to a stable isotope, but could also disintegrate with a relatively long mean life with emission of light particles. As bombarding particles they used α -particles from polonium, and found that the light particle emitted was generally a positron. Similar results were obtained on several elements by other experimenters using α -particles, and artificially accelerated protons and deutons.‡

The use of charged particles for the bombardment, limits the possibility of an activation only to light elements. Indeed, only about ten elements up to the atomic number 15 could be activated by these methods.

It seemed therefore convenient to try the effect of a neutron bombardment, as these particles can reach the nucleus even of the heaviest elements. Available neutron sources are, of course, much less intense than α -particles or proton or deuteron sources. But it was reasonable to assume that this factor would be partly compensated by the higher efficiency of neutrons in producing disintegrations. Indeed, experiment showed that more than forty elements out of about sixty investigated could be activated by this method.

* Fermi, 'Ric. Scient.,' vol. 1, pp. 283, 330 (1934); Amaldi, D'Agostino, Fermi, Rasetti and Segrè, 'Ric. Scient.,' vol. 1, pp. 452, 652, 21 (1934); Fermi, Rasetti and D'Agostino, 'Ric. Scient.,' vol. 1, pp. 533 (1934); Fermi, 'Nature,' vol. 133, pp. 757, 898 (1934). See also Fermi, 'Nuovo Cim.,' vol. 11, p. 429 (1934); Amaldi, Fermi, Rasetti and Segrè, 'Nuovo Cim.,' vol. 11, p. 442 (1934); Amaldi and Segrè, 'Nuovo Cim.,' vol. 11, p. 452 (1934); 'D'Agostino 'Gazz. Chim. Ital.,' in press (1934).

† 'C.R. Acad. Sci. Paris,' vol. 198, pp. 254, 561 (1934).

‡ Frisch, 'Nature,' vol. 133, p. 721 (1934); Wertenstein, 'Nature,' vol. 133, p. 564 (1934); Cockcroft, Gilbert and Walton, 'Nature,' vol. 133, p. 328 (1934); Neddermeyer and Anderson, 'Phys. Rev.,' vol. 45, p. 498 (1934); Lauritsen, Crane and Harper, 'Science,' vol. 79, p. 234 (1934).

2—*The Experimental Method*

The neutron source consisted of a sealed glass tube about 6 mm in diameter and 15 mm in length, containing beryllium powder and radon in amounts up to 800 millicuries. According to the ordinarily assumed yield of neutrons from beryllium, the number of neutrons emitted by this source ought to be of the order of 1000 neutrons per second per millicurie. These neutrons are distributed over a very wide range of energies from zero up to 7 or 8 million volts, besides a very small percentage having energies about twice as high as this limit.

The neutrons are mixed with a very intensive γ -radiation. This does not, however, produce any inconvenience, as the induced activity is tested after irradiation, and it was shown that radon without beryllium produced no effect. The neutrons from beryllium are accompanied by a γ -radiation harder than any emitted by the radon products (5 to 6 million volts—about one γ -quantum per neutron). It seems, however, most unlikely that the observed effects are in any way connected with this γ -radiation, as a γ -radiation of enormously greater intensity and only slightly lower energy produces no effect.

The emission of electrons from the activated substances was tested with Geiger-Müller counters about 5 cm in length and 1.4 cm diameter. The walls of the counter were of thin aluminium foil, 0.1 to 0.2 mm in thickness. The applied voltage ranged between 1000 and 1500 volts. The amplified impulses were counted on a mechanical meter worked by a thyratron.

The substances to be investigated were generally put into form of cylinders, which could be fitted round the counter in order to minimize the loss in intensity through geometrical factors. During irradiation the material was located as close as possible round the source. Substances which had to be treated chemically after irradiation were often irradiated as concentrated water solutions in a test tube.

The decay curves of the induced activity were for many elements simple exponentials. Sometimes they could be analysed into two or more exponentials; it was then convenient to irradiate the substance for different lengths of time in order to activate the various components with different intensity. The existence of several mean lives is, sometimes, certainly due to different isotopic constituents of the element; when a single isotope is present it may be attributed to alternative processes of disintegration, and sometimes (uranium) to a chain of disintegrations. The intensity of activation varies within a wide range among the different elements: In some the effect is hardly measurable,

the number of impulses produced by the irradiated substance being of the order of magnitude of the number of spontaneous impulses in the counter. In others the activation is so strong that when the substance is placed too near the counter the number of impulses is of the order of some thousands per minute, so that they cannot be counted because of lack of resolving power.

No accurate measurement of the intensity of activation of the different elements was carried out, as it would require experimenting in well-defined geometrical condition, and a knowledge of the efficiency of our counters in counting electrons, and of the absorption in the substance and in the aluminium foil. However, a very rough evaluation of these factors was made, and for some elements a number expressing the intensity of activation (i) is given. This intensity is defined as the number of disintegrations per second which take place in 1 gm of the element, placed at the distance of 1 cm from a neutron source consisting of one millicurie of radon (in equilibrium with its decay products) and beryllium powder. The substance was always irradiated until saturation of the active product was reached. The efficiency of our counters (including absorption in the aluminium foil and geometrical factors) was about $1/20$, as determined by the measurement of the impulses from known quantities of potassium and uranium.

From this number expressing the intensity it is easy to obtain the cross-section for the activating neutron impact, if the number of neutrons emitted per second by a one millicurie source is known. Assuming this number to be 1000, one finds immediately the cross-section

$$\sigma = 2 \cdot 10^{-26} i \cdot A,$$

A being the atomic weight of the element.

In order to be able to discuss the nuclear reaction giving rise to the active element, it is essential to identify it chemically. It is reasonable to assume that the atomic number of the active element should be close to the atomic number Z of the bombarded element. As the amount of the active substance is exceedingly small (in the most favourable cases about 10^9 atoms), there is no hope of separating it by ordinary methods. The irradiated substance was therefore dissolved, and small amounts of the inactive elements, which are suspected of being isotopic with the active product, were added. These added elements and the irradiated element were then chemically separated from each other, and separately tested for activity. It is generally found that the activity follows definitely one element. The active product can then be considered as identified with this element.

A preliminary investigation of the penetrating power of the β -rays of the new radio-elements has been carried out. For this purpose counters of the standard type were used, and the substance, instead of being put quite close to the counter, was shaped in the form of a cylinder of inner diameter somewhat larger than the diameter of the counter in order to allow cylindrical aluminium screens of different thicknesses to be interposed. In this way absorption curves of a more or less exponential type were obtained. As the geometrical conditions of this absorption measure are different from the standard ones, and moreover, the number of impulses instead of the total ionization is computed, we checked the method by measuring the absorption coefficients for known radioactive substances; as expected, we found a difference (about 20%). The data are corrected for this factor.

In several cases the absorption by 2 mm of lead was not complete; this was assumed as a proof of the existence of a γ -radiation.

It was very important to determine whether the emitted particles were positive or negative electrons. Owing to the weakness of the radiation it seemed convenient to use for this purpose Thibaud's* method of the inhomogeneous magnetic field. Even by this intensive arrangement this investigation had to be limited to elements which could be strongly activated (Al, Si, P, S, Cr, As, Br, Rh, Ag, I, Ir, U). In every case only negative electrons were observed. This, however, does not exclude that a small percentage (up to about 15%) of the emitted particles might be positrons.

For a few very strongly activated elements the emitted electrons could be also photographed in a Wilson chamber.

3—*Experimental Results*

The elements investigated are here arranged in order of atomic number; a summary of the results is to be found in a table at the end of the paper.

1—*Hydrogen*—Shows no effect when water is irradiated 14 hours with a 670-millicuries source.

3—*Lithium*—The hydroxide irradiated 14 hours with 750 millicuries is inactive.

4—*Beryllium*—Shows an extremely weak activity which might well be due to impurities.

5—*Boron*—Same as beryllium.

* 'C.R. Acad. Sci. Paris,' vol. 197, p. 447 (1933).

6—*Carbon*—Paraffin irradiated 15 hours with 220 millicuries is inactive.

7—*Nitrogen*—Guanidine carbonate (about 35% N) irradiated 14 hours with 500 millicuries is inactive.

8—*Oxygen*—No activity: see hydrogen.

9—*Fluorine*—This element irradiated as calcium fluoride can be strongly activated ($i = 0.7$). As calcium proves to be inactive, the effect is due to fluorine. The activity decreases with a very short half period, about 9 seconds. No chemical separation was possible in this case. However, as it is known that fluorine disintegrates under neutron bombardment with emission of an α -particle, the active nucleus is probably N^{16} . This unstable isotope goes over to stable O^{16} with emission of an electron. The remarkable stability of the latter nucleus agrees with the observed very high energy of the β -rays; the intensity reduces to half value in $0.24 \text{ gm/cm}^2 \text{ Al}$. This and all the following absorption data are given for aluminium.

11—*Sodium*—This element has been irradiated as carbonate. Sodium shows a fairly strong activation, decreasing with a period of about 40 seconds.

12—*Magnesium*—This element can be fairly strongly activated, and the decay curves show the existence of two periods, of about 40 seconds and 15 hours. Half-value thickness for the long period 0.06 gm/cm^2 .

The active element decaying with the 15 hours' period could be chemically separated. The irradiated magnesium was dissolved, and a sodium salt was added. The magnesium was then precipitated as phosphate and found to be inactive, while the sodium which remains in the solution carries the activity. The active atom is thus proved not to be an isotope of magnesium, and as neon also can be excluded, we assume it to be an isotope of sodium, formed according to the reaction:



13—*Aluminium*—This element acquires a strong activity under neutron bombardment. The decay curves indicate two periods of about 12 minutes ($i = 0.8$) and 15 hours ($i = 0.5$). Half-value thickness respectively, 0.07 and 0.06 gm/cm^2 .

The long-period activity could be chemically separated by dissolving the irradiated aluminium and adding to it small quantities of sodium and magnesium. Aluminium and magnesium are then precipitated as hydroxides and phosphates, and are found to be inactive. The solution containing sodium is then dried up, and shows an activity decaying with the 15 hours' period.

The active element is probably the same as in the former case of magnesium, as the identity of the periods and of the half-value thickness suggests. In the present case the nuclear reaction is

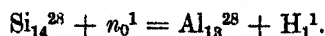


This active isotope Na^{24} then goes over to the stable isotope Mg^{24} with emission of an electron.

The active product with the 12-minute period has not been separated. However, we consider it likely to be Mg^{27} , as the other two possible cases, Al^{28} and Al^{26} , are probably to be excluded, the first because Al^{28} , as we shall next see, is a radioactive isotope with a period of 3 minutes, and the latter because Al^{26} should probably disintegrate with emission of positrons.

14—*Silicon*—Silicon is also strongly active ($i = 0.7$), and has a period probably somewhat shorter than 3 minutes. Half-value absorption thickness of the β -rays, 0.16 gm/cm^2 .

The chemical separation of the active element has been performed by evaporating irradiated silica with hydrofluoric and sulphuric acids, after addition of aluminium and magnesium. Silicon is eliminated as fluoride, and aluminium precipitated from the residue is found to contain the activity. The active product is therefore probably an isotope of aluminium, and the nuclear reaction is

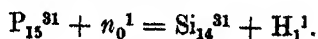


This is in accordance with the hypothesis of Curie, Joliot and Preiswerk* about the identity of this active isotope with the one which is formed by the impact of α -particles on Mg^{25} , and which has actually the same period.

15—*Phosphorus*—This element shows a strong activity ($i = 0.6$) decaying with a period of about 3 hours, and also an activity ten times less intense with a period of 3 minutes, first noticed by Curie, Joliot and Preiswerk. The half-value thickness for the β -rays of the 3 hours' product is 0.09 .

The 3 hours' active product could be chemically separated. For this purpose phosphorus was irradiated as a concentrated solution of phosphoric acid. This solution was afterwards diluted with water, adding sulphuric acid and a small amount of sodium silicate. The substance is dried up to render silica insoluble, and then dissolved in water and filtered. The activity is found with the silica.

The nuclear reaction is then probably



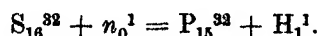
* 'C.R. Acad. Sci. Paris,' vol. 198, p. 2089 (1934).

The 3 minutes' active product has not been chemically separated. The identity of period suggests that it might be the same Al^{33} obtained from silicon.

16—*Sulphur*—Sulphur shows a fairly strong activity, decaying with a period of about 13 days (rather inaccurately measured). Half-value absorption thickness of the β -rays 0.10 gm/cm^2 .

A chemical separation of the active product was carried out as follows: irradiated sulphuric acid was diluted, a trace of sodium phosphate added, and phosphorus precipitated as phosphomolibdate by addition of ammonium molibdate. The activity was found in the precipitate.

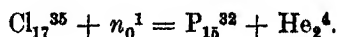
We think, in consequence, that the nuclear reaction is



This active P^{32} is transformed by emission of an electron into the stable isotope S^{32} .

17—*Chlorine*—Half-period and penetration of the β -rays of this element are about the same as for sulphur. Intensity, $i = 0.1$. The active substance was separated with a method quite similar to that used for sulphur. Irradiated ammonium chloride was dissolved in diluted nitric acid, and then phosphorus added and separated as in the former case. This element carried the activity as before.

The nuclear reaction which gives rise to the same active phosphorus as obtained from sulphur is



20—*Calcium*—No activity could be detected.

22—*Titanium*—A very weak effect, with a period of a few minutes, could be observed. However, it cannot be excluded that it might be due to impurities.

23—*Vanadium*—This element shows a medium activity. The half-period is about 4 minutes, and coincides within experimental error with those observed in chromium and manganese, which are due to isotopes of vanadium. This suggests the hypothesis that the active element might be V^{52} . The half-value thickness is also the same as for chromium, 0.16 gm/cm^2 .

24—*Chromium*—Metallic chromium becomes fairly strongly active under neutron irradiation. The half-period is, as in the former case, about 4 minutes. Half-value absorption thickness, 0.16 gm/cm^2 .

In order to identify the active element, we proceeded as follows: to irradiated ammonium chromate some sodium vanadate was added, and vanadium precipitated by addition of ammonium chloride. The activity being found

in the precipitate, it is certainly not due to an isotope of chromium. To see whether it was an isotope of titanium, a titanium salt was added besides vanadium to the irradiated chromium compound, and titanium precipitated by hydrolysis. The precipitate showed no activity. In consequence, we consider the active substance to be probably the same isotope V^{52} as before, formed according to the nuclear reaction



25—*Manganese*—We irradiated manganese dioxide and found a fairly intense activity decaying with two periods: about four minutes and two and a half hours. Half-value absorption thickness for the electrons of the 2.5 hours' product, 0.16 gm/cm².

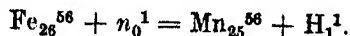
The activity with the long period cannot be separated from manganese by adding chromium and vanadium and precipitating them respectively as chromate and vanadate of lead. It is therefore probably due to an isotope of manganese, Mn^{56} , the same which is extracted from irradiated iron and cobalt, as the identity of the half-life periods suggests.

In order to identify the 4-minute active element, we irradiated manganese nitrate, added a vanadium compound and precipitated vanadium as vanadate of lead. The activity was carried down in the precipitate. A similar reaction was carried out with chromium, and also in this case the precipitate was found to be active, but apparently with a definitely lower yield. The active principle is probably the isotope V^{52} , and the nuclear reaction is



The same active vanadium is thus probably obtained from chromium, vanadium and manganese, fig. 1.

26—*Iron*—This element shows a fairly intense activity ($i = 0.05$), decaying with a period of 2.5 hours.* Half-value absorption thickness, 0.16 gm/cm². The active product can be separated as follows: the irradiated iron is dissolved in nitric acid, a small amount of a soluble manganese salt is added, and then the Mn is precipitated as MnO_2 by addition of sodium chlorate. The activity is found in the manganese precipitate. The active element is probably formed according to the reaction



and is the same as obtained from manganese.

* See also Fleischmann, 'Naturw.', vol. 22, p. 434 (1934).

27—*Cobalt*—Cobalt can be activated, and the decay curves show the same half-period as iron. The active product can be chemically separated with manganese by the same method as that described for iron. This suggests that it may be again the isotope Mn^{56} . In the present case the nuclear reaction would be

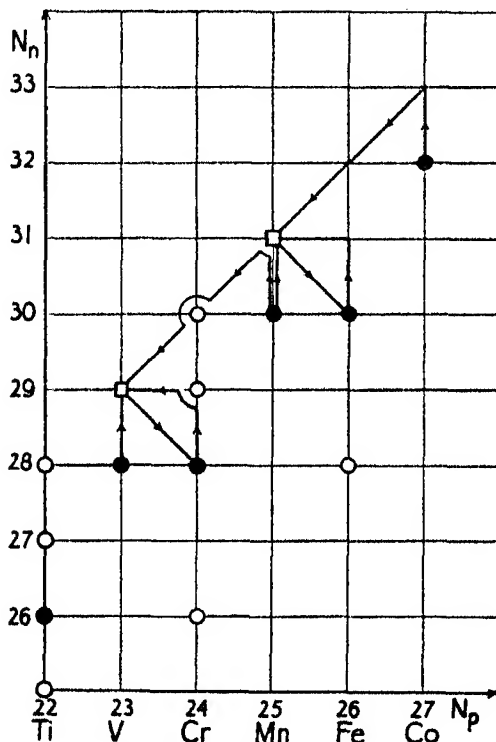


FIG. 1—The figure shows a possible scheme for the transformations which take place in the elements of atomic number 23 to 27, plotted in a proton-neutron diagram. Stable isotopes are indicated by dots (●) when representing more than 20% of the element, otherwise by circles (○). Active isotopes are indicated by small squares (□). The arrows indicate the transformations.

The active isotope Mn^{56} appears to originate from cobalt, iron and manganese (see fig. 1).

28—*Nickel*—The metal, irradiated 13 hours with 250 millicuries, was found to be inactive.

29—*Copper*—This element shows a medium activity, decaying with a period of about 6 minutes. We suggest as a possibility that the active nucleus might be the same as that which is produced from zinc, that is, an isotope of copper.

30—*Zinc*—Shows a weak activity, whose decay curve is composed of two periods, one of about 6 minutes and the other much longer and not yet measured.

The active element with the 6-minute period has been chemically separated, dissolving the irradiated metal, adding copper and nickel, and then precipitating copper as sulphide, or depositing it electrochemically on a zinc plate. In both cases copper carries the activity. The added nickel, precipitated with dimethylglyoxime, was found to be inactive. The active element is thus probably an isotope of copper.

31—*Gallium*—This element shows a moderately intense activity, decaying with a period of about 30 minutes.

33—*Arsenic*—Has a strong effect, the activity decaying with a period of about one day. Half-value absorption thickness, 0.16 gm/cm^2 . We have tried to separate the active substance by adding gallium and germanium and precipitating the former as ferrocyanide, the latter as sulphide after elimination of the arsenic. While the precipitation of the gallium appeared to be complete, in the case of germanium we are not sure that this element had been completely separated. In both cases the substance separated was found to be inactive, suggesting as probable that the activity belongs to an isotope of arsenic. However, as the reaction with germanium gave a somewhat uncertain result, we cannot give this conclusion as proved beyond doubt.

34—*Selenium*—This element could be weakly activated. The half-period is about 35 minutes.

35—*Bromine*—Ammonium bromide was found to be strongly activated by neutron irradiation. The decay curves show two periods, of about 30 minutes and 6 hours. In order to identify the active substance we added arsenic and selenium, and separated the former as sulphide, the latter electrochemically. Both were found to be inactive. The active elements seem thus to be isotopes of bromine. As a control we added arsenic and selenium and precipitated bromine as silver bromide, and found that the precipitate carried down the activity. We suggest that the two periods may be due to two active isotopes, Br^{80} and Br^{82} , formed from the two ordinary isotopes, Br^{79} and Br^{81} .

37—*Rubidium*—Rubidium nitrate showed a very weak activity, decaying with a period of about 20 minutes.

38—*Strontium*—This element irradiated 13 hours with 400 mC was found inactive.

39—*Yttrium*—This element irradiated 30 minutes with 750 mC was found inactive.

Artificial Radioactivity produced by Neutron Bombardment 493

40—*Zirconium*—Zirconium oxide showed an extremely weak activity with a period of a few minutes. It is possibly due to impurities.

42—*Molybdenum*—This element shows a very weak activity. The decay curves indicate at least two periods, one of about 15 minutes and one longer than a day.

44—*Ruthenium*—This element irradiated 40 minutes with 750 mC was found inactive.

45—*Rhodium*—Metallic rhodium could be strongly activated, and the decay curves found are consistent with the existence of two periods, one of about 50 seconds and the other of 5 minutes. Most of the activity belongs to the shorter period. Half-value thickness for the electrons of the 5 minutes' active product, 0.10 gm/cm^2 .

46—*Palladium*—This element becomes moderately active under neutron bombardment. The decay curves are not very accurate, but indicate a period of the order of six hours. Half-value thickness, 0.03 gm/cm^2 .

47—*Silver*—A strongly active element. The decay curves show a period of about 20 seconds and one of about 2 minutes (intensity of the latter, $i = 0.5$; half-value thickness, 0.08 gm/cm^2).

48—*Cadmium*—Metallic cadmium could be only weakly activated. The decay curves indicate a period slightly longer than one hour.

50—*Tin*—This metal showed an extremely weak activity, perhaps due to impurities.

51—*Antimony*—The same as tin.

52—*Tellurium*—Shows a weak activity decaying with a period of about half an hour.

53—*Iodine*—We irradiated both the element and ammonium iodide. Both showed a strong activity, decaying with a period of 30 minutes. Intensity, $i = 0.4$. Half-value thickness, 0.09 gm/cm^2 . The active element follows the iodine when this substance is precipitated by adding nitric acid to the solution of the irradiated ammonium iodide, to which tellurium and antimony had been added. It also follows the same element when precipitated as silver iodide in presence of tellurium and antimony. It is very likely that we have here the formation of an active isotope of iodine.

55—*Cæsium*—Cæsium (tartrate) showed a very weak activity, whose period has not yet been measured with any accuracy.

56—*Barium*—We irradiated the hydroxide and found it weakly active. The curves indicate a period of about 3 minutes.

57—*Lanthanum*—This element irradiated 40 minutes with 400 mC was found inactive.

58—*Cerium*—This element irradiated 30 minutes with 400 mC was found inactive.

59—*Praseodymium*—This element, as well as the other rare earths—Nd, Sm, and Pr—were kindly given to us by Professor Rolla, of the University of Florence. They are very pure, and in the form of oxides.

Praseodymium shows a rather weak activity. The decay curves indicate a period of about 5 minutes, and perhaps a longer one.

60—*Neodymium*—Shows a rather weak activity. Period about one hour.

62—*Samarium*—Also has a rather weak activity. Period about 40 minutes.

73—*Tantalum*—This element irradiated 2.5 hours with 750 mC was found inactive.

74—*Tungsten*—This element shows an extremely weak activity of probably long period. This might possibly be due to impurities.

75—*Rhenium*—This element irradiated 10 minutes with 750 mC was found inactive.

76—*Osmium*—This element irradiated 15 hours with 450 mC was found inactive.

77—*Iridium*—This element has a strong activity, decaying with a period of about 20 hours. Half-value thickness, 0.13 gm/cm^2 .

In order to establish the chemical nature of the activity, we irradiated the tetrachloride, added osmium and rhenium, and separated the former by distillation of the tetroxide, and the latter as sulphide. Both were found to be inactive. Iridium still contained the activity, which appears to be due to an isotope of this element.

78—*Platinum*—Pure platinum from Heraeus showed an extremely weak activity of short period.

79—*Gold*—We irradiated the metal, which showed a fairly intense activity. The period is about two days. Half-value thickness 0.33 gm/cm^2 .

We tried to separate the active substance by dissolving the irradiated gold foil in aqua regia, adding platinum and iridium, and precipitating these elements as respectively chloroplatinates and chloroiridates. Both were found to be inactive, while the activity was still found in gold, thus indicating an isotope of this element as the active nucleus. The activity remains with gold also when mercury is added and evaporated.

80—*Mercury*—This element, strongly irradiated, showed an extremely weak activity which might be due to impurities.

81—*Thallium*—The same as mercury.

82—*Lead*—This element irradiated 10 hours with 500 mC was found inactive.

83—*Bismuth*—The same as lead.

90—*Thorium*—This element has not been investigated sufficiently at present. Thorium nitrate, freed of its ordinary β -active decay products and irradiated, becomes strongly active. The decay curves indicate at least two periods, of less than 1 minute and about 15 minutes.

92—*Uranium*—We give here only the main results on this element, as its behaviour has been discussed recently elsewhere.*

Besides the half-periods of 10 seconds, 40 seconds and 13 minutes, we have identified later one more of about 1.5 hours. The intensity of the activation is of the order of 0.5 for each of these lives. We have already discussed experiments which appear to prove that the 13 minutes' active product is not isotopic with any of the elements with atomic number from 86 to 92 (emanation, ekacæsium, radium, actinium, thorium, protactinium, uranium). These experiments have been repeated under different conditions, chiefly in order to obtain a negative proof of the identity of the 13-minute product with protactinium, this proof being the most difficult to establish on account of the short period of the available Pa isotope, UX_2 . The manganese reaction which has already been described gives a yield of about 15% for the 13-minute product. Its yield for UX_2 depends widely upon the conditions of the reaction, and may be varied between 2% and 10%, account being taken of the natural decay of this substance. A more effective reaction for obtaining the 13-minute active product is the following: irradiated uranium nitrate is dissolved in diluted hydrochloric acid; some rhenium nitrate is added, and then rhenium is precipitated as sulphide by addition of sodium thiosulphate. This precipitate carries about 50% of the activity; and sometimes more. The percentage of UX_1 and of UX_2 found in the rhenium precipitate varies also with the conditions of the reaction (particularly with the acidity), but can be made very low, probably less than 1%. It was actually possible to separate the 13-minute active product and to measure its period using uranium which had not been purified at all from UX. The 90-minute active product has apparently chemical properties very analogous to those of the 13-minute active product, as in every type of reaction they are always obtained in about the same percentage. These activities seem, therefore, both to be due to products with atomic number higher than 92, and possibly to isotopes of a same element.

* Fermi, 'Nature,' vol. 133, p. 898 (1934).

4—*Theoretical Discussion*

We want here to discuss, from the theoretical point of view, the processes that may take place under neutron bombardment. At the present state of the nuclear theory these considerations can have only a provisional character. We can resume the empirical results of the preceding sections in the following points.

(a) A large percentage of elements of any atomic weight can be activated from this point of view no special difference can be noticed between light and heavy elements.

(b) The cross-sections for neutron impact for the elements which can be most intensely activated are of the order of the geometrical cross-section of the nucleus. This means that a large percentage of the neutrons which hit the nucleus produce an active atom.

(c) The active product is sometimes an isotope of the original atom (atomic number Z); in other cases its atomic number is lower by one or two units. In this respect there appears to be a difference between light and heavy elements. For light elements the atomic number of the active product is usually lower than Z , while in the five cases investigated for heavy, non-spontaneously radioactive elements, the active product is always an isotope of the bombarded element.

(d) The emitted electrons always have a negative charge, or at least no positrons could ever be detected.

There seems to be no special difficulty in explaining the general mechanism of the activation for light elements. This seems to consist usually in the capture of the impinging neutron, followed immediately by the expulsion of an α -particle or a proton. If the energy of the emitted α -particle or proton is of some million volts, it results from Gamow's theory that the time which is necessary to emit the particle is extremely short, and there is therefore a fairly high probability for the process to happen before the neutron has left the nucleus. After this process, which may last a time of the order of 10^{-20} seconds, the nucleus has been transformed into a new one having, on the average, an atomic weight higher than would belong to its nuclear charge, as the processes of absorbing a neutron and emitting an α -particle or a proton increase the neutron/proton ratio in the nucleus. This is probably the reason why an emission of negative electrons is always observed. The process of the electron emission re-establishes the correct value for neutron/proton ratio, and corresponds to the formation of a stable isotope.

As the atomic weight of the bombarded element increases, the potential barrier around the nucleus becomes an increasingly strong obstacle to the emission of heavy, positively-charged particles; it is therefore easy to understand why processes with emission of protons and α -particles become very improbable.

The reactions whose theoretical interpretation seems to meet with difficulties are those, normally occurring among heavy elements, in which the activated atom is isotopic with the original atom. The simplest hypothesis would be to assume a capture of the impinging neutron, giving rise to an unstable isotope of the bombarded element with an atomic weight higher by one unit than before the process. This hypothesis, which would be in agreement with the observed fact of the emission of negative electrons, gives rise, however, to serious theoretical difficulties when one tries to explain how a neutron can be captured by the nucleus in a stable or quasi-stable state. It is generally admitted that a neutron is attracted by a nucleus only when its distance from the centre of the nucleus is of the order of 10^{-12} cm. It follows that a neutron of a few million volts' energy can remain in the nucleus (i.e., have a strong interaction with the constituent particles of the nucleus) only for a time of the order of 10^{-21} seconds; that is, of the classical time needed to cross the nucleus. The neutron is captured if, during this time, it is able to lose its excess energy (e.g., by emission of a γ -quantum). If one evaluates the probability of this emission process by the ordinary methods one finds a value much too small to account for the observed cross-sections. In order to maintain the capture hypothesis, one must then either admit that the probability of emission of a γ -quantum (or of an equivalent process, as, for example, the formation of an electron-positron pair) should be much larger than is generally assumed; or that, for reasons that cannot be understood in the present theory, a nucleus could remain for at least 10^{-16} seconds in an energy state high enough to permit the emission of a neutron.

An alternative hypothesis is to admit that the impinging neutron is not captured, but causes the expulsion of another neutron from the nucleus. This process could be described as follows: the primary neutron loses part of its energy, bringing the nucleus into an excited state by a sort of inelastic impact. One can easily understand theoretically that these processes may take place in a large percentage of the collisions between nuclei and neutrons. If the excitation energy is large enough, a neutron can be emitted before the nucleus loses its energy by emission of a γ -quantum. The atom formed by such a process is an isotope of the original one, with atomic weight lower by one unit.

An objection which may be raised against this hypothesis is that if the number of neutrons decreases instead of increasing, it is, *a priori*, more likely that the atom, in the following disintegration, should emit a positron than a negative electron as observed. However, in the few cases investigated of heavy elements which are activated by neutron bombardment and are transformed into their isotopes, when the isotopic constitution of the neighbouring elements is known, there always exists a stable isotope of the element $Z + 1$, having atomic weight one unit less than the original element, as a possible end-product of the transformation.

One has, moreover, to bear in mind that if an unstable nucleus has energetically the possibility of emitting both an electron and a positron, the theory of the β -rays* gives *ceteris paribus* the emission of an electron as the most probable.

In conclusion, the choice between these two alternatives seems at present rather uncertain, and further experiments must be performed to test this point.

The radon sources were supplied by Professor G. C. Trabacchi, Laboratorio Fisico della Sanità Pubblica, Rome, without whose kind help these researches would have been impossible. To him, therefore, our warmest thanks are due. A fund for this work was granted to us by the Consiglio Nazionale delle Ricerche, Rome. Our thanks are due also to Professor N. Parravano and Professor L. Rolla, who have supplied us some rare chemicals.

* Fermi, 'Z. Physik,' vol. 88, p. 161 (1934).

5—Tabular Summary

The main results of this investigation are summarized in the table. Column 1 contains the atomic number and symbol of the elements investigated. Column 2 gives the isotopic constitution; numbers in bold type refer to isotopes which represent more than 20% of the element. Column 3 gives the observed half-periods; a heavy — means that the activity was sought for and not found. Column 4 gives a rough evaluation of the intensity *s* (strong), *m* (medium), *w* (weak). Column 5 gives the average energy of the electrons in million volts; this was obtained from the absorption measurement by a rather rough extrapolation based on the absorption coefficients of ordinary β -active substances without strong γ -rays (Ra E and UX₂). Column 6 shows whether γ -rays were observed or not; a line means that γ -rays have been sought for and not observed. Column 7 gives a probable active product; for simplicity we have always assumed that the neutron is captured; if, instead, a neutron was emitted, the corresponding atomic weights should be decreased by two units. When two or more periods are present, the data of columns 4, 5, 6 and 7 refer to the different periods in their order.

Atomic number.	Isotopes.	Half-period.	Intensity.	Mean energy of β -rays in 10 ⁶ volts.	γ -rays.	Active isotope.
1 H	1, 2	—	—			
3 Li	6, 7	—	—			
4 Be	9	?	?			
5 B	10, 11	?	?			
6 C	12, 13	—	—			
7 N	14, 15	—	—			
8 O	16, 17, 18	—	—			
9 F	19	9 s.	<i>s</i>	2	yes	N ¹⁹ (?)
11 Na	23	40 s.	<i>m</i>			
12 Mg	24, 25, 26	40 s.; 15 h.	<i>m</i> ; <i>m</i>	—; .5	?; yes	—; Na ²⁴
13 Al	27	12 m.; 15 h.	<i>s</i> ; <i>s</i>	.6; .5	yes; yes	—; Na ²⁴
14 Si	28, 29, 30	3 m.	<i>s</i>	1.3	yes	Al ²⁸
15 P	31	3 m.; 3 h.	<i>m</i> ; <i>s</i>	—; .7	?	Si ³¹
16 S	32, 33, 34	13 d.	<i>m</i>	.8	—	P ³²
17 Cl	35, 37	13 d.	<i>m</i>	.8	—	P ³²
20 Ca	40, 42, 43, 44	—	—			
22 Ti	46, 47, 48, 49, 50	3 m.	<i>w</i>			
23 V	51	4 m.	<i>m</i>	1.3		V ⁵² (?)
24 Cr	50, 52, 53, 54	4 m.	<i>m</i>	1.3	yes	V ⁵²
25 Mn	55	4 m.; 150 m.	<i>m</i> ; <i>m</i>	—; 1.3		V ⁵² ; Mn ⁵⁴
26 Fe	54, 56	150 m.	<i>m</i>	1.3	yes	Mn ⁵⁴
27 Co	59	150 m.	<i>w</i>			Mn ⁵⁴
28 Ni	58, 60, 61, 62	—	—			
29 Cu	63, 65	6 m.	<i>m</i>			
30 Zn	64, 66, 67, 68, 70	6 m.; ?	<i>w</i> ; <i>w</i>			Cu; —
31 Ga	69, 71	30 m.	<i>m</i>			
33 As	75	1 d.	<i>s</i>	1.3	yes	As ⁷⁶
34 Se	74, 76, 77, 78, 80, 82	35 m.	<i>w</i>			
35 Br	79, 81	30 m.; 6 h.	<i>s</i> ; <i>s</i>	—; .7 (?)	—	Br ⁸⁰ ; Br ⁸²
37 Rb	85, 87	20 m.	<i>w</i>			
38 Sr	86, 87, 88	—	—			
39 Y	89	—	—			
40 Zr	90, 91, 92, 94, 96	?	<i>w</i>			
42 Mo	92, 94, 95, 96, 97, 98, 100	15 m.; (?)	<i>w</i> ; <i>w</i>			
44 Ru	96, 98, 99, 100, 101, 102, 104	—	—			
45 Rh	—	50 s.; 5 m.	<i>s</i> ; <i>m</i>	.8	—	
46 Pd	—	6 h. (?)	<i>w</i>	.3	—	
47 Ag	107, 109	20 s.; 2 m.	<i>s</i> ; <i>s</i>	—; .7	—	
48 Cd	110, 111, 112, 113, 114, 116	70 m.	<i>w</i>			
50 Sn	112, 114, 115, 116, 117, 118, 119, 120, 121, 122, 124	—	—			

500 *Artificial Radioactivity produced by Neutron Bombardment*

Tabular Summary—(continued).

Atomic number.	Isotopes.	Half-period.	Intensity.	Mean energy of β -rays in 10^6 volts.	γ -rays.	Active isotope.
51 Sb	121, 123	?	?			
52 Te	122, 123, 124, 125, 126 , (127), 128, 130	30 m. (?)	<i>w</i>			
53 I	127	30 m.	<i>s</i>	·7	—	I ¹²⁸
55 Cs	133	(?)	<i>w</i> (?)			
56 Ba	135, 136, 137, 138	3 m.	<i>w</i>			
57 La	139	—	—			
58 Ce	140, 142	—	—			
59 Pr	141	5 m.	<i>w</i>			
60 Nd	142, 143, 144, 145, 146	1 h.	<i>w</i>			
62 Sm	144, 147, 148, 149, 150, 152, 154	40 m.	<i>w</i>			
73 Ta	181	—	—			
74 W	182, 183, 184, 186	(?)	<i>w</i> (?)			
75 Re	185, 187	—	—			
76 Os	186, 187, 188, 189, 190 , 192	—	—			
77 Ir	—	20 h.	<i>s</i>	1·1	yes	Ir
78 Pt	—	(?)	<i>w</i> (?)			
79 Au	—	2 d.	<i>s</i>	·3	—	Au
80 Hg	196, 197, 198, 199, 200 , 201, 202, 203, 204	(?)	(?)			
81 Tl	203, 205	(?)	(?)			
82 Pb	203, 204, 205, 206, 207 , 208, 209	—	—			
83 Bi	209	—	—			
90 Th	232	1 m. (?); 15 m.	<i>s</i> ; <i>s</i>			
92 U	238	15 s.; 40 s.; <i>s</i> ; <i>s</i> ; <i>s</i> ; <i>s</i> 13 m. 100 m.			yes	*

* See p. 495.

The Formation of Emulsions in Definable Fields of Flow

By G. I. TAYLOR, F.R.S., Royal Society Yarrow Professor

(Received May 9, 1934)

[PLATES 4 AND 5]

The physical and chemical condition of emulsions of two fluids which do not mix has been the subject of many studies, but very little seems to be known about the mechanics of the stirring processes which are used in making them. The conditions which govern the breaking up of a jet of one fluid projected into another have been studied by Rayleigh* and others, but most of these studies have been concerned with the effect of surface tension or dynamical forces in making a cylindrical thread unstable so that it breaks into drops. The mode of formation of the cylindrical thread has not been discussed. As a rule in experimental work it has been formed by projecting one liquid into the other under pressure through a hole. It seems that studies of this kind which neglect the disruptive effect of the viscous drag of one fluid on the other, though interesting in themselves, tell us very little about the manner in which two liquids can be stirred together to form an emulsion.

When one liquid is at rest in another liquid of the same density it assumes the form of a spherical drop. Any movement of the outer fluid (apart from pure rotation or translation) will distort the drop owing to the dynamical and viscous forces which then act on its surface. Surface tension, however, will tend to keep the drop spherical. When the drop is very small, or the liquid very viscous, the stresses due to inertia will be small compared with those due to viscosity.

Recently the present writer made a rough theoretical estimate, based on the hydrodynamical equations of a spherical drop in a shearing fluid, of the maximum size of drop which surface tension might be expected to hold together against the disruptive forces due to the viscous drags of the shearing fluid. Since the drop must depart very markedly from the spherical form before it bursts, this theoretical estimate is unlikely to be of much value except as an indication of the conditions under which marked deviations from the spherical form began to occur. It seemed worth while therefore to make some experiments on the deformation and bursting of a drop of one fluid in another under

* 'Proc. Roy. Soc.,' vol. 29, p. 71 (1879).

controlled conditions measuring the interfacial tension of the two liquids their viscosities and the rate of deformation of the outer fluid.

Among the infinite variety of possible fields of flow two have been chosen which can easily be produced in an actual fluid and at the same time can be represented by simple mathematical equations. The first is that represented by

$$u = Cx, \quad v = -Cy, \quad (1)$$

the stream lines of which are rectangular hyperbolas. The second is that represented by

$$u' = \alpha y', \quad v' = 0. \quad (2)$$

"Four Roller" Apparatus

To produce approximately the field of flow represented by (1) the apparatus represented in the sketch of fig. 1 was constructed. Four brass cylinders

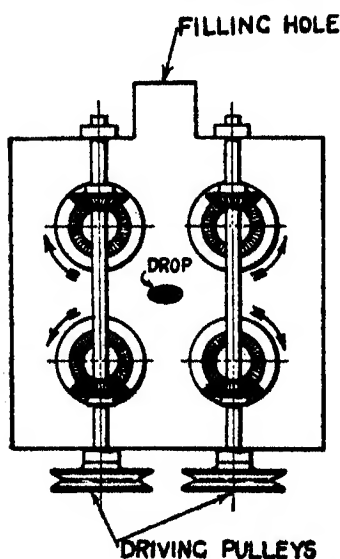


FIG. 1—"Four roller" apparatus.

3.81 cm \times 2.39 cm diameter were mounted at the corners of a square the sides of which were 3.18 cm. Their axes ran in brass bearings fixed in two glass plates which formed the sides of a box the internal dimensions of which were 7.6 \times 7.6 \times 3.9 cm. The remaining sides were brass and one of them was pierced by a large hole through which the apparatus could be filled with liquid. The cylinders were driven in the directions indicated by arrows in fig. 1 by means of two vertical shafts and bevel wheels. These two shafts were rotated at the same speed but in opposite directions by a motor through reduction gears. The box was filled with golden syrup, illuminated by an electric lamp, and observed by means of a long focus camera

(magnification 2.5) set with its axis on the centre line in a direction parallel to the axes of the cylinders.

Slight variations in the water content of the golden syrup caused streaks to appear in the image on the camera screen as soon as the apparatus was set in motion. These streaks mark out stream lines and the photograph, fig. 2, Plate 4, shows that at any rate in the centre of the field they are very

like the rectangular hyperbolas which are stream lines of the flow represented by (1).

To compare the velocity in the field of flow actually produced with equation (1) a series of lines were ruled horizontally and vertically on the screen of the camera at distances ± 0.5 , ± 1.0 , ± 1.5 , ± 2.0 , and ± 2.5 cm from the centre. The times at which images of small particles in the golden syrup passed successive lines were observed and also the time τ of one revolution of the vertical shafts. In one set of such measurements τ was 48.7 seconds and the corresponding times for covering the 0.5 cm distances between successive lines are given in Table I.

Table I

Distances, in cm, from centre	Time, in secs	Value of C from formula (3)
0.5 to 1.0	7	0.099
1.0 to 1.5	3.9	0.104
1.5 to 2.0	2.7	0.106
2.0 to 2.5	2.0	0.111

If the field of flow is represented by (1) the velocity of a particle is $dx/dt = Cx$ so that the time of passage of a particle from x_1 to x_2 is $C^{-1}(\log x_2 - \log x_1)$. Hence

$$C = (\log x_2 - \log x_1) \div (\text{time from } x_1 \text{ to } x_2). \quad (3)$$

The values of C corresponding with this formula are given in Table I. It will be seen that C is nearly constant over the range from 0.5 to 2.5 cm from the centre of the camera screen which corresponds with the range 0.2 to 1.0 cm from the centre of the field in the apparatus itself.

The values of C in any experiment are proportional to the speed of rotation of the cylinder, *i.e.*, to $1/\tau$. Taking the average value of C in this set of measurements as 0.105 corresponding with $\tau = 48.7$ it will be seen that in any other experiment for which τ is measured the flow will be represented by (1) provided

$$C = (48.7) (0.105) \tau^{-1} = 5.1/\tau. \quad (4)$$

The number 5.1 is a dimensionless constant of the apparatus.

"Parallel Band" Apparatus

To produce the flow represented by (2) two endless celluloid bands of cinema film 35 mm wide were stretched between rollers, one of which in each case was fitted with pins to engage in the regularly spaced holes at the edge of the film. The two bands could be driven at any speed in either direction, the ratio of

their speeds being controlled by a continuously variable gear. The bands and rollers were contained in a glass sided box the width of which was 3 mm greater than that of the film. The apparatus is illustrated in the sketch fig. 3.

With this construction the speed of the band was definitely related to the speed of the rollers so that each revolution of a driving pulley moved the corresponding endless band through 7.10 cm.

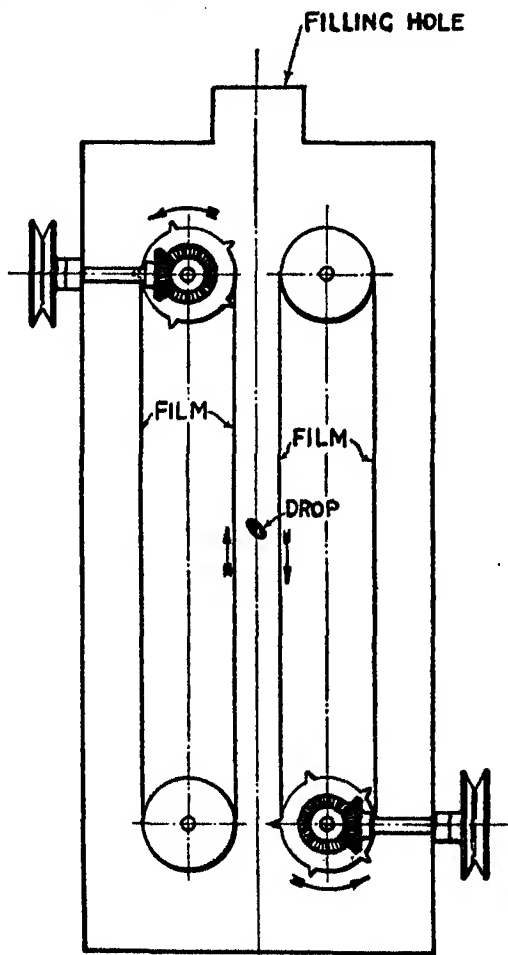


FIG. 3—"Parallel band" apparatus.

The distance apart of the bands was 1.36 cm so that if the shearing motion of the liquid between them is represented by $u' = \alpha y'$, y' being measured perpendicular to the bands,

$$\alpha = \frac{7.10}{1.36} \left(\frac{1}{\tau_1} + \frac{1}{\tau_2} \right) = 5.22 \left(\frac{1}{\tau_1} + \frac{1}{\tau_2} \right), \quad (5)$$

where τ_1 and τ_2 are the times of revolution of the two driving pulleys. If the constant C in (1) is chosen to be equal to $\frac{1}{2}\alpha$ and if the whole system (2), i.e., the axes of co-ordinates (x', y') is given a rotation with angular velocity $\frac{1}{2}\alpha$ and if the axes (x', y') are instantaneously at 45° to the axes (x, y) then at that instant the two fields of flow are identical. Effects therefore which depend only on the instantaneous distribution of velocity and are unaffected by a rotation of the whole system will be identical in the two pieces of apparatus when they are operated at corresponding speeds, i.e., so that $C = \frac{1}{2}\alpha$. On the other hand, effects which do not depend only on the instantaneous distribution of velocity but are dependent on a sequence of such distributions are very different in the two.

To illustrate the significance of these remarks consider the effect of the two kinds of flow of a very viscous fluid on an elongated symmetrical solid body, say a prolate spheroid, placed with its long axis in the plane xy . If this body is placed in the field of flow (1) with its long axis at angle θ to the axis of x its surface will be subjected to exactly the same stresses that would act on it in the field of flow (2) if its long axis were placed at $45^\circ + \theta$ to the axis of x' . The resultant effects of the two fields of flow on the motion of the body over a period of time are, however, very different. In the field of flow (1) the body will set itself permanently with its long axis parallel to the axis of x , whereas in the flow (2) the body will continually roll over and over rotating, at a variable speed, about an axis perpendicular to the plane $x'y'$.

Calculation of Small Deformations

Before describing the experimental results obtained with the two forms of apparatus we may see how far theory can predict the effects of the two fields of fluid flow (1) and (2) on drops of another fluid immersed in them.

Suppose that a spherical drop of a fluid of viscosity μ' is immersed in a fluid of viscosity μ and that the latter is caused to flow in the velocity distribution represented by $(u = Cx, v = -Cy)$. If the flow is very slow the viscous drag will deform the drop only slightly from the spherical form. This small deformation will cause only a small change in the distribution of stresses in either fluid, accordingly in the stress conditions which must be satisfied at the surface of the drop, namely, (a) continuity of tangential stress, and (b)

$$T(r_1^{-1} + r_2^{-1}) = \text{constant} + p_i - p_o, \quad (6)$$

the stresses may be reckoned as those which occur when the drop is held

spherical by a distribution of normal force at the surface. In equation (6) T is the interfacial surface tension between the two liquids, p_i and p_o are the normal pressures inside and outside the drop, r_1 and r_2 are the principal radii of curvature of the deformed drop.

It follows that the analysis previously given by the present writer* for the flow in the neighbourhood of a spherical drop can be applied directly in the present work. The value of $p_i - p_o$ is therefore

$$p_i - p_o = \frac{1}{2}C\mu \frac{19\mu' + 16\mu}{\mu' + \mu} \left(\frac{x^2 - y^2}{a} \right) + \text{constant.} \quad (7)$$

Comparing (6) and (7) it will be seen that it is necessary to find the shape of the nearly spherical drop for which the variation in $(r_1^{-1} + r_2^{-1})$ is proportional to $(x^2 - y^2)a^{-2}$. It can be verified that for the surface whose equation is

$$r = a + b(x^2 - y^2)a^{-2} \quad (8)$$

$$r_1^{-1} + r_2^{-1} = 2a^{-1} + 4b(x^2 - y^2)a^{-4}. \quad (9)$$

Combining (6), (7), and (9) and equating coefficients of the variable part of the pressure it will be seen that (8) represents the deformed drop provided

$$\frac{1}{2}C\mu \frac{19\mu' + 16\mu}{\mu' + \mu} = \frac{4Tb}{a^3}. \quad (10)$$

A convenient method for expressing the results of experiment is to measure L , the length of the drop in the direction of the x axis, and B , the breadth in the direction of the y axis. These measurements are connected with the constant b of equation (8) by the formula

$$\frac{L - B}{L + B} = \frac{b}{a}, \quad (11)$$

so that (10) becomes

$$\frac{L - B}{L + B} = F \frac{19\mu' + 16\mu}{16\mu' + 16\mu}, \quad (12)$$

where

$$F = 2C\mu a/T. \quad (13)$$

F is non-dimensional.

It will be noticed that over the whole range of ratios μ'/μ from 0 to α $(19\mu' + 16\mu)/(16\mu' + 16\mu)$ varies only from 1.0 to 1.187, so that $(L - B)/(L + B)$ is nearly equal to F .

* "The viscosity of a fluid containing small drops of another fluid," 'Proc. Roy. Soc.,' A, vol. 138, p. 41 (1932). The expression here given in (7) is identical with equation (21) of that paper except that $2C$ has been substituted for α .

For the flow ($u' = \alpha y'$, $v' = 0$) the deformation of the drop at slow rates of flow should also be represented by (12), but in that case

$$F = \mu \alpha x / T, \quad (14)$$

and the long axis should lie in the direction making 45° with the axis of x' (i.e., at 45° to the celluloid film as shown in fig. 3).

Method of Experiment

In all the experiments to be described the apparatus was filled with golden syrup (which is a concentrated sugar solution) diluted with a small quantity of water till the viscosity was between 50 and 150 c.g.s. A number of liquids which do not mix with water were used for the drop so as to cover a large range of values of μ'/μ . For low values of μ'/μ a mixture of carbon tetrachloride with the paraffin oil sold as "Nujol" was made up to be of the same density as the syrup and was coloured purple with dissolved iodine. For values of μ' rather smaller than μ a lubricating oil sold as "BB" was used. For values of μ' equal to μ a black lubricating oil was used. For values of μ' considerably greater than μ a mixture of coal tar and pitch was made up so that its viscosity was about 2000 c.g.s. These values together with the interfacial surface tensions are given in Table II.

Table II

	μ' (c.g.s.)	T (c.g.s.)
CCl_4 and paraffin	0.034	23
"BB" oil	60	17
Black lubricating oil	100	8
Tar-pitch mixture	2000	(23)

Before setting the apparatus in motion the drop was introduced into the syrup by means of a pipette which was lowered through the hole in the top of the apparatus. The drop became spherical under the influence of surface tension and was photographed in that condition in order to measure its radius. The apparatus was then set in motion at a slow speed and adjusted till the drop was steady and stationary. A photograph was then taken. The speed was then increased and another photograph taken, these operations being repeated till some limiting condition such as the bursting of the drop was reached.

Experiments with the "Four Roller" Apparatus

After introducing the drop at the top of the apparatus the latter was slowly set in motion so as to carry the drop towards the middle of the field. After prolonged running the drop gradually took up a position in the central horizontal plane. It was, however, highly unstable so far as horizontal motion was concerned tending to move off to the right or left if it got displaced from the centre. This instability was controlled by varying the speed of the right- or left-hand pair of rollers. It has already been mentioned that the two rollers on the right were driven by one shaft and the two on the left by another. Each pair was driven by a belt which could be made to slip. When uncontrolled neither of the belts slipped so that all four rollers rotated at the same speed. If the drop was observed to get slightly off centre to the right, the right-hand pair of rollers was retarded and the drop moved back towards the centre. After a little practice it was possible to keep the drop very close to the centre of the field.

The photograph of fig. 4, Plate 4, shows a drop which had been maintained in this way symmetrically in the middle of the field for a time which was long enough to ensure that the drop and surrounding fluid was in a steady state. One-quarter of each of the four rollers is shown in the corners of the photograph and the direction of rotation of each is shown by means of an arrow. Each of the photographs taken with this apparatus was similar to that of fig. 4, but in order to economize space only the part of the field immediately surrounding the drop is shown in the remaining photographs.

$\mu'/\mu = 0.0003$ —The sequence of photographs of fig. 5, Plate 4, shows the effect of the field of flow represented by equation (1) on drops of the CCl_4 and paraffin mixture ($\mu' = 0.034$). At each setting of the apparatus the time of revolution τ of the rollers was observed, the apparatus being uncontrolled during the exposure, and for sufficient time before it, to ensure steady conditions. Using equation (4), the constant C was found. The diameter $2a$ of the undistorted drop was measured on the photograph and T were measured independently by the methods described in the Appendix so that the non-dimensional quantity $F = 2c\mu a/T$ could be calculated.

The analysis of the slightly distorted drop shows that the shape of the drop should depend on the two non-dimensional quantities μ'/μ and F . The shape of the drop can be defined by the ratio $(L - B)/(L + B)$ where L is the greatest length and B the breadth. For any given value of μ'/μ the experimental

results can, therefore, be expressed by means of a single curve giving $(L-B)/(L+B)$ for all values of F . In each case the maximum and minimum diameters of the photographs of distorted drops were measured and $(L-B)/(L+B)$ was found. Under each photograph of fig. 5 the measured values of F and $(L-B)/(L+B)$ are given and over each photograph the radius a of the drop in centimetres.

In the first series of photographs (fig. 5) it will be seen that at the slowest speed, $F = 0.18$, the drop is only slightly distorted from the spherical form, and the distortion, measured by $(L-B)/(L+B)$, is 0.15. In this drop $\mu'/\mu = 0.034/100 = 0.00034$ so that the predicted relationship (12) is nearly exactly $F = (L-B)/(L+B)$. The experiment therefore is in good agreement with the theory.

In the second photograph of fig. 5 $F = 0.28$ and $(L-B)/(L+B) = 0.26$, so that the theory still appears to represent the experimental conditions. In the third photograph the drop has developed into a form which is very far from spherical, indeed the ends have become pointed, so that the theory can no longer be applied. It will be noticed, however, that $F = 0.41$, $(L-B)/(L+B) = 0.44$, so that the theoretical relationship for small deformations is still nearly correct. The drop shown in photograph 3, fig. 5, was not in a truly steady state, for after developing the point shown in the photograph a thin skin appeared to slip off its surface and the ends of the drop again became rounded. This condition persisted, as shown in the fourth photograph, till $F = 0.54$. At $F = 0.65$ (fifth photograph) the ends of the drop again became pointed and these points remained as F increased up to the highest speed at which the apparatus could be operated.

The sixth, seventh, and eighth photographs, fig. 5, show a pointed drop which increases in length and decreases in thickness with increasing speed. Thus as F increases from 0.65 to 2.45 $(L-B)/(L+B)$ increases from 0.51 to 0.87. It was not possible to realize values of F higher than 2.45 because the ends of the drop got into the region where the field of flow ceased to be even approximately that represented by (1). There was no sign, however, that the drop would have burst even if considerably higher speeds had been attained.

The results described above, together with some others for which the drop is not here reproduced, are shown graphically in fig. 6 where values of F and $(L-B)/(L+B)$ are plotted in a diagram. The theoretical relationship $F = (L-B)/(L+B)$ applicable to small values of F is shown by means of a broken line.

$\mu'/\mu = 0.9$ —Using black lubricating oil for which $\mu' = 100$ c.g.s. in syrup for which $\mu = 110$ c.g.s. the value of μ'/μ was 0.91. The interfacial surface tension T was found to be 8.0 c.g.s. A drop of oil 0.144 cm diameter was used and the series of photographs shown in fig. 7, Plate 5, were obtained. In the first of these the time of revolution of the rollers was 97 seconds so that from (4) and (13)

$$F = \frac{10.2 (0.144) (110)}{(8.0) (97)} = 0.21.$$

The value of $(L - B)/(L + B)$ obtained by measuring the photograph was 0.19 and its theoretical value from (12) is $1.09F = 0.23$. It will be seen,

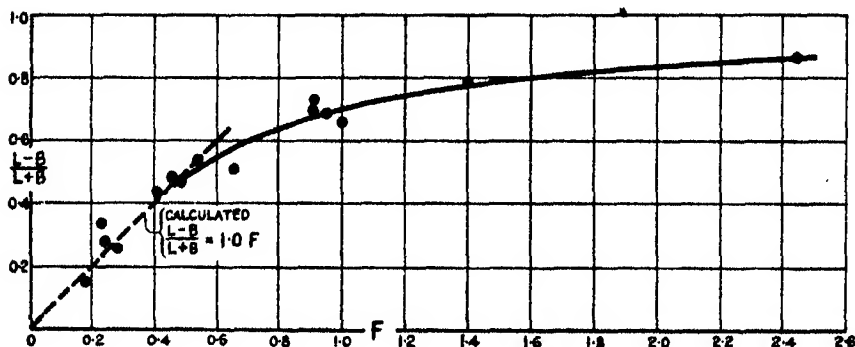


FIG. 6— CCl_4 -paraffin. "Four roller" apparatus, $\mu'/\mu = 0.0003$.

therefore, that the observed value 0.19 is in fair agreement with its theoretical value 0.23. The error is certainly not greater than that which arises from the uncertainties involving in measuring T .

The second photograph shows the drop at $F = 0.30$ when the theoretical value of $(L - B)/(L + B)$ was $1.09 (0.30) = 0.33$. The observed value was 0.29 so that again the theory is confirmed. In the third photograph $F = 0.37$ and the drop has become much elongated. The observed value of $(L - B)/(L + B) = 0.54$ is now considerably greater than the value $(1.09) (0.37) = 0.40$ obtained by extrapolating the theory.

When the speed reached the point at which $F = 0.39$ the drop began to pull out into a thread-like form. This is shown in the fourth and fifth photographs of fig. 7 which were taken while the drop was bursting in this way. Shortly after taking the fifth photograph the apparatus was stopped. The thread of oil which had seemed quite stable while the apparatus was in motion then gradually broke up into a number of small drops. The final appearance of the oil in this condition is shown in the sixth photograph of fig. 7.

These results are shown graphically in fig. 8. It will be seen that when $\mu'/\mu = 0.9$ the drop remains coherent so long as $F < 0.39$ but burst as soon as F reaches this value. This is indicated by the broken line continuation of the curve.

$\mu'/\mu = 20$ —To investigate the effect of high viscosity of the drop a mixture of tar and pitch was made with viscosity 2000 c.g.s. This had a density not far from that of the syrup, namely, 1.40. In these experiments the viscosity of the syrup was 99 c.g.s. No way was found for making an independent

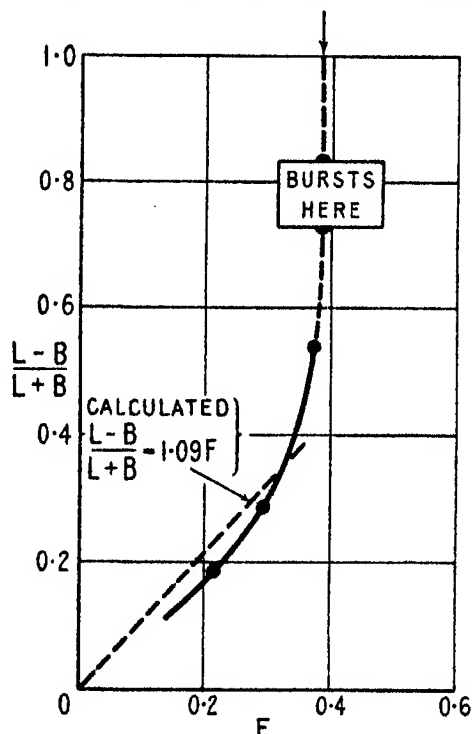


FIG. 8—"Four roller" apparatus. Black lubricating oil, $\mu'/\mu = 0.9$.

and reasonably accurate measurement of the interfacial surface tension. On the other hand, if the truth of the theory of slightly deformed drops is assumed equations (12) and (13) can be applied to find T .

A drop 0.16 cm radius was used. The first photograph, fig. 9, Plate 4, shows this drop in its undeformed condition. The apparatus was set in motion so that the time of revolution τ of the rollers was 54 seconds and the second photograph of fig. 9 was taken. By measuring this photograph it was found that $(L - B)/(L + B) = 0.15$. Taking μ'/μ as 20 in (12) the theoretical

value of $(L - B)/(L + B)$ is $1.18F$ so that if the theory is correct $F = 0.15/1.18 = 0.13$. Referring to equation (13) it will be seen that when $a = 0.16$, $\tau = 54$, $\mu = 99$, then the value of F is 0.13 provided $T = 23$. This value is given in Table II in brackets and is available for use in further experiments with the tar-pitch mixture.

On increasing the speed of the rollers till $\tau = 24$ seconds the drop was found to be bursting. The third photograph of fig. 9, Plate 4, shows the drop in the

act of bursting. Using $T = 23$ c.g.s. the corresponding value of F was 0.28 . It appears, therefore, that when $\mu'/\mu = 20$ the drop bursts for some value of F rather less than 0.28 .

These results are indicated in the diagram, fig. 10.

Experiments with the "Parallel Band"

Apparatus

This apparatus was driven by a motor through various reduction gears and a variable gear so that the speed could be varied and also, independently, the ratio of the speeds of the two bands. A drop of fluid was placed in the apparatus and photographed. The apparatus was then set in motion. If the drop happened to be placed exactly mid-way between the bands it would remain at rest when they both moved at the same speed. If the drop was not quite central then it could be brought to rest by adjusting slightly the ratio of the speeds of the two bands.

When the conditions had become steady a photograph was taken and the speeds of both bands measured by timing the revolutions of the driving rollers.

$\mu'/\mu = 0.0003$ —A drop of the same mixture of CCl_4 and paraffin as that used in the "four roller" apparatus was introduced. The first photograph of fig. 11, Plate 5, shows this drop before starting the apparatus. The dark horizontal lines at the top and bottom are the celluloid bands which in the apparatus itself were vertical. The arrow above the whole series of pictures shows the direction of motion of the band which is at the top of the photograph.

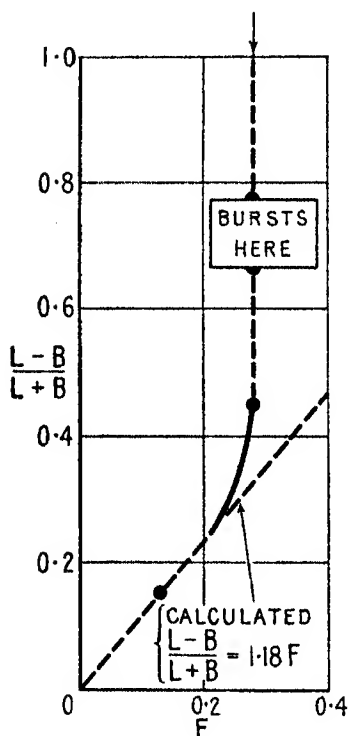


FIG. 10—"Four roller" apparatus, tar-pitch mixture, $\mu'/\mu = 20$.

The other band moves in the opposite direction. Measurement of the first photograph showed that the radius of the drop was 0.157 cm.

The second photograph of fig. 11 shows the drop distorted by viscous drag, the two periods of revolution of the driving rollers being $\tau_1 = 192$ seconds, $\tau_2 = 233$ seconds. It will be seen that the long axis of the distorted drop lie at about 45° to the bands, *i.e.*, in the direction in which lines of particles are elongating at the greatest rate. In this experiment it was found that $\mu = 123$ c.g.s., so that from (5) and (14)

$$F = (5.22) (0.157) (123) T^{-1} (\tau_1^{-1} + \tau_2^{-1}).$$

If T is taken as 23 c.g.s. this becomes $F = 4.4 (\tau_1^{-1} + \tau_2^{-1})$ so that $F = 0.04$. Measurement of the photograph gives $(L - B)/(L + B) = 0.08$ so that the theoretical relationship $F = (L - B)/(L + B)$ is not fulfilled.

The third photograph taken when $F = 0.10$ gives $(L - B)/(L + B) = 0.22$ so that again the observed value of $(L - B)/(L + B)$ is about twice as great as the prediction. The consistency of the error makes it seem probable that the surface tension of the drop in the syrup was considerably less during this series of experiments than it had been previously, probably owing to impurities in the syrup. The sequence of drops shown in the eight photographs of fig. 11 shows that as the speed of the apparatus is increased the drop elongates but does not burst even at the highest speed obtainable. The highest value of F shown in fig. 11 is 2.30, but this photograph was obtained with a different filling of syrup from the others. One experiment, however, was tried with a very large drop ($a = 0.54$) and it was found that this drop was still coherent at $F = 5.3$ if $T = 23$ (or $F = 11$ if $T = 11$).

It will be noticed that the fifth photograph of fig. 11 shows a thin streak coming off from each end of the drop. This was a transient phenomenon and is evidently the same as that previously described in connection with the third photograph of fig. 5, Plate 4.

The results obtained with two fillings of syrup are set out in fig. 12 as "First series" and "Second series."

$\mu'/\mu = 0.5$ —Using fresh syrup and a drop of "BB" oil the results set forth in Table III were obtained. T was measured independently and found to be 17 c.g.s. In the first set of observations μ was 135 c.g.s. while in the second it was 110 c.g.s. The second set is shown in the photograph, fig. 13, Plate 5. It will be seen that for low values of F the drop is, as predicted, an ellipse with its long axis at 45° to the celluloid bands. As the speed of the apparatus is

increased the drop becomes elongated till at $F = 1.43$ a steady motion ceases to be possible and the drop elongates into a thread-like form.

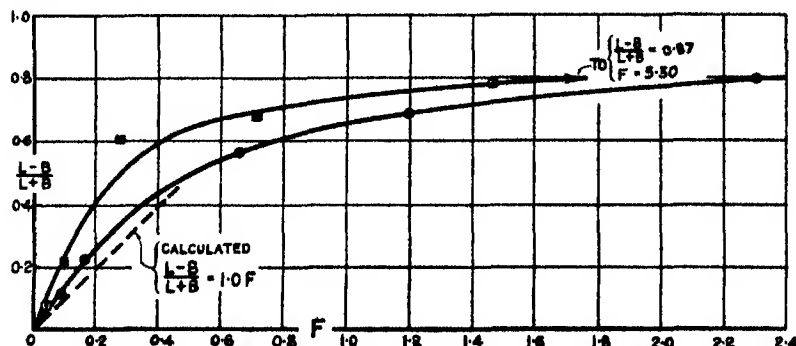


FIG. 12—"Parallel band" apparatus. CCl_4 -paraffin. $\mu'/\mu = 0.0003$. ● First series; □ Second series.

Table III—"BB" oil drop in "parallel band" apparatus. $\mu' = 60$, $T = 17$

a (cm)	μ	τ_1 (secs)	τ_2 (secs)	F	$\frac{L-B}{L+B}$
0.140	110	62	51	0.17	0.17
0.167	135	157	828	0.05	0.07
0.123	135	99	87	0.11	0.10
0.123	135	83	85	0.12	0.19
0.123	135	24	25	0.42	0.45
0.101	135	9.5	10.5	0.84	0.60
0.100	135	7.0	8.0	1.12	0.81
0.100	135	5.5	6.2	1.43	burst

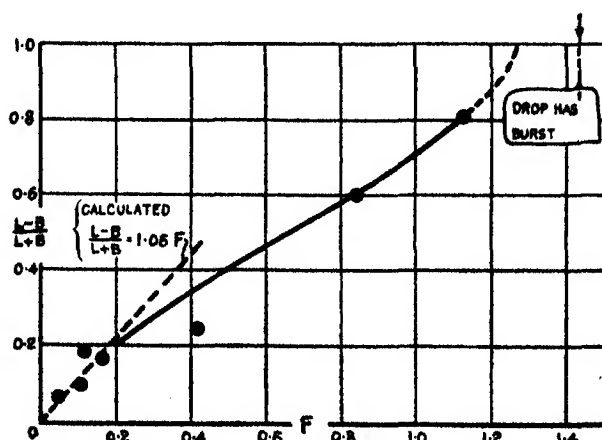


FIG. 14—"Parallel band" apparatus. "BB" oil. $\mu'/\mu = 0.5$.

These results are set out graphically in fig. 14. For $\mu'/\mu = 0.5$ the theoretical relationship (12) is $(L-B)/(L+B) = 1.06F$. This is represented in fig. 14 by a broken line. It will be seen that the agreement is good.

$\mu'/\mu = 0.9$ —With the same black lubricating oil which had previously been used in the “four roller” apparatus, the results given in Table IV were obtained. Some of the photographs are shown in fig. 15, Plate 5. It will be noticed that when $F = 0.28$ the drop is not symmetrical, one end being more pointed than the other. This asymmetry is still more pronounced when $F = 0.55$. It always occurred when there was a large difference in density between the drop and the syrup.

Table IV—Black lubricating oil in syrup, “parallel band” apparatus.

$\mu = 110, \mu' = 100, T = 8.0$				
a	τ_1 (secs)	τ_2 (secs)	F	$\frac{L-B}{L+B}$
0.097	262	207	0.06	0.07
0.097	141	111	0.11	0.15
0.097	92	71	0.17	0.22
0.097	57	44	0.28	0.45
0.086	40	31	0.36	0.53
0.086	22	23	0.55	burst

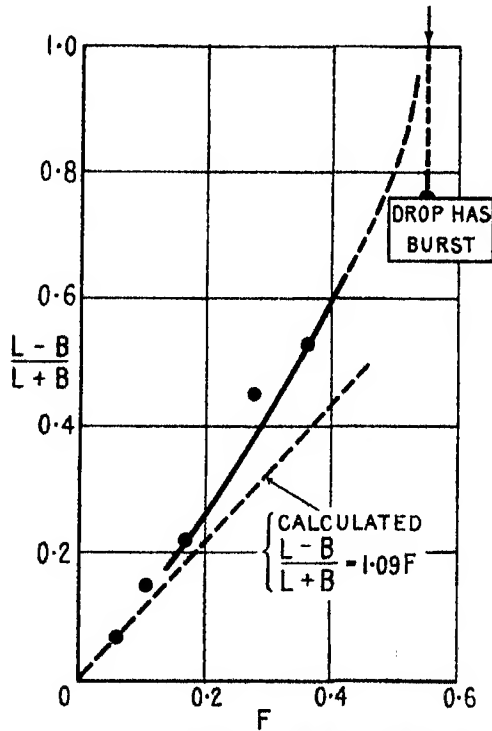


FIG. 16—“Parallel band” apparatus. Black lubricating oil. $\mu'/\mu = 0.9$.

The relationship between $(L-B)/(L+B)$ and F is shown in fig. 16 and the theoretical relationship for $\mu'/\mu = 0.9$, namely, $(L-B)/(L+B) = 1.09F$, is there shown by a broken line.

$\mu'/\mu = 20$ —Using the pitch and tar mixture for which μ' was about 2000 c.g.s. the drop again became elliptical with its long axis at 45° to the celluloid bands when the apparatus was run at very slow speeds. This is shown in the second photograph of fig. 17, Plate 5, taken when $F = 0.08$.* As the speed increased to $F = 0.27$, third photograph, fig. 17, the drop became slightly more elongated, but its long axis became more nearly parallel to the celluloid bands. At $F = 1.13$, fourth photograph, fig. 17, its deformation was only slightly greater than at $F = 0.27$ and its long axis was still more nearly parallel to the bands. At $F = 1.69$, fifth photograph, fig. 17, its shape and orientation were almost identical with those at $F = 1.13$.

In comparing these results with those shown in fig. 9, Plate 4, which were obtained with the "four roller" apparatus, a very striking difference will be noticed. In the "four roller" apparatus the drop burst at a very low speed represented by $F = 0.28$. In the "parallel band" apparatus the drop did not burst however fast the apparatus was run. On the contrary, it attained at high speeds a constant condition in which $(L - B)/(L + B)$ was 0.26 and the long axis was parallel to the bands.

The explanation of this phenomenon is simple. In the "four roller" apparatus, which produces the field of flow (1), the lines of particles which are extending at the greatest rate, namely, those parallel to the axis of x , remain in the direction of maximum rate of elongation as long as the flow continues. The disruptive stress due to the viscous drag of the syrup is therefore always tending to extend the drop in the same direction. As soon as this stress is able to overcome the cohesive effect of surface tension the drop bursts.

In the "parallel band" apparatus the lines of particles which lie in the direction of maximum rate of elongation, namely, at 45° to the bands, are continually being rotated away from that position towards the line parallel to the bands which is neither elongating nor contracting. After attaining this position further rotation brings the line of particles into an orientation where they are contracting. When the drop is very viscous compared with the surrounding medium it rotates almost like a slightly plastic solid body, lines of particles in it elongating slowly while they are within 45° of the direction of maximum rate of elongation and contracting slowly while they are within 45° of the direction of maximum rate of contraction. In this way the surface of the drop attains a permanent position with its long axis parallel to the bands. The tar-pitch mixture rotates round inside this fixed envelope; in fact, accidental

* The values of F are found by assuming $T = 23$ C.g.s., see Table II, and p. 507.



FIG. 2



FIG. 4

$a =$ 0.20 0.20 0.25 0.16 0.12



$F =$ 0.18 0.28 0.41 0.54 0.65
 $\frac{L-B}{L+B} =$ 0.15 0.26 0.44 0.54 0.51

FIG. 5A

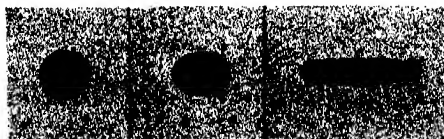
$a =$ 0.25 0.25 0.25



$F =$ 0.95 1.40 2.45
 $\frac{L-B}{L+B} =$ 0.69 0.79 0.87

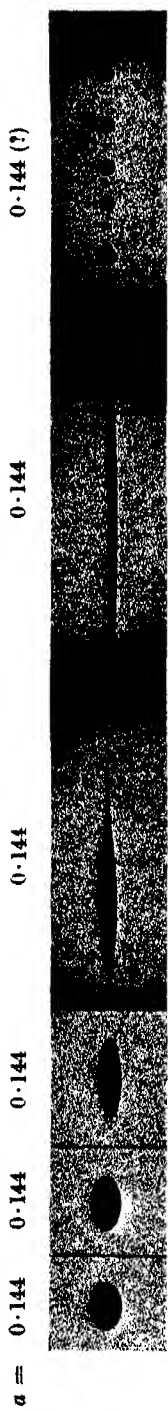
FIG. 5B

$a =$ 0.16 0.16 0.16



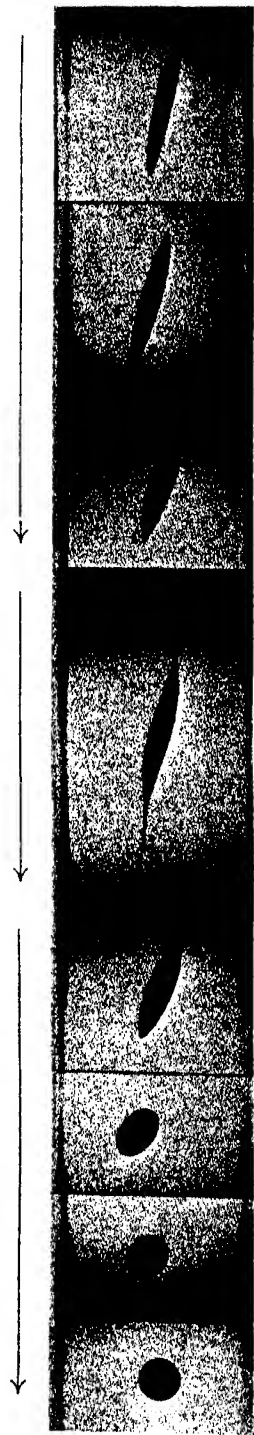
$F =$ 0 0.13 0.28
 $\frac{L-B}{L+B} =$ 0 0.15 Bursting

FIG. 9



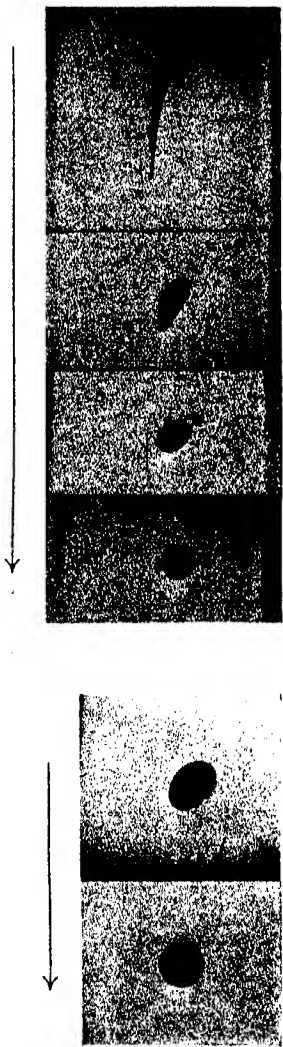
$F = 0.21$	0.30	0.37	0.39	0
$L-B$				
$L+B = 0.19$	0.29	0.54	—	—

Fig. 7



$F = 0$	0.04	0.10	0.27	0.71	0.71	1.46	2.30
$L-B$							
$L+B = 0$	0.08	0.22	0.61	Unsteady	0.68	0.76	0.80
$a = 0.16$	0.16	0.16	0.16	0.16	0.16	0.16	0.15

Fig. 11

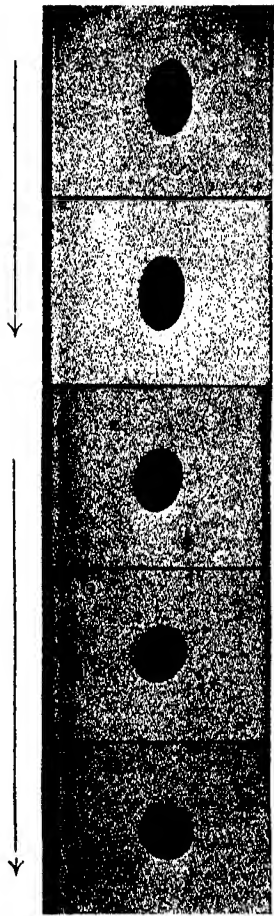


$F = 0$ 0.17
 $\frac{L-B}{L+B} = 0$ 0.17
 $a = 0.14$ 0.14

FIG. 13

0 0.11 0.28 0.55
0 0.15 0.45 Bursting
0.097 0.097 0.097 0.086

FIG. 15



$F = 0$
 $\frac{L-B}{L+B} = 0$
 $a = 0.17$

0.08 0.27 1.13 1.69
0.08 0.15 0.28 0.26
0.17 0.17 0.17 0.17

FIG. 17

small unevennesses could be seen to move round the contours of the drops. As the speed increases the viscous stresses in the surrounding medium and in the drop itself increase in the same ratio. The stresses due to surface tension do not increase so that ultimately at comparatively high speeds the drop assumes a form which is quite independent of surface tension.

Analytical Treatment of very Viscous Drop

The idea just put forward can be analysed mathematically in the case when μ' is large compared with μ and the speed is so great that the forces due to surface tension can be neglected compared with those due to viscosity.

Referring to the treatment* previously given for finding the distribution of flow inside and outside a drop held spherical by surface tension the conditions of continuity of velocity at the surface of the drop must be satisfied so that equations (8) and (9) of the previous paper still hold. These are

$$\frac{1}{2}A_{-3} - 5B_{-3} = -\frac{2}{21}A_2 \quad (8A)$$

$$2B_{-3} + \frac{1}{2}\alpha = \frac{5}{21}A_2 + 2B_2. \quad (9A)$$

The condition of continuity of tangential stress is

$$A_{-3} - 16B_{-3} + \alpha = \frac{\mu'}{\mu} \left(\frac{16}{21}A_2 + 4B_2 \right). \quad (17A)$$

Neglecting the effect of surface tension the condition of continuity of normal stress p_{rr} is

$$\mu(\gamma - \beta) = \mu'(\gamma' - \beta')$$

or

$$\mu(-3A_{-3} + 24B_{-3} + \alpha) = \mu'(-\frac{3}{21}A_2 + 4B_2). \quad (17B)$$

The solution of equations (8A), (9A), (17A), (17B) is

$$\left. \begin{aligned} A_{-3} = 10B_{-3} = -5\alpha \left(\frac{\mu' - \mu}{2\mu' + 3\mu} \right) \\ A_2 = 0, \quad B_2 = \frac{5\alpha\mu}{4(2\mu' + 3\mu)} \end{aligned} \right\} \quad (15)$$

Referring to equation (5) of the previous paper (*loc. cit.*, p. 43) the components of velocity at the surface are

$$u = 2B_2a \cos \phi \sin \theta, \quad v = -2Ba \sin \phi \sin \theta, \quad w = 0, \quad (16)$$

* "The Viscosity of a Fluid Containing small drops of another fluid," 'Proc. Roy. Soc.,' A, vol. 138, p. 41 (1932).

where

$$x = a \cos \phi \sin \theta, \quad y = a \sin \phi \sin \theta.$$

When μ'/μ is large these are

$$u = \frac{1}{4} \frac{\mu}{\mu'} a \alpha \cos \phi \sin \theta, \quad v = -\frac{1}{4} \frac{\mu}{\mu'} a \alpha \sin \phi \sin \theta. \quad (17)$$

This expression gives the instantaneous rate of deformation of the drop referred to Polar co-ordinates (θ, ϕ) at 45° to the celluloid bands of the apparatus.

In the central plane $\theta = \frac{1}{2}\pi$ the radial component of velocity is

$$\frac{1}{4} a \alpha \frac{\mu}{\mu'} \cos 2\phi. \quad (18)$$

It has already been pointed out that the condition of a drop in the shearing field ($u' = \alpha y$, $v' = 0$) is identical with that in the field ($u = \frac{1}{2}\alpha x$, $v = -\frac{1}{2}\alpha y$) when $(x'y')$ is at 45° to (xy) when the latter is rotated with angular velocity $\frac{1}{2}\alpha$.

If the result of this rotation and this rate of deformation is to keep the outer surface of the drop in a fixed position in the apparatus though the particles move round on it, and if this surface is nearly spherical its central section may be represented by the equation

$$r = a \{1 + bf(\phi)\}. \quad (19)$$

The condition that this surface may remain fixed in space is that the component of velocity normal to the surface due to rotating it at angular velocity $\frac{1}{2}\alpha$ shall be equal to the radial component of velocity of deformation. Thus

$$\frac{1}{2} \alpha a b \frac{d}{d\phi} f(\phi) = \frac{1}{4} a \alpha \frac{\mu}{\mu'} \cos 2\phi. \quad (20)$$

The solution of (20) is

$$bf(\phi) = \frac{1}{4} \frac{\mu}{\mu'} \sin 2\phi,$$

and the equation to the surface is therefore

$$r = a \left(1 + \frac{1}{4} \frac{\mu}{\mu'} \sin 2\phi\right). \quad (21)$$

Remembering that $\phi = 0$ is the line at 45° to the celluloid bands of the apparatus it will be seen that (21) indicates:—

(a) that the long axis of the drop is parallel to the bands.

(b) the ratio $(L - B)/(L + B)$ is equal to $\frac{1}{4} (\mu/\mu')$, (22)

and this ratio is independent of the size of drop and speed of the apparatus.

Photographs were taken with a view to verifying the formula (22). In each case the value of $(L - B)/(L + B)$ was about 0.25, while the value of $\frac{1}{2} \mu/\mu'$ was about 0.07, so that (22) was not verified quantitatively, though the prediction that the drop will assume a permanent shape with its long axis parallel to the bands was verified (see fig. 18).

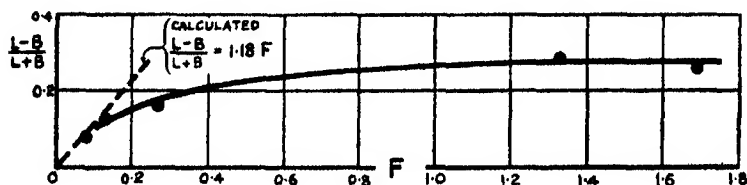


FIG. 18—"Parallel band" apparatus, tar-pitch mixture. $\mu'/\mu = 20$.

Conclusions

It has been shown that when a drop is slightly distorted from the spherical form by the stresses in a viscous fluid which is in motion round it the deformation depends only on the instantaneous conditions. The drop becomes elongated in the direction along which lines of particles are elongating at the greatest rate. Thus in the "four roller" apparatus the long axis of the drop is horizontal while in the "parallel band" apparatus it is at 45° to the bands. The shape of a slightly deformed drop is in complete agreement with a theory which shows that

$$\frac{L - B}{L + B} = \frac{19\mu' + 16\mu}{16\mu' + 16\mu} F.$$

As the viscous drag on the surface of the drop increases the drop elongates, but its shape no longer depends on the instantaneous conditions of flow. Thus the two types of apparatus produce different effects. The ultimate fate of the drop as the speed of distortion of the outer fluid increases depends also very much on the ratio μ'/μ . For very small values of μ'/μ , e.g., 0.0003, the drop remains coherent in spite of the fact that it gets very long and narrow in both types of apparatus.

As the viscosity of the drop increases the speed necessary to burst it gets less with both kinds of flow: thus, with the "parallel band" apparatus, it bursts when $F = 1.2$ approximately, for $\mu'/\mu = 0.5$. For $\mu' = \mu$ it bursts at $F = 0.5$ with the parallel band apparatus, and $F = 0.4$ with the "four roller" apparatus.

When μ'/μ has increased to 20 the two kinds of disrupting field have very different effects. In the "four roller" apparatus the drop bursts at $F = 0.28$, whereas the "parallel band" apparatus seems incapable of bursting the drop even at the highest speeds attainable. At high speeds in the latter apparatus the drop, in fact, attains a constant shape which depends only on μ/μ' . In this condition theoretical considerations lead to the prediction that

$$(L - B)/(L + B) = 5\mu/4\mu',$$

but this formula is not confirmed by these experiments except that the drop does assume a constant shape.

It is remarkable that in the "parallel band" apparatus the ease with which the drop can be burst increases as the viscosity of the drop rises from small values to be equal to that of the surrounding medium, but when the viscosity of drop rises to be several times as great as that of the outer fluid the viscous drag of the latter is incapable of bursting it however big the viscous stresses may be. The drop merely rotates, remaining nearly spherical.

Finally the manner in which the drops burst is of interest. The act of bursting is always an elongation to a threadlike form. When this thread breaks up it degenerates into drops which are of the order of 1/100th of the size of the original drop. This seems to be related to the known fact that when an emulsion is formed mechanically it contains drops which cover a very large range of sizes.

The experiments here described were carried out in the Cavendish Laboratory through the kindness of Lord Rutherford, to whom the author wishes to express his thanks.

Summary

The distortion of a drop of one fluid by the viscous forces associated with certain mathematically definable fields of flow of another fluid which surrounds it is discussed. An expression is found for small distortions from the spherical form which occur at slow speeds. If L is the greatest, and B the least diameter, $(L - B)/(L + B) = F$ approximately, where F is a non-dimensional quantity, proportional to the speed of flow, which involves the surface tension, viscosity, and the radius of the drop.

Apparatus for producing in golden syrup two definable fields of flow were constructed and their effects on drops of various oily liquids were observed and registered photographically.

Agreement with theory was found in the range of low speeds where agreement might be expected. At higher speeds the effect produced by the flow varies greatly with μ'/μ , μ and μ' being the viscosities of the syrup and drop.

For $\mu'/\mu = 0.0003$ the drop elongates almost indefinitely, but does not burst at the highest speeds attainable. For $\mu'/\mu = 0.5$ the drop burst at $F = 1.4$. For $\mu = \mu'$ the drop burst at about $F = 0.5$. For $\mu'/\mu = 20$ the drop burst at $F = 0.3$ in one type of field, but in the other the drop did not burst even at the highest speed attainable.

The difficulty experienced in bursting drops of viscous fluid by a disruptive field of flow in a surrounding fluid of considerably less viscosity is shown to be qualitatively in accordance with a theory of drops in a laminar shearing field of flow when F and μ'/μ are both large.

According to this theory $(L - B)/(L + B) = 5\mu/4\mu'$.

APPENDIX

Measurement of Viscosity—For the oils, and the syrup viscosity was measured by weighing the amount of fluid flowing in a given time through a glass tube. This method was unsuitable for measuring the viscosity of the highly viscous mixture of tar and pitch, accordingly the apparatus shown in the sketch of fig. 19 was constructed.

A brass cylinder A 1.27 cm diameter \times 3.9 cm long was hung by a fine steel wire from the torsion head B. A small metal dish containing a washer 1.2 mm thick was placed below it and the torsion head gently lowered till the bottom of the cylinder was just in contact with the washer. The washer was then removed and some of the tar-pitch mixture was dropped into the dish so that the depth was slightly more than 1.2 mm. The brass cylinder was then carefully dropped on to the surface of the mixture so that it was separated from the dish by a disc of the mixture 1.2 mm thick \times 1.27 cm diameter. A light pointer C served to mark the position of the cylinder as it rotated about its vertical axis.

If the torsion head was rotated suddenly through an angle θ_0 the cylinder would begin to rotate in the same direction, the rate of rotation being proportional to $\theta_0 - \theta$ where θ is the angle of rotation of the cylinder from its

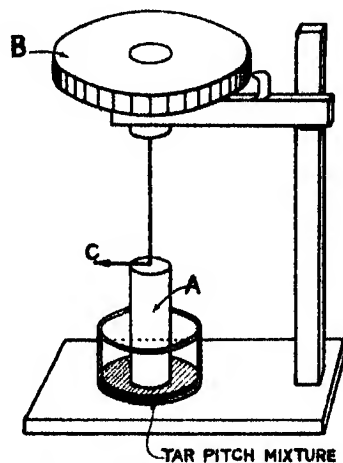


FIG. 19—Viscometer for very viscous liquids.

initial position. If the torsional couple of the wire is $K(\theta_0 - \theta)$ and this is equal to the couple due to action of viscosity μ' on the base of the cylinder, then the equation of motion is

$$K(\theta_0 - \theta) = \mu' \frac{d\theta}{dt} \int_0^a \frac{2\pi r^3 dv}{d}, \quad (23)$$

where d is the thickness of the disc of fluid which in this case was 0.12 cm and $2a = 1.27$ cm. The right-hand side of (23) is in c.g.s. units $2.12 \mu' d\theta/dt$. To find K the cylinder was allowed to oscillate freely and its period timed. In this way it was found that $K = 2.11 \times 10^3$ in c.g.s. units. Hence (23) becomes on integration

$$\log \left(\frac{\theta_0}{\theta_0 - \theta} \right) = \frac{211}{2.12} \frac{t}{\mu'} = 100t/\mu'. \quad (24)$$

In making measurements it was found convenient to turn the torsion head suddenly through half a turn so that $\theta_0 = \pi$. The time taken for the cylinder to turn through $\frac{1}{2}\pi$ and $3\pi/4$ was observed and it was found, as would be expected, that the time for $3\pi/4$ was exactly twice that for $\frac{1}{2}\pi$.

Using formula (24) it will be seen that the time corresponding with $\theta = \frac{1}{2}\pi$ is $\mu' \log_2 2/100$, while that corresponding with $\theta = 3\pi/4$ is $\mu' \log_2 4/100$.

This apparatus was used in making a mixture of tar and pitch of the desired viscosity. In the mixture chosen for some of the experiments the time for $\theta = \frac{1}{2}\pi$ was found to be 14 seconds while that for $\theta = 3\pi/4$ was 28 seconds, so that $\mu' = (100)(14)/\log_2 2 = 2 \times 10^3$ c.g.s.

Measurement of Surface Tension—In measuring the interfacial surface tension between two liquids one or both of which are very viscous it is advisable to avoid the use of any apparatus containing an appreciable length of capillary tube, for this may unduly prolong the time necessary for the system to attain equilibrium. In the present work the surface tension was measured by means of the apparatus shown in fig. 20. This sketch is self-explanatory. The syrup-oil interface was at the end of a very short length of capillary tube whose internal diameter was 0.37 mm. The syrup was in an open glass-walled box and the interface could be observed through a microscope. The oil was in a U-tube and the pressure of the air over the air-oil surface, which was of large area, could be varied and measured by a manometer.

The air pressure was first adjusted till the syrup-oil interface appeared flat in the microscope (the oil wetted the glass) and then measured. The air pressure was then increased till it attained its maximum steady value when the interface was hemispherical. The difference between the air pressure when

the interface is flat and the air pressure when it is hemispherical with radius a is $2T/a$.

With this apparatus the values given in Table II were measured.

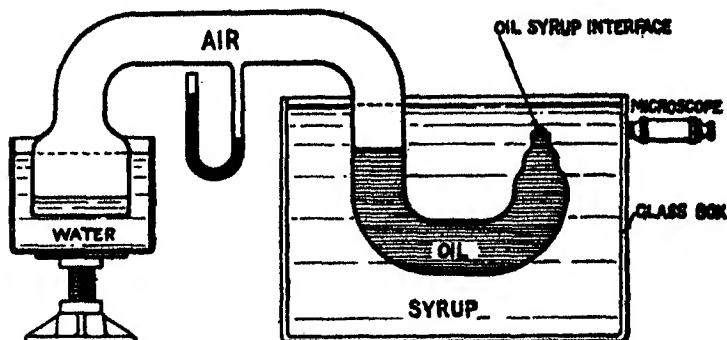


FIG. 20—Apparatus used for measuring surface tension between oil and syrup.

DESCRIPTION OF PLATES 4 AND 5

FIG. 2—Stream lines in "four roller" apparatus.

FIG. 4—Large drop in "four roller" apparatus.

FIG. 5—Drops of CCl_4 -paraffin mixture in "four roller" apparatus.

FIG. 7—Drops of black lubricating oil in "four roller" apparatus.

FIG. 9—Drop of tar-pitch mixture in "four roller" apparatus.

FIG. 11—Drops of CCl_4 -paraffin mixture in "parallel band" apparatus.

FIG. 13—Drops of "BB" oil in "parallel band" apparatus.

FIG. 15—Drop of black lubricating oil in "parallel band" apparatus.

FIG. 17—Drop of tar-pitch mixture in "parallel band" apparatus.

The Emission of Electrons under the Influence of Chemical Action
 Part IV—*The Reactions of Liquid NaK₂ with Gaseous SOCl₂, S₂Cl₂, SO₂Cl₂, HgCl₂, Sulphur Dichloride and with Mixtures of Gases and a New Method of Determining the Contact Potential Difference*

By A. K. DENISOFF, University of London, King's College, and O. W. RICHARDSON, F.R.S., Yarrow Research Professor of the Royal Society

(Received June 5, 1934)

§ 1—*Introduction*

In two earlier papers,* which we shall refer to as Part I and II in the sequel, we described a very detailed investigation of the electron emission phenomena which occur when the liquid alloy of sodium and potassium reacts with phosgene, COCl₂, at very low pressures. In Part II we also gave a brief account of some of our principal conclusions from the results of experiments in which 22 gases were examined. In a third paper,† Part III, we gave a detailed description of the corresponding phenomena observed with a variety of gases, namely, Cl₂, NOCl, HCl, Br₂, I₂, COS, N₂O, and H₂O. A comparison of the data obtained with Cl₂, COCl₂, and NOCl disclosed a linear relation between the dissociation energy involved in the reaction and the maximum energy of the emitted electrons. A theory of the way in which we supposed this connection to originate had already been given in Part II. With the particular purpose of testing further the generality of this relation, as well as of widening the basis of our information as to the details of the energy distribution among the electrons emitted in different reactions, we selected for our next experiments a group of gases containing chlorine. The gases chosen were SOCl₂, S₂Cl₂, SO₂Cl₂, HgCl₂, and S₂Cl₄.‡ We expected that one of the immediate results of the reaction of these gases with the liquid alloy would be, as in the case of Cl₂, COCl₂, and NOCl, the adsorption of a Cl⁻ ion on the surface of the alloy; consequently the same theory should apply to all of them.

The parts of this paper which follow immediately are concerned with a description of the results of the experiments with these five additional gases

* 'Proc. Roy. Soc.,' A, vol. 132, p. 22 (1931), Part I; vol. 144, p. 46 (1934), Part II.

† 'Proc. Roy. Soc.,' A, vol. 145, p. 18 (1934), Part III.

‡ We believe that under the conditions of our experiments the molecules of sulphur dichloride are in the dimerous form (S₂Cl₄); see § 5).

containing chlorine. We next describe experiments which we made with mixtures of COCl_2 with COS , and with S_2Cl_2 , and of SOCl_2 with S_2Cl_2 . The object of these was to test the additive property of the chemical electron emission. We then go on to describe a new method of determining the contact potential difference between the alloy drop and the surrounding platinum electrode in presence of the different gases. We regard the results given by this method as of great importance in establishing the interpretation of the experimental data on a firm basis. This is followed by an analysis of the electronic spectra of the gases to be described in this paper. The primary object of the analysis consists in identifying the different groups in a composite electronic spectrum with the corresponding mechanisms of the reaction; the analysis is conducted in the light of our previous experience with the reactions involving halogens and also in the light of some new general considerations of the kinetics and of the electronic yield of the chemical reactions. The electronic spectra, having been thus analysed, are then applied to test the fundamental relation between the dissociation energy, involved in a certain reaction, and the maximum energy of the emitted electrons of the group originating from the reaction with the corresponding mechanism. Finally we present the energy distribution functions obtained with the gases under consideration.

§ 2—*The Experimental Results for SOCl_2 , S_2Cl_2 , SO_2Cl_2 , HgCl_2 ,
and S_2Cl_4*

The substances under investigation, SOCl_2 , S_2Cl_2 , SO_2Cl_2 , HgCl_2 , and sulphur dichloride, were supplied in the purest form obtainable by Schering-Kahlbaum, A.G., Berlin. All of them except HgCl_2 are liquids at room temperatures, and at 0°C have vapour pressures within a range of about 5 to 50 mm of mercury. To ensure the purity of the gases used in the experiments about half a cubic centimetre of the liquid was first conveyed to a vertical glass tube (No. 10 in fig. 1, Part I), about 1 cm in diameter, immersed in liquid air and connected to the main vacuum system. The tube with the liquid was then pumped out, through a side tube having a constriction for sealing off, by a rough vacuum pump which gives a vacuum of about 1 mm of Hg; at the same time the temperature of the liquid was gradually increased from about -180°C towards 0°C . The pumping out continued until there was no more visible evolution of gas from the liquid; the glass tube with the liquid was then sealed off from the rough vacuum pump. Any remaining volatile impurities were

pumped out of the liquid by the high-vacuum pump, through the main glass system, at various intervals of temperature between about -50°C and -180°C .

The experiments with the liquid substances were made in the same way and with the same apparatus as those with the other gases which we have described in the previous papers. As mercury chloride is in a solid state at room temperatures and has a very low vapour pressure (about 5×10^{-5} mm at 15°C , as extrapolated from the data for the range 60 – 200°C), a new method for supplying the active gas was used to obtain the necessary pressure conditions in the reaction chamber. The method is illustrated schematically in fig. 1; the tube, containing some crystals of HgCl_2 , was placed between two glass spheres which were connected together by means of a low resistance glass tube and a tap which had a large opening about 8 mm in diameter. With such an arrangement it was possible to obtain in the reaction chamber a

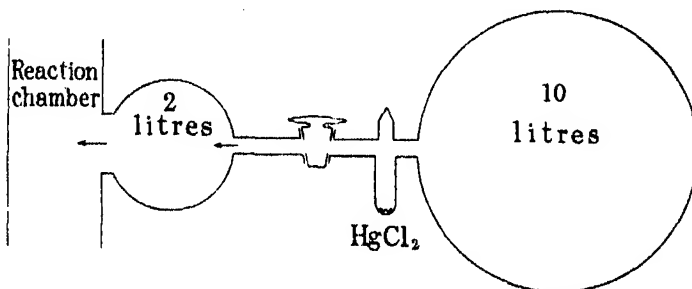


FIG. 1

pressure of HgCl_2 about 1×10^{-5} mm, when the room temperature was about 20°C . The apparatus showed a great permanence of pressure conditions, as can be judged by the electron current which was constant within 2% during 2 hours of the actual experiment.

The effect of the pressure of each of these gases on the contact potential difference was of the same general character as that observed with the gases already investigated. But the magnitude of the variation in contact potential difference with pressure was considerably less than, for instance, for Cl_2 .

A reverse current was observed with each gas except HgCl_2 . For this gas the direct current is so small that a detectable reverse current is hardly to be expected. In Table I we give the ratios of the reverse current (i'_0) to the direct saturation current (i_0) due to electron emission for the different gases at a number of pressures. It will be seen from Table I that the ratio i'_0/i_0 was small and comparable with 10^{-4} . For HgCl_2 , owing to the small absolute

value of i_0 , only an upper limit for the ratio can be estimated which is about 3×10^{-4} . On account of the smallness of the reverse currents we cannot say that the variation of this ratio with the pressure exceeds the experimental error with any of the gases.

Table I

Gas :	SOCl ₂			S ₂ Cl ₂		SO ₂ Cl ₂		S ₂ Cl ₄		
Pressure in 1×10^{-6} mm	0.2	0.5	2.0	0.4	1.8	0.1	0.3	0.05	0.2	10
i'_0/i_0 in 10^{-4}	13	4	4	10	8	0.0	0.4	1	3	6

The general form of the function $i_0 = f(p)$ is the same for all the gases. Unfortunately, this relation for S₂Cl₂ was obtained only in the region of low

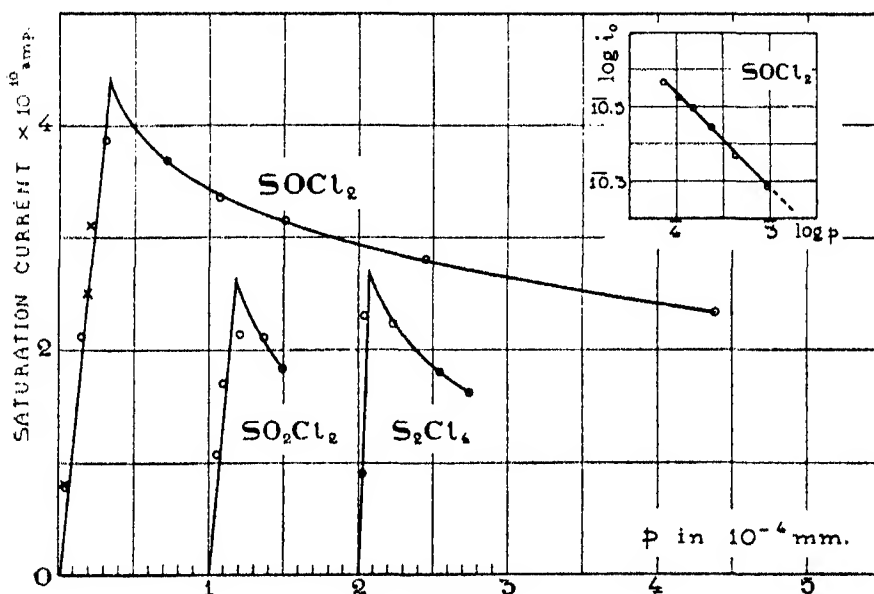


FIG. 2

pressures; the experimental points for this gas are indicated by crosses in fig. 2 and it can be seen that they follow exactly the trend of the SOCl₂ curve, the experimental points of which are indicated by circles. The vertical scale readings for the S₂Cl₂ data should be multiplied by 4.5. An accurate determination of the function $f(p)$ for HgCl₂ could not be made on account of its low vapour pressure; nevertheless, a general observation definitely showed that i_0 is a very sensitive function of the pressure, quite similar to that of all the other gases. The vertical scale readings for the curves obtained with SO₂Cl₂ and S₂Cl₄, which are shown in fig. 2, should be multiplied by 10 and

the curves are also arbitrarily shifted to the right from $p = 0$ by 1 and 2 units respectively. All the curves in fig. 2 were obtained at approximately the same time of drop T and time of exposure dt , namely, the SOCl_2 curve at $T = 30$ sec, $dt = 25$ sec, the S_2Cl_2 data at $T = 40$ sec, $dt = 30$ sec, the SO_2Cl_2 curve at $T = 38$ sec, $dt = 30$ sec, and the S_2Cl_4 curve at $T = 35$ sec, $dt = 30$ sec. At a pressure p about 3×10^{-5} mm (absolute values of the gas pressure are rather uncertain, owing to the Pirani gauge having been calibrated only in N_2) the relation $i_0/p = \text{constant}$ changes sharply and becomes transformed at higher pressures into another form $(i_0)^\alpha \cdot p = \text{constant}$, where α is a constant for a given gas, which depends on the rate of formation of the drops and on the time of exposure. This can be seen from the straight line which is obtained when $\log_{10} i_0$ is plotted against $\log_{10} p$. A plot of this kind for SOCl_2 is shown as an inset in fig. 2.

We shall now give the characteristic curves and the $\log(i/i_0)$ vs. V_1 plots which we have obtained for each of the five gases investigated. The characteristic curves are obtained by plotting i/i_0 against V_1 where i is the actual measured negative emission current when the potential difference between the drop of alloy and the surrounding platinum electrode is V_1 and i_0 is its maximum or saturation value which it assumes when V_1 becomes greater than a certain value. V_1 is not equal to the true difference of potential V between the electrodes. They are connected by the relation $V = V_1 + K$, where K is the contact potential difference between the drop and the outer electrode.

1 *Thionyl Chloride* (SOCl_2)—From the four independent sets of experiments, which give practically identical results, we have selected two characteristic curves, as representing the most accurate observations. These curves are shown in fig. 3; the observations marked \bigcirc were obtained at $p = 5 \times 10^{-6}$ mm, $T = 30$ sec, $dt = 25$ sec, $i_0 = 1.2 \times 10^{-10}$ amp, and those marked \bullet refer to $p = 2.0 \times 10^{-5}$ mm, $T = 32$ sec, $dt = 25$ sec, $i_0 = 3.6 \times 10^{-10}$ amp. The latter curve is arbitrarily shifted to the right from $V_1 = 0$ by 0.5 volt. The corresponding logarithmic plots are shown in fig. 4. In all the diagrams the true zeros ($V = 0$) are indicated by arrows.

2 *Sulphur Chloride* (S_2Cl_2)—Figs. 3 and 4 show two characteristic curves and the corresponding logarithmic plots for S_2Cl_2 . The circles in figs. 3 and 4 are arbitrarily shifted to the right from $V_1 = 0$ by 0.8 and 1.3 volts respectively, and the dots are shifted by 1.4 and 2 volts respectively. The experimental conditions for \bigcirc were: $p = 1.8 \times 10^{-5}$ mm, $T = 45$ sec, $dt = 30$ sec, $i_0 = 1.0 \times 10^{-9}$ amp, and for \bullet : $p = 0.36 \times 10^{-5}$ mm, $T = 38$ sec, $dt = 30$ sec, $i_0 = 3.0 \times 10^{-10}$ amp.

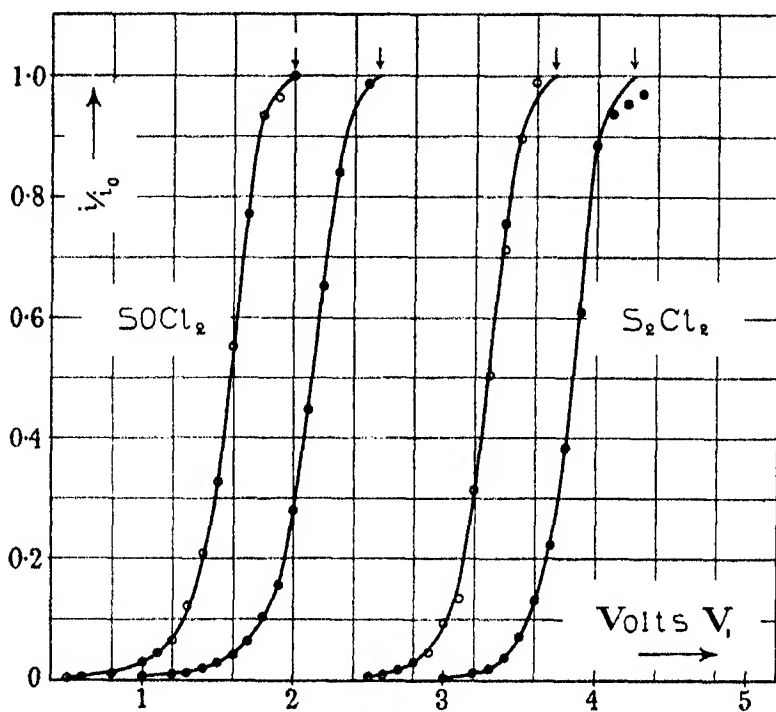


FIG. 3

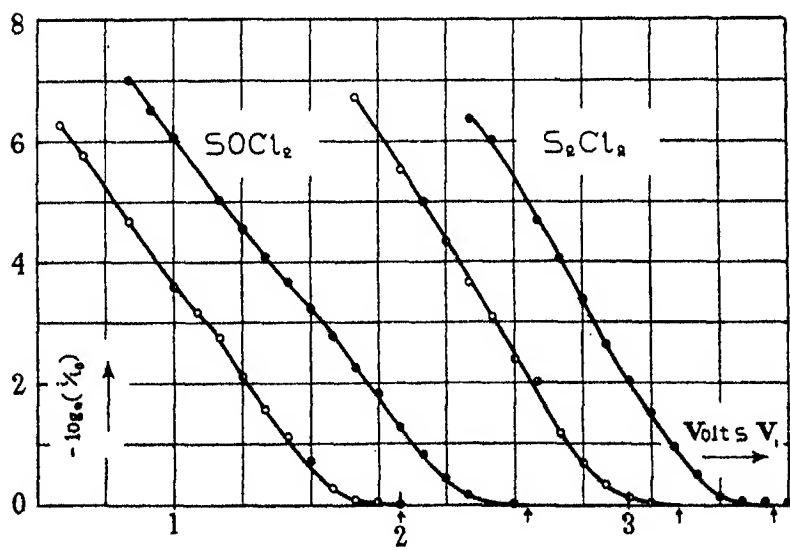


FIG. 4

3 *Sulphuril Chloride* (SO_2Cl_2)—Figs. 5 and 6 exhibit two characteristic curves and the corresponding logarithmic plots for SO_2Cl_2 . In each figure the points marked \circ were obtained at $p = 2.5 \times 10^{-6}$ mm, $T = 40$ sec, $dt = 30$ sec, $i_0 = 6.0 \times 10^{-9}$ amp, and those marked \bullet at $p = 1.0 \times 10^{-6}$ mm, $T = 38$ sec, $dt = 30$ sec, $i_0 = 2.2 \times 10^{-9}$ amp. The circles are correctly placed with respect to the V_1 scale and the dots in figs. 5 and 6 are arbitrarily moved to the right by 0.7 and 0.6 volt respectively.

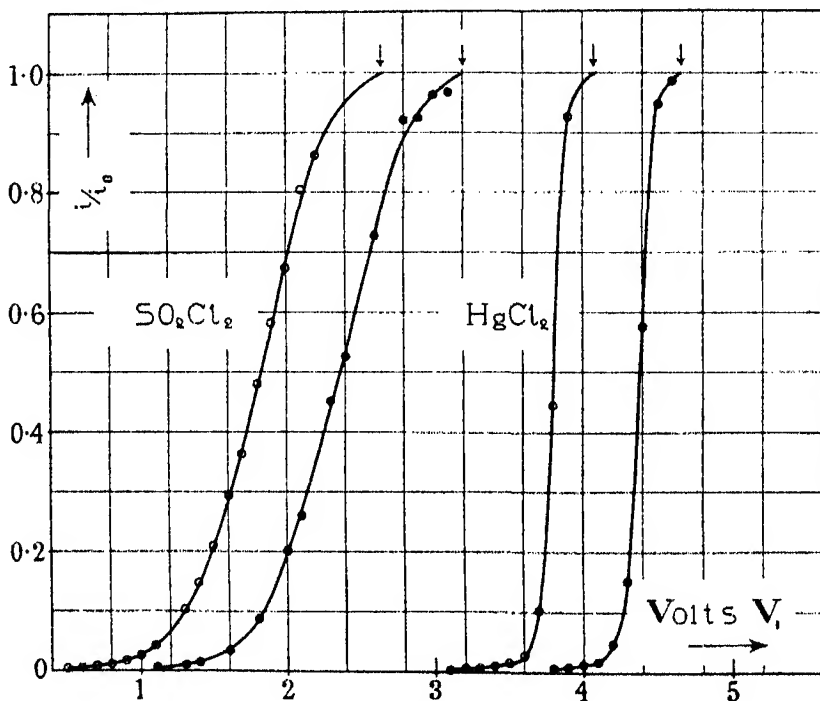


FIG. 5

4 *Mercury Chloride* (HgCl_2)—Two characteristic curves for HgCl_2 are shown on the right of fig. 5. The curve marked \circ was obtained at $p = ca. 10^{-5}$ mm, $T = 32$ sec, $dt = 1$ min 30 sec, $i_0 = 3.8 \times 10^{-11}$ amp, and that marked \bullet at $p = ca. 10^{-5}$ mm, $T = 27$ sec, $dt = 50$ sec, $i_0 = 3.8 \times 10^{-11}$ amp. The curves are shifted to the right along the volt axis by 1.3 and 2 volts respectively. The logarithmic plots are shown in fig. 7 and the experimental points are marked to correspond with fig. 5. Curve (\bullet) is shifted to the right from $V_1 = 0$ by 0.8 volt. It will be noticed that the absolute values of i_0 are quite identical in the two sets of observations, which were obtained under identical pressure conditions but on different days.

5 *Sulphur Dichloride* (S_2Cl_4)—Two characteristic curves for S_2Cl_4 , and the corresponding logarithmic plots, are given in figs. 8 and 9. The experimental conditions for the points marked \circ : $p = 1.0 \times 10^{-4}$ mm, $T = 35$ sec, $dt = 30$ sec, $i_0 = 1.5 \times 10^{-8}$ amp, for those marked \bullet : $p = 0.5 \times 10^{-6}$ mm, $T = 35$ sec, $dt = 30$ sec, $i_0 = 2.0 \times 10^{-9}$ amp. The characteristic and the logarithmic curves (\bullet) are shifted to the right from $V_1 = 0$ by 1.4 and 0.8 volt respectively.

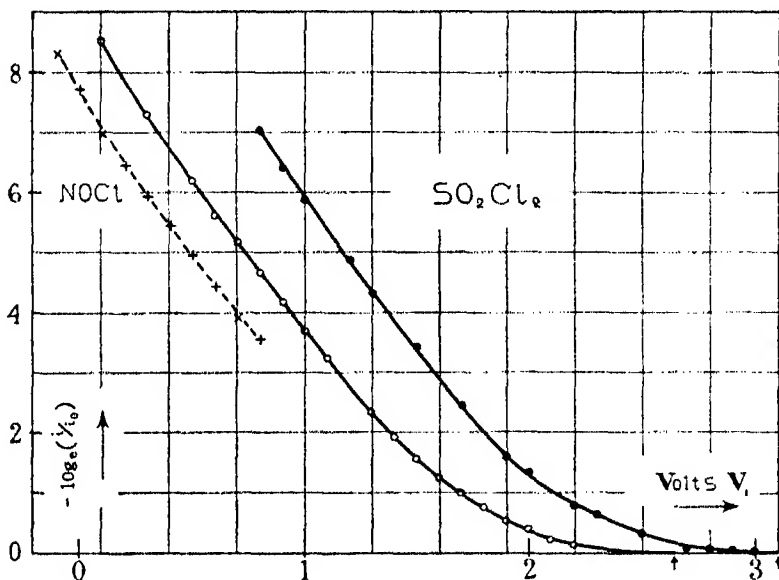


FIG. 6

§ 3—Experiments with Mixtures of Gases. The Principle of Superposition

In all our experiments with the different gases we never noticed any appreciable effect of pressure of the gas on the distribution of energy among the emitted electrons. Some of our experiments with COCl_2 were carried out in a wide range of pressures from 2×10^{-7} to 5×10^{-3} mm of mercury. We saw in Part II, § 6, that the time required for the actual chemical transformation responsible for the electron emission, and for the dissipation of the energy developed as a result of the transformation, is of the order of 10^{-15} sec; during this time, and at the lowest pressure at which measurements were made, only about 4×10^{-2} molecules strike 1 sq cm of the surface of the alloy drop. Therefore there is only one instantaneously active centre of reaction to about 20 sq cm of the surface, on the average. Furthermore, the experi-

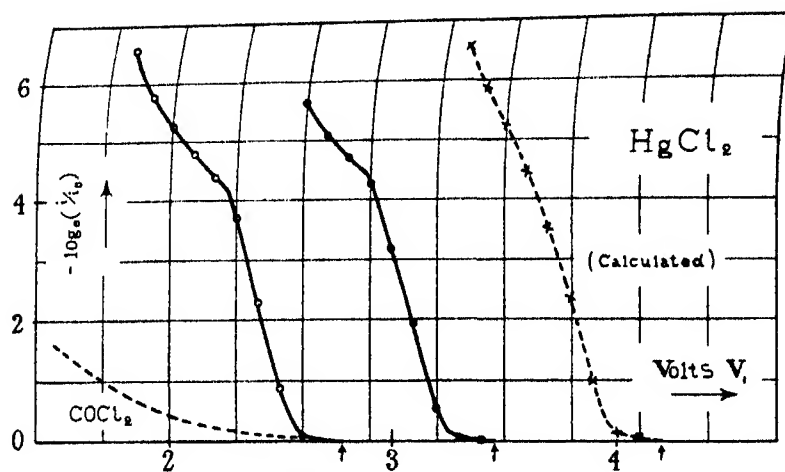


FIG. 7

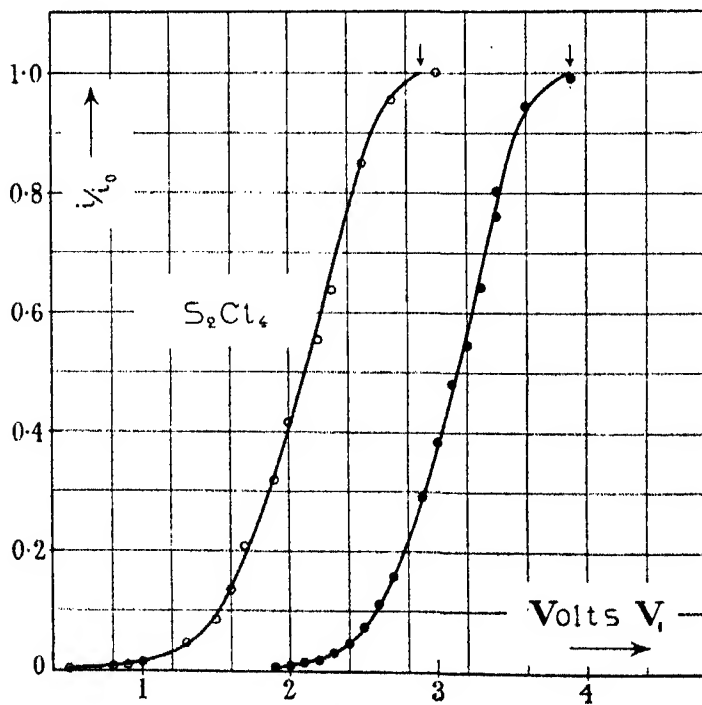


FIG. 8

ments show that the surface of the drop is covered with a monomolecular layer of the reaction products at a pressure of about 3×10^{-5} mm. At pressures lower than this the part of the surface which is covered will be approximately proportional to the pressure; so that, at the pressure $p = 2 \times 10^{-7}$ mm only $2 \times 10^{-7} \div 3 \times 10^{-5}$, i.e., one hundredth part of the surface is covered. Therefore, the average value of the area of the alloy surface, which surrounds each completed centre of reaction, after the usual half-a-minute exposure, is about 100 times as large as the area occupied by an individual member of the reaction products.

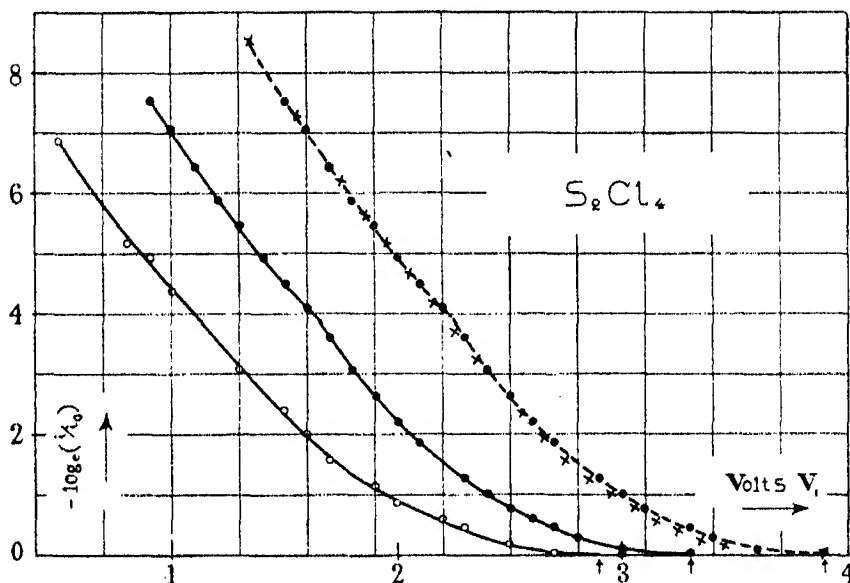


FIG. 9

It is evident from this that the electron emission is the result of the interaction between an *individual* gas molecule and the alloy and the energy distribution is something which is definitely determined by such an individual interaction. A necessary consequence of this statement will be that the distribution for a mixture of non-interfering gases can be obtained by superposing, in suitable proportions, the distributions for the separate constituents. It is a matter of great importance to prove experimentally the exact validity of the superposition principle, as our interpretation of the electronic spectra for the reactions with a complicated mechanism of dissociation is based entirely on the assumption of its exact validity. That is, it is required to prove that the current i which flows against an opposing potential difference V , in a

reaction with a mixture of gases, is equal to the sum of the currents i' and i'' which would flow against the same potential difference if the gases were reacting separately at the same pressures as their partial pressures in the mixture. The superposition principle stated in this form can be, of course, true only for comparatively low total pressures of a mixture of gases, since the proportionality between the electron emission and the pressure breaks down at a critical pressure which is high enough to keep the surface of the alloy completely covered with the reaction products.

We should like first to describe some experiments with those mixtures of two gases in which one of the gases is either non-reactive, or a gas which gives a negligibly small electron emission. The effect of mixing the non-reactive gas nitrogen with phosgene was already described in Part I (p. 42). To COCl_2 at a pressure of 3.5×10^{-5} mm we added pure N_2 at a pressure of 3.85×10^{-4} mm, thus raising the total pressure to 4.2×10^{-4} mm. As we should expect, this caused no appreciable change in the total emission and no change in the energy distribution among the emitted electrons. A similar result was observed with a mixture of COCl_2 and COS . We determined first the distribution of energy among the emitted electrons with COCl_2 at a pressure $p \approx 0.3 \times 10^{-5}$ mm, the saturation current i'_0 being 5.2×10^{-10} amp. The observations made in this experiment are shown in the form of a $\log i/i_0$ vs. V_1 plot, as circles, on the left-hand side of fig. 10. Then at this pressure of COCl_2 a quantity of COS was added, the total pressure being thus raised to 4.0×10^{-5} mm. As this pressure is higher than the critical value (about 3×10^{-5} mm), this was found to decrease the electron saturation current, which fell from 5.2 to 2.8×10^{-10} amp. On admitting the COS a change in the glitter of the drops was observed, showing that the COS was reacting with the alloy. The observations made with this mixture are shown as crosses in fig. 10. In spite of the partial pressure of the COS being 10 times as high as that of the COCl_2 , to which it was added, it has caused no detectable change in the velocity distribution of the emitted electrons. Any difference in the observations on the $\log i/i_0$ vs. V_1 plot for the pure COCl_2 and for the mixture with COS which exceed the experimental errors are due to a small change in the contact potential difference between the drop and the platinum electrode which is brought about when the COS is added. Although the partial pressure of the COS is so much higher than that of the COCl_2 the electron emission from it is much smaller, being less than 10^{-14} amp (see Part III, p. 33) as compared with more than 10^{-10} amp. The distribution of energy for the mixture is the sum of the distributions for the separate constituents, since the contribution coming

from the COS is always negligible compared with that from the COCl_2 . We have here, therefore, an example of the principle of superposition.

The next experiments with mixtures were made with COCl_2 and S_2Cl_2 . This is one of the most instructive combinations of two gases, as each of the two gases gives approximately the same yield of electrons and at the same time the energy distribution functions of these gases are widely different. The pressure of the COCl_2 was low, being 0.18×10^{-5} mm, and $i'_0 = 3.6 \times 10^{-10}$ amp. To this gas the S_2Cl_2 was added at such a pressure $p = 0.3 \times 10^{-5}$ mm, calculated from the ratio $i_0/p = \text{constant}$ ($p < 3 \times 10^{-5}$ mm) which had

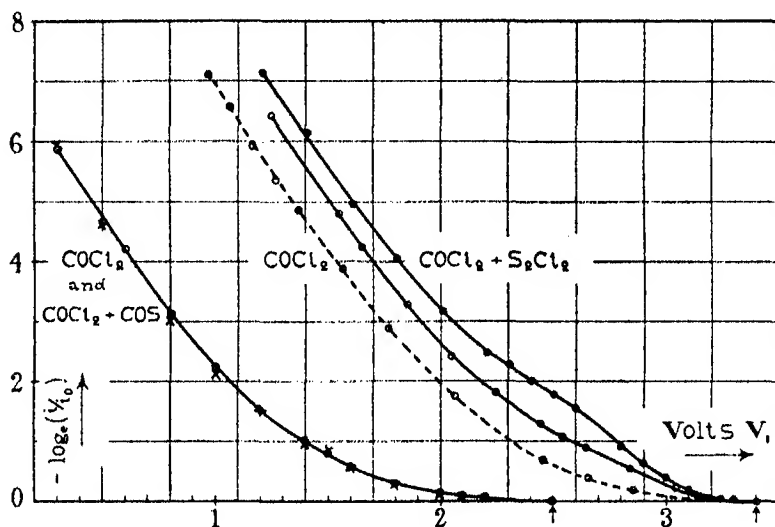


FIG. 10

previously been determined for S_2Cl_2 , as would make i''_0 for the S_2Cl_2 present approximately equal to i'_0 for the COCl_2 in the mixture. On measuring i_0 for the mixture of $\text{COCl}_2 + \text{S}_2\text{Cl}_2$ it was found to be 7.0×10^{-10} amp; the addition of the S_2Cl_2 had thus approximately doubled the emission, in accordance with the calculation. For this experiment T was 27 sec, $dt = 25$ sec. The results of the observations are shown, as circles, on the i/i_0 vs. V_1 and $\log i/i_0$ vs. V_1 plots in figs. 11 and 10 respectively. The full line curve (\circ) on the right of fig. 10 is arbitrarily shifted to the right from $V_1 = 0$ by 1.04 volts. After taking the set of measurements just described a new portion of S_2Cl_2 was added to the mixture in such a quantity that the partial pressure of the S_2Cl_2 would exceed the partial pressure of the COCl_2 by a considerable amount. The total pressure was, in fact, brought up to 2.1×10^{-5} mm, and the total

current i_0 to 18.4×10^{-10} amp, time of drop T being approximately as before, about 30 sec. The resulting i/i_0 vs. V_1 and $\log i/i_0$ vs. V_1 observations for this mixture are shown as dots in figs. 11 and 10 respectively. Curve (●) in fig. 11 is arbitrarily shifted to the right from $V_1 = 0$ by 0.5 volt; in fig. 10 curve (●) is shifted to the left along the volt axis by 0.24 volt relative to curve (○) in such a way that the true zeros of these curves would coincide. On the right-hand side of fig. 11 two characteristic curves for S_2Cl_2 and $COCl_2$ are drawn as dotted lines; the curves are arbitrarily shifted to the right from

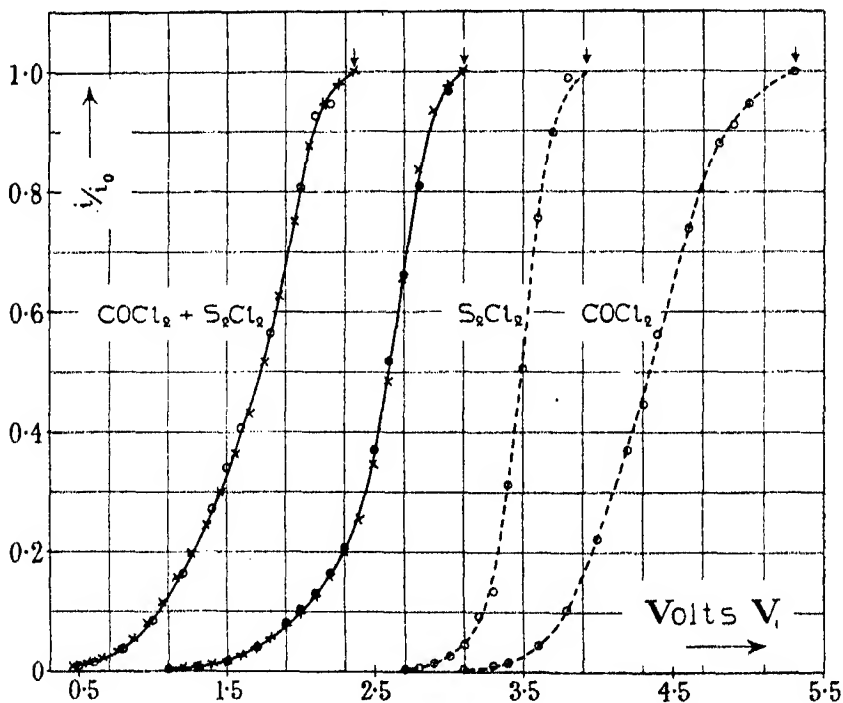


FIG. 11

$V_1 = 0$ by 1.5 and 2.8 volts respectively. These curves for the pure gases were not obtained on the same day as those for the mixtures $COCl_2 + S_2Cl_2$ but previously at approximately the same pressures as the partial pressures in the experiment with the mixture; this is not important, however, as characteristic curves do not depend upon pressure. The values of the ratio i/i_0 calculated by means of the $COCl_2$ and S_2Cl_2 curves are given in Table II, column 5, and in fig. 11 the calculated points are shown as crosses.

As can be seen from fig. 11 and Table II, columns 5 and 6, complete agreement, within the limits of the experimental error, between the calculated and

observed values of i/i_0 is obtained for both the mixtures. This, therefore, proves the exact validity of the principle of superposition.

It has to be pointed out that on constructing curve (●) it was found that the calculated curve disagreed slightly with the observed one and that the

Table II

Volts	i' COCl ₂	i'' S ₂ Cl ₂	$i = i' + i''$	i/i_0 calculated	i/i_0 observed
Mixture (○)					
0	3.60	3.40	7.00	1	—
0.1	3.546	3.305	6.851	0.979	—
0.2	3.485	3.135	6.620	0.946	0.945
0.3	3.413	2.720	6.133	0.876	0.875
0.4	3.308	1.938	5.246	0.749	0.750
0.5	3.168	1.207	4.375	0.625	0.630
0.6	2.963	0.646	3.609	0.516	0.525
0.7	2.664	0.330	2.994	0.428	0.440
0.8	2.340	0.190	2.530	0.361	0.370
0.9	1.994	0.102	2.096	0.299	0.305
1.0	1.656	0.054	1.710	0.244	0.245
1.1	1.350	0.027	1.377	0.197	0.195
1.2	1.080	0.014	1.094	0.156	0.150
1.3	0.792	0.008	0.800	0.114	0.110
1.4	0.558	0.004	0.562	0.080	0.075
1.5	0.371	—	0.373	0.053	0.050
1.6	0.245	—	0.246	0.035	0.030
1.7	0.158	—	0.158	0.022	0.020
1.8	0.094	—	0.094	0.013	0.012

Mixture (●)

0	4.50	13.90	18.40	1	—
0.1	4.433	13.511	17.94	0.975	0.965
0.2	4.356	12.816	17.17	0.933	0.925
0.3	4.266	11.120	15.39	0.836	0.810
0.4	4.136	7.923	12.06	0.655	0.660
0.5	3.960	4.935	8.895	0.483	0.505
0.6	3.704	2.641	6.345	0.345	0.365
0.7	3.330	1.348	4.678	0.254	0.265
0.8	2.925	0.778	3.703	0.201	0.205
0.9	2.493	0.417	2.910	0.158	0.160
1.0	2.070	0.222	2.292	0.125	0.130
1.1	1.688	0.111	1.799	0.098	0.100
1.2	1.350	0.056	1.406	0.076	0.080
1.3	0.990	0.028	1.018	0.055	0.055
1.4	0.698	0.017	0.715	0.039	0.040
1.5	0.464	—	0.472	0.026	0.025
1.6	0.306	—	0.310	0.017	0.017
1.7	0.198	—	0.200	0.011	0.010
1.8	0.117	—	0.118	0.0064	0.007

cause of the disagreement was in the slightly too high value of the ratio i''_0/i'_0 . The above complete agreement between the calculated and observed curves was obtained with a value of i'_0 equal to 4.5×10^{-10} amp. which is about 25% higher than the original value 3.6×10^{-10} amp. It is therefore necessary

to admit that the partial pressure of the COCl_2 in the reaction chamber increased by about 25% when the second large portion of S_2Cl_2 had been added to mixture (○). This is quite a possible thing if we remember that the ultimate magnitude of the pressure in the reaction chamber is a result of the dynamic equilibrium conditions. It is probably due to the fact that the high pressure (2.1×10^{-5} mm) of S_2Cl_2 has decreased the output of the vacuum system, namely, the amount Q_3 (see Part I, p. 26) of the COCl_2 , by forming a more complete layer of the reaction products on the surface of the alloy in the lower bottle and has thus raised up the partial pressure of the COCl_2 in the reaction chamber. This layer of the reaction products in the lower bottle is not stationary but regularly breaks into pieces by the falling alloy drops. The fact of the output of the vacuum system being slightly out of proportion with pressure in the neighbourhood of the critical pressure (about 3×10^{-5} mm) probably also accounts for some irregularities in the relation $i_0/p = \text{constant}$ for the pure gases, which were usually observed in this region of pressures.

The dotted curve of fig. 10 is the logarithmic plot for the pure COCl_2 ; the true zero of this curve is made to coincide with the true zeros of the curves for the mixtures. The dotted curve is a repetition of one of those previously published (see curve I, fig. 1, p. 52, Part II); it corresponds to a pressure $p \approx 2.2 \times 10^{-5}$ mm, and represents an accurate determination of the high energy part of the spectrum. The characteristic curve for the pure COCl_2 , corresponding to a low pressure $p \approx 0.3 \times 10^{-5}$ mm, given in fig. 11 and on the left-hand side of fig. 10 was specially obtained on purpose to determine accurately the low energy part of the spectrum; it has a comparatively low accuracy in the extreme high energy part of the spectrum. We wish to draw attention to the following features of these curves.

(1) In the higher energy part of the spectrum the curves for the mixtures are practically parallel to the curve for COCl_2 . This shows that the energy distribution in the region of higher energy for the mixtures is practically the same as that for the pure COCl_2 , and is little affected by the presence of the S_2Cl_2 . This is in agreement with the theoretical considerations of § 2, Part III. In a mixture of two groups of electrons with markedly different average energies the group of lower energy will be stopped by the higher opposing fields, and the faster electrons from the group of higher energy alone will reach the collecting electrode.

(2) Curve (○) for $\text{COCl}_2 + \text{S}_2\text{Cl}_2$ has practically retained the shape of the curve for the pure COCl_2 , even in the low energy part of the spectrum, in spite of the fact that the ratio i''_0/i'_0 is as high as 1. Only curve (●), correspond-

ing to $i''_0/i'_0 = 3$, begins to show the point of inflexion characteristic of a mixture (cf. § 2, Part III).

(3) In spite of the fact that the high energy part of the curves is unaffected by the presence of the S_2Cl_2 the maximum energy of the emitted electrons, as determined directly from the diagram, will be appreciably less than that for the pure $COCl_2$. This is because of the high energy part of the curves being displaced, along the volt axis, to the right from the curve for the pure $COCl_2$. The displacements are about 0.15 and 0.25 volt for curve (○) and (●) respectively, and therefore the *apparent* maximum energies of the electrons, originating from the reaction with the $COCl_2$, are less than the true maximum energies by the same amounts.

It is evident that the amount of displacement depends upon the ratio i''_0/i'_0 of the individual currents. It is easy to show that there is a simple relation between the amount of the vertical displacement along the $\log i/i_0$ axis, and the ratio i''_0/i'_0 . In fact, the total current i for any value of V will be given by

$$\frac{i}{i_0} = \frac{i'_0}{i_0} f'(V) + \frac{i''_0}{i_0} f''(V), \quad (1)$$

where i_0 is the total saturation current $i'_0 + i''_0$ for the two reactions for which the individual currents in the pure gases are given by

$$i' = i'_0 f'(V) \quad \text{and} \quad i'' = i''_0 f''(V). \quad (2)$$

When the opposing V is so large that the weaker group of electrons, indicated by two dashes, is stopped equation (1) reduces to

$$\frac{i}{i_0} = \frac{i'_0}{i_0} f'(V) = \frac{i'_0}{i_0} \frac{i''}{i'_0}, \quad (3)$$

or

$$\log(i/i_0) = \log(i'/i'_0) - \log\left(\frac{i''}{i'_0} + 1\right). \quad (4)$$

Thus the $\log(i/i_0)$ vs. V_1 plot (for the mixture) will lie above the $\log(i'/i'_0)$ vs. V_1 plot (for the more energetic pure gas) by an amount equal to $\log\left(\frac{i''}{i'_0} + 1\right)$.

The amounts of the displacement 0.67 and 1.4₁, thus calculated for mixtures (○) and (●), agree, within the limits of the experimental error, with the values measured from fig. 10, 0.85 and 1.4₅ respectively.

The last mixtures experimented with were of $SOCl_2$ and S_2Cl_2 . Two sets of experiments were made with these mixtures.

In the first set at the start there was SOCl_2 at $p = 2.0 \times 10^{-5}$ mm, and $i'_0 = 1.43 \times 10^{-10}$ amp. S_2Cl_2 was then added to this up to such a partial pressure p_1 , calculated from the known ratio $i_0/p_1 = \text{constant}$ (for S_2Cl_2), as would make i_0 for the mixture about double the i'_0 for the pure SOCl_2 , on the assumption that the emissions were additive. For this purpose it was necessary to add only a quite small pressure of S_2Cl_2 , about 0.3×10^{-5} mm, so that the total pressure was $p = 2.3 \times 10^{-5}$ mm, and i_0 was found to be 3.5×10^{-10} amp. The observations are indicated by circles on a logarithmic plot in fig. 12, curve II. As soon as these observations were completed a new portion of S_2Cl_2 was added to the previous mixture of gases. This increased

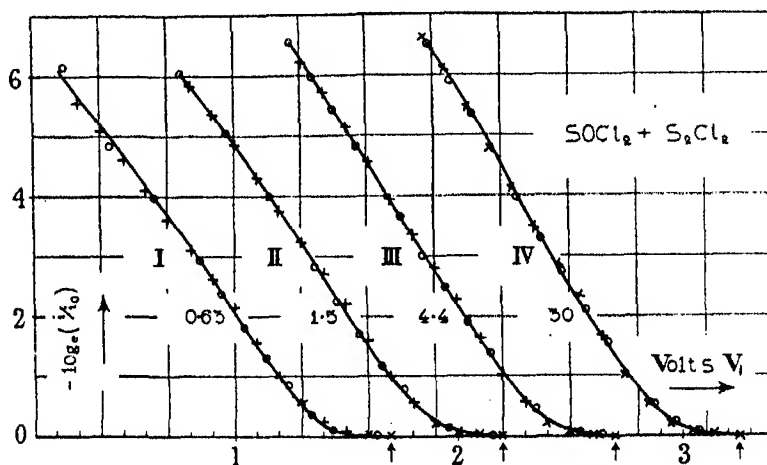


FIG. 12

the total pressure to $p = 3.6 \times 10^{-5}$ mm, and i_0 was found to be 7.7×10^{-10} amp. The observations made on the new mixture are shown as circles in fig. 12, curve III. The contact potential difference for curves II and III was 2.23 and 2.35 volts respectively; in fig. 12 the true zeros are indicated by arrows. Throughout the set of experiments just described T was 50 sec, and dt 30 sec.

In the next set of experiments with these gases the initial pressure of the SOCl_2 was considerably less, being 0.3×10^{-5} mm, and $i'_0 = 4.0 \times 10^{-11}$ amp. A very small amount of S_2Cl_2 was then added so that the total pressure became 0.35×10^{-5} mm, and the total current was found to be 6.5×10^{-11} amp. The observations made with this mixture are shown as circles in fig. 12, curve I. As soon as these observations had been completed a relatively large additional amount of S_2Cl_2 was added, so that the total pressure of $\text{SOCl}_2 +$

S_2Cl_2 became 2.0×10^{-5} mm, and the total current was found to be 12.0×10^{-10} amp. The observations made with this mixture are shown as circles in fig. 12, curve IV. The contact potential difference for curves I and IV was 2.26 and 2.37 volts respectively. Throughout this set of observations, which started with the SOCl_2 at a pressure of 0.3×10^{-5} mm, T was 23 sec, and dt 20 sec.

In fig. 12 the four curves are placed, and numbered, in the order of their increasing ratio i''_0/i'_0 which is equal to 0.63, 1.5, 4.4, and 30 respectively. By means of these values of i''_0/i'_0 and by means of curve (●) for SOCl_2 , and curve (○) for S_2Cl_2 , which are shown in fig. 3, we have calculated the values of i/i_0 for the different mixtures. The calculated data are indicated by crosses on logarithmic plots in fig. 12; it will be seen that the calculated data are in complete agreement with the observed, as the discrepancy does not exceed the limits of the experimental error. This proves again that the chemical electron emission possesses the additive property. It may be noticed that for these calculations exactly the same S_2Cl_2 curve was used as for the mixtures of $\text{COCl}_2 + \text{S}_2\text{Cl}_2$.

§ 4—*The Determination of the True Zero on the Voltage Scale*

This is a matter of very great importance for the correct interpretation of the results of these investigations. The differences in the energy distribution curves and in the $\log(i/i_0)$ vs. V_1 (or σV vs. V_1) plots for the large number of gases which have now been investigated show that the detailed peculiarities of all such curves are essential characteristics of the particular reactions involved and are not due to defects in the method of experimenting or similar secondary factors. For example, for COCl_2 , in the investigation of which so much use has been made of the σV vs. V_1 plots, we must now regard the curved part of the plots to the right of the tangent to the straight part (see, for instance, Part I, figs. 1, 2, or 6) as of equal importance with the rest. This immediately destroys the validity of using the intersection of the tangent with the V_1 axis as a method of determining the zero of the true potential difference V ($= V_1 - K$, K = contact potential difference) on the V_1 scale.

This reduces the number of methods which have hitherto been regarded as available for determining the position of the $V = 0$ point on the V_1 axis from two to one. This is a very serious defect because every determination of the actual energy of the emitted electrons must rest on this zero and the photo-electric method, which is the one remaining, has important limitations in this

application. These have been mentioned in an earlier publication.* It will be convenient at this stage briefly to review the history of this matter as it will enable us to put right some statements and inferences in earlier papers which we now believe to be erroneous or misleading.

We shall start with a quotation from a book published by one† of us in 1921. "If we take the true zero (determined photoelectrically) to lie anywhere within this region we see that, broadly speaking, and disregarding a little abnormality in the neighbourhood of zero volts, the chemical currents are saturated for all accelerating voltages and show a rapid diminution for all retarding voltages." Evidently at that time it was believed that the $V = 0$ point coincided with the point on the V_1 axis at which the currents reached saturation. This is what we now believe and believe to have firmly and finally established as a result of the experiments described in § 3, as we shall show in a moment. However, with the misinterpretation of the tangents to the σV vs. V_1 plots there came into being an independent method of determining the $V = 0$ point as the intersection of these tangents with the V_1 axis. The points thus determined were called "chemical" zeros. For brevity we shall call the other two "photoelectric" and "saturation" zeros. Now the saturation and photoelectric zeros were found, as in 1921, to coincide but to differ from the chemical zero by about 0.7 volt. At least we found (Parts I and II) such a difference between the chemical and saturation zeros for NaK_2 and Richardson and Brotherton (*loc. cit.*) found the same difference, within their limits of error, for seven alloys which differed in composition from NaK_2 . For NaK_2 they found the chemical and photoelectric zeros to coincide. This was held to establish the correctness of the chemical zero. But it is inconsistent with all the other well-established data. An examination of Richardson and Brotherton's paper (*loc. cit.*, Table VII, p. 35) shows that this identification of the chemical and photoelectric zeros rests entirely on the high value, $6.2 \times 10^{14} \text{ sec}^{-1}$, of the photoelectric threshold in presence of COCl_2 of a single specimen of alloy, F.77, of the composition NaK_2 . It is very suspicious that this change in the threshold, as compared with the other alloys, was not accompanied by an equal change in the stopping potential for light of a given frequency. The determination itself contains very doubtful elements. It rests solely on measurements of the photoelectric yield from two mercury lines the relative intensities of which the authors state varied in a manner they did

* Richardson and Brotherton, 'Proc. Roy. Soc.,' A, vol. 115, p. 31 (1927).

† Richardson, "The Emission of Electricity from Hot Bodies," 2nd ed., p. 312, London (1921).

not understand. They themselves admit that it was difficult to make any reliable determinations in the region where this threshold was located. We think that all that those experiments prove with certainty about the photoelectric threshold of this particular alloy is that it was more than 5.4×10^{14} sec⁻¹. We also think that there is no certain evidence that the gap between the chemical and photoelectric zero for this alloy was very different from the values given by the alloys of other composition.

The superposition principle applied to mixtures of gases provides us with an independent method for determining whether the true zero is the chemical zero or the saturation zero. This last does not differ from the photoelectric zero by more than the combined errors of both methods. With gases like SOCl₂ and S₂Cl₂ where the σV vs. V_1 (or $\log(i/i_0)$ vs. V_1) plots are straight lines practically down to the V_1 axis the chemical zero differs little from the saturation zero, probably by not more than the error involved in ascertaining the latter. Now suppose we mix such a gas with a gas like COCl₂, in which the chemical is a long way from the saturation zero, and observe the characteristic curve when the alloy reacts with the mixture. The superposition principle enables us to calculate the characteristic curve of the mixture from those of the individual constituents, but the answer it gives depends entirely on how we make the superposition. If we assume that the $V = 0$ points coincide with the chemical zeros we get one characteristic curve for the mixture, if we assume that they coincide with the saturation zeros we get another. In the preceding section we applied this method to the two different mixtures of COCl₂ and S₂Cl₂, and the method shows unequivocally that the true zeros are the saturation zeros and that the chemical zeros are no unique values on the voltage scale.

It follows, as the converse of this, that *the electron currents originating from chemical action exhibit saturation with true zero applied potential difference.*

It is interesting to note that the contact potential difference determined by this method has a value of the order of -2.5 volts. This is a reasonable magnitude since the active gases have the effect of reducing the work function of platinum. (The photoelectric work function of pure Pt may vary between 4.5 and 6.3 volts depending on the process of outgassing.*)

We regard these experiments as establishing beyond doubt that the curved part of the low energy end (the so-called foot) of the σV vs. V_1 (or $\log(i/i_0)$ vs. V_1) plots in such gases as COCl₂, NOCl, Cl₂, etc., is a real and essential part of

* Cf. Hughes and Du Bridge, "Photoelectric Phenomena," p. 76 (1932).

the energy spectrum of the emitted electrons and not due to some difficulty of uncertain origin in attaining saturation. However, as this is an important question, we should like to mention some other facts which lead to the same conclusion. The strongly individual character of the distributions in this region given by reactions with different gases seems otherwise incomprehensible. The result of the experiment with the mixture of COCl_2 and COS is also very striking in this connection. In spite of the fact that the partial pressure of the COS was more than 10 times the partial pressure of the COCl_2 and that the COS was actually reacting with the alloy, the electron spectrum for COCl_2 was quite unchanged and the shape of the "feet" entirely unaltered. The following considerations also furnish strong evidence that the curved parts of the plots in the low energy region are really determined by the true energy distribution and are thus of equal importance with the rest. If we suppose that the electrons liberated by the chemical action are affected by the fields of force of the individual members, or by the patches, of the reaction products we should expect that the magnitude of this effect will be negligible at a pressure $p \approx 2 \times 10^{-7}$ mm (the lowest pressure at which measurements were made), as compared with that at a pressure $p \approx 10^{-3}$ mm. This follows from the facts that the electron emission at low pressures is proportional to the pressure, and therefore the heterogeneous chemical reaction takes place uniformly over the surface of the alloy, and that at the pressure $p \approx 2 \times 10^{-7}$ mm only one-hundredth part of the surface is covered with the reaction products while at the pressure $p \approx 10^{-3}$ mm the surface of the alloy is covered with a more or less complete layer of the reaction products. The experiments show, however, that there is no noticeable difference in the electron spectrum over this range of pressures. The effect of the reaction products has thus no marked influence on the energy distribution function, and therefore it cannot be responsible for the "feet."

Richardson and Brotherton (*loc. cit.*, p. 37) attempted to justify the difference between the chemical zero and the photoelectric zero by the theory of patches. This attempted justification must now be abandoned. It can, in fact, be shown that their own data do not really support it. They find that on this theory, if D is the difference in volts between the stopping potential with light of a given frequency ν and the chemical zero, then $-D = \frac{h}{e}(\nu - \nu_c)$, where ν_c is the threshold frequency for the clean metal. The mean of six experimental determinations of D made by them for the alloy B.50, for example, is 0.36 volt and the individual values range from 0.31 to 0.44 volt, whereas

their value of $\frac{h}{e}(\nu - \nu_c)$ for this alloy was 0.83 volt. In fact, the theory of patches seems to locate the true zero about where we now find it, instead of at the chemical zero. At the time, Richardson and Brotherton were not inclined to attach much significance to this discrepancy of 0.4 to 0.5 volt in the two methods of determining D . This is perhaps not surprising as their determinations of D had a range of 0.19 volt and those of $\frac{h}{e}\nu_c$ a range of which the lower limit was 0.16 volt and the upper limit unknown. At present the theory of patches hardly seems to be required in connection with chemical electron emission phenomena; but, whatever it may do, it certainly cannot explain the difference between the old chemical zeros, got by drawing tangents to the straight portions of the σV vs. V_1 plots, and the photoelectric and saturation zeros.

§ 5—*The Electronic Spectra and the Mechanism of the Reactions*

As we have stated in the Introduction, the main object of the investigations which we describe in this paper, was to test further the generality of the relation, which exists between the maximum energy E_m of the emitted electrons and the chemical energy E_c , and which is of the form

$$E_m = E_c - \phi, \quad (5)$$

where ϕ is the work function of the sodium-potassium alloy.

For the reactions with the gas molecules containing one halogen atom and a non-reactive radicle, like NOCl, there is only one possible mechanism of dissociation, namely, into the halogen atom and into the radicle, and the electronic spectrum has a structure which can be fairly well expressed in a simple mathematical form. It is, therefore, assumed that the electronic spectrum consists of only one group of electrons which is identified with the above mechanism of dissociation. The maximum energy E_m , determined from the spectrum, can be thus directly compared with the chemical energy E_c , calculated by means of the relation

$$E_c = C - D, \quad (6)$$

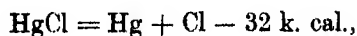
where C is a constant (provided the average collision diameter does not depend markedly upon the gas) for all the reactions which result in the adsorption of a particular negative halogen ion on the surface of the alloy, and D is the energy of dissociation relating to the corresponding reaction mechanism.

When molecules of an active gas contain more than one atom capable of entering into the reaction with the alloy the spectrum of the emitted electrons may contain more than one group of electrons, with different average energies, according to the number of the reaction mechanisms responsible for the observed electronic spectrum. In the latter case the problem therefore consists: (1) in ascertaining the number of the groups of which the observed electronic spectrum is composed; (2) in correlating these groups of electrons with the reaction mechanisms available; and (3) in estimating the relative total number of electrons (*i.e.*, the relative electronic current) of the different groups. As we have seen in § 3, the apparent maximum energy E_m , as measured directly from the i/i_0 vs. V_1 , or $\log(i/i_0)$ vs. V_1 , plots, depends upon the ratio of the individual electronic currents.

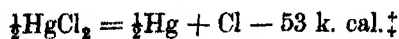
The above problem, stated for a general case, is considerably simplified if the molecules of an active gas contain only two, identical, halogen atoms and a non-reactive radicle. We believe that the gases which are described in this paper belong to this category. The reasons for this are the following: (1) A comparative study of the various data (especially the general form of the function $i_0 = f(p)$) obtained with a large number of different gases leads to the conclusion that the rate of the reaction involving the radicles of these gases is negligible. (2) As we shall show in a moment, for all the radicles in a free state, *i.e.*, S_2 , SO, SO_2 , and Hg, there will be little chance of reacting with the alloy, since the kinetic energy they receive in the moment of their liberation will make them fly off into the surrounding space. (3) It is most unlikely that one of the sulphur, or oxygen, atoms of the molecules S_2Cl_2 , $SOCl_2$, or SO_2Cl_2 will first, or even simultaneously with the chlorine atom, enter into the reaction with the alloy, as such a process is connected with a high energy of dissociation (probably of the order of 100 k. cal.), and also probably requires a small amount of true energy of activation (*cf.* the reaction with N_2O , Part III, p. 47). A similar process involving the Hg atom of the $HgCl_2$ molecule will probably be endothermic, and therefore also unimportant. The only gas which cannot be put in the above category is sulphur dichloride, as its molecules probably contain four halogen atoms; the results obtained with this gas will be considered separately from the others, on account of this and also some other complicating factors.

We can show that the electronic spectra, obtained with the gases belonging to the above category, consist in general of not more than two groups of electrons. These two groups of electrons originate from the one-stage reaction, corresponding to the dissociation process $\frac{1}{2}[(R) + 2(Cl)]$, and from

the first stage of the two-stage reaction, corresponding to the dissociation process $(\text{RCl}) + (\text{Cl})$; the group which originates from the second stage of the two-stage reaction, corresponding to the dissociation process $(\text{R}) + (\text{Cl})$, is immeasurably small. We saw (§ 2, Part III) from some theoretical considerations of the $\log(i/i_0)$ vs. V plots that one of the criteria of an electronic spectrum for which more than one reaction mechanism is responsible is that the graph of $\log(i/i_0)$ against V shall show inflexions. According to this criterion we were able to establish, in accordance with some other experimental facts, that the electronic spectra for Br_2 and I_2 contained, as an admixture, a small group of high average energy electrons; but the observed data were insufficient to establish experimentally whether this high average energy group of electrons comes from the one-stage reaction or from the second stage of the two-stage reaction or from both of them. We pointed out (see Part III, p. 39), however, that we should expect that the atom, or the radicle, which is liberated as a result of the first stage of the two-stage reaction, will have little chance of reacting with the metal drop, as the kinetic energy, which it receives during its liberation from the first atom, will make it in general fly off into the surrounding space. A beautiful example of separation of two groups of electrons with widely different average energies, with which the reaction with HgCl_2 presents us (see fig. 7), allows us to prove that the small admixture of high average energy electrons, which is present in the HgCl_2 spectrum, originates from the one-stage reaction. This result therefore confirms the conclusion that the rate of the second stage of the two-stage reaction is in general too small to be observed experimentally. In fact, according to the spectroscopic data of Sponer*



and according to the thermochemical data†



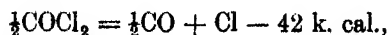
A comparison of the second, high average energy, distribution in the electronic spectrum of HgCl_2 (see fig. 7) with the electronic spectrum of COCl_2 (the part of this spectrum, from $V = 0$ to $V = 1.3$ volts, is drawn as a dotted line in fig. 7) shows that the former has a lower average energy of electrons (*cf.* § 2,

* 'Z. phys. Chem.,' B, vol. 11, p. 425 (1931).

† Braune and Knoke, 'Z. phys. Chem.,' A, vol. 152, p. 409 (1931).

‡ Throughout this paper all chemical symbols refer to the gaseous state except where otherwise indicated.

Part III), therefore it must correspond to a higher dissociation energy. As the dissociation energy, corresponding to the COCl_2 spectrum, is



this proves that the high average energy admixture in the HgCl_2 spectrum does come from the one-stage reaction.

Whenever an electronic spectrum consists of two resolved groups of electrons these groups can be easily identified with the corresponding reaction mechanisms, and the ratio of the individual electronic currents can be approximately estimated directly from the $\log(i/i_0)$ vs. V_1 plots. It is evident that we cannot adopt this procedure when the electronic spectrum consists of two unresolved groups of electrons. Such a spectrum will be always observed when the individual electronic current, originating from the group with the lower average energy electrons, is less than, or of the same order of magnitude as, the individual electronic current originating from the group with the higher average energy electrons. It follows from the considerations of electronic spectra given in § 2, Part III, that the extreme high energy part of such a spectrum will practically represent the distribution of only one group, namely, that corresponding to the higher average energy electrons. For such spectra the ratio of the individual electronic currents of the two groups can be approximately estimated from the amount of the displacement, along the $\log(i/i_0)$ axis, of the higher average energy distribution, as is shown in § 3, equation (4). For this it is necessary to know, however, the whole of the logarithmic plot of the high average energy group down to the value $V = 0$; the question then involves finding a gas which gives a spectrum consisting of one group of electrons having a similar average energy, but to find such a gas is not always possible. To avoid this difficulty we can apply an indirect method of estimating the ratio of the individual electronic currents, which is based on the observation of the electronic yield. We shall show, when we come to a detailed consideration of the experimental results, that there exists a simple relation, experimentally established, between the chemical energy E_c and the yield c of electrons, calculated per *one halogen atom which entered* into the reaction with the alloy and liberated the chemical energy E_c . We shall call the yield c , which is composed of the electrons all belonging to the same group, the "specific" yield, and denote by Y the composite yield, also calculated per one halogen atom entering into the reaction, which is composed of the electrons originating from both the groups. Since the specific yield c is composed of the electrons

all belonging to one group, it is independent of the reaction mechanism* and it is a function of the chemical energy E_c only, that is

$$c = F(E_c). \quad (7)$$

We can derive a relation between c , Y and the ratio of the individual electronic currents by means of which the latter quantity can be calculated, if c and Y are known.

Let us consider a gas the molecules of which contain, as before, two halogen atoms and a non-reactive radicle. Let N be the total number of halogen atoms entering into the reaction with the alloy in unit time and let N_1 and N_2 be the number of halogen atoms entering, in unit time, into the one-stage and into the two-stage reactions respectively. If c_1 and c_2 are the specific yields, and i_1 and i_2 are the electronic currents, referring to the one-stage and to the two-stage reactions respectively we can write, according to the definition, $c_1 = i_1/N_1$ and $c_2 = i_2/N_2$; now, $N_1 = \alpha N$ and $N_2 = (1 - \alpha) N$, where $\alpha < 1$ is a constant for a given gas. The total electronic current i may be represented in the form

$$i = i_1 + i_2 = c_1 \alpha N + c_2 (1 - \alpha) N. \quad (8)$$

The composite electronic yield Y , calculated per one halogen atom entering into one of the two types of the reaction with the alloy, will then be

$$Y = i/N = c_1 \alpha + c_2 (1 - \alpha). \quad (9)$$

In the study of the kinetics of gas reactions it is customary to deal with reaction rates, that is, with the number of molecules of a gas which enter into a certain reaction in unit time. We may introduce, instead of the coefficient α , the ratio R of the rates of the two reactions. Taking into account the fact that when the gas molecule enters into the two-stage reaction the second halogen atom of the molecule does not enter into the reaction with the alloy at all but flies off into the surrounding space, we can write

$$R = \frac{\text{rate of two-stage reaction}}{\text{rate of one-stage reaction}} = \frac{2(1 - \alpha)}{\alpha}. \quad (10)$$

By means of equations (8), (9), and (10) we can finally obtain the following relations between Y , R , i_2/i_1 , and c_2/c_1 :

$$R = \frac{2(c_1 - Y)}{(Y - c_2)}, \quad (11)$$

* This statement requires some additional qualification. We intend to return to it in a later paper.

$$Y = \frac{c_1}{\frac{1}{2}R + 1} + c_2 \frac{R}{R + 2} \quad (12)$$

$$\frac{i_2}{i_1} = \frac{1}{2} \cdot \frac{c_2}{c_1} \cdot R = \frac{c_2}{c_1} \cdot \frac{(c_1 - Y)}{(Y - c_2)}. \quad (13)$$

To calculate the ratio i_2/i_1 of the individual electronic currents by means of relation (13) we must know the composite electronic yield Y . This quantity cannot be directly calculated from the measurements of the total electronic current and the pressure of the gas, as might at first sight appear. To calculate Y we require to know, besides the total electronic current, not the number n of the gas molecules striking the surface of the alloy in unit time, which is proportional to the pressure and the coefficient of proportionality depends upon the molecular weight of the gas only, but the number N of the halogen atoms which *actually enter* into the reaction with the alloy. The latter number N may not be proportional to n , as it may occur that not every collision of the gas molecules with the alloy is effective and this may depend upon the nature of the gas molecules. There exists, however, one convenient method of estimating the quantity Y , which is independent of the absolute values of the pressures of the different gases, and thus it is free from the uncertainty which is introduced in our Pirani gauge method of absolute measurements of pressure. In fact, the method is based on the measurement of the maximum value of the total saturation current i_0 obtained from the relation $i_0 = f(p)$. As we know, for all the gases containing chlorine the function $f(p)$ has a sharp maximum at a certain pressure p_0 , and we showed (see Part I, p. 46) that this maximum value of i_0 corresponds to the condition when the surface of the alloy becomes covered with a more or less complete layer of reaction products. Therefore, for all those reactions for which we have reason to believe that they result in the formation of the same reaction products the values of $(i_0)_{\max.}$, obtained with the different gases, will be proportional to Y , provided the time of drop T and the time of exposure dt remain approximately constant. If for some gases the functions $f(p)$ were by chance obtained at different T it is not difficult to introduce a correction for this, as soon as we have a set of the functions $f(p)$, corresponding to different T , obtained for one and the same gas. To obtain the absolute values of Y it is sufficient to calculate this value for one of the gases. It is convenient to choose NOCl for this purpose, as the molecules of this gas contain only one halogen atom. Assuming that each molecule of this gas, striking the surface of the alloy drop, enters into the reaction with the alloy, and taking for the average value of the surface of the alloy drop about

0.3 cm², we obtain the following approximate absolute value of Y, which gives the number of electrons emitted per one adsorbed Cl⁻ ion,

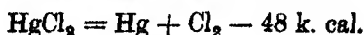
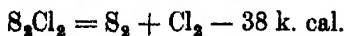
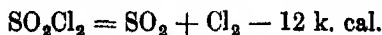
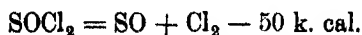
$$Y \approx 1.0 \times 10^{-3} \frac{\text{amp}}{\text{mm}} \approx 1.0 \times 10^{-4} \frac{\text{electrons}}{\text{ad. Cl}^- \text{ ions}} .$$

The values of Y for the other gases we shall thus compare with this value of Y for NOCl.

One accidental circumstance which makes the interpretation of the electronic spectra of the gases under consideration difficult is that there are no spectroscopic, or any other, data available with regard to the energy of dissociation of the first, or the second, halogen atom of the molecules SOCl₂, SO₂Cl₂, S₂Cl₂, and sulphur dichloride. The only data available are thermochemical data relating to the dissociation process Cl₂ + Radicle, and, in particular, for sulphur dichloride even these data are absent.

The way of overcoming the difficulties arising from the absence of the spectroscopic data is to compare the electronic spectra of these gases with the electronic spectra of those gases for which all the data, relating to the different dissociation processes, are available. For the gases which give an electronic spectrum consisting of resolved groups of electrons, such a comparison of the electronic spectra, coupled with the thermochemical data, allows us to estimate approximately the chemical energy E_c, corresponding to the two-stage reaction, and therefore allows us to test the fundamental equation (5). On the other hand, when the electronic spectrum consists of unresolved groups of electrons the chemical energy E_c, available in the two-stage reaction, can be approximately estimated by means of the relation $c = F(E_c)$. For this it is necessary to know the ratio c_2/c_1 which can be calculated from (13). The quantity Y is obtained from the relation $i_0 = f(p)$ and the ratio i_2/i_1 can be approximately estimated (when it is possible) by the method of displacement, from equation (4).

The accuracy of the estimation of E_c greatly depends upon the accuracy of the thermochemical data. Unless other references are given the thermochemical data tabulated below are taken from Landolt-Börnstein, 'Physikalisch-Chemische Tabellen,' 1924-1931 :



These data refer to room temperature and probably have to be regarded as uncertain to within several units of k. cal., and especially, the value 50 k. cal. relating to SOCl_2 . This value is not obtained from a pure thermochemical equation, as there are no thermochemical data relating to the heat of formation of SO. The above value was obtained by means of the following spectroscopic data :

$$\text{S}_2 = \text{S} + \text{S} - 102.5 \text{ k. cal.}$$

$$\text{O}_2 = \text{O} + \text{O} - 117.4 \text{ k. cal.}$$

$$\text{SO} = \text{S} + \text{O} - 116.2 \text{ k. cal.}$$

The value of the dissociation energy of SO equal to 116.2 k. cal., which has been recently obtained by Martin,* differs greatly from the value 148 k. cal., given by Henri† ; such a great discrepancy finds its explanation in the fact that spectroscopic determinations of dissociation energies, though being usually very accurate, are only correct subject to a correct general interpretation of the band spectrum of the corresponding molecule. It seems to be generally accepted now that the value 148 k. cal. is incorrect, as it is greater than the heat of dissociation of the oxygen molecule.

We shall reserve the discussion of the results obtained with the sulphur dichloride gas until all of the available data on the chlorine compounds shall have been considered. The absence of the thermochemical data about the heat of formation of the sulphur dichloride molecule, and also some other complicating factors, make it impossible to give an interpretation, of the data obtained with this gas, which is not subject to a considerable uncertainty.

A general inspection of the electronic spectra of the gases SOCl_2 , S_2Cl_2 , SO_2Cl_2 , and HgCl_2 , as given by the $\log(i/i_0)$ vs. V_1 plots and represented by figs. 4, 6, and 7, leads us to the conclusion that all these spectra, except that for SO_2Cl_2 which requires a further examination, are composed of two groups of electrons with different average energies, since the logarithmic plots show an inflexion characteristic for such composite spectra.

HgCl_2 gives a most instructive example of a composite electronic spectrum. Because of the great difference of the average energies of the electrons of the two groups, and of a comparatively large ratio i_2/i_1 of the individual currents, there is practically no interference between them, except near the point of intersection. The higher average energy group of electrons of this spectrum, which corresponds to the dissociation energy 53 k. cal., has a distribution

* 'Phys. Rev.', vol. 41, p. 167 (1932).

† Cf. 'Leipziger Vorträge,' p. 147 (1931).

which shows some resemblance to that of the main group of the S_2Cl_2 spectrum. We may assume that the main group of the $HgCl_2$ spectrum at higher energies continues the trend of the straight line, which is obtained at lower energies; then, by adding a suitable proportion of the S_2Cl_2 distribution we can obtain a composite curve. This curve is indicated by a dotted line on the right of fig. 7. It represents well the main features of the observed curve for $HgCl_2$ and gives a ratio i_2/i_1 , of the electronic currents of the two groups of the $HgCl_2$ spectrum, equal to about 20. Because of the low saturation pressure, at room temperatures, of the $HgCl_2$ crystals it was impossible to obtain the relation $i_0 = f(p)$, and thus, to measure the value $(i_0)_{max}$. We are able to give only a lower limit for the value of the composite electronic yield, it is $Y \geq 0.01 \times 10^{-5}$ electrons per adsorbed Cl^- ion.

The $\log(i/i_0)$ vs. V_1 plot for S_2Cl_2 , shown in fig. 4, has a very unsharp inflexion at the top end of the curve; this shows that the spectrum is composed of one very large group of electrons and of one very small group of high average energy electrons (*cf.* the spectrum for I_2 given in fig. 6, Part III). The calculation of the above composite curve for $HgCl_2$ has revealed that the main group of the S_2Cl_2 spectrum corresponds to a somewhat higher dissociation energy than 53 k. cal., we can therefore ascribe it to about 58 k. cal. A similar conclusion can also be derived from a comparison of the i/i_0 vs. V_1 plot for S_2Cl_2 , fig. 3, with those for $COCl_2$, fig. 11, and $HgCl_2$, fig. 5. It will be seen that the curve for S_2Cl_2 differs greatly from the curve for $COCl_2$, corresponding to $D = 42$ k. cal., and is nearer, in respect to its resemblance, the $HgCl_2$ curve, corresponding to $D = 74$ k. cal. It is rather difficult in this case to estimate accurately the ratio i_2/i_1 , as there is no suitable spectrum (corresponding to a dissociation energy of about 48 k. cal.) available for comparison. An approximate estimation, by the same method as that used for $HgCl_2$, gives a value of i_2/i_1 of the order of 20. The electronic yield Y for this gas, as estimated from the $i_0 = f(p)$ relation, is $Y \approx 0.45 \times 10^{-5}$.

An examination of the electronic spectrum for $SOCl_2$, fig. 4, shows that the spectrum contains quite a large group of the higher average energy electrons, since the point of inflexion is in the middle of the curve and the general form of the plot in the region of low energies does not differ much from that in the region of high energies. The stronger group can but originate from the one-stage reaction corresponding to $D = 54$ k. cal.; in fact, it shows a great resemblance with the second group of the $HgCl_2$ spectrum, corresponding to $D = 53$ k. cal. The i/i_0 vs. V_1 plot for $SOCl_2$, fig. 3, is very like that for S_2Cl_2 , but this indicates that the dissociation energy, corresponding to the weaker

group of the SOCl_2 spectrum, must be appreciably larger than $D = 58$, since there is a considerable interference between the two groups of the SOCl_2 spectrum. This conclusion is also confirmed by the low value of the yield observed with this gas; it is $Y \approx 0.1 \times 10^{-5}$, i.e., about one-fourth of the value observed with S_2Cl_2 . We can obtain some further information about this unknown value of D by considering the magnitude of the ratio i_2/i_1 of the electronic currents. On the one hand, the ratio i_2/i_1 cannot be much less than 1, since the logarithmic plot has a noticeable inflexion; on the other hand, it cannot be much larger than 1, since the amount of the displacement of the high energy part of the logarithmic plot for HgCl_2 , relative to that for SOCl_2 , approximately corresponds to the value of $i_2/i_1 = 20$ obtained previously for HgCl_2 . Therefore, the ratio i_2/i_1 for SOCl_2 must be of the order of 1. To obtain by calculation, using this value of i_2/i_1 , a characteristic curve similar to that observed for SOCl_2 , fig. 3, it is necessary that the unknown value of D must be considerably less than 74 k. cal., referring to the characteristic curve of HgCl_2 ; it must be, in fact, about 65 k. cal.

As we have already mentioned, the SO_2Cl_2 spectrum requires a special examination, since the logarithmic plot, fig. 6, shows that this electronic spectrum consists either of two unresolved groups or of only one group. Very fortunately the value of the dissociation energy referring to the one-stage reaction with this gas, equal to 35 k. cal., nearly coincides with the value 38 k. cal. corresponding to the reaction with NOCl . The high energy part of the NOCl spectrum is drawn in fig. 6 and its point of zero is made to coincide with the point of zero for curve (O) obtained with the SO_2Cl_2 . The high energy part of the SO_2Cl_2 spectrum does show a great resemblance with the NOCl spectrum, and furthermore, the comparison proves that the SO_2Cl_2 spectrum contains a considerable group of lower average energy electrons, since there is a considerable displacement between the logarithmic plots. The ratio i_2/i_1 of the individual currents, as determined from equation (4), is about 3. As the logarithmic plot for this gas has no inflexion, in spite of this high value of the ratio, it shows that the dissociation energy corresponding to the weaker group is not much higher than 35 k. cal. In fact, the characteristic curve for this gas, fig. 5, which under such conditions is little affected by the slightly stronger group, is only just a little steeper than that for COCl_2 , fig. 11. The dissociation energy of the weaker group of the SO_2Cl_2 spectrum must be therefore about 45 k. cal. We can show that this value coincides with that which can be calculated from relation (13) which is based on the measurements of the yield of electrons.

To show this it is necessary to obtain a relation between the specific yield c and the chemical energy E_c . In Tables III and IV we have summed up the results of our examination of the electronic spectra of the gases dealt with in

Table III

Gas	Mechanism of dissociation	Dissociation energy D in k. cal.	Chemical energy E_c in k. cal.	Specific yield $c \times 10^4$	Composite yield $Y \times 10^4$
S_2Cl_2	$S_2Cl + Cl$	58	105	0.45	0.45
	$\frac{1}{2}[S_2 + 2Cl]$	48	115	2.3	
	$S_2 + Cl$	38	—	—	
$SOCl_2$	$SOCl + Cl$	65	98	0.05	0.10
	$\frac{1}{2}[SO + 2Cl]$	54	109	0.87	
	$SO + Cl$	43	—	—	
$HgCl_2$	$HgCl + Cl$	74	89	0.013	≥ 0.01
	$\frac{1}{2}[Hg + 2Cl]$	53	110	1.1	
	$Hg + Cl$	32	—	—	
SO_2Cl_2	$SO_2Cl + Cl$	45	118	3.8	5.0
	$\frac{1}{2}[SO_2 + 2Cl]$	35	128	15	
	$SO_2 + Cl$	25	—	—	
$COCl_2$	$COCl + Cl$	80	83	0.002	2.5
	$\frac{1}{2}[CO + 2Cl]$	42	121	5.8	
	$CO + Cl$	4	—	—	
Cl_2	$Cl + Cl$	58	105	0.43	12
	$\frac{1}{2}[Cl + Cl]$	29	134	31	
	Cl	0	—	—	
$NOCl$	$NO + Cl$	38	125	10	10

Table IV

Gas	Ratio c_1/c_2 of specific yields	Ratio i_1/i_2 of currents	Ratio R of rates of 2-stage reaction / 1-stage reaction
S_2Cl_2	5.1	ca. 20 (observed)	200 (calculated from (13))
$SOCl_2$	8.7	ca. 1 (observed)	20 (calculated from (13))
$HgCl_2$	85	20 (observed)	3000 (calculated from (13))
SO_2Cl_2	4.0	3 (observed)	20 (calculated from (13) or (11))
$COCl_2$	2900	0.0006 (calculated from (13))	3 (calculated from (11))
Cl_2	72	0.02 (calculated from (13))	3 (calculated from (11))

this paper, and also of $COCl_2$, Cl_2 , and $NOCl$ which were examined in Parts II and III. It will be seen from Table III, column 3, that for all the gases whose molecules contain two atoms of chlorine the chemical energy E_c liberated in

the one-stage reaction is always larger than that liberated in the first stage of the two-stage reaction, therefore the ratio c_1/c_2 is always > 1 . It is $\gg 1$ if the chemical energies of these two reactions are markedly different, since the yield c is a very sensitive function of E_c . Now, equation (13) shows that when the ratio $i_2/i_1 > 1$ and $c_1/c_2 \gg 1$, then the ratio $R \gg 1$ and the composite yield Y , according to (12), is then equal to $(1 + i_1/i_2) c_2$, if we regard $2/R$ as negligible. It is therefore approximately equal to c_2 when i_1/i_2 is small. The gases S_2Cl_2 and $SOCl_2$, thus, give us two values of the function $F(E_c)$ defined on p. 549, corresponding to $E_c \approx 105$ and $E_c \approx 98$ k. cal. A third value, corresponding to $E_c = 125$ k. cal., we can obtain from $NOCl$; in this case $Y = c$, since the electronic spectrum has only one group of electrons. These three values of $F(E_c)$ are indicated by circles in fig. 13 which represents a graph of $\log_{10} c$ against $1/E_c$. The points fall on a straight line

$$-\log_{10} c \approx 903.4 \times \frac{1}{E_c} - 3.222. \quad (14)$$

As a matter of fact, we can obtain a fourth value of $F(E_c)$ and thus furnish some more experimental evidence for equation (14). We have seen that the dissociation energy of the one-stage reaction with SO_2Cl_2 is nearly the same as for $NOCl$, therefore we can put c for SO_2Cl_2 about 10×10^{-5} , i.e., the same as for $NOCl$. From the observed values of i_2/i_1 and Y , and this value of c_1 , we obtain, by means of equation (13), $c_2 \approx 4.3 \times 10^{-5}$ and, by means of equation (14), $E_c \approx 118.5$ or $D \approx 44.5$ k. cal. The latter value compares with the 45 k. cal. which we have just estimated directly by comparison of the characteristic curves for SO_2Cl_2 and $COCl_2$. The value of $F(E_c) \approx 4.0 \times 10^{-5}$ corresponding to $D \approx 45$ k. cal. is indicated by a double circle in fig. 13. Again, the relation seems to give the right order of magnitude for the yield Y observed with $HgCl_2$; the calculated value 0.013×10^{-5} compares with the observed value $\geq 0.01 \times 10^{-5}$.

We think, thus, that there is sufficient experimental evidence that in this range of E_c , from about 90 to about 130 k. cal., the function $F(E_c)$ is really near the form given by (14) which can also be written as

$$c \approx 1.67 \times 10^3 \times e^{-\frac{2080}{E_c}} \frac{\text{electrons}}{\text{ad. Cl}^- \text{ ions}}. \quad (15)$$

The theoretical interpretation of this equation will be dealt with in a later paper.

In Table III, column 5, we give the values of the specific yield c , partly observed and partly calculated from (14), referring to the different reaction

mechanisms and the different gases. By means of these data we were able to calculate the order of magnitude of the ratio R of the rate of the two-stage reaction to the rate of the one-stage reaction. The latter is given in Table IV, column 4; the calculated data reveal some new interesting facts and explain many puzzling features observed with some gases. It appears that in general the ratio $R > 1$, i.e., only one of the two Cl atoms of the gas molecule normally enters into the reaction with the alloy. Though, for the diatomic gas chlorine the chance of the above event is only slightly higher than the chance of the two Cl atoms, of the chlorine molecule, simultaneously entering into the reaction with the alloy. It is interesting to compare this value of R for chlorine

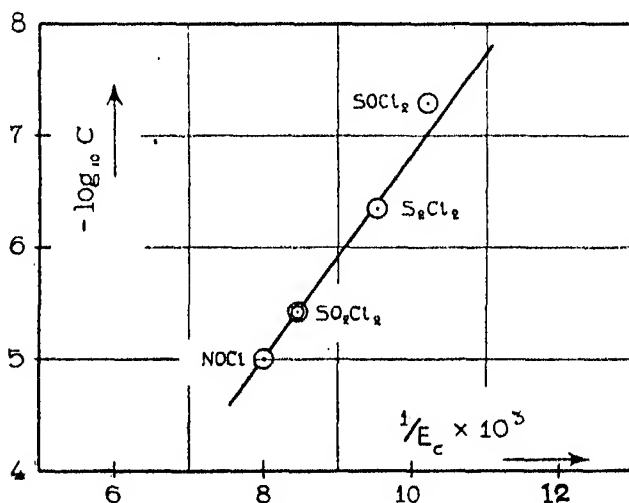
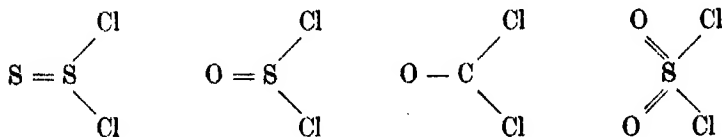


FIG. 13

with those for bromine and iodine. We saw in Part III, fig. 6, that the electronic spectra for Br₂ and I₂ consist of one large group of the lower average energy electrons, and of a very small admixture of the higher average energy electrons. Assuming that the ratio i_2/i_1 is of the order of 20, the ratio R , as calculated from (13), is then of the order of 500, i.e., about 100 times as large as that for chlorine. The value is subject to a considerable uncertainty, but is probably of the right order of magnitude. The estimation is based on the relation $c = F(E_c)$ obtained with the chlorine compounds only and the absolute values of E_c , for the different halogens, are uncertain within ± 10 k. cal. (this latter circumstance cannot affect the estimated value very seriously, however, as we are only concerned with the ratio c_1/c_2 of the electronic yields). We notice that HgCl₂ has an abnormally high value of R , as compared with

the majority of the gases. This can be easily explained by the fact that the HgCl_2 molecule has, in contrast with the others, a linear shape with the widely separated (4.56×10^{-8} cm) Cl atoms.* The shapes of the other molecules are very similar to each other†



The shapes of these molecules were deduced from Raman frequencies, and it seems the correctness of the interpretation of the Raman spectra of these compounds is generally accepted with the exception of S_2Cl_2 . The structure of this compound may be that shown above or $\text{Cl}-\text{S}-\text{S}-\text{Cl}$.‡ It may be noted that the ratio R observed with S_2Cl_2 has a higher value as compared, for example, with that for SOCl_2 . The value for S_2Cl_2 is probably one of the most uncertain, owing to the difficulty of an accurate estimation of i_2/i_1 for this gas. Still, it is hardly probable that it can be much less than 100, as it is the upper limit of i_2/i_1 which is rather uncertain. This seems to indicate somewhat larger average separation of the Cl atoms of these molecules.

On the basis of the yield measurements we were able to calculate, by means of equation (13), the ratio i_2/i_1 of the electronic currents for COCl_2 and Cl_2 . The calculated values (see Table IV, column 3), in conjunction with the values of R , explain at once why the electronic spectra of these gases contain practically one group of electrons. In Part II, p. 72, we suggested that the predominance of the one group of electrons in the COCl_2 spectrum indicates that two Cl atoms of the COCl_2 molecule normally enter into the reaction with the metal simultaneously; accordingly that conclusion must now be modified. We can also understand now why the yield from COCl_2 was so small, as compared with the yield from NOCl , contrary to the comparatively small change in the general form of the electronic spectra, and in the chemical energy E_c , of these two gases. The calculated data also explain why the yield from Cl_2 appears not to be high enough.

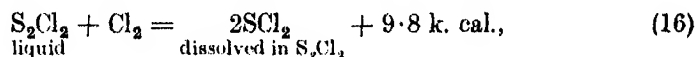
We come now to a brief consideration of the results obtained with sulphur dichloride. A remarkable fact observed with this gas is that its electronic

* Braune and Knoke, 'Z. phys. Chem.,' B, vol. 23, p. 163 (1933).

† Cf. 'Leipziger Vorträge,' 1931, pp. 23 and 131; Lorenz and Samuel, 'Z. phys. Chem.,' B, vol. 14, p. 219 (1931).

‡ Cf. Hibben, 'Chem. Rev.,' vol. 13, p. 345 (1933).

spectrum is practically identical with the SO_2Cl_2 spectrum. It can be seen from fig. 9 that the logarithmic plot for SO_2Cl_2 , which is a repetition of the curve (○) of fig. 6, with the experimental points indicated by crosses is very well superimposed on the dotted curve for sulphur dichloride, experimental points indicated by dots, which is a repetition of the curve (●) for sulphur dichloride arbitrarily shifted to the right from $V_1 = 0$ by 1.4 volts. The results are still more remarkable as not only the energy distributions but also the functions $i_0 = f(p)$ are identical for these gases (see fig. 2). The identity of the electronic spectra, and of the yields, suggests strongly that the dissociation energies of the processes $\text{R} + \text{Cl}_2$, and $\text{RCl} + \text{Cl}$, referring to the sulphur dichloride, must be about the same as for the SO_2Cl_2 gas, i.e., about 12 and 45 k. cal. respectively. Now, it was shown by Trautz* that



and we can therefore take for the energy of dissociation of the process $2\text{SCl}_2 = \text{S}_2\text{Cl}_2 + \text{Cl}_2$ a value of the order of 10 k. cal.† Our results can be at once accounted for if we assume that at very low pressures and at room temperatures there is a comparatively large number of the sulphur dichloride molecules in the dimerous form $(\text{SCl}_2)_2$, since then $(\text{SCl}_2)_2 = \text{S}_2\text{Cl}_2 + \text{Cl}_2 - 12$ k. cal., if $(\text{SCl}_2)_2 = 2\text{SCl}_2 - \text{ca. } 2$ k. cal. Trautz observed that at temperatures about 100–200° C and at atmospheric pressures the number of the $(\text{SCl}_2)_2$ molecules was not appreciable in comparison with the number of the SCl_2 molecules. This cannot be considered, however, as evidence against the existence of the sulphur dichloride molecules in the dimerous form under our conditions. It is important that the decomposition of the dimer into the monomer should be, at least slightly, endothermic‡; it is then quite probable that at room temperatures the decomposition of the $(\text{SCl}_2)_2$ is a bimolecular reaction (that is, the dissociation occurs chiefly by means of collisions), and therefore the rate of this reaction will be negligibly small at pressures of the order of 10^{-5} mm. On the other hand, the rate of recombination of the SCl_2 molecules may be comparatively very large at such pressures, as the reaction of recombination may proceed as a heterogeneous reaction on the glass walls. To account for our results it is sufficient to assume that the number of the $(\text{SCl}_2)_2$ molecules is approximately of the same order of magnitude as the

* 'Z. Elektrochem.', vol. 35, p. 110 (1929).

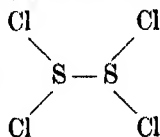
† Cf. also Trautz, *ibid.*, p. 133.

‡ Cf. Trautz, *loc. cit.*

number of the SCl_2 molecules, since the effect of the latter group is negligibly small. In fact, it is easy to show on the ground of the above thermochemical data that the dissociation energy of the process $\text{SCl}_2 = \text{S} + \text{Cl}_2$ is as large as about 75 k. cal.

Among the complicating factors which increase the uncertainty of the interpretation is that the liquid sulphur dichloride at room temperatures seems to be dissociated to a measurable extent into sulphur chloride and chlorine.* The effect from the small amount of the S_2Cl_2 , as having a low yield Y , will be hardly noticeable (this is also definitely confirmed by the observed data), but the small amount of the Cl_2 , as having a large Y , may seriously affect the distribution (the observed data seem to show a slight dependence of the distribution upon the pressure; this is probably due to the free chlorine), though not to such extent as to change considerably its low energy part which is important for our general interpretation of the phenomena.

Finally, it may be noted that the structure of the $(\text{SCl}_2)_2$ molecule is probably

very similar to that of the SO_2Cl_2 molecule, *i.e.*, it is , and this

fact may explain the close values of the ratio i_2/i_1 , and therefore of the yield Y , for these gases. Probably a comparatively large separation of the two pairs of halogen atoms may also explain why only two groups of electrons can be found in the electronic spectrum.

As we have now the necessary data about the dissociation energy D and the ratio i_2/i_1 of the individual currents we can test the fundamental equation (5). It is convenient to combine (5) and (6) into one equation and to write it in the form

$$E_m + D = \text{constant.} \quad (17)$$

The apparent maximum energy E_m is given in Table V, column 2; it was determined directly from the i/i_0 vs. V_1 plots and by using exactly the same method as that employed in Parts II and III. The true maximum energy E_m is given in column 3. For S_2Cl_2 and HgCl_2 , as having large values of i_2/i_1 , the true E_m refers to the weaker group; by assuming that the distribution of the main group continues the trend of the straight line obtained at lower energies the maximum energy of this group was determined from the logarithmic plots by the same method. For SOCl_2 and SO_2Cl_2 , as having small values

* Lowry and Jessop, 'J. Chem. Soc.', p. 1421 (1929).

of i_2/i_1 , the true E_m refers to the stronger group, and it was obtained from the apparent E_m by introducing a correction for the displacement of the distribution of the stronger group. The corresponding dissociation energies are given in columns 4 and 5. By choosing the above groups of electrons for the determination of the true E_m we reduce, at the same time, the uncertainty of the values of D to a minimum, since all these values, except 58 k. cal., are taken from the tables of physical and chemical constants.

Table V

Gas	E_m (apparent) in volts	E_m (true) in volts	D in k. cal.	D in volts	$E_m + D$ in volts
S_2Cl_2	1.5 ₄	1.5 ₀	58	2.5 ₂	4.0 ₂
$HgCl_2$	1.1 ₀	0.7 ₆	74	3.2 ₄	3.9 ₇
$SOCl_2$	1.8 ₀	1.9 ₀	54	2.3 ₆	4.2 ₆
SO_2Cl_2	2.4 ₀	2.6 ₃	35	1.5 ₃	4.1 ₅

It will be seen from column 6 that $E_m + D$ is really a constant, within the limits of the experimental error and uncertainty of the thermochemical data, and, moreover, it compares with an average, more accurately determined, of 4.2₂ volts obtained with $NOCl$, $COCl_2$, and Cl_2 (see Part III, p. 42). This proves that the maximum energy E_m of the emitted electrons is in satisfactory agreement with the fundamental equation $E_m = E_c - \phi$ over a wide range of values of E_m from about 3.0 volts to about 0.7 volt.

§ 6—The Energy Distribution Functions

The energy distribution functions for the gases investigated are shown in figs. 14 and 15. The ordinates $\Delta (i/i_0)$ of these curves are proportional to the fraction of the total number of electrons which have kinetic energies within the range eV to $e(V + \Delta V)$, ΔV being taken equal to 0.1 volt. The curve for S_2Cl_4 is displaced vertically upwards by the arbitrary amount, 0.1 unit, and the curves for $SOCl_2$ and $HgCl_2$ are displaced along the volt axis to the right from $V = 0$ by 1.6 and 3.4 volts respectively. For $HgCl_2$ the vertical scale reading on the figure should be multiplied by 2. The true zeros of the curves are indicated by arrows, and the experimental points of all the curves are marked in the same way as the corresponding data in figs. 3, 5, and 8 from which they are derived.

It will be seen that the curves for SO_2Cl_2 , S_2Cl_4 , and $SOCl_2$ show a second slightly resolved maximum, just after the main one. This is in accordance with the results of our analysis of the logarithmic plots of these gases that

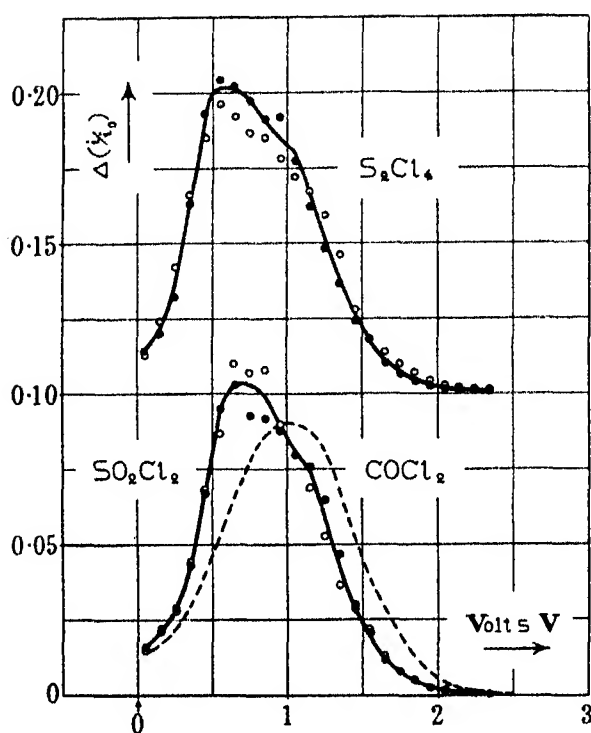


FIG. 14

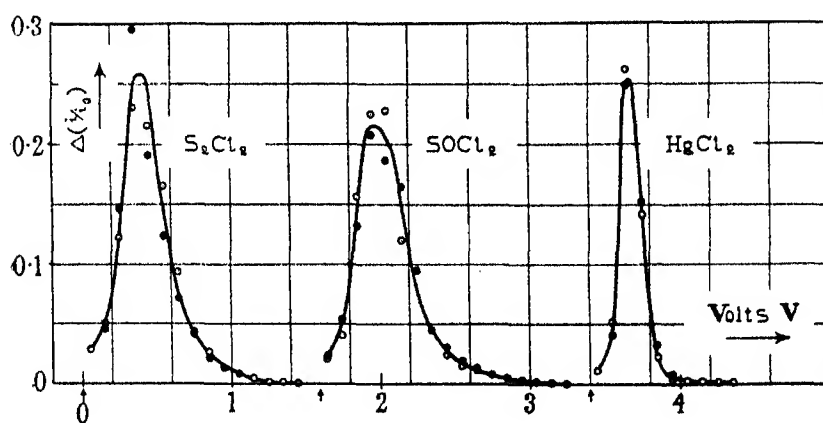


FIG. 15

their electronic spectra consist of two nearly equal groups of electrons with different average energies. The composite character of these curves is especially noticeable if they are compared with the electronic spectra of similar average energy but containing one group only. This can be seen, for example, from fig. 14, where the SO_2Cl_2 curve is compared with the COCl_2 curve indicated by a dotted line. It may be noted that the curves are not very suitable for a detailed analysis with the object of detecting different groups of electrons, first, because they have been obtained by graphical differentiation of the smooth characteristic curves and second, because the process of differentiation usually magnifies any errors in the original observations.

As with the gases described in Parts II and III, the energy distribution function for S_2Cl_2 , which contains practically one group of electrons, can be approximately represented for energies $> V_m$ and $< E_m$ by the equation

$$N(V) = Ae^{-k(V - V_m)^c}, \quad (18)$$

where V_m , the energy corresponding to the maximum of the curve, is equal to 0.41 volt and the values of the constants A , k and c are $A = 10^{-0.65}$, $k = 2.30 \times 2.2_0 = 5.0_6$ volt $^{-1}$ and $c \approx 1$.

In concluding we should like to take this opportunity of acknowledging our indebtedness to the Department of Scientific and Industrial Research for a grant which has made it possible to carry out these investigations.

Summary

The electron emission from NaK_2 when acted on by SOCl_2 , S_2Cl_2 , SO_2Cl_2 , HgCl_2 , and $(\text{SCl}_2)_2$, at very low pressures, has been investigated and some experiments with mixtures of gases are also described. The latter experiments have proved that the electron currents originating from chemical action (1) possess the additive property, and (2) exhibit saturation with true zero applied potential difference.

A general method of analysis of electronic spectra is given; the method is based on the comparative study of different electronic spectra and on some considerations of the kinetics and the electronic yield of the chemical reactions. The analysis has shown that (1) the maximum energy E_m of the emitted electrons is, over a wide range of E_m from about 3.0 volts to about 0.7 volt, in satisfactory agreement with the fundamental equation $E_m = E_c - \phi$, where E_c is the energy available in the corresponding elementary chemical

reaction responsible for E_m and ϕ is the work function of the metal, (2) in this range of E_c , the number c of electrons emitted per one Cl atom entering into the reaction with the metal is approximately an exponential function of the chemical energy E_c , and (3) the reaction mechanism of most frequent occurrence is that in which only one of the two Cl atoms of the gas molecule reacts with the alloy.

ERRATUM.

In Part III, vol. 145, p. 33, fig. 7, delete the \bigcirc , at ordinate 5 and abscissa 0.15.

*Studies on Explosive Antimony I—The Microscopy of Polished Surfaces**

By C. C. COFFIN and STUART JOHNSTON

(Communicated by A. S. Eve, F.R.S.—Received March 5, 1934)

[PLATES 6, 7 and 8]

Introduction

In 1855 Gore† reported the discovery of a peculiar soft and lustrous form of antimony obtained by the electrolysis of antimony trichloride solutions. This deposit when heated or scratched underwent a sudden change in which a considerable quantity of heat was developed, the metal was badly shattered, and white fumes of occluded antimony trichloride were evolved. The metal after "explosion" was indistinguishable from ordinary antimony.

Different aspects of the phenomenon have since been the subject of several investigations of which the most comprehensive is that carried out by Cohen and his co-workers‡ during the years 1904–05. More recently Cohen and Coffin§ have succeeded in determining the factors governing the deposition

* Contribution from the Laboratory of Physical Chemistry, Dalhousie University, Halifax, Canada.

† 'Phil. Mag.,' vol. 9, p. 73 (1855); 'J. Chem. Soc.,' vol. 17, p. 365 (1863); 'Proc. Roy. Soc.,' vol. 12, p. 185 (1858); 'Phil. Trans.,' vol. 148, pp. 185, 797 (1858); vol. 152, p. 323 (1862).

‡ Cohen and Ringer, 'Z. phys. Chem.,' vol. 47, p. 1 (1904); Cohen, Collins and Strengers, *ibid.*, vol. 50, p. 291 (1905); Cohen and Strengers, *ibid.*, vol. 52, p. 129 (1905).

§ *Ibid.*, A, vol. 149, p. 417 (1930).

of the explosive form, and Böhm,* Steinwehr and Schulze,† and Kersten‡ have made X-ray studies of its structure.

It appears from the existing data that the explosive metal is amorphous, and that the explosion is simply a rapid exothermic crystallization. As an amorphous metal and its crystallization are of considerable interest from several points of view, an extended investigation of the nature of the substance and its explosion has been undertaken in this laboratory. The present paper is concerned with the microscopic examination of polished surfaces before and after explosion and is necessarily of a descriptive character. Detailed discussion of the phenomena described is reserved until the completion of several different lines of investigation now in progress.

Experimental

Antimony was deposited in the explosive form upon flat copper or copper-plated zinc cathodes about the size of microscope slides from well-stirred antimony trichloride solutions containing one or more antimony anodes. The temperature and concentration of the solution and the current density were adjusted to bring the deposit well within the "explosive region" mapped out by Cohen and Coffin (*loc. cit.*). The solutions were made up by dissolving a weighed amount of antimony trichloride in a known weight of 10% HCl solution. C.P. materials were used throughout. Cathodes were deposited from solutions containing 5, 40 and 70% antimony trichloride and thus from the data of Cohen and Ringer§ contained respectively about 2, 7, and 10% occluded salt.

The explosive deposits were ground flat with a water suspension of fine emery, and were polished with fine rouge on wet chamois leather. Great care was necessary in working with the cathodes from the more dilute solutions on account of the ease with which explosion occurs. Many deposits from the 5%, a few from the 40%, and an occasional one from the 70% solution exploded while being polished. Fortunately the metal from the 5% solution was usually so smooth that very little grinding or polishing was necessary.

The polished cathodes were exploded by a spark from an induction coil, or Leyden jar, or by touching them with a hot needle. Microscopic observa-

* 'Z. anorgan. Chem.,' vol. 149, p. 217 (1925).

† 'Z. Physik,' vol. 63, p. 815 (1930).

‡ 'Physics,' vol. 2, p. 276 (1932).

§ 'Z. phys. Chem.,' vol. 47, p. 1 (1904).

tions and photographs were made with reflected light ; magnifications were determined by photographing a micrometer slide.

Appearance of Exploded Deposits

A polished surface of amorphous antimony before explosion, fig. 1, Plate 6, resembles that of any other soft bright metal. No distinctive features beyond polishing scratches and faults in the deposit are visible. After explosion, however, the surface is covered by many well-defined equally spaced parallel lines, which, if viewed far enough from the point at which the explosion started, appear to be straight, fig. 2, Plate 6. However, if the slide is moved so that the spot where the explosion started is brought closer and closer to the field of view the lines become more and more curved and eventually, if the curvature is followed back to the origin, appear as concentric circles about the point where the spark or hot needle struck the metal. Fig. 3, Plate 6, and fig. 4, Plate 6, are photographs of the spot where a spark hit a cathode deposited from a 40% solution. The concentric circles are plainly visible. Fig. 5, Plate 6, is a view of a typical "crater" made by touching polished metal from a 40% solution with a hot needle ; fig. 6, Plate 6, shows the crater made by touching it obliquely with a hot copper wire. The deposit is frequently badly cracked and the surface distorted by the explosion, so that it is sometimes impossible to get the whole field in focus at the same time, *e.g.*, fig. 3.

If the deposit is not too thin or too porous the spacing of the lines is remarkably constant. Many counts on exploded deposits from the different solutions reveal that there are from 2000 to 4000 lines per centimetre, and that any departure from parallelism can usually be traced to some hole or fault in the metal. The counting was done either through a microscope with a micrometer eyepiece or by throwing the image of the negative on a screen which had been calibrated with the image of the micrometer slide.

That these lines are not merely a surface phenomenon but exist throughout the body of the metal is evinced in several ways. They can be readily polished off so that the surface of an exploded deposit resembles that shown in fig. 1. However, a few minutes etching with a mixture of tartaric and nitric acids or a short time as an *anode* in an electrolytic cell will bring up the lines just as clearly as before. The surface as a whole is somewhat darkened by the etching, and through the microscope shows brilliant interference colours which are probably due to a film of oxide from the nitric acid treatment. The examination of two polished exploded surfaces at right angles to one another also reveals that the lines are to be found throughout the body of the metal, and

that they are in no way related to the orientation of the deposit with respect to the copper cathode. Fig. 7, Plate 7, is a photograph of the face of an electrode from a 40% solution exploded by a spark to its edge. The crater is on the cross hairs. Fig. 8, Plate 7, is a view of the same crater from the side or edge of the electrode. Fig. 9, Plate 7, shows the face of a deposit from a 70% solution exploded on the edge by touching it with the side of a hot needle. Fig. 10, Plate 7, is a view of the same crater from the edge of the deposit and like fig. 8 shows the lines spreading spherically through the metal. The two electrodes from which figs. 7-10 were taken were polished before explosion. Exactly similar views are obtained by sawing through an exploded deposit near the crater on its face, grinding at right angles to the face until the crater is just on the edge, and finally polishing and etching. It is thus evident that the lines are due to a regular crystallization brought about by the spherical and autogenous heat wave travelling through the mass of metal.

The wavelike appearance of the crystallization lines suggested several "interference" and "shadow" experiments. Fig. 11, Plate 7, is a photograph of the region between two craters, about 2 mm apart, made simultaneously by causing a spark to jump from a needle point to the metal and from the metal to a second needle point. The "waves" meet at a very clearly defined straight line. Fig. 12, Plate 7, is a view of part of the same line. No interference in the ordinary sense is visible as the passing "wave" leaves the medium "frozen." The dark spots on fig. 11 are holes in the deposit and the manner in which they affect the propagation of the explosion is evident. The "shadow" of a hole or obstruction usually appears as a sort of line, like that in figs. 11 and 12, where the "waves" rounding each side meet at an angle.

The rate at which the crystallization wave travels through the metal can obviously be determined by measuring the distance from the line of meeting of two sets of waves, one of which is made a known fraction of a second after the other, to each of the two craters. An investigation of the effect of temperature, thickness of deposit, amount of occluded salt, etc., on the rate of crystallization is in progress and will be reported in detail elsewhere. It appears that the velocity is approximately 23 cm/sec at room temperature.

When a thin (< 0.1 mm) film of the explosive metal is deposited on heavy copper the crystallization will not travel more than a fraction of a millimetre from the starting-point. The large heat capacity and good heat conductivity of the underlying copper evidently reduce the heat wave to such an extent that it is unable to bring about further crystallization. Fig. 13, Plate 8, and fig. 14, Plate 8, show the result of scratching a 0.07 mm thick deposit

from a 5% solution with a hot needle. Many craters appear along the line of the scratch and the crystallization always ceases abruptly after travelling a fraction of a millimetre. Curious "interference" effects are often visible along such scratches.

In slightly thicker films the whole deposit may explode, or the explosion may stop suddenly after travelling a considerable distance. Fig. 15, Plate 8, and fig. 16, Plate 8, are typical photographs of the line where the crystallization of a 0.17 mm deposit from a 5% solution suddenly stopped after travelling several centimetres. The line between exploded and non-exploded metal is very sharp and owing to the difference in reflecting power is easily visible to the naked eye. A curious spacing of the crystallization lines in groups of two or three is discernible in fig. 15. In such thin films little or no cracking occurs on explosion.

If the deposit is still thicker (> 0.2 mm) the crystallization is complete, and is accompanied by a violent shattering of the metal which is often stripped from the copper in circular sheets or rings concentric with one another about the crater. Fig. 17, Plate 8, and fig. 18, Plate 8, are typical of such deposits. The former is a view at some distance from the crater; the latter is the crater itself. The explosion was started by a single spark from a Leyden jar. From the direction of the crystallization lines on opposite sides of the cracks it would appear that the cracking occurred after the formation of the lines. In the explosion of deposits thicker than about 0.5 mm the cracks are not so numerous and the tendency of the metal to strip from the copper is not so noticeable.

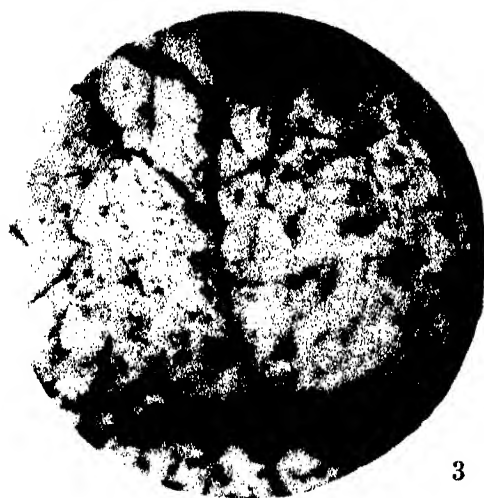
Amorphous antimony prepared from a solution of any concentration explodes violently between 110 and 125° C when heated slowly in a test tube immersed in an oil bath. Polishing and etching of pieces exploded in this way shows that the usual crystallization lines are not present. The metal can also be made to lose its explosive property gradually by heating for an hour or more at 100°, when no explosion occurs and no crystallization lines appear on etching. As the metal treated in this way has undoubtedly become crystalline it would seem that exposure to a uniform high temperature results in a random crystallization in which the definite crystal orientation brought about by a heat wave is entirely absent. With craters made by touching the metal with a hot object there is often a relatively large area which shows no crystallization line, *e.g.*, figs. 5, 6, Plate 8, and fig. 14, Plate 8. It seems probable that the crystallization in this region is completely random due to uniform heating, and that the regular crystal orientation occurs only in the wake of a moving



1



2



3



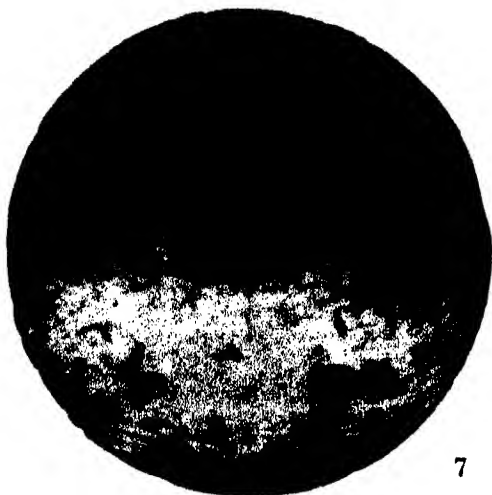
4



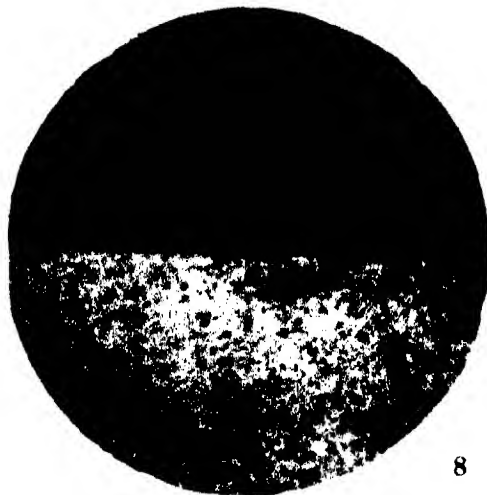
5



6



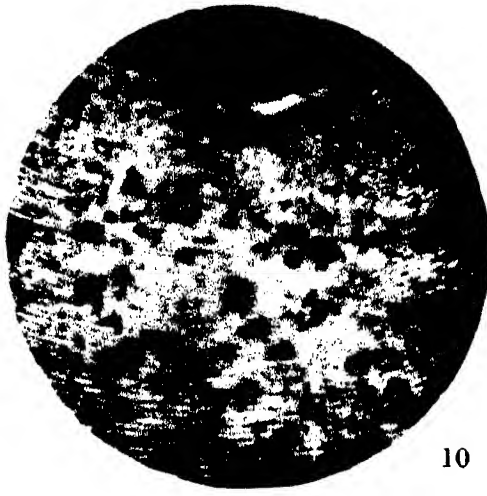
7



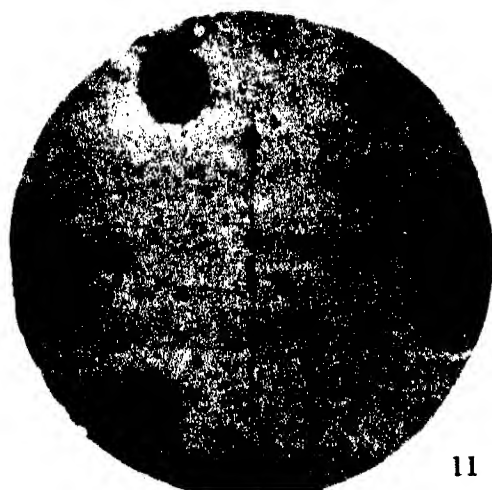
8



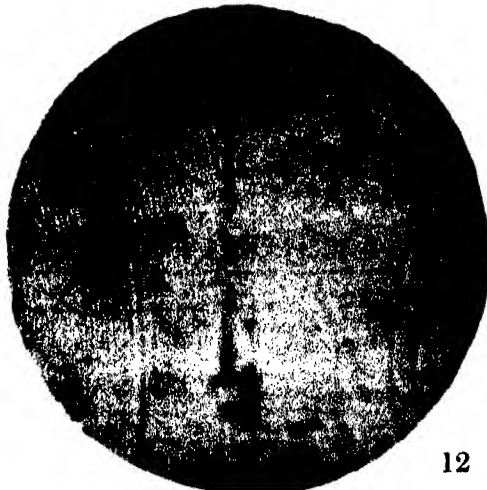
9



10



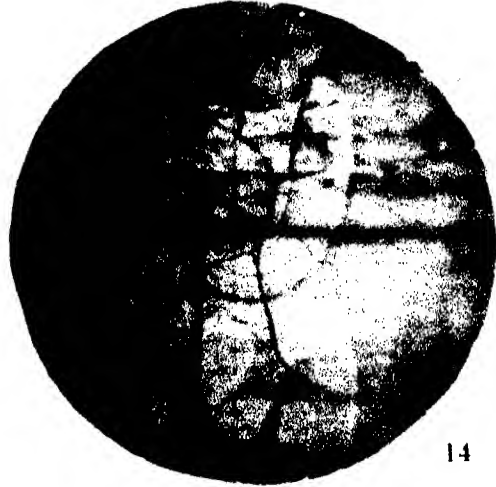
11



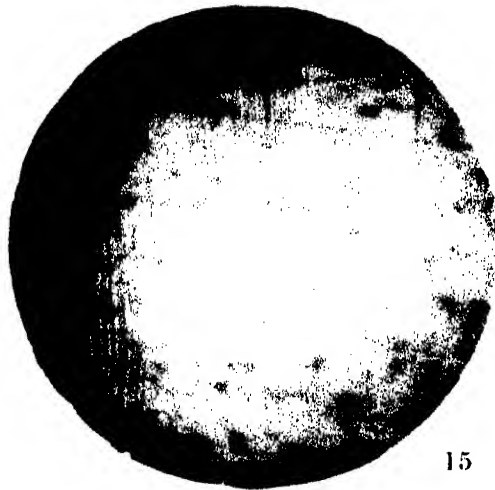
12



13



14



15



16



17



18

temperature gradient or heat wave. An attempt is being made to determine the rate of crystallization at temperatures below that at which explosion occurs with the object of obtaining the activation energy of the reaction.

The exact topography of a crystallized polished surface has so far not been determined. The possibility of optical illusions, diffraction effects, etc., must not be overlooked in attempting to analyse photographs of a periodic phenomenon of this type. Efforts to measure the distance between troughs and crests by depth of focus have yielded no reasonable or consistent results. The same is true of attempts to secure an "end on" picture of the "waves." Our opinion, however, after viewing many specimens and inspecting some sixty photographs is that the surface after crystallization is much like a ploughed field or the roof of a building covered with short thick slates. It is believed that the spaces between the lines or, to return to the simile, the weather faces of the slates, is a crystal face making a small angle with the surface plane and that the "lines" are due to another face making a large angle with the surface. The clearer portions of fig. 12, Plate 7, for example, suggest that this is the correct interpretation. Attempts are being made to prepare a crystallized surface uniform enough to be used as a diffraction grating and it is expected that more detailed information with regard to the surface structure will then be forthcoming.

It gives us pleasure to acknowledge our indebtedness to Professor G. V. Douglas for the loan of microscopes and accessories, and to Professor C. B. Nickerson for assistance with the photography.

DESCRIPTION OF PLATES

PLATE 6

- FIG. 1—Polished metal from 40% SbCl_3 solution before explosion. $\times 150$.
FIG. 2—Polished metal from 40% SbCl_3 solution after explosion. $\times 150$.
FIG. 3—Crater where spark hit, and exploded polished metal from 40% solution. $\times 150$.
FIG. 4—Crater where spark hit, and exploded polished metal from 70% solution. $\times 37.5$.
FIG. 5—Crater caused by touching metal from a 40% solution with a hot needle. $\times 150$.
FIG. 6—Crater caused by touching metal from a 40% solution obliquely with a hot wire. $\times 150$.
FIG. 7—Edge of face of electrode from 40% solution exploded by spark to edge. $\times 150$.

PLATE 7

- FIG. 8—Side view of same crater as fig. 7. $\times 37.5$.
FIG. 9—Edge of face of electrode from 70% solution exploded at edge with a hot needle. $\times 37.5$.
FIG. 10—Side view of same crater as fig. 9. $\times 150$.
FIG. 11—Two craters made by simultaneous sparks on metal from 40% solution. $\times 37.5$.
FIG. 12—Same as fig. 11. $\times 150$.

PLATE 8

FIG. 13—Craters along needle scratch on thin deposit from 5% solution. $\times 37.5$.

FIG. 14—Same as fig. 13.

FIG. 15—Line where explosion stopped in thin deposit from 5% solution. $\times 150$.

FIG. 16—Same as fig. 15. $\times 37.5$.

FIG. 17—Typical exploded thin deposit from 5% solution. $\times 150$.

FIG. 18—Crater made by single spark on thin deposit from 5% solution. $\times 37.5$.

The Crystal Structure of Copper Sulphate Pentahydrate, $\text{CuSO}_4 \cdot 5\text{H}_2\text{O}$

By C. A. BEEVERS and H. LIPSON, George Holt Physics Laboratory, University of Liverpool

(Communicated by W. L. Bragg, F.R.S.—Received April 4, 1934)

[PLATE 9]

Introduction

Despite their frequent appearance in the laboratory, few of the structures of hydrated salts have as yet been found. This may be due to the large numbers of parameters usually involved, which, in the absence of any general laws concerning water of crystallization, makes the analysis very difficult. It was thought that clues to such general laws might be obtained from a determination of the structure of copper sulphate pentahydrate which has many interesting properties and which has been studied from many different points of view. For example, the decomposition on heating proceeds in three distinct stages,



reactions which should be explainable from a knowledge of the structure.

Also, four of the waters are replaceable by ammonias, while the other one is retained. This suggests that one of the waters is very different from the others.

Furthermore, Jordahl* has predicted a grouping around the copper atoms of an octahedron of oxygens, based on measurements of magnetic susceptibilities. It is of importance that this conclusion should be verified by the direct results of X-ray analysis.

* 'Phys. Rev.', vol. 45, p. 87 (1934).

Copper sulphate also has an historical interest, since it was the crystal with which Friedrich, Knipping and Laue* established the undulatory nature of X-rays.

Unit Cell and Space Group

Copper sulphate pentahydrate crystallizes in the triclinic system, and possesses centro-symmetry. Its space group is thus C_1 .¹

The axial ratios and angles are given by Tutton† as

$$a : b : c = 0.5715 : 1 : 0.5575$$

$$\alpha = 82^\circ 16', \quad \beta = 107^\circ 26', \quad \gamma = 102^\circ 40'.$$

The crystal, as is well known, grows from saturated solution at ordinary temperatures, and has a well-developed [001] zone.

Oscillation photographs were taken with the crystal rotating about the three axes, and estimations of intensities were made from the rotations about the *b* and *c* axes.

From the photographs a unit cell was deduced with

$$a_0 = 6.12 \text{ \AA}, \quad b_0 = 10.7 \text{ \AA}, \quad c_0 = 5.97 \text{ \AA} \pm 1\%,$$

in agreement with the crystallographic ratios. The volume of this unit cell is 363 \AA^3 and it contains two molecules of $\text{CuSO}_4 \cdot 5\text{H}_2\text{O}$.

Determination of the Copper and Sulphur Positions

We had estimated from our photographs the strengths of about 700 spots, in the usual classes: vs—very strong, s—strong, m-s—medium-strong, m—medium, w-m—weak-medium, w—weak, v—very weak, and o—absent.

Many of these were observed several times, and the strengths recorded in this paper are estimated averages. Bernal's method‡ was used in assigning the indices.

A close inspection of the intensities showed that those with $h + k$ even were in general stronger than those with $h + k$ odd. This effect is illustrated in fig. 6, Plate 9 which is a 30° oscillation photograph taken with the crystal rotating about the zone axis [112]. The spots on the even layer lines thus have $h + k$ even, and on the odd ones, $h + k$ odd. It will be seen that the

* 'Ann. Physik,' vol. 41, p. 971 (1913).

† "Crystallography and Practical Crystal Measurement," vol. 1, p. 297 (Macmillan, 1922).

‡ 'Proc. Roy. Soc.,' A, vol. 113, p. 117 (1927).

even layer lines contain a much larger proportion of strong spots than do the odd ones.

This suggests that there is a face-centred arrangement of some of the heavy atoms in the (001) plane. There are two possibilities: (a) the sulphurs face-centre the coppers, or (b) the two coppers themselves have the face-centred arrangement.

Differentiation between these was made by comparison with the intensities of reflection from copper selenate, $\text{CuSeO}_4 \cdot 5\text{H}_2\text{O}$ which is isomorphous with copper sulphate. A face-centring of copper and selenium would show up very well, since the two atoms have atomic numbers which are nearly equal. Fig. 7, Plate 9, shows a photograph similar in every way to fig. 6, Plate 9, except that a crystal of copper selenate was used. It will be seen that the predominance of the $h+k$ even spots is less marked, and the conclusion was reached that the face-centring is that of the coppers themselves.

There are only two essentially different ways in which this face-centring can have a centre of inversion: the coppers must be on (000) and $(\frac{1}{2}\frac{1}{2}0)$ (i.e., on the centres of inversion) or on $(\frac{1}{4}\frac{1}{4}0)$ and $(\frac{3}{4}\frac{3}{4}0)$.

The distinction between these was made possible by a further regularity of intensities. It was observed that those spots for which $h+k$ is even showed a tendency to be independent of h . This is shown in Table I.

Table I—General Reflections with $\sin \theta > 0.5$

h	<i>kl</i>							
	71	91	71	91	72	92	72	92
5			m	m-s			m-s, m	
3	w	m-s	o	s, m-s	w-m, w	m	m	v
1	v	m	w-m, w	o	w-m	w-m, w	m	w-m, w
$\bar{1}$	m	m-s, m	w-m	m	s, m-s	m-s	m	m
3	w-m	w-m	w	m	m	w	w-m, w	w-m, w
5	w	m	w		m-s	m-s	m	
7	v				s, m-s			
h	<i>kl</i>							
	81	101	81	101	82	102	82	
6			m, w-m					
4	s, m-s		m	m-s, m			m-s	
2	m-s, m	o	m, w-m	m	v	m-s, m	m-s	
0	m-s, m	w	w	w-m	w-m, w	o	m	
2	m-s	o	w-m		v	m	w-m	
4	m	w-m, w	m		m	m	m	
6	m	v			m, w-m	s, m-s		

This regularity must be due to the sulphur having the same x as one of the coppers. Comparison of sulphate and selenate reflections showed that the sulphur or selenium must have a large contribution to the odd orders of 100; this is shown in Table II.

Thus the z parameters of sulphur and copper cannot be $\frac{1}{2}$ and consequently the coppers must be on the centres of inversion at (000) and ($\frac{1}{2}\frac{1}{2}0$).

The second regularity of intensities made it possible to detect immediately those reflections which have a large oxygen effect, and it thus provided reliable data for the estimation of the sulphur parameters. From the intensities $hk0$ the y parameter was estimated to be 0.28. (The calculations of relative amplitudes of reflection were made on the assumption that the f -number of Cu is twice that of S at all angles. This made it possible to consider groups of planes with the same k and l .)

The intensities $h0l$ were used to find the z sulphur parameter, which was estimated to be ± 0.36 . Both signs must be considered here since the points ($o y z$) and ($o y \bar{z}$) are not equivalent.

Table II—Comparison of Orders of Reflection from (100)

	1	2	3	4	5	6	7
CuSO ₄	s, m-s	s	o	s	v	m-s, m	m
CuSeO ₄	s	s	w-m	s	m	m	s, m-s

The general $h k l$ intensities showed that the z parameter was -0.36 .

Thus the parameters found were (000), ($\frac{1}{2}\frac{1}{2}0$) for the coppers, and (0 0.28 0.64) for the sulphur.

The Complete Structure

The establishment of the fact that the two copper atoms lie on the centres of inversion leads to the conclusion that the groups of waters round them are plane, and probably square. Six degrees of freedom are therefore involved. The sulphate group and the extra water also involve six degrees of freedom, so that 12 parameters are still needed to define the complete structure. It was found that the difficulties involved in handling such a large number of parameters were too great for the problem to be solved directly.

Thus it was decided to use Fourier methods* to determine the projection of the unit cell on the (001) plane. Using a crystal slip† the intensities were measured of 89 $hk0$ reflections; these were the reflections which we had estimated from our photographs as being in the classes higher than weak, and having $\sin \theta/\lambda < 0.65$.

The observed F 's (corresponding with one molecule of CuSO₄ · 5H₂O) are shown in Table III.

* W. L. Bragg, 'Proc. Roy. Soc.,' A, vol. 123, p. 537 (1929).

† Bragg and West, 'Z. Kristallog.,' vol. 69, p. 120 (1928).

Table III—Values of F_{hko}

		h																
		8	7	6	5	4	3	2	1	0	1	2	3	4	5	6	7	8
k	0	8	11	12	0	28	0	33	26	129	26	33	0	28	0	12	11	8
	1		0	0	0	10	19	10	18	0	30	18	21	0	20	0	11	
	2		0	9	0	10	7	17	32	12	17	0	21	0	0	0	0	
	3		8	6	16	7	18	17	50	11	23	20	26	7	18	0	0	
	4			10	0	8	10	17	0	0	17	27	8	26	13	18	0	
	5			0	0	10	0	13	11	14	0	0	12	0	0	0	0	
	6			0	0	9	0	15	14	12	0	18	0	7	0	0	0	
	7				15	7	19	0	18	15	21	15	19	9	13	0	7	
	8				0	0	0	11	0	12	8	16	0	0	0	10	0	
	9					0	7	0	0	0	0	11	0	0	0	0	0	
	10					12	0	10	0	16	7	14	0	12	0	8		
	11						7	0	8	0	17	0	12	0	13			
	12							0	0	0	0	0	0	0	0			
13								7	0	11	0	0	0					

The signs of the F 's were assumed to be those of the Cu and S contributions except where the selenate photographs indicated the opposite.

The resulting contour map is shown in fig. 1. It will be seen that, apart from the Cu and S, eight other peaks are indicated in each half of the unit cell. There are three much smaller peaks also shown in the diagram, but apart from these, the background is everywhere between ± 70 . Three of these peaks, labelled 1, 2, and 3, form a triangle around S, and the tetrahedral nature of the SO_4 group suggests that another oxygen atom, 4, is directly in line with the S and consequently irresolvable from it. Estimation of the electron content of the peaks verified this.

The estimates were :—

$$\text{Cu at } (000) = 26 \text{ electrons}$$

$$\text{Cu at } (\frac{1}{2}\frac{1}{2}0) = 29 \quad ,,$$

$$\text{S} + 4(\text{O}) = 22\frac{1}{2} \quad ,,$$

$$1(\text{O}) = 10.2 \quad ,,$$

$$2(\text{O}) = 6.9 \quad ,,$$

$$3(\text{O}) = 8.6 \quad ,,$$

$$5(\text{H}_2\text{O}) = 7.7 \quad ,,$$

$$6(\text{H}_2\text{O}) = 5.7 \quad ,,$$

$$7(\text{H}_2\text{O}) = 6.6 \quad ,,$$

$$8(\text{H}_2\text{O}) = 7.7 \quad ,,$$

$$9(\text{H}_2\text{O}) = 8.5 \quad ,,$$

Ionized sulphur would have 10 electrons, so that it is clear that if 4 is about the average of the other O's, S must approximate more closely to the un-ionized condition. The oxygen and water peaks are too small on the average, and the

total count for $\text{CuSO}_4 \cdot 5\text{H}_2\text{O}$ is 112 electrons, which is much smaller than the required 120. This is partly due to the three "ghosts."

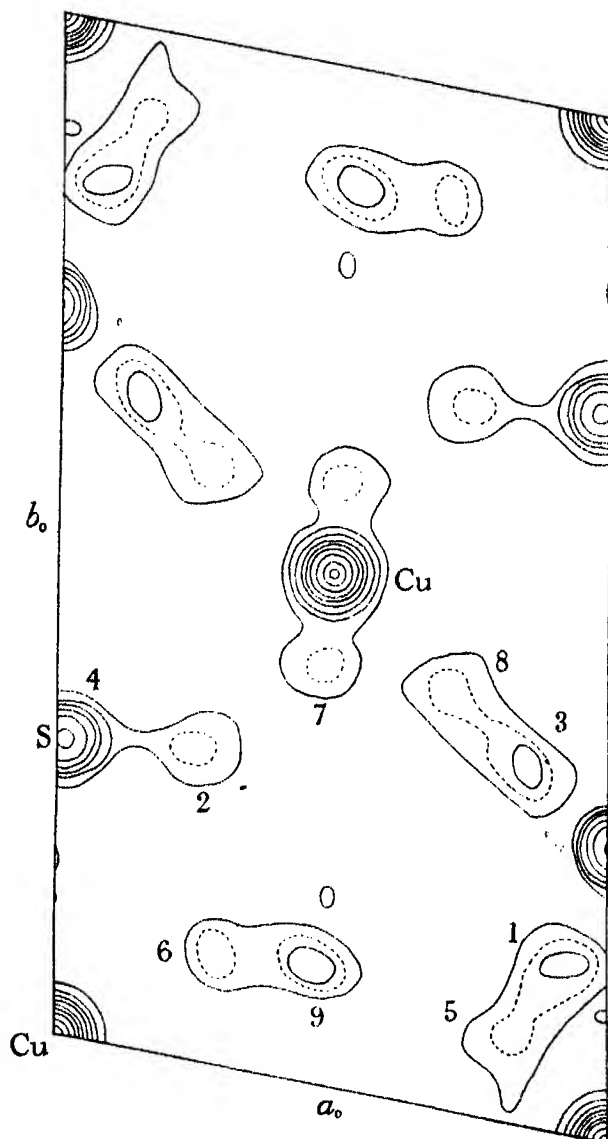


FIG. 1.—Fourier synthesis of the projection of the structure on (001). Contours are drawn at levels of 100, 200, 300, etc., and in the oxygen peaks, of 150, shown by the dotted lines.

The Fourier synthesis gives the sulphur position as (0.01 0.29) instead of (0.00 0.28).

The x and y parameters obtained can be accounted for by tetrahedral SO_4 groups, and square groups of waters round copper, assuming a distance of 2.5 Å between oxygens in the former, and 2.8 Å between waters in the latter. There are, however, for each of the groups two possible positions, which are connected by a plane of symmetry through the central atom and perpendicular to the c axis. In only one of the eight possibilities was there a good fitting together of the groups themselves.

Even in this structure it was found that some of the interatomic distances were rather less than the usually accepted values, but small rotations of the groups could be made which increased these. The parameters finally chosen were :—

1	(O)	0.89	0.15	0.69
2	(O)	0.24	0.31	0.82
3	(O)	0.86	0.38	0.64
4	(O)	0.02	0.30	0.38
5	(H_2O)	0.83	0.08	0.16
6	(H_2O)	0.29	0.11	0.17
7	(H_2O)	0.48	0.41	0.32
8	(H_2O)	0.76	0.42	0.01

The z parameter of 9 (H_2O) may easily be found from considerations of space, and turned out to be 0.65, so that we had—

9	(H_2O)	0.43	0.12	0.65
---	--------------------------------	------	------	------

The structure was verified by the comparison of calculated and observed intensities; this comparison is shown in Table IV. The f curves used were those of Cu, S (neutral) and O^{-2} in the tables of James and Brindley.*

The ($h k 0$) intensities of copper selenate were also calculated and showed excellent agreement with observed intensities.

Discussion of the Determined Structure

Fig. 2 is a representation of the projection of the structure on a plane perpendicular to the c axis. The numbers in the circles representing the atoms are the z parameters, and the numbers outside the circles are the numbers given in the previous paragraph.

The copper and sulphur positions give a typically ionic structure. The copper at (000) has round it four sulphurs, two at 3.55 Å and two at 5.2 Å,

* 'Z. Kristallog.,' vol. 78, p. 470 (1931).

and the copper at ($\frac{1}{2}\frac{1}{2}0$) has eight, in pairs, at 3.6 Å, 5.5 Å, 5.3 Å, and 4.8 Å.

Round the sulphur are six coppers at the distances just given. It will be noticed that the sulphur is very close to two coppers.

The arrangement of the oxygens and waters is of particular interest. Although the two coppers are not equivalent, they have similar groups of atoms round them, namely, octahedra composed of four waters and two oxygens. The octahedra are not regular: their dimensions are given in fig. 3.

Table IV—Calculated Intensities in Order of θ

<i>hkl</i>	Calcu- lated	Observed	<i>hkl</i>	Calcu- lated	Observed	<i>hkl</i>	Calcu- lated	Observed
001	1700	m-s	401	800	m-s	205	150	m
101	650	m-s	402	750	m-s, m	603	360	m
101	480	m-s	204	250	w-m	308	4	o
121	2200	s	004	8	v	006	1000	m-s
201	22	w-m	302	8	w, v	505	97	m, w-m
002	340	m, w-m	203	1500	s	406	480	m-s, m
102	410	m-s, m	304	24	v	604	3	o
221	6400	s	403	640	m-s	601	220	m
141	610	m-s	104	200	m	106	18	w, v
212	11	o	401	160	w-m	404	200	w-m
202	17	v	421	180	w-m	503	48	w
102	200	m	303	25	w	508	39	m
201	110	m	404	49	w	605	580	s, m-s
241	960	s, m-s	501	55	w	702	4	v
212	20	o	502	64	w, v	701	120	w-m, w
232	1100	v-s, s	105	25	v	703	63	o
103	89	m	205	100	m, w-m	107	108	m, w-m
301	2	v	402	160	m, w-m	307	45	v, o
242	1800	s	204	2	v, o	602	140	m
132	1300	v-s, s	005	530	m-s	407	200	m
331	920	v-s, s	503	12	o	007	70	w
003	3000	s	305	56	w-m	704	510	m-s, m
312	1100	s, m-s	501	1	v, o	606	420	m-s, m
203	3900	v-s	105	20	w-m, w			
302	17	o	405	320	m-s, m			
202	1800	s	504	100	w-m, w			
341	305	s	403	360	m			
212	800	s	602	200	m			
103	96	w	206	240	m			
301	140	m	305	17	w-m, w			
181	6	v	601	0	o			
303	3	v, o	108	2	o			
104	59	w-m	502	10	o			

(There are difficulties in the estimation of the probable error of these distances, but we believe that it is less than 0.1 Å.) The sulphate group is, of course, tetrahedral, with O-O distances equal to 2.5 Å.

Apart from the atoms in its own group, every water touches two oxygens, if the extra water be counted as an oxygen. The contacts correspond to distances which are included in the range 2.75 ± 0.2 Å, and there are no other distances less than 3.2 Å.

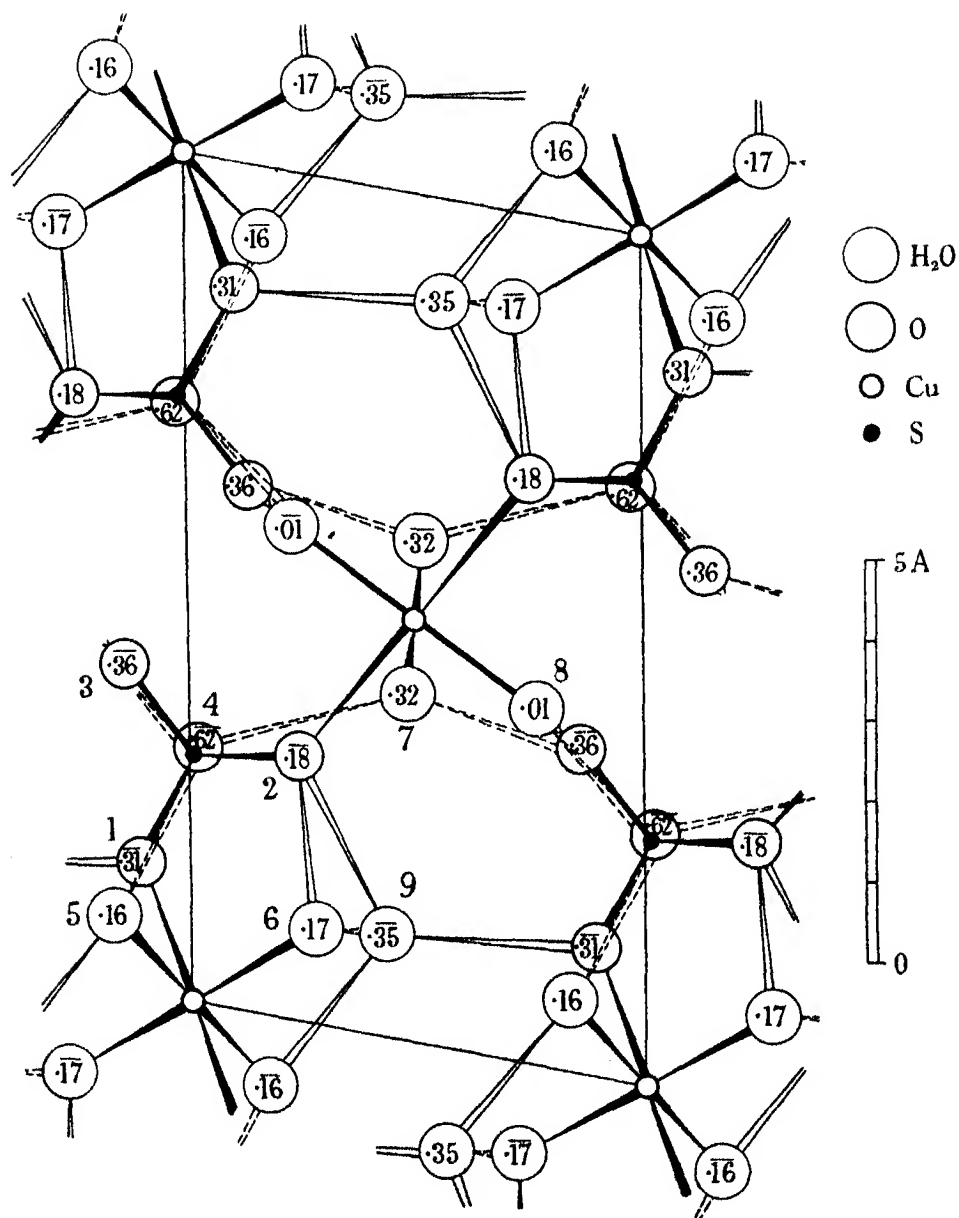


FIG. 2.—Representation of the projection of the structure on a plane normal to the c axis, showing the bonds between the atoms. Bonds between atoms in the same group are drawn in black; others between atoms with the z parameters actually shown are drawn with full lines, and the bonds to atoms c , removed from these are shown by broken lines.

The two bonds from water to oxygen probably correspond with the two hydrogens in the molecule. If this be so, there cannot be bonds between waters and oxygens in the same group. The small distance of the coppers

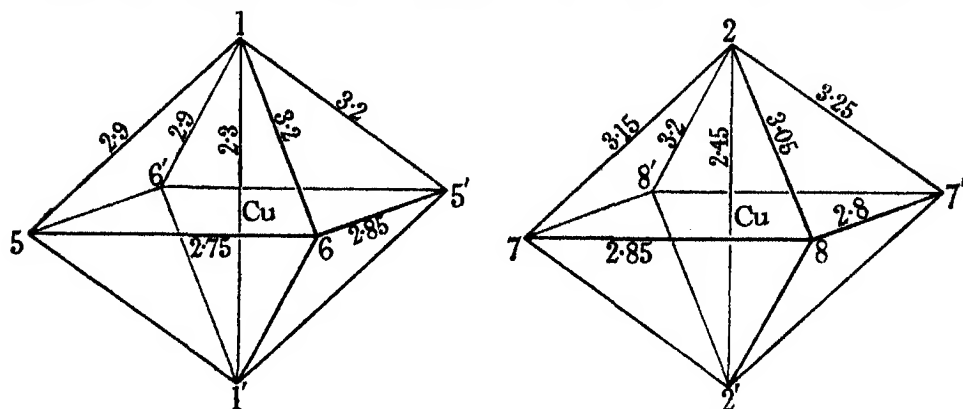


FIG. 3—Dimensions of the groups round the copper atoms.

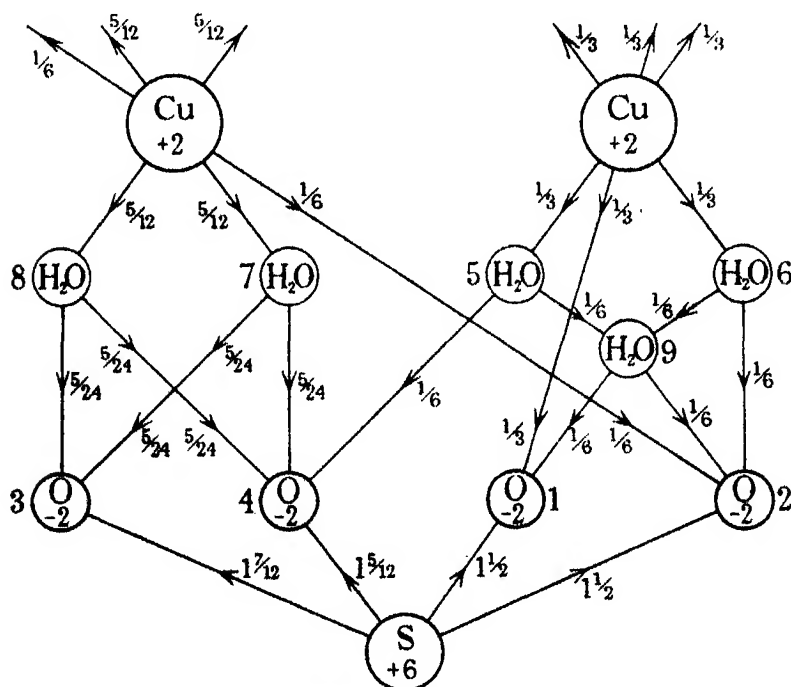


FIG. 4—Bond Structure.

from the oxygens of the octahedra suggests that there are direct bonds between them. With these assumptions it is possible to build different bond structures, of which that given in fig. 4 is an example. It was not found possible to get

exactly equal bonds to the sulphate oxygens, as these are all making different contacts, but in fig. 4 they are approximately equal.

It will be seen from fig. 2 that the copper at ($\frac{1}{2}\frac{1}{2}0$) is linked to the eight sulphate groups around it, in six instances by water contacts and in two by direct bonds to oxygen. The copper at (000) also is linked directly to two SO_4 groups, and by means of water contacts to two more; but also by contacts to the extra water, it is linked to two more SO_4 groups, making six in all.

The sulphate oxygens are all making different contacts. 1 touches Cu and H_2O ; 2, Cu and $2\text{H}_2\text{O}$'s; 3, $2\text{H}_2\text{O}$'s; and 4, $3\text{H}_2\text{O}$'s.

A theory of the structure of water has been proposed by Bernal and Fowler.* In this theory the water molecule resembles a tetrahedron with two corners of positive and two of negative charge. There is only one water molecule in the copper sulphate structure which can be directly compared with this, i.e., 9, which has four bonds, two to water and two to oxygen. The two bonds to water should be due to the negative charges and the bonds to oxygens to the positive charges.

It will be seen from fig. 2 that the four bonds do form a tetrahedral arrangement. The angle between the two bonds to the oxygens is 121° , and between the two to the waters 108° ; the other angles between the bonds are 126° , 92° , 114° , and 95° , and the average is 109° which is exactly the tetrahedral angle. The probable error in our determinations of the angles is not easily estimated, but if all the three distances which determine a particular angle were wrong by 0.1 Å, the error in the angle may amount to 10° : in general it should be much less than that. It appears therefore that a certain amount of variation from the tetrahedral angle is possible.

The theory cannot be applied exactly to the other waters since they have only three bonds, the two negative ones both going to the same copper atom. These distributions of bonds are as shown in fig. 5.

It will be seen that the three bonds to both 7 and 8 are exactly coplanar, while those to 5 and 6 are only approximately so. The angles between the two bonds to oxygen are on the average distinctly greater than the tetrahedral angle of 109° , actually the mean is almost exactly 120° . This point was tested on the crystals $\text{BeSO}_4 \cdot 4\text{H}_2\text{O}$ † and $\text{NiSO}_4 \cdot 6\text{H}_2\text{O}$ ‡ in which also each water touches two oxygens. In the former there is only one $\text{O}-\text{H}_2\text{O}-\text{O}$ angle, and it is exactly 120° ; in the latter there are three, which are 99° , 125° ,

* 'J. Chem. Phys.,' vol. 1, p. 515 (1933).

† Beevers and Lipson, 'Z. Kristallog.,' vol. 82, p. 297 (1932).

‡ *Ibid.*, vol. 83, p. 123 (1932).

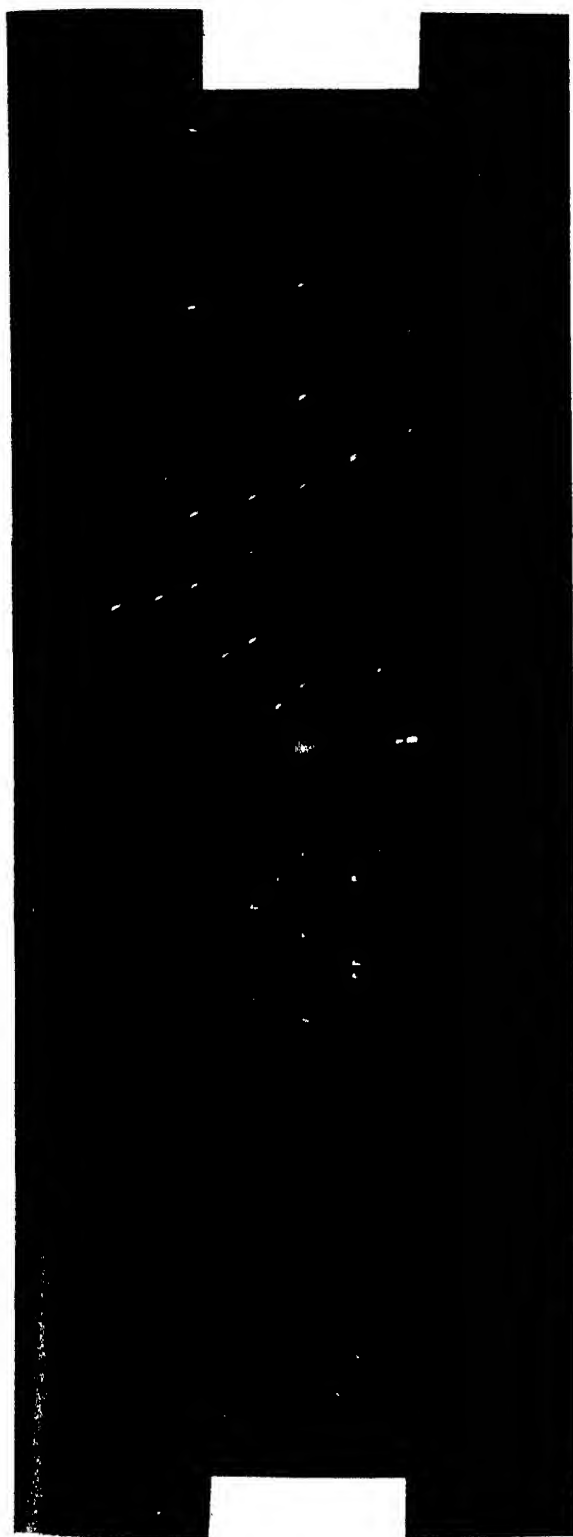


FIG. 6

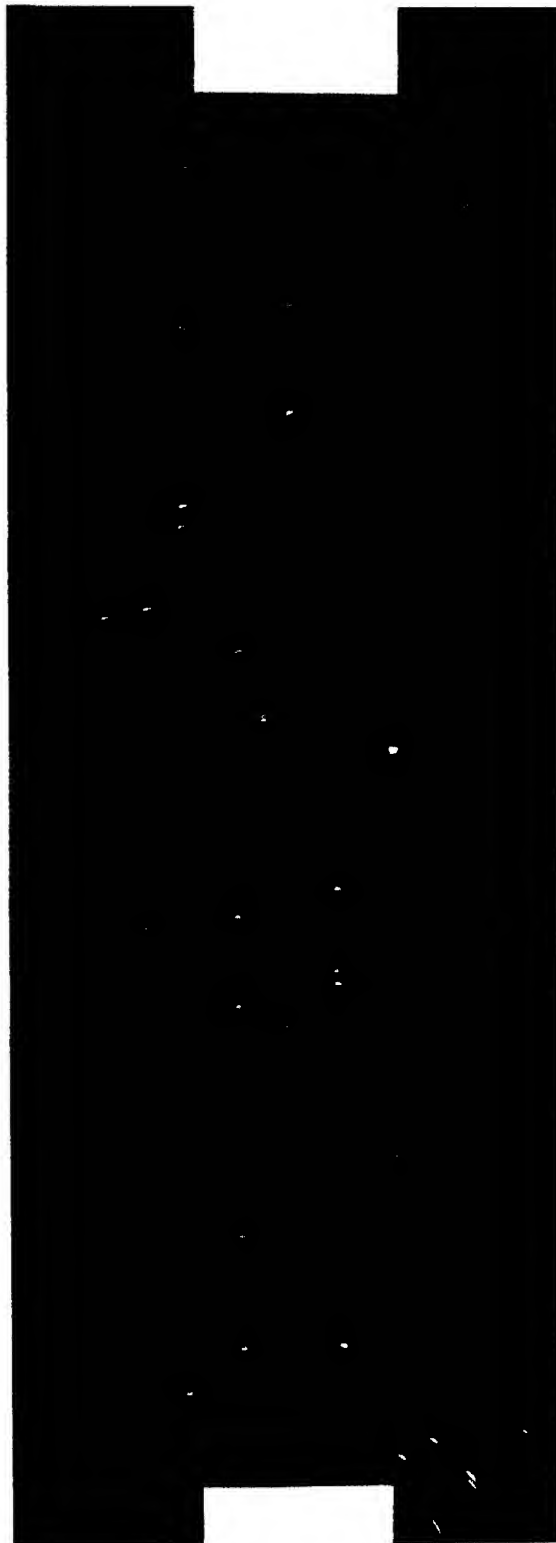


FIG. 7

(Facing p. 589.)

and 132° , of which the mean is 119° . The large variation in this latter crystal is to be expected; its remarkable cleavage plane suggests that the $\text{O}-\text{H}_2\text{O}$ bonds across it are not very strong. It may therefore be said that the positions of the water molecules in copper sulphate agree well with the theory of Bernal and Fowler, but that when the water molecule is one of a positive co-ordination complex the angle between the two bonds to the negative atoms is about 120° rather than 109° . It may be pointed out that this deviation is less than that

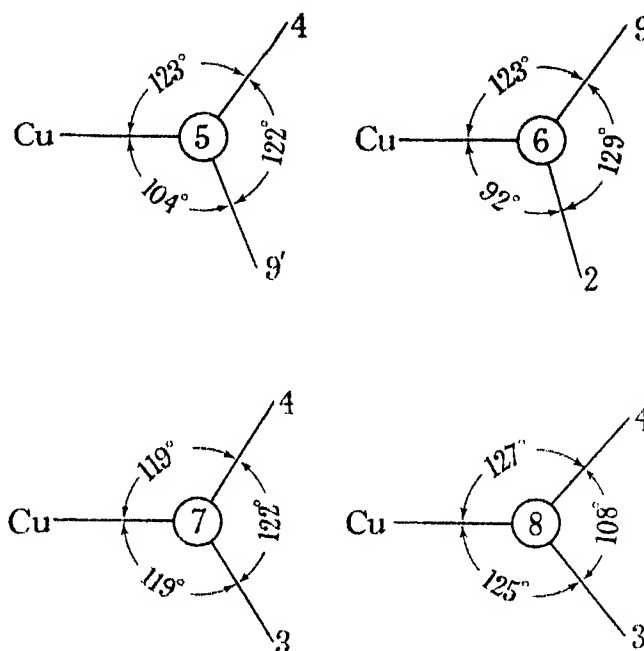


FIG. 5—Disposition of bonds around the four waters.

which is proposed in the quartz-like structure of water: in this the bond angles are 132° .

The structure of copper sulphate explains well the existence of the three successive stages of dehydration, which correspond with the breaking up of the group round one of the coppers, then of the other group, and finally the expulsion of the odd water molecule. It is tempting to push the theory further. The last water molecule is very firmly bound with a tetrahedral arrangement of bonds. The molecules of the group round $(\frac{1}{2}\frac{1}{2}0)$ have a coplanar system of three bonds which one would expect to be much less stable, while the molecules of the ground round (000) have a distorted coplanar arrangement, which should be weaker still. Thus it is to be expected that the group round

(000) would break up first, a conclusion which is also reached by consideration of the bond strengths. That this theory is very incomplete is evident from the argument that it cannot be presumed that the bonds to the odd water would retain their tetrahedral arrangement after the disruption of the other groups. Definite evidence might be obtained by a determination of the structure of $\text{CuSO}_4 \cdot 3\text{H}_2\text{O}$.

According to Jordahl,* the variation of the mean susceptibility of $\text{CuSO}_4 \cdot 5\text{H}_2\text{O}$ with temperature can be explained by groupings of oxygens around the copper atoms with approximately cubic symmetry. Measurements also suggest that the atoms form an octahedron rather than a tetrahedron or a cube. The structure affords a complete verification of this theory.

We have to thank Professor W. L. Bragg for his constant interest and for allowing us to make the necessary absolute measurements at Manchester.

Summary

In $\text{CuSO}_4 \cdot 5\text{H}_2\text{O}$ the copper atoms lie on the special positions (000) and $(\frac{1}{2}\frac{1}{2}0)$ and the sulphur upon the general position (0.01 0.29 0.64). Four of the waters are arranged in squares around the coppers, and two oxygens make with these approximate octahedra. The fifth water is not co-ordinated, but is in contact with two oxygens and two waters. All the waters show two oxygen bonds each, in accordance with recent ideas.

* 'Phys. Rev.,' vol. 45, p. 87 (1934).

*The Kinetics of the Oxidation of Gaseous Hydrocarbons II—The
Oxidation of Ethane*

By E. W. R. STEACIE and A. C. PLEWES

(Communicated by H. T. Barnes, F.R.S.—Received April 6, 1934)

Introduction

It has been repeatedly stated that aldehydes are of importance in the oxidation of saturated hydrocarbons.† Thus in discussing the question Kassel‡ says "Taking the results of these two investigations together it is clear that the general nature of hydrocarbon oxidation involves aldehyde formation followed by a chain oxidation of the aldehyde . . . Under favourable conditions the excited molecules which carry the chain may crack a considerable amount of the original hydrocarbon."

In the previous paper of this series§ it was shown that the addition of acetaldehyde to ethylene-oxygen mixtures had no effect. Hence normal acetaldehyde molecules and their products of oxidation were not effective in the propagation or continuation of the chain process.

This behaviour appears to be in sharp contrast to the work of Bone and Hill.|| who reported instant inflammation on adding acetaldehyde to ethane-oxygen mixtures. This difference in behaviour seemed to warrant a further investigation of the question, and the present paper deals with the oxidation of ethane in the presence of added substances.

Experimental

The apparatus and experimental method were the same as in the previous investigation.

Ethane of 90% purity was obtained in cylinders from the Ohio Chemical and Manufacturing Company. It was purified by two fractional distillations, the middle third being retained each time. The final product was 96–98% ethane, most of the remainder being nitrogen.

Oxygen, ethylene and acetaldehyde were as previously described.

† Pease, 'J. Amer. Chem. Soc.,' vol. 51, p. 1839 (1929); Pope, Dykstra and Edgar, *ibid.*, vol. 51, pp. 1875, 2203, 2213 (1929).

‡ "Kinetics of Homogeneous Gas Reactions," p. 289 (1932).

§ Steacie and Plewes, p. 72.

|| 'Proc. Roy. Soc.,' A, vol. 129, p. 434 (1930).

Experimental Results

Throughout the investigation mixtures consisting of $1\text{C}_2\text{H}_6 + 2.3 - 2.4 \text{O}_2$ were used at 452°C . As may be seen from fig. 1 the reaction process consists of three distinct phases (a) a period of inhibition, (b) an induction period, and (c) the main reaction period. The general form of the pressure-time curves is in agreement with the investigations mentioned above.

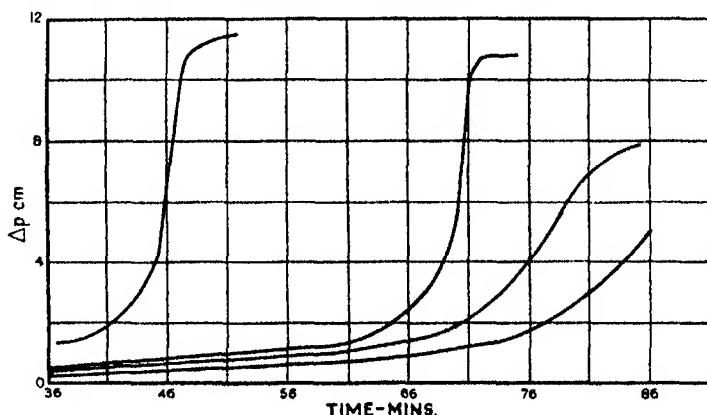


FIG. 1—Typical pressure-time curves; $\text{C}_2\text{H}_6 + 2.3\text{O}_2$; 452°C

The Pressure Change accompanying the Reaction—Some typical pressure increases at completion, relative to the initial partial pressure of ethane are given in Table I.

Table I—Pressure Increase at Completion. $1\text{C}_2\text{H}_6 + 2.3\text{O}_2$. 452°C

Initial partial pressure of C_2H_6 , cm	% pressure increase at completion
7.41	105
8.56	105
7.49	106
9.27	104
7.68	105
9.79	102
7.74	107
10.57	104
13.03	104

It is evident that there is no drift in the pressure increase with changing pressure. The reaction $\text{C}_2\text{H}_6 + 2.5\text{O}_2 = 2\text{CO} + 3\text{H}_2\text{O}$ would lead to a pressure increase of 150%. The reaction $\text{C}_2\text{H}_6 + 3.5\text{O}_2 = 2\text{CO}_2 + 3\text{H}_2\text{O}$ would give 50%.

As will be seen later both CO and CO_2 are formed. It is evident that both processes are occurring. No exact agreement between pressure change and

analyses can be expected, however, since (a) some ethane is always left over at the end of the reaction (b) a certain amount of condensable products is undoubtedly formed.

The Products of the Reaction—Some typical analyses of the gaseous products, made at various times throughout the investigation are listed in Table II.

Table II—The Products of the Reaction

Sample taken at	1 hour after completion	Completion		50% pressure change	End of inhibitory period
CO ₂	12.4	11.5	11.4	3	0.5
C ₂ H ₄	4.4	3.8	4.5	10.3	0.2
O ₂	10.9	10.0	10.6	50.5	64.5
CO	45.3	46.1	47.7	10.7	0
C ₂ H ₆	4.7	—	7.2	11.2	26.7
H ₂	3.0	—	4.5	—	0
CO/CO ₂	3.7	4.0	4.1	3.6	—

The original mixture contained 67.2% oxygen, 27.5% C₂H₆, as shown by analysis. The residue was mainly nitrogen.

The Rate of Reaction—Some typical pressure-time curves are given in fig. 1, and the complete data for a few runs in Table III.

Table III—Data for Typical Runs. Initial pressure, cm

6.23		7.20		10.36		10.96	
Time mins	% ΔP	Time mins	% ΔP	Time mins	% ΔP	Time mins	% ΔP
0	0	0	0	0	0	0	0
10	0	10	1.0	10	0.3	10	1.1
25	1.8	25	2.5	30	1.8	20	2.0
40	4.3	40	5.4	50	7.1	30	6.9
50	8.0	50	10.7	57	15.2	40	17.5
60	15.3	60	21.4	59	20.6	43	35.0
65	21.2	64	30.0	61	29.6	44	56.5
70	27.3	66	40.5	62	37.3	45	98.3
74	63.6	68	56.0	63	56.2	47	103.7
76	81.7	70	79.0	64	89.6	49	103.7
80	101.1	72	98.4	65	103.7	—	—
85	105.0	74	104.5	66	103.7	—	—
87	105.0	76	104.5	—	—	—	—

In order to obtain a measure of the rate of reaction, it is necessary to eliminate the effect of the long and rather erratic period of inhibition. The later stages of the process are quite reproducible. To make sure of eliminating the induction and inhibition periods, we have chosen as a measure of the rate the times for the pressure to increase from 50 to 60%, and from 60 to 70%, relative to ethane. The data are given in Table IV.

If we plot $\log T_{70}-T_{60}$ against $\log PC_2H_6$, we obtain a fairly good straight line, and find that the apparent order is about 3.5. It will be noticed that

the ratio of $T_{70}-T_{60}$ to $T_{60}-T_{50}$ remains more or less constant until we reach high ethane pressures. At high pressures the ratio diminishes. This is due to the fact that at high pressures the induction period is suppressed. This is shown by fig. 1.

It was found that the time of pumping, history of the bulb, etc., had no appreciable effect on the rate as inferred from $T_{70}-T_{60}$ and $T_{60}-T_{50}$. The inhibition period, however, was extremely sensitive to the history of the bulb. This will be discussed in connection with the effect of added substances.

Table IV— $1C_2H_6 + 2.3O_2$. $452^\circ C$

Run No.	PC_{2H_6} , cm	$T_{60}-T_{50}$, min	$T_{70}-T_{60}$, min	$\frac{T_{70}-T_{60}}{T_{60}-T_{50}}$	Remarks
2.....	6.23	1.32	1.34	1.01	Mixed outside
7.....	6.29	1.69	1.49	0.89	" "
11.....	6.45	1.64	1.34	0.82	C_2H_6 first, O_2 last
8.....	7.79	1.10	1.02	0.93	Mixed outside
3.....	7.90	1.28	1.13	0.89	" "
12.....	8.22	0.95	0.93	0.98	" "
23.....	10.38	0.55	0.42	0.77	" "
22.....	10.92	0.50	0.29	0.57	" "
28.....	11.07	0.50	0.27	0.54	" "

The Effect of Added Substances—The effect of added substances on the main reaction is given in Table V, and on the induction period in Table VII.

In calculating the percentage pressure change, and the values of T_{70} , T_{60} and T_{50} for runs with added acetaldehyde, a correction has been made for the pressure change accompanying the oxidation of the acetaldehyde. This has been shown in the former paper to amount to a 55% increase at $452^\circ C$.

In considering the results given in Table V it must be remembered that on account of the form of the pressure-time curves it is not possible to obtain a very high degree of reproducibility in the values of $T_{70}-T_{60}$ and $T_{60}-T_{50}$. Within the experimental error, however, it is apparent that acetaldehyde and its products of oxidation are without effect on the main body of the reaction. This is in disagreement with the conclusions drawn by Bone and Hill from their experiments. It is worth mentioning that according to Prettre† aldehyde-hydrocarbon-air mixtures will only explode at high partial pressures of aldehyde.

The fact that aldehyde is without appreciable effect on the main body of the reaction is confirmed by analyses of the products made after runs with added aldehyde. Some typical examples are given in Table VI.

† 'Bull. Soc. Chim.,' vol. 51, p. 1132 (1932).

Table V— $\text{C}_2\text{H}_6 + 2\cdot3\text{O}_2$ + foreign substances

Run No.	PC_2H_6 , cm	Added substance	% pressure increase at completion	$T_{80}-T_{10}$, min	$T_{70}-T_{80}$, min	$\frac{T_{70}-T_{80}}{T_{80}-T_{10}}$
16	5.82	0.2 cm CH_3CHO	105	2.21	1.69	0.77
17	8.88	0.1 cm CH_3CHO	104	0.87	0.82	0.94
27	10.98	0.5 cm CH_3CHO	104	0.32	0.31	0.96
38	10.40	1.0 cm CH_3CHO	104	0.75	0.64	0.86
4	5.88	1.88 cm CH_3CHO	97	1.35	1.19	0.88
9	7.05	1.55 cm CH_3CHO at end of inhibitory period (70 mins)	100	1.24	1.12	0.90
10	6.07	1.44 cm CH_3CHO after 14 mins	100	1.97	1.11	0.56
21	7.65	5 mm H_2	103	0.97	0.92	0.95
24	5.91	14.08 cc H_2	51% followed by decrease			
13	7.79	2 mm products taken from previous run at completion	104	1.12	0.86	0.79
15	6.50	3 mm products taken from previous run at end of in- hibitory period	107	1.52	1.18	0.78
18	6.10	14.5 cm N_2	106	1.71	1.29	0.76

Table VI— $\text{C}_2\text{H}_6 + 2\cdot3\text{O}_2$

Aldehyde added	0.4%	1.1%	2.7%
CO_2	11.0	14.2†	14.3
C_2H_4	3.3	0.4	6.3
O_2	13.5	5.3	9.5
CO	43.0	40.0	48.4

† The second analysis was done on a sample taken from a reaction mixture which exploded on account of the high total pressure. Hence the CO_2 is rather higher than usual, O_2 is lower, most of the C_2H_4 has disappeared. The residue from this run was mainly hydrogen.

Nitrogen and traces of the products of reaction are also without effect on the main body of the reaction. Small quantities of hydrogen are also without effect. Large quantities of hydrogen enter into the actual reaction.

It is apparent from Table VI that the inhibition period is much more erratic than the main body of the reaction. This is in agreement with the work of Kowalsky, Sadownikow, and Tschirkow,† and of Taylor and Riblett.§

In spite of the erratic behaviour, however, it is possible to draw certain general conclusions.

(a) The length of the inhibition period diminishes with increasing ethane concentration.

(b) The inhibition period is shortened by diminishing the time of pumping or by adding traces of products. Under these conditions the reproducibility is much better than in a thoroughly pumped out vessel.

† 'Phys. Z. Sowjet.', vol. 1, p. 451 (1932).

§ 'J. Phys. Chem.', vol. 35, p. 2667 (1931).

(c) In the same vessel, there is a slight diminution in the inhibition period in successive runs.

(d) The inhibition period is intensified in a new bulb, or by baking out 750 °C.

(e) The effect of hydrogen is similar to that of traces of the products.

(f) The addition of large amounts of nitrogen seems to increase the inhibition period.

Table VII—The Inhibition Period

Run No.	PC ₂ H ₆ , cm	Added substance	Inhibition† period, min	Remarks
26	11.70	None	16	Pumped 24 hours
29	11.30	"	10	" 24 "
28	11.10	"	13	" 24 "
22	11.00	"	18	" 48 "
23	10.40	"	31	" 5 "
12	8.23	"	60	" 48 "
8	7.80	"	40	" 1 "
37	7.53	"	25	Pumped 1 hour after No. 36
36	7.27	"	48	Heated to 750° C and pumped 0 hours
3	7.20	"	30	Pumped 1 hour
6	7.03	"	30	" 24 hours
35	6.97	"	60	" 4 "
34	6.54	"	70	" 48 "
11	6.45	"	50	Pumped 24 hours, ethane put in first, oxygen later
7	6.29	"	70	Pumped 24 hours
2	6.23	"	35	" 1 hour
1	5.77	"	62	First run in new bulb
13	7.78	2 mm products taken at completion	36	—
15	6.52	3 mm products taken at end of inhibition period	38	—
18	6.10	15.50 cm N ₂	83	Pumped 1 hour
19	5.95	14.14 cm N ₂	65	" 24 hours
21	7.65	5 mm H ₂	30	Pumped 1 hour
24	5.92	14.14 cm H ₂	36	" 36 hours
25	7.02	16.74 cm H ₂	28	" 0.5 hour
17	8.90	Trace of CH ₃ CHO	35	—
27	11.00	5 mm CH ₃ CHO	8	—
5	6.59	1.4 cm CH ₃ CHO	0.5	—
4	5.89	2.1 cm CH ₃ CHO	1	—
38	10.40	1 cm CH ₃ CHO added after 6 mins. Reaction began immediately		
10	6.06	1.7 cm CH ₃ CHO added after 14 mins. Reaction began immediately		
16	5.83	2 mm CH ₃ CHO	8	Bulb filled with CH ₃ CHO. Stood for 5 mins. Pumped down to 2 mm
20	7.53	1 cm of products from a CH ₃ CHO-O ₂ run	45	—

† The inhibition period has been taken as the time from the start of the reaction until the pressure increases 2.0 mm.

(g) Traces of acetaldehyde, or of the products of acetaldehyde oxidation have an effect similar to that of the products of the reaction. 2 or 3 mm of aldehyde cut down the period enormously, while larger quantities practically eliminate it.

It is evident that the inhibition period must have its origin in a surface effect. Aldehyde, although it exerts no influence on the main process in the gas, must have a very pronounced effect on the processes connected with the inhibition period.

The Oxidation of Ethylene-Ethane Mixtures

Four runs were made with ethane-ethylene-oxygen mixtures. The data are given in Table VIII.

Table VIII

I		II		III		IV	
$C_2H_4 = 5.68$ cm		5.29 cm		9.00 cm		9.42 cm	
$C_2H_6 = 8.21$ cm		7.65 cm		1.31 cm		1.37 cm	
$O_2 = 30.59$ cm		28.40 cm		22.70 cm		23.78 cm	
Time mins	ΔP , cm	Time, mins	ΔP , cm	Time, mins	ΔP , cm	Time, mins	ΔP , cm
0	0	0	0	0	0	0	0
3	0.04	3	0.10	19	0.22	15	0.10
5	0.35	5	0.25	25	0.55	22	0.40
7	4.55	6	0.75	29	1.00	28	1.11
8	10.05	7	2.00	33	2.10	31	2.43
9	10.75	8	5.90	35	3.74	33	4.10
10	10.75	9	10.28	36	5.59	34	6.74
12	10.75	10	10.28	37	8.45	35	10.02
15	10.75	11	10.28	38	10.02	36	10.60
				40	10.02	38	10.60
ΔP at completion assuming 55% for C_2H_4 and 10% for C_2H_6		10.47		9.76		10.17	
						10.65	

The fact that the pressure change at completion in the mixtures is the same as that calculated for the separate reactants shows that there is no fundamental change in mechanism.

In runs III and IV the C_2H_4 concentration is so low that, in the absence of C_2H_6 , it would give an inhibition period of 15–20 minutes. The C_2H_6 pressure is such as to give one of about 15–20 minutes also. Hence it is not surprising that the inhibition period is unaffected by the addition of C_2H_4 . It is evident that C_2H_4 and C_2H_6 are not interchangeable in the processes which occur in the inhibitory stage. The main body of the reaction is likewise unaffected to any great degree, as may be shown by calculating T_{70} – T_{80} and T_{80} – T_{90} .

The data for run II are plotted in fig. 2. It will be seen that there is an inhibition period of about 4 minutes. This corresponds to the behaviour of C_2H_4 alone at the partial pressure used here. After the inhibition period the reaction proceeds very rapidly (curve A). Curves B and C show the rates at which C_2H_6 and C_2H_4 at the partial pressures used would react if they were entirely independent of one another. It is apparent that the rate of oxidation of the mixture is much greater than the sum of the rates for the single components. Curve D shows the rate of oxidation of pure C_2H_6 at a pressure approaching the sum of those of the hydrocarbons in curve A. The similarity in the two curves shows that C_2H_4 and C_2H_6 are evidently interchangeable so far as the chain process is concerned.

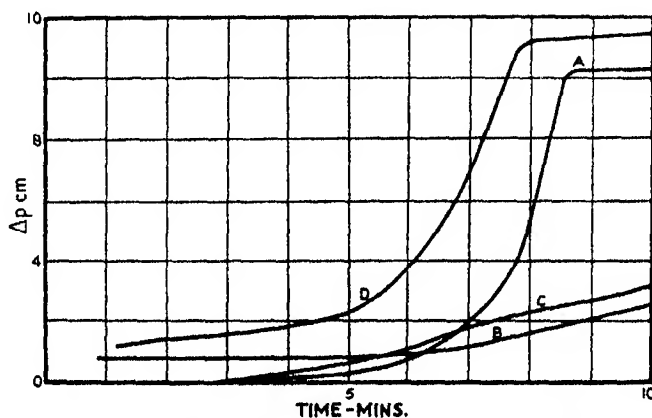


FIG. 2—The oxidation of mixtures of ethane and ethylene. A, 5.29 cm C_2H_6 + 7.65 cm. C_2H_4 + 28.40 cm O_2 ; B, 5.29 cm C_2H_6 + 11.62 cm O_2 ; C, 7.65 cm C_2H_4 + 16.83 cm O_2 ; D, 11.07 cm C_2H_6 + 25.30 cm O_2 .

The Effect of Surface

Runs were made with C_2H_6 - O_2 mixtures in a reaction vessel packed with short lengths of quartz tubing. With fresh surfaces the inhibition period was decreased. Thus in two runs at about 10 cm pressure the inhibition periods were 6 and 8 minutes. This is about one-sixth the value for the empty bulb under similar conditions, and the ratio of new surface to old was approximately 6:1. It is therefore evident that the processes involved in the inhibitory period are surface reactions. The process subsequent to the inhibitory period was greatly suppressed, pointing to a breaking of chains at the wall.

In the empty bulb the ageing of the walls was very slight. In the packed bulb the effect was enormous, and after a few runs the reaction was practically

stopped. This was probably due to a slight deposit of carbon which was formed. No such deposit occurred in the empty bulb.

In the packed bulb the addition of acetaldehyde and of ethylene had comparatively little effect.

It is apparent that the reaction process is considerably altered in the packed bulb. Thus the pressure change at completion is reduced from 105 to about 45%. This is in line with the results of analyses, as shown in Table IX.

Table IX—Analyses in Packed Bulb

	Original mixture	At end of inhibitory period, %	At completion %
CO ₂	—	0.6	23.6
C ₂ H ₄	—	1.2	5.7
O ₂	67.0	65.0	0.8
CO	—	0.0	28.4
C ₂ H ₆	28.5	18.0	5.0
H ₂	—	4.1	0

Discussion

Previous Work—Before discussing the present work, it is necessary to review briefly the results of previous investigations on the oxidation of ethane.

Bone and Hill (*loc. cit.*) studied the reaction in a silica bulb at temperatures between 290 and 323° C, and at total pressures from 400 mm to 790 mm. Their main interest was in the products of the oxidation, and very little attention was paid to the kinetics of the reaction. They observed a very long inhibition period followed by a typical autocatalytic pressure-time curve. Increase in pressure decreased the inhibition period. Packing the vessel strongly retarded the reaction. They also investigated the effect of a number of foreign substances on the inhibition period, and found that iodine, water, hydrogen peroxide, ethyl alcohol and formaldehyde cut down the period of inhibition, while acetaldehyde caused instant inflammation. As a result of analyses at the end of the inhibition period, they concluded that there was no detectable reaction during this period.

The results of analyses at completion are in general agreement with those reported here. Exact agreement can hardly be expected in view of the difference in the temperature ranges of the two investigations. Their analytical results favoured Bone's hydroxylation scheme for the products of oxidation.

The only disagreement between the results of Bone and Hill and the present investigation arises in connection with the effect of added acetaldehyde on the rate of oxidation of ethane. The pressures used by them were much higher

than those reported here, it is true, but if explosion occurs at 310° C, it would certainly be expected at 450° C, and in the present work no explosions were obtained even with 20% acetaldehyde. The discrepancy may possibly be explained by the observations of Prettre who found that acetaldehyde-air mixtures would explode within a certain temperature range, but not at higher temperatures.

Taylor and Riblett (*loc. cit.*) investigated the kinetics of the ethane-oxygen reaction from 450° to 480° C in a pyrex bulb. They used pressures comparable to those used here. They found an average inhibition period of about two minutes. The pressure increase at completion was about 21% relative to the total initial pressure, which is rather lower than that of the present investigation. They found that packing the vessel caused only a slight diminution in the rate. If, however, the vessel was packed with pyrex glass coated with KCl, the reaction was virtually stopped. The inhibition period was found to be entirely erratic. It is apparent that silica and pyrex behave quite differently. Their results, however, are in general agreement with ours. They suggested that the inhibition period was caused by a reaction accompanied by little or no pressure change.

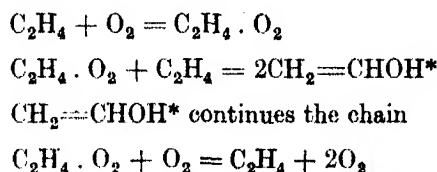
Finally, the work of Kowalsky, Sadownikow, and Tschirkow was done at about 600° C and 7 cm pressure. Here again a very short inhibition period of about 30 seconds was found. The results were quite erratic, and the surface appeared to age. This is in agreement with the present work. The authors concluded that the ageing effect was due to the removal of an adsorbed layer by the reactants.

If the reaction vessel were heated to 1000° C and evacuated, the rate at 600° C was found to be faster than before. This is in contrast to the present work, since we have found that heating to 750° C and evacuating intensifies the inhibition period. It is possible, however, that heating to 1000° C may have caused a permanent change in the quartz surface, since some devitrification occurs at such a temperature. The maximum pressure increase relative to ethane was found by them to be 50%. This is definitely lower than that found here, but at the much higher temperatures which they used oxidation of CO to CO₂ would occur.

The Theory of Hydrocarbon Oxidation—The hydroxylation theory of Bone furnishes a very valuable scheme for the prediction of the products of gaseous oxidation reactions. It makes no attempt, however, to discuss the mechanism of the process. The first attempt in this direction was that of Egerton† who

† 'Nature,' vol. 121, p. 10 (1928).

assumed that the oxidation proceeded through the initial formation of a peroxide. Thompson and Hinshelwood† suggested a fusion of the peroxide and hydroxylation ideas for the oxidation of ethylene, viz. :—



or

= stable oxidation products.

One of the most useful developments of the peroxide theory was made by Bodenstein.‡ He attempted to explain both the products and the kinetics of the process. Thus for ethylene his scheme may be represented as :—

- (1) $\text{C}_2\text{H}_4 = \text{C}_2\text{H}_4^*$
- (2) $\text{C}_2\text{H}_4^* + \text{O}_2 = \text{C}_2\text{H}_4 \cdot \text{O}_2$
- (3) $\text{C}_2\text{H}_4 \cdot \text{O}_2 + \text{C}_2\text{H}_4 = \text{C}_2\text{H}_4^* + \text{CHOH} = \text{CHOH}$
- (4) $\text{C}_2\text{H}_4 \cdot \text{O}_2 + \text{O}_2 = \text{Products of oxidation}$
- (5) $\text{C}_2\text{H}_4 \cdot \text{O}_2 = \text{Products of oxidation.}$

The main objection to this scheme is that it leads to an induction period only if we assume the presence of some inhibitor. Semenov§ claims that the Bodenstein scheme is not applicable to the oxidation of saturated hydrocarbons.

A number of investigations|| have suggested that the oxidation of saturated hydrocarbons is initiated by a primary dehydrogenation of the paraffin.

The work of Pease on the oxidation of propane and butane gave definite indications that the following three homogeneous overall reactions occurred :—

- (1) $\text{C}_3\text{H}_8 = \text{C}_3\text{H}_6 + \text{H}_2$
- (2) $\text{C}_3\text{H}_8 + \frac{1}{2}\text{O}_2 = \text{C}_3\text{H}_6 + \text{H}_2\text{O}$
- (3) $\text{C}_3\text{H}_8 + 2\text{O}_2 = \text{CO} + 2\text{H}_2\text{O} + \text{CH}_3\text{CHO.}$

At lower temperatures reaction (3) predominated and showed the characteristics of a chain reaction. At higher temperatures reactions (1) and (2) became

† 'Proc. Roy. Soc.,' A, vol. 125, p. 277 (1929).

‡ 'Z. phys. Chem.,' B, vol. 12, p. 141 (1931).

§ 'Phys. Z. Sowjet.,' vol. 4, p. 553 (1932).

|| Brunner, 'Helv. Chim. Acta.,' vol. 11, p. 881 (1928); Berl, Heise and Winnacker, 'Z. phys. Chem.,' A, vol. 139, p. 453 (1928); Pease, 'J. Amer. Chem. Soc.,' vol. 51, p. 1839 (1929); Lewis, 'J. Chem. Soc.,' p. 1555 (1927), p. 759 (1929), p. 58 (1930).

important. Experiments in a packed bulb indicated that the surface played a definite part in the process.

Conclusions from this Investigation—The following are the main conclusions which can be drawn from the present work.

(1) There is a long period of inhibition, which decreases as the total pressure is raised. Heating to a high temperature, or long pumping intensifies the inhibition period, while packing cuts it down.

(2) Aldehydes, hydrogen, and the products of the reaction reduce or eliminate the inhibition period. Nitrogen seems to increase it.

(3) Chains started by ethylene can be continued by ethane.

(4) Analysis shows that hydrogen and ethylene are present at the end of the inhibitory period, and throughout the reaction.

(5) The main reaction is strongly suppressed by packing.

Discussion

The erratic nature of the inhibition period and its dependence on the history of the reaction vessel make it apparent that it is a surface effect. The fact that packing decreases the inhibition period shows that it is dependent on a heterogeneous reaction rather than on a chain breaking effect at the surfaces. It may therefore be assumed that the progress of the main reaction is dependent upon the accumulation of products formed heterogeneously during the inhibition period.

The explanation of the action of aldehydes, hydrogen and the products of the reaction in cutting down the inhibition period must necessarily be *ad hoc*. It is first necessary to decide what reactions occur at the surface during the inhibition period. Since ethylene is formed the most likely processes are



and



The first process is probably too slow relative to the second to be of much importance. The second reaction will occur when an adsorbed ethane molecule finds itself adjacent to an atom of oxygen. We may possibly explain the effect of added substances on the rate of reaction by assuming that on a clean surface oxygen is irreversibly adsorbed in the manner postulated by Langmuir to explain processes occurring on tungsten filaments. Ethane is thus kept off the surface and no reaction occurs. The presence of products, aldehydes, etc., prevents the formation of a complete layer, and on their evaporation

ethane may be adsorbed in the gaps and further free the surface of oxygen by reacting with it.

In any case, no matter what the mechanism of the surface may be, the inhibition process unquestionably leads to the formation of ethylene.

The main reaction is a homogeneous chain process. The effect of packing indicates that the chains are started in the gas and broken at the wall. It has already been suggested that the primary process in the oxidation of ethane is dehydrogenation. The present work strongly confirms this idea in a modified form, viz., that the main chain process is the oxidation of ethylene, but that chains started by ethylene may be carried by ethane, ethylene being regenerated in the process. The evidence for this view is of several kinds.

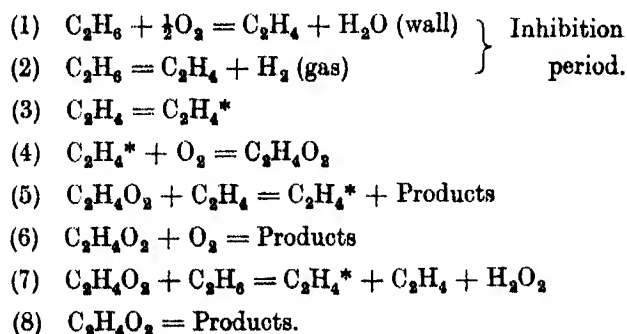
(1) Ethylene was always present during the reaction. In one experiment in which a sample was withdrawn at the half-way stage, the ethylene present amounted to 63% of the ethane which had reacted.

(2) It is apparent from fig. 2 that ethane and ethylene are interchangeable during the main chain process.

(3) In the packed bulb the chain process is almost entirely suppressed as in the oxidation of ethylene. This would naturally occur if the reaction consists mainly of ethylene-oxygen chains which can be continued in ethane.

(4) Acetaldehyde has no effect on the main chain process as with ethylene-oxygen mixtures.

The following mechanism for the reaction may therefore be suggested :—



On this basis reactions (4), (5) and (7) constitute the chain process. The chains are broken by (6), (8) or by the wall.

From the above we have

$$-\frac{d}{dt}(\text{C}_2\text{H}_6) = K_7(\text{C}_2\text{H}_6)(\text{C}_2\text{H}_4\text{O}_2).$$

Evaluating $(C_2H_4O_2)$ by putting its rate of formation equal to its rate of destruction in the steady state we obtain

$$-\frac{d}{dt}(C_2H_6) = \frac{K_7K_8(C_2H_4)(C_2H_6)}{K_6(O_2) + K_8}.$$

It is obviously not entirely justifiable to treat the steady state concentration of C_2H_4 in the same way as that of $C_2H_4O_2$. However, this method will give a result which is approximately correct, and we obtain

$$(C_2H_4) = \frac{K_7(C_2H_6)(C_2H_4O_2)}{K_2 + K_5(C_2H_4O_2)}.$$

K_3 is obviously negligible compared to $K_5(C_2H_4O_2)$, since the one represents the initial rate of formation of $C_2H_4^*$, and the other its formation in the chain process. Hence we have

$$(C_2H_4) = \frac{K_7(C_2H_6)}{K_5},$$

whence

$$-\frac{d}{dt}(C_2H_6) = \frac{K_7^2K_8(C_2H_6)^2}{K_5K_6(O_2) + K_5K_8}.$$

On the basis of the above equation the reaction should be retarded by excess oxygen, and more or less independent of oxygen when ethane is in excess. This is in general agreement with the work of Taylor and Riblett and with the work of Pease on the higher saturated hydrocarbons.

On account of the form of pressure-time curves it is very difficult to infer the order of the reaction with respect to ethane from experimental data. Depending on the stage of the reaction chosen for comparison the apparent ethane order lies between 1.5 and 3.5. The equation therefore, in spite of the approximations involved, reproduces the experimental facts in a satisfactory manner.

The fundamental basis of the above scheme is the Bodenstein mechanism for the oxidation of ethylene, together with the assumption that ethane participates in the ethylene-oxygen chains and is dehydrogenated in the process. It is suggested that the oxidation of all saturated hydrocarbons proceeds in an analogous manner.

Further work is in progress on the oxidation of acetylene, ethylene, ethane and methane.

Summary

An investigation has been made of the oxidation of ethane and its mixtures with acetaldehyde and ethylene.

Acetaldehyde virtually eliminates the inhibition period but has no effect on the subsequent reaction. In the main chain process ethane and ethylene are practically interchangeable.

It is concluded that—

(a) The inhibition period is a surface process which leads to the production of ethylene.

(b) The oxidation of saturated hydrocarbons occurs through a primary dehydrogenation, followed by a chain oxidation of the olefine thus produced. Further cracking of the saturated hydrocarbon occurs during the oxidation of the olefine.

Problem of the Sedimentation Equilibrium in Colloidal Suspensions

By S. LEVINE, Department of Physics, University of Toronto

(Communicated by J. C. McLennan, F.R.S.—Received April 10, 1934)

§ 1. *Introduction*

As is well known, in 1909, Perrin investigated the sedimentation equilibrium of colloidal suspensions and obtained a logarithmic decrease in concentration with the height, the result being confirmed by other workers. This was in agreement with the distribution law for “ideal” behaviour of the sol,

$$\log n = \log n_0 + v_p g d (\rho_1 - \rho_2)/kT, \quad (1)$$

where n and n_0 are the number of particles per cubic centimetre at depths d and 0 respectively, v_p is the volume of a single particle, ρ_1 and ρ_2 are densities of particles and dispersing medium respectively, g , k , T having their usual meaning. Costantin,* however, obtained departures from this condition for n greater than 8×10^{10} and interpreted his results in terms of repulsive forces due to the charges on the particles. Perrin modified equation (1) by assuming a law of the van der Waals' type and obtained agreement with observations up to the highest concentrations investigated ($n = 6 \times 10^{11}$). In all these results normal behaviour was found up to values of n greater than 10^{10} .

Burton,† however, working with vessels about 100 cm long, has shown that the concentration is permanently uniform below a very thin layer near the

* ‘Ann. Physik,’ vol. 3, p. 101 (1915).

† Burton and Bishop, ‘Proc. Roy. Soc.,’ A, vol. 100, p. 414 (1921); Burton and Currie, ‘Phil. Mag.,’ vol. 47, p. 721 (1924).

upper surface. To explain this there was introduced the concept of "limiting concentration" arising as a result of the repulsive forces between the particles. Porter and Hedges* and Barkas,† using cells of length of the order of 1 cm, have obtained similar results. To account for these deviations Porter introduced a correcting term in the osmotic pressure of the sol similar to the "b" in van der Waals' equation. In contrast with the earlier work, in all these experiments uniform concentration was obtained at depths exceeding 1 mm corresponding to departures from the ideal laws at $n = 10^6$, uniform concentration being attained for $n = 10^7$. Using tubes of 21–24 cm long Laird‡ has reported a uniform distribution throughout the greater portion of the sol. However, he does not give the values of n and his first reading is a few centimetres from the surface.

More recently confirmation of the results of earlier experiments has been obtained by Johnston and Howell§ and by McDowell and Usher||. Using cells 8.3 mm in height the former report ideality, but do not state their maximum value of n , the only value quoted being 4×10^8 . The latter found no deviation down to a depth of 9 mm with concentration up to $n = 10^{12}$.

§ 2. *Plan of the Paper*

Due to the apparent contradictions described above, it would be very desirable to find theoretically the distribution law for the sedimentation equilibrium. A method for deriving such an expression is given in this paper. The assumption is made that owing to the charges on the colloidal particles and the surrounding ions of the electrolyte present, forming the so-called "ionic atmosphere," two particles repel one another when their atmospheres overlap. The development is carried out in the following stages.

In § 3, using the Boltzmann distribution law, equation (1) is modified by the addition of a term for the potential energy of the particles associated with their charges and atmospheres. By an application of the methods of statistical mechanics an expression for this energy is obtained in a form $A_1n + A_2n^2 + A_3n^3 + \dots$, where A_1, A_2, A_3, \dots , are constants of which only the first three are evaluated. Here A_r , for example, is given by an integral, involving the

* 'Trans. Faraday Soc.,' vol. 18, p. 91 (1922); vol. 19, p. 1 (1923); 'Phil. Mag.,' vol. 44, p. 641 (1922).

† 'Trans. Faraday Soc.,' vol. 21, p. 66 (1925).

‡ 'J. Phys. Chem.,' vol. 31, p. 1034 (1927).

§ 'Phys. Rev.,' vol. 35, p. 374 (1930).

|| 'Proc. Roy. Soc.,' A, vol. 138, p. 133 (1932).

energy of r particles considered as isolated from all the others, taken over the $3r$ -dimensional phase space.

To evaluate these integrals it is necessary to obtain E_{12} , the change in electrostatic energy involved in an encounter of two particles. This is carried out in § 4 and § 5. In § 4 the potential about a particle is derived by using the differential equation employed by Debye and Hückel in their theory of electrolytic solutions. In § 5 an attempt is made to solve this equation for a binary encounter. Then E_{12} is found by integrating the electrical energy density over the surface of the two particles and their surrounding atmospheres.

In § 6, the constants A_1 , A_2 , and A_3 are found for different values of the charges on the particles and of the concentrations of the electrolyte. The results indicate departure from (1) when n reaches values ranging from $n = 1.6 \times 10^{13}$ to $n = 4.0 \times 10^{14}$ with corresponding limiting concentrations lying between $n = 2.1 \times 10^{14}$ and $n = 5.5 \times 10^{15}$. These values are compared with those of the different experiments mentioned above.

With a slight modification the formula derived for the distribution is applied to sedimentation in the centrifuge and numerical cases are given in § 6.

In § 7, a discussion of the method is given, with a suggestion for a more accurate treatment. The questions of hydration of the particles and the hydrostatic pressure due to the electrostrictive forces are mentioned.

§ 3. Development of the Basic Formula

Using the Boltzmann distribution law,

$$n = n_0 \exp [1/kT (mgd - E + E_0)], \quad (2)$$

where E and E_0 are the energies of the particles at depths d and 0 (the top of the column) associated with their charges and ionic atmospheres, and $m = v_p (\rho_1 - \rho_2)$. To find E we use the method of partition functions as developed by Ursell.* The sol is divided into small elements each of which, treated as an independent assembly, contains a large number ν of particles, and occupies a volume v . The partition function for the electrostatic energy is defined by

$$B(\vartheta) = \int \dots \int \vartheta^w \prod_{r=1}^{\nu} (dx \, dy \, dz)_r,$$

* 'Proc. Camb. Phil. Soc.,' vol. 23, p. 685 (1927); see also Fowler, "Statistical Mechanics," chap. 8.

where $\vartheta = \exp(-1/kT)$, $w = vE$ is the energy of the v particles and depends only on the position co-ordinates; the integration is to be extended over the $3v$ -dimensional phase-space. The average potential energy of the assembly is at once given by the relation

$$w = \vartheta \frac{\partial}{\partial \vartheta} \log B(\vartheta). \quad (3)$$

Thus the problem reduces to the evaluation of $B(\vartheta)$.

In order to make successive approximations to $B(\vartheta)$ and hence to \bar{w} by including particle encounters of increasing order we use the formula given by Ursell,*

$$B(\vartheta) = v^v e^{vh}, \quad (4)$$

where h is a function of a certain quantity x_r to be defined below such that

$$h = x_2, \quad (5, i)$$

if we consider only binary encounters,

$$h = x_2 - 2x_2^3 + x_3, \quad (5, ii)$$

on including ternary encounters,

$$h = x_2 + (x_3 - 2x_2^3) + (x_4 - 6x_2x_3 + 20x_2^3/3), \quad (5, iii)$$

with encounters of the fourth order and so on. As the concentration increases, the contribution from these higher orders becomes more and more important.

Let ϑ_r represent $\vartheta^{E_{12\dots r}}$, where $E_{12\dots r}$ is the mutual potential of r particles, all others being considered absent. Since the contribution to $E_{12\dots r}$ from gravity has been accounted for in the term mgd in (2) we need only treat the purely electrostatic energy. It will be seen that we may linearly superpose the fields due to the individual particles in a close encounter, so that

$$E_{123} = E_{12} + E_{23} + E_{13}, \quad E_{1234} = E_{12} + E_{23} + E_{31} + E_{14} + E_{24} + E_{34}, \text{ etc.} \quad (6)$$

We introduce a set of quantities u_r , the general form being given by Ursell (*loc. cit.*)† and the first four of which are

$$\left. \begin{aligned} u_1 &= 1, & u_2 &= \vartheta_2 - 1, & u_3 &= \vartheta_3 - \Sigma \vartheta_2 + 2 \\ u_4 &= \vartheta_4 - (\Sigma \vartheta_3 + \Sigma \vartheta_2 \vartheta'_2) + 2\Sigma' \vartheta_2 - 6 \end{aligned} \right\} \quad (7)$$

* See footnote, p. 599.

† See Fowler, *op. cit.*, p. 179.

where

$$\left. \begin{aligned} \Sigma \vartheta_2 &= \vartheta^{E_{11}} + \vartheta^{E_{22}} + \vartheta^{E_{12}}, & \Sigma \vartheta_3 &= \vartheta^{E_{111}} + \vartheta^{E_{112}} + \vartheta^{E_{121}} \\ \Sigma \vartheta_2 \vartheta'_2 &= \vartheta^{E_{11}+E_{22}} + \vartheta^{E_{11}+E_{12}} + \vartheta^{E_{12}+E_{22}} \\ \Sigma \vartheta'_2 &= \vartheta^{E_{11}} + \vartheta^{E_{22}} + \vartheta^{E_{12}} + \vartheta^{E_{11}} + \vartheta^{E_{22}} + \vartheta^{E_{12}} \end{aligned} \right\}. \quad (8)$$

Then x_r is defined by the relation

$$x_r v^r r! / v^{r-1} = \int u_r \prod_{a=1}^r (dx dy dz)_a, \quad (9)$$

the integral being taken over the $3r$ -space of the r particles.

For a binary encounter ($r = 2$) (3), (4), and (5, i) give

$$\bar{w} = v \vartheta \frac{\partial x_2}{\partial \vartheta}. \quad (10)$$

Using (7) and (9) for $r = 2$

$$x_2 = \frac{v}{2v} \int (\vartheta_2 - 1) dx dy dz = \frac{2\pi v}{v} \int_{2a}^{\infty} (\vartheta_2 - 1) r_{12}^2 dr_{12}, \quad (11)$$

where x, y, z are the relative co-ordinates of the two particles, r_{12} is the distance between them and a is the radius of either particle. Then from (10),

$$\bar{w} = \frac{2\pi v^2}{v} \int_{2a}^{\infty} E_{12} \vartheta_2 r_{12}^2 dr_{12} = A_1 v^2, \text{ say.} \quad (12)$$

For a ternary encounter ($r = 3$) from (3), (4), and (5, ii)

$$\bar{w} = v \left[(1 - 2x_2) \frac{\partial x_2}{\partial \vartheta} + \frac{\partial x_3}{\partial \vartheta} \right]. \quad (13)$$

Here

$$v (1 - 2x_2) \frac{\partial x_2}{\partial \vartheta} = \left[1 - \frac{4\pi v}{v} \int_{2a}^{\infty} (\vartheta_2 - 1) r_{12}^2 dr_{12} \right] \left[\frac{2\pi v^2}{v} \int_{2a}^{\infty} E_{12} \vartheta_2 r_{12}^2 dr_{12} \right]. \quad (14)$$

From (7) and (9) for $r = 3$

$$v \vartheta \frac{\partial x_3}{\partial \vartheta} = \frac{v^2}{v^3 3!} \left[v \vartheta \frac{\partial}{\partial \vartheta} \int [\vartheta_3 - \Sigma \vartheta_2 + 2] dw_3 \right], \quad (15)$$

where $dw_r = \prod_{a=1}^r (dx dy dz)_a$. By (6),

$$v \vartheta \frac{\partial}{\partial \vartheta} \int \vartheta_3 dw_3 = v \int E_{123} \vartheta_3 dw_3 = 3v \int E_{123} \vartheta_3 dw_3, \quad (16)$$

since the integral is symmetrical with respect to the three particles. From (8) owing to the identical role played by each pair of particles

$$\int \Sigma \vartheta_2 dw_3 = 3 \int \vartheta^{E_{12}} dw_3,$$

giving

$$v\vartheta \frac{\partial}{\partial \vartheta} \int \Sigma \vartheta_2 dw_3 = 3v \int E_{12} \vartheta^{E_{12}} dw_3. \quad (17)$$

Substitution of (16) and (17) in (15) gives

$$v\vartheta \frac{\partial x_3}{\partial \vartheta} = \frac{v^3}{2v^3} \int E_{12} (\vartheta_3 - \vartheta^{E_{12}}) dw_3 = \frac{v^3}{2v^3} \int E_{12} \vartheta^{E_{12}} (\vartheta^{E_{12}+E_{23}} - 1) dw_3. \quad (18)$$

To evaluate (18) we consider a configuration of three particles P_1 , P_2 , and P_3 and integrate in steps in the following manner. We keep P_1 and P_2 inside volume elements dw_1 and dw'_1 at a distance r_{12} apart and allow P_3 to move over the whole space available. Introduce elliptic co-ordinates

$$\xi = \frac{r_{13} + r_{23}}{r_{12}}, \quad \eta = \frac{r_{13} - r_{23}}{r_{12}}, \quad \phi, \quad (19)$$

where ϕ is the azimuthal angle about line P_1P_2 , r_{13} and r_{23} being the distances from P_3 to P_1 and P_2 respectively. Putting

$$dx dy dz = \frac{r_{12}^3}{8} (\xi^2 - \eta^2) d\xi d\eta d\phi,$$

and integrating for all positions available to P_3 , the contribution to (18) is

$$\frac{\pi}{8} \frac{v^3}{v^3} E_{12} r_{12}^3 dw_1 dw'_1 \iint G d\xi d\eta, \quad (20)$$

where $G = (\vartheta^{E_{12}+E_{23}} - 1) (\xi^2 - \eta^2)$ and where we have integrated with respect to ϕ . From the conditions $r_{13} \geq 2a$, $r_{23} \geq 2a$ the region of integration in (20) is all space external to two spheres with centres P_1 and P_2 and radius $2a$. The surfaces of these spheres are given by

$$\eta = \frac{4a}{r_{12}} - \xi, \quad (r_{13} = 2a), \quad \eta = \xi - \frac{4a}{r_{12}}, \quad (r_{23} = 2a). \quad (21)$$

On integrating over all space the integral in (20) is $\int_1^\infty d\xi \int_{-1}^{+1} G d\eta$. We must subtract from this the integrals taken inside the spheres $r_{13} = 2a$ and $r_{23} = 2a$;

the first of these is $\int_1^\delta d\xi \int_{-1}^{\frac{4a}{r_{12}} - \xi} G d\eta$ and the second is $\int_1^\delta d\xi \int_{\xi - \frac{4a}{r_{12}}}^1 G d\eta$,

where $\delta = \frac{4a + r_{12}}{r_{12}}$. Using these results, (20) becomes

$$\frac{\pi}{8} \frac{v^3}{v^3} E_{12} r_{12}^3 dw_1 dw'_1 \left[\int_\delta^\infty d\xi \int_{-1}^{+1} G d\eta + \int_1^\delta d\xi \int_{\frac{4a}{r_{12}} - \xi}^1 G d\eta \right].$$

It is to be observed that this holds only for $r_{12} \geq 4a$. The necessary modification when $r_{12} < 4a$ is indicated in § 6.

We now put $dw'_1 = r_{12}^2 \sin \theta_{12} d\theta_{12} d\phi_{12} dr_{12}$, where r_{12} , θ_{12} , and ϕ_{12} are the polar co-ordinates of P_2 with P_1 as origin, and we integrate for all positions of P_2 . To account finally for integration with respect to P_1 , dw_1 is replaced by v . Thus (18) reads

$$\vartheta v \frac{\partial x_3}{\partial \vartheta} = \frac{\pi^2}{2} \frac{v^3}{v^3} \int_{2a}^\infty E_{12} \vartheta^{E_{12}} r_{12}^5 dr_{12} \left[\int_\delta^\infty d\xi \int_{-1}^{+1} G d\eta + \int_1^\delta d\xi \int_{\frac{4a}{r_{12}} - \xi}^1 G d\eta \right], \quad (22)$$

integration of θ_{12} and ϕ_{12} giving 4π . Using (14) and (22), (13) may be written in the form $\bar{w} = A_1 v^2 + A_3 v^3$.

For an encounter of the 4th order ($r = 4$), according to (3), (4), and (5, iii)

$$\begin{aligned} \bar{w} &= v\vartheta \left[\frac{\partial x_3}{\partial \vartheta} + \frac{\partial x_3}{\partial \vartheta} - 2x_2 \frac{\partial x_2}{\partial \vartheta} + \frac{\partial x_4}{\partial \vartheta} + 6x_3 \frac{\partial x_2}{\partial \vartheta} - 6x_2 \frac{\partial x_3}{\partial \vartheta} + 20x_2^2 \frac{\partial x_2}{\partial \vartheta} \right] \\ &= A_1 v^2 + A_2 v^3 + A_3 v^4, \end{aligned} \quad (23)$$

where

$$A_3 v^4 = v\vartheta \left[\frac{\partial x_4}{\partial \vartheta} + 6x_3 \frac{\partial x_2}{\partial \vartheta} - 6x_2 \frac{\partial x_3}{\partial \vartheta} + 20x_2^2 \frac{\partial x_2}{\partial \vartheta} \right]. \quad (24)$$

Use of (11) and (22) leads to the expressions for all the quantities (24) except x_3 and $v\vartheta \frac{\partial x_4}{\partial \vartheta}$.

Applying (6), (7), and (8), (9) reads for $r = 3$

$$\begin{aligned} x_3 &= \frac{v^2}{3! v^3} \int [\vartheta^{E_{11} + E_{22} + E_{33}} - \vartheta^{E_{11}} - \vartheta^{E_{22}} - \vartheta^{E_{33}} + 2] dw_3 \\ &= \frac{v^2}{3! v^3} \int [(\vartheta^{E_{11}} - 1)(\vartheta^{E_{22} + E_{33}} - 1) + (\vartheta^{E_{11}} - 1)(\vartheta^{E_{22}} - 1)] dw_3. \end{aligned} \quad (25)$$

The first term in the integrand gives, similarly to (22),

$$\frac{\pi^2 v^2}{6 v^3} \int_{2a}^\infty (\vartheta^{E_{11}} - 1) r_{12}^5 dr_{12} \left[\int_\delta^\infty d\xi \int_{-1}^{+1} G d\eta + \int_1^\delta d\xi \int_{\frac{4a}{r_{12}} - \xi}^1 G d\eta \right]. \quad (26, i)$$

To evaluate the second term we imagine P_3 and P_2 to be fixed in volume elements dw'_1 and dw'_1 and allow P_1 to move over all available space. The contribution is then

$$\frac{v^2}{3! v^3} dw'_1 dw''_1 (\vartheta^{E_{11}} - 1) \int (\vartheta^{E_{11}} - 1) dw_1, \quad (27)$$

the region of integration excluding the volumes $r_{12} \leq 2a$ and $r_{13} \leq 2a$. If we exclude only $r_{12} \leq 2a$ then the integral in (27) is independent of r_{23} and so on integrating for all positions of P_2 and P_3 (27) becomes

$$\frac{v^2}{3! v^3} \left[\int (\vartheta_2 - 1) dw_1 \right]^2. \quad (26, ii)$$

We can therefore find x_3 from (26, i) and (26, ii) and the term $6x_3 v \vartheta \frac{\partial x_3}{\partial \vartheta}$ in (24) is known.

From (7), (8), and (9) for $r = 4$

$$\begin{aligned} x_4 &= \frac{v^3}{v^4 4!} \int [\vartheta_4 - (\Sigma \vartheta_3 + \Sigma \vartheta_2 \vartheta'_3) + 2\Sigma' \vartheta_2 - 6] dw_4 \\ &= \frac{v^3}{v^4 4!} \int [\vartheta^{E_{1111}} - 4\vartheta^{E_{111}} - 3\vartheta^{E_{11}+E_{21}} + 12\vartheta^{E_{11}} - 6] dw_4 \end{aligned}$$

by symmetry of the integral with respect to the four particles. Using (7), by symmetry again

$$\begin{aligned} v \vartheta \frac{\partial x_4}{\partial \vartheta} &= \frac{v^4}{v^4 4!} \int 6E_{12} [\vartheta^{E_{1111}} - 2\vartheta^{E_{111}} - \vartheta^{E_{11}+E_{21}} + 2\vartheta^{E_{11}}] dw_4 \\ &= \frac{v^4}{v^4 4!} \int 6E_{12} \vartheta^{E_{11}} [(\vartheta^{E_{11}+E_{21}+E_{31}} - 1)(\vartheta^{E_{11}+E_{21}} - 1) \\ &\quad + \vartheta^{E_{22}}(\vartheta^{E_{11}+E_{22}} - 1) - (\vartheta^{E_{11}+E_{22}} - 1)] dw_4. \end{aligned}$$

We may replace the second term in the integrand by $\vartheta^{E_{22}}(\vartheta^{E_{11}+E_{22}} - 1)$ and so obtain

$$\begin{aligned} v \vartheta \frac{\partial x_4}{\partial \vartheta} &= \frac{v^4}{v^4 4!} \int 6E_{12} \vartheta^{E_{11}} [(\vartheta^{E_{11}+E_{21}} - 1)(\vartheta^{E_{11}+E_{21}+E_{31}} - 1) \\ &\quad + (\vartheta^{E_{11}+E_{22}} - 1)(\vartheta^{E_{22}} - 1)] dw_4. \end{aligned}$$

Neglecting the volumes of P_1 , P_2 , and P_3 , when P_4 moves over the available space the second term in the integrand gives

$$\frac{v^4}{v^4 4!} \left[\int (\vartheta_2 - 1) dw_1 \right] \left[\int 6E_{12} \vartheta^{E_{11}} (\vartheta^{E_{11}+E_{22}} - 1) dw_2 \right], \quad (28, i)$$

which can be evaluated by using (11) and (22). Replacing $\vartheta^{E_{11}+E_{22}+E_{33}}$ by $\vartheta^{3E_{11}}$ the first term in the integrand gives

$$\frac{v^4}{v^4 4!} \left[\int \{(\vartheta_2)^3 - 1\} dw_1 \right] \left[\int 6E_{12} \vartheta^{E_{11}} (\vartheta^{E_{11}+E_{22}} - 1) dw_3 \right], \quad (28, ii)$$

which can similarly be calculated. It will be seen that the errors produced in the approximations in (26, ii), (28, i), and (28, ii) are small.* We now have expressions for all the terms in (24) and thus know A_2 . We shall not consider encounters of higher order.

Putting $v = 1$ cc (23) reads $\bar{w} = A_1 n^2 + A_2 n^3 + A_3 n^4$, and thus

$$E = \frac{\bar{w}}{n} = A_1 n + A_2 n^2 + A_3 n^3. \quad (29)$$

It is found that for $n_0 \leq 10^{12}$, $\exp(-E_0/kT)$ is very close to unity. Then substituting (29) for E in (2) we obtain as the law of distribution

$$n = n_0 \exp \left[\frac{1}{kT} (mgd - A_1 n - A_2 n^2 - A_3 n^3) \right]. \quad (30)$$

To evaluate A_1 , A_2 , and A_3 an expression for E_{12} is found in the next two sections. If only the term $A_1 n$ be retained then (30) is equivalent to the distribution laws obtained by Perrin and Porter when they assume laws of van der Waals' type.

§ 4. Potential about a Colloid Particle

Before finding E_{12} , we evaluate the potential ψ about a colloidal particle due to its charge and the surrounding ionic atmosphere. We assume that the electrolyte present, a uni-univalent salt, is of uniform concentration in the sol.

The method of Debye and Hückel† is employed. The density of charge at any point in the atmosphere is

$$\rho = -2n_i \epsilon \sinh \epsilon \psi / kT, \quad (31)$$

where ϵ is the electronic charge, and $n_i = \frac{\gamma N}{1000}$, γ being the concentration in mols per litre and N Avogadro's number. Then the potential satisfies the differential equation

$$\nabla^2 \psi = \frac{8\pi n_i \epsilon}{D} \sinh \epsilon \psi / kT, \quad (32)$$

* Numerical work in § 6 shows that the last term in (24), which is evaluated exactly, forms the main contribution to A_3 .

† 'Phys. Z.', vol. 24, p. 185 (1923).

or, for a spherical particle,

$$\frac{1}{r^2} \frac{d}{dr} \left(r^2 \frac{d\psi}{dr} \right) = \frac{8\pi n_1 \epsilon}{D} \sinh \epsilon \psi / kT, \quad (33)$$

r being the distance from the centre of the particle. Making the approximation

$$\sinh \epsilon \psi / kT = \epsilon \psi / kT, \quad (34)$$

(32) reduces to

$$\nabla^2 \psi = \kappa^2 \psi, \quad (35)$$

and (33) becomes

$$\frac{1}{r^2} \frac{d}{dr} \left(r^2 \frac{d\psi}{dr} \right) = \kappa^2 \psi, \quad (36)$$

the solution being

$$\psi = \frac{Q}{D} \frac{e^{\kappa a}}{(1 + \kappa a)} \frac{e^{-\kappa r}}{r}. \quad (37)$$

Here Q is the charge on the particle, a is its radius and $\kappa^2 = \frac{8\pi n_1 \epsilon^2}{DkT}$. The value

of ψ for colloidal particles is too large to permit the approximation (34) so that a more exact solution of (33) must be used.

According to Gronwall, La Mer, and Sandved* the potential at the surface of the particle is given by the infinite series

$$\psi_0 = \sum_{m=1}^{\infty} \frac{\epsilon^{2m-1} z^m}{(Da)^m (-kT)^{m-1}} \psi_m(x_0, x_0), \quad (38)$$

where $x_0 = \kappa a$, $Q = ze$ in our notation, and ψ_m are certain functions of which we shall require only the first few. For a uni-univalent salt, a symmetrical type, $\psi_m = 0$ if m is even. When m is odd

$$\psi_m(x, x) = X_m(x),$$

where $X_1(x) = \frac{1}{1+x}$, and tables of values are given† for $X_3(x)$ and $X_5(x)$.

We shall use the first three terms only in (38) to find ψ_0 , viz.,

$$\psi_0 = \frac{ze}{Da(1+x_0)} + \frac{z^3 \epsilon^5}{(Da)^3 (-kT)^2} X_3(x_0) + \frac{z^5 \epsilon^9}{(Da)^5 (-kT)^4} X_5(x_0). \quad (39)$$

When $z \geq 200$, more terms would need to be evaluated, but it is simpler to make use of Gyemant's‡ investigations. He showed that if ρ_s is the effective

* 'Phys. Z.,' vol. 29, p. 558 (1928) (equations (23A), (73)).

† Gronwall, La Mer, and Sandved (*loc. cit.*).

‡ 'Z. Physik,' vol. 17, p. 190 (1923).

surface density on a sphere of radius r , concentric to and containing the particle, the relation

$$\rho_s = \frac{D}{2\pi} [\sqrt{\sigma} \sinh \epsilon \psi/2 + \psi/2r] \quad (40)$$

is approximately true where $\sigma = \frac{8\pi kNT\gamma}{1000D}$. Substituting $\rho_s = \frac{Q}{4\pi a^2}$ we give Q different values and solve (40) for ψ . Comparison with the values of ψ from (39) for $z = 50$ and $z = 100$ shows close agreement and so we shall use (40) for $z = 200$.

The values of ψ_0 for different values of γ and z are given in Table I, with $a = 10^{-6}$ cm, $T = 291^\circ\text{K}$, $D = 81$, $k = 1.372 \times 10^{-16}$, $N = 6.06 \times 10^{23}$.

Table I

z	50		100		200	
γ	10^{-3}	10^{-4}	10^{-3}	10^{-4}	10^{-3}	10^{-4}
$10^4 \psi_0$ by (39), c.s.u.....	1.38	2.12	2.6	3.6	—	—
$10^4 \psi_0$ by (40), c.s.u.....	1.36	2.08	2.4	3.6	3.8	5.3

We now find convenient upper and lower limits to the potential curve $\psi = \psi(r)$. Putting $x = \kappa r$, $y = \epsilon x \psi / kT$, (33) becomes

$$\frac{d^2y}{dx^2} = x \sinh y/x. \quad (41)$$

Multiply (41) by dy/dx and integrate from $x = \infty$ to $x = x$, i.e., from $y = 0$ to $y = y$, obtaining

$$\frac{1}{2} \left(\frac{dy}{dx} \right)^2 = \int_0^y x \sinh y/x dy. \quad (42)$$

From the inequalities $x_0 \sinh y/x_0 > x \sinh y/x > y$ for $x > x_0$ we get on integrating $\int_0^y x_0 \sinh y/x_0 dy > \int_0^y x \sinh y/x dy > \int_0^y y dy$. Using (42) this reads

$$2x_0 \sinh y/2x_0 > -\frac{dy}{dx} > y.$$

From the inequality $-\frac{dy}{dx} > y$, integrating from $x = x_0$ to $x = x$, we have $y = y_0 e^{ax} e^{-x}$. An upper limit for the potential curve is then

$$y = x_0 y_0 e^{x_0} e^{-x}/x \quad \text{or} \quad \psi = A e^{-\kappa r}/r, \quad (43)$$

where $A = \psi_0 e^{x_0} a$. It is to be observed that (43) has the value $\psi = \psi_0$ at $r = a$.

The condition $2x_0 \sinh y/2x_0 > -\frac{dy}{dx}$, on integrating from $x = x_0$ to $x = x$, leads to $\tanh y/4x_0 > \tanh y_0/4x_0 e^{x_0} e^{-x}$ and *a fortiori* to

$$y > 4x_0 \tanh y_0/4x_0 e^{x_0} e^{-x}.$$

These two inequalities give lower limits

$$\tanh y/4x_0 \tanh y_0/4x_0 e^{x_0} e^{-x} \quad \text{or} \quad \tanh \beta r \psi = C e^{-\kappa r}, \quad (44)$$

where

$$\beta = \varepsilon/4akT, \quad C = e^{x_0} \tanh \varepsilon \psi_0/4kT,$$

and

$$y = 4x_0 e^{x_0} e^{-x} \tanh y_0/4x_0, \quad \text{or} \quad \psi = B e^{-\kappa r}/r, \quad (45)$$

where $B = \frac{4akT}{\varepsilon} e^{x_0} \tanh \varepsilon \psi_0/4kT$. Here (44) gives the proper values of $d\psi/dr$ and ψ at $r = a$ and is the better limit though (45) is more convenient.

To obtain narrower limits, the value of ψ at $r = 2a$ is found and formulæ corresponding to (43) and (45) which are valid for $r \geq 2a$ are developed. Gronwall, La Mer, and Sandved give a general expansion for all values of r , but they do not examine enough terms to give satisfactory values for ψ at $r = 2a$. We therefore use an approximate relation between ψ and r given by Gyemant, this being sufficiently accurate for our purpose. He suggests as solution

$$4r \sqrt{\frac{a}{\alpha}} \tanh \alpha \psi/4 + \psi = G e^{-\kappa r} (1 + \kappa r)/r, \quad (46)$$

where $\alpha = \frac{F}{kNT}$, F is a Faraday (96,540 Coulombs) and G is an undetermined constant.

To find G the initial condition $\psi = \psi_0$ at $r = a$ are introduced. It is seen from the graphs, fig. 1, that the curves (46) lie between the upper and lower limits (43) and (44). The value of ψ at $r = 2a$ is obtained from (46) and is substituted in (43) and (45). In this way new limits, valid for $r \geq 2a$ are derived for the potential curves in the forms $\psi = A' e^{-\kappa r}/r$ and $\psi = B' e^{-\kappa r}/r$ the constants A' and B' replacing A and B . We shall assume that

$$\psi = \Lambda e^{-\kappa r}/r \quad (47)$$

represents the potential where $\Lambda = \frac{A' + B'}{2}$. It is seen that this gives values a little below the true potential for $a \leq r \leq 2a$. Table II gives the results.

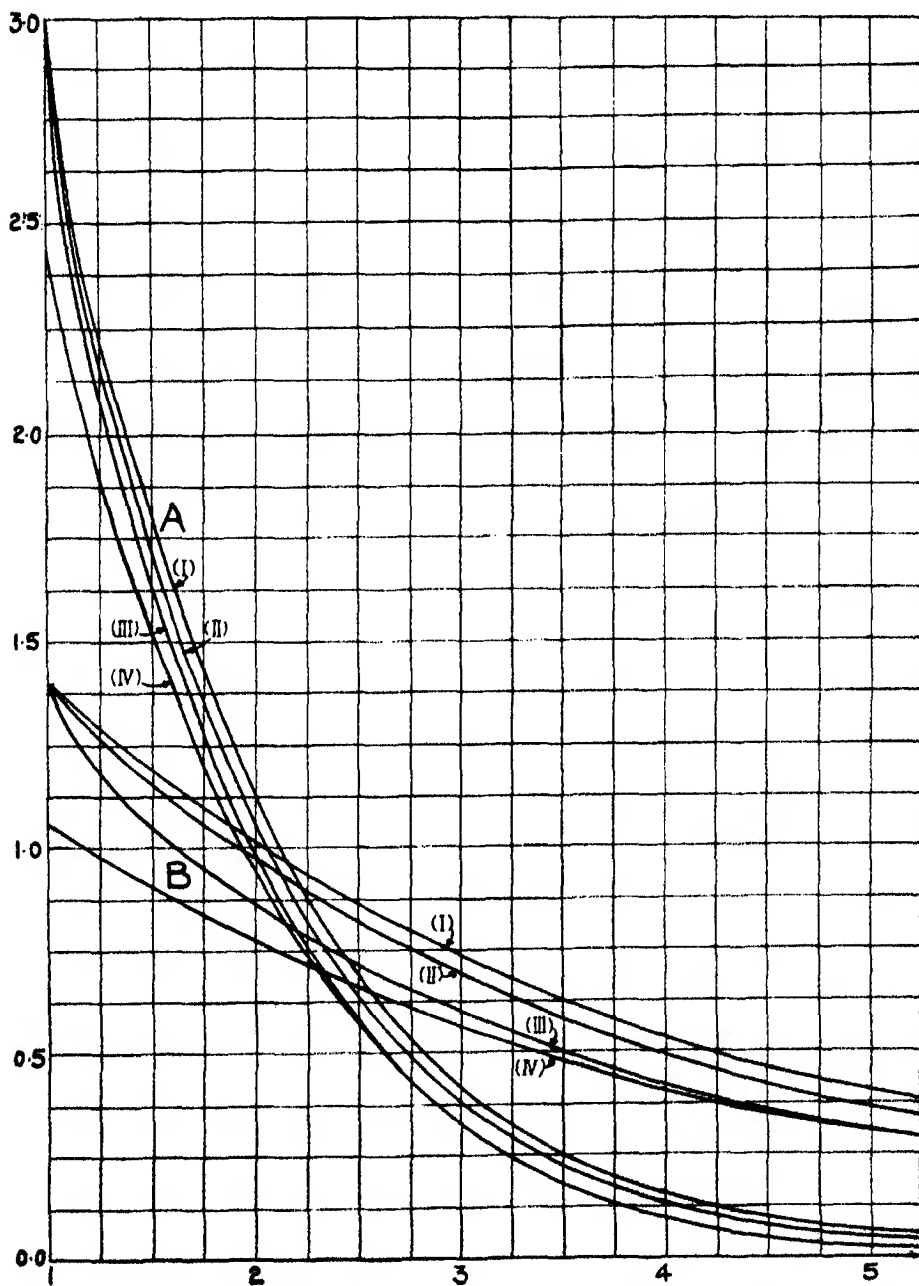


FIG. 1—Various limits for the potential curves. A, $z = 100$, $\gamma = 10^{-3}$; B, $z = 100$, $\gamma = 10^{-4}$. (i) $y = y_0 e^{x_0} e^{-\kappa r}$; (ii) equation (46) in $y-r$ co-ordinates; (iii) $\tanh \frac{y}{4x_0} = \tanh \frac{y_0}{4x_0} e^{x_0} e^{-\kappa r}$; (iv) $y = 4x_0 \tanh \frac{y_0}{4x_0} e^{x_0} e^{-\kappa r}$.

Table II

z γ	50		100		200	
	10^{-2}	10^{-4}	10^{-2}	10^{-4}	10^{-2}	10^{-4}
$10^{10} A'$	3.77	2.84	6.44	4.70	9.11	6.77
$10^{10} B'$	3.77	2.81	6.42	4.51	9.05	6.22
$10^{10} A$	3.77	2.83	6.43	4.60	9.08	6.50

§ 5. *Evaluation of Energy Involved in a Binary Encounter*

To find E_{12} for two particles A and B we solve (35), making the necessary corrections when (32) should be used. From the solution, the details of which are given in the appendix, the potential Ψ_0 at the surfaces of A and B is obtained. The change in energy associated with the particles alone is therefore $Q(\Psi_0 - \psi_0)$.

There only remain the contributions of the ionic atmosphere to E_{12} . Let r_1 and r_2 be the distances of any point P from the centres of A and B, which are at a distance b apart. According to (90) the potential obtained on linear superposition of the ψ 's is sufficiently exact for $b \geq 4a$ so that, by (47), we may assume the potential at P to be

$$\psi_P = \psi_1 + \psi_2 = \Lambda \frac{e^{-\kappa r_1}}{r_1} + \Lambda \frac{e^{-\kappa r_2}}{r_2}. \quad (48)$$

This form for ψ_P implies no distortion of the atmospheres and hence, using (31), the density of charge at P is

$$\rho_P = \rho_1 + \rho_2 = -2n_i \epsilon [\sinh \epsilon \psi_1 / kT + \sinh \epsilon \psi_2 / kT]. \quad (49)$$

Applying (48) and (49) the energy associated with the ionic atmosphere is given by

$$\begin{aligned} \frac{1}{2} \iiint \rho_P \psi_P dx dy dz &= \frac{1}{2} \iiint (\rho_1 + \rho_2) (\psi_1 + \psi_2) dx dy dz \\ &= \iiint (\rho_1 \psi_1 + \rho_2 \psi_2) dx dy dz, \end{aligned} \quad (50)$$

since A and B play identical roles. The integration is to be extended over all space excluding the two particles.

Since only the change in energy on the approach of A and B is desired, we must subtract from (50) the energy at infinite separation. This is given for the atmosphere of one particle (say A) by $\frac{1}{2} \iiint \rho_1 \psi_1 dx dy dz$, integrating over all space external to it. Subtracting twice this amount from the first term in (50) we obtain

$$2n_i \epsilon \Lambda \iiint (e^{-\kappa r_1} / r_1) \sinh \epsilon \psi_1 / kT dx dy dz, \quad (51)$$

where we have substituted for ρ_1 and ψ_1 ; the region of integration is now the interior of particle B. It is convenient to put

$$\sinh \epsilon \psi_1 / kT \equiv \sinh \epsilon \Lambda e^{-\kappa r_1} / kT r_1 = \frac{\epsilon \Lambda}{kT} \frac{e^{-\kappa r_1}}{r_1} + \lambda \frac{e^{-\mu r_1}}{r_1}, \quad (52)$$

which is a good approximation on proper choice of the constants λ and μ , which depend on Q and γ , and are found graphically. Their values are given in Table III. Transforming to the co-ordinates r_1, r_2, ϕ where ϕ is the azimuthal angle about the line AB, and integrating with respect to ϕ , (51) reads

$$\begin{aligned} \frac{2n_1 \epsilon \Lambda}{bkT} \iiint e^{-\kappa r_1} \sinh \frac{\epsilon \psi_1}{kT} r_2 dr_1 dr_2 d\phi &= \frac{4\pi n_1 \epsilon \Lambda}{bkT} \int_0^a r_2 dr_2 \int_{b-r_1}^{b+r_1} e^{-\kappa r_1} \sinh \frac{\epsilon \psi_1}{kT} dr_1 \\ &= \frac{4\pi n_1 \epsilon \Lambda}{bkT} \left[\int_b^{b+a} e^{-\kappa r_1} \sinh \frac{\epsilon \psi_1}{kT} dr_1 \int_{r_1-b}^a r_2 dr_2 \right. \\ &\quad \left. + \int_{b-a}^b e^{-\kappa r_1} \sinh \frac{\epsilon \psi_1}{kT} dr_1 \int_{b-r_1}^a r_2 dr_2 \right], \end{aligned}$$

on interchanging the order of integration. Substituting (52) in this it becomes

$$\begin{aligned} \frac{2\pi n_1 \epsilon^2 \Lambda^2}{bkT} &\left[(a^2 - b^2) \int_{b-a}^{b+a} \frac{e^{-2\kappa r_1}}{r_1} dr_1 + \frac{e^{-2\kappa b}}{\kappa} \left\{ \left(b - \frac{1}{2\kappa} \right) \sinh 2\kappa a + a \cosh 2\kappa a \right\} \right] \\ &+ \frac{2\pi n_1 \epsilon \lambda \Lambda}{b} \left[(a^2 - b^2) \int_{b-a}^{b+a} \frac{e^{-(\kappa+\mu)r_1}}{r_1} dr_1 \right. \\ &\left. + \frac{2e^{-(\kappa+\mu)b}}{\kappa + \mu} \left\{ \left(b - \frac{1}{\kappa + \mu} \right) \sinh (\kappa + \mu) a + a \cosh (\kappa + \mu) a \right\} \right]. \quad (53) \end{aligned}$$

To evaluate the second term in (50) we change to elliptic co-ordinates $\xi = \frac{r_1 + r_2}{b}, \eta = \frac{r_1 - r_2}{b}, \phi$, similar to (19). Here, however, the spheres excluded are $r_1 \ll a$ and $r_2 \ll a$ and $\delta = \frac{2a+b}{b}$. Then

$$\begin{aligned} \iiint \rho_2 \psi_1 dx dy dz &= - \frac{n_1 \epsilon b^3 \Lambda}{4} \iiint \frac{e^{-\kappa r_1}}{r_1} \sinh \frac{\epsilon \psi_2}{kT} (\xi^2 - \eta^2) d\xi d\eta d\phi \\ &= - \frac{n_1 \epsilon b^3 \Lambda}{4} \left[\int_\delta^\infty d\xi \int_{-1}^{+1} \{ \dots \} d\eta + \int_1^\delta d\xi \int_{\frac{2a}{\delta} - \xi}^{\frac{2a}{\delta}} \{ \dots \} d\eta \right]. \quad (54) \end{aligned}$$

Substituting from (52), the integration of (54) yields

$$\begin{aligned}
 & -\frac{\pi n_i \epsilon^2 b \Lambda^2}{2kT} \left[\frac{e^{-\kappa b}}{\kappa b} \left(1 + \frac{1}{\kappa b} - \frac{2a}{b} \right) - \frac{e^{-\kappa b \delta}}{\kappa^2 b^2} \right] \\
 & -\frac{4\pi n_i \epsilon \Lambda \lambda b}{t^2 - u^2} \left[e^{-t} \left\{ \cosh \left(1 - \frac{2a}{b} \right) u + \frac{t}{u} \sinh \left(1 - \frac{2a}{b} \right) u \right\} \right. \\
 & \quad \left. - e^{-u} \left(\cosh u + \frac{u}{t} \sinh u \right) \right] \quad (55)
 \end{aligned}$$

where $t = \frac{b}{2}(\mu + \kappa)$, $u = \frac{b}{2}(\mu - \kappa)$.

Adding (53) and (55), we obtain the (negative) contribution of the atmosphere to E_{12} and subtraction of the result from $Q(\Psi_0 - \psi_0)$ gives E_{12} . It was found that for $b > 10a$, $\gamma = 10^{-3}$ and for $b > 15a$, $\gamma = 10^{-4}$, E_{12} is negative, implying an attractive force. But since we are subtracting two quantities subject to some error to obtain a much smaller quantity, this apparent discrepancy is not surprising. From the positive values of E_{12} only, it was found possible to use an empirical formula $E_{12} = \chi e^{-\tau b}$ the constants χ , τ being given in Table III. We may conclude that the approximate method adopted to find E_{12} may produce an appreciable error and a more rigorous treatment is desirable.

To find E_{12} more accurately we may suppose ψ is of the form $\psi = \psi_1 + \psi_2 + \zeta$ where ζ is a correcting factor. If we assume ζ is small enough to permit the approximation $\sinh \epsilon \zeta / kT = \epsilon \zeta / kT$, then

$$\nabla^2 \zeta = \frac{8\pi n_i \epsilon^2}{DkT} \left[\cosh \frac{\epsilon}{kT} (\psi_1 + \psi_2) \right] \zeta$$

remembering that ψ_1 and ψ_2 both satisfy (32). This equation is now being investigated.

Table III

z γ	50		100		200	
	10^{-3}	10^{-4}	10^{-3}	10^{-4}	10^{-3}	10^{-4}
$10^{11} \chi$	1.26	0.398	4.07	0.794	10.5	1.59
$10^{-6} \tau$	1.50	0.553	1.44	0.601	1.40	0.577
$10^5 \lambda$	5.62	2.57	28.2	8.91	159.0	31.6
$10^{-6} \mu$	2.10	4.51	2.02	4.37	2.16	4.49

§ 6. Calculation of the Coefficients A_1 , A_2 , and A_3

To find A_1 we substitute the relation $E_{12} = \chi e^{-\tau b}$ in (12) giving (for $v = 1$)

$$A_1 = 2\pi\chi \int_{2a}^{\infty} e^{-\tau r_{12}} \exp \left(-\frac{\chi}{kT} e^{-\tau r_{12}} \right) r_{12}^2 dr_{12}, \quad (56)$$

the integral being evaluated numerically. We can determine the contribution to A_s from (14) similarly, and to obtain that from (22) we put

$$\begin{aligned} G &= \left\{ \exp \left[-\frac{\chi}{kT} \left(e^{-\tau r_{12}} + e^{-\tau r_{13}} \right) \right] - 1 \right\} (\xi^2 - \eta^2) \\ &= \left\{ \exp \left[-\frac{2\chi}{kT} e^{-\tau r_{12}} \cosh \tau r_{12} \eta \right] - 1 \right\} (\xi^2 - \eta^2), \end{aligned} \quad (57)$$

on introducing the co-ordinates (19). In the relation (true for $r_{12} \geq 4a$)

$$\begin{aligned} \int_0^\infty d\xi \int_{-1}^{+1} G d\eta + \int_1^\infty d\xi \int_{\frac{4a}{r_{12}} - \xi}^{\xi - \frac{4a}{r_{12}}} G d\eta &= \int_1^\infty d\xi \int_{-1}^{+1} G d\eta \\ &- \int_1^\infty d\xi \left[\int_{-1}^{\xi - \frac{4a}{r_{12}}} G d\eta + \int_{\xi - \frac{4a}{r_{12}}}^1 G d\eta \right], \end{aligned} \quad (58)$$

which was used to obtain (22), the second term on the right gives the integration inside the spheres $r_{13} = 2a$ and $r_{23} = 2a$, for which regions as seen from the values of χ and τ

$$G = -(\xi^2 - \eta^2), \quad (59)$$

very nearly. If we now substitute (59) in the second term and multiply it by $\int_0^{2\pi} \frac{r_{12}^3}{8} d\phi = \frac{\pi r_{12}^3}{4}$, the result is the sum of the volumes of the two spheres, i.e., $v_a = \frac{64\pi a^3}{3}$. Thus (58) becomes

$$\begin{aligned} \int_0^\infty d\xi \int_{-1}^{+1} G d\eta + \int_1^\infty d\xi \int_{\frac{4a}{r_{12}} - \xi}^{\xi - \frac{4a}{r_{12}}} G d\eta &= \int_1^\infty d\xi \int_{-1}^{+1} G d\eta + \frac{256}{3} \frac{a^3}{r_{12}^3} \\ &= 2 \int_1^\infty d\xi \int_0^1 G d\eta + \frac{256}{3} \frac{a^3}{r_{12}^3} = I + \frac{256}{3} \frac{a^3}{r_{12}^3}. \end{aligned} \quad (60)$$

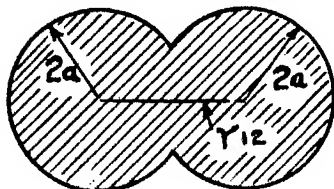


FIG. 2.—Volume v'_a to be excluded.

If $r_{12} < 4a$ then v_a is replaced by the volume shown shaded in fig. 2 this being

$$v'_a = \frac{\pi}{3} \left[12a^2 r_{12} - \frac{r_{12}^3}{4} + 32a^3 \right].$$

To find I, we choose values of r_{12} and calculate $\int_1^\infty G d\xi$ for $\eta = 0, \frac{1}{2}$ and 1 by numerical integration, and then integrate I with respect to η . Then (22) reduces to

$$\frac{\pi^2 \chi}{2} \int_{2a}^\infty (1 + v_a) e^{-\tau r_{12}} \exp\left(-\frac{\chi}{kT} e^{-\tau r_{12}}\right) r_{12}^5 dr_{12}, \quad (61)$$

which is evaluated. It was found that the term involving I formed the main contribution to (61), implying that a neglect of the size of the particles would produce only a small error. Hence our approximations in (26, ii), (28, i), and (28, ii) are quite reasonable.

In the expression for $A_3 v^4$ we have shown in § 3 that all the terms can be reduced to forms involving (56) and (61), or other integrals similar to these.

In this way A_1 , A_2 , and A_3 are found for different values of Q and γ the results being given in Table IV. For silver colloidal particles, density 10.5 and radius 10^{-6} cm, we have $mg = 3.9 \times 10^{-14}$. Substituting this value for

Table IV

z	50		100		200	
γ	10^{-3}	10^{-4}	10^{-5}	10^{-6}	10^{-7}	10^{-8}
A_1	$2.9 \cdot 10^{-30}$	$4.4 \cdot 10^{-29}$	$4.0 \cdot 10^{-30}$	$5.1 \cdot 10^{-30}$	$6.9 \cdot 10^{-30}$	$6.0 \cdot 10^{-29}$
A_2	$7.5 \cdot 10^{-48}$	$1.4 \cdot 10^{-43}$	$2.2 \cdot 10^{-48}$	$1.8 \cdot 10^{-43}$	$5.8 \cdot 10^{-46}$	$3.5 \cdot 10^{-43}$
A_3	$9.0 \cdot 10^{-61}$	$2.8 \cdot 10^{-57}$	$5.9 \cdot 10^{-60}$	$4.1 \cdot 10^{-57}$	$2.5 \cdot 10^{-59}$	$1.2 \cdot 10^{-56}$
Limiting concentration ..	$5.5 \cdot 10^{13}$	$3.6 \cdot 10^{14}$	$2.9 \cdot 10^{13}$	$2.6 \cdot 10^{14}$	$8.3 \cdot 10^{14}$	$2.1 \cdot 10^{14}$

mg and the values of A_1 , A_2 , and A_3 we obtain the sedimentation law of a suspension of colloidal particles. The $\log n$ is plotted against d , fig. 3, and it is seen that deviations from Perrin's law appear for values of n ranging between 1.6×10^{13} and 4.0×10^{14} , the corresponding limiting concentrations being given in Table IV. It is to be noticed that the latter are reached only at depths greater than 5 cm. In plotting the curves, an estimate of the order of magnitude of A_4 was made, since it was found to have an appreciable effect on the limiting concentration.

We may now compare these results with those obtained experimentally. The value $n = 8 \times 10^{10}$ at which deviations occurred in Costantin's investigations is smaller than in ours owing to the larger size of the particles ($a = 3 \times 10^{-5}$ cm). In the work of Laird the first reading is at depths of 4–6 cm ($a = 8 \times 10^{-7}$ cm) where the concentration of particles would almost have reached its maximum value. Johnston and Howell worked with solutions which were too dilute to indicate deviations ($n = 4 \times 10^8$, $a = 3.6 \times 10^{-6}$ cm).

The results of McDowell and Usher ($a = 1.5 \times 10^{-6}$ cm) confirm the fact that no deviations occur below $n = 10^{12}$.

The much smaller values of the limiting concentrations obtained by Burton, Porter and Hedges, and Barkas may possibly be attributed to the existence of a larger charge Q on the colloidal particles. If so, there would be a considerable contribution from the polarization and electrostrictive forces, discussed in

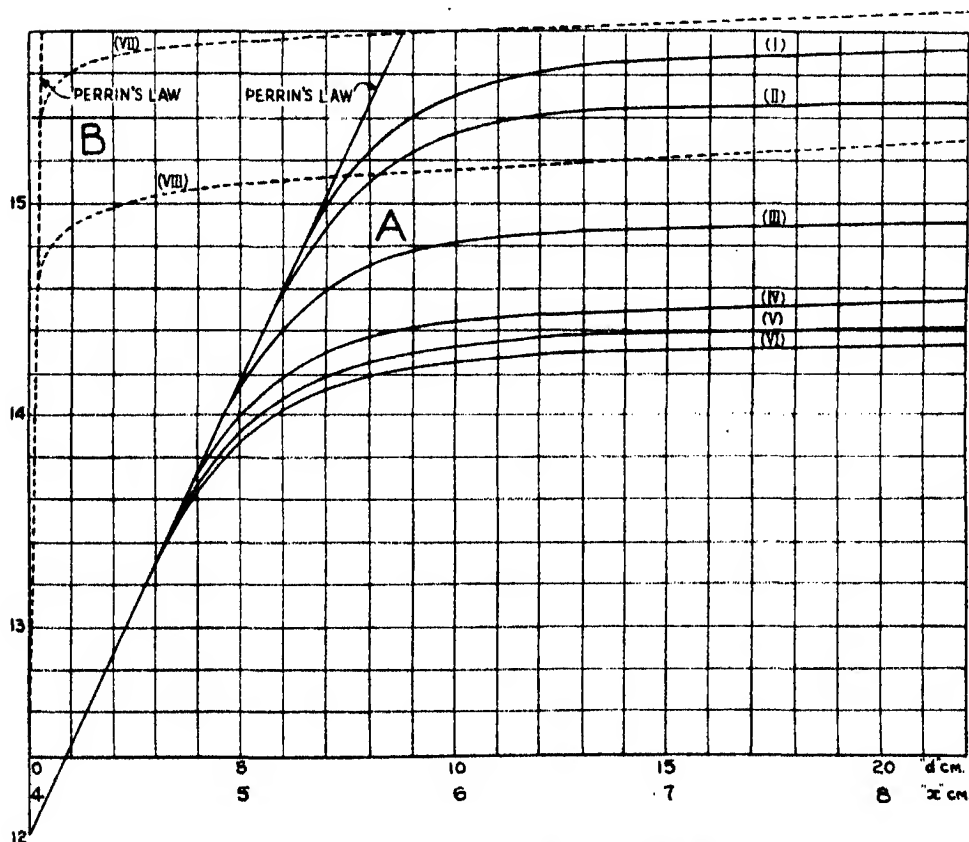


FIG. 3—Distribution curves for colloidal suspensions.

$$A \text{ --- } n = n_0 \exp \left[\frac{1}{kT} (mgd - A_1 n - A_2 n^2 - A_3 n^3 \dots) \right]$$

$$B \text{ --- } n = n_0 \exp \left[\frac{1}{kT} \left\{ \frac{m\omega^2}{2} (x^2 - x_0^2) - A_1 n - A_2 n^2 - A_3 n^3 \dots \right\} \right]$$

	z	γ		z	γ
(i)	50	10^{-2}	(v)	100	10^{-4}
(ii)	100	10^{-2}	(vi)	200	10^{-4}
(iii)	200	10^{-2}	(vii)	100	10^{-2}
(iv)	50	10^{-4}	(viii)	100	10^{-4}

§ 7. Under these conditions, the method for finding E_{12} as given in § 4 and § 5 is not valid, since the dielectric constant D is no longer constant. In fact, calculations by the above method for $z = 1000$ have given limiting concentrations, which are quite close to those for $z = 200$, and this cannot be considered as correct.

To apply (30) to sedimentation equilibrium in the centrifuge we replace it by

$$n = n_0 \exp \left[\frac{1}{kT} \left\{ \frac{mw^2(x^2 - x_0^2)}{2} - A_1n - A_2n^2 - A_3n^3 \right\} \right], \quad (62)$$

where w is the angular velocity of the centrifuge, x is the distance of the point under consideration in the sol from the centre of rotation, and x_0 refers to the base of the container facing the centre. We let $x_0 = 4$ cm and $w = 20,000$ r.p.m. and the distribution curves for $z = 100$, $\gamma = 10^{-3}$ and $\gamma = 10^{-4}$ are shown in fig. 3. The deviations from Perrin's distribution would begin less abruptly if we included the coefficients A_6, A_6, \dots , which are more important here than in a simple gravitational field.

§ 7. Discussion of the Method

Ursell's method of finding the partition function is not readily applicable to high concentrations. In our method the force of repulsion between two particles was replaced by a simple empirical expression to facilitate integration. A more satisfactory treatment may be based on the work of Kramers* who, for electrolytes, starts with the phase integral, which corresponds to the partition function, and endeavours to find a solution for it.

Fowler (*loc. cit.*) has criticized the method of Debye and Hückel, the three doubtful points being those of "smoothing," the form of the average density, and the neglect of fluctuation terms. In our method, however, with relatively large colloidal particles these are points of less importance.

In calculating the force between two particles of a hydrophobic sol, the principal factors are the charge and the ionic atmospheres. But with hydrophilic sols, the hydration must be considered, the orientation polarization of the dipole water molecules at the surface of the colloidal particle playing an important role. A method for calculating the contribution to E_{12} due to this phenomenon is suggested by the work of Webb,† who finds the energy of hydration of an ion by using the classical theory of dielectrics.

* 'Proc. Amst. Akad. Sci.,' vol. 30, p. 145 (1927).

† 'J. Amer. Chem. Soc.,' vol. 48, p. 2589 (1926).

In addition to this effect there exists, in the vicinity of the ions, electrostrictive forces which produce very high hydrostatic pressures. On the approach of two particles there will be an additional compression work involved, and this will contribute to E_{12} . The method used by Zwicky* in his treatment of the specific heat of solutions can be extended to calculate this contribution. Consideration of the hydration and pressure effects should give a larger value for E_{12} and hence smaller values for the limiting concentrations. This is to be expected as the experimental values of the limiting concentration range from $n = 5 \times 10^{15}$ to $n = 10^{13}$.

The method of Kramers is now being developed, consideration of the finite dimensions of the ions and particles being taken into account, and it is hoped to publish a communication shortly. The problems of the hydration and pressure effects are also being investigated.

APPENDIX

Solution of Equation $\nabla^2\psi = \kappa^2\psi$ for two Particles†

Consider two spherical particles A and B at a distance b apart. Transforming

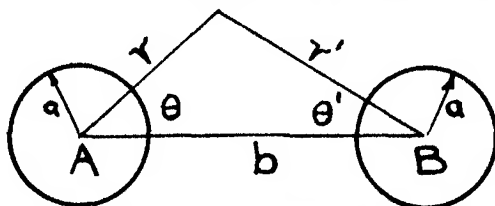


FIG. 4—Encounter of two particles A and B.

(35) to polar co-ordinates r, θ, ϕ with the centre of A as origin, and the z axis the line joining the centres of A and B, we obtain

$$\frac{\partial^2\psi}{\partial r^2} + \frac{2}{r} \frac{\partial\psi}{\partial r} + \frac{1}{r^2 \sin \theta} \frac{\partial}{\partial \theta} \left(\sin \theta \frac{\partial\psi}{\partial \theta} \right) + \frac{1}{r^2 \sin \theta} \frac{\partial^2\psi}{\partial \phi^2} - \kappa^2\psi = 0. \quad (63)$$

Introducing the condition that the solution shall be finite everywhere and remembering that $\frac{\partial^2\psi}{\partial \phi^2} = 0$, due to symmetry about the z axis, the solution is‡

$$\psi = \sum_{n=0}^{\infty} A_n P_n(\mu) K_{n+\frac{1}{2}}(\kappa r) r^{-\frac{1}{2}}, \quad (64)$$

given by the standard process of separation of variables, where $\mu = \cos \theta$.

* 'Phys. Z.', vol. 26, p. 664 (1925); vol. 27, p. 271 (1926); 'Proc. Nat. Acad. Sci. Wash.', vol. 12, p. 86 (1926); Evjen and Zwicky, 'Phys. Rev.', vol. 33, p. 860 (1929).

† Equation (35) has been solved by Scatchard and Kirkwood for two ions, but with different boundary conditions: 'Phys. Z.' vol. 33, p. 297 (1932).

‡ See Watson, "Theory of Bessel Functions," p. 77, for definition of $K_{n+\frac{1}{2}}$, $I_{n+\frac{1}{2}}$.

Since the two boundary conditions at the surfaces of A and B must be satisfied, we must have two sets of arbitrary constants. If the origin is taken at B with polar co-ordinates r' , θ' , ϕ' , by symmetry the solution is of the form

$$\psi = \sum_{n=0}^{\infty} B_n P_n(\mu') K_{n+\frac{1}{2}}(\kappa r') r'^{-\frac{1}{2}}.$$

As the two particles play identical roles there is no loss of generality in writing $A_n = B_n$ and thus the general solution is

$$\psi = \sum_{n=0}^{\infty} A_n P_n(\mu) K_{n+\frac{1}{2}}(\kappa r) r^{-\frac{1}{2}} + \sum_{n=0}^{\infty} A_n P_n(\mu') K_{n+\frac{1}{2}}(\kappa r') r'^{-\frac{1}{2}}. \quad (65)$$

In a given finite region of space any solution of (65) can be expressed as

$$\sum_{s=0}^{\infty} C_s P_s(\mu) K_{s+\frac{1}{2}}(\kappa r) r^{-\frac{1}{2}} + \sum_{s=0}^{\infty} D_s P_s(\mu) I_{s+\frac{1}{2}}(\kappa r) r^{-\frac{1}{2}}. \quad (66)$$

In particular we can write

$$P_n(\mu') K_{n+\frac{1}{2}}(\kappa r') r'^{-\frac{1}{2}} = \sum_{s=0}^{\infty} C_{ns} P_s(\mu) K_{s+\frac{1}{2}}(\kappa r) r^{-\frac{1}{2}} + \sum_{s=0}^{\infty} D_{ns} P_s(\mu) I_{s+\frac{1}{2}}(\kappa r) r^{-\frac{1}{2}}. \quad (67)$$

To find the coefficients C_{ns} and D_{ns} use is made of an expansion due to Gegenbauer.* If $r < b$ then

$$\frac{K_{n+\frac{1}{2}}(\kappa r')}{(r')^{n+\frac{1}{2}}} = \frac{2^{n+\frac{1}{2}} \Gamma(n+\frac{1}{2})}{(\kappa r b)^{n+\frac{1}{2}}} \sum_{s=0}^{\infty} (s+\frac{1}{2}+n) K_{s+\frac{1}{2}+n}(\kappa b) I_{s+\frac{1}{2}+n}(\kappa r) C_s^{n+\frac{1}{2}}(\mu), \quad (68)$$

where

$$(1 - 2\alpha t + \alpha^2)^{-\nu} = \sum_{n=0}^{\infty} C_n^{\nu}(t) \alpha^n. \quad (69)$$

In particular, this formula is valid in the neighbourhood of the particle A.

If we put $n = 0$, $\mu = \mu' = 1$, i.e., $r' = b - r$, (68) becomes

$$K_{\frac{1}{2}}[\kappa(b-r)](b-r)^{-\frac{1}{2}} = \frac{2^{\frac{1}{2}} \Gamma(\frac{1}{2})}{(\kappa r b)^{\frac{1}{2}}} \sum_{s=0}^{\infty} (s+\frac{1}{2}) K_{s+\frac{1}{2}}(\kappa b) I_{s+\frac{1}{2}}(\kappa r) C_s^{\frac{1}{2}}(\mu), \quad (70)$$

and (67) reads

$$K_{\frac{1}{2}}[\kappa(b-r)](b-r)^{-\frac{1}{2}} = \sum_{s=0}^{\infty} C_{0s} K_{s+\frac{1}{2}}(\kappa r) r^{-\frac{1}{2}} + \sum_{s=0}^{\infty} D_{0s} I_{s+\frac{1}{2}}(\kappa r) r^{-\frac{1}{2}}. \quad (71)$$

* Watson, *loc. cit.*, chap. XI.

On comparing (70) and (71) we see that $C_{0s} = 0$ for all s and

$$D_{0s} = \frac{2^{3/2} \Gamma(\frac{3}{2})}{(\kappa b)^{3/2}} (s + \frac{1}{2}) K_{s+\frac{1}{2}}(\kappa b) C_s^{\frac{3}{2}}(1). \quad (72)$$

In particular,

$$D_{00} = \frac{\pi}{2\kappa b} e^{-\kappa b}, \quad D_{01} = 3 \left(\frac{\pi}{2\kappa b} \right) \left(1 + \frac{1}{\kappa b} \right) e^{-\kappa b}. \quad (73)$$

If we write $n = 1$, $\mu = \mu' = 1$ (68) reads

$$\begin{aligned} K_{3/2}[\kappa(b-r)](b-r)^{-1/2} \\ = \frac{2^{3/2} \Gamma(\frac{3}{2})}{(\kappa b)^{3/2}} \frac{(b-r)}{r} \sum_{s=0}^{\infty} (s + \frac{3}{2}) K_{s+\frac{3}{2}}(\kappa b) I_{s+\frac{3}{2}}(\kappa r) C_s^{3/2}(1) r^{-1/2}, \end{aligned} \quad (74)$$

and (67) becomes

$$K_{3/2}[\kappa(b-r)](b-r)^{-1/2} = \sum_{s=0}^{\infty} C_{1s} K_{s+\frac{3}{2}}(\kappa r) r^{-1/2} + \sum_{s=0}^{\infty} D_{1s} I_{s+\frac{3}{2}}(\kappa r) r^{-1/2}. \quad (75)$$

Using the recurrence relation

$$\frac{I_{s+\frac{3}{2}}(\kappa r)}{\kappa r} = \frac{I_{s+\frac{1}{2}}(\kappa r) - I_{s+\frac{5}{2}}(\kappa r)}{2s+3} \quad (76)$$

in (74) and rearranging the terms in ascending order in $I_{s+\frac{3}{2}}(\kappa r)$, we immediately obtain an expansion of the form

$$K_{3/2}[\kappa(b-r)](b-r)^{-1/2} = \sum_{s=0}^{\infty} D_{1s} I_{s+\frac{3}{2}}(\kappa r) r^{-1/2}. \quad (77)$$

It follows, on comparison with (75), that $C_{1s} = 0$. We shall only need the first two terms in (77), viz.,

$$\left. \begin{aligned} D_{10} &= \frac{2^{3/2} \Gamma(\frac{3}{2})}{2(\kappa b)^{3/2}} K_{3/2}(\kappa b) C_0^{3/2}(1) = \frac{\pi}{2\kappa b} \left(1 + \frac{1}{\kappa b} \right) e^{-\kappa b} \\ D_{11} &= \frac{2^{3/2} \Gamma(\frac{3}{2})}{2(\kappa b)^{3/2}} K_{5/2}(\kappa b) C_1^{3/2}(1) - \frac{3}{2} \frac{2^{3/2} \Gamma(\frac{3}{2})}{(\kappa b)^{3/2}} K_{3/2}(\kappa b) C_0^{3/2}(1) \\ &= 3 \left(\frac{\pi}{2\kappa b} \right) \left(\frac{2}{\kappa b} + \frac{3}{(\kappa b)^2} \right) e^{-\kappa b} \end{aligned} \right\}. \quad (78)$$

We can examine in a similar manner the cases $n = 2, 3, \dots$, but it will be seen that there is hardly need for it. We would finally be lead to the relations $C_{ns} = 0$ and

$$P_n(\mu') K_{n+\frac{1}{2}}(\kappa r') r'^{-1/2} = \sum_{s=0}^{\infty} D_{ns} P_s(\mu) I_{s+\frac{1}{2}}(\kappa r) r^{-1/2}, \quad (79)$$

valid for all positive integrals n and s , with $r < b$. The general solution (65) becomes

$$\psi = \sum_{n=0}^{\infty} A_n P_n(\mu) K_{n+\frac{1}{2}}(\kappa r) r^{-\frac{1}{2}} + \sum_{n=0}^{\infty} \sum_{s=0}^{\infty} A_n D_{ns} P_s(\mu) I_{s+\frac{1}{2}}(\kappa r) r^{-\frac{1}{2}}. \quad (80)$$

To find A_n the boundary conditions are introduced. If Ψ_0 is the potential at the surface of A, (80) gives

$$\Psi_0 = \sum_{n=0}^{\infty} A_n P_n(\mu) K_{n+\frac{1}{2}}(\kappa a) a^{-\frac{1}{2}} + \sum_{n=0}^{\infty} \sum_{s=0}^{\infty} A_n D_{ns} P_s(\mu) I_{s+\frac{1}{2}}(\kappa a) a^{-\frac{1}{2}}. \quad (81)$$

Multiplying by $P_0(\mu)$ and integrating from $\mu = -1$ to $\mu = +1$,

$$\Psi_0 = A_0 K_{\frac{1}{2}}(\kappa a) a^{-\frac{1}{2}} + I_{\frac{1}{2}}(\kappa a) a^{-\frac{1}{2}} \sum_{n=0}^{\infty} A_n D_{n0}. \quad (82)$$

The value of Ψ_0 is determined by the condition

$$-\frac{4\pi Q}{D} = \iint \left(\frac{\partial V}{\partial r} \right)_{r=a} dS = \int_0^{2\pi} \int_0^{\pi} \left(\frac{\partial V}{\partial r} \right)_{r=a} a^2 \sin \theta d\theta d\phi,$$

where the integral is taken over the surface of A. This reduces to

$$-\frac{2Q}{Da^2} = \int_{-1}^{+1} \left(\frac{\partial V}{\partial r} \right)_{r=a} d\mu. \quad (83)$$

The corresponding boundary conditions at the particle B are satisfied at the same time owing to the symmetry of the solution with respect to A and B. Using (80), the condition (83) becomes

$$\begin{aligned} -\frac{Q}{Da^2} &= A_0 \frac{d}{dr} [K_{\frac{1}{2}}(\kappa r) r^{-\frac{1}{2}}]_{r=a} + \sum_{n=0}^{\infty} A_n D_{n0} \frac{d}{dr} [I_{\frac{1}{2}}(\kappa r) r^{-\frac{1}{2}}]_{r=a} \\ &= A_0 \kappa K_{3/2}(\kappa a) a^{-\frac{1}{2}} - \kappa I_{3/2}(\kappa a) a^{-\frac{1}{2}} \sum_{n=0}^{\infty} A_n D_{n0} \end{aligned} \quad (84)$$

from the relations

$$\frac{d}{dr} [K_{\frac{1}{2}}(\kappa r) r^{-\frac{1}{2}}]_{r=a} = -\kappa K_{3/2}(\kappa a) a^{-\frac{1}{2}}, \quad \frac{d}{dr} [I_{\frac{1}{2}}(\kappa r) r^{-\frac{1}{2}}]_{r=a} = \kappa I_{3/2}(\kappa a) a^{-\frac{1}{2}}.$$

We now make successive approximations to Ψ_0 by including an increasing number of terms in the series $\sum_{n=0}^{\infty} A_n D_{n0}$. If we only retain the first term $A_0 D_{00}$

neglecting all the others, we can eliminate A_0 from (81) and (84) and obtain

$$\begin{aligned}\Psi_0 &= Q [K_{\frac{1}{2}}(\kappa a) + I_{\frac{1}{2}}(\kappa a) D_{00}] / Da^2 \kappa [K_{3/2}(\kappa a) - I_{3/2}(\kappa a) D_{00}] \\ &= \frac{Q [e^{-\kappa a} + \frac{e^{-\kappa b}}{\kappa b} \sinh \kappa a]}{Da [e^{-\kappa a} (1 + \kappa a) - \frac{e^{-\kappa b}}{\kappa b} (\kappa a \cosh \kappa a - \sinh \kappa a)]},\end{aligned}$$

using (73).

As a second approximation the terms $A_0 D_{00}$ and $A_1 D_{10}$ are included, and we neglect all the A_r 's for $r \geq 2$. Then multiplying (81) by $P_1(\mu)$ and integrating from $\mu_1 = -1$ to $\mu = +1$

$$0 = A_1 K_{3/2}(\kappa a) a^{-\frac{1}{2}} + [A_0 D_{01} + A_1 D_{11}] I_{3/2}(\kappa a) a^{-\frac{1}{2}}.$$

Thus

$$A_1 = -A_0 D_{01} I_{3/2}(\kappa a) / (K_{3/2}(\kappa a) + D_{11} I_{3/2}(\kappa a)) = -E_1 A_0, \quad (86)$$

introducing E_1 for convenience. On dividing (82) by (84) and substituting (86) for A_1

$$\begin{aligned}\Psi_0 &= \frac{Q [K_{\frac{1}{2}}(\kappa a) + (D_{00} - E_1 D_{10}) I_{\frac{1}{2}}(\kappa a)]}{Da^2 \kappa [K_{3/2}(\kappa a) - (D_{00} - E_1 D_{10}) I_{3/2}(\kappa a)]} \\ &= \frac{\frac{Q}{Da (1 + \kappa a)} + \frac{Q e^{\kappa a}}{Da (1 + \kappa a)} \left(\frac{e^{-\kappa b}}{\kappa b} - \frac{2}{\pi} E_1 D_{10} \right) \sinh \kappa a}{1 - \left(\frac{e^{-\kappa b}}{\kappa b} - \frac{2}{\pi} E_1 D_{10} \right) (a \kappa \cosh \kappa a - \sinh \kappa a) / e^{-\kappa a} (1 + \kappa a)}, \quad (87)\end{aligned}$$

where

$$\frac{2}{\pi} E_1 D_{10} = \frac{\frac{3}{(\kappa b)^2} \left(1 + \frac{1}{\kappa b} \right)^2 (\kappa a \cosh \kappa a - \sinh \kappa a) e^{-\kappa b}}{(1 + \kappa a) e^{-\kappa a} + \frac{3}{\kappa b} \left[\frac{2}{\kappa b} + \frac{3}{(\kappa b)^2} \right] e^{-\kappa b} (\kappa a \cosh \kappa a - \sinh \kappa a)}.$$

The first term in the numerator of (87) is due to A itself, the second term is the contribution from B . Since it was found that $E_1 D_{10} \ll D_{00}$ for $b \geq 4a$ in which range we obtain the greatest contributions to A_1 , A_2 , and A_3 , the next approximation is not necessary.

If linear superposition of the potentials is assumed, then the potential at any point P on the surface of A is

$$\psi_P = \psi'_P + \frac{Q}{Da (1 + \kappa a)},$$

where, by (37), $\psi'_P = \frac{Q e^{\kappa a}}{D(1 + \kappa a)} \frac{e^{-\kappa r'}}{r'}$ is due to the particle B. The density of charge at P being $\sigma = \frac{Q}{4\pi a^2}$, the energy associated with the charge on the particle alone is given by

$$\frac{1}{2} \frac{Q^2}{Da(1 + \kappa a)} + \frac{1}{2} \int \sigma \psi'_P dS = \frac{Q^2}{2Da(1 + \kappa a)} + \frac{Qe^{\kappa a} \sinh \kappa a}{Da(1 + \kappa a)} \frac{e^{-\kappa b}}{\kappa b}.$$

Hence in this case (87) is replaced by

$$\Psi_0 = \frac{Q}{Da(1 + \kappa a)} + \frac{Qe^{\kappa a} \sinh \kappa a}{Da(1 + \kappa a)} \frac{e^{-\kappa b}}{\kappa b}. \quad (88)$$

Thus if the particles are sufficiently far apart the two expressions (87) and (88) are practically identical.

When Q is too large to permit the approximation (34) a modification is made in (87). We replace $\frac{Q}{Da(1 + \kappa a)}$, the potential at $r = a$ as given by (37), by ψ_0 (Table I), and use $\psi = \frac{\Lambda e^{-\kappa r}}{r}$ in place of (37) for the potential. Then we get instead of (87)

$$\Psi_0 = \frac{\psi_0 + \frac{\Lambda \sinh \kappa a}{a} \left(\frac{e^{-\kappa b}}{\kappa b} - \frac{2}{\pi} E_1 D_{10} \right)}{1 - \left(e^{-\kappa b} / \kappa b - \frac{2}{\pi} E_1 D_{10} \right) (\kappa a \cosh \kappa a - \sinh \kappa a)} \frac{e^{-\kappa a} (1 + \kappa a)}{e^{-\kappa a} (1 + \kappa a)} \quad (89)$$

which, for $b \gg 4a$, may be replaced by

$$\Psi_0 = \psi_0 + \frac{\Lambda \sinh \kappa a}{a} \frac{e^{-\kappa b}}{\kappa b} \quad (90)$$

as obtained by linear superposition of the fields.

In conclusion, the author wishes to express his sincere appreciation for the many valuable suggestions received from Professor E. F. Burton, Dr. Colin Barnes and other members of the staff in the Physics Department.

Summary

An expression for the distribution law for the sedimentation equilibrium in colloidal suspensions is derived. Using the Boltzmann distribution law a

term involving the energy of a single particle, associated with its charge and surrounding "ionic atmosphere," is introduced. This term is evaluated as a power series in the concentration of particles by using the methods of statistical mechanics, assuming the electrostatic energy E_{12} associated with two colloidal particles to be known. To obtain E_{12} the differential equation used by Debye and Hückel to find the potential about an ion is solved for two particles. The potential and the charge distribution of the ions about the two particles are thereby derived and integration of the energy density gives E_{12} . The results indicate departure from Perrin's law varying, according to the charges on the particles and the concentration of electrolyte present, from $n = 1.6 \times 10^{13}$ to $n = 4.0 \times 10^{14}$ with corresponding limiting concentrations lying between $n = 2.1 \times 10^{14}$ and $n = 5.5 \times 10^{15}$. The expression for the distribution is also applied to sedimentation in the centrifuge.

Experiments on Heavy Hydrogen. III.—The Electrolytic Separation of the Hydrogen Isotopes*

By ADALBERT FARKAS and LADISLAS FARKAS, Colloid Science Laboratory,
Cambridge University

(Communicated by Eric K. Rideal, F.R.S.—Received April 16, 1934)

Introduction

The object of the present paper is to call attention to a fact which may play an important role hitherto not considered in the electrolytic separation of the hydrogen isotopes.

As is well known the most common mode of preparation of heavy hydrogen is the electrolytic method† based on the original discovery of Washburn and Urey. If water containing a certain amount of heavy water be electrolysed under suitable conditions, the light water is more readily decomposed than the heavy water and the heavy hydrogen remains preferentially in the residual

* Part I, 'Proc. Roy. Soc.,' A, vol. 144, p. 467 (1934); Part II, *Ibid.*, p. 481.

† Lewis and Maconald, 'J. Chem. Phys.,' vol. 1, p. 341 (1933).

water. The separation of the heavy hydrogen proceeds formally according to the formula

$$\frac{H_0}{H} \cdot \left(\frac{D}{D_0}\right)^s = \left(\frac{V_0}{V}\right)^{s-1},$$

where H_0 and D_0 , H and D denote the initial and final concentrations of light and heavy hydrogen respectively in the water, and V_0 and V are the initial and final volumes of the electrolysed water. s is the so-called "separation factor" or "separation coefficient" indicating how many times more readily the light water is decomposed than the heavy one.

In the preparation of heavy hydrogen an efficient separation, *i.e.*, a large separation coefficient is desired which is found, in favourable conditions, to be about 7 but the average value is some 4-5.

In attempting to derive an explanation for the electrolytic separation of the two isotopes so far chiefly three processes have been considered :—

- (1) The transport of the ions from the electrolyte to the electrodes.
- (2) The discharge of the ions at the electrodes.
- (3) The formation and liberation of molecular hydrogen at the cathode.

The importance of these factors has recently been investigated theoretically in detail by Fowler.*

Since the transport of H^+ and D^+ ions cannot be responsible for the separation, on account of the relatively small difference in their mobilities (in alkaline solution the H^+ and D^+ ion do not take part at all in the current carrying process), it was believed that either or both of processes (2) and (3) effect the electrolytic fractionation of the hydrogen isotopes.

It has been shown from quantum mechanical considerations that the transition of an electron from the cathode metal to the adsorbed hydrogen ion to discharge it proceeds by jumping over an energy barrier,† and we might assume that the height of this barrier would be different for H^+ and D^+ respectively thus giving a different probability of discharge.

On the other hand, both from measurements on the adsorption of hydrogen and from catalytic experiments, it is known that the recombination of hydrogen atoms on metal surfaces proceeds with a finite activation energy; thus we could expect different activation energies for the recombination of light and heavy hydrogen effecting a separation when molecular gas is formed.

* 'Proc. Roy. Soc.,' A, vol. 144, p. 452 (1934).

† Gurney, 'Proc. Roy. Soc.,' A, vol. 134, p. 137 (1931).

Which of these two processes* might really be the decisive factor in the electrolytic separation could not be established with certainty, but it has hitherto been generally assumed that the separation factor is due to different velocities of evolution comparable, for example, to the different velocities of diffusion of light and heavy hydrogen through palladium (*cf.* I, *loc. cit.*, p. 475) or with the different reaction velocities in some chemical reactions involving light and heavy hydrogen. In these examples the processes involving heavy hydrogen always proceed more slowly than those with light hydrogen since there is an additional activation energy on account of the smaller zero point energy of the heavy isotope.

In investigating the decomposition of sodium formate by *Bacterium coli* and by palladium black,† it was found that the liberated hydrogen had at 40° C an H/D ratio which was about 3·3 times higher than that of the water in which the formate was dissolved, and that the liberated hydrogen was in true equilibrium with the water. This was proved by showing that neither the bacteria nor the palladium black effected any change in the composition of the gas when left in contact with the water. (It had been definitely proved by detailed experiments that both bacteria and palladium black efficiently catalysed the water-hydrogen exchange reactions of Horiuti and Polanyi‡). We are thus forced to the conclusion that the observed factor of 3, 3 is very nearly the equilibrium constant of the reaction (see below)

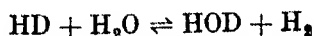


in agreement with the equilibrium measurement of Bonhoeffer and Rummel.§

The fact that the isotopic fractionation or separation in the hydrogen evolved by the enzymatic or catalytic decomposition of formate was due to the formation of hydrogen corresponding to the water-hydrogen equilibrium (1) suggested the investigation of the question whether the isotopic fractionation occurring in the electrolysis of water is due, at least partially, to the same cause.

Experimental

In order to answer this question the following experiments were carried out. Firstly the equilibrium



* It is remarkable that the same questions arise in the problem of overvoltage, but there is no other direct connection between overvoltage and the electrolytic separation of the hydrogen isotopes.

† Farkas, Farkas and Yudkin, 'Proc. Roy. Soc.,' B, vol. 113, p. 373 (1934).

‡ 'Nature,' vol. 132, p. 765 (1933).

§ 'Naturwiss.,' vol. 22, p. 45 (1934).

was determined by bringing into contact about 20 cc of ordinary hydrogen at 30 mm pressure with 0.2 cc of water containing 26.2% D in presence of a few milligrammes of freshly prepared palladium black at 20° C. From time to time samples of the gas were withdrawn and their D-content determined by the micro-thermal conductivity method already described (*cf.* Part I, *loc. cit.*).

Table I shows the attainment of the equilibrium.

Table I*

Time in mins	D % of the gas
0	0
30	5.0
48	7.5
55	9.5
93	10.2
115	9.8
120	10.1

* Since the sample was not shaken the progress of the exchange reaction was somewhat modified by diffusion effects.

From the final value 10.1% D we can derive the expression

$$\frac{(\text{H/D})_{\text{gas}}}{(\text{H/D})_{\text{water}}} = \frac{89.9}{10.1} : \frac{73.8}{26.2} = 3.16,$$

which is, to a first approximation—the equilibrium constant of the reaction



In the next experiment 0.6 cc of the same water (containing 26.2% D) was electrolysed at 20° C in a small U-tube after the addition of 5 mg NaOH* (0.2 N NaOH). As electrodes 0.7 mm nickel wires were used, the current was about 50–200 mA, and the current density 0.5–2 amp/cm². After having evacuated the cell the electrolysis was started and in a few minutes the evolved hydrogen attained a pressure of several millimetres. In three different runs the D-content of the evolved hydrogen was determined and found to be 9.6, 10.6, 9.5%, giving a mean of 9.9%.

This result shows quite definitely that in this experiment the preferential liberation of light hydrogen in the electrolysis of water is only due to the position of the hydrogen-water equilibrium, and that none of the above-mentioned processes, involving differences in velocity are responsible for the

* The determination of the D content was carried out after the addition of NaOH.

electrolytic separation occurring in this experiment. To confirm this the electrolytically evolved hydrogen containing 9.9% D was brought into contact with the original water, 26.2% D, in the presence of palladium black when only a very slight change in the D-content of the gas could be detected as shown in Table II.

Table II

Time in mins	D-content of the gas
0	9.9
21	10.2
35	10.1

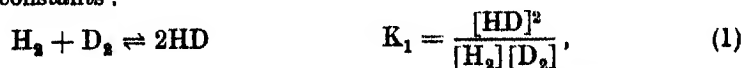
If we consider that in the electrolytic separation of the hydrogen isotopes a separation factor of about 4 is imposed on the system by the hydrogen-water equilibrium, we can understand why the separation factor observed under different conditions (different metal-electrodes, current densities, p_{H} of the electrolyte) does not differ very much from this value. Naturally the water-hydrogen equilibrium is not the only factor to be considered in the electrolytic separation, since in the most efficient fractionation experiments the factor is always higher than 6, and the velocities of discharge of the ions and the formation of molecular hydrogen may affect the separation.

Furthermore it is clear that this factor determining the electrolytic separation must also intrude in the chemical separation of the isotopes occurring when metals are dissolved in water or acids* or steam is decomposed by iron or carbon at high temperatures, although we originally attributed this separation to different velocities of the dissolution in light and heavy water.

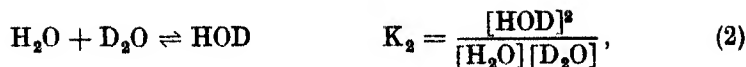
Considering all the different processes such as electrolysis, the catalytic decomposition of formate and the liberation of hydrogen by dissolving metals, we may anticipate that whenever hydrogen is evolved in aqueous solution by any process the hydrogen water reaction is, more or less, always operative thus causing, when light and heavy water are present, an isotopic fractionation. This is especially interesting in the preparation of heavy water by electrolysis as we might always expect a separation factor of the order 4—since the attainment of the equilibrium can be easily effected experimentally, *e.g.*, by coating the electrodes with palladium or platinum.

The connection between the hydrogen water equilibrium and the electrolytic or chemical "separation factor" can be established as follows.

The complete equilibrium is given by the three following equations and equilibrium constants:



† A. Farkas and L. Farkas, 'Nature,' vol. 133, p. 139 (1934).



It can be easily shown that all other exchange reactions between the different sorts of hydrogen and water molecules may be derived from these three equations, *e.g.*,



K_1 was originally calculated theoretically by Urey and Rittenberg* and their results were later experimentally confirmed,† K_1 being about 3.27 at room temperatures. K_2 has not yet been determined, but it will probably not differ very much from K_1 . The equation (3) expresses the complete equilibrium alone for low D-contents in gas and water, when only the molecules H_2 , HD, and H_2O HOD are present.

Then

$$K_3 = \frac{[\text{HOD}][\text{H}_2]}{[\text{H}_2\text{O}][\text{HD}]} \approx \frac{[\text{HOD}]}{[\text{HD}]} \approx \frac{D_{\text{water}}}{D_{\text{gas}}}.$$

If we introduce H and D content of gas and water, *i.e.*, the magnitudes

$$\begin{aligned} H_{\text{gas}} &= [\text{H}_2] + \frac{1}{2}[\text{HD}], \\ D_{\text{gas}} &= [\text{D}_2] + \frac{1}{2}[\text{HD}], \\ H_{\text{water}} &= [\text{H}_2\text{O}] + \frac{1}{2}[\text{HOD}], \\ D_{\text{water}} &= [\text{D}_2\text{O}] + \frac{1}{2}[\text{HOD}], \end{aligned}$$

the separation factor defined by

$$s = \frac{(H/D)_{\text{gas}}}{(H/D)_{\text{water}}},$$

can be expressed using the equations (1), (2), and (3) as a function of K_1 , K_2 , and K_3 .

This expression is very complicated for the particular case, but is reduced to a rather simple form $K_1 = K_2 = 4$ (which does not involve a large error).

* 'J. Chem. Phys.', vol. 1, p. 137 (1933).

† Part I and 'Nature,' vol. 132, p. 874 (1933); Bleakney and Urey, 'J. Chem. Phys.', vol. 2, p. 48 (1934).

We then obtain

$$s = K_3,$$

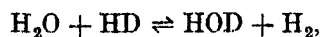
i.e., that this ratio is in effect a species of equilibrium constant, being independent of the H and D content.

It must be remarked, however, that in the exact treatment where the assumption $K_1 = K_3 = 4$ is not fulfilled, this ratio is not necessarily independent of the D-concentration.

We are very much indebted to Professor E. K. Rideal, F.R.S., for his interest in our work and for the communication of this paper.

Summary

It is shown that when in the electrolysis of a mixture of light and heavy water a preferential liberation of light hydrogen takes place, the gas evolved may reach equilibrium with the water corresponding to the reaction



the equilibrium constant of this reaction being about 3.8 at room temperature. It is pointed out that the position of this equilibrium is an important factor in the electrolytic separation of the hydrogen isotopes.

*Experiments on Heavy Hydrogen IV—The Hydrogenation and
Exchange Reaction of Ethylene with Heavy Hydrogen*

By A. FARKAS, L. FARKAS, and ERIC K. RIDEAL, F.R.S., Laboratory of
Colloid Science, The University, Cambridge

(Received June 5, 1934)

Hitherto it has generally been assumed that the catalytic hydrogenation of ethylene linkages in organic compounds at surfaces such as nickel or platinum involves merely the direct addition of a molecule of hydrogen across the double bond. In view of the fact that chemi-adsorbed hydrogen on catalytically active metallic substrates is in the atomic form it seemed possible that the reaction was indeed a more involved one than that suggested by the simple hypothesis referred to. By employing mixtures of light and heavy hydrogen it is possible to follow the reaction in more detail since the fate of the "labelled" heavy hydrogen atoms can be determined. Ethylene itself was used as a suitable substance for examination since it is readily hydrogenated at relatively low temperatures and complications due to other reactions are under these conditions absent.

Experimental

The experimental arrangement was very simple and is shown in fig. 1. The catalyst employed was in the form of a nickel wire, 0.1 mm diameter and 15 cm long, which was "activated" by oxidation, at 600° C, and reduction, at 300° C, several times in succession. The temperature of the wire was controlled by measuring its resistance in a Wheatstone-bridge. The trap D which was cooled by acetone carbon dioxide mixture served to protect the catalyst from poisoning by tap grease or by mercury vapours.

The ethylene used was distilled several times *in vacuo*. The mixture of light and heavy hydrogen was kept in the burette B after purification by passage through a palladium tube. The ethylene and hydrogen were both introduced into the reaction vessel V (volume 50 cc) and the pressure measured on the mercury manometer M.

In the course of the reaction between the ethylene and the hydrogen in addition to the change in the pressure the deuterium content of the hydrogen present in the vessel was measured from time to time using the micro-thermo

conductivity method.* The samples which were withdrawn through the lock L (volume 0.2 cc) passed through a trap (T) cooled by solid nitrogen of 63° K in order to freeze out every trace of ethylene and ethane which would affect the conductivity measurement. This D-determination could be performed relatively rapidly and each determination did not take longer than 2 to 3 minutes, and on account of the small amount of gas required for each measurement the decrease of the pressure caused by withdrawing the sample was practically negligible.

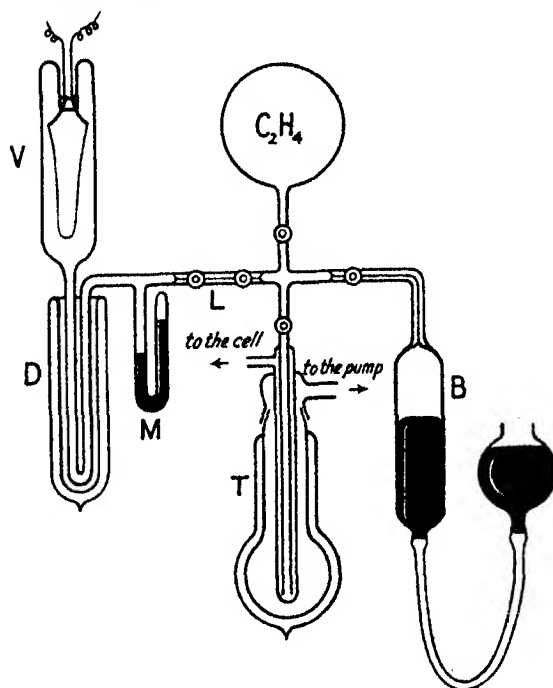


FIG. 1

The most striking features of the interaction of ethylene and heavy hydrogen are revealed by the experiments given in Tables I and II.

Table I—Temperature 20° C

Time in mins	Ethylene pressure in mm Hg	Hydrogen pressure in mm Hg	D-content %
0	21.5	32.5	30.6
10	13.5	24.5	30.0
25	5.5	16.5	33.2
37	1.0	12.0	33.8

* A. and L. Farkas, 'Proc. Roy. Soc.,' A, vol. 144, p. 467 (1934).

Table II—Temperature 120° C

Time in mins	Ethylene pressure in mm Hg	Hydrogen pressure in mm Hg	D-content in %
0	12	14	30.1
7	8	10	18.9
13	5	7	15.4
21	4	6	12.9
46	2	4	11.1

If the hydrogenation proceeds at low temperatures the D-content of the hydrogen does not suffer any marked change, an indication that both light and heavy hydrogen are consumed by the ethylene at nearly identical velocities. Actually a slight increase in the D-content is obtained indicating a small difference in the rates of the reaction between ethylene and light and heavy hydrogen respectively which is, however, much smaller than one would anticipate from analogy with other reactions. We shall refer to this point below.

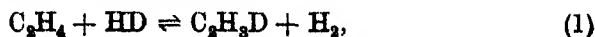
At higher temperatures in the progress of the reaction a considerable decrease in the D-content is to be observed, a fact which cannot be accounted for by assuming that this might be due to a higher rate of consumption of heavy hydrogen compared with the light isotope. Not only is this assumption highly improbable but direct experimental evidence against this view can be provided by the following data. Table III shows the results of an experiment carried out at 120° C.

Table III

Time in mins	Ethylene pressure in mm Hg	Ethane pressure in mm Hg	Hydrogen pressure in mm Hg	D-content of hydrogen in %
0	15	0	25	63.8
27	0	15	10	26.0

The decrease of the D-content in this case could only be caused by a preferential reaction of the heavy hydrogen on the assumption that the light one did not react at all.

The actual cause for this decrease is an exchange reaction occurring between ethylene and hydrogen according to the equation



as it is obvious from the experimental data cited in Tables IV and V.

Table IV—Temperature 155° C

	Pressure in mm Hg			D-content of hydrogen in %
	ethylene	ethane	hydrogen	
Initial	20	0	24	62
Final	13	7	17	22

The hydrogen containing 22% D in the gas mixture was replaced by pure hydrogen and the mixture of pure hydrogen, heavy and light ethylene and ethane re-admitted to the reaction vessel. After reaction the results given in Table V were obtained.

Table V—Temperature 155° C

	ethylene	Pressure in mm Hg ethane	hydrogen	D-content of hydrogen in %
Initial	13	7	16	0
Final	10	10	13	13

In the second run the exchange reaction causes an increase in the D-content of the freshly added ordinary hydrogen since the ethylene which was used already contained a considerable amount of D from the previous experiment.

It is clear that this exchange reaction can only be detected by using heavy hydrogen as reactant and by measuring the D-content during the process of hydrogenation. A comparison of reaction rates by measuring the pressure change alone would at these relatively high temperatures give us merely a measure of the rate of hydrogenation of ethylene by H_2 and the rate of hydrogenation of a partially D-substituted ethylene with a partially diluted mixture of light and heavy hydrogen.*

In equation (1) we have assumed that only ethylene but not ethane undergoes the exchange reaction. By conducting separate experiments it was found that ethane showed no interaction at all with heavy hydrogen under conditions in which in the presence of ethylene the exchange reaction proceeded readily. In the absence of the catalyst no homogeneous exchange reaction between ethylene and heavy hydrogen could be observed up to 250° C.†

The experiments recorded in Tables IV and V indicate that we are dealing with a reversible reaction. The equilibrium of this reaction can be actually established provided that the exchange reaction proceeds much faster than the hydrogenation since the ethane molecules formed in the hydrogenation are not able to undergo the exchange reaction. Above 120° C the exchange reaction on the catalyst actually employed was fast enough to approach this

* It must be observed that if pure H_2 and pure D_2 react at different rates with a certain substance they do not necessarily do so, when present in a mixture of light and heavy hydrogen, since exchange reactions similar to that described above may be operative. Thus to what an extent a separation of the hydrogen isotopes occurs in a chemical reaction proceeding in a mixture of the two can only be determined by direct experiment.

† This exchange would naturally be operative in a temperature region where the equilibrium $C_2H_4 \rightleftharpoons C_2H_6 + H_2$ comes into play.

equilibrium. In Table VI the results of some experiments are shown together with the final D-content calculated on the assumption that at equilibrium the D is equally distributed between ethylene and hydrogen.

Table VI—Temperature 120–150° C

Pressures in mm Hg		D-content %		Final D % calculated
ethylene	hydrogen	initial	final	
8.7	11.8	30.0	11.0	11.5
10	21	30.0	13.5	15.4
7	19	30.0	15.2	17.3
15	25	63.8	26.0	29.1

From these figures it would appear that the equilibrium constant of the reaction (1)

$$K_1 = \frac{(C_2H_3D)(H_2)}{(C_2H_4)(HD)}, *$$

is somewhat higher than unity, *i.e.*, the heavy hydrogen is preferentially present in the ethylene. It is very probable that the exact value of this constant is even higher than that indicated by these results since in our experiments the ratio of the rates of the exchange reaction to that of the hydrogenation reaction was not large enough to ensure a complete exchange before any ethane was formed.

Over the temperature range between 20 and 100° C both the addition and the exchange of hydrogen proceed simultaneously, the latter reaction coming to an end when the ethylene is used up. Table VII shows the results obtained at different temperatures.

In order to measure the change in the D-content during the course of the reaction at different temperatures catalysts of different activity were employed.† Thus the dependence of the hydrogenation and exchange reaction on temperature was not directly determined but rather the ratio of the temperature dependence of these two reaction velocities. This ratio was found to be independent of the activity of the catalyst.

* This equilibrium constant determines the distribution of light and heavy hydrogen between ethylene and hydrogen only for comparatively low D-contents in the hydrogen. For higher D-contents we must evidently take into consideration the equilibrium between the mono- and the different di- and poly- deuterio-ethylene molecules, and between H_2 , HD, and D_2 .

† This method is identical with that employed in investigating the distribution of oxygen between carbon monoxide and hydrogen by Hurst and Rideal, 'J. Chem. Soc.', vol. 125, p. 685 (1924).

Table VII

Temperature °C	C ₂ H ₄ : H ₂	D-content in %		Final D % calculated with K ₁ = 1	Equilibrium attained in %
		initial	final		
20	1 : 1	29.7	35.4	9.9	~0
58	0.6 : 1	65.9	48.5	30.0	48
78	0.5 : 1	63.6	43.5	31.8	65
120	0.58 : 1	65.0	28.0	30.2	~100

In column 6 the attainment of the equilibrium is given in %, i.e., the expression $100 [D_{\text{initial}} - D_{\text{final}} / D_{\text{initial}} - D_{\text{calculated}}]$.

These results show quite definitely that the exchange reaction and the addition reaction proceed independently of each other since they have different temperature coefficients. Whereas at low temperatures the addition of the hydrogen occurs without the exchange, at higher temperatures the latter is the faster process.

In order to obtain some information about the state and concentration of the hydrogen and ethylene on the surface of the catalyst a comparison of the rate of hydrogenation with the reconversion of parahydrogen was made. According to Bonhoeffer and Farkas* on a catalyst such as nickel the mechanism of the parahydrogen conversion is attributed to the loosing of the bond between the hydrogen atoms in the adsorption layer, to such an extent that the individual atoms are bound more firmly to the catalyst than to each other. When the hydrogen evaporates the atoms recombine in such a manner that the orthopara hydrogen content of the gas leaving the surface corresponds to the equilibrium at the temperature of the catalyst. Thus we can use the rate of the parahydrogen conversion as a measure of the adsorption and desorption velocity of hydrogen.

In fig. 2 is shown the conversion of 45% parahydrogen into normal hydrogen (25% *p*-H₂) at 20° C and 25 mm pressure. The rate of conversion is not altered by the presence of 17 mm of ethane. (The slight shift is due to the time delay caused by the diffusion with which the concentration change in the reaction vessel, V, fig. 1, reaches the lock 1.)

Fig. 3 refers to a hydrogenation experiment carried out in mixture of 19 mm ethylene and 23 mm 45% *p*-H₂ showing the consumption of ethylene and the rate of conversion. It is noted that the presence of ethylene strongly inhibits the parahydrogen conversion which, however, sets in immediately the bulk

* 'Z. phys. Chem.,' B, vol. 12, p. 231 (1931). 'Trans. Faraday Soc.,' vol. 28, pp. 242, 561 (1931).

of the ethylene is used up. The inhibition by ethylene of the ortho-para conversion of hydrogen is thus a phenomenon identical with the inhibition of the dissociation of hydrogen at a hot tungsten wire by traces of oxygen examined by Langmuir,* and a similar inhibition caused by traces of oxygen on the hydrogenation of ethylene.† When the inhibitor is removed by reaction the main reaction proceeds at a normal rate. This inhibition of the parahydrogen conversion by ethylene is completely reversible for the same rate of conversion was obtained before and after the hydrogenation experiment.

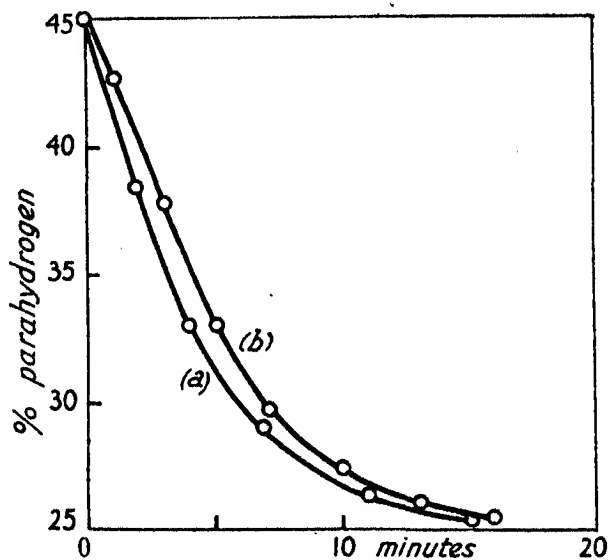


FIG. 2—(a) 25 mm H₂. (b) 25 mm H₂ + 17 mm C₂H₄.

Fig. 3 shows, furthermore, that the decrease of ethylene pressure is exactly linear in the first 30 minutes of the hydrogenation indicating a zero order reaction.

Discussion

These experiments give us some information about the mechanism of the hydrogenation of ethylene. The strong inhibition of the parahydrogen conversion by the ethylene suggests that at 20° C and at pressures of some 10 mm ethylene the surface of the nickel catalyst is very nearly completely covered with a layer of C₂H₄, which prevents the adsorption of hydrogen and thus the

* 'J. Amer. Chem. Soc.,' vol. 37, p. 1162 (1915); 'Trans. Faraday Soc.,' vol. 16 (1921).

† Rideal, 'J. Chem. Soc.,' vol. 121, p. 313 (1922).

parahydrogen conversion. The hydrogenation occurs whenever by evaporation of a C_2H_4 or a C_2H_6 molecule a gap can be filled by hydrogen which then reacts with the ethylene before leaving the surface. According to this view C_2H_4 is on the surface of the catalyst in a state in which it is ready to take up the hydrogen reaching it. The hydrogen which reacts with the ethylene on the catalyst is not necessarily dissociated into atoms, especially at low temperatures, although this probably occurs on a nickel surface. This mechanism explains the observed zero order of the reaction since the rate of reaction is determined simply by the rate of evaporation of C_2H_4 which is independent of

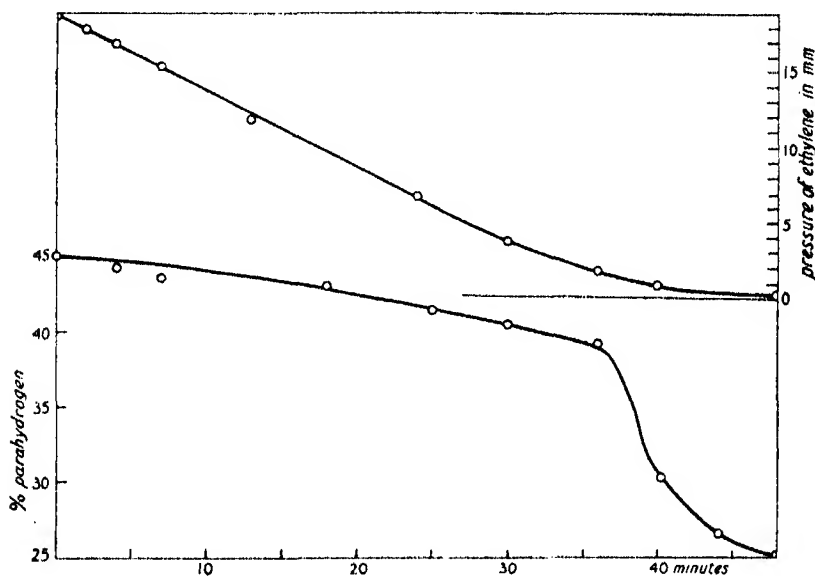


FIG. 3

the hydrogen and ethylene pressure until the adsorption layer becomes unsaturated. [From the experimental data this is so at $20^\circ C$ down to 1–2 mm C_2H_4 pressure, whereas at higher temperatures (about $60^\circ C$) the reaction ceases to be one of zero order, an indication that the adsorption layer is no longer saturated.]

This reaction mechanism is furthermore consistent with the fact that at $20^\circ C$ the light and heavy hydrogen are added to C_2H_4 at nearly the same speed, since the consumption of the molecules H_2 , HD , and D_2 takes place at the relative rates of their impingement on the gaps in the surface layer. The slight concentration increase in the D-content observed during the reaction (Table I) can be accounted for by the different molecular velocities of these

species. This is the reason why there is no difference in the reaction rates for light and heavy hydrogen, due to different activation energies, on account of the difference in their zero point energies as has been shown to hold for the diffusion through palladium,* for the union with chlorine,† and bromine‡ for the catalytic reaction with nitrous oxide and oxygen§ and anticipated theoretically by Polanyi and Cremer|| and by Eyring.¶

On increasing the temperature the surface of the catalyst does not remain saturated with ethylene but will be covered partially by a mixture of hydrogen and ethylene. At the same time the C—H bond becomes loosened in a manner similar to that which the H—H bond undergoes when hydrogen is adsorbed and undergoes the parahydrogen conversion. Since simultaneously light and heavy hydrogen molecules or rather atoms are present in the adsorption layer the exchange reaction,



will occur when the $\text{>C}=\text{C}<$ radical picks up new hydrogen atoms. The evaporating ethylene will now contain heavy hydrogen atoms corresponding to the concentration of the latter provided that a complete dissociation of the C_2H_4 into $\text{>C}=\text{C}<$ has taken place. At still higher temperatures even a complete dissociation involving a breaking of the double bond may occur.

The decrease of the ethylene concentration in the adsorption layer with increasing temperature accounts for the fact that the rate of hydrogenation of ethylene is not markedly temperature dependent.

Since the exchange reaction proceeds more slowly than the addition reaction below about 60°C and more rapidly above this temperature we can conclude that there are two factors which are responsible for this marked change in relative velocities. In the first case it is clear that in the addition reaction the steric factor is more important than in the exchange reaction for it is only at highly localized areas on the adsorbed molecule that addition can actually take place. Since the reactions have different temperature coefficients this involves the assumption of different energies of activation, that for the addition reaction being the smaller.

* A. and L. Farkas, 'Proc. Roy. Soc.,' A, vol. 144, p. 467 (1934).

† A. and L. Farkas, 'Naturwiss.,' vol. 22, p. 218 (1934); cf. Rollefson, 'J. Chem. Phys.,' vol. 2, p. 144 (1934).

‡ Bonhoeffer and Bach, 'Z. phys. Chem.,' A, vol. 168, p. 313 (1934).

§ Melville, 'J. Chem. Soc.,' p. 797 (1924).

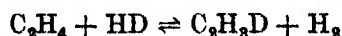
|| 'Z. phys. Chem.,' vol. 319, p. 443 (1932).

¶ 'Proc. Nat. Acad. Sci. Wash.,' vol. 19, p. 78 (1933).

These experiments raise the question as to how general this exchange reaction may be. For ethylene this phenomenon is most probably connected with its strong adsorptivity. Since the adsorption of ethylene on metals is much stronger than one would anticipate from its boiling point (*cf.* ethane) it is evident that it is due to forces of a definitely chemical nature which are also operative in the adsorption of hydrogen. Whether these chemical forces are based on the interaction of the double bond with the metal or on the loosening effect of the double bond on the C—H linkage and then on the interaction of the H and the $>C=C<$ radical* cannot be decided at the moment. The latter possibility receives some support from the fact that in acetylene where this loosening is caused by the triple bond the hydrogen atom can be directly replaced by metals.†

Summary

An examination of the interaction of ethylene and light and heavy hydrogen at a catalytically active nickel surface has revealed the fact that two reactions are involved ; an exchange reaction which may be written



and the more usual addition reaction



The steric factors and the temperature coefficients of these two reactions are not identical. By examining the rate of hydrogenation simultaneously with the rate of paraortho hydrogen conversion some light is thrown on the mechanism of hydrogenation reactions.

* According to this view tetra-methyl-ethylene should not be strongly adsorbed.

† With both acetylene and benzene we have failed so far to find an exchange reaction, but the catalyst underwent rapid irreversible poisoning. It is hoped that such poisons may be capable of being removed by suitable purification.

The Compressibility of Aqueous Solutions II

By W. G. THOMAS and E. P. PERMAN

(Communicated by A. W. Porter, F.R.S.—Received April 17, 1934)

Introduction

In an earlier communication, Perman and Urry* described the measurement, by a direct method, of the compressibility coefficients of aqueous solutions of urea, cane sugar, potassium chloride, and calcium chloride, over a range of temperatures and concentrations. Their work was over the pressure range 0–200 atmospheres excess pressure. They were able to apply their results, together with other data obtained by their co-workers, to an extension of Porter's theory of compressible solutions, and thus obtained values for the osmotic pressures of those solutions which agreed very well with the values obtained by more direct methods.

The present work is a continuation of this and subsequent work (unpublished) by these authors. It was intended, especially, to investigate the effect of the nature of the solute molecule upon the compressibility, and, for this reason, the choice of solutes was particularly important. A number of series of chemically related compounds were used where only one part of the molecule varied in a progressive manner from substance to substance. In another series there was no chemical relationship, but the members had the same empirical formula and their molecular weights were therefore simple multiples of each other.

Finally it was intended to use as fully as possible the experimental results of Perman and Urry.

Experimental Procedure

The experimental procedure was, fundamentally, the same as that of Perman and Urry, but the results were obtained at one temperature only, namely, 30° C, at which temperature the thermostat was very accurately maintained at all times. The thermostatic arrangements were superior to those of the earlier workers. Electrical immersion heaters in the bath were controlled by a thermo-regulator-relay system, but, contrary to the usual

* 'Proc. Roy. Soc.,' A, vol. 126, p. 44 (1929).

procedure, the relay, when activated, did not cut off the current supply to the heaters; it introduced, in series, a resistance which was so adjusted that the current supply to the heaters was reduced until it was just insufficient to maintain the bath at constant temperature. When the relay was inactive, this resistance was short-circuited, and the current in the heaters was regulated by another resistance until it was only slightly in excess of that required to maintain the bath at 30° C. The variation of current in the heaters was, therefore, very small, whereas, in the customary method, the variation was from the maximum to zero. This arrangement also assisted greatly in reducing sparking at the relay contacts.

A further increase in accuracy was considered necessary in the calibration of the capillary tubes. It was noted that the equation $V = \pi r^2 (L - 2/3r)$, giving the radius of the tube in terms of the length and volume of the mercury thread used in the calibration, did not admit direct solution. If the effect of hemispherical ends were ignored, as is usual in such calibrations, where the length of the thread is great compared with its radius, there would be an error of nearly 4% in the value of r^2 , since L cannot be greater than 15 mm and r is about 0.75 mm for the tubes used. Furthermore, the ends are not spherical, as was assumed in deriving the above equation. An alternative method of procedure was therefore adopted. A very long thread was introduced into the tube and its length L_1 measured. A small portion (about 1.3 cm) was run out into a tared weigh-tube and the length of the remainder L_2 measured. During the measurements of L_1 and L_2 , one end of the long thread was adjusted to coincide accurately with the etched mark on the tube. Then the portion of thread which had been removed was considered as an equivalent cylinder with one end concave and the other convex (not necessarily spherical, but some definite constant shape), having a volume $V = \pi r^2 (L_1 - L_2)$, its mean position being $\frac{1}{2} (L_1 + L_2)$ from the etched mark. This procedure was repeated, small lengths of mercury being run out and weighed until the whole tube was emptied.

This method of calibration was also considered very suitable because it bore a great resemblance to the method of measuring volume changes in the capillaries due to pressure during actual experiments. In practice, r need not be calculated, but a graph may be plotted for each capillary tube showing its internal volume (i.e., the weight of the mercury thread divided by density of mercury) against the distance from the etched calibration mark.

With these exceptions, the general experimental procedure was the same as that of Perman and Urry, and, since the same kind of glass was used in the

construction of the piezometers, use could be made of the elastic constants for glass obtained by them.*

The Solutions Studied

Three series of compounds were considered, care being taken that the compounds selected were sufficiently soluble to give a good range of concentration.

The first, consisting of potassium chloride, potassium bromide, and potassium iodide, gave an example of an inorganic salt series where the acid radicals varied from salt to salt, but themselves belonged to a chemically related series.

The second series was chosen where the metallic radicals varied from salt to salt, but which were all members of the same periodic series, and consisted of the bromides of calcium, strontium, and barium. The values for the solutions of calcium chloride studied by Perman and Urry were compared with those for this series.

The third series consisted of very soluble organic compounds having the same empirical formula but having no close chemical resemblances. Formalde-

Table I—Series I

Grams per 100 grams	Grams per 100 cc	n/N	D_4^{20}	Compressibility (0–100 atmospheres)
Potassium Chloride (Perman and Urry)				
2.59	2.62	0.0063	1.011	428×10^{-7}
5.37	5.53	0.0134	1.029	412
10.40	11.04	0.0276	1.062	385
12.23	13.15	0.0337	1.075	375
17.92	19.95	0.0526	1.113	347
22.19	25.38	0.0690	1.144	328
Potassium Bromide				
3.23	3.32	0.0050	1.027	430×10^{-7}
9.60	10.34	0.0161	1.077	401
14.60	16.39	0.0259	1.123	378
19.51	22.77	0.0367	1.166	358
25.51	30.98	0.0519	1.218	337
31.16	39.42	0.0685	1.265	317
32.10	40.70	0.0716	1.268	314
Potassium Iodide				
6.32	6.62	0.0073	1.048	422×10^{-7}
12.41	13.66	0.0154	1.101	399
19.86	23.14	0.0268	1.165	374
31.02	39.68	0.0488	1.279	336
38.76	53.46	0.0687	1.379	313
47.53	62.09	0.0983	1.476	302

* 'Proc. Phys. Soc.,' vol. 40, p. 186 (1928).

hyde and acetic acid formed this series which was compared with the sugar solutions of Urry (see Appendix).

Tables I-III give the experimental results, the concentrations being expressed as (a) grams of solute per 100 grams of solution, (b) grams of solute per 100 cc of solution, and (c) the ratio of the number of molecules of solute n to the number of molecules of solvent, N .

Table II—Series II

Grams per 100 grams	Grams per 100 cc	n/N	D_4^{20}	Compressibility (0-100 atmospheres)
Calcium Bromide				
13.29	15.04	0.0138	1.132	382×10^{-7}
26.84	34.77	0.0331	1.295	322
40.36	59.74	0.0810	1.480	272
52.76	87.74	0.1007	1.663	221
60.04	109.76	0.1354	1.798	204
Strontium Bromide				
13.03	14.67	0.0109	1.126	388×10^{-7}
24.70	31.17	0.0239	1.262	342
33.98	47.13	0.0375	1.387	309
42.17	64.01	0.0531	1.518	279
50.24	80.66	0.0735	1.655	248
55.60	97.97	0.0912	1.763	226
Barium Bromide				
8.74	9.40	0.00581	1.075	412×10^{-7}
15.85	18.25	0.01142	1.151	382
24.19	30.07	0.01934	1.243	351
31.87	40.44	0.02836	1.341	322
42.93	64.44	0.04560	1.502	283
53.01	92.40	0.06839	1.743	246

Table III—Series III

Grams per 100 grams	Grams per 100 cc	n/N	D_4^{20}	Compressibility (0-100 atmospheres)
Formaldehyde				
7.95	8.11	0.0518	1.020	416×10^{-7}
11.5	11.82	0.0780	1.028	406
16.4	17.06	0.1177	1.040	379
22.1	25.42	0.1703	1.055	361
29.0	31.12	0.2460	1.073	340
33.1	35.68	0.2970	1.078	326
40.2	43.70	0.4034	1.087	303
Acetic Acid				
10.0	10.05	0.0334	1.005	433×10^{-7}
20.5	20.83	0.0774	1.016	417
30.7	31.50	0.1329	1.026	395
42.6	44.13	0.2227	1.036	381
57.3	59.89	0.4028	1.046	351

Fig. 1 shows the compressibility-concentration curves drawn from these figures, but, owing to the smallness of the scale of plotting, the individual curves for each member of any series cannot be distinguished from those of the other members of the same series; accordingly, the curve for the middle member of each series only is given except for Series III where the curves are sufficiently spaced to allow separate plotting.

The values for solutions of calcium chloride (Perman and Urry) would, if plotted on the same diagram, almost coincide with the curve for Series II which includes calcium bromide.

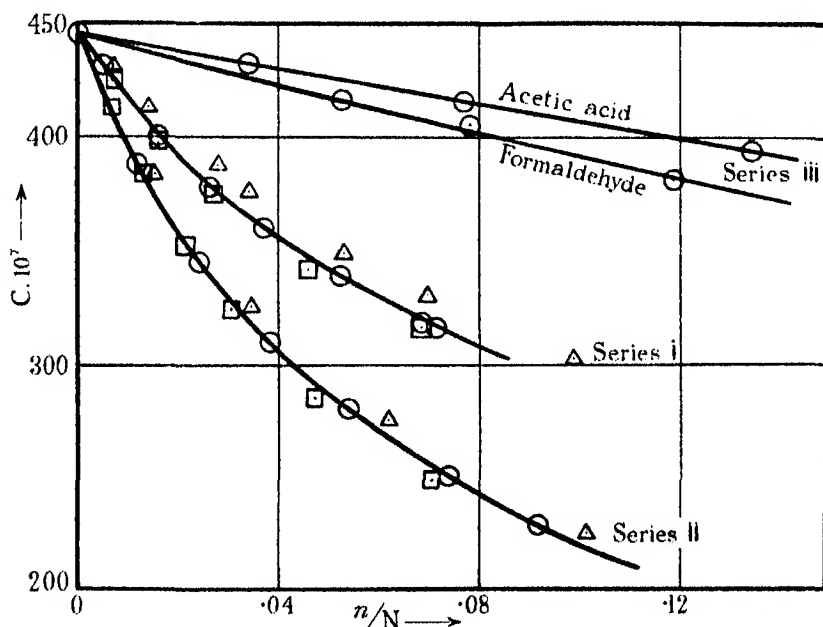


FIG. 1

Discussion

Inspection of small scale graphs at once suggests that the compressibility curves for substances closely related chemically lie very close to each other, whereas, when there are few or no chemical resemblances, as in Series III, the curves are widely spaced. In this connection, compare the diagram on p. 64 of Perman and Urry's earlier paper showing compressibility-concentration (molecular) curves at 30° C for potassium chloride, calcium chloride, urea, and cane sugar solutions. There, too, no relationship is suggested between the curves of chemically unlike substances.

A more careful plotting of the results on a larger scale reveals further information for the series of chemically related substances.

In Series I, the molecular weights differ by steps of about 45 units. It would be expected that an increase of this amount to the molecular weight of the chloride would cause a greater effect than the same addition to that of the bromide. This is, in fact, seen to be so, since the curve of potassium bromide lies slightly closer to that of the iodide than it does to the chloride curve.

This effect is also seen in the large scale diagram for Series II. In Series I, the weight variation between the compounds was greater than the weight of the common radical; in Series II, the heavier part of the molecules, the bromide radical, is fixed and the variation is small in comparison. Hence the curves for this series should lie closer than those of Series I. This is so, and moreover it can be seen that the curves for the two heavier bromides, barium and strontium, are more closely related than those of the lighter pair, calcium and strontium.

On this basis, too, it would be anticipated that the curves for solutions of calcium chloride (Urry) and calcium bromide should resemble one another more than those of potassium chloride and potassium bromide. The experimental results amply confirm this.

According to the electron theory, the members of these series differ amongst themselves by the number of electron orbits completed, the valency group upon which the chemical properties largely depend being common in any series. It is known that usually an increase in the number of completed orbits means an increase in the general stability of the compound and so, on this basis too, the differences between the properties of the chloride and bromide solutions should be greater than the differences between the properties of the bromide and iodide solutions. A similar statement might be made for the other series.

The compounds of Series III consisted of the same elements in exactly the same proportions by weight, but no obvious chemical properties are common to the compounds. Accordingly, no similarity was expected, worthy of notice, between the compressibility curves for the series, and none was observed.

Mention may be made here of a series of results obtained by Urry (private communication) for three sugars, a monosaccharide, a disaccharide, and a trisaccharide, namely, glucose, sucrose, and raffinose (see Appendix). The curves drawn from the data do not lie so close as those of Series I or II above, but are sufficiently close to indicate that there is some relationship between them. The compounds, being sugars, have many chemical resemblances, and we suppose that the molecules are built up of very similar units. The general

symmetry of the whole molecule would, however, differ very much along the series and it would be expected, therefore, that the curves for this series would not bear the close similarity of those of such a series as the salt series considered above, but would show a greater relationship to each other than the curves of a series such as the Series III considered above. The experimental results support this view.

Consideration of the data available, namely, that in Perman and Urry's earlier communication, Urry's unpublished results for the sugar solutions, and our own results given above, suggests, therefore, that there is some connection between the nature of the solute molecule and its effect upon the compressibility of the solvent, water.

Firstly, it is seen in all substances examined that the depression of compressibility is some function of the concentration of the solution, but, unless there is a close chemical relationship between the solutes, there is little similarity between the effects of different solutes. Where this similarity does exist, such as in one of the salt series described above, the effects are quite orderly and appear to depend directly upon the closeness of the relationship between the compounds considered. Unfortunately, however, the data available are very scanty for such a qualitative survey of so large a field; there are many indications, however, that there is a chemical as well as a physical aspect of solution and theories of solution.

It is well known that there is some chemical connection between solute and solvent, sufficient indeed to suggest a loose chemical combination between the molecules. The theories of co-ordinate linkages put forward by Sidgwick and others already furnish a mechanism for such solute-solvent combinations, and it is reasonable, therefore, to suggest that the effect of the solute upon the physical properties of the solvent depends to a greater extent upon the chemical properties of the solute than upon its molecular weight.

In the compressibility results given this is definitely confirmed.

In all the above considerations the curves studied have been those in which the molecular concentration (n/N) has been plotted against the compressibility. The method of expressing the concentrations can be varied, but, although curves for any series may then become more widely spaced, the general arguments outlined above still hold.

When, however, the concentrations are expressed in terms of the weight of solute per unit weight of solution, the curves (not reproduced here), plotted from the data, nearly always approximate to straight lines. This is mentioned in Perman and Urry's paper, pp. 62-64, but no theoretical inference was

drawn. The weight-concentration-compressibility curves for sucrose and potassium chloride are straight for all temperatures; that for urea showed very slight curvature which, the authors suggested, was due to a slight hydrolysis which is known to take place. The calcium chloride curves, however, show considerable curvature over the whole range, the explanation probably being the great and varying hydration which occurs in solution.

Weight-concentration-compressibility curves for the present results show the same fairly close approximation to the straight line. The curves for Series I show very slight curvature for potassium iodide, and even less for the bromide, whilst the chloride curve is straight. In Series II, where the curves lie even closer, this is even more apparent, and a marked contrast is seen in the calcium chloride curve if this is plotted on the same diagram, although, as already stated above, it lies very close to the other curves when the concentrations are expressed as the ratio of the numbers of molecules. In Series III, the formaldehyde curve is straight whilst that for acetic acid shows but slight curvature due probably to such changes as hydration, ionization, and association.

Thus, in most substances studied, a linear equation would approximately relate the compressibility and the concentration, the latter being expressed as the weight w of solute per unit weight of solution. Hence the depression of the compressibility Δc can be defined by such an equation as $\Delta c = k \cdot w$. If n is the number of solute molecules of molar weight M , in unit weight of solution, $w = n \cdot M$. This can be substituted in the first equation giving the relationship $\Delta c = k \cdot n \cdot M$, and since, for any one solute M is normally a constant, $\Delta c = K \cdot n$, where K is a constant depending partly upon M . This final equation is also linear, and so the compressibility-concentration curves, replotted to express the concentrations in terms of moles of solute per unit weight of solution, would be straight lines too, differing from the weight (in grams) per unit weight of solution curves only in the gradient.

Provided that the concentrations are expressed in this manner, the curves for all solutions studied, with the exception of calcium chloride, are either straight lines or curves differing only very slightly from straight lines. The gradients of the curves, however, differ considerably even amongst members of the same related series, and to see best the family relationship between the members of any series, the concentrations should be expressed as the ratio of the numbers of molecules n/N .

In the series of three sugars (see Appendix), however, the three curves plotted in this way have the same gradient, *i.e.*, are coincident straight lines. This would suggest that every raffinose molecule has exactly three times the

effect, and every sucrose molecule twice the effect of a glucose molecule. The fact that the lines are straight is to be anticipated after considering the information given above, since the sugars, as solutes, usually behave in a more orderly manner than inorganic salts, acetic acid, urea, etc. It is also to be expected that the heavier raffinose molecule would affect the compressibility more than the lighter sugars, but it is not difficult to suggest reasons for the effects following the ratio of the molecular weights.

Two explanations may be put forward to account for this, the one being purely physical, and the other purely chemical:—

(a) Polysaccharide molecules are considered as consisting of monosaccharide molecules linked to each other by single bonds. The monosaccharide molecules are assumed to be unchanged in structure, except for this link, and it is reasonable to assume, therefore, that a trisaccharide molecule would have approximately three times the volume of one of its constituent monosaccharide molecules. When a liquid suffers compression, it is assumed, after consideration of the available experimental material, that at the lower pressures at least (up to about 5000 atmospheres), the main result is to force the molecules closer together, so reducing the spaces between them. The molecules themselves are assumed to be only very slightly affected. In a solution, the solute molecules must necessarily occupy the spaces between the solvent molecules, whether attached to the latter or not. On this basis it might be assumed therefore, that, as the compressibility at the pressures we are considering depends on the change of volume of the intermolecular (solvent) spaces, the effect of a solute would depend directly on the volume of the solute molecule. Raffinose would, therefore, be expected to affect the compressibility three times, and sucrose twice as much as glucose.

(b) It has been pointed out above that the effects of a solute upon compressibility depend very largely upon the chemical structure of the molecule. Then, as raffinose has three 6-carbon units, sucrose two, and glucose one, all bearing a general resemblance to each other, it might be expected that each unit produces its own effect as if the others were not present. In the general properties of sugars, this is seen. It is known that, when monosaccharide molecules combine to form di- and tri-saccharides, their chemical properties are not submerged in a new set of properties of the di- or tri-saccharide. Accordingly, on a chemical basis, too, we might anticipate that a raffinose molecule would affect compressibility three times as much as a glucose molecule, and so the compressibility-concentration (grams/100 grams) curves would approximately coincide.

Finally, the compressibility-concentration (weight) curve for formaldehyde solutions would, if plotted upon the same diagram as those of the three sugars, bear a very close relationship to the sugar curves. There is not that remarkable coincidence that is seen between the sugar curves, but the closeness suggests that, whatever explanation is put forward to explain the coincidence of the sugar curves, the same explanation must also apply to the formaldehyde solutions in which one molecule of formaldehyde would produce approximately one-sixth the effect of a molecule of glucose.

Both the above reasons, chemical and physical (volumetric), can be applied if a sugar molecule be regarded as a chain or ring of formaldehyde molecules joined through the carbons, but naturally the accuracy of the coincidence of the curves cannot be expected to be as good as between the sugars themselves.

Similar reasoning would suggest that the acetic acid molecule would have quite a different volume and effect from two formaldehyde molecules or one-third of a glucose molecule, and no relationship to formaldehyde or the sugars is expected, or found.

APPENDIX

We are very grateful to Dr. W. D. Urry for permission to include his values, hitherto unpublished, for the compressibility coefficients of glucose and raffinose solutions. These results are given in Table IV. The concentrations were

Table IV—Temperature 30° C. Pressure range 0–100 atmospheres

Grams per 100 grams	n/N	D_t^{80}	Compressibility
Glucose			
4.21	0.0044	1.0105	434.0×10^{-7}
8.79	0.0096	1.0279	417
15.28	0.0180	1.0526	396
26.83	0.0367	1.0973	358
36.23	0.0568	1.1369	327.5
Sucrose			
5.12	0.0027	1.016	430×10^{-7}
13.95	0.0085	1.051	400
20.62	0.0137	1.080	378
35.62	0.0293	1.150	331
47.14	0.0473	1.210	292
55.19	0.0648	1.253	268
61.67	0.0848	1.293	247
Raffinose			
6.96	0.0027	1.0233	425.5×10^{-7}
11.15	0.0045	1.0410	411
20.71	0.0093	1.0836	377
25.44	0.0122	1.1054	361

determined polarimetrically and are expressed (a) as grams of sugar per 100 grams of solution, and (b) as the ratio of the number of molecules of sugar to the number of molecules of solvent (n/N).

For purposes of comparison, the results for cane sugar solutions are also repeated here, and thus the whole series consists of a monosaccharide, a disaccharide, and a trisaccharide.

The relationship of the curves to each other has been discussed above.

Summary

(1) Slight improvements and modifications of Perman and Urry's method of measuring the compressibility of solutions are described.

(2) Results are given for solutions of potassium chloride, potassium bromide, potassium iodide, calcium bromide, strontium bromide, barium bromide, acetic acid, and formaldehyde. The measurements were made at 30° C and over the pressure range 0–100 atmospheres excess.

In an Appendix, results for solutions of glucose, sucrose, and raffinose, obtained by W. D. Urry, over the same pressure range, are given.

(3) The results are discussed with regard to compressibility in equi-molecular solutions, and to the effect upon the solvent of differently constituted solute molecules.

Approximate Phases in Electron Scattering

By F. L. ARNOT, Ph.D., Lecturer in Natural Philosophy, and G. O. BAINES,
M.A., The University, St. Andrews

(Communicated by H. S. Allen, F.R.S.—Received April 18, 1934)

Introduction

During the last five years considerable attention has been devoted to the scattering of electrons by atoms and molecules of a gas or vapour. On the experimental side a large number of scattering curves have been obtained showing the angular distribution of the electrons scattered from a primary beam by atoms and molecules of many different gases and vapours. The most characteristic feature of these curves is the presence of diffraction maxima and minima. On the theoretical side expressions, valid under different conditions, have been obtained showing the variation of scattered intensity with angle. Where a comparison between theoretical and experimental curves has been made good agreement is obtained, and the theory is able to account for the observed diffraction effects.

However, assuming the atomic field is accurately known, the calculations required to obtain an accurate theoretical curve for even the elastically scattered electrons are exceedingly laborious and consequently approximations have generally been made. These consist in using approximate solutions of the wave equation, from the asymptotic solution of which the phases are determined.

Two approximate expressions for the phases have been used, one due to Jeffreys and the other to Born. In the present paper a number of phases for krypton have been calculated by both Jeffreys' and Born's method, and these are compared with the exact phases determined by Holtsmark. A theoretical scattering curve for 121-volt electrons in krypton has also been calculated using phases determined by Jeffreys' and Born's methods, and this is compared with Arnot's experimental curve.

Jeffreys' Approximation

The elastic scattering of electrons by a spherically symmetrical field is given by

$$I(\theta) = \frac{1}{4k^2} \left| \sum_{n=0}^{\infty} (2n+1) [e^{2i\delta_n} - 1] P_n(\cos \theta) \right|^2,$$

where $I(\theta)$ is the scattered intensity at an angle θ and

$$k = 2\pi/\lambda = (8\pi^2 m E / h^2)^{1/2},$$

λ being the wave-length and E the energy of the incident electrons. Separating the expression into its real and imaginary parts, and taking the square of the modulus we obtain

$$I(\theta) = \frac{1}{4k^2} \left[\sum_{n=0}^{\infty} (2n+1) (\cos 2\delta_n - 1) P_n \right]^2 + \frac{1}{4k^2} \left[\sum_{n=0}^{\infty} (2n+1) \sin 2\delta_n P_n \right]^2. \quad (1)$$

The phases δ_n in (1) are obtained from the asymptotic solution of the wave equation,

$$\frac{d^2\psi}{dr^2} + a\psi = 0, \quad (2)$$

where

$$a = k^2 - \frac{8\pi^2 m}{h^2} V(r) - \frac{n(n+1)}{r^2}, \quad (3)$$

$V(r)$ being the potential energy of the incident electron in the field of the scattering atom.

If $V(r)$ is zero, the solution of (2) which is zero at the origin is of the form

$$\psi \sim J_{n+1/2}(kr)$$

which has the asymptotic value*

$$\psi \sim \sin(kr - \frac{1}{2}n\pi). \quad (4)$$

If $V(r)$ is not zero, it is not possible to obtain an analytical solution of (2). However, as r increases the two last terms of (3) tend to zero, and when r is large a is constant and equal to k^2 . Thus the *asymptotic* solution of (2) which is zero at the origin is of the form

$$\psi \sim \sin(kr - \frac{1}{2}n\pi + \delta_n). \quad (5)$$

This defines the phases δ_n occurring in (1), and we see from (4) and (5) that δ_n is zero when $V(r)$ is zero. δ_n is thus the phase difference between the asymptotic solution of (2) when $V(r)$ is zero, and its asymptotic solution when $V(r)$ has its value corresponding to the atomic field.

Now when $V(r)$ is not zero an accurate solution of (2) can be found only by a very laborious numerical integration. However, Jeffreys† has shown that

* Watson, "Bessel Functions."

† 'Proc. Lond. Math. Soc.,' vol. 23, p. 437 (1924).

an approximate solution of (2) can be obtained provided a does not vary too rapidly with r . If a is strictly constant, the solutions of (2) are

$$\psi = A \exp [\pm ia^{\frac{1}{2}}r].$$

Jeffreys takes

$$\psi = A(r) \exp \left[\pm i \int a^{\frac{1}{2}} dr \right]. \quad (6)$$

Substituting in (2) we obtain

$$A'' + 2iA'a^{\frac{1}{2}} + iAa^{\frac{1}{2}'} = 0,$$

where the dashes denote differentiation with respect to r . Since A is practically constant $A'' \ll A'a^{\frac{1}{2}}$. Neglecting A'' we have

$$2A'a^{\frac{1}{2}} + Aa^{\frac{1}{2}'} = 0,$$

which gives

$$A = Ba^{-\frac{1}{2}},$$

where B is an arbitrary constant. Therefore our approximate solutions of (2) are

$$\psi = Ba^{-\frac{1}{2}} \exp \left[\pm i \int_0^r a^{\frac{1}{2}} dr \right]. \quad (7)$$

Now if a has a zero r_0 , such that a is negative for $r < r_0$ and positive for $r > r_0$ then the solutions (7) will be exponential up to r_0 , and oscillatory beyond. Jeffreys has shown that the solution which decreases exponentially below r_0 , becoming zero at the origin, has the asymptotic form

$$\psi \sim \sin \left[\frac{1}{4}\pi + \int_{r_0}^{\infty} a^{\frac{1}{2}} dr \right]. \quad (8)$$

Similarly if $V(r)$ in (3) were zero we should obtain

$$\psi \sim \sin \left[\frac{1}{4}\pi + \int_{r'_0}^{\infty} b^{\frac{1}{2}} dr \right], \quad (9)$$

where

$$b = k^2 - \frac{n(n+1)}{r^2}. \quad (10)$$

Since δ_n is the phase difference between (8) and (9) we have

$$\delta_n = \int_{r_0}^{\infty} a^{\frac{1}{2}} dr - \int_{r'_0}^{\infty} b^{\frac{1}{2}} dr, \quad (11)$$

where r_0 and r'_0 are the zeros of the respective integrands.

The Special Case of δ_0

The derivation of equation (11) requires both a and b to have a definite zero between $r = 0$ and $r = \infty$. Now for all values of n except zero it is clear that a and b will have definite zeros for both repulsive and attractive fields.

If n is zero it is clear that b has no zero, and if the field is attractive $V(r)$ in (3) is negative and consequently a has no zero. To obtain an expression for δ_0 in this case we must choose from the solutions (7) the one which is zero at the origin. This is clearly

$$\psi = Ba^{-1} \sin \left[\int_0^r a^{\frac{1}{2}} dr \right],$$

which has the asymptotic form

$$\psi \sim \sin \left[\int_0^\infty a^{\frac{1}{2}} dr \right]. \quad (12)$$

Similarly if $V(r)$ is zero we obtain

$$\psi \sim \sin \left[\int_0^\infty b^{\frac{1}{2}} dr \right], \quad (13)$$

and hence

$$\delta_0 = \int_0^\infty a^{\frac{1}{2}} dr - \int_0^\infty b^{\frac{1}{2}} dr. \quad (14)$$

We can therefore use the expression (11) for δ_0 in an attractive field if we replace the lower limits of both integrals by zero. In a repulsive field, however, a does have a zero, since $V(r)$ in (3) is now positive. Therefore our asymptotic solution (8) remains valid, but we must replace (9) by (13), since b has no zero. We thus obtain for δ_0 in a repulsive field

$$\delta_0 = \frac{1}{4}\pi + \int_{r_0}^\infty a^{\frac{1}{2}} dr - \int_0^\infty b^{\frac{1}{2}} dr. \quad (15)$$

The Error in Jeffreys' Approximation when $V(r)$ is Zero

When $V(r)$ is zero the asymptotic form of the solution of (2) which is zero at the origin is given by (4), and is

$$\psi \sim \sin(kr - \frac{1}{2}n\pi). \quad (16)$$

Jeffreys' approximation (9) gives

$$\psi \sim \sin \left[\frac{1}{4}\pi + \int_{r_0}^\infty \left(k^2 - \frac{n(n+1)}{r^2} \right)^{\frac{1}{2}} dr \right]. \quad (17)$$

To evaluate this integral consider

$$\int_{r'_0}^{\infty} \left[\left(1 - \frac{s^2}{r^2} \right)^{\frac{1}{2}} - 1 \right] dr = s, \quad (18)$$

where

$$s^2 = \frac{n(n+1)}{k^2},$$

and r'_0 is the zero of $\left(1 - \frac{s^2}{r^2} \right)$, i.e., $r'_0 = s$.

Integrating (18) by parts, and substituting $r = s \sec \theta$ in the result we find that (18) is equal to $-s \frac{\pi}{2}$. Multiplying (18) throughout by k we obtain

$$\int_{r'_0}^{\infty} \left[\left(k^2 - \frac{s^2 k^2}{r^2} \right)^{\frac{1}{2}} - k \right] dr - kr'_0 = -\sqrt{n(n+1)} \frac{\pi}{2},$$

and hence for large r

$$\int_{r'_0}^{\infty} \left(k^2 - \frac{n(n+1)}{r^2} \right)^{\frac{1}{2}} dr = kr - \sqrt{n(n+1)} \frac{\pi}{2}.$$

Substituting this value for the integral in (17) we obtain

$$\psi \sim \sin \left[kr - (\sqrt{n(n+1)} - \frac{1}{2}) \frac{\pi}{2} \right].$$

Comparing this with (16) we see that Jeffreys' value of the angle is greater than the exact value by

$$(n + \frac{1}{2} - \sqrt{n(n+1)}) \frac{\pi}{2}. \quad (19)$$

For all values of n except zero this is very small; for $n = 1$ the error amounts to 0.13; for $n = 2$ it is only 0.08.

When n is zero the error would appear to be $\frac{1}{4}\pi$. However, as has been pointed out in § 2, the approximation (17) breaks down when n is zero, and we must use in place of (17) the expression (13). This is less than (17) by the term $\frac{1}{4}\pi$, and hence the error is zero, as would be expected; for when n is zero, b in (13) is constant, and consequently Jeffreys' solution is exact.

It should be pointed out that the error discussed in this section is that of Jeffreys' approximate solution of the wave equation (2) when $V(r)$ is zero, and not the error in Jeffreys' approximate expression for the phases. The expression (11) for the phases contains two terms, and the error discussed here is that in the second term only. The error in the first term of (11) will depend upon the form of $V(r)$. We shall see in the next section that the error in the

phases, and hence the error in the first term of (11) is sometimes considerably greater than the error in the second term, which is given above.

Comparison of Approximate and Exact Phases

We have seen that Jeffreys' approximate expression for the phases in an attractive field is

$$\left. \begin{aligned} \delta_n &= \int_{r_0}^{\infty} a^{\frac{1}{2}} dr - \int_{r'_0}^{\infty} b^{\frac{1}{2}} dr \\ \text{where} \\ a &= k^2 - \frac{8\pi^2 m}{h^2} V(r) - \frac{n(n+1)}{r^2} \\ \text{and} \\ b &= k^2 - \frac{n(n+1)}{r^2} \end{aligned} \right\}, \quad (20)$$

and r_0 and r'_0 are the greatest positive zeros of the respective integrands. For the special case of δ_0 we put $r_0 = r'_0 = 0$.

This approximation will be satisfactory provided a does not vary too rapidly with r . We have already seen in § 3 that it is quite satisfactory for the term involving b .

For very small phases, such that $\sin \delta_n \sim \delta_n$ we may use Born's approximation

$$\delta_n = \frac{\pi}{2} \cdot \frac{8\pi^2 m}{h^2} \int_0^{\infty} r V [J_{n+\frac{1}{2}}(kr)]^2 dr. \quad (21)$$

This is obtained by Mott* from an approximate solution of the wave equation (2) on the assumption that the second term in (3) is so small that we may neglect any term involving its square.

Using Hartree's atomic field for $V(r)$ with a correction applied for polarization we have calculated a number of phases in krypton by both Jeffreys' formula (20), and Born's formula (21). These are given in Table I together with Holtsmark's exact phases,† calculated from the same field with the same polarization correction (Holtsmark's field No. 2). The phase δ_3 has been omitted for $k=2$ since Holtsmark does not give a value for this phase.

With the exception of δ_0 we see that the difference between the exact phase and Jeffreys' approximate phase is always small, the approximate formula always giving a slightly high value. The rather higher difference that occurs

* 'Proc. Camb. Phil. Soc.,' vol. 25, p. 304 (1929).

† 'Z. Physik,' vol. 66, p. 49 (1930).

in δ_2 for $k = 1$ is possibly due to an error in Holtsmark's exact phase, for we have carefully checked our value. It should be remarked that it is the actual difference between the two values that is of importance in judging the success of an approximate formula, and not the percentage error in the phase, since even multiples of 2π in any phase have no effect on the formula (1) for the scattered intensity.

Table I—Exact and Approximate Phases for Krypton

k^2 volts	k atomic units	Phase	Exact phase	Jeffreys' approx.	Born's approx.	Exact phase minus Jeffreys' approx.	Exact phase minus Born's approx.
0	0	δ_0	12.568	15.310		-2.742	
13.54	1	δ_0	10.996	12.024		-1.028	
		δ_1	8.489	8.781		-0.292	
		δ_2	4.368	4.880		-0.512	
		δ_3	0.226	0.286	0.242	-0.060	-0.016
		δ_4	0.107	0.107	0.107	0.000	0.000
54.15	2	δ_0	9.696	10.612		-0.916	
		δ_1	7.452	7.710		-0.258	
		δ_2	4.469	4.748		-0.279	
		δ_3	1.238	1.410	0.779	-0.172	+0.459
		δ_4	0.445	0.557	0.414	-0.112	+0.031
		δ_5	0.143	0.180	0.144	-0.037	-0.001

The most important feature of this work is that the error in Jeffreys' approximate phase *decreases* as the order of the phase increases. It has always been assumed that Jeffreys' approximation is only valid for phases of low order, having a value greater than unity. Although this may be so for a repulsive field,* we see from Table I that it is not true for an attractive field, at any rate for a heavy atom such as krypton. For $k = 1$ the error in Jeffreys' phase is zero for δ_4 which has a value of only 0.107.

Another surprising result is the large error in δ_0 . In order to see how this error varied with the atomic field we calculated δ_0 for $k = 0$ for the rare gases, krypton, argon, neon, and helium, using the Hartree field† in each case. The exact phase is an integral multiple of π for each atom. The results are given in Table II.

* Massey and Mohr find that Jeffreys' approximation gives far too low a value for phases less than unity in the collision of two helium atoms with $k = 2$ ('Proc. Roy. Soc.,' A, vol. 144, p. 188 (1934)).

† The Hartree field for the rare gases is given in the following papers: For Kr, Holtsmark, 'Z. Physik,' vol. 66, p. 49 (1930). For Ar, Holtsmark, 'Z. Physik,' vol. 55, p. 437 (1929). For Ne, Brown, 'Phys. Rev.,' vol. 44, p. 214 (1933). For He, McDougall, 'Proc. Roy. Soc.,' A, vol. 136, p. 549 (1932).

Table II— δ_0 Phases for $k = 0$ for the Rare Gases

Atom	Exact phase	Jeffreys' approx. phase
Kr	4π	$4\pi + 2.740$
Ar	3π	$3\pi + 1.040$
Ne	2π	$2\pi + 0.852$
He	π	$\pi + 0.180$

We see that for each gas Jeffreys' approximation gives too high a value, and that the error is less the smaller the atomic number of the atom.

In order to see how the error in δ_0 varied with k we calculated δ_0 by Jeffreys' formula for each value of k for which Holtsmark gives exact phases in krypton. These results are given in Table III and fig. 1.

Table III—Exact and Approximate Values of δ_0 in Krypton

k atomic units	Exact value	Jeffreys' approx.	Difference
0	12.568	15.310	2.742
0.1	12.709	14.418	1.709
0.2	12.597	13.956	1.359
0.5	11.975	13.050	1.075
0.7	11.536	12.620	1.084
1.0	10.996	12.024	1.028
2.0	9.696	10.612	0.916

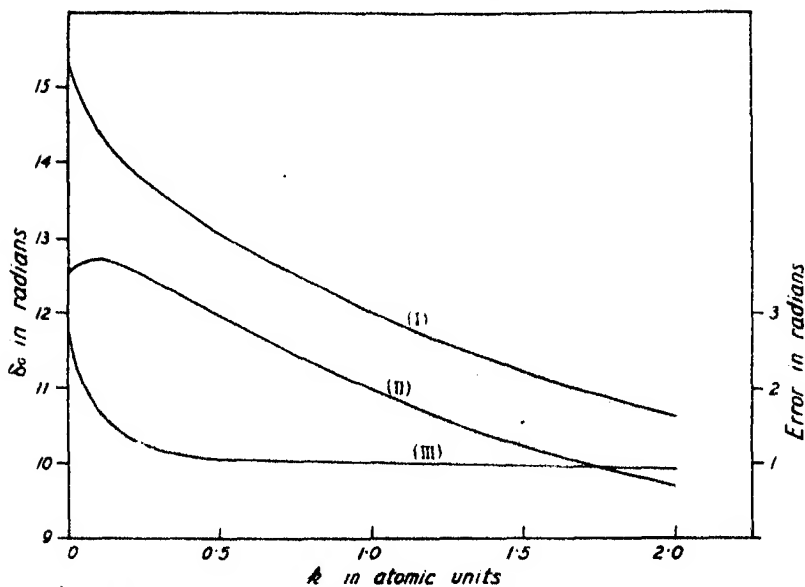


FIG. 1—Jeffreys' value (i) and exact value (ii) of δ_0 in krypton. Showing variation of the error (iii) with k .

We see from fig. 1 that as k increases the error in δ_0 decreases rapidly at first and then becomes nearly constant. Over the range from $k = 0.5$ to

$k = 2.0$ the error curve is a straight line, and consequently it would probably be justifiable to extrapolate linearly to obtain the correction for δ_0 for higher values of k .

The relatively large error in δ_0 compared with the other phases is readily explained if we remember that Jeffreys' approximation is deduced on the assumption that

$$a = k^2 - \frac{8\pi^2 m}{h^2} V(r) - \frac{n(n+1)}{r^2}$$

varies only slowly with r . Now in an attractive field V is negative and varies inversely with some power of r . The rate of variation of a will thus depend mainly upon the rate of variation of the potential field, and this rate decreases as r increases. We see from equation (20) that we are only concerned with the potential field beyond the zero of a . Now this zero r_0 is greater the greater the value of n , and consequently the rate of variation in the effective portion of the potential field is less the greater the value of n . This explains why the error in Jeffreys' approximation decreases as the order of the phase increases.

For the zero order phase δ_0 we must integrate right into $r = 0$, where the variation in the potential field is very great, and consequently we must expect a much greater error in δ_0 than in the phases of higher order.

Also since the rate of variation in the potential field near $r = 0$ is less for lighter atoms we should expect the error in δ_0 to decrease with the atomic number of the atom, as is shown to occur in Table II.

Since V is positive in a repulsive field the second and third terms in a have the same sign and consequently the variation in the third term will increase the total rate of variation of a with r instead of decreasing it as in an attractive field. This may cause the error in the phase to increase with the order in a repulsive field. Also since a has a zero in a repulsive field, even for $n = 0$, the error in the zero order phase should not be so large as it is in an attractive field.

Referring to formula (1) for the scattered intensity we see that it is the phase whose value is most nearly equal to $\frac{1}{2}\pi$ that mainly determines the form of the scattering curve, and therefore the error in δ_0 should not be very serious provided δ_0 is large (say, greater than 2π). The error, however, would be very serious if δ_0 was of the order of $\frac{1}{2}\pi$, and would entirely change the shape of the angular scattering curve. This might occur for a high value of k and a heavy atom. It would then be necessary to find δ_0 by numerical integration of equation (2). The other phases could, of course, be determined by the approximate methods of Jeffreys and Born.

As regards Born's approximation we see that this gives a satisfactory value for all phases less than about 0.5, and that for phases below this value Born's approximation is a little better than Jeffreys', the error in either approximation being for most purposes negligible.

In the calculation of phases it has been customary to use Jeffreys' approximation for phases greater than unity, and Born's approximation for the phases less than 0.5 or 0.2, the intermediate phases being then obtained by interpolation on a phase-order diagram. In this procedure the error in the phases obtained by interpolation may sometimes be quite large owing to the very rapid change in slope of the phase-order curve in the region between 1.0 and 0.2.

The results given in Table I show that this procedure is unnecessary, since Jeffreys' approximation may be used for phases down to quite small values, the error actually decreasing as the value of the phase decreases.

Angular Distribution Curve for 121-volt Electrons in Krypton

Using the Hartree field with the polarization correction given by Holtsmark we have calculated the phases for $k = 3$, corresponding to an energy of 121.6 volts, and used these in equation (1) to determine the angular distribution of electrons of this energy scattered in krypton. The phases are given in Table IV, and the scattered intensity* in atomic units in Table V. The phases δ_0 to δ_4 were calculated by Jeffreys' method, and δ_5 and δ_6 were obtained from Born's approximation.

Table IV—Phases for $k = 3$ for Krypton

δ_0	δ_1	δ_2	δ_3	δ_4	δ_5	δ_6
9.824	7.003	4.411	1.830	0.980	0.460	0.302

Table V—Scattered Intensity $I(\theta)$ in Atomic Units for 121-volt Electrons in Krypton

θ°	0	10	20	30	40	50	60	70	80	90
$I(\theta)$	75.21	55.76	22.18	3.35	0.608	1.57	2.13	2.00	0.749	0.007
θ°	100	110	120	130	140	150	160	170	180	
$I(\theta)$	0.293	0.721	0.335	0.218	0.122	0.009	0.676	2.56	3.83	

* The scattered intensity $I(\theta)$ is defined thus. If a beam of electrons passes through a gas containing N atoms per unit volume, then $NI(\theta)$ is the proportion of the beam elastically scattered in the direction θ per unit solid angle, and per unit length of the beam. $I(\theta)$ has the dimensions of an area.

In fig. 2 is given the theoretical curve with Arnot's experimental points* for 121-volt electrons fitted to it. The agreement is seen to be extremely good.

In conclusion, we wish to express our thanks to Dr. C. B. O. Mohr for advice in the calculation of the phases. One of us (G. O. B.) wishes to thank the Carnegie Trust for the Universities of Scotland for a Research Scholarship.

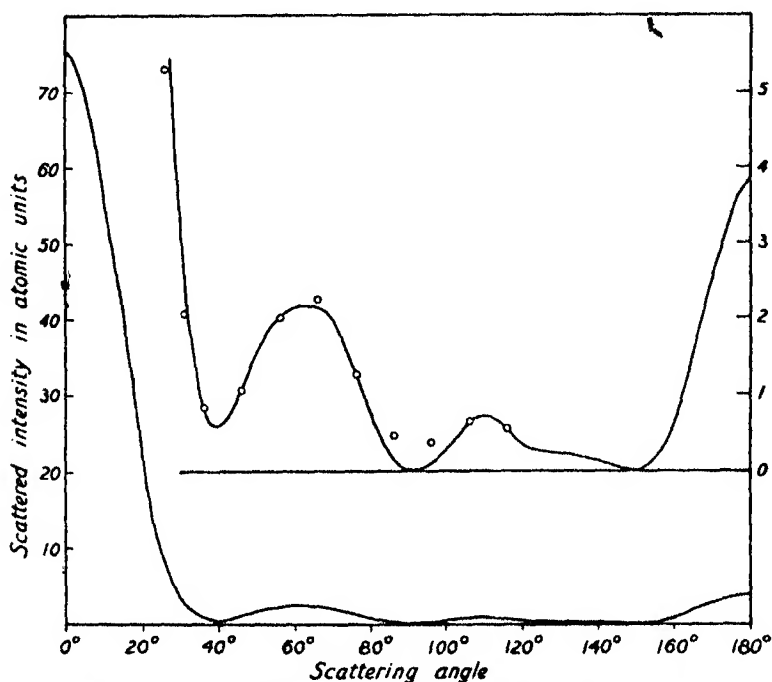


FIG. 2.—Theoretical curve and experimental points for the scattering of 121-volt electrons in krypton.

Summary

A discussion of Jeffreys' approximate expression for the value of phases is given. It is shown that in the special case of the zero order phase Jeffreys' expression is greater for a repulsive field than for an attractive field by the term $\frac{1}{4}\pi$.

A number of phases in krypton have been calculated by Jeffreys' and Born's approximate expressions, and these are compared with Holtsmark's exact values. The error in Jeffreys' phase is found to decrease as the order of the

* 'Proc. Roy. Soc.,' A, vol. 133, p. 615 (1931).

phase increases, and is small for all phases except that of zero order. The large error found in the zero order phase is shown to decrease with decrease in the atomic number of the atom, and with increase in energy. The cause of this error is discussed, and it is pointed out that the error is not likely to affect seriously the form of the angular distribution curve provided the phase is itself large. Born's approximation is found to be satisfactory for phases having a value less than 0.5.

A theoretical angular distribution curve is calculated for 121-volt electrons scattered in krypton, and very good agreement is obtained between this and Arnot's experimental curve.

The Scattering of Electrons in Bromine Vapour

By F. L. ARNOT, Ph.D., Lecturer in Natural Philosophy, and
J. C. McLAUCHLAN, M.A., The University, St. Andrews

(Communicated by H. S. Allen, F.R.S.—Received April 18, 1934)

Introduction

The angular distribution of the electrons scattered elastically from a primary beam in passing through the vapours of halogens and their compounds has recently been measured by one of us.* Diffraction maxima and minima were found in all the curves; and although the scattering was produced by molecules the form of each curve was similar to those previously obtained by the author for the adjacent monatomic rare gases.

We have now calculated theoretical curves for the same energies for which experimental curves were obtained in diatomic bromine. These results are given in the present paper, and a comparison is made between the theoretical and experimental scattering curves.

Elastic Scattering by Atoms

The elastic scattering of electrons by a spherically symmetrical field is given by

$$I_a(\theta) = \frac{1}{4k^2} \left| \sum_{n=0}^{\infty} (2n+1) [e^{2i\delta_n} - 1] P_n(\cos \theta) \right|^2, \quad (1)$$

* Arnot, 'Proc. Roy. Soc.,' A, vol. 144, p. 360 (1934).

where $I_a(\theta)$ is the scattered intensity at an angle θ and

$$k = 2\pi/\lambda = (8\pi^2 m E / h^2)^{1/2},$$

λ being the wave-length and E the energy of the incident electrons.

The phases δ_n in (1) are given to a sufficiently close approximation (p. 651) by Jeffreys' formula

$$\delta_n = \int_{r_0}^{\infty} \left[k^2 - \frac{8\pi^2 m}{h^2} V(r) - \frac{n(n+1)}{r^2} \right]^{1/2} dr - \int_{r_0'}^{\infty} \left[k^2 - \frac{n(n+1)}{r^2} \right]^{1/2} dr, \quad (2)$$

where r_0 and r_0' are the zeros of the respective integrands except in the special case of δ_0 , for which we set $r_0 = r_0' = 0$ and $V(r)$ is the potential energy of the incident electron in the field of the scattering atom.

For phases having a value less than 0.5 a slightly more accurate value is given by Born's approximation

$$\delta_n = \frac{1}{2}\pi \cdot \frac{8\pi^2 m}{h^2} \int_0^{\infty} r V [J_{n+1/2}(kr)]^2 dr. \quad (3)$$

Elastic Scattering by Molecules

The theory of the elastic scattering of electrons by molecules is far more complicated than for atomic scattering since the molecular field is not spherically symmetrical, and also because the wave equation for the motion of an electron in the field of the molecule is not separable as in atomic fields, unless a very much simplified molecular field is used, such as has been adopted by Stier.* Stier's method, however, is only applicable to very slow electrons (below about 10 volts).

For very fast electrons we may use Born's approximation for the scattered intensity; and for an axially symmetrical molecule which has no permanent dipole moment, such as diatomic bromine, we may assume the axis of the molecule to be orientated at random, and so average the scattering over all orientations to obtain the experimental conditions. It can be shown† that the scattered intensity for a homonuclear diatomic molecule is given approximately by

$$I_m(\theta) = 2I_a(\theta) \left[1 + \frac{\sin x}{x} \right], \quad (4)$$

where $I_a(\theta)$ is the scattered intensity for a single free atom obtained from Born's approximation. This expression neglects the effect of the binding

* 'Z. Physik,' vol. 76, p. 439 (1932).

† Massey and Bullard, 'Proc. Camb. Phil. Soc.,' vol. 29, p. 511 (1933).

between the two atoms, but it has been shown that this is quite small for hydrogen* and nitrogen,†

The term

$$1 + \frac{\sin x}{x},$$

where

$$x = 2kd \sin \frac{1}{2}\theta,$$

d being the equilibrium distance between the two nuclei, represents the interference between the waves scattered separately from the two atoms forming the molecule. For Br_2 , $d = 2.28 \text{ \AA} = 4.3$ atomic units.‡

For electrons with energy less than a few thousand volts Born's approximation for $I_a(\theta)$ breaks down for large angle scattering in bromine. However, (4) might prove fairly satisfactory if we use Faxen and Holtsmark's exact expression (1) for $I_a(\theta)$ in place of Born's formula. Massey and Bullard using Hund's§ molecular field for $V(r)$ in the calculation of the phases, find that this gives satisfactory results for nitrogen.

In the following calculations for bromine we have used the expression (4), determining $I_a(\theta)$ from (1), and using for $V(r)$ in (2) and (3) an approximate Hartree atomic field for bromine calculated from Hartree's results for rubidium.

The Hartree Atomic Field for Bromine

Before we can evaluate the phases we must determine the atomic field. The most accurate value of $V(r)$ is obtained by the self-consistent field method of Hartree.|| Using Hartree's atomic units we have

$$\frac{8\pi^2 m}{h^2} V(r) = \frac{2Z_p}{r},$$

where Z_p is the effective nuclear charge for potential. This is related to the effective nuclear charge Z by

$$Z_p(r) = -r \int_r^\infty \frac{Z}{r^2} dr. \quad (5)$$

However, in the actual calculation of Z_p from Z this equation does not prove

* Massey and Bullard, 'Proc. Camb. Phil. Soc.', vol. 29, p. 511 (1933).

† Massey and Mohr, 'Proc. Roy. Soc.,' A, vol. 135, p. 258 (1932).

‡ Wierl, 'Ann. Physik,' vol. 8, p. 521 (1931).

§ 'Z. Physik,' vol. 77, p. 12 (1932).

|| 'Proc. Camb. Phil. Soc.,' vol. 24, p. 89 (1927).

to be numerically satisfactory. We have consequently used the following modified form of (5) kindly supplied by Professor Hartree,

$$Z_p = N - r \int_r^\infty \frac{N - Z}{r^2} dr, \quad (6)$$

where N is the value of Z for $r = 0$, *i.e.*, the atomic number.

The field for bromine was calculated from the Hartree field for singly ionized rubidium.* The contributions to Z for bromine from the different atomic sub-shells were determined from the contributions from corresponding sub-shells to Z for ionized rubidium by expanding the linear scale in the ratio

$$\frac{N(\text{Rb}^+) - s}{N(\text{Br}) - s},$$

where N is the atomic number and s a screening constant which varies for the different sub-shells.

For the outermost incomplete $4p^5$ sub-shell the following correction was applied. It is known that

$$\frac{5}{3}Z(\text{Cl}, r) \sim Z(\text{K}^+, \frac{3}{4}r)$$

where $Z(\text{Cl}, r)$ is the contribution to Z at radius r from the outermost sub-shell of the chlorine atom, and $Z(\text{K}^+, r)$ is the corresponding quantity for K^+ . Therefore

$$\frac{5}{3}Z(\text{Cl}, r) - Z(\text{K}^+, \frac{3}{4}r)$$

was plotted against

$$Z(\text{K}^+, \frac{3}{4}r)$$

so giving a correction graph for the calculation of $Z(\text{Cl}, r)$ from $Z(\text{K}^+, \frac{3}{4}r)$. The correction for bromine was then obtained from this graph by assuming that $\frac{5}{3}Z(\text{Br}, r) - Z(\text{Rb}^+, \alpha r)$ was the same function of $Z(\text{Rb}^+, \alpha r)$ where α is a constant.

The contributions to Z from the various sub-shells are given in Table 1 together with the total effective nuclear charge Z , and the effective nuclear charge for potential Z_p calculated from Z by (6).

Professor Hartree informs us that the error in the contributions to Z from each sub-shell from $1s^2$ to $3p^6$ should be less than 0.05 for all values of r . The error in the contributions from the $3d^{10}$ and $4s^2$ groups may be a little greater, but not more than 0.1; whereas for the outermost $4p^5$ group the error may possibly be as much as 0.3 in places.

* The method and data were kindly supplied by Professor D. R. Hartree, F.R.S.

Table I—Contributions to Z , Total Z and Z_p for the Bromine Atom

r	$1s^2$	$2s^2$	$2p^4$	$3s^2$	$3p^4$	$3d^{10}$	$4s^2$	$4p^4$	Z	Z_p
0.000	2.00	2.00	6.00	2.00	6.00	10.00	2.00	5.00	35.00	35.00
0.005	1.99	2.00	6.00	2.00	6.00	10.00	2.00	5.00	34.99	34.13
0.010	1.94	1.99	6.00	2.00	6.00	10.00	2.00	5.00	34.93	33.29
0.015	1.82	1.98	6.00	2.00	6.00	10.00	2.00	5.00	34.80	32.50
0.020	1.68	1.97	6.00	1.99	6.00	10.00	2.00	5.00	34.64	31.76
0.025	1.50	1.95	6.00	1.99	6.00	10.00	2.00	5.00	34.44	31.06
0.030	1.31	1.94	5.99	1.99	6.00	10.00	2.00	5.00	34.23	30.40
0.035	1.13	1.93	5.97	1.99	6.00	10.00	2.00	5.00	34.02	29.78
0.040	0.96	1.92	5.95	1.99	5.99	10.00	2.00	5.00	33.81	29.19
0.05	0.67	1.92	5.87	1.99	5.98	10.00	2.00	5.00	33.43	28.08
0.06	0.44	1.92	5.76	1.99	5.96	10.00	2.00	5.00	33.07	27.05
0.07	0.29	1.92	5.59	1.98	5.93	10.00	2.00	5.00	32.71	26.07
0.08	0.18	1.90	5.38	1.98	5.91	10.00	2.00	5.00	32.35	25.16
0.09	0.11 ₅	1.88	5.12	1.98	5.88	9.99	2.00	4.99	31.96	24.29
0.10	0.07	1.84	4.82	1.98	5.84	9.99	2.00	4.99	31.33	23.46
0.12	0.02	1.71	4.18	1.95	5.77	9.98	2.00	4.99	30.60	21.93
0.14	0.01	1.52	3.50	1.92	5.71	9.95	1.99	4.98	29.58	20.57
0.16		1.30	2.84	1.90	5.67	9.91	1.99	4.98	28.59	19.35
0.18		1.07	2.27	1.89	5.65	9.84	1.99	4.97	27.68	18.25
0.20		0.86	1.76	1.88	5.64	9.74	1.99	4.97	26.84	17.25
0.25		0.45	0.85	1.87	5.62	9.35	1.99	4.97	25.10	15.07
0.30		0.20	0.38	1.85	5.53	8.82	1.98	4.97	23.73	13.22
0.35		0.09	0.16	1.78	5.26	8.12	1.98	4.97	22.36	11.58
0.40		0.03 ₅	0.06	1.65	4.83	7.32	1.96	4.95	20.81	10.16
0.45		0.01 ₅	0.02 ₅	1.46	4.28	6.47	1.94	4.93	19.12	8.93
0.50		0.00 ₇	0.01	1.25	3.68	5.65	1.92	4.90	17.42	7.89
0.6				0.82	2.54	4.12	1.89	4.85	14.22	6.31
0.7				0.50	1.62	2.90	1.88	4.84	11.74	5.21
0.8				0.28	0.98	2.00	1.88	4.82	9.96	4.41
0.9				0.15	0.55	1.32	1.87	4.82	8.71	3.82
1.0				0.07	0.30	0.87	1.84	4.80	7.88	3.33
1.2				0.02	0.08	0.36	1.66	4.78	6.90	2.59
1.4					0.02	0.14	1.39	4.38	5.93	2.00
1.6						0.05	1.09	3.98	5.12	1.53
1.8						0.02	0.82	3.48	4.32	1.14
2.0						0.01	0.59	3.02	3.62	0.86
2.2							0.41	2.57	2.98	0.62
2.4							0.28	2.15	2.43	0.44
2.6							0.18	1.76	1.94	0.30
2.8							0.12	1.43	1.55	0.20
3.0							0.08	1.16	1.24	0.11
3.5							0.02 ₅	0.66	0.69	0.03
4.0							0.01	0.37	0.38	0.00
4.5								0.20	0.20	
5.0								0.11	0.11	
5.5								0.04	0.04	
6.0								0.02	0.02	
6.5								0.01	0.01	

Results

The phases δ_0 to δ_3 were calculated by Jeffreys' method from (2) and δ_3 to δ_6 were determined from Born's formula (3). These are given in Table II and fig. 1. In the calculation of the scattering we have used Jeffreys' value for δ_3 for each value of k .

Table II—Phases for Bromine

k	1.05	1.74	2.43	3.00	5.00
Volts	15	41	80	121	339
δ_0	11.05	10.20	9.58	9.15	8.06
δ_1	7.75	7.23	6.75	6.44	5.61
δ_2	3.66	3.94	3.89	3.81	3.65
δ_3 { J.	0.035	0.535	1.05	1.24	1.72
B.	0.040	0.302	0.607	0.810	1.18
δ_4		0.092	0.290	0.452	0.792
δ_5		0.024	0.129	0.244	0.557
δ_6				0.127	0.380

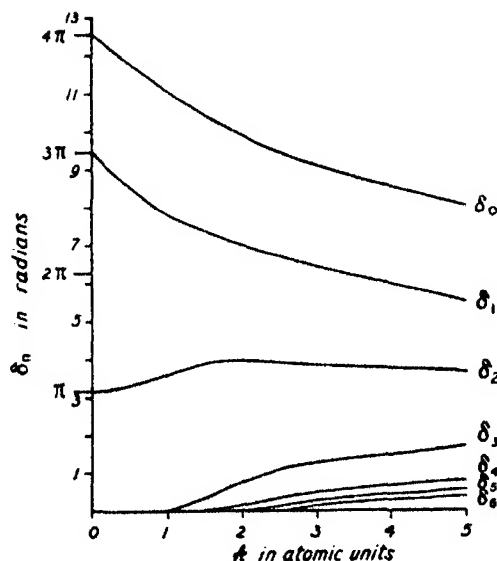


FIG. 1—Phase curves for bromine

The scattered intensity for the atom was then determined from (1) and that for the molecule from (4). These results are given in atomic units in Table III.

In order to illustrate the nature of the interference factor $\left(1 + \frac{\sin x}{x}\right)$ the values of $I_a(\theta)$ for the atom have been tabulated together with the interference factor, instead of the final result for the molecule which is obtained simply by multiplying the two together and the result by two.

The interference factor falls from its maximum value of 2.0 at zero angle to a minimum of 0.783, rises again to a maximum of 1.128, after which it oscillates about unity with slowly decreasing amplitude. The factor will therefore have its main effect on the scattering over the angular range between its initial value of 2.0 and its first minimum. For $k = 1.05$ this range is from 0° to 60° , while for $k = 5$ it is only from 0° to 12° .

Table III—Scattered Intensity in Atomic Units for the Bromine Atom with Interference Factor for the Diatomic Molecule

λ Volts	1.05 15	1.74 41	2.43 80	3.00 121	5.00 339
θ°	$I(\theta)$	$I(\theta)$	$I(\theta)$	$I(\theta)$	$I(\theta)$
0	2.000	2.000	2.000	2.000	2.000
10	1.899	1.738	1.528	1.346	0.846
20	1.637	1.198	0.868	0.783	1.125
30	1.307	0.828	0.860	1.061	0.911
40	1.017	0.822	1.109	1.059	1.058
50	0.834	1.009	1.059	0.401	0.967
60	0.783	1.125	0.918	1.52	0.780
70	0.830	1.083	1.34	0.960	0.149
80	0.924	0.977	0.709	0.350	0.104
90	1.019	0.914	0.131	0.058	0.054
100	1.087	0.921	0.023	0.198	0.131
110	1.122	0.974	0.249	0.446	0.309
120	1.128	1.030	0.399	0.469	0.293
130	1.114	1.063	0.256	0.296	0.178
140	1.094	1.071	0.030	0.041	0.056
150	1.072	1.066	0.084	0.063	0.037
160	1.055	1.053	0.573	0.048	0.290
170	1.046	1.049	1.24	1.018	1.143
180	1.041	1.044	1.56	1.60	2.48
					3.22
					0.980

The small effect of the interference factor at greater angles is seen from figs. 2 and 3, where the continuous curve represents the theoretical angular distribution curve for the molecule, and the broken curve is that for two separate atoms scattering independently. It will be seen that the two curves are practically coincident at large angles.

The small circles in figs. 2 and 3 are the experimental points taken from a previous paper.* These have been fitted to the theoretical curve for the molecule at 90° in the 15- and 41-volt curves, and at 120° in the 80- and 121-volt curves, the fitting factor for the last two curves being the same. As no experimental results were obtained for 339-volt electrons ($k = 5$), this curve has not been included in the figures.

In view of the approximate nature of the expression (4) the agreement between theory and experiment is really quite satisfactory. The forms of the theoretical and experimental curves agree for all energies, the positions of the maxima and minima in both occurring at approximately the same angle. The chief discrepancy occurs in the magnitude of the first maximum. This is probably caused by neglecting the effect of the binding between the two atoms.

In the 15-volt and 41-volt curves we see that the theory predicts too much scattering at small angles. This discrepancy would be decreased, if not entirely removed, if the molecular field were used, for this is less than the atomic field at large distances, and it is the outer field of the molecule which is mainly responsible for the small angle scattering. As would be expected the agreement progressively improves as the energy is increased. This is due to the fact that as k increases the outer field of the molecule has progressively less effect on the scattering, and so the error caused by using the atomic field in place of the molecular field becomes less. Since the scattering of 15-volt electrons, even at large angles, is caused by the outer field of the molecule it is surprising that the agreement for this energy is as good as it is, especially in view of the marked change in the shape of the curve at this energy.

The reason for the change in shape of the curve from the form $|P_3|^2$ to $|P_1|^2$ between 41 volts and 15 volts is evident from Table II, for we see that above 41 volts the phase having a value most nearly equal to $\frac{1}{2}\pi$ is δ_3 ; while at 15 volts $\delta_1 \sim 2\pi + \frac{1}{2}\pi$, and since δ_3 is close to π the form* of the curve at 15 volts will be that of the harmonic $|P_1|^2$.

It is unfortunately not possible to find in these results any very definite evidence for the interference of the waves scattered by the two atoms, for in

* Arnot, 'Proc. Roy. Soc.,' A, vol. 144, p. 360 (1934).

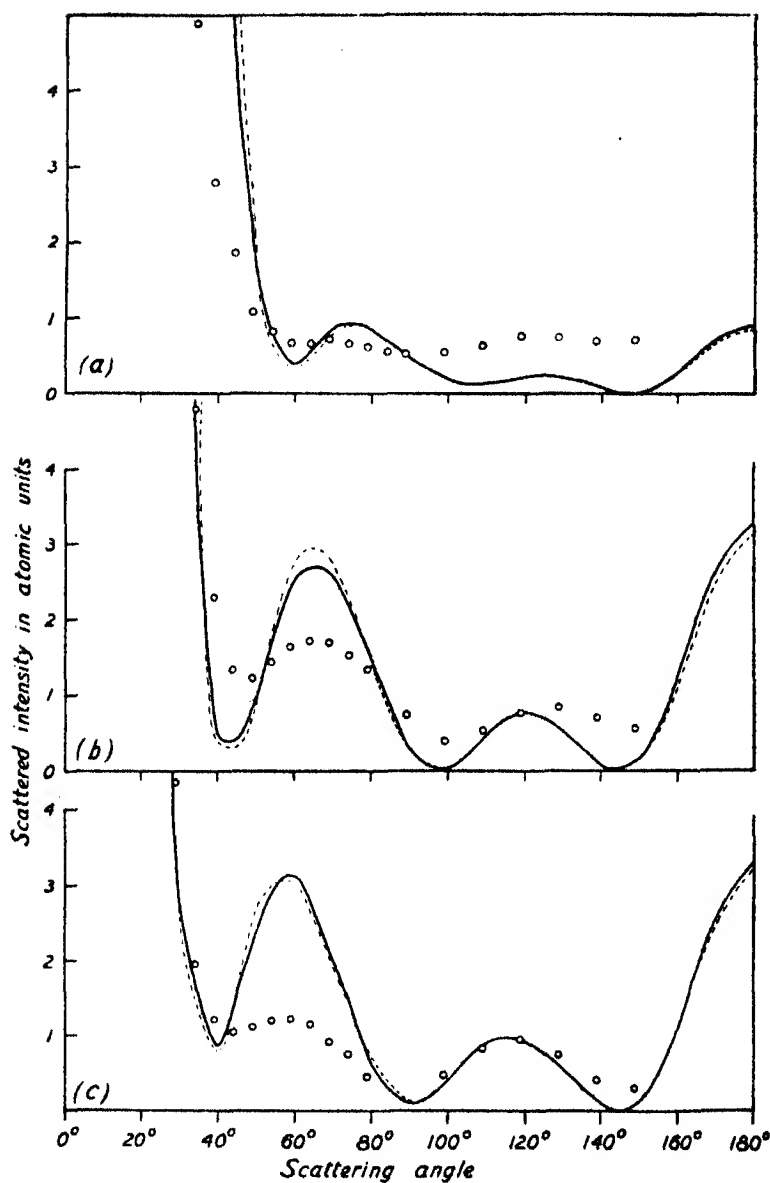


FIG. 2—Theoretical curves and experimental points for bromine. Continuous curve represents scattered intensity for the diatomic molecule. Broken curve is for the atom. (a) $k = 1.74 = 41$ volts; (b) $k = 2.43 = 80$ volts; (c) $k = 3.00 = 121$ volts.

the higher energy curves the interference factor has a marked effect only at very small angles where no experimental results have been obtained, and for the lower energy curves, in which the effect of the interference factor extends to larger angles, the agreement is not good enough to enable one to decide

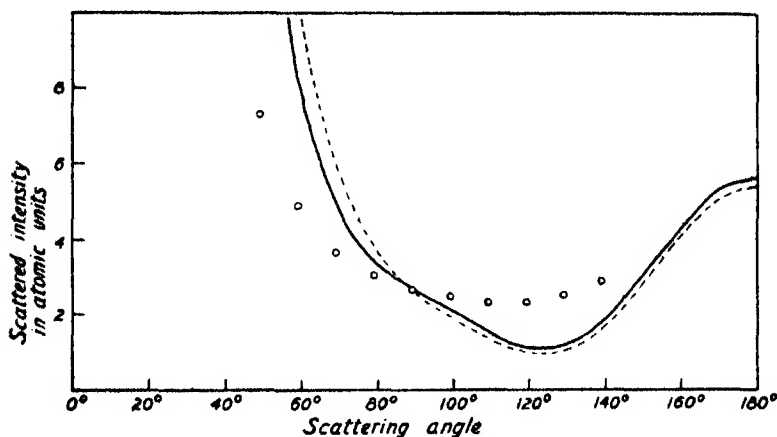


FIG. 3—Theoretical curves and experimental points for bromine. Continuous curve represents scattered intensity for the diatomic molecule. Broken curve is for the atom. $k = 1.05 = 14$ volts.

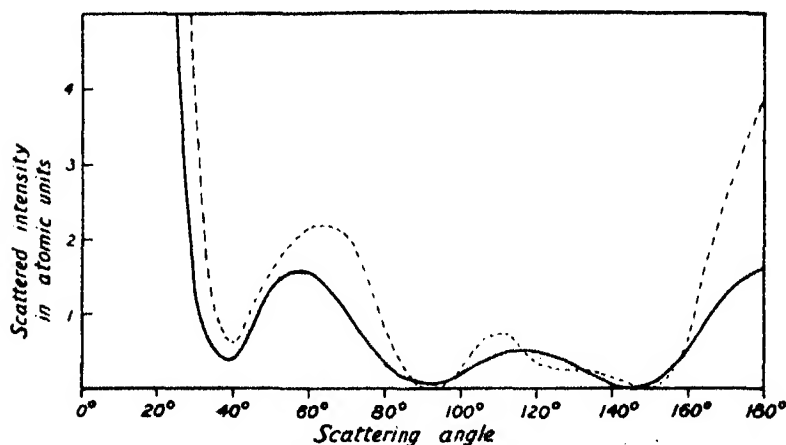


FIG. 4—Theoretical curves for 121-volt electrons. — atomic bromine. - - - - krypton.

definitely between the two curves. However, it will be seen that wherever the factor is in evidence, it is in the right direction to improve the agreement.

In fig. 4 are given two theoretical curves for 121-volt electrons ($k = 3$). The continuous curve is for *atomic* bromine, and the broken curve is for krypton

taken from the previous paper by Arnot and Baines. It will be seen that the curves are very similar as would be expected since the bromine and krypton atoms differ only in the structure of the outer shell which has but little effect on the scattering of electrons of this energy. The same similarity is found in the experimental scattering curves for atoms occupying adjacent positions in the Periodic Table.

Summary

Theoretical angular distribution curves for elastically scattered electrons of various energies from 15 volts to 339 volts are given for bromine. These are compared with the experimental results of Arnot, and satisfactory agreement is obtained. Phases for various energies and an approximate Hartree atomic field for bromine are also given.

Molecular Structure as Determined by a new Electron Diffraction Method. I—Experimental

By HENRY DE LASZLO, M.A., Ph.D. (The Sir William Ramsay Laboratories of Inorganic and Physical Chemistry, and Imperial Chemical Industries, Ltd., University College, London)

(Communicated by F. G. Donnan, F.R.S.—Received April 27, 1934)

Introduction and Theory

In this and the following paper a method will be described* of obtaining good high order interference photographs of electron beams scattered by the vapour of any stable substance, organic or inorganic, whose vapour pressure exceeds 10 cm at 1000° C, as well as an interpretation of the results achieved with this improved technique, using a simplified method of calculation. The apparatus has been so developed that it is now as easy to obtain electron interference patterns of vapours as it is to make measurements of the Raman effect, dipole moment, infra-red and ultra-violet absorption spectra; the results enable us to clear up a number of doubts that still exist concerning the spatial structure of certain compounds.

* de Laszlo, 'Nature,' vol. 131, p. 803, June 3 (1933).

Debye and Ehrenfest* showed theoretically that if a beam of monochromatic X-rays was passed through a gas consisting of randomly orientated polyatomic molecules with fixed interatomic distances, then an interference effect might be expected. Later Debye† worked out the general case for a molecule containing 1-*i-j-n* atoms each having a scattering factor *F*. He averaged in every orientation, and since the coherent scattered intensity *J* is a function of the scattering angle θ , he then showed that

$$J(\theta) = k \sum_1^n i \sum_1^n j F_i F_j \frac{\sin x_{i-j}}{x_{i-j}}, \quad (1)$$

in which

$$x_{i-j} = 4\pi l_{i-j} \frac{\sin \theta/2}{\lambda}, \quad (2)$$

λ being the wave-length of the incident radiation; for electrons λ may be calculated by de Broglie's‡ formula from their velocity *V* in volts after a small relativity correction has been applied according to the equation:—

$$\lambda = \sqrt{\frac{150}{V}} \cdot \frac{1}{(1 + 4.91 \times 10^{-7} V)} \cdot 10^{-8} \text{ cm}, \quad (3)$$

l_{i-j} is the distance in Å between atoms *i* and *j*, and *k* is a constant for the given experimental conditions.

Mark and Wierl§ have shown that Debye's formula may also be applied to the case when a beam of monochromatic electrons is used instead of X-rays with the following modifications. Mott|| and Bethe's¶ theoretical work on the coherent scattering of electrons by monatomic gases gives us a modified Rutherford scattering formula for use with electrons. Thus the X-ray scattering factors *F_i* and *F_j* for the atoms *i* and *j* must be replaced by electron-scattering factors ψ_i and ψ_j by means of their formula

$$\psi_i \sim \frac{Z_i - F_i}{\left(\frac{\sin \theta/2}{\lambda}\right)^2} \sim \frac{(Z_i - F_i)^2}{\left(\frac{\sin \theta/2}{\lambda}\right)^4}, \quad (4)$$

where *Z* is the atomic number and *F* the atomic scattering factor for the atom *i*.

* 'Ann. Physik,' vol. 46, p. 809 (1915); 'Proc. K. Akad. Wet. Amst.,' vol. 23, p. 1132 (1915).

† 'Phys. Z.,' vol. 31, p. 419 (1930).

‡ 'Ann. Physique,' vol. 3, p. 22 (1925).

§ 'Z. Physik,' vol. 60, p. 141 (1930).

|| 'Proc. Camb. Phil. Soc.,' vol. 25, p. 304 (1929).

¶ 'Ann. Physik,' vol. 87, p. 55 (1928); vol. 5, p. 325 (1930).

Values of F for any element have been calculated by Pauling and Sherman* from the electron distributions corresponding to Schrödinger's "Eigenfunctionen" for hydrogen like atoms.

To the above "coherent" scattering of the electrons should also be added the "incoherent" scattering factor S by the atoms i - j - n in the molecule as a function of $(\sin \theta/2)/\lambda$.

This incoherent scattering was first calculated by Heisenberg† and later put into a simple form by Fermi‡ for any element of atomic number Z .

$$\frac{\sin \theta/2}{\lambda} = \frac{v \cdot 3\sqrt{Z^2}}{4\pi \times 0.176}, \quad (5)$$

where v has the values calculated by Bewilogua.§

Experimental

Since the apparatus had to be built up *ab initio*, it was thought best to make it as simple and universal as possible so that not only vapours but also the intimate surface structure of solid matter could be conveniently examined. It is shown in section in fig. 1. It can be divided into two distinct parts, the camera, and the diffraction chamber proper.

Considerable difficulty was experienced in obtaining pore-free castings for the camera and various alloys were investigated. Eventually PMG metal was found to be suitable, doubtless owing to its very fine grain structure and its high fluidity at the casting temperature. All movable connections in the high vacuum side of the apparatus were made with 1/10 taper ground joints. We have never found a leak taking place at such joints and with the aid of a set of high-speed 1/10 taper reamers they are easy to make and standardize.

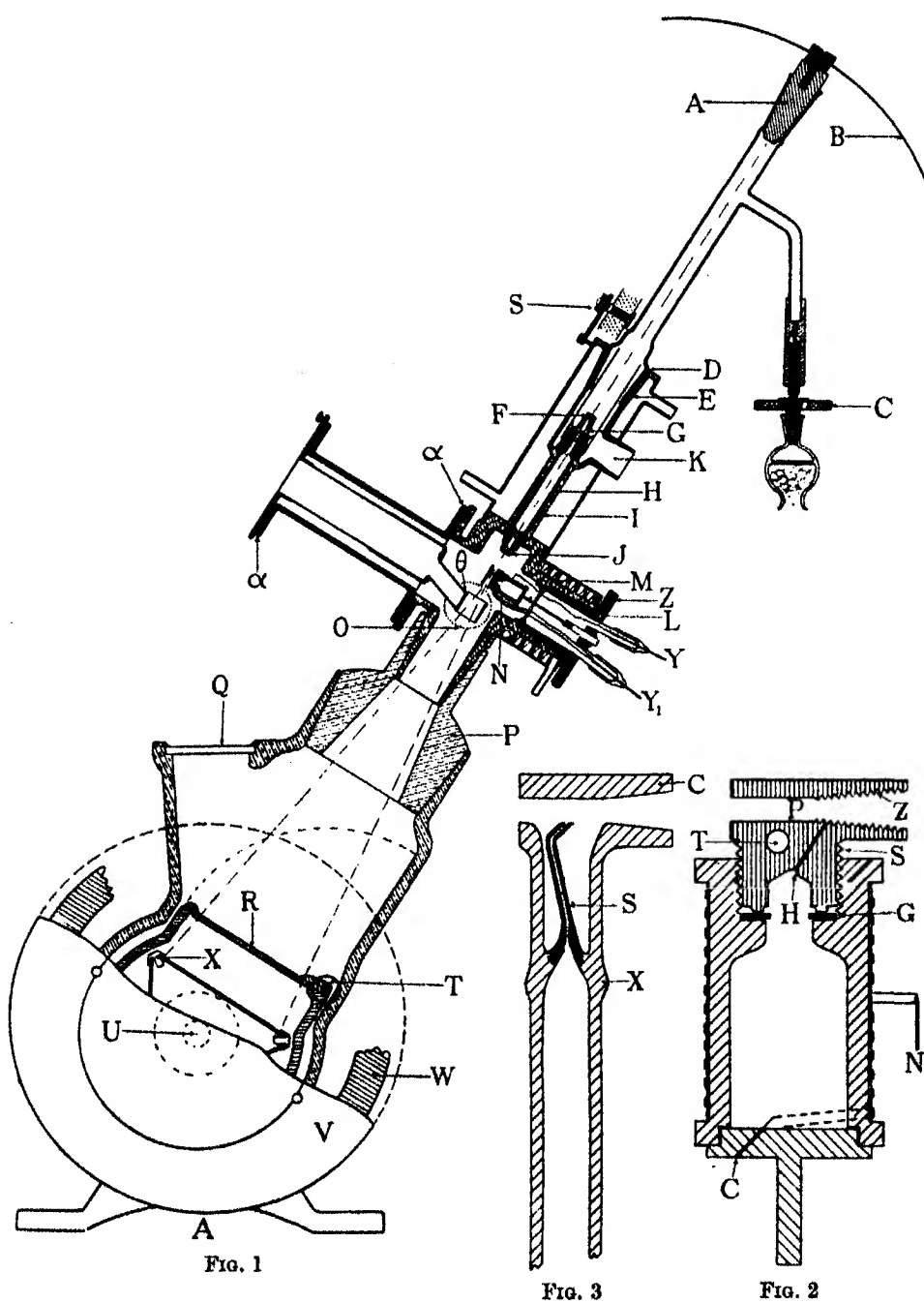
Since we were primarily interested in the examination of vapours, it was decided to use a gas discharge tube rather than a hot cathode as a source of electrons. With the latter the vapours of volatile substances diffused through the electron beam jets into the discharge tube proper, spoiling the necessary high vacuum and thus giving rise to irregularities in electron emission, and hence to variations in voltage. The vapours usually poisoned the electron emitter which had, therefore, to be frequently changed. For work on metal

* 'Z. Kristallog.,' vol. 81, p. 1 (1932).

† 'Phy. Z.,' vol. 32, p. 737 (1931).

‡ 'Leipziger Vorträge,' p. 95 (1928).

§ 'Phys. Z.,' vol. 32, p. 741 (1931).



FIGS. 1, 2, and 3—Sectional view of complete electron diffraction apparatus with enlarged drawing of vaporizers.

films and crystal structure, however, the hot cathode is preferable since all the variable electrical factors are under control. Thomson* has shown that even with a source of high voltage with as bad a characteristic as that produced by an induction coil, the gas discharge tube gives an electron beam of surprising constancy. We have been able to substantiate this claim in countless experiments,† and have proved it by the fineness of the diffraction images obtained with mica.

Various types of discharge tube were tried out. Pyrex glass was used at first, but at high potentials sparking took place near the cathode, owing to electrolysis having taken place in the glass itself under the big potential difference, leading to slight decomposition and devitrification, with resulting loss in dielectric strength and ultimate breakdown. Quartz glass was found to be free from these objections, and by narrowing down the 20-cm long discharge tube to about 15 mm internal diameter, we obtained very constant and highly concentrated pencils of cathode rays.

Various metals were used as the cathode, and "electron metal" was chosen for general use. This is a 97% magnesium alloy and hence splutters rather less than aluminium. It is easily worked in the lathe and takes a high polish. A rod of "electron" is turned down to a 1/10 taper and ground into the quartz tube. The actual cathode surface is turned off at right angles to the axis of the discharge tube and polished with household metal polish. The cathode, A, is cemented into the tube with "picein" which, however, is only allowed to flow round the top half of the joint. The cathode is cooled by screwing on to it a spherical aluminium spinning, B, which also increases the concentration of the electron beam, owing perhaps to the focussing action of the electrostatic field between the charged curved surface and the rest of the apparatus. A beryllium‡ cathode was tried and was satisfactory as regards spluttering, but only lasted twice as long as magnesium. However, when it had to be turned down and re-polished, it was found to be too hard and brittle to work. After about 5 hours of use the cathode is removed, re-faced and polished. The quartz tube is cleaned with fuming nitric acid and heated to redness before re-inserting the cathode. While heating these quartz tubes to just below red heat a curious greenish-blue fluorescence is observed even in daylight, which lasts for several seconds. It appears to travel up the tube with the heating flame and may be due to thermal activation of magnesium

* "The Wave Mechanics of Free Electrons," Oxford Univ. Press.

† de Laszlo and Coslett, 'Nature,' vol. 130, p. 59 (July 9, 1932).

‡ Kindly presented by H. A. Sloman, M.A., of the N.P.L., Teddington.

vapour that has been spluttered on to the interior of the discharge tube. The discharge was first tried in hydrogen, but the result was no better than in air and was therefore abandoned. Dry, filtered air is allowed to leak in through the Leybold valve, C. By varying the applied voltage and the pressure in the discharge tube by adjustment of the valve (the rate of pumping remaining constant), an electron beam of any desired voltage between 20 and 60 kv can easily be obtained. The pressure in the discharge tube for the formation of a concentrated electron beam was measured and found to be very critical; it lies between 1.0 and 1.3×10^{-2} mm. For a good spot it is best to run the tube as hard as possible consistent with the required voltage.

The bottom of the discharge tube is made in the form of a ground joint, D, which fits into the water-cooled sleeve, E. A thin layer of Apiezon grease, or "Selloseal" is used on the top half of the joint. All parts must be accurately aligned in order that the electron beam may pass down the axis of the discharge tube. To achieve this the latter is gripped in a lathe chuck by the cathode, A, and is softened a little with an oxy-hydrogen flame whilst rotating slowly, until the joint, D, is co-axial with A. The electron beam strikes a platinum-iridium plate, F, which is hard soldered to the jet, G. This alloy is used owing to its resistance to heat and corrosive vapours. The jet is ground into a very accurately turned cylinder of brass, H, which fits into I, with not more than 1/100 mm play. A hole of 0.3 mm diameter is drilled centrally through F. The beam emerges through a similar jet, J, where the diaphragm is 0.12 mm diameter and 0.2 mm long followed by a hole 0.8 mm long and 0.14 mm diameter. This particularly long canal cuts off electrons and soft X-rays scattered from the edge of the smaller hole which would otherwise tend to fog the plate. Watchmaker's drills were used for this work, tallow being the lubricant. The electron beam may be finally adjusted with the aid of a small bar magnet fixed to a universal joint outside D. H has only a very thin layer of grease on it and is water cooled. The discharge tube is thus only connected to the camera via the two holes, F and J, and is evacuated separately at K by a three-stage quartz Volmer diffusion pump. The size of the electron spot is somewhat less than 0.5 mm.

After leaving J the beam either impinges on the gas or surface which is being investigated. A tapered brass fitting, L, is ground into the water-cooled joint, M. Any form of vaporizing apparatus, N, or specimen holder, affixed to this joint may be introduced into the diffraction chamber. In order to get good centring N is usually arranged off the axis of L so that the rotation of L gives

a small translational motion to N. It is of the greatest importance that the beam should pass as nearly as possible down the axis of the vaporizing nozzle, as otherwise poor photographs will be obtained. To achieve this, the whole of the diffraction chamber is taken off the camera, a source of light is substituted for A, and N adjusted by rotation until the spot of light appears to be in the centre of the vaporizing nozzle. The camera and diffraction chamber are evacuated through a ground joint, O, connected by a piece of flexible Tombac tubing to a large Lyebold three-stage steel diffusion pump via a liquid air trap. Tubes of different length, P, may be inserted between the diffracting chamber and the camera to provide varying distances between the diffracting centre and the photographic plate. The interference pattern is observed through a window, Q, on a luminescent screen, R, attached to the lid of the plate box. Zinc silicate, though brilliantly fluorescent, shows no after-glow and has therefore been chosen for the screen. As soon as a pattern appears on the screen the electron beam is cut off by switching on an electromagnet, S. The lid, R, of the plate box is opened by turning a ground joint, T, and the exposure is made by short-circuiting the magnet through a time switch. Any exposure up to 6 ± 0.1 seconds may be made in this way. The lid is then closed.

The plate box is made of aluminium and can contain various types of plate or film holders. For plates, a triangular holder, X (9×12 cm), or a hexagonal one (for 6×12 cm) is in use. After exposure the holder is rotated by a second ground joint, U, until a new plate comes into position. Recently we have been using Ilford X-ray film which is stretched over a cylinder of $4\frac{1}{2}$ inches diameter. A diaphragm with a 2×12 cm slit cut in it only permits a strip of film to be exposed at a time. By rotating the film by the ground joint U about 15 exposures may be taken on the same film strip, one beneath the other, at varying voltages and times of exposure. The plate box has a light-tight cover on the side which is taken off in the dark room to remove the plate or film holders for development. The side of the camera is closed by a thick brass disc, V, which has been ground on the inner side on to a similar flat machined flange which is an integral part of the camera casting. A special gas-freed rubber gasket, W, is placed between the two flat surfaces and furnishes a vacuum-tight joint. The rubber and metal surface must be kept very clean. The rubber is occasionally washed with a 5% solution of Apiezon oil in benzol which renders the surface slightly tacky.

Vaporizers

Wierl* was the first who attempted to obtain electron diffraction photographs of a substance which required heating in order to give a sufficiently high vapour pressure. His experiments were conducted on carbon tetrabromide. He found narrow, clearly defined rings on his plates, which indicated that diffraction must have taken place on the random orientated, spontaneously formed, polycrystalline mist that had condensed out of the jet of vapour. He tried many modifications, none of which were any more successful.

Since this was one of the primary objects of the investigation, much time was spent in arriving at a solution. The first experiments were all made on ovens of the "direct" type, *i.e.*, ovens in which the substance is heated in a sealed container with only one fine orifice or jet from which the vapour issues straight into the evacuated space surrounding it. Various difficulties were met and overcome in turn.

I—The interior of the oven must at times be accessible, firstly for filling with the desired substance, and secondly for cleaning at the end of an experiment. During the experiment, however, the oven must be hermetically sealed except for the orifice through which the vapour emerges. It was found best to arrange for the orifice to be contained in a solid head or nozzle which could be easily attached to the body of the oven by one of two methods: (a) a fine screw thread, S, which was rendered gas-tight by a washer of some soft metal with a coefficient of expansion slightly greater than the substance of which the head and body were made. In our work, see fig. 2, pure gold washers, G, were used with a silver head and oven. (b) The head may be attached to the oven by a 1/10 taper ground joint which has been well lapped in. In this case we must choose a material for the head with a coefficient of expansion that is preferably the same or slightly greater than that of the oven.

In both these methods the joint remains gas-tight while the temperature of the oven rises.

II—Electric heating was used for all types of oven. External heating as in fig. 2 was the best for temperatures up to 500° C. A thin wash of "Crolite" cement is painted on to a single layer of thin asbestos paper wound round the body of the oven. One end of a piece of 1 mm × 0.05 mm nichrome resistance strip, N, is inserted in a fine saw cut, C, at one end. A tap with a hammer on the cut will cause the strip to be firmly gripped by the silver rim. About half-way down the oven the strip is doubled on itself and spot welded together.

* 'Ann. Physik,' vol. 8, pp. 536, 550 (1931).

Winding is continued and the strip secured in a saw cut at the other end. The current is brought in through the doubled strip and out through the body of the oven. The outside is then covered with another layer of "Crolite."

For higher temperatures two holes are drilled in the solid steel body of the oven parallel to the container. In these holes are placed spirals of tungsten wire insulated from the steel body by "Crolite" and a magnesia washer at the top end. The bottom end is connected directly with the oven by small screws. The two spirals are heated in parallel. Temperatures up to 1000°C may be reached with this method of indirect heating. For higher temperatures a cylindrical radiation shield of polished nickel is used to prevent the body of the apparatus becoming too warm.

One insulated lead only is required for heating these ovens and this is brought in through a Pyrex to copper seal,* Y.

The temperature of the issuing vapour is found by inserting a fine copper-constantan thermocouple via a taper plug into a taper hole, T, fig. 2, as near to the gas exit as possible. The leads for it are brought out through a separate copper-pyrex seal, Y'. The temperature is read off continuously on a Cambridge millivoltmeter.

In order that the oven may quickly assume the correct temperature and that the body of the apparatus should not get too hot, it is thermally insulated by being mounted on a 1 mm diameter invar rod, Z.

III—In the early experiments the jet, being rather thin and long, was at a slightly lower temperature than the body of the oven. This often caused condensation of the vapour and hence gave rise to blockage of the fine hole. The heads are therefore now made of massive silver and are thermally well connected to the body of the oven.

IV—The various types of direct ovens had jets which consisted of fine holes varying in diameter from 0.05 to 0.30 mm, and in length from 0.5 to 3.0 mm, or were slits about 0.05 mm wide by 1.5 mm broad. The former were made by drilling with fine spiral drills. The latter were first holes into which was inserted a piece of steel of nichrome ribbon of the desired size. On squeezing the metal the hole then became a slit. The ribbon was removed by warming.

With these direct jets it was just possible to obtain a photograph, especially when the ribbon jet was used parallel to the electron beam. However, very careful adjustment was necessary to obtain a result, and the beam had almost to graze the top of the jet in order to pass through a layer of sufficiently high molecular concentration. This often gave rise to spurious results, owing to the

* de Laszlo, 'J. Sci. Instr.', vol. 10, p. 296 (1933).

diffraction and reflexion effects from the metal of the jet top. Even in the best cases, however, the interference photographs obtained were never evenly exposed all over. The bottom half—nearest the jet—had more distinct and darker rings than the top half.

This matter was investigated separately, and it was found that with the small difference in pressure available between the interior and exterior of the oven (5–25 cm Hg) the vapour beam issued in the form of a wide-angle cone of approximately 110° . This was determined by permitting the vapour of a substance such as diphenyl to condense on a polished, plane, liquid-air-cooled, copper surface situated at right angles to the axis of the oven. The condenser surface could also be moved to various distances from the jet. The diameter of the condensed ring or band could then be directly measured.

Owing to the big angular spread, the vaporized substance, if of high melting point, would condense on the second electron jet, J, and block it up, unless it were placed a long way—5 cm—from the oven. This indicated that a method had to be devised whereby a greater constant molecular concentration of vapour could be attained over a fairly long distance—a few mm—without affecting the vacuum in the body of the apparatus.

V—A method which overcomes all these difficulties is that of not permitting the issuing vapour to pass straight into the evacuated space. A capillary hole, H, fig. 2, 0.2 mm diameter, is bored in the head at an angle of 45° so as to lead the gas from the oven into a passage, P, fig. 2, 2 mm diameter, which is bored at right angles to the axis of the oven. Electrons pass down the axis of this hole where they meet the gas molecules which have issued from H. These molecules are caused to collide, and bump by reflexion from the screw threads, Z, which line the tapered mouth of the passage. Owing to the angle of H, the molecules enter P with a component in the direction of the photographic plate, *i.e.*, away from the electron jet. After leaving P, they are at once condensed on the liquid-air-cooled platinum-plated copper tube θ . The concentration of randomly orientated gas molecules is therefore very high within the space P–Z, and is, above all, fairly constant throughout any unit cross-section. We can thus get the maximum interference effect for any particular substance by suitably adjusting the temperature of the oven and its head. The point where the electron beam strikes a sufficiently high concentration of molecules to cause interference is taken to be where the canal enters the main hole, P. This is important for measuring the distance from where interference takes place to the photographic plate, which is necessary for the interpretation of the results.

The same system can be applied to very volatile substances which do not require heating, in lieu of the original direct jet method of Wierl. Superior results are likewise obtained owing to the higher and more uniform molecular concentration. In this case the heads are made of pyrex or quartz glass, fig. 3. A suitable piece of 1.5 mm bore capillary tubing, C, is made into a T with a piece of $\frac{1}{4}$ -inch thin walled tubing. The former is then cracked off to approximately the correct length. One end of the capillary portion is then ground out into a cone with the aid of a tapered phosphor-bronze rod. The ends are ground square. A piece of very fine capillary tubing is then prepared by pulling down from a piece of $\frac{1}{4}$ -inch tubing. The interior diameter should be about 0.1 mm. Having made a suitable piece, the end is allowed to drop through about 45° by heating with a very fine flame. The end is cut off to the right length and the tip ground off parallel to the axis of C. The fine capillary, S, is then inserted into T and joined at X. By working in the flame the point of S can easily be made to assume the correct position. These heads are very robust, can be cleaned with acids, etc., and will stand heating in order to remove all traces of moisture. They are adjusted in the apparatus by sealing through the tapered brass joint L with the aid of "picein." The bulbs containing the volatile materials are joined to the head either by fusion or by a ground joint, depending on the substance. While evacuating the apparatus the reservoir is cooled with liquid air to avoid unnecessary loss.

Liquid Air Trap

The trap is made of seamless German silver tubing of $\frac{1}{2}$ mm wall thickness. About 5 cm of its length are turned down on a mandrill until the wall thickness is between $\frac{1}{10}$ and $\frac{1}{20}$ of a millimeter. This fact coupled with its low thermal conductivity avoids the unduly rapid evaporation of the liquid air within it. The German silver is brazed on to the actual copper condenser, θ . The whole is platinum plated to avoid corrosion and contamination of the condensed material.

In order to adjust the exact position of the trap relative to the nozzle, two flat lapped joints, α and α' , are employed with a distance piece of pyrex. The latter is made by blowing a 4-inch bulb in the middle of a piece of 40 mm tubing which is fixed at either end into the synchronously rotating chucks of a glass-blowing lathe. When the bulb is soft, the glass tube is pushed together and the bulb collapsed on itself by squeezing with a large carbon-faced forceps. We thus obtain a solid ring of glass about 8 cm diameter in the middle of the

tube. The process is repeated at 10 cm from the first ring. After careful annealing, the outer tubes are cracked off at the rings, which are ground flat with carborundum on a face plate. All joints of the trap are soldered with a 50% alloy of pure tin and lead, which does not tend to form large crystals at low temperatures, thus giving rise to leaks. The vaporized material may be conveniently recovered after the experiment by scratching or dissolving off the trap.

Photographic Plates

All our preliminary work was done with Paget process plates. We found these gave excellent results for transmission diffraction photographs of thin metal foils. The images are of fine grain and contrast well with the clear, unfogged background, which makes them ideal for photometry. They are, however, relatively insensitive to electrons and have a very steep blackening curve. This results in the portion round the central spot being over-exposed, leaving the edge very under-exposed. Great variations in exposure must be given for the same substance so that measurements on the outside rings may be made on over-exposed plates and *vice versa*.

The Ilford X-ray emulsion is far more sensitive to electrons and has a greater range of blackening than the Paget. It permits of visual measurement of all the existing interference maxima on the same plate. There is, however, a lot of general fogging which does not affect the measurements. The plates are developed for the same period of time in a tank at constant temperature. The Ilford tank formula for X-ray plates is used.

Production and Measurement of Constant Voltage

Three values are required for calculating the $(\sin \theta/2)/\lambda$ value for any particular ring maxima according to the formula $\frac{\sin \theta/2}{\lambda} = \frac{D}{4n\lambda}$, where D is the diameter of the ring, and n the distance of the diffracting centre to the photographic plate. λ is the wave-length which is derived directly from the voltage V at which the exposure was made by equation (3).

n and D could be measured with a respective accuracy of a quarter of 1% and 1%. However, if the mean of the values of $(\sin \theta/2)/\lambda$ for a number of plates are taken, then the order of accuracy to which D can be determined will be increased to about the same as n . V alone is difficult to determine.

Since the interference maxima obtained by passing electrons through vapours are necessarily rather broad and indistinct, all causes which could give rise to an even greater lack of definition than is inherent in the method must be eliminated. The voltage must therefore be kept very steady during an exposure. Wierl used a Siemens Stabilivolt high-voltage equipment as designed for medical X-ray work, which has a ripple of at least $\pm 3\%$, besides probable fluctuations in the A.C. mains. We decided to eliminate errors arising from ripple by using high-frequency A.C. of 500–1000 \sim . This was obtained from a Mackie $\frac{1}{2}$ kw. rotary converter with specially shaped pole pieces to improve the wave form. This is driven by the Institute accumulator cells which are of ample capacity to provide a constant source of D.C. for the motor side of the converter.

Great difficulty was experienced in finding a suitable transformer to operate up to 60,000 volts at this high frequency with the small amount of power available. Two transformers were specially made, but either broke down in use or drew too much current from the converter owing to the high saturation current taken by the core. Various makes of induction coil were then tried, but only one type survived the test and has been in use for the last two years without a breakdown.

This coil was made by Butt for service in the tropics. It is layer wound in two sections. The innermost layer of each of the secondaries was joined and earthed, thus forming the mid-point of our transformer. The two outer ends of the secondary are connected directly to the filaments of two E.H.T. 3 rectifying valves.* The filaments of the valves are heated by insulated 12-volts car accumulators to avoid variation in filament temperature if operated off the A.C. mains. The 60,000 volts Meirowski condenser of 0.05 mf. capacity is connected between the earthed mid-point and the high tension side of the system, and is mounted horizontally on two brackets near the ceiling of the room. The very smooth high voltage D.C. (1/10 of 1% ripple) is connected to the cathode of our discharge tube via a 3-megohm wire-wound Philips resistance and a 0.5 mA meter.

Voltage Measurement

The voltage at which a photograph is taken has until recently been determined either with a sphere cap or an electrostatic voltmeter. With neither of these methods can the actual voltage at the moment of the exposure be

* Presented by Osram Lamp Works through kindness of Mr. Smith.

measured with a greater accuracy than $\pm 2\%$.* From the very beginning therefore we have used high resistances of the order of 50 megohms connected across the discharge tube, through a Weston precision milliammeter, to earth. Any variation in the voltage during the exposure at once becomes apparent in the meter. The first resistance used was made of 100 "Varley" $\frac{1}{2}$ megohm wire-wound cartridges soldered together 20 at a time in 10-glass tubes. Each resistance was first calibrated with a Cambridge precision bridge and the sum total compared with actual diffraction photographs obtained with gold leaf. Owen† value of 4.071 Å for the space lattice of gold was taken as our standard. This resistance, however, was soon abandoned, owing to the high temperature coefficient of the nickel-chromium wire used in its construction. Actual breaks, which were difficult to locate, would take place in some of the cartridges, due to expansion and contraction.

The resistance now in use is made of 25 Siemens 2-megohm (Hochkonstant type 4a) resistances,‡ each capable of carrying two watts. These are soldered together and mounted in a glass tube which forms part of a closed system round which transformer oil circulates, keeping the resistances at fairly constant temperature. After running for 5 minutes a constant condition is reached and gives very reliable readings with the meter. The resistance is checked once a month with gold diffraction photographs.

Measurement of Plates

Eight of the best photographs are selected out of the two dozen that are usually taken of each substance with varying exposures and voltages. They are selected firstly according to the visibility of the rings of maximum and minimum intensity, and secondly each must have been taken at a different voltage varying between 15 and 60 kv. With compounds that give very closely spaced rings such as p-p'-di-iodo diphenyl, a distance piece is inserted in the apparatus so as to increase the resolving power. The selected plates are cleaned and preserved in transparent envelopes made of cellophane "sausage skin."

We have tried using evenly illuminated surfaces of opal glass, altering the light intensity with a rheostat, and the colour with gelatin filters, but varying results in ring diameter were found, depending on the conditions used. In the end a 60-watt lamp with interior etching of the bulb was selected as a standard,

* Finch and Quarrell, 'Proc. Roy. Soc.,' A, vol. 141, p. 404 (1933).

† 'Phil. Mag.,' vol. 13, p. 1020 (1932).

‡ Hartmann and Dossman, 'Z. Tech. Physik,' vol. 9, p. 434 (1928).

and all ring measurements have been made with its aid under identical conditions in a dark room. The bulb etching is of such a grain size that the intensity distribution over the bulb falls off steeply from the centre outwards. This tends to compensate the rapid falling-off in blackening of the plate. An opal glass half-watt lamp gave very poor results, as its intensity distribution is far too even over its surface.

Trendelenburg* has recently published a method of removing the diffuse background scattering from electron diffraction photographs by the use of a revolving sector so dimensioned as simultaneously to compensate for the steep falling-off in blackening of the photographic plate, especially near the centre. If his method were used on interference photographs of vapours, it would increase the accuracy and facilitate the measurement of the maxima as well as providing prints that are more suitable for reproduction than the original plates.

The plate is held up in front of the light and the diameters of the rings measured at their apparent points of maximum and minimum density with a 10 cm white celluloid millimeter ruler. Scales of glass or transparent celluloid are far more difficult to use. Where no visual maxima is seen, the ring edge is measured. Results are consistent and may be repeated on different days with a reproducibility of $\frac{1}{2}\%$.

Let D be the diameter in millimetres for any particular ring of a substance which has been photographed at a certain λ and at a distance n mm from the diffracting centre. Let θ be the semi-angle subtended by the ring diameter.

Then since we are dealing with small angles

$$\sin \theta = \tan \theta = D/2n$$

and dividing by 2λ we get

$$\frac{\sin \theta/2}{\lambda} = \frac{D}{4n\lambda}, \quad (6)$$

$(\sin \theta/2)/\lambda$ will therefore be a constant for the same ring of the same substance, even though taken at varying λ and a , and is also the expression that is present in equations (2), (4), (5).

The $(\sin \theta/2)/\lambda$ values are calculated for the rings of our eight plates, and the arithmetical mean is taken.

From (4) we see that the intensity falls off $\sim \frac{1}{\left(\frac{\sin \theta/2}{\lambda}\right)^4}$. The eye discounts this fact and physiologically one has the impression of a number of light and

* 'Wiss. Veröff. Siemens-Konz.', vol. 13, p. 48 (1934).

dark rings of varying intensity with but a gradual falling-off in blackening towards the edge of the plate. As Brockway* has pointed out, with two rings that are badly resolved or have very different rates of decline in apparent density at either side, the St. John† effect appears. The apparent separation of such rings is greater than actual fact, by anything from 5 to 10%. Owing to the intense blackening of the central spot, the first minimum is shifted outwards by about 10%. For purposes of structure determination, it is best to select those maxima or minima that are clearly defined and as far from the centre as possible. Slight variations in chemical structure only become apparent at values of $(\sin \theta/2)/\lambda$ greater than 0.6. As Wier‡ first showed, microphotometer records of these interference patterns usually give a very steep falling-off in intensity (in perfect accordance with theory), the visual maxima being but points of inflexion. Such records are not very helpful, since we do not know what positions on these inflexions correspond with those determined visually. Only with certain substances where the maxima and minima are, for structural reasons, very intense, as in hexabromethane and carbon tetrabromide, can true photometric maxima and minima be obtained. They have been found to correspond with our visual measurements. The photometer cannot be used for measuring ring diameters for high values of $(\sin \theta/2)/\lambda$. For such small differences in intensity as occur here the eye is infinitely more sensitive than any instrument yet made.§ Since these are the most vital rings for structural investigation, one must conclude that the photometer may usually be dispensed with in electron-scattering work on vapours, in view of the improved technique which permits the registration of all existing rings of high order.

Interpretation and Calculation

Having determined experimentally the $(\sin \theta/2)/\lambda$ values of the maxima and a few of the sharpest minima of our substance, we proceed to construct a theoretical intensity curve for it, which depends on its supposed chemical constitution. If the $(\sin \theta/2)/\lambda$ values of the maxima and minima of the latter coincide with the former, then the spatial structure of that particular compound may be taken as proved, otherwise a new model or a modification of the first must be undertaken.

* 'Proc. Nat. Acad. Sci.,' vol. 19, p. 872 (1933).

† 'Astrophys. J.,' vol. 44, p. 35 (1916).

‡ 'Ann. Physik,' vol. 8, p. 539 (1931).

§ J. S. Haldane, Inaug. Add. Edin. R. Med. Soc., October 13, 1933.

After investigating and calculating the curves for over 200 substances, we have found as a general rule that a simplified equation for intensity distribution may be employed, especially for substances of molecular weight greater than 150. We substitute Z (atomic number) for ψ in equation (4) and leave out the incoherent scatterings.* If we are using maxima and minima of high order between $(\sin \theta/2)/\lambda$ 0.6 and 1.5, to characterize our substances, then they would scarcely be shifted towards the origin if we were to employ the complete equations (1) and (4): This would, however, increase the labour of calculation about six times, which in the circumstances is not warranted. Our object is to determine interatomic distances and the spatial arrangements of these atoms in various molecules. Nothing can be gained by this very slight increase in accuracy. We are satisfied if the high order maxima and minima of our theoretical values do not differ from those determined experimentally by more than $\pm (\sin \theta/2)/\lambda$ 0.005.

The exact procedure of the calculations will be shown in Part II.

In conclusion, I should like to thank Imperial Chemical Industries for having made this piece of work possible, and Professor F. G. Donnan, F.R.S., for having put the facilities of his laboratories at my disposal.

Summary

The technique of obtaining photographic records of the scattering of fast electron beams by vapours and gases has been simplified and perfected in the following way.

A—The interference pattern of the vapour of any substance that will vaporize *in vacuo* up to 1000° C without decomposition can be photographed by means of a small oven, equipped with an original type of vaporizing nozzle. This permits the investigation of a great variety of molecules which could not have been measured by the older methods.

B—This nozzle, either in conjunction with the oven or by itself when using substances with a high vapour pressure at room temperature, coupled with the use of Ilford X-ray emulsions, enables us to record many more interference maxima than had previously been possible.

* Sherman's four-figure table of $\sin \pi/x$ values† has been found invaluable for this work in conjunction with 50 cm precision "Nestler" slide rules and a simple form of adding machine.

† 'Z. Kristallog.', vol. 85, p. 404 (1933).

C—These new high order maxima are particularly sensitive to changes in chemical structure. Hence we can now make an accurate determination of interatomic distances and the molecular architecture of many compounds whose spatial configuration has hitherto been unknown.

D—The high potential source used for the electron beam is very constant and free from ripple, the voltage being measured by a simple resistance method which has proved more accurate than the usual electrostatic instruments.

E—The high $(\sin \theta/2)/\lambda$ values of the maxima that are now available warrant the use of a simplified method of calculating the theoretical scattering curves, with which the experimental results are compared, with a consequent saving in time.

These technical improvements have turned the electron diffraction method into a quick, reliable, and accurate tool for the determination of chemical structure in the vapour phase. It should now be possible to clear up most of those debatable points in chemistry where a knowledge of the spatial structure is essential. Over two hundred substances have been examined by this method and the results will be recorded in subsequent papers.

Molecular Structure as Determined by a new Electron Diffraction Method II—The Halogen-Carbon Bond Distance in some Simple Benzene Derivatives

By HENRY DE LASZLO M.A., PH.D. (The Sir William Ramsay Laboratories of Inorganic and Physical Chemistry and Imperial Chemical Industries, Ltd., University College, London)

(Communicated by F. G. Donnan, F.R.S.—Received April 27, 1934)

[PLATES 10 and 11]

The object of this investigation was to get replies to the following questions concerning the structure of certain simple benzene derivatives in the vapour phase :—

- (1) Is the benzene ring a flat, regular hexagon ?
- (2) What is the carbon-carbon distance in the benzene ring, and is this a constant independent of the number of substituents ?
- (3) What is the halogen-carbon distance for Cl, Br, and I, substitution products of benzene ?
- (4) Is this distance constant and independent of the number of halogen atoms substituted in any particular compound ?

Lonadale* has shown that the carbon-carbon distance in crystalline hexachlorobenzene is about 1.42 Å provided one takes the ring as being plane, and the carbon-chlorine distance must be greater than 1.675 Å. Robertson† finds 1.41 Å for carbon-carbon in the benzene ring of crystalline 1.2.4.5 tetramethyl benzene. Wierl‡ examined benzene vapour by electron diffraction and came to the conclusion that it was a regular flat hexagon with carbon-carbon = 1.39 Å. Hendricks§ has used the same method on *p*-di-iodobenzene vapour and finds reasonable concordance with experimental results assuming a flat regular ring, with carbon-carbon = 1.42 Å and carbon-iodine = about 2.00 Å. Owing to his technique he had only the first three maxima to go on instead of ten as in our work, which accounts for the approximate accuracy of

* 'Proc. Roy. Soc.,' A, vol. 133, p. 536 (1931).

† 'Proc. Roy. Soc.,' A, vol. 142, p. 659 (1933).

‡ 'Ann. Physik,' vol. 8, p. 559 (1931).

§ 'J. Chem. Phys.,' vol. 1, p. 550 (1933).

his result. Recently Pierce* has measured *p*-dichlorobenzene vapour by X-ray diffraction and considers that 1.4 Å for C-C and 1.8 Å for C-Cl are sufficiently accurate values to account for a plane hexagonal benzene molecule with Cl atoms lying in or near the plane of the ring. Except for the work of Lonsdale and Robertson, the order of accuracy of the experimental results $< (\pm 5\%)$ does not justify the conclusions.

In order to achieve our purpose, the vapours of the following substances were examined as to their electron diffraction in the apparatus described in Part I. These substances were all recrystallized several times before use, and had correct melting points. The oven temperature range at which the vapours were photographed are noted beside each substance.

- (1) { Hexa-chlorobenzene (B.D.H.), 165°–185° C
Hexa-brombenzene (Schuchardt), 204°–224° C
- (2) { 1-3-5 tribrom benzene (Schuchardt), 110°–120° C
1-3-5 tri-iodo benzene (gift of Professor G. M. Bennett), 320°–340° C
- (3) { *p*-dibrom benzene (Kodak), 82°–92° C
p-di-iodo-benzene (Kodak), 120°–140° C.

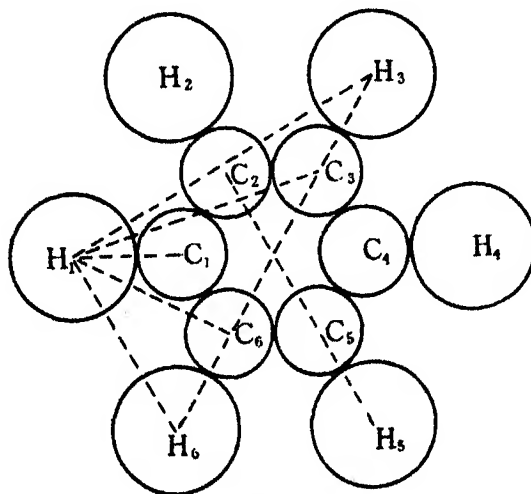


FIG. 1

Fig. 1 will serve as a universal diagrammatic representation of the structure of the above substances, C_1 – C_6 being the centres of the six C atoms of the benzene ring with the centres of the six halogen atoms H_1 – H_6 situated such

* 'J. Chem. Phys.,' vol. 2, p. 1 (1934).

that their valancy directions with respect to the C atoms of similar denominations join at the centre of the benzene ring. Let them also lie in the plane of the benzene ring. In making the calculations of the theoretical curves various values of the C-C distance in the benzene ring were tried and without any doubt 1.41 Å was found to answer for all the substances examined in this paper. Half a dozen different halogen-carbon distances were tried for each of the halogens until a value was found that made the theoretical curve J agree with the experimental facts.

In the columns of figures given below, the corresponding experimental and theoretical maxima and minima will be shown side by side with a shortened description of their character. In the equations representing the theoretical intensity distribution curves, the distance in Å between the two diffracting atoms, say (Br₁-C₁) will be placed before the hyphen. This distance being (*l*), it must be multiplied by 4π before use. But $4\pi l_{i,j} \frac{\sin \theta/2}{\lambda} = x_{i,j}$, therefore

in making out calculation 4π*l* is multiplied by values of (sin θ/2)/λ from 0.150 up to 1.5 in steps of 0.01 and the values of sin *x*/*x* corresponding to each value of *x* is looked up in Sherman's* tables. The same operation is repeated for each interatomic distance *l_i - j* present in the molecule.

If a factor is shown outside the brackets of the *l* values, then each term within must be multiplied by it. When all the *l* values of a molecule have been worked out, those corresponding to a particular (sin θ/2)/λ value are summed. The resulting sums are plotted as ordinates against (sin θ/2)/λ as abscissae.

In figs. 2, 3 and 4 the theoretical scattering curves are shown as a continuous line. The numbered arrows denote the positions of the experimentally determined maxima and minima.

As we see from equation †(1) all distances *l_{i,j}*, in the molecule must be taken twice over. Since this is the same for every term it may be disregarded in making the calculation and will not appear in the equations of intensity distribution. With the benzene derivatives under examination we have for the sake of brevity and clarity left out the terms arising from the benzene ring itself, namely, the six interferences due to C¹⁻⁴¹-C and those due to carbon and hydrogen. The intensity of these interferences is so small compared with those caused by halogen-carbon and halogen-halogen that they do not measurably affect the resultant intensity curve.

* 'Z. Kristallog.', vol. 85, p. 404 (1933).

† Pt. I., p. 673.

Hexabrombenzene

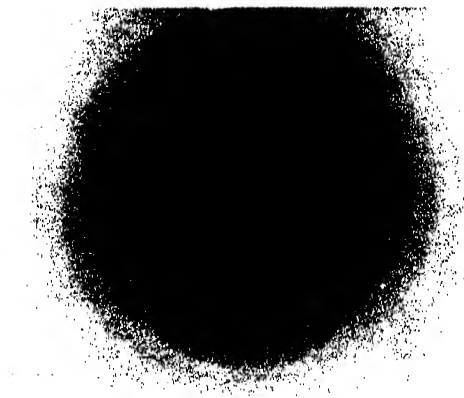


FIG. 5
 $\lambda = 0.0790 \text{ \AA}$
0.5 secs

Hexachlorbenzene



FIG. 6
 $\lambda = 0.0647 \text{ \AA}$
2 secs

Tri-iodobenzene

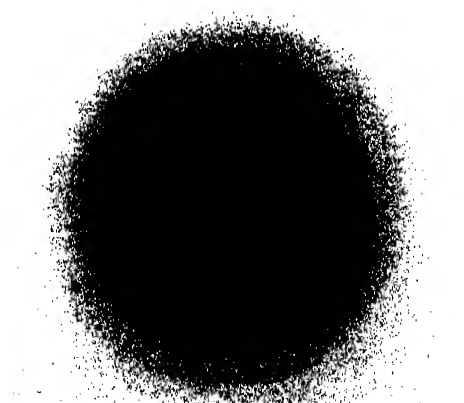
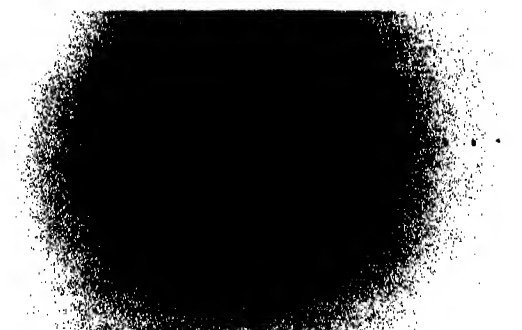


FIG. 7
 $\lambda = 0.0810 \text{ \AA}$

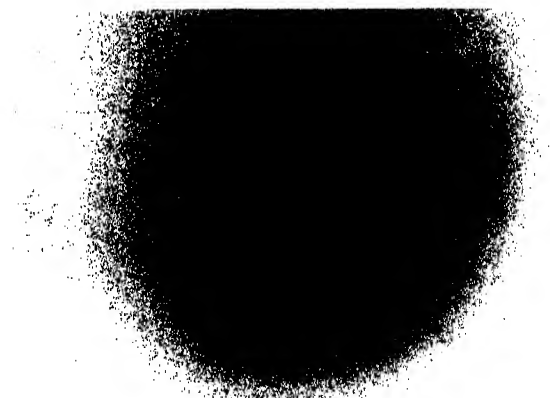
Tribrombenzene

FIG. 8
 $\lambda = 0.0635 \text{ \AA}$



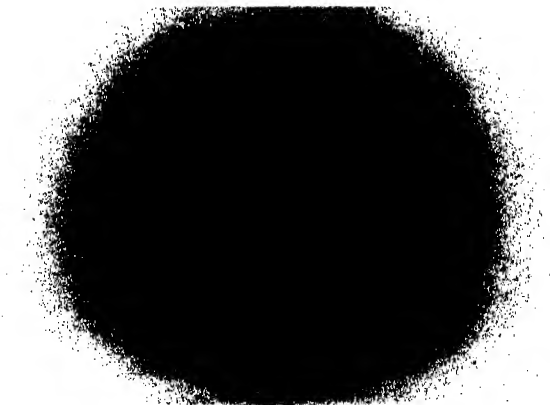
p-di-iodobenzene

FIG. 9
 $\lambda = 0.0733 \text{ \AA}$
0.5 secs



p-di-brombenzene

FIG. 10
 $\lambda = 0.0684 \text{ \AA}$
1.5 secs



In the reproductions of the original plates shown on Plates 10 and 11, it has been found impossible to do justice to the original negatives, owing to the rapid falling-off in photographic density from the centre outwards. The distance between the diffracting centre and plate was 28 cm.

In the six substances investigated in this paper we have found that the following halogen-carbon distances give theoretical intensity curves that agree very well with the experimental facts :—

$$\text{C} - \text{Cl} = 1.69 \text{ \AA}$$

$$\text{C} - \text{Br} = 1.88 \text{ \AA}$$

$$\text{C} - \text{I} = 2.05 \text{ \AA}$$

Hexabrom Benzene

$$\begin{aligned} J = & 6 \times 35^2 [(H_1^{3.29} - H_0) + (H_1^{5.697} - H_3)] + 3 \times 35^2 (H_2^{6.58} - H_4) \\ & + 12 \times 35 \times 6 [(H_1^{2.859} - C_6) + (H_1^{4.177} - C_3)] \\ & + 6 \times 35 \times 6 [(H_1^{1.88} - C_1) + (H_5^{4.70} - C_2)]. \end{aligned}$$

Divide through by (3×35^2) .

Experimental and Theoretical Results

Ring No.	$\frac{\sin \theta/2}{\lambda}$ expt.	$\frac{\sin \theta/2}{\lambda}$ theor.	Description
1	0.186	0.190	Very intense
2	0.278	0.275	Faint edge
3	0.377	0.370	Very, very intense
4	0.472	0.475	Intense and narrow
5	0.549	0.545	Intense and narrow
6	0.638	0.635	Very intense and narrow
7	0.665	0.690	Minimum
8	0.727	0.730	} Doublet faint and broad
9	0.798	0.800	
10	0.839	0.850	Minimum
11	0.898	0.910	} Doublet badly resolved and faint
12	0.980	0.980	
13	1.040	1.040	Minimum
14	1.087	1.085	Faint, very narrow

In order to show the mechanism of the calculation we give below, as an example, a few short sections covering one or two of the maxima and minima for hexabrom benzene.

The complete theoretical curve is shown in fig. 2 and an example of the original photographs in fig. 5, Plate 10.

$\frac{\sin \theta/2}{\lambda}$	3.29 Å	5.697 Å	6.58 Å	4.177 Å	2.859 Å	1.88 Å	4.70 Å	
	41.83×2	71.55×2	32.65	52.47×0.686	35.92×0.686	23.62×0.343	59.03×0.343	
0.620 } max.	+366	+162	+163	+190	-84	+204	-83	+918
30	+606	+388	+188	+207	-182	+170	-46	+1331
40	+732	+426	+92	+170	-250	+126	+7	+1308
50	+736	+256	-54	+89	-287	+75	+55	+870
0.690 } min.	+124	-410	-61	-171	-184	-74	+54	-682
90	-164	-322	+80	-189	-93	-119	+8	-799
0.700 } min.	-416	-86	+167	-155	+4	-152	-38	-676
1.030 } min.	-466	-270	-32	-73	-119	-100	-50	-1110
40	-390	-226	-107	-115	-193	-76	-55	-1162
50	-254	-66	-106	-123	+3	-45	-41	-632
1.070 } max.	+106	+244	+53	-49	+121	+20	+18	+493
90	+278	+244	+108	+17	+158	+51	+43	+899
1.100 } max.	+388	+132	+94	+73	+174	+77	+53	+991
	+438	-40	+23	+108	+169	+100	+46	+844

Hexachlor Benzene

$$J = 6 \times 17^2 [(H_1^{3.10} - H_6) + (H_1^{5.27} - H_3)] + 3 \times 17^2 (H_3^{6.20} - H_6) \\ + 12 \times 17 \times 6 [(H_1^{1.688} - C_6) + (H_1^{3.10} - C_3)] \\ + 6 \times 35 \times 6 [(H_1^{1.69} - C_1) + (H_5^{4.51} - C_2)].$$

Divide through by 3×17^2 .

Ring No.	$\frac{\sin \theta/2}{\lambda}$ expt.	$\frac{\sin \theta/2}{\lambda}$ theor.	Description
1	0.202	0.200	Very intense
2	0.396	0.395	Very intense
3	0.502	0.502	Very clear and narrow
4	0.585	0.580	Very clear and narrow
5	0.675	0.670	Very intense and narrow
6	0.725	0.728	Minimum
7	0.782	0.780	Intense
8	Visible, not measurable	0.820	Very faint and broad
9	1.030	1.025	Very faint and broad
10	1.101	1.095	Minimum
11	1.156	1.153	Weak but clear

The theoretical intensity curves for the above are shown in fig. 2 and an original photograph in fig. 6, Plate 10.

Sym. Tri-Iodo Benzene

$$J = 3 \times 53^2 (H_1^{5.99} - H_3) + 6 \times 53 \times 6 [(H_1^{3.0135} - C_6) + (H_1^{4.34} - C_3)] \\ + 3 \times 53 \times 6 [(H_1^{2.05} - C_1) + (H_2^{4.87} - C_2)].$$

Divide through by $3 \times 53 \times 6$.

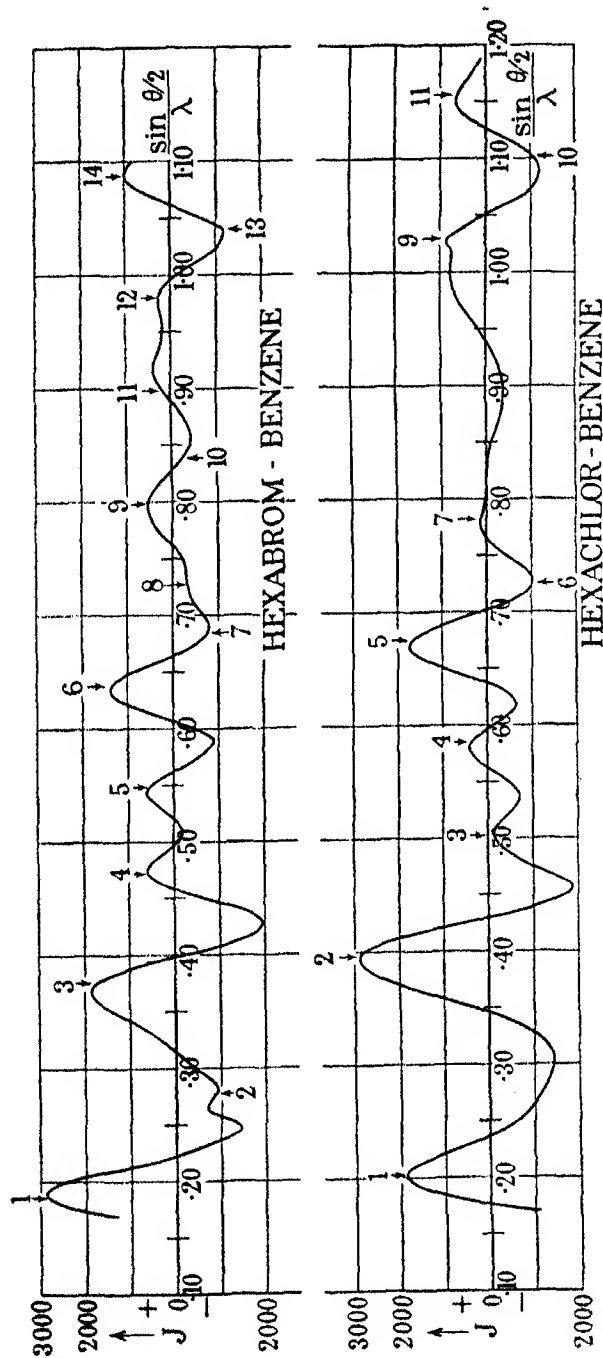


FIG. 2

Ring No.	$\frac{\sin \theta/2}{\lambda}$ expt.	$\frac{\sin \theta/2}{\lambda}$ theor.	Description
1	0.187	0.190	Intense and narrow
2	0.265	0.265	Intense and broad
3	0.354	0.355	Very intense and narrow
4	0.436	0.435	Weak and broad
5	0.517	0.522	Clear, very narrow
6	0.604	0.605	Faint
7	0.690	0.695	Faint and narrow
8	0.757	0.762	Very faint and blurred
9	0.847	0.850	Faint and clear

Sym. Tribrom Benzene

$$J = 3 \times 35^2 (H_1^{5.697} - H_2) + 6 \times 53 \times 6 [(H_1^{2.859} - C_6) + (H_1^{4.177} - C_2)] \\ + 3 \times 35 \times 6 [(H_1^{1.88} - C_1) + (H_2^{4.70} - C_5)].$$

Divide through by $3 \times 35 \times 6$.

Ring No.	$\frac{\sin \theta/2}{\lambda}$ expt.	$\frac{\sin \theta/2}{\lambda}$ theor.	Description
1	0.205	0.200	Very narrow and intense
2	0.291	0.280	Clear edge
3	0.375	0.375	Very, very intense
4	0.469	0.465	Edge
5	0.548	0.550	Narrow, very intense
6	0.636	0.635	Narrow and intense
7	0.730	0.730	Narrow and weak
8	0.817	0.815	Very weak edge
9	0.894	0.895	Narrow and weak
10	0.986	0.985	Narrow and very weak
11	1.089	1.085	Narrow and weak

The theoretical intensity curves of tri-iodo and tribrom benzene are shown in fig. 3, and reproductions of original photographs in figs. 7 and 8, Plates 10 and 11.

Para-di-iodo Benzene

$$J = 53^2 (H_2^{6.92} - H_6) + 4 \times 53 \times 6 [(H_1^{2.0155} - C_6) + (H_1^{4.24} - C_2)] \\ + 2 \times 53 \times 6 [(H_1^{2.05} - C_1) + (H_2^{4.87} - C_5)].$$

Divide through by $2 \times 53 \times 6$.

Ring No.	$\frac{\sin \theta/2}{\lambda}$ expt.		$\frac{\sin \theta/2}{\lambda}$ theor.	Description
	de Laszlo	Hendricks*		
1	0.160	0.156	0.160	Very intense
2	0.236	0.230	0.238	Very intense and narrow
3	0.306	—	0.308	Edge, faint
4	0.378	0.376	0.375	Very intense and narrow
5	0.457	—	0.455	Edge, faint
6	0.520	—	0.525	Very intense and narrow
7	0.598	—	0.595	Clear edge
8	0.671	—	0.675	Very faint
9	0.734	—	0.735	Clear narrow
10	0.812	—	0.820	} Very faint and diffuse doublet
11	0.876	—	0.875	
12	0.955	—	0.955	Very faint, narrow

* 'J. Chem. Phys.,' vol. 1, p. 550 (1933).

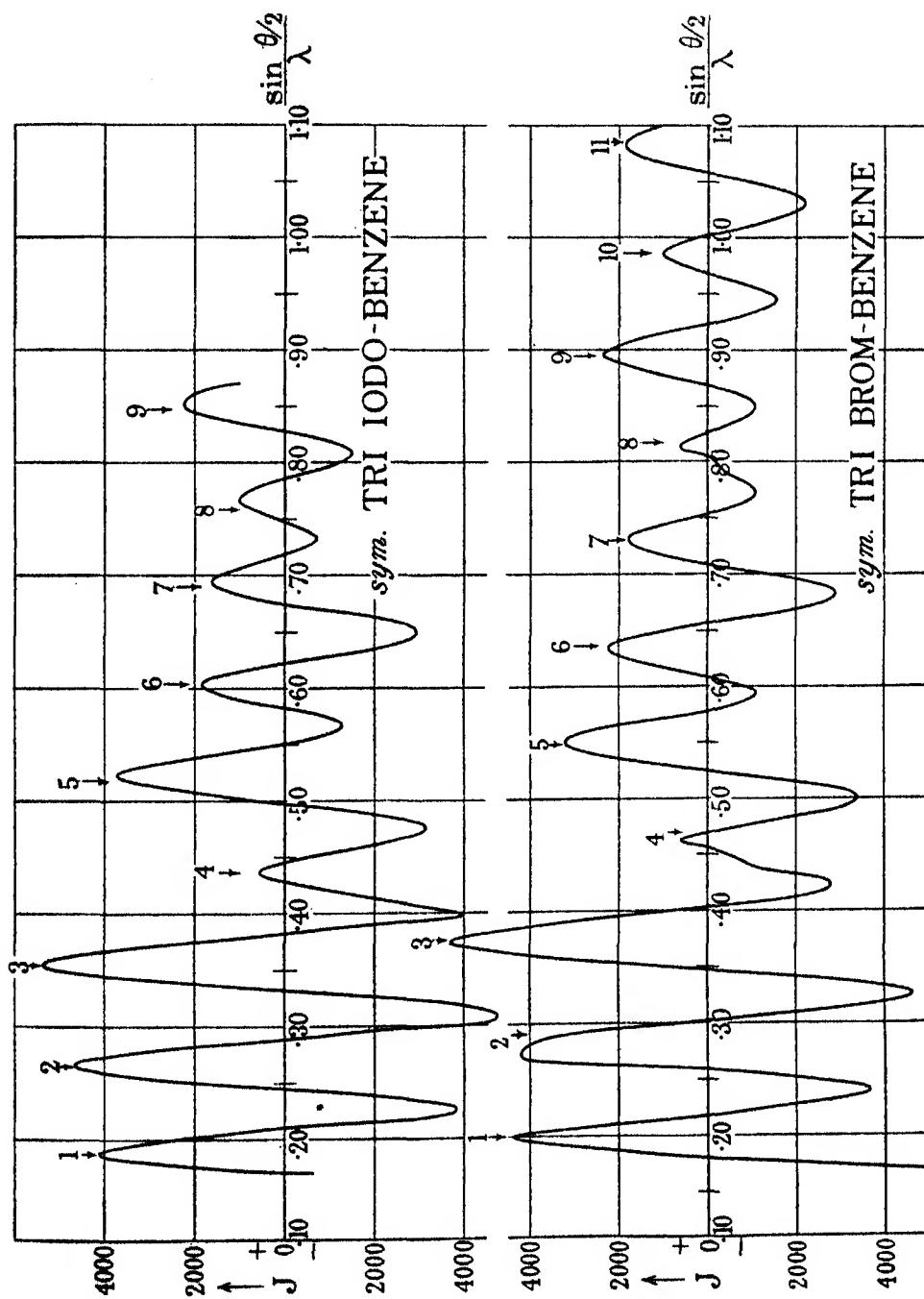


FIG. 3

Para-dibrom Benzene

$$J = 35^2 (H_3^{6.58} - H_6) + 4 \times 35 \times 6 [(H_1^{2.858} - C_6) + (H_1^{4.177} - C_3)] \\ + 2 \times 35 \times 6 [(H_1^{1.88} - C_1) + (H_2^{4.70} - C_5)].$$

Divide through by $2 \times 35 \times 6$.

Ring No.	$\frac{\sin \theta/2}{\lambda}$ expt.	$\frac{\sin \theta/2}{\lambda}$ theor.	Description
1	0.176	0.170	Intense
2	0.248	0.250	Very intense and narrow
3	0.370	0.360	Very, very faint
4	0.392	0.392	Very intense and narrow
5	0.480	0.480	Very faint
6	0.555	0.555	Faint edge
7	0.637	0.625	Faint edge
8	Not measurable	0.740	Very, very vague
9	0.780	0.774	Faint edge
10	0.870	0.870	} Faint doublet
11	Not measurable	0.920	
12	1.085	1.092	Very faint, clear

The complete theoretical curves of *p*-di-iodo and *p*-dibrom benzene are seen in fig. 4, and experimental results in figs. 9 and 10, Plate 11.

Discussion and Summary of Results

A remarkable agreement between the theoretical maxima of the intensity curves and the experimental results has been found for the six substances under investigation. We feel therefore that the following answers may safely be given to the questions stated at the commencement of this paper:—

- (1) and (2)—The benzene ring exists in the vapour phase as a flat regular hexagon with a C-C distance of 1.41 Å.
- (3) and (4)—The halogen-carbon distances for substituted benzene derivatives in the state of vapour are:—

$$C - Cl = 1.69 \text{ Å} \pm 0.01 \text{ Å}$$

$$C - Br = 1.88 \text{ Å} \pm 0.01 \text{ Å}$$

$$C - I = 2.05 \text{ Å} \pm 0.01 \text{ Å}$$

These distances appear to remain constant and are independent of the number of similar atoms substituted at the same time in the benzene ring.

It will be seen that the carbon-halogen distances in substituted benzene

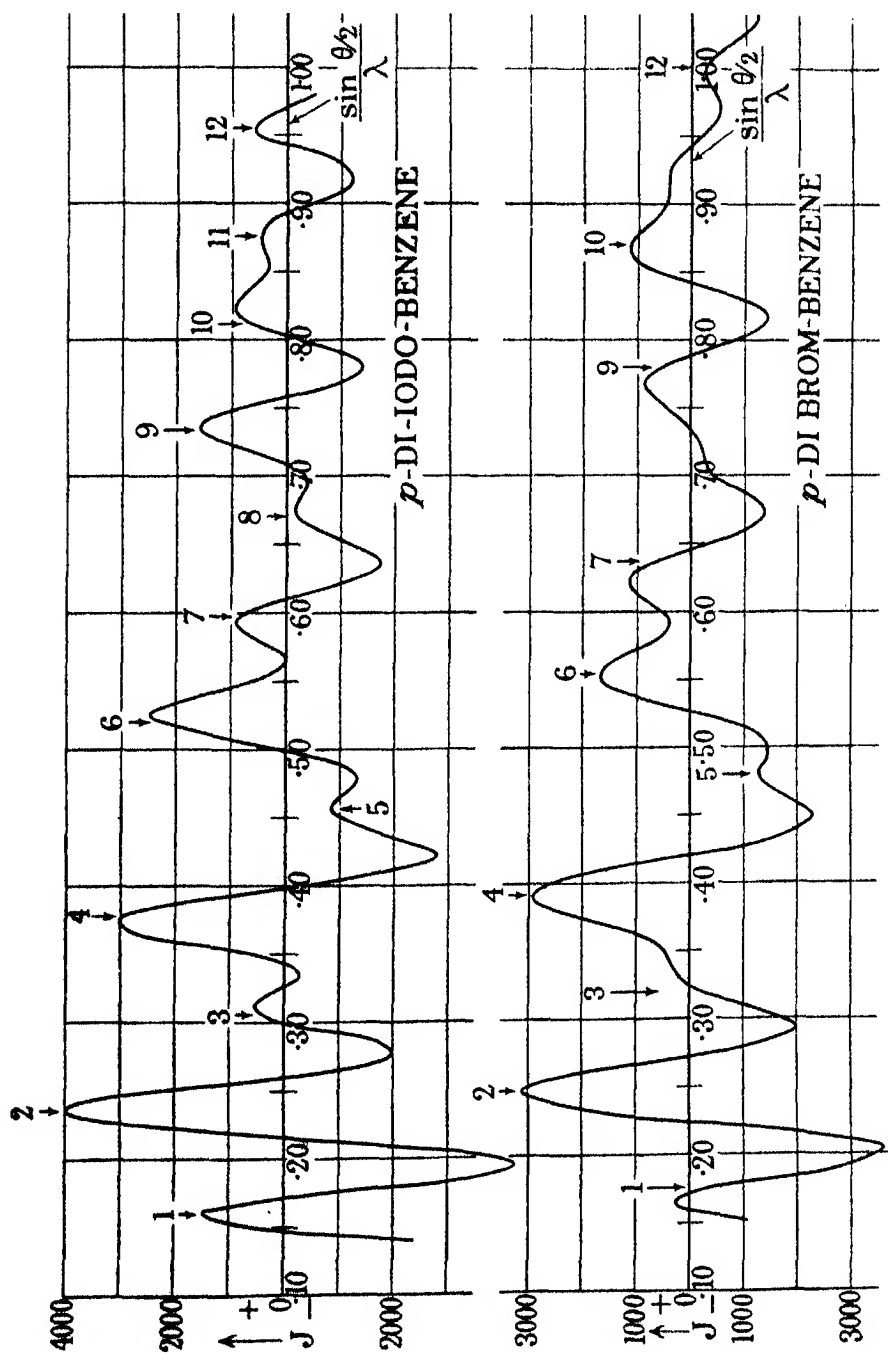


FIG. 4

derivatives are always less than those generally accepted for aliphatic compounds, the discrepancy being of the order of 0.06 Å.

Summary

The electron diffraction of the following six benzene derivatives have been measured in the vapour phase: hexa-chlor and hexa-brom benzene; sym. tribrom and tri-iodo benzene; *p*-dibrom and di-iodo benzene.

The experimental results agree well with the theoretical scattering curves based on a model where benzene is a regular flat hexagonal ring with carbon-carbon distance 1.41 Å.

The halogen-carbon distances were found to be: $\text{C} - \text{Cl} = 1.69 \text{ Å} \pm 0.01 \text{ Å}$, $\text{C} - \text{Br} = 1.88 \text{ Å} \pm 0.01 \text{ Å}$, $\text{C} - \text{I} = 2.05 \text{ Å} \pm 0.01 \text{ Å}$.

These distances appear to remain constant and to be independent of the number of similar atoms substituted at the same time in the benzene ring, and all the atoms lie in the same plane as the benzene ring.

These carbon-halogen distances are always less than those generally accepted for aliphatic compounds, the discrepancy being of the order of 0.06 Å.

Wind Structure and Evaporation in a Turbulent Atmosphere

By O. G. SUTTON, B.Sc.

(Communicated by G. C. Simpson, F.R.S.—Received May 2, 1934)

PART 1—THE GENERAL EQUATION OF TRANSFER AND THE VARIATION
OF THE WIND WITH HEIGHT*Introduction*

1—It is now generally recognized that in a turbulent medium, such as the lower atmosphere, the processes of the diffusion of mass, heat, and momentum are dominated by the action of eddies in the wind. The exact mechanism by which the typical frictional and diffusion effects are set up by the turbulence is still obscure, and at the present time there appears to be little hope of the presentation of a comprehensive theory of turbulent motion. The object of the present paper is to set forth a theory which, while admittedly non-exact and based partly upon an empirical assumption, appears to afford a satisfactory basis for the preliminary consideration of the allied problems of wind structure and the natural evaporation from a freely exposed plane surface in the lower atmosphere.

2—It is noticeable that most of the theories of turbulence which have been advanced treat the diffusion phenomena by means of a model which is suggested by the kinetic theory of gases. The eddies are regarded as distinct masses of fluid which behave like the molecules of the kinetic theory in that they are assumed to move along a kind of "free path," and thereby to transfer mass, heat, and momentum from one layer of the fluid to another by a process which is regarded as being substantially identical with that described by the collision dynamics of the kinetic theory. Briefly, it is assumed that a certain mass of fluid, of dimensions small compared with those of the total volume of fluid under consideration, breaks away from its surroundings under the influence of some mechanical or thermal disturbing force, and moves to another region of the medium, carrying with it a content of mass, heat, and momentum typical of the layer from which it originated. Having moved a certain distance (the *Mischungsweg* of Prandtl*) the eddy is then conceived to mix instantaneously

* 'Proc. 2nd Int. Cong. Appl. Maths.' (1926). See also the article on 'Hydrodynamics' by Prandtl in Müller-Pouillet's "Lehrbuch der Physik." References will be made to the English translation of this work, "The Physics of Solids and Fluids," by Ewald, Pöschl and Prandtl, translated by Dougall and Deans (1930).

with the surrounding fluid, much in the same manner as a molecule transfers a portion of its energy when it comes into collision with another molecule.

The basic idea of the present treatment is that mixing by turbulence should not be regarded as the kind of "explosive" action contemplated in these theories, but rather as a continuous process which takes place along the whole path of the eddy. This concept will be elaborated and subjected to mathematical treatment by making use of Professor G. I. Taylor's work on "Diffusion by Continuous Movements."* This appears to be the only theory which has yet been advanced which deals with eddy motion, not as a series of independent impulses, but as a succession of connected movements. The present theory, although departing in many respects from the methods developed by Taylor, may therefore be considered as a sequel to Taylor's work on this subject.

The General Equation of Transfer

3—Consider a rectangular system of axes, and let the components of the wind velocity at any instant be u , v , and w , taken along the x , y , and z axes respectively. Let mean velocities \bar{u} , \bar{v} , and \bar{w} be defined for an interval of time T as follows

$$\bar{u} = \frac{1}{T} \int_{t-\frac{1}{2}T}^{t+\frac{1}{2}T} u \, dt; \quad \bar{v} = \frac{1}{T} \int_{t-\frac{1}{2}T}^{t+\frac{1}{2}T} v \, dt; \quad \bar{w} = \frac{1}{T} \int_{t-\frac{1}{2}T}^{t+\frac{1}{2}T} w \, dt; \quad (1)$$

where t is time. The eddy velocities u' , v' , and w' are defined (following Reynolds) by

$$u = \bar{u} + u'; \quad v = \bar{v} + v'; \quad w = \bar{w} + w'. \quad (2)$$

Let the orientation of the system of axes be such that the x -axis is along the direction of the mean wind, the y -axis across wind and the z -axis vertically upwards. We shall assume that the heights we are dealing with are sufficiently small to enable us to neglect any change with height in the direction of the mean wind, and that the orientation of the system of axes, relative to the earth, does not change in the periods of time with which we are concerned. It is further assumed that there is no mean velocity in the vertical direction. These assumptions are likely to be realized on most occasions in the lower atmosphere (say, up to 20 metres above the ground) for periods of 1 hour or less.

* 'Proc. Lond. Math. Soc.,' vol. 20, p. 196 (1922).

With our assumptions, and the above system of axes, we have

$$\left. \begin{aligned} \bar{v} = \bar{w} = 0 \\ \bar{u}' = \bar{v}' = \bar{w}' = 0 \end{aligned} \right\} (z \geq 0). \quad (3)$$

Let the surface of the earth be the plane $z = 0$, and let it be assumed that \bar{u} , u' , v' , and w' are functions of height only. The air is supposed to be homogeneous as regards wind structure, water vapour content, etc., in all directions except the vertical. Observations have shown that the elements of wind in flat country show little variation over areas up to 20 square miles or so, so that the last assumption is also in reasonable accord with fact. We are thus dealing with the case of a laminar mean motion having superimposed upon it a fluctuating eddy motion.

Consider a mass of air (an "eddy"), the volume of which is supposed small compared with the total volume of the atmosphere under consideration, moving away from its surroundings under the influence of some external disturbing force. It is assumed that the air constituting the eddy has acquired the typical mean properties of its surroundings. Suppose now that the atmosphere possesses some transferable conservative property, such as vapour or smoke content, temperature, or momentum, and let E be the amount of the transferable entity per unit volume. The effect of the vertical motion w' is to cause a transfer of the entity E associated with the layer of air at height z to a new height $z + l$, and by analogy with the kinetic theory, it is easily shown that the mean rate at which E is communicated to unit area of a horizontal area of thickness δz is

$$\frac{\partial}{\partial z} \left(\overline{\rho w' l} \frac{\partial \bar{E}}{\partial z} \right) \delta z, \quad (4)$$

where ρ is the density of the air, which is assumed not to vary with height. The quantity $\overline{\rho w' l}$ here plays the part of a coefficient of diffusion, heat conduction, or viscosity, though not necessarily one which has the same value at all points in the field, as in the case of molecular transfer. The problem under consideration thus amounts to finding an expression for $\overline{\rho w' l}$ in terms of the mean motion \bar{u} and the height z , so that it may be possible to integrate the equations of transfer.

The term *Austauschkoeffizient* has been used by Schmidt* for the quantity $\overline{\rho w' l}$; the term "interchange coefficient" will be used throughout this paper.

* "Der Massenaustausch in freier Luft," vol. 7, "Probleme der Kosmischen Physik."

Let us assume that the motion is such that the mean eddying energy in the vertical direction does not vary with time over the periods with which we are concerned. That is, we assume $\overline{w'^2}$ to be independent of time. For periods of the order of 1 hour or less, this condition is fairly well satisfied in the lower atmosphere.

Let R_ξ be the correlation coefficient between the vertical motion $w'(t)$ associated with a mass of fluid at time t and the vertical motion $w'(t + \xi)$ associated with the same mass at time $t + \xi$. Thus, by definition of a correlation coefficient

$$R_\xi = \frac{\overline{w'(t) w'(t + \xi)}}{\overline{w'^2}}. \quad (5)$$

We now proceed to attach a physical meaning to the variation of R_ξ with ξ .

4—In a turbulent fluid, the length l , which, following Prandtl (*loc. cit.*) we term the "mixing path," corresponds to the "free path" of the kinetic theory of gases. It is "the path traversed by masses of the fluid relative to the rest of the fluid before they lose their individuality again by mixing with the turbulent fluid by which they are surrounded."*

The collision dynamics of the kinetic theory admits of a precise definition of the molecular free path as the distance traversed by the molecule between successive collisions. No such precision appears to be feasible in the present connection, since we must admit the possibility of mixing being a continuous process which takes place at all points on the path. We are also confronted with the difficulty of framing a mathematical definition of "mixing."

If we fix our attention upon a particular eddy, it seems reasonable to assume that the eddy shares out its excess or defect of matter, heat, or momentum whilst blending with the surrounding fluid until a stage is reached when the blending has proceeded so far that it becomes impossible to distinguish the eddy from the main body of the fluid, and it ceases to act as a transport agent. We may express this mathematically by saying that the correlation between its initial vertical velocity and its subsequent vertical velocity is continually decreasing, until at the end of the mixing path, all correlation has disappeared. That is, the eddy has mixed with the surrounding fluid so that an interchange of characteristics has taken place, and the later motion of the mass of fluid constituting the eddy tends to be governed by conditions which are unrelated to the original impulses causing the early motion of the eddy. Mixing may,

* Prandtl, "The Physics of Solids and Fluids," p. 278.

therefore, be defined in our case as a loss of correlation between the initial and subsequent relative motion of the eddy, and the mixing path may now be defined as the distance through which the eddy moves during the period necessary for the correlation between the velocity relative to the mean motion at the beginning and at the end of the path to vanish or become negligibly small.

5—Let t_0 be the time taken by the eddy to transverse the vertical distance l . It has been shown by Taylor* that

$$\int_0^{t_0} \overline{w'(t) w'(t + \xi)} d\xi = \overline{w'(t)} \int_0^{t_0} \overline{w'(\xi)} d\xi = \overline{w'^2} \int_0^{t_0} R_\xi d\xi. \quad (6)$$

But

$$\overline{w'l} = \overline{w'(t) \int_0^{t_0} w'(\xi) d\xi},$$

so that

$$\overline{w'l} = \overline{w'^2} \int_0^{t_0} R_\xi d\xi. \quad (7)$$

We have now to assign a suitable form for R_ξ . The conditions that have to be satisfied are clearly, in view of the meaning attached to R_ξ above :

$$\left. \begin{array}{ll} \text{(i)} & R_\xi = 1 \text{ for } \xi = 0 \\ \text{(ii)} & R_\xi \text{ decreases as } \xi \text{ increases} \\ \text{(iii)} & R_\xi \text{ is negligibly small for } \xi = t_0 \end{array} \right\}. \quad (8)$$

In a previous paper† dealing with the diffusion of matter in a turbulent medium, the writer has shown that expressions which appear to fit the facts of observations on the distribution of smoke or other suspended matter in the atmosphere are obtained by taking for R_ξ a simple form equivalent to

$$R_\xi = (\bar{u}\xi)^{-n},$$

where n is a positive constant. In the present treatment it has been found necessary to modify this assumption somewhat, and R_ξ has been taken to behave like $[(\bar{u})^2 \xi]^{-n}$. This modification does not affect the form of the expressions previously obtained for the distribution of matter, but necessitates a slightly different definition of the diffusion coefficient. The present work may, therefore, be regarded as a continuation of the previous investigations on the diffusion of matter.

* *Loc. cit.*, p. 207.

† 'Proc. Roy. Soc.,' A, vol. 135, p. 143 (1932).

We define R_t as

$$R_t = \left(\frac{\nu}{\nu + \overline{w'^2} \xi} \right)^n \quad (9)$$

the quantity ν being a constant of dimensions L^2T^{-1} , and small compared with $\overline{w'^2} t_0$. Since Taylor* and Scrase† have shown that in the lower atmosphere $\overline{w'^2}$ is proportional to $(\overline{u})^2$, it will be seen that R_t behaves like $[(\overline{u})^2 \xi]^{-n}$.

It will be shown later that ν can be identified as the kinematic viscosity of the medium. In the atmosphere, ν is of the order of 10^{-1} cm²/sec, whilst $\overline{w'^2}$ is of the order of 10^4 cm²/sec² under normal conditions. The time t_0 , estimated from the wind tunnel experiments of Relf and Lavender,‡ and from Scrase's§ measurements in the lower atmosphere, appears to be greater than 10^{-1} secs, and thus $\overline{w'^2} t_0$ is greater than 10^3 cm²/sec. We are thus justified in assuming that ν is small compared with $\overline{w'^2} t_0$ when ν is taken to be the kinematic viscosity of the air. We have still to enquire if R_t is small for $\xi = t_0$. It will be shown later that in the absence of thermal disturbances, $n = \frac{1}{2}$ and so, taking $\overline{w'^2} t_0 = 10^3$ cm²/sec we find $R_t = 0.1$ approximately. Such a value for R_t indicates an almost complete absence of correlation and condition (iii) of (8) is thus satisfied in practice.|| In the presence of convection currents, n decreases, but since at the same time the magnitude of $\overline{w'^2}$ increases, it is probable that the effects balance each other and so keep R_t small.

6—The functional form which has been suggested here for R_t has several advantages. In the first place it is, mathematically regarded, perhaps the simplest type of function satisfying conditions (8) which leads to tractable expressions when substituted in the differential equation of transfer. Secondly, there is the advantage that, starting from the expression for R_t as a simple power, with one adjustable constant n which specifies the rapidity of mixing, and is thus a simple measure of the degree of turbulence present in the medium, we reach expressions for the distribution of the elements in a turbulent fluid as simple power laws. Most of the experimental work on turbulence has been expressed in terms of power laws, and thus comparison with experimental data is facilitated. It is probable that R_t can be represented by a power series in which (9) is the dominant term, and for the present it appears that it is unnecessary to retain any other terms.

* 'Q. J. Roy. Met. Soc.,' vol. 53, p. 201 (1927).

† Meteorological Office, Geophys. Mem. No. 52 (1930).

‡ 'Advisory Cttee. Aero., R. and M.,' No. 597 (1918).

§ *Loc. cit.*, p. 15.

|| See D. Brunt, "The Combination of Observations," 2nd ed., p. 157.

In the above expression for R_t , the quantity n is an indicator of the degree of turbulence present in the medium. It appears that, to a first approximation, n is independent of the mean velocity and the height, and is primarily affected only by those factors which tend to damp out or enhance the turbulence. For meteorological purposes, n is thus to be regarded as a function of the vertical gradient of temperature and of the roughness of the surface, and at present it does not appear possible to express the variation of n with these factors other than empirically. It is, however, easy to see that, to ensure physical reality, n must be restricted to lie between 0 and 1. For, considering the scatter of a group of particles in a turbulent medium, Taylor* has shown that, if X be the vertical distance travelled by a particle in time T , then

$$\overline{X^2} = 2\overline{w'^2} \int_0^T \int_0^t R_t d\xi dt,$$

or, approximately, using our definition of R_t ,

$$\overline{X^2} = \frac{2v^n}{(1-n)(2-n)} \overline{w'^2} T^{2-n},$$

since $\overline{X^2}$ is essentially positive, and the scatter of the particles must increase with time, it is clear that n must lie between 0 and 1.

We have now

$$\begin{aligned} \overline{w'l} &= \overline{w'^2} \int_0^{t_0} \left(\frac{v}{v + \overline{w'^2} \xi} \right)^n d\xi \\ &= \frac{v^n}{1-n} \{ (v + \overline{w'^2} t_0)^{1-n} - v^{1-n} \}. \end{aligned}$$

Since v is assumed to be small compared with $\overline{w'^2} t_0$ and $n < 1$, we may write the above as

$$\overline{w'l} = \frac{v^n}{1-n} (\overline{w'^2} t_0)^{1-n}, \quad (10)$$

the terms neglected being of the order v at the most. This approximation really amounts to neglecting molecular forces in comparison with eddy forces.

7—It does not appear possible to give a rigorous expression for $\overline{w'^2} t_0$ in terms of the mean velocity and the height unless we know how $\overline{w'^2}$ depends upon the boundary conditions and the stability of the motion, and the manner in which \bar{u} depends upon the height. We may, however, obtain a reasonable

* 'Proc. Lond. Math. Soc.,' vol. 20, p. 196 (1922).

approximation in the following manner, in which use is made of ideas due to Prandtl* and Th. v. Kármán.†

If $|w'|$ denote the absolute magnitude of the vertical component of the eddy velocity we have, following Prandtl,

$$|w'| = l' \left| \frac{\partial \bar{u}}{\partial z} \right|$$

where l' is an individual mixing path. Hence

$$\overline{|w'|} = l \left| \frac{\partial \bar{u}}{\partial z} \right|$$

where l is the mean mixing path. It has been shown by Hesselberg and Bjordkal‡ that the eddy velocities are distributed according to Maxwell's law. Thus we have the well-known relationship

$$\overline{w'^2} = \frac{1}{2}\pi (\overline{|w'|})^2$$

and so

$$\overline{w'^2} = \frac{1}{2}\pi l^2 \left(\frac{\partial \bar{u}}{\partial z} \right)^2.$$

The time t_0 is given by

$$t_0 = \int_z^{z+l} \frac{dz}{w'}.$$

Replacing w' by its mean absolute value $\overline{|w'|}$, we have

$$t_0 = \frac{l}{\overline{|w'|}} = \left(\left| \frac{\partial \bar{u}}{\partial z} \right| \right)^{-1}$$

approximately. Hence

$$\overline{w'^2} t_0 = \frac{1}{2}\pi l^2 \left| \frac{\partial \bar{u}}{\partial z} \right|.$$

It has been shown by v. Kármán (*loc. cit.*) and also by Betz§ that the assumption that the eddy velocities at different points in the region are dynamically similar leads to a particularly simple expression for l . Making this assumption in our case we have v. Kármán's expression

$$l = k \cdot \frac{\left| \frac{\partial \bar{u}}{\partial z} \right|}{\left| \frac{\partial^2 \bar{u}}{\partial z^2} \right|}, \quad (11)$$

* "The Physics of Solids and Fluids," p. 278.

† 'Nachr. Ges. Wiss., Gottingen,' p. 58 (1930).

‡ 'Beitrage Phys. frei. Atmos.,' vol. 15 (1929).

§ 'Z. angew. Math. Mech.,' vol. 11, p. 391 (1931).

where k is a dimensionless constant, whose value is approximately 0.4. Thus finally

$$\overline{w'^2 t_0} = 0.08 \pi \left(\left| \frac{\partial \overline{u}}{\partial z} \right| \right)^3 \left(\left| \frac{\partial^2 \overline{u}}{\partial z^2} \right| \right)^{-2}$$

approximately. We thus deduce as our expression for the interchange coefficient

$$\begin{aligned} A &= \overline{\rho w' l} = \frac{\rho v^n}{1-n} (\overline{w'^2 t_0})^{1-n} \\ &= \frac{(0.251)^{1-n}}{1-n} \rho v^n \left\{ \left(\left| \frac{\partial \overline{u}}{\partial z} \right| \right)^3 \left(\left| \frac{\partial^2 \overline{u}}{\partial z^2} \right| \right)^{-2} \right\}^{1-n}. \end{aligned} \quad (12)$$

The Variation of Wind with Height

8—It was conjectured by Schmidt, and has recently been proved by Ertel*, that if the interchange coefficient has in the lower layers of the atmosphere the form

$$A(z) = A(1) \left(\frac{z}{z_1} \right)^{\frac{p-1}{p}},$$

then the law of variation of wind with height is

$$\overline{u} = \overline{u}_1 \left(\frac{z}{z_1} \right)^{1/p},$$

where $A(1)$ and \overline{u}_1 are the values of the interchange coefficient and the mean velocity at a fixed height z_1 . This implies also that

$$A(z) \frac{\partial \overline{u}}{\partial z} = \text{constant}$$

in the lower layers of the atmosphere. Substituting (12) for $A(z)$ we find

$$\frac{(0.251)^{1-n}}{1-n} \rho v^n \left(\frac{\partial \overline{u}}{\partial z} \right)^{4-3n} \left(\frac{\partial^2 \overline{u}}{\partial z^2} \right)^{2n-2} = \text{constant},$$

from which we deduce the law of variation of wind with height as

$$\overline{u} = \overline{u}_1 \left(\frac{z}{z_1} \right)^{\frac{n}{2-n}} \quad (13)$$

on the assumption that there is no velocity at the surface ($u = 0$ for $z = 0$). For $n = 1$, (13) yields the form of the law for $A = \text{constant}$, viz.,

$$\overline{u} = \overline{u}_1 z / z_1, \quad (14)$$

* 'Met. Z.', vol. 50, p. 386 (1933).

while as n approaches zero, the law tends to the form

$$\bar{u} = \bar{u}_1, \quad (15)$$

i.e., a velocity constant with height.

A considerable amount of research has been devoted by meteorologists to the question of the variation of the wind with height near the surface of the earth, and it appears to be well established that, except perhaps in the immediate vicinity of the surface (within a few centimetres of the ground), the wind structure is represented by a power law such as (13).^{*} The interest lies in the question as to whether or not all possible variations are included in the limits set by (14) and (15).

It has been shown by the present writer[†] and by Barkat Ali[‡] that the index occurring in the power law of wind structure is subject to a marked diurnal variation. This is particularly evident in the curves given by Barkat Ali, where, in one instance, the variation in the index is from 0.87 at midnight to 0.02 at noon. This range is included in that which is covered by the index $n/(2-n)$ of equation (13) for $0 < n < 1$.

It is obvious that changes in the value of the index are associated with the diurnal variation of turbulence in the lower atmosphere, which in turn is associated with the diurnal variation of the vertical gradient of temperature. The variation of the index with the vertical gradient of temperature is shown in the papers by Barkat Ali and the present writer quoted above, and reference may also be made to the very detailed investigations carried out in recent years at the Royal Airship Works, Cardington. In the memoirs dealing with these investigations the ratio of the mean wind velocity at 150 feet above the ground to the mean wind velocity at 50 feet above the ground is tabulated for various temperature differences between heights of 143 feet and 4 feet above the ground. From this table it may be calculated that, assuming the power law of wind structure to hold over these heights, the index varies from 0.009 for the greatest lapse (temperature decreasing with height, i.e., very turbulent air) to 0.62 in the greatest inversion (temperature increasing with height, i.e., air in which turbulence tends to be damped out). These values, which represent the collected results of several years' observations, again lie within the range indicated by the theory.

^{*} The evidence for power laws of wind structure has been summarized by R. Geiger in "Das Klima der Bodennahen Luftschicht," p. 70.

[†] 'Q. J. Roy. Met. Soc.,' vol. 58, p. 74 (1932).

[‡] *Ibid.*, vol. 58, p. 285 (1932).

[§] "Meteorological Office, Geophys. Mem.," No. 54 (1932).

To sum up, it may be said that the wind structure near the ground is represented by the equation

$$\bar{u} = \bar{u}_1 \left(\frac{z}{z_1} \right)^{\frac{n}{2-n}},$$

in which n varies from a value which is nearly zero to one which approaches unity. The quantity n is to be regarded as a function of the degree of turbulence present. For meteorological purposes, this is best expressed by the statement that n is primarily a function of the vertical gradient of temperature and also, but almost certainly to a lesser degree, of the roughness of the ground.

Comparison with Pipe Flow Experiments

9.—Much of the above analysis may be equally well applied to problems connected with the flow of air in pipes* or wind tunnels, a subject which has received a considerable amount of attention from the experimental standpoint. In these problems, thermal influences are absent, and n is thus a function of the Reynolds' number and of the degree of roughness of the pipe only. It has been found by experiment that n varies but slowly with the Reynolds' number, and for most purposes may be considered as an absolute constant in these problems.

The shearing stress in the air in the pipe is given by

$$\tau = A(z) \frac{\partial \bar{u}}{\partial z},$$

where z now denotes distance from the wall of the pipe. From (12) and (13) this is

$$\begin{aligned} \tau &= \frac{(0.251)^{1-n}}{1-n} \rho v^n \left(\frac{\partial \bar{u}}{\partial z} \right)^{4-2n} \left(\frac{\partial^2 \bar{u}}{\partial z^2} \right)^{2n-2} \\ &= (0.251)^{1-n} \frac{n^{2-n}}{(1-n)(2n-2)^{2-2n} (2-n)^n} \rho \frac{v^n}{z_1^n} \bar{u}_1^{2-n}. \end{aligned} \quad (16)$$

Large numbers of experiments on pipe flow have shown that for smooth tubes and for a wide range of Reynolds' number the velocity varies with distance from the wall according to the law†

$$\bar{u} = \bar{u}_1 \left(\frac{z}{z_1} \right)^\dagger.$$

* Comparisons between pipe flow and natural winds in the atmosphere have been made by Prandtl and Tollmien, 'Z. Geophysik,' jahrg. 1, heft 1/2 (1925) and by Bryant, 'Aero. Res. Ctee., R. and M,' No. 1047 (1931).

† "The Physics of Solids and Fluids," p. 281.

Comparison with (13) shows that

$$\frac{n}{2-n} = \frac{1}{7}$$

or

$$n = \frac{1}{4}.$$

Putting $n = \frac{1}{4}$ in (16) we find

$$\tau = \frac{0.020}{z_1^{\frac{1}{4}}} \rho v_1^{\frac{1}{4}} \bar{u}_1^{\frac{1}{4}}$$

The experimental result is*

$$\tau = \frac{0.023}{z_1^{\frac{1}{4}}} \rho v_1^{\frac{1}{4}} \bar{u}_1^{\frac{1}{4}},$$

where v_1 is the kinematic viscosity of the medium. This enables us to identify the constant v which has been used in the definition of R_t as the kinematic viscosity of the medium.

The closeness of the agreement between the numerical constants 0.020 and 0.023 in the above expressions is probably accidental, in view of the approximate methods which have been employed to deduce the expression for $w'^2 t_0$ in terms of the height and the mean velocity, but the fact that these constants are of the same order of magnitude may be taken as an indication that the theory as developed above is in reasonable accord with fact.

PART II—EVAPORATION

1—The hydrodynamical aspects of the problem of evaporation into a turbulent medium under varying degrees of turbulence have received somewhat meagre treatment, despite the fact that a very large number of investigations has been carried out on the experimental side. It is proposed in the following to investigate the natural evaporation from a plane horizontal surface, using the theory developed in Part I of this paper, and making the assumption that the transfer of mass in a turbulent atmosphere follows the same laws, and is governed by the same interchange coefficient, as the transport of momentum.

The present investigation is confined to two problems—

- (i) the variation of the rate of evaporation with the size and shape of the evaporating surface;
- (ii) the variation of the rate of evaporation with the mean wind velocity in air streams possessing varying degrees of turbulence.

* "The Physics of Solids and Fluids," p. 282.

Both of these questions are of interest in meteorology, and, in particular, the first problem is of importance in that it introduces the scale factor which is required in assessing the rate of evaporation from large areas, such as reservoirs, from observations upon small scale areas, such as the evaporimeter as used at many observatories.

These problems have been attacked by Jeffreys* for the case of a constant interchange coefficient, and a wind independent of height. Jeffreys' results are (i) the rates of total evaporation from surfaces of the same shape and the same orientation to the wind are to each other as the three-quarter powers of their respective areas, and (ii) the rate of evaporation is proportional to the square root of the wind velocity.

It is well known that the interchange coefficient shows a considerable variation with height under normal conditions in the lower atmosphere. Further, whilst under conditions of very large temperature inversions, the stable density gradient may damp out most of the eddy motion and the atmosphere approach a state of streamline flow (constant interchange coefficient), under such conditions the shear of the wind is most marked. It is therefore necessary to generalize Jeffreys' results as so to apply to the case of evaporation in a turbulent atmosphere in which the interchange coefficient is given by (12) and the wind structure near the surface by (13).

2—Let the evaporating surface be level with the surface of the earth, and let it be of such dimensions that it produces no sensible variations in the normal wind structure, and also such that the increase in the vapour content of the air, as it flows over the surface, is never large enough to affect the rate of evaporation from the leeward side of the surface. In practice this latter limitation, owing to the rapid air exchange taking place normally over the surface, would exclude from our consideration only very large natural surfaces.

When the evaporating liquid is one whose vapour is not a normal constituent of the atmosphere, let $\chi(x, y, z)$ be the amount of vapour present per unit volume of air. If the evaporating liquid be water, χ must be defined as that portion of the air mass per unit volume of the atmosphere which is due solely to water vapour evaporated from the surface considered. With these definitions, χ vanishes at great heights and is zero at all points to the windward of the surface.

* 'Phil. Mag.,' vol. 35, p. 273 (1918).

Let x be measured downwind from the windward edge of the evaporating surface, y across wind and z vertically upwards as before. Let \bar{u} be the mean wind velocity; we again assume that \bar{u} is a function of height only.

The equation for the diffusion of vapour from the surface is

$$\rho \frac{D\chi}{Dt} = \frac{\partial}{\partial x} \left\{ A(x) \frac{\partial \chi}{\partial x} \right\} + \frac{\partial}{\partial y} \left\{ A(y) \frac{\partial \chi}{\partial y} \right\} + \frac{\partial}{\partial z} \left\{ A(z) \frac{\partial \chi}{\partial z} \right\}, \quad (17)$$

where

$$\frac{D\chi}{Dt} = \frac{\partial \chi}{\partial t} + \bar{u} \frac{\partial \chi}{\partial x} + \bar{v} \frac{\partial \chi}{\partial y} + \bar{w} \frac{\partial \chi}{\partial z},$$

$A(x)$, $A(y)$, and $A(z)$ being the interchange coefficients in the directions x , y , and z respectively.

Following Jeffreys, we consider only the two-dimensional problem obtained by neglecting

$$\frac{\partial}{\partial x} \left\{ A(x) \frac{\partial \chi}{\partial x} \right\} \quad \text{and} \quad \frac{\partial}{\partial y} \left\{ A(y) \frac{\partial \chi}{\partial y} \right\}$$

in comparison with the remaining terms, and since x is measured along the direction of the mean wind, it follows that $\bar{v} = \bar{w} = 0$. Equation (17) thus becomes, in the steady case ($\partial \chi / \partial t = 0$)

$$\bar{u} \frac{\partial \chi}{\partial x} = \frac{1}{\rho} \frac{\partial}{\partial z} \left\{ A(z) \frac{\partial \chi}{\partial z} \right\}, \quad (18)$$

this being the equation (with \bar{u} and $A(z)$ constant) which is considered by Jeffreys.

Substituting (13) in our expression for $A(z)$ we find

$$\begin{aligned} A(z) &= \left| \frac{(0.251)^{1-n} (2-n)^{1-n} n^{1-n}}{(1-n)(2n-2)^{2(1-n)}} \right| \rho v^n \frac{\bar{u}_1^{1-n}}{z_1^{n-1}} \left(\frac{z}{z_1} \right)^{\frac{2(1-n)}{2-n}} \\ &= \rho a \bar{u}_1^{1-n} z^{\frac{2(1-n)}{2-n}}, \text{ say,} \end{aligned} \quad (19)$$

in which a is a quantity which depends only upon n and the physical constants of the atmosphere, and which will be treated here as an absolute constant. It is important to notice that a does not depend in any way upon \bar{u}_1 . Thus equation (18) becomes

$$\frac{\bar{u}_1^n}{a} z^{\frac{n}{2-n}} \frac{\partial \chi}{\partial x} = \frac{\partial}{\partial z} \left\{ z^{\frac{2(1-n)}{2-n}} \frac{\partial \chi}{\partial z} \right\},$$

or, writing $m = n/(2-n)$

$$\frac{\bar{u}_1^n}{a} \frac{\partial \chi}{\partial x} = z^{-m} \frac{\partial}{\partial z} \left\{ z^{1-m} \frac{\partial \chi}{\partial z} \right\}. \quad (20)$$

3—In order to formulate the problem mathematically, we assume that (i) at the evaporating surface $\chi = \chi_0$ (which may be regarded as the saturation value) and (ii) no vapour arising from the surface is present to the windward of the surface, so that $\chi = 0$ for $x < 0, z \geq 0$. The presence of vapour at the actual evaporating surface must be regarded as being due to the action of molecular diffusion in a very thin layer of air immediately above the surface, since the eddy motion has been assumed to vanish on the plane $z = 0$. These assumptions introduce a discontinuity in χ at the point $x = 0, z = 0$, but elsewhere they are physically acceptable, and, as will be shown, lead to results which are in good agreement with experimental data. They are also the simplest mathematical assumptions we can make.

Let x_0 be the length of the evaporating surface downwind. Then we require a solution $\chi(x, z)$ of equation (20), valid in the semi-infinite strip $0 < x \leq x_0, 0 < z$ such that

$$\begin{aligned} (1) \quad \lim_{z \rightarrow 0} \chi(x, z) &= \chi_0 & (0 < x \leq x_0) \\ (2) \quad \lim_{z \rightarrow \infty} \chi(x, z) &= 0 & (0 \leq x \leq x_0) \\ (3) \quad \lim_{x \rightarrow 0} \chi(x, z) &= 0 & (0 < z). \end{aligned}$$

Make the transformations

$$\xi = \frac{x}{x_0}, \quad \zeta = \left(\frac{u_1^n}{ax_0} \right)^{\frac{1}{n}} z^{m+1}.$$

Equation (20) becomes

$$\frac{\partial \chi}{\partial \xi} = \frac{\partial^2 \chi}{\partial \zeta^2} + \frac{1}{(2m+1)\zeta} \frac{\partial \chi}{\partial \zeta} \quad (21)$$

and the boundary conditions (1), (2), and (3) now become

$$\begin{aligned} (1') \quad \lim_{\zeta \rightarrow 0} \chi(\xi, \zeta) &= \chi_0 & (0 < \xi \leq 1) \\ (2') \quad \lim_{\zeta \rightarrow \infty} \chi(\xi, \zeta) &= 0 & (0 \leq \xi \leq 1) \\ (3') \quad \lim_{\xi \rightarrow 0} \chi(\xi, \zeta) &= 0 & (0 < \zeta). \end{aligned}$$

The evaporating surface is now defined by $0 \leq \xi \leq 1, \zeta = 0$. It is to be noted that none of a, u_1, x_0 occur explicitly in the problem constituted by equation (21) and the transformed boundary conditions (1'), (2'), and (3'), so

that if $F(\xi, \zeta)$ is the solution of this latter problem, the solution of the original problem is

$$\chi(x, z) = F\left\{\frac{x}{x_0}, \left(\frac{u_1^n}{ax_0}\right)^{\frac{1}{2}} z^{m+\frac{1}{2}}\right\}. \quad (22)$$

We now proceed to find $F(\xi, \zeta)$.*

In equation (21) write

$$\chi = \zeta^p \Omega(\xi, \zeta),$$

where

$$p = \frac{m}{2m+1} = \frac{n}{2+n}$$

so that, since $0 < n < 1$, we have $0 < p < 1/3$. Then

$$\frac{\partial \Omega}{\partial \xi} = \frac{\partial^2 \Omega}{\partial \zeta^2} + \frac{1}{\zeta} \frac{\partial \Omega}{\partial \zeta} - \frac{p^2}{\zeta^2} \Omega. \quad (23)$$

It is easily verified that

$$\Omega(\xi, \zeta) = \frac{C}{\xi - h} \exp\left\{-\frac{\zeta^2 + 4\alpha^2}{4(\xi - h)}\right\} K_p\left(\frac{\alpha\zeta}{\xi - h}\right),$$

where $K_p(\omega)$ denotes the Modified Bessel Function of the second kind,† is a solution of (23) for all values of the constants h , α , and C . Taking $h = 0$, and choosing C as a suitable function of α , we are led to the expression

$$\begin{aligned} F(\xi, \zeta) &= \zeta^p \Omega(\xi, \zeta) \\ &= \frac{2\chi_0}{\pi} \tan p\pi \zeta^p \int_0^\infty \frac{(2\alpha)^{1-p}}{\xi} \exp\left\{-\frac{(\zeta^2 + 4\alpha^2)}{4\xi}\right\} K_p\left(\frac{\alpha\zeta}{\xi}\right) d\alpha. \end{aligned}$$

Using this, we can easily show by making use of the expansion of $\omega^p K_p(\omega)$ near $\omega = 0$, and the asymptotic expansion of $K_p(\omega)$ for large positive ω , that $F(\xi, \zeta)$ satisfies equation (21) for $0 < \xi \leq 1$, $0 < \zeta$, and that

- (i) $F(\xi, \zeta) \rightarrow \chi_0$ as $\zeta \rightarrow 0$ for $0 < \xi \leq 1$ and also for $\xi \rightarrow 0$ with ζ , provided that $\zeta/\xi \rightarrow 0$.
- (ii) $F(\xi, \zeta) \rightarrow 0$ as $\zeta \rightarrow \infty$ for $0 \leq \xi \leq 1$.
- (iii) $F(\xi, \zeta) \rightarrow 0$ as $\xi \rightarrow 0$ for $0 < \zeta$, and also for $\zeta \rightarrow 0$ with ξ , provided that $\zeta/\xi \rightarrow \infty$.

* The actual form of $F(\xi, \zeta)$ is not necessary for the results we wish to obtain. However, since the discontinuity in the boundary conditions makes a direct appeal to the usual theorems of existence and uniqueness of solution impossible, it seems simplest to construct the solution whose existence is implied. An outline of the construction is therefore given above.

† Whittaker and Watson, "Modern Analysis," 3rd ed., p. 373.

These are sufficient to establish the validity of the treatment which follows, in which the object is to establish the scale factors and the wind velocity law only.

We have

$$\chi(x, z) = F\left\{\frac{x}{x_0}, \left(\frac{\bar{u}_1^n}{ax_0}\right)^{\frac{1}{2}} z^{m+\frac{1}{2}}\right\}.$$

The mean quantity of vapour passing in unit time through a unit surface perpendicular to the direction of the mean wind is $\chi\bar{u}$; hence the total mass of vapour removed in unit time (*i.e.*, the rate of evaporation) is found by integrating this quantity over the height of the atmosphere. We have, then, for the mean amount of vapour carried across the plane $x = x_0$ in unit time

$$\begin{aligned} E &= \int_0^\infty \bar{u}_1 z^m F\left\{1, \left(\frac{\bar{u}_1^n}{ax_0}\right)^{\frac{1}{2}} z^{m+\frac{1}{2}}\right\} dz \\ &= \int_0^\infty \bar{u}_1 \left(\frac{\bar{u}_1^n}{ax_0}\right)^{-\frac{(1+m)}{2m+1}} F(1, \zeta) \frac{d\zeta}{\zeta^{\frac{2(m+1)}{2m+1}}} \\ &= \bar{u}_1^{1 - \frac{n(m+1)}{2m+1}} (ax_0)^{\frac{m+1}{2m+1}} K, \end{aligned}$$

where

$$K = \int_0^\infty F(1, \zeta) \frac{d\zeta}{\zeta^{\frac{2(m+1)}{2m+1}}}$$

is a constant, independent of u_1 , a , and x_0 .

Since $m = n/(2 - n)$ we get

$$\begin{aligned} \frac{m+1}{2m+1} &= \frac{2}{2+n}, \\ 1 - \frac{n(m+1)}{2m+1} &= \frac{2-n}{2+n}. \end{aligned}$$

Hence the mean rate of evaporation from a surface of unit breadth and length x_0 downwind is

$$E = K \bar{u}_1^{\frac{2-n}{2+n}} a^{\frac{2}{2+n}} x_0^{\frac{2}{2+n}}.$$

4—We shall now consider certain special cases.

(1) *Rectangular area, length x_0 downwind, and breadth y_0 across wind*—The evaporation from a strip length x_0 downwind and breadth dy across wind is

$$dE = K \bar{u}_1^{\frac{2-n}{2+n}} a^{\frac{2}{2+n}} x_0^{\frac{2}{2+n}} dy.$$

Hence the total rate of evaporation from the whole area is

$$E = \int_0^{y_0} K \bar{u}_1^{\frac{2-n}{2+n}} a^{\frac{2}{2+n}} x_0^{\frac{2}{2+n}} dy = K \bar{u}_1^{\frac{2-n}{2+n}} a^{\frac{2}{2+n}} x_0^{\frac{2}{2+n}} y_0.$$

(2) *Elliptic area, semi axes r_1 (downwind), and r_2 (across wind)*—As above, we have for a strip of length x and breadth dy

$$dE = K \bar{u}_1^{\frac{2-n}{2+n}} a^{\frac{2}{2+n}} x^{\frac{2}{2+n}} dy.$$

Writing $x = r_1 (1 + \cos \theta)$ $y = r_2 \sin \theta$, the total rate of evaporation is

$$\begin{aligned} E &= K \bar{u}_1^{\frac{2-n}{2+n}} a^{\frac{2}{2+n}} \int_0^\pi r_1^{\frac{2}{2+n}} (1 + \cos \theta)^{\frac{2}{2+n}} r_2 \cos \theta d\theta \\ &= K' \bar{u}_1^{\frac{2-n}{2+n}} a^{\frac{2}{2+n}} r_1^{\frac{2}{2+n}} r_2, \end{aligned}$$

where

$$K' = \sqrt{\pi} 2^{\frac{2}{2+n}} \left\{ \frac{2\Gamma\left(\frac{10+3n}{4+2n}\right)}{\Gamma\left(\frac{6+2n}{2+n}\right)} - \frac{\Gamma\left(\frac{6+n}{4+2n}\right)}{\Gamma\left(\frac{4+n}{2+n}\right)} \right\} K.$$

(3) *Circular area, radius r* —This is immediately deduced from the elliptic area case by putting $r_1 = r_2 = r$. We have

$$E = K' \bar{u}_1^{\frac{2-n}{2+n}} a^{\frac{2}{2+n}} r^{\frac{4+n}{2+n}}.$$

In general, we have the result that for similar figures similarly orientated with respect to the direction of the mean wind, the mean rate of evaporation is proportional to $L^{\frac{4+n}{2+n}}$, where L is a linear dimension.

We are now able to supply an answer to the two problems. Thus if the wind structure near the surface be represented by an equation of the form

$$\bar{u} = \bar{u}_1 \left(\frac{z}{z_1} \right)^{\frac{n}{2-n}},$$

then the mean rate of evaporation under steady conditions varies as $\bar{u}_1^{\frac{2-n}{2+n}}$, and if L be a linear dimension of the evaporating surface, then the rate of evaporation from similar figures similarly orientated with respect to the direction of the mean wind varies as $L^{\frac{4+n}{2+n}}$.

Comparison with Experiments

5—(a) *The Effect of the Dimensions of the Evaporating Surface*—The only investigations which appear to have been made upon the effect of the dimensions of the evaporating surface upon the rate of evaporation are those of Gallenkamp,* and Thomas and Ferguson.† Gallenkamp, in his indoor experiments upon the rate of evaporation of water, arranged shallow rectangular and circular vessels upon a cross which was rotated in the stagnant air of a laboratory, so that the linear velocity of the air past the dishes was between $\frac{1}{2}$ m/sec and 1 m/sec. It is fairly certain that at such slow speeds the motion of the air relative to the dishes is almost non-turbulent, so that the diffusion of vapour is entirely by molecular processes and the interchange coefficient becomes the (constant) coefficient of molecular diffusion. The dishes used by Gallenkamp varied in their diameters from 2 cm to 8 cm. Jeffreys (*loc. cit.*) concludes that for indoor experiments the problem of evaporation may be treated as two-dimensional provided that the radii of the areas lie between 1 cm and 25 metres, so that we are justified in applying our results to Gallenkamp's experiments.

In our equations, the solution for $A = \text{constant}$ has the same form as that obtained by putting $n = 1$ in the results. Thus the theory gives for evaporation due to the molecular diffusion of vapour from rectangular areas

$$E = K\bar{u}_1^{\frac{1}{2}} a^{\frac{1}{2}} x_0^{\frac{1}{2}} y_0.$$

Gallenkamp found the relation

$$E \propto x_0^{0.6} y_0$$

in good agreement with the theoretical result. For circular dishes the result obtained was

$$E \propto r^{1.6},$$

where r is the radius of the dish. The theory gives

$$E \propto r^{1.67},$$

also in good agreement.

The experiments of Thomas and Ferguson, which are mainly concerned with the "rim" effect (*i.e.*, the variation of the rate of evaporation with the depth of the surface below the rim of the vessel), may also be shown to be in fair agreement with the present theory, by making use of methods due to Jeffreys (*loc. cit.*, p. 275).

* 'Met. Z.', vol. 36 (1919).

† 'Phil. Mag.' vol. 34, p. 308 (1917).

The above are controlled laboratory experiments, and the present writer has been unable to find records of any experiments upon evaporation in the open with simultaneous records of wind gradient. Certain wind tunnel experiments, giving the rates of evaporation in turbulent air are available, and these will be dealt with next.

(b) *The Effect of Wind Velocity*—The problem of evaporation into turbulent air under controlled conditions has been studied by Himus* and Hine† who have made measurements on the loss of weight from dishes containing various liquids placed in wind tunnels, using velocities well above the critical.

In a turbulent medium, in the absence of thermal influences, the variation of the mean velocity with height above a fixed surface, for a wide range of Reynolds' number, is given by

$$\bar{u} = \bar{u}_1 \left(\frac{z}{z_1} \right)^{\frac{1}{n}}$$

Comparing this with (13) we find $n = \frac{1}{4}$. Hence, if the above theory is correct we should find

$$E \propto \bar{u}_1^{\frac{1}{4}} = u_1^{0.78} \text{ approximately,}$$

where \bar{u}_1 is the velocity at unit height. It is clearly immaterial, if we are considering a pipe of constant dimensions, if we replace \bar{u}_1 by \bar{u}_m , where \bar{u}_m is the mean velocity over the cross-section. Hence we should expect

$$E \propto \bar{u}_m^{0.78}.$$

Himus, as the result of a long series of carefully conducted experiments on water gives as his final result

$$E \propto \bar{u}_m^{0.77},$$

which is in excellent agreement with the theory.

As far as the writer can ascertain, the only results which have been published on the effect of wind velocity on the rate of evaporation of liquids other than water are those of Hine, who employed nitro-benzene, toluene, *m*-xylene, and chlorobenzene. Hine's results, expressed in mols per hour divided by the vapour pressure (which enables different liquids evaporating at different temperatures to be compared), have been grouped for like wind velocities and plotted logarithmically against the wind velocity in fig. 1. Despite a somewhat large scatter of points, there does not appear to be any pro-

* Inst. of Chemical Engineers, Conference on Vapour Absorption and Adsorption (1929).

† 'Phys. Rev.,' vol. 24 (1924).

nounced curvature, and so we conclude that the rate of evaporation is proportional to a power of the wind velocity. The line corresponding to

$$E \propto \bar{u}_m^{0.78}$$

has been drawn so as to take its optimum position, and it will be seen that there is fair agreement between theory and practice. For the sake of comparison, the line corresponding to $E \propto \bar{u}_m$ (a relation assumed by many writers, including Hine) has been drawn so as to pass through the main cluster of points. It is clear that this relationship is inferior to that proposed by the theory.

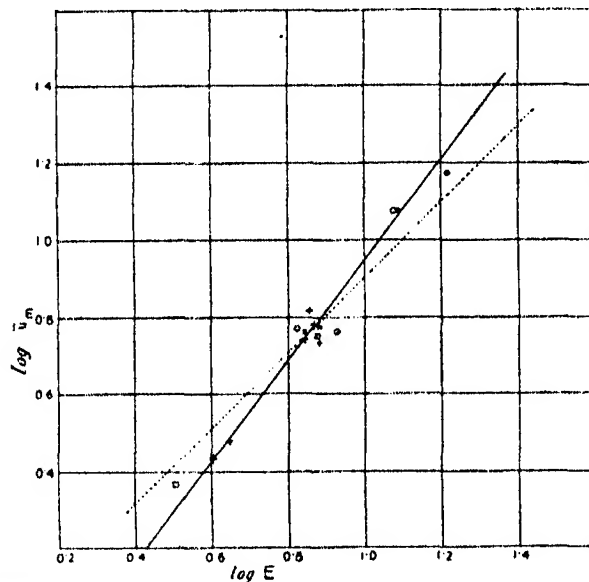


FIG. 1—The variation of the rate of evaporation with wind velocity. \odot nitrobenzene, $+$ toluene, \bullet *m*-xylene, \square chlorbenzene, — $E \propto \bar{u}_m^{0.78}$, --- $E \propto \bar{u}_m$.

Thus it appears that, despite a lack of confirmatory experiments, there is good reason for stating that the processes of evaporation, as regards wind velocity and size and shape of area, are connected with the wind shear in the manner set forth in the present theory. From this it appears that the transfer of momentum and the diffusion of matter in a turbulent atmosphere are governed by the same type of interchange coefficient, but the same conclusion does not seem to apply to the transfer of heat in the lower atmosphere. Researches on the thermal structure of the lower atmosphere by A. C. Best appear to point to the conclusion that the laws of eddy conduction of heat near the ground cannot be deduced in the above straightforward manner from

the shear of the wind. In other words, in our general equation (4) E may stand for momentum in a fixed azimuth or mass, but not for temperature. For a full discussion of this point, reference must be made to a forthcoming memoir by Best.

The writer wishes to acknowledge the valuable criticisms which he has received during the preparation of this paper from Mr. D. Brunt, M.A., Mr. E. Ll. Davies, M.Sc., and Mr. A. C. Best, B.Sc., of the Meteorological Office, and from Mr. W. G. L. Sutton, M.A., of the University College of Wales, Aberystwyth.

Summary

A theory of the transfer of momentum and mass in a turbulent medium is developed, which starts from the concept of an eddy as a mass of fluid which for some reason leaves its initial surroundings and moves as a discrete body continuously blending with the main mass of the fluid. The mixing path is defined as that distance through which an eddy moves relative to the main body of the fluid during the period necessary for the correlation between its initial and final relative velocities to become negligibly small. An empirical expression is suggested for the correlation coefficient and from this the law of variation of wind with height above the earth's surface is deduced. The theory is then extended to the problem of evaporation, on the assumption that the diffusion of mass follows the same laws as the diffusion of momentum, and expressions are found which are in good agreement with experimental data.

The Annihilation of Fast Positrons by Electrons in the K-Shell

By H. J. BHABHA and H. R. HULME, Gonville and Caius College, Cambridge

(Communicated by R. H. Fowler, F.R.S.—Received May 4, 1934)

The probability of the simultaneous annihilation of a positron and an electron, with the emission of two quanta of radiation, has been calculated by Dirac† and several other authors. From considerations of energy and momentum it follows that an electron and positron can only annihilate one another with the emission of one quantum of radiation in the presence of a third body. An electron bound in an atom could, therefore, annihilate a positron, represented by a hole on the Dirac theory, by jumping into a state of negative energy which happens to be free, the nucleus taking up the extra momentum. The process is now mathematically analogous to the photoelectric transitions to states of negative energy in the sense that the matrix elements concerned are the same, and we might expect that the effect would be most important for the electrons in the K-shell. Fermi and Uhlenbeck‡ have calculated the process approximately, for the condition where the kinetic energy of the positron is of the order of magnitude of the ionization energy of the K-shell. The result they obtained was very small compared with the two quantum process, which is to be explained by the fact that for these small energies, the positron does not get near the nucleus. In view of the fact that positrons of energies of the order $100mc^2$ occur in considerable quantities in the showers produced by cosmic radiation, and that the primary cosmic radiation itself may consist, in part, of positrons, it becomes of interest to calculate the cross-section for the annihilation of positrons of high energy by electrons in the K-shell, and their absorption in matter, and also to compare this process with the two quantum process for high energies.

In the photoelectric effect for hard γ -rays, the electron leaves the atom in states of different angular momentum (described by the azimuthal quantum number l), and the terms which give the largest contribution are roughly those for which l is of the order of the energy of the γ -ray in terms of mc^2 . For high energies, therefore, a calculation by the method of Hulme,§ in which the last step is carried out numerically, is out of the question, and we must

† 'Proc. Cam. Phil. Soc.,' vol. 26, p. 361 (1930).

‡ 'Phys. Rev.,' vol. 44, p. 510 (1933).

§ 'Proc. Roy. Soc.,' A, vol. 133, p. 381 (1931).

find some approximate method of effecting a summation. We shall use an adaptation of Sauter's† method, in which we shall treat as small the product of the fine structure constant and the nuclear charge. This method may be expected to give a good approximation for small nuclear charge. Our method has the further restriction that it is valid only when the kinetic energy of the positron is *not small* compared with mc^2 .

As stated above, we have taken into account the interaction of the positron and the nucleus, and the electron and the nucleus. We neglect, however, the interaction between the positron and the electron. There is, at the moment, no adequate theory of this interaction. We further assume for the K-shell electrons, the wave functions of a hydrogen-like atom in the ground state.

In § 1 we give the general theory of the annihilation. It will there be shown that if we require only the total annihilation, and do not consider the direction of the emitted γ -ray, then it is proportional to the total photoelectric effect from the K-shell to states of negative energy, assuming all these to be unoccupied. In § 2 we proceed to work out this stimulated photoelectric effect, and in § 3 we discuss the results.

§ 1. *General Theory of the Annihilation*

The actual problem we are considering is the probability of the spontaneous transition of an electron from the K-shell to a state of negative energy, which, of course, can only happen if the state of negative energy is unoccupied. We therefore consider the atom in the presence of a beam of positrons. In the absence of the atom, the beam of positrons is represented by a plane wave, but in the presence of an atomic nucleus this is slightly perturbed, and we must express the beam, not as a plane wave, but as a superposition of a number of states with wave functions $\psi(E, l, m)$. Here, $\psi(E, l, m)$ is the wave function of an electron of energy E , with azimuthal quantum number l , and magnetic quantum number m , in the presence of a nucleus. A pure plane wave, associated with an energy E , cannot be expressed in terms of the wave functions $\psi(E, l, m)$, since these are of the form $\exp(i\kappa r - n \log 2\kappa r)$ for large values of r , but we can make our wave function, obtained by superposition, approximate as closely as we like to that of a plane wave, by taking r large enough; that is, when the perturbation due to the presence of the nucleus is sufficiently small. It would be possible to express the plane wave in terms of $\psi(E, l, m)$ if we

† 'Ann. Physik,' vol. 9, p. 217 (1931); referred to as A; vol. 11, p. 454 (1931), referred to as B.

had the complete energy range at our disposal, but we do not wish to do this, as each positron is to be regarded as an unoccupied state $\psi(E, l, m)$, the whole approximating to a plane wave at great distances only. The states $\psi(E, l, m)$ occurring in the beam may now be considered as unoccupied, and the required transition probability may be calculated.

For an atom in the ground state, with two electrons in the K-shell, this transition probability is independent of the direction of the beam of positrons. We may, therefore, average over all directions of the beam, or, what is equivalent, we may consider the atom in an atmosphere of positrons, so that the probability of collision of any particular positron with quantum numbers l, m is the same; that is, the probability of any particular state $\psi(E, l, m)$ being free is independent of l and m . This may be justified by actual expansion of the plane wave in terms of $\psi(E, l, m)$, and subsequent averaging over all directions of the wave.

A considerable simplification is thus introduced, as we may now calculate the transition probability as if all the states of negative energy were free, and then multiply by the factor giving the ratio of the actual number of collisions (of positrons) to the number occurring if all the states of negative energy were free.

Let us now consider the calculation of this ratio, which we shall call θ . Suppose we have a beam of positrons such that one crosses unit area normal to the path per second, per unit energy range. As stated, we may consider the beam averaged over all directions, and then we have the number in any element of solid angle, $d\omega$, crossing unit area normal to the path, per second, per unit energy range as $d\omega/4\pi$. The wave function of such a stream, confined to a small element of solid angle, $d\omega$ around the x -axis, and containing positrons of energies lying in the range E to $E + dE$, is

$$Ae^{2\pi i p x/\hbar},$$

where p is the momentum of a positron, A is a matrix of one row and four columns if we use the Dirac wave functions, and

$$AA^* = \frac{d\omega dE}{4\pi v},$$

v being the velocity of the positrons.

If all the states of negative energy are unoccupied, then in each element of phase space of volume $dx dy dz dp_x dp_y dp_z$ there are

$$(2/\hbar^3) dx dy dz dp_x dp_y dp_z$$

possible states for the electron. On transforming to polar co-ordinates this becomes

$$(2/h^3) p^2 dp d\omega dx dy dz.$$

The wave function of the part of these states which are confined to a small element $d\omega$ along the x -axis and to the momentum range p to $p + dp$ is therefore

$$Be^{2\pi i p x/h},$$

where

$$BB^* = (2/h^3) p^2 dp d\omega.$$

The ratio θ is given by

$$\begin{aligned} \theta &= AA^*/BB^* \\ &= \frac{h^3}{8\pi p^2}, \end{aligned} \quad (1)$$

since $dE = v dp$.

Suppose now that the atom is in a beam of γ -rays confined to a small solid angle $d\omega$, such that the total energy which crosses unit area normal to the direction of propagation is one erg per unit energy range per second. Let P_{st} be the probability of an electron being stimulated by this beam to make a transition from the K-shell to a state of negative energy, assuming all these to be unoccupied. We are interested in the corresponding spontaneous transition, and the factor giving the ratio of the number of spontaneous transitions to the number induced by this particular beam, both taken per unit energy range, is easily found to be $4\pi v^3/c^2$, so that the number of spontaneous transitions is $(4\pi v^3/c^2)P_{st}$, when all the negative energy states are unoccupied.

Hence

$$\begin{aligned} N &= \theta \frac{4\pi v^3}{c^2} P_{st} \\ &= \frac{h^3 v^3}{2p^2 c^2} P_{st}, \end{aligned} \quad (2)$$

where N is the number of positrons absorbed per unit energy range from a beam of positrons such that one positron crosses unit area normal to the path per unit energy range per second.

§ 2. Calculation of the Stimulated Annihilation

Let a beam of γ -rays of unit intensity be travelling along the z -axis, and be represented by the vector potential

$$\begin{aligned} A_y &= \sqrt{\left(\frac{2c}{\pi}\right) \frac{1}{v_0}} \cos 2\pi v_0 \left(t - \frac{z}{c}\right) \\ A_x &= A_z = 0 \end{aligned} \quad (3)$$

The transitions stimulated by this beam, of frequency ν_0 , will then be equal to the number of transitions stimulated over unit energy range by the beam of γ -rays considered in the previous section.

Following Sauter,[†] we write the equation of motion of the electron in the form

$$\left\{ \begin{aligned} & \left\{ \gamma_1 \frac{\partial}{\partial x} + \gamma_2 \frac{\partial}{\partial y} + \gamma_3 \frac{\partial}{\partial z} + \gamma_4 \left(\frac{1}{ic} \frac{\partial}{\partial t} - \frac{\alpha}{r} \right) + \lambda E_0 + i\gamma_2 \lambda e A_y \right\} \Psi = 0, \\ & \text{where} \\ & \gamma_1 = \begin{bmatrix} 0 & 0 & 0 & 1 \\ 0 & 0 & -1 & 0 \\ 0 & -1 & 0 & 0 \\ 1 & 0 & 0 & 0 \end{bmatrix}, \quad \gamma_2 = \begin{bmatrix} 0 & 0 & 0 & -i \\ 0 & 0 & -i & 0 \\ 0 & i & 0 & 0 \\ i & 0 & 0 & 0 \end{bmatrix}, \\ & \gamma_3 = \begin{bmatrix} 0 & 0 & -i & 0 \\ 0 & 0 & 0 & i \\ i & 0 & 0 & 0 \\ 0 & -i & 0 & 0 \end{bmatrix}, \quad \gamma_4 = \begin{bmatrix} 1 & 0 & 0 & 0 \\ 0 & 1 & 0 & 0 \\ 0 & 0 & -1 & 0 \\ 0 & 0 & 0 & -1 \end{bmatrix}, \\ & \text{and} \\ & \lambda = \frac{2\pi}{\hbar c}, \quad E_0 = mc^2, \quad \alpha = \frac{2\pi e^2 Z}{\hbar c} \sim \frac{Z}{137}. \end{aligned} \right\} \quad (4)$$

We get[‡] for Ψ , omitting the irrelevant part dealing with transitions to positive energies,

$$\Psi = \psi_0 e^{-2\pi i E_1 t / \hbar} + \psi^- e^{-2\pi i (E_1 - \hbar \nu_0) t / \hbar}$$

with

$$\psi^- = \frac{\lambda \pi e A}{\beta} \sum_{l, m} \psi_{as.} \int \bar{\psi} \gamma_2 \psi_0 e^{-2\pi i \nu_0 \cdot \mathbf{r} \cdot \mathbf{c} / c} d \text{ vol}, \quad (5)$$

where

$$A = (2c/\pi)^{\frac{1}{2}} \nu_0^{-1},$$

and $\psi_{as.}$ denotes the asymptotic part of the wave function of the unperturbed equation (4) containing $\exp(-i\kappa r)$. (For the definition of κ see equation (10).) This represents a diverging wave *when the energy is negative*, the part containing $\exp(i\kappa r)$ represents the converging wave in this case, and vanishes, as shown by Bethe.[§] Our symbols have here the same meaning as in Sauter's

[†] *Loc. cit.* A.

[‡] $\bar{\psi} = \psi^* \gamma_4$, that is, the matrix product of the conjugate complex of ψ and γ_4 .

[§] 'Ann. Physik,' vol. 4, p. 443 (1930).

papers. ψ_0 is the initial state of the electron with energy E_1 , $\bar{\psi} = \psi^* \gamma_4$, and

$$\beta = v/c = (1 - E_0^2/E^2)^{1/2},$$

where v is the velocity of the electron emitted.

For the initial state we have two normalized solutions given by

$$\psi_{01} = \begin{bmatrix} -iU_0 \\ 0 \\ V_0 \cos \theta \\ -iV_0 \sin \theta e^{i\phi} \end{bmatrix}, \quad \psi_{02} = \begin{bmatrix} 0 \\ U_0 \\ -V_0 \sin \theta e^{-i\phi} \\ -iV_0 \cos \theta \end{bmatrix}, \quad (6)$$

where

$$\left. \begin{aligned} U_0 &= \frac{N_0}{2} \sqrt{\left(\frac{1+j_0}{2}\right)} e^{-k_0 r} r^{j_0-1} \\ V_0 &= \frac{N_0}{2} \sqrt{\left(\frac{1-j_0}{2}\right)} e^{-k_0 r} r^{j_0-1} \end{aligned} \right\}, \quad (6A)$$

with

$$N_0^2 = \frac{(2k_0)^{2j_0+1}}{\Gamma(2j_0+1)}, \quad j_0 = (1 - \alpha^2)^{1/2}, \quad k_0 = \frac{2\pi}{hc} E_0 \alpha.$$

The solutions of the unperturbed equation (4), *i.e.*, without the last term, we write in the form

$$\psi_I = N_{\theta\phi} \begin{bmatrix} i(l-m) P_l^m e^{im\phi} U_I \\ P_l^{m+1} e^{i(m+1)\phi} U_I \\ -(l+m) P_{l-1}^m e^{im\phi} V_I \\ -iP_{l-1}^{m+1} e^{i(m+1)\phi} V_I \end{bmatrix}, \quad \psi_{II} = N_{\theta\phi} \begin{bmatrix} -i(l+m) P_{l-1}^m e^{im\phi} U_{II} \\ P_{l-1}^{m+1} e^{i(m+1)\phi} U_{II} \\ (l-m) P_l^m e^{im\phi} V_{II} \\ -iP_l^{m+1} e^{i(m+1)\phi} V_{II} \end{bmatrix}. \quad (7)$$

The normalizing factor $N_{\theta\phi}$ for the angular part is given by

$$N_{\theta\phi}^2 = \frac{1}{4\pi} \frac{(l-m-1)!}{(l+m)!}$$

and P_l^m is defined by the equation

$$P_l^m = \sin^m \theta \left(\frac{d}{d \cos \theta} \right)^{m+1} \frac{(\cos^2 \theta - 1)^l}{2^l l!}. \quad (8)$$

Following Gordon,[†] we write the normalized U , V , for the negative energy states in the form

$$\left. \begin{aligned} U &= \frac{i\kappa}{\sqrt{\pi}} \sqrt{\left(1 - \frac{E_0}{|E|}\right)} \frac{|\Gamma(n+j)|}{\Gamma(2j+1)} e^{\frac{i\pi n}{2}} e^{-i\kappa r} (2\kappa r)^{j-1} (X+Y) \\ V &= \frac{\kappa}{\sqrt{\pi}} \sqrt{\left(1 + \frac{E_0}{|E|}\right)} \frac{|\Gamma(n+j)|}{\Gamma(2j+1)} e^{\frac{i\pi n}{2}} e^{-i\kappa r} (2\kappa r)^{j-1} (X-Y) \end{aligned} \right\}, \quad (9)$$

[†] 'Z. Physik,' vol. 48, p. 11 (1928).

with

$$\kappa = \frac{2\pi}{\hbar c} (E^2 - E_0^2)^{\frac{1}{2}}, \quad n = -\frac{i\alpha E}{(E^2 - E_0^2)^{\frac{1}{2}}} \quad \text{and} \quad j = (l^2 - \alpha^2)^{\frac{1}{2}}, \quad (10)$$

where E is to be taken with its proper sign, and

$$\left. \begin{aligned} X &= (\mp l + nE_0/E) F(-n + j, 2j + 1; 2i\kappa r) \\ Y &= (j - n) F(-n + j + 1, 2j + 1; 2i\kappa r) \end{aligned} \right\}, \quad (9A)$$

the top sign being taken for the solutions (I) and the bottom sign for the solutions (II).

The asymptotic forms of U and V are given by

$$\begin{aligned} U_{as.} &= \frac{i(1 - E_0/|E|)^{\frac{1}{2}}}{2\sqrt{\pi}} |\Gamma(n + j)| \left\{ \frac{e^{-i\kappa r + n \log 2\kappa r + \frac{1}{2}i\pi j}}{r \cdot \Gamma(n + j)} \left(\frac{\mp l + nE_0/E}{j + n} \right) \right. \\ &\quad \left. + \frac{e^{i\kappa r - n \log 2\kappa r - \frac{1}{2}i\pi j}}{\Gamma(-n + j)} \right\}, \\ V_{as.} &= \frac{(1 + E_0/|E|)^{\frac{1}{2}}}{2\sqrt{\pi}} |\Gamma(n + j)| \left\{ \frac{e^{-i\kappa r + n \log 2\kappa r + \frac{1}{2}i\pi j}}{r \cdot \Gamma(n + j)} \left(\frac{\mp l + nE_0/E}{j + n} \right) \right. \\ &\quad \left. - \frac{e^{i\kappa r - n \log 2\kappa r - \frac{1}{2}i\pi j}}{\Gamma(-n + j)} \right\}. \end{aligned}$$

We notice that the first term in the curly bracket is not exactly the conjugate complex of the second, but has in addition the phase factor

$$\frac{\mp l + nE_0/E}{j + n} = \varepsilon \quad \text{say,}$$

of modulus unity. This is the cause of the increased complexity of our calculation over Sauter's. We require the part $\exp(-i\kappa r)$, which we shall write in the form

$$\left(\frac{U'_{as.}}{V'_{as.}} \right) \left(\frac{\mp l + nE_0/E}{j + n} \right), \quad (9B)$$

with

$$\begin{aligned} U'_{as.} &= \frac{i(1 - E_0/E)^{\frac{1}{2}}}{2\sqrt{\pi}} \frac{|\Gamma(n + j)|}{\Gamma(n + j)} e^{-i\kappa r + n \log 2\kappa r + \frac{1}{2}i\pi j} / r, \\ V'_{as.} &= \frac{(1 + E_0/E)^{\frac{1}{2}}}{2\sqrt{\pi}} \frac{|\Gamma(n + j)|}{\Gamma(n + j)} e^{-i\kappa r + n \log 2\kappa r + \frac{1}{2}i\pi j} / r. \end{aligned}$$

Our calculation now follows Sauter's† more or less closely, except that for the important difference mentioned above, that we have $\exp(-2\pi i v_0 z/c)$ and $\exp(-i\kappa r)$ in the expression (5).

† We should like to thank Dr. Sauter for a letter giving us some of the details of his calculations.

We now get for (5), carrying out the integration, according as our initial state is ψ_{01} or ψ_{02} , the expressions

$$\psi_{-1} = \begin{bmatrix} i(F_2 e^{-i\phi} + G_2 e^{i\phi}) \\ -(F_1 + G_1 e^{2i\phi}) \\ -(F_4 e^{-i\phi} + G_4 e^{i\phi}) \\ i(F_3 + G_3 e^{2i\phi}) \end{bmatrix}, \quad \psi_{-2} = \begin{bmatrix} i(F_1 + G_1 e^{-2i\phi}) \\ (F_2 e^{i\phi} + G_2 e^{-i\phi}) \\ -(F_3 + G_3 e^{-2i\phi}) \\ -i(F_4 e^{i\phi} + G_4 e^{-i\phi}) \end{bmatrix}, \quad (11)$$

where the F's and G's are given by

$$\left. \begin{aligned} F_1 &= \frac{\lambda e A}{4\beta} \sum_l U'_{as} \left\{ -\frac{l - nE_0/E}{j+n} l P_l A_1 + \frac{l + nE_0/E}{j+n} l P_{l-1} A_2 \right\} \\ F_2 &= \frac{\lambda e A}{4\beta} \sum_l U'_{as} \left\{ -\frac{l - nE_0/E}{j+n} P_l A_1 - \frac{l + nE_0/E}{j+n} P_{l-1} A_2 \right\} \\ F_3 &= \frac{\lambda e A}{4\beta} \sum_l V'_{as} \left\{ -\frac{l - nE_0/E}{j+n} l P_{l-1} A_1 + \frac{l + nE_0/E}{j+n} l P_l A_2 \right\} \\ F_4 &= \frac{\lambda e A}{4\beta} \sum_l V'_{as} \left\{ -\frac{l - nE_0/E}{j+n} P_{l-1} A_1 - \frac{l + nE_0/E}{j+n} P_l A_2 \right\} \\ G_1 &= \frac{\lambda e A}{4\beta} \sum_l U'_{as} \left\{ \frac{l - nE_0/E}{j+n} \frac{1}{l(l+1)} P_l^2 A_3 \right. \\ &\quad \left. + \frac{l + nE_0/E}{j+n} \frac{1}{l(l-1)} P_{l-1}^2 A_4 \right\} \\ G_2 &= \frac{\lambda e A}{4\beta} \sum_l U'_{as} \left\{ -\frac{l - nE_0/E}{j+n} \frac{l-1}{l(l+1)} P_l A_3 \right. \\ &\quad \left. + \frac{l + nE_0/E}{j+n} \frac{l+1}{l(l-1)} P_{l-1} A_4 \right\} \\ G_3 &= \frac{\lambda e A}{4\beta} \sum_l V'_{as} \left\{ \frac{l - nE_0/E}{j+n} \frac{1}{l(l+1)} P_{l-1}^2 A_3 \right. \\ &\quad \left. + \frac{l + nE_0/E}{j+n} \frac{1}{l(l-1)} P_l^2 A_4 \right\} \\ G_4 &= \frac{\lambda e A}{4\beta} \sum_l V'_{as} \left\{ -\frac{l - nE_0/E}{j+n} \frac{1}{l} P_{l-1} A_3 \right. \\ &\quad \left. + \frac{l + nE_0/E}{j+n} \frac{1}{l} P_l A_4 \right\} \end{aligned} \right\}, \quad (12)$$

with the A's given by

$$\left. \begin{aligned} A_1 &= 2\pi i \int (V_I^* U_0 P_{l-1} + U_I^* V_0 P_l \cos \theta) e^{-iqr \cos \theta} r^2 dr d \cos \theta \\ A_2 &= 2\pi i \int (V_{II}^* U_0 P_l + U_{II}^* V_0 P_{l-1} \cos \theta) e^{-iqr \cos \theta} r^2 dr d \cos \theta \\ A_3 &= 2\pi i \int (U_I^* V_0 P_l \sin \theta) e^{-iqr \cos \theta} r^2 dr d \cos \theta \\ A_4 &= 2\pi i \int (U_{II}^* V_0 P_{l-1} \sin \theta) e^{-iqr \cos \theta} r^2 dr d \cos \theta \end{aligned} \right\}, \quad (13)$$

writing

$$q = \frac{2\pi}{hc} h\nu_0 = \frac{2\pi}{hc} \{ |E| + E_0 (1 - \alpha^2)^{\frac{1}{2}} \}.$$

These expressions are similar to those obtained by Sauter (equations (35) and (34) of A), the only differences being the presence of the phase factors

$$\frac{\mp l + nE_0/E}{j + n} = \epsilon,$$

and the fact that we have $\exp(-iqr \cos \theta)$ in the A's, instead of $\exp(iqr \cos \theta)$. So far our calculation is exact, but it cannot be carried further without approximations. We approximate by writing l in place of $j = (l^2 - \alpha^2)^{\frac{1}{2}}$ in the expressions (6A), (9), (9A), and (12). We now make a second approximation, which is only valid in certain circumstances. We have

$$n = \frac{i\alpha |E|}{(E^2 - E_0^2)^{\frac{1}{2}}},$$

and tends to $i\alpha$ as $|E|$ tends to infinity. For $|E| = 2E_0$ it is equal to $2i\alpha/\sqrt{3}$, and is less for greater values of $|E|$. We, therefore, consider it a quantity of the order α , which imposes the restriction that our further calculation is not valid when $|E| \sim E_0$. It is valid for $|E| \geq 2E_0$; that is, when the kinetic energy, $|E| - E_0$, is not small compared with E_0 .

We expand the phase factors ϵ in ascending powers of n , i.e., virtually α , and approximate by taking the lowest power only, which is equivalent to putting the factors equal to ∓ 1 .

With this approximation we should expect our results to be valid only when $\alpha (= Z/137) \ll 1$; that is, for elements of small atomic number.

With this restriction, the quantities F , etc., can be evaluated as in Sauter's paper. We shall not reproduce the working, which is cumbersome but follows Sauter's closely, the only difference being due to the presence of the quantity $\exp(-iqr \cos \theta)$ mentioned above.

We have, finally, keeping only the lowest terms in α ,

$$\begin{aligned} F_1 &= Mi \left[\frac{1+\gamma}{\gamma} \sin \theta \right], \\ F_2 &= Mi \left[-\frac{1+\gamma}{\gamma} \cos \theta + \frac{(1-\gamma)(1+2\gamma)}{\gamma(1-\gamma^2)^{\frac{1}{2}}} \right], \\ F_3 &= M \left[\frac{1+2\gamma}{\gamma} \sin \theta \right], \\ F_4 &= M \left[\frac{1+2\gamma}{\gamma} \cos \theta - \frac{(1+\gamma)^2}{\gamma(1-\gamma^2)^{\frac{1}{2}}} \right], \\ G_1 &= 0, \\ G_2 &= Mi \left[-\frac{1-\gamma}{(1-\gamma^2)^{\frac{1}{2}}} \right], \\ G_3 &= M [-\sin \theta], \\ G_4 &= M [-\cos \theta], \end{aligned}$$

where

$$M = \frac{C \cdot f\alpha}{2\sqrt{2} q^2} \frac{\beta^2 \sin \theta}{(1 - \beta \cos \theta)^2},$$

$$C = \frac{\pi e A N_0}{2hc\sqrt{(2\pi)}} e^{i\pi n} \Gamma(-n+1),$$

writing γ for $E_0/|E| = (1 - \beta^2)^{\frac{1}{2}}$.

These expressions differ from the corresponding ones in Sauter's paper (equations (28) of B), in the fact that γ has the opposite sign; that is, in putting $-E$ for E . The reason for this is that both these expressions are the first terms of a series in ascending powers of α , and to this order the factors ϵ in (12) do not make a difference. Our next term would, however, differ from Sauter's. $\beta = c|p|/|E|$, has, of course, the same sign in both expressions.

The density is given by

$$\bar{\psi}\gamma_4\psi = H + 2K \cos 2\phi \pm 2L \sin 2\phi,$$

the upper sign to be taken for the initial state ψ_{01} and the lower for ψ_{02} , with

$$\left. \begin{aligned} H &= \sum_{\nu=-1}^4 (F_{\nu}^* F_{\nu} + G_{\nu}^* G_{\nu}) \\ K &= R \left\{ \sum_{\nu=-1}^4 G_{\nu}^* F_{\nu} \right\} \\ L &= I \left\{ \sum_{\nu=-1}^4 G_{\nu}^* F_{\nu} \right\} \end{aligned} \right\} \quad (15)$$

where R, I denote the real and imaginary parts. For large distances from the nucleus the current, which is radial, is given by

$$S_r = ec\beta\bar{\psi}\gamma_4\psi,$$

and on putting the expressions (14) in (15) we get for either initial state

$$S_r = \frac{2C^*C\alpha^2ce}{q^4} \beta^3 \frac{\sin^2 \theta}{r^2} \left[-\frac{\gamma \sin^2 \phi}{(1 - \beta \cos \theta)^4} + \frac{(1 + \gamma) \sin^2 \phi}{2\gamma(1 - \beta \cos \theta)^3} + \frac{(1 + \gamma)^2}{4\gamma^2(1 - \beta \cos \theta)^3} \right] \quad (16)$$

with

$$CC^* = \frac{8\pi^3 e^2 m^3 c^2 \alpha^3}{h^5 v_0^2},$$

to the approximation used.

On integrating over a large sphere we obtain, for the total number of electrons crossing a large sphere about the nucleus per unit time, stimulated by radiation of unit intensity, the expression

$$\frac{e^2 c^7 m^3 \alpha^5 \beta^3}{h^5 v_0^6 \gamma^3} \left[-\frac{4}{3} + \frac{1 + 2\gamma}{\gamma(1 - \gamma)} \left\{ 1 + \frac{\gamma^2}{2\beta} \log \frac{\gamma^2}{(1 + \beta)^3} \right\} \right]. \quad (17)$$

This again differs from Sauter's expression in having γ replaced by $-\gamma$.

We may expand the expression in square brackets of (17) as a series in ascending powers of β and get

$$\left[\frac{8}{3} + \frac{7}{15} \beta^2 + \frac{151}{420} \beta^4 \dots \right],$$

the expression being always positive.

§ 3. Results

Multiplying by $2xh^3v_0^3/2c^3p^2$ we get for the total number of annihilation processes with a beam of positrons of unit intensity falling on the atom,

i.e., the annihilation cross-section, due to *two* electrons in the K-shell, the expression

$$\frac{he^2}{m^2c^3} \alpha'^5 Z^5 \left[\frac{\beta\gamma^2}{(1+\gamma)^3} \left\{ -\frac{4}{3} + \frac{1+2\gamma}{\gamma(1-\gamma)} \left\{ 1 + \frac{\gamma^2}{2\beta} \log \frac{\gamma^2}{(1+\beta)^2} \right\} \right\} \right], \quad (18)$$

where we have written $\alpha = \alpha'Z$ for greater clarity.

This expression, expanded in ascending powers of β , gives

$$\frac{he^2}{m^2c^3} \alpha'^5 Z^5 \left\{ \frac{1}{3} \beta - \frac{1}{40} \beta^3 - \dots \right\}.$$

We should, however, emphasize that our expressions are only valid when the kinetic energy of the positrons is not small compared to their rest mass; that is, for $\beta \sim 0.8$ or greater.

In the limit of very large energies, $\gamma \rightarrow 0$, and we may neglect the second term in curly brackets of (18) compared to unity, and the first term in square brackets compared to the second, and we get for the total annihilation due to two K electrons

$$\begin{aligned} & \frac{e^2h}{m^2c^3} \alpha'^5 Z^5 \frac{mc^2}{|E|} \\ &= 6.8 \times 10^{-23} \alpha'^5 Z^5 \frac{mc^2}{|E|}. \end{aligned} \quad (19)$$

This formula does not differ from the more exact formula (18) by more than 2% for energies greater than $100mc^2$ and the deviation is less than 15% for energies greater than $10mc^2$.

We give a table of σ , the annihilation cross-section (18), for various energies and elements of interest in experiments on cosmic radiation.

Atomic number, Z	8 (O)	13 (Al)	26 (Fe)	82 (Pb)
σ for $\frac{ E }{E_0} = 2$	1.08×10^{-23}	1.23×10^{-23}	3.93×10^{-27}	1.23×10^{-24}
σ for $\frac{ E }{E_0} = 100$	4.59×10^{-31}	5.20×10^{-30}	1.65×10^{-28}	5.21×10^{-26}

The last column is only given as an indication, because here $Z/137$ can no longer be regarded as small compared with unity.

We may calculate the rate of destruction in lead, given by σnv , where $n = 3.3 \times 10^{22}$ is the number of atoms of lead per cc, and get 1.0×10^9 per second, which is in satisfactory agreement with the value of 10^9 given by Fermi and Uhlenbeck, for positrons of energy approximately $3mc^2$, although

their non-relativistic calculation is not valid in this region, not because Z is too large, as in our case, but because the velocity is too high. The agreement, however, serves to indicate that this value is probably of the right order of magnitude. Combining our results with those of Fermi and Uhlenbeck, we see that the annihilation cross-section is largest for an energy very roughly about $2mc^2$.

It has been suggested by Rossi† that in primary cosmic radiation, which seems to consist partly of positrons, these positrons may by annihilation give rise to secondary γ -rays of high energy. If this be correct, the cross-section for such an annihilation process in lead can be calculated from the observed absorption coefficient of the primary radiation, 0.006 cm^{-1} ,‡ and we get $\sigma = 1.8 \times 10^{-25} \text{ cm}^2$. These particles must have energies of at least $1000 mc^2$, and for such energies our theoretical cross-section (19) gives a value of $0.05 \times 10^{-25} \text{ cm}^2$, a cross-section which is too small, although our approximations are not valid for lead. We may further calculate the probability of a positron being annihilated in its passage through the atmosphere by this process, and get, for positrons of energy $1000 mc^2$, a probability of 1.2×10^{-7} . We must remember, however, that the Dirac equation cannot be expected to describe phenomena accurately for energies greater than about $137 mc^2$.

Lastly we compare our formula (18) with the formula of Dirac (*loc. cit.*) for the cross-section per atom for annihilation by the two quantum process,

$$\frac{\pi e^4 Z}{m^2 c^3 v} \frac{1}{\alpha(\alpha+1)} \left[\frac{\alpha^2 + 4\alpha + 1}{(\alpha^2 - 1)^3} \log \{ \alpha + (\alpha^2 - 1)^{1/2} \} - (\alpha + 3) \right].$$

Here α is the energy of the positron in units of mc^2 , and not, as above, $Z/137$. We see that for large energies this cross-section is proportional to

$$\frac{mc^2}{|E|} \log \left\{ \frac{|E|}{mc^2} \right\}.$$

whereas ours is proportional to $mc^2/|E|$, so that for increasing energies, the ratio of these two will increase. Further, this cross-section is proportional to Z whereas ours is proportional to Z^3 , so that the two quantum process will be relatively more important for the lighter elements. For energies $2mc^2$ and $100mc^2$ we get annihilation cross-sections per atom in oxygen of 1.88×10^{-24} and $0.90 \times 10^{-25} \text{ cm}^2$, and in lead of 1.93×10^{-23} and $0.92 \times 10^{-24} \text{ cm}^2$

† 'Nature,' vol. 132, p. 173 (1933).

‡ Bhabha, 'Z. Physik,' vol. 86, p. 120 (1933).

respectively, due to the two quantum process. We see, therefore, that even for lead, the two quantum process is roughly 20 times larger. For oxygen, the two quantum process is greater by a factor of order 10^5 .

This calculation was begun in Cambridge, and finished by one of us (H. J. B.) at the Institute of Physics in Rome, and he would like to thank Professor E. Fermi for the very pleasant and instructive time spent in the institute, and for suggestions in the writing of this paper.

Summary

The rate of annihilation of fast positrons by electrons in the K-shell is considered. The probability of a stimulated transition of an electron from the K-shell to a state of negative energy is calculated for the condition where all the states of negative energy are unoccupied. From this can be calculated the probability of the corresponding spontaneous transition when only certain of the negative energy states are unoccupied, namely, those represented by the beam of positrons.

The Dirac wave functions for an electron in the presence of a nucleus are used, but a closed formula can be obtained only if we treat $Z/137$ as small, Z being the atomic number, and further assume that $|E| \gtrsim 2mc^2$, where E is the energy of the positrons.

Results for various elements are given for $|E|/mc^2 = 2$, and 100, and it is found that for large values of $|E|$ the absorption is given by $\sigma = \text{const } Z^5/|E|$. The probability of annihilation is always very small compared with the probability of annihilation by free electrons, where two quanta are emitted.

The Kinetics of the Reaction between Hydrogen and Nitrous Oxide
Part II

By H. W. MELVILLE, Senior Student, Exhibition of 1851

(Communicated by J. Kendall, F.R.S.—Received May 8, 1934)

An analysis of the mechanism of the thermal hydrogen-nitrous oxide reaction in silica vessels by the kinetic method has shown that it is a chain process.* The experiments were confined to a comparatively narrow pressure range and the evidence for chain propagation, although quite definite, required confirmation. The present paper is therefore concerned with the kinetics under a much wider variety of conditions. First, the experiments have been extended to pressures below 30 mm; second, photochemical methods have been employed to shed more light on the individual steps of the reaction and to demonstrate unequivocally its chain character; third, in view of the close similarity of the hydrogen-nitrous oxide and hydrogen-oxygen reactions, a detailed study has been made of the effect of small amounts of oxygen on the former reaction. The results of these experiments all lend additional strong support to the chain hypothesis.

Small alterations to the apparatus were made. A glass spring gauge was employed for measuring low pressures. One end of the furnace was provided with a quartz lens in order to focus the light from the mercury lamp on the reaction bulb; the cathode of the lamp was water cooled. Arrangements were also made for inserting a hollow silica cell between the lamp and the lens so that filters could be used for controlling the intensity and wave-length of the light reaching the bulb. Direct photo dissociation of the nitrous oxide molecule was not attempted since (a) absorption of photochemically active light at low pressures in small bulbs is not complete, (b) the intensity of the lines of the mercury arc in the absorption region of nitrous oxide is weak. Recourse was therefore made to mercury sensitization in spite of a little additional complication.

Low Pressure Dark Reaction

Several questions arise when the reaction is carried out at somewhat lower pressures. The high pressure experiments indicated the importance of gas

* Melville, 'Proc. Roy. Soc.,' A, vol. 142, p. 524 (1933).

phase termination with but a small proportion of wall inhibition. At low pressures, it would be anticipated that the mechanism would involve wall processes to a much greater extent. In the thermal decomposition of nitrous oxide, it has been shown that the collisions leading to activation below 50 mm are different from those above this pressure, for example, the energy of activation increases from 50 to 58 k. cal. (Musgrave and Hinshelwood put the upper limit at 64 k. cal.) It was thus of importance to find if there was, in consequence, any fundamental alteration in the kinetics of the hydrogen-nitrous oxide reaction. Further, the chain length at high pressures increases with decreasing pressure and there is therefore a chance that the reaction might become explosive, if the pressure were reduced sufficiently, in the sense that an upper explosion limit had been passed.

The lower limit to the pressure range was fixed at about 2 mm. It was undesirable with this type of apparatus to go below this pressure, for several complicating factors intrude. The withdrawal of water vapour by the phosphorus pentoxide gives rise virtually to a small water vapour diffusion pump which would make the manometer readings unreliable. Similarly, the effect of thermal effusion would be difficult to calculate in the transition region where the mean free path of the molecules begins to become comparable with the dimensions of the connecting tubes.

The total order of the reaction was determined by finding the effect of pressure on (a) the initial rate (R), and (b) the time required (t_1) for the reaction to go half-way to completion. If there is concordance in these two methods, nitrogen cannot exert any appreciable influence on the course of the reaction. The data are given in Table I.

In fig. 1, $\log_{10} R$ and $\log_{10} t_1$ have been plotted against $\log_{10} p$, but the lines obtained are not quite straight; the slope tending to decrease at high pressures. For the $\log_{10} R$ - $\log_{10} p$ curve, the mean slope is 1.8 and hence the order of the reaction, as measured by the influence of p on R , is very nearly two. The slope of the $\log_{10} t_1$ - $\log_{10} p$ curve is -0.7 and again, therefore, the order is almost two. The decrease in the order at higher pressures is in accordance with the results in Part I, where the total order has fallen to unity.

The effect of nitrogen, and probably that of argon too, should thus be negligible in view of the correspondence in the values obtained for the orders. A few experiments are quoted in Table II, in which nitrogen or argon was present initially, and inspection of the values of Δp show these to be practically independent of the pressure of inert gas.

Table I

Temperature 750° C, 5 cm tube, 1 : 1 mixture

Initial pressure	27.0	18.38	12.98
Time	Δp	Δp	Δp
mins			
0	0.0	0.0	0.0
0.5	1.4	0.80	0.56
1.0	3.4	2.02	1.18
1.5	5.2	3.06	1.93
2	6.4	3.96	2.41
3	8.2	4.96	3.13
4	9.3	5.74	3.66
6	10.5	6.58	4.30
8	11.1	7.18	4.68
10	—	7.50	4.96

 p is in mm of mercury.

Initial pressure	6.52	3.20	1.60
Time	Δp	Δp	Δp
mins			
0	—	—	—
0.5	0.12	0.03	—
1	0.40	0.10	—
2	0.70	0.42	—
3	1.05	—	—
4	1.30	0.58	0.20
6	1.66	0.67	0.27
8	1.85	—	—
10	2.06	0.96	0.35

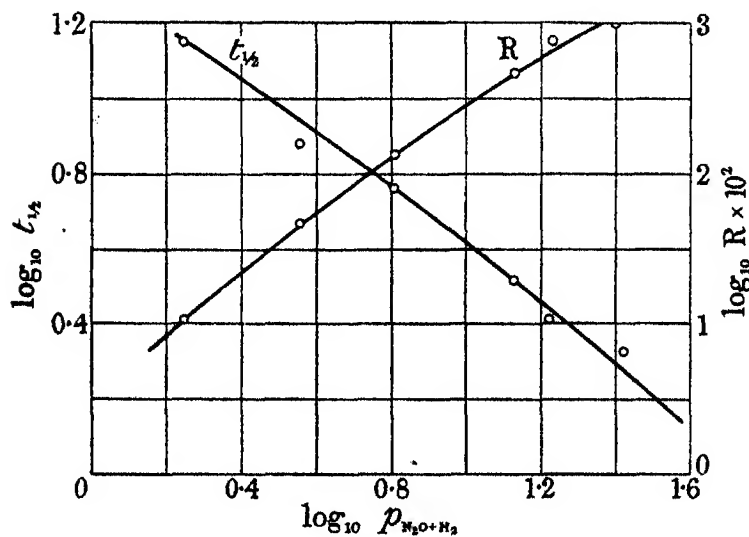


FIG. 1

Table II
750° C, 1 : 1 mixture

$p_{H_2 + N_2O}$	9.63	9.92	9.57	9.75	$p_{H_2 + N_2O}$	9.89	9.59	9.94
p_A	—	4.80	9.61	14.40	p_{N_2}	—	4.61	9.60
t	Δp	Δp	Δp	Δp		Δp	Δp	Δp
2	1.93	1.74	1.58	1.25		2.15	1.82	1.76
3	2.30	2.40	2.20	2.10		2.56	2.40	2.54
4	2.70	2.84	—	2.70		2.91	2.80	2.94
5	—	—	2.96	—		—	—	—
6	3.20	3.32	—	3.35		3.46	3.32	3.45
8	3.55	3.60	—	3.55		3.76	3.64	3.74

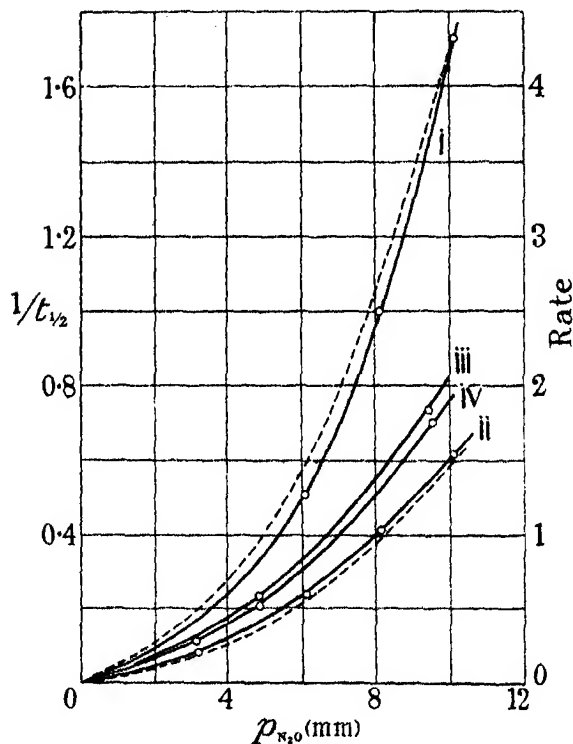


FIG. 2

Effect of H_2 and N_2O —Although the total order of the reaction has increased, the question arises whether the concentration of the nitrous oxide is still the most important factor controlling the rate. The results of a number of experiments are summarized in Table III, in which p_{H_2} and p_{N_2O} have been varied, and are plotted in figs. 2 and 3. Curves i and ii in fig. 2 respectively show R and $t_{1/2}^{-1}$ plotted against p_{N_2O} for experiments 281 to 284; curves iii and iv refer to experiments 362–364. The dotted lines are drawn assuming that the rate is proportional to the square of p_{N_2O} . These results demonstrate that the

Table III

Experiments 281-284, 725° C. Experiments 358-364, 750° C.

Experiment No.	p_{H_2}	p_{N_2O}	R	t_1	t_1^{-1}
282	2.02	3.23	0.20	9.0	0.111
283	1.98	6.07	0.60	1.95	0.51
281	2.02	8.11	1.04	1.00	1.00
358	4.77	4.91	0.64	4.10	0.244
359	9.61	4.81	0.79	3.36	0.297
360	16.22	4.93	0.96	2.86	0.35
361	24.40	4.95	0.96	2.86	0.35
362	4.83	4.85	0.58	5.0	0.20
363	4.80	9.58	1.85	1.42	0.70
364	4.86	15.10	2.50	1.00	1.00

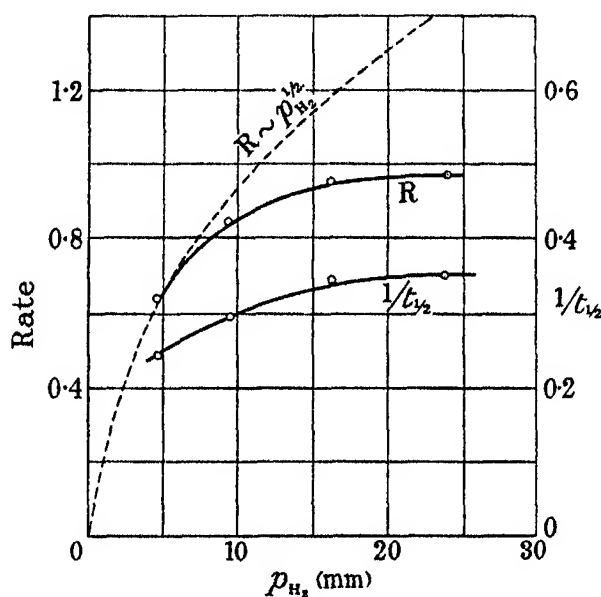


FIG. 3

order with respect to the nitrous oxide pressure is nearly two. Hydrogen has, however, very little effect as can be seen from fig. 3. For comparison a curve $R \sim p_{H_2}^{1/2}$ has been drawn to show that R varies even less than the square root of the hydrogen pressure. The increase in the total order is thus due entirely to the nitrous oxide.

Packing Experiments—The general change in the kinetics has also its counterpart in the effect of packing the reaction vessel. The procedure was exactly the same as that employed in experiments 243-247 in I, the same bulb and packing material being employed. Effectively the diameter is decreased from 2.5 to 0.7 cm. That wall inhibition has increased is fully borne out by the

results in Table IV, where the rate decreases six times compared with a two-fold decrease at 100 mm. If the chains were terminated solely on the walls, the decrease should be $(2.5/0.7)^2$ or 13 times. Even at 5 mm there must therefore be a small amount of gas phase termination.

Table IV
Temperature 768° C. 1 : 1 mixture

Empty		Packed		Empty	
Initial pressure	4.94		4.92		4.71
<i>t</i>	Δp	<i>t</i>	Δp	<i>t</i>	Δp
0	—	0	—	0	—
0.5	0.07	1	0.03	0.5	0.08
1	0.24	3	0.06	1	0.17
1.5	0.36	6	0.23	2	0.34
2	0.48	11	0.43	3	0.47
3	0.62	16	0.55	4	0.59
4	0.84			6.5	0.86
6	1.09			9	1.03
8	1.24				
R	0.24	0.034			0.17 mm/min

Temperature Coefficient—Likewise there is a change in the temperature coefficient of the reaction. The apparent energy of activation (*E*) rises from 30.5 k. cal. at 200 mm to 43.4 at 13 mm, as is shown by the data in Table V.

Table V
1 : 1 mixture. Initial pressure 13.20 mm

Temperature ° C	R	<i>t</i> ₁
655	0.120	—
683	0.250	6.50
718	0.67	2.52
749	1.33	1.28
778	2.45	0.70
799	3.05	0.62

E, 43.4 k. cal. *t*₁ time for 25% reaction.

These calculations of *E* are not quite exact, for constant pressures instead of concentrations were used. The corrected values are, however, easily obtained for the kinetics of the reactions are known; at high pressure *E* is 36.5 k. cal. and at low, *E* is 49.5 k. cal.

Explosions—As with the high pressure reaction, explosions could be obtained if the temperature was raised sufficiently. There were no signs of any sharp limiting pressures, either upper or lower.

Mechanism of the Reaction

In further elaborating the scheme of reactions put forward in I, the following observations have to be accounted for, the increase in the total order, in

packing effect and in the apparent energy of activation. It will be supposed that the mechanism of initiation and propagation remain unaltered, but the strong inhibition by walls shows definitely that most of the chains are terminated there. To simplify the equations, gas phase termination will be neglected. The equations expressing the stationary concentrations of H and of OH will therefore be :

$$\frac{d[H]}{dt} = I + k_6[OH][H_2] - k_4[H][N_2O] - k_9[H] = 0, \quad (1)$$

$$\frac{d[OH]}{dt} = I + k_4[H][N_2O] - k_5[OH][H_2] - k'_9[OH] = 0, \quad (2)$$

the notation being the same as in I. k_9 and k'_9 represent the rate of diffusion of H atoms and of OH radicals to the walls. If it be further assumed that $k_5[H_2] \gg k'_9$, then the last term of (2) may be neglected, so that solution of these equations yields

$$-\frac{d[N_2O]}{dt} = \frac{2k_4}{k_9}[N_2O]^2\{k_1[N_2O] + k_2[H_2]\}, \quad (3)$$

if, as before, the chains are long. Reinstatement of the last term in (2) leads to an apparently considerable amount of additional complication. In this circumstance,

$$[H] = \frac{2I - k'_9[OH]}{k_9} \quad \text{and} \quad [OH] = \frac{2I/k_9 + I}{k_5[H_2] + k_9 + k'_9k_4[N_2O]/k_9},$$

whence

$$-\frac{d[N_2O]}{dt} = \frac{k_5[H_2]\{2k_4[N_2O]/k_9 + 1\}[N_2O]\{k_1[N_2O] + k_2[H_2]\}}{k_5[H_2] + k_9 + k'_9k_4[N_2O]/k_9}. \quad (4)$$

An examination of (4) will show that if $k'_9 = 0$, this equation reduces to (3). First of all, (4) can be much simplified on account of a previous valid assumption, namely, that the chains are long, i.e., k_9 can be neglected compared with $k_4[N_2O]$ and $k_5[H]$. k'_9/k_9 can be approximately calculated from the diffusion theory, and for a 1 : 1 mixture is equal to 0.25. (4) reduces to

$$\frac{d[N_2O]}{dt} = \frac{2k_5[H_2]k_4[N_2O]^2\{k_1[N_2O] + k_2[H_2]\}}{k_9\{k_4[N_2O]/4 + k_5[H_2]\}}. \quad (5)$$

At high pressures, the theoretical equation agreeing best with the results was based on the assumption that $k_5 \gg k_4$. In (5), this inequality is still further increased by taking into account the different rates of diffusion of H and OH. On making this further simplification, (5) reduces to (3). Again it may be

pointed out that the experimentally observed order is rather less than the theoretical value. At low pressures, k_0 should be inversely proportional to the total pressure which would accentuate the difference between theory and experiment. The absence of acceleration of the reaction by argon and nitrogen, however, indicates that there may be sufficient gas phase termination to render k_0 effectively constant in the pressure range employed. (5) also shows that the increase in order is due to N_2O , which is in agreement with experiment. It is surprising to find that p_{H_2} does not affect R as much as (5) would allow. This might be due to a surface effect, in that adsorption of hydrogen on the wall may increase with pressure causing a concomitant increase in the efficiency of chain-breaking collisions.

The temperature coefficient of a chain reaction may be interpreted most simply by considering the reaction to consist of three separate parts: initiation (I), propagation (P), termination (T), each having its own temperature coefficient. At high and at low pressures, the kinetic equations may be generalized as follows:—

$$R = \frac{P \cdot I'}{T'} \exp \{(E_T - E_P - E_{I'})/RT\} = \frac{P \cdot I'}{T'} \exp (-E'_R/RT),$$

(low pressure)

$$R = P \cdot (I''/T'')^{\frac{1}{2}} \exp \{(E_{T''/2} - E_{I''/2} - E_P)/RT\} = P \cdot (I''/T'')^{\frac{1}{2}} \exp (-E''_R/RT),$$

(high pressure)

where T' and T'' refer to the low and high pressure reactions and E'_R and E''_R to the apparent energies of activation. Termination at high pressures is mainly due to ternary collisions, a reaction which, so far as is known, has practically no energy of activation, $E_{T''} = 0$ and since $-E''_R = E_{T''/2} - E_{I''/2} - E_P$, $E_P = 7.5$ k. cal., assuming $E_{I''} = 58$ k. cal. E_P represents the energy of activation of the reaction $H + N_2O = OH + N_2$. This value is perhaps somewhat low if the following calculation is made. It will be shown later that, at 10 mm and $700^\circ C$, the chain length is of the order 10^2 . A hydrogen atom, under these conditions, if generated in the middle of the bulb, would make about 10^6 collisions before reaching the wall. If it is further assumed that on every collision with the wall, the atom is adsorbed and rendered incapable of further chain propagation, then it must make $10^6/2 \times 10^2$ or 5×10^3 collisions with N_2O before reaction occurs. This corresponds to a value of E_P of 17 k. cal., and is of course a minimum, for if the collisions with the walls are partly elastic, E_P will be correspondingly increased.

Substituting $E_T = 7.5$ k. cal. in (6) and putting $E_T = 50$ k. cal. $E_{T'} = 8$ k. cal. It may be remarked that $E_{T'}$ agrees moderately well with the values for the wall termination process in the H_2-O_2 reaction obtained by Grant and Hinshelwood* for silica surfaces (12.8 k. cal.), and by Frost and Alyea† for a KC coated Pyrex surface (13.5 k. cal.), which are also based on the assumption that termination in a ternary collision requires no activation.

Whatever may be the true significance of $E_{T'}$, there is no doubt about its sign, which shows that the efficiency of wall removal of the carriers increases with the temperature. A similar behaviour might be expected in analogous reactions, for example, the combination of organic radicals. In practice, however, methyl and ethyl radicals are *less* easily destroyed as the temperature of the surface is raised,‡ that is, the sign of E_T is different. It must be pointed out that in the latter experiments, the results were obtained directly, whereas in the H_2-N_2O and H_2-O_2 reactions, $E_{T'}$ is calculated indirectly on assumptions which may not be exact.

As at high pressures, the rate of the H_2-N_2O reaction is considerably faster than the decomposition of N_2O . For example, at 650° , the rate of water formation was 1.21 mm per minute at 22.52 mm (1:1 mixture). In the same 5 cm tube, N_2O decomposed at 0.14 mm per minute at 740° , the initial pressure being 12.58 mm. At 650° and 11 mm, the rate would be 0.017. The ratio is 95 and will not alter much with pressure since the orders of the two reactions are equal. Similarly, temperature will have little effect on the ratio.

Effect of NO_2 —The primary object of studying the effect of this molecule was to determine whether it might induce the explosive combination of H_2 and N_2O at temperatures where the normal rate is small. No such phenomenon was observed, although the NO_2 slightly accelerated the rate. Another point of dissimilarity thus exists between the present reaction and those chain oxidations in which the addition of NO_2 leads to explosive combination at lower temperatures.§

Photochemical Experiments

A number of problems have arisen in the discussion of the low and high pressure reactions which may be solved by employing photochemical methods.

* 'Proc. Roy. Soc.,' A, vol. 141, p. 29 (1933).

† 'J. Amer. Chem. Soc.,' vol. 55, p. 3227 (1933).

‡ 'Trans. Faraday Soc.,' vol. 30, p. 186 (1934).

§ H_2-O_2 , Gibson and Hinshelwood, 'Trans. Faraday Soc.,' vol. 24, p. 559 (1928); Thompson and Hinshelwood, 'Proc. Roy. Soc.,' A, vol. 124, p. 219 (1929); Norrish and Griffiths, *ibid.*, vol. 139, p. 147 (1933). $CO-O_2$, Semenov and others, 'Z. phys. Chem.,' B, vol. 6, p. 307 (1930).

By this means, the initiation of chains can be independently controlled so that the propagation and termination factors may be observed operating together. The first important point was to demonstrate that a photochemically produced hydrogen atom could induce the reaction of several molecules of N_2O , and thus show without doubt that the reaction is of the chain type. Further, it was also necessary to find if the chain length calculated from the thermal experiments agreed with that obtained photochemically, in order to support the hypothesis about initiation by oxygen atoms. Experiments on the effect of intensity of the radiation should provide confirmation of the mechanism of the termination of the chains. Having obtained this information, the next problem to be elucidated is the form of the propagation factor and how it is influenced by H_2 , N_2O and by temperature.

It will be shown later that small amounts of oxygen exert a very marked accelerating influence on the H_2 - N_2O reaction, and the question arises whether this effect is due to a change in the initiation or the propagation factor; both may be affected.

In obtaining the photochemical chain length, the measurements were made from room temperature up to temperatures where the thermal becomes comparable with the photochemical reaction. The pressures were so chosen that a constant concentration of gas was present in the reaction vessel; the data are given in Table VI. For comparison, a run with a 1:1 H_2 - O_2 mixture at room temperature was carried out.

The results in Table VI are further tabulated in Table VII. The net photochemical rate in Table VII is the observed rate of reaction with the light on minus the rate of the thermal reaction. It will be observed that in experiments 757 and 759, the rates of the H_2 - N_2O and H_2 - O_2 reaction are nearly the same. In Table VII, it has been assumed for the purposes of calculation that the quantum yield of the former reaction at 25° C is unity. It may be greater than this, but would certainly not exceed two. The photochemical chain length is then simply calculated by finding the ratio of the rates at the higher temperature and at 25° C. The assumption made is that the quenching of the mercury resonance radiation is not appreciably influenced by temperature; this is supported, at any rate for hydrogen, by the measurements of Cario and Franck.*

The photochemical chain length at 650°, (116) is somewhat greater than the ratio of the rates of the H_2 - N_2O reaction, and the decomposition of N_2O . The

* 'Z. Physik,' vol. 37, p. 619 (1926).

Table VI

1 : 1 mixture. 5 cm tube

757 25° C		759 23° C		766 294° C		767 400° C	
<i>t</i>	<i>p</i>	<i>t</i>	<i>p</i>	<i>t</i>	<i>p</i>	<i>t</i>	<i>p</i>
0	9.65	0	0.56	0	15.15	0	16.67
5	9.59	10	9.39	2	15.03	2	16.27
10	9.49	21	9.21	5	14.72	4	15.78
20	9.36	30	9.08	10.5	14.34	6	15.35
30	9.20	40	8.95	15	13.98	8	14.98
40	9.09	52	8.87	21	13.55	10	14.55
50	8.90	(H ₂ -O ₂)		25	13.22	15	13.75
R	0.015	0.017		0.082		0.234	

* 768 502° C		763 558° C		765 603° C		764 603° C (thermal)	
<i>t</i>	<i>p</i>	<i>t</i>	<i>p</i>	<i>t</i>	<i>p</i>	<i>t</i>	<i>p</i>
0	18.67	0	19.13	0	19.13	0	20.18
1	17.94	0.5	18.37	0.5	18.05	1	19.88
2	17.06	1	17.60	1	16.75	2	19.59
3	16.32	1.5	16.70	1.5	15.68	4	19.22
4	15.68	2	16.00	2	14.83	6	18.88
6	14.33	3	14.70	2.5	14.07	8	18.55
8	13.41	4	13.50	3	13.42	10	18.27
10	12.47	6	12.00	4	12.50	12	17.94
		8	11.13	5	11.93		
R	0.76	1.70		2.60		0.265	

770 650° C (photo)		771 650° C (thermal)		773 740° C (thermal)		772 740° C Decom. of N ₂ O	
<i>t</i>	<i>p</i>	<i>t</i>	<i>p</i>	<i>t</i>	<i>p</i>	<i>t</i>	<i>p</i>
0	22.40	0	22.50	0	25.54	0	12.58
0.25	21.10	0.5	21.86	0.25	23.82	5	12.93
0.50	19.90	1	21.40	0.50	22.78	10.5	13.35
0.75	19.04	1.5	20.84	1	18.23	15	13.60
1	18.24	2	20.48	1.5	17.27	20	13.83
1.5	17.02	3	19.84	2	16.70	25	14.10
2	16.02	4	19.28	3	15.83	30	14.39
2.5	15.33	6	18.48				
3	14.72	8	17.60				
5	13.43						
R	5.25	1.21		8.9		0.140	

Table VII

Temp. ° C	Photo. rate	Thermal rate	Net photo. rate	Photo. chain length (ν)	$\log_{10} \nu$	$10^3/T$
25	1.55×10^{-3}	—	1.55×10^{-3}	1	0.00	3.36
294	5.43×10^{-3}	—	5.43×10^{-3}	3.5	0.544	2.203
400	1.40×10^{-2}	—	1.40×10^{-2}	9.0	0.954	2.141
502	4.07×10^{-2}	—	4.07×10^{-2}	26.2	1.418	1.764
558	8.90×10^{-2}	—	8.90×10^{-2}	57.3	1.76	1.485
603	1.36×10^{-1}	1.31×10^{-2}	1.23×10^{-1}	79.0	1.90	1.790
650	2.34×10^{-1}	5.4×10^{-2}	1.80×10^{-1}	116.0	2.06	1.154
740	—	3.5×10^{-1}	—	—	—	1.088

The rates of the reactions are expressed as R/p.

discrepancy is increased if, as has been assumed, one oxygen atom from the nitrous molecule initiates two chains, but the numbers are of the same order of magnitude. The conclusions which may therefore be drawn are (a) that chains can be propagated in $\text{H}_2\text{-N}_2\text{O}$ mixtures, (b) that nearly every oxygen atom derived from the thermal dissociation of an N_2O molecule leads to the initiation of two chains. In these calculations no account has been taken, in the thermal reaction, of the possibility of hydrogen molecules activating N_2O by collision; this would have the effect of decreasing the thermal chain length. It may be that when such a collision takes place, H_2O is formed immediately after, so the collision is unfruitful so far as chain starting is concerned. The close proximity of N_2 would facilitate the formation of H_2O by removing a considerable amount of the energy which would normally cause H_2O to dissociate.

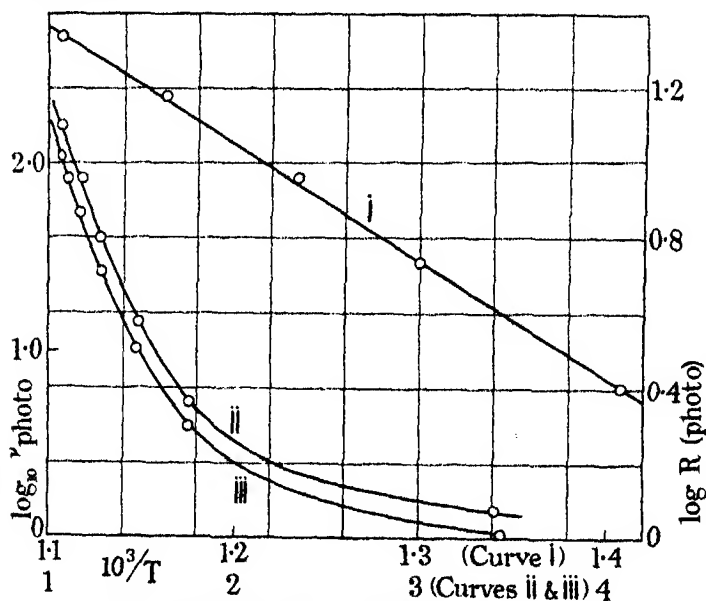


FIG. 4—Curve ii is displaced upwards for clarity.

It is also improbable that $v_{\text{ther.}} < v_{\text{photo.}}$, on account of the O atom reacting with N_2O to yield NO, since Harteck* found that reaction of O with H_2 is very much faster than with N_2O . Another anomaly is that $v_{\text{photo.}}$ increases with, but $v_{\text{ther.}}$ is independent of, temperature.

The results in Table VII and other data are illustrated in fig. 4 in which $\log v_{\text{photo.}}$ is plotted against $1/T$. The slope of the curve is not constant but

* 'Z. phys. Chem.,' B, vol. 12, p. 327 (1931).

increases from 25° to 400°, thereafter remaining constant. A similar variation in the slope of $\log R - 1/T$ curves is also obtained in the mercury photo-sensitized H_2-O_2 reaction, which Taylor and Salley* ascribe to branching. The curvature is, however, most pronounced at high temperatures. It is very doubtful whether such an explanation would hold in the present instance. What is more reasonable to suppose is that there is a change in the mechanism of the reaction as the temperature is raised from 25° to 400° C; for instance in deducing the kinetic equation, the assumption was made that the chains were long: Table VII shows this is no longer valid. Curve i in fig. 4 has been plotted with a larger $1/T$ scale in order to demonstrate more clearly that there is no curvature between 440° and 630° C; the energy of activation is 13.8 k. cal., which may be compared with zero for the thermal reaction. At high pressures on the other hand, the apparent energy of activation (36.5 k. cal.) is lower than that of the initiation process (58), and consequently the chain length must decrease with temperature. The origin of this phenomenon is due primarily to self-neutralization of the chains in the gas, as may be seen from the following equations,

$$R_{H,-N_2O} = P \left(\frac{I''}{T''} \right)^{\frac{1}{2}} \exp \{ (-E_P - E''_I/2 + E''_T/2)/RT \},$$

$$R_{N_2O} = I'' \exp (-E''_I/RT).$$

But

$$v_{ther.} = \frac{2R_{H,-N_2O}}{R_{N_2O}} = \frac{P}{(I''T'')^{\frac{1}{2}}} \exp \{ (-E_P + E''_I/2)/RT \},$$

since $E''_T = 0$.

In order that dv/dT be negative, $E''_I/2$ must be greater than E_P .

Effect of N_2O and of H_2 —In Table VIII, the effect of total pressure on the rate is given and in Table IX, the effect of hydrogen. The thermal reaction was negligible at 533° C. It will be observed that the initial rate of reaction increases with pressure, but the values of $T/2$ ($T/2$ time for 50% reaction) also increase with pressure and hence the order must lie between zero and unity. If the values of Δp in Table IX be compared for different hydrogen pressures, it will be seen that a five-fold variation has hardly any influence. Nitrous oxide must then be responsible for the increase in rate of Table VIII.

The initiation term in the kinetic equation will now be $\frac{[H_2]}{[H_2] + [N_2O]}$, assuming to a first approximation that (a) atomic hydrogen starts the reaction

* 'J. Amer. Chem. Soc.,' vol. 55, p. 96 (1933).

(b) N_2O merely deactivates Hg' , (c) the quenching radii of the two molecules is the same. Let $I = \frac{K [H_2]}{[H_2] + [N_2O]}$, K is a constant and is proportional to mercury vapour pressure and to the intensity of the light. On substituting this value of I in equations (1) and (2) and performing the simplifications in deriving (5),

$$-\frac{d[N_2O]}{dt} = \frac{k_4[N_2O]}{k_9} \cdot \frac{K[H_2]}{[H_2] + [N_2O]}$$

Table VIII

5 cm tube, 1 : 1 mixture, 533° C

t	$p_{H_2+N_2O}$	6.73	10.04	13.44	16.80	22.40
	Δp	Δp	Δp	Δp	Δp	Δp
0.5	0.33	0.33	0.38	0.48	0.50	0.90
1	0.58	0.69	0.66	0.82	1.46	1.65
2	1.00	1.14	1.28	2.58	3.40	2.80
4	1.61	1.97	2.18	4.04	4.86	3.90
6	1.99	2.54	2.90	5.78	6.00	4.80
8	2.28	2.96	3.64	7.08	8.4	5.78
10	2.50	3.34	4.11	8.4	9.7	7.08
15	2.82	3.96	4.90			
T/2 (min)	4.3	5.8	7.4			

Table IX

t	p_{N_2O}	4.81	4.80	4.77	4.86	4.77
	p_{H_2}	9.57	14.40	19.23	23.98	4.80
t	Δp	Δp	Δp	Δp	Δp	Δp
0.5	0.36	0.31	0.32	0.36	0.27	0.62
1	0.82	0.63	0.66	0.70	1.44	1.63
2	1.48	1.30	1.32	1.34	2.21	2.83
3	1.94	1.95	1.88	2.00	3.39	3.87
4	2.48	2.42	2.30	2.48		
6	—	3.17	3.10	3.14		
8	—	3.67	3.58	—		
10	—	—	—	—		

The small effect of hydrogen would seem to indicate that I is independent of $[H_2]$ and hence there is evidence of quenching by H_2 being more efficient than that by N_2O . I would then become equal to K . The important point is that, compared with the thermal reaction, the order with respect to $[N_2O]$ has fallen sufficiently to show that N_2O is not only responsible for initiation in the thermal reaction, but that the propagation factor is very nearly proportional, to $[N_2O]$. The general features of the thermal reaction are thus supported by photochemical data.

Effect of Argon—Argon does not deactivate Hg' very efficiently so that I should be unaffected by its presence; any effect would therefore be due to its influence on propagation or termination. None was found, using 10 mm of A

and 10 mm of a 1 : 1 mixture. Again, there is agreement between the photo and thermal data.

Effect of Intensity—It has been shown in deducing (6) that at low pressures, the rate of reaction should be proportional to the intensity. At high pressures, the equation for the photochemical reaction will be

$$-\frac{d[\text{N}_2\text{O}]}{dt} = k_4[\text{N}_2\text{O}] \left(\frac{K[\text{H}_2]}{[\text{H}_2] + [\text{N}_2\text{O}]} \cdot \frac{1}{k_8\{[\text{N}_2\text{O}] + [\text{H}_2]\}} \right)^{\frac{1}{2}},$$

and therefore the rate ought to be proportional to the square root of the intensity.

Preliminary experiments were carried out with a sector wheel containing two apertures, the angle of which could be varied. If the mean life of the chains is greater than the time between successive exposures, then, effectively, variation in this angle will alter the (mean) intensity of the light admitted to the reaction vessel.* If, however, the chains are of very short duration, alteration of the sector opening will merely change the time of exposure and thus will not provide the information on the intensity law which is being sought. In the latter circumstance, the data may show whether or no there is an induction period or a reaction after the light has been cut off.

The results of two experiments are illustrated in fig. 5, the upper curve referring to the low pressure reaction (16 mm of 1 : 1 mixture) at 570°, the lower curve was obtained at a pressure of 100·5 mm and 510° C. The wheel was rotated at about 120 r.p.m., *R* is the initial rate of reaction. The points at 180° show the value of the rate without the rotating sector. It will be observed, first of all, that the lines are straight and pass through the 180° points. This alone would indicate that there is no appreciable dark reaction after the light is cut off, for if there were, the 180° points would lie below the prolongation of the *R*- ϕ lines. These lines, however, do not pass through the origin and hence there would appear to be some dark reaction. In varying the time of illumination by altering the angle of the aperture, the interval between exposures is likewise changed, owing to the method of construction of the discs. That this time of darkness does not account for any significant part of the variation of *R* with ϕ is shown by the data in Table X. The rate of rotation of the sector was reduced so that the interval of darkness was increased from 0·12 to 5 seconds, but the values of Δp are nearly identical and hence the after-effect must be complete in less than 0·12 second.

* Cf. Griffith and McKeown, "Photo Processes," p. 664.

Table X

Sector angle 90°, pressure 16 mm, temperature 570° C, 1 : 1 mixture

Speed	<i>t</i>	0.5	0.75	1.0	1.5	2	2.5	3
3 r.p.m.	Δp	0.54	0.75	1.20	1.56	2.06	2.46	2.86
120 "	Δp	0.53	—	1.05	1.63	2.13	2.57	2.96

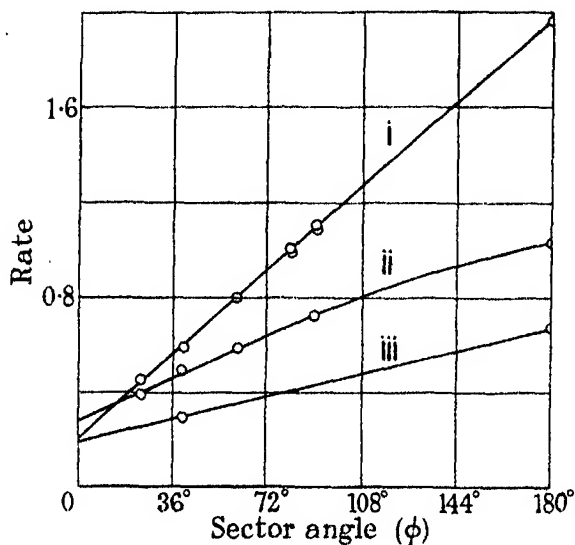


FIG. 5—(i) Low pressure, 570° C; (ii) high pressure, 510° C; (iii) high pressure, 470° C.

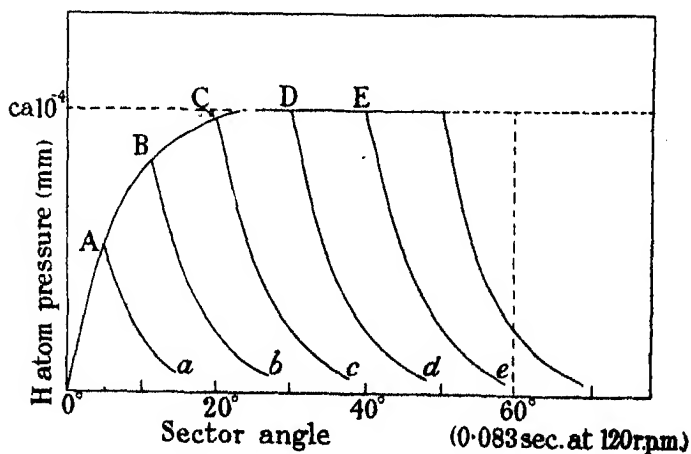


FIG. 6

The course of the reaction during the time of exposure and the interval before the next period of illumination occurs may be illustrated by fig. 6, which is only approximately drawn to scale, the H atom concentration being

plotted against the sector angle or time of illumination for a given velocity of rotation. The reaction velocity is assumed to be so small that the stationary concentration of atomic hydrogen does not alter appreciably owing to the decrease in $[H_2]$ and $[N_2O]$. When the light is first switched on at O, $[H]$ rises, attains a certain steady value and then falls at E when illumination ceases. The lines Aa, Bb, . . . , show how $[H]$ falls when the light is cut off at A, B, C, etc. The number of H_2O molecules formed in time t is proportional to $\int_0^t [H] dt$ and for a sector opening corresponding to E, will be proportional to the area OAEe. The rate of decrease of $[H]$ will depend on the method of termination of the chains. At low pressures, $-d[H]/dt = k_9[H]$, whereas at high pressures, $-d[H]/dt = k'_9[H]^2$.

Consider the low pressure reaction first, then the equation giving the value of $[H]$ at any time during illumination is

$$\frac{d[H]}{dt} = I - k_9[H],$$

or

$$[H] = I/k_9 (1 - e^{-k_9 t}).$$

During the ensuing dark period,

$$-\frac{d[H]}{dt} = k_9[H],$$

or

$$[H] = [H]_T e^{-k_9 t},$$

where $[H]_T$ is the value $[H]$ attains before the light is cut off after time T. The rate R is proportional to the number of H_2O molecules produced for a given time of experiment. If the proportionality factor be K then

$$R = K \int_0^T [H]_L dt + K \int_0^{T_0-T} [H]_D dt,$$

where L and D refer to the reaction in the light and in the dark. T_0 is the time required for the disc to rotate 180° . Substituting from the above equations

$$R/K = I/k_9 \int_0^T (1 - e^{-k_9 t}) dt + \int_0^{T_0-T} I/k_9 (1 - e^{-k_9 T}) e^{-k_9 t} dt,$$

or

$$R/K = \frac{I}{k_9} T - \frac{I}{k_9^2} (1 - e^{-k_9 T}) e^{-k_9 (T_0-T)}.$$

When $k'_6{}^{-1}$ is small compared with T , the second term may be neglected, and therefore

$$R/K = I \cdot T/k_6.$$

The R - ϕ curves should be straight and pass through the origin. It will also be observed from the above equation that if $T = 0$, then $R = 0$.

The results at high pressures may be treated in a similar way. During illumination

$$1/k'_6 \cdot \frac{d[H]}{dt} = I/k'_6 - [H]^2,$$

or

$$[H] = (I/k'_6)^{1/2} \tanh \sqrt{Ik'_6} t,$$

where $k'_6 [H]^2$ is the rate at which H atoms are removed in ternary collisions. In the dark

$$-\frac{d[H]}{dt} = k'_6 [H]^2$$

or

$$[H] = \{k'_6 t + 1/[H]_T\}^{-1/2},$$

whence

$$\begin{aligned} R/K &= \int_0^T [H]_L dt + \int_0^{T_0-T} [H]_D dt \\ &= \int_0^T (I/k'_6)^{1/2} \tanh \sqrt{Ik'_6} dt + \int_0^{T_0-T} \{k'_6 t + 1/[H]_T\}^{-1/2} dt \\ &= 1/k'_6 \cdot \log \cosh \sqrt{Ik'_6} T + 1/k'_6 \log \left\{ \frac{T_0 - T + 1/k'_6 I \cdot \coth \sqrt{Ik'_6} T}{1/k'_6 I \cdot \coth \sqrt{Ik'_6} T} \right\}. \end{aligned}$$

If $T = 0$, $R/K = 0$. When T is large so that $e^{(Ik'_6)^{1/2}T} > e^{-(Ik'_6)^{1/2}T}$, then

$$R/K = 1/k'_6 \left\{ (Ik'_6)^{1/2} T + \log \frac{(Ik'_6)^{1/2} T + 1}{2} \right\}.$$

When $(Ik'_6)^{1/2} T > 1$, the second term in the above equation will be relatively unimportant compared with the first and again therefore, a straight line passing through the origin is to be expected, the slope of which should be proportional to the square root of the intensity of the light from the lamp. The cause of the positive intercept on the rate axis is not revealed by this analysis. In the course of the photochemical experiments, it was observed that after the light was cut off, the reaction still continued but at a much reduced speed. It was somewhat difficult to obtain accurate measurements, but the effect lasted some 30 seconds, and hence would not be revealed by the variation in section speed employed in Table X. Moreover, the dark reaction could not be due to the

gradual decrease in the concentration of hydrogen atoms for these diffuse to the wall in a time very much less than 30 seconds (*cf.* p. 744). It may happen that although the H atoms are removed by the walls very rapidly, they do not immediately recombine and so may be capable of starting new chains from the surface long after the light has been cut off. Virtually, then, a dark reaction is superposed on the photo reaction, but its existence depends primarily on the previous illumination of the gas. The magnitude of the rate is not, however, sufficiently great to cause the $R-\phi$ curves (at high pressure) to follow the relation $R \sim \phi^{\frac{1}{2}}$. Since the 180° point lies on the same line as the other points, the dark reaction will become of greater importance as the sector angle decreases; the relation will be a linear one for the interval between successive periods of illumination is small compared with half-life of the dark reaction. The intercept (0.2 mm/min) therefore represents the velocity of the dark reaction. Direct measurements of the after-effect showed that the rate was about 0.2 at 16 mm and 570°C ; for instance, in one experiment in which the light was switched on and off at 1 minute intervals, the dark reaction amounted to 0.20, 0.13 and 0.10 mm after 25%, 50% and 60% reaction respectively.

Similar photochemical after-effects have been observed* in the ammonia sensitized $\text{H}_2\text{-O}_2$ reaction where some reactive atom or radical is deposited on the walls after explosion and is capable of exploding a fresh mixture without requiring illumination. The after-effect for the mercury photosensitized stable reaction was also observed in the present experiments, but the results were not very reproducible. It may be mentioned in this connection that a lag between the adsorption and subsequent re-evaporation of chain carriers has formed a successful postulate† in explaining some of the features of the induction period in certain chain reactions, such as hydrocarbon oxidations.

According to the calculations made on p. 744, the life of a reaction chain or hydrogen atom is at least 10^{-2} seconds, if it reaches the wall. Even at higher pressures, the mean life of the hydrogen atom is probably of the same order of magnitude since there is still wall-inhibition. This calculation gives a minimum value for the energy of activation of $\text{H} + \text{N}_2\text{O}$. The sector experiments yield a maximum value. Had the mean life of the hydrogen atom been greater than 10^{-1} second, then the $R - \phi$ at high pressures should have exhibited a well-defined curvature. As the line is straight, the mean life is

* Farkas, Haber and Harteck, 'Z. Electrochem.,' vol. 36, p. 711 (1930).

† Semenoff, 'Z. phys. Chem.,' B, vol. 11, p. 464 (1931); 'Phys. Z. Sowjet,' vol. 1, p. 543 (1932); 'Trans. Faraday Soc.,' vol. 28, p. 878 (1932).

less than 10^{-1} seconds, which corresponds to an energy of activation of 21.5 k. cal.

So far as these experiments go, they cannot provide the information on the rate intensity relationship which is being sought. Recourse was therefore made to wire screens, but these were not satisfactory; finally a liquid filter consisting of a solution of carbon tetrachloride in specially pure *n*-hexane was employed.*

The data at high and at low pressures are given in Table XI.

Table XI

Pressure 16.0 mm, temperature 568° C					
Intensity.....	1.00	0.91	0.80	0.68	0.51
<i>t</i>	Δp	Δp	Δp	Δp	Δp
0.5	0.53	0.52	0.35	0.30	0.24
1.0	1.07	0.95	0.86	0.66	0.52
1.5	1.57	1.36	1.22	0.95	0.66
2	2.01	1.79	1.59	1.27	0.95
3	2.77	2.48	2.17	1.85	1.32
4	3.27	2.95	2.65	2.26	1.71
5	3.84	3.47	3.18	2.70	2.06

Pressure 100.0 mm, temperature 510° C				
Intensity.....	1.00	0.68	0.51	0.38
<i>t</i>	Δp	Δp	Δp	Δp
2	1.5	1.2	0.9	0.7
4	3.4	2.6	2.2	1.6
6	4.9	4.0	3.2	2.3
8	6.5	5.0	4.2	3.0
10	7.9	6.2	5.0	3.6
15	11.1	8.4	—	4.8

The results in Table XI and some others are plotted in fig. 7. The full line represents $R \sim I$, and the dotted curve $R \sim I^{\frac{1}{2}}$. It will be observed that the low pressure results lie close to the line, whereas the high pressure experiments lie nearer the curve; therefore the termination reaction involves the participation of one carrier at low pressure and two at high pressure. The $R \sim I^{\frac{1}{2}}$ law could not be expected to hold exactly at 100 mm for it was shown in Part I that there is still a considerable amount of termination on the walls. The important point, however, is that these measurements support the hypothesis already put forward to explain the way in which the chains are stopped.

Discussion

It remains now to mention a few points not specifically dealt with in the discussion of the data. The interpretation of the present results does not

* Melville and Walls, 'Trans. Faraday Soc.', vol. 29, p. 1255 (1933).

alter the scheme of reactions set forth in Part I. The equivalence of the thermal and photochemical chain lengths shows that a hydrogen or an oxygen atom can set off a similar reaction cycle, but unfortunately, the calculations are not sufficiently exact to demonstrate whether hydrogen molecules can activate nitrous oxide molecules by collision. It would also seem most probable, at low pressures, that the combination of H atoms is responsible for termination. Schemes involving OH radicals do not give kinetic equations in agreement with the facts. The intensity measurements quite definitely show that only one carrier is concerned, and in conjunction with the packing experiments there is no doubt that a wall reaction is responsible for termination.

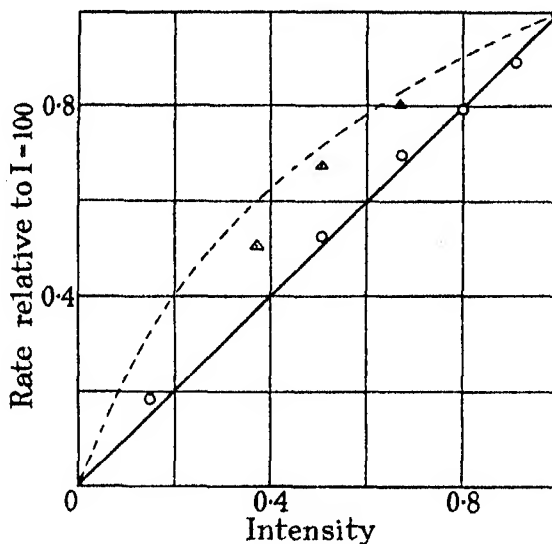
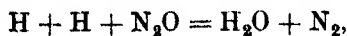
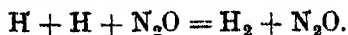


FIG. 7

Since Part I was written, new data* have become available on the effect of various gases in promoting the combination of hydrogen atoms. Argon is about as effective as the hydrogen molecule. Now in the high pressure experiments, argon does not inhibit the reaction (for a 1:1 mixture) and hence neither can H_2 ; N_2O must therefore be more efficient than H_2 as a third body. This greater effective collision diameter may possibly be due to the chemical reaction,



rather than to the physical removal of energy,



* L. Farkas, private communication.

But N_2O cannot be very much more efficient than H_2 , for the rate of reaction becomes independent of $[\text{H}_2]$ when this is large. Such a result implies that an inhibition term containing $[\text{H}_2]$ appears in the denominator of the kinetic equation.

In all the reactions studied, the effect of hydrogen is, in general, small, the nitrous oxide concentration mainly controlling the rate. This is consistent with the theory that the propagation and initiation factors (in the thermal reactions) contain $[\text{N}_2\text{O}]$. In outline, then, the experimental facts are in agreement with the theory, except that the total order is usually a little lower than that expected theoretically. There are, nevertheless, some inconsistencies in the scheme, concerning in particular the values of the energies of activation of the several reactions. The value of E for $\text{H} + \text{N}_2\text{O}$ is only 7 k. cal. (calculated from the high pressure temperature coefficient) and hence if the value of 15 be accepted for $\text{OH} + \text{H}_2 = \text{H}_2\text{O} + \text{H}$, then the latter reaction would be much slower than the former, whereas the present theory would incline to the opposite view. In the thermal low pressure reaction, the chain length is independent of temperature, but in the photo reaction there is an increase, although it happens that in the region where comparison can be made, the chain lengths agree within an order of magnitude. The energy of activation of $\text{H} + \text{N}_2\text{O}$ could be measured and since the values for the initiation processes are known, it would then be practicable to estimate directly the energy of activation of termination (i.e., the combination of hydrogen atoms) in a three body collision and in presence of a wall.

The discrepancy between Hinshelwood's experiments and those described above is probably due to the higher pressures employed and to the accumulation of water vapour, both of which make the chain length short. It is, however, difficult to understand how Dixon and Higgins succeeded in obtaining spontaneous inflammation at comparatively low temperatures. The composition of the gas in a flow system could, of course, vary within wide limits, but it is hardly possible for this to give a velocity sufficiently great to inflame the gases.

The author desires to thank the Royal Commissioners for the Exhibition of 1851 for a Senior Studentship and the Trustees of the Moray Research Fund of Edinburgh University for a grant.

Summary

The kinetics of the hydrogen-nitrous oxide reaction have been studied in the pressure region 1-30 mm and at temperatures from 500° to 750° C. Under

these conditions, the rate of reaction is proportional to the square of the nitrous oxide concentration, is nearly independent of that of the hydrogen, is markedly retarded by packing the vessel, but is not affected by nitrogen or argon. The energy of activation is 49 k. cal. The kinetics are different from those of the high pressure reaction studied previously, but practically complete correlation may be obtained by postulating that the chains now end by the combination of H atoms on the walls.

Chains may also be started by H atoms produced by optically excited mercury atoms. The photochemical chain length agrees with that of the thermal reaction, the latter being based on the measured rate of dissociation of N_2O . At low pressures, the photo reaction rate is proportional to the N_2O concentration, to the intensity of the light, but is independent of the concentration of H_2 , N_2 and A. The energy of activation is 17 k. cal. At high pressures, the rate varies as the square root of the intensity, which shows that the chains end by self-neutralization, thus supporting the theory given for the thermal high pressure reaction.

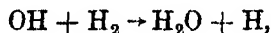
Experiments on the photo reaction with a rotating sector are described. The results are shown to be consistent with the remainder of the data.

The Kinetics of the Reaction between Hydrogen and Nitrous Oxide
 III—*Effect of Oxygen*

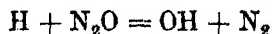
By H. W. MELVILLE (Senior Student, Exhibition of 1851)

(Communicated by J. Kendall, F.R.S.—Received May 8, 1934)

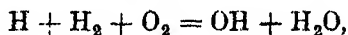
One of the most striking dissimilarities between the hydrogen-oxygen and hydrogen-nitrous oxide reactions is the absence in the latter of sharp explosion limits, a feature characteristic of the former. Another important difference is that propagation of chains in the $\text{H}_2\text{-N}_2\text{O}$ mixtures is rather less easy than in $\text{H}_2\text{-O}_2$, for the photochemical chain length is smaller for $\text{H}_2\text{-N}_2\text{O}$ than for $\text{H}_2\text{-O}_2$ at the same temperatures and pressures (see below). It has, however, been postulated that the carriers in the two reactions are identical and that at least one step, viz.,



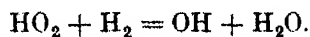
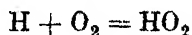
is common to both reactions. The differences in the propagation factors would therefore be due to these reactions



and



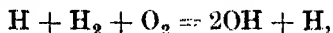
or



It may be anticipated that termination processes will be somewhat similar, and consequently the observed differences in the thermal reactions will also be partly due to initiation reactions.

In this paper, an attempt has been made to study the two reactions under similar conditions so that propagation and initiation reactions may be separated from each other. Experiments have therefore been made on the effect of small quantities of oxygen on the high and low pressure thermal reactions and on the high and low pressure photo reactions. As will be shown below, oxygen exerts a very marked effect in increasing the rate. Its addition has been controlled so that the increase is comparable with the rate of reaction of the oxygen-free mixtures, in order that the stationary concentration of the chain carriers and the nature of the termination reactions should be similar for the two reactions.

To account for the sharp explosion limits in $\text{H}_2\text{-O}_2$ mixtures, branching is supposed to occur in one of the reaction cycles, and the reaction presumed to be responsible for this is



or some slight modification of such a reaction. The nature of the process leading to branching need not be so particularly specified, the essential condition being that in a branching collision two carriers of one type (OH) are produced from one of the other type (H). If this happens once (on the average) before the chain is terminated, the chain length will increase indefinitely and explosion ensue. But with $\text{H}_2\text{-N}_2\text{O}$ there is no possibility of such an occurrence with H atoms or with OH radicals. In the $\text{H}_2\text{-O}_2$ reaction branching becomes possible because the oxygen molecule is diatomic; it is the splitting of this into two parts which ultimately yields the two carriers requisite for branching. Nitrous oxide, on the other hand, has only one atom available and cannot therefore give rise to two OH radicals even in a ternary collision such as $\text{H} + \text{N}_2\text{O} + \text{N}_2\text{O}$.

Although a very definite mechanism for the $\text{H}_2\text{-O}_2$ reaction has been adopted, which perhaps is not correct in detail, it will be of importance to find if homogeneous reactions between nitrous oxide and simple combustible molecules do exhibit well-defined lower and especially upper limits for explosion. If they do not, then the following statement would appear to sum up the behaviour of these reactions: In combustion processes involving nitrous oxide, branching chains and therefore chain explosion limits do not occur. The lower limits observed are due to thermal explosions, initiated homogeneously or heterogeneously, of a type similar to those discussed by Semenov* some time ago. The reaction must, of course, take place under such conditions that these phenomena are usually observed. For instance, the mixture should be capable of propagating chains; the chain length should increase at low pressures and decrease at high pressures. These conditions can be realized with $\text{H}_2\text{-N}_2\text{O}$, but no sharp limits are observed. The sharpness of a limit may be masked by the occurrence of a relatively fast reaction outside the explosion region, such as occurs with $\text{H}_2\text{-O}_2\text{-NO}_2$ mixtures.†

The Photochemical Low Pressure Reaction

To eliminate the possibility of thermal initiation, the experiments recorded in Table I were made at low temperatures, using the mercury lamp with mer-

* 'Z. Physik,' vol. 48, p. 571 (1928).

† Norrish and Griffiths, 'Proc. Roy. Soc.,' A, vol. 139, p. 147 (1933).

cury vapour present in the reaction tube. In Table II the oxygen content of the mixture was varied, maintaining the total pressure unaltered. It will be observed that oxygen accelerates the reaction from 340 to 600° C, but the increase does not change much with temperature, the ratio of the rates increasing 50% for a 20-fold increase in the rate. The energies of activation of the two reactions $\text{H} + \text{N}_2\text{O} = \text{OH} + \text{N}_2$ and $\text{H} + \text{O}_2 + \text{H}_2 = \text{H}_2\text{O} + \text{OH}$ must therefore be nearly equal. If the values of R in Table II be plotted against the percentage of O_2 in the gas, a linear relation is obtained up to 33%.

Table I—5 cm tube. Composition of mixture 19.5 mm O_2 , 300 mm of H_2 and of N_2O

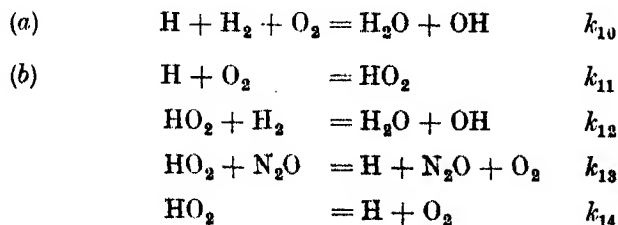
Temperature °C	340	400	460	525	600
Initial pressure	15.95	16.00	17.67	18.24	19.68
Rate	0.26	0.52	0.92	2.50	7.0
Rate (O_2 -free)	0.115	0.23	0.41	0.92	2.20
RO_2/R	2.25	2.3	2.3	2.7	3.2

Table II—Temperature 390° C

Composition of mixture	O_2	—	10	20	40	100	100
	H_2	100	100	100	100	100	100
	N_2O	100	100	100	100	100	—
	(O_2 %	0	4.8	9.1	16.6	33.3	50
Pressure		16.00	16.33	16.00	16.23	16.12	16.12
Rate		0.330	1.05	1.97	3.75	8.40	6.30

Small quantities of a foreign gas can exert a large influence on a chain reaction only by destroying the carriers before they would normally end, or by increasing the rate of initiation. It is improbable, in the present work, that O_2 molecules affect the rate of starting, for the quenching radius of O_2 is only twice as great as that of H_2 .* The acceleration will therefore be due to the participation of oxygen in the propagation reactions.

Two possibilities may be distinguished :



* Zemanski, 'Phy. Rev.', vol. 36, p. 919 (1930).

(a) will be considered first. The stationary concentrations of H and of OH will be given by the equations

$$\frac{d[H]}{dt} = I + k_5 [OH][H_2] - k_4 [H][N_2O] - k_{10} [H][H_2][O_2] - k_9 [H] = 0,$$

$$\frac{d[OH]}{dt} = k_4 [H][N_2O] + k_{10} [H][H_2][O_2] - k_5 [OH][H_2] - k'_9 [OH] = 0,$$

whence

$$\frac{d[H_2O]}{dt} = \{k_4 [N_2O] + k_{10} [H_2][O_2]\} I/k_9.$$

There are difficulties in accepting this simple scheme, for it would be expected that a triple collision with an energy of activation similar to that of $H + N_2O$ would occur much less frequently than the latter reaction, whereas in fact, the rate of removal of H atoms by O_2 is faster than that by N_2O . By postulating the formation of the complex, HO_2 , this difficulty can, in part, be overcome. For (b), therefore,

$$\frac{d[HO_2]}{dt} = k_{11} [H][O_2] - k_{12} [HO_2][H_2] - k_{13} [HO_2][N_2O] - k_{14} [HO_2] = 0,$$

$$[HO_2] = \frac{k_{11} [H][O_2]}{k_{12} [H_2] + k_{13} [N_2O] + k_{14}}.$$

$$\frac{d[H]}{dt} = I + k_5 [OH][H_2] - k_4 [H][N_2O] - k_{11} [H][O_2] - k_9 [H] = 0,$$

$$\frac{d[OH]}{dt} = k_4 [H][N_2O] + k_{12} [HO_2][H_2] - k_5 [OH][H_2] - k'_9 [OH] = 0,$$

$$\frac{d[H_2O]}{dt} = \left\{ k_4 [N_2O] + \frac{k_{11} [O_2] \cdot k_{12} [H_2]}{k_{12} [H_2] + k_{13} [N_2O] + k_{14}} \right\} I/k_9.$$

If k_{13} and k_{14} are small compared with k_{12} then

$$\frac{d[H_2O]}{dt} = \{k_4 [N_2O] + k_{11} [O_2]\} I/k_9.$$

This equation is in agreement with experiment in that the rate should increase linearly with $[O_2]$. At 390° the ratio $k_{11}/k_4 = 13.3$. Oxygen molecules increase the rate of production of water by reaction with the atomic hydrogen of the H_2 - N_2O chains. At higher temperatures, the combination of H_2 and O_2 may also increase the rate of initiation.

High Pressure Thermal Reaction

Having established that oxygen can affect the propagation, the next question is whether the homogeneous or heterogeneous combination of hydrogen and oxygen may give rise to molecules or atoms capable of initiating chains in hydrogen-nitrous oxide. First of all, experiments were made on the effect of O_2 on the thermal reaction; the results are given in Table III. The mixtures

Table III—1.7 cm tube. Temperature 585° C

% O_2	4.75	2.37	1.18	0.59	0.0
Total pressure	100.5	103.0	99.0	100.0	99.0
Rate	15.0	6.0	3.8	1.75	0.26

were made up separately in a gas holder before admission to the reaction bulb. As might be expected, oxygen considerably increases the rate, which may, of course, be due to the propagation. Examination of the values of Δp (not given) will not, however, sustain this explanation entirely. Comparison of the experimental with the calculated values of Δp indicated that hydrogen and oxygen do react to yield H or OH which then start off the chains. In order to find whether this additional source of carriers is due to a wall or to a homogeneous process, the kinetics of the reaction were further investigated with respect to $[N_2O]$, $[H_2]$ and packing. R is directly proportional to $[O_2]$, as may be seen if the results are plotted. Hydrogen and nitrous oxide are inhibitors, for the initial rate of reaction is very nearly independent of pressure, as is shown in fig. 1, where $\Delta p - t$ curves are plotted for a mixture containing 3.3% oxygen. One prominent point is that the curves bend round comparatively rapidly, especially at low pressures, long before the reaction has gone to completion. The oxygen must therefore be consumed in the initial stages. To investigate the individual effects of hydrogen and of nitrous oxide, the following procedure was adopted: p_{N_2O} was fixed at 50 mm, p_{O_2} at 2.4 mm, and p_{H_2} was varied within measurable limits. A similar set of experiments was made with $p_{N_2O} = 150$ mm. A third series was carried out in which p_{H_2} and p_{O_2} were respectively 50 and 2.6 mm, and p_{N_2O} was varied. The results are summarized in Table IV where it will be observed that hydrogen and nitrous oxide exert about the same inhibitory action. The approximate constancy of $R \cdot p_{H_2}^{\frac{1}{2}}$ and $R \cdot p_{N_2O}^{\frac{1}{2}}$ shows that the rate is inversely proportional to the square root of the pressure, but when the pressure of nitrous oxide is considerably greater than that of hydrogen, the latter ceases to have any effect.

Table IV—5 cm bulb. Temperature 568° C

$p_{\text{N}_2\text{O}}$	p_{O_2}	p_{H_2}	R	$Rp_{\text{H}_2}^{\dagger}$
48.2	2.4	24.2	15.0	7.5
48.2	2.4	50.0	11.4	8.1
48.2	2.4	100.2	7.2	7.3
48.4	2.4	199.8	4.6	6.5
48.0	2.4	299.6	4.0	6.9
140.0	7.0	150.0	5.6	6.9
138.6	7.0	100.4	5.6	5.6
143.2	7.0	50.0	6.6	4.6
141.1	7.1	25.0	6.0	3.0
199.5	2.6	48.5	2.1	3.0
148.7	2.7	48.7	2.8	3.4
99.1	2.7	49.1	3.6	3.6
48.4	2.7	48.4	5.2	3.6

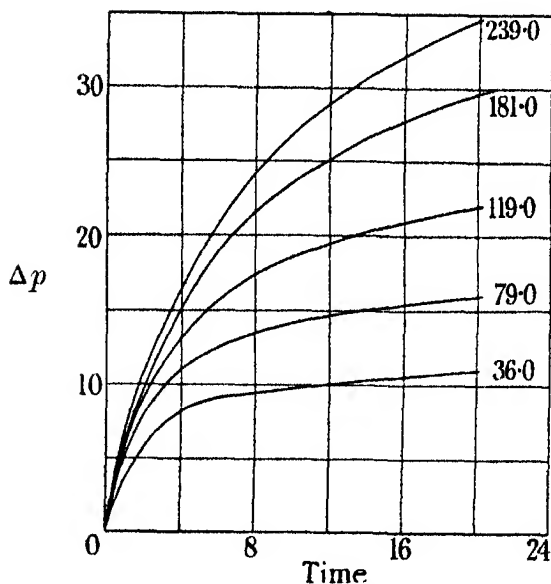


FIG. 1—Effect of total pressure, thermal high pressure reaction, 3.3% oxygen, temperature 532° C

Argon does not cause any inhibition when added to the extent of 200 mm to 100 mm of $\text{H}_2\text{-O}_2\text{-N}_2\text{O}$ mixture. Packing experiments were also made to determine the nature of chain termination, using exactly the same tube and packing material as employed in the thermal high pressure experiments (Part I, p. 532). For comparison, the results are given in full in Table V. A decrease of 50% occurs in the rate, which is the same as that found for O_2 -free mixtures.

Table V—2.5 cm tube. Packing 0.7 cm tubes. Temperature 640° C.
Composition of mixture, 100O₂, 250H₂, 250N₂O. Total pressure 100 mm

<i>t</i>	Packed		Empty	
	Δp	Δp	Δp	Δp
1	6.5	6.5	12.0	11.5
2	10.0	12.0	21.5	20.5
3	13.5	15.0	28.0	27.0
4	17.0	19.0	33.0	32.0
6	21.0	23.5	40.0	38.5
8	24.5	26.0	42.0	41.0
10	26.0	28.0	43.5	—

Since the discussion of the temperature coefficients of the different reactions has shown that there may be a possibility of assigning separate values to the various steps in the reaction, measurements were made of the apparent energy of activation of the present reaction, Table VI.

Table VI—Composition of mixture, 100O₂, 150H₂, 150N₂O

Temperature °C	510	555	572	590	606	649
Rate	2.9	6.0	8.5	11.2	13.7	20.5

E = 17.4 k. cal.

The change in the kinetics of the reaction is complete. The effect of packing and of inert gases show, however, that similar termination reactions occur. The initiation factor is quite different and the fall in the apparent energy of activation shows that nitrous oxide no longer plays any important part in the first stages. It has been seen how oxygen affects the propagation factor, and in order to make certain that these fundamental changes in the kinetics were partly due to initiation, the following series of runs was made. Conditions for reaction were so arranged that the rates of the four reactions—thermal H₂-N₂O, thermal H₂-N₂O-O₂, photo H₂-N₂O, photo H₂-N₂O-O₂, were all comparable. If oxygen affects the propagation factor only, then the acceleration of the thermal and of the photo reactions should be the same. On the other hand, if the initiation factor is also affected, then the acceleration of the photo reaction will be somewhat smaller than that of the thermal. The reasons for these statements can be readily seen if the general velocity equations are set down for the four conditions:

$$R_T = P_T \cdot I_T^{\frac{1}{2}}, * \quad (1)$$

$$R_{T, O_2} = (P_T + P_{O_2}) (I_T + I_{O_2})^{\frac{1}{2}}, \quad (2)$$

$${}_PR_T = P_T \cdot (I_T + I_P)^{\frac{1}{2}}, \quad (3)$$

$${}_PR_{T, O_2} = (P_T + P_{O_2}) (I_T + I_{O_2} + I_P)^{\frac{1}{2}}. \quad (4)$$

* The termination factors are identical for all four reactions, and for simplicity are not inserted in the equations.

If $I_{O_2} = 0$,

$$R_{T, O_2} - R_T = {}_P R_{T, O_2} - {}_P R_T$$

If $I_{O_2} \neq 0$ and $I_T \doteq I_{O_2} \doteq I_P$,

$$R_{T, O_2} - R_T > {}_P R_T - {}_P R_{T, O_2}$$

P and I are propagation and initiation factors. The suffixes T, O_2 , P refer respectively to the thermal, the O_2 , and the photo reactions. From these equations, the relative values of I_T , I_{O_2} , and I_P may be calculated. Let $P_{O_2} = \alpha P_T$, α can be computed from the oxygen content of the mixture and the results in Table VII. Equations (1) and (3) yield

$$I_T = I_P \{R_T^2 / ({}_P R_T^2 - R_T^2)\},$$

and (1), (2), (3), and (4) give

$$I_{O_2} = I_P \left(\frac{a+b}{a-b} \right),$$

where $a = {}_P R_{T, O_2}^2 - (1 + \alpha)^2 R_T^2$ and $b = R_{T, O_2}^2 - (1 + \alpha)^2 R_T^2$.

Table VII—5 cm tube. Composition of mixture, 50% O_2 , 24.7% H_2 , 24.7% N_2O .
 $\alpha = 0.30$

Temp. °C	Pres- sure	R_T	R_{T, O_2}	${}_P R_T$	${}_P R_{T, O_2}$	$(R_{T, O_2} - R_T)$	$({}_P R_{T, O_2} - {}_P R_T)$
550	100	0.60	2.75	1.95	3.45	2.15	1.50
578	50	0.70	4.36	2.40	5.00	3.56	2.6
572	100	1.05	4.20	3.3	5.9	3.15	2.6
572	150	1.96	4.9	3.2	6.0	3.0	2.8
618	100	3.4	8.7	5.9	10.5	5.3	4.6

I_T	:	I_P	:	I_{O_2}		I_T	:	I_P	:	I_{O_2}
1		9.6		11.7		0.14		1		1.22
1		10.6		21.9		0.095		1		2.07
1		8.9		8.9		0.112		1		1.00
1		1.66		2.60		0.60		1		1.57
1		2.01		2.87		0.50		1		1.43

The results for a few different pressures and temperatures are collected in Table VII. The acceleration of the two reactions is not equal, as will be observed from an examination of columns 7 and 8. This is more clearly shown by the calculations on the relative magnitudes of I. In the first set, $I_T = 1$ and in the second $I_P = 1$. I_P is nearly independent of temperature and pressure and hence the variation of the other quantities is given in better perspective. The second set of calculations demonstrates that the thermal reaction, compared with the photo, is greater as the temperature and pressure increase. The first shows that initiation by oxygen is of greatest importance

at low pressures and temperatures. This is in accordance with the value of E for the oxygen reaction being smaller than E for the normal reaction. Furthermore, since it has been found that the temperature coefficients of the propagation factors are nearly the same, the effect of packing is identical and there is initiation by O_2 , it must be concluded that, under these conditions, the initiation reaction involves both H_2 and O_2 and takes place in the gas phase with an energy of activation considerably less than that for the decomposition of nitrous oxide.

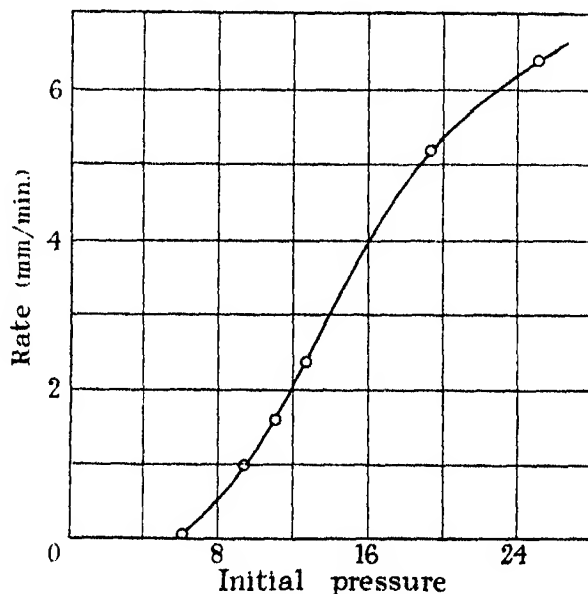


FIG. 2.—Effect of total pressure, thermal low pressure reaction, temperature $602^{\circ}C$, 2.91% oxygen

The Low Pressure Reaction

It has been mentioned previously that, above 50 mm the pressure of a given $H_2-N_2O-O_2$ mixture does not affect the initial rate. As the pressure is reduced below this value, the rate diminishes linearly as is indicated by fig. 2. The curve does not pass through the origin, but makes an intercept on the pressure axis. The reaction velocity would thus appear to drop to a very small value when the pressure is below a certain critical point, in the present instance, 8 mm. If the individual runs are examined, it is found that Δp increases quite rapidly at first, but later changes only very slowly, although the reaction has not proceeded to completion. For example, with an initial pressure of 19.4 mm, Δp is almost steady after attaining 4 mm, which is equivalent to 40% of the

total possible increase. Had the observed value of Δp been due to the $\text{H}_2\text{-O}_2$ reaction alone, the pressure decrease would have been 0.6 mm. The comparatively abrupt bending over of the $\Delta p - t$ curves is due to the pressure of the mixture falling below the critical value. An essentially similar phenomenon is obtained when the oxygen content of a $1:1\text{H}_2\text{-N}_2\text{O}$ mixture at constant pressure is altered (Table VIII). Above 12.5% O_2 , the reaction is rapid and increases if the oxygen percentage is raised to 5. At 0.63%, however, the rate has dropped to a very small value. On raising the temperature to 650° , a conveniently measurable velocity is obtained, which does not greatly depend on the oxygen content and is, indeed, not much faster than that for the oxygen-free gases.

Table VIII

Temp. $^\circ\text{C}$...	570	570	570	560
% O_2	5	1.25	0.63	0.63
Pressure	12.80	13.06	12.84	12.80
	Δp	Δp	Δp	Δp
	0.25 2.25	0.25 0.46	0.5 0.00	0.5 0.38
	0.50 3.46	0.50 0.76	2 0.04	1 0.62
	0.75 4.16	0.75 0.88	4 0.06	2 1.00
	1.0 4.44	1 1.02		3 1.30
	1.25 4.54	1.5 1.36		4 1.56
	1.75 4.82	2 1.54		6 1.88
		3 1.82		8 2.10
		6 2.06		10 2.30
Temp. $^\circ\text{C}$...	650	650	650	
% O_2	0.31	0.16	—	
Pressure	12.71	12.98	12.80	
	t Δp	t Δp	t Δp	
	1 0.26	1.5 0.38	1 0.20	
	2 0.56	3 0.70	2 0.38	
	4 0.93	4 0.80	4 0.80	
	6 1.28	7 1.40	6 1.04	
	8 1.60	10 1.78	10 1.62	
	10 1.88	15 2.36	14 2.16	
	15 2.36	21 2.78		
	20 2.78			

If the $\Delta p - t$ curves are plotted, the same tendency to bend over is not so marked at 650° . The oxygen pressure would thus seem to control the position of the critical point. If the reaction above the critical pressure is to be identified with that at high pressures, it would be expected that, as with O_2 -free gases, the apparent energy of activation would decrease with pressure. This is borne out by the data in Table IX, where it will also be noted that, for a given mixture at a constant pressure, there is a critical value for the temperature, below which the rate is slow.

Table IX—Composition 12O_2 , $200\text{N}_2\text{O}$, 200H_2 . Pressure 12.8 mm
5 cm tube

Temperature °C	510	519	525	540	580	625
Rate	0.01	0.95	1.25	2.05	3.3	8.2

$E = 30.6 \text{ k. cal.}$

Finally, packing experiments show clearly the importance of inhibition by walls. For example, in the 5-cm tube at 550° with a mixture containing 2.9% O_2 , the critical pressure was 6 mm, the rates at 7.67 and 20.10 mm being respectively 1.00 and 2.40 mm/min. On packing the tube completely with

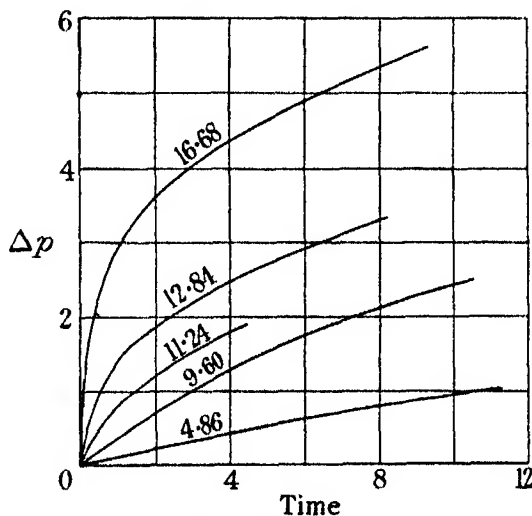


FIG. 3—Effect of total pressure, packed reaction bulb. Temperature 710°C , 2.9% O_2 .

0.7 cm tubes, no measurable reaction occurred at all and the temperature had to be raised to 710° to get a conveniently observable rate, which for a pressure of 16 mm was 1.55 mm/min. The rate of the $\text{H}_2\text{-N}_2\text{O}$ reaction was now 0.50 mm/min. In the packed tube, however, there was still evidence of the existence of a critical pressure, for it will be seen from fig. 3, where $\Delta p - t$ curves are plotted for different total pressures, the form of the curves changes between 9.60 and 11.24 mm. This is brought out more clearly in Table X where a comparison is shown for an O_2 -free and an O_2 -containing mixture at 16.00 and at 8 mm, i.e., above and below the critical pressure. The acceleration of the reaction is much greater at 16 than at 8 mm.

It should be mentioned that, in all these experiments, the mixtures were made up previously in a separate gas holder, for it was neither convenient nor

accurate to add small amounts of oxygen to the $\text{H}_2\text{-N}_2\text{O}$ mixture. A considerable number of experiments was carried out in which the gases were added separately to the bulb and the important observation was made that, if only hydrogen and oxygen were admitted without nitrous oxide, there was immediate explosion and the pressure fell extremely rapidly. This occurred with pressures and temperatures above the critical values for the $\text{H}_2\text{-N}_2\text{O-O}_2$ reaction.

Table X—Composition of mixture as in Table IX

Above transition point				Below transition point			
O ₂ free				O ₂ free			
<i>p</i>	16.04	16.24			8.06	8.00	
<i>t</i>	<i>Δp</i>	<i>t</i>	<i>Δp</i>		<i>t</i>	<i>Δp</i>	<i>t</i>
0.5	1.64	1	0.40		0.5	0.09	0.5
1.1	2.60	2	0.84		1	0.26	1
2.1	3.24	4	1.74		2	0.59	2
4	3.94	6	2.46		3	0.85	3
6	4.54	8	3.02		5	1.26	5
8	5.04	10	3.44		7.5	1.65	7.5
R ₀ 3.30		R 0.42		R ₀ 0.295		R 0.175	
R ₀ /R = 7.9				R ₀ /R = 1.69			

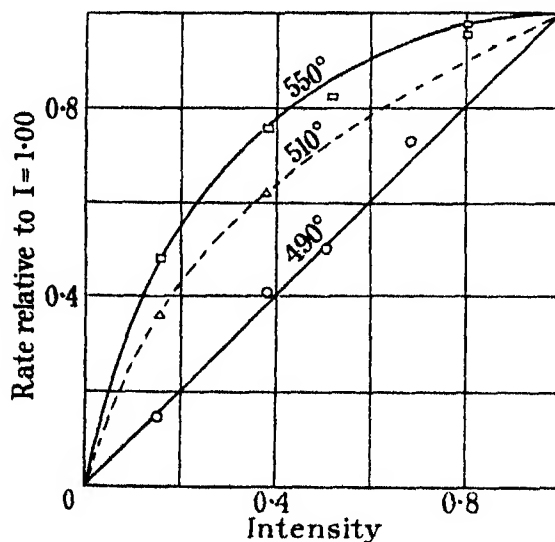


FIG. 4

The unusual character of the reaction is further borne out by experiments on the effect of the intensity of the light in the photochemical reaction in the region of the transition point. The rate-intensity curves are given in fig. 4 for three temperatures. The dark reactions were not greater than 5% of the total. At 492°, a linear relation is obtained as might be expected, but at 510°

and still more so at 550°, curvature is marked in such a way as to indicate that the exponent of I at 510° is 0.5 and even less at 550° for the dotted curve refers to $R \sim I^{\frac{1}{2}}$. The interpretation of the results at 510° might simply be that the increase in rate has altered the termination process from a wall to a gas phase reaction. Although this may in part be true, the fact that at 550°, $R \sim I^{1/n}$ where $n > 2$ and that in the ordinary photo reaction, H_2-N_2O , at a rate of the order of 1 mm per minute surface termination is still predominant, shows that this explanation is not sufficient.

Discussion of the Mechanism

The critical point observed in the low pressure O_2 -reaction bears a remarkable similarity to the lower limit in H_2-O_2 mixtures. The reaction above this point is not, however, an explosion, for it was quite easy to get spontaneous inflammation at low pressures if the temperature was raised sufficiently. Since the H_2-O_2 mixture itself is spontaneously explosive and, above the critical point initiation is largely due to the H_2-O_2 reaction, it may be that the stable reaction observed is not unlike the degraded ("entartete") explosions of Semenov.* It would appear that there is some additional inhibition factor coming into operation which prevents effective branching of the chains. The intensity-rate relationships support this argument, for at the highest temperature 550°, the rate has become almost independent of intensity; that is, initiation ceases to play any important role in determining the course of the reaction. This latter effect is one of the characteristics of a pure lower explosion limit. Nitrous oxide is, in fact, an inhibitor of the H_2-O_2 reaction for, although it reduces the lower limiting pressure for explosions like argon or helium,† the critical pressure rises again as the amount of N_2O increases, *e.g.*,

Temperature 515° C

$p_{H_2+O_2}$	1.60	1.27	1.21	1.23	1.61
p_{N_2O}	—	3.20	4.81	6.57	9.61

The limit was determined by admitting a 2 : 1 H_2-O_2 mixture until inflammation was observed. A short time was allowed for the water formed in the explosion to be withdrawn by the P_2O_5 , when the residual pressure was noted. Nitrous oxide was then added and the foregoing procedure repeated.

* 'Z. phys. Chem.,' B, vol. 2, p. 464 (1931).

† Hinshelwood and Moelwyn-Hughes, 'Proc. Roy. Soc.,' A, vol. 138, p. 311 (1932).

Some curious observations were made during these experiments. If the $\text{H}_2\text{-O}_2$ mixture was quickly admitted to the tube and the lower limit passed, a much more violent explosion occurred at about 10 mm, which was accompanied by rapid vibration of the manometer pointer. If the flow of hydrogen and oxygen was arrested, the pressure fell very quickly as the water was removed. During this period, successive explosions were observed in the reaction tube, resembling those obtained with $\text{P}_4\text{-O}_2$ mixtures when the lower limit is passed. There may be some connection between these two types of explosion and the experiments of Ouellet* who used a quantum counter for investigating the lower limit of the $\text{P}_4\text{-O}_2$ reaction. In these, the lower limit was succeeded at a higher pressure by another explosion with a flash of a different colour, which alone affected the counter (it may be noted that the counter was only sensitive to radiation of $\lambda < 280 \text{ m}\mu$) and hence it was concluded that there were two kinds of explosion in so far as the nature of the chemiluminescence was concerned.

The modification of the previous theory of the effect of oxygen to allow for branching is simply made. It will be assumed that branching occurs in the step $\text{HO}_2 + \text{H}_2$ and that as usual $(\alpha - 1)$ is the efficiency of branching, *i.e.*, the probability of two OH radicals being produced when one H atom disappears. The equations for the stationary concentrations of H and of OH are therefore

$$\frac{d[\text{H}]}{dt} = \text{I} + k_5 [\text{OH}] [\text{H}_2] - k_4 [\text{H}] [\text{N}_2\text{O}] - k_9 [\text{H}] - k_{11} [\text{H}] [\text{O}_2] = 0,$$

$$\frac{d[\text{OH}]}{dt} = \text{I} + k_4 [\text{H}] [\text{N}_2\text{O}] - k_5 [\text{OH}] [\text{H}_2] + \alpha k_{11} [\text{HO}_2] [\text{H}_2] = 0,$$

whence

$$\frac{d[\text{H}_2\text{O}]}{dt} = \{k_4 [\text{N}_2\text{O}] + k_{11} [\text{O}_2]\} \frac{\text{I}}{k_9 + (1 - \alpha) k_{11} [\text{O}_2]}.$$

At low temperatures, α is very nearly unity and hence the second term in the denominator vanishes. The condition for explosion is $k_9 = (\alpha - 1) k_{11} [\text{O}_2]$ and therefore the limit should be sharp as in the thermal $\text{H}_2\text{-O}_2$ reaction. In the present reaction, however, a rather peculiar position arises. It has been seen that there is a little gas phase termination in the low pressure reaction. If the stationary concentration of H or of OH be raised much above that obtaining under the conditions employed in these experiments, for example, by a branching mechanism, gas phase termination will become of ever-increasing importance. The functioning of this additional inhibitory factor may, at any

* 'Trans. Faraday Soc.,' vol. 29, p. 486 (1933).

rate in a small region, prevent effective branching and thus allow the stable reaction to be measured. The transition point is therefore reached when $[H]$ attains a certain value, which will naturally be affected by packing, temperature, and oxygen content of the mixture, in a somewhat similar manner to a lower limit. At high pressures gas termination is so important that a sharp transition is not obtained; likewise, when the chains are short, as in a packed tube, transitional characteristics are only slightly in evidence.

On p. 762 it was shown that although oxygen is more effective than N_2O in producing OH radicals from a hydrogen atom, yet the energies of activation of the two reactions are almost identical. First of all, this rules out the possibility of the simple reaction $H + H_2 + O_2 = H_2O + OH$ since, if such a ternary collision required the same energy of activation as $H + N_2O$, the probability of its happening would be extremely small. Recently, L. Farkas* has measured the rate at which H atoms are removed in a mixture of H_2 and O_2 at room temperature and found that the velocity was about 1/50 of that calculated from the number of ternary collisions $H + H_2 + O_2$, and is not changed by temperature. This discrepancy can be explained by supposing that the removal of an H atom is not accompanied by the production of OH . This latter process requires as much activation as the reaction $H + N_2O$. But the oxygen molecule is more effective than the N_2O molecule in yielding OH , and therefore the rate of $HO_2 + H_2 = H_2O + OH$, although possessing the same energy of activation, is faster than $H + N_2O = OH + N_2$. The concentration of HO_2 must consequently be greater than that of H ; from the results in Table I, the order of magnitude is 10.

The author desires to thank Dr. E. B. Ludlam and Professor J. Kendall for their continued help and encouragement throughout the course of this work, which was carried out in the Chemistry Department of the University of Edinburgh and subsequently at the Department of Colloid Science of the University of Cambridge. He also thanks the Royal Commissioners of the Exhibition of 1851 for a Senior Studentship.

Summary

The effect of the addition of oxygen on the kinetics of the hydrogen-nitrous oxide reaction has been investigated in order to compare the H_2-N_2O and H_2-O_2 reactions under similar conditions.

* Private Communication.

Summary of Reactions

Reaction	Kinetic equation (observed) $R \sim$	Kinetic equation (calculated) $R \sim$	E (total)	E (initiation)
Thermal high pressure } Thermal low pressure }	$[N_2O][H_2]^{0.5*}$	$[N_2O] \sqrt{\frac{[N_2O]([N_2O] + [H_2])}{([N_2O] + [H_2])^2}}$	36.5	57
Photo high pressure } Photo low pressure }	I†	$[N_2O] \sqrt{\frac{[H_2]}{([N_2O] + [H_2])^2}} I$	<36	0
Thermal high pressure + O_2 } Thermal low pressure + O_2 }	$[O_2] \cdot [N_2O]^{-0.5} \cdot [H_2]^{-0.5}$	$([N_2O] + \alpha [O_2]) \sqrt{\frac{?}{([N_2O] + [H_2])}}$	17	<57
Photo high pressure + O_2 } Photo low pressure + O_2 }	—	$([N_2O] + \alpha [O_2]) \sqrt{\frac{[H_2]}{([N_2O] + [H_2])^2}}$	31‡ <17§	<50 0
	$[O_2] \cdot I(1 \rightarrow 0)†$	$([N_2O] + \alpha [O_2]) \cdot \frac{[H_2]}{[N_2O] + [H_2]}$	14	0

* These exponents are to some extent a function of $[N_2O]$.

† Exponent depends on temperature.

‡ Measured above the transition point.

§ Estimated from the data in Table VII.

|| The coefficients for $[H]$ and $[N_2O]$ are not inserted.

The thermal and mercury photosensitized reactions have been studied in the pressure range 1–300 mm.

At high pressures, the addition of small quantities of oxygen increases the velocity, the kinetics change entirely and the energy of activation falls off. By using photochemical methods it is shown that oxygen participates in the initiation and in the propagation of the chains. From packing experiments it is also shown that initiation is homogeneous.

At low pressures in the thermal reaction, a transition point is observed above which the reaction is comparatively rapid and below which it is slow, provided wide bulbs are used. This point depends on the oxygen content and the temperature of the gases; it is displaced to higher temperatures on packing the reaction tube. The phenomenon has some definite connection with the lower limit of the H_2 - O_2 reaction. Photo experiments confirm these observations in that as the temperature is raised the value of the exponent n in the equation $\text{Rate} = \text{const.} \times (\text{intensity})^n$ decreases from unity to almost zero.

The Exchange of Energy between a Platinum Surface and Gas Molecules

By W. B. MANN, Physics Department, Imperial College of Science, London

(Communicated by G. P. Thomson, F.R.S.—Received May 8, 1934)

Recent experiments by Roberts* have shown, not only that the accommodation coefficients of helium and neon atoms impinging on a clean heated tungsten surface are extraordinarily low, but also that these values increase with time after cleaning the surface. To explain this increase he suggests the gradual formation of adsorbed films on the surface of the tungsten due to residual impurities in the gas. The primary object in starting the investigations to be described in this paper was to gain some information as to the nature of these films, the existence of which has also been postulated by Blodgett and Langmuir.† For this purpose experiments have been carried out in which the emission of energy from electrically heated wires of platinum, a metal relatively resistant to contamination, has been investigated under varied conditions.

Apparatus

A pure platinum wire about 20 cm long and 0.025 mm diameter was silver-soldered to platinum leads of 0.4 mm diameter and mounted loosely in a vertical glass tube of approximately 5 cm diameter. The wire was connected, by double leads, to a Thomson bridge, by means of which the resistance could be determined and also controlled by suitable adjustment of the current. The potential drop along the wire was measured by means of a Siemens and Halske potentiometer. The mean temperature of, and the heat developed in, the wire could thus be determined.

The tube containing the wire was connected by glass tubing of 1.5 cm bore to a flask of about 10 litres and to a pipette system which has been described by Knudsen,‡ by means of which small quantities of gas at a known

* 'Proc. Roy. Soc.,' A, vol. 129, p. 146 (1930); vol. 135, p. 192 (1932); vol. 142, p. 519 (1933).

† 'Phys. Rev.,' vol. 40, p. 78 (1932).

‡ 'K. danske vidensk. Selsk. Skr.,' vol. 7, p. 15 (1927).

pressure could be expanded into the apparatus to give accurate pressure increments of any value from 0.01 dyne/cm².

To determine the residual pressure in the apparatus after evacuation a radiometer gauge was constructed in which a vertically hanging aluminium leaf, 0.5 μ thick, 3 mm wide, and about 5 cm long, was repelled by an electrically heated vertical platinum blade, 1.5 μ thick, 3 mm wide, and 4.5 cm long. The blade was included in one arm of a Wheatstone net and its resistance, and hence its temperature, was controlled by adjustment of the current flowing through it. For a mean temperature of the blade of about 45° C a deflection of 2.5 microscope scale divisions per 1 dyne/cm² was obtained, the aluminium leaf being at room temperature.

The tube containing the wire was immersed in a vaseline oil bath which was kept stirred by means of compressed air. A mercury in glass thermometer, standardized by the Deutsche Physikalische Reichsanstalt, was used to determine the temperature of the bath.

Experimental Procedure

After weighing and mounting a wire it was annealed at red heat in air to remove strain; a necessary procedure in order to obtain reproducible values of the resistance, and the temperature coefficient of resistance, of the wire. The resistance of the wire was then determined at room temperature and at the boiling point of water and the temperature coefficient of resistance deduced. This was found to have a mean value of 0.003901 per degree C. With the tube in the oil bath the apparatus was evacuated and the current flowing through the wire adjusted until its resistance corresponded to a mean temperature of about 100° C. The radiation heat loss was determined and then gas was admitted to a known pressure. The bridge was then rebalanced and the new heat loss from the wire at the same mean temperature determined. The ratio of the difference of these two heat losses to the theoretical difference of heat loss deduced by Knudsen* for the given differences in pressure and temperature gives the accommodation coefficient. The observed heat development in the wire must always be corrected for the energy loss through the ends of the wire.

Readings were taken for a series of pressure increments, up to about 800 dynes/cm² for helium, in order to determine the range of pressure over which the relation given by Knudsen for the molecular heat conduction is valid.

* 'Ann. Physik,' vol. 34, p. 593 (1911).

With a fresh specimen of gas in the apparatus the temperature of the wire was now raised, usually to 1000°C , and the accommodation coefficient was determined from readings taken at that temperature. In general the accommodation coefficient fell exponentially with time, many hours, in one instance 50, being needed before the heat loss from the wire became constant.

A constant value having been obtained the mean temperature of the wire was lowered to different temperatures between 100° and 1000°C , and the variation of the accommodation coefficient of the surface with time determined at each of these temperatures, the wire being raised to 1000°C between each set of determinations. The apparatus was now evacuated and the radiation heat loss determined for the "clean" wire at each temperature. Readings were repeated using fresh specimens of gas, but, in general, it was found that after the first "conditioning" of the wire it was not necessary to keep it very long at 1000°C before the minimum constant value was reached; the time depending to a very great extent on the length of the period during which the wire had been left at a lower temperature.

After a complete set of readings with a given specimen of gas, the current through the wire was lowered so that the temperature of the wire was only a few degrees above that of the bath. Resistance readings were taken for different values of the wattage and a linear extrapolation made to zero wattage to give the resistance of the wire at the temperature of the bath.

When not in use the apparatus was left evacuated. It was found to be necessary, however, to keep the wire always at a higher temperature than its surroundings in order to prevent condensation of mercury, from the mercury seals in the pipette system, on to the wire. Considerable difficulty had been experienced with the first wire, results for which are not given, through such a condensation. A current, therefore, sufficient to keep its temperature at about 100°C was always left flowing through the wire.

A liquid air trap between the pipette system and the tube containing the wire could be used to remove mercury from the apparatus during an experiment, the last mercury seal being provided with a ground glass float seal which prevented mercury from distilling into the apparatus. This seal was also closed when the apparatus was not being used.

Results for the accommodation coefficients with respect to three platinum wires are given. For convenience of comparison these three wires will be identified by the letters A, B, and C. No correction has been made for the thermal expansion of the platinum surface. Such a correction would amount to only 1% at 1000°C .

Results and Discussion

A brief preliminary outline of the general results obtained will serve to render the detailed observations for individual gases more readily intelligible.

In general, on lowering the mean temperature of the wire to, say, 100°C ., after cleaning at about 1000°C ., the accommodation coefficient was observed to increase with time, a quite rapid rise being observed in the first few minutes after lowering the temperature of the wire. This is illustrated by the curve shown in fig. 1 where the mean temperature of the wire has been lowered from 1000° to 100°C . On again raising the temperature to 1000°C the wire is

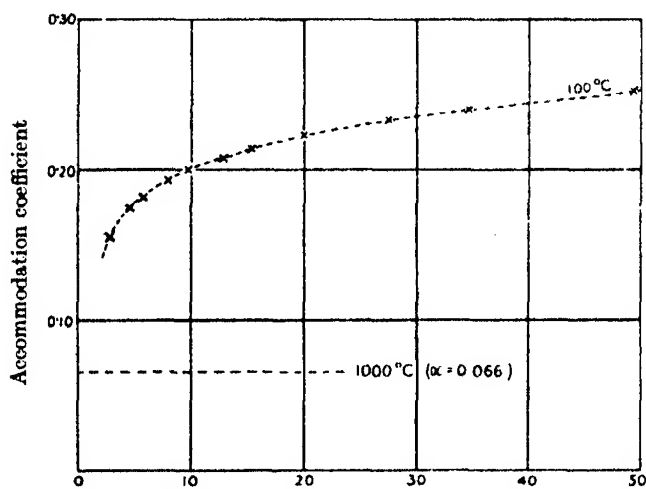


FIG. 1—Helium

usually cleaned in a very short time, even though the initial cleaning of the wire may have taken as long as 40 hours. The contamination on lowering the temperature of the wire always seemed to be of a superficial nature.

The form of the curves obtained on lowering the temperature of the wire, make it somewhat difficult to make any satisfactory extrapolation to zero time in order to obtain the accommodation coefficient with respect to a clean wire at a temperature of 100°C . Roberts uses an almost linear extrapolation. It would seem, however, that the contamination occurs most rapidly within the first 2 minutes after lowering the temperature of the wire, in which case such an extrapolation would be invalid.

It was found that oxygen had a quite remarkable effect on the platinum wire. It was found to attack the wire at 1000°C , a quite appreciable mass of

platinum being removed. After this action the susceptibility of the wire to contamination on lowering the temperature was most markedly decreased; no increase in the accommodation coefficient being observed at temperatures at which, previously, there had been a quite appreciable increase. For different gases the following results were obtained.

1 *Helium*—Preliminary experiments were carried out using a specimen of helium 96% pure. From these it was concluded that the wire could be thoroughly cleaned at about 1200° C, no increase in the heat emission being observed on lowering the temperature of the wire from 1400° to 1200° C and only a slight increase on lowering to 1000° C. This wire (A) was accidentally fused during these experiments and a new wire (B) was mounted.

Results were now obtained using a specimen of spectroscopically pure helium, such low values having been obtained for the accommodation coefficient (*e.g.*, 0.04) for the impure helium that it was to be expected that small quantities of impurity might influence the results quite considerably.

Before cleaning the new wire, by heating to 1000° C, experiments were made with the wire at a mean temperature of 100° C, at different pressures, in order to determine the range of pressure over which the heat conduction through the gas is a linear function of the pressure; that is, to determine the limiting pressure below which the mean free path of the gas molecules is sufficiently large compared with the dimensions of the wire for the assumption of pure molecular conduction to be justified.

This assumption will be valid so long as the radius of the wire is so small, compared with the mean free path of the gas molecules, that the probability of a molecule re-colliding with the wire with only one intermediate molecular collision is negligibly small.

The results shown in Table I were obtained, the decrease in the accommodation coefficient with increase of pressure being due to the falling away of the heat conduction from the value given by the linear relation.

Table I

Pressure of helium in dynes/cm ²	120.9	234.8	342.1	443.1	538.3
Accommodation coefficient	0.353	0.353	0.352	0.351	0.350
Pressure of helium in dynes/cm ²		627.9	712.2	791.5	866.0
Accommodation coefficient		0.349	0.347	0.346	0.345

As it is not possible to obtain absolute values of the accommodation coefficient to a greater accuracy than about 2 or 3%, it will be seen from these results that to work at a pressure of about 500 dynes/cm² will be legitimate.

The wire was now heated to 1000°C at which temperature, during 27 hours, the accommodation coefficient fell to a minimum value of 0.066. The temperature of the wire was now lowered to 100°C and the variation of the accommodation coefficient with time, at that temperature, is shown in fig. 1. The temperature was lowered, simultaneously with the starting of a stop-watch, by bringing an appropriate resistance into the circuit by means of a double-pole switch. After a period of 17 hours at this temperature the accommodation coefficient had risen to 0.306 and finally rose to 0.314 after standing for a further 50 hours. While the absolute values of the accommodation coefficient are of little value beyond the second place of decimals, it is, however, quite legitimate to take account of the third figures in the consideration of the variation of the accommodation coefficient for any given set of conditions, the only variable upon which this variation depends being an accurately determined potential difference.

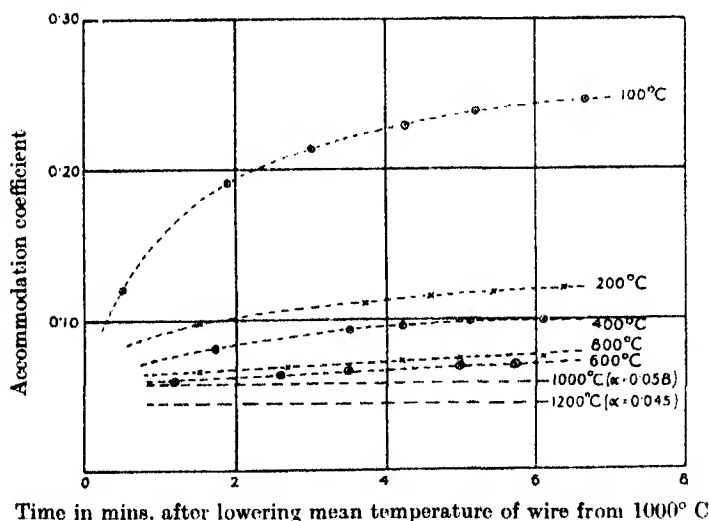


FIG. 2.—Helium

With a fresh sample of gas, this and all subsequent samples being taken from the same bulb of spectroscopically pure helium, the wire was cleaned at 1000°C , and the accommodation coefficient determined at different temperatures of the wire. The results are shown in fig. 2 in which the temperatures given refer to the wire. The values at 1200° and 1000°C were constant, but at all other temperatures a variation with time was observed. It will be noticed, however, that all the curves tend to converge to a common value between 0.045 and about 0.07. This is of importance in that it shows that

the variation of the accommodation coefficient with the temperature of the wire is small provided that the condition of the surface of the wire be kept unaltered. It must be remembered, however, that, when the temperature of the wire is increased from 100° to 1000° C, there is only a small change in the mean temperatures of the gas atoms leaving the wire, namely, from about 25° to 80° C. The only fundamental difference would seem to be that at 1000° C the wire is protected from contamination.

With regard to these results, it should be remarked that after the accommodation coefficient of the surface had risen to 0.25 at 100° C it required only some 15 minutes heating at 1000° C in order to reduce it to 0.059 at that temperature. In the initial cleaning of the wire after it had been standing several weeks in air it required, however, more than 2 hours heating at 1000° C in order to reduce the accommodation coefficient from 0.14 to 0.070, and a further 18 hours at that temperature to reduce it from 0.070 to 0.066. It would seem therefore that, although the surface becomes contaminated very rapidly, especially within the first 2 minutes, the contamination is purely superficial. After very long periods, however, this or some other contamination would seem to become more deeply absorbed and, correspondingly, more difficult to remove.

It is also interesting to note from these results that, as the ultimate value of the accommodation coefficient at 100° C is about twice as great as the ultimate value at 200° C, it requires almost the same amount of energy to maintain the wire at 200° C as to maintain it at 100° C. It so happens, indeed, that less energy is required to maintain the wire at 200° C after $1\frac{1}{2}$ minutes from the time of lowering the temperature from 1000° C than is required to maintain it at 100° C after 7 minutes. A range of almost unstable equilibrium thus exists in which any increase of current at 100° C will result in a cleaning of the wire and consequent rise in temperature. This was first observed when, with the wire at 100° C, I tried to anticipate the rise in accommodation coefficient by increasing the current. The temperature rose, however, and the accommodation coefficient fell. It is thus necessary to alter the current to rebalance the bridge in following the rise in accommodation rather carefully in order to get a true relation between the increase of accommodation and time at a temperature of 100° C.

The wire was now heated to about 1000° C in oxygen at a pressure of 570 dynes/cm² for 20 hours. During this period the resistance of the wire was observed to increase and subsequent weighing revealed that its mass had correspondingly decreased by some 5%. After this treatment lower values

were obtained for the accommodation coefficient with respect to helium, the results being shown in fig. 3. In addition the wire showed a very marked decrease in its susceptibility to contamination. Where, previously, the heat loss from the wire had increased with time at 800° C, after cleaning at 1000° C, no such rise is now observed until the mean temperature of the wire is lowered to 400° C. At 100° C the rate of increase is also greatly reduced as will be observed by comparison between figs. 2 and 3. The limits, between which the extrapolated values to zero time seem to lie, are also very much closer after the oxygen treatment, the upper and lower limits being 0.035 and 0.030 respectively. It must be remembered, however, that the mean temperature

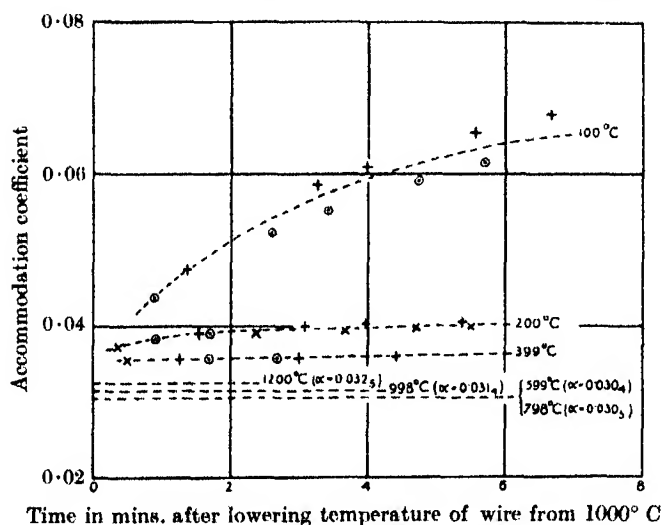


FIG. 3—Helium

increment of the atoms at impact with the wire at 1000° C is now only 30° C, the gas atoms leaving the wire having a mean temperature of about 50° C. Readings at 1000° C, when the pressure was varied, gave values of 0.0340, 0.0342, and 0.0345 for the accommodation coefficient for values of the pressure equal to 186.0, 362.0, and 528.4 dynes/cm² respectively, thus justifying the assumption of pure molecular conduction at this temperature.

In addition, experiments were made in which the apparatus was evacuated with, and without, liquid air on the trap between the wire and the mercury seals, in order to determine what effect the presence of mercury vapour might have on the accommodation coefficient. In the two experiments, with and without the liquid air, helium was admitted to pressures of 407 and 348 dynes/cm² respectively.

A set of readings was also taken in which the tube containing the wire was immersed in a liquid air bath at 80° K.

These results are shown in Table II.

Table II

Mean temperature of wire in degrees C	1000	800	600	400	200
Accommodation coef. (without mercury)	0.032	0.032	0.031	—	0.035
Accommodation coef. (with mercury)	0.033	0.032	0.032	0.037	0.036
Accommodation coef. (liquid air bath)	0.040	0.040	0.039	0.039	—

With regard to the experiments with and without the mercury there was very little difference in the results obtained. The increase at 100° C was found to be a little more rapid with the mercury present, the accommodation coefficient rising from about 0.042 to 0.096 in 6 minutes as compared with a rise from about 0.033 to 0.068 in the same time without mercury.

With the readings in the liquid air bath, the accommodation coefficient, instead of remaining constant on lowering the mean temperature of the wire to 800° C, was now observed to increase slightly with time at that temperature. At 600° C a more rapid increase was observed. For the readings when the helium atoms striking the hot wire were at room temperature no increase of accommodation with time was observed until the mean temperature of the wire was lowered to 400° C. The difference may possibly be due to the helium atoms being more readily adsorbed, since they have a much smaller translational energy at the temperature of liquid air.

Filament B was now removed and weighed and a fresh piece of wire, filament C, mounted. Results were obtained with this wire before and after heating at 1000° C in oxygen for 48 hours, during which time the mass of the wire, as shown by subsequent weighing, decreased by 8%. The values of the accommodation coefficient before the oxygen treatment were between about 0.060 (at 116° C) and 0.038, and between about 0.044 (at 83° C) and 0.032 after treatment. The same very remarkable decrease in the susceptibility of the wire to contamination was again observed; the accommodation coefficient rising from about 0.044 to 0.052 in 6 minutes, with the wire at 83° C, after treatment as compared with a rise from about 0.06 to 0.18 in the same time, with the wire at 116° C, before treatment.

These values of the accommodation coefficient of helium are of the same order as those obtained with filaments A and B. They are, however, not included in detail as they were less carefully obtained, the main object of the experiments with filament C being to verify the rather surprising action of oxygen.

2 Argon—Using a specimen of argon, 99·5% pure, measurements of the accommodation coefficient were made with respect to filament B after treatment with oxygen. The pressure in the apparatus was first raised to atmospheric for about 2 hours, by admitting dry air, in order to re-grease the taps. The apparatus was then evacuated and, without raising the temperature of the wire above 100° C, a value of 0·748 was obtained for the accommodation coefficient of argon, the argon being admitted slowly, with liquid air on the last trap, to a pressure of 540 dynes/cm². The wire was then heated at 1000° C in a vacuum, argon was admitted and new readings taken, at different temperatures of the wire, without raising the temperature of the wire above 600° C. The results are shown graphically in fig. 4 by the upper set of points. On

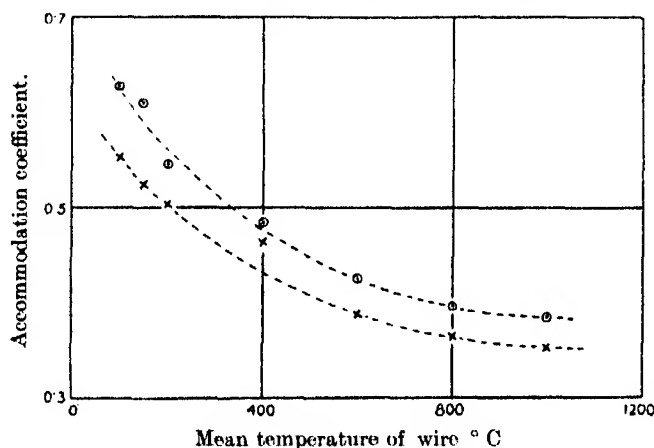


FIG. 4—Argon

raising the temperature to 800° and 1000° C values of the accommodation coefficient were immediately obtained, which are shown. It was found, however, that the accommodation at 1000° C was falling. This fall was followed until a constant value of the accommodation coefficient of 0·355 was reached asymptotically. With a fresh specimen of gas another set of readings at different temperatures was taken. The accommodation coefficient at 1000° C was found to be 0·353 and the complete results are shown by the lower set of points in fig. 4.

It will be observed that the results for argon differ from those obtained for helium in that the accommodation coefficient is not constant for different temperatures of the wire. The rise of the accommodation coefficient in the case of argon, on lowering the temperature of the wire, is, moreover, immediate and does not seem to be due to contamination. Thus for temperatures down

to 400°C there is no increase of the accommodation coefficient with time after lowering the temperature. On lowering the temperature to 100°C there was a slight increase with time which necessitated an almost linear extrapolation to zero time; the value rising, in the second set of results, to 0.558 within 40 seconds, and to 0.579 after 6 minutes. After a further 12 hours the accommodation coefficient had risen to 0.666.

With argon, on account of its large accommodation coefficient, the atoms undergo a considerable change in temperature on impinging with the wire at 1000°C . Whereas with helium the temperature increment was only 30°C with the wire at 1000°C , after the oxygen treatment; the temperature increment with argon, for the same temperature of the wire, is about 350°C . With argon we are, therefore, dealing with a considerably larger range of temperature. It was observed, however, in the experiments with helium that the accommodation coefficient at the temperature of liquid air was approximately equal to that at room temperature. In his last paper, Roberts draws attention to the difference in the temperature variations of the accommodation coefficients of helium and neon atoms with a tungsten surface due to the much larger attractive force exerted by the tungsten surface on an atom of neon. The above results for argon with respect to platinum show, when compared with the results for helium, an even greater variation with temperature which, together with the high value of the coefficient itself, may probably be ascribed to the still larger attractive forces existing in the case of this atom relative to helium.

3 *Mercury*—From the "radiation" readings for the experiments on helium in which the apparatus was evacuated with and without liquid air on the trap between the mercury seals and the wire, it is possible to obtain an approximate value of the accommodation coefficient of mercury. With the apparatus evacuated, the difference in the heat loss from the wire, at mean temperatures of 100° and 200°C with and without mercury vapour, together with the vapour pressure of mercury at room temperature gave values of 1.02 and 0.93 respectively for the accommodation coefficient of mercury vapour. It would appear, therefore, that the accommodation coefficient with respect to mercury vapour is about unity; a variation of 10% is not unduly large, the heat conducted by the mercury being given as the difference between two quantities already small.

4 *Hydrogen*—Using filament A, before making the measurements with helium, results were obtained for the accommodation coefficient of hydrogen. Before attempting to clean the wire, experiments were first performed using

increments of pressure at constant filament temperatures of 100°, 203°, and 367° C, the values of the accommodation coefficient obtained being respectively equal to 0.39, 0.30, and 0.26.

The wire was now heated to 1000° C in order to clean it. The behaviour in hydrogen was exceptional, however, as the wire appeared to absorb hydrogen at 1000° C. Thus, even though the wire might be rid of all other contamination at this temperature, a minimum value of the accommodation coefficient could not be obtained owing to the fact that hydrogen itself was apparently absorbed by the wire. Thus with hydrogen in the apparatus at a pressure of 381 dynes/cm² the mean filament temperature was set at 1021° C. During a period of 50 hours at this temperature the accommodation coefficient fell from 0.257 to a constant value of 0.112; the fall during the last 4 hours being from 0.113 to 0.112. On lowering the temperature of the wire from 1021° to 813° C, however, the accommodation started to decrease still more. This decrease was followed until, after 18 hours, the accommodation had again reached a practically constant value. At the end of this period the temperature of the wire was raised, for 90 seconds only, to 1021° C and then lowered again to 813° C. The accommodation at 813° C was found to have been increased so much by this that it required a further 4 hours heating at 813° C to reduce the accommodation once more to its previous minimum value at that temperature. The most reasonable conclusion seems to be that platinum at a temperature of 1000° C absorbs hydrogen.

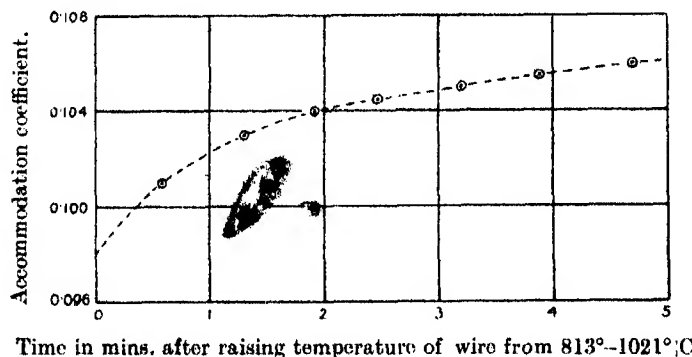


FIG. 5—Hydrogen

After cleaning the wire at 813° C readings were obtained at different lower temperatures of the wire and, lastly, at 1021° C; a rise of accommodation with time was always observed. The time variation of the accommodation coefficient, with the wire at 1021° C, is shown in fig. 5. It was observed that,

while the accommodation coefficient, with the wire at 104°C , rose from 0.11 to nearly 0.15 in 2 minutes, it required only a few minutes heating at 813°C to reduce the accommodation coefficient to its previous value at 813°C . On the other hand, the contamination, after the wire had been heated at 1021°C , was much more difficult to remove, requiring some 4 hours heating at 813°C . These results indicate that, at lower temperatures, the contamination is due to adsorption, while at 1000°C , in hydrogen, the process is one of absorption.

The values (extrapolated to zero time) obtained at different filament temperatures are shown in fig. 6. While it cannot be certain that there is

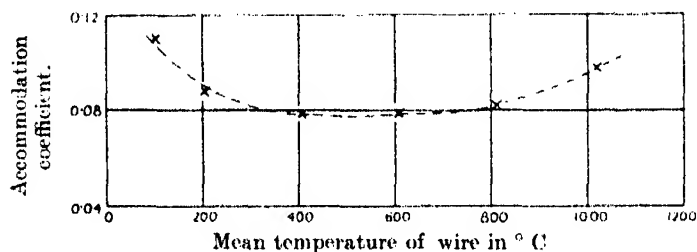


FIG. 6—Hydrogen

no absorption at 813°C it seems reasonable to assume that this effect is small and that the results are representative of a clean wire. They may at least be said to represent the upper limit for the accommodation coefficient of hydrogen with a clean platinum surface and, therefore, show that the values obtained by Rowley and Bonhoeffer* are probably about 100% too great. This is not surprising in view of the fact that the time for which they heated their wire, in order to clean it, seems to be little over an hour, the wire being "glowed" in oxygen for half an hour of that time.

As, with a polyatomic gas, the internal energy of the molecules bears a different ratio to the translational energy at different temperatures, the molecular heat conduction is no longer an exactly linear function of the temperature difference. To evaluate the accommodation coefficient for hydrogen, and later also for oxygen, it has been necessary to calculate the actual mean temperatures of the molecules leaving the wire. For this purpose values of the ratio of the specific heats at different temperatures have been obtained from the 'International Critical Tables' (vol. 5, p. 82). The values of the accommodation coefficient given are thus the ratios of the actual to the possible changes of kinetic energy, as distinct from the changes of total energy of the molecules.

* 'Z. phys. Chem.,' B., vol. 21, p. 84 (1933).

5 *Oxygen*—With oxygen at a pressure of 573 dynes/cm² a value of 0.43 was obtained for the accommodation coefficient with respect to filament B at 1000° C. The wire was then left at this temperature for about 20 hours, at the end of which period the wire had decreased in mass by about 5%. The coefficient at 950° C was now found to be 0.44. With a fresh specimen of oxygen, distilled from oxygen which had been liquefied, at a pressure of 540 dynes/cm² a series of readings at different temperatures was obtained. A value of 0.45 was obtained at 1001° C, and the complete results at that and other temperatures are shown plotted in fig. 7. At all temperatures, with the exception of 100° C, no increase with time was observed. At 100° C the increase was from 0.555 at 15 seconds to 0.585 after 6 minutes.

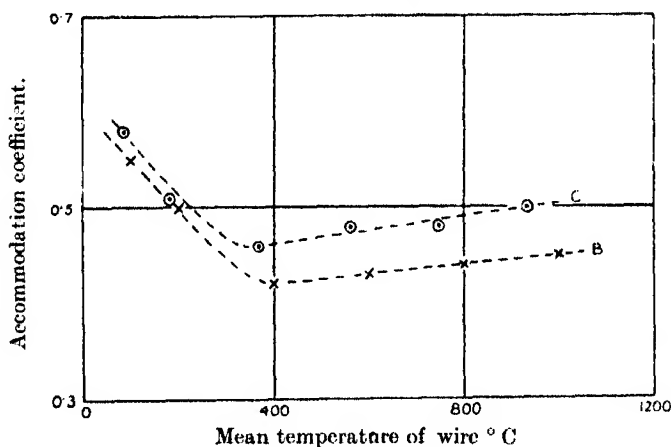


FIG. 7—Oxygen

With filament C slightly higher results, shown by the upper set of points in fig. 7, were obtained. This would correspond to a rougher surface of the wire. In this set, too, there was no appreciable increase with time until the temperature was lowered to 83° C, the accommodation coefficient at 181° C increasing by only two parts in five hundred in 5 minutes, while at higher temperatures it was constant.

The Radiation Heat Loss

Aschkinass* has shown that the energy radiated from a conductor at a temperature T_1 ° K, the surroundings being at a temperature of T_2 ° K, should be given by an equation of the form:—

$$Q_r = k (\sqrt{s_1} T_1^{4.5} - \sqrt{s_2} T_2^{4.5}),$$

* 'Ann. Physik,' vol. 17, p. 960 (1905).

where s_1, s_2 are the specific resistances of the conductor at the temperatures T_1, T_2 ° K. I have found that this relation agrees quite well with experiment over a very wide range of temperature. Slightly better agreement is obtained over a wider range of temperature if the absolute temperature be raised to the power of 4.6 instead of 4.5. In Table III the observed radiation is compared with values calculated by means of a relation of the type given using both 4.5 and 4.6 as the index.

For platinum the radiation heat loss may be best expressed in the form :—

$$Q_r = k' (\sqrt{1 + \alpha \cdot pt_1} T_1^n - \sqrt{1 + \alpha \cdot pt_2} T_2^n),$$

where pt is the temperature on the platinum scale and α is the temperature coefficient of resistance. The constant k' seemed to be dependent to a slight extent upon the condition of the wire. For the results shown in Table III the values taken for k' were 2.180×10^{-15} for $n = 4.5$ and 1.066×10^{-15} for $n = 4.6$. Both these values involve the surface area of the wire, which was equal to 0.1544 cm^2 .

Table III

Mean temperature of wire (° C)	Observed radiation, in watts	Calculated radiation, in watts ; $n = 4.5$	Calculated radiation, in watts $n = 4.6$
100.3	0.000580	0.000687	0.000613
150.7	0.00137	0.00154	0.00139
200.2	0.00265	0.00289	0.00263
400.1	0.0179	0.0181	0.0170
599.8	0.0672	0.0663	0.0639
799.6	0.186	0.184	0.181
999.3	0.427	0.427	0.427
997.6	0.429	0.424	0.424
1200.6	0.868	0.876	0.888

The first seven readings shown in the table were taken with filament B immediately before the second set of results for argon, while the last two readings were obtained 9 days earlier just after the wire had been acted upon by oxygen.

The constant k' is calculated from the observed radiation for a mean temperature of the wire equal to 999.3°C . In the radiation calculations the value of the absolute zero has been taken as -273.2°C .

In conclusion, I wish to express my gratitude to Professor Martin Knudsen for his help in permitting me to carry out the above research in his laboratory. My thanks are also due to the University of London for the award of a travelling studentship which made it possible for me to go to Copenhagen.

Summary

Using wires of pure platinum the following results have been obtained for the accommodation coefficients of different gases with respect to the clean wire :—

Helium—0·03 at room temperature and 0·04 at 80° K for a range of mean filament temperatures between 100° and 1000° C.

Argon—At room temperature, 0·55 to 0·35 for mean filament temperatures between 100° and 1000° C. respectively.

Mercury vapour—At room temperature about unity for mean filament temperatures of 100° and 200° C.

Hydrogen—At room temperature between 0·11 and 0·08 for mean filament temperatures between 100° and 1000° C.

Oxygen—At room temperature, between 0·42 and 0·55 for mean filament temperatures between 100° and 1000° C.

These results refer for every gas, except hydrogen, to the same wire, filament B.

From the results it would seem natural to conclude that the process of contamination is one of adsorption. From the effect of oxygen it would appear that contamination of the wire is dependent, not so much on the residual impurities which may be present in the gas, but more on the actual nature of the surface of the wire. Thus the adsorbing properties of the surface in two samples of the same specimen of helium were quite markedly changed by a process somewhat analogous to etching.

With hydrogen the accommodation is increased at higher temperatures by absorption.

The removal of the initial contamination takes several hours at wire temperatures of 1000° C, the last traces being removed very slowly. Once removed the wire again becomes contaminated if its temperature be reduced to, say, 100° C. This causes the accommodation to increase, at first very rapidly and then more slowly.

The experimentally observed temperature variation of the energy radiated from the wire has been compared with theoretical relations.

The Freezing Point of Platinum

By F. H. SCHOFIELD, B.A., D.Sc., Physics Department, National Physical Laboratory, Teddington, Middlesex

(Communicated by Sir Joseph Petavel, F.R.S.—Received May 9, 1934)

I—Introduction

The International Temperature Scale, which has been in force since 1927,* is based on certain values assigned to the boiling and freezing points of pure substances and on specified means of interpolation between, or extrapolation beyond, these points. The highest basic point of the scale is the freezing point of gold, defined as $1063\cdot0^{\circ}\text{C}$, while for extrapolation from this temperature use is made of the Wien law of radiation, with a certain value of the constant C_2 . Though any temperature above 1063°C is thus completely defined without reference to further fixed points, determinations of such points are of considerable value. In particular, they serve to indicate the degree of reproducibility of the scale by the various users of it, and, when well authenticated, to provide secondary standards for its realization. Of such fixed points the most important has been the freezing point of palladium (1555°C), but the latest developments in furnace technique and refractory materials should now enable the freezing point of platinum to be used with equal, if not greater, advantage. The qualities of platinum which render it especially valuable in this connection are as follows: its freedom from oxidation; its high standard of purity, for which a convenient electrical test is available; its high freezing point (about 1775°C) which approaches the important zone of temperature covered by the electric lighting industry. These qualities also make the platinum point especially suitable as the basis for a standard of light, as has been proposed by a number of experimenters.

It is with the two objects indicated above that the National Physical Laboratory has undertaken an investigation concerning the freezing point of platinum, the precise scope of which may be defined as follows:—

- (1) To determine the value of the freezing point in terms of the International Temperature Scale.

* 'Trav. Mem. Bur. Int. Pds. et Mes.,' vol. 18, p. 94 (1927).

- (2) To obtain evidence as to the suitability of the specification proposed by the Bureau of Standards, U.S.A., for a Primary Standard of Light based on the freezing point.

Both objectives involve measurements of radiation from a black body held at the temperature of freezing platinum, but, whereas for the purposes of the second, the black body has to be realized under strictly defined conditions, no such limitation applies to the first objective. The procedure adopted has been to set up a radiator in accordance with the proposed specification and to try modifications suggested by the experience gained. The present paper is concerned with the furnace arrangements, the setting up and modification of the radiators, and the other factors involved in the determination of the freezing point. The same apparatus was used, for their observations on the proposed standard of light, by the Photometry Division of the Electricity Department, who will deal with this subject in a subsequent paper.

II—*Method of Experiment*

According to the International Temperature Scale any temperature t , above the freezing point of gold (1063°C), is determined by means of the ratio of the intensity J_2 of monochromatic visible radiation of wave-length λ cm, emitted by a black body at the temperature t , to the intensity J_1 of radiation of the same wave-length emitted by a black body at the gold point, by means of the following formula, derived from the Wien equation

$$\log_e \frac{J_2}{J_1} = \frac{C_2}{\lambda} \left[\frac{1}{1336} - \frac{1}{(t + 273)} \right],$$

the constant C_2 being taken as 1.432 cm degrees. Though the definition refers to monochromatic radiation, the common practice is to use for the temperature measurement a pyrometer of the disappearing filament type fitted with a red glass transmitting a comparatively wide band of radiation. As is well known the "effective wave-length" of such a glass for any temperature interval, *i.e.*, the wave-length to which the above formula is strictly applicable, can readily be calculated from the spectral transmission of the glass and the visibility curve of the eye.

Having obtained the effective wave-length, the process of temperature measurement consists in determining the ratio J_2/J_1 . For moderate temperatures this is done by employing a rotating sector disc of such aperture as will

out down the radiation from a black body at the higher temperature to match in intensity the radiation from a black body at the gold point.

For the freezing point of platinum, however, this ratio, for a wave-length of 0.66μ , is of the order of 300 to 1, so that if a sector disc with two symmetrically placed apertures* were used, each aperture would only be 0.6 degrees of angle. The cutting of such an aperture with the requisite precision and its measurement to an accuracy of at least 1 part in 500, or 4 seconds of arc, would be a matter of great difficulty.

Consequently it is convenient to carry out the reduction in intensity from the platinum to the gold point in two stages. This allows of the use of sectors of considerable aperture which are easily constructed and measured. It is true that the double set of observations would tend to a decrease in precision. Against this it may be mentioned that, with a pyrometer of normal construction, the field intensity most favourable to accurate observation lies considerably above the gold point. Hence, by choice of an appropriate sector, the observations, which are most limited in time, namely, those on the black body at the platinum point, can be taken at a favourable intensity, while unlimited time is available for those at less favourable intensity. On the whole, therefore, considerable advantage accrues from the system of two-stage reduction of the platinum point.

The several processes involved in a determination of the freezing point of platinum may now be summarized.

1—The determination of the spectral transmission of the red glass and calculation of its effective wave-length for the two ranges.

2—The construction and measurement of two sector discs of such apertures that the product of their transmissions gives approximately the ratio of radiation intensity of black bodies at the gold and platinum points for red light of about 0.66μ .

3—The setting up of a black-body radiator at the freezing point of platinum and the measurement of the current through the pyrometer lamp required to match the intensity of the radiator as reduced by the rotation of one of the sector discs.

4—The adjustment of another radiator to such temperature as will, without the interposition of a sector, require approximately the same current as in 3 to give a match with the pyrometer lamp.

* It is advantageous to use two apertures since they are self-compensating for errors in centring and require a lower speed to eliminate flicker.

5—The measurement of the current through the pyrometer lamp required to match the intensity of the radiator, referred to in 4, as reduced by the rotation of the second sector disc.

6—The setting up of a black body radiator at the freezing point of gold and the measurement of the current through the pyrometer lamp required to match the intensity of this black body.

It is not necessary that the operation 4 should give exactly the same current as 3 since corrections for small departures can readily be determined ; similarly it is not necessary that the combined effect of 4 and 5 should give exactly the same current as 6.

III—*Apparatus*

1—*The Optical Pyrometer*—The optical pyrometer used in the investigation was of the disappearing filament type of Holborn-Kurlbaum. It calls for no detailed description since its main features follow those of the instrument developed at the Nela Research Laboratory with improvements based on the work of Fairchild and Hoover. Thus use was made of their type of lamp, which has a cylindrical envelope provided with flat ends designed to allow the filament and object to be viewed at high magnification without distortion. It may be added that the filament employed had a diameter of 0.05 mm and that with diaphragms giving angles of 0.054 and 0.022 radians on the objective and eyepiece sides of the lamp respectively, a satisfactory disappearance of the filament was obtained.

The red filter used in the eyepiece of the pyrometer was of the Corning Glass, known as "high transmission red 50%," and was 6 mm in thickness. Its effective wave-length was calculated in the usual way* from the spectral transmission† of the glass and the visibility curve for the eye, taking for this latter the agreed international data.‡ As is well known, the effective wave-length varies with the temperature of the glass itself, so that a correction has to be applied to any readings obtained with a sector on account of the variations in atmospheric temperature. The magnitude of this correction increases with a decrease in the transmission of the sector. It so happened in the present investigation that the observations with the sector of smaller transmission had to be taken in a laboratory subject to wide changes in temperature and it

* For a specimen calculation see Fairchild, Hoover, and Peters, 'Bur. Stand. J. Res.,' vol. 2, p. 951 (1929).

† This was determined by the Optics Division, National Physical Laboratory.

‡ 'C. R. Comm. Int. Eclairage,' p. 67 (1924).

was thought well, therefore, to control the temperature of the glass at the maximum likely to be reached, about 25°C . For this purpose the screw-on cell for attaching the red glass to the pyrometer was provided with a water circulation which could be maintained at the required temperature.

Another point which may be mentioned in connection with the pyrometer was the use of a totally reflecting prism. Normally this formed an integral part of the instrument, being attached to the end of the objective tube in such a way that the prism had one face always normal to the axis of the tube but that it could be rotated about this axis so as to allow the sighting of the pyrometer in a vertical, horizontal, or intermediate direction. Except where otherwise stated, all observations were taken with the prism attached to the pyrometer as indicated.

2—Rotating Sectors—As already stated, the reduction in intensity from the platinum to the gold point was effected in two stages. The intermediate temperature could, of course, range over wide limits and the considerations governing its choice in the present work were as follows. In addition to determining the platinum point (about 1773°C) in terms of the gold point it is useful to correlate its value with that for the palladium point (about 1555°C). A single sector could be used twice over to determine either of these points in a two-stage operation and the intermediate temperatures would then be 1340°C for platinum and 1270°C for palladium. It is obvious, therefore, that if either of these temperatures were chosen for the intermediate point, a total of two sectors would enable both the platinum and palladium points to be determined by the two-stage method in terms of the gold point and in relation to each other. In view of the simplification which could thus be obtained and of the fact that the temperatures in question were in a region giving a comfortable brightness of field in the pyrometer, it was decided to work at one of the temperatures and the choice was given to 1270°C . Two sectors were, therefore, constructed, one giving a reduction from 1773°C to 1270°C , and the other from 1270°C to 1063°C , the latter to be used subsequently for a determination of the palladium point. The sectors were cut from aluminium discs 0.5 mm thick and 39 cm in diameter, and were in pairs of approximately equal angles and situated opposite to each other. The peripheries of the discs were not cut through and the risk of damage to the edges was thereby diminished. The edges were trued against a radial jig and were covered with a thin layer of dull black paint.

The angular apertures of the sectors were determined by measurement of chord and radius as magnified by a simple lever system. For this purpose the

disc was clamped to a flat steel strip, 1.5 metres in length, so as to be concentric with a pivot situated near one end of the strip and about which it could be rotated in a horizontal plane. A microscope having its axis approximately vertical was sighted with its cross wires on one edge of the aperture to be measured and the lever was rotated until the second edge came under the cross wires. The resulting movement of a mark on the remote end of the lever, situated at a known distance from the centre of rotation, was measured by means of a travelling microscope. The arrangement gave about an eight-fold magnification.

With this apparatus no difficulty was experienced in measuring the apertures, even of the smaller sector, to 1 part in 1000. As a check on the absence of reflection from the painted edges of the sector, the transmission of the sector of smaller aperture was compared in the pyrometer with that of a sector, of about the same opening, prepared by mounting knife edges on an aluminium disc to form the apertures. The calibrations of the two types were found to be consistent to within the limits of observation. For prolonged series of readings the comparative absence of noise with a plain disc is a considerable advantage and this type was used throughout the investigation.

3—*Black-body Radiators at Platinum Point*—As already indicated, the investigation has been largely concerned with radiators set up in accordance with the specification* recommended by the Bureau of Standards for the realization of a black body at the freezing point of platinum for the purposes of a primary standard of light. The general design of the radiator will be understood by reference to fig. 1 which shows a section of it mounted in a furnace as used in the present investigation. The following are some of the main points of the specification :—

- (1) The crucible, etc., to be of material which does not contaminate platinum (*e.g.*, thoria) and the thermal insulation to be of the same material.
- (2) The dimensions of the several parts to be as follows: internal diameter of crucible at top 22 ± 2 mm, and at bottom 17 ± 2 mm; internal height of crucible 45 ± 5 mm; inside diameter of sight tube 2.5 ± 0.2 mm; wall thickness of sight tube 0.25 to 0.5 mm; opening in cover at least 0.8 mm less than internal diameter of sight tube; depth of powder in sight tube 10 to 15 mm.
- (3) Platinum to be of such purity as to give an α coefficient of at least 0.390.

* 'Rep. Com. Consult. d'Electr., Bur. Int. des Pds. Mes.,' p. 178 (1930).

- (4) Electromagnetic heating to be used, freezing points only to be taken and power supply to be so controlled as to give a constant intensity for 3 minutes during the freeze.

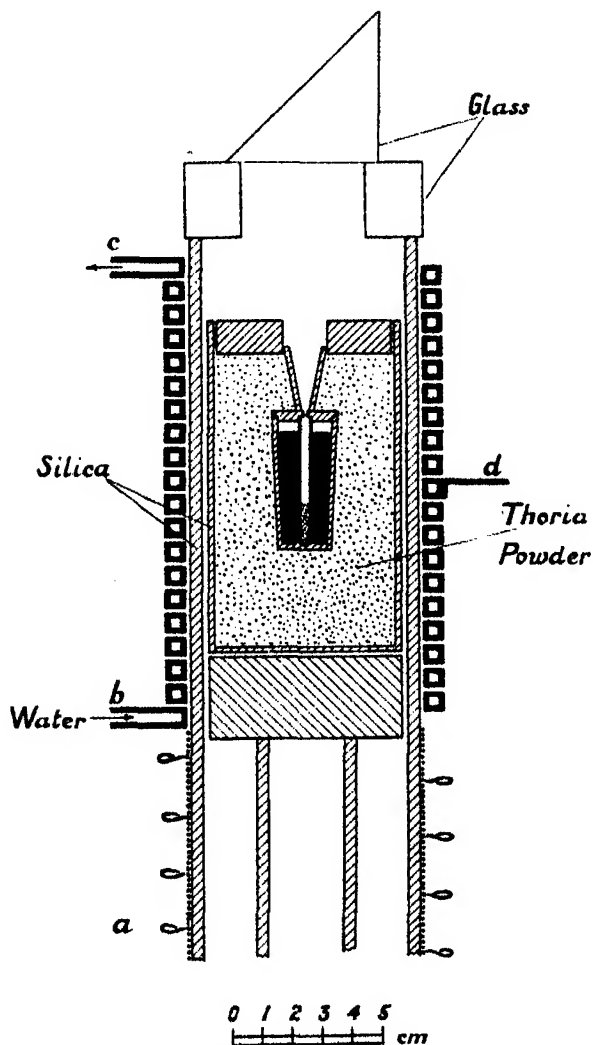


FIG. 1.—Furnace assembly for platinum melting point with B.S. crucible

It is convenient at this stage to point out the slightly divergent objects of the two investigations undertaken at the Laboratory in relation to the above-mentioned specification. The investigation on the Standard of Light was concerned primarily with the reproducibility of the standard defined by the detailed specification and only secondarily with the question whether that

standard complies with the conditions required of a black-body radiator. On the other hand, the determination of the freezing point depends fundamentally on the realization of a black body, no matter how obtained, and the specification has to be considered only from this point of view.

Unfortunately no simple test is available for compliance with black-body conditions. It is therefore necessary, for this purpose, to rely on such indirect evidence as the constancy of the results obtained at the freezing point under variation in the conditions of experiment, *e.g.*, in the rate of cooling and the amount of induced undercool, the constancy of the results obtained at the melting point, and the agreement between the freezing and melting points. In the present work there appeared to be a small but definite difference between the values of the melting and freezing points obtained with the specified apparatus shown in fig 1 and it was thought advisable to try some modifications of that assembly. Assuming the most likely cause of the difference to be a departure from black-body conditions due to a longitudinal gradient of temperature in the sight tube, it was considered that such an effect might be produced either by the tapering of the ingot resulting in a differential effect in the inductive heating, or by the fact that the direction of maximum heat loss was obviously upwards. Effects of this description could, of course, be additive or subtractive, and were probably the latter in the present instance.

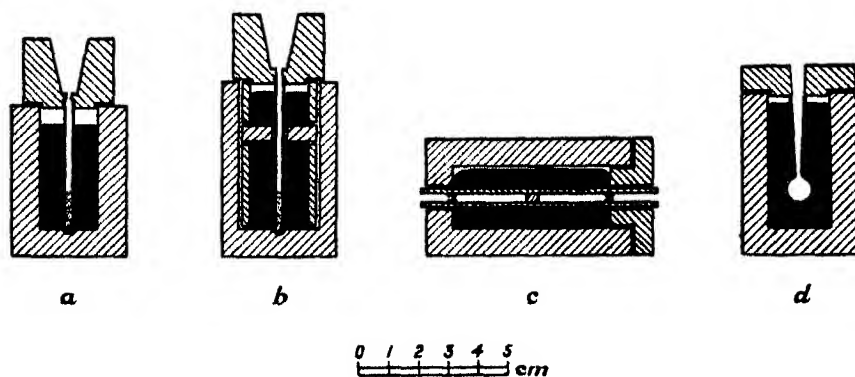


FIG. 2.—Modified crucible assemblies for platinum melting point

In the modification shown in fig. 2 (a), the radiating tube and top are similar to those in fig. 1, but the crucible is made strictly cylindrical in form, so as to eliminate the supposed unequal heating of the ingot. In fig. 2 (b) the ingot is shown divided by a horizontal partition of refractory material, with the idea of modifying, and perhaps reducing, the upward conduction of heat.

Both of these modifications gave satisfactory results, which are summarized later in this paper.

It is perhaps of interest to mention two other modifications which did not prove to be successful. In the first of these, fig. 2 (c), the attempt was made to eliminate temperature gradient in the central region of the radiator on which the pyrometer was sighted, by a symmetrical arrangement giving equal heat loss from the two ends. It is obvious that, other things being the same, the ingot would have to be longer with this arrangement than with assymetric arrangements such as those in figs. 1 or 2 (a), and further that the ingot is most conveniently placed with its axis horizontal. The use of the assembly, shown in fig. 2 (c), had been suggested as the result of promising experiments on a similar arrangement of a gold ingot, heated in a resistor furnace, and also those on a very small platinum ingot, $\frac{1}{4}$ inch in diameter and $\frac{3}{4}$ inch in length, heated inductively. This latter ingot was contained in a crucible of alumina and had a sight tube of alumina glazed on the outside by partial fusion.* The bore of the sight tube was 1 mm and the object sighted on was a tiny fragment of alumina at its centre. This assembly gave passable melting points, having a duration of halt of from 1 to 3 minutes, and values of the same order as those obtained with larger scale apparatus. The freezing points were less satisfactory owing to the tendency of the undercool to obscure the halt though this defect could no doubt have been minimized by taking special measures to eliminate the fluctuations in the supply voltage so as to allow a finer regulation of the rate of cooling. However, it was obviously desirable to work on a larger scale and the assembly shown in fig. 2 (c) was accordingly tried. In the first trial the crucible had a cavity at the top, not shown in fig. 2 (c), containing an extra piece of platinum which it was hoped would melt and fill the crucible to its full capacity. Unfortunately this extra piece did not entirely coalesce with the ingot and the irregular shape seems to have resulted in unsatisfactory curves being obtained for the six freezes observed. Finally the experiment broke down through the gradual bending upwards of the middle of the tube, under the hydrostatic pressure, so as to render the sighting unsatisfactory. The tube in this case was of thoria 2.5 mm in bore and 0.25 mm in wall thickness. The results were considered to be sufficiently promising to justify a second trial with a tube of the same bore but 1 mm in wall thickness. However, a breakdown again occurred through the bending of the tube and the method was accordingly abandoned.

* See description of process by Adcock and Turner in 'J. Sci. Instr.', vol. 7, p. 327 (1930).

The other arrangement, fig. 2 (*d*), has been successfully used at lower temperatures,* but in the present work it yielded curves of unsatisfactory form on the only occasion on which it was tried. The reasons for failure were not explored; probably heavy gradients were induced in the ingot by radiation from the conical surface above the bulb. The arrangement is only mentioned here because of the possible interest attaching to the refractory material used. The bulb and tube, fig. 2 (*d*), were made in one unit of pure alumina by means of a process described by Mr. Turner in the note on refractory materials appended to this paper. When heated to about 1950° C in the molten metal the material of the radiator re-crystallized into the translucent form which has great mechanical strength. It was noteworthy that, at the conclusion of the experiments, the radiator was withdrawn from the molten metal and exposed immediately to the atmosphere without fracture occurring.

The following comments may be added with regard to the refractories used for melting platinum. Except where otherwise mentioned, these were of pure thoria. The crucible assemblies of the form of fig. 1 were made at the Bureau of Standards from thoria fused by a special process as described by Swanger and Caldwell,† and the other assemblies in the Metallurgy Department of the Laboratory from shrunk thoria as described in Appendix I. The behaviour of the two types did not seem to be very different and examples could be quoted of prolonged usage with each. Thus one of the shrunk thoria type, fig. 2 (*a*), was intact when it came to be broken up after some 50 melts while one of the fused thoria type, fig. 1, actually survived 300 melts. No cracks were observed in the former type of crucible, which was thick-walled, but they seemed prone to develop in the thinner-walled type of fig. 1. The most common cause of failure in both kinds of assembly arose from the particular manner of anchoring the sight tube by fitting it into recesses in the lid and the base of the crucible as recommended in the proposed specification for the Standard of Light. Any imperfection of fit, or differential shrinkage of the crucible and the tube, was liable to cause the latter to shift in position if not to come adrift. The main cause of failure with both types being as stated, it might be preferable to adopt a closed-end sight tube rigidly attached to the lid.

4—*Black-body Radiators at the Gold Point*—With gold, as with platinum, the ingot method provides the best means for realizing a black body at the freezing

* Hoffmann and Meissner, 'Ann. Physik,' vol. 60, p. 201 (1919), also Schofield, 'Proc. Roy. Soc.,' A, vol. 125, p. 517 (1929).

† 'Bur. Stand. J. Res.,' vol. 6, p. 1131 (1931).

point. A much wider range of experimental conditions is, however, practicable at the gold point. This feature is of value in that it provides a possible means for detecting systematic error inherent in the platinum determinations, since those at the gold point can be made both with and without the restrictions applying at the higher temperature. Accordingly, a series of measurements was carried out, for the purposes of the present investigation, with a gold ingot assembled as shown in fig. 2 (a) and heated by means of the longer coil employed for most of the experiments on platinum (see 6, p. 803). In addition a large number of experiments have been made with ingots heated in ordinary resistor types of furnace. The use of such a furnace has the advantage over inductive

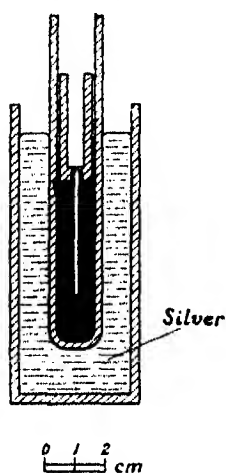


FIG. 3—Crucible assembly for gold melting point in resistor type furnace

heating as a finer control is possible at the change point since the alteration of electrical resistance on melting of most metals, including platinum and gold, does not, as in the inductive system, tend to accelerate the process of melting or freezing. Further, the provision of special means for attaining temperature uniformity can more readily be made in the resistor type of furnace.

As already mentioned a gold ingot assembled as in fig. 2 (c) was used in a resistor furnace and this gave satisfactory melting and freezing curves so long as there was an absence of longitudinal temperature gradient at the centre of the ingot. To prove the absence of gradient involves, however, the somewhat laborious process of taking simultaneous observations with two pyrometers sighted into opposite ends of the radiator and fortunately an alternative method of securing the desired uniformity came to light as a result of a parallel investigation* into the melting point of gold by means of platinum thermocouples. It was then shown that a high degree of temperature uniformity could be secured by the expedient of interposing a bath of silver between the ingot of gold and the furnace tube and this arrangement was accordingly adopted for the purposes of the present investigation in the manner indicated in fig. 3. The radiator shown consists of a fireclay tube which is cemented into a block of "mabor" material resting on the surface of the gold ingot. The ingot is contained within a "pythagoras" tube which is immersed in a bath of silver, the whole being inserted into a tubular furnace (not shown in the figure) which was wound with platinum ribbon.

* An account of this investigation will be published in due course.

5—*Radiator at Intermediate Temperature* (1270°C)—Any hot object having the required brightness temperature, in this case about 1270°C , could apparently be used for the purposes of the operations 4 and 5 described in Section II above, irrespective of its spectral distribution of energy. It was found convenient to employ a radiator similar to that at the gold point (see fig. 3) but without the supplementary silver bath. This assembly was inserted into a resistor furnace and maintained at a steady temperature, as indicated by a thermocouple fixed beside the crucible, over the period required for the taking of the observations with and without the sector.

6—*High Frequency Induction Furnace*—In heating all the ingots the high frequency induction furnace designed by Bell* was employed, some modifications† being made to meet the particular requirements of the investigation. Thus for the anode coil ba ‡ it was found advantageous to use an air-cooled coil consisting of 50 turns of cotton-covered copper wire of 18 gauge spaced at 16 turns to the inch and provided with tapings at each fifth turn. The coil was covered with bakelite paint and was air-cooled by fans. For the main heating coil, bc , two arrangements were used each consisting of $\frac{1}{4}$ inch square section copper pipe with water cooling, one coil having 14 turns in a length of $5\frac{1}{2}$ inches and the other 20 turns in a length of $6\frac{3}{4}$ inches. The power condensers used were of 0.003 and 0.005 microfarads respectively.

IV—Measurements

In this section the observations at the gold point, the intermediate point (1270°C) and the platinum point are dealt with in order of rising temperature. A single pyrometer lamp of known constancy was used throughout the investigation, and occasional comparisons with other lamps showed no appreciable change in its calibration. All the measurements were made by two observers whose readings were in close agreement, and the values given below represent the mean of their observations.

At Gold Point—As already explained, two types of assembly were used for the determination of the freezing point of gold, namely, that shown in fig. 2 (a), which was heated inductively, and that shown in fig. 3, which was heated in a resistor furnace. Examples of freezing and melting point curves, obtained with the two types of apparatus, are plotted in fig. 4. The ordinates are

* See 'Proc. Phys. Soc.', vol. 40, p. 193 (1928).

† Suggested and carried out by A. Grace.

‡ The lettering in fig. 1 agrees with that of figs. 3 and 4 of Bell's paper.

pyrometer readings expressed in terms of temperature as derived from the mean reading of all the freezing points taken as 1063.0°C . Differences in reading can readily be estimated from the fact that individual observations are represented as circles of radius 0.5°C . It will be noted that in inductive heating the melting point curve shows a comparatively short halt. This was characteristic of the series and apparently arises from the considerable increase

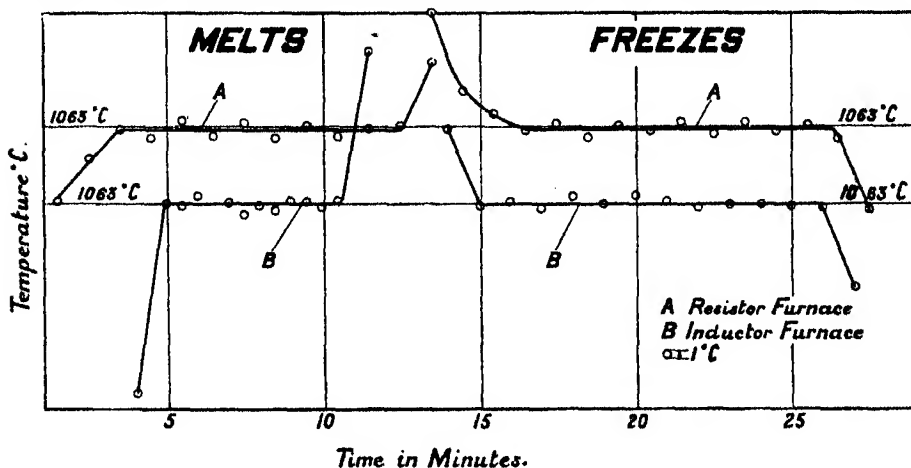


FIG. 4—Examples of curves for melting and freezing points of gold. Mean of all freezing points taken as 1063°C .

of electrical resistance of gold on melting. The results of all the experiments are summarized in Table I.

It will be seen that the mean values of freezing point given by the two methods are indistinguishable, while the mean values of the melting point in the two methods are respectively higher and lower by 0.2°C than the mean freezing points. These differences though small appear to be quite definite.

Table I—Calibration of Pyrometer at Gold Point—Pyrometer readings expressed in temperature relative to the mean of the readings for all the freezing points taken as 1063.0°C .

Assembly	Melting points				Freezing points			
	No.	Average deviation of, from mean	Mean	Probable error of mean	No.	Average deviation of, from mean	Mean	Probable error of mean
		$^{\circ}\text{C}$	$^{\circ}\text{C}$	$^{\circ}\text{C}$		$^{\circ}\text{C}$	$^{\circ}\text{C}$	$^{\circ}\text{C}$
Fig. 2 (a)	26	0.4	1062.8	± 0.08	27	0.2	1063.0 ₁	± 0.04
Fig. 3	24	0.2	1063.2	± 0.03	25	0.2	1062.9 ₆	± 0.04
		Mean	1063.0			Mean	1063.0	

It may be added that the mean value taken for the freezing point is based on some 400 individual observations.

At Intermediate Point (1270° C)—Over 350 individual observations were taken for the purpose of linking the intermediate temperature with the gold point. They do not call for any special comment.

At Platinum Point—Before dealing with the measurements on which the actual determination of the freezing point depends it may be of interest to refer to certain preliminary experiments.

At the commencement of the investigation it was thought that, since both the work on the freezing point and the standard of light involved the use of right-angled prisms to reflect the radiation from the black body in a horizontal direction, it would be convenient to adopt a common form of mounting for the prism. This mounting is shown in fig. 1. It will be seen that the prism rests on two bars of glass which span the end of the furnace tube. A slow stream of air was blown through the gap between the glass bars in order to cool the prism. This arrangement was, however, found to be unsatisfactory for two reasons. In the first place there was the possibility of error owing to the axis of the pyrometer not being normal to the face of the prism, which might result in an appreciable loss of light. An optical test was devised to check the correctness of adjustment in this respect, but was found to be somewhat troublesome to apply in conjunction with other necessary adjustments of the pyrometer. A second and more serious source of error came to light during the course of the investigation, namely, the deposit of a slight film on the face of the prism nearest the furnace. The material of this film was not identified, but it seems not improbable that it consisted of platinum.* When the film was present its absorption no doubt caused a lowering in the apparent value of the freezing point which in one extreme case amounted to 5° C. On discovering the presence of film the attempt was first made to prevent it, by greatly increasing the strength of the draught on the exposed face of the prism, but this was found to lead to error owing to the cooling of the radiator. Subsequently resort was had to cleaning the prism before commencing observations on each melt and freeze, but finally the apparatus was re-arranged so as to allow the prism to be fixed to the pyrometer tube as previously described. In this

* Incidentally it may be mentioned in support of this view that after being maintained for some hours near the melting point, the inner surface of the cone (see figs. 1 or 2) was found to have a deposit of platinum which apparently could have reached this position only by vapourization.

position it was situated at 14 inches from the top of the furnace and no further difficulty with the formation of a film was experienced.

Another point dealt with in the preliminary work was in relation to the two induction coils described in Section III 6 above. The first experiments were made with the short coil, and gave freezing points which were higher by 1°C or 2°C than the melting points. It was considered that possibly this difference might be due to lack of uniform heating caused by variations in the strength of the inductive field covering the ingot. Observations were accordingly taken with the ingot in various positions inside the longer coil. It was found that the values of the freezing and melting points remained sensibly constant for movements of the ingot of about 1.5 cm from the central position. Though the experiments indicated that the shorter coil was probably adequate in length, the longer coil was, in fact, used for most of the experiments.

Turning now to the definitive observations, we give in fig. 5 the whole of the readings taken in a single series of experiments, in order that an idea may be formed of their general characteristics. This set has been chosen for illustration because it represents the greatest variation of conditions in a consecutive batch of experiments. Thus it will be seen that there was a variation of the order of two to one in the duration of melt or freeze and that in the latter the magnitude of the undercool ranges from zero to 70°C . Attention may also be drawn to the following points: the "spread" of the observations, from their mean values, averages less than $\pm 1^{\circ}\text{C}$; the values of melting or freezing point seem to be independent of the duration of the halt and the value of the freezing point also independent of the amount of undercool; the curves for the melts were superior to those of the freezes in sharpness of breakaway at the end of the halt.

Observations of melting and freezing points were taken on five separate ingots. The data used for calculating the absolute values are given in Appendix II and the results obtained are summarized in Table II. It will be observed that the table is divided into two parts according as the ingot is cylindrical (see fig. 2) or tapered (see fig. 1), the object of adopting this division being to throw light on the possibility of systematic difference between the two types. In the result no such difference was found and each form gave satisfactory curves.

The data in Table II may be supplemented by the following information:

Cylindrical Ingot C.1—The curves for melt and freeze were of about equal quality, the latter being somewhat better than those in fig. 5. No undercools of any magnitude were recorded.

With regard to the comparatively large drop in the value of R_{100}/R_0 which occurred with this ingot, it may be mentioned that the process of purifying the shrunk and ground thoria, used for making crucibles, was improved after the experiments with this ingot (see Appendix I).

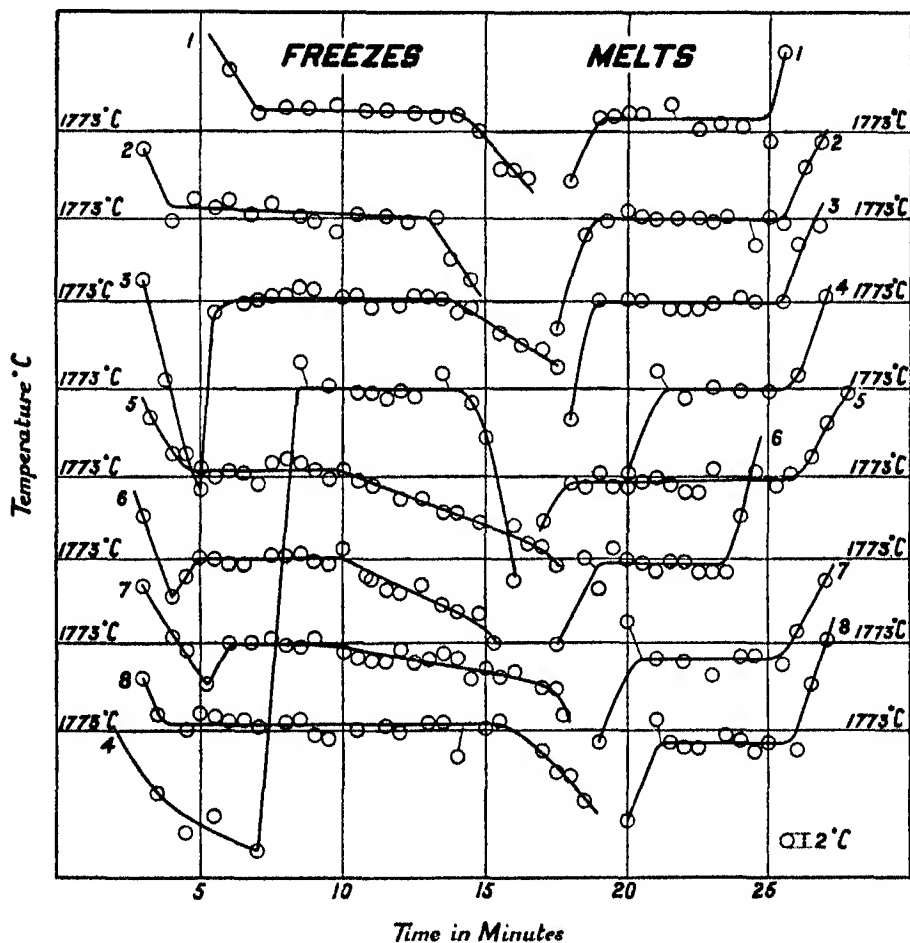


FIG. 5—Examples of curves for melting and freezing point of platinum with C.2 ingot.

Cylindrical Ingot C.2—These curves are dealt with in fig. 5 and have already been commented upon. A high value of R_{100}/R_0 is seen to have been maintained.

Cylindrical Ingot C.3—The curves for melt and freeze were the best obtained in the whole series of experiments. More than half the freezes gave curves of the same quality as those obtained with gold, fig. 4, and only slight undercools were observed.

Table II—Melting and Freezing Points of Platinum. Summary of Values

Particulars* of assembly	No. of previous melts	Melting points				Freezing points				R ₁₀₀ /R ₀		
		No.	Average deviation of, from mean	Mean	Probable error of mean	No.	Average deviation of, from mean	Mean	Probable error of mean	less melting point	Before	After
C.1, fig. 2 (a)	0	5	0.3	1772.3	° C	5	0.4	1773.4	° C	1.1	1.3916	1.3884
C.2, fig. 2 (a)	0	8	1.0	1772.6	±0.12	8	0.6	1773.6	±0.14	1.0	1.3919	1.3911
C.3, fig. 2 (b)	0	18	1.0	1772.1	0.29	17	0.8	1773.2	0.24	1.1	1.3895	1.3887
		Mean (C)	1772.3	0.22	Mean (C)	1773.3	0.14			
B.S.1, fig. 1	75	3	0.3	1771.7	° C	5	1.1	1772.7	° C	1.0	1.3910	—
	200	22	1.4	1770.4	±0.12	25	1.2	1774.3	±0.43	3.9	—	1.3903
B.S.2, fig. 1	10	7	1.0	1771.3	±0.24	7	0.9	1772.9	0.20	1.6	—	1.3916
		Mean (B.S.)	1771.1	0.31	Mean (B.S.)	1773.3	0.24			

* C.1, C.2, C.3 refer to separate ingots of cylindrical form according to the figure indicated.

B.S.1, B.S.2 refer to separate ingots of tapered form according to the specification proposed by the Bureau of Standards.

The ingot was prepared by mixing portions of ingots which had already been much used and consequently the initial value of R_{100}/R_0 was lower than usual. The fall after use was, however, small.

Tapered Ingot B.S.1—The assembly was still in working condition when it came to be broken up after the ingot had been melted some 300 times for several distinct purposes, *i.e.*, experiments on the standard of light, the colour temperature scale, and the freezing point determination. In its final form the ingot was somewhat irregular in shape owing to the extrusion of metal through fissures in the crucible. A considerable number of the earlier freezing points observations, prior to the 75th melt, had to be rejected for various reasons, mainly because of the suspected presence of film on the prism as already described. Though the absolute values could not be taken into account, it should be recorded that the freezing points were higher on the average than the melting points by between 1 and 2° C.

A similar difference is seen in the short series of observations, after the 75th melt, entered in the table. In the later series, after the 200th melt, the difference had increased to about 4° C, though the curves for the melts and the freezes, without undercools, were of fairly good form. However, included in the 25 freezes were a number in which heavy undercools had been deliberately induced with the result that a series of freezing point curves were obtained of about the same average quality as those shown in fig. 5, Nos. 3 and 4. Examples of three such curves, with undercools varying from 25° to 40° C, are given in fig. 6.

In Table III the 25 freezes are divided into two groups according to the amount of undercool.

Table III—Analysis according to the amount of undercool of the 25 freezing points with B.S.1 ingot, taken after 200 previous melts

No. of determinations	Undercool		Mean freezing point, ° C
	Amount, ° C	Average, ° C	
13	0 to 5	2	1775.0
12	25 to 55	38	1773.5
25 (total)	—	—	1774.3

Taking from Table II the most probable value of the freezing point as 1773.3° C, we see that the first value in Table III, with a very small average undercool, is higher than this by 1.7° C, while the value of the melting point, given in Table II, is lower than 1773.3° C by 2.9° C. Presumably, therefore, some factor was operative in opposite directions during melt and freeze. For

example, we might surmise that material extruded from the ingot, as already mentioned, would affect the temperature distribution both as a source of heat, by electrical induction, and a sink of heat, by thermal conduction, and that one effect might predominate during melting and the other during freezing, so as actually to cause a reversal of the longitudinal gradient in the two conditions, and give rise to the differences noted.

With regard to the other group in Table III, the undercools were induced by raising the temperature of the ingot considerably above the melting point.

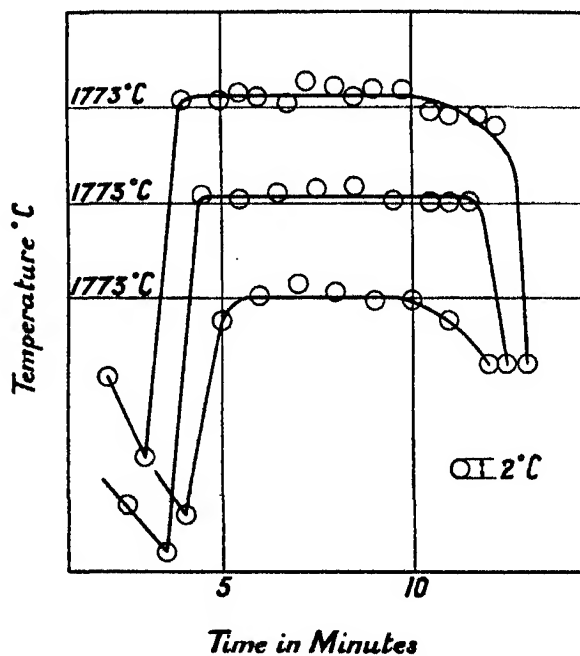


FIG. 6—Examples of freezing point curves with B.S.1. ingot after 200 melts.

The tendency of undercool was thereby increased, but it could often be terminated at will by tapping the apparatus. The sudden evolution of heat, which occurs on freezing after an undercool, might be expected to override the prevailing temperature gradients and give, for an appreciable time, a flat on the curve corresponding with the true freezing point. Although after any undercool the reading cannot apparently rise above the true freezing point, there is a certain danger that if the liquid is cooled too far the freezing point may never be reached in the subsequent rebound. When, however, curves are of the form shown in fig. 6, and with a reasonable length of halt, there seems to be very little possibility of a depression in value. In

all the experiments on platinum no evidence of such depression was found with undercools ranging up to 70°C , and even with an undercool of 150°C the difference in the single instance observed was only 2°C which is hardly outside the range of error of a single determination.

In the circumstances it would seem that the second value in Table III is entitled to considerably greater weight than the first.

Tapered Ingot B.S.2—The melts and freezes gave curves of about average quality, those for the freezes being without appreciable undercools.

Mean Values in Table II—In view of the small range of the values given in Table II the precise method of arriving at the means for each group is not of great importance. For the C ingots the values have been weighted according to the number of determinations, while for the B.S. ingots the arithmetic mean has been taken, since, for the reasons already indicated, the second value in the table, though representing many determinations, is not considered to be of greater weight than the other two. Alternatively if the second freezing point value is replaced by the more reliable second value of Table III, and the mean taken according to the number of determinations, practically no alteration would result.

V—Discussion of Results

The object of the investigation dealt with in this paper is to determine the temperature of equilibrium of the solid and liquid phases of platinum at normal atmospheric pressure, which temperature has been referred to throughout, for the sake of brevity, as the "freezing point of platinum." Such an equilibrium temperature should be given by observation either of the freezing or the melting point at any atmospheric pressure, the extreme variation of this pressure being of quite negligible effect in metals. Where, however, as not infrequently happens, the values obtained from the freezing and melting points differ it is generally recognized that the former gives the more reliable indication. Thus in the specification for the International Temperature Scale it is laid down that, for the purpose of realizing the Scale at the gold and silver points by means of platinum thermocouples, the equilibrium temperature is that given by the freezing point subject to a test for freedom from the influence of external conditions. The test can be either a raising or lowering of the couple in the ingot by 1 cm without altering the reading by more than 0.1°C , or alternatively an agreement between the melting and freezing points to 0.2°C . Unfortunately an exploratory test is hardly feasible under the

conditions applying in the present investigation, while a persistent difference of at least 1°C has been noted between the freezing and melting points (see Table II). It is therefore necessary to adduce other reasons for the acceptance of the value found for the former point. In the first place a number of arguments can be advanced in support of the greater reliability of the freezing point in the particular circumstances of the work. For example :—

(1) Electrical induction is known to have a stirring action on the liquid which would tend to promote temperature uniformity at the onset of solidification.

(2) Heating by high frequency induction being a skin effect, departures from the true cylindrical form of ingot, arising, for example, from the original shape of the crucible, or extrusion of metal through its walls, would be more likely to produce non-uniformity of temperature in the metal when melting. This seems a reasonable deduction from the fact that the energy dissipated in the skin of the ingot is relatively large during melting, being required for raising the temperature of the surroundings in addition to that of the ingot, whereas during freezing only a small amount of energy is needed to retard the natural process of cooling.

(3) Apart from the more permanent effects indicated in (2) casual irregularity of shape may arise from the contraction of the ingot on each solidification. For example, an ingot frequently solidifies with a smooth continuous skin on its top surface and a cavity may then be formed either in the body of the metal or against the side wall of the crucible. In either state non-uniformity of temperature is likely to be caused on melting.

(4) The conditions at the freezing point permit of greater variation as use may be made of the phenomenon of undercooling. Examples have been given above of the satisfactory results which can be obtained by inducing undercooling. It is not, of course, advocated that the undercool should be habitually employed, but, when used with due caution, it seems to afford a valuable means of check.

For the general reasons given above, the freezing point is to be preferred to the melting point as a means of obtaining the equilibrium temperature. In favour of acceptance of the particular value found for the freezing point of platinum in the present investigation the following special reasons may be urged : the mean values yielded by the experiments on five separate ingots, with considerable variation of assembly, have only ranged through 1.6°C , or 0.9°C if the higher value in Table III is rejected ; no appreciable change in the value of the freezing point has been found with a two-fold variation in

the length of freeze, or by undercooling ranging from 0° to 70° C: the probability of freedom from systematic error is increased by the fact that a similar apparatus used for gold gave values for the freezing point agreeing perfectly with those obtained with a different assembly and with a different type of heating.

So far nothing has been said concerning the effect of the uncertainties arising in various processes involved in obtaining the absolute value of the freezing point. An estimate of the limits of the most obvious of these sources of error is given in Table IV.

Table IV—Estimate of Errors

Source of error	Effect at platinum point $^{\circ}$ C
Photometric matching at gold, intermediate, and platinum points.....	± 0.6
Transmission of sectors	± 0.4
Effective wave-length	± 0.4
Maximum error (if all of one sign)	± 1.4

For the transmission of the sectors an uncertainty of 1 part in 1000 has been allowed on each and treated as additive. The allowance for effective wave-length is intended to represent the probable error in the transmission curve for the glass. It has been assumed that the visibility curves for two observers are identical with that adopted for the average eye by the international agreement already referred to. It is hardly practicable to determine the visibility data for each individual engaged in work of this type, but the occurrence of any abnormality in the present work is rendered unlikely by the facts that the Y/B ratios* of the two observers were found to be 1.00 and 1.02 respectively, and that no discrepancies appeared in their readings when working with or without sectors.

No allowance has been made for possible depression of the freezing points owing to impurities in the metals. The specimens of gold used were of the highest purity prepared by Messrs. Johnson Matthey & Co., while the resistance coefficient of the platinum does not, in the worst specimen, point to impurities totalling more than a few parts in 100,000,† the precise effect of which is very difficult to assess.

* See Crittenden and Richtmeyer, 'Bull. Bur. Stand.,' vol. 14, p. 87 (1918). The ratios given here were determined by the Photometry Division, National Physical Laboratory.

† Cf. analyses in paper by Wensel, Roeser, Barbrew, and Caldwell, 'Bur. Stand. J. Res.,' vol. 6, p. 1108 (1931).

On the whole it would seem that the value found for the freezing point may be taken as 1773.2°C with an uncertainty of the order of $\pm 1^{\circ}\text{C}$. It is of interest to compare this figure with former values obtained by optical pyrometer methods. For this purpose we reproduce a table of values, Table V, taken from a paper by Roeser, Caldwell, and Wensel,* and have added our own value thereto.

Table V—Determinations of the Melting Point of Platinum with Optical Pyrometer by the Ratio of Brightness Method

Observers	Date	Scale used		Value reported	Value on International Temperature Scale
		C ₁	Au point		
			$^{\circ}\text{C}$	$^{\circ}\text{C}$	$^{\circ}\text{C}$
Nernst and Von Wartenburg	1906	1.46	1064	1745	1763
Holborn and Valentiner	1907	1.42	1064	1789	1777
Waidner and Burgess	1907	1.45	1064	1753	1764
Hoffmann	1924	1.430	1063	1771	1769.5
Ribaud and Mohr	1931	1.432	1063	1762	1762
Roeser, Caldwell, and Wensel	1931	1.432	1063	1773.5	1773.5*
Author	1934	1.432	1063	1773.5	1773.5*

* Freezing point determinations.

The determination of Roeser, Caldwell, and Wensel at the Bureau of Standards in 1931 was the first made by the ingot or crucible method, which is no doubt greatly superior to those previously employed. It is satisfactory to note that, following this method with variations as described above, the present investigation has yielded a value indistinguishable from that found at the Bureau of Standards.

VI—Acknowledgments

Acknowledgments have been made in the course of the paper for assistance received in various ways, but special thanks are due to the Bureau of Standards who kindly presented the Laboratory with a number of crucible assemblies and to Mr. Turner, of the Metallurgy Department, National Physical Laboratory, who was responsible for the making of all the other crucible assemblies used for melting platinum. In addition the author desires to record his personal indebtedness to Mr. C. R. Barber, B.Sc., Assistant in the Physics Department, not only for sharing in the observations throughout, but for his skill in constructing apparatus and for making many valuable suggestions. Mr. A. Grace, Assistant in the Physics Department, also rendered valuable assistance by his suggestions and skill in constructional work.

* 'Bur. Stand. J. Res.,' vol. 6, p. 1121 (1931).

Summary

The freezing point of platinum on the International Temperature Scale has been determined by measuring the ratio of brightness, for a certain wavelength, of black-body radiators held at the freezing points of platinum and gold, the latter being the basic point of the scale for all high temperatures. The radiators consisted of hollow enclosures of refractory materials immersed in ingots of the metals which were heated by electro-magnetic induction and also for gold, in an ordinary resistor type of furnace. Observations on five ingots of platinum and two of gold yielded a mean value of $1773.3^{\circ}\text{C} \pm 1^{\circ}\text{C}$ for the freezing point of platinum. This value is indistinguishable from the only previous one obtained by the same method.

APPENDIX I

Note on the Refractory Articles made for the Investigation into the Freezing Point of Platinum

By D. TURNER, B.Sc. (Tech.)

Most of the articles to which reference is made are illustrated in fig. 2 of the paper. They were all made of pure thoria except for the unit, consisting of lid tube and bulb, shown in fig. 2 (*d*), which was made of alumina. An account of the methods developed at the Laboratory for the preparation of special refractories, including the two mentioned, has been published by the author of this note elsewhere.* The following additional information may be given with regard to the special articles referred to in the paper.

The thoria used was of the highest quality obtainable and contained only small traces of impurity. Its treatment consisted in a preliminary calcination to a temperature of about 1650°C with the object of reducing the subsequent shrinkage during the firing and use of the article, after which the calcined powder was crushed in a steel end runner mill, for a period determined by its hardness and temperature of firing, so as to obtain a suitable grain size and particle distribution. Accurate grading of the powder was not necessary, but the whole of the material would pass a 120 I.M.M. sieve and a considerable percentage of the powder would pass a 200 mesh sieve. The powdered refrac-

* 'Trans. Faraday Soc.,' vol. 27, p. 112 (1931); 'Trans. Ceramic Soc.,' vol. 33, p. 33 (1934); (with F. Adcock) 'J. Sci. Instr.,' vol. 7, p. 327 (1930).

tory was then treated with hydrochloric acid to remove the iron introduced during the grinding process, after which filtration and thorough washing of the material was essential for maintaining its purity. In the first crucible made (referred to as C.1 in the paper) slight contamination of the platinum charge occurred which was presumably due to inadequate washing, but subsequently no trouble of this kind was experienced.

Both slip casting and moulding processes for making thoria crucibles have been developed at the Laboratory, but in the present work the latter method was employed since only thick walled crucibles were required. The prepared thoria powder was mixed with a quantity of water sufficient to provide cohesion and was then fed in small quantities into a metal mould, each filling being tamped down hard by hand, using a small wooden rod. The moulded crucible, which was sufficiently strong to be removed from the mould and to withstand careful handling, was finally fired at 1650° C. It is understood that these crucibles showed no sign of failure from cracking in spite of the further shrinkage which occurred in their use at temperatures as high as 1900° C.

A similar moulding process was used for making the lids and the large diameter tubes shown in fig. 2 (b).

The small bore thoria tubing was prepared by extrusion through the usual type of die, the necessary plasticity being obtained by the addition of cellulose acetate solution to the calcined and powdered material. The volatile constituents of the solution evaporated rapidly as the material left the die and the resulting tube hardened almost immediately. In this condition the tubes were strong and possessed considerable flexibility. They could be closed, cut, joined, or otherwise manipulated with ease, and could be fired immediately.

All the thoria articles, referred to above, if suitably prepared, were strong, hard, and dense after firing at 1650° C.

In articles made from alumina, which was obtained as a very pure calcined powder, no preliminary heat-treatment was required, but similar grinding and acid treatment of the material was carried out, the powdered material being prepared as an aqueous casting "slip." The tube and bulb of fig. 2 (d) was slip cast in one piece in a two-part coreless plaster-of-Paris mould. This portion was then fired after which the lid itself was cast around the fired tube and the whole assembly subsequently refired to 1600° C.

The small bore alumina tubing mentioned in the paper was prepared by extrusion and was glazed by surface fusion as described elsewhere.*

* Turner and Adcock, 'J. Sci. Instr.,' vol. 7, p. 327 (1930).

APPENDIX II

Data for Calculation of Freezing Point of Platinum on International Temperature Scale

Sectors—These had transmissions of 0.03136 and 0.11143 respectively.

Effective Wave-length of Red Glass—This was as follows for the two intervals :

For temperature 25° C, and interval 1270°–1773° C, 0.6585 μ .*

For temperature 15° C, and interval 1063°–1270° C, 0.6588 μ .

Pyrometer Observations—Mean current to match radiator at gold point was 0.19804 amp and $di/dt = 0.00025$ amp/° C.

Mean current to match radiator at platinum point as reduced by the two sectors (see operations 3–5 on p. 794) was 0.19784 amp. This latter current is seen to be equivalent to a temperature of 1062.2° C and by application of the formula in Section II above for the two sectors in succession, a temperature of 1773.3° C is obtained for the mean freezing point. The values of individual freezing points were obtained by difference from the mean value.

* This was obtained from the calculated value 0.6574 μ for 15° C by adding 0.00011 μ per ° C. The value of the temperature coefficient of this type of glass was determined by Mr. Buckley ; see also Fairchild, Hoover, and Peters, 'Bur. Stand. J. Res.,' vol. 2, p. 951 (1928), and Forsythe, 'Trans. Faraday Soc.,' vol. 15, p. 21 (1920), for temperature coefficients of similar glasses.

Intensity Measurements in a Fine Structure Multiplet of AsII

By S. TOLANSKY, Ph.D., 1851 Exhibition Senior Student, and J. F. HEARD,
Ph.D., 1851 Exhibition Scholar, Imperial College of Science, London

(Communicated by A. Fowler, F.R.S.—Received May 15, 1934)

[PLATE 12]

Introduction

The present work was undertaken with the object of testing the fine structure intensity formulæ deduced by Hill.* Up to the present very few intensity measurements have been made on the fine structures arising from nuclear spin. The principal difficulty in such measurements arises from the smallness of the structures which are usually incompletely resolved by the interferometers employed. The use of the interferometer in any event necessitates careful corrections for the instrumental intensity distribution.

Schüler and Keyston† have made photometric determinations of the intensity ratios in the fine structures of two CdI lines and have verified the intensity rules for these lines. An inherent difficulty in the examination with a Fabry-Perot interferometer of CdI structures lies in the presence of an intense even isotope line within the pattern due to the nuclear spin of the odd isotopes. The even isotope component contributes 77% of the intensity of the line and the remaining 23% is distributed amongst the members of the nuclear spin multiplet. The authors do not describe their method of coping with this difficulty which, judging from the experience of the present writers, must have been serious.

D. A. Jackson‡ has made a number of intensity measurements upon fine structures of resonance lines with the object of determining nuclear spins, assuming the validity of the intensity rules. The examination of resonance lines introduces difficult corrections associated with self-absorption, and in most of Jackson's experiments the high values of the nuclear spins introduce some uncertainty into the interpretation of his results.

It appeared desirable to carry out intensity measurements in a fine structure multiplet where the above difficulties would not be encountered and so test

* 'Proc. Nat. Acad. Sci. Wash.,' vol. 16, p. 68 (1930).

† 'Z. Physik,' vol. 67, p. 433 (1931).

‡ 'Proc. Roy. Soc., A, vol. 139, p. 674 (1933); 'Nature,' vol. 127, p. 924 (1931).

the formulæ more rigorously. The ideal circumstances would be the following :

- (a) that the atom possess one isotope only ;
- (b) that the nuclear spin be known with certainty ;
- (c) that the nuclear spin and J-values be small in order to have intensity ratios which could be measured with accuracy ;
- (d) that the line patterns be completely resolved by the interferometer ;
- (e) that the source preclude effects due to self-absorption, high pressure, high temperature, etc.

The present observations are concerned with $\lambda 5231$ ($5s\ ^3P_1-5p\ ^3P_0$) of AsII which satisfies these requirements :

- (a) Arsenic has only one isotope, namely, 75.*
- (b) The nuclear spin has been determined by an extended fine structure analysis of AsII by Tolansky† and confirmed by Crawford and Crooker,‡ in AsIV.
- (c) The spin is $3/2$ and the structure arises from the $5s\ ^3P_1$ term so that the line pattern is a triplet with theoretical intensity ratios $1:2:3$; values eminently suited for measurement by photographic photometry.
- (d) With a 11 mm silvered Fabry-Perot interferometer the components are well spaced and, the lines being in the green region, the instrumental background intensity is small.
- (e) The source of light, namely, a water-cooled hollow cathode operated in helium, can be made free from self-absorption, temperature, pressure, etc., effects. $\lambda 5231$ is, moreover, reasonably intense and is well separated from its neighbours. No other line in AsII is so well suited for the experiments.

The manner in which the fine structure of $\lambda 5231$ arises is shown in fig. 1.

Experimental

The AsII spectrum was excited in a water-cooled hollow cathode of iron containing a little arsenic at the bottom. It has been shown elsewhere§ that previous failure to excite the arsenic spectrum in the hollow cathode was probably due to the presence of oxide. The cathode was 4 cm long and the

* Aston, " Mass Spectra and Isotopes " (1933).

† ' Proc. Roy. Soc.,' A, vol. 137, p. 541 (1932) ; ' Z. Physik,' vol. 87, p. 210 (1933).

‡ ' Nature,' vol. 131, p. 655 (1933).

§ Tolansky, ' Proc. Roy. Soc.,' A, vol. 146, p. 182 (1934).

bore measured 1 cm. Helium was circulated continuously through the discharge tube at a pressure of about 1 mm of mercury. A 1000-volt D.C. generator was used to operate the discharge. The pressure and voltage conditions necessary for stable operation were found to be critical.

The fine structure patterns were produced by means of a silvered Fabry-Perot interferometer with quartz plates of 6 cm aperture used at a separation of 11.0 mm. The silverings were obtained by sputtering in argon. To separate the coarse structure in the spectrum the interferometer was crossed

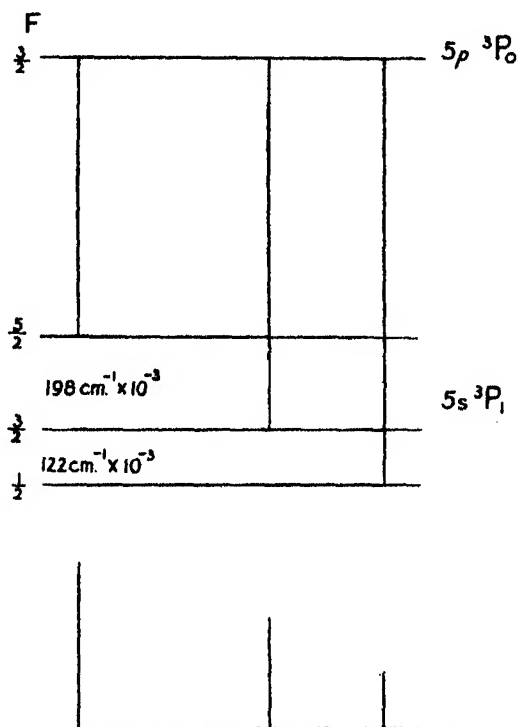


FIG. 1—Term analysis of fine structure of λ 5231.

with a large aperture two-prism glass spectrograph having a dispersion of 30 Å per mm in the region λ 5200. The interferometer was tilted so that only one side of the ring system fell on the photographic plate, and about twelve orders were photographed in a space of about 12 mm, when the size of the image on the slit was about 6 mm.

The intensity calibration of the plates was effected by means of the stepped slit method. A series of eight short slits ranging in width from 0.2 to 1.4 mm were placed immediately before the widely opened slit of the spectrograph.

White light from a small diffuse source fell upon these slits and produced a series of continuous spectra, the intensities of which at any wave-length were proportional to the widths of the respective slits. Each photographic plate was exposed to these spectra immediately after the exposure to the AsII spectrum. The exposure times for the line pattern and the density marks were of the same order. Freshly coated backed Ilford hypersensitive panchromatic and soft gradation panchromatic plates were used. The plates were developed for 7 minutes in pyro-soda, and were continuously agitated during the development.

Microphotometer recordings of the plates were made with a Cambridge Instrument Company's recording microphotometer. Each tracing consisted of a run across the density marks at the approximate wave-length λ 5231, and a run across the Fabry-Perot fringes of the fine structure multiplet. A recording across the fringes is shown in Plate 12.

Method of Reduction

In evaluating the true intensities of the components from the photometer tracings, three independent factors must be taken into consideration, namely :—

- (i) the source itself has an intensity distribution such that there is a maximum brightness at the centre which falls off regularly towards the walls of the hollow cathode ;
- (ii) a Fabry-Perot interferometer produces a definite intensity distribution from order to order ; a theoretically uniform extended source gives a maximum of intensity in the central orders, the intensity falling off regularly towards the outer order fringes ;
- (iii) the intensity distribution between two orders of any component contributes to the intensity of every other component lying between these two orders. This contribution is a function of the line width and the reflection coefficient of the interferometer, the instrumental factor being the more important.

The present method of reduction deals with these factors in the following way : A smooth curve was drawn through the peaks of successive orders of each component as shown by the dotted lines in Plate 12. They represent the resultant intensity distribution due to (i) and (ii) above. The intersections of any Y ordinate with these curves gives the relative heights of the peaks

corrected for the intensity distributions across the fringe system. In effect this is equivalent to shrinking the three components into superposition in the fringe system. These heights, converted into units of intensity by means of a blackening curve, represent the intensities of the peaks corresponding to the three components. In order to obtain the true intensities of the components from the "peak intensities" it is necessary to evaluate the mutual contributions described in (iii) above; and to evaluate these requires a knowledge of the intensity distribution between two adjacent orders of a single fringe. This distribution was determined from a microphotometer recording of a structure-free line in the same spectral region, namely, λ 5385. (The errors introduced by the small difference in wave-length are negligible.) Then from the measured separation of the peaks of λ 5231 the contribution to each component by each of the others, expressed as a fraction of the latter, was determined. Thus the peak intensity corresponding to each component could be expressed as the sum of three parts, namely, the intensity of the component itself plus small fractions of the intensities of the other two components. This gave three simultaneous equations, one for each peak, which were solved to give the three true intensities. If A, B, C are the peak intensities in diminishing order and I_1, I_2, I_3 are the desired true intensities also in diminishing order, then the experimentally determined equations were

$$\begin{aligned} I_1 + 0.075 I_2 + 0.12 I_3 &= A \\ 0.075 I_1 + I_2 + 0.13 I_3 &= B \\ 0.12 I_1 + 0.13 I_2 + I_3 &= C \end{aligned}$$

An attempt was made to determine the effect of scattered light which is not corrected for in the above method. This effect was found to be too small for photometric determination and so can introduce no appreciable errors in the results.

Results

In order to examine systematically the intensities in λ 5231 for any possible effects due to self-absorption, temperature, etc., the observations of the intensity ratios were made for a number of different discharge tube currents. The range of currents was from 80 to 165 milliamperes; with currents less than 80 milliamperes the light was too feeble for the thick Fabry-Perot silverings employed, with currents greater than 165 milliamperes the rise in arsenic vapour pressure made the discharge unstable.

From a number of plates seven were chosen on which the densities fell into the best regions of the calibration curves. For each plate the microphotometer recording was taken across about eight orders. Seven equidistant ordinates were drawn and thus, in the manner of reduction described above, each recording yielded seven values for the intensity ratios. From these, mean values of the ratios were determined for each plate. These mean values are, given in Table I where, for convenience of comparison with theory, the central component has been given an intensity of 2.

Table I—Fine Structure Intensity Ratios in λ 5231 ($5s\ ^3P_1$ — $5p\ ^3P_0$)
(Theoretical Ratios 1 : 2 : 3)

Current (milliamperes)	Observed intensity ratios
80	0.91 : 2 : 3.10
100	0.98 : 2 : 2.92
100	0.97 : 2 : 3.07
150	0.99 : 2 : 2.86
150	1.00 : 2 : 2.84
165	1.03 : 2 : 3.13
Mean ratios	$0.98 \pm 0.04 : 2 : 2.99 \pm 0.12$

The deviations from the mean are not systematic enough to indicate any dependence of the ratios on current, and within the probable error of 4% the theoretical ratios of 1 : 2 : 3 are verified. Since the upper term of λ 5231 is single ($J = 0$), the results show without ambiguity that for the $5s\ ^3P_1$ term the quantum weights of the fine structure levels are proportional to $2F + 1$, F being the fine structure quantum number of any level.

In conclusion, the writers wish to express their best thanks to Professor A. Fowler, F.R.S., for his kind assistance and encouragement and for the excellent experimental facilities which have been enjoyed in his laboratory during this investigation.

Summary

Accurate measurements of the intensity ratios in the fine structure triplet of AsII λ 5231 ($5s\ ^3P_1$ — $5p\ ^3P_0$) have been made by a method of photographic photometry. The spectrum was excited in a water-cooled hollow cathode discharge and examined by means of a silvered Fabry-Perot interferometer. A method of reduction is described which takes into consideration the intensity distributions in the source and in the interferometer. The mean values of the triplet ratios obtained from 42 independent observations on six spectrograms

are 0.98 : 2 : 2.99 which, within the 4% probable experimental error, are in agreement with the theoretical values 1 : 2 : 3. This proves that the quantum weights of the fine structure levels in the $5s\ ^3P_1$ term are proportional to $2F + 1$.

DESCRIPTION OF PLATE

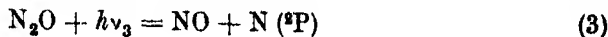
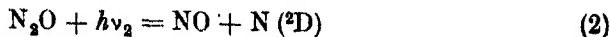
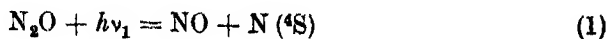
The plate shows a photograph of the Fabry-Perot fringes of $\lambda\ 5231$ (11 mm etalon) and a microphotometer recording of the fringes illustrating the method of reduction.

Fluorescent Radiation from N₂O

By P. K. SEN GUPTA, Department of Physics, University of Allahabad, Allahabad, India

(Communicated by M. N. Saha, F.R.S.—Received May 15, 1934)

The action of light on N₂O was studied by Leifson* and continued in recent years by Wulf and Melvin,† Dutta,‡ and the present author§ from experiments on its absorption spectra. The experimental data so far known indicate that under the action of light quanta of suitable wave-length N₂O dissociates into a normal NO and N which may be in different excited metastable states as shown below.



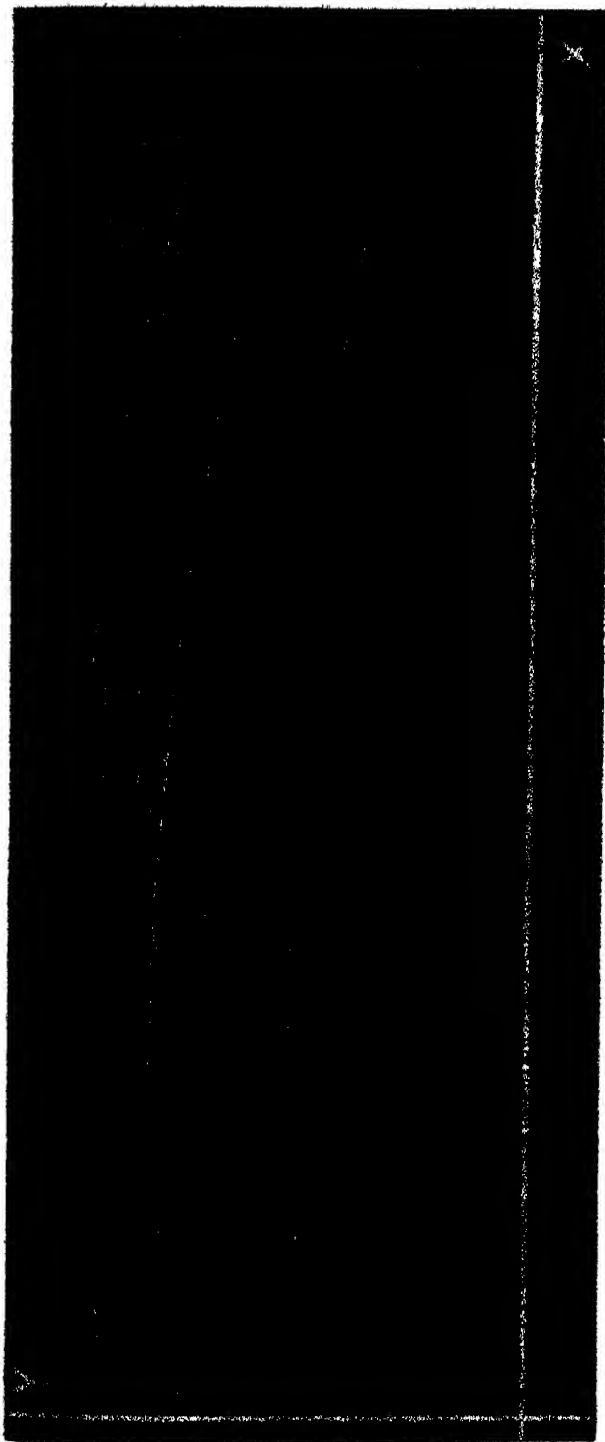
These processes are inferred from the various starting points of continuous absorptions from a long wave-length limit, and with retransmitted patches of light occurring between these beginnings. The energies corresponding to $h\nu_1$, $h\nu_2$, and $h\nu_3$ are given by the different long wave beginnings of absorption at $\lambda\ 2750$, $\lambda\ 1850$, and $\lambda\ 1580$; the differences of energy between these light quanta are respectively the values of $^4S-^2D$ and $^2D-^2P$ of N.

* 'Astr. phys., J.,' vol. 63, p. 73 (1926).

† 'Phys. Rev.,' vol. 39, p.180 (1932).

‡ 'Proc. Roy. Soc.,' A, vol. 138, p. 84 (1932).

§ 'Bull. Acad. Sci. U.P., Allahabad,' vol. 3, p. 197 (1934).

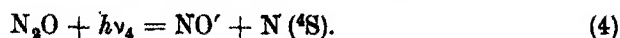


Microphotometer recording of λ 5231 Fabry Perot fringes.



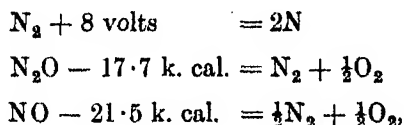
Fabry Perot fringes of λ 5231 [Gap — 11 mm]

But so far no evidence of the production of an excited NO molecule, as the result of light absorption has been found, according to the process,



For explaining the non-occurrence of such a process let us find out theoretically the value of $h\nu_4$. We have $h\nu_4 = h\nu_1 + \epsilon$, where ϵ is the energy required to excite the NO molecule. For $h\nu_1$, Mecke* has given a value of 105 k. cal., while Dutta (*loc. cit.*) from his absorption experiments gives 104 k. cal. The agreement seems to be quite good, but Dutta's value seems to be high on account of the fact that in the process of absorption, transition takes place from the ground state to an excited one for which the Franck-Condon curve is rather sloping,† indicating repulsion. Taking into account Lozier's‡ latest determination of the heat of dissociation of nitrogen, which appears to be correct, the value of $h\nu_1$ has been recalculated here.

Since



we obtain from equation (1)

$$h\nu_1 = 95 \text{ k. cal.}$$

The ground states of the NO molecule are $^2\Pi_a$, and the next excited states are $^2\Sigma$ and $^2\Pi_b$. The γ -bands corresponding to $^2\Pi_a \leftarrow ^2\Sigma$ transition require an energy of 125.4 k. cal. for their excitation, while the β -bands corresponding to $^2\Pi_a \leftarrow ^2\Pi_b$ transition require 128.8 k. cal.§ Thus ϵ is either 125.4 or 128.8 k. cal. according as the NO molecule is excited to the $^2\Sigma$ or $^2\Pi_b$ state. In the former state,

$$\begin{aligned} h\nu_4 &= h\nu_1 + \epsilon \\ &= 95 + 125.4 = 220.4 \text{ k. cal.} \end{aligned}$$

This corresponds to a wave-length of 1300 Å. In the latter state,

$$\begin{aligned} h\nu_4 &= 95 + 128.8 \\ &= 223.4 \text{ k. cal.,} \end{aligned}$$

corresponding to λ 1290 Å.

* 'Z. phys. Chem.,' B, vol. 7, p. 126 (1930).

† Sen Gupta, 'Z. Physik,' vol. 88, p. 647 (1934).

‡ 'Phys. Rev.,' vol. 44, p. 575 (1934).

§ Jevons, 'Report on Band Spectra of Diatomic Molecules,' p. 288 (1932).

This explains why we do not get the absorption corresponding to the photochemical process (4), as it would lie almost at the limit of the fluorite spectrograph. Other absorptions indicative of the interaction of excited NO as well as excited N would lie still further off in the ultra-violet beyond the fluorite region.

If the photochemical processes indicated above occur, the excited atoms or molecules should return to the normal states and we should get the corresponding lines or bands in emission. In the reactions mentioned we may expect the lines of N given in Table I.

The transitions indicated are all forbidden and, therefore, the probability of appearance of these lines in emission is extremely small. The lines due to $^2\text{D}-^4\text{S}$ and $^2\text{P}-^4\text{S}$ are claimed to have been obtained in astrophysical sources by Boyce, Menzel, and Payne.* Of the three transitions the most probable is that of $^2\text{P}-^2\text{D}$, but the corresponding line lies in the extreme infra-red region where photography is inapplicable.

Table I

Transition	λ in A units	Exciting λ in N_2O
$^2\text{P}-^2\text{D}$	16000	$h\nu_1 + (h\nu_1 - h\nu_2) = 8.06 \text{ volts } (\lambda 1580)$
$^2\text{P}-^4\text{S}$	3470	$h\nu_1 + (h\nu_1 - h\nu_2) = 8.06 \text{ volts } (\lambda 1580)$
$^2\text{D}-^4\text{S}$	5210	$h\nu_1 + (h\nu_1 - h\nu_2) = 6.87 \text{ volts } (\lambda 1850)$

On the other hand, as transition corresponding to the state in which NO is excited are not forbidden, the corresponding bands are easier to obtain if N_2O is irradiated by light of suitable wave-length. Both the β and γ bands of NO correspond to transition to the fundamental state as shown by Sponer and Hopfield† from the photographs of Leifson (*loc. cit.*), and later supported by Mulliken. But in the visible region only the β -bands are obtained. Here we are concerned only with the visible part of the spectrum, because the camera available had only glass lenses.

The experimental method was quite simple. A 500 cc glass globe was filled with N_2O (prepared from ammonium nitrate and dried by phosphorus pentoxide) at an average pressure of 0.01 mm of mercury. The gas was illuminated with light from a hydrogen-discharge tube through a fluorite window, so that light up to $\lambda 1200$ could be obtained easily. The illuminated part was observed at right angles to the direction of light with the aid of

* 'Proc. Nat. Acad. Sci. Wash.', vol. 19, p. 581 (1933).

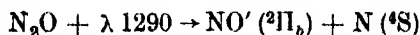
† 'Phys. Rev.', vol. 27, p. 640 (1926).

constant deviation spectrograph. A special camera* having high light gathering power was chosen. Photographs were taken on Ilford golden iso-zenith plates, and the copper arc was used for comparison.

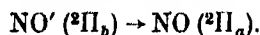
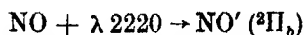
After an exposure of 50 hours the β -bands of NO came out very clearly on the plate in the region λ 5000–3700 Å. The lines could be compared with those of Jenkins, Barton, and Mulliken† and Johnson and Jenkins.‡ In my plate also the intensities were maintained; that is, the lines at 3800, 4041, and 4589 were very strong. The dispersion being necessarily small, the doublet separations were not distinct and some of the lines were too faint to be recorded with certainty.

There were also a few hydrogen lines which were due to the scattering of the Balmer lines by the gas. These could easily be eliminated by direct comparison with the spectrogram of a vacuum hydrogen tube.

The excitation of the β -bands of NO requires 5.6 volts. The bands which are observed may be due to fluorescence of free NO, which may be present as an impurity or may be produced permanently in small quantities owing to the continued action of light on N₂O. (Frequent fillings of the globe with fresh N₂O, and subsequent evacuations, reduced the possibility of production of free NO to a minimum.) To test this point, another experiment was done in which another exposure of 50 hours was given under exactly similar conditions except that N₂O was now illuminated by light having the short wave limit at λ 1850 (H₂-spectrum through quartz window). By this method the dissociation of N₂O into NO excited was avoided. The result was negative. This proved that the β -bands in the previous experiment were really due to the photochemical steps—



and not due to the excitation of any free NO in the globe as represented by



The work is being continued with some experimental improvements to obtain the forbidden atomic transitions.

* I am grateful to Dr. S. B. Dutt, Reader in Organic Chemistry of the Allahabad University, for the loan of the camera.

† 'Phys. Rev.', vol. 30, p. 150 (1927).

‡ 'Phil. Mag.', vol. 2, p. 626 (1930).

I am very grateful to Professor M. N. Saha, D.Sc., F.R.S., for helpful suggestions and guidance in connection with this work.

Summary

The β -bands of NO were obtained in fluorescence when N_2O was illuminated by light of suitable wave-length, showing that NO, which is one of the products of photochemical dissociation of N_2O is also excited during the process.

Inert Gas Effects in the Photosynthesis of Hydrogen Bromide

By MOWBRAY RITCHIE, B.Sc., Ph.D., Department of Chemistry, University of Edinburgh

(Communicated by J. Kendall, F.R.S.—Received May 23, 1934)

Recent studies of many chemical gas reactions which involve the production and behaviour of atoms, have shown that the effect of the surface of the reaction vessel on the atom concentration can seldom be regarded as a small disturbing factor to be allowed for by a semi-empirical correction, but must be adequately considered in relation to the other processes determining the velocity of reaction. In this connection, therefore, alteration in the pressure of any one reactant must involve an effect depending on the diffusion coefficient of the atom concerned, with regard to the reactant, this effect being, of course, superimposed on the normal effect to be expected from the mass action principles of the chemical kinetics. Examples of this simple diffusion effect are well known.*

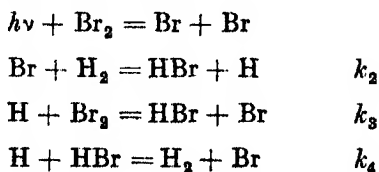
The results to be expected on these lines are sometimes complicated by the existence of other factors consequent on increase in pressure in the reacting system. In the photosynthesis of hydrogen bromide, where bromine atoms are involved, it has been shown† that increase in total pressure, by the introduction of an otherwise inert gas, produces a relative decrease in reaction velocity, where the application of the simple diffusion theory as above would

* Cf. *inter alia*, Semenoff, 'Z. phys. Chem.,' B, vol. 2, p. 161 (1929); Melville, 'Trans. Faraday Soc.,' vol. 28, pp. 302, 814 (1932); Norrish and Griffiths, 'Proc. Roy. Soc.,' A, vol. 139, p. 147 (1933); vol. 135, p. 69 (1932).

† Jost and Jung, 'Z. phys. Chem.,' B, vol. 3, p. 83 (1929).

lead one to expect an increase in velocity by prevention of the removal of bromine atoms by the walls. This decrease has been attributed to the stabilization of the bromine "quasi-molecule"* by the added gas molecule, the removal of bromine atoms being thus facilitated by what is virtually a triple collision. Similar considerations apply to the photochemical formation of phosgene.†

The mechanism of reaction universally accepted for the photo-combination of hydrogen and bromine‡ is as follows:—



The removal of bromine atoms is accomplished by mutual recombination or by wall action. In either reaction, however, the rate of formation of hydrogen bromide can be obtained from the above in the form

$$\frac{d(\text{HBr})}{dt} = \frac{2k_2 \cdot k_3 \cdot [\text{H}_2] \cdot [\text{Br}_2] \cdot [\text{Br}]}{(k_3 [\text{Br}_2] + k_4 [\text{HBr}])}$$

The rate of reaction is thus proportional to the concentration of bromine atoms. If the bromine atoms are considered as being removed solely by the triple collision process



then

$$\frac{d(\text{HBr})}{dt} = \frac{2k_2 \cdot k_3 [\text{Br}_2] \cdot [\text{H}_2] \sqrt{\frac{2I_{\text{abs.}}}{k_5 [\text{M}]}}}{(k_3 \cdot [\text{Br}_2] + k_4 [\text{HBr}])}$$

In the calculation by Jost§ of velocity coefficients in this reaction, the effect of total pressure from the point of view of the triple collision effect was allowed for by the introduction of a single term ($\sqrt{p_M}$) in which no distinction was made between the relative efficiencies of the different gases. From the general trend of the rates of reaction, however, it appeared that the relative efficiencies were expressed by the series $\text{H}_2 > \text{O}_2 > \text{N}_2 > \text{A} > \text{He}$. In the present work, preliminary experiments indicated that the efficiency of hydrogen as

* Jost and Jung, 'Z. phys. Chem.,' B, vol. 3, p. 83 (1929).

† Schumacher and Stieger, 'Z. phys. Chem.,' B, vol. 13, pp. 157, 169 (1931).

‡ Bodenstein and Lütkenmeyer, 'Z. phys. Chem.,' vol. 114, p. 208 (1924).

§ 'Z. phys. Chem.,' B, vol. 3, p. 95 (1929)

an inert gas in this connection was more of the order of that of helium and argon; systematic examination of the different effects was therefore begun.

Briers and Chapman* have shown that as the surface removal of bromine atoms becomes progressively greater in relation to the recombination of bromine atoms, the experimentally determined relation between the rate of HBr formation and the amount of light absorbed changes from

$$\frac{d(\text{HBr})}{dt} \propto (I_{\text{abs}})^{\frac{1}{2}},$$

where surface effect is negligible, to

$$\frac{d(\text{HBr})}{dt} \propto (I_{\text{abs}})^n,$$

where n tends towards unity.

These relationships have been confirmed in the present investigation. In relation to the formation of HBr in the gas phase, therefore, the removal of bromine atoms by the surface does not involve a term in $[\text{Br}]^2$. Correspondingly, the experimental conditions in which surface effects might be expected to predominate are low pressures of bromine and low intensities of illumination, together with small reaction vessels with suitably low total pressures. On the other hand, high concentrations of bromine atoms, produced by high light intensities and high pressures of bromine, will tend at high total pressures to favour the removal of bromine atoms by the triple collision process involving the square of the bromine atom concentration. The results of the present work are considered in relation to these two extremes of classification.

Experimentally, relative values of the rates and quantum efficiencies of HBr formation at 200° C were obtained for fixed pressures of H_2 , Br_2 , and HBr, the incident light intensity being kept at a constant value, while other gases (He , A , N_2 , CO_2 , O_2 , CCl_4) were added in various proportions. The rate of reaction was calculated from the rate of removal of bromine as determined by a photometric method.

Apparatus

A diagram of the apparatus is given in fig. 1. All experiments were carried out at 200° C, this temperature being maintained in the electric heater F, by means of a 100-volt battery system with suitable resistances. Little difficulty was experienced in keeping the temperature constant to $\pm 0.2^\circ \text{C}$,

* 'J. Chem. Soc.,' p. 1802 (1926).

as measured by mercury thermometer, by means of a sliding resistance worked by hand. The heater itself was constructed in two similar sections to facilitate the introduction of the quartz reaction vessel V, the heating coils being wound round the inner glass cylinders occupying the centre of each section, while several layers of asbestos paper placed just inside the outer metal cover rendered the production of the necessary steady temperature a comparatively easy matter. Light from the 500-watt lamp S, run at 190 v from 230 v. A.C. mains by hand controlled resistance, was rendered parallel by a system of

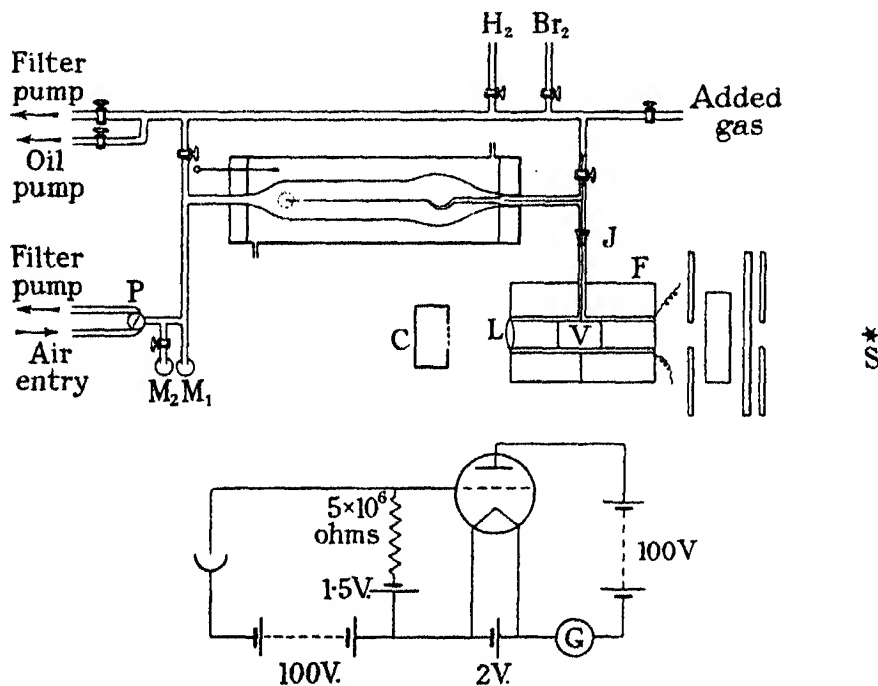


FIG. 1

lenses and circular apertures, and passed into the inner tube of the heater through the plane glass plate closing the end, traversing then the reaction vessel, and being finally focussed by the lens L on the aperture of the photo-electric cell C (potassium metal, vacuum type). The photo-electric current was magnified by thermionic valve and recorded by galvanometer, fig. 1, an arrangement which at all times gave accurately reproducible results.

The quartz reaction vessel, cylindrical in shape and of optically plane ends, was of 32 cc internal volume and approximately 60 sq. cm internal surface, being connected by capillary tubing to the Bourdon glass-spring gauge and

to the various gas reservoirs through the ground joint J. The gauge itself, kept at constant temperature by the surrounding water jacket, was usually used as a null instrument only, for the measurement of the total gas pressure in the reaction vessel. The pointer of the gauge, observed by telescope, was thus brought back to the same position on the telescope eyepiece scale by the admission or withdrawal of dry air by the two-way tap P, the balancing pressure of air being read off on the mercury manometer M_1 , used in conjunction with the standard manometer M_2 .

The tap grease used throughout was Apiezon L, which absorbed bromine to a small extent only at the pressures used in the experiments. No abnormalities in reaction velocity were ascribed to its use. In calculating rates of reaction, correction was applied for the small decrease in pressure which occurred during the course of an experiment and which was due to such absorption.

All parts of the apparatus could readily be evacuated to a pressure less than 0.01 mm by means of filter pump and Hyvac oil pump.

Bromine, carbon tetrachloride, and carbon dioxide were distilled through phosphorus pentoxide and purified by repeated fractionation. Hydrogen and oxygen were prepared by electrolysis of sodium hydroxide solution passed over hot copper and copper oxide respectively, and dried by phosphorus pentoxide. Nitrogen and argon were obtained from cylinders and passed through liquid air traps before use. Helium was used as supplied by the British Oxygen Company.

Determination of Bromine Concentration

The light beam was rendered approximately monochromatic ($\lambda \doteq 420 \mu\mu$) by an aqueous solution of cupric ammonium sulphate (6 cm length of 1% solution) used in conjunction with an aqueous solution of quinine hydrochloride (2 cm length of 1% solution). By Beer's law, for monochromatic and parallel light,

$$[\text{Br}_2] \propto \log I_0/I,$$

where $[\text{Br}_2]$ represents pressure of bromine, I_0 the transmitted light intensity at zero pressure, and I the transmitted light intensity at the pressure $[\text{Br}_2]$. Determinations of $\log I_0/I$ were carried out with bromine pressures up to 50 mm, I_0 and I being taken as the corresponding deflections of the galvanometer. The temperature was that at which actual rates of HBr formation were recorded, namely 200° C. The linear relationship given above was found to be valid, the pressure of bromine being given by $77.0 \log I_0/I$.

It was found in accordance with the results of Jost,* and others, that the introduction of other gases altered the absorption coefficient of the bromine, this effect being akin to the broadening of the absorption bands by added gas molecules. A small increase in absorption which necessitated a correction in the calculations was always observed. This correction was estimated at the beginning of each experiment.

Experimental Procedure

After the required steady temperature of 200° C had been attained, and the system had been thoroughly evacuated by oil-pump, repeated observations of I_0 (representing transmitted intensity of blue light when no bromine was present in the reaction vessel) were recorded. The reaction vessel was then "washed out" once with pure bromine vapour, bromine added to the required pressure, and the value of I , the transmitted intensity, recorded. Addition of inert gas to the required pressure was followed by redetermination of the transmitted light, this value being slightly less than the previous value by reason of the increased absorption due to the presence of inert gas. At this stage the mixture was illuminated for a short time (5–10 minutes) to minimize the effect of possible inhibitors. Hydrogen was added last, observations of the transmitted light being again rapidly recorded.

Towards the end of the necessary period of illumination repeated observations of the transmitted light were again made. The small decrease in total pressure occurring during the illumination was measured by the gauge pointer and telescope eyepiece scale. Evacuation and redetermination of I_0 completed the experiment.

Experimental Results

As carried out in the above manner, each experiment gave values of $\log I_0/I$ for the beginning and end of each period of illumination, and these were converted to actual pressures of bromine by means of the calibration graphs of $\log I_0/I$ against $[Br_2]$. The small decrease in total pressure recorded by the gauge pointer was attributed, for purposes of calculation, to absorption of bromine alone by the tap grease, and a correction (approximately equal to 2% of the total change in bromine concentration) applied accordingly. Table I is typical of the results obtained. The average pressure of the reactants is given in millimetres, the total hydrogen bromide produced by the illumina-

* 'Z. phys. Chem.,' B, vol. 3, p. 95 (1929).

tion being in each case twice the value recorded under the heading (HBr), while γ is the relative quantum efficiency calculated by the formula

$$\gamma' = \frac{10^4 \times 2 \times \text{HBr}}{t \times I_{\text{abs.}}}$$

Here $I_{\text{abs.}} = (I_0 - I)$, and I represents the transmitted intensity at the mean bromine pressure. The values under the heading γ have been calculated to $[\text{H}_2] = 200.0$ mm from γ' on the assumption that the reaction velocity and relative quantum efficiency are proportional to $[\text{H}_2]$.

Table I—Blue light. No inert gas present. $[\text{H}_2] = 200.0$ mm $[\text{Br}_2] \doteq 15.0$ mm $[\text{HBr}] \doteq 4.5$ mm

$[\text{H}_2]$ mm	$[\text{Br}_2]$ mm	$[\text{HBr}]$ mm	t mins	$I_{\text{abs.}}$ divs	γ'	γ
201.0	15.3	3.65	60.5	13.3	91.0	90.5
202.5	15.8	4.25	61.0	14.5	90.2	95.0
202.4	14.5	4.35	60.0	15.1	95.6	94.5
202.7	14.2	4.37	60.5	15.0	96.0	94.5
199.0	14.5	4.59	61.0	15.9	95.0	95.5
203.5	14.2	4.69	62.0	15.5	97.5	96.0

Average $\gamma = 94.3$

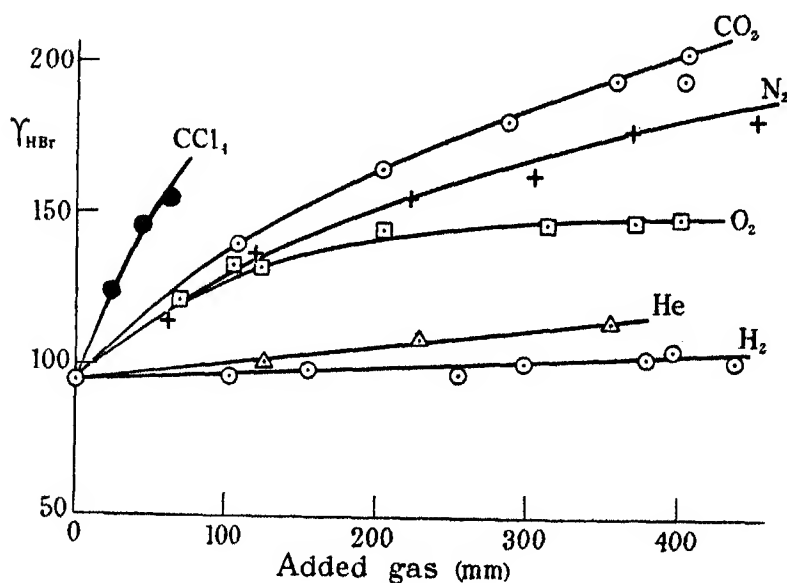


FIG. 2

With similar values of $[\text{H}_2]$, $[\text{Br}_2]$, $[\text{HBr}]$ and $I_{\text{abs.}}$, rates of reaction were measured for various concentrations of other gases. Results are given in Table II, and are shown graphically in fig. 2.

The curve representing the inert gas effect of hydrogen was obtained by reducing the appropriate values of γ' (obtained for the various values of $[\text{H}_2]$) to $[\text{H}_2] = 200.0$ mm by assuming in accordance with the mechanism previously quoted, that the rate of reaction, apart from diffusion and triple collision effects, is directly proportional to the hydrogen concentration. The corresponding "inert gas" concentrations were obtained by subtracting 200 from the actual values of $[\text{H}_2]$ with which the experiments were carried out.

Table II

Added gas	$[\text{H}_2]$	$[\text{Br}_2]$	$[\text{HBr}]$	t	$I_{\text{abs.}}$	γ'	γ
	mm	mm	mm	mins	divs		
$\text{CO}_2 =$	284.5	201.5	14.4	4.95	40.5	13.4	181
	106.5	198.2	13.9	5.15	58.0	12.75	140
	202.1	200.2	14.0	5.08	47.0	12.65	165
	355.4	201.3	14.5	5.65	39.5	14.6	195
	400.3	201.1	14.5	4.17	30.1	14.2	196.5
	403.0	198.7	14.8	4.75	36.0	13.0	204
$\text{N}_2 =$	60.3	200.5	14.05	4.95	61.0	14.2	114
	303.4	205.6	12.85	5.43	48.5	13.5	163
	118.0	200.6	13.7	5.92	60.0	14.3	137.5
	367.1	200.8	13.9	5.85	45.0	14.5	179
	221.1	200.8	13.8	6.32	55.0	14.6	157
	449.0	199.6	13.7	5.70	45.0	13.9	182.5
$\text{O}_2 =$	312.6	202.5	14.0	5.1	60.0	11.3	150.5
	103.5	199.0	13.4	4.15	60.0	10.5	132
	203.3	201.7	13.9	5.32	60.0	12.1	146.5
	400.2	216.2	13.6	4.25	45.0	11.65	161.5
	68.1	199.2	14.5	5.50	62.0	14.8	120
	122.0	199.6	14.5	6.2	61.0	15.4	132
	370.0	198.1	12.8	6.55	62.0	14.4	146.5
							148
$\text{He} =$	124.9	201.0	14.3	3.33	57.0	11.6	101
	228.2	200.9	15.1	4.31	57.0	13.7	110
	355.4	201.4	14.6	4.27	57.0	13.0	116
$\text{CCl}_4 =$	21.5	201.0	13.5	5.0	60.5	13.2	125
	43.0	201.0	13.5	4.65	50.0	12.6	147.5
	61.0	201.0	13.7	2.80	30.0	12.0	156
$\text{H}_2 =$	436.0	636.0	12.8	6.52	30.0	13.4	324
	254.0	454.0	13.1	6.05	41.0	13.35	221
	154.4	354.4	13.7	6.35	53.0	13.7	174.5
	378.3	578.3	14.7	6.35	30.5	13.95	299
	396.2	596.2	13.8	6.50	31.0	13.3	316
	101.8	301.8	14.75	4.47	45.0	13.75	144
	298.1	498.1	15.2	5.08	30.0	13.5	251
							101.0

If hydrogen had no effect other than that to be attributed to the chemical reaction mechanism, then the curve so obtained would be a straight line parallel to the concentration axis. Fig. 2 shows, however, that as hydrogen is added, the rates so obtained become progressively greater than would be expected on the above basis, and this relative increase must therefore be attributed to

the decreased rate of removal of bromine atoms by the wall. The other curves, with the possible exception of that with oxygen as added gas, are explicable on the same basis.

The theory previously outlined indicates that under such circumstances the rate of reaction would approximate to the first power of $I_{abs.}$, while, on the other hand, complete removal of bromine atoms by recombination in the gas phase would render the rate proportional to $(I_{abs.})^{\frac{1}{2}}$. Experiments were carried out in two series, the first in which no inert gas was present, and the second in which approximately 450 mm carbon dioxide were added. The incident light intensity was reduced by placing blue glass plates in the path of the light beam. The results are given in Table III, where γ_1 represents actually measured values (γ') calculated to $[H_2] = 400.0$ mm as before.

Table III

$[CO_2]$	$[H_2]$	$[Br_2]$	$[HBr]$	t	$[I_{abs.}]_1$	γ'	γ_1
mm	mm	mm	mm	mins	divs		
0	397.0	15.5	4.30	61	6.25	226	228
0	403.5	14.7	4.00	60	5.85	228	226
0	402.0	14.5	3.80	60	5.74	221	220

The mean value of $\gamma_1 = 225$ can be taken as representing the conditions $[H_2] = 400$, $[Br_2] = 15.0$, $[HBr] = 4.0$, $[I_{abs.}]_1 = 5.9$; this is to be compared with $\gamma_2 = 198$ for $[H_2] = 400$ mm, $[Br_2] = 15.0$ mm, $[HBr] = 5.0$ mm, and $(I_{abs.})_2 = 15.0$ divs (*cf.* fig. 2, and Table II). If now

$$\frac{d(HBr)}{dt} \propto (I_{abs.})^n,$$

then

$$\frac{\gamma_1}{\gamma_2} = \left[\frac{(I_{abs.})_1}{(I_{abs.})_2} \right]^{n-1},$$

and the value of n is here calculated as equal to 0.86.

The results for the other series are given in Table IV, where the values of γ_1 are those of γ' calculated to $H_2 = 200.0$ mm; γ_2 values are the corresponding efficiencies given by the CO_2 curve of fig. 2, where $I_{abs.} = 13.5$ divs.

Table IV

$[CO_2]$	$[H_2]$	$[Br_2]$	$[HBr]$	t	$(I_{abs.})$	γ	γ_1	γ_2	$(I_{abs.})_2$	n
mm	mm	mm	mm	mins	divs					
420.0	202.0	16.9	3.5	51	6.00	230	228	203	13.5	0.86
441.5	202.3	14.3	3.77	62	4.90	248	245	206	13.5	0.83
471.0	200.0	15.8	3.06	45	5.68	240	240	210	13.5	0.84

Calculation gives values of n slightly less than but of the same magnitude as before. It is thus apparent that the addition of inert gas as above involves a small change only in the relationship between rate of reaction and energy absorbed. In general the results indicate that bromine atoms, under the above conditions, are removed by wall action to a greater extent than that involved in mutual recombination.

It has been shown by Melville and Ludlam* that the increase in chain lengths in certain thermal oxidation reactions due to the addition of inert gas can be expressed approximately by the factor

$$1 + \left(\frac{\mu p_x}{p_R + p_{O_2}} \right),$$

where p_x , p_{O_2} , and p_R represent pressures of inert gas, oxygen, and oxidizable substance respectively, and μ is a constant inversely proportional to the diffusion coefficient of the reactive centres through the gas mixture. If μ is truly constant, then the graph of the rate of reaction against p_x is a straight line. Departure from linearity indicates that the inert gas is causing the chains to end in some other manner.

Similarly, curves showing the accelerating effect of inert gases on the photosynthesis of hydrogen bromide would be truly linear if the addition of inert gas involved no factor other than diffusion. The fact that for the conditions of the experiments of Tables I and II, the rate of reaction is proportional to $(I_{abs})^n$, where n is not unity but approximately 0.85, shows that the recombination effect cannot be neglected. In view of the fact, however, that the departure from linearity in the curves of fig. 2 is not large and that the change in n is small, it is possible to calculate from a knowledge of the molecular weights and diameters of hydrogen, bromine, and hydrogen bromide, relative values of the molecular diameters of the added inert gases, and in this way confirm the theoretical treatment.

If the atomic recombination be entirely neglected, it can be shown in the usual way that

$$\frac{d(\text{HBr})}{dt} = \frac{2k_1 \cdot k_2 \cdot k_3 \cdot [\text{H}_2] \cdot [\text{Br}_2] \cdot I_{abs}}{(k_3 [\text{Br}_2] + k_4 [\text{HBr}]) S},$$

where S represents the rate at which bromine atoms reach the wall of the vessel and are removed. For constant values of $[\text{H}_2]$, $[\text{Br}_2]$ and $[\text{HBr}]$,

$$\gamma_{\text{HBr}} = \frac{d(\text{HBr})}{dt} / I_{abs} = \frac{k}{S}.$$

* 'Proc. Roy. Soc.,' A, vol. 132, p. 108 (1931).

Consider now the bromine atom diffusing through a mixture of the four gases, Br_2 , H_2 , HBr , inert gas, for which the diffusion coefficients for each gas separately are D_1 , D_2 , D_3 , D_4 , respectively.

If t be the time required to diffuse a given distance, then it can be taken that

$$t \propto \left(\frac{1}{D_1} + \frac{1}{D_2} + \frac{1}{D_3} + \frac{1}{D_4} \right).$$

Now S is inversely proportional to t and hence

$$S \propto \left(\frac{1}{D_1} + \frac{1}{D_2} + \frac{1}{D_3} + \frac{1}{D_4} \right)^{-1}.$$

For the diffusion of a binary mixture, by the Stefan-Maxwell theory,

$$D \propto \frac{1}{[X] \sigma_{AX}^2 \left(\frac{1}{M_A} + \frac{1}{M_X} \right)^{-1}},$$

where

M_A = molar weight of particle diffusing

M_X = molar weight in inert gas

$[X]$ = pressure of inert gas

σ_{AX} = sum of radii of gas molecule and diffusing particle.

Substituting this in the expression for γ_{HBr} and remembering that $[\text{HBr}]$ and $[\text{Br}_2]$ are constant, we have

$$\gamma_{\text{HBr}} = \frac{k}{S} = k \left\{ k' + [X] \sigma_{AX}^2 \left(\frac{1}{M_A} + \frac{1}{M_X} \right)^{-1} \right\},$$

where k' is a constant readily calculated for the appropriate pressures of H_2 , Br_2 , and HBr , if the corresponding molecular radii are known. When no added inert gas X is present,

$$\gamma_{\text{HBr}} = kk'.$$

The ratio of the quantum efficiencies with and without inert gas X is therefore

$$\mu = \left\{ 1 + \frac{[X] \sigma_{AX}^2 \left(\frac{1}{M_A} + \frac{1}{M_X} \right)^{-1}}{k'} \right\}.$$

It is thus possible, for the above conditions, to calculate the molecular radii of the added inert gas molecules, if the radius of the bromine atom be known. Since, however, an appreciable fraction of the bromine atoms were

removed by triple collision as indicated by the experimental connection between $d(\text{HBr})/dt$ and $I_{\text{abs.}}$, such calculated radii must be expected to be less than the commonly accepted values. In view of the fact that the departure from linearity in the curves of fig. 2 is not great, and that any possible differences in triple collision efficiency will have only a secondary effect, relative values of the radii are calculable with a fair approximation to accuracy.

The values of μ for each inert gas were obtained from the appropriate curves of fig. 2 by extrapolation to $[\text{X}] = 0$; they thus represent the slope of the line that would be obtained if the addition of inert gas involved no effects other than the diffusion process. In Table V are given the relative increases (μ_{100}) in rate of reaction afforded on this basis by the introduction of 100 mm inert gas, and the calculated values of σ_{AX} .

$$\text{Table V—}\sigma_{\text{AX}}^2 = \frac{(\mu_{100} - 1)k'}{100} \cdot \left(\frac{1}{M_{\text{A}}} + \frac{1}{M_{\text{X}}} \right)^{-1}$$

$$k' = 2.00 \times 10^{-13}, \quad \sigma_{\text{Br}} = 2 \times 0.84 \times 10^{-8} \text{ cm.} \quad \sigma_{\text{Br}_2} = 2 \times 1.68 \times 10^{-8} \text{ cm.}$$

$$\sigma_{\text{HBr}} = 2 \times 1.40 \times 10^{-8} \text{ cm.} \quad \sigma_{\text{H}_2} = 2 \times 1.15 \times 10^{-8} \text{ cm.}$$

Inert gas	μ_{100}	$(\mu_{100} - 1)k' \times 10^{13}$	$\left(\frac{1}{M_{\text{A}}} + \frac{1}{M_{\text{X}}} \right)^{-1}$	$\sigma_{\text{AX}}^2 \times 10^{16}$	$\sigma_{\text{AX}} \times 10^8$
N_2	1.47	0.94	0.219	2.06	1.43
O_2	1.47	0.94	0.209	1.96	1.40
CO_2	1.57	1.14	0.187	2.13	1.46
CCl_4	2.95	2.90	0.138	4.00	2.00
He	1.09	0.18	0.461	0.83	0.91
H_2	1.04	0.08	0.715	0.57	0.76

As expected, calculated values are low, as compared with the usually accepted figures. Relative values are therefore considered by taking nitrogen as standard with $\sigma_{\text{A-N}_2} = (1.55 + 0.84) \cdot 10^{-8} = 2.39 \times 10^{-8} \text{ cm}$, the other values being raised correspondingly by the same factor. Results are given in Table VI.

Table VI

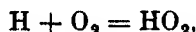
Gas	$0.5 \sigma_{\text{X}} \times 10^8$ (from viscosity)	$0.5 \sigma_{\text{X}} \times 10^8$ (calculated)
N_2	1.55	1.55
O_2	1.45	1.49
CO_2	1.60	1.60
CCl_4	2.55	2.50
He	0.95	0.70
H_2	1.15	0.42

The value for hydrogen is the only one which shows a marked divergence from the usually recognized figure. It is to be noted that a small error in μ_{100} when μ is small produces a marked effect on the finally calculated value and the difference may thus be due to experimental error.

The anomalous nature of the oxygen curve of fig. 2 remains to be considered. The values for the molecular weight and diameter of the oxygen molecule would indicate here a diffusion curve approximating in position to the nitrogen curve. Where the pressure of added gas is less than 100 mm the curve is normal in its position, but higher pressures obviously involve the introduction of a factor which is not connected with the diffusion process. The lower rate values then obtained are regarded as due to the removal of hydrogen atoms by oxygen. The effect of this reaction depends on its relation to the removal of hydrogen atoms by bromine, the deciding factors being the relative pressures of bromine and oxygen, as well as the collision efficiencies of both reactions. If the two opposing reactions are



and



and are of equal collision efficiencies, then the addition of 15 mm oxygen to 15 mm bromine would reduce the rate to half its original value; correspondingly the addition of 450 mm oxygen would mean a retardation factor of 1/31. Since the addition of 450 mm oxygen actually gives a retardation factor of 1/1.36 (by comparison with the nitrogen curve), the efficiency of the reaction involving oxygen must be 1.2×10^{-2} times that of the reaction involving bromine. Taking as the collision efficiency of this latter Bodenstein's value of 10^{-1} *, the collision efficiency of the former is 1.2×10^{-3} . The assumption is here made that the triple collision efficiencies are not appreciably different for oxygen and nitrogen; later results show that oxygen is more efficient in this respect than nitrogen, and therefore the true value will be slightly less than this figure. Bodenstein (*loc. cit.*) gives 10^{-3} as the efficiency of this reaction; Bates and Lavin† indicate a maximum value of 10^{-3} , and Norrish and Ritchie‡ give 10^{-4} at 25° C. The introduction of the reaction $\text{H} + \text{O}_2 + \text{H}_2 = \text{H}_2\text{O} + \text{OH}$ as an additional means of hydrogen atom removal would reduce the probable value of the HO_2 reaction a little further.

Results with Higher Concentrations of Bromine Atoms

Increased pressures of bromine were employed in conjunction with the maximum intensity of light provided by the filters. The method of experiment

* 'Trans. Faraday Soc.,' vol. 27, p. 415 (1931).

† 'J. Amer. Chem. Soc.,' vol. 55, p. 81 (1933).

‡ 'Proc. Roy. Soc.,' A, vol. 140, p. 713 (1933).

and the measurement of reaction velocity render inconvenient the use of very high pressures of bromine. The quantum efficiency (arbitrary units) was 320 for $[N_2] = 250$ mm, $[H_2] = 300$ mm, $[Br_2] = 39.0$ mm, $[HBr] = 15.0$ mm, and $I_{abs.} = 37.0$ divs. Experiments for similar concentrations of reactants but with $I_{abs.} = 20.4$ divs gave $\gamma = 412$, the incident intensity being reduced by blue glass plates placed in the path of the light beam. Taking as before

$$\frac{d(HBr)}{dt} \propto (I_{abs})^n, \quad \text{and} \quad \gamma = \frac{d(HBr)}{dt} / I_{abs.},$$

the ratios of the above quantum efficiencies for the two intensity values yield a value of n equal to 0.53, indicating that under such conditions, practically all bromine atoms were removed by mutual recombination, and not by the agency of the surface of the reaction vessel.

Since definite conclusions as to the triple collision effects of the different gases could not be reached with the maximum intensity of blue light obtainable as above, further experiments were carried out with white light from which light of wave-length less than $365 \mu\mu$ was removed by means of quinine hydrochloride solution. The 500 watt lamp was employed as before as the source, the rate of reaction being then some six times faster than before. The change in bromine concentration was determined by means of blue light as already described; the incident intensity of white light was taken as the galvanometer deflection produced by the white light, and $I_{abs.}$ calculated by applying the blue light absorption coefficient per mm bromine to this I_0 . Since neither I_0 nor the distribution of energy in the white light spectrum changed appreciably throughout the series of experiments, relative values of the quantum efficiency were obtained as before. The assumption is here made that the small increase in the light absorption of the bromine due to the presence of added gases is (with regard to each individual gas) relatively the same for white light as for blue light. This assumption cannot involve an error of any magnitude in view of the fact that the absorption coefficient of bromine is at its maximum in the blue region of the spectrum. Experimental results are given in Table VII, and shown graphically in fig. 3, "constant" conditions being $[H_2] = 100$ mm, $[Br_2] = 38$ mm, $[HBr] = 16$ mm, $[N_2] = 100$ mm, $I_{abs.} = 64$ divs, the other gases being added in varying concentrations. In the nitrogen series the total nitrogen present is given in the first column. The hydrogen results have been treated as before. To avoid confusion, the helium and hydrogen curves are given at the top of fig. 3.

Table VII

Added gas	[N ₂]	[H ₂]	[Br ₂]	[HBr]	t	I _{abs.}	γ'	γ	
mm	mm	mm	mm	mm	mins				
He	100.1	100.0	99.2	37.9	15.3	15.75	59.8	325	328
	220.3	100.1	101.0	38.0	16.1	16.5	60.6	322	319
	288.0	100.7	96.1	36.9	17.2	18.5	61.0	305	318
	379.6	99.6	100.5	38.1	16.3	17.3	60.5	311	309
A	122.3	99.3	99.3	38.5	14.6	13.5	62.7	345	348
	301.3	100.4	101.6	38.2	15.1	13.5	65.2	343	338
	201.3	99.1	100.5	38.4	15.6	13.5	66.4	348	347
	381.0	101.8	100.8	37.7	15.3	14.0	64.6	337	334
	435.3	100.0	100.3	38.0	15.6	15.0	64.8	321	320
CO ₂	342.0	102.7	100.0	40.0	13.9	16.0	63.9	272	272
	222.1	100.6	110.6	39.5	14.7	14.0	63.2	332	301
	65.3	100.4	100.3	38.5	15.2	14.75	61.1	337	336
	109.7	99.9	102.1	37.2	14.6	14.75	59.4	333	326
	301.3	100.9	100.3	37.8	15.85	17.0	64.3	290	289
	112.4	101.6	100.3	38.2	14.6	14.0	64.9	321	320
	479.0	100.6	102.7	39.7	11.8	15.25	63.7	243	237
	442.6	100.2	101.0	38.6	13.3	16.75	63.4	250	247
O ₂	80.0	101.0	99.1	37.3	14.4	15.5	60.3	308	311
	300.0	101.4	98.0	37.7	15.1	19.5	60.5	256	261
	0.0	95.1	100.0	38.0	16.0	16.0	60.6	330	330
	101.5	100.0	100.9	39.5	14.8	15.0	61.5	321	318
	380.0	100.2	100.4	38.4	13.25	19.0	60.4	231	230
	459.1	101.2	102.9	39.5	12.25	18.0	61.3	222	216
	210.8	99.6	102.7	38.9	13.35	15.0	59.8	298	291
H ₂	206.8	100.7	306.8	36.6	15.75	5.0	63.1	995	324
	294.0	100.5	394.0	37.4	13.9	3.5	65.6	1210	307
	382.5	100.9	482.5	36.8	15.7	3.5	63.6	1410	292
	453.0	99.3	553.0	36.0	18.0	3.75	62.0	1550	280
N ₂	466.0		98.1	38.0	14.6	15.0	67.7	289	295
	283.0		96.6	39.4	15.5	14.0	68.7	322	333
	436.0		97.6	38.5	15.6	15.0	67.7	307	315
	493.2		98.4	38.9	14.0	15.0	67.7	276	281
	547.4		110.0	38.8	14.3	14.0	66.7	306	278
	101.2		100.2	37.7	15.55	14.5	64.8	331	330
	196.8		99.1	35.9	15.3	14.0	65.7	332	335
	347.1		102.3	39.4	15.3	14.0	67.3	325	318

Examination of fig. 3 shows that in some determinations, a small diffusion effect is still appreciable when the added gas concentration is relatively low, this being apparent in the initial increases in quantum efficiencies. Further addition of inert gas, however, is attended by a decrease in reaction velocity; the proportion of bromine atoms which is then removed by wall action must be small, the conditions being comparable to those already cited, where the rate of reaction was proportional to $(I_{\text{abs.}})^{0.53}$.

When all bromine atoms are removed by recombination, the quantum efficiency of hydrogen bromide formation is

$$\gamma = \frac{d(\text{HBr})}{dt} / I_{\text{abs.}} = \frac{2 \sqrt{2} \cdot k_2 \cdot k_3 [\text{Br}_2] \cdot [\text{H}_2]}{\sqrt{I_{\text{abs.}} (k_3 [\text{Br}_2] + k_4 [\text{HBr}])} \sqrt{k_5 M}}$$

When variation of $[M]$ is alone considered, $I_{abs.}$ and the concentrations of the other reactants being constant as above,

$$\gamma = \frac{k}{\sqrt{k_5[M]}}, \text{ or } k_5[M] = \frac{k^2}{(\gamma)^2}.$$

Now $k_5[M]$ refers to all the gases present in the system, each of which must be taken as having a different efficiency so far as the triple collision is concerned, and hence $k_5[M]$ must be replaced by

$$k_{H_2}[H_2] + k_{HBr}[Br_2] + k_{Br_2}[Br_2] + k_x[X].$$

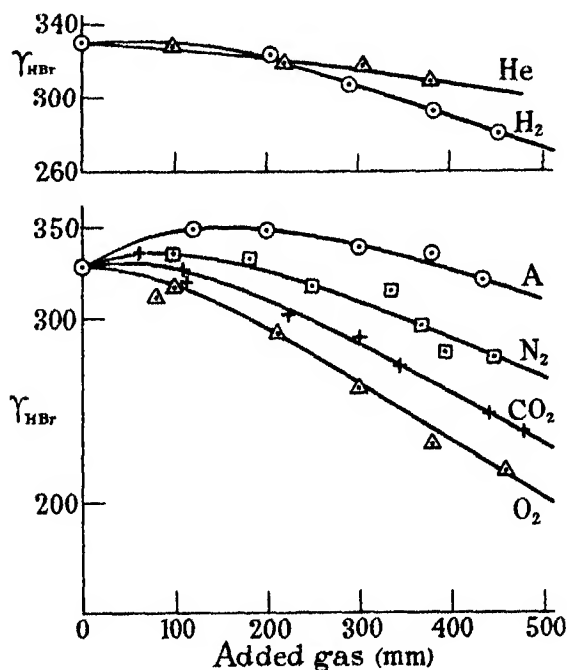


FIG. 3

The first three of these terms are constant, by the experimental conditions, and therefore

$$k' + k_x[X] = \frac{k^2}{\gamma^2},$$

where X refers to the added foreign gases of fig. 3. Thus the graphs of $1/\gamma^2$ against X should be a series of straight lines with a common intercept k'/k^2 , the slopes of these lines giving relative values of k_x .

The values of fig. 3 are thus considered in this connection, the results being shown graphically in fig. 4. The oxygen values of fig. 3 have been corrected for the reaction $\text{H} + \text{O}_2 = \text{HO}_2$ by the factor given previously. When the pressure of added gas is low, the diffusion effect is considerable, but approximately straight lines are obtained for the higher pressures of carbon dioxide, oxygen, nitrogen, and argon, the common intercept being $k'/k^2 = 0.35 \times 10^{-5}$. From the straight line portions, values of k_x/k^2 are: CO_2 , 0.29×10^{-7} ; O_2 , 0.29×10^{-7} ; N_2 , 0.21×10^{-7} ; A, 0.135×10^{-7} . Corresponding values for helium and hydrogen cannot be obtained with any precision by this method, for the reason that the diffusion effect is not overcome unless by the addition of very large pressures of these gases.

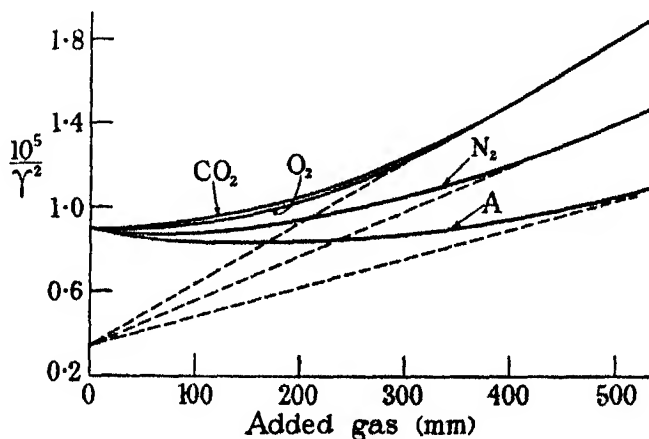


FIG. 4

If all bromine atoms were removed by recombination in the gas phase, *i.e.*, if $n = 0.50$,

$$\gamma^2 = \frac{1}{(0.35 \times 10^{-5} + \frac{k_x}{k^2} [\text{X}])}$$

and the rate which would have been obtained if $[\text{X}] = 0$ and no surface removal of atoms occurred, would be $\gamma = \frac{\sqrt{10^5}}{0.35} = 535$. This is considerably greater than the actually recorded value of 330, and hence by determining the slope of the argon curve where $[\text{A}] = 0$, a straight line can be drawn, points on which give a good approximation to the rates of reaction to be expected if the addition of argon produced no effect other than a rise in velocity referable to that fraction of bromine atoms removed by the wall. Once the argon line has

been established it is an easy matter, on the theoretical basis given previously to calculate from the molecular weights and diameters the positions of the corresponding lines for helium and hydrogen. The relative effects of argon, helium and hydrogen on the rate of HBr formation are therefore estimated by considering the increases which would have been obtained if no further triple collision processes had occurred on the addition of inert gas, and comparing these with the actually recorded values. Thus, taking the value of μ_{100} as 1.07 for argon, the other calculated values are $\mu_{H_2} = 1.017$, $\mu_{He} = 1.019$. Retardation factors (ratios of experimentally determined rates to rates calculated on the basis of no further triple collision processes) can then be tabulated.

Table VIII—Retardation Factors

Pressure mm.	A	H ₂	He
0	1.00	1.00	1.00
100	0.98	0.985	0.975
200	0.92	0.935	0.94
300	0.85	0.88	0.905
400	0.775	0.825	0.865
500	0.695	0.76	0.795

In accordance with the above considerations, the most accurate comparisons will be obtained at low pressures of added gas, considered in conjunction with experimental error.

The rate of reaction is proportional to the concentration of bromine atoms, and the number of bromine quasi-molecules then forming is proportional to $[Br]^2$; and therefore the relative effects of, say, 300 mm foreign gas, on the number of quasi-molecules forming is given by the squares of the corresponding retardation factors, *i.e.*, 0.72 (A), 0.78 (H₂), 0.82 (He). The relative efficiencies of these gases in the triple collision process are then approximately 0.28 : 0.22 : 0.18.

We can now complete the series of triple collision efficiencies as follows :—

$$\begin{array}{ccccccc} \text{He} & < & \text{H}_2 & < & \text{A} & < & \text{N}_2 < \text{CO}_2 \\ & & & & & & & \text{O}_2 \\ (0.086) & & (0.106) & & (0.135) & & (0.21) & (0.29) \end{array}$$

From the value of $k'/k^2 = 0.35 \times 10^{-5}$, a value for Br₂ can be estimated as 0.15; but in view of the possible error in k'/k^2 , this value can only be interpreted as indicating a very rough order of magnitude.

The above numbers give the relative triple collision efficiencies when the added gas concentrations are expressed in millimetres. Correcting for the fact that the number of collisions (for a given pressure) depends on the mass and

radius of the molecule or atom, the series becomes, taking the CO_2 value as unity :—

$$\begin{array}{ccccccc} \text{H}_2 & < & \text{He} & < & \text{A} & < & \text{N}_2 & < & \text{O}_2 & < & \text{CO}_2 \\ (0.12) & & (0.15) & & (0.52) & & (0.62) & & (0.95) & & (1.00). \end{array}$$

In considering generally the removal of energy in the triple collision process, it seems reasonable to conclude that comparison cannot rightly be made between the above series and the series of gas effects associated with quenching of fluorescence (*e.g.*, mercury, iodine, nitrogen dioxide), on the basis that the latter involves electronic energy, while the former is concerned mainly with energy of vibration. The removal of energy in the quenching phenomena might thus be expected to be specific in action, with due regard to the amount of energy to be removed and the existence of possible resonance levels in the quenching molecule. Stern and Volmer* have drawn the conclusion that the more pronounced the electronegative character of the gas, then the greater the efficiency of energy removal. Thus oxygen would have a greater effect than nitrogen, as above; but the definite effect of the inert gas argon in itself indicates that the triple collision series above cannot be explained satisfactorily on this basis. In the same way the number of degrees of freedom of the foreign gas molecule gives little idea of the effect to be expected in such a process.

A similar series of effects does occur in the stabilization of the ozone molecule by the triple collision



Thus Schumacher and Beretta† have shown that the rate of decomposition of ozone in red or ultra-violet light is decreased by the addition of other gases as above. The series in this work was found to be

$$\begin{array}{ccccccc} \text{He} & < & \text{Ar} & < & \text{N}_2 & < & \text{CO}_2 \\ & & & & & & \text{O}_2. \\ (0.5) & & (1) & & (6) & & (10) \end{array}$$

Carbon dioxide and oxygen again have efficiencies which are approximately equal, the oxygen molecule being more efficient than the nitrogen molecule, a difference perhaps unexpected on general grounds, but also indicated by Schumacher and Stieger for the recombination of chlorine atoms.

Considering the question from the general point of view, the removal of energy from the energy-rich complex by collision with another gas molecule

* 'Z. wiss. Photogr.,' vol. 19, p. 275 (1920).

† 'Z. phys. Chem.,' B, vol. 17, p. 417 (1932).

might be expected to be a process analagous to the collision of a gas molecule with a hot wire. It has been established that in this latter reaction the temperature of the wire is not, in general, attained by the colliding gas molecule, the efficiency of the collision in this respect varying with the nature of the gas, and being expressed by the "accommodation coefficient"* A table of such coefficients has recently been given by Dickinst† from measurements on the thermal conductivity of the gases concerned by the hot wire method, and while the actual values of the coefficients are dependent on the state of the metal surface, yet for comparable conditions there seems no reason to doubt that the order of efficiency thus obtained is dependent mainly on the nature of the gas. The series is as follows, the accommodation coefficients being quoted also :—

$$\begin{array}{ccccccc} \text{H}_2 & < & \text{He} & < & \text{A} & = & \text{N}_2 & < & \text{O}_2 & < & \text{CO}_2 \\ (0.36) & & (0.50) & & (0.89) & & (0.89) & & (0.90) & & (0.91) \end{array}$$

It will be observed that the differences between A, N₂, O₂ and CO₂ are small, the efficiency of energy removal being high, but as a whole the series bears a decided resemblance to that obtained for the stabilization of the quasi-bromine molecule. In particular may be noted the position of hydrogen and the relatively high values of argon. The series of efficiencies of gases in the triple collision process here studied thus corresponds to the accommodation coefficient series as determined from thermal conductivity measurements.

The author desires to acknowledge the interest and encouragement afforded to him by Dr. E. B. Ludlam and Professor J. Kendall. His thanks are also due to the Earl of Moray Endowment Fund for the provision of the quartz reaction vessel.

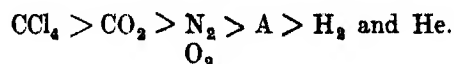
Summary

Investigation has been made of the rates of photochemical formation of hydrogen bromide at 200° C in the presence of various "foreign" gases, from two points of view (a) the removal of bromine atoms from the gas phase by diffusion to the wall of the reaction vessel and (b) the removal of bromine atoms by the recombination process involving a third molecule as stabilizer.

* Cf. Knudsen, 'Ann. Physik,' vol. 46, p. 641 (1915); Soddy and Berry, 'Proc. Roy. Soc.,' A, vol. 83, p. 284 (1910); vol. 84, p. 576 (1911).

† 'Proc. Roy. Soc.,' A, vol. 143, p. 538 (1934).

In (a), addition of foreign gas is accompanied by increase in the rate of reaction, the relative accelerations corresponding to those calculated on kinetic theory considerations and being expressed by the series



In (b), addition of foreign gas decreases the rate of reaction by facilitating the recombination of bromine atoms. The series representing the efficiencies of the triple collision process is given by



Attention is drawn to the parallelism existing between this series and that of the corresponding accommodation coefficients as determined from thermal conductivity measurements.

The Thermal Decomposition of Ozone

By MOWBRAY RITCHIE (B.Sc., Ph.D.), Department of Chemistry, University of Edinburgh

(Communicated by J. Kendall, F.R.S.—Received May 23, 1934.)

The thermal decomposition of ozone has been generally regarded as essentially a bimolecular reaction. The exact determination of the nature of the mechanism has, however, been attended by the discovery of several conflicting influences, the interpretations of which have been matters of no small difficulty and interest. It can scarcely be said that the mechanism of decomposition has been definitely established.

General discussion has centred round the calculation of the absolute rate of reaction from the experimentally determined energy of activation, from which it appears that the velocity coefficient, calculated in the usual way, is much less than the experimentally determined value when the decomposition is regarded as bimolecular. Thus Riesenfeld and Wassmuth* inclined to the idea of an energy chain reaction, the length of the chains being sufficient to explain the discrepancy, while Schumacher and Sprenger† considered that

* 'Z. phys. Chem.,' B, vol. 8, p. 314 (1930).

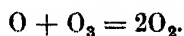
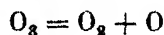
† 'Z. phys. Chem.,' B, vol. 6, p. 446 (1930).

the energy of activation cannot adequately be considered on the "two squared terms" basis, but that allowance must be made for the possible other degrees of freedom of the ozone molecule. This view is regarded as supported by recent work of Glissmann and Schumacher.*

Jahn† and Perman and Greaves‡ concluded that the rate of decomposition varied inversely as the pressure of oxygen present, and Jahn suggested that the course of the reaction was not the simple one



but consisted of the stages



The first stage was assumed rapid and reversible, and the observed rate determined by the second reaction. This mechanism, however, was rejected by Wulf and Tolman§ on the basis of a calculation showing the number of collisions between ozone molecules and oxygen atoms as too small to account for the observed rate of reaction.

In the previous paper on the photochemical formation of hydrogen bromide, the effects of foreign gases have been arranged in two series, one corresponding to an acceleration of the rate of reaction by virtue of the suppression of a wall reaction, and the other to a retarding action attributed to a triple collision process. In the thermal decomposition of ozone, a surface action and an accelerating influence of inert gases have been reported, while a retarding influence of oxygen has been observed in certain circumstances||; it therefore appeared possible that where no definite effect of oxygen could be observed, the explanation was the cancelling of the accelerating and inhibiting influences.

The thermal decomposition of ozone therefore has here been examined from this point of view. The results now to be reported are interpreted as indicating that the primary decomposition of ozone is the "unimolecular" process



In the absence of oxygen, inert gases such as argon, helium, and nitrogen,

* 'Z. phys. Chem.,' B, vol. 21, p. 323 (1933).

† 'Sitzber. K. Akad. Wiss.,' Berlin, vol. 48, p. 1126 (1901).

‡ 'Proc. Roy. Soc.,' A, vol. 80, p. 353 (1908).

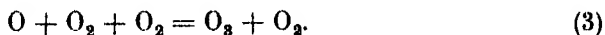
§ 'J. Amer. Chem. Soc.,' vol. 49, p. 1650 (1927).

|| Cf. Hinshelwood, 'Kinetics of Chemical Change in Gaseous Systems,' 3rd Ed., p. 80.

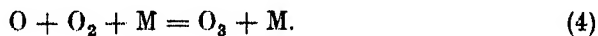
increase the rate of reaction by preventing the diffusion of the oxygen atoms to the wall and thereby facilitating the reaction



Addition of oxygen at first increases the rate of reaction by the above diffusion effect, but this is succeeded by a decrease in total reaction velocity by virtue of the triple collision



The addition of other gases to ozonized oxygen mixtures of sufficiently high oxygen content produces a similar decrease in rate of decomposition, by the reaction



In the presence of large pressures of oxygen, the mechanism is then such as to render the total rate of decomposition apparently bimolecular with respect to the ozone; the apparent heat of activation obtained under these conditions involves the velocity coefficients of the reactions quoted above.

Experimental

The apparatus used has been described in detail in the preceding paper. The same quartz reaction vessel was employed, experiments being carried out at 80°, 90° and 100° C., the increase in pressure due to the decomposition being accurately measured by the calibrated telescope-Bourdon gauge system. Ten divisions of the eyepiece scale corresponded to 1.7 mm Hg, and since readings were accurate to 0.1 division, changes in pressure down to 0.015 mm could be recorded.

Ozone was prepared in a single ozonizer (Berthelot type, employing copper sulphate solution) by subjecting dry oxygen to the silent discharge provided by an induction coil. In the ozonizer itself the oxygen was kept at atmospheric pressure, while the liquid air trap in which the ozone was collected was evacuated by water filter-pump to approximately 10 mm pressure, the connecting tap thus controlling the rate of flow of oxygen through the ozonizer. The vapour pressure of ozone at the temperature of liquid air is very small (< 0.05 mm): residual oxygen was removed finally by direct application of a Hyvac oil pump. Analysis of ozone samples prepared in such a manner and collected in an analysing bulb (200 cc volume) by manipulation similar to that involved in the introduction of ozone into the reaction vessel for any

thermal decomposition experiment, gave concordant values of 95–96% purity, as estimated by the neutral potassium iodide-thiosulphate method.* Complete decomposition, by a hot platinum wire, of similar samples gave values of 97%; the ozone as prepared above and as introduced into the reaction vessel contained, therefore, only a small proportion of oxygen.

Nitrogen, argon, helium and oxygen were obtained as described in the preceding paper.

Rates of reaction were recorded immediately the ozone had been introduced into the reaction vessel. The sensitivity of the glass spring gauge was such as to render possible accurate measurement of the rate of reaction in the initial stages where the amount of oxygen formed by the decomposition remained relatively small. Correspondingly the rate was measured over a small change in ozone concentration.

Results

Ozone-nitrogen Mixtures—Table I gives details of experiments showing the influence of nitrogen on the rate of decomposition. The initial pressure of ozone was calculated on the basis of the analyses already recorded, showing that 100 mm gas, as introduced into the reaction vessel, contained 5 mm oxygen. The average pressure of ozone was taken as the arithmetic mean of initial and final concentrations. The increase in pressure (Δp) is given in divisions of the telescope eyepiece scale for the time t (seconds), while the rate of decomposition $r_{\text{exp.}}$ is calculated in millimetres ozone decomposing per second over the range. Since an increase in pressure of Δp represents a decrease in ozone pressure of $2(\Delta p)$,

$$r_{\text{exp.}} = \frac{2(\Delta p)}{t} \times F,$$

Table I—Temperature = 90.0° C

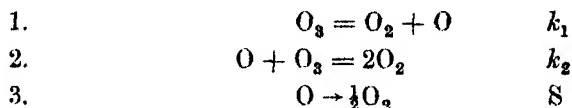
[N ₂] mm	Initial [O ₃]	Av. [O ₃]	Av. [O ₂]	Δp divs	t secs	$r_{\text{exp.}} \times 10^3$
0.0	19.5	18.3	2.7	6.8	570	4.06
0.0	19.5	18.3	2.8	6.95	600	3.94
127.0	20.0	18.8	4.8	7.3	450	5.50
241.1	19.5	18.1	8.1	8.1	480	5.75
43.0	19.8	18.6	3.8	7.2	510	4.80
65.8	19.3	17.7	4.3	8.95	600	5.07
0.0	19.8	18.7	2.6	6.4	540	4.03
285.4	19.2	17.7	8.2	8.7	510	5.80
88.0	19.5	18.2	5.0	7.4	510	5.00
184.2	19.6	18.3	6.5	7.8	480	5.52
0.0	19.4	18.2	2.8	7.0	600	3.96

* Cf. Mellor, 'Inorganic and Theoretical Chemistry,' vol. 1, p. 904; also Riesenfeld and Schwab, 'Ber. deuts. chem. Ges.,' vol. 55, p. 2088 (1922).

where F is the factor (0.17) converting eyepiece divisions to millimetres of mercury. The results are given in the order in which they were obtained.

The nitrogen used in these experiments was found by analysis to contain approximately 1.5% oxygen; this correction has been included in the numbers of Table I. The differences in $\text{Av. } [\text{O}_3]$ and $\text{Av. } [\text{O}_2]$ for the various experiments are small, and for the present purpose it is sufficient to consider the results as applying to the values $[\text{O}_3] = 18.0$ mm and $[\text{O}_2] = 4.0$ mm for the different concentrations of nitrogen. The results are thus shown graphically in fig. 1; the increase in rate of decomposition on the addition of nitrogen is immediately apparent.

This increase on the addition of such a foreign gas suggests at once the gradual lessening of the wall effect reported by many observers for low pressure conditions. The reaction mechanism which is here put forward on the basis of the above and subsequent results is founded on the recognition of the oxygen atom as the reactive diffusing body; for the conditions of Table I the scheme is represented as follows:—



The coefficient S represents the rate at which oxygen atoms reach the wall and are destroyed. The total rate of decomposition then depends on the relative effects of reactions 2 and 3; obviously the addition of an inert gas such as nitrogen will increase the rate of reaction by preventing the oxygen atoms from reaching the wall. On the basis of the above mechanism, then,

$$\frac{d(\text{O})}{dt} = k_1[\text{O}_3] - k_2[\text{O}][\text{O}_3] - S[\text{O}] = 0,$$

whence

$$[\text{O}] = \frac{k_1[\text{O}_3]}{(k_2[\text{O}_3] + S)}.$$

The rate of ozone decomposition is thus

$$-\frac{d(\text{O}_3)}{dt} = k_1[\text{O}_3] \left[1 + \frac{k_2[\text{O}_3]}{(k_2[\text{O}_3] + S)} \right]. \quad (a)$$

The effect of the surface is hence most appreciable at low pressures of ozone; conversely, if sufficient inert gas be present to render the surface effect negligible, the rate of ozone decomposition is given by

$$-\frac{d(\text{O}_3)}{dt} = 2k_1[\text{O}_3].$$

If now D_{O_2} and D_X are the diffusion coefficients of the oxygen atom with respect to ozone and to a foreign gas such as nitrogen respectively (neglecting the small amount of oxygen for the present),

$$S \propto \left(\frac{1}{D_{O_2}} + \frac{1}{D_X} \right)^{-1}.$$

For a binary mixture (atom A and foreign gas M)

$$D_M \propto \frac{1}{[M] \sigma_{AM}^2 \left(\frac{1}{M_A} + \frac{1}{M_M} \right)^{-1}},$$

where σ_{AM} is the sum of the radii of atom and inert gas, and M is the molecular or atomic weight, and hence we can put

$$S = V \left(\frac{1}{D_{O_2}} + \frac{1}{D_X} \right)^{-1},$$

where V is a constant which will otherwise vary with the shape and material of the reaction vessel. For a given temperature, the ratio of rates of ozone decomposition with and without added inert gas X is then calculated as

$$R = \frac{[2 [O_3] \{P [O_3] + Q [X]\} + V/k_2] [[O_3] \{P [O_3]\} + V/k_2]}{[[O_3] \{P [O_3] + Q [X]\} + V/k_2] [2 [O_3] \{P [O_3]\} + V/k_2]}, \quad (b)$$

where

$$P = \sigma_{O-O_2}^2 \left(\frac{1}{M_O} + \frac{1}{M_{O_2}} \right)^{-1}$$

$$Q = \sigma_{O-X}^2 \left(\frac{1}{M_O} + \frac{1}{M_X} \right)^{-1}.$$

The nitrogen curve of fig. 1 was constructed on this basis; the standard rate of decomposition when $[N_2] = 0$ was taken from the results of Table I as 4.00×10^{-8} mm ozone per second for the conditions $[O_3] = 18.0$ mm. The following values were employed in the calculations:—

$$\sigma_{O_2} = 3.6 \times 10^{-8} \text{ cm}, \sigma_{N_2} = 3.1 \times 10^{-8} \text{ cm}, \sigma_{O_2} = 3.0 \times 10^{-8} \text{ cm}$$

$$\sigma_O = 1.5 \times 10^{-8} \text{ cm}, V/k_2 = 30000 \times 10^{-18}.$$

The rates calculated by formula (b) above are compared in Table II with those obtained experimentally.

The figures of the last column show that experimental rates are well expressed by the above expression and, correspondingly, reliance is placed in the value obtained for $[N_2] = \infty$. This rate, as previously pointed out, represents the

Table II—Temperature = 90.0° C $[O_3] = 18.0$ mm

$[N_2]$	$r_{\text{exp.}} \times 10^3$	$r_{\text{calc.}} \times 10^3$	$r_{\text{exp.}}/r_{\text{calc.}}$
mm	mm/sec	mm/sec	
43.0	4.80	4.64	1.03
65.8	5.07	4.90	1.03
88.0	5.00	5.11	0.98
127.0	5.50	5.36	1.03
184.2	5.52	5.60	0.99
241.1	5.75	5.78	1.00
285.4	5.80	5.87	0.99
∞		6.52	

rate of ozone decomposition when surface action is negligible, and is related to k_1 by the formula

$$-\frac{d(O_3)}{dt} = 2k_1 [O_3].$$

The velocity coefficient k_1 is thus calculated from these figures as

$$\frac{6.52 \times 10^{-3}}{2 \times 18.0} = 1.81 \times 10^{-4} \text{ sec}^{-1} \text{ at } 90^\circ \text{ C.}$$

Ozone-argon and Ozone-helium Mixtures—The value of V/k_2 having been determined as $30,000 \times 10^{-16}$ in the appropriate units, it is possible to calculate on the above basis rates of reaction in the presence of inert gases other than nitrogen, from a knowledge of the corresponding molecular weights and diameters. Experimentally, rates of decomposition were determined as before for ozone-argon and ozone-helium mixtures. In Table III these are given and compared with values calculated as above, σ_A and σ_{He} being taken, for purposes of calculation, as 2.85×10^{-8} and 1.90×10^{-8} cm respectively.

The ratios of the final column ($r_{\text{exp.}}/r_{\text{calc.}}$) show that experimental rates are again in good agreement with those calculated on the basis of the diffusion theory.

Table III—Temperature = 90.0° C $[O_3] \doteq 18$ mm

Added gas	Initial $[O_3]$	Av. $[O_3]$	Av. $[O_3]$	Δp	t	$r_{\text{exp.}} \times 10^3$	$r_{\text{calc.}} \times 10^3$	$r_{\text{calc.}}/r_{\text{ex.}}$
	mm			divs	secs			
Argon	32.8	19.0	17.6	2.0	8.0	4.53	4.40	0.98
	79.3	19.4	18.1	2.0	7.7	4.85	4.95	1.02
	151.0	19.7	18.4	1.9	7.6	5.38	5.40	1.00
	221.9	19.2	17.9	1.9	7.5	5.66	5.68	1.00
Helium	0	19.1	17.9	1.8	6.86	4.08	4.00	1.02
	59.0	19.1	17.8	1.9	7.5	4.25	4.31	0.99
	75.0	19.3	18.0	1.9	7.4	4.42	4.39	1.01
	103.5	19.4	18.1	2.0	7.7	4.36	4.52	0.96
	196.0	19.5	18.4	1.7	6.5	4.60	4.85	0.96

Mixtures containing Oxygen—Further experiments were carried out in which oxygen was introduced as the foreign gas, the temperature and concentration of ozone being kept as in the preceding series. Results are given in Table IV.

Table IV—Temperature = 90.0° C $[O_3] \doteq 18$ mm

Av. [O ₂]	Initial [O ₂]	Av. [O ₂]	Δp	t	$r_{\text{exp.}} \times 10^3$	$r_{\text{calc.}} \times 10^3$	$r_{\text{exp.}}/r_{\text{calc.}}$
			divs	secs			
2.0	19.1	17.8	8.1	660	4.17	4.03	1.03
38.5	19.4	18.0	8.2	660	4.22	4.48	0.94
60.6	19.2	17.8	8.2	600	4.64	4.63	1.00
90.6	19.1	17.8	8.2	600	4.64	4.60	1.01
104.3	19.5	18.2	8.1	630	4.37	4.47	0.98
2.1	19.3	17.9	8.2	690	4.04	4.03	1.00
203.8	19.4	17.9	8.8	960	3.12	3.21	0.97
250.1	19.4	18.1	8.05	1020	2.68	2.70	1.00
309.7	19.4	18.1	7.8	1200	2.21	2.10	1.05
373.5	19.0	17.7	7.9	1560	1.72	1.62	1.06

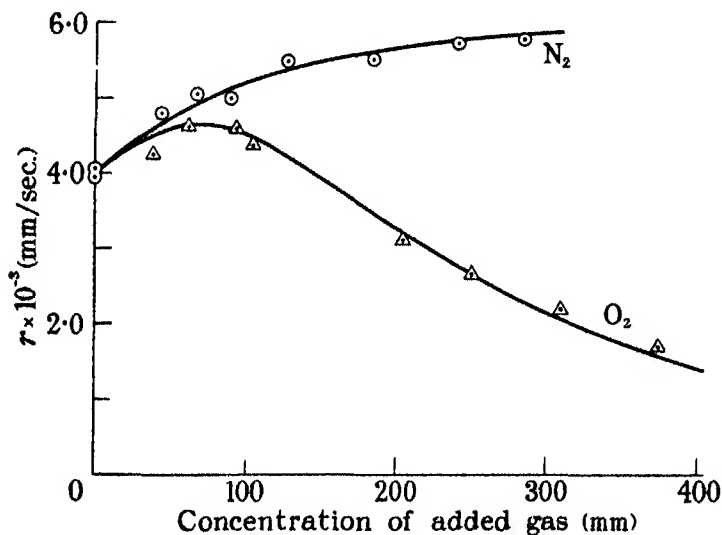


FIG. 1

The average ozone concentrations being in each experiment approximately 18 mm as before, the results are also shown graphically in fig. 1. Addition of oxygen at first increases the rate of ozone decomposition by reason of the diffusion effect, but this is rapidly succeeded by a decrease in the rate of reaction, 350 mm oxygen reducing the rate to approximately half its original value. Before discussing these effects, it is of advantage to give another set of experimental results, Table V, when the rate of reaction was recorded for $[O_3] = 18$ mm, as before, while the initial concentration of oxygen was approximately 100 mm, and nitrogen or argon were added to various pressures.

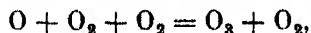
Table V—Temperature = 90.0° C

Added gas		Av. [O ₃]	Initial [O ₃]	Av. [O ₃]	Δp	t	$r_{\text{exp.}} \times 10^3$	$r_{\text{calc.}} \times 10^3$	$r_{\text{exp.}}/r_{\text{calc.}}$
		mm			diva	secs			
Argon	50.1	109.8	19.3	17.8	8.6	750	3.90	4.14	0.95
	83.6	103.1	19.7	18.3	8.1	690	4.00	4.03	0.99
	130.1	103.3	19.2	17.9	7.5	660	3.86	3.74	1.03
	154.7	103.3	19.6	18.2	8.2	780	3.58	3.58	1.00
	200.2	102.4	19.4	18.0	8.0	840	3.41	3.36	1.01
Nitrogen	0	2.0	19.8	18.4	8.0	690	3.94	4.00	0.99
	80.4	103.3	19.4	18.0	8.5	780	3.70	3.76	0.98
	130.6	102.5	19.5	18.1	8.2	840	3.32	3.31	1.00
	180.0	102.6	19.4	18.2	6.95	780	3.03	2.95	1.03
	244.1	102.6	20.0	18.5	9.0	1320	2.32	2.56	0.91
	0	1.8	19.2	18.0	7.1	600	4.03	4.00	1.01

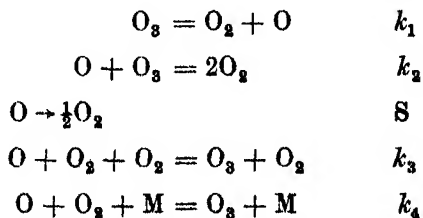
From the results of Table V, it is evident that the addition of "inert" gas to the oxygen ozone mixtures, more particularly when the "inert" gas is nitrogen, decreases the rate of ozone decomposition, in contradistinction to the increase in reaction velocity observed when no oxygen was present; the diffusion effect due to nitrogen must occur as before, but, under the conditions, is small and overshadowed by some reaction in which both oxygen and nitrogen are involved. This reaction is then most probably a triple collision involving the nitrogen molecule, the oxygen molecule and the oxygen atom, reformed ozone being stabilized by the triple collision,



Thus the retardation by oxygen alone is represented by



where oxygen molecules themselves play the part of the third colliding body. On this basis we formulate the reaction mechanism as follows:—



The rate of ozone decomposition is then obtained as before as

$$-\frac{d(\text{O}_3)}{dt} = \frac{k_1 [\text{O}_3] [2k_2 [\text{O}_3] + \text{S}]}{(k_2 [\text{O}_3] + k_3 [\text{O}_2]^2 + k_4 [\text{O}_2] [\text{M}] + \text{S})}. \quad (c)$$

In this expression, S represents the rate at which oxygen atoms are removed

from the gas phase by wall action and can therefore be replaced as in the theory given previously by

$$V ([O_3] P + [O_2] Q + [X] R)^{-1},$$

where

$$P = \sigma_{O-O_3}^2 \left(\frac{1}{M_O} + \frac{1}{M_{O_3}} \right)^{-\frac{1}{2}},$$

$$Q = \sigma_{O-O_2}^2 \left(\frac{1}{M_O} + \frac{1}{M_{O_2}} \right)^{-\frac{1}{2}},$$

and

$$R = \sigma_{O-X}^2 \left(\frac{1}{M_O} + \frac{1}{M_X} \right)^{-\frac{1}{2}}.$$

The value of V/k_2 at 90° C has already been determined as $30,000 \times 10^{-16}$ in the appropriate units. For oxygen-ozone mixtures, the ratios of rates with and without added oxygen are then given by

$$R = \frac{[2 [O_3] \{P [O_3] + Q [O_2]\} + V/k_2] [[O_3] \{P [O_3]\} + V/k_2]}{\{ [O_3] + \frac{k_3}{k_2} [O_2]^2 \} \{P [O_3] + Q [O_2]\} + V/k_2 [2 [O_3] \{P [O_3]\} + V/k_2]}. \quad (d)$$

The values of $r_{calc.}$ in Table IV have been obtained by means of this expression by taking as standard the rate of 4.00×10^{-3} mm ozone per second for $[O_3] = 18.0$ mm, with $\sigma_{O-O_3} = 2.55 \times 10^{-8}$ cm, $\sigma_{O-O_2} = 2.25 \times 10^{-8}$ cm, and $k_3/k_2 = 4.5 \times 10^{-4}$. Again the ratios of the final column of Table IV show that the experimental rates are well reproduced by the above expression.

For oxygen-argon-ozone and oxygen-nitrogen-ozone mixtures, the ratios of rates with and without added oxygen and nitrogen or argon are given by

$$R = \frac{[2 [O_3] \{P [O_3] + Q [O_2] + R [X]\} + V/k_2] [[O_3] \{P [O_3]\} + V/k_2]}{\{ [O_3] + \frac{k_3}{k_2} [O_2]^2 + \frac{k_4}{k_2} [X] [O_2] \} \{P [O_3] + Q [O_2] + [X] [R]\} + V/k_2 [2 [O_3] \{P [O_3]\} + V/k_2]}.$$

where X refers to nitrogen or argon. The values of $r_{calc.}$ in Table V have been obtained by taking $k_4/k_2 = 6.4 \times 10^{-4}$ for argon, and $k_4/k_2 = 10.2 \times 10^{-4}$ for nitrogen, in conjunction with the previously determined values of k_3/k_2 and V/k_2 . Again satisfactory agreement is to be observed between experimental and calculated values, Table V.

Velocity Coefficients and Energies of Activation

Examination of formula (c) above indicates that in the presence of large pressures of oxygen, when S will be small, the total rate of decomposition will

be approximately proportional to the square of the ozone concentration, since under these circumstances the denominator remains approximately constant. The reaction under these conditions will appear bimolecular, as has been observed by many workers. The apparent heats of activation obtained from experiments in which mixtures of ozone and oxygen were used will in general depend on the relative concentrations of ozone and oxygen as well as on the velocity coefficients k_1 , k_2 and k_3 .

From Tables I and II, comprising the results for ozone-nitrogen mixtures, the value of k_1 has been found to be $1.81 \times 10^{-4} \text{ sec}^{-1}$ at 90.0°C . Corresponding series of experiments were carried out with ozone-nitrogen mixtures at 80.0°C and 100.0°C with a view to obtaining by similar calculation the variation of k_1 for such a change in temperature, and from this the true energy of activation in this reaction. Results are given in Tables VI and VII.

Table VI—Temperature = 100.0°C

N_2	Initial [O_3]	Av. [O_3]	Av. [O_2]	$4p$	t	$r_{\text{exp.}} \times 10^3$	$r_{\text{calc.}} \times 10^3$	$r_{\text{exp.}}/r_{\text{calc.}}$
mm	mm	mm	mm	divs	secs			
0	19.4	18.1	1.9	7.1	300	8.05	7.8	1.03
78.5	19.5	18.3	3.2	6.9	240	9.75	9.8	0.99
125.0	19.5	18.1	5.0	8.0	270	10.1	10.45	0.97
175.0	19.7	18.2	5.2	8.7	270	11.0	10.9	1.01
237.0	19.3	18.0	6.8	7.6	240	10.9	11.2	0.97
292.3	19.0	17.6	7.0	8.0	240	11.3	11.5	0.98
0.0	19.5	18.2	2.1	7.6	330	7.8	7.8	1.00
∞		18.0					13.0	

Table VII—Temperature = 80.0°C

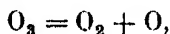
0	19.2	17.9	1.9	7.6	1440	1.79	1.80	1.00
70.0	19.3	18.0	3.0	7.6	1140	2.27	2.23	1.02
113.4	19.7	18.4	4.0	7.4	1080	2.33	2.37	0.98
198.0	19.8	18.6	5.8	7.25	960	2.56	2.54	1.01
261.9	19.8	18.5	5.2	7.4	990	2.54	2.63	0.97
339.0	19.6	18.4	7.8	7.35	930	2.67	2.68	1.00
0.0	19.3	18.0	2.0	7.7	1440	1.82	1.80	1.01
∞		18.0					3.00	

Again addition of inert gas raises the rate of reaction, 300 mm nitrogen increasing the rate by the factor 1.45 as at 90°C . The calculated rates of Tables VI and VII have been obtained by means of formula (b), the value of V/k_2 being taken as $30,000 \times 10^{-16}$ as before. This term V/k_2 must vary with temperature, but experimental results are satisfactorily represented by the constant value; both V and k_2 apparently increase with rise in temperature in such a way as to render the quotient practically independent of the temperature over the range concerned. The standard rates ($N_2 = 0$) were $7.85 \times 10^{-3} \text{ mm}$ per second at 100.0°C and $1.80 \times 10^{-3} \text{ mm}$ per second at 80.0°C .

Calculating the appropriate value of k_1 from τ_∞ at each temperature, we can summarize the numbers obtained as follows:—

Temperature °C	k_1 (sec ⁻¹)
80.0 ..	0.835×10^{-4}
90.0 ..	1.81×10^{-4}
100.0 ..	3.61×10^{-4}

The energy of activation calculated in the usual way is found to be 19,600 cal., from results at 80° and 90° C, 18,600 from results at 90° and 100° C, and 19,000 from the results at 80° and 100° C. The value thus taken as representing the energy of activation of reaction 1



is 19,000 calories, from results at $[\text{O}_3] = 18$ mm.

It has already been pointed out that the energy of activation calculated in the usual way for oxygen-ozone mixtures will vary with the composition of the mixtures. Clement* used ozonized oxygen in vessels where the surface factor would be small by reason of the temperatures employed (150–200° C), the apparent value of E being 26,000 calories. Wulf and Tolman† found for ozonized oxygen of 2% ozone $E = 29,600$, Belton, Griffith and McKeown‡ give $E = 27,800$ for roughly 10% ozone-oxygen mixtures. The values obtained by Glissmann and Schumacher ($E > 23,000$) are considered later.

Details of three experiments on approximately 10% mixtures at 100° C are now given in Table VIII, these having been carried out in the manner already described.

Table VIII—Temperature = 100.0° C

Av. $[\text{O}_3]$ mm	Initial $[\text{O}_3]$	Av. $[\text{O}_3]$	Δp divs	t secs	$\tau_{\text{exp.}} \times 10^3$	$\tau_{\text{calc.}} \times 10^3$	$\tau_{\text{exp.}}/\tau_{\text{calc.}}$
200.2	19.7	18.3	7.7	360	7.3	7.4	0.97
231.1	19.9	18.5	7.9	390	6.9	6.8	1.02
225.0	19.5	18.1	7.8	390	6.8	6.85	0.99
400.0		18.0				3.64	

The values of $\tau_{\text{calc.}}$ were obtained by formula (d) by inserting the appropriate concentrations of oxygen with $k_3/k_2 = 3.2 \times 10^{-4}$, and $V/k_2 = 30,000 \times 10^{-16}$. Ratios of total decomposition rates at oxygen concentrations of 0, 200, and

* 'Ann. Physik,' vol. 14, p. 341 (1904).

† 'J. Amer. Chem. Soc.,' vol. 49, p. 1210 (1927).

‡ 'J. Chem. Soc.,' p. 3153 (1926).

400 mm may then be examined for the two temperatures 100.0 and 90.0° C (cf. fig. 1).

Table IX

[O ₂]	$r \times 10^3$	$r \times 10^3$	r_{100}/r_{90}	E'
mm	90°	100° C		
0	4.00	7.9	1.95	18100
200	3.30	7.4	2.24	22000
400	1.45	3.64	2.51	25000

E' is the apparent heat of activation calculated from these figures; it will be observed to increase as the percentage oxygen increases, becoming 25,000 for an ozone-oxygen mixture of approximately 5% ozone. It appears probable therefore that the high values obtained by the workers cited above are to be explained at least partly on this basis.

The results of Tables IV and VIII indicate that k_3/k_2 has the value 4.5×10^{-4} at 90.0° C, and the value 3.2×10^{-4} at 100° C. Thus $(k_2^{100}/k_2^{90})/(k_3^{100}/k_3^{90}) = 1.4$. Replacing in both instances (k^{100}/k^{90}) by $e^{-E/2 \times 373}/e^{-E/2 \times 353}$, we calculate $E_2 - E_3$ as equal to 9000 cal. This figure may be checked by considering the collision efficiencies of reactions 2 and 3 (e'_2 and e'_3 respectively) in conjunction with the ratio R' of total binary collisions to total ternary collisions at, say, 100 mm pressure of ozone and of oxygen. Since $k_3/k_2 = 4.5 \times 10^{-4}$ at 90° C,

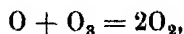
$$\frac{2.2 \times 10 \times e'_3}{e'_2} = R'.$$

By taking $e' = e^{-E/RT}$ for both reactions as before, with $E_2 - E_3 = 9000$ cal., R' is calculated as approximately 5×10^4 , a figure in good agreement with the accepted value for the pressures under consideration.

For very dilute ozone-oxygen mixtures, i.e., when the pressure of oxygen is very high and surface effects correspondingly negligible, the rate of reaction will be proportional to $k_1 k_2/k_3$ (cf. formula (c)), and the apparent heat of activation would then be $E_1 + E_2 - E_3$; on the basis of the above results the maximum apparent heat of activation which could be observed would be in the neighbourhood of $19000 + 9000 = 28000$ calories.

At 90° C, the maximum rate of decomposition obtained with $[O_2] = 18.0$ mm is 6.52×10^{-3} mm O₃ per second ($= 2k_1[O_3]$), no oxygen atoms being then removed by wall action. On the other hand, if all oxygen atoms were removed at the wall, the rate would be half this value, namely, 3.26×10^{-3} mm per second. For $[O_3] = 18.0$ mm, no inert gas being present, the actual recorded rate was 4.00×10^{-3} ; in other words the ratio of oxygen atoms removed by collision with ozone molecules to those removed by the wall in the particular

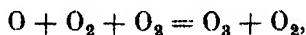
reaction vessel is $\frac{4.00 - 3.26}{6.52 - 4.00} = 0.294$. If now at any instant during the decomposition N_1 atoms of oxygen are produced per cc per sec by reaction (1) these N_1 atoms make $\pi\sigma^2_{O.O}N_1n_2\sqrt{\bar{u}_1^2 + \bar{u}_2^2}$ collisions with ozone molecules where n_2 is the number of ozone molecules per cc and \bar{u}^2 represents the mean square velocity as calculated in the usual way. If E_2 be the energy of activation of reaction (2)



the fraction of impacts which are effective is $e^{-E_2/RT}$ and the number of effective collisions per sec per cc is $\pi\sigma^2_{O.O}N_1n_2\sqrt{\bar{u}_1^2 + \bar{u}_2^2} \cdot e^{-E_2/RT}$. For $[O_3] = 18.0$ mm, under the experimental conditions the number of atoms removed by such a process is $0.294 N_1$ and therefore

$$0.294 N_1 = \pi\sigma^2_{O.O}N_1n_2\sqrt{\bar{u}_1^2 + \bar{u}_2^2} \cdot e^{-E_2/RT}.$$

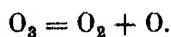
The value of E_2 is then calculated as 14200 cal. Now $E_2 - E_3$ has been found experimentally to be 9100 calories, and hence the energy of activation E_3 of the triple collision



is approximately 5000 calories. This small value is in accordance with general considerations regarding the rates of reaction when three bodies are involved, in the sense that an appropriate ternary collision is an event of comparative rarity. At the temperature of the above experiments, for the above triple collision, the value of $e^{-E_3/RT}$ is 1.03×10^{-3} , i.e., roughly 1 collision in 1000 is efficient.

The Initial Stage

We may now proceed with a further discussion of the initial step in the scheme for the decomposition of ozone, namely,



On the basis of the kinetics developed above, this reaction is "unimolecular," i.e., the rate of decomposition in this equation would be directly proportional to the number of molecules of ozone. In recent years, considerable attention has been directed to the probable mechanism of such a process, and in particular Lindemann* has shown that molecules may receive their energy of activation

* 'Trans. Faraday Soc.,' vol. 17, p. 598 (1922).

by collision with other molecules, but nevertheless may be transformed chemically at a rate independent of the pressure over a very large range.

A knowledge of the energy of activation E as obtained experimentally should give a calculated velocity constant much greater than the value recorded in the region where the reaction follows the unimolecular law; but this calculation leads to the result that unimolecular reactions in general proceed at a rate many times greater than the expression $Ze^{-E/RT}$ requires. It then appears that unimolecular reactions are characteristic of complex molecules possessing a necessary number of internal degrees of freedom. The decomposition of ozone, if unimolecular, should be of considerable interest in view of the comparatively simple nature of the molecule. The correction for the number of internal degrees of freedom would presumably be small, and hence the rate calculated on the ordinary basis might still be greater than that experimentally determined. At the same time, it is to be remembered that the existence of the unimolecular reaction depends on the time lag between activation and chemical transformation, and this time lag can reasonably be assumed to be connected with the complexity of the molecule; on this view, the less the complexity the more quickly would the unimolecular reaction tend to become bimolecular on reducing the pressure.

A series of experiments was therefore carried out with varying pressures of ozone. The removal of oxygen atoms by the surface of the reaction vessel was rendered small by the addition of a suitable quantity of nitrogen; under these circumstances the rate of the initial reaction is approximately half the experimentally recorded rate. The results are given in Table X, values of k_1 being calculated by means of the general expression previously derived:

$$-\frac{d(O_3)}{dt} = \frac{k_1 [O_3] (2k_2 [O_3] + S)}{(k_2 [O_3] + k_3 [O_2]^2 + k_4 [O_3] [N_2] + S)}.$$

Table X—Temperature = 90.0° C

$$V/k_2 = 30,000 \times 10^{-16}, \quad k_3/k_2 = 4.5 \times 10^{-4}, \quad k_4/k_2 = 10.2 \times 10^{-4}.$$

Experi- ment	Initial [O ₃]	Av. [O ₃]	Av. [O ₂]	[N ₂]	Δp	t	$r_{exp.} \times 10^8$	$k_1 \times 10^4$
	mm	mm	mm	mm	divs	secs	mm/sec	(sec) ⁻¹
1	10.5	7.9	6.9	284.0	6.4	1800	1.21	1.19
2	19.2	17.7	8.2	285.4	8.7	510	5.80	2.02
3	31.8	28.4	9.6	270.5	17.3	480	12.2	2.52
4	53.0	45.6	14.6	184.6	16.8	240	23.8	2.92
5	68.1	58.8	17.7	245.1	25.0	240	35.4	3.37
6	80.2	70.2	19.5	239.7	30.9	240	43.7	3.56
7	96.4	84.4	23.0	174.0	30.2	180	56.8	3.66
8	104.1	89.6	26.9	197.0	32.5	180	61.3	3.76

It will be observed that a five-fold variation in $[O_3]$ (from 18 to 90 mm) corresponds to an approximately ten-fold variation in the rate of the initial reaction; if this reaction were strictly bimolecular, the rate would, of course, have increased 25 times. At the same time the adoption of a bimolecular mechanism for the initial stage would mean, on the basis of the results already reported, that in oxygen-rich mixtures the total rate of decomposition would be proportional to $[O_3]^n$, where $n > 2$; experiment gives little or no evidence in support of this point of view.

Of considerable interest in this connection are the results of Bowen, Moelwyn-Hughes, and Hinshelwood* on the decomposition of ozone in carbon tetrachloride solution. The decomposition is found to be strictly unimolecular, as would be expected from the above general ideas—oxygen content small and surface effect negligible. The rate of decomposition is given by the relation

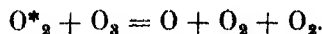
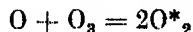
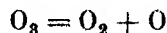
$$k = 5.82 \times 10^{12} \times e^{-26169/RT} \text{ sec}^{-1},$$

which becomes $5.2 \times 10^{-4} \text{ sec}^{-1}$ at 80° C . This figure corresponds to the total rate $2k_1$ in the preceding mechanism; hence half this value will represent the rate of the initial stage, namely, $2.6 \times 10^{-4} \text{ sec}^{-1}$, and is to be compared with the k_1 values of the gas phase experiments. In Table X the values of k_1 range from 2×10^{-4} to $4 \times 10^{-4} \text{ sec}^{-1}$ at 90° C ; at 80° C , k_1 will be approximately half these values. It can easily be shown from the above figures that the reciprocal of k_1 varies linearly with the reciprocal of $[O_3]$; extrapolation gives a value of approximately 2.3×10^{-4} for infinite pressure. The agreement between the two sets of experimental results thus affords strong support to the recognition of the first step in the thermal decomposition of ozone at ordinary pressures as predominantly unimolecular.

It may be mentioned that the ozone employed in experiments 7 and 8 of Table X was heated, before use in these experiments, in a large glass bulb at 100° C until approximately one-third had been decomposed. The residual ozone was condensed out by means of liquid air, oxygen removed by evacuation, and experiments 7 and 8 then carried out. The object of this procedure was to destroy any "impurities" which might increase the rate of reaction; the substance O_4 for example, might conceivably have been formed initially in the ozonizer and might be responsible for the higher values of k_1 , obtained. The results of experiments 7 and 8 are, however, in reasonable agreement with the rates to be expected from examination of the general results of Table X.

* 'Proc. Roy. Soc.,' A, vol. 134, p. 211 (1931-2).

It is possible also that this relative increase on the further addition of ozone is due to a chain reaction of short duration, this being perhaps formulated as follows :—



One might expect, however, that at low pressures of ozone and high pressures of nitrogen, this effect would be small, the nitrogen presumably acting as a deactivator of the O^*_2 molecules; at low pressures, however, the discrepancy does not disappear but appears to be accentuated (*cf.* Experiment 1, Table X).

Glissmann and Schumacher† have carried out an extensive series of experiments on the thermal decomposition of ozone with and without the addition of oxygen and other gases. The general results show a decided similarity to the results reported in this paper; surface action is recognized, which becomes relatively less as the total pressure becomes greater, together with the acceleration of the rate of reaction by inert gases such as carbon dioxide, nitrogen, and argon when little oxygen is present, the acceleration by oxygen when the oxygen concentration is not too high, and the increase in the apparent heat of activation as the oxygen content increases. In the reaction mechanism advanced by these workers, however, the initial step is regarded as strictly bimolecular, and the oxygen atom is not regarded as playing a dominant part in the total rate of decomposition. It is admitted by Glissmann and Schumacher that the increased rate of reaction in ozone-inert gas mixtures is not definitely accounted for.

The value of the energy of activation adopted by Glissmann and Schumacher for ozone containing little oxygen is larger (24500) than that obtained by the writer (19000). This latter value was obtained for a relatively low pressure of $[\text{O}_3]$, namely, 18 mm, while the experiments of Glissmann and Schumacher were carried out at higher pressures. The temperature ranges considered are the same. Examination of their results and comparison with the result for 18 mm obtained by the writer indicates that the higher the pressure of ozone, the higher the calculated heat of activation. Glissmann and Schumacher give a mean value of approximately 24000 cal. for the range 25–100 mm O_3 , but values of 27300, 29700, 25100, and 27000 calories are recorded for pressures of 144, 172, 284 and 376 mm respectively. This increase might be explained

† 'Z. phys. Chem.,' B, vol. 21, p. 323 (1933).

by reference to the possible chain reaction involving activated oxygen molecules as already mentioned; if this be so, the value of 19000 calories would be nearer to the correct value for the initial reaction. On the other hand, a decrease in apparent energy of activation as calculated in the ordinary way, has been recorded in reactions which are definitely regarded as of the unimolecular type, in that region where the decomposition is showing definite bimolecular characteristics.* Comparison may also be made by reason of the fact that the reciprocal of k_1 bears here a linear relationship to the reciprocal of the pressure. The value of 19000 calories obtained by the writer for ozone at 18 mm pressure is less than the usually recognized figure for the heat of the (endothermic) reaction, namely, 24000 calories; under such conditions the simple expression $\frac{d(\log k)}{dt} = \frac{E}{RT^2}$ is not strictly applicable. A more reasonable value of the energy of activation would be the value recorded by Glissmann and Schumacher for the higher pressures of ozone (28000 cal.) or that obtained for the decomposition of ozone in carbon tetrachloride solution, where the reaction is strictly unimolecular; according to Bowen, Moelwyn-Hughes, and Hinshelwood (*loc. cit.*), this is 26160 calories. The rate of decomposition then calculated in the ordinary way from this latter figure is approximately $4 \times 10^{-5} \text{ sec}^{-1}$ at 90° and is thus one-tenth the experimental value; the adoption of Glissmann and Schumacher's heat of activation increases the divergence; the difference between calculated and experimental values is then to be ascribed to the part played by the internal energy of the ozone molecule.

The author desires to acknowledge the interest and encouragement afforded to him by Dr. E. B. Ludlam and Professor James Kendall. His thanks are also due to the Earl of Moray Endowment Fund for the quartz reaction vessel used.

Summary and Conclusions

The thermal decomposition of ozone has been investigated manometrically for the temperature range $80\text{--}100^\circ \text{C}$, the pressure of ozone being varied from 10 to 100 mm. The initial stage is recognized as the pseudo-unimolecular reaction

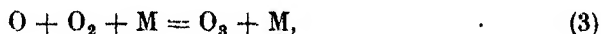


* Cf. Linhorst and Hodges, "Decomposition of N_2O_5 " ('J. Amer. Chem. Soc.', vol. 56, pp. 840-841 (1934)); also decomposition of azomethane, cf. Kassel "Kinetics of Homogeneous Reactions" 1932, p. 193.

the oxygen atom thus formed leading to further ozone decomposition by the reaction



In the absence of appreciable amounts of oxygen, addition of inert gases increases the rate of total decomposition by preventing the diffusion of oxygen atoms to the wall. In the presence of oxygen, due allowance having been made for the diffusion effect, the rate of decomposition is retarded by the triple collision effect

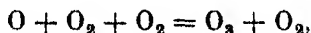


where M may be a molecule of oxygen or of other added gas. The apparent heat of activation depends then on the relative concentrations and the velocity coefficients of reactions (1), (2) and (3).

At the higher pressures of ozone employed, reaction 1 is regarded as predominantly unimolecular: k_1 is approximately $4 \times 10^{-4} \text{ sec}^{-1}$ at 90°C and agrees satisfactorily with the value of k_1 , obtained by other workers, for the decomposition of ozone in carbon tetrachloride solution. At the lower pressures, bimolecular characteristics become increasingly evident.

The heat of activation of reaction 1, calculated in the usual way, is 19000 calories, from results at 18 mm pressure of ozone; comparison with results of other workers indicates that this activation energy when calculated in the usual way depends on the pressure of ozone in this transition region.

The energy of activation of reaction 2 is estimated as 14000 calories and that of the triple collision



as 5000 calories.

The Physical Basis of the Biological Effects of High Voltage Radiations

By W. V. MAYNEORD, D.Sc., F.Inst.P.

(Communicated by H. Hartridge, F.R.S. Received May 26, 1934)

Although both the physical properties of penetrating X-rays and gamma rays and their biological effects have been carefully studied, the mechanism of the action of the rays is little known. The question of the relative effects of the same absorbed energy per cubic centimetre of tissues when different wave-lengths are used is a particularly important and obscure one. The present paper is an attempt to apply recent theories of high-speed electron production to this problem.

Radiations, such as high voltage X-rays or gamma rays, on suffering real absorption give rise to high speed negative electrons, either in photoelectric absorption whereby nearly the whole of the quantum is transferred to the electron, or in a Compton recoil process in which only part of the energy is transferred. The mean fraction given to the electrons rises gradually as the radiations become more penetrating. The relative importance of these two types of process varies in a complex manner with the wave-length and absorbing materials, but in this paper it is proposed to confine discussion to the absorption of "hard" radiations in light elements, of which living materials are mostly constructed.

It will be remembered that the photoelectric absorption coefficient (τ) is proportional approximately to the cube of the wave-length while the real energy absorption coefficient (σ_a) associated with recoil varies in a complex way with wave-length, reaching a flat maximum at about 0.024 Å. It may be shown that for wave-lengths below about 0.1 Å the recoil process preponderates, while for wave-lengths greater than 0.3 Å the photoelectric effect is much the more important absorption type. It is proposed to attempt the discussion of the effects of high voltage radiations in terms of these high-speed electrons emitted from the material. The theory is intimately connected with previous ideas put forward by Dessauer* in 1922, and developed by Blau and Altenburger,† and known as the "point-heat theory." It is found that the total energy absorption of a high voltage radiation which is required to cause profound biological effects is such as only to cause a very small rise of

* 'Z. Physik,' vol. 12, p. 38 (1922-23).

† *Ibid.*, vol. 12, p. 315 (1922-23).

temperature of the material as a whole, and it is therefore assumed that the energy is localized in very small volumes scattered throughout the irradiated mass, a view evidently consistent with the quantum structure of radiation. Blau and Altenburger developed very considerably the mathematical aspects of the theory, calculating on probability grounds the number of "hits" of cells with varying dosage, and giving survival curves corresponding to conditions under which one, two, three, or larger numbers of quantum impacts on a cell were required to cause the death of the unit. Crowther,* employing similar ideas in terms of the ions produced, showed that this quantum theory of action of X-rays was capable of interpreting the results of Strangeways and Oakley on tissue cultures, and later Crowther† performed much theoretical and experimental work on a protozoon, *Colpidium colpoda*, with the same object. Other workers on the subject, such as Condon and Terrill,‡ Holweck and Lacasagne.§ have further exemplified the importance of the ideas. A fundamental question remains, namely, as to whether the important quantity determining the biological effect is the number of quantum impacts, or the number of electronic impacts, or total absorbed energy. Thus Crowther deduces from Strangeways' and Oakley's results that the "sensitive volume" requiring to be hit before the cell is prevented from going into mitosis has a diameter of approximately 4×10^{-5} cm, the assumption being implied in the calculation that each pair of secondary ions causes the observed biological change in one cell. On the other hand, Condon and Terrill assume, while analysing certain biological effects observed by Packard, that a whole quantum of radiation is required to produce the effect. Both possibilities are envisaged by Crowther‡ in a later paper. Glocker,|| in more recent work, has shown the importance of electron range in this connection and has performed detailed calculations on the subject.

The decision as to the correct assumption seems, then, to depend on the speed of the electrons produced by radiation in the material considered. If we irradiate a mass of cells with a radiation of long wave-length, say, 0.7 Å, then the range of the photoelectrons in a material composed of light elements and of density one is of the order of 0.01 mm, and one photoelectron will affect only one or two cells of normal dimensions. The products of absorption of a

* 'Proc. Roy. Soc.,' B, vol. 96, p. 207 (1924).

† *Ibid.*, vol. 100, p. 390 (1926).

‡ 'J. Cancer Res.,' vol. 11, p. 324 (1927).

§ 'Cong. int. Electricité,' Rep. 15, Paris (1932).

|| 'Z. Physik,' vol. 77, p. 653 (1932).

quantum are therefore confined to one or two cells only and the energy absorption per unit volume is very high near the point of impact. If, on the other hand, we irradiate with hard gamma rays from RaC, then the range of the recoil electrons will be some 4 mm, and the energy absorbed is now spread over some hundreds of cells. That is, one absorbed quantum now affects a large number of cells whereas previously only one or two were "hit," if by a "hit" we mean an electron passage. Of course the gamma ray quantum is a much larger total energy, but we may easily see, since the range of a high-speed electron is proportional to the square of its energy, that even for a given total energy absorption the gamma ray electrons will pass through a much larger number of cells. The energy left behind per electron passage will, however, be correspondingly smaller and may not be sufficient to cause the biological effect contemplated, and, therefore, the number of passages may have to be greater for the higher speed electrons, the two effects partially cancelling out. These problems are considered in greater detail below.

Physical Phenomena

It may be convenient to recapitulate some of the main points concerning the absorption processes in light elements such as carbon, oxygen, and nitrogen. If short wave-length radiation falls on a light element it may be absorbed in three ways: (a) photoelectrically, (b) by the production of recoil electrons, and (c) by the recently discovered interaction with the nucleus with the production of positive electrons. We may neglect the last method for the present purposes as it appears to apply only to very short wave-lengths and is probably of relatively little importance for light elements. We will commence with the consideration of photoelectric phenomena.

Let

λ = wave-length of the radiation.

n = frequency.

h = Planck's constant.

m = mass of the electron.

e = charge on the electron.

On absorption of a quantum, a photoelectron is emitted with a velocity v given by (omitting the relativity corrections)

$$hn - W = \frac{1}{2}mv^2, \quad (1)$$

where W represents the work done in removing the electron from its parent atom. For hard rays and light elements such as C, O, N, W is small compared with the energy of the incident quantum. This is easily seen from the values of the energy levels of the K electrons or the wave-lengths of the $K\alpha$ X-ray lines (carbon 45 Å, oxygen 23.8 Å, nitrogen 31.8 Å). Since only wave-lengths shorter than about 0.4 Å are being considered, W may therefore be neglected and the energy of the photoelectrons set approximately equal to that of the quantum. The speed of the photoelectrons, therefore, increases rapidly with frequency of incident radiation, while the range increases still more sharply.

Range of Photoelectrons

The theory of the passage of high-speed electrons through matter is very complex, but both experiment* and theory†‡ suggest that over a wide range of speed the total distance traversed is roughly proportional to the square of its initial energy, or the fourth power of its velocity. The number of pairs of ions formed in traversing gases is roughly inversely proportional to the square of the speed* if the energy of the electron is far above the ionization potential of the material traversed. For very high speeds $H_p > 3000$, this specific ionization appears to approach a limiting value.§ More recent wave mechanical investigations predict both of these results. The experimental work on the subject shows a rather slower rise of range with speed, and we have therefore used the experimental data of Varder,|| and Schonland¶ as a basis of this investigation. It appears both experimentally and theoretically that the range in gm/cm² is nearly independent of the material, and we have therefore used the data for aluminium as applicable to tissues. The ranges are given in Table I.

Column 1 gives the product H_p for the electrons, H being the strength of the magnetic field required to bend an electron moving perpendicular to it into a path of radius ρ . H_p is a measure of the momentum of the particles. Column 2 gives the wave-lengths of the radiations which would produce photoelectrons with H_p given in column 1. These values are graphically interpolated from values given in tables of electronic constants. Column 3

* Wilson, 'Proc. Roy. Soc.,' A, vol. 85, p. 240 (1911).

† Thomson, 'Phil. Mag.,' vol. 23, p. 429 (1912).

‡ Bethe, 'Ann. Physik,' vol. 5, p. 325 (1930).

§ Rutherford, Chadwick, and Ellis, "Radiations from Radioactive Substances," p. 426.

|| 'Phil. Mag.,' vol. 29, p. 725 (1915).

¶ 'Proc. Roy. Soc.,' A, vol. 108, p. 187 (1925).

gives the ranges R_0 in mm for the various photoelectrons, while column 4 gives the ranges in cells assuming the latter to be 5μ in diameter. These numbers, however, give the cells affected per absorbed quantum; that is, for an amount of energy proportional to the frequency of the radiation. On multiplication by the appropriate wave-length, we obtain, therefore, column 5, the relative electronic path per unit absorbed energy. This is the quantity we set out to find, since it may be used in the later calculations as the probability of an electron passage through a cell per unit absorbed energy, representing as it does the value of the total path (we shall refer to it as the "integral path") of all the electrons evolved during the absorption of the same amount of energy for different wave-lengths.

Table I

1 H_p	2 λ in Å	3 R_0 mm	4 R_0 in 5μ units	5 $R_0 \lambda$ for photo- electrons	6 $R_0 \lambda \xi$ recoil electrons	7 Mean integral range
627	0.360	0.0232	4.64	1.67	0.150	1.51
694	0.304	0.0341	6.80	2.07	0.186	1.69
916	0.182	0.070	14.0	2.54	0.280	1.41
1010	0.148	0.095	19.0	2.80	0.364	1.09
1040	0.143	0.108	21.6	2.89	0.404	1.10
1380	0.085	0.180	36.0	3.06	0.765	0.97
1930	0.046	0.64	128	5.88	2.41	2.41
2535	0.031	1.24	248	7.69	3.77	3.77
3790	0.021	2.79	558	11.7	6.40	6.40
5026	0.010	4.40	880	8.80	5.71	5.71

Recoil Electrons

The calculation of "integral path" for recoil electrons is much more difficult but is attempted below. The complexity arises from the fact that for a given incident radiation recoil electrons of a very wide variety of speeds are emitted, corresponding to their varying angles of emission, ϕ . The numerical distribution of recoil electrons with angle is also a complex function of direction and wave-length.

If I_0 be the intensity of the incident radiation, then it may be shown* that, I , the energy scattered per electron per unit solid angle in a direction θ to that of the original radiation is given by

$$I = I_0 \cdot \frac{e^4}{2m^2c^4} \cdot \frac{1 + \cos^2 \theta}{(1 + \alpha(1 - \cos \theta)^2)} \left[1 + \frac{\alpha^2(1 - \cos \theta)^2}{(1 + \cos^2 \theta)(1 + \alpha(1 - \cos \theta))} \right]$$

$$= I_0 \frac{e^4}{2m^2c^4} \cdot f(\theta), \quad \text{where} \quad \alpha = \frac{h\nu}{mc^2} = \frac{22.2}{\lambda}, \quad (2)$$

λ being measured in X units.

* Klein and Nishina, 'Z. Physik,' vol. 52, p. 853 (1929).

On multiplication by $d\Omega/hn'$ where n' represents the modified frequency appropriate to θ and α , we obtain the number of quanta scattered per electron in the direction θ within a solid angle $d\Omega$, whence we transfer very easily to the number of quanta scattered in a cone bounded by θ and $\theta + d\theta$. But each of these scattered quanta has a recoil electron associated with it at an angle ϕ given by

$$-(1 + \alpha) \tan \phi = \cot \theta/2. \quad (3)$$

Let $N_\theta d\theta$ represent the number of scattered quanta in the elementary cone $d\theta$, and $N_\phi d\phi$ the number of recoil electrons in the cone $d\phi$. Then

$$N_\phi = N_\theta \frac{d\theta}{d\phi}. \quad (4)$$

But $N_\theta d\theta$ = number of quanta scattered between θ and $\theta + d\theta$

$$= 2\pi \sin \theta \cdot f(\theta) \cdot \frac{n}{n'} \cdot \frac{1}{hn} \cdot \frac{c^4}{m^2 c^4} \cdot d\theta. \quad (5)$$

Also $n/n' = 1 + 2\alpha \sin^2 \theta/2$ and from (3)

$$d\theta/d\phi = \frac{2(1 + \alpha) \sin^2 \theta/2}{\cos^2 \phi}. \quad (6)$$

Whence we have

$$N_\phi d\phi = \frac{\pi c^4}{m^2 c^4} f(\theta) \cdot \sin \theta \cdot \frac{(1 + \alpha)(2 \sin^2 \theta/2)(1 + 2\alpha \sin^2 \theta/2)}{\cos^2 \phi} \cdot \frac{1}{hn} \cdot d\phi. \quad (7)$$

This solves the problem of the number of recoil electrons and we now turn to their ranges. Let R_ϕ be the range of the electrons emitted at the angle ϕ . The energy E_ϕ of these electrons may be written.

$$E_\phi = E_0 \left[\frac{2\alpha \sin^2 \theta/2}{1 + 2\alpha \sin^2 \theta/2} \right],$$

where

$$E_0 = \text{energy of the quantum.}$$

Whence assuming the range proportional to the square of the energy we have

$$R_\phi = R_0 \left[\frac{2\alpha \sin^2 \theta/2}{1 + 2\alpha \sin^2 \theta/2} \right]^2, \quad (8)$$

where

$$R_0 = \text{range of the photoelectrons appropriate to } \alpha.$$

The total range of all the recoil electrons set free in the angular cone $d\phi$ is therefore the product $N_\phi R_\phi d\phi$ which may be written down from equations

(7) and (8). The total absorbed energy per unit incident energy is clearly σ_a per electron, and the integral range of photoelectrons corresponding to this energy absorption is $\sigma_a R_0 / hn$. Whence we find that the ratio ξ of the integral range of the recoil electrons to the integral range of the photoelectrons for the same total energy absorption of the same wave-length may be written

$$\begin{aligned} \xi &= \int \frac{\pi e^4}{m^2 c^4} \cdot f(\theta) \frac{\sin \theta}{\cos^2 \phi} \cdot \alpha (1 + \alpha) (2 \sin^2 \theta/2)^2 \left[\frac{2\alpha \sin^2 \theta/2}{1 + 2\alpha \sin^2 \theta/2} \right] \frac{d\phi}{\sigma_a} \\ &= \int_{\phi=0}^{\phi=\pi/2} N_\phi R_\phi d\phi \cdot \frac{hn}{\sigma_a R_0}. \end{aligned} \quad (9)$$

$f(\theta)$ having its previous significance.

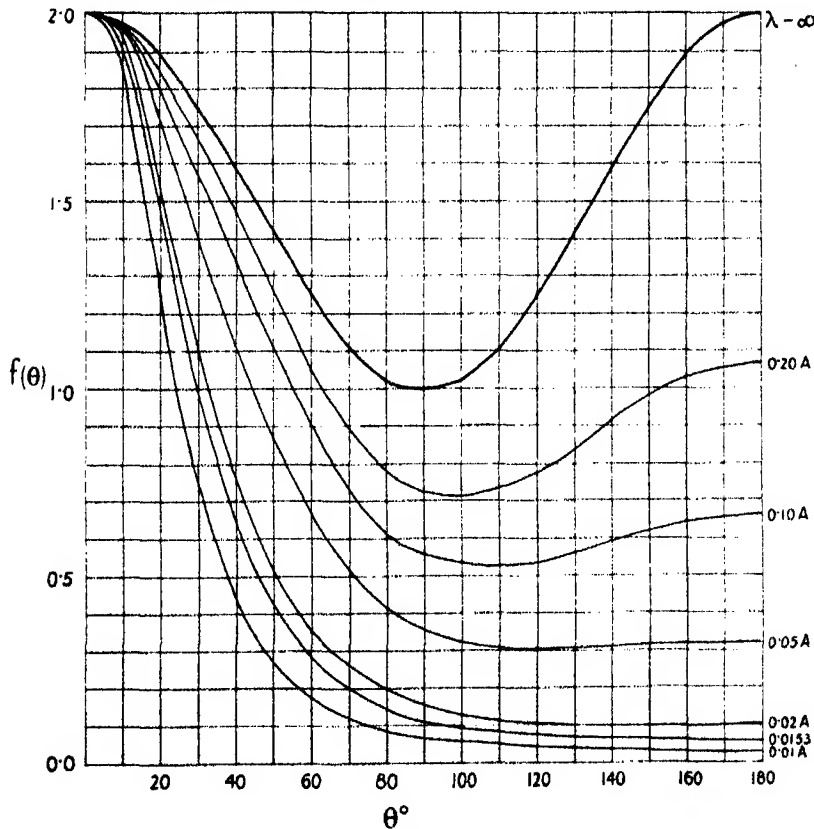


FIG. 1

The integration has been performed graphically, the rather laborious arithmetic being carried out for several wave-lengths in the region of interest. The values of $f(\theta)$, the scattering function, are given in fig. 1. Their general shapes

are well known. The values of $N_\phi R_\phi$ are given in fig. 2, while the curve representing the variation of

$$\xi = \int N_\phi R_\phi d\phi \cdot \frac{hn}{\sigma_a R_0},$$

with wave-length is given in fig. 3. It will be seen that the recoil processes give smaller integral ranges than the photoelectric processes, as is obvious

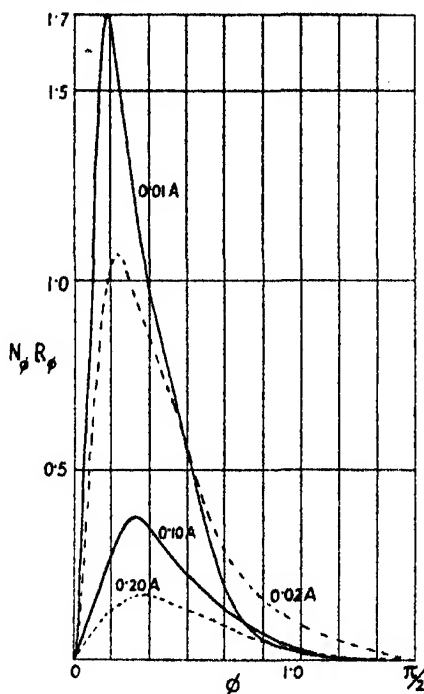


FIG. 2

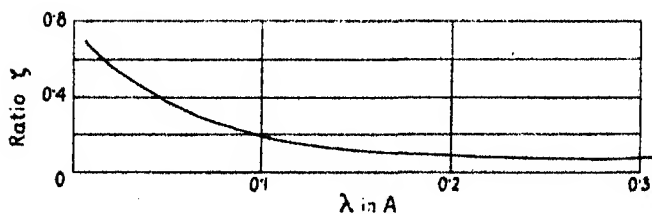


FIG. 3

from elementary considerations. The value of ξ is, in fact, nearly $1.4 \left[\frac{\sigma_a}{\sigma_a + \sigma_s} \right]$ as suggested by the theory of scattering due to Bothe. The ratio ξ enables us immediately to calculate the integral range for the recoil electrons by simple

multiplication by the appropriate R_0 and thus we obtain the probability of an electron passage per unit energy absorption for recoil absorption, Table I, column 6. In general at each wave-length both types of absorption occur, the recoil becoming more and more important at short wave-lengths. We have, therefore, taken the appropriate fraction of the total energy absorption of each type, photoelectric and recoil, for each wave-length, and obtained in this way the final integral range per unit energy absorption over the whole wave-length region, column 7. This result is given in fig. 4, where the relative number of cells traversed is plotted against wave-length.

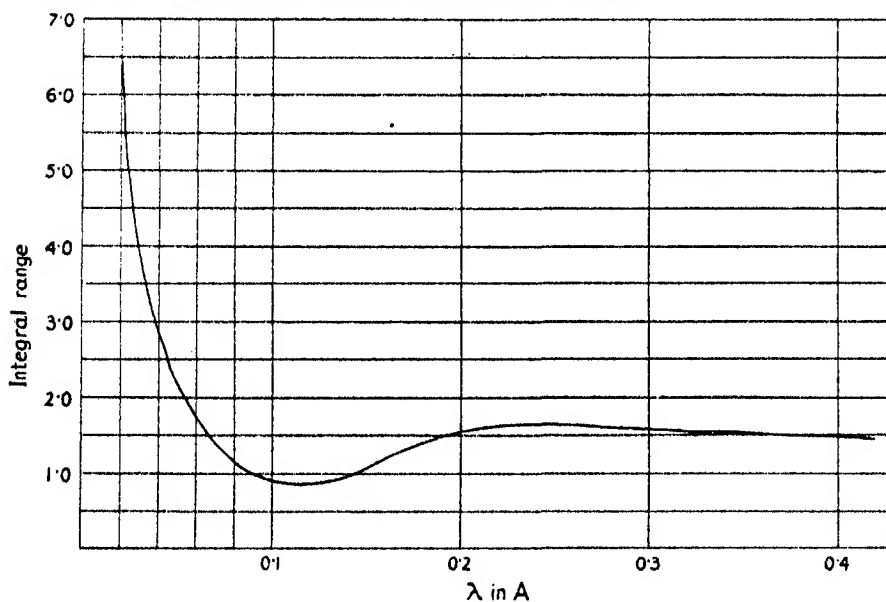


FIG. 4

This curve is of interest indicating, as it does, the probability of a cell being traversed by an electron per unit energy absorption. On a simple photoelectric law, assuming range proportional to the square of the energy, the curve would rise over the whole region, but the variation is checked by the gradual transition of type of absorption process from photoelectric to recoil as we proceed towards shorter wave-lengths, and also by the slower increase of range with speed found experimentally than that calculated theoretically.

"Survival" Phenomena

We may now turn to the second part of the theory dealing with the variation of probability of an electron passage through a cell and "dose" of radiation.

It may be shown* that if N_0 be the number of organisms initially present and p the probability of a "hit" by unit dose of radiation, then N the number of systems left unaffected by a dose q if r hits are required to cause the biological effect, may be written:—

$$N = N_0 e^{-pq} \left(1 + pq + \frac{p^2 q^2}{2!} + \dots + \frac{p^{r-1} q^{r-1}}{(r-1)!} \right). \quad (10)$$

This number N we may imagine to represent the number of survivals after a dose q . The physical meaning of p may be seen more readily by considering a simple case in which one hit only is required. Then

$$N = N_0 e^{-pq}, \quad (11)$$

or the surviving number decreases exponentially with dose. We may write (11) slightly differently as

$$dN/N = -pdq, \quad (12)$$

or p is the fractional decrease in the number of unaffected cells per unit small increase of dose. The general shape of the curves representing N against q for various values of r are given by Blau and Altenburger (*loc. cit.*). In view of equation (12), we may evidently set p as proportional to the integral range of the electrons as already discussed, while r may be taken to have various values according to different circumstances.

Let us now consider three examples of survival curves.

1—Suppose a single electron passage through a cell is sufficient to cause a given biological change, however high the speed of the electron. This we may imagine to occur for changes caused by very small amounts of energy left in the cell. Then in (10) we put $r = 1$ and may calculate, putting $p =$ integral range as in fig. 4, the survival curve for different wave-lengths. This has been carried out for two wave-lengths 0.15 Å and 0.02 Å for which p_1 and p_2 are 1.1 and 6.2 respectively. The result is shown in fig. 5. It will be seen that the hard gamma radiation is much more destructive than the longer wave-length.

2—Suppose the energy required to cause a certain other change is higher and of the order of the energy left in the cell during a single passage of the slower electrons corresponding to the longer wave-length, r_1 still equals one. But more passages of the higher speed electron will be required and we may assume a value of r_2 for this shorter wave-length equal to 5.6 ($= 6.2/1.1$)

* Blau and Altenburger, 'Z. Physik,' vol. 12, p. 315 (1923); Crowther, 'Proc. Roy. Soc.,' B, vol. 100, p. 390 (1926).

since the values of p are referred to unit energy absorption. Thus in the example, still considering the same pair of wave-lengths, we see that the integral range of the shorter wave-length is 5.6 times greater than for the longer. This implies that on the average 5.6 times less energy is left behind per unit path and we therefore assume a larger number r_2 (actually 5.6) of electron passages to be required to cause the same effect per cell for the higher speed electrons. The survival curve for 5.6 hits at 0.02 A is also given in fig. 5, where it will be seen that the shape of the curve is different from that for one hit at 0.15 A, but the dose required to cause a change in about 70% the cells is now of the same order in the two examples.

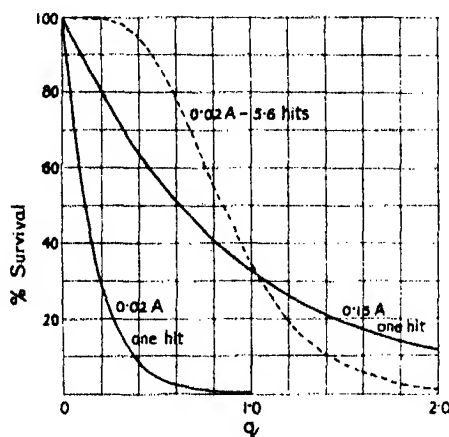


FIG. 5

3—Finally we may assume a certain number r_1 (greater than unity) passages of the low speed electrons necessary and a still greater number $5.6 r_1 = r_2$, for the higher speeds. The curves are given in fig. 6, for the case $r_1 = 8$ and $r_2 = 45$, where it will be seen that the survival curves for the two wave-lengths are more nearly identical, being more exactly alike as r_1 increases. The curves are calculated by the use of tables of the incomplete Γ function.*

It may be seen therefore that even on the simple basis assumed here, the questions of "selective action" and "differential action" are very complex, but intimately related to each other. If the energy required to cause a change is very small, gamma rays would be expected for small doses to be much more active than longer wave-length X-rays, while if the energy required per cell is large the difference between various wave-lengths would probably be

* Pearson, "Tables of incomplete Γ function," 1922.

negligible in biological experiments. Some such considerations as these may be the basis of the "action élective" found by such workers as Regaud* when considering the action of radiations on rapidly growing cells side by side with muscular tissue. It is observed that the relative destruction of malignant to normal cells increases as the wave-length decreases. This may, as above, be due to the smaller energy required to kill the malignant cell. Clearly no simple relation of selectivity to wave-length is to be expected since different biological effects show different relative effects with varying wave-length according to the energy absorption per cell required to bring them about. If we may imagine that either the sensitive volume of the cell or the energy required to cause a given change varies periodically during the life cycle, the

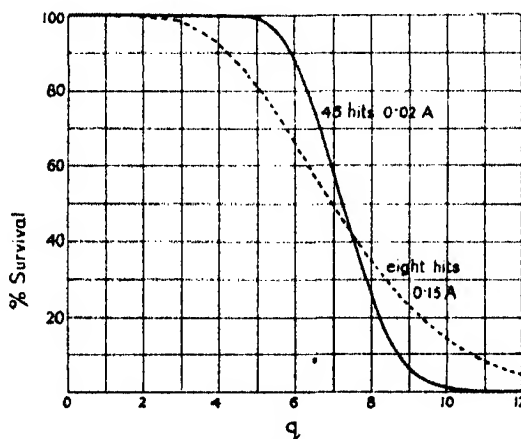


FIG. 6

energy being perhaps considerably less during some stage of mitosis, then the alleged "action élective" on rapidly growing cells is explicable, as well as the possibly greater sensitivity of rapidly growing tissues.†

A multitude of complexities such as time effects, inequality of ionization along an individual track, or variations of speed of tertiary electrons may be suggested, but it is hoped that the simple considerations suggested here are of some interest in the theory of the subject.

A complexity which may be of considerable significance but not usually contemplated is the geometrical form of the biological object irradiated. For example, if the latter be a very thin sheet of material irradiated in a direction perpendicular to its plane, then the recoil electrons will only pass through cells

* 'Radiophysiol. and Radiotherap.,' vol. 1, pp. 2, 177 (1927); vol. 2, p. 360 (1931).

† Begonié and Tribondeau, 'C. R. Acad. Sci. Paris,' vol. 143, p. 983 (1906).

during the early part of their paths. If the object be indefinitely thin, evidently the considerations relative to integral paths previously advanced are of no significance, the number of absorbed quanta being the important parameter, and for a given absorbed energy as normally measured a smaller biological effect of shorter wave radiations is to be expected.

Now that means are available of measuring radiations of varying wavelength in the same unit, it is hoped to carry out experimental work on the subject.

Summary

The possible importance of the range of the secondary electrons produced in living materials by high voltage X-rays and gamma rays is discussed. Using the Klein-Nishina formulæ, the total path of all the electrons set free per unit energy absorption is calculated and shown to rise rapidly in the gamma ray region of wave-lengths.

Supposing one or more electron passages suffice to cause a biological change in a cell, the survival curves of a mass of cells irradiated with different wave-lengths are calculated. The differences in these survival curves according to the energy absorption required to cause the biological changes are discussed.

The Collisions of Slow Electrons with Atoms—IV

By H. S. W. MASSEY, Ph.D., Independent Lecturer in Mathematical Physics,
Queen's University, Belfast, and C. B. O. MOHR, Ph.D., Cavendish
Laboratory, Cambridge

(Communicated by R. H. Fowler, F.R.S.—Received May 26, 1934)

The collision of a slow moving electron with an atom is known to be a very complicated phenomenon involving a number of processes which are themselves complex. To obtain even an approximate description of such phenomena the only method of attack is to consider the effects of the different individual processes separately in order to estimate the nature and magnitude of their contributions to the resultant scattering.

In both elastic and inelastic scattering the principal processes occurring may be stated as follows :—

1—Scattering by the field of the atom considered as undisturbed by the incident electron, the latter being also thought of as only slightly affected by the collision.

2—The distortion of the incident and scattered electron waves by the potential field of the atom, the latter field being taken as the undisturbed atomic field.

3—The exchange of electrons between the incident and scattered electron waves and the atom.

4—The disturbance of the atomic field by the incident electron waves.

Of these the first is taken into account in the first approximation of Born's theory of collisions, and detailed calculations have been carried out using Born's first approximation for a great number of atomic collision phenomena.† It is therefore very convenient to describe the effects of the remaining three processes in terms of the deviations they produce from the behaviour given by Born's first approximation. In general this approximation predicts an angular distribution of scattered electrons per unit solid angle in which the scattered intensity falls off continually with increase of scattering angle, this rate of fall being much faster for inelastic than for elastic scattering.

† Mott and Massey, "The Theory of Atomic Collisions," Oxford Univ. Press, chapter IX.

The third process stated above, electron exchange, was first discussed by Oppenheimer.[†] In four previous papers by the present authors,[‡] and in papers by Feenberg[§] and by Allis and Morse^{||} the theory of electron exchange has been elaborated, and it is now possible to state the conditions under which exchange effects may be important, and contributions to the scattering due to this exchange are often recognized.

The second effect, distortion of the colliding electron waves, can be accurately discussed for elastic collisions by the method of Faxén and Holtsmark, which has been applied to the consideration of a number of collisions of slow electrons with atoms.[¶] The general result of the distortion effect is to introduce maxima and minima in the angular distribution curves and, in certain cases, also in the cross-section-velocity curves, for elastic scattering. The detailed application of a theory of inelastic collisions which includes the distortion of the incident and inelastically scattered electron waves by the fields of the normal and excited atom respectively, is very complicated. However, in Papers II and III it was shown that distortion does not greatly affect the total probability of a given inelastic collision, but has a considerable influence on the angular distribution of the scattered electrons at large angles of scattering. The experimental results show that, provided the incident electron energy is considerably greater than the excitation energy of the atom involved in the inelastic collision, the angular distribution of the inelastically scattered electrons closely resembles that of the elastic,** and in papers II and III it was shown in general how this arises from distortion effects. In this paper we apply the theory developed in the previous papers to a detailed consideration of the angular distributions of electrons scattered inelastically by argon and neon atoms, and in this way good agreement is obtained with experimental curves when this is to be expected.

The second portion of this paper is devoted to the consideration of the fourth effect stated above, so far as the elastic scattering is concerned. The disturbance of the atomic field by the incident electron may be regarded as a polariza-

[†] 'Phys. Rev.,' vol. 32, p. 361 (1928).

[‡] 'Proc. Roy. Soc.,' A, vol. 132, p. 605 (1931), referred to subsequently as paper A; 'Proc. Roy. Soc.,' A, vol. 136, p. 289 (1931), referred to subsequently as paper I; 'Proc. Roy. Soc.,' A, vol. 139, p. 187 (1932), referred to subsequently as paper II; 'Proc. Roy. Soc.,' A, vol. 140, p. 613 (1933), referred to subsequently as paper III.

[§] 'Phys. Rev.,' vol. 40, p. 40 (1932) and vol. 42, p. 17 (1932).

^{||} 'Phys. Rev.,' vol. 44, p. 269 (1933).

[¶] Mott and Massey, "The Theory of Atomic Collisions," chapter X.

** Nicoll and Mohr, 'Proc. Roy. Soc.,' A, vol. 142, pp. 320, 647 (1933).

tion effect or alternatively, as arising from the interaction of the inelastically scattered electrons with the elastic. Considered in this last way, the polarization effect can be dealt with by using the second approximation of Born's theory of collisions, and a detailed discussion and application of this approximation is carried out in the second section of this paper. In paper III it was shown qualitatively that the effect of polarization is to increase the elastic scattering at small angles of scattering, and the detailed theory of this paper confirms this result and gives approximately quantitative results for the scattering of electrons by hydrogen and helium.

Finally, a summary of the results of the application of quantum theory to the description of the experimental observations on slow electron scattering will be given.

Section I—The Angular Distribution of Inelastically Scattered Electrons

We adopt the same notation as in previous papers. It was shown in paper II that, if one includes the distortion effect but neglects exchange and polarization, the angular distribution per unit solid angle of electrons scattered after exciting the n th state of a given atom, is given by

$$I_n(0) = \frac{k_n}{k} \frac{4\pi^2 m^2}{h^4} |f_n(k_n, k, \theta)|^2, \quad (1)$$

where

$$\left. \begin{aligned} f_n(k_n, k, \theta) &= \int V_{0n}(\mathbf{r}') F_0(r', \theta') \mathfrak{F}_n(r', \pi - \Theta) d\tau' \\ V_{0n}(\mathbf{r}) &= \int V(\mathbf{r}, \mathbf{r}_a) \psi_0(\mathbf{r}_a) \psi_n^*(\mathbf{r}_a) d\tau_a \end{aligned} \right\} \quad (2)$$

In this formula $V(\mathbf{r}, \mathbf{r}_a)$ is the interaction energy between the incident electron (co-ordinates \mathbf{r}) and the atomic electrons (co-ordinates \mathbf{r}_a) and $\psi_0(\mathbf{r}_a)$, $\psi_n(\mathbf{r}_a)$ are the initial and final atomic wave functions: $k/2\pi$, $k_n/2\pi$ are the wave-numbers of the colliding electrons before and after the impact. $F_0(r, \theta)$ is the solution of the equation

$$\nabla^2 F + \left\{ k^2 - \frac{8\pi^2 m}{h^2} V_{00}(r) \right\} F = 0, \quad (3)$$

which is finite everywhere and has the asymptotic form

$$F \sim e^{ikr \cos \theta} + r^{-1} e^{ikr} f(\theta), \quad (4)$$

while $\mathfrak{F}_n(r, \theta)$ is the corresponding solution of

$$\nabla^2 F + \left\{ k_n^2 - \frac{8\pi^2 m}{h^2} V_{nn}(r) \right\} F = 0; \quad (5)$$

θ is the angle of scattering and Θ is given by

$$\cos \Theta = \cos \theta \cos \theta' + \sin \theta \sin \theta' \cos \phi'. \quad (6)$$

In Born's theory of collisions the first approximation gives a formula similar to the above but with F_0 , \mathfrak{F}_n replaced by plane waves $e^{ikr' \cos \theta'}$, $e^{ik_n r' \cos \theta}$. The formula (1) thus includes the effect of the distortion of these waves by the fields V_{00} , V_{nn} of the normal and excited atoms respectively.

We consider in all cases a transition associated with a dipole moment so that $V_{0n}(r')$ takes the form †

$$V_{0n}(r') \begin{cases} \cos \theta' \\ 2^{-\frac{1}{2}} \sin \theta', \pm \phi' \end{cases} \quad (7)$$

It follows that

$$I_n(\theta) = \frac{k_n}{k} \frac{4\pi^2 m^2}{h^4} \{ |f_c(k, k_n, \theta)|^2 + 2 |f_s(k, k_n, \theta)|^2 \}, \quad (8)$$

where f_c arises from the form with $\cos \theta'$, f_s from $2^{-\frac{1}{2}} \sin \theta' e^{-i\phi'}$. Also we have

$$F_0(r', \theta') = \sum_s (2s+1) i^s e^{is\gamma_s} F_0^s(r') P_s(\cos \theta'), \quad (9)$$

where $rF_0^s(r)$ is that solution of the equation

$$\frac{d^2}{dr^2} (rF_0^s) + \left\{ k^2 - \frac{s(s+1)}{r^2} - \frac{8\pi^2 m}{h^2} V_{00}(r) \right\} (rF_0^s) = 0, \quad (10)$$

which is zero at the origin and tends asymptotically to the form

$$k^{-1} \sin(kr - \frac{1}{2}s\pi + \delta_s).$$

Similarly

$$\mathfrak{F}_n(r', \pi - \Theta) = \sum_s (2s+1) i^{-s} e^{i\gamma_s} F_n^s(r') P_s(\cos \Theta), \quad (12)$$

where F_n^s , γ_s correspond respectively to F_0^s , δ_s in (9) with 0 replaced by n . Now on substitution of (9) and (12) in (8) we may integrate over the angular co-ordinates θ' , ϕ' leaving f_c and f_s as an infinite series of integrals involving

† The quantity $1/\sqrt{2}$ appears when one normalizes the two terms to the same value.

F_0^s , F_n^s , and $V_{0n}(r')$. This series is very slowly converging so we rewrite (9) and (12) in the form

$$F_0(r', \theta) = e^{ikr' \cos \theta} + \sum_s (2s+1) i^s \left[e^{i\delta_s} F_0^s(r') - \left(\frac{\pi}{2kr'} \right)^{\frac{1}{2}} J_{s+\frac{1}{2}}(kr') \right] P_s(\cos \theta) \quad (13)$$

$$F_n(r', \pi - \Theta) = e^{-ik_n r' \cos \Theta} + \sum_s (2s+1) i^{-s} \left[e^{i\gamma_s} F_n^s(r') - \left(\frac{\pi}{2k_n r'} \right)^{\frac{1}{2}} J_{s+\frac{1}{2}}(k_n r') \right] P_s(\cos \Theta), \quad (14)$$

In this way each function is written as the sum of a plane wave and a series, the terms of which arise from the differences between the functions F_0^s , F_n^s , and the corresponding function in the expansion of a plane wave in zonal harmonics. The series terms thus represent the distortion due to the atomic field. On substitution of the formulæ (13), (14) in (2) the plane wave terms give Born's approximation while the series terms give rise to additional contributions to the scattered amplitude due to distortion. The formulæ are

$$f_c(k, k_n, \theta) = \int V_{0n}(r') \cos \theta' \exp \{ir' (k \cos \theta' - k_n \cos \Theta)\} d\tau' + 4\pi i \int r'^2 V_{0n}(r') D_c(r', \theta) dr', \quad (15)$$

$$2if_s(k, k_n, \theta) = \int V_{0n}(r') \sin \theta' \exp \{i(kr' \cos \theta' - k_n r' \cos \Theta \pm i\phi')\} d\tau' + 4\pi i \int r'^2 V_{0n}(r') D_s(r', \theta) dr', \quad (16)$$

$$\begin{aligned} D_c(r', \theta) = & \exp \{i(\gamma_0 + \delta_1)\} F_n^0 F_1^0 - L_n^0 L'_n \\ & + \sum_{s=1}^{\infty} P_s(\cos \theta) [(s+1) \exp \{i(\gamma_s + \delta_{s+1})\} F_n^s F_0^{s+1} \\ & - s \exp \{i(\gamma_s - \delta_{s-1})\} F_n^s F_0^{s-1} - (s+1) L_n^s L_0^{s+1} \\ & + s L_n^s L_0^{s-1}], \end{aligned} \quad (17)$$

$$\begin{aligned} D_s(r', \theta) = & \sum_{s=1}^{\infty} P_s^1(\cos \theta) [\exp \{i(\gamma_s + \delta_{s+1})\} F_n^s F_0^{s+1} \\ & - \exp \{i(\gamma_s + \delta_{s-1})\} F_n^s F_0^{s-1} - L_n^s L_0^{s+1} - L_n^s L_0^{s-1}]. \end{aligned} \quad (18)$$

In these formulæ we have written

$$\left(\frac{\pi}{2kr'} \right)^{\frac{1}{2}} J_{s+\frac{1}{2}}(kr') = L_0^s, \quad \left(\frac{\pi}{2k_n r'} \right)^{\frac{1}{2}} J_{s+\frac{1}{2}}(k_n r') = L_n^s.$$

To calculate the terms arising from D_c and D_s , a convenient approximation may be made without appreciable error. The function $r^2 V_{0n}(r)$ is a maximum near the outer shell of the atom concerned and vanishes like r^3 for small distances, whereas the functions F_0^s , F_n^s only deviate appreciably from their asymptotic forms

$$\left(\frac{k}{k_n} r\right)^{-1} \sin \left\{ \frac{k}{k_n} r - \frac{1}{2} s \pi + \frac{\delta_s}{\gamma_s} \right\}, \quad (19)$$

at such small atomic distances that $r^2 V_{0n}(r)$ is then quite small. This region therefore contributes very little to the integrals involved in the second terms of (15) and (16), and so we may replace all the functions in (17) and (18) by their asymptotic forms. We then obtain

$$k k_n r'^2 D_c(r', \theta) = \sum_{s=1}^{\infty} P_s(\cos \theta) \left\{ (s + \frac{1}{2}) T_s + \frac{1}{2} S_s \right\} \\ - \exp \{i(\gamma_0 + \delta_1)\} \sin(k_n r + \gamma_0) \cos(kr + \delta_1), \quad (20)$$

$$k k_n r'^2 D_s(r', \theta) = \sum_{s=1}^{\infty} P_s^1(\cos \theta) S_s, \quad (21)$$

where

$$\left. \begin{aligned} 2S_s \} &= \pm \exp \{i(\gamma_s + \delta_{s+1})\} \sin(k_n r + \gamma_s - \frac{1}{2} s \pi) \cos(kr + \delta_{s+1} - \frac{1}{2} s \pi) - \\ 2T_s \} &= - \exp \{i(\gamma_s + \delta_{s+1})\} \sin(k_n r + \gamma_s - \frac{1}{2} s \pi) \cos(kr + \delta_{s+1} - \frac{1}{2} s \pi). \end{aligned} \right\} \quad (22)$$

On substitution in (15) and (16) it will be seen that the integrals

$$\int_0^{\infty} V_{0n}(r') \frac{S_s}{T_s} dr' \quad (23)$$

are required. These may be written down for all s in terms of the integrals

$$\left. \begin{aligned} \int_0^{\infty} V_{0n}(r) \sin \lambda r dr &= A(\lambda) \\ \int_0^{\infty} V_{0n}(r) \cos \lambda r dr &= B(\lambda) \end{aligned} \right\} \quad (24)$$

For example

$$2 \int_0^{\infty} S_s V_{0n}(r') dr' = \exp \{i(\gamma_s + \delta_{s+1})\} \left\{ \cos(\delta_{s+1} - \gamma_s) A(k - k_n) \right. \\ + \sin(\delta_{s+1} - \gamma_s) B(k - k_n) + (-1)^{s+1} \{ \cos(\delta_{s+1} + \gamma_s) \\ \times A(k + k_n) + \sin(\delta_{s+1} + \gamma_s) A(k + k_n) \} \} \\ + \text{similar terms with } \delta_{s-1} \text{ in place of } \delta_{s+1}. \quad (25)$$

A similar type of expression holds for the integral involving T_1 . We thus see that the contribution to the scattered amplitude arising from the distortion terms can be written down in terms of the phase quantities δ_s , γ_s and the four integrals $A(k \pm k_n)$, $B(k \pm k_n)$. At angles greater than about 25° the contribution to the amplitudes f_s , f_c arising from the undisturbed plane waves (Born's first approximation) is very small and so the distortion terms give rise to the complete form of the angular distribution in this region.

Application to Argon and Neon—In applying the formulæ of the preceding section to the inelastic scattering of electrons by argon and neon atoms it will be assumed that the transition involved is concerned with only one atomic electron which is considered as jumping from a p to an s state. The wave functions ψ_0 , ψ_n for this electron were then obtained by using Slater's rules† and are :—

$$\left. \begin{aligned} \psi_0 &= N_0 r^2 e^{-2.25 r/a_0} \\ \psi_n &= N_0 r e^{-2.02 r/a_0} \end{aligned} \right\} \begin{aligned} &\cos \theta \\ &\sin \theta e^{\pm i\phi} \end{aligned} \quad \left. \begin{aligned} \psi_n &= N_n r^{2.7} e^{-0.55 r/a_0} \text{ (for argon)} \\ \psi_n &= N_n r^2 e^{-0.68 r/a_0} \text{ (for neon)} \end{aligned} \right\} \quad (26)$$

$V_{0n}(r)$ can then be calculated using these functions. V_{00} and V_{nn} must then be obtained in order to calculate the δ_s and γ_s . V_{00} may be obtained in both cases from the Hartree fields‡ but V_{nn} must be derived from the field of the normal atom by allowing for the transfer of one electron from the outer shell to the unoccupied shell of total quantum number greater by unity, and for the reaction of this transfer on the effective nuclear charges acting on the remaining electrons. These terms were also computed using atomic wave functions given by Slater's rules. The forms of V_{00} and of V_{nn} calculated in this way for neon are compared in fig. 1, showing the increased potential at large distances due to the excitation. Having obtained the potentials V_{00} and V_{nn} the phases δ_s , γ_s may then be calculated with sufficient accuracy using Jeffreys' method of approximation (fig. 2).§

Calculations were carried out in this way for the scattering of 20, 40 and 80 volt electrons after exciting the resonance level of argon (11.6 volts above the ground level), and of 26 and 60 volt electrons after exciting the resonance level of neon (16.6 volts above the ground level). The resulting angular distributions are illustrated in figs. 3 and 4. For comparative purposes curves are also given for the angular distribution of electrons with the same

† 'Phys. Rev.', vol. 36, p. 57 (1930).

‡ Holtsmark, 'Z. Physik,' vol. 55, p. 437 (1929); Brown, 'Phys. Rev.', vol. 44, p. 214 (1933).

§ Mott and Massey, "The Theory of Atomic Collisions," chapter VII, 3.

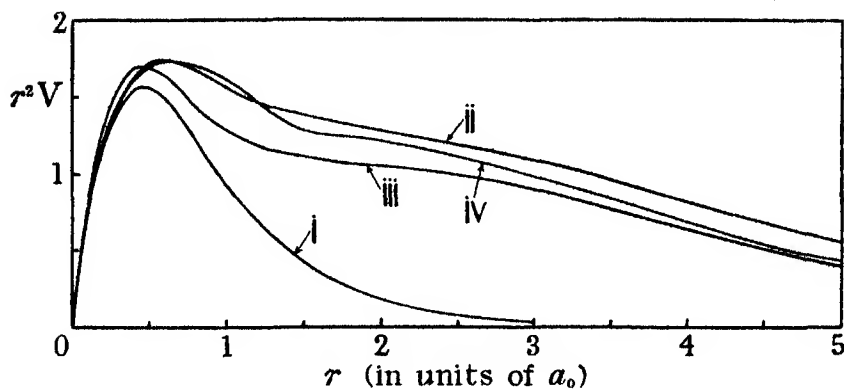


FIG. 1—Fields of normal and excited neon. Curve i is the Hartree field of normal neon; curve ii that of excited neon, calculated from i as described in the text; curve iii is the Hartree field of normal sodium which is to be compared with curve iv for normal sodium, calculated from i in the same way as ii.

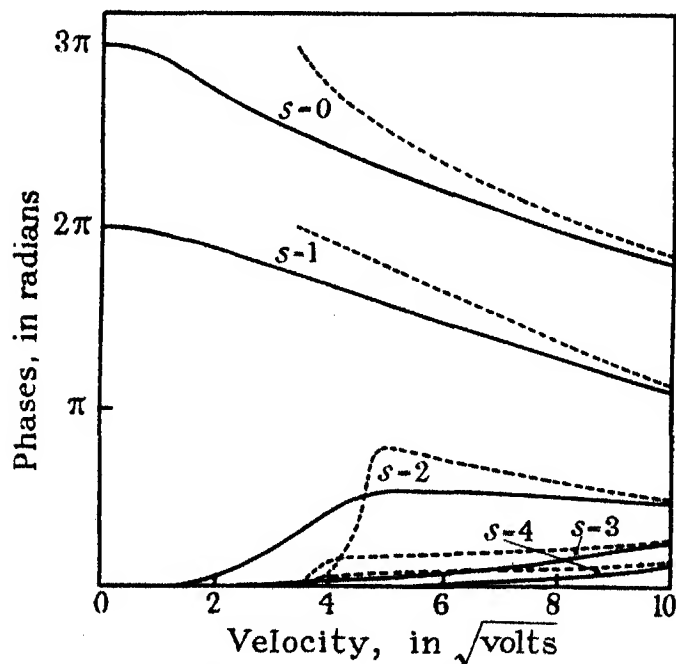


FIG. 2—Variation of the phases with velocity of the incident electrons, for argon. — δ_s (incoming wave in normal field); - - - γ_s (corresponding outgoing wave in excited field).

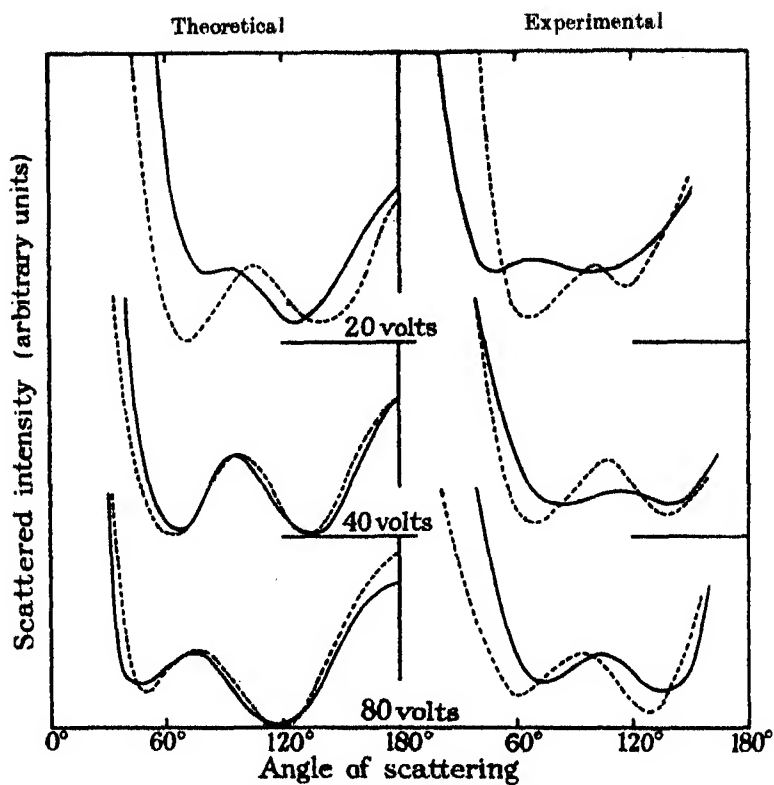


FIG. 3—Calculated and observed angular distributions in argon. - - - elastic
— inelastic.

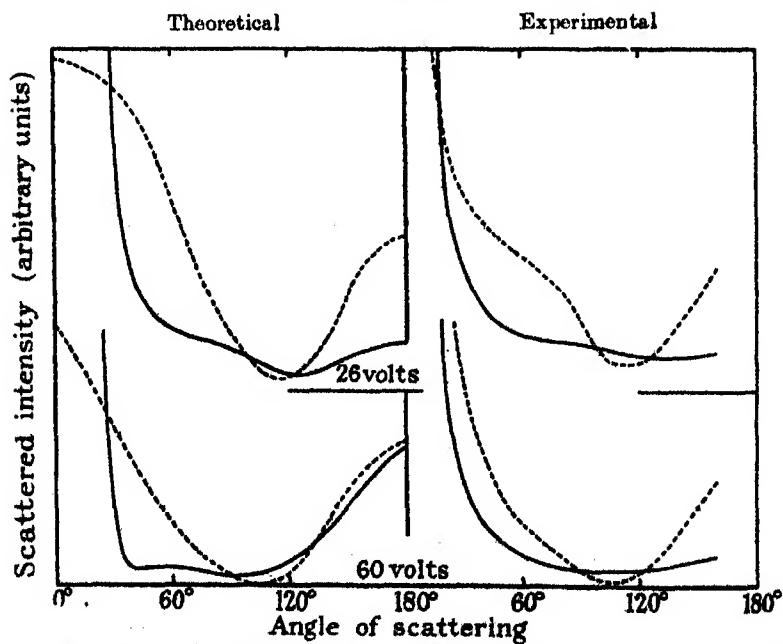


FIG. 4—Calculated and observed angular distributions in neon. - - - elastic
— inelastic.

incident energy scattered elastically, the calculation being carried out by using Faxén and Holtsmark's formula†

$$I(\theta) = \left| \frac{1}{2ik} \sum_n (e^{2i\delta_n} - 1) (2n + 1) P_n(\cos \theta) \right|^2. \quad (27)$$

Experimental curves, obtained by Nicoll and Mohr,‡ are included to check the accuracy of the theory.

The striking feature of the calculated curves for argon for the higher voltages is the very close similarity between the form of the elastic and inelastic scattering curves. At the lowest voltages, where the excitation energy involved is comparable with the incident electron energy the similarity begins to disappear. The reason for this has already been given in general terms in papers II and III. This result was first obtained experimentally and examination of the observed curves illustrated in fig. 3 reveals this same general similarity. For 80-volt electrons in argon the agreement with observation is very good, but for 40-volt electrons the calculated elastic and inelastic curves resemble each other more closely than do the corresponding observed curves. Again the agreement of theoretical and observed curves for 20-volt electrons is not very close. For neon, fig. 4, it will be seen that the general agreement between theory and experiment is quite good even at the lower voltage. It is of interest to note, however, that, unlike argon, there is a definite disagreement between theory and experiment for the lowest voltage elastic scattering curve, the kink in the experimental curve in the region of 60° being absent from the theoretical. This effect must be due to the contribution to the scattering from second order harmonics being relatively underestimated in the theory. It is probable that this discrepancy is due to neglect of electron exchange which could produce interference effects, reducing the contributions from the zero and first order harmonics and so making the second order contributions more apparent.

It is clear from figs. 3 and 4 that the main features of large angle inelastic scattering may be considered as arising from the diffracting effect of the static potential fields of the normal and excited atoms, respectively, on the incident and inelastically scattered electron waves, and so confirms the general considerations of papers II and III. The lack of close agreement with observation at the low voltages is to be expected, as it is under these conditions that one would expect the neglected effects of polarization and exchange to become important.

† Mott and Massey, "The Theory of Atomic Collisions," chapter II.

‡ 'Proc. Roy. Soc.' A, vol. 142, pp. 320, 647 (1933).

Section II—The Effect of Polarization on the Elastic Scattering of Electrons

We now consider the effect of the disturbance of the atomic field by the colliding electron on the elastic scattering of the electron, showing how it may be considered alternatively as arising from the interaction of the inelastically scattered electrons with the elastic.

The function $F_0(\mathbf{r})$ which describes the elastic scattering satisfies the equation

$$[\nabla^2 + k^2] F_0 = \frac{8\pi^2 m}{h^2} \sum_n F_n(\mathbf{r}) V_{n0}(\mathbf{r}), \quad (28)$$

with

$$[\nabla^2 + k_n^2] F_n = \frac{8\pi^2 m}{h^2} \sum_m F_m(\mathbf{r}) V_{mn}(\mathbf{r}). \quad (29)$$

The potentials are as defined in the preceding section. Born's first approximation is obtained from these equations by taking

$$F_0 = e^{ik\mathbf{n}_0 \cdot \mathbf{r}}, \quad F_n = 0 \quad n \neq 0,$$

on the right-hand side of (28). This assumes that the perturbation of the incident wave is so small that it can be neglected on the right-hand side of (28) and we obtain, using Green's theorem and remembering that

$$\begin{aligned} F_n &\sim r^{-1} e^{ik_n \mathbf{r}} f_n(\theta, \phi), \quad F_0 \sim e^{ik\mathbf{n}_0 \cdot \mathbf{r}} + r^{-1} e^{ikr} f(\theta, \phi), \\ F_n(\mathbf{r}) &= -\frac{2\pi m}{h^2} \int V_{0n}(\mathbf{r}_2) \frac{\exp\{ik_n |\mathbf{r} - \mathbf{r}_2|\}}{|\mathbf{r} - \mathbf{r}_2|} \exp\{ik\mathbf{n}_0 \cdot \mathbf{r}_2\} d\tau_2 \quad n \neq 0 \\ F_0(\mathbf{r}) &= e^{ik\mathbf{n}_0 \cdot \mathbf{r}} - \frac{2\pi m}{h^2} \int V_{00}(\mathbf{r}_2) \frac{\exp\{ik |\mathbf{r} - \mathbf{r}_2|\}}{|\mathbf{r} - \mathbf{r}_2|} \exp\{ik\mathbf{n}_0 \cdot \mathbf{r}_2\} d\tau_2. \end{aligned} \quad (30)$$

We now obtain an equation from which to derive a second approximation, viz. :—

$$\begin{aligned} [\nabla^2 + k^2] F_0 &= \frac{8\pi^2 m}{h^2} V_{00}(\mathbf{r}) e^{ik\mathbf{n}_0 \cdot \mathbf{r}} - \frac{16\pi^2 m^2}{h^4} \sum_n V_{n0}(\mathbf{r}) \\ &\quad \times \int V_{0n}(\mathbf{r}_2) \frac{\exp\{ik_n |\mathbf{r} - \mathbf{r}_2|\}}{|\mathbf{r} - \mathbf{r}_2|} e^{ik\mathbf{n}_0 \cdot \mathbf{r}_2} d\tau_2. \end{aligned} \quad (31)$$

In order to sum the series involved in this equation we restrict ourselves to such velocities of impact that $k_n \simeq k$ for all values of n which contribute appreciably to the sum. With this assumption we may use the result

$$\sum V_{n0}(\mathbf{r}) V_{0n}(\mathbf{r}_2) = \int V(\mathbf{r}, \mathbf{r}_a) V(\mathbf{r}_2, \mathbf{r}_a) |\psi_0(\mathbf{r}_a)|^2 d\tau_a, \quad (32)$$

where $V(\mathbf{r}, \mathbf{r}_a)$ is the interaction energy between an electron of co-ordinate (\mathbf{r}) and the atom. This gives

$$[\nabla^2 + k^2] F_0 = \frac{8\pi^2 m}{\hbar^2} V_{00}(\mathbf{r}) e^{ik\mathbf{n}_0 \cdot \mathbf{r}} - \frac{16\pi^2 m^2}{\hbar^4} \times \iint V(\mathbf{r}, \mathbf{r}_a) V(\mathbf{r}_2, \mathbf{r}_a) |\psi_0(\mathbf{r}_a)|^2 \frac{\exp\{ik|\mathbf{r} - \mathbf{r}_2|\}}{|\mathbf{r} - \mathbf{r}_2|} \exp\{ik\mathbf{n}_0 \cdot \mathbf{r}_2\} d\tau_2 d\tau_a. \quad (33)$$

Let us now change the origin of co-ordinates to the point \mathbf{r} for the calculation of the right-hand integral, and denote the polar co-ordinates with respect to the point \mathbf{r} by ρ, ϑ, ψ so, if $\rho_0, \vartheta_0, \psi_0$ are the co-ordinates of the initial origin

$$\rho_0 = r, \quad \vartheta_0 = \pi - \theta, \quad \psi_0 = \phi.$$

We then have

$$(\nabla^2 + k^2) F_0(\mathbf{r}) = \frac{8\pi^2 m}{\hbar^2} e^{ik\mathbf{n}_0 \cdot \mathbf{r}} \{V_{00} + v_{00}\},$$

where

$$v_{00} = -\frac{2\pi m}{\hbar^2} \iint \exp\{ik(\rho_2 + \mathbf{n}_0 \cdot \rho_2)\} V(\mathbf{r}, \rho_a - \mathbf{r}) V(\rho_2 - \mathbf{r}, \rho_a - \mathbf{r}) \times |\psi_0^2(\rho_a - \mathbf{r})|^2 \rho_2^{-1} d\rho_2 d\rho_a. \quad (34)$$

The effect of the second approximation can thus be regarded as the introduction of extra scattering potential v_{00} . This, however, includes the first approximation to the distortion effect which is obtained by considering the equation

$$(\nabla^2 + k^2) F_0 = \frac{8\pi^2 m}{\hbar^2} V_{00} F_0. \quad (35)$$

Solving this by successive approximations in the same way as the above, gives for the second approximation

$$(\nabla^2 + k^2) F_0 = \frac{8\pi^2 m}{\hbar^2} e^{ik\mathbf{n}_0 \cdot \mathbf{r}} (V_{00} + u_{00}),$$

where

$$u_{00} = -\frac{2\pi m}{\hbar^2} V_{00}(\mathbf{r}) \int V_{00}(|\rho_2 - \mathbf{r}|) \rho_2^{-1} \exp\{ik(\rho_2 + \mathbf{n}_0 \cdot \rho_2)\} d\rho_2. \quad (37)$$

u_{00} is thus a contribution due to V_{00} , and as such must be regarded as due to distortion rather than atomic polarization. We call the potential $v_{00} - u_{00}$ the true polarization potential, which arises from the interaction of the inelastically scattered waves F_n with the elastically scattered and can be regarded as an additional term due to the modification of the atomic potential.

The general considerations discussed in paper III would make it seem probable that the second approximation effects due to $v_{00} - u_{00}$ should represent the effect of the reaction of the inelastic on the elastic scattering with some accuracy, but there is no reason to suppose that u_{00} gives a good representation of the distortion effect, which is a diffraction phenomenon arising from the large magnitude of V_{00} for small values of r . Moreover we are able to calculate the distortion effect accurately by exact solution of equation (35) by Faxén and Holtsmark's method. Hence to compare with experiment, the scattered amplitude due to the potential $(V_{00} + v_{00} - u_{00})$ is calculated using Born's first approximation and the additional amplitude due to distortion determined immediately by comparing Born's formula for the scattering by the field V_{00} with Faxén and Holtsmark's formula (27). In this way we obtain the scattered amplitude as the sum of these terms:—

(a) that given by Born's first approximation calculated for the undisturbed field V_{00} ;

(b) a term given by calculating the scattering due to the "true" polarization potential $v_{00} - u_{00}$ using Born's first approximation;

(c) a term arising from distortion calculated by comparison of (a) with Faxén and Holtsmark's expression.

Alternatively we may regard the resultant amplitude as the sum of that given by Faxén and Holtsmark's formula (which includes distortion but not polarization) and of a polarization term obtained by calculating the scattering by the field $v_{00} - u_{00}$ using Born's approximation. Actually in practice it is more convenient to use the former method.

Calculation for Hydrogen and Helium—The calculation of $v_{00} - u_{00}$ is a very lengthy procedure and it can only be evaluated in a series of zonal harmonics. For convenience we will consider v_{00} and u_{00} separately.

(a) Calculation of v_{00} . Considering only one atomic electron with normalized wave function

$$\psi_0(r) = \left(\frac{\mu^3}{8\pi}\right)^{\frac{1}{2}} e^{-\frac{1}{2}\mu r} \quad (38)$$

we have

$$V(r, r_a) = -e^2 \left(\frac{1}{r} - \frac{1}{|r - r_a|} \right), \quad (39)$$

and so

$$v_{00} = \frac{e^4 m \mu^3}{4\hbar^2} (-I_1 + I_2 + I_3 - I_4), \quad (40)$$

where

$$\left. \begin{aligned} I_1 &= r^{-1} \iint \exp \{ik (\rho_2 + \mathbf{n}_0 \cdot \rho_2) - \mu \rho_{02}\} (\rho_{02} \rho_2)^{-1} d\rho_2 d\rho_a \\ I_2 &= \iint \exp \{ik (\rho_2 + \mathbf{n}_0 \cdot \rho_2) - \mu \rho_{02}\} (\rho_a \rho_2 \rho_{02})^{-1} d\rho_2 d\rho_a \\ I_3 &= r^{-1} \iint \exp \{ik (\rho_2 + \mathbf{n}_0 \cdot \rho_2) - \mu \rho_{02}\} (\rho_{2a} \rho_2)^{-1} d\rho_2 d\rho_a \\ I_4 &= \iint \exp \{ik (\rho_2 + \mathbf{n}_0 \cdot \rho_2) - \mu \rho_{02}\} (\rho_a \rho_{2a} \rho_2)^{-1} d\rho_2 d\rho_a \end{aligned} \right\} \quad (41)$$

Using now the expansions

$$\begin{aligned} e^{ik\rho_1 \cos \theta_1} &= \left(\frac{\pi}{2k\rho}\right)^{\frac{1}{2}} \sum_{n=0}^{\infty} (2n+1) i^n J_{n+\frac{1}{2}}(k\rho) P_n(\cos \theta) \\ \rho_{12}^{-1} &= \sum_{n=0}^{\infty} \gamma_n(\rho_1, \rho_2) P_n(\cos \gamma) \\ e^{-\mu \rho_{12}} &= -(\rho_1 \rho_2)^{-\frac{1}{2}} \sum_{n=0}^{\infty} (2n+1) \eta_n(\rho_1, \rho_2) P_n(\cos \gamma) \end{aligned}$$

where

$$\left. \begin{aligned} \gamma_n &= \rho_2^n \rho_1^{-n-1} \\ \eta_n &= \frac{\partial}{\partial \mu} \{K_{n+\frac{1}{2}}(\mu \rho_1) I_{n+\frac{1}{2}}(\mu \rho_2)\} \end{aligned} \right\} \rho_1 > \rho_2,$$

and

$$\cos \gamma = \cos \theta_1 \cos \theta_2 + \sin \theta_1 \sin \theta_2 \cos(\phi_1 - \phi_2); \quad (42)$$

together with the orthogonal properties of spherical harmonics, we obtain

$$\left. \begin{aligned} I_1 &= -16 \left(\frac{\pi^5}{2k}\right)^{\frac{1}{2}} \sum_n i^{-n} P_n(\cos \theta) r^{-3/2} \iint \gamma_n(r, \rho_a) e^{ik\rho_1} \\ &\quad J_{n+\frac{1}{2}}(k\rho_2) \eta_0(r, \rho_a) \rho_2^{\frac{1}{2}} \rho_a^{3/2} d\rho_2 d\rho_a, \\ I_2 &= -16 \left(\frac{\pi^5}{2k}\right)^{\frac{1}{2}} \sum_n i^{-n} P_n(\cos \theta) r^{-\frac{1}{2}} \iint \gamma_n(r, \rho_a) e^{ik\rho_1} \\ &\quad J_{n+\frac{1}{2}}(k\rho_2) \eta_0(r, \rho_a) \rho_2^{\frac{1}{2}} \rho_a^{\frac{1}{2}} d\rho_2 d\rho_a, \\ I_3 &= -16 \left(\frac{\pi^5}{2k}\right)^{\frac{1}{2}} \sum_n i^{-n} P_n(\cos \theta) r^{-3/2} \iint \gamma_n(\rho_2, \rho_a) e^{ik\rho_1} \\ &\quad J_{n+\frac{1}{2}}(k\rho_2) \eta_n(r, \rho_a) \rho_2^{\frac{1}{2}} \rho_a^{3/2} d\rho_2 d\rho_a, \\ I_4 &= -16 \left(\frac{\pi^5}{2k}\right)^{\frac{1}{2}} \sum_n i^{-n} P_n(\cos \theta) r^{-\frac{1}{2}} \iint \gamma_n(\rho_2, \rho_a) e^{ik\rho_1} \\ &\quad J_{n+\frac{1}{2}}(k\rho_2) \eta_n(r, \rho_a) \rho_2^{\frac{1}{2}} \rho_a^{\frac{1}{2}} d\rho_2 d\rho_a. \end{aligned} \right\} \quad (43)$$

The polar axis is taken in the direction of the unit vector \mathbf{n}_0 .

(b) Calculation of u_{00} . With the wave function (38) we have

$$V_{00}(r) = \left(\frac{\alpha}{r} + \frac{\mu}{2} \right) e^{-\mu r}, \quad (44)$$

where, in atomic units, $\alpha = 1$ and $\mu = 2$ for hydrogen.

Substituting in (37) and using the expansions (42) gives

$$\begin{aligned} u_{00} = & - \left(\frac{2^5 \pi^5}{k} \right) \frac{me^4}{\hbar^2} \left(\frac{\alpha}{r} + \frac{\mu}{2} \right) e^{-\mu r} \left(\alpha - \frac{\mu}{2} \frac{\partial}{\partial \mu} \right) \\ & \sum_n i^{-n} (2n+1) P_n(\cos \theta) \left\{ r^{-\frac{1}{2}} K_{n+\frac{1}{2}}(\mu r) \right. \\ & \int_0^r I_{n+\frac{1}{2}}(\mu \rho_2) e^{i k \rho_2} J_{n+\frac{1}{2}}(k \rho_2) d\rho_2 + r^{-\frac{1}{2}} I_{n+\frac{1}{2}}(\mu r) \\ & \left. \int_r^\infty K_{n+\frac{1}{2}}(\mu \rho_2) e^{i k \rho_2} J_{n+\frac{1}{2}}(k \rho_2) d\rho_2 \right\}. \end{aligned} \quad (45)$$

The further calculation of u_{00} and v_{00} can only be carried out by using the explicit expressions for the Bessel functions involved. After this substitution the integrations may be carried out without difficulty, but even for the zero order terms the complications of algebra are very great. It is found in this way that v_{00} has the asymptotic form

$$v_{00} \sim - \frac{e^2}{a_0 \mu^2 k} \left[\frac{2i}{r^3} + \frac{(1-3\cos\theta)}{r^4 k} \left\{ 1 - \frac{\mu^6 e^{2ikr}}{(\mu^2 + 4k^2)^3} \right\} + O\left(\frac{1}{r^6}\right) \right]. \quad (46)$$

It will be clear without further calculation that the effect of the true polarization potential will be to increase the small angle scattering owing to the presence of a term (purely imaginary), which falls off as slowly as r^{-3} for large r . In fact with this form for $v_{00}(r)$ the scattering per unit solid angle becomes logarithmically infinite at $\theta = 0$, although the scattering per unit angle still tends to zero as the angle of scattering is decreased. The real part of the second term in the asymptotic expansion of $v_{00}(r)$ corresponds to the classical polarization effect, and a semi-empirical potential with this asymptotic form was actually introduced by Holtsmark in calculating the scattering of slow electrons by argon and krypton.

With regard to the convergence of the series (43) and (45), which will be better the smaller the incident electron energy, we note that the zero order term vanishes more slowly at infinity than the remaining terms, and so is always much the most important in determining the small angle scattering. It was found then that, when the incident electron energy is sufficiently great

to make the convergence poor for other values of r , the effect of $v_{00} - u_{00}$ at the larger angles of scattering (determined by the form of $v_{00} - u_{00}$ for these values of r) is small compared with the true distortion effect and Born's first approximation. Hence it was fortunately only necessary to take into account the first two terms in the expansions (43) and (45).

To carry out the detailed calculation of the scattered amplitude due to $v_{00} - u_{00}$ we substitute $V_{00} + v_{00} - u_{00}$ for V_{00} in Born's approximate formula, to obtain

$$f(\theta) = -\frac{2\pi m}{h^2} \int (V_{00} + v_{00} - u_{00}) e^{ik(\mathbf{a}_s - \mathbf{a}_i) \cdot \mathbf{r}} d\tau \quad (47)$$

and carry out the integration. The resulting formulæ, even for the zero order term of $v_{00} - u_{00}$, are too complicated for reproduction here, but in fig. 5 the contributions arising from the various terms are illustrated for scattering by hydrogen. It will be seen from this figure that the imaginary amplitude due to the polarization effect produces a great increase at small angles, but has only a small effect at large angles. The rapid convergence of the contributions from the various terms in the series (43) and (45) is also clear.

Comparing the results for hydrogen and helium it is found that the polarization effect persists at much higher voltages in helium than in hydrogen. This follows from the fact that, apart from a numerical factor which is nearly unity for hydrogen and helium, the ratio of the polarization amplitude to that given by Born's first approximation is a function of μ/k . Since

$$\frac{\mu_{\text{helium}}}{\mu_{\text{hydrogen}}} = 1.69,$$

$$\frac{k_{\text{helium}}}{k_{\text{hydrogen}}} = 1.69 = \frac{\sqrt{\text{volts}_{\text{helium}}}}{\sqrt{\text{volts}_{\text{hydrogen}}}} \text{ for constant } \mu/k,$$

and the effect is approximately the same for 230-volt electrons in helium as for 80-volt electrons in hydrogen.

In figs. 6 and 7 angular distributions calculated in the manner described above are compared with experimental curves for hydrogen† (molecular) and helium.‡ The agreement is seen to be very good. The experimental curves for hydrogen have each been arbitrarily fitted to the theoretical curves. The experimental results for helium include also the relative magnitudes of the scattering curves at different voltages, and so in fig. 7 only one arbitrary

† Arnot, 'Proc. Roy. Soc.,' A, vol. 133, p. 615 (1931)

‡ Hughes, McMillen and Webb, 'Phys. Rev.,' vol. 41, p. 154 (1932).

adjustment was made, the 350 volt experimental and theoretical curves being fitted together; it was then found that the curves for the other voltages also fitted each other. Assuming that the scattering of 700 volt electrons is given

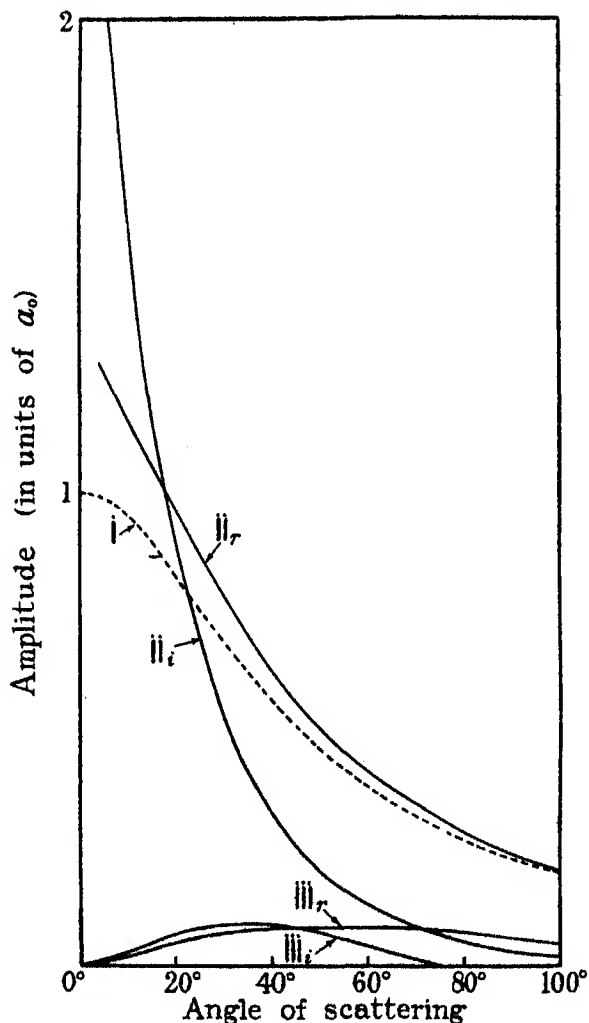


FIG. 5—Illustrating the correction to Born's approximation due to polarization and distortion, for 54-volt electrons in hydrogen. i, Born's approximation; ii, after taking polarization and distortion into account also, zero order term; iii, ditto, first order term. Suffices r and i denote real and imaginary amplitudes respectively.

accurately by Born's approximation, absolute values may be assigned to the experimental results, but these values are 0.45 times smaller than those calculated. Also the evidence from determinations of ionization and total

cross-sections in helium would seem to indicate a smaller elastic cross-section than the theoretical. However, the accuracy of experimental determinations of *absolute* values of scattered intensities is not high, and to be quite certain of the position, it would be advisable to have independent observations

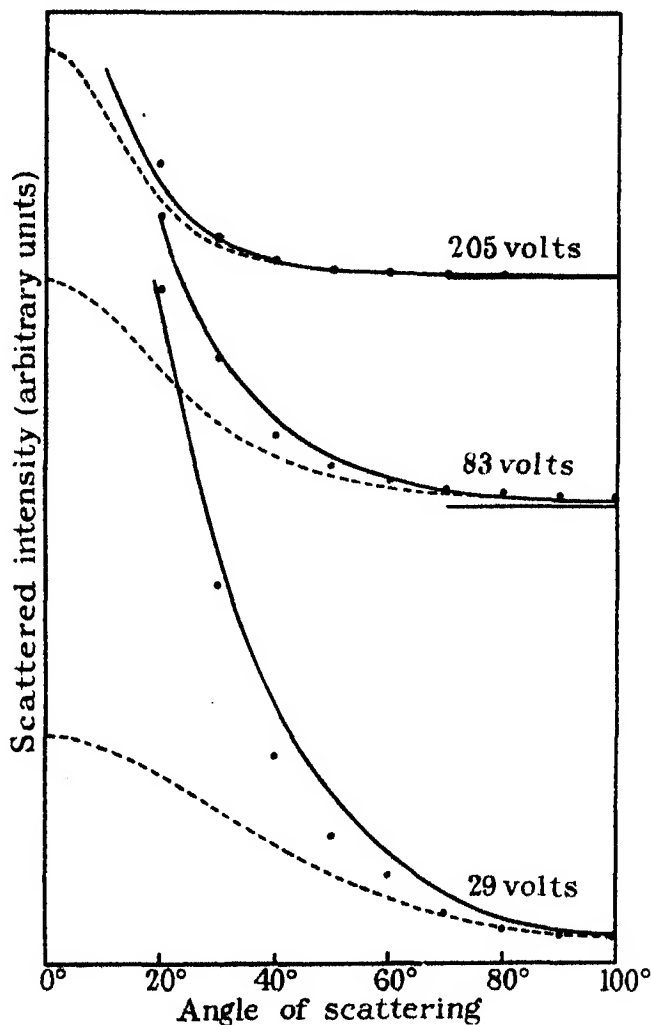


FIG. 6—Elastic angular distributions in hydrogen. - - - calculated using Born's approximation; — calculated taking polarization and distortion into account also; . . . observed values.

of the elastic cross-section in helium and its ratio to the total cross-section for a range of velocities. Nevertheless, there is no doubt that the observed departure from Born's approximation at small angles is due to the effect we

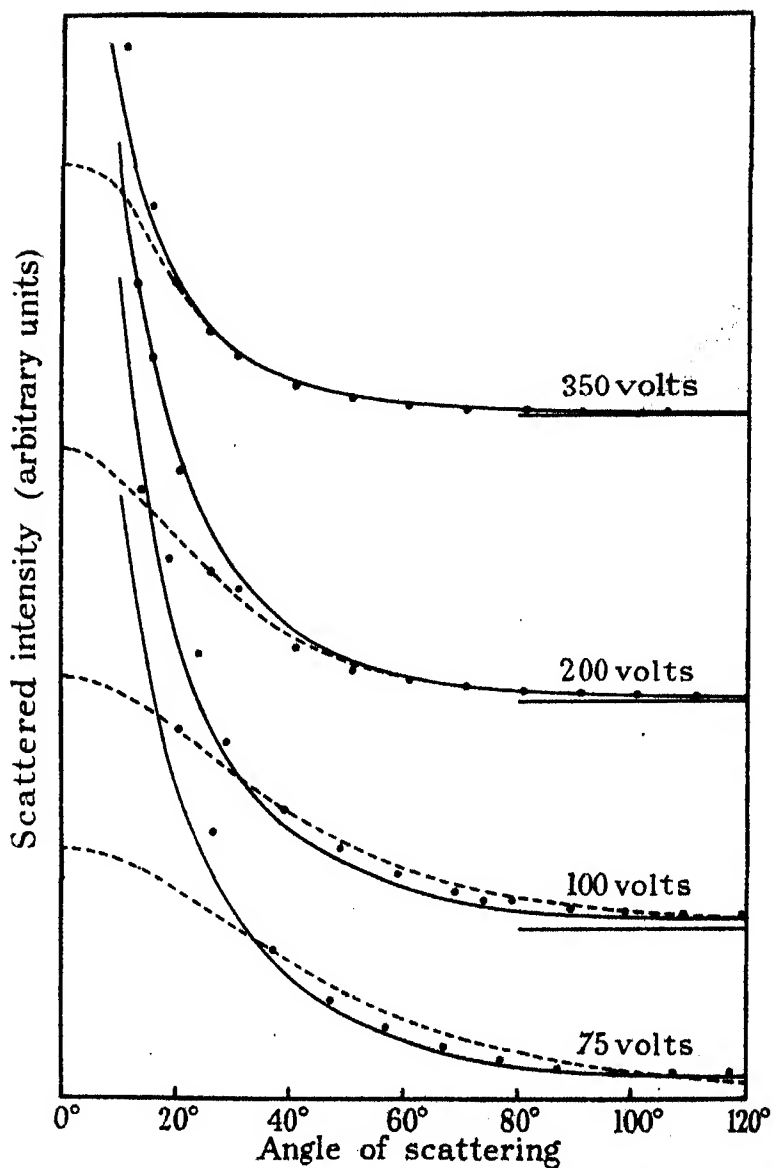


FIG. 7—Elastic angular distributions in helium. - - - calculated using Born's approximation; — calculated taking polarization and distortion into account also; . . . observed values.

have denoted by polarization. The qualitative explanation given in paper III is therefore definitely established.

Further confirmation of the theory is provided by the recent results obtained by Whiddington† for the scattering in helium at still smaller angles (2° – 5°). The theory predicts the scattering at 2° to be about twice that at 5° for energies between 100 and 400 volts; the experiments indicate this rate of variation of scattering at 200 volts, though somewhat slower and faster variations respectively at 100 and 400 volts. However, these preliminary experimental results are based on the questionable assumption that the inelastic scattering is given accurately by Born's approximation at angles as small as 2° . Since the elastic scattering as given by Born's approximation does not change sensibly between 2° and 5° at these voltages, these results can be regarded as further evidence in favour of the theory. It is interesting to note that as the angle of scattering decreases to zero, the scattering as given by the present approximation of the theory increases slowly but continually, instead of approaching a constant value as predicted by Born's approximation. The total cross-section still remains finite, however, since the scattering increases only logarithmically at very small angles.

Discussion

The detailed investigations of this paper have confirmed the qualitative description of the effect of the distortion of the electron waves by the atomic field on the inelastic scattering, and the effect of polarization of the atomic field on the elastic scattering. We may, therefore, summarize the present position of knowledge of the way in which the effects of the different individual processes are manifest in experimental observations. This is done in Table I.

It will be seen that, although it is possible to recognize most of the effects of the processes, it is not yet possible to give a quantitative account of the effect of exchange and polarization on the inelastic scattering, although a qualitative account of the effect of the latter on the total probability of an inelastic collision can be given. A quantitative account of this effect of polarization on the inelastic scattering would be very complicated, but, in view of the success of the method of Section II in discussing the effect of polarization on the elastic scattering, it is probable that a similar method could be applied to discuss the effect on the inelastic scattering.

† 'Nature,' vol. 133, p. 685 (1934).

Table I

Process involved	Effect on	
	Elastic scattering	Inelastic scattering
1—Scattering by the undisturbed field of the atom in which the incident wave is only slightly disturbed.	Small intensity of scattering. Angular distribution monatomic, intensity decreasing with angle.	Angular distribution monatomic and decreasing more rapidly with angle than for elastic scattering.
2—Distortion of incident and scattered waves by atomic field.	Maxima and minima in cross-section-velocity curves (Ramsauer effect). Maxima and minima in angular distributions, these being most marked for heavy atoms and disappearing at low velocities of impact.	No marked effect on cross-section-velocity curves. Maxima and minima in angular distributions at large angles, closely resembling the corresponding elastic angular distributions except for very low velocities of impact.
3—Electron exchange.	Apparent for light atoms (H, He) at low velocities of impact in producing greater variability of form in the angular distributions (i.e., He below 20 volts).	Leads to possibility of excitation of optically disallowed transitions (i.e., excitation of He triplets). Effect on angular distributions not yet known.
4—Disturbance of atomic field (polarization) or, alternatively, effect of interaction of scattered waves on each other.	Greatly increased scattering at small angles. Increase of total probability of an elastic collision.	Decrease of probability of an inelastic collision. Effect on angular distribution not yet known.

Our thanks are due to the Department of Scientific and Industrial Research for a Senior Grant to one of us (C. B. O. M.), and to Mr. J. McDougall for providing us with an approximate Hartree field for sodium.

Summary

A quantitative account is given of the effect of two factors which are of importance in determining the scattering of slow electrons by atoms. The first section discusses the form of the angular distribution of inelastically scattered electrons as determined by the distortion of the incident and outgoing electron waves by the field of the atom. The numerical application of the formulæ to neon and argon shows good agreement with the observed diffraction effects. In the second section the effect of the disturbance of the atomic field by the colliding electron on the elastic scattering is dealt with, and this theory is applied numerically to the scattering by hydrogen and helium. Comparison with experiment then shows that the marked excess of scattering observed at small angles above that given by Born's approximation is clearly due to this polarization effect. A summary of the present position of the theory of the scattering of slow electrons is also given.

Spectrum of the Afterglow of Sulphur Dioxide

By A. G. GAYDON, A.R.C.S., D.I.C., M.Sc., Research Student, Imperial College,
South Kensington

(Communicated by A. Fowler, F.R.S.—Received May 28, 1934)

[PLATES 13 and 14]

Introduction

Following a previous investigation of the afterglow of carbon dioxide* it was decided to examine sulphur dioxide under similar conditions of experiment. An afterglow of considerable intensity and duration had, in fact, already been noted by Professors Sir J. J. and G. P. Thomson† as occurring when sulphur dioxide was excited in a ring discharge, but no observations on its spectrum appear to have been recorded. Strutt‡ has recorded an afterglow when ozone is passed over sulphur, but no glow was recorded with sulphur dioxide.

The spectrum yielded by SO_2 in vacuum tubes varies greatly according to the conditions of excitation. With sufficiently powerful condensed discharges and a rather low pressure of the gas, the molecules are dissociated into atoms and the spectrum consists of lines of oxygen and sulphur. With uncondensed discharges of moderate intensity and a suitable pressure of gas, the spectrum shows a strong system of bands degraded to the red which have been analysed by Henri and Wolff§ and attributed to the diatomic molecule SO ; these bands are most intense in the region λ 2442 to λ 3941. Still weaker excitation yields an entirely different system of bands extending from the blue to about λ 2000, and there is evidence that these bands are due to undissociated molecules of SO_2 || The absorption of SO_2 is characterized by a large number of bands, which are most intense in the region λ 2800 to λ 3150. Owing to the continuous spectrum emitted by the gas during electrical excitation, this absorption may appear superposed on the emission spectrum in some

* Fowler and Gaydon, 'Proc. Roy. Soc.,' A, vol. 142, p. 362 (1933).

† 'Conduction of Electricity through Gases,' vol. 2, p. 443.

‡ 'Proc. Phys. Soc.' vol. 23, p. 149 (1911).

§ 'J. Phys.,' vol. 10, p. 81 (1929).

|| Tung-Ching Chow, 'Phys. Rev.,' vol. 44, p. 638 (1933).

forms of discharge tube. Recently Lotmar* has reported on a band system excited in SO_2 by fluorescence.

While much work has been done on the subject, our knowledge of the energy levels associated with the SO_2 molecule is far from complete and it was thought that any further information as to the spectrum which could be obtained by different means of excitation might be of assistance in completing the analysis.

Experimental

Liquid sulphur dioxide, purified by freezing out *in vacuo*, was used. After purification it was let into a 2-litre flask R, fig. 1, as reservoir. This reservoir

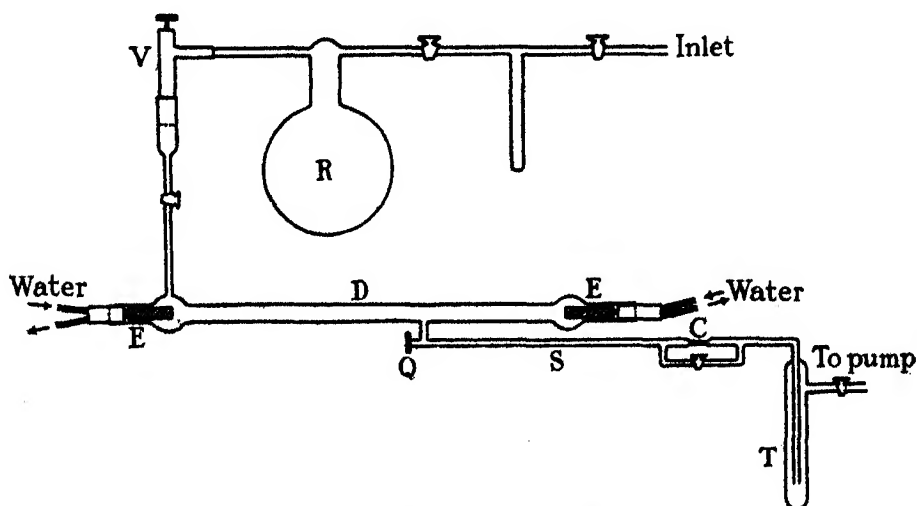


FIG. 1—Diagram of vacuum system

was connected to the discharge tube through an adjustable valve V. The discharge tube consisted of a Pyrex tube D about 60 cm long and 1.5 cm internal diameter. The electrodes EE consisted of stout aluminium rods screwed into water-cooled copper cylinders; this water cooling was found to be essential owing to the great heat produced by the intense discharge in some of the experiments. The electrodes were waxed into the ends of the discharge tube. The afterglow was observed in the side tube S, which was some 30 cm long and 0.4 cm internal diameter. Observation was made through the quartz window Q. The connection between the side tube and the discharge tube was made as short as convenient (about 2 cm) because the afterglow, being of short

* 'Z. Physik,' vol. 83, p. 765 (1933).

duration, did not extend far from the discharge. After passage through the discharge tube and constriction C, which was shunted by a tap for quick evacuation of the system, the gas was frozen out by a liquid air trap T. The pump (a good mechanical pump giving a pressure estimated at 0.001 mm) was kept going to remove any oxygen formed by decomposition of the gas. By adjusting the valve V a continuous stream of gas at any desired pressure was passed through the discharge tube.

For investigation at high pressure (1 to 5 mm) the afterglow was observed and photographed in the side tube, but at low pressures this method was not found satisfactory as stray discharges down the side tube tended to mask the afterglow. To overcome this difficulty the mercury break adapted as a rotating shutter in a previous examination of the afterglow of carbon dioxide* was employed. This entailed a slight modification in the design of the discharge tube so that it could be viewed end on; the dimensions, however, were approximately the same. A continuous stream of gas was used, as before, to prevent accumulation of oxygen formed by decomposition of the gas.

The discharge was maintained by a powerful induction coil taking up to 20 amperes through the primary from the 110 volts mains.

Occurrence of the Afterglow

A bright blue-violet afterglow was observed. At a low pressure (about 0.1 mm) the afterglow was very persistent and could be seen for about 5 to 10 seconds in a completely darkened room, and for a short time even in daylight. At higher pressure (estimated at 2 to 5 mm) the afterglow was of very short duration ($\frac{1}{4}$ second or less) but still very intense; it was drawn only about 5 cm down the side tube, but could be photographed quite easily with a quartz E2 spectrograph in half an hour. It was noticed that the afterglow was rather faint for the first few minutes after the current was switched on, but increased in intensity as the discharge tube became heated. A little sulphur was deposited both in the discharge tube and in the side tube.

An attempt to examine the effect of the presence of small quantities of possible impurities produced only negative results. Small quantities of carbon dioxide, air, and water vapour were admitted, but produced no observable change in the duration, intensity, or colour of the afterglow, although if air was present in appreciable quantity the "second positive" bands of nitrogen appeared in the spectrum of the afterglow. During examination of the afterglow

* 'Proc. Roy. Soc.,' A, vol. 142, p. 362 (1933).

the spectrum of the ordinary discharge was free from impurities except that at very low pressure the hydrogen lines H_α and H_β were faintly present. It seems, therefore, quite safe to assume that the afterglow is stimulated by SO_2 or one of its decomposition products and not by any impurity.

Photography of the Spectrum

Preliminary work was carried out with a medium size quartz spectrograph (Hilger E2). A small quartz instrument (E31) was also used for exploration in the far ultra-violet. It was found, however, that the interesting portion of the spectrum was in the region 4000 Å and hence it was determined to use instruments giving a larger dispersion in this region.

A large aperture glass prismatic spectrograph giving a dispersion in the blue and violet of about 45 Å per mm was then used, this instrument being extremely fast and very useful for studying the effect of variation of pressure and electrical excitation on the spectrum of the afterglow. Using the side tube, good spectrograms were obtained in about 20 minutes on fast plates, but when using the rotating shutter this time was reduced to about 10 minutes. A grating-on-prism spectrograph giving a rather larger dispersion (26 Å per mm) was also used; the spectrum only extended from the red to about 3925 Å, but the instrument gave good definition and was suitable for a rather detailed examination of the spectrum under various conditions, and also for studying the ordinary discharge with very weak excitation. This spectrograph was much slower than the large aperture instrument, but enabled the afterglow to be photographed in about $\frac{1}{2}$ to 3 hours according to its intensity.

For exploration work, Ilford Monarch and Double-X-Press plates were used, these being extremely fast. Owing to the coarse grain, spectrograms on these plates were difficult to measure under a microscope, and hence it was necessary to use slower plates when the best results were desired. As no spectrum was observed in the red, there was no advantage in using panchromatic plates, although an unsuccessful trial was made to see if anything further was obtained. In order to display the bands of the afterglow relative to the continuous background it was desirable to use a contrasting developer, and hydroquinone was therefore used for most of the work.

Spectrum of the Afterglow

The spectrum may be divided into two portions, a continuum and a band system.

The continuum was very intense from far in the ultra-violet (2400 Å or less) to the blue-green; it did not extend into the red. The SO_2 absorption bands from λ 2800 to λ 3150 were superposed on the continuum; these are to be attributed to absorption in the space between the afterglow and the quartz window, this distance being about 3 cm when examining through the side tube, and about 5 cm when using the rotating shutter. There were no emission bands in the ultra-violet.

The band system, λ 3828 to λ 4699, when photographed in an afterglow under favourable conditions, using a narrow slit and contrasting developer, was well displayed. It consisted of about 20 narrow but rather diffuse bands, often occurring in pairs. The bands were not clearly degraded preferentially in either direction, and hence exact measurements of the wave-lengths could not be obtained; the values given in Table I are estimates of the wave-lengths of the centres of the bands; intensities have been estimated on a scale of 0 to 4.

Table I—Wave-lengths, intensities, and wave numbers of the bands of the afterglow of SO_2

λ	I	ν	λ	I	ν
4699	1	21277	4244.6	4	23553
4677	0	21375	4200.1	0	23802
4588	2	21780	4152.9	4	24073
4564.8	2	21901	4130.1	1	24170
4483.6	1	22297	4060.5	4	24584
4461.0	3	22411	4048.3	3	24694
4441.0	0	22512	4007.2	1	24949
4361.1	3	22925	3963.7	4	25222
4339.7	2	23037	3883.0	2	25746
4265.3	3	23440	3828	0	26116

The band system, relatively to the continuum, was more pronounced at fairly high pressure, estimated at about 2 to 5 mm, and with a weak exciting discharge, although the afterglow as a whole was less intense; under these conditions little or no sulphur was deposited. With very powerful excitation, or at low pressure the continuous background was much more intense and the bands were almost obscured; a considerable amount of sulphur was deposited, necessitating occasional cleaning of the quartz window. Under similar conditions of pressure and electrical excitation, the spectrum was found to be the same whether observed along the side tube or through the rotating shutter.

Analysis of the Band Spectrum

The emission band system is quite simple in appearance, and although very accurate values of the wave-lengths have not been obtained, the wave number

differences have been determined with sufficient accuracy to leave no doubt as to their identity. Intervals of about 1140 and 520 occur (also 620, the difference between 1140 and 520). It is convenient to arrange the bands as shown in Table II to show this regularity. This arrangement shows certain differences from similar schemes for diatomic molecules, and suggests that the afterglow spectrum is not due to a diatomic emitter. The intervals 1140 and 520 are, in fact, to be identified with those found in other ways for the triatomic molecule SO_2 . All the bands except three have been arranged into this scheme.

Table II—Arrangement of afterglow bands to show wave number differences of about 1140 and 520. The differences are printed in italics. Intensities are in brackets following wave numbers of bands

		22512 (0)		21375 (0)	
		<i>525</i>	<i>1137</i>	<i>526</i>	
24170 (1)		23037 (2)		21901 (2)	
	<i>1133</i>		<i>1136</i>		
<i>524</i>		<i>516</i>		<i>510</i>	
24094 (3)		23553 (4)		22411 (3)	21277 (1)
	<i>1141</i>		<i>1142</i>	<i>1134</i>	
<i>528</i>		<i>520</i>		<i>514</i>	<i>513</i>
25222 (4)		24073 (4)		22925 (3)	21790 (2)
	<i>1149</i>		<i>1148</i>	<i>1135</i>	
<i>524</i>		<i>511</i>		<i>515</i>	<i>507</i>
25746 (2)		24584 (4)		23440 (3)	22297 (1)
	<i>1162</i>		<i>1144</i>	<i>1143</i>	

In absorption, Chow* finds intervals of 521 decreasing, 1150 and two other rather uncertain ones. In fluorescence, Lotmar† finds 520 decreasing to 430, 1150 decreasing to 1110, and, in addition, 1370. In the Raman effect, Dickinson and West‡ report intervals of 524, 1146, and 1340; and in infra-red investigations Bailey and Cassie§ give 524, 1152, and 1361. These intervals have been definitely attributed to the ground state. It thus appears that the band system of the afterglow is due to SO_2 , and is produced by transitions to the various vibrational levels of the ground state.

The intensity distribution of the bands arranged in Table II is smooth and indicates fairly definitely that the band at $\nu = 25746$ is that corresponding to a transition to the lowest state as indicated. The larger interval seems to

* 'Phys. Rev.', vol. 44, p. 638 (1933).

† 'Z. Physik,' vol. 83, p. 765 (1933).

‡ 'Phys. Rev.', vol. 35, p. 1126 (1930).

§ 'Proc. Roy. Soc.,' A, vol. 137, p. 622 (1932).

decrease for the higher vibrational levels, and 1150, 1145, and 1140 have been chosen as the most probable values for the three levels. The smaller wave-number interval does not appear to alter appreciably with increase of quantum number, and a mean value of 518 has been adopted. Both differences decrease towards the top right-hand corner of Table II; this may be a real change caused by some interaction of the two vibrations for the higher quantum numbers, or perhaps can be explained by assuming that the centres of the bands as measured do not correspond to their origins, so that a systematic change in the differences is to be expected. The third vibrational interval of about 1360 associated with the ground state has not been observed in the afterglow spectrum.

Since all except three of the bands are due to transitions from one upper level to these lower levels, and the remaining three bands (wave numbers 26116, 24949, and 23802) show the 1150 interval between themselves, it must be concluded that only two vibrational levels of the upper state are involved. The energy of the lower level of this upper state must be at least 25746 units of wave number, but it seems unlikely that it is the same state as found for the emission of SO_2 in the ultra-violet (in the region 2300 Å), as this would imply that only very high vibrational levels of the ground state are involved, which appears unlikely with a gas in a cool side tube, and also from the intensity distribution of the bands. The majority of the transitions (17 bands) occur from the lower vibrational level of the upper state, and the remaining three bands are from the next vibrational level to the ground state. The separation of the two vibrational levels of this upper state would then appear to be about 365^* cm^{-1} (or perhaps $365 +$ one of the other intervals, 520, or 1150, or an integral multiple of these). If this is assumed to be true, then we obtain an energy level scheme as shown in fig. 2. The 365 interval for the upper state is not very certain. The two series of levels in the lower state correspond to two forms of vibration of the triatomic molecule which can occur independently; hence any value of the total vibrational energy of the lower state made from a combination of these levels is possible. The spectrum affords no means of determining the value of the vibrational quantum number associated with the

* The three bands which do not fit into Table II show the 1150 interval among themselves, and are displaced about 365 cm^{-1} from the three corresponding bands in Table II, thus

25746		24584		23440
	1162		1144	
370		365		362
26116		24949		23802
	1167		1147	

frequency of 1360, but if the bands belong to the system obtained by Watson and Parker* in absorption it must have a value about five.

The bands observed do not appear to have been recorded previously, at any rate as a group, although some of them coincide roughly with some of Lotmar's fluorescence bands. In view of the large number of bands in his spectrum, however, the agreement is probably accidental.

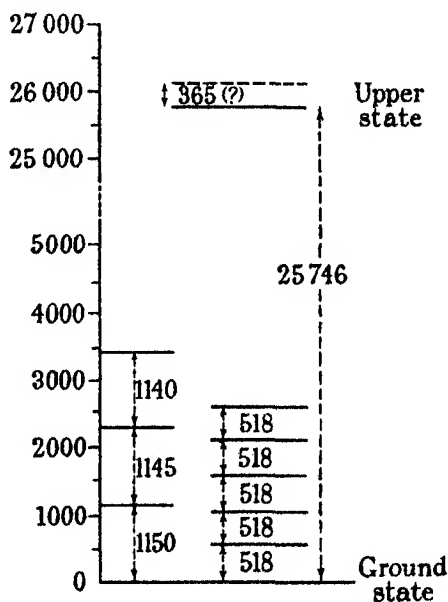


FIG. 2

Spectrum of the Exciting Discharge and its Relation to the Cause of the Afterglow

It has been shown already that the band system of the afterglow is produced by molecules of SO_2 , but it was thought desirable, if possible, to obtain some evidence as to the cause of these molecules being or remaining in an excited state. Hence the spectrum of the exciting discharge was examined.

The spectrum of the exciting discharge was in general very complex, and varied considerably with the intensity of the discharge. The most prominent features between 5000 Å and 2200 Å were numerous bands which have been attributed to SO and SO_2 . The SO bands have been described by Henri and

* 'Phys. Rev.', vol. 37, p. 1013 (1931).

Wolff, and the SO_2 emission bands in the ultra-violet by Chow. Bands in the blue violet have also been attributed to this molecule by Bhaduri at the Imperial College, although an analysis of these bands has not yet been published. The more intense bands of the afterglow are also shown on spectrograms of the discharge under suitable conditions, but this does not necessarily imply that they are present in the initial spark, as the afterglow is, of course, included. A few lines were observed at times, including the aluminium lines λ 3961 and λ 3944 at the electrodes, the sulphur triplet, $4s\ ^5\text{S}_2-5p\ ^5\text{P}_{1,2,3}$, at λ 4696, and the oxygen line at λ 4368. Bands of S_2 were present only with relatively very powerful, but still uncondensed, excitation. With weak excitation the most prominent features were the SO bands, the SO_2 system observed by Chow in the ultra-violet, and bands in the blue and violet including the more intense afterglow bands, now also attributed to this molecule. The sulphur triplet was faint but definitely present. With powerful excitation the SO_2 bands were less pronounced and the spectrum consisted chiefly of SO bands, the oxygen line and the sulphur triplet, the last named being very strong.

Under the conditions most favourable to the production of the band system of the afterglow, we see that the constituents of the gas were SO_2 , SO, S, and presumably oxygen. The sulphur lines, although present, were faint, and it is unlikely that the afterglow depends on the presence of atomic sulphur. The strength of the afterglow was unaffected by the rate of flow of the gas through the tube; since the rate of flow should affect the proportion of oxygen formed by decomposition, it seems improbable that the afterglow is stimulated by oxygen alone. It has recently been shown* that sulphur monoxide, SO, can be condensed out after passage of an electric discharge through sulphur dioxide; this would imply that the SO molecules although unstable have an appreciable life. We have spectroscopic evidence of the presence of these molecules in the discharge, and it seems quite probable that the afterglow is produced by some reaction in which they take part. It is possible that they combine with oxygen to form SO_2 , giving rise to something in the nature of a flame which yields the observed spectrum of the afterglow. This is similar to the explanation, put forward in a previous paper, to account for the occurrence of the afterglow of carbon dioxide.

In conclusion, I wish to express my sincere thanks to Professor A. Fowler, F.R.S., under whose guidance the research has been carried out, and to Dr. R. W. B. Pearse for much helpful discussion.

* Cordes and Schenk, 'Trans. Faraday Soc.', vol. 30, p. 31 (1934).

Summary

Sulphur dioxide, when excited to luminescence in an electrical discharge at low pressure, has been found to possess a blue-violet afterglow of considerable intensity. The conditions of its production and the effect of change of pressure and electrical excitation on the spectrum have been investigated.

The spectrum of the afterglow has been studied between 2400 Å and 6000 Å, and found to consist of about 20 narrow but headless bands in the region λ 3828 to λ 4699 and a continuum from 2400 Å to about 4500 Å. The band system has been analysed and found to give wave number intervals of about 1140 and 520 and a few intervals of 365. The first two of these intervals are known intervals of the ground state of sulphur dioxide. This indicates that the afterglow bands are due to the triatomic molecule SO_2 . It is suggested that the lower of the excited states may have an energy equivalent to about 25746 cm^{-1} , with a vibrational level of an additional 365 cm^{-1} associated with it.

From a consideration of the spectrum of the exciting discharge it seems probable that the afterglow is caused by the recombination of SO and oxygen in the form of a flame which gives the observed spectrum.

DESCRIPTION OF PLATES

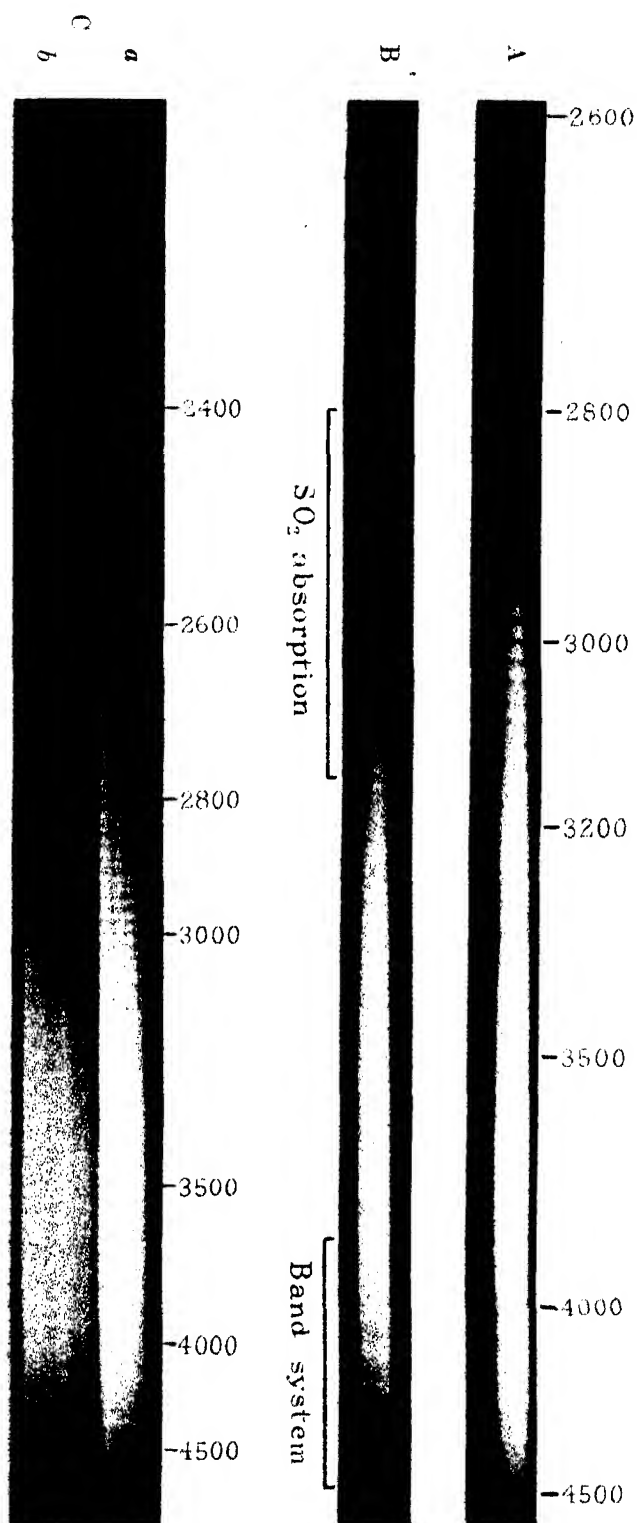
PLATE 13

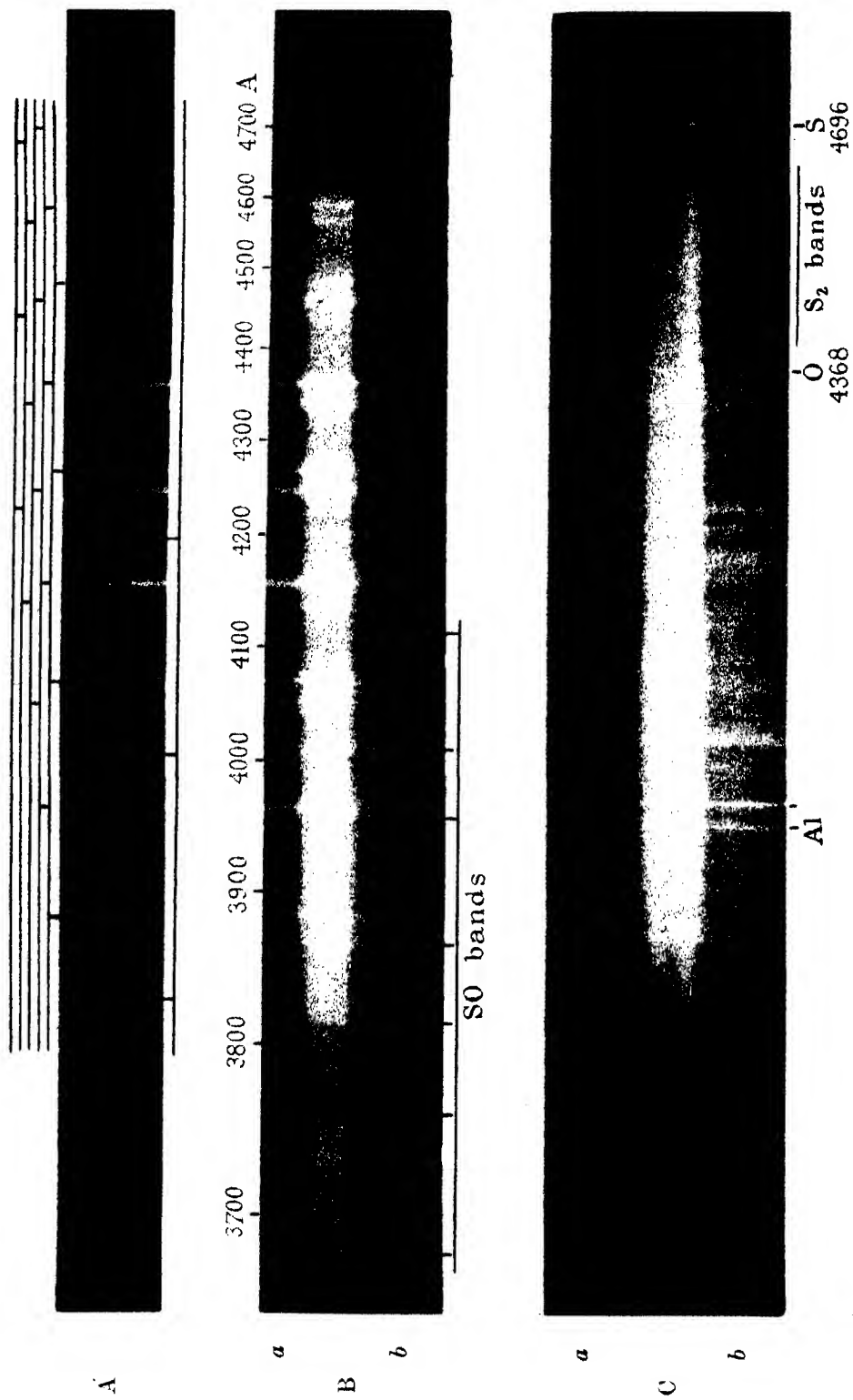
- A— SO_2 afterglow spectrum, observed by drawing through side tube, on medium quartz spectrograph. Fairly powerful excitation; low pressure; exposure 15 minutes.
 B—As above. Higher pressure; exposure 20 minutes.
 C—Small quartz spectrograph. Weak excitation; high pressure. (a) Exciting discharge; exposure 50 seconds. (b) Afterglow observed through rotating shutter; exposure 30 minutes.

PLATE 14

All these spectrograms were taken with the large aperture instrument, the afterglow being observed through the rotating shutter.

- A— SO_2 afterglow (see details under B (a) below). Transitions between the lower vibrational level of the upper state and the various vibrational levels of the ground state are marked above the spectrogram. The 1150 cm^{-1} intervals are marked in horizontal rows, and the 518 intervals correspond to the shifts between adjacent rows. The transitions from the upper vibrational level of the upper state to the ground state are marked below the spectrogram.
 B—(a) SO_2 afterglow at high pressure and with weak excitation. Exposure 1 hour. (b) Exciting discharge. Exposure 2 minutes; weak afterglow bands and some SO bands are the chief features.
 C—(a) Afterglow at moderate pressure with very powerful excitation; exposure 1 minute. The continuum is pronounced and the bands are almost absent. (b) Exciting discharge; exposure 5 seconds. A few lines are present, and there are also some S_2 bands.





The Speed of Positive Ions in Nitrogen

By J. H. MITCHELL and K. E. W. RIDLER, Wills Physical Laboratory,
University of Bristol

(Communicated by A. M. Tyndall, F.R.S.—Received May 31, 1934)

In a previous paper* from this laboratory it was suggested that when helium ions move under the influence of an electric field through helium gas, the positive charge carried by an ion does not remain long associated with a single atom, but is repeatedly passed on from ion to atom at collision by the process of electron capture.† This process may be regarded as equivalent to an increase in the target area presented by the atoms to the positive helium ions and must therefore lead to a reduction in their mobility. When foreign ions move in a given gas the conditions of resonance necessary for electron capture would not normally occur. If therefore in the absence of electron capture the mobility of a foreign ion in a given gas is found to afford an unambiguous measure of its mass, we may expect the value of the mobility of the ions of the gas itself to be less than that predicted from their mass, owing to the operation of this process.

From the study of a number of ions in various gases we now know that helium is not a satisfactory gas in which to demonstrate the effect. Even with simple ions like Rb^+ , Cs^+ , In^+ , Tl^+ the size of the ion has a profound effect on its mobility, so that the fact that He^+ ions in helium move more slowly than the much heavier sodium ions cannot be definitely attributed to an exchange process. The exchange hypothesis offers a very probable, but not a certain, explanation of the relatively low mobility of the helium ions.

In nitrogen, however, it was found‡ that the mobility K_m of an ion of atomic weight m is given to an accuracy of within about 1% by the relation

$$K_m = B \left(1 + \frac{28}{m} \right)^{\frac{1}{2}}$$

cm/sec/unit field, where B is a numerical constant; this relation holds for a number of ions including such widely different ions as Na^+ , $(\text{Na}, \text{NH}_3)^+$ and

* Tyndall and Powell, 'Proc. Roy. Soc.,' A, vol. 134, p. 125 (1931).

† Kallmann and Rosen, 'Z. Physik,' vol. 61, p. 261 (1930).

‡ Tyndall and Powell, 'Proc. Roy. Soc.,' A, vol. 136, p. 146 (1931); Powell and Brata, *ibid.*, vol. 138, p. 117 (1932); Brata, *ibid.*, vol. 141, p. 454 (1933).

Th^+ . On Langevin's classical theory this result follows if the "size" of an ion has no appreciable influence on its mobility. In this paper we show that this relation is also true for the molecular ion NH_3^+ as well as for the ions Kr^+ , Xe^+ and Hg^+ ; moreover, from the mobility value obtained for ions of molecular nitrogen we obtain in this case evidence of electron capture. In addition evidence for electron capture is obtained indirectly from the study of the breakdown of Langevin's law ($\text{mobility} \times \text{pressure} = \text{constant}$), when the velocity is increased above a certain value.

Experimental Method

The metal parts of the apparatus used in these experiments are shown diagrammatically in fig. 1. With the exception of the alkali ions obtained

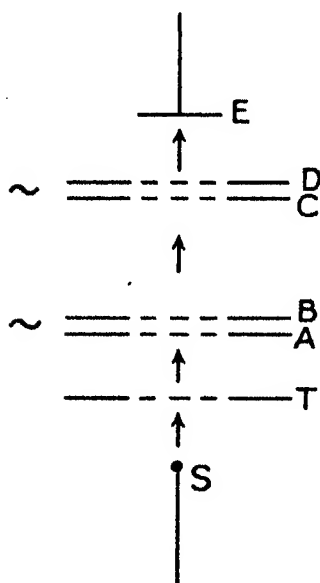


FIG. 1

from Kunsman sources the positive ions were formed by a glow discharge in the gas between a rounded point electrode S and a perforated cathode T, and were dragged by a suitable field up to the shutter AB and thence to the shutter CD and to the electrometer plate E. The mobility of the ions, which may be regarded as typical of those in the positive column of the discharge, was then determined by the four gauze method which has been adequately described in previous papers.

Nitrogen was produced by heating pure sodium azide, diluted by the addition of silver sand in order to avoid explosive decomposition. The silver sand was previously heated in air in an electric furnace to 1000°C to drive off water and organic impurities. The mixture was placed in a quartz tube which was itself enclosed in

an evacuated tube of pyrex. It was heated for many hours *in vacuo* at 300°C and then the nitrogen was driven off by raising the temperature slowly to 380°C the first gas evolved being pumped off. The sodium, which is formed as a product of the decomposition of the azide, removes any residual water and oxygen. The gas was sometimes passed into a tube containing heated copper oxide to remove possible traces of hydrogen, and finally into the apparatus through a trap immersed in liquid oxygen.

The ions formed in the gas obtained by this method have a mobility of 2.67 cm/sec/volt/cm, and a typical curve is shown in fig. 2 (curve *a*). Here the electrometer current is plotted against fp/E in arbitrary units where f is the frequency, p the pressure and E the field. This quantity is proportional to the mobility. We have obtained the peak due to this group of ions in a great many samples of gas, and for reasons detailed below, we regard the

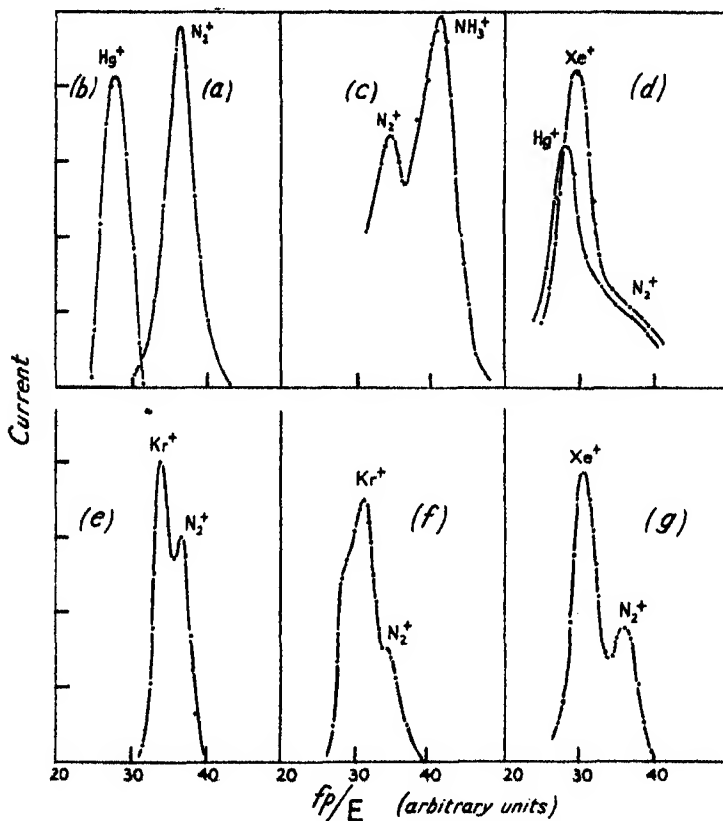


FIG. 2

group as characteristic of pure nitrogen. Fig. 3 is a curve showing the mobility in nitrogen of various ions plotted with their mass. Those previously examined* are indicated by a dot including Ba^+ at 2.23 obtained by Powell and Brata previously unpublished; other ions referred to later in the paper are indicated by a cross. The point for pure nitrogen is shown by a circle and it will be seen that with this exception the mobility gives an unambiguous measure of

* Tyndall, Powell and Brata, *loc. cit.*

the mass of all the ions tested, though the dispersion at high masses is very small. The dotted curve is that given by the equation

$$K_m = B \left(1 + \frac{28}{m} \right)^{\frac{1}{2}}$$

with the ordinate fitted at the sodium point.

If the ions produced in a glow discharge in pure nitrogen are diatomic molecular ions then according to fig. 3 we might expect them to have a mobility of 2.89. There are three possible explanations of the low value obtained in these experiments :

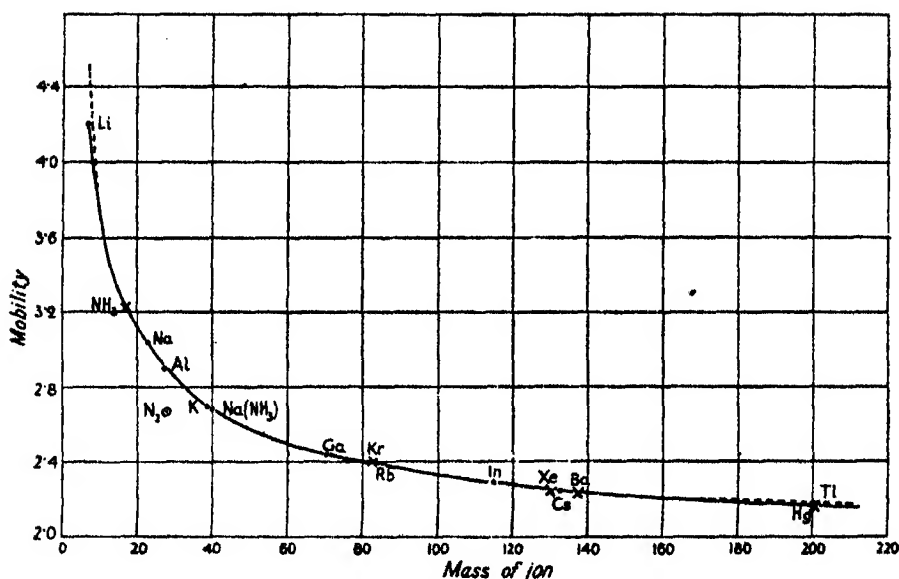


FIG. 3

(1) Although every precaution was taken to secure pure nitrogen, the ions might possibly be charged atoms or molecules of impurity produced by various collision processes in the glow discharge. If so we can deduce from the mass curve that the ions must have a mass 40 ± 1 .

(2) In recent experiments by Luhr* evidence has been obtained for the formation of triatomic and tetratomic molecular ions by a glow discharge in nitrogen, the number of these ions increasing with the number of collisions that the ions make with the neutral gas molecules. We may therefore assume, as a second possibility, that the ions are triatomic molecular ions of mass 42.

* 'Phys. Rev.', vol. 44, p. 459 (1933).

They cannot be ions of atomic nitrogen or of tetratomic nitrogen for then their mobility would in the former case be 3.54 and in the latter 2.50.

(3) The ions may be molecular nitrogen, the low mobility being explained by the phenomenon of electron exchange.

Some light is thrown on the first suggestion by some experiments which were undertaken to extend the range of application of the mobility mass relation in nitrogen by studying the ions produced when controlled amounts of various impurities were added to pure nitrogen. The results are shown by the remaining curves in fig. 2. Curve (b) shows the effect on the mobility of the ions of allowing mercury vapour, saturated at room temperature, to enter the pure gas. It will be seen that the original group of ions has disappeared completely, and that it is replaced by a group of mobility 2.16. Assuming that this group is due to Hg^+ ions of mass 206 we obtain another point which lies approximately 1.5% below the mass mobility curve (fig. 3) drawn through the points representing the results of previous experiments.

Similarly the addition of less than 0.8% of hydrogen to the nitrogen resulted in the appearance of a group of ions of mobility 3.22* as well as the group attributed to N_2^+ , fig. 2 (curve c). From fig. 3 we deduce that the mass of the ions of this mobility is 17 and we therefore identify them as NH_3^+ . The ammonia is continuously produced by the action of the glow discharge on the gas mixture and although the gas had access to a trap cooled in liquid oxygen to -178°C , the equilibrium vapour pressure of ammonia in the mobility chamber is sufficiently great to give a large proportion of NH_3^+ ions in the glow discharge. The remaining curves, d, e, f, g, show peaks in nitrogen due to Xe^+ at mobility 2.23 and Kr^+ at mobility 2.41 which are identified by these values in fig. 3. The conditions under which these curves were obtained will be discussed later.

Other impurities were tried with results not at present susceptible to analysis, but there was no evidence of a peak of mobility 2.67 due to the added impurity. We therefore feel confident that the ions produced in the uncontaminated gas are really characteristic of pure nitrogen.

It remains to decide whether they are due to N_2^+ or N_3^+ . The peak due to N_3^+ of mass 42 should occur at 2.63 which is near that which was observed. But it is very improbable that more than a small percentage of the ions drawn from the glow discharge are triatomic; they could not therefore be responsible for the whole of the single peak observed. There remains only the third

* When the added impurity differs considerably from nitrogen in density, a small density correction has been applied in deducing the mobility.

possibility that the observed single group is due to ions of diatomic nitrogen reduced 7.5% in mobility by the process of electron exchange. This is rendered still more probable by indirect evidence from experiments described in the following paragraph.

Breakdown in Langevin's Law

In the absence of an external electric field, a positive ion executes a Brownian movement in a gas. When a field is applied, an acceleration of the ions in the direction of the field takes place between successive collisions; this motion is imposed on the random movement of the ions, and the charge drifts through the gas. On the classical theory at low field-strengths and high pressures this drift velocity, W , through nitrogen gas, of an ion of atomic weight m is given by the relation

$$W = \frac{AE}{p} \left(1 + 28/m\right)^{\frac{1}{2}}, \quad (1)$$

where A is a constant, E is the electric field and p the pressure. It follows that we may expect the velocity W of a given ion to be proportional to the quantity E/p . But the theory assumes that the rate of drift in the electric field is small compared with the velocity of thermal agitation. At higher values of E/p this will not be true and we may therefore expect that the law will break down and that the velocity of the ions will exceed that given by equation (1).

We have studied this breakdown in Langevin's law for a number of different ions in nitrogen. In fig. 4 the experimental results are expressed by plotting the quantity Wp/E against E/p for the ions Li^+ , Na^+ , K^+ , Rb^+ , Cs^+ , NH_4^+ and $\text{Na}^+(\text{NH}_3)$. For convenience E is measured in volts/cm and p in mm of mercury. It will be seen that as long as E/p is sufficiently low, the experimental points lie on a horizontal straight line in accordance with the simple theory. At the higher values, however, Wp/E seems to increase approximately linearly with E/p . The velocity of an ion after breakdown presumably follows some law such as

$$W = \alpha (E/p) + \beta (E/p)^2.$$

With some of the lighter ions there is evidence that the discontinuity is quite sharp; for this reason the curves are so drawn, giving a critical value $(E/p)_c$ for breakdown. By an indirect method Huxley obtained a similar graph for helium ions moving through helium gas. But the results of Tyndall and Powell in this gas suggest that his method was less satisfactory for quantitative measurements.

It will be seen from fig. 4 that the critical value of E/p where the breakdown of Langevin's law begins is characteristic of the ion, being greater the smaller the mass of the ion. A second empirical characteristic of the curves which may be noticed is that the slope of the lines after breakdown also increases with decrease of ionic mass. It will also be seen that the value of $(E/p)_c$ for the ions (Na^+ , NH_3), of mass 40, is practically coincident with that for K^+ , of

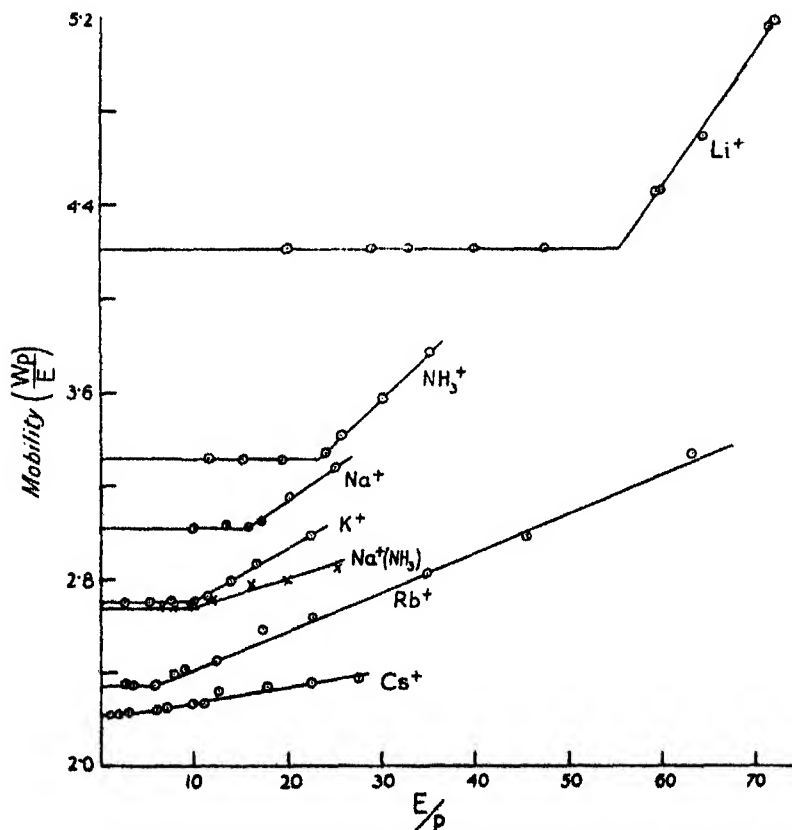


FIG. 4.

mass 39, although the slopes of the two curves after breakdown are very different. Similar curves have been obtained for the ions produced in pure nitrogen and the results are shown in fig. 5.

In fig. 6 the value of $(E/p)_c$ is plotted against the reciprocal of the mass of the ions. The results lie approximately on a straight line through the origin with the single exception of the result shown by a cross for the ions produced by a glow discharge in pure nitrogen. This line affords a second method of

distinguishing the mass of an ion in nitrogen by mobility measurements, though here again the dispersion is smallest with ions of the greatest mass.

It was shown above that of the three possible ways of explaining the values of mobility obtained in the purest nitrogen, the view that the ions were those

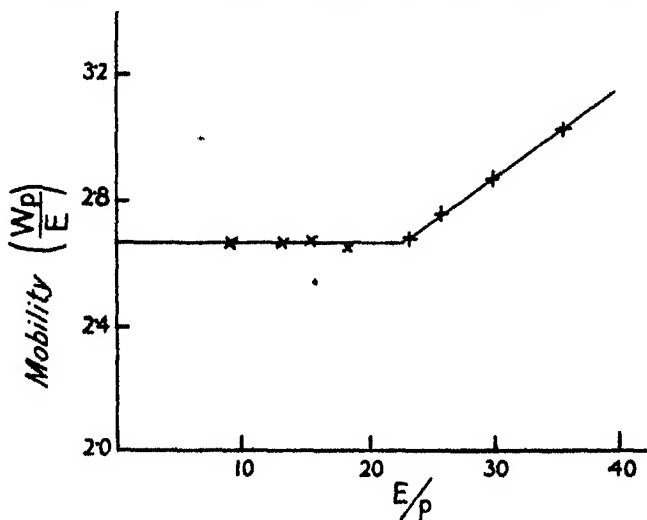


FIG. 5—Nitrogen ions

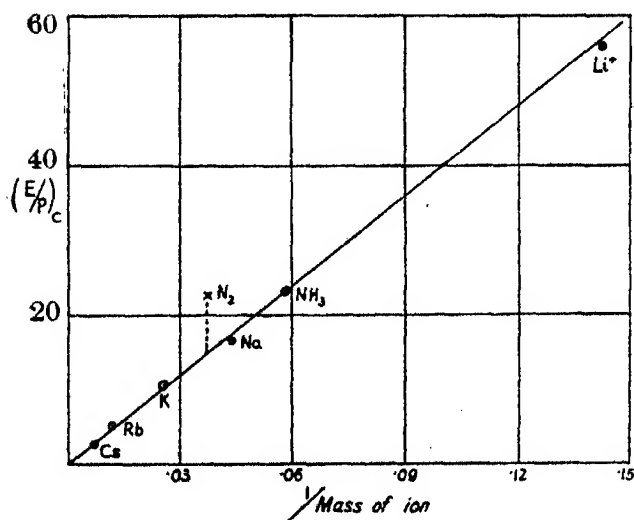


FIG. 6

of diatomic nitrogen with a mobility reduced by the process of exchange was the most probable. The fact that the pure nitrogen point, if it is assumed to be due to N_2^+ , is off the line in fig. 6 is further evidence in favour of this

explanation. The mobility results at low values of E/p show that the ions in pure nitrogen move as though they had a mass of 40. If this were their true mass the value of $(E/p)_c$ from fig. 6 should be 9.7; actually it is 22.5. In order to place this value on the straight line we should have to assume their mass to be 17.4. Such an ion would have a mobility of 3.2 instead of the value 2.67 actually found.

On the other hand if the ions are due to N_2^+ , this anomaly is easily explained on the exchange hypothesis. By comparison with most experiments on positive ions carried out at low pressure we are here dealing with very slow ions, and the collision time, the period during which the ion remains in the field of force of a colliding atom, is comparatively long.

In addition to direct collisions which take place for all ions, there may be an appreciable probability that the N_2^+ ions transfer their charge to a neutral molecule at relatively distant collisions, since this process requires no energy change. Whenever this exchange of charge occurs there is an additional loss of momentum in the direction of the field which leads to a reduction in mobility. Indeed we may think of an exchange of charge as equivalent to a head-on collision with no exchange. Its effect, therefore, is the same as that of an increase in gas pressure. Consequently if we suppose that Langevin's law breaks down when the average momentum of an ion exceeds a certain value a higher field will be required to produce this value when exchange is operating. Thus the phenomenon of exchange explains why both the mobility and the breakdown value of E/p for the N_2^+ ion in nitrogen differ from those characteristic of another ion of the same mass.

The Effects of Added Impurities

It is well known that small quantities of impurity may have a profound effect on the spectrum of a gas discharge. It has even become a matter of industrial importance in attempts to produce a "white" discharge lamp. A number of facts have been accumulated in this laboratory on the ions produced by glow discharge in various gases contaminated with known amounts of impurity and it is clear that the two problems are closely related. While further information is necessary before the results can be analysed in the light of a comprehensive theory, this seems to be a convenient opportunity for recording the data for nitrogen. One striking result was that obtained by removing a liquid oxygen trap so that mercury vapour was added to pure nitrogen at a concentration of about 0.018%. This is referred to above and

is plotted in fig. 2, curve (b). A comparison with curve (a) shows the complete suppression of N_2^+ ions and their replacement by Hg^+ . The pressure of the nitrogen was 5.2 mm. It should, however, be mentioned that in all these experiments the number of positive ions dragged to the shutter AB had to be made sufficient to give a peak current adequate for accurate measurement. This was secured by altering the voltage of the discharge and dragging field by amounts which varied with the nature and percentage of the added impurity. The words "suppression of ions" is therefore used here in the sense that the percentage of them entering the measuring apparatus is negligible under the changed conditions but not necessarily under all conditions of applied voltage.

When 0.03% of pure xenon was added to pure nitrogen the upper curve (d) shows the presence of a strong Xe^+ peak, with a tail probably due to N_2^+ . This Xe^+ peak was suppressed by 0.018% Hg (lower curve) even when the concentration of Xe was raised to 1%. Curve (e) shows the result of adding 0.19% of pure krypton to nitrogen at 8.31 mm giving both Kr^+ and N_2^+ peaks. In curve (f) the concentration of Kr was raised to 0.27% and the pressure of the mixture reduced to 4.46 mm. In this curve a bulge is shown on the low mobility side of the Kr^+ peak indicating the presence of a heavier ion. At a still higher concentration of krypton (0.74%) this is quite clearly identified in curve (g) as Xe^+ , the krypton ions being suppressed. Presumably the xenon was present as an impurity in the krypton although this was stated by the makers to be over 99% pure.

Now the ionization potentials of N_2 , Kr, Xe, and Hg are 16.7, 13.9, 12.1, and 10.4 respectively. At first sight it may seem that the results may be interpreted by one mechanism of ionization alone, that of direct electron impact. Thus mercury displaces both Xe and N_2 because, owing to its low ionization potential, it acts as a barrier and prevents the electrons from ever obtaining a high enough energy to ionize xenon or nitrogen themselves. For the same reason xenon displaces krypton. On this view, however, without more knowledge of the distribution of electron velocities in the discharge, the following results are a little surprising:—(1) the entire suppression of nitrogen by such a very low concentration of mercury; (2) the suppression of Xe by mercury when the ratio of their concentrations is 60 to 1 and the difference in their ionization potentials only 1.7 volts; (3) the suppression of krypton by xenon in the krypton nitrogen mixtures *without* the suppression of nitrogen.

On the other hand it is probable that metastable atoms play a role in the production of ions in many gas discharges. But the best experimental evidence

suggests that the metastable nitrogen molecule carries an energy of about 8.3 volts and this is insufficient to ionize any of the impurities added to nitrogen in the present experiments. It may be that we have to deal with some combined process of excitation in which both gas and impurity atoms coupled with electron impacts are concerned. A study of the intensity distribution of the lines of the spectrum of the positive column in pure and in contaminated nitrogen should throw some light on the problem.

We are indebted to Professor Tyndall for his encouragement and advice during the course of the work and to Dr. C. F. Powell for the benefit of his experience in mobility measurement. We have also to thank the Colston Research Society of the University of Bristol for a grant in aid.

Summary

The mobility of the positive ions produced by glow discharge in pure nitrogen at a pressure of from 4 to 9 mm has been found to be 2.67 cm/sec/volt/cm. Values of the mobilities of NH_3^+ , Kr^+ , Xe^+ and Hg^+ in nitrogen have also been obtained by adding small quantities of these substances to the gas. Of the 17 ions in nitrogen, which have now been studied in this laboratory, all lie on a smooth curve connecting the mobility of an ion with its mass, except those in pure nitrogen.

Evidence is advanced for the view that the ions found in pure nitrogen are N_2^+ and that their mobility is 7.5% less than that appropriate to their mass owing to the phenomenon of electron exchange.

Further evidence of exchange is afforded by a study of the breakdown in the law which states that the speed of an ion is proportional to the field E and inversely proportional to the pressure p . A linear relation is found for seven ions between the critical value of E/p for breakdown and the reciprocal of the mass of the ion. Again the ion N_2^+ is anomalous.

Examples are given of the suppression of ions of one kind and their replacement by ions of an impurity present in small concentration.

*Separation of the Isotopes of Lithium and some Nuclear
Transformations observed with them*

By M. L. OLIPHANT, Royal Society Messel Research Fellow, E. S. SHIRE, and
B. M. CROWTHER, Cavendish Laboratory, Cambridge

(Communicated by Lord Rutherford, O.M., F.R.S.—Received June 11, 1934)

In studying the transformations of elements by bombarding particles, it is of great importance to examine separately the effects due to each isotope of composite elements. It is to be anticipated that the nature of the transformations will be very different for the individual isotopes, and in a study of a complex element it may prove difficult to decide with certainty which isotope is responsible for the effects under consideration. For these reasons experiments have been made to devise methods of separation of isotopes in sufficient quantity for direct observation of the nature of the transformations produced in them.

With the exception of the isotopes of hydrogen, by far the most promising method for the complete separation of isotopes is by means of some form of mass spectrograph. Unfortunately the quantities separable in this way are very small. In the mass spectrographs of Aston, Bainbridge, etc., the isotope beams produced are of the order of 10^{-8} ampere or less, while for lithium a beam of a microampere would deposit only a quarter of a microgram of Li^7 per hour. The probability of disintegration of lithium by protons and deuterons is, however, so large that monomolecular layers suffice for an experiment and quantities of the order of a tenth of a microgram are ample. Attention was therefore directed to obtaining quantities of this order by means of a mass spectrograph designed to give large ion beams.

Two spectrographs have been built, both using the combined action of crossed electrostatic and magnetic fields to separate the isotopes. This method has two advantages over that employing a magnetic field alone. Since the ions may be made to travel in approximately straight lines, the apparatus required is simple to make and adjust, while the separation of the isotope beams may be made much greater with both electrostatic and magnetic fields than with a magnetic field alone. In both spectrographs the ions were obtained from a platinum filament coated with a mixture of $3\text{Li}_2\text{CO}_3$, Al_2O_3 , 3SiO_2 , as described by Jones.* These sources proved very reliable and satis-

* 'Phys. Rev.,' vol. 44, p. 707 (1933).

factory, provided that they were first overheated until a sudden increase in emission indicated that the surface had been activated in some way. After this activation an ion current of several hundred microamperes could be taken from the source for several hours. The isotopes were collected on small metal plates carried on a glass tube filled with liquid nitrogen. After collection the isotopes were fixed by admitting a puff of HCl into the apparatus to form lithium chloride. Details of the two spectrographs will now be given.

Spectrograph 1

The apparatus, fig. 1, was of small and simple design, and was in the form of a rectangular tube, the sides of which were made up of soft iron magnetic pole pieces 14 cm long, and the top and bottom of two electrostatic deflecting plates 10 cm long fixed between them at a distance of 2 mm apart, the upper of the two plates being insulated. The electric deflecting plates D formed a defining

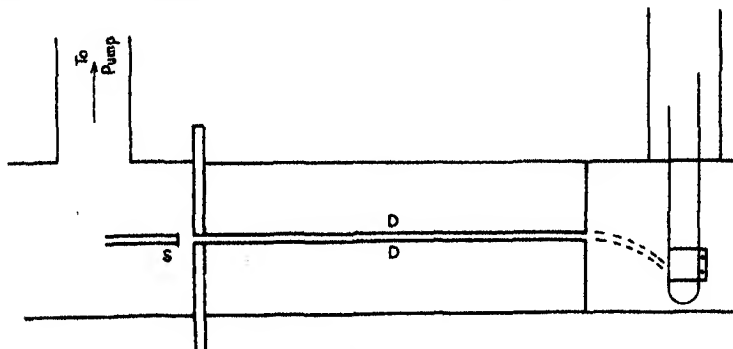


FIG. 1

channel of cross-section $2\text{ cm} \times 2\text{ mm}$ through which was passed a beam of positive ions of lithium of about 800 volts energy, from a flat source S, prepared as described above, and placed 4 mm from the mouth of the channel. With a magnetic field of about 4000 gauss, and the electric deflecting field so adjusted (600 volts/cm) as to allow the ions of one isotope to follow a straight path, the ions of the other isotope would be deflected in a distance of 10 cm through about 1.5 cm, and so would have no chance of passing out of the other end of the channel. The ions entering the crossed fields require to be homogeneous in velocity within about 7%, and this was easily accomplished with the source and accelerating voltage used. The magnetic field was arranged to extend 4 cm beyond the region of the electric field; consequently the ion beam, after passing straight through the crossed fields, was deflected through about 1 cm

by the magnetic field alone. This deflection of the ion beam separated it from the atomic beam, which was condensed on the liquid air tube opposite the slit.

Difficulty was experienced in getting a reasonably large current through the slit, owing to the fact that there was a considerable leakage in the magnetic field in the space between the source and the slit, and no appreciable electric field to balance it. By suitably orientating and tilting the source, a current of about 2.5×10^{-6} amps of Li^7 , or a tenth of that of Li^6 , could be received on a nickel collector strapped round the liquid air tube. After a few minutes running an easily discernible trace was made on the nickel sheet. This trace was quite sharply defined, and of width slightly less than 2 mm. This showed that the ion beam emerging from the electric field was homogeneous in velocity, and could only consist of one isotope. The only possibility of contamination would be due to the diffusion of uncharged atoms through the channel.

The isotopes were collected one at a time. Targets were prepared, of Li^7 by collecting a current of about 2.5×10^{-6} amps for 5 minutes, and of Li^6 by collecting 0.25×10^{-6} amps for 50 minutes. The quantities separated were therefore of the order of 5×10^{-8} gm.

The low accelerating voltage used (800 volts) reduced the possibility of the lithium atoms being knocked off the target; the purity of the separated isotopes is shown by the results of the disintegration experiments.

Spectrograph 2

In this spectrograph the ion beams were brought to a sharp focus after passing through the crossed fields by means of the electrostatic fields accelerating the ions leaving the source. Ions from the filament F, fig. 2, prepared as described above, were accelerated by a potential difference of about 4000 volts between the electrodes E_1 and E_2 and by a further 6000 volts between E_2 and E_3 . Ions diverging from the slit S in E_2 were made to converge by the field between E_2 and E_3 , the position of the resulting focus depending on the ratio of the potential difference between the filament and E_2 and that between E_2 and E_3 . For the separation of the lithium isotopes the focus was made to come slightly in front of the collecting plates CC. On applying an electrostatic field between the plates PP and a magnetic field perpendicular to it over the region within the dotted line of fig. 2, the focal spot split into two, corresponding to the two isotopes, and these spots were arranged to fall on the collectors CC. The focal spots, as determined by a willemite screen and by the

traces on the collectors, measured about $8 \times 2\frac{1}{2}$ mm. For ions accelerated by 10,000 volts, the magnetic field available would have permitted a separation of the two beams of Li_6 and Li_7 of over 4 cm. As the deflecting plates were only 2 cm apart such a separation would have made it impossible to collect both isotopes simultaneously, so the magnetic field was reduced until the separation was 15 mm, when both isotopes could be collected at the same time. For this separation a magnetic field of 1300 gauss was required and an electrostatic field of 600 volts per cm. The accelerating and deflecting potentials were obtained from transformers and rectifiers connected to the A.C. mains and the D.C. mains were used to excite the magnet. The separation of the two isotope beams was not seriously affected by mains fluctuations and any simultaneous drift of the beams was indicated by a galvanometer connected to two electrodes N, placed between the collecting plates and connected to earth through 10 megohm resistances.

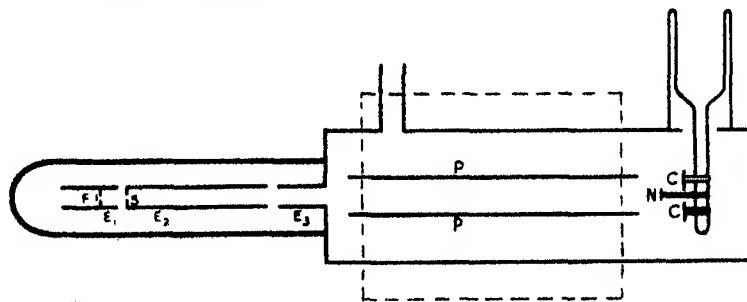


FIG. 2.

With this apparatus beams of 5 microamps of Li_7 and 0.4 microamps of Li_6 were easily obtained, but owing to the sputtering action of the incident ions on the lithium already present on the collectors it was impossible to collect more than a few tenths of a microgram of either isotope in a single run. The apparatus is being modified to overcome this defect by slowing down the ions before collection.

Transformation Experiments with the Separated Isotopes

In general, for purposes of experiments on the differences in their properties, separated isotopes are required in much larger amounts than we have been able to obtain so far. From the point of view of nuclear structure the most important experiments are the transformations observed when lithium is bombarded by fast particles. Oliphant and Rutherford* have shown that it

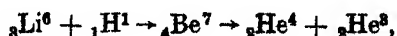
* 'Proc. Roy. Soc.,' A, vol. 141, p. 259 (1933).

is possible to observe the products of transformation from a fraction of a monomolecular layer of lithium when bombarded by protons or by deuterons, and therefore quantities such as are collected in the present experiments are ample for accurate work. Accordingly the copper and nickel discs, upon which the separated isotopes had been deposited, were mounted upon the target system of the apparatus described elsewhere* and they were bombarded successively with protons and with ions of heavy hydrogen accelerated through a potential of about 160 kv. The range distribution among the resulting charged particles was measured by absorption in mica, while neutrons were searched for by observation of the ionization produced by recoil nuclei in the counting chamber. A linear amplifier and oscillograph were used to record the particles.

It will be seen that the Li^6 and Li^7 targets behave very differently under bombardment by protons or deuterons, the range and nature of the escaping particles being characteristic of the particular isotope. The details of the observations are included below.

Li^6 Bombarded with Protons

Large numbers of doubly charged particles of range 11.5 mm were detected under these conditions. We were unable to observe below a range of about 9 mm as the mica window through which particles escaped into the counting chamber had a stopping power equivalent to about 6 mm of air and we required an extra 3 mm in order that the particles should be recorded. Oliphant, Kinsey, and Rutherford† have reported the presence of two short range groups of particles from lithium under proton bombardment, one range being identical with that observed in the present experiments, and a shorter range group travelling 6–8 mm in air. Some expansion chamber photographs obtained by Dee‡ suggest that these particles are emitted in opposite pairs, a particle of 11.5 mm range appearing opposite an 8 mm particle. The reaction suggested by Oliphant and Rutherford (*loc. cit.*) to account for the presence of these groups is



the He^4 corresponding to the 8 mm group and the He^3 to the 11.5 mm group. The energy of the He^3 particle can be determined from its range, and it can be shown that the observed ranges satisfy momentum considerations as

* Oliphant, Hartek, and Rutherford, 'Proc. Roy. Soc.,' A, vol. 144, p. 692 (1934).

† 'Proc. Roy. Soc.,' A, vol. 141, p. 722 (1933).

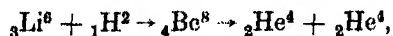
‡ 'Nature,' vol. 133, p. 564 (1934).

closely as the accuracy of the experimental results will allow. It is then possible to calculate the mass of He^3 . Using the mass for Li^6 given by Bainbridge* the mass of He^3 comes out to be 3.0166, while the mass of Li^6 calculated from disintegration data† gives 3.0178.

In addition to the short range group of particles discussed above, the Li^6 targets gave a few particles of range 8.4 cm. It is clear from the experiments described later for the Li^7 isotope, that these 8.4 cm particles arise from a slight contamination of the Li^6 target with atoms of lithium of mass 7. The relative number of these particles varied widely for different targets, but was never greater than 1% of the number of short range particles observed, so that the contamination of the Li^6 targets by Li^7 could never have been greater than a few per cent. No other groups were observed.

Li^6 Bombarded by Heavy Hydrogen Ions

The Li^6 targets all gave a large emission of 13.2 cm α -particles when bombarded by ions of heavy hydrogen. These particles have been discussed by Oliphant, Kinsey, and Rutherford (*loc. cit.*) and expansion chamber photographs have been obtained by Dee and Walton.‡ It seems certain that the reaction which gives rise to them is



the two α -particles being emitted in opposite directions. Energy and momentum relations are satisfied if the mass of Li^6 is assumed to be about 6.0157, which is further from Bainbridge's value of 6.0145 than the experimental errors in the mass or the range determinations would seem to allow. It is perhaps significant that the value 6.0157, derived from the range data, gives calculated results closer to the experimental values in some other atomic transformations.§

In the experiments with heavy hydrogen the Li^6 target also gave two groups of protons of ranges about 14 and 30 cm. The 14 cm group of protons is present with all target materials and it is natural to assume that it arises from bombardment of a deposit on the target of heavy hydrogen from the beam.

* 'Phys. Rev.,' vol. 44, p. 56 (1933).

† See next paragraph.

‡ 'Proc. Roy. Soc.,' A, vol. 141, p. 733 (1933).

§ Cf. Oliphant, Harteck, and Rutherford, 'Proc. Roy. Soc.,' A, vol. 144, p. 692 (1934).

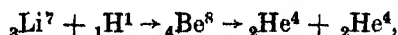
The 30 cm group has been observed by Cockcroft and Walton* who concluded that it must arise from the transformation



The Li^6 targets did not give rise to a neutron emission which was greater than that observed from bombardment of iron or copper by heavy hydrogen ions, and this small emission probably arose from contamination with heavy hydrogen.

Li^7 Bombarded by Protons

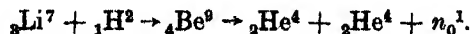
An emission of α -particles of 8.4 cm range was observed. This is the group of particles first found by Cockcroft and Walton,† and of which expansion chamber photographs have been obtained by Kirchner,‡ and by Dee and Walton (*loc. cit.*). The nuclear reaction which results in the production of the group is



and the measured range agrees very well with that calculated from the mass of Li^7 given by Bainbridge (*loc. cit.*). The best of the Li^7 targets gave no trace of any other group of particles, and in the others there was just a trace of the short range group characteristic of Li^6 .

Li^7 Bombarded by Heavy Hydrogen Ions

When heavy hydrogen was substituted for the ordinary hydrogen, using a Li^7 target, a continuous distribution of α -particles was found from 1 cm up to about 8 cm range. Oliphant, Kinsey, and Rutherford (*loc. cit.*) have discussed the mechanism of production of this inhomogeneous group of particles, and they came to the conclusion that it was a three body reaction in which two α -particles and a neutron are emitted.



We have observed deflections of the oscillograph produced by recoil particles which result from collisions between neutrons and the nuclei of the gas in our ionization chamber, and have shown that the number of such recoils was much greater from the Li^7 target than from the Li^6 or from iron. It seems probable,

* 'Proc. Roy. Soc.,' A, vol. 144, p. 704 (1934).

† 'Proc. Roy. Soc.,' A, vol. 137, p. 229 (1932).

‡ 'Naturwiss.,' vol. 21, p. 473 (1933).

therefore, that the above reaction does express correctly what happens in this case.

Discussion

The experimental results which we have described seem to establish beyond all doubt that the methods which we have used have resulted in the preparation of very pure samples of the separated isotopes of lithium. The quantities which we have dealt with have been very small, of the order of 10^{-8} gram, but the methods are capable of development to give about a milligram of the separated isotopes per day. The limiting factors are the intensity of the ion beam which it is possible to obtain and the difficulties of collection introduced by the sputtering action of the incident ions. The intensity of a beam of positive ions is seriously limited by space-charge effects and this factor sets an upper limit to the current which can be used, for it causes the two divergent beams of ions to spread and overlap one another if the intensity is too high. The sputtering action may be eliminated by reducing the velocity of the ions to a few volts immediately before collection, or alternatively by collecting the deposited lithium ions in a deep and cooled depression in a block of metal.

The possibility of using other sources of positive ions is being explored, and it is hoped to be able to separate the isotopes of boron and of some other elements which are required for transmutation experiments.

Summary

A description is given of the methods used to separate the isotopes of lithium in quantities of the order of 10^{-8} gram. The completeness of the separation effected, and the possibility of using such small quantities of material for definite experiments on the transmutation effects observed during bombardment by protons and by ions of heavy hydrogen, is confirmed by the further experiments described. In these the targets were mounted and bombarded with hydrogen ions at about 160,000 volts energy, and the particles emitted were examined. The results are summarized in the following table.

Bombarding particles	Lithium 6	Lithium 7
Protons	α -particles of 11.5 mm range	α -particles of 8.4 cm range
Diplons	α -particles of 13.2 cm range	α -particles up to 8 cm range
	Protons of 30 cm range	Neutrons

On Born's Theory of the Electron

By J. FRENKEL, Physical Technical Institute, Leningrad

(Communicated by P. A. M. Dirac, F.R.S.—Received June 22, 1934)

The equations of the electromagnetic field are derived in Born's theory* from the variation principle $\delta \int \mathcal{L} d\tau = 0$ with the Lagrangian

$$\mathcal{L} = b^2 (1 - \sqrt{1 - (E^2 - H^2)/b^2})$$

where $E = -\nabla\phi - \frac{1}{c} \mathbf{A}$ and $H = \text{curl } \mathbf{A}$, b being the maximum value of E . In order to obtain the equation of motion Born and Infeld† use instead of the Lagrangian the Hamiltonian H putting $\delta \int H d\tau = 0$. This seems to me a hardly justifiable procedure.

Born and Infeld's main results (1) the finite value of the electromagnetic mass of a punctual electron, and (2) the fact that it is acted upon by an external field in the same way as if it was an extended ("free") charge, can, however, be obtained by a very simple method which seems to be wholly unobjectionable.

Besides giving the correct dependence of the mass on the velocity, this method yields the correct ratio (c^2) between the rest-energy and the rest-mass of the electron.

1.—In order to obtain the mass of the electron we consider the electromagnetic momentum of the field produced by it when in uniform motion. The density of the electromagnetic momentum is given in Born's theory by the vector

$$\mathbf{g} = \frac{1}{c} \frac{\mathbf{E} \times \mathbf{H}}{\sqrt{1 - (E^2 - H^2)/b^2}} \quad (1)$$

(where my H corresponds to Born's B and *vice versa*).

The values of E and H can easily be derived from the value E' of the electric field produced by the electron in a co-ordinate system S' with respect to which it is at rest (i.e., which is moving with respect to the original system with the same velocity v as the electron) with the help of the familiar transformation formulæ of the relativity theory

$$\left. \begin{aligned} E_x &= E'_x, & E_y &= \gamma E'_y, & E_z &= \gamma E'_z, \\ H_x &= 0, & H_y &= \gamma \frac{v}{c} E'_z, & H_z &= -\gamma \frac{v}{c} E'_y \end{aligned} \right\} \quad (2)$$

x being the direction of relative motion and $\gamma = (1 - v^2/c^2)^{-1/2}$.

* 'Proc. Roy. Soc.,' A, vol. 143, p. 410 (1934).

† 'Proc. Roy. Soc.,' A, vol. 144, p. 425 (1934).

Noting further that $E^2 - H^2 = E'^2$ (since $H' = 0$) we get

$$g_x = \frac{\gamma^2}{c^2} v \frac{E'_x{}^2 + E'_y{}^2}{\sqrt{1 - E'^2/b^2}}, \quad (3)$$

the total momentum G being equal to $\iiint g_x dx dy dz$ (and parallel to v).

In carrying out the integration we can transform from the original co-ordinate system S to the moving one S' by putting $dx = \frac{1}{\gamma} dx'$, $dy = dy'$, $dz = dz'$, that is $dx dy dz = \frac{1}{\gamma} dV'$, dV' being the element of volume in S' . Since, further, the electrostatic field produced by a point charge resting at the origin of S' is radially symmetrical we can replace

$$\int \frac{E'_x{}^2 + E'_y{}^2}{\sqrt{1 - E'^2/b^2}} dV' \quad \text{by} \quad \frac{2}{3} \int \frac{E'^2}{\sqrt{1 - E'^2/b^2}} dV',$$

which gives

$$G = \frac{2}{3} \frac{\gamma v}{c^2} \int \frac{E'^2}{\sqrt{1 - E'^2/b^2}} dV'. \quad (4)$$

This expression is of the usual form $G = \frac{m_0 v}{\sqrt{1 - v^2/c^2}}$ if the rest-mass of the electron is defined by

$$m_0 = \frac{1}{c^2} \frac{2}{3} \int \frac{E^2}{\sqrt{1 - E^2/b^2}} dV, \quad (5)$$

where for the sake of simplicity we have dropped the dashes indicating that all the quantities concerned refer to the system with respect to which the electron is at rest. In the classical theory of the extended spherical electron this expression reduces to $m_0 = \frac{1}{c^2} \frac{2}{3} \int E^2 dV$ ($b = \infty$), i.e., $m_0 = \frac{1}{c^2} \frac{4}{3} U$,

$U = \frac{1}{2} \int E^2 dV$ being the electron's own (electrostatic) energy. The factor $4/3$ is in contradiction with the relativity theory which requires that m_0 should be *exactly* equal to U/c^2 . This difficulty has been considered by a number of different authors, in particular by Fermi, but the solutions proposed seem to me artificial and unsatisfactory.

Now it is a very pleasant feature of Born's theory that in the case of the *punctual* electron (and *only* in this case) the integral in (5) reduces to $\frac{2}{3} U$ (instead of $2U$), thus giving the desired relativistic relation between mass and energy.

To see this let us note that the energy density is given according to Born's theory (in the absence of a magnetic field) by the expression

$$\eta = b^2 \left(\frac{1}{\sqrt{1 - E^2/b^2}} - 1 \right), \quad (6)$$

which in the limiting case $b \rightarrow \infty$ reduces to the ordinary one $\eta = \frac{E^2}{2}$. Introducing the vector $D = \frac{E}{\sqrt{1 - E^2/b^2}}$ (corresponding to the "momentum" in mechanics or to the "electrical induction" in the ordinary theory of a polarizable medium with the dielectric coefficient $\epsilon = \frac{1}{\sqrt{1 - E^2/b^2}}$, we have further $\frac{1}{\sqrt{1 - E^2/b^2}} = \sqrt{1 + D^2/b^2}$ and consequently

$$\eta = b^2 (\sqrt{1 + D^2/b^2} - 1) = b (\sqrt{b^2 + D^2} - b). \quad (7)$$

We get in a similar way

$$\begin{aligned} \frac{E^2}{\sqrt{1 - E^2/b^2}} &= b^2 \left(\frac{1}{\sqrt{1 - E^2/b^2}} - \sqrt{1 - E^2/b^2} \right) \\ &= b^2 \left(\sqrt{1 + D^2/b^2} - \frac{1}{\sqrt{1 + D^2/b^2}} \right), \end{aligned}$$

whence

$$\int \frac{E^2}{\sqrt{1 - E^2/b^2}} dV = b^2 \int (\sqrt{1 + D^2/b^2} - 1) dV + b^2 \int \left(1 - \frac{1}{\sqrt{1 + D^2/b^2}} \right) dV.$$

The first of these two integrals is equal to the electrostatic energy U . In order to evaluate the second one we note that it can be written in the form

$$-b^2 \frac{\partial}{\partial b} \int (\sqrt{b^2 + D^2} - b) dV = -b^2 \frac{\partial}{\partial b} \left(\frac{U}{b} \right).$$

Now in the case of a punctual electron $U = \kappa \cdot \frac{e^2}{r_0}$, where κ is a numerical constant of the order of 1 (which is immaterial for us) and r_0 the electron's effective radius defined by $\frac{e}{r_0^2} = b$. We thus have $U \propto b^3$ and $\frac{U}{b} \propto b^2$ whence

$$-b^2 \frac{\partial}{\partial b} \left(\frac{U}{b} \right) = \frac{2}{3} U,$$

and consequently

$$\int \frac{E^2}{\sqrt{1 - E^2/b^2}} dV = \frac{5}{3} U.$$

Substituting this in the expression (5) we see that the factor $\frac{1}{2}$ cancels out and thus obtain the relativistic relation between mass and energy

$$m_0 = \frac{U}{c^2}.$$

2---We shall now turn to the question as to the force acting on an electron in a given external field, limiting ourselves for the sake of simplicity to the case of an electrostatic field.

It should be mentioned that in a dynamical theory of the electromagnetic field ("unitarian" theory according to Born) the notion of "force" becomes meaningless, the *total* force acting on the electron always vanishing (it is just this principle that determines the laws of motion). The really important quantity is the electromagnetic energy (or more exactly the energy tensor, the equations of motion being derived from the principle of its conservation). The separation of the total field into two parts—that due to the electron under consideration and another due to the external system of charges—is not possible for the electromagnetic field \mathbf{E} , \mathbf{H} is not additive with respect to its "sources." This additivity must hold, however, at least approximately for

the induction vectors $\mathbf{D} = \frac{\mathbf{E}}{\sqrt{1 - (\mathbf{E}^2 - \mathbf{H}^2)/b^2}}$ and $\mathbf{B} = \frac{\mathbf{H}}{\sqrt{1 - (\mathbf{E}^2 - \mathbf{H}^2)/b^2}}$ since they are connected in Born's theory with the true distribution of electric charge and current by exactly the same equations, as in the ordinary theory. In the particular case of an electrostatic field due to a system of punctual charges at rest we have, for example, $\text{div } \mathbf{D} = 0$ everywhere outside these charges. Since, however, $\text{curl } \mathbf{D}$ is in general different from zero (whereas $\text{curl } \mathbf{E} \equiv 0$) it must not be thought that the additivity law for \mathbf{D} is exactly valid. The departure from it can be shown, however, to be the smaller the larger the distance between the electrons concerned compared with r_0 .

Let us consider the *total* electrostatic energy U of the given electron and some other relatively remote system of charges and let us put $\mathbf{D} = \mathbf{D}_1 + \mathbf{D}_2$ where \mathbf{D}_1 is the induction due to the former, and \mathbf{D}_2 , that due to the latter. The energy density of the resulting field $\eta = b^2(\sqrt{1 + \mathbf{D}^2/b^2} - 1)$ in the neighbourhood of the electron in question ($\mathbf{D}_1 \gg \mathbf{D}_2$) can be written approximately in the form

$$\eta = b^2(1 + \mathbf{D}_1^2/b^2)^{\frac{1}{2}} \left[1 + \frac{\mathbf{D}_1 \cdot \mathbf{D}_2}{b^2(1 + \mathbf{D}_1^2/b^2)} \right] - b^2 = \eta_{1,1} + \eta_{1,2},$$

where

$$\eta_{1,1} = b^2(\sqrt{1 + \mathbf{D}_1^2/b^2} - 1)$$

is the part corresponding to the electron's own energy while

$$\gamma_{1,2} = \frac{\mathbf{D}_1 \cdot \mathbf{D}_2}{\sqrt{1 + D_1^2/b^2}} \quad (8)$$

is the part defining the mutual action between the electron (1) and the "external system" (2). The "external force" acting on the electron can thus be calculated as the negative gradient (with respect to its co-ordinates) of the mutual potential energy $U_{1,2} = \int \gamma_{1,2} dV$, the integration being practically extended over a small volume containing the electron, where D_2 remains small compared with D_1 . Under these conditions we can put $\mathbf{D}_2 \approx \mathbf{E}_2$; since further

$\frac{\mathbf{D}_1}{\sqrt{1 + D_1^2/b^2}} = \mathbf{E}_1$ we get

$$U_{1,2} = \int \mathbf{E}_1 \cdot \mathbf{E}_2 dV, \quad (9)$$

which is *exactly* the same expression as that defining the *mutual* potential energy of two systems of electrical charges in the ordinary theory (it reduces in particular to $\frac{e_1 e_2}{r_{1,2}}$ in the case of two point charges at a distance $r_{1,2}$ apart).

Putting $\mathbf{E}_2 = -\nabla\phi_2$ we can transform (9) to the familiar form

$$U_{1,2} = \int \phi_2 \operatorname{div} \mathbf{E}_1 dV, \quad (10)$$

which is the same as in the ordinary theory, if the distribution of the electron's charge is described not by the divergence of the vector \mathbf{D}_1 (corresponding to a punctual charge) but by the divergence of the vector \mathbf{E}_1 . This is the "free charge" of Born's theory, the above derivation being quite similar to that of Born and Infeld, but being free from the objection of using an unjustified (and I think unjustifiable) variation principle for its derivation. The preceding results are easily generalized for an arbitrary electromagnetic field.

Summary

The formula of Born and Infeld for the mass and the equations of motion of an electron are derived by a direct method which avoids the variation principle used by these authors.

Remarks on the paper by Frenkel on Born's Theory of the Electron

By M. BORN and L. INFELD

Frenkel's derivation of the electromagnetic mass and the equations of motions of the electron are very suggestive and simple. But we cannot admit that our method of reasoning is unjustified. There are two points :

(1) We have proved exactly that the two variation principles using the Lagrangian and the Hamiltonian are entirely equivalent, both leading to the same results (p. 436). The reason why we have to use the Hamiltonian, not the Lagrangian, for the derivation of the equations of motion is the additivity of the $p_{kl}(\mathbf{D}, \mathbf{H})$ and not of the $f_{kl}(\mathbf{E}, \mathbf{B})$ in accordance with Frenkel's statement ; we regret that we have stated this important point only in a footnote (p. 449).

(2) Frenkel's calculation of the energy and momentum for a uniformly moving co-ordinate system is entirely equivalent to our derivation of the so-called Laue-theorem (p. 446), which states that in the proper co-ordinate system all space integrals of the components of the energy-tensor T_{kl} vanish, except the energy $E_0 = m_0 c^2 = \frac{1}{4}\pi \int T_{44} dx dy dz$. From this follows immediately that in any co-ordinate system (of special relativity)

$$\frac{1}{4}\pi \int T_{14} dx dy dz = m_0 \frac{v}{\sqrt{1 - \frac{v^2}{c^2}}},$$

in accordance with Frenkel's equation (4).

We are very grateful to Mr. Frenkel for having given to us the opportunity of reading his manuscript.

INDEX TO VOL. CXLVI (A)

- Acetaldehyde and ethylene, mixtures, kinetics of oxidation (Steacie and Plewes), 72.
- D'Agostino (O.) *See* Fermi and others.
- Aldehyde molecules, modes of activation in decomposition reactions (Hinshelwood and others), 327.
- Aldehyde, propionic, thermal decomposition (Winkler and others), 345.
- Aldehydes and ketones, rotatory dispersion (Lowry and Allsopp), 313.
- Allsopp (C. B.) Refractive dispersion of organic compounds. Part V—Oxygenated derivatives of cyclohexane. The inadequacy of the Ketteler-Helmholtz equation, 300.
- Allsopp (C. B.) *See also* Lowry and Allsopp.
- Aluminium, artificial disintegration by radium C' α -particles (Duncanson and Miller), 396.
- Amaldi (E.) *See* Fermi and others.
- Antimony, explosive, studies (Coffin and Johnston), 564.
- Antimony, nuclear spins and magnetic moments of isotopes (Tolansky), 182.
- Arnot (F. L.) and Baines (G. O.) Approximate phases in electron scattering, 651.
- Arnot (F. L.) and McLaughlan (F. C.) The scattering of electrons in bromine vapour, 603.
- Arsenic II, intensity measurements in a fine structure (Tolansky and Heard), 818.
- Aston (F. W.) Isotopic constitution and atomic weights of the rare earth elements, 46.
- Atoms, collisions with slow electrons, IV (Massey and Mohr), 880.
- Baines (G. O.) *See* Arnot and Baines.
- Band systems, excitation by electron impact (Langstroth), 166.
- Beevers (C. A.) and Lipson (H.) The crystal structure of copper sulphate pentahydrate, $\text{CuSO}_4 \cdot 5\text{H}_2\text{O}$, 570.
- Benzene ring and related compounds, theory of stability (Penney), 223.
- Bethe (H.) and Heitler (W.) On the stopping of fast particles and on the creation of positive electrons, 83.
- Bhabha (H. J.) and Hulme (H. R.) The annihilation of fast positrons by electrons in the K-shell, 723.
- Blackett (P. M. S.) Technique of the counter controlled cloud chamber, 281.
- Childs (E. C.) and Woodcock (A. H.) The scattering of slow electrons by organic molecules. I—Acetylene, ethylene, and ethane, 199.
- Chloral, kinetics of decomposition and its catalysis by iodine (Verhoek and Hinshelwood), 334.
- Chrysene, X-ray analysis of structure (Iball), 140.
- Cloud chamber, technique of the counter controlled (Blackett), 281.
- Coffin (C. C.) and Johnston (S.) Studies on explosive antimony. I—The microscopy of polished surfaces, 564.
- Cohen (L. L.) *See* Townend, Cohen and Mandlekar.
- Copper sulphate pentahydrate, crystal structure (Beevers and Lipson), 570.
- Corrosion, velocity from electrochemical standpoint (Evans and Mears), 153.

- Crowther (B. M.) *See* Oliphant and others.
- Cyclohexane, refractive dispersion of oxygenated derivatives (Allsopp), 300.
- Darwin (C. G.) The refractive index of an ionized medium, 17.
- Decomposition reactions (Hinshelwood and others), 327, 334, 345, 357.
- Denisoff (A. K.) and Richardson (O. W.) The emission of electrons under the influence of chemical action. Part IV—The reactions of liquid NaK_2 with gaseous SOCl_2 , S_2Cl_2 , SO_2Cl_2 , HgCl_2 , sulphur dichloride and with mixtures of gases and a new method of determining the contact potential difference, 524.
- Dibenzyl, X-ray analysis of crystal structure (Robertson), 473.
- Dirac's theory of the positive electron (Peierls), 420.
- Discussion on energy distribution in molecules in relation to chemical reactions (Hinshelwood and others), 239.
- Dispersion, refractive, of organic compounds. (Allsopp and Lowry, and Allsopp), 300, 313.
- Dispersion, supersonic in gases (Richardson), 56.
- Duncanson (W. E.) and Miller (H.) Artificial disintegration by radium C' α -particles—aluminium and magnesium, 396.
- Electron, Born's theory (Frenkel), 930.
- Electron, positive, vacuum in Dirac's theory (Peierls), 420.
- Electron scattering, approximate phases (Arnot and Baines), 651.
- Electron scattering, in bromine vapour (Arnot and McLauchlan), 663.
- Electrons, emission under influence of chemical action, Part IV (Denisoff and Richardson), 524.
- Electrons in the K-shell, annihilation of fast positrons (Bhabha and Hulme), 723.
- Electrons, positive, creation (Bethe and Heitler), 83.
- Electrons, slow, collisions with atoms, IV (Massey and Mchr), 880.
- Electrons, slow, scattering by organic molecules, I (Childs and Woodcock), 199.
- Ellis (C. D.) and Henderson (W. J.) Artificial radioactivity, 206.
- Emulsions, formation in definable fields of flow (Taylor), 501.
- Energy distribution in molecules, discussion (Hinshelwood and others), 239.
- Ethyl alcohol, sorption by silica gels (Foster), 129.
- Ethylene and acetaldehyde, mixtures, kinetics of oxidation (Steaie and Plewes), 72.
- Ethylene, hydrogenation and exchange reaction with heavy hydrogen (Farkas and others), 630.
- Evans (U. R.) and Mears (R. B.) Velocity of corrosion from the electro-chemical standpoint, III, 153.
- Evaporation in a turbulent atmosphere (Sutton), 701.
- Farkas (A.) and Farkas (L.) Experiments of heavy hydrogen. III—The electrolytic separation of the hydrogen isotopes, 623.
- Farkas (A.), Farkas (L.) and Rideal (E. K.) Experiments on heavy hydrogen. IV—The hydrogenation and exchange reaction of ethylene with heavy hydrogen, 630.
- Farkas (L.) *See* Farkas and Farkas.
- Farkas (L.) *See also* Farkas, Farkas and Rideal.
- Fermi (E.), Amaldi (E.), D'Agostino (O.), Rasetti (F.) and Segrè (E.) Artificial radioactivity produced by neutron bombardment, 483.
- Fisher (R. A.) Probability likelihood and quantity of information in the logic of uncertain inference, 1.

- Fisk (J. B.) and Taylor (H. M.) Internal conversion of γ -rays, 178.
 Fletcher (C. J. M.) *See* Hinshelwood and others.
 Fletcher (C. J. M.) Thermal decomposition of formaldehyde, 357.
 Fletcher (C. J. M.) *See also* Winkler and others.
 Flow, formation of emulsions in definable fields (Taylor), 501.
 Formaldehyde, thermal decomposition (Fletcher), 357.
 Foster (A. G.) The sorption of methyl and ethyl alcohol by silica gels, 129.
 Frenkel (J.) On Born's theory of the electron, 930.
- Gamma rays, internal conversion (Fisk and Taylor), 178.
 Gamma-rays, physical basis of the biological effects (Mayneord), 867.
 Gamow (G.) Nuclear spin of radioactive elements, 217.
 Gas-air mixtures, inflammable, influence of pressure on spontaneous ignition, III (Townend and others), 113.
 Gases, supersonic dispersion (Richardson), 56.
 Gas Molecules, exchange of energy with platinum surface (Mann), 776.
 Gaydon (A. G.) Spectrum of the afterglow of sulphur dioxide, 901.
- Heard (J. F.) *See* Tolansky and Heard.
 Heitler (W.) *See* Bethe and Heitler.
 Henderson (W. J.) *See* Ellis and Henderson.
 Hinshelwood (C. N.) *See also* Verhoek and Hinshelwood.
 Hinshelwood (C. N.) *See also* Winkler and others.
 Hinshelwood (C. N.), Fletcher (C. J. M.), Verhoek (F. H.) and Winkler (C. A.) The modes of activation of aldehyde molecules in decomposition reactions, 327.
 Hulme (H. R.) *See* Bhabha and Hulme.
 Hydrocarbons, gaseous, kinetics of the oxidation (Steacie and Plewes), 583.
 Hydrogen bromide, photosynthesis, inert gas effects (Ritchie), 828.
 Hydrogen, heavy, III (Farkas and Farkas, and Farkas and Rideal), 623, 630.
 Hydrogen isotopes, electrolytic separation (Farkas and Farkas), 623.
 Hydrogen, kinetics of the reaction with nitrous oxide, II and III (Melville), 737.
- Iball (J.) X-ray analysis of the structure of chrysene, 140.
 Index, refractive, of an ionized medium (Darwin), 17.
 Inference, logic of uncertain, probability, likelihood and quantity of information (Fisher), 1.
 Ions, positive, speed in nitrogen (Mitchell and Ridler), 911.
 Iron, magneto-caloric effect and other magnetic phenomena (Potter), 362.
 Isotopes and atomic weights of rare earth elements (Aston), 46.
- Jeffreys (H.) Probability and scientific method, 9.
 Johnston (S.) *See* Coffin and Johnston.
- Kinetics of oxidation of gaseous hydrocarbons (Steacie and Plewes), 583.
 Kinetics of oxidation of mixture of ethylene and acetaldehyde (Steacie and Plewes), 72.
- Langstroth (G. O.) Excitation of band systems by electron impact, 166.
 Laszlo (H. de) Molecular structure as determined by a new electron diffraction method.
 I—Experimental. II—The halogen-carbon bond distance in some simple benzene derivatives, 672, 690.

- Levine (S.) Problem of the sedimentation equilibrium in colloidal suspensions, 597.
- Lipson (H.) *See* Beevers and Lipson.
- Lithium, separation of the isotopes and some nuclear transformations observed with them (Oliphant and others), 922.
- Lowry (T. M.) and Allsopp (C. B.) Refractive dispersion of organic compounds. Part VI—Refractivities of the oxygen, carbonyl and carboxyl radicals. Origin of optical rotatory power and of the anomalous rotatory dispersion of aldehydes and ketones, 313.
- McLauchlan (F. C.) *See* Arnot and McLauchlan.
- Magnesium, artificial disintegration by radium C' α -particles (Duncanson and Miller), 396.
- Mandlekar (M. R.) *See* Townend, Cohen and Mandlekar.
- Mann (W. B.) The exchange of energy between a platinum surface and gas molecules, 776.
- Massey (H. S. W.) and Mohr (C. B. O.) The collisions of slow electrons with atoms, IV, 880.
- Mayneord (W. V.) The physical basis of the biological effect of high voltage radiations, 867.
- Mears (R. B.) *See* Evans and Mears.
- Medium, ionized, refractive index (Darwin), 17.
- Melville (H. W.) The kinetics of the reaction between hydrogen and nitrous oxide, II, 111, 737.
- Mercury fluorescence, dark interval (Rayleigh), 272.
- Metals, liquid, resistance (Mott), 465.
- Metals, theory of surface photoelectric effect (Mitchell), 442.
- Methyl and ethyl alcohol, sorption by silica gels (Foster), 129.
- Methyl nitrite, gaseous, homogeneous unimolecular decomposition (Steacie and Shaw), 388.
- Miller (H.) *See* Duncanson and Miller.
- Mitchell (J. H.) and Ridler (K. E. W.) The speed of positive ions in nitrogen, 911.
- Mitchell (K.) Theory of the surface photoelectric effect in metals, 442.
- Mohr (C. B. O.) *See* Massey and Mohr.
- Molecular structure, as determined by a new electron diffraction method (Laszlo), 672, 690.
- Molecules, discussion on energy distribution in relation to chemical reactions (Hinshelwood and others), 239.
- Mott (N. F.) The resistance of liquid metals, 465.
- Neutron bombardment, artificial radioactivity produced (Fermi and others), 483.
- Nitrogen, speed of positive ions (Mitchell and Ridler), 911.
- Nitrous oxide, fluorescent radiation (Sen Gupta), 824.
- Nitrous oxide, kinetics of the reaction with hydrogen, II and II (Melville), 737.
- Oliphant (M. L.), Shire (E. S.) and Crowther (B. M.) Separation of the isotopes of lithium and some nuclear transformations observed with them, 922.
- Ozone, thermal decomposition (Ritchie), 828.
- Particles, fast, stopping (Bethe and Heitler), 83.
- Peierls (R.) Vacuum in Dirac's theory of the positive electron, 420.
- Penney (W. G.) Theory of the stability of the benzene ring and related compounds, 223.
- Perman (E. P.) *See* Thomas and Perman.
- Photoelectric effect, surface, theory in metals (Mitchell), 442.

- Platinum, freezing point (Schofield), 792.
- Platinum surface, exchange of energy with gas molecules (Mann), 776.
- Plewes (A. C.) *See* Steacie and Plewes.
- Positrons, fast, annihilation by electrons in the K-shell (Bhat ha and Hulme), 723.
- Potter (H. H.) Magneto-caloric effect and other magnetic phenomena in iron, 362.
- Probability and scientific method (Jeffreys), 9.
- Probability likelihood and quantity of information in the logic of uncertain inference (Fisher), 1.
- Radiations, high voltage, physical basis of the biological effects (Mayneord), 867.
- Radioactivity, artificial (Ellis and Henderson), 206.
- Radioactivity, artificial, produced by neutron bombardment (Fermi and others), 483.
- Radium C' α -particles, artificial disintegration—aluminium and magnesium (Duncanson and Miller), 396.
- Rasetti (F.) *See* Fermi and others.
- Rayleigh (Lord) The Dark interval in mercury fluorescence, 272.
- Refractivities of the oxygen, carbonyl and carboxyl radicals (Lowry and Allsopp), 313.
- Richardson (E. G.) Supersonic dispersion in gases, 56.
- Richardson (O. W.) *See* Denisoff and Richardson.
- Rideal (E. K.) *See* Farkas, Farkas and Rideal.
- Ridler (K. E. W.) *See* Mitchell and Ridler.
- Ritchie (M.) Inert gas effects in the photosynthesis of hydrogen bromide, 828.
- Ritchie (M.) The thermal decomposition of ozone, 848.
- Robertson (J. M.) X-ray analysis of the crystal structure of dibenzyl. I—Experimental and structure by trial, 473.
- Schofield (F. H.) The freezing point of platinum, 792.
- Sedimentation equilibrium in colloidal suspensions (Levine), 597.
- Segrè (E.) *See* Fermi and others.
- Sen Gupta (P. K.) Fluorescent radiation from N_2O , 824.
- Shaw (G. T.) *See* Steacie and Shaw.
- Shire (E. S.) *See* Oliphant and others.
- Silica gels, sorption of methyl and ethyl alcohol (Foster), 129.
- Solutions, aqueous, compressibility, II (Thomas and Perman), 640.
- Spectrum of afterglow of sulphur dioxide (Gaydon), 901.
- Spectrum of AsII, intensity measurements (Tolansky and Heard), 818.
- Spin, nuclear of radioactive elements (Gamow), 217.
- Steacie (E. W. R.) and Plewes (A. C.) Kinetics of the oxidation of mixtures of ethylene and acetaldehyde, 72.
- Steacie (E. W. R.) and Plewes (A. C.) The kinetics of the oxidation of gaseous hydrocarbons. II—The oxidation of ethane, 583.
- Steacie (E. W. R.) and Shaw (G. T.) Homogeneous unimolecular decomposition of gaseous methyl nitrite, 388.
- Sulphur dioxide, spectrum of the afterglow (Gaydon), 901.
- Suspensions, colloidal, sedimentation equilibrium problem (Levine), 597.
- Sutton (O. G.) Wind structure and evaporation in a turbulent atmosphere, 701.
- Taylor (G. I.) The formation of emulsions in definable fields of flow, 501.
- Taylor (H. M.) *See* Fish and Taylor.

- Thomas (H. G.) and Perman (E. P.) The compressibility of aqueous solutions, II, 640.
- Tolansky (S.) Nuclear spins and magnetic moments of the isotopes of antimony, 182.
- Tolansky (S.) and Heard (J. F.) Intensity measurements in a fine structure multiplet of AsII, 818.
- Townend (D. T. A.), Cohen (L. L.) and Mandlekar (M. R.) The influence of pressure on the spontaneous ignition of inflammable gas-air mixtures. III—Hexane-and isobutane-air mixtures, 113.
- Verhoek (F. H.) and Hinshelwood (C. N.) The Kinetics of the decomposition of chloral and its catalysis by iodine, 334.
- Verhoek (F. H.) *See also* Hinshelwood and others.
- Wind structure and evaporation in a turbulent atmosphere (Sutton), 701.
- Winkler (C. A.), Fletcher (C. J. M.) and Hinshelwood (C. N.) Thermal decomposition of propionic aldehyde, 345.
- Winkler (C. A.) *See also* Hinshelwood and others.
- Woodcock (A. H.) *See* Childs and Woodcock.
- X-rays, physical basis of the biological effects (Mayneord), 867.

L. A. R. 76

IMPERIAL AGRICULTURAL RESEARCH
INSTITUTE LIBRARY
NEW DELHI

Date of issue.	Date of issue.	Date of issue.
2-11-21		
2-15-22		
3-4-58		
2-4-2-60		
27 AUG 1961		